frontiers | Research Topics

Movement and connectivity of large pelagic sharks

Edited by
R. J. David Wells, J. Marcus Drymon, Clive N. Trueman,
Yannis Peter Papastamatiou, Johann Mourier and
Mark Meekan

Published in
Frontiers in Marine Science

ISSN 1664-8714
ISBN 978-2-8325-1178-7
DOI 10.3389/978-2-8325-1178-7

About Frontiers

Frontiers is more than just an open access publisher of scholarly articles: it is a pioneering approach to the world of academia, radically improving the way scholarly research is managed. The grand vision of Frontiers is a world where all people have an equal opportunity to seek, share and generate knowledge. Frontiers provides immediate and permanent online open access to all its publications, but this alone is not enough to realize our grand goals.

Frontiers journal series

The Frontiers journal series is a multi-tier and interdisciplinary set of open-access, online journals, promising a paradigm shift from the current review, selection and dissemination processes in academic publishing. All Frontiers journals are driven by researchers for researchers; therefore, they constitute a service to the scholarly community. At the same time, the *Frontiers journal series* operates on a revolutionary invention, the tiered publishing system, initially addressing specific communities of scholars, and gradually climbing up to broader public understanding, thus serving the interests of the lay society, too.

Dedication to quality

Each Frontiers article is a landmark of the highest quality, thanks to genuinely collaborative interactions between authors and review editors, who include some of the world's best academicians. Research must be certified by peers before entering a stream of knowledge that may eventually reach the public - and shape society; therefore, Frontiers only applies the most rigorous and unbiased reviews. Frontiers revolutionizes research publishing by freely delivering the most outstanding research, evaluated with no bias from both the academic and social point of view. By applying the most advanced information technologies, Frontiers is catapulting scholarly publishing into a new generation.

What are Frontiers Research Topics?

Frontiers Research Topics are very popular trademarks of the *Frontiers journals series*: they are collections of at least ten articles, all centered on a particular subject. With their unique mix of varied contributions from Original Research to Review Articles, Frontiers Research Topics unify the most influential researchers, the latest key findings and historical advances in a hot research area.

Find out more on how to host your own Frontiers Research Topic or contribute to one as an author by contacting the Frontiers editorial office: frontiersin.org/about/contact

Movement and connectivity of large pelagic sharks

Topic editors
R. J. David Wells — Texas A&M University at Galveston, United States
J. Marcus Drymon — Mississippi State University, United States
Clive N. Trueman — University of Southampton, United Kingdom
Yannis Peter Papastamatiou — Florida International University, United States
Johann Mourier — Université de Montpellier, France
Mark Meekan — University of Western Australia, Australia

Citation
Wells, R. J. D., Drymon, J. M., Trueman, C. N., Papastamatiou, Y. P., Mourier, J., Meekan, M., eds. (2023). *Movement and connectivity of large pelagic sharks*. Lausanne: Frontiers Media SA. doi: 10.3389/978-2-8325-1178-7

Table of contents

frontiers in Marine Science

ORIGINAL RESEARCH
published: 01 September 2020
doi: 10.3389/fmars.2020.566364

Seasonal Movements and Habitat Use of Juvenile Smooth Hammerhead Sharks in the Western North Atlantic Ocean and Significance for Management

Ryan K. Logan[1,2]*, Jeremy J. Vaudo[1,2], Lara L. Sousa[3], Mark Sampson[4], Bradley M. Wetherbee[1,5] and Mahmood S. Shivji[1,2]*

[1] Guy Harvey Research Institute, Nova Southeastern University, Dania Beach, FL, United States, [2] Save Our Seas Foundation Shark Research Center, Nova Southeastern University, Dania Beach, FL, United States, [3] Wildlife Conservation Research Unit, Department of Zoology, The Recanati-Kaplan Centre, University of Oxford, Tubney, United Kingdom, [4] Fish Finder Adventures, Ocean City, MD, United States, [5] Department of Biological Sciences, University of Rhode Island, Kingston, RI, United States

OPEN ACCESS

Edited by:
Yannis Peter Papastamatiou,
Florida International University,
United States

Reviewed by:
James Ketchum,
Independent Researcher, La Paz,
Mexico
Camrin Braun,
University of Washington,
United States

***Correspondence:**
Ryan K. Logan
rlogan@nova.edu;
rklogn@gmail.com
Mahmood S. Shivji
mahmood@nova.edu

Specialty section:
This article was submitted to
Marine Megafauna,
a section of the journal
Frontiers in Marine Science

Received: 27 May 2020
Accepted: 12 August 2020
Published: 01 September 2020

Citation:
Logan RK, Vaudo JJ, Sousa LL,
Sampson M, Wetherbee BM and
Shivji MS (2020) Seasonal
Movements and Habitat Use
of Juvenile Smooth Hammerhead
Sharks in the Western North Atlantic
Ocean and Significance
for Management.
Front. Mar. Sci. 7:566364.
doi: 10.3389/fmars.2020.566364

Upper trophic level predators dramatically impacted by fisheries include the large-bodied hammerhead sharks, which have become species of conservation concern worldwide. Implementing spatial management for conservation of hammerhead populations requires knowledge of temporal distribution patterns and habitat use, identification of essential habitat for protection, and quantification of interactions with human activities. There is little such information for the smooth hammerhead shark, *Sphyrna zygaena*. We used fin-mounted satellite tags to examine the movements and habitat use of juvenile smooth hammerheads, a demographic segment particularly threatened by exploitation. Six sharks were tagged off the US mid-Atlantic and tracked for 49–441 days (mean 187 ± 136 days). Sharks consistently showed area-restricted movements within a summer core area in waters of the New York Bight and a winter core area off Cape Hatteras, North Carolina, with directed movements between them in autumn. There was high overlap of shark winter core area use and the Mid-Atlantic Shark Area (MASA) – a 7 month per year, bottom-longline fishery closure – indicating that this area closure offers seasonal reduction in fishing pressure for this species. Based on timing of shark movements and the MASA closure, protection for juvenile smooth hammerheads may be increased by beginning the closure period 1 month earlier than currently scheduled. Generalized additive mixed models revealed that area-restricted movements of sharks in their summer and winter core areas coincided with high primary productivity, and elevated sea surface temperature. Consistency in use of summer and winter core areas suggests that the coastal waters of the New York Bight and Cape Hatteras, North Carolina could be considered for Essential Fish Habitat designation for this species. This study reveals the first high resolution movements and habitat use for smooth hammerheads in the western North Atlantic to inform management planning for this population.

Keywords: ***Sphyrna zygaena*, movement ecology, behavior, conservation, satellite telemetry**

INTRODUCTION

The rapid expansion of elasmobranch fisheries and trade globally are principal drivers of population decline for many shark species (Dulvy et al., 2014). Some species, such as the large-bodied hammerhead sharks (great – *Sphyrna mokarran,* scalloped – *S. lewini,* and smooth – *S. zygaena* hammerheads), are especially vulnerable to fishing pressure because of their slow rates of population growth (Cortés et al., 2010) and high at-vessel and post-release mortality due to elevated stress response to capture (Morgan and Carlson, 2010; Eddy et al., 2016; Gallagher and Klimley, 2018). In addition, hammerhead sharks are taken in large numbers because of the high demand for their superior-quality fins (large size and high ceratotrichia count) in the global shark fin trade (Abercrombie et al., 2005; Clarke et al., 2006a,b; Cardeñosa et al., 2018). While population declines of the large-bodied hammerhead shark species complex is thought to be largely driven by declines of scalloped hammerheads (Jiao et al., 2011), low catch rates in various parts of the world for all species suggest a significant historical decline in the abundance of all large-bodied hammerhead sharks (Baum et al., 2003; Baum and Blanchard, 2010; Ferretti et al., 2010).

Fishery exploitation of smooth hammerhead sharks via targeting or bycatch has been identified as the major threat to this species, particularly for juveniles (Casper et al., 2009; Cortés et al., 2010; Miller, 2016). The conservation of this species is an international priority, e.g., Vulnerable listing on the International Union for Conservation of Nature (IUCN) Red List (Casper et al., 2009); Appendix II listing on the Convention on International Trade in Endangered Species of Wild Fauna and Flora (CITES); Appendix II listing on the Convention on Migratory Species of Wild Animals (CMS). Furthermore, an ecological risk assessment of sharks caught in Atlantic pelagic longline fisheries highlighted smooth hammerheads as a species in urgent need of biological data necessary for stock assessment (Cortés et al., 2010). However, conservation-relevant data on many aspects of the biology of smooth hammerheads are extremely limited, including information relating to their movements, seasonal distributions and habitat use (Miller, 2016; Gallagher and Klimley, 2018).

Achieving sustainable populations of fishery exploited species is critically dependent on the recruitment of immature individuals. Thus, identification and conservation of essential habitat for juvenile and sub-adult sharks is of paramount importance, requiring an understanding of this key demographic segment's spatiotemporal patterns of occurrence and associated oceanic environmental drivers (Kinney and Simpfendorfer, 2009; Schlaff et al., 2014). Equipped with adequate information on how environmental parameters influence seasonal movements, spatial management measures such as temporal closures of targeted areas can be enacted to promote recovery of overfished stocks. For example, based on understanding of temporal and spatial habitat use of dusky sharks (*Carcharhinus obscurus*), the Mid-Atlantic Shark Area (MASA) – a region closed to bottom longline fishing for 7 months each year – was established in 2005 as a means of reducing fishing mortality and enhancing recovery of this species (NMFS, 2009).

Smooth hammerheads have a circumglobal distribution in coastal and oceanic waters and occupy a wider latitudinal range than other sphyrnids (Compagno, 1984). Catch records from a variety of locations suggest that juveniles and sub-adults [<265 cm total length (TL)] are more common in inshore waters over coastal shelves, with larger individuals (>265 cm TL) found more frequently offshore (Diemer et al., 2011; Clarke et al., 2015; Francis, 2016; Deacy et al., 2020). This species is capable of long distance movements (e.g., 6,610 km over 150 days; Santos and Coelho, 2018), but also shows high levels of resident behavior within restricted areas (at least 80 days; Diemer et al., 2011).

To date, just two studies have reported on the finer-scale movements of smooth hammerheads via satellite telemetry. Horizontal and vertical movements of juveniles in the temperate western South Pacific appear to vary seasonally (Francis, 2016); in contrast, juvenile and adult smooth hammerheads in the tropical eastern Atlantic demonstrated relatively stable temporal diving behavior (Santos and Coelho, 2018). These studies illustrate the possibility that movements and behavior of smooth hammerheads may be influenced by thermal heterogeneity of their environment. Very little information on relationships between other environmental variables (primary productivity, oceanic fronts, water depth) and movements of smooth hammerheads exists (Couto et al., 2018), although these variables have been shown to greatly influence movement and habitat selection of highly mobile sharks (Block et al., 2011; Queiroz et al., 2016; Vaudo et al., 2017). Understanding interactions between patterns of habitat use and environmental variables would contribute toward construction of habitat models and an improved ability to predict the distribution of smooth hammerheads under climate change scenarios, as well as reveal potential interactions with human activities throughout their range.

Given minimal information on the spatial ecology of smooth hammerheads in general and conservation concerns for this species, our goal was to quantify habitat use and horizontal movements of juvenile smooth hammerheads in the western North Atlantic Ocean via satellite tag telemetry. Only very coarse scale information exists on movements of smooth hammerheads in this region, obtained from the recapture of just seven individuals out of 269 (0.02%) tagged with conventional identification tags over 52 years (Kohler and Turner, 2019). Our study objectives were to: (1) determine seasonal movements and distribution patterns; (2) identify core areas of habitat use; (3) evaluate the potential of the MASA seasonal closure for providing protection from fishing pressure, and (4) investigate relationships between movement behavior and environmental conditions, for juvenile smooth hammerheads.

MATERIALS AND METHODS

Capture and Tagging

Between 22 July 2016 and 9 September 2017 six female, juvenile smooth hammerhead sharks were caught via rod and reel off the coast of Ocean City, Maryland United States (38.1° N, 74.5° W). Sharks were brought on board the fishing vessel where a saltwater hose was inserted into the mouth to irrigate the gills and then the sharks were measured, sexed, and fitted with a satellite-linked radio tag (SPOT-196 tag; Wildlife Computers, Redmond, WA, United States) on the dorsal fin. These tags directly communicate with the Argos tracking system[1] when the shark's dorsal fin breaks the sea surface exposing the tag to air, providing an estimated position (latitude and longitude) and an associated location class. Location class is determined by the number of transmissions received and the number of Argos satellites receiving transmissions, and categorized from most to least accurate as 3, 2, 1, 0, A and B. Estimated errors (1 *SD*) for each location class are LC 3: < 250 m, LC 2: 250–500 m; LC 1: 500–1500 m, and LC 0: > 1500 m; there is no spatial estimate of accuracy for LC A and B (CLS, 2016). The two tags deployed in 2016 were programmed to transmit for 1 h every other hour; the four tags deployed in 2017 were programmed to transmit for 1 h every 4 h to try to obtain longer duration tracks.

Movements, Distribution, and Behavior

Because Argos positions of sharks varied in temporal frequency and spatial accuracy, we obtained standardized positions (hereafter "positions") at 12 h intervals that were comparable between individuals and over time by processing Argos locations using a behavioral switching state-space model (SSM) within a Bayesian framework developed by Jonsen et al. (2005). Since parameter estimation is improved when conducted jointly across multiple individual datasets (Jonsen, 2016), we produced most probable tracks using a hierarchical joint estimation model (hSSM) that produced temporally regular positional estimates based on the Argos location class, mean turning angle, and autocorrelation in speed and direction. Previous research has shown that the accuracy of the hSSM parameter estimates declines in response to outlier locations (from poor quality satellite positions) and long gaps in detection data (Bailey et al., 2008); therefore, prior to fitting hSSMs, each track was filtered using the *argosfilter* package (Freitas et al., 2008) in R Core Team (2014) with parameters listed in Vaudo et al. (2017). To reduce spurious results associated with long detection gaps, tracks were broken into multiple segments when gaps between Argos locations were >10 days. Resulting segments <20 days in duration were excluded from the hSSM (Block et al., 2011). Given that 84.7% of gaps between positions in our tracks were ≤12 h (**Supplementary Figure S1**), we used a time step of 12 h in the hSSM to produce two positions per day for each shark.

The hSSM model was fit by running two Markov Chain Monte Carlo (MCMC) chains in parallel for a total of 60,000 samples, with the first 50,000 being discarded as burn-in, and the remaining 10,000 samples thinned by retaining every 10th sample to reduce autocorrelation (n = 1,000 per chain). Each MCMC iteration provides not only a most probable track but also assigns each estimated location to one of two possible behavior modes (resident and transient). The final estimated track is the average of all 2,000 MCMC samples and the final output for each behavioral state represents the proportion of samples for a given position classified as resident (MCMC diagnostics given in **Supplementary Figure S5**). When the proportion is high (resident) or low (transient) the classification can be confidently assessed. Consequently, following Breed et al. (2009), we classified proportions ≤0.3 as transient, ≥0.7 as resident, and proportions of 0.3–0.7 as uncertain. The hSSM was fit using the *bsam* package (Jonsen et al., 2015) in R.

Using the hSSM positions, a seasonal utilization distribution (UD) was calculated for all sharks pooled across the meteorological seasons (summer: June–August, autumn: September–November, winter: December–February, and spring: March–May) using the *adehabitat* package in R (Calenge, 2006). The UD estimate was calculated following methods described in Vaudo et al. (2017).

To investigate vertical diel behavior in the absence of transmitted depth data, we used successful Argos transmissions as a proxy for surfacing behavior since locations are only obtained when sharks are at the surface (Doyle et al., 2015). Using the Argos Satellite Pass Prediction tool[2], satellite pass data was obtained for all six available satellites from June 2017–September 2018. Because each satellite can simultaneously detect all transmitters within an approximately 5,000 km diameter circle below it (CLS, 2016), satellite pass data was obtained for 40°N and 74°W, which encompassed all shark positions received. Because the number of satellites passing overhead varies by hour of the day (in effect increasing the amount of listening effort when more satellites are present; **Supplementary Figure S2**), surfacing behavior was determined by summing the number of Argos locations obtained per shark per hour (Eastern Standard Time), and dividing by the cumulative amount of time that all satellites were overhead during each hour (in general, each satellite takes roughly 10 min to pass over a stationary object). The resulting value represents a standardized number of Argos locations per hour of satellite coverage (hereafter termed "surfacing index"), providing information on temporal patterns of surfacing, regardless of the number of satellites overhead. The surfacing index (square root transformed) was compared among hours of the day using a linear mixed effects (LME) model as surfacing index $\sim$ hour + ID, where surfacing index was the response variable, hour of day was the explanatory variable and shark ID was a random factor using the lmer function in the *lme4* R package (Bates et al., 2014). Tests of multiple comparisons were obtained using the glht function in the *multcomp* package (Hothorn et al., 2008). This analysis of diel surfacing behavior was limited to Sharks 3–6 because satellite pass data is only retained by the Argos system for 1 year and this analysis was not undertaken until 2018; thus, satellite pass data could only be obtained for the four sharks tagged in 2017.

Environmental Variables

Water depth (m) and sea surface temperature (SST; °C) values were obtained using the NOAA ETOPO1 Global Relief Model (one arc-minute resolution) and the Multi-scale Ultra-high Resolution (MUR) SST dataset[3] (0.01° resolution), respectively, using the "xtractomatic" package in R (Mendelssohn, 2017). SST gradient (a proxy for temperature fronts) was calculated as the maximum difference in SST

---

[1] www.argos-system.org

[2] https://argos-system.clsamerica.com

[3] http://mur.jpl.nasa.gov/

across a moving window of a 15 × 15 grid cell matrix (totaling ~0.15° area covered) using the *raster* package (Hijmans et al., 2017) in R. Finally, using the *rerddap* (Chamberlain et al., 2019) and *rerddapXtracto*[4] packages in R, we obtained 8-day composite primary productivity (PP) (mg C/m^2/day; 0.0125° resolution) data from the National Aeronautics and Space Administration's (NASA) Aqua satellite with its Moderate Resolution Imaging Spectroradiometer sensor (MODIS-Aqua).

Generalized additive mixed models (GAMMs) were used to determine the best environmental predictors of smooth hammerhead shark resident behavior. Prior to inclusion in the global model, univariate models were constructed with potential environmental predictors standardized by their mean and standard deviation, and tested using a likelihood ratio test. Significant predictor variables were then tested for collinearity using a Pearson's rank correlation matrix (Zuur et al., 2009) and all non-spatial combinations were <0.7 (**Supplementary Figure S3**). The proportion of behavioral states categorized as resident for each position by the hSSM was used as the response variable and all predictor variables were included in the global model. The model was run using a Gaussian response distribution and identity link. The importance of various combinations of autocorrelation structures was tested while holding other variables constant. Similarly, to determine the best random effects structure aimed at accounting for any temporal effect (e.g., increasing temporal gaps between positions since tagging or season) or individual effect imposed on the sharks' behavior, we considered shark ID, season and days at liberty as possible random effects. The performance of the final model output was assessed using the C index, where values closer to 1 indicate better performance, and the corresponding Somers' Dxy rank correlation, which is a measure of ordinal association between the response and predictor variables (Lea et al., 2018).

RESULTS

The six juvenile smooth hammerheads TL (mean ± *SD*) 184.2 ± 18.5 cm were tracked for periods of 49–441 days and generated a total of 3,488 Argos locations. The number of Argos locations d^{-1} ranged from 0 to 21 (mean 3.1 ± 3.3). The mean time interval between Argos positions was 7.7 ± 33.8 h (median = 2.5 h). The number of days with Argos locations for each shark ranged from 46 to 263 days (mean 131 ± 72.5 days), resulting in a total of 786 days with locations out of 1121 days at liberty (mean 187 ± 136 days) (**Table 1**). Among all sharks, this equates to being detected on 77.2 ± 0.1% of days at liberty. Once the Argos locations were filtered and standardized to a 12 h time interval using the hSSM, positions were removed for days lacking an Argos location. As a result, 1,531 positions remained, which served as the basis of subsequent analyses.

Most individuals displayed similar movements and habitat use throughout the course of the study (**Figure 1A**). In general, the hSSM indicated that sharks were resident in shallow water off southern Long Island, New York during the summer, with some southern movement to the waters off New Jersey, Delaware and Maryland in late summer. During autumn, directed southern movements through the mid-Atlantic region were common to all sharks, showing little affinity to any one region in the area, as indicated by the observation that 57% of positions were classified as transient during autumn. During winter and early spring, sharks displayed area restricted movements, primarily focused near the southeastern outer banks of Pamlico Sound, North Carolina (**Figure 1A** and **Supplementary Figure S4**).

One shark (shark #5), tagged 17 June 2017 was tracked for 441 days (**Figure 1b** and **Table 1**). This shark was tagged near Ocean City, Maryland and remained there for almost 2 weeks after tagging, then moved north into the New York Bight in early July, where it remained until September when it began a 3 month journey south reaching the area off Cape Hatteras, North Carolina on 15 November. It remained in this area until 3 May 2018 and was not detected again until 9 July 2018 off New Jersey; the shark then moved to waters of the New York Bight until 1 September 2018. Another individual (Shark #1) moved south from the New York Bight similarly to other sharks, but continued moving south east Cape Hatteras eventually reached the coast of central Florida on 12 December 2016 at the time of the last detection 144 days after tagging (**Figure 1a**).

Seasonal utilization distributions showed similar seasonal movements as indicated by the hSSM (**Figure 2**). Core areas (50% UD) of the seasonal distributions were primarily centered in the New York Bight in the summer, expanded southward during the autumn as sharks moved south, and were concentrated off Cape Hatteras, North Carolina in the winter (**Figure 2**). The individual tracked for greater than 1 year moved north in late April/early May, in a similar manner to the northward movements of sharks shortly after tagging off Ocean City, Maryland (**Figures 1b**, **2d**).

TABLE 1 | Summary information for SPOT tag deployments on juvenile smooth hammerhead sharks.

Shark ID	TL (cm)	Sex	Date tagged	Tagging location	Days detected	Track duration (days)	Track distance (km)	Argos locations day^{-1}
1	221	F	22-Jul-16	38.22, −75.03	126	144	3305.2	6.6 ± 4.9
2	183	F	18-Sep-16	38.27, −74.8	118	155	2554.1	3.7 ± 3.6
3	163	F	4-Jun-17	37.96, −74.63	139	217	4359.4	2.4 ± 2.3
4	173	F	12-Jun-17	37.98, −74.75	94	115	2252.2	2.6 ± 1.9
5	190	F	17-Jun-17	37.95, −74.71	263	441	7319.5	2.2 ± 2.5
6	175	F	13-Sep-17	38.25, −74.8	46	49	1345.8	3.0 ± 2.2

Track distance reflects the sum of distances between estimated track positions. TL: shark total length.

---

[4] https://github.com/rmendels/rerddapXtracto

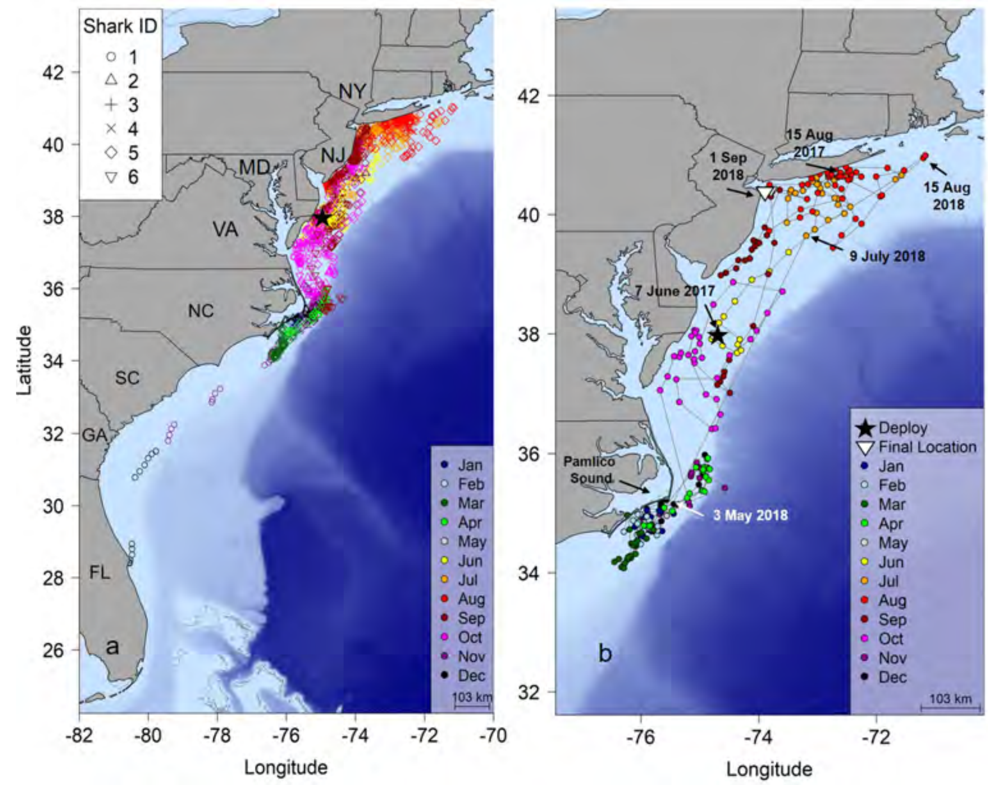

FIGURE 1 | (a) Twelve-hour position estimates for six juvenile smooth hammerhead sharks determined by a hierarchical Bayesian state space movement model (hSSM). **(b)** Shark #5 tracked 441 days revealing a complete migration. Black star, tagging location; NY, New York; NJ, New Jersey; MD, Maryland; VA, Virginia; NC, North Carolina; SC, South Carolina; GA, Georgia; FL, Florida.

For sharks with transmissions extending to the winter and spring of the year following tag deployment ($n = 4$), 96.7% (315 of 326) of locations fell within the boundaries of the Mid-Atlantic Shark Area (MASA) off North Carolina (**Figure 3**); 101 (32%) of these positions occurred during the month of December, when the area is open to commercial bottom longline fisheries (closure period: 1 January–31 July). Positional data was not available to determine when shark #5 (the individual tracked for >1 year) left the MASA (**Figure 1b**), and transmissions from all other sharks stopped prior to exiting the MASA, so time spent within the MASA could not be assessed.

Because tags (sharks 3–6) deployed in 2017 were programmed to transmit just one out of every 4 h, diel vertical behavior is only described for the hours tags were set to transmit (0000–0100, 0400–0500, 0800–0900, 1200–1300, 1600–1700, and 2000–2100 h). Significant fixed effects for the 0400–0500 and 2000–2100 h blocks (0400–0500 LME Estimate = 0.25, SE = 0.07, $t = 3.4$, $p = 0.004$; 2000–2100 LME Estimate = 0.23, SE = 0.07, $t = 3.1$, $p = 0.007$) indicated that surfacing index varied over the 24 h diel period, and multiple comparisons revealed that sharks surfaced most frequently just before dawn, at midday, and just after dusk (**Figure 4**). The total number of Argos locations for all sharks pooled was greatest during the time interval 0400–0500 and 2000–2100 h (308 and 700 total Argos locations, respectively). The 2000–2100 h time interval coincided with the greatest number of satellite passes in the study area (all satellites combined = 794 passes, **Supplementary Figure S2**), resulting in 165.3 h of listening time, which yielded an overall surfacing index of 4.23 for all sharks combined. However, although the 0400–0500 h block only had 40.8 total h of satellite listening time, it had the highest surfacing index of 4.35 for all sharks combined (i.e., on average, there was roughly one position per shark per hour of satellite coverage just before and just after dawn and dusk, respectively; **Figure 4**).

After testing the importance of various combinations of autocorrelation structures while holding other variables constant, we found that the GAMM without an autocorrelation term was deemed more robust with better wAIC and ΔAIC (wAIC = 0.31; **Supplementary Table S1**); thus, no autocorrelation structure was used in the final model. Additionally, wAIC and ΔAIC revealed that treating shark ID and season as random effects resulted in the most parsimonious model, thus, days at liberty was not included (**Supplementary Table S2**). The final GAMM predicting residency behavior explained 34% of the sample variance (C index = 0.72, Dxy = 0.45, *SD* = 0.001, $n = 1432$). Mean SST, log of primary productivity and water depth were included in the best fit model, while SST gradient was removed given its lack of significance ($p = 0.2$) and improved model fit after removal (ΔAIC = 2.4, wAIC = 0.76). Model output indicated that most of the variation in the observed resident

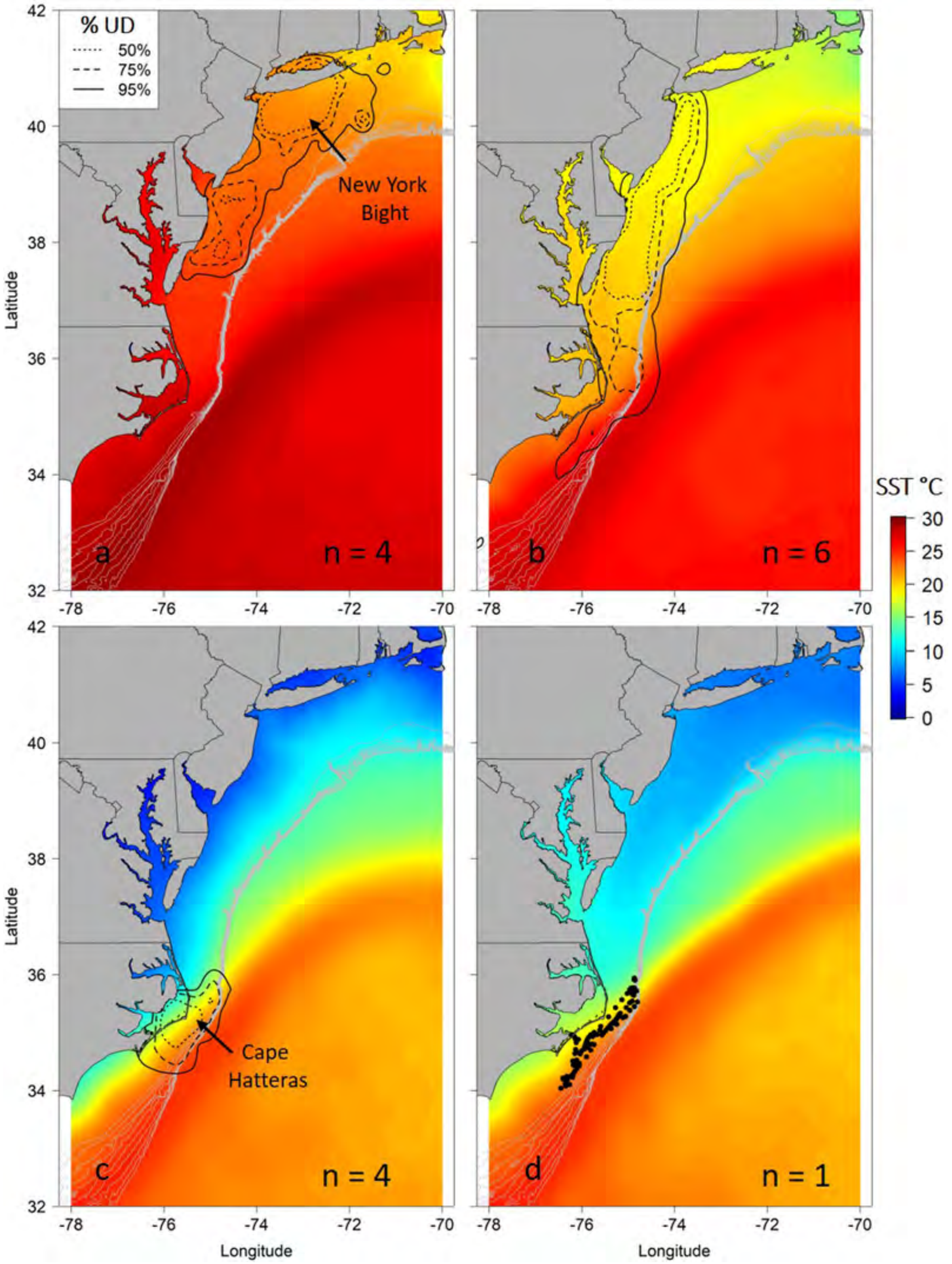

FIGURE 2 | Seasonal utilization distributions (UD) for juvenile smooth hammerhead sharks overlaid on mean seasonal sea surface temperature (SST) during the tracking period. Seasons are summer (**a**; June–August), autumn (**b**; September–November), winter (**c**; December–February) and spring (**d**; March–May). Solid line is the 95% UD, dashed line is the 75% UD and dotted line is the 50% UD. N refers to the number of individuals that were analyzed in each season. Because only one individual represents the spring locations, points of locations are shown. Gray contour lines represent depth contours from 100 to 1000 m depth.

behavior was attributable to geographical location, followed by primary productivity concentration and depth (**Table 2**). Probability of displaying resident behavior was highest at latitudes associated with the New York Bight (>40° N), high primary productivity concentration [7.82 log(mg C/m^2/day) (**Figure 5B**)], and inshore neritic waters (<100 m; **Figure 5C**). In addition, SST of ~18, 23 and ≥26°C resulted in increased probability of sharks displaying resident behavior as these represented the temperatures experienced in core habitat areas (**Figure 5A** and **Table 2**).

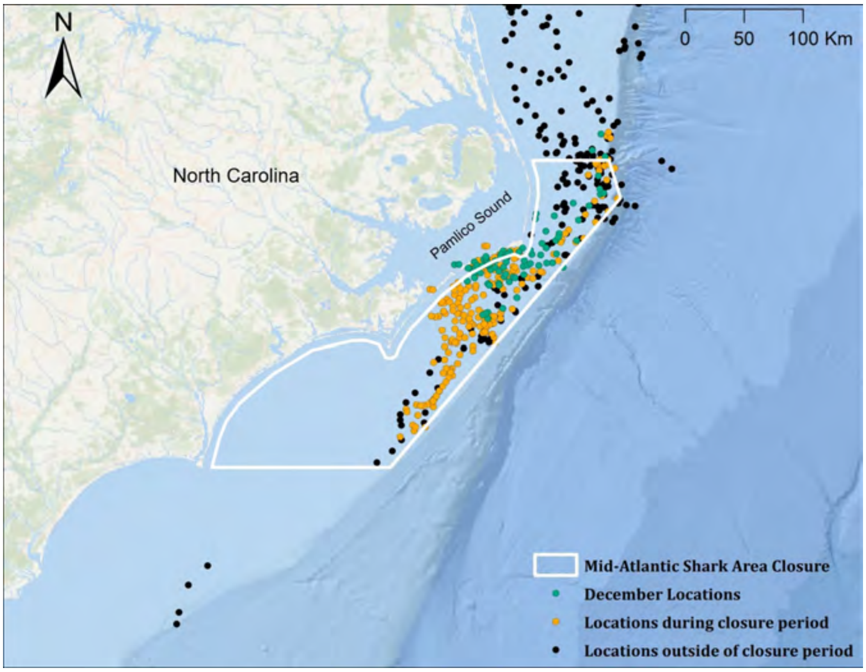

FIGURE 3 | Locations of juvenile smooth hammerhead sharks (*n* = 4 for all groupings) within the mid-Atlantic Shark Area (MASA) during the closure period (January 1–July 1; orange points), and outside of the closure period (black points). Nearly all December locations (green points) fall within the MASA boundary but not within the closure period.

DISCUSSION

We provide the first detailed view of the movement dynamics of smooth hammerhead sharks in the western North Atlantic. Previous work has reported that smooth hammerhead sharks spend a large proportion of their time in surface or near-surface (<10 m) waters (Francis, 2016; Santos and Coelho, 2018), potentially making them good candidates for SPOT tags which only transmit data when exposed to air. Indeed, the sharks tracked here were detected on average 3.1 ± 3.3 times per day, and 84.7% of Argos locations occurred within 12 h of a previous location. The high frequency of satellite transmissions and Argos locations allowed for reconstruction of smooth hammerhead movements at a much higher resolution than has previously been described.

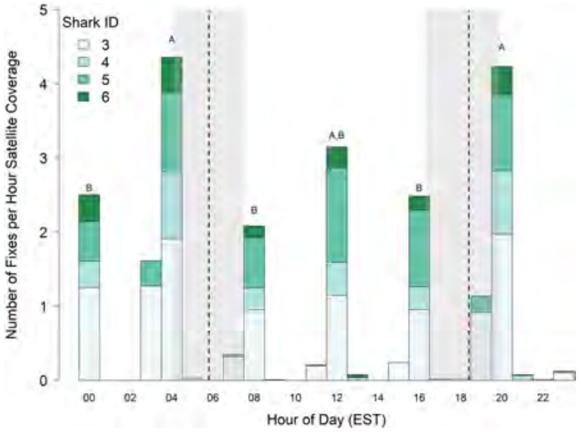

FIGURE 4 | Surfacing index (number of locations per hour of satellite time) of juvenile smooth hammerhead sharks. Vertical dashed lines and shading represent the minimum, mean and maximum times of sunrise and sunset experienced by sharks. Bars labeled with different letters differ at α = 0.05, and bars without letters were not included in statistical comparisons. Data only includes four sharks tagged in 2017. EST, Eastern Standard Time.

The sharks we tracked in the western North Atlantic Ocean displayed consistent seasonal movements between core areas of activity off Long Island, New York in summer and off Cape Hatteras, North Carolina in winter. Although seasonal movements of this species have been hypothesized previously based on surface sightings (Couto et al., 2018) and fisheries catch per unit effort data (Santos and Coelho, 2019) in the eastern North Atlantic, the telemetry results here provide a direct, fishery independent demonstration of this behavior by smooth hammerheads. Based on environmental characteristics of the core areas, sea surface temperature and productivity appear to be important drivers of their seasonal movement patterns, as has been demonstrated in other highly migratory marine megafauna (Weng et al., 2008; Block et al., 2011; Curtis et al., 2014; Kajiura and Tellman, 2016; Vaudo et al., 2017).

Seasonal movements and habitat use in other hammerhead species have been documented, but thus far suggest they are driven more so by foraging or reproduction, rather than dynamic oceanographic processes. For example, seasonal changes in abundance of scalloped hammerheads at offshore

TABLE 2 | GAMM output for juvenile smooth hammerhead resident behavior in relation to environmental variables.

Variable	edf	Ref.df	*F*	*p*-value
s(SST)	6.8	6.8	4.2	<0.001
s[log(Primary Productivity)]	3.9	3.9	25.3	<0.001
s(Depth)	1	1	25.4	<0.001
te(Lon, Lat): Summer	10	10	42.1	<0.001
te(Lon, Lat): Autumn	11.6	11.6	19.4	<0.001
te(Lon, Lat): Winter	4.2	4.2	11.9	<0.001
te(Lon, Lat): Spring	4.1	4.1	19.5	<0.001

islands in the eastern tropical Pacific have been suggested as possibly related to movements for reproductive purposes and/or parturition, but currents and chlorophyll concentrations may also play a role in long term movements (Bessudo et al., 2011; Ketchum et al., 2014; Nalesso et al., 2019). Wells et al. (2018) found scalloped hammerhead movements in the northern Gulf of Mexico to be primarily driven by static bathymetric features rather than dynamic environmental variables and did not observe any seasonal patterns in shark movements. Furthermore, great hammerhead repeated seasonal presence and residency within the Bahamas is also believed to be related to reproduction or foraging, rather than climatic processes (Guttridge et al., 2017). However, sharks tracked here represent the juvenile to sub-adult size class of this species, and physiological tolerances to environmental conditions vary across ontogeny and may result in juveniles selecting different habitats than adults (Grubbs, 2010). Given that only one smooth hammerhead in our study was tracked for over a full year, it remains unclear how typical seasonal migratory behavior and environmental driven movement is in this species throughout its geographic and size range.

Seasonal movement patterns of smooth hammerheads along the US East Coast was characterized by resident behavior during the summer and late winter/early spring. The timing of resident behavior coincided with increased levels of primary productivity, presumably tied to prey availability (Ware and Thomson, 2005; Priede and Miller, 2009). Stomach contents show that the major prey of smooth hammerheads is cephalopods (mainly ommastrephid squid) and small schooling fishes (Smale, 1991; Rogers et al., 2012; Bornatowski et al., 2014). The longfin squid *Doryteuthis pealeii* and shortfin squid *Illex illecebrosus* are the most common species of squid in the western North Atlantic from Georges Bank to Cape Hatteras, and both species undergo seasonal spawning migrations at northern and inshore locations in late spring/early summer and deeper, southern locations along the continental shelf edge in late autumn/early winter (Dawe et al., 2007; Jereb and Roper, 2010). Seasonal movements and aggregations in relation to high prey abundance has been reported in several species of sharks (Klimley et al., 1992; Heyman et al., 2001; Mourier et al., 2016), however, little information exists on smooth hammerhead diet in the study region to determine if they are taking advantage of this potential resource. Nevertheless, spawning and seasonal movements of these squid in the western North Atlantic spatially and temporally overlap with core areas used by smooth hammerheads tracked in this study.

The diel surfacing behavior patterns of smooth hammerheads tracked in our study may also be related to foraging. Highest surfacing indices were recorded shortly before dawn and after dusk, similar to the pattern observed in a juvenile smooth hammerhead (139 cm TL) tracked off the coast of New Zealand (Francis, 2016). Francis (2016) also reported diel differences in depth distribution of another juvenile smooth hammerhead tracked with a popup satellite transmitter, with a shallower distribution at night compared to daylight hours. In contrast, scalloped hammerhead sharks have been observed to remain in shallow waters during the day and dive at night presumably to forage (Klimley and Nelson, 1984; Hoffmayer et al., 2013), or show continuous deep diving behavior throughout the 24 h cycle (Spaet et al., 2017). Similarly, Santos and Coelho (2018) found that similarly sized smooth hammerheads to those in this study [T-test; $T_{(6\cdot5)} = 1.1$, $p = 0.3$] tracked using depth and temperature archival transmitters off the west coast of

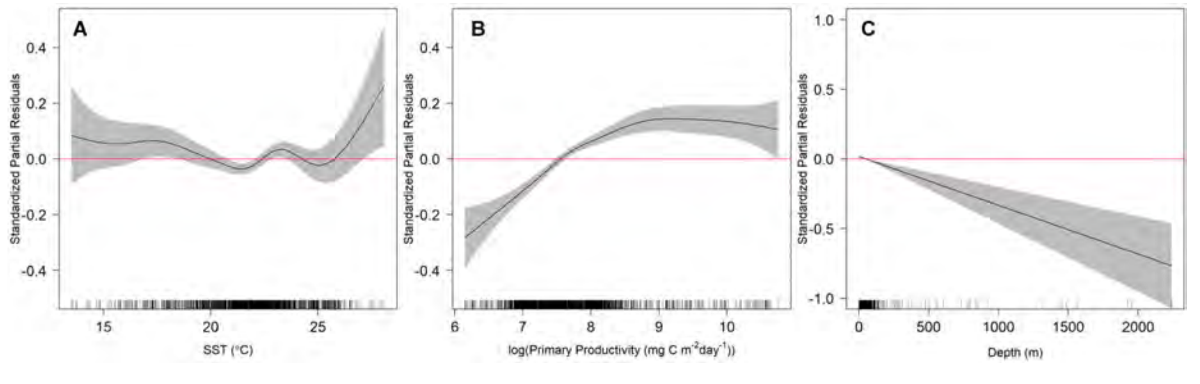

FIGURE 5 | Relationship of sea surface temperature (SST; **A**), log of primary productivity **(B)** and seafloor depth **(C)** with resident behavior exhibited by juvenile smooth hammerhead sharks. Values with 95% confidence intervals that do not overlap with 0 (red line) indicate either increased (positive values) or decreased probability of resident behavior (negative values; transient behavior). Black ticks along the x-axis represent the distribution of the independent variable values examined. Note y-axis scales differ.

equatorial Africa occupied deeper, cooler water during the night compared to day. Our findings contrast somewhat with those of Santos and Coelho (2018); however, this difference may be an artifact of study location, where sharks tracked in Santos and Coelho (2018) were experiencing temperatures at depth several degrees warmer (26–27°C) than SSTs observed here in the temperate western North Atlantic (mean 21.7 ± 2.2°C). In addition, the surfacing index presented here is limited to when a sharks' dorsal fin breaks the surface and appropriate satellite coverage is overhead, so patterns observed here may not be fully representative of smooth hammerhead diel depth distribution in the western North Atlantic.

Decreasing population trends of smooth hammerheads have prompted conservation listings (e.g., IUCN, CITES, CMS) and calls for additional management. Because of high at- vessel (Coelho et al., 2012) and estimated post-release mortality of smooth hammerheads caught in fisheries (Braccini et al., 2012), reducing exposure to capture rather than relying on release after capture is a more effective management method for reduced fishing mortality. While acknowledging that our inferences are based on the four animals with long enough tracks, the consistent finding of the winter core area of activity largely falling within the boundaries of the MASA management zone during winter and spring, and high proportion of transmissions occurring within the MASA during the shark bottom longline fishery closure period (1 January–31 July), suggests the potential of the MASA for reducing fishing mortality of this species. Furthermore, as reported for sand tiger sharks (*Carcharias taurus*) (Teter et al., 2015), the smooth hammerhead spatial and temporal patterns of movement suggest that beginning the MASA closure on 1 December, rather than 1 January, would provide additional and extended protection from commercial fisheries for this species also.

Though there was some individual variability in movements of smooth hammerheads tracked in our study with a limited number of individuals, the high degree of spatial and temporal consistency demonstrated by the sharks in use of both summer and winter core areas as well as behaviors associated with foraging suggest that the coastal waters of the New York Bight and Cape Hatteras, North Carolina could be considered for designation of Essential Fish Habitat (EFH) for this species in the western North Atlantic, an important designation for protection consideration in U.S. fisheries management practices (NMFS, 2009)[5]. Seasonal movement between southern areas of increased presence in winter and northern areas of concentrated activity in summer have been reported for other species of sharks in the western North Atlantic, including sandbar sharks *Carcharhinus plumbeus* (Grubbs et al., 2007; McCandless et al., 2007; Conrath and Musick, 2008), dusky sharks *Carcharhinus obscurus* (Musick and Colvocoresses, 1986), sand tiger sharks *Carcharias taurus* (Teter et al., 2015) and white sharks *Carcharodon carcharias* (Curtis et al., 2018), and has led to delineation of nurseries and designation of EFH for several of these species (NMFS, 2009). Likely due to the lack of available data, there is currently no EFH in U.S. waters for smooth hammerhead sharks.

Successful management of populations is dependent on the survival of young individuals and recruitment to reproductive stock; therefore, understanding movement patterns, habitat use and EFH of juveniles is vital. In this study we have identified both winter and summer core areas of concentrated activity for juvenile smooth hammerheads in the western North Atlantic, as well as pathways traveled between those seasonal core areas. In addition, environmental conditions associated with resident behavior within these core areas and timing of directed movements between them enables improved ability to predict inter- and intra-annual distribution of smooth hammerheads, and how this may change over time with changing environmental conditions (e.g., increasing sea surface temperatures). These advances in understanding patterns of distribution and habitat use of juvenile smooth hammerheads in the western North Atlantic are directly applicable to effective management of this demographic component of their population. Future work should include studying the movement ecology of adult smooth hammerhead sharks of both sexes since their movements and habitat use patterns are likely to be different from those of juveniles.

DATA AVAILABILITY STATEMENT

The raw data supporting the conclusions of this article will be made available by the authors, without undue reservation, to any qualified researcher.

ETHICS STATEMENT

The animal study was reviewed and approved by the Nova Southeastern University IACUC #DB1.

AUTHOR CONTRIBUTIONS

BW and MSS designed and implemented the research. MS led the fieldwork. RL led the analysis of the data with assistance from LS and JV. RL led the writing of the manuscript with assistance from all authors.

FUNDING

This work was supported by grants to MSS from the Guy Harvey Ocean Foundation (GHOF18-1), Save Our Seas Foundation (SOSF157), Shark Foundation/Hai-Stiftung (HF-19-2), the Levitetz Family Foundation (LFF-19), and a scholarship to RL from Fish Florida.

SUPPLEMENTARY MATERIAL

The Supplementary Material for this article can be found online at: https://www.frontiersin.org/articles/10.3389/fmars.2020.566364/full#supplementary-material

---

[5] https://www.fisheries.noaa.gov/resource/map/essential-fish-habitat-mapper

REFERENCES

Abercrombie, D. L., Clarke, S. C., and Shivji, M. S. (2005). Global-scale genetic identification of hammerhead sharks: application to assessment of the international fin trade and law enforcement. *Conserv. Genet.* 6, 775–788. doi: 10.1007/s10592-005-9036-2

Bailey, H., Shillinger, G., Palacios, D., Bograd, S., Spotila, J., Paladino, F., et al. (2008). Identifying and comparing phases of movement by leatherback turtles using state-space models. *J. Exp. Mar. Biol.* 356, 128–135. doi: 10.1016/j.jembe.2007.12.020

Bates, D., Maechler, M., Bolker, B., and Walker, S. (2014). *lme4: Linear mixed-effects models using Eigen and S4. R package version 1*. doi: 10.18637/jss.v067.i01

Baum, J. K., and Blanchard, W. (2010). Inferring shark population trends from generalized linear mixed models of pelagic longline catch and effort data. *Fish. Res.* 102, 229–239. doi: 10.1016/j.fishres.2009.11.006

Baum, J. K., Myers, R. A., Kehler, D. G., Worm, B., Harley, S. J., and Doherty, P. A. (2003). Collapse and conservation of shark populations in the Northwest Atlantic. *Science* 299, 389–392. doi: 10.1126/science.1079777

Bessudo, S., Soler, G. A., Klimley, A. P., Ketchum, J. T., Hearn, A., and Arauz, R. (2011). Residency of the scalloped hammerhead shark (*Sphyrna lewini*) at Malpelo Island and evidence of migration to other islands in the Eastern Tropical Pacific. *Environ. Biol. Fishes* 91, 165–176. doi: 10.1007/s10641-011-9769-3

Block, B. A., Jonsen, I. D., Jorgensen, S. J., Winship, A. J., Shaffer, S. A., Bograd, S. J., et al. (2011). Tracking apex marine predator movements in a dynamic ocean. *Nature* 475, 86. doi: 10.1038/nature10082

Bornatowski, H., Braga, R., Abilhoa, V., and Corrêa, M. (2014). Feeding ecology and trophic comparisons of six shark species in a coastal ecosystem off southern Brazil. *J. Fish Biol.* 85, 246–263. doi: 10.1111/jfb.12417

Braccini, M., Van Rijn, J., and Frick, L. (2012). High post-capture survival for sharks, rays and chimaeras discarded in the main shark fishery of Australia?. *PLoS One* 7:e32547. doi: 10.1371/journal.pone.0032547

Breed, G. A., Jonsen, I. D., Myers, R. A., Bowen, W. D., and Leonard, M. L. (2009). Sex-specific, seasonal foraging tactics of adult grey seals (*Halichoerus grypus*) revealed by state–space analysis. *Ecology* 90, 3209–3221. doi: 10.1890/07-1483.1

Calenge, C. (2006). The package adehabitat for the R software: a tool for the analysis of space and habitat use by animals. *Ecol. Modell.* 197, 516–519. doi: 10.1016/j.ecolmodel.2006.03.017

Cardeñosa, D., Fields, A. T., Babcock, E. A., Zhang, H., Feldheim, K., Shea, S. K., et al. (2018). CITES-listed sharks remain among the top species in the contemporary fin trade. *Conserv. Lett.* 11:e12457. doi: 10.1111/conl.12457

Casper, B., Domingo, A., Gaibor, N., Heupel, M., Kotas, E., Lamonaca, A., et al. (2009). *Sphyrna zygaena. The IUCN Red List of Threatened Species*. Available a: http://www.iucnredlist.org (Accessed August 16, 2018).

Chamberlain, S., Tupper, B., and Mendelssohn, R. (2019). *rerddap: General Purpose Client for 'ERDDAP' Servers, R package version 0.4.2.9130*.

Clarke, S., Coelho, R., Francis, M., Kai, M., Kohin, S., Liu, K., et al. (2015). *Report of the Pacific Shark Life History Expert Panel Workshop: Final Report*. Kolonia: Western and Central Pacific Fisheries Commission Scientific Committee.

Clarke, S. C., Magnussen, J. E., Abercrombie, D. L., McAllister, M. K., and Shivji, M. S. (2006a). Identification of shark species composition and proportion in the Hong Kong shark fin market based on molecular genetics and trade records. *Conserv. Biol.* 20, 201–211. doi: 10.1111/j.1523-1739.2005.00247.x

Clarke, S. C., McAllister, M. K., Milner-Gulland, E. J., Kirkwood, G., Michielsens, C. G., Agnew, D. J., et al. (2006b). Global estimates of shark catches using trade records from commercial markets. *Ecol. Lett.* 9, 1115–1126. doi: 10.1111/j.1461-0248.2006.00968.x

CLS (2016). *Argos Users Manual*. Available online at: http://www.argos-system.org/wp-content/uploads/2016/08/r363_9_argos_users_manual-v1.6.6.pdf (accessed September 15, 2018).

Coelho, R., Fernandez-Carvalho, J., Lino, P. G., and Santos, M. N. (2012). An overview of the hooking mortality of elasmobranchs caught in a swordfish pelagic longline fishery in the Atlantic Ocean. *Aquat. Living Resour.* 25, 311–319. doi: 10.1051/alr/2012030

Compagno, L. J. (1984). *Sharks of The World: An Annotated and Illustrated Catalogue of Shark Species Known to Date, pt. 2: Carcharhiniformes*. Rome: FAO.

Conrath, C. L., and Musick, J. A. (2008). Investigations into depth and temperature habitat utilization and overwintering grounds of juvenile sandbar sharks, *Carcharhinus plumbeus*: the importance of near shore North Carolina waters. *Environ. Biol. Fishes* 82, 123–131. doi: 10.1007/s10641-007-9263-0

Cortés, E., Arocha, F., Beerkircher, L., Carvalho, F., Domingo, A., Heupel, M., et al. (2010). Ecological risk assessment of pelagic sharks caught in Atlantic pelagic longline fisheries. *Aquat. Living Resour.* 23, 25–34. doi: 10.1051/alr/2009044

Couto, A., Queiroz, N., Ketchum, J. T., Sampaio, E., Furtado, M., Cid, A. A., et al. (2018). Smooth hammerhead sharks (*Sphyrna zygaena*) observed off the Portuguese southern coast. *Environ. Biol. Fishes* 101, 1261–1268. doi: 10.1007/s10641-018-0773-8

Curtis, T. H., Metzger, G., Fischer, C., McBride, B., McCallister, M., Winn, L. J., et al. (2018). First insights into the movements of young-of-the-year white sharks (*Carcharodon carcharias*) in the western North Atlantic Ocean. *Sci. Rep.* 8:10794. doi: 10.1038/s41598-018-29180-5

Curtis, T. H., Zeeman, S. I., Summers, E. L., Cadrin, S. X., and Skomal, G. B. (2014). Eyes in the sky: linking satellite oceanography and biotelemetry to explore habitat selection by basking sharks. *Anim. Biotelemetry* 2:12. doi: 10.1186/2050-3385-2-12

Dawe, E., Hendrickson, L., Colbourne, E., Drinkwater, K., and Showell, M. (2007). Ocean climate effects on the relative abundance of short-finned (*Illex illecebrosus*) and long-finned (*Loligo pealeii*) squid in the northwest Atlantic Ocean. *Fish. Oceanogr.* 16, 303–316. doi: 10.1111/j.1365-2419.2007.00431.x

Deacy, B. M., Moncrief-Cox, H. E., and Carlson, J. K. (2020). First verified record of the smooth hammerhead (*Sphyrna zygaena*) in coastal waters of the northern gulf of mexico with a review of their occurrence in the Western North Atlantic Ocean. *South. Nat.* 19, 1–7. doi: 10.1656/058.019.0105

Diemer, K., Mann, B., and Hussey, N. (2011). Distribution and movement of scalloped hammerhead *Sphryna lewini* and smooth hammerhead Sphyrna zygaena sharks along the east coast of southern Africa. *Afr. J. Mar. Sci.* 33, 229–238. doi: 10.2989/1814232X.2011.600291

Doyle, T. K., Bennison, A., Jessopp, M., Haberlin, D., and Harman, L. A. (2015). A dawn peak in the occurrence of 'knifing behaviour' in blue sharks. *J. Anim. Biotelemetry* 3:46. doi: 10.1186/s40317-015-0084-1

Dulvy, N. K., Fowler, S. L., Musick, J. A., Cavanagh, R. D., Kyne, P. M., Harrison, L. R., et al. (2014). Extinction risk and conservation of the world's sharks and rays. *eLife* 3:e00590. doi: 10.7554/eLife.00590

Eddy, C., Brill, R., and Bernal, D. (2016). Rates of at-vessel mortality and post-release survival of pelagic sharks captured with tuna purse seines around drifting fish aggregating devices (FADs) in the equatorial eastern Pacific Ocean. *Fish. Res.* 174, 109–117. doi: 10.1016/j.fishres.2015.09.008

Ferretti, F., Worm, B., Britten, G. L., Heithaus, M. R., and Lotze, H. K. (2010). Patterns and ecosystem consequences of shark declines in the ocean. *Ecol. Lett.* 13, 1055–1071. doi: 10.1111/j.1461-0248.2010.01489.x

Francis, M. (2016). Distribution, habitat and movement of juvenile smooth hammerhead sharks (*Sphyrna zygaena*) in northern New Zealand. *N. Zeal. J. Mar. Freshw. Res.* 50, 506–525. doi: 10.1080/00288330.2016.1171244

Freitas, C., Lydersen, C., Fedak, M. A., and Kovacs, K. M. (2008). A simple new algorithm to filter marine mammal Argos locations. *Mar. Mamm. Sci.* 24, 315–325. doi: 10.1111/j.1748-7692.2007.00180.x

Gallagher, A. J., and Klimley, A. P. (2018). The biology and conservation status of the large hammerhead shark complex: the great, scalloped, and smooth hammerheads. *Rev. Fish Biol. Fish.* 28, 777–794. doi: 10.1007/s11160-018-9530-5

Grubbs, R. D. (2010). "Ontogenetic shifts in movements and habitat use," in *Sharks and Their Relatives II*, eds M. Heithaus, J. C. Carrier, and J. A. Musick (Boca Raton, FL: CRC press), 335–366. doi: 10.1201/9781420080483-c7

Grubbs, R. D., Musick, J. A., Conrath, C. L., and Romine, J. G. (2007). "Long-term movements, migration, and temporal delineation of a summer nursery for juvenile sandbar sharks in the Chesapeake Bay region," in *Proceedings of the American Fisheries Society Symposium*, (Bethesda, MD: American Fisheries Society).

Guttridge, T. L., Van Zinnicq Bergmann, M. P., Bolte, C., Howey, L. A., Finger, J. S., Kessel, S. T., et al. (2017). Philopatry and regional connectivity of the great hammerhead shark, *Sphyrna mokarran* in the US and Bahamas. *Front. Mar. Sci.* 4:3. doi: 10.3389/fmars.2017.00003

Heyman, W. D., Graham, R. T., Kjerfve, B., and Johannes, R. E. (2001). Whale sharks Rhincodon typus aggregate to feed on fish spawn in Belize. *Mar. Ecol. Prog. Ser.* 215, 275–282. doi: 10.3354/meps215275

Hijmans, R. J., van Etten, J., Cheng, J., Mattiuzzi, M., Sumner, M., Greenberg, J. A., et al. (2017). *Package 'Raster'*. Vienna: R Foundation for Statistical Computing.

Hoffmayer, E. R., Franks, J. S., Driggers, W. B., and Howey, P. W. (2013). Diel vertical movements of a scalloped hammerhead, *Sphyrna lewini*, in the northern Gulf of Mexico. *Bull. Mar. Sci.* 89, 551–557. doi: 10.5343/bms.2012.1048

Hothorn, T., Bretz, F., and Westfall, P. (2008). multcomp: simultaneous inference in general parametric models. R package version 1.4-6. *Biometr. J.* 50, 346–363. doi: 10.1002/bimj.200810425

Jereb, P., and Roper, C. (2010). *Cephalopods of the world. An annotated and illustrated catalogue of species known to date. Volume 2. Myopsid and Oegopsid Squids*. Rome: Food and Agriculture Organization of the United Nations.

Jiao, Y., Cortés, E., Andrews, K., and Guo, F. (2011). Poor-data and data-poor species stock assessment using a Bayesian hierarchical approach. *Ecol. Applic.* 21, 2691–2708. doi: 10.1890/10-0526.1

Jonsen, I. (2016). Joint estimation over multiple individuals improves behavioural state inference from animal movement data. *Sci. Rep.* 6:20625. doi: 10.1038/srep20625

Jonsen, I., Bestley, S., Wotherspoon, S., Sumner, M., and Flemming, J. M. (2015). *bsam: Bayesian State-Space Models For Animal Movement. R package. R Foundation for Statistical Computing version 0.43. 1*.

Jonsen, I. D., Flemming, J. M., and Myers, R. A. (2005). Robust state–space modeling of animal movement data. *Ecology* 86, 2874–2880. doi: 10.1890/04-1852

Kajiura, S. M., and Tellman, S. L. (2016). Quantification of massive seasonal aggregations of blacktip sharks (*Carcharhinus limbatus*) in Southeast Florida. *PLoS One* 11:e0150911. doi: 10.1371/journal.pone.0150911

Ketchum, J. T., Hearn, A., Klimley, A. P., Peñaherrera, C., Espinoza, E., Bessudo, S., et al. (2014). Inter-island movements of scalloped hammerhead sharks (*Sphyrna lewini*) and seasonal connectivity in a marine protected area of the eastern tropical Pacific. *Mar. Biol.* 161, 939–951. doi: 10.1007/s00227-014-2393-y

Kinney, M. J., and Simpfendorfer, C. A. (2009). Reassessing the value of nursery areas to shark conservation and management. *Conserv. Lett.* 2, 53–60. doi: 10.1111/j.1755-263x.2008.00046.x

Klimley, A. P., Anderson, S. D., Pyle, P., and Henderson, R. (1992). Spatiotemporal patterns of white shark (*Carcharodon carcharias*) predation at the South Farallon Islands, California. *Copeia* 1992, 680–690. doi: 10.2307/1446143

Klimley, A. P., and Nelson, D. R. (1984). Diel movement patterns of the scalloped hammerhead shark (*Sphyrna lewini*) in relation to El Bajo Espiritu Santo: a refuging central-position social system. *Behav. Ecol. Sociobiol.* 15, 45–54. doi: 10.1007/bf00310214

Kohler, N. E., and Turner, P. A. (2019). Distributions and movements of atlantic shark species: a 52-year retrospective atlas of mark and recapture data. *Mar. Fish. Rev.* 81, 1–93. doi: 10.7755/mfr.81.2.1

Lea, J. S., Wetherbee, B. M., Sousa, L. L., Aming, C., Burnie, N., Humphries, N. E., et al. (2018). Ontogenetic partial migration is associated with environmental drivers and influences fisheries interactions in a marine predator. *ICES J. Mar. Sci.* 75, 1383–1392. doi: 10.1093/icesjms/fsx238

McCandless, C., Pratt, H., Kohler, N., Merson, R., and Recksiek, C. (2007). "Distribution, localized abundance, movements, and migrations of juvenile sandbar sharks tagged in Delaware Bay," in *Shark Nursery Grounds of the Gulf of Mexico and the East Coast Waters of the United States*, eds C. McCandless, N. Kohler, and H. Pratt (Bethesda, MD: American Fisheries Society), 45–62.

Mendelssohn, R. (2017). *Package 'xtractomatic: Accessing Environmental Data from ERD's ERDDAP Server'*. Vienna: R Foundation for Statistical Computing.

Miller, M. H. (2016). *Endangered Species Act Status Review Report: Smooth Hammerhead Shark (Sphyrna zygaena)*. Silver Spring, MD: National Marine Fisheries Service, Office of Protected Resources.

Morgan, A., and Carlson, J. K. (2010). Capture time, size and hooking mortality of bottom longline-caught sharks. *Fish. Res.* 101, 32–37. doi: 10.1016/j.fishres.2009.09.004

Mourier, J., Maynard, J., Parravicini, V., Ballesta, L., Clua, E., Domeier, M. L., et al. (2016). Extreme inverted trophic pyramid of reef sharks supported by spawning groupers. *Curr. Biol.* 26, 2011–2016. doi: 10.1016/j.cub.2016.05.058

Musick, J., and Colvocoresses, J. (1986). "Seasonal recruitment of subtropical sharks in Chesapeake Bight, USA," in *Workshop on Recruitment in Tropical Coastal Demersal Communities. Intergovenmental Oceanographic Commission Workshop Report 44*, eds A. Yanez, Y. Arancibia, and D. Pauley (Campeche: FAO/UNESCO), 301–311.

Nalesso, E., Hearn, A., Sosa-Nishizaki, O., Steiner, T., Antoniou, A., Reid, A., et al. (2019). Movements of scalloped hammerhead sharks (*Sphyrna lewini*) at Cocos Island, Costa Rica and between oceanic islands in the Eastern Tropical Pacific. *PLoS One* 14:e0213741. doi: 10.1371/journal.pone.0213741

NMFS (2009). *Final Amendment 1 to the 2006 Consolidated Atlantic Highly Migratory Species Fishery Management Plan, Essential Fish Habitat*. Silver Spring, MD: NMFS.

Priede, I. G., and Miller, P. I. (2009). A basking shark (*Cetorhinus maximus*) tracked by satellite together with simultaneous remote sensing II: new analysis reveals orientation to a thermal front. *Fish. Res.* 95, 370–372. doi: 10.1016/j.fishres.2008.09.038

Queiroz, N., Humphries, N. E., Mucientes, G., Hammerschlag, N., Lima, F. P., Scales, K. L., et al. (2016). Ocean-wide tracking of pelagic sharks reveals extent of overlap with longline fishing hotspots. *Proc. Natl. Acad. Sci. U.S.A.* 113, 1582–1587. doi: 10.1073/pnas.1510090113

R Core Team (2014). *R: A Language and Environment for Statistical Computing*. Vienna: R Foundation for Statistical Computing.

Rogers, P. J., Huveneers, C., Page, B., Hamer, D. J., Goldsworthy, S. D., Mitchell, J. G., et al. (2012). A quantitative comparison of the diets of sympatric pelagic sharks in gulf and shelf ecosystems off southern Australia. *ICES J. Mar. Sci.* 69, 1382–1393. doi: 10.1093/icesjms/fss100

Santos, C. C., and Coelho, R. (2018). Migrations and habitat use of the smooth hammerhead shark (*Sphyrna zygaena*) in the Atlantic Ocean. *PLoS One* 13:e0198664. doi: 10.1371/journal.pone.0198664

Santos, C. C., and Coelho, R. (2019). Distribution patterns and indicators of the smooth hammerhead shark (*Sphyrna zygaena*) in the Atlantic Ocean. *Fish. Res.* 212, 107–113. doi: 10.1016/j.fishres.2018.12.015

Schlaff, A. M., Heupel, M. R., and Simpfendorfer, C. A. (2014). Influence of environmental factors on shark and ray movement, behaviour and habitat use: a review. *Rev. Fish Biol.* 24, 1089–1103. doi: 10.1007/s11160-014-9364-8

Smale, M. (1991). Occurrence and feeding of three shark species, *Carcharhinus brachyurus*, *C. obscurus* and *Sphyrna zygaena*, on the Eastern Cape coast of South Africa. *South Afr. J. Mar. Sci.* 11, 31–42. doi: 10.2989/025776191784287808

Spaet, J. L., Lam, C. H., Braun, C. D., and Berumen, M. L. (2017). Extensive use of mesopelagic waters by a Scalloped hammerhead shark (*Sphyrna lewini*) in the Red Sea. *Anim. Biotelemetry* 5:20. doi: 10.1186/s40317-017-0135-x

Teter, S. M., Wetherbee, B. M., Fox, D. A., Lam, C. H., Kiefer, D. A., and Shivji, M. (2015). Migratory patterns and habitat use of the sand tiger shark (*Carcharias taurus*) in the western North Atlantic. *Mar. Freshw. Res.* 66, 158–169. doi: 10.1071/mf14129

Vaudo, J. J., Byrne, M. E., Wetherbee, B. M., Harvey, G. M., and Shivji, M. S. (2017). Long-term satellite tracking reveals region-specific movements of a large pelagic predator, the shortfin mako shark, in the western North Atlantic Ocean. *J. Appl. Ecol.* 54, 1765–1775. doi: 10.1111/1365-2664.12852

Ware, D. M., and Thomson, R. E. (2005). Bottom-up ecosystem trophic dynamics determine fish production in the Northeast Pacific. *Science* 308, 1280–1284. doi: 10.1126/science.1109049

Wells, R., TinHan, T. C., Dance, M. A., Drymon, J. M., Falterman, B., Ajemian, M. J., et al. (2018). Movement, behavior, and habitat use of a marine apex predator, the scalloped hammerhead. *Front. Mar. Sci.* 5:321. doi: 10.3389/fmars.2018.00321

Weng, K. C., Foley, D. G., Ganong, J. E., Perle, C., Shillinger, G. L., and Block, B. A. (2008). Migration of an upper trophic level predator, the salmon shark *Lamna ditropis*, between distant ecoregions. *Mar. Ecol. Prog. Ser.* 372, 253–264. doi: 10.3354/meps07706

Zuur, A., Ieno, E., Walker, N., Saveliev, A., and Smith, G. (2009). *Mixed Effects Models and Extensions in Ecology with R*. New York, NY: Springer.

Conflict of Interest: MS was employed by the company Fish Finder Adventures.

The remaining authors declare that the research was conducted in the absence of any commercial or financial relationships that could be construed as a potential conflict of interest.

frontiers in Marine Science

ORIGINAL RESEARCH
published: 10 November 2020
doi: 10.3389/fmars.2020.576343

St. Helena: An Important Reproductive Habitat for Whale Sharks (*Rhincodon typus*) in the Central South Atlantic

Cameron T. Perry[1]*, Elizabeth Clingham[2], D. Harry Webb[3], Rafael de la Parra[4], Simon J. Pierce[5], Annalea Beard[6], LeeAnn Henry[6], Beth Taylor[7], Kenickie Andrews[7], Rhys Hobbs[6], Gonzalo Araujo[8] and Alistair D. M. Dove[1,3]

[1] School of Biological Sciences, Georgia Institute of Technology, Atlanta, GA, United States, [2] Foreign Commonwealth Office, St Helena Government, Jamestown, Saint Helena, [3] Research and Conservation Department, Georgia Aquarium, Atlanta, GA, United States, [4] Ch'ooj Ajauil AC, Cancun, Mexico, [5] Marine Megafauna Foundation, Truckee, CA, United States, [6] Environment and Natural Resources Directorate, St Helena Government, Jamestown, Saint Helena, [7] Saint Helena National Trust, Jamestown, Saint Helena, [8] Large Marine Vertebrates Research Institute Philippines, Bohol, Philippines

OPEN ACCESS

Edited by:
David Wells,
Texas A&M University at Galveston,
United States

Reviewed by:
Mourier Johann,
Institut de Recherche Pour le Développement, France
Eric Hoffmayer,
Southeast Fisheries Science Center (NOAA), United States

***Correspondence:**
Cameron T. Perry
cperry60@gatech.edu;
perrycnbc@gmail.com

Specialty section:
This article was submitted to Marine Megafauna, a section of the journal Frontiers in Marine Science

Received: 25 June 2020
Accepted: 05 October 2020
Published: 10 November 2020

Citation:
Perry CT, Clingham E, Webb DH, de la Parra R, Pierce SJ, Beard A, Henry L, Taylor B, Andrews K, Hobbs R, Araujo G and Dove ADM (2020) St. Helena: An Important Reproductive Habitat for Whale Sharks (Rhincodon typus) in the Central South Atlantic. Front. Mar. Sci. 7:576343. doi: 10.3389/fmars.2020.576343

A reliable aggregation of whale sharks (*Rhincodon typus*) takes place in waters surrounding the remote South Atlantic island of St. Helena from December to May each year, peaking in January. Using photographic identification (photo-ID), a total of 277 individual sharks were identified over the course of the study, consisting of a 1.1:1 sex ratio of male and female sharks, ranging from 5 to 12 m in total length, with 86% of males and 51% of females likely to be mature. Modified maximum likelihood methods of the photo-ID data estimated ∼102 individual whale sharks at any one time, each residing within the study site for a mean of 19 days with a decline to complete absence at ∼75 days following initial identification. Interannual periodicity was observed for some ($n = 34$) sharks at the site. Eyewitness accounts of mating behavior have been reported by reliable local observers on two separate occasions, which comprise the first observations of copulation in this species and are consistent with the size and sex demographics of the population. Horizontal movements away from the island proved difficult to track, due to deep-diving behavior that either damaged or caused premature detachment of the archival satellite tags, however, some individuals showed large scale movement away from the island towards both Africa and South America. Acoustic telemetry showed that animals use the habitats around the entire island, but are focused on the leeward side, particularly from James Bay to Barn Cap. Due to its likely role in the reproductive ecology of the whale shark, St. Helena represents a critical habitat for this endangered species and deserves concerted research and conservation efforts.

Keywords: mating, movement ecology, diving, aggregation, demographics, remote, elasmobranch

INTRODUCTION

The whale shark (*Rhincodon typus*) can be found circumglobally in tropical and warm temperate seas, and often forms reliable coastal aggregations, typically in response to high prey abundance (Rowat and Brooks, 2012). The species has suffered $a > 50\%$ decline in global population over the last 75 years, leading to a conservation status of "Endangered" on the IUCN Red List of Threatened

Species (Pierce and Norman, 2016). Understanding the ability of whale shark populations to recover from these declines is vital for the conservation of the species, but little is known about their reproduction and some life-history characteristics. Genetic evidence suggests that whale shark populations are distinct between the Atlantic and Indo-Pacific, with clear differentiation between sharks sampled in the Gulf of Mexico and Indo-Pacific locations (i.e., Vignaud et al., 2014). Coupled with movement information from broad-scale whale shark photo-identification studies, such as Norman et al. (2017), this indicates that whale sharks in the Atlantic represent a functionally separate population from those in the Indo-Pacific (Pierce and Norman, 2016). The lack of movement or genetic data form outside the Gulf of Mexico and Caribbean region within the Atlantic makes it difficult to identify finer-scale structure within this ocean basin. In addition, there is a lack of information about the biology and ecology of whale shark populations in the South Atlantic relative to other ocean basins (Norman et al., 2017). Data are lacking on the formation of coastal feeding aggregations of juvenile sharks in this region, which tend to occur in areas of seasonal upwelling (de la Parra Venegas et al., 2011) or other high-productivity habitats. Similarly, the ecology of adult whale sharks, which are often sighted at volcanic islands far removed from continental shelf habitats (Ramírez-Macías et al., 2017), is poorly understood in general and in the Atlantic in particular.

The tropical South Atlantic Ocean has only a few oceanic islands in the habitable range of whale sharks, namely St. Peter and St. Paul Rocks (Brazil), Fernando de Noronha (Brazil), Trindade and Martim Vaz (Brazil), Ascension (United Kingdom), and St. Helena (United Kingdom), whereas the Pacific, North Atlantic, and Indian oceans are replete with oceanic islands. Whale sharks have been sighted at all of these Atlantic locations; however, the significance and role of these areas in whale shark biology and ecology is understudied (Hazin et al., 2008). Previous work at the archipelago of St. Peter and St. Paul in the Equatorial Atlantic region documented putative reproductive behaviors and indicators of sexual activity in whale sharks. Examples of this included a mature male shark that exhibited mating behaviors in proximity to a vessel, and large females that were observed with distended abdomen and potential mating scars suggesting pregnancy and/or possible mating attempts, respectively (Macena and Hazin, 2016). These results suggest the importance of the tropical Atlantic in terms of whale shark population demographics and reproductive ecology, although further research is needed to confirm these observations.

Whale shark aggregations can be explored through a variety of different research methods and techniques. Photographic identification is a non-invasive tool that uses stable markings to identify individuals within a population and has been employed on a variety of marine species, including turtles (Schofield et al., 2008), cetaceans (Hammond et al., 1990), and manta rays (Marshall et al., 2011). Whale sharks also have natural body markings that make them suitable study targets for photographic identification (Arzoumanian et al., 2005) and this technique has been commonly used to estimate population demographics and structure, such as sex ratios and size ranges, throughout all sites where whale sharks are encountered (Norman et al., 2017). Furthermore, photographic identification can be used to explore aggregation structure such as seasonality and individual residency by documentation of repeat encounters with individuals over time (McCoy et al., 2018). These repeat encounters can be used in mark-recapture models to estimate population sizes (e.g., McCoy et al., 2018) and residency through modified maximum likelihood methods (e.g., Fox et al., 2013), such as lagged identification rates, providing a valuable tool to explore whale shark sites globally.

Satellite and acoustic telemetry are two other techniques that have been commonly used on whale sharks worldwide to explore a variety of research questions relating to movement ecology. These methods involve attaching satellite and/or acoustic transmitters that passively record or actively report a suite of data depending on the tag. Satellite telemetry is a vital tool to explore horizontal movements as well as vertical diving behavior and profiles. Insights from these tags have shown that whale sharks are capable of very large horizontal movements (e.g., Hueter et al., 2013) and able to conduct deep dives into the bathypelagic zone (e.g., Tyminski et al., 2015). Acoustic telemetry can help explore residency patterns (such as site use and fidelity) (Cagua et al., 2015), fine-scale horizontal movements, and validate photographic identification data (Cochran et al., 2019). Used in combination, these techniques can elucidate both the large and fine-scale movements of whale sharks in a particular area.

To redress the lack of information on whale sharks in the South Atlantic, and to help understand their reproductive biology, here we report the first data on the biology of whale sharks around St. Helena Island. We have compiled historical data curated by the St. Helena Government (SHG) and collected new information during research expeditions to the island in 2015, 2016, 2018, and 2019. We used photographic identification from these dedicated expeditions to explore the population demographics of St. Helena whale sharks. Additionally, satellite and acoustic telemetry were used in combination to explore the large and fine-scale movement and residency patterns. Finally, we used modified maximum likelihood methods to further understand the population demographics of whale sharks at St. Helena.

MATERIALS AND METHODS

Study Site

Saint Helena is a rocky volcanic island in the South Atlantic Ocean, approximately 2,000 km west of Angola, and 3,500 km east of Brazil (**Figure 1**). It is one of the most remote inhabited islands in the world, with a population of *ca.* 4,300 people, and is part of the United Kingdom Overseas Territory (UKOT) of St. Helena, Ascension, and Tristan da Cunha. The island is surrounded by steep cliffs on all sides and the water depth increases sharply as you move away from the island in all directions, down to the South Atlantic abyssal plain at approximately 4,200-4,500 m depth. The island has a mild and stable subtropical climate, heavily influenced by southeast trade winds, which also create a stark difference in navigability between the calmer leeward side facing the

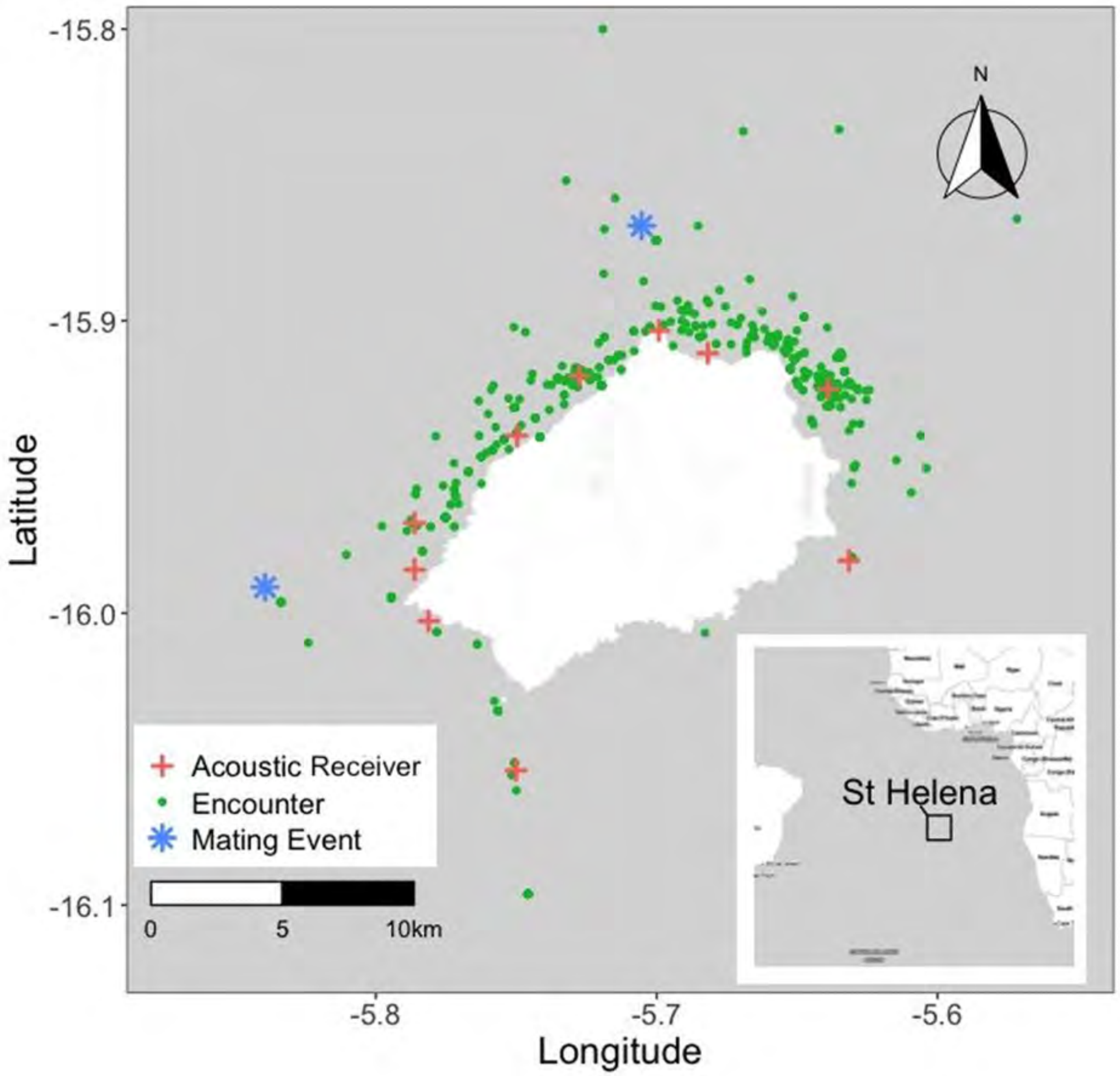

FIGURE 1 | St. Helena study site, showing whale shark sightings from 1999 to 2019 inclusive as green dots. Asterisks show sites of eyewitness accounts of mating behavior. Crosses show the sites of receivers in the acoustic array deployed since 2016. Inset: location of St. Helena in the South Atlantic.

northwest, and the rougher windward side facing southeast. The island is home to a substantial portion of UK marine biodiversity (Brown, 2013; Bormpoudakis et al., 2019) and has high rates of endemism for both terrestrial (Gray et al., 2019) and marine life (Roberts et al., 2002).

Visual Observations

The Environment Natural Resources and Planning Directorate (ENRD) of St. Helena Government has maintained an incidental sightings database of whale sharks, which are locally also called bone sharks, since 1999. Any boater, fisher or member of the general public who saw a whale shark was encouraged to report the sighting to ENRD resource managers for inclusion in the database. This database represents opportunistic sightings of whale sharks by marine users and is mainly driven by fishermen, some recreational users, and three tourism operators, all of whom are on the water year-round. Sightings form the first four Georgia Aquarium expeditions dedicated to the study of whale sharks in St. Helena are also included in this database. These took place in January 2015, January-February 2016, February 2018, and March 2019 and their timing was determined by seasonal occurrence trends noted in the earlier sightings database.

During these four expeditions, visual observations took place from cabin-cruiser style boats. On the expeditions in 2015 and 2016, an equal effort search pattern was deployed that incorporated the entire circumference of the island. In subsequent years, search effort was focused on areas of known whale shark abundance to improve efficiency. Upon seeing a whale shark near the surface, snorkelers were deployed to observe and photograph animals for submission to the Wildbook for Whale Sharks photographic identification database[1] (Arzoumanian et al., 2005). Whale sharks were sexed visually by the presence/absence of claspers, measured with laser photogrammetry following Rohner et al. (2011), and photographed to document distinguishing features and/or injuries. Maturity in males was determined by the external morphology of the claspers. Sharks with claspers extending beyond the pelvic fins, with a thick and calcified appearance, were considered mature; claspers extending past the pelvic fins but not being calcified in appearance were considered sub-adult (i.e., immature), and claspers not extending past the pelvic fins and not calcified were also classes as immature (Norman and Stevens, 2007). Maturity in females cannot be accurately assessed externally, however, maturity is thought to occur ∼9.0 m total length (Acuña-Marrero et al., 2014), although size at maturation may differ between ocean regions (Hueter et al., 2013). Conservatively, female whale sharks over 9 m were considered mature while those under 8 m were considered immature. Those in the ambiguous 8-9 m range were excluded from maturity assessments due to uncertainty in female size at maturity (Macena and Hazin, 2016). In 2016, multiple laser photogrammetry photos were taken during each encounter to generate mean values and improve accuracy of size estimates (Rohner et al., 2011). The number of sightings was compared across years and months to explore seasonal and interannual trends in sighting reports from the ENRD dataset. Sex ratios, number of individuals, size estimates, and resighting rates were explored from the Wildbook dataset. Maps were created using the *ggmap* package in R studio (Kahle and Wickham, 2019). Figures were created using the *ggplot2* package in R studio (Wickham, 2016).

Telemetry

Satellite Telemetry

Multiple types of satellite tags were used to address questions of whale shark movements on a regional spatial scale. These tags included pop-up satellite archival tags (Wildlife Computer Mk10/MiniPAT and Desert Star SeaTagMOD/SeaTagGeo) and smart position only (Wildlife Computer SPOT253-C/SPOT6/SPLASH10) tags. All tags were attached to the dorsal surface of the whale shark, along the lateral aspect at the base of the first dorsal fin. Wildlife Computers SPOT253-C tags in towed configuration were used to track whale shark movements in near-real-time using Doppler locations generated by the CLS-ARGOS satellite system. These tags were affixed to a whale shark on a long braided stainless wire leader attached to a Wildlife Computers titanium intradermal dart applied by pole spear. The section of leader in the skin of the animal was covered in heat-shrink wrap to minimize abrasion. Wildlife Computers MiniPAT archival tags were used to generate horizontal movement tracks using light-based location estimates, as well as recording vertical movements and water temperature. Sensors were set to sample at 3-min intervals. The MiniPAT tag has a self-preservation circuit that severs the tag from the leader if the tag depth exceeds a pre-set value of either 1,650 or 1,850 m. MiniPAT tags were affixed to the animals with short leaders of Dyneema braided synthetic material that was heat shrink wrapped to minimize skin abrasion. Wildlife Computers SPLASH10 towed archival tags were also used on a leader similar to that of the SPOT253-C tags.

Transmissions that had quality scores[2] under 1 were removed from further analyses as these transmissions are accompanied by greater uncertainty and error. Tracks were then filtered to remove floating tags from the dataset using methods similar to Hearn et al. (2013). Briefly, changes in latitude and longitude were assessed on each tag and compared to observations from known floating tags to apply a filtering method for all tags. The tracks that fit these criteria were determined to be floating and removed from further analysis. MiniPAT most probable tracks (MPT) were generated using the GPE3 processing tool in the Wildlife Computers web portal[3], which estimates animal movements from tag data and user input variables such as maximum animal swim speed. Datasets were explored to look for any unrealistic movements such as >200 km/day. No tags were physically recovered during this study and therefore complete time-series datasets were not available for further analyses.

Acoustic Telemetry

To investigate fine-scale habitat usage and observer-independent seasonality, an acoustic array was established around the island in 2016 (six receivers) and 2017 (an additional four receivers). This consisted of Vemco VR2 passive acoustic receivers deployed at prominent features on the bottom, within no-decompression diving depth of the surface, i.e., <30 m depth. The array aimed to allow coverage around the entire island; however, accessibility on the southeast windward side of the island was limited due to weather and safe diving conditions. Depending on the site, receivers were affixed with plastic cable-ties to mooring ropes on subsurface buoys or to rebar embedded in plastic 20 L buckets filled with concrete. The acoustic receivers were not range tested due to field constraints; however, we speculate the range would be on the upper end of previous range tests (>530 m) due to the open ocean, steeply sloped, and deep nature of the water surrounding St. Helena (Cagua et al., 2013). Vemco V16 acoustic transmitters were affixed to whale sharks using leaders similar to those of the MiniPAT tags described above in both the 2016 and 2018 field seasons. Receivers were downloaded and maintained on an approximately annual basis.

Site use and fidelity were explored by analyzing the number of detections, individuals, and days that were documented at each receiver location. Receivers that had high total numbers of detections likely represent areas where sharks were remaining for periods of time and therefore may be indicative of site fidelity. Total number of individuals detected by each receiver was explored to investigate sites that may indicate habitats frequented by multiple individuals. Lastly, the number of days that each receiver detected an individual shark was explored to investigate site fidelity, as receivers that were visited multiple

---

[1] www.whaleshark.org

[2] https://www.argos-system.org/support-and-help/faq-localisation-argos

[3] https://my.wildlifecomputers.com/

times throughout the course of the study may be important fidelity sites or nearby migratory routes. Spatial residence ($R_{spatial}$) was calculated by dividing the number of days a shark was detected by an individual receiver by the total number of days it was documented in the array. When comparing between years $R_{spatial}$ values were only calculated for receivers that were active for both years because the addition of receivers in later years could influence results as they could increase the number of days an individual was detected in the array through increased search effort.

Individual residency was explored by analyzing the number of detections by individuals throughout the year and calculating both minimum (R_{min}) and maximum (R_{max}) residence indices. Sharks that were not detected on the array were removed from analysis as these would skew results and may be indicative of tag loss or failure rather than residence patterns. Minimum residence index (R_{min}) was calculated by dividing the number of days an individual was detected in the array by the period between initial tagging and the end of the study. Maximum residence index (R_{max}) was calculated by dividing the number of days an individual was detected in the array by the total number of days between initial tagging and last detection. Both indices are directly affected by study duration, which can bias animals that were tagged later in the course of the study or individuals that were detected over short periods of time (Cochran et al., 2019), therefore, both results are reported in an attempt to provide upper and lower values for true residency.

Lagged Identification Rate

The photographic identification data were downloaded from Wildbook for Whale Sharks and used to calculate the lagged identification rate (LIR), which is the probability that an individual will be re-sighted at the site after a certain time lag (Whitehead, 2001). The LIR was estimated using the "Movement" module in program SOCPROG 2.7 (Whitehead, 2009). Eight models were fitted against various parameters for population closure, emigration, reimmigration and mortality (**Table 1**). The quasi-Akaike information criterion (QAIC) was used to account for data overdispersion (Whitehead, 2007). We used the ΔQAIC to select the best-fit model based on a ΔQAIC of ≤ 2 providing considerable support (Burnham and Anderson, 2003), whilst subjectively weighing the number of biologically relevant parameters estimated, and the comparability to other studies using these methods. The best-fit model was then bootstrapped for 100 repetitions to generate confidence intervals (95%) and standard errors (Buckland and Garthwaite, 1991).

TABLE 1 | Model results for maximum likelihood methods using parameters to test for population closure, mortality or permanent emigration, reimmigration, and residency as preset in program SOCPROG 2.7 (Whitehead, 2009).

Model name	Parameters	ΔQAIC
A	Closed (1/a1 = N)	23.83
B	Closed (a1 = N)	1901.50
C	Emigration/mortality (a1 = emigration rate; 1/a2 = N)	1.83
D	Closed: Emigration + reimmigration (a1 = emigration rate; a2/(a2+a3) = proportion of population in study area at any time)	2.06
E	Emigration/mortality (a1 = N; a2 = Mean residence time)	1.83
F	Emigration + reimmigration + mortality	5.83
G	Emigration + reimmigration (a1 = N; a2 = Mean time in study area; a3 = Mean time out of study area)	2.06
H	Emigration + reimmigration + mortality/permanent emigration	0.00

N, population size; QAIC, quasi-Akaike information criterion.

RESULTS

Visual Observations

Sighting Database

The ENRD sighting database contained 985 whale shark sightings between February 1999 and May 2019 (**Figure 2**). These data do not represent individual identification of whale sharks, but rather the total number of encounters over the time period. Most of these sightings were unaccompanied individual sharks, with only 150 encounters documenting more than one individual. There was distinct seasonality in whale shark encounters with 85.5% of all encounters being documented in the months of January, February, and March. This season appears to begin with whale sharks arriving around the island in November and December, however, sightings increased sharply starting in January. January had the highest number of sightings, with 38.5% of the total (**Figure 3**), whereas February and March had the next highest number of sightings with 28.9% and 18.1%, respectively. Encounters from visual observations showed a drastic decline in sightings from April to December with sharks seen infrequently in the surrounding waters over these months. Annually, whale shark sightings have increased towards the end of the study period with peaks corresponding with dedicated research expeditions and associated increased search effort.

On any given day 1-40 whale sharks were seen around St. Helena from both the ENRD database and dedicated research expeditions. A few extraordinary aggregations of over 30 individuals were noted, including an event off Egg Island on the 17th of January 2014, at Barn Cap on the 21st of January 2015, off Sugarloaf on 22nd of January 2015, and another in Flagstaff Bay on 13th February 2019. These aggregations were remarkable for being feeding events whereas most other sightings around St. Helena did not involve obvious feeding behavior. Whale sharks at St. Helena were seen feeding at the surface using the active surface suction-feeding mode described by Motta et al. (2010), but more often, they were observed swimming calmly 1-5 m below the surface. A range of different sizes was seen at these feeding events; however, the sharks involved were not visibly different in size (at ∼7-9 m) from those encountered at other times. Qualitative plankton tows taken at the time of the 2015 aggregation event indicated the presence of substantial numbers of fish eggs, associated with nearby schools of skipjack tuna (*Katsuwonus pelamis*) that were suspected to be spawning at the surface.

Mating Events and Reproductive Behavior

Putative mating behaviors of whale sharks were reported to ENRD staff on two occasions during the reporting period. These

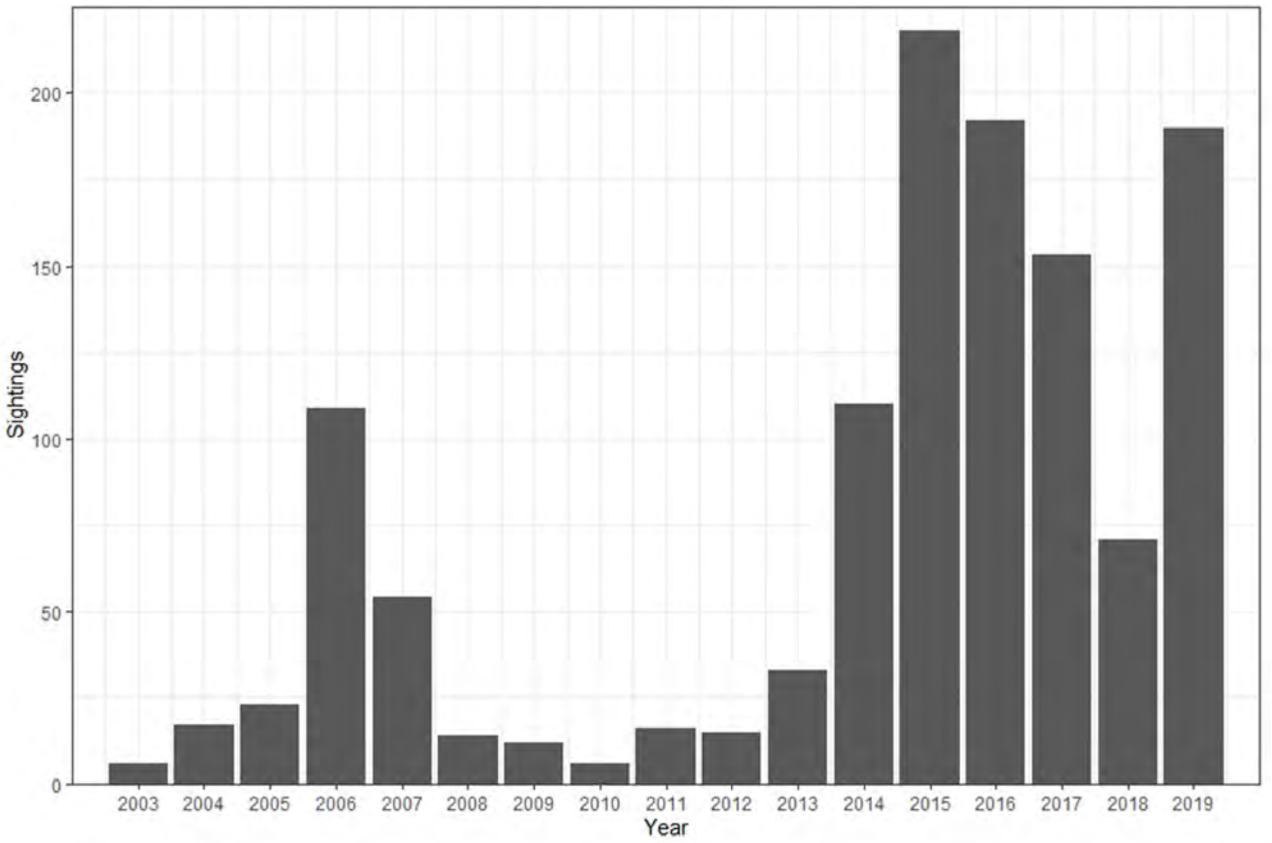

FIGURE 2 | Sightings per year of whale sharks since 2003. Dedicated expeditions were conducted in 2015, 2016, 2018, and 2019. Note year 1999 is not displayed on the figure to eliminate gaps in coverage.

events took place in 2005 and 2007 at opposite ends of the island, both on popular fishing grounds, both approximately 16 km from shore. The observations were made by two different people and each was unaware of the observations of the other. The 2005 event was reported by the island's chief fisheries officer at the time, whereas the 2007 event was reported by a career professional fisherman. On January 28, 2005 on the New Shoval fishing ground (5°50′21.97″W, 15°59′28.12″S; see **Figure 1**) the chief fisheries officer reported:

"*Two whale sharks mating! Came together -- one on* [its] *back swimming below the other one, then came belly to belly, very near to the surface for a few minutes. Came alongside the boat, lifted its head out of the water. Quite a few remoras on them -- were pale white*."

On February 15, 2007 on the Dawson's fishing ground (15°52′2.83″S, 5°42′19.25″W and see **Figure 1**) a professional fisherman reported:

"*Saw two smaller ones (male) and one larger female. The two males were trying to mate with the female. Saw the male going belly to belly with female and other male also trying to get in there!*"

While photo and video documentation were not made of these events, both observers are competent naturalists and would be expected to recognize mating behavior among sharks. In addition, during the 2019 expedition photo documentation was made of potential pre-copulatory behaviors and post-copulatory wounds. A male whale shark followed a female whale shark and positioned his rostrum towards the posterior of the female which resulted in contact of the female's caudal fin against the male's snout (**Figure 4**). Furthermore, a female whale shark was encountered with abrasions on her left pectoral fin that may be indicative of recent mating attempts (**Figure 5**).

Photographic Identification

The Wildbook database contained 462 encounters from April 2013 to May 2019 with 277 individual sharks identified. The majority of all individual sharks (n = 180, 65.4%) were encountered only once across the study period (**Supplementary Figure 1**). Of the individuals that were encountered more than once (n = 97), a total of 35% (n = 34) were seen between seasons with an average of 1.4 seasons per individual (range:1-4 seasons). Sex was determined for 257 sharks. Of these 53% (n = 137) were males, and 47% (n = 120) were females, an approximately even sex ratio. Sex ratios did not differ between month, with January exhibiting a 1.07:1 sex ratio and February and March exhibiting a 1.42:1 sex ratio of males to females. Of the male sharks, 108 were assessed for clasper morphology with 86.1% (n = 93) being identified as mature and 13.8 % (n = 15) identified as subadult (n = 9) and immature (n = 6). Size estimates

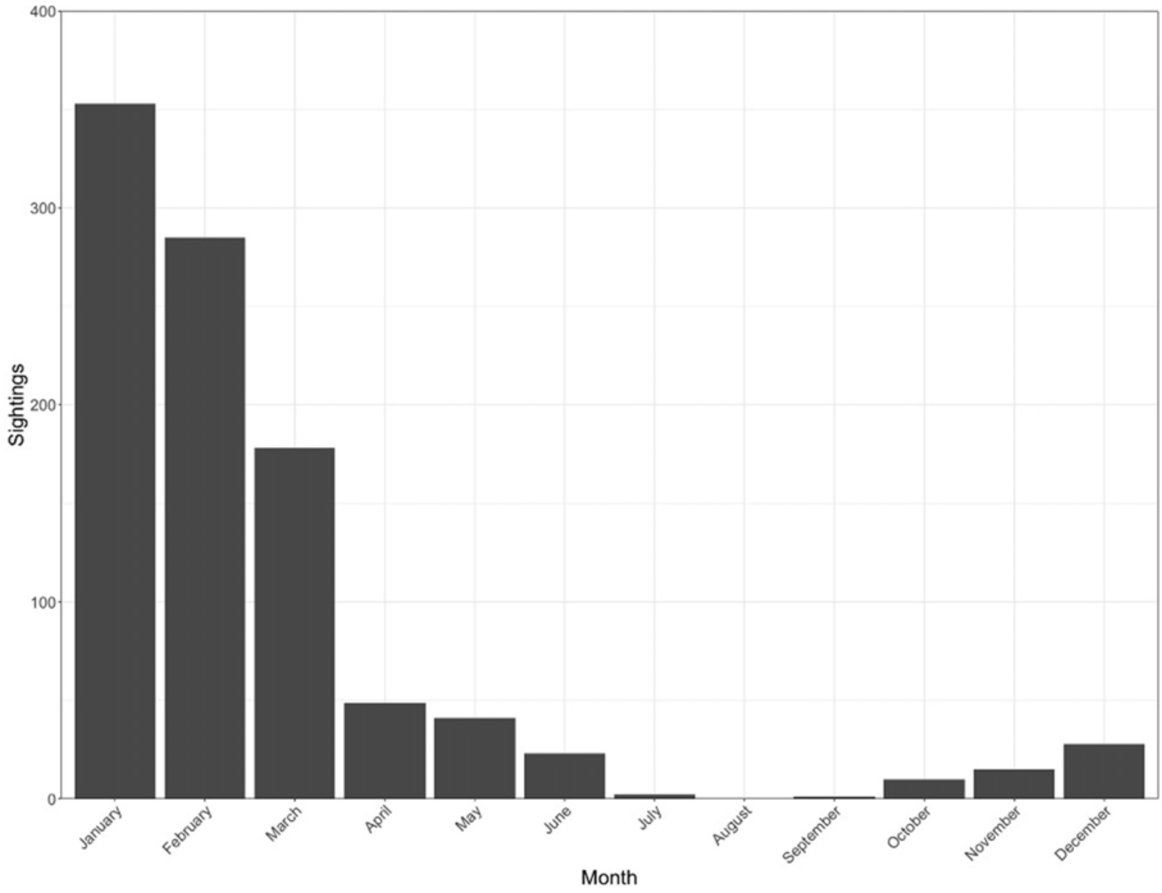

FIGURE 3 | Sightings per month aggregated across all years since 1999, showing seasonality peaking between January and March.

were documented for 89 female and 107 male whale sharks and yielded an average size of 8.1 m (**Figure 6**). The average estimated size was 7.9 and 8.4 m for male and female whale sharks, respectively. Assuming a size at maturity of 9 m for female whale sharks and removing eight sharks in the ambiguous 8-9 m range, 50.6 % ($n = 41$) of female sharks with length estimates were conservatively determined to be mature. Laser photogrammetry from the 2016 expedition yielded an average total length of

FIGURE 4 | Solicited contact between a male and female whale shark with the male positioning his snout on the caudal fin of the female.

FIGURE 5 | Abrasions on the pectoral fin of a female whale shark that may be indicative of recent mating behavior.

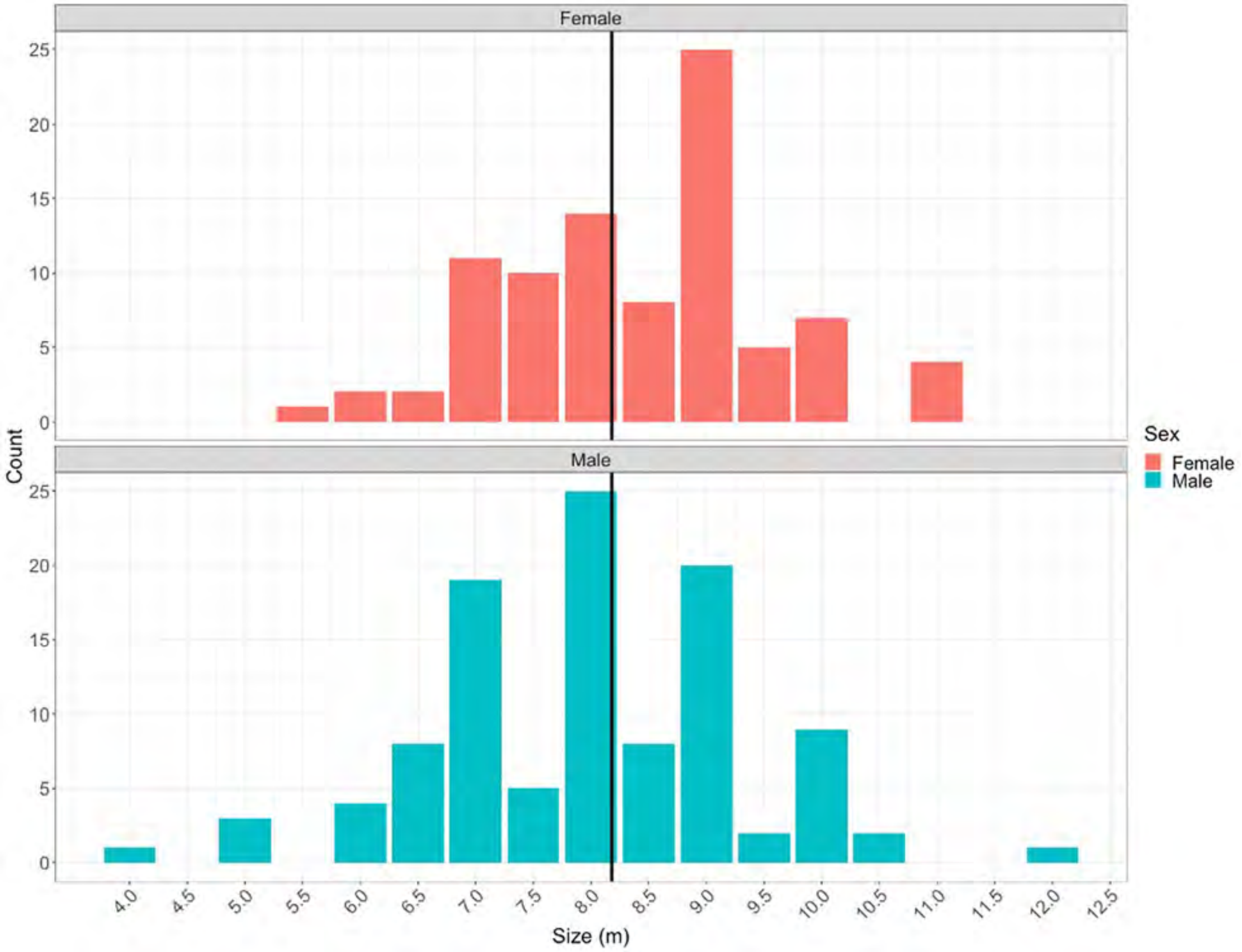

FIGURE 6 | Size frequency of male (teal) and female (red) whale sharks encountered in St. Helena. The black vertical line represents the average of all sharks encountered at 8.1 m.

9.51 m ± 0.18 (mean ± s.e) (8.55–10.79 m, n = 15). During the 2018 and 2019 expeditions, a total of 154 unique individuals were sighted and detailed observations of injuries were documented. Injuries were documented on 56.4% (n = 87) of all individuals and were mainly minor and well-healed in nature. A few instances of well-healed major injuries were documented including a shark with its entire dorsal fin missing, a shark with some very large apparent bite marks, and a shark with entanglement wounds around its head and mouth, however, major wounds and fresh wounds were not a common occurrence.

Telemetry

Satellite Telemetry

Horizontal and vertical movements

While a total of fifty satellite tags were placed on whale sharks, only thirty reported reliable data from which horizontal movements could be evaluated. There were no unrealistic movements (>200 km/day) observed in any of the tag datasets. Among tags that reported data, an average deployment duration of 74.84 ± 19.71 days was obtained (**Table 2**). The average straight-line distance between tagging and pop-off was 465 km with a median distance of 97 km. The majority of tags (n = 21) remained near St. Helena (**Figure 7**) and sixteen sharks reported straight-line distances of less than 100 km between tagging and pop-off locations, over an average of 24.8 days. No obvious habitat use was observed in the tracks as there appeared to be substantial individual variation in how animals moved around the island. Additionally, many tags (n = 14) released prematurely due to the crush depth being reached shortly after the animals left the proximity of St. Helena.

Five tagged individuals were seen to venture away from St. Helena, recording straight-line distances of over 1,000 km over an average of 131 days (**Table 2**). One tagged individual (tag #173924) swam to the northeastern coast of Brazil, near the archipelago of Fernando de Noronha, a distance of 3,395 km from the tagging location (**Figure 9**). These were class 1 location reports representing reliable transmissions with improved accuracy, but no other data packets were received, and thus a complete track could not be generated. Another individual (tag #173920) traveled 1,054 km east of the tagging

TABLE 2 | Summary of the whale sharks that were tagged with satellite tags from 2015 to 2019.

Tag number	*Tag type*	*Sex*	*Tagging date*	*Pop-off date*	*Days*	*Straight-line distance*
173920	MiniPAT	F	1/29/18	3/5/18	35	1054.56
142271	Desert Star SeaTag MOD	M	1/18/15	5/11/15	113	2612.04
173924	SPOT6	F	2/10/18	8/3/18	174	3395.59
154785	SPOT6	U	1/8/16	8/12/16	217	565.65
154790	MiniPAT	F	1/8/16	9/4/16	240	1320.02
158435	Desert Star SeaTag MOD	F	1/9/16	3/13/16	64	663.46
173923	SPOT6	M	2/5/18	4/22/18	76	621.88
177970	MiniPAT	F	3/16/19	4/11/19	26	581.85
177990	SPLASH10	F	3/7/19	6/10/19	95	1445.49
152640	Desert Star SeaTag MOD	U	1/11/16	2/12/16	32	12.27
152641	Desert Star SeaTag MOD	U	1/7/16	1/23/16	16	98.89
152643	Desert Star SeaTag MOD	F	1/14/16	4/14/16	91	131.14
154784	SPOT6	U	1/8/16	3/15/17	432	178.85
154788	MiniPAT	M	1/8/16	1/9/16	1	22.14
154789	MiniPAT	M	1/8/16	7/31/16	205	319.4
154794	Desert Star SeaTag GEO	F	5/13/16	5/31/16	138	270.87
157580	Desert Star SeaTag MOD	U	1/11/16	1/12/16	1	4.76
157581	Desert Star SeaTag MOD	F	1/11/16	1/13/16	2	20.45
157582	Desert Star SeaTag MOD	F	1/10/16	1/18/16	8	2.94
158432	Desert Star SeaTag MOD	M	1/11/16	2/11/16	31	15.57
158434	Desert Star SeaTag MOD	F	1/9/16	3/15/16	66	64.13
158436	Desert Star SeaTag MOD	M	1/9/16	3/4/16	55	31.3
158438	Desert Star SeaTag MOD	M	1/14/16	2/17/16	34	153.13
158439	Desert Star SeaTag MOD	F	1/20/16	1/23/16	3	33.37
173921	SPOT6	F	1/28/18	1/29/18	1	8.07
174109	SPLASH10	M	2/15/18	4/3/18	47	31.51
177968	MiniPAT	M	3/5/19	4/22/19	48	63.39
177969	MiniPAT	M	3/6/19	3/24/19	18	96.25
177971	MiniPAT	M	3/15/19	4/18/19	34	95.04
177972	MiniPAT	F	3/15/19	4/18/19	34	36.12

Note these tags represent those that reported data for analysis.

location, towards the western coast of Namibia and Angola (**Figure 9**). One individual (tag #142271) moved to the Gulf of Guinea near the coast of Nigeria, over 2,500 km distance (**Figure 9**). This tag washed ashore shortly after detachment, before it was able to relay its data payload, and therefore a track could not be generated for this individual. Three sharks (#177990, #154790, and #154785) traveled towards Ascension Island, with one individual (tag #154785), returning towards St. Helena, after which its tag released in August of 2016 (**Figure 8**). Two sharks were in close proximity to Ascension Island during the months of April, May, and June.

In general, there was north westerly movement away from the island, with only a handful ($n = 4$) of individuals venturing east. Variations in individual movement patterns showed that some individuals left the surrounding water relatively quickly after being tagged, whereas others appeared to spend more time navigating in closer proximity to St. Helena. Eight out of nine MiniPAT tagged sharks (5 males and 3 females) reported diving data for analysis. There were 509 daily dives reported, with a median daily maximum depth of 619 m and a maximum depth overall of 1,879 m (**Figure 10**). The 500-700 m depth range accounted for 65.6% ($n = 334$) of all maximum daily dives. It is also worth noting that 6.6% of all daily dives were to depths greater than 1,000 m ($n = 34$); evidently these dives took place once the individuals left the proximity of St. Helena.

Acoustic Telemetry

Data were downloaded in both the 2018 and 2019 field seasons, representing information from the 2016 and 2018 field seasons. There was an initial total of six receivers deployed in 2016 with coverage around the island (Barn Cap, Darkdale, Sugarloaf, Speery Cap, George Island, and Torm's Ledge). An additional five receivers (Frontier, Bird Island, Flagstaff, Torm's Ledge replacement, and Egg Island) were deployed in 2017 to reduce gaps in coverage (**Figure 11**). A total of 43 individual sharks were tagged with acoustic transmitters. Eight tagged individuals (18.6%) were not detected on any of the receivers and two receivers, Torm's Ledge and Bird Island, did not have any detections recorded in the dataset. Tagged individuals were detected 49.6 ± 9.37 times at 2.5 ± 0.24 receivers over both years (**Figure 12**). There were 903 detections of 19 individuals over 78 distinct days in 2016. In 2018, there were 649 detections of 16

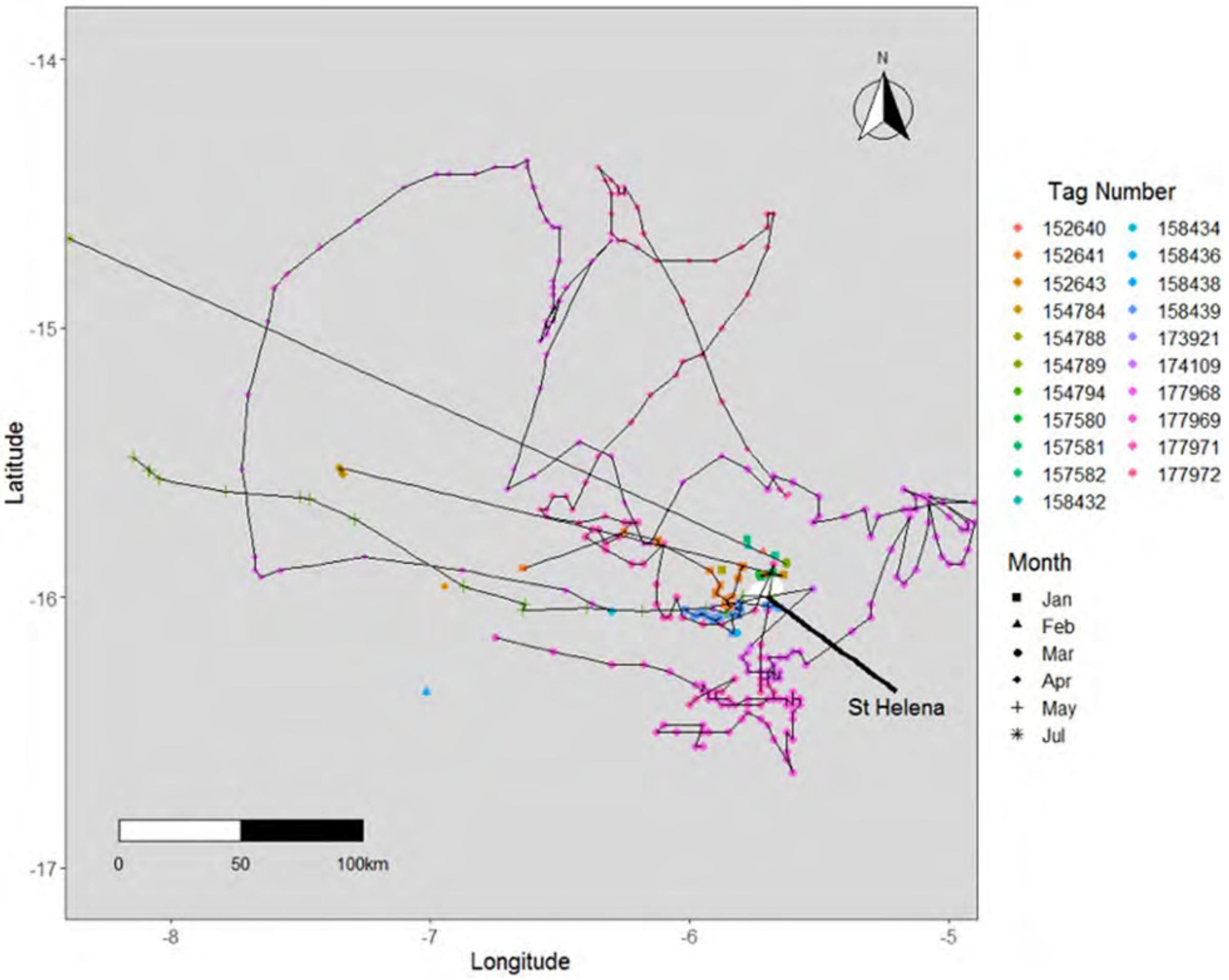

FIGURE 7 | Tracks of satellite-tagged whale sharks from St Helena 2015-2019 representing individuals that have travelled short distances (<300 km) from St. Helena.

individuals over 31 distinct days (**Table 3**). Individual sharks were detected in the array over an average of 5.7 (range 1-27) days.

Barn Cap and the wreck of the Darkdale recorded 73.5 and 73.9% of all detections in 2016 and 2018, respectively. $R_{spatial}$ values were calculated for each receiver from each individual and showed similar site use and fidelity results. In 2016, Darkdale and Barn Cap led receivers with values of 0.42 and 0.35, respectively. In 2018, Barn Cap and the Darkdale reported values of 0.61 and 0.25, respectively. When comparing $R_{spatial}$ values from receivers that were active for both years similar patterns were seen, however, annual variations in receiver use were also documented with Barn Cap increasing from 0.34 to 0.64 from 2016 to 2018 (**Table 3**).

The majority of individual detections were documented in January and declined steadily until June, in which detections were effectively zero (**Figure 12**). When removing detections that were recorded at the start of a second season, there were on average 35.8 days (range 0-185) between first and last detection. On average whale sharks exhibited an R_{max} of 0.24 (range: 0-1) and an R_{min} value of 0.008 (**Supplementary Table 1**). Three individual sharks were recorded returning to St. Helena waters at the beginning of a new season after their initial tagging seasons. These individuals returned during the months of September and November and were documented at Darkdale, Barn Cap, and Speery Cap.

There was one confirmed instance of tag loss, wherein an individual that was acoustically tagged in 2018 was re-sighted in 2019 and no acoustic tag was present. However, the overall frequency of tag shedding at this location is unknown. Of further note, the George Island receiver was not recovered for maintenance during the 2018 field season and therefore battery life was uncertain and tagged individuals in 2018 were likely not detected due to low battery. Furthermore, the receiver at Speery Cap in 2016 recorded 938 (81.9% of all detections) detections of one tagged individual (#56232) over the course of 31 h, with detections being recorded every few minutes during that period. The likely cause for this observation is the shedding of a transmitter in close proximity to the receiver, leading

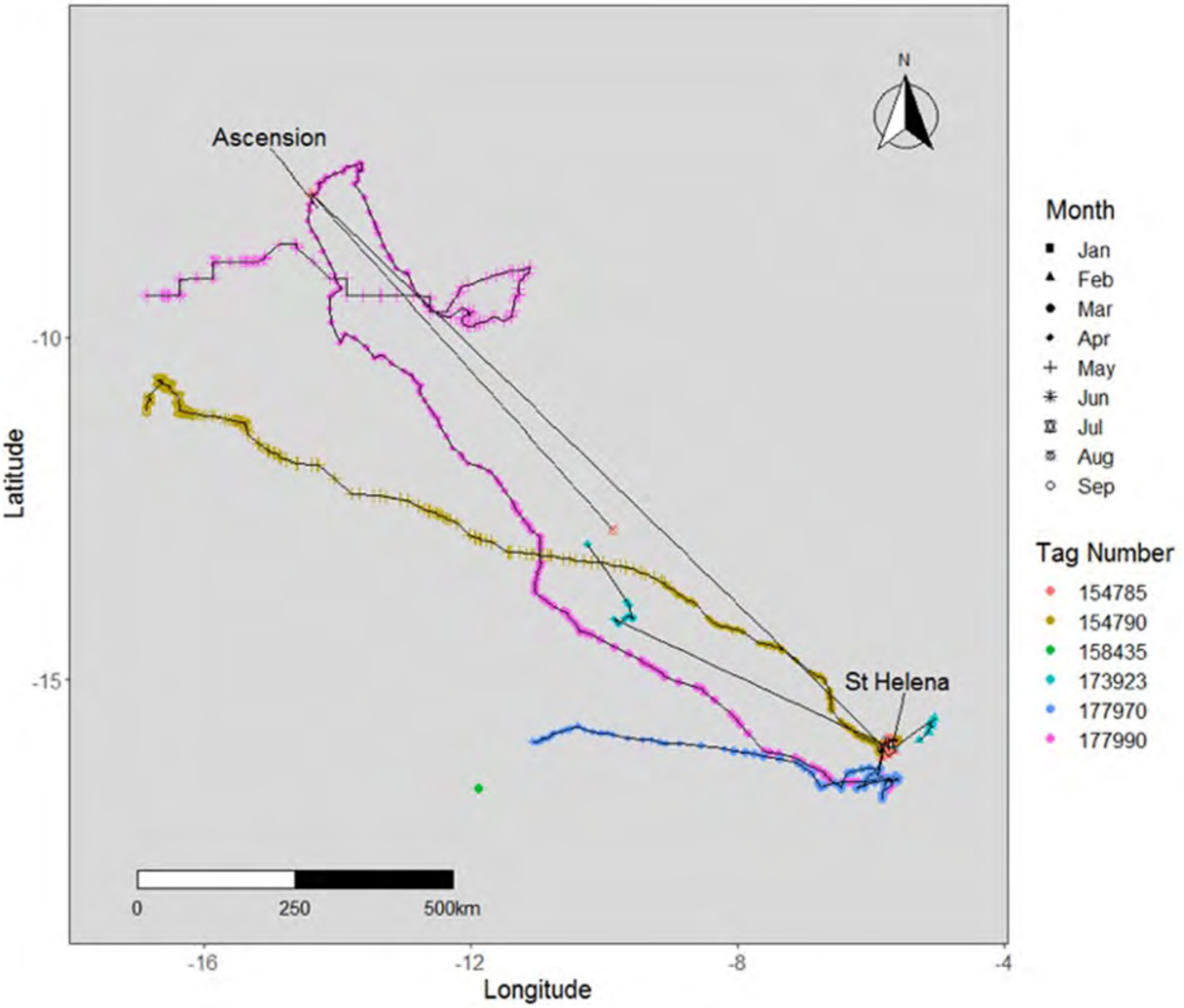

FIGURE 8 | Tracks of satellite-tagged whale sharks from St Helena 2015-2019 representing individuals that have traveled intermediate distances (500-1500 km) toward Ascension Island from St. Helena.

to continuous detections over that time period. This tagged individual was only recorded at Speery Cap and was removed from further analysis. It should also be noted that the maximum depth rating for the acoustic tags was significantly less than the average daily maximum dive depth for whale sharks at St. Helena (determined from archival satellite tags), so it is likely that a significant number of tags were lost due to crushing at depth.

Lagged Identification Rate

Models C, E, and H had substantial support (ΔQAIC < 2; **Table 1**). However, models C and E produced fewer parameter estimates than did model H, whilst biasing towards single-sighting data. Model H best-fit the empirical data (ΔQAIC = 0), described through a combination of residency, population size, reimmigration and mortality or permanent emigration. The LIR declined steadily to zero, from 1 to 64 – 88 (mean 75.4) days, followed by an increase between 268 and 470 (mean 376.9) days and again at mean 742.4, 1306.4, and at 2218.4 days, suggesting an interannual periodicity of some sharks at the site (**Supplementary Figure 2**). The model estimated a mean 102.1 ± 35.7 (95% CI 21.1 – 146.4) whale sharks at the study site at any one time, each residing a mean 18.9 ± 22.5 (95% CI 0.5 – 70.8) days at the study site whilst spending 32.8 ± 50.7 (95% CI 2.5 – 164.4) days outside the site. Mortality or permanent emigration was estimated at 0.00056 ± 0.00039 (95% CI 0.0001 – 0.0014), an apparent survival of 0.796 ± 0.857 year^{-1}.

DISCUSSION

Population Characterization

The whale shark population that visits St. Helena is a seasonal aggregation of mostly adult male and female animals in approximately equal ratio. This is unusual in two ways; first, because most known aggregation sites are dominated by juvenile animals, and second, because most aggregations are dominated

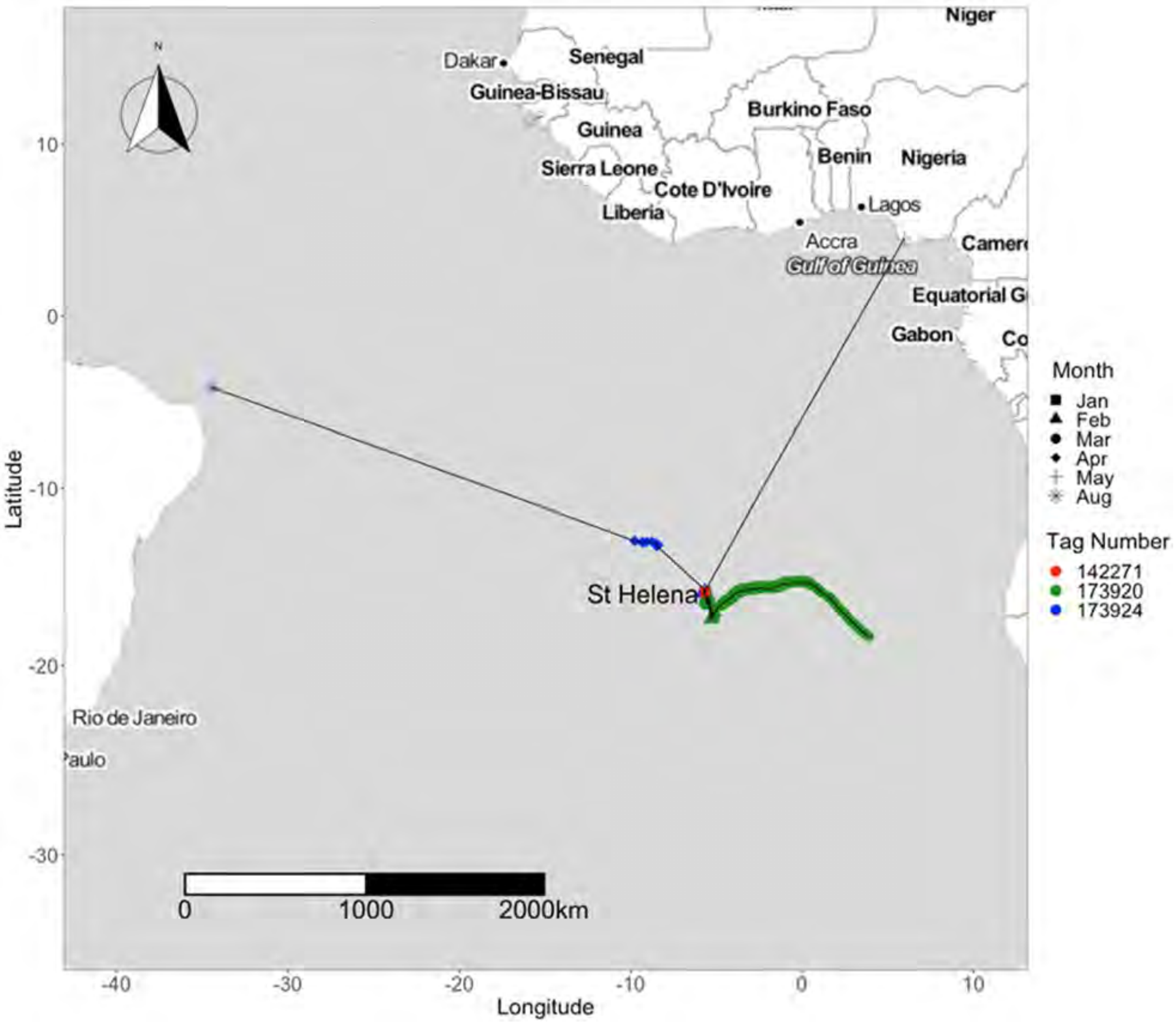

FIGURE 9 | Tracks of satellite-tagged whale sharks from St Helena 2015-2019 representing individuals that have traveled greater distances (>1000 km) from St. Helena.

by males, in ratios varying from 3:1 to 10:1 or more (Norman et al., 2017). Macena and Hazin (2016) found a similar trend in seasonality and size in the Equatorial Atlantic at St. Peter and St. Paul Rocks, with peak whale shark sightings occurring between January and June, and sharks averaging 8.27 m (2.5-14 m) in total length. However, the sex ratio of 14 sharks observed at that location differs from St. Helena, with a 3.6:1 ratio of females to males recorded. These authors also reported reproductive behaviors and suggested that these oceanic islands in the Atlantic play a significant role in whale shark reproduction. The unique presence of approximately equal numbers of mature adults of both sexes at St. Helena supports this hypothesis. St. Helena is unique in hosting a significant population of adult whale sharks, with similar numbers of both sexes, and appears to play an important role in their reproductive ecology.

The whale sharks documented at St. Helena were estimated 4-12 m in length with average lengths around 8 m, which is the upper end of those seen at most coastal aggregations (4.5-8.5 m), but smaller than some of large females regularly seen at Darwin's Arch in the Galapagos (9-13.5 m) (Norman et al., 2017). However, there are known biases of visual estimates with larger sharks often being underestimated in size (Perry et al., 2018). Laser photogrammetry of 15 sharks yielded an average length of 9.15 m, and the average sizes of whale sharks encountered in St Helena may be closer to the laser photogrammetry data, although that sample size is small. During some expeditions there were individuals that were visually estimated to be larger than 12 m total length, however, visual estimates should all be assessed with caution (Perry et al., 2018). Uncertainties and errors in visual length estimates can easily influence the maturity assessment for female whale sharks reported here and should be

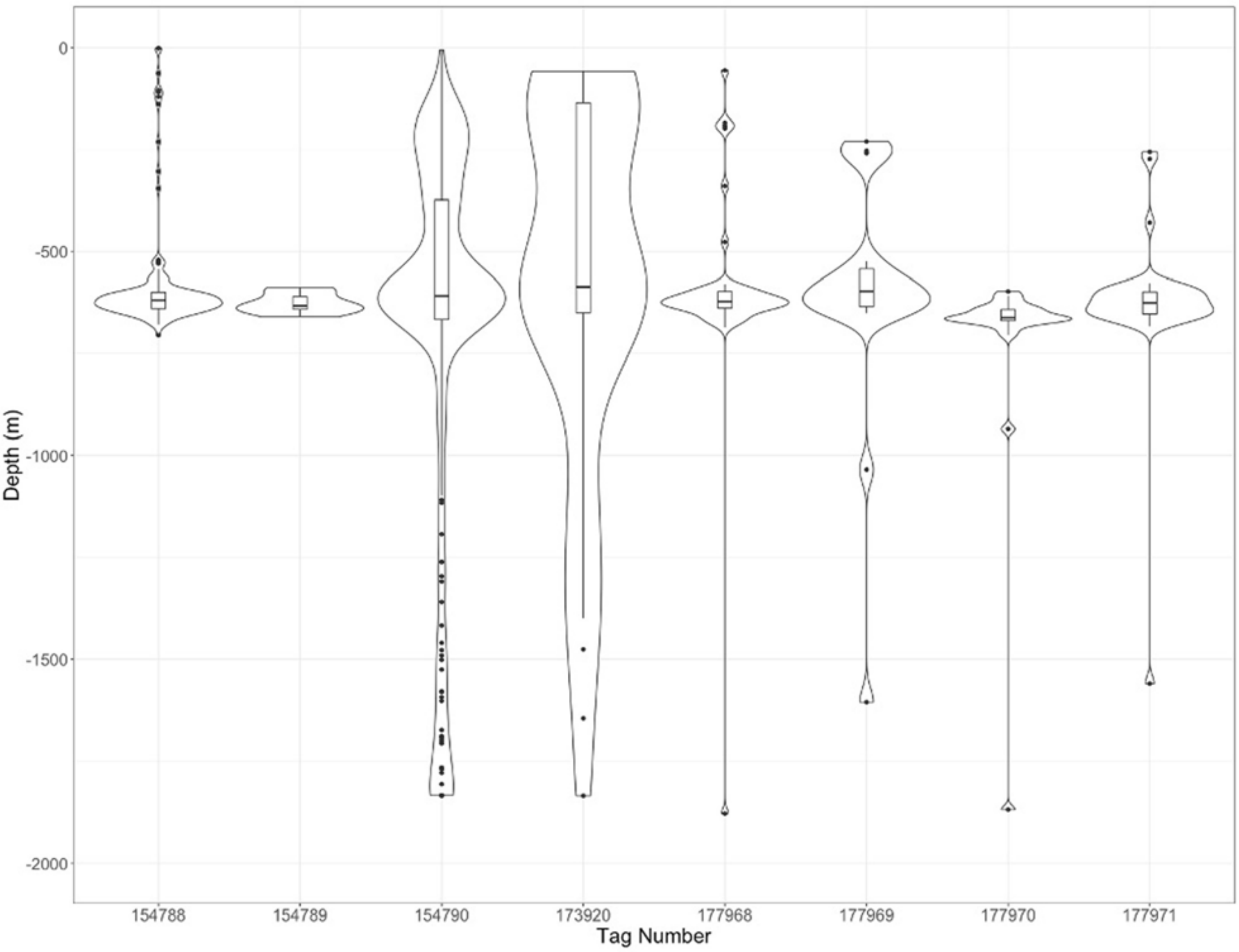

FIGURE 10 | Diving behavior of individual whale sharks from St. Helena. Black line in boxplot represents the mean diving depth while the extent of the boxes represent the interquartile range.

interpreted cautiously until more accurate methods to ascertain female maturity status are developed. Nonetheless, the size ranges and clasper morphology of whale sharks in St. Helena further confirms the mature status of the population (Rowat and Brooks, 2012), although immature and smaller (~5 m) sharks were also occasionally encountered. The large number of individuals that have been encountered only once or a handful of times shows the transient and open nature of this population. The presence of feeding whale sharks may indicate that sharks are seasonally arriving in St. Helena to feed allowing them opportunistic chances to mate due to the presence of mature conspecifics of the opposite sex, or that the feeding is opportunistic, and that mating is the main driver of their presence at the island.

Saint Helena appears to be a globally important site for whale sharks, not only due to the occurrence of adults and possible mating, but due to the number of animals. The maximum likelihood methods estimated a mean ~102 whale sharks at any one time, considerably higher than that estimated at coastal sites in the Indo-Pacific using the same methods (e.g., 16, Southern Leyte, Philippines, Araujo et al., 2017; 35, Mafia Island, Tanzania, Prebble et al., 2018), yet similar to that observed in offshore Qatar (116, Prebble et al., 2018) or in the Gulf of Mexico (136, de la Parra, unpub. data). This is a considerable number of whale sharks, and highlights the importance of St. Helena for the species. The LIR revealed that some whale sharks have an interannual periodicity at the site, following a complete absence of individuals after ~75 days – an interesting feat given the remoteness of the site and the large proportion of single-sighted whale sharks. However, this result follows the seasonal nature of the aggregation with peaks occurring between January and March, ~90 days. This philopatry to the site has also been observed in adult whale sharks at Ningaloo Reef in Australia (Norman and Morgan, 2016) and at Donsol, Philippines (McCoy et al., 2018), and is common amongst juvenile-dominated coastal aggregations (Norman et al., 2017).

Although a high level of transience was overall observed, they do appear to spend some time in St. Helena as estimated through the LIR and acoustic telemetry. Whale sharks spent a mean 19 days in St. Helena before departing the site, similar to that observed in Qatar (18 days, Prebble et al., 2018), the

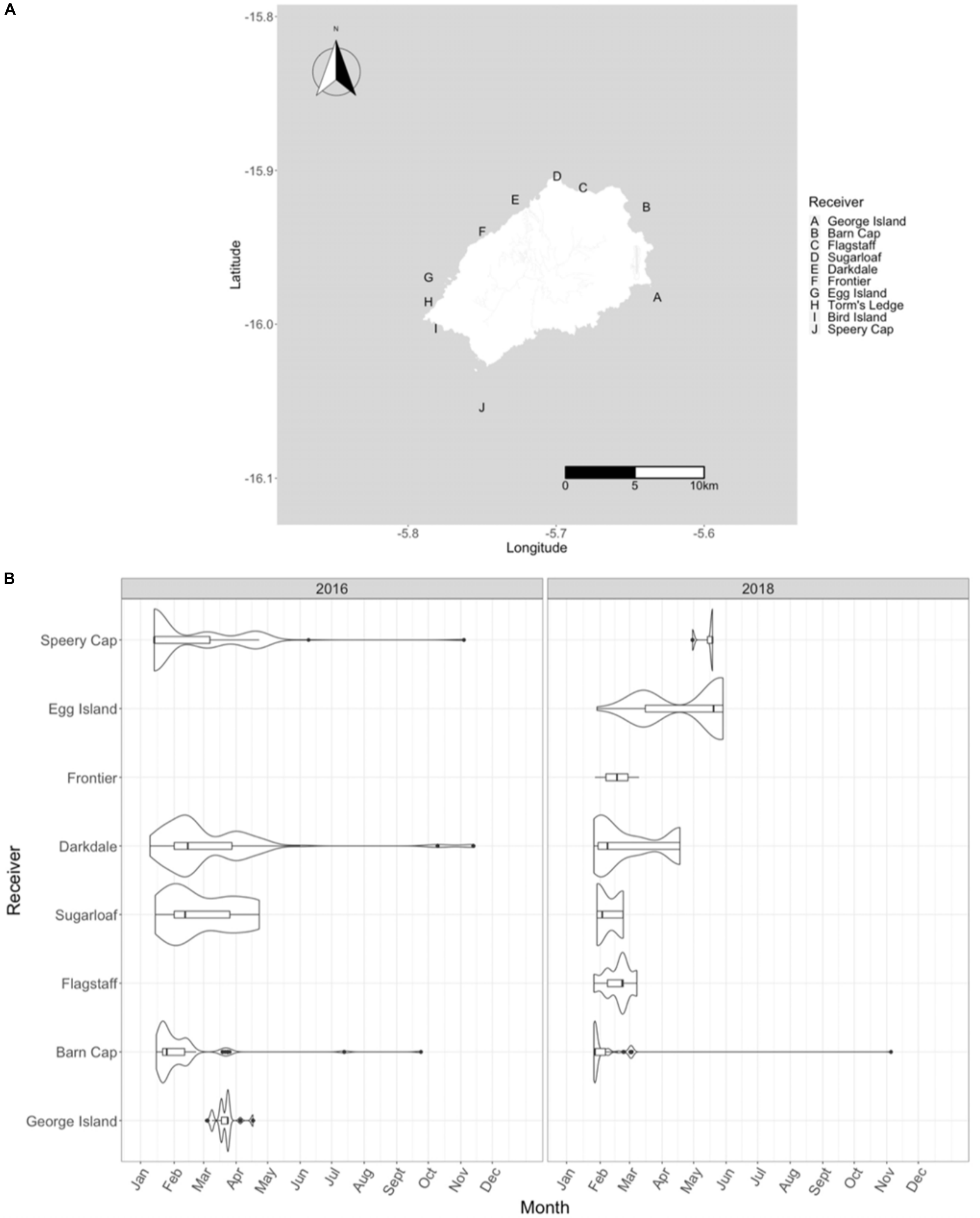

FIGURE 11 | Acoustic telemetry data from tagged whale sharks in St. Helena. Panel **(A)** shows the names and locations of the acoustic receivers. Panel **(B)** is a violin plot of the number of detections per year. The line in each boxplot represents the mean while the extent of the boxes represent the interquartile range. Further information regarding each receiver is provided in **Table 3**.

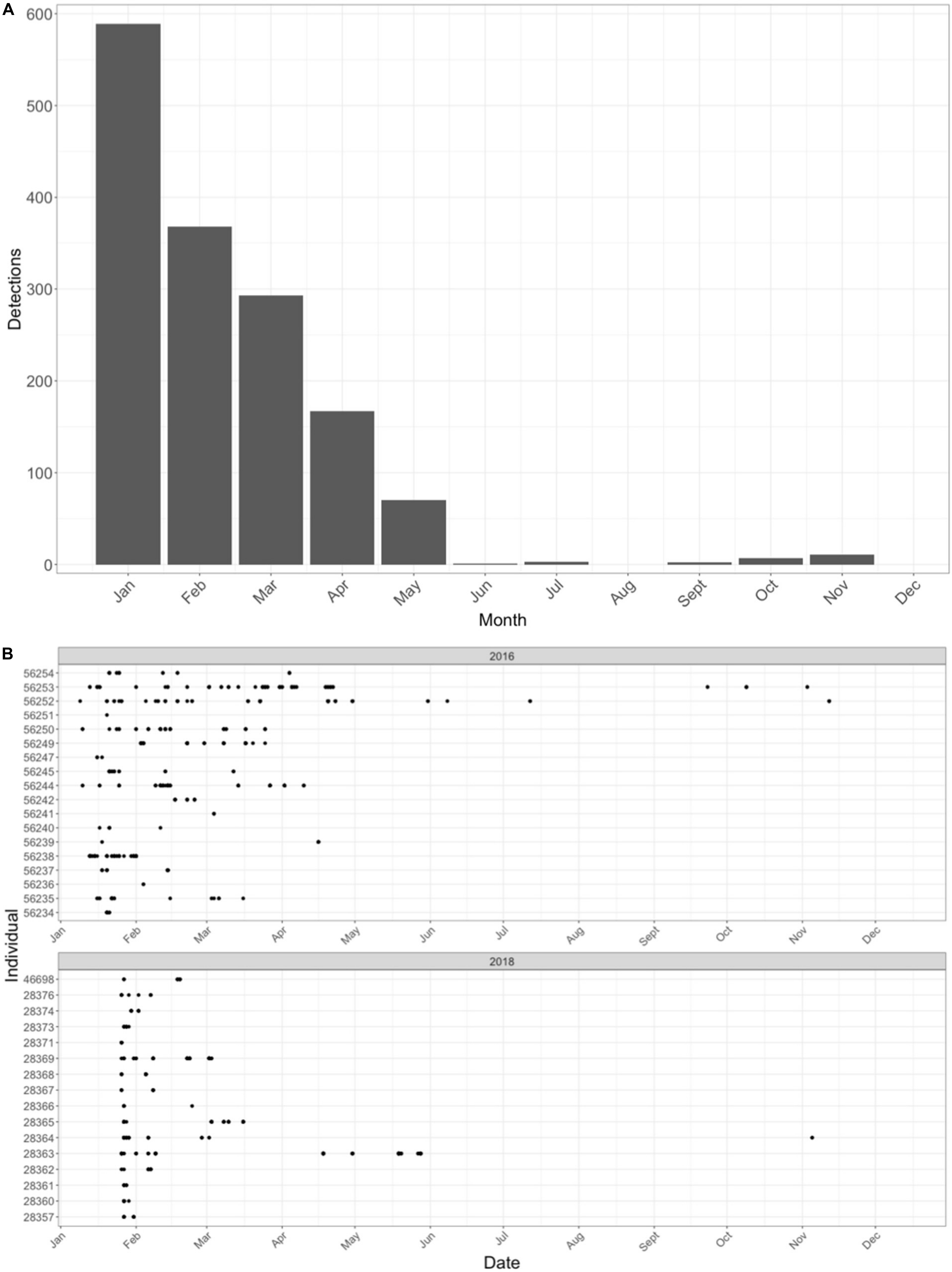

FIGURE 12 | Acoustic telemetry data from tagged whale sharks in St. Helena. Panel **(A)** shows the number of detections per month. Panel **(B)** shows the detections of individual sharks in 2016 and 2018 over the course of the year.

TABLE 3 | Summary of the acoustic receiver data from 2016 to 2018.

2016| 2018								
Receiver	Detections	Individuals	Days	Detections/Individual	Detections/Day	Individuals/Day	$R_{spatial}$	Compared $R_{spatial}$
George Island	122 | N/a	8 | N/a	9 | N/a	15.25 | N/a	13.56 | N/a	0.88 | N/a	0.14 | N/a	
Barn Cap	234 | 358	13 | 16	28 | 16	18 | 22.38	8.36 | 22.38	0.46 | 1	0.35 | 0.61	0.34 | 0.64
Flagstaff	N/a| 54	N/a | 4	N/a | 5	N/a | 13.5	N/a | 10.8	N/a | 0.8	N/a | 0.11	
Sugarloaf	36 | 10	6 | 3	15 | 4	6 | 3.33	2.4 | 2.5	0.4 | 0.75	0.10 | 0.04	0.20 | 0.16
Darkdale	430 | 123	12 | 10	46 | 13	35.83 | 12.3	9.35 | 9.46	0.26 | 0.77	0.42 | 0.23	0.61 | 0.52
Frontier	N/a | 5	N/a | 3	N/a | 3	N/a | 1.67	N/a | 1.67	N/a | 1	N/a | 0.02	
Egg Island	Na | 51	N/a | 4	N/a | 6	N/a | 12.75	N/a | 8.5	N/a | 0.67	N/a | 0.07	
Torm's Ledge	N/a | 0	N/a | 0	N/a | 0	N/a | 0	N/a | 0	N/a | 0	N/a | 0	
Bird Island	N/a | 0	N/a | 0	N/a | 0	N/a | 0	N/a | 0	N/a | 0	N/a | 0	
Speery Cap	81 | 48	6 | 1	12 | 2	13.5 | 48	6.75 | 24	0.5 | 0.5	0.04 | 0.01	0.17 | 0.08
Total	903 | 649	19 | 16	78 | 31	47.52 | 40.56	11.57 | 20.94	0.24 | 0.52		

Data points that contain an N/a indicate receivers that either were not currently deployed or considered lost. $R_{spatial}$ *values are the mean values of all sharks detected.*

Red Sea (12 days, Cochran et al., 2016) or Honduras (12 days, Fox et al., 2013), yet lower than that estimated at coastal sites such as Donsol (50 days, McCoy et al., 2018) or Tanzania (31 days, Prebble et al., 2018). These estimates of residency using photo-ID data are supported by the acoustic telemetry findings, where detection peaks at various stations were 2–3 weeks apart (**Figure 12**). The estimated apparent survival was high given the inferred transience within this population. However, it is similar to that observed in Donsol (0.78 year^{-1}, McCoy et al., 2018), Southern Leyte (0.74 year^{-1}, Araujo et al., 2017), or among non-scarred individuals at Ningaloo Reef (Australia) as estimated through different methods (0.82 year^{-1}, Lester et al., 2020), and contrasting with that observed in Tanzania (0.97 year^{-1}, Prebble et al., 2018) or scarred individuals at Ningaloo Reef (0.88 year^{-1}, Lester et al., 2020). However, this could be attributed to the lack of the model's ability to distinguish mortality from permanent emigration (Holmberg et al., 2008). Some permanent emigration is likely as evidenced by the LIR falling to zero after around 75 days (Whitehead, 2001).

Mating Events and Reproductive Behavior

Reproductive behaviors in elasmobranchs have proven difficult to study due to a lack of direct observations. However, existing knowledge of elasmobranch reproductive behaviors as summarized by Pratt and Carrier (2001); Carrier et al. (2004) can help elucidate the suspected mating and reproductive behavior that was documented for whale sharks in St. Helena. Generally, elasmobranch courtship begins when one individual signals to another that they are reproductively receptive, with either olfaction and/or motor displays being primary sensory cues. During this time males may cease feeding, become aggressive, and display dominance behaviors to others. A female may be approached by either a solitary male or group of males that follow her and focus on or "nose" her cloaca. The male's mouth is then used to make and maintain contact with the female, typically by grasping the pectoral fin. After attaining a hold of the female, copulatory behaviors likely vary by species/female cooperation and can occur anywhere in the water column from the seafloor to the sea surface. In successful copulation, clasper insertion occurs and the female becomes relatively motionless with copulation taking anywhere from a few seconds to hours.

Pre-copulatory, copulatory, and post-copulatory behaviors were all observed at St. Helena. The two eyewitness accounts of mating in the ENRD/SHG sightings database support the notion that the Central Atlantic plays a role in whale shark reproductive ecology and, to our knowledge, are the only documented observations of mating in this species. One of these accounts was provided by the island's chief fisheries officer at the time, and the other by a career professional fisher, and we found both to be credible witnesses. On the 2019 expedition, members of our team witnessed following behavior and solicited contact between the snout of a male and the caudal fin of a female suggesting that this may be pre-copulatory behavior. However, copulatory behaviors such as rotation or insertion of claspers were not observed. Dominance behavior was observed in St. Helena between two male whale sharks with the larger male (est. 9 m) positioning himself above and behind the smaller male (est. 8 m) shark and appearing to actively direct him towards the bottom of the water column, similar in description to two male sand tiger sharks (*Carcharias taurus*) in captivity that circled and tailed one another until the alpha male forced the beta male out of the area prior to copulation (Gordon, 1993). Whether dominance hierarchies and behaviors are common in whale sharks has yet to be proven as they were rarely documented throughout the rest of the expeditions. Furthermore, one female whale shark was encountered in St. Helena that appeared to bear tell-tale pectoral mating scars that were similar to those reported by Macena and Hazin (2016). However, the relatively low frequency of pectoral mating scars on females may not be unusual as whale sharks are filter feeders and their teeth are not as prominent as other species potentially making mating scars less noticeable. Direct mating observations of great white sharks reported by a fur seal observer mentioned that they had positioned belly-to-belly and became motionless (Francis, 1996), a shared observation between both reports of mating in St. Helena. Taken together, these pieces of evidence support the idea that St. Helena is a mating area for whale sharks.

Although observations of mating have remained elusive for whale sharks, there have been some reports of whale shark reproductive behaviors that have been observed elsewhere. Whale shark tour guides operating in Donsol, Philippines have reported reproductive-like behaviors (McCoy et al., 2018) and researchers have observed an 8 m male whale shark unfurling its clasper and banking in this same area (Miranda et al., in revision). Additionally, four male whale sharks were observed at a nearby shoal displaying belly to belly behaviors, however, no female was observed in close proximity, although visibility was poor (Miranda et al., in revision). These behaviors are similar to aerial footage of a male whale shark rolling over on its back in proximity to another smaller, presumably female, individual that was recorded at Ningaloo Reef, Australia (T. Klein, pers. comm.). A 9.5 m male whale shark was observed rolling over and rotating his claspers in proximity to a boat in the Seychelles (D. Rowat, pers. comm in Macena and Hazin, 2016.). Additionally, male whale sharks at the Georgia Aquarium and Okinawa Churaumi Aquarium have also been recorded doing this behavior as well (A. Dove unpub. data; Matsumoto et al., 2019). A male shark near St. Peter and St. Paul's rocks exhibited similar behavior, rolling over in proximity to a fishing vessel and repeating this behavior three times over the course of 10 minutes (Macena and Hazin, 2016). A mature male whale shark Okinawa Churaumi Aquarium has been observed biting the pectoral fins of the females in the exhibit, a display of pre-copulatory behaviors (R. Matsumoto pers. comm.). Large females with distended bellies were also observed at St. Peter and St. Paul's Rocks with markings on their pectoral fins that the authors suggested were caused by mating attempts.

In addition to observed mating and reproductive behavior, there have been a few sightings of neonates in the Central Atlantic. Three male neonate whale sharks (~56 cm total length) were captured in the Central Atlantic in the Gulf of Guinea near the Equator (Wolfson, 1983). All of these individuals were captured by fishing fleets in waters that ranged in depth from 2,600 to 4,700 m. Additionally, two more neonates were observed in close proximity to St. Peter and St. Paul's Rocks (Kukuyev, 1996). One individual, a 59 cm female, was captured in a landing net beyond the continental slope off Sierra Leone while the other was found in the stomach of a blue shark caught in the Central Tropical Atlantic (Kukuyev, 1996). Furthermore, two sharks were observed at 1.8–2 m in size from St. Peter and St. Paul's rocks (Hazin et al., 2008), a size range that is rarely encountered anywhere. These observations further support the idea that the Central Atlantic is a prime area for whale shark reproductive ecology.

Horizontal and Vertical Movements

Whale shark habitat use at St. Helena appeared to incorporate all sides of the island to greater or lesser degree, but the anecdotal perceptions of local residents that whale sharks are concentrated on the leeward side do seem to be somewhat supported by the acoustic array data. Two receiver stations in the north of the island, Barn Cap and the wreck of the Darkdale, recorded 68.3% (1145/1677) of all reception events. Additionally, these receivers led in $R_{spatial}$ calculations confirming their value as important sites for whale sharks in St. Helena. The Speery Cap receiver recorded 15.1% (254/1677) of all detections and may represent another important location for whale sharks around St. Helena, although this location is on the windward side of the island and limited by surface search effort and accessibility. Furthermore, when exploring $R_{spatial}$ values between years there were changes in these values suggesting that habitat and site use may vary between seasons. Seasonality of detections in the array matched those of surface-based assessments, *viz* animals begin to arrive at the island in November and December, with the aggregation peaking in January and petering out by May. This confirms the value of validating visual observations with unsupervised passive acoustic monitoring as suggested by Cagua et al. (2015); Cochran et al. (2019). Residence indices were similar to those from other seasonal sites (Shib Habil: R_{max} = 0.36, R_{min} = 0.05) and in contrast to sites that had cryptic residency of whale sharks year-round (Mafia: R_{min} = 0.24) further supporting the seasonal nature observed from the sighting data (Cagua et al., 2015; Cochran et al., 2019). The maximum residence indexes calculated for tagged sharks shows that they spend roughly 23% of their time, or ~84 days, in St. Helena waters. This value is similar to the permanent emigration of ~75 days predicted by the LIR model and both are representative of the seasonality observed in the sighting data.

Our attempts to learn about connectivity between whale shark populations in St. Helena and other geographic locations were hampered by the remoteness of the island and the extreme deep-diving behavior of the tagged animals in adjacent oceanic waters. Remoteness is a problem because any given tag must remain functional on the animal for at least 1,120 km in order to reach the nearest land (Ascension Island) and more than 2,000 km to reach a continental coast. The extreme deep diving behavior of the tagged animals, however, tended to mean that the tags detached prematurely due to the triggering of the crush depth safety release mechanism, long before animals reached another site. In other words, extreme vertical movements prevented us from properly documenting horizontal movements. The deep-diving capabilities of the whale shark appears to exceed current technological capacity to document their biology; new telemetry tools will need to be devised in order to properly document their movement patterns.

The general horizontal movement patterns of whale sharks tagged in this study revealed a northwest movement away from the island. This may indicate that whale sharks are following the prevailing currents which primarily head west towards Brazil and this could potentially be an energy efficient or thermoregulatory-mandated way to travel away from the island, however, they may also be traveling towards other key features as well. The horizontal movements that were documented in this study included several tracks towards Ascension and sometimes back again, which is perhaps not surprising since it is the closest land and one of the only other oceanic islands in the tropical South

Atlantic. There was no documentation of any archival or real-time tracks that would suggest use of the habitats of Sysoev, Cardno, and Bonaparte seamounts near St. Helena. Nonetheless, not all sharks exhibited this northwest horizontal movement pattern away from the island, and there appeared to be variation in each individual's travel pattern. Among one of the most distant tag detachments detected by ARGOS took place in an offshore oilfield near the Niger Delta of Nigeria, in the Gulf of Guinea, some 2,612 km to the NE of St. Helena, on May 11th of 2015. Unfortunately, this tag washed up on a beach near Lagos shortly afterwards, before it had appreciable time floating at the surface to transmit its data payload. Another tag detached from an individual halfway between St. Helena and the coast of Angola and Namibia on March 3, 2018. Sequeira et al. (2014) analyzed a comprehensive data set from logbooks of tuna purse seine fisheries, covering 31 years from 21°N to 15°S and 34°E to 14°E, which showed significant reports of whale sharks along the western coast of Africa south of the Gulf of Guinea. The highest number of documented sightings was from July-September (1153) with April-June having similar numbers (1070); in contrast January–March only had seven encounters over the same time period. A similar hotspot off the coast of Gabon was found from April-September and is thought to be linked to increases in primary productivity related to nutrient runoff from the Congo river, which peaks in April–June (Capietto et al., 2014; Escalle et al., 2016). Whether this means that whale sharks are leaving St. Helena around April to venture to the feed on the western coast of Africa warrants further investigation.

A different tag transmitted a handful of data packets from a location near Fernando de Noronha Island, Brazil, on August 3rd, 2018, more than 3,300 km to the west-northwest of St. Helena, but not enough data were received to generate a track for that tag. In a different study, one female whale shark that was tagged in the Gulf of Mexico traveled 7,213 km over 150 days through the Caribbean Sea, across the equator, and into the South Atlantic Ocean before her tag came off in January (Hueter et al., 2013). This location was in close proximity to where our tag transmitted data, potentially connecting the Gulf of Mexico and the South Atlantic. These results were both tantalizing and frustrating, but they hint that whale sharks may be capable of basin-wide movements across the South Atlantic. This would be consistent with large scale movements by several tagged individuals (Eckert et al., 2002; Hueter et al., 2013).

Two distinct patterns of vertical movement were documented among the animals tagged in this study. Immediately following tagging, and for the duration of their time spent in the waters surrounding the island, all tagged animals dove almost every day to a maximum depth of around 600 m between the hours of 06:00 and 19:00. After leaving the island, the diving pattern abruptly changed from daily 600 m dives, to a much more sporadic diving pattern, but many of these dives attained far greater maximum depths in the bathypelagic zone that were deep enough to trigger tag release/destruction. Extreme diving behavior of the sort has been previously documented in whale sharks and these dives have caused premature release of tags just as reported here (Tyminski et al., 2015). However, many coastal aggregation sites are not adjacent to depths that could result in tag damage. Tyminski et al. (2015) documented a dive to 1,928 m in the Gulf of Mexico, which was determined to be on the bottom at that location, and this observation made the whale shark the deepest diving fish known to science. The purpose of whale sharks' dives into the bathypelagic zone is not known, however, the dive profiles tend to be V-shaped rather than U-shaped (Tyminski et al., 2015), which suggests that they are not primarily feeding dives. Gleiss et al. (2011) proposed, based on the geometry of the dive profile, that it may provide a mechanism for whale sharks to travel long horizontal distances efficiently (see also Lawson et al., 2019). In considering this possibility, it helps to imagine the behavior not as a dive *per se*, but rather a glide into the depths at a very shallow angle of descent. Whatever the reason for these dives is, it must be compelling because it subjects the animal to an environmental temperature change from 25°C to around 3°C, and a pressure change of nearly 200 atmospheres, both of which have profound effects on enzyme kinetics, toxicity of certain biochemical species, and cell membrane permeability (Yancey et al., 2002). The net effect of this behavior was that most realized tag missions were less than 1 month in duration, regardless of the programmed mission length. Deep diving behavior of whale sharks clearly warrants dedicated investigation.

CONCLUSION

Waters adjacent to St. Helena are home to a reliable seasonal population of adult male and female whale sharks and there have been multiple documented instances of sexual behaviors, which leads us to conclude that it is most likely a mating ground for this species, and the only one yet documented. Since the whale shark is an endangered species on the IUCN Red List (Pierce and Norman, 2016), this makes St. Helena waters a particularly important and possibly critical habitat for this species. Future studies around St. Helena should further characterize the extremely regular diving behavior immediately surrounding the island and the extraordinarily deep-diving behavior that takes place over abyssal depths farther from shore, as well as confirming reproduction through either direct observation of reproductive behaviors, or indirect measurements such as blood hormone analysis or underwater ultrasound. Regardless of what future research reveals, it is clear that St. Helena is important habitat for whale sharks and deserving of concerted research efforts.

DATA AVAILABILITY STATEMENT

The raw data supporting the conclusions of this article will be made available by the authors, without undue reservation.

ETHICS STATEMENT

The animal study was reviewed and approved by the Georgia Institute of Technology and was carried out in accordance with the St. Helena Government environmental ordinance under permit number 2019-SRE-1.

AUTHOR CONTRIBUTIONS

AD and EC conceived the study. AD designed the survey. AD, EC, CP, DW, RP, SP, AB, LH, BT, KA, and RH conducted the field work. CP, AD, DW, GA, and RP analyzed the data. CP and AD prepared the manuscript with critical input from SP and GA. All authors contributed to the article and approved the submitted version.

FUNDING

This research was made possible by funding from the Georgia Aquarium, the St. Helena Government, the Saint Helena National Trust, and grant DPLUS039 from the Darwin Foundation.

ACKNOWLEDGMENTS

We appreciate the citizens of St. Helena for diligently reporting bone shark (whale shark) sightings to ENRD/SHG and thank the past and present staff of ENRD for curating those data. Thanks to Her Excellency Lisa Honan, Governor of St. Helena for her support and hospitality during three of our expeditions. We also appreciate the tour operators who provided boat support: Jonny Herne, Keith Yon, Craig Yon, Donnie O'Bey, Karl Thrower, Alex Benjamin, and Anthony Thomas. Special thanks to Graham Sim for answering so many questions about his eyewitness account of whale shark mating behavior, and Dr. Judith Brown for helping in the early stages of conceptualizing the expeditions. AD appreciates the support and participation of the Saint Helena National Trust Marine Team, Katie Hindle, Morgan Riley, Lourens Malan, Ross Leo, Alexandra Watts, and Georgia Aquarium's zoological operations, dive operations and research staff in conducting four difficult expeditions to such a remote location, and the patience of his wife and two children in tolerating his prolonged absences as a result.

SUPPLEMENTARY MATERIAL

The Supplementary Material for this article can be found online at: https://www.frontiersin.org/articles/10.3389/fmars.2020.576343/full#supplementary-material

REFERENCES

Acuña-Marrero, D., Jiménez, J., Smith, F., Doherty, P. F. Jr., Hearn, A., Green, J. R., et al. (2014). Whale shark (*Rhincodon typus*) seasonal presence, residence time and habitat use at Darwin Island, galapagos marine reserve. *PLoS One* 9:e115946. doi: 10.1371/journal.pone.0115946

Araujo, G., Snow, S., So, C. L., Labaja, J., Murray, R., Colucci, A., et al. (2017). Population structure, residency patterns and movements of whale sharks in Southern Leyte, Philippines: results from dedicated photo-ID and citizen science. *Aquat. Conserv. Mar. Freshw. Ecosyst.* 27, 237–252. doi: 10.1002/aqc.2636

Arzoumanian, Z., Holmberg, J., and Norman, B. (2005). An astronomical pattern-matching algorithm for computer-aided identification of whale sharks *Rhincodon typus*. *J. Appl. Ecol.* 42, 999–1011. doi: 10.1111/j.1365-2664.2005.01117.x

Bormpoudakis, D., Fish, R., Leo, D., and Smith, N. (2019). *South Atlantic Natural Capital Project; Cultural ecosystem services in St Helena*. Peterborough: JNCC.

Brown, J. (2013). *Mapping St Helena's Marine Biodiversity to Create A Marine Management Plan. 1st Annual Report*. Available at https://urlzs.com/fFXV (accessed November 14, 2019).

Buckland, S. T., and Garthwaite, P. H. (1991). Quantifying precision of mark-recapture estimates using the bootstrap and related methods. *Biometrics* 47, 255–268. doi: 10.2307/2532510

Burnham, K. P., and Anderson, D. (2003). *Model Selection and MultiModel Inference*. New York, NY: Springer.

Cagua, E. F., Berumen, M. L., and Tyler, E. (2013). Topography and biological noise determine acoustic detectability on coral reefs. *Coral Reefs* 32, 1123–1134. doi: 10.1007/s00338-013-1069-2

Cagua, E. F., Cochran, J. E., Rohner, C. A., Prebble, C. E., Sinclair-Taylor, T. H., Pierce, S. J., et al. (2015). Acoustic telemetry reveals cryptic residency of whale sharks. *Biol. Lett.* 11:20150092. doi: 10.1098/rsbl.2015.0092

Capietto, A., Escalle, L., Chavance, P., Dubroca, L., de Molina, A. D., Murua, H., et al. (2014). Mortality of marine megafauna induced by fisheries: insights from the whale shark, the world's largest fish. *Biol. Conserv.* 174, 147–151. doi: 10.1016/j.biocon.2014.03.024

Carrier, J. C., Pratt, H., and Castro, J. I. (2004). "Reproductive biology of elasmobranchs," in *Biology of Sharks and Their Relatives*, eds J. C. Carrier, J. A. Musick, and M. R. Heithaus (Milton Park: Taylor & Francis), 269–286. doi: 10.1201/9780203491317.ch10

Cochran, J., Braun, C., Cagua, E., Campbell, M. Jr., Hardenstine, R., Kattan, A., et al. (2019). Multi-method assessment of whale shark (*Rhincodon typus*) residency, distribution, and dispersal behavior at an aggregation site in the Red Sea. *PLoS One* 14:e0222285. doi: 10.1371/journal.pone.0222285

Cochran, J., Hardenstine, R., Braun, C., Skomal, G., Thorrold, S., Xu, K., et al. (2016). Population structure of a whale shark *Rhincodon typus* aggregation in the Red Sea. *J. Fish Biol.* 89, 1570–1582.

de la Parra Venegas, R., Hueter, R., Cano, J. G., Tyminski, J., Remolina, J. G., Maslanka, M., et al. (2011). An unprecedented aggregation of whale sharks, *Rhincodon typus*, in Mexican coastal waters of the Caribbean Sea. *PLoS One* 6:e18994. doi: 10.1371/journal.pone.0018994

Eckert, S. A., Dolar, L. L., Kooyman, G. L., Perrin, W., and Rahman, R. A. (2002). Movements of whale sharks (*Rhincodon typus*) in South-east Asian waters as determined by satellite telemetry. *J. Zool.* 257, 111–115. doi: 10.1017/s0952836902000705

Escalle, L., Gaertner, D., Chavance, P., De Molina, A. D., Ariz, J., and Merigot, B. (2016). Consequences of fishing moratoria on catch and bycatch: the case of tropical tuna purse-seiners and whale and whale shark associated sets. *Biodivers. Conserv.* 25, 1637–1659. doi: 10.1007/s10531-016-1146-2

Fox, S., Foisy, I., De La Parra Venegas, R., Galván Pastoriza, B., Graham, R., Hoffmayer, E., et al. (2013). Population structure and residency of whale sharks *Rhincodon typus* at Utila, Bay Islands, Honduras. *J. Fish Biol.* 83, 574–587. doi: 10.1111/jfb.12195

Francis, M. P. (1996). Observations on a pregnant white shark with a review of reproductive biology. *Great White Sharks* 157:172.

Gleiss, A. C., Norman, B., and Wilson, R. P. (2011). Moved by that sinking feeling: variable diving geometry underlies movement strategies in whale sharks. *Funct. Ecol.* 25, 595–607. doi: 10.1111/j.1365-2435.2010.01801.x

Gordon, I. (1993). Pre-copulatory behaviour of captive sandtiger sharks, *Carcharias taurus*. *Environ. Biol. Fishes* 38, 159–164. doi: 10.1007/978-94-017-3450-9_14

Gray, A., Wilkins, V., Pryce, D., Fowler, L., Key, R. S., Mendel, H., et al. (2019). The status of the invertebrate fauna on the South Atlantic island of St Helena: problems, analysis, and recommendations. *Biodivers. Conserv.* 28, 275–296. doi: 10.1007/s10531-018-1653-4

Hammond, P. S., Mizroch, S. A., and Donovan, G. P. (1990). *Individual Recognition of Cetaceans: Use of Photo-Identification and Other Techniques to Estimate Population Parameters: Incorporating the Proceedings of The Symposium and Workshop on Individual Recognition and the Estimation of Cetacean Population Parameters*. Cambridge, MA: International Whaling Commission.

Hazin, F., Vaske Júnior, T., Oliveira, P., Macena, B., and Carvalho, F. (2008). Occurrences of whale shark (*Rhincodon typus* Smith, 1828) in the Saint Peter and Saint Paul archipelago, Brazil. *Braz. J. Biol.* 68, 385–389. doi: 10.1590/s1519-69842008000200021

Hearn, A. R., Green, J. R., Espinoza, E., Peñaherrera, C., Acuña, D., and Klimley, A. P. (2013). Simple criteria to determine detachment point of towed satellite tags provide first evidence of return migrations of whale sharks (Rhincodon typus) at the Galapagos Islands, Ecuador. *Anim. Biotelem.* 1:11. doi: 10.1186/2050-3385-1-11

Holmberg, J., Norman, B., and Arzoumanian, Z. (2008). Robust, comparable population metrics through collaborative photo-monitoring of whale sharks *Rhincodon typus*. *Ecol. Appl.* 18, 222–233. doi: 10.1890/07-0315.1

Hueter, R. E., Tyminski, J. P., and de la Parra, R. (2013). Horizontal movements, migration patterns, and population structure of whale sharks in the Gulf of Mexico and northwestern Caribbean Sea. *PLoS One* 8:e71883. doi: 10.1371/journal.pone.0071883

Kahle, D., and Wickham, H. (2019). ggmap: spatial visualization with ggplot2. *R J.* 5, 144–161. doi: 10.32614/rj-2013-014

Kukuyev, E. (1996). The new finds in recently born individuals of the whale shark *Rhiniodon typus* (*Rhiniodontidae*) in the Atlantic Ocean. *J. Ichthyol.* 36:203.

Lawson, C. L., Halsey, L. G., Hays, G. C., Dudgeon, C. L., Payne, N. L., Bennett, M. B., et al. (2019). Powering Ocean giants: the energetics of shark and ray Megafauna. *Trends Ecol. Evol.* 34, 1009–1021. doi: 10.1016/j.tree.2019.07.001

Lester, E., Meekan, M. G., Barnes, P., Raudino, H., Rob, D., Waples, K., et al. (2020). Multi-year patterns in scarring, survival and residency of whale sharks in Ningaloo Marine Park, Western Australia. *Mar. Ecol. Prog. Ser.* 634, 115–125. doi: 10.3354/meps13173

Macena, B. C., and Hazin, F. H. (2016). Whale shark (*Rhincodon typus*) seasonal occurrence, abundance and demographic structure in the mid-equatorial Atlantic Ocean. *PLoS One* 11:e0164440. doi: 10.1371/journal.pone.0164440

Marshall, A. D., Dudgeon, C., and Bennett, M. (2011). Size and structure of a photographically identified population of manta rays Manta alfredi in southern Mozambique. *Mar. Biol.* 158, 1111–1124. doi: 10.1007/s00227-011-1634-6

Matsumoto, R., Matsumoto, Y., Ueda, K., Suzuki, M., Asahina, K., and Sato, K. (2019). Sexual maturation in a male whale shark (*Rhincodon typus*) based on observations made over 20 years of captivity. *Fish. Bull.* 117, 78–86. doi: 10.7755/fb.117.1-2.9

McCoy, E., Burce, R., David, D., Aca, E. Q., Hardy, J., Labaja, J., et al. (2018). Long-term photo-identification reveals the population dynamics and strong site fidelity of adult whale sharks to the coastal waters of Donsol, Philippines. *Front. Mar. Sci.* 5:271. doi: 10.3389/fmars.2018.00271

Motta, P. J., Maslanka, M., Hueter, R. E., Davis, R. L., De la Parra, R., Mulvany, S. L., et al. (2010). Feeding anatomy, filter-feeding rate, and diet of whale sharks Rhincodon typus during surface ram filter feeding off the Yucatan Peninsula, Mexico. *Zoology* 113, 199–212.

Norman, B. M., Holmberg, J. A., Arzoumanian, Z., Reynolds, S. D., Wilson, R. P., Rob, D., et al. (2017). Undersea constellations: the global biology of an endangered marine megavertebrate further informed through citizen science. *BioScience* 67, 1029–1043. doi: 10.1093/biosci/bix127

Norman, B. M., and Morgan, D. L. (2016). The return of "Stumpy" the whale shark: two decades and counting. *Front. Ecol. Environ.* 14, 449–450. doi: 10.1002/fee.1418

Norman, B. M., and Stevens, J. D. (2007). Size and maturity status of the whale shark (*Rhincodon typus*) at Ningaloo Reef in Western Australia. *Fish. Res.* 84, 81–86. doi: 10.1016/j.fishres.2006.11.015

Perry, C. T., Figueiredo, J., Vaudo, J. J., Hancock, J., Rees, R., and Shivji, M. (2018). Comparing length-measurement methods and estimating growth parameters of free-swimming whale sharks (*Rhincodon typus*) near the South Ari Atoll, Maldives. *Mar. Freshw. Res.* 69, 1487–1495. doi: 10.1071/mf17393

Pierce, S. J., and Norman, B. (2016). *Rhincodon typus. The IUCN Red List of Threatened Species 2016: e.T19488A2365291*. Available online at: http://dx.doi.org/10.2305/IUCN.UK.2016-1.RLTS.T19488A2365291.en (accessed August 08, 2019).

Pratt, H. L., and Carrier, J. C. (2001). A review of elasmobranch reproductive behavior with a case study on the nurse shark, *Ginglymostoma cirratum*. *Environ. Biol. Fishes* 60, 157–188. doi: 10.1007/978-94-017-3245-1_11

Prebble, C. E., Rohner, C. A., Pierce, S. J., Robinson, D. P., Jaidah, M. Y., Bach, S. S., et al. (2018). Limited latitudinal ranging of juvenile whale sharks in the Western Indian Ocean suggests the existence of regional management units. *Mar. Ecol. Prog. Ser.* 601, 167–183. doi: 10.3354/meps12667

Ramírez-Macías, D., Queiroz, N., Pierce, S. J., Humphries, N. E., Sims, D. W., and Brunnschweiler, J. M. (2017). Oceanic adults, coastal juveniles: tracking the habitat use of whale sharks off the Pacific coast of Mexico. *PeerJ* 5:e3271. doi: 10.7717/peerj.3271

Roberts, C. M., McClean, C. J., Veron, J. E., Hawkins, J. P., Allen, G. R., McAllister, D. E., et al. (2002). Marine biodiversity hotspots and conservation priorities for tropical reefs. *Science* 295, 1280–1284. doi: 10.1126/science.1067728

Rohner, C., Richardson, A., Marshall, A., Weeks, S., and Pierce, S. (2011). How large is the world's largest fish? Measuring whale sharks *Rhincodon typus* with laser photogrammetry. *J. Fish Biol.* 78, 378–385. doi: 10.1111/j.1095-8649.2010.02861.x

Rowat, D., and Brooks, K. (2012). A review of the biology, fisheries and conservation of the whale shark *Rhincodon typus*. *J. Fish Biol.* 80, 1019–1056. doi: 10.1111/j.1095-8649.2012.03252.x

Schofield, G., Katselidis, K. A., Dimopoulos, P., and Pantis, J. D. (2008). Investigating the viability of photo-identification as an objective tool to study endangered sea turtle populations. *J. Exp. Mar. Biol. Ecol.* 360, 103–108. doi: 10.1016/j.jembe.2008.04.005

Sequeira, A. M., Mellin, C., Fordham, D. A., Meekan, M. G., and Bradshaw, C. J. (2014). Predicting current and future global distributions of whale sharks. *Glob. Change Biol.* 20, 778–789. doi: 10.1111/gcb.12343

Tyminski, J. P., de la Parra-Venegas, R., Cano, J. G., and Hueter, R. E. (2015). Vertical movements and patterns in diving behavior of whale sharks as revealed by pop-up satellite tags in the eastern Gulf of Mexico. *PLoS One* 10:e0142156. doi: 10.1371/journal.pone.0142156

Vignaud, T. M., Maynard, J. A., Leblois, R., Meekan, M. G., Vázquez-Juárez, R., Ramírez-Macías, D., et al. (2014). Genetic structure of populations of whale sharks among ocean basins and evidence for their historic rise and recent decline. *Mol. Ecol.* 23, 2590–2601. doi: 10.1111/mec.12754

Whitehead, H. (2001). Analysis of animal movement using opportunistic individual identifications: application to sperm whales. *Ecology* 82, 1417–1432. doi: 10.1890/0012-9658(2001)082[1417:aoamuo]2.0.co;2

Whitehead, H. (2007). Selection of models of lagged identification rates and lagged association rates using AIC and QAIC. *Commun. Stat. Simul. Comput.* 36, 1233–1246. doi: 10.1080/03610910701569531

Whitehead, H. (2009). SOCPROG programs: analysing animal social structures. *Behav. Ecol. Sociobiol.* 63, 765–778. doi: 10.1007/s00265-008-0697-y

Wickham, H. (2016). *ggplot2: Elegant Graphics for Data Analysis*. New York, NY: Springer-Verlag.

Wolfson, F. (1983). Records of seven juveniles of the whale shark, *Rhiniodon typus*. *J. Fish Biol.* 22, 647–655. doi: 10.1111/j.1095-8649.1983.tb04224.x

Yancey, P. H., Blake, W. R., and Conley, J. (2002). Unusual organic osmolytes in deep-sea animals: adaptations to hydrostatic pressure and other perturbants. *Comp. Biochem. Physiol. A Mol. Integr. Physiol.* 133, 667–676. doi: 10.1016/s1095-6433(02)00182-4

Conflict of Interest: The authors declare that the research was conducted in the absence of any commercial or financial relationships that could be construed as a potential conflict of interest.

frontiers in Marine Science

BRIEF RESEARCH REPORT
published: 12 November 2020
doi: 10.3389/fmars.2020.581775

Inferring Life History Characteristics of the Oceanic Whitetip Shark *Carcharhinus longimanus* From Vertebral Bomb Radiocarbon

Michelle S. Passerotti[1]*, Allen H. Andrews[2] and Lisa J. Natanson[3]

[1] Department of Biological Sciences, University of South Carolina, Columbia, SC, United States, [2] Department of Oceanography, University of Hawaii, Honolulu, HI, United States, [3] Apex Predators Program, National Marine Fisheries Service, Narragansett, RI, United States

Oceanic whitetip sharks *Carcharhinus longimanus* are a cosmopolitan epipelagic species that was once prolific throughout the tropics and subtropics but was recently listed as Critically Endangered by the International Union for the Conservation of Nature and as Threatened under the United States Endangered Species Act. Although historically conspicuous in oceanic fisheries catches, relatively little is known about their habitat use, movement, and life history during migration. Given the paucity of data on migratory patterns and lack of age estimate validation available for this species, we evaluated vertebral growth bands for bomb radiocarbon (^{14}C) patterns to derive additional information on these metrics. Individual growth bands (n = 62) were milled from vertebrae of eight individuals caught in the northwestern Atlantic Ocean. Age estimates based on vertebral growth bands ranged 1–13 years, with capture dates spanning 1978–2004. Plots of vertebral $\Delta^{14}C$ relative to regional coral, shark, and fish otolith reference curves suggest age estimates based on presumed annual growth bands were accurate, although specimens were not old enough to capture the most informative portion of the bomb radiocarbon reference period. The magnitude of $\Delta^{14}C$ varied among individuals, and individual chronologies demonstrated semi-cyclic patterns of $\Delta^{14}C$ depletion and subsequent enrichment, which may be indicative of changes to diet as a function of annual migratory patterns and is supported by recently published telemetry, diet, and stable isotope studies. Although these data are preliminary in nature, they provide some evidence that $\Delta^{14}C$ patterns in vertebrae can serve as a multi-purpose tool for life history studies of oceanic sharks.

Keywords: carbon-14, age validation, migration, diet, vertebrae, family Carcharhinidae

Edited by:
David Wells,
Texas AM University at Galveston,
United States

Reviewed by:
Paul Brickle,
South Atlantic Environmental
Research Institute, Falkland Islands
Phillip Sanchez,
Texas A&M University at Galveston,
United States

****Correspondence:***
Michelle S Passerotti
mpasserotti@gmail.com

Specialty section:
This article was submitted to
Marine Megafauna,
a section of the journal
Frontiers in Marine Science

Received: *09 July 2020*
Accepted: *21 October 2020*
Published: *12 November 2020*

Citation:
Passerotti MS, Andrews AH and
Natanson LJ (2020) Inferring Life
History Characteristics of the Oceanic
Whitetip Shark Carcharhinus
longimanus From Vertebral Bomb
Radiocarbon.
Front. Mar. Sci. 7:581775.
doi: 10.3389/fmars.2020.581775

INTRODUCTION

Oceanic whitetip sharks, *Carcharhinus longimanus*, were once among the most prevalent sharks in tropical and temperate surface waters of the world's equatorial oceans (Compagno, 1984), but are now among the most threatened. Distinctive in appearance with characteristic large, white-tipped dorsal and pectoral fins, this epipelagic, cosmopolitan species has comprised a disproportionate share of fisheries catches over the past 50 years which has resulted in severe depletion of the global population (see Young et al., 2017;

Rigby et al., 2019; Young and Carlson, 2020 for reviews). Recently enacted conservation measures include the listing of *C. longimanus* by the International Union for the Conservation of Nature (IUCN) as Critically Endangered worldwide (Rigby et al., 2019), by the US Endangered Species Act as Threatened in US waters (83 FR 4153; January 30, 2018), and by the Convention on International Trade in Endangered Species (CITES) as prohibited from international trade in accordance with Appendix II classification (CITES, 2013), as well as designation of catch as prohibited across many regional fishery management organizations (Young and Carlson, 2020).

Life history information on *C. longimanus* is lacking (Rigby et al., 2019, but see Young and Carlson, 2020 for a thorough review) and data are difficult to obtain given the oceanic nature of the species and recent declines in population numbers. Studies published to date suggest *C. longimanus* exhibit slow to moderate, regionally variable growth rates, and intermediate longevity with maximum ages from direct growth band counts of up to 19 years (Seki et al., 1998; Lessa et al., 1999; Joung et al., 2016; D'Alberto et al., 2017). Annual growth band deposition has been verified with marginal increment analysis (Seki et al., 1998; Lessa et al., 1999; Joung et al., 2016), but aging methods and longevity have not been fully validated. Individuals in the northern Atlantic Ocean are known to undertake philopatric migrations between shallow reef habitats and oceanic waters (Howey-Jordan et al., 2013) as well as to exhibit vertical migrations to depths up to ∼1000 m potentially associated with foraging behavior (Howey-Jordan et al., 2013; Howey et al., 2016). Similar movements and site fidelity have been documented off northeast Brazil (Tolotti et al., 2015). Overall movement patterns elsewhere are less known. As a whole, published information on *C. longimanus* provides an incomplete picture of longevity, age validation, and migration patterns, all of which affect management ability and conservation potential on both regional and global scales.

Owing to the need for comprehensive life history data on *C. longimanus*, we set out to evaluate radiocarbon signatures from vertebral growth bands in hopes of validating annual growth band deposition and associated aging methods, as well as to evaluate ontogenetic habitat use patterns via examination of dietary carbon signatures over individual lifespans. Bomb radiocarbon dating has proven to be one of the only true methods of age validation suitable for marine fishes (Campana, 2001; Cailliet et al., 2006) owing to the permanent record of ^{14}C from the environment recorded in calcified tissues. In elasmobranch species, ^{14}C is dietary in origin (Fry, 1988) and can also enable identification of broad habitat shifts via related dietary changes and their effect on ^{14}C (e.g., Kerr et al., 2006; Kneebone et al., 2008; Passerotti et al., 2014). Herein, we present preliminary results of bomb radiocarbon analyses of vertebral growth bands for archival specimens of *C. longimanus* from the western North Atlantic Ocean (WNA).

MATERIALS AND METHODS

Vertebral specimens were sourced from the archival collection of the NMFS Apex Predators Program (Narragansett, RI, United States), and were collected from latitudes 38°N to 18°N in the WNA between 1978 and 2004 (**Figure 1**). At the time of collection, vertebrae were dissected from under the branchial chamber and stored frozen until analysis. To prepare for sectioning, frozen vertebrae were thawed and excess tissue removed. A total of three centra from each shark were sectioned: one for thin sectioning (age reading) and two additional for thick sectioning (radiocarbon analyses). For age reading, one centrum from each specimen was sectioned laterally through the focus to a thickness of 0.5mm using gross sectioning (Natanson et al., 2006), and sections were subsequently stored in capsules in 70% ethanol. Thin sections were imaged while wet using a Nikon DSR121 digital camera (Nikon Corp., Tokyo, Japan) attached to a Nikon SMZ1500 stereo microscope (Nikon Instruments, Inc., Melville, NY, United States). Magnification varied with the size of the section, and a scale was included in each photo. Band pairs (consisting of one opaque and one translucent band; Casey et al., 1985) were counted and marked independently by each author in individual image layers using image editing software (Adobe Photoshop Elements 6, Adobe, Inc., San Jose, CA, United States) following Natanson et al. (2018b). Counts were compared for each sample, and those not in agreement had band assignments compared via image layers to determine consensus on band placement. Additional independent counts were then carried out, and consensus age reached when two of three age reader counts were in agreement.

For radiocarbon analysis, two additional centra from each shark were sectioned through the core to a thickness of ∼ 1.5 mm each using twin diamond-tipped blades separated by spacers. Sections were pressed between glass slides and air dried overnight to prevent warping and facilitate proper extraction with a micromill. Dried sections were mounted onto double-wide glass slides using two layers of warmed Parafilm, into which the sections were firmly pressed until cool. Prior to micromilling the growth bands visualized from thin sections were used to guide the marking of corresponding bands on all growth axes of both thick sections. Milling was done using a New Wave Research (Elemental Scientific Lasers, LLC, Bozeman, MT, United States) micromilling machine with a 0.5 mm diameter burr (Brasseler, Savannah, GA, United States). For each sample, serial drill holes were made targeting identical years of growth along each of the four growth axes of the corpus calcareum (**Figure 2**). Depth of milling was just short of passing completely through the section to avoid Parafilm. Resulting powdered material was collected and pooled from other growth axes to comprise a single sample sufficient for ^{14}C analyses. In an effort to evaluate precision of radiocarbon measurements across vertebral centra within the same shark, replicate material was taken from the second thick-section mirroring the growth sampled from the first. Because *C. longimanus* vertebrae are small and width of growth band pairs decreases with age (and thus available sample material), in many cases it was necessary to pool multiple years of growth per sample. Year(s) of formation (YOF) for each sample were assigned on the basis of estimated shark age and collection year according to the thin section used for age estimation. For samples comprising multiple years of growth, year of formation was plotted as the midpoint of the growth records sampled, including a fractional

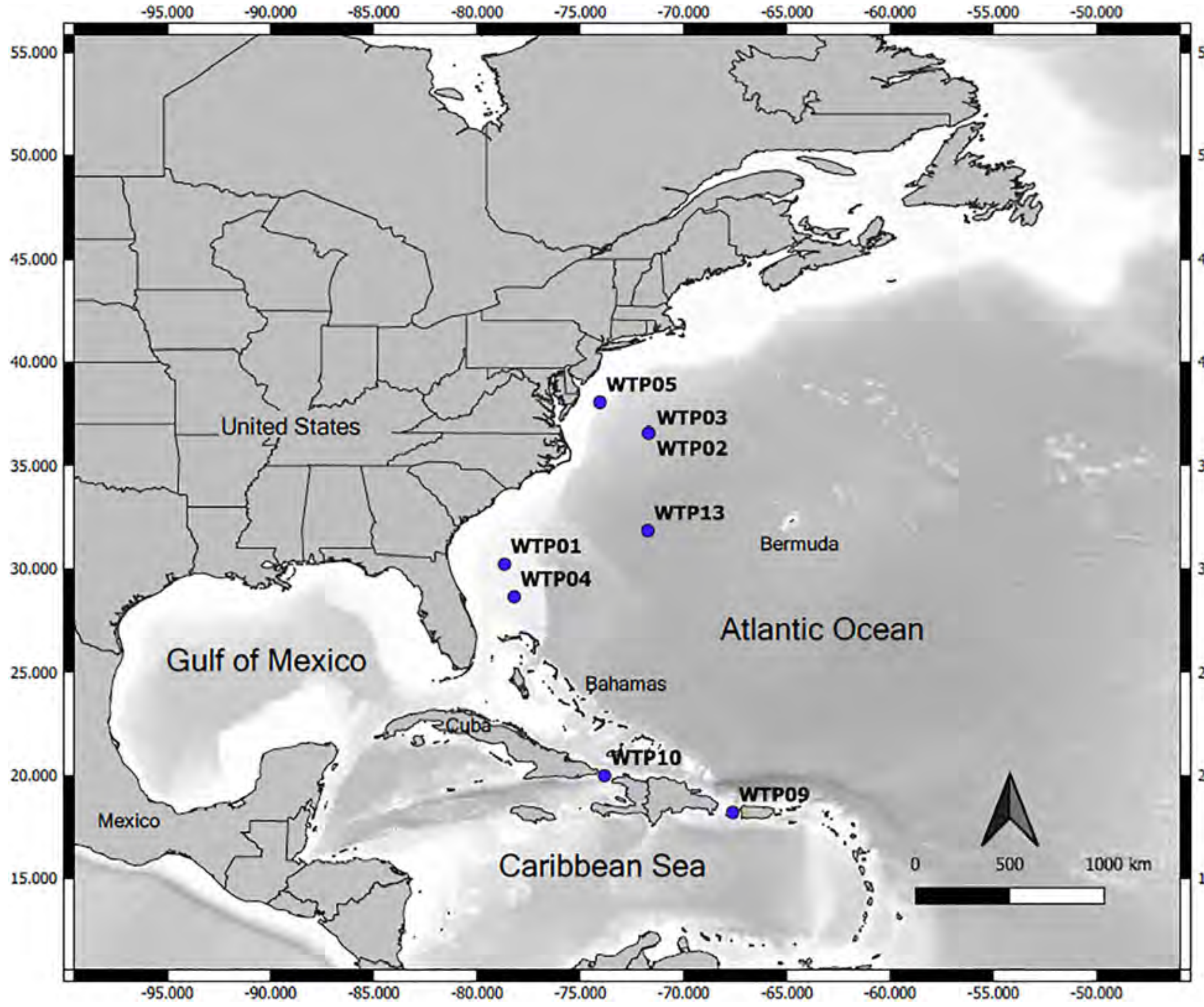

FIGURE 1 | Map of catch locations for sampled *Carcharhinus longimanus*. Shading of ocean waters denotes rough bathymetry for depth comparison, with light areas indicative of shallow continental shelf waters and darker shading indicative of deeper oceanic waters. WTP 02 and WTP 03 were caught at the same time and location.

year adjustment based on month of capture when available. In addition to material beyond the birth band, we also sampled pre-birth material from the core of the vertebrae, near the apex of the section, for four sharks and these samples were not replicated. Growth-band pairs were milled from a total of 14 vertebral sections sampled from 8 sharks. Samples were taken along the section beginning with the band pair immediately following the birth band and ranging from one to nine additional samples for each individual (**Figure 2**).

Powdered samples were analyzed at the National Ocean Sciences Accelerator Mass Spectrometry Facility (NOSAMS) at Woods Hole Oceanographic Institution (WHOI), Woods Hole, Massachusetts, for organic combustion, accelerator mass spectrometry (AMS) ^{14}C assay. Radiocarbon measurements are reported as the Fraction modern (F_m, Reimer et al., 2004), which was used to calculate Δ^{14}C with a correction for natural isotopic fractionation (Stuiver and Polach, 1977). F_m is the measured deviation of the ^{14}C:^{12}C ratio from a 'modern' sample. This reference is defined as 95% of the radiocarbon concentration of the NBS Oxalic Acid I Standard (SRM 4990B) normalized to δ^{13}C Vienna Pee Dee Belemnite geological standard (VPDB; -19%) in 1950AD (Olsson, 1970). Coral references herein are relevant to the present study because they document mixed layer ocean chemistry of the tropics, similar to the known geographical range of *C. longimanus* in the WNA (Howey-Jordan et al., 2013; Kohler and Turner, 2019), and because they can be considered the timeliest bomb-produced ^{14}C response for the marine environment—the hermatypic coral ^{14}C records chosen were from southern Florida, Puerto Rico, and Bermuda (Druffel, 1989; Moyer and Grottoli, 2011), as well as validated shark vertebrae ^{14}C data from porbeagle (*Lamna nasus*, Campana et al., 2002) and a fish otolith reference (Campana et al., 2008), both from the WNA. Measured Δ^{14}C values for the assigned dates were compared with regional Δ^{14}C reference

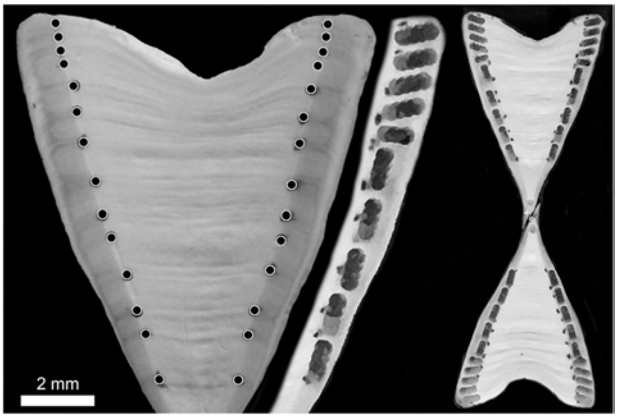

FIGURE 2 | Composite image of a *Carcharhinus longimanus* vertebra (WTP-05, estimated as 13 years old) showing the marked growth bands **(left)** on a thick section with milled bands (offset edge of the full section showing age alignments) and the full vertebra after all extractions **(right)**. Milled extractions were pooled across all growth axes for the same age classes or groups.

chronologies to assess the accuracy of age estimates from growth band counting. Generally, correctly estimated ages will yield sample formation years that align with the regional reference chronologies when plotted relative to sample Δ^{14}C values. A shift in alignment to the right, relative to reference chronologies, indicates age underestimation, and a shift to the left indicates age overestimation.

RESULTS

A total of 62 samples were available for analysis (**Table 1**) after the loss of seven measurements during AMS processing and three additional measurements were discarded due to presumed contamination during milling (depleted values likely due to inclusion of paraffin). Consensus age estimates ranged 1–13 years for fish with lengths of 94–247 cm total length (TL), which were consistent with estimated age-at-length from other published growth models for the region (**Figure 3**). Based on our age estimates, the earliest sampled YOF assigned to post-birth material was 1966.5 for WTP 04-2, meaning the majority of samples analyzed herein did not form during the informative initial rise period of Δ^{14}C (∼1958–1965), and therefore were largely uninformative for the purpose of age validation. Chronologies from sharks aged ≥4 years fell near the peak of the rise period and hence did not exhibit the strong pre- and post-peak environmental signatures evident in reference chronologies. However, because none of the sample chronologies exhibited the sharp ^{14}C rise exhibited by the reference chronologies, it is certain that the largest and oldest specimens were not considerably older. Likewise, the earliest samples from WTP 04-2 show several years of relatively static or slightly increasing values, which may represent the beginning of the plateau after the initial rise period and suggests that over-aging beyond 1–2 years did not occur. Coupled with the favorable fit with published growth curves of the age-length data for estimated ages, we believe annual growth band deposition is occurring over the ages sampled in this study. In total, our results suggest age estimates based on single, annual band pair deposition are accurate, although additional samples to definitively capture the initial rise period are needed to refine age estimates beyond a few years' accuracy.

The novel replicate sampling design of our study provides a first estimation of variation in ^{14}C across vertebrae within the same shark, with remarkable precision in ^{14}C estimates, even when multiple years of growth were pooled. Hence, it seems the resulting patterns in Δ^{14}C over time were not spurious variation due to sampling error but instead represent actual fine-scale patterns in ^{14}C uptake that likely reflect migration history via shifts in available prey. Young sharks (aged 4 years or younger) mostly exhibited Δ^{14}C levels near those of coral references, with the exception of WTP 03 which fell more in line with the upper range of porbeagle and NWA otolith references (**Figure 4A**). Adult sharks also exhibited variation in baseline Δ^{14}C levels: WTP 01 remained intermediate between coral and otolith/porbeagle reference curves for all years sampled (**Figure 4B**), WTP 02 followed the porbeagle reference (**Figure 4B**), and both WTP 04 (**Figure 4C**), and WTP 05 (**Figure 4D**) exhibited marked increases in Δ^{14}C in later years relative to values near the porbeagle/otolith references in early life. For WTP 04, this increase was followed by a return to more depleted Δ^{14}C, whereas WTP 05 remained less depleted for the remaining years. Additionally, all sharks except WTP 04 exhibited a drop in Δ^{14}C around years 2–3, which could signify ontogenetic dietary shifts and/or initiation of offshore migrations as part of philopatric movements. Continued oscillation in Δ^{14}C patterns of all older sharks seems to support the idea that these shifts are associated with migratory behavior between disparate feeding environments, as reflected in the regional ^{14}C reference records.

Pre-birth tissue sampled from the apex of centra from WTP 1, 2, 10, and 13 had Δ^{14}C levels between ∼60 and 75‰ for all specimens. Relative to timing, pre-birth values fell near the mean Δ^{14}C of the corresponding individual chronology, meaning they were closest to the coral reference in WTP 10 and 13 and to the otolith reference in WTP 01 and 02, although aging error of 1-2 years in older sharks would alternatively place them closer to the coral reference. Gestation in *C. longimanus* is characterized as viviparous placental, meaning resources used to form tissues *in utero* are derived at least in part from the maternal blood supply (Buddle et al., 2019). Hence, all pre-birth material ostensibly reflects maternal dietary carbon sourced during gestation, although the narrow Δ^{14}C range of these samples might suggest more influence from the ambient radiocarbon levels (i.e., closer alignment to coral records that trace DIC in the mixed layer environment) while *in utero*.

DISCUSSION

Preliminary analysis of vertebral radiocarbon from *C. longimanus* herein suggests annual band-pair deposition to at least 13 years of age, although further confirmation of this as well as

TABLE 1 | Specimen information, sample description, and results of radiocarbon analysis for all *Carcharhinus longimanus* vertebral samples analyzed in this study.

Specimen	Sex	Length (cm FL)	Capture year	Age (years)	Birth year	Sample ID	Description	Growth years	YOF	F_m	F_m err	$\Delta^{14}C$
WTP 01-1	F	181	1980	10	1970	WTP 01-1-1	Core (pre-birth)	1969	1969.5	1.083	0.003	80.1
						WTP 01-1-3	Year 2	1972	1972.5	1.098	0.002	95.4
						WTP 01-1-4	Year 3–4	1973–1974	1974	1.093	0.002	89.6
						WTP 01-1-5	Year 5–6	1975–1976	1976	1.101	0.002	97.9
						WTP 01-1-7	Year 9–10	1979–1980	1979.6	1.092	0.002	88.0
WTP 01-2			1980	10	1970	WTP 01-2-4	Year 5–6	1975–1976	1976	1.099	0.004	95.2
						WTP 01-2-6	Year 9–10	1979–1980	1979.6	1.081	0.002	77.2
WTP 02-1	M	160	1978	10	1968	WTP 02-1-1	Core (pre-birth)	1967	1967.5	1.072	0.003	70.1
						WTP 02-1-2	Year 1	1969	1969.5	1.043	0.002	40.9
						WTP 02-1-3	Year 2	1970	1970.5	1.030	0.003	27.5
						WTP 02-1-4	Year 3–5	1971–1973	1972.5	1.050	0.002	46.7
						WTP 02-1-6	Year 8–10	1976–1978	1977.5	1.062	0.002	58.4
WTP 02-2			1978	10	1968	WTP 02-2-1	Year 1	1969	1969.5	1.047	0.003	44.9
						WTP 02-2-2	Year 2–3	1970–1971	1971	1.029	0.002	26.6
						WTP 02-2-3	Year 4–5	1972–1973	1973	1.051	0.002	48.0
						WTP 02-2-4	Year 6–7	1974–1975	1975	1.041	0.003	37.5
						WTP 02-2-5	Year 8–10	1976–1978	1977.5	1.067	0.002	63.5
WTP 03-1	M	143	1978	4	1974	WTP 03-1-1	Year 1	1975	1975.5	1.083	0.003	79.6
						WTP 03-1-2	Year 2	1976	1976.5	1.071	0.002	67.3
						WTP 03-1-3	Year 3	1977	1977.5	1.070	0.002	66.5
						WTP 03-1-4	Year 4	1978	1978.5	1.072	0.002	68.3
WTP 03-2			1978	4	1974	WTP 03-2-1	Year 1	1975	1975.5	1.075	0.002	72.1
						WTP 03-2-2	Year 2	1976	1976.5	1.065	0.002	61.4
						WTP 03-2-3	Year 3	1977	1977.5	1.075	0.002	71.6
						WTP 03-2-4	Year 4	1978	1978.5	1.078	0.003	74.5
WTP 04-1	M	163	1978	13	1965	WTP 04-1-1	Year 1–2	1966–1967	1967	1.039	0.003	36.4
						WTP 04-1-2	Year 3–4	1968–1969	1969	1.044	0.002	41.8
						WTP 04-1-3	Year 5–6	1970–1971	1971	1.047	0.003	44.5
						WTP 04-1-4	Year 6–8	1972–1973	1972.5	1.029	0.002	26.0
						WTP 04-1-5	Year 8–10	1974–1975	1974.5	1.056	0.003	53.0
						WTP 04-1-6	Year 10–12	1976–1977	1976.5	1.079	0.002	75.8
						WTP 04-1-7	Year 12–13	1978	1977.6	1.057	0.002	53.5
WTP 04-2			1978	13	1965	WTP 04-2-1	Year 1	1966	1966.5	1.048	0.002	46.0
						WTP 04-2-2	Year 2–3	1967–1968	1968	1.045	0.002	42.7
						WTP 04-2-3	Year 4–5	1969–1970	1970	1.047	0.002	44.8
						WTP 04-2-4	Year 6–7	1971–1972	1972	1.040	0.003	37.1
						WTP 04-2-5	Year 8–9	1973–1974	1974	1.049	0.002	46.0
						WTP 04-2-6	Year 9–11	1974–1976	1975.5	1.081	0.002	77.7
						WTP 04-2-7	Year 11–13	1976–1978	1977	1.059	0.003	55.9
WTP 05-1	F	205	1983	13	1970	WTP 05-1-1	Year 1	1971	1971.5	1.051	0.002	48.3
						WTP 05-1-2	Year 2–3	1972–1973	1973	1.050	0.002	47.3
						WTP 05-1-3	Year 3–4	1973–1974	1974	1.038	0.003	34.7
						WTP 05-1-4	Year 4–5	1974–1975	1975	1.055	0.002	51.7
						WTP 05-1-5	Year 5–6	1975–1976	1976	1.078	0.004	74.1
						WTP 05-1-6	Year 7–8	1977–1978	1978	1.084	0.004	80.1
						WTP 05-1-7	Year 9	1979	1979.5	1.066	0.002	62.5
						WTP 05-1-8	Year 10	1980	1980.5	1.082	0.002	78.0
WTP 05-2			1983	13	1970	WTP 05-2-1	Year 1	1971	1971.5	1.060	0.002	57.0
						WTP 05-2-2	Year 2–3	1972–1973	1973	1.052	0.002	48.9
						WTP 05-2-3	Year 3–4	1973–1974	1974	1.038	0.002	35.0
						WTP 05-2-4	Year 4–5	1974–1975	1975	1.053	0.002	49.6
						WTP 05-2-5	Year 6	1976–1977	1977	1.079	0.002	75.5
						WTP 05-2-7	Year 9	1979	1979.5	1.074	0.002	69.8
						WTP 05-2-8	Year 10	1980	1980.5	1.074	0.002	69.5

(Continued)

TABLE 1 | Continued

Specimen	Sex	Length (cm FL)	Capture year	Age (years)	Birth year	Sample ID	Description	Growth years	YOF	F_m	F_m err	$\Delta^{14}C$
						WTP 05-2-9	Year 11	1981	1981.5	1.079	0.002	75.1
						WTP 05-2-10	Year 12–13	1982–1983	1982.7	1.072	0.002	68.1
WTP 09	F	84	2001	1	2000	WTP 09-1	Year 1	2001	2001.5	1.073	0.003	66.4
WTP 10	M	100	2004	2	2002	WTP 10C	Core (pre-birth)	2001	2001.5	1.076	0.003	69.2
						WTP 10-1	Year 1	2003	2003	1.068	0.003	61.1
						WTP 10-2	Year 1–2	2003–2004	2004	1.067	0.003	60.3
WTP 13-1	F	104	2001	1	2000	WTP 13-1-C	Core (pre-birth)	1999	1999.5	1.076	0.003	69.3
WTP 13-2			2001	1	2000	WTP 13-2-1	Year 1	2001	2001	1.072	0.002	65.3

Specimen length was measured to the nearest cm fork length (FL) at time of capture, and lengths were converted to total length (TL) using data from Kneebone (unpublished) for additional analyses herein. Birth year was calculated as the difference in capture year and age (years). Sampled vertebral material is described by the relative years of growth captured in each sample, with core (pre-birth) samples taken from near the apex of vertebral centra where noted. Growth years denote the calendar range of years comprising each sample, with year of formation (YOF) calculated as the decimal midpoint of the range of growth years, accounting for birth month where available. Fraction modern (F_m) and associated error (F_m err, ± 2 SD of the mean) are reported along with $\Delta^{14}C$ (‰) calculated from F_m. Alternating specimen numbers are shaded to facilitate viewing.

maximum lifespan are needed. By employing a novel, multi-centra approach to measuring replicate growth bands within individual sharks, we have demonstrated that the fine-scale patterns in vertebral $\Delta^{14}C$ apparent for this species are genuine records of $\Delta^{14}C$ variation, which are conserved across centra within the individual, and may allow for precise reconstruction of dietary shifts corresponding to movement patterns over the lifespan of the shark. Previous documentation of philopatric movement patterns for *C. longimanus* support these findings.

Vertebral radiocarbon is typically used to determine growth band periodicity and to test the validity of age reading protocol, with the potential to determine maximum lifespan in sharks (Kalish and Johnston, 2001; Campana et al., 2002; Natanson et al., 2018a). Its use has led to discoveries of "missing time" in the vertebrae due to cessation of growth in later years of life (Francis et al., 2007; Andrews et al., 2011; Passerotti et al., 2014; Andrews and Kerr, 2015) and in many cases significant underestimation of age (Harry, 2018). The sharks sampled for this study were the oldest/largest available from archival material, yet YOF for the earliest formed material did not fall early enough to validate annual band-pair deposition with certainty. However, species found to have "missing time" generally have ages validated from early life through maturity, with a loss of years documented later in life (Harry, 2018). Hence, given indirect verification of annual deposition of growth bands in *C. longimanus* using marginal increment analysis (Seki et al., 1998; Lessa et al., 1999; Joung et al., 2016), and that size-at-age using our age estimates fell as expected along the published growth curve for Atlantic *C. longimanus* (Lessa et al., 1999) and within range of all published growth curves (**Figure 3**), the assumption of annual growth band deposition to 13 years of age is supported.

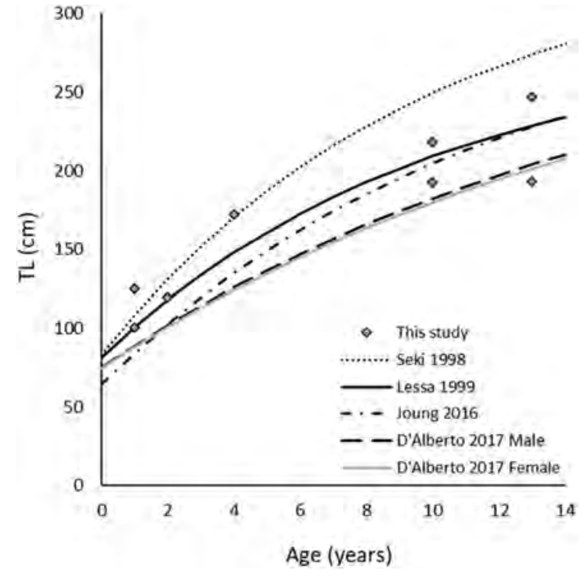

FIGURE 3 | Total length (TL) at age for *Carcharhinus longimanus* specimens aged in this study plotted against published VB growth curves from Seki et al. (1998); Lessa et al. (1999), Joung et al. (2016), and D'Alberto et al. (2017). Fork length (FL) to TL conversions for samples analyzed in this study were calculated using unpublished length data from the western North Atlantic (Kneebone, unpublished data).

Aside from age information, vertebral ^{14}C has also been interpreted to reflect shifts in dietary patterns, related to habitat use across the lifespan. Because carbon uptake in elasmobranchs is accomplished via feeding (dietary source; Fry, 1988)—as opposed to direct uptake of dissolved inorganic carbon from seawater, as in teleosts (Kalish, 1993)—changes in prey composition occurring due to habitat shifts can often be detected in vertebral radiocarbon (Natanson et al., 2018a). Depth-related changes and the consequent change in prey items was well-supported as the reason for an attenuated and phase-lagged bomb ^{14}C signal for porbeagle shark (Campana et al., 2002). In contrast, ^{14}C from early growth of tiger shark, *Galeocerdo cuvier,* (Kneebone et al., 2008) and sand tiger shark, *Carcharias taurus,* (Passerotti et al., 2014) demonstrated an affinity for nearshore habitat by having well-constrained ^{14}C values from young sharks aligned with coral references, while the vertebrae from older sharks indicated there was a dietary shift to more depleted ^{14}C values that may indicate life in offshore waters and thus consumption of prey from these deeper waters. Additional

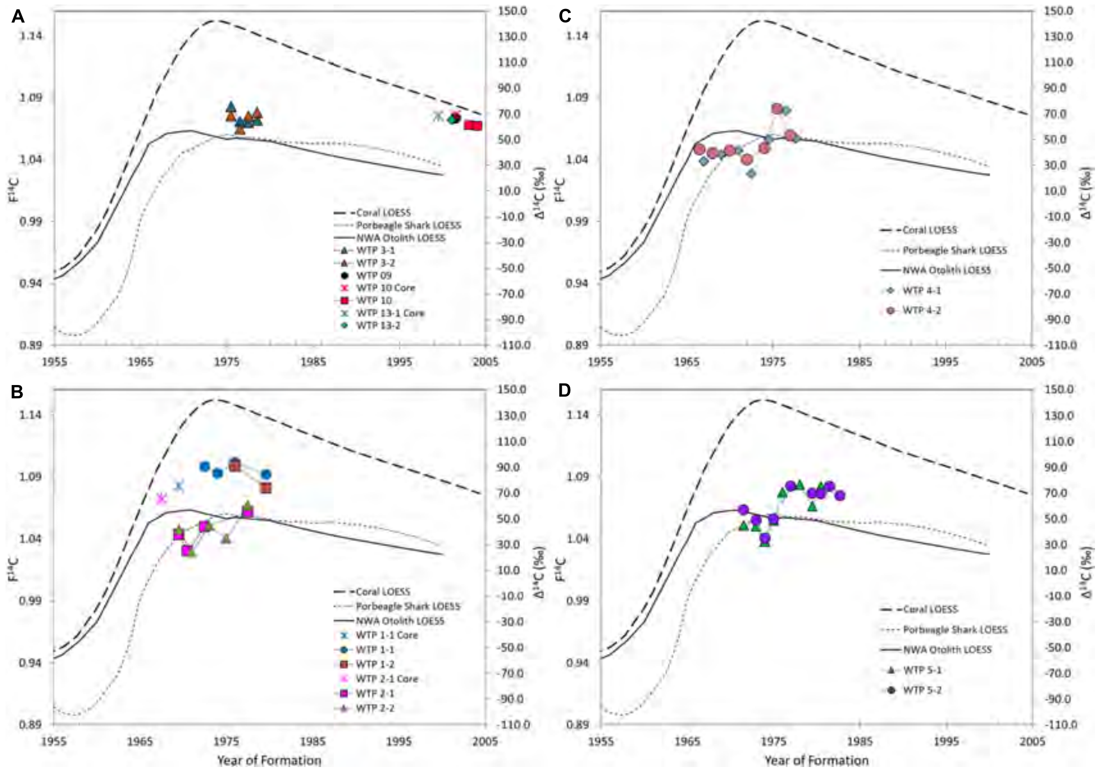

FIGURE 4 | Vertebral radiocarbon results for *Carcharhinus longimanus* plotted over the estimated life span of each individual and relative to the regional ^{14}C reference records (Loess curves for coral, porbeagle, and otoliths). The year of formation for each sample is plotted based on age estimates from growth band counting in the vertebral thin sections. Plots for *C. longimanus* aged ≤4 years are included in panel **(A)**, followed by sharks aged 10 years in panel **(B)**, and aged 13 years in **(C,D)**. Samples corresponding to pre-birth material are denoted by star shaped icons in panels **(A,B)**. Complete sample information can be found according to specimen ID in **Table 1**.

studies have hypothesized that post-rise differences in ^{14}C magnitude between adults can signal individual differences in diet or location, as in white sharks, *Carcharodon carcharias,* (Kerr et al., 2006; Hamady et al., 2014). Young *C. longimanus* caught in shallow nearshore areas (WTP 09 and 10) provided similar time-constrained references for residence in shallow waters possibly near where they were pupped, while WTP 03 caught offshore at higher latitude shows a more depleted $\Delta^{14}C$ signature. We could similarly hypothesize that WTP 13, caught offshore between Bermuda and the US mainland but exhibiting enriched $\Delta^{14}C$, may have been pupped in shallow waters before moving offshore. The overall range of vertebral $\Delta^{14}C$ among sampled sharks was narrow relative to that measured across habitats, hence complete validation of habitat-specific influence on vertebral $\Delta^{14}C$ patterns cannot be made without additional samples. However, the relative correlation of young shark habitat with $\Delta^{14}C$ evident in our study samples suggests that the oscillations seen in $\Delta^{14}C$ for older *C. longimanus* reflect annual to biennial migrations.

Published tagging, diet, and stable isotope studies for *C. longimanus* provide empirical evidence to support the interpretation of radiocarbon signatures to reflect movement patterns. Catch locations of most sampled sharks in this study overlapped *C. longimanus* movement tracked near Cat Island, Bahamas, by Howey-Jordan et al. (2013) as well as diet studies for individuals tagged in the Bahamas including stable isotope and stomach contents analyses (Madigan et al., 2015). Howey-Jordan et al. (2013) documented philopatric movements for many sharks, but disparate movement patterns among individuals were also evident despite most being the same sex and maturity (mature females). Some exhibited philopatric movements to the original tagging location over a scale of months, relatively fewer initiated longer (to ∼1900 km) offshore migrations (including to near Bermuda), while several others remained near the tagging location for the duration of the tracking period (up to ∼150 days). Repeated annual sightings of individuals are also reported from the Bahamas (Madigan et al., 2015). Vertical migration patterns also varied among individuals across multiple tagging studies, with some sharks initiating deep dives to >1000 m potentially associated with foraging behavior or thermoregulation (Howey-Jordan et al., 2013; Tolotti et al., 2017; Andrzejaczek et al., 2018).

The Bahamas population of *C. longimanus* is well-established, and this region provides access to abundant epipelagic prey such as billfish and tunas which are an important component of diet for sharks in the area (Madigan et al., 2015). Short term (blood plasma) stable isotope data showed higher proportions of large pelagic teleosts in the diet while sharks were in the Bahamas, while squid and smaller planktivorous teleosts were more prevalent in the diet in the long term (muscle) and appear to be important prey during oceanic portions of the life cycle (Madigan et al., 2015). Other diet studies have reported mammals in the diet of *C. longimanus* (Bass et al., 1973; Cortés, 1999). Squid are depleted in δ^{13}C (∼−18 per mil) relative to pelagic teleosts (∼−16.5 per mil, Madigan et al., 2015), and mammals tend to be relatively depleted in δ^{13}C and Δ^{14}C (Stewart et al., 2006; Madigan et al., 2015). Post-bomb Δ^{14}C of Atlantic seawater is variable and ranges to −100‰ across depths dependent on residence time and mixing rates (Druffel et al., 1992); hence, any planktivorous prey taken during deep dives would likely reflect the depleted profile of the deeper water column. A recent observation of a *C. logimanus* in the Pacific with scars from an interaction with a large, deep-dwelling cephalopod (likely either *Architeuthis*, *Thysanoteuthis* or *Megalocranchia*; Papastamatiou et al., 2020) lend further evidence to the theory that foraging occurs in deep waters. While sub-annual patterns of offshore-onshore movements might not cause year-to-year oscillations in Δ^{14}C, the sharks undertaking longer offshore migrations may remain offshore substantially beyond the time recorded by tagging, and thus consume proportionally more depleted prey items for the year as a whole. Alternatively, even a small proportion of highly depleted prey in the diet can likely cause depleted vertebral Δ^{14}C (Kerr et al., 2006). The porbeagle reference chronology (Campana et al., 2002) lends solid evidence of the effect that deep foraging can have on Δ^{14}C signatures in sharks.

The maternally derived pre-birth Δ^{14}C measurements reported herein for C. *longimanus* are only the second species to be reported in the literature. White shark pre-birth Δ^{14}C was reported from the Pacific (Kerr et al., 2006), and Atlantic (Hamady et al., 2014). Aside from reporting the values as part of the larger studies, the pre-birth data were not used to inform any conclusions, although Natanson and Skomal (2015) used the Atlantic pre-birth value to align the sample chronology for age validation. Our results are likewise presented for informational purposes, with hopes that future work will determine applicability of these measurements to life history research. If pre-birth vertebral material can be used as a proxy for maternal ^{14}C during gestation, then chronologies including both pre- and post-birth samples may be useful for exploring movement and diet related to gestation, parturition, and ontogeny of pups.

An important aspect of this study is the replication of ^{14}C measurements for most vertebral growth bands, which provides insight on the variation of ^{14}C uptake across vertebrae. These findings, coupled with empirical evidence, support life history insights about ontogenetic movements gained from fine-scale patterns in vertebral ^{14}C. These analyses are generally expensive and studies involving large numbers of samples (and thus replicates) are usually cost-prohibitive. Hence, this study provides novel insights into the measurement precision attainable for vertebral ^{14}C and its potential utility for applications outside of age validation, such as deciphering life history ecology in the years following the more informative bomb-produced ^{14}C rise period.

DATA AVAILABILITY STATEMENT

All datasets presented in this study are included in the article/supplementary material.

AUTHOR CONTRIBUTIONS

LN provided archival vertebrae and sectioned and photographed vertebrae for aging. MP sectioned and marked vertebrae, performed all laboratory analyses, data analysis, and prepared the first draft of the manuscript. AA milled vertebrae for radiocarbon analysis, contributed to data analysis, and provided images. All authors designed the study, aged vertebrae, and contributed to the final version of the manuscript.

FUNDING

This work was made possible by a Graduate Student Fellowship from the National Ocean Sciences Accelerator Mass Spectrometry (NOSAMS) laboratory at Woods Hole Oceanographic Institute, Woods Hole, Massachusetts. Funds for open access publication fees were provided by the University of South Carolina.

ACKNOWLEDGMENTS

Our overwhelming thanks go to Kathryn Elder and Mark Roberts of NOSAMS for their advisory role in this work, as well as to Tess Walther and other NOSAMS staff for assistance in sample processing. We also thank Bryan Frazier and the South Carolina Department of Natural Resources for providing lab space and equipment for sample preparation. Additional thanks go to the NOAA staff and fisheries observers who collected the specimens used in this study. NOAA Pacific Islands Fisheries Science Center provided infrastructural support.

REFERENCES

Andrews, A. H., and Kerr, L. A. (2015). Estimates of maximum age for white sharks of the northeasternPacific Ocean: altered perceptions of vertebral growth shed light on complicated bomb Δ^{14}Cresults. *Environ. Biol. Fish.* 98, 971–978. doi: 10.1007/s10641-014-0326-8

Andrews, A. H., Natanson, L. J., Kerr, L. A., Burgess, G. H., and Cailliet, G. M. (2011). Bomb radiocarbon andtag-recapture dating of sandbar shark (*Carcharhinus plumbeus*). *Fish. Bull.* 109, 454–465.

Andrzejaczek, S., Gleiss, A. C., Jordan, L. K., Pattiaratchi, C. B., Howey, L. A., Brooks, E. J., et al. (2018). Temperature and the vertical movements of oceanic whitetip sharks. *Carcharhinuslongimanus*. *Sci. Rep.* 8, 1–12.

Bass, A. J., D' Aubrey, J. D., and Kistnasamy, N. (1973). Sharks of the east coast of southern Africa. I. The genus *Carcharhinus* (Carcharhinidae). *Oceanogr. Res. Inst.* 33:168.

Buddle, A. L., Van Dyke, J. U., Thompson, M. B., Simpfendorfer, C. A., and Whittington, C. M. (2019). Evolution of placentotrophy: using viviparous sharks as a model to understand vertebrateplacental evolution. *Mar. Freshw. Res.* 70, 908–924. doi: 10.1071/mf18076

Cailliet, G. M., Smith, W. D., Mollet, H. F., and Goldman, K. J. (2006). Age and growth studies ofchondrichthyan fishes: the need for consistency in terminology, verification, validation, andgrowth function fitting. *Env. Biol. Fish.* 77, 211–228. doi: 10.1007/S10641-0069105-5

Campana, S. E. (2001). Accuracy, precision and quality control in age determination, including a reviewof the use and abuse of age validation methods. *J. Fish Biol.* 59, 197–242. doi: 10.1111/J.1095-8649.2001.TB00127.X

Campana, S. E., Casselman, J. M., and Jones, C. M. (2008). Bomb radiocarbon chronologies in the Arctic,with implications for the age validation of lake trout (*Salvelinus namaycush*) and other Arcticspecies. *Can. J. Fish. Aquat. Sci.* 65, 733–743. doi: 10.1139/f08-012

Campana, S. E., Natanson, L. J., and Myklevoll, S. (2002). Bomb dating and age determination of largepelagic sharks. *Can. J. Fish. Aquat. Sci.* 59, 450–455. doi: 10.1139/f02-027

Casey, J. G., Pratt Jr, H. L., and Stillwell, C. E. (1985). Age and growth of the sandbar shark (*Carcharhinus plumbeus*) from the western North Atlantic. *Can. J. Fish. Aquat. Sci.* 42, 963–975.

CITES (2013). "Convention on International Trade in Endangered Species of Wild Fauna and Floraconsideration of proposals for amendment of Appendices I and II". in *Sixteenth Meeting of the Conference of the Parties Bangkok (Thailand), 3–*14, 2013. (Thailand: CITES).

Compagno, L. J. V. (1984). *FAO Species Catalogue Vol 4. Sharks of the world: an annotated and illustratedcatalogue of shark species known to date. Parts 1 and 2. FAO Fisheries Synopsis No. 125*. Italy: FAO, 655.

Cortés, E. (1999). Standardized diet compositions and trophic levels of sharks. *ICES J. Mar. Sci.* 56, 707–717. doi: 10.1006/jmsc.1999.0489

D'Alberto, B. M., Chin, A., Smart, J. J., Baje, L., White, W. T., and Simpfendorfer, C. A. (2017). Age, growthand maturity of oceanic whitetip shark (*Carcharhinus longimanus*) from Papua New Guinea.Mar. *Freshw. Res.* 68, 1118–1129. doi: 10.1071/mf16165

Druffel, E. M. (1989). Decadal time scale variability of ventilation in the North Atlantic: high-precisionmeasurements of bomb radiocarbon in banded corals. *J. Geoph. Res.* 94, 3271–3285. doi: 10.1029/jc094ic03p03271

Druffel, E. M., Williams, P. M., Bauer, J. E., and Ertel, J. R. (1992). Cycling of dissolved and particulateorganic matter in the open ocean. *J. Geophys. Res* 97, 15639–15659. doi: 10.1029/92jc01511

Francis, M. P., Campana, S. E., and Jones, C. M. (2007). Age under-estimation in New Zealand porbeaglesharks (*Lamna nasus*): Is there an upper limit to ages that can be determined from sharkvertebrae? *Mar. Freshw. Res.* 58, 10–23. doi: 10.1071/mf06069

Fry, B. (1988). Food web structure on Georges Bank from stable C. N and S isotopic compositions. *Limnol.Oceanogr.* 33, 1182–1190. doi: 10.4319/lo.1988.33.5.1182

Hamady, L. L., Natanson, L. J., Skomal, G. B., and Thorrold, S. R. (2014). Vertebral bomb radiocarbonsuggests extreme longevity in white sharks. *PloS One* 9:e84006. doi: 10.1371/journal.pone.0084006

Harry, A. V. (2018). Evidence for systemic age underestimation in shark and ray ageing studies. *Fish Fisheries* 19, 185–200. doi: 10.1111/faf.12243

Howey, L. A., Tolentino, E. R., Papastamatiou, Y. P., Brooks, E. J., Abercrombie, D. L., Watanabe, Y. Y., et al. (2016). Into the deep: the functionality of mesopelagic excursions by an oceanicapex predator. *Ecol. Evol.* 6, 5290–5304. doi: 10.1002/ece3.2260

Howey-Jordan, L. A., Brooks, E. J., Abercrombie, D. L., Jordan, L. K., Brooks, A., Williams, S., et al. (2013). Complex movements, philopatry and expanded depth range of aseverely threatened pelagic shark, the oceanic whitetip (*Carcharhinus longimanus*) in thewestern North Atlantic. *PloS One* 8:e56588. doi: 10.1371/journal.pone.0056588

Joung, S. J., Chen, N. F., Hsu, H. H., and Liu, K. M. (2016). Estimates of life history parameters of theoceanicwhitetip shark, *Carcharhinus longimanus*, in the western North Pacific Ocean. *Mar.Biol. Res.* 12, 758–768. doi: 10.1080/17451000.2016.1203947

Kalish, J. M. (1993). Pre-and post-bomb radiocarbon in fish otoliths. *Earth Plan. Sci. Lett.* 114, 549–554. doi: 10.1016/0012-821x(93)90082-k

Kalish, J. M., and Johnston, J. (2001). "Determination of school shark age based on analysis of radiocarbonin vertebral collagen," in *Use of the bomb radiocarbon chronometer to validatefish age. Final Report. FDRC Project 93/109*, ed. J. M. Kalish (Canberra: Fisheries Research and Development Corporation), 116–122.

Kerr, L. A., Andrews, A. H., Cailliet, G. M., Brown, T. A., and Coale, K. H. (2006). "Investigations of Δ^{14}C,δ^{13}C, and δ^{15}N in vertebrae of white shark (*Carcharodon carcharias*) from the eastern NorthPacific Ocean," in *Special Issue: Age and Growth of Chondrichthyan Fishes: New Methods,Techniques and Analysis*, eds John K Carlson and Kenneth J Goldman (Dordrecht: Springer), 337–353. doi: 10.1007/978-1-4020-5570-6_14

Kneebone, J., Natanson, L. J., Andrews, A. H., and Howell, W. H. (2008). Using bomb radiocarbonanalyses to validate age and growth estimates for the tiger shark, *Galeocerdo cuvier*, in thewestern North Atlantic. *Mar. Biol.* 154, 423–434. doi: 10.1007/S00227-008-0934-Y

Kohler, N. E., and Turner, P. A. (2019). Distributions and Movements of Atlantic Shark Species: A 52-YearRetrospective Atlas of Mark and Recapture Data. *Mar. Fish. Rev.* 81, 1–94. doi: 10.7755/mfr.81.2.1

Lessa, R., Santana, F. M., and Paglerani, R. (1999). Age, growth and stock structure of the oceanicwhitetip shark, *Carcharhinus longimanus*, from the southwestern equatorial Atlantic. *Fish. Res.* 42, 21–30. doi: 10.1016/s0165-7836(99)00045-4

Madigan, D. J., Brooks, E. J., Bond, M. E., Gelsleichter, J., Howey, L. A., Abercrombie, D. L., et al. (2015). Diet shift and site-fidelity ofoceanicwhitetip sharks *Carcharhinus longimanus* along the Great Bahama Bank. *Mar. Ecol. Prog.Ser.* 529, 185–197. doi: 10.3354/meps11302

Moyer, R. P., and Grottoli, A. G. (2011). Coral skeletal carbon isotopes (δ^{13}C and Δ^{14}C) record the deliveryof terrestrial carbon to the coastal waters of Puerto Rico. *Coral Reefs* 30:791.

Natanson, L. J., and Skomal, G. B. (2015). Age and growth of the white shark, *Carcharodon carcharias*, inthe western North Atlantic Ocean. *Mar. Freshw. Res.* 66, 387–398. doi: 10.1071/mf14127

Natanson, L. J., Andrews, A. H., Passerotti, M. S., and Wintner, S. P. (2018a). "History and Mystery of Ageand Growth Studies in Elasmobranchs," in *Shark Research: Emerging Technologies and Applications forthe Field and Laboratory*, eds J. C. Carrier, M. R. Heithaus, and C. A. Simpfendorfer (Boca Raton, FL: CRC Press), 177–200.

Natanson, L. J., Skomal, G. B., Hoffmann, S. L., Porter, M. E., Goldman, K. J., and Serra, D. (2018b). Age andgrowth of sharks: do vertebral band pairs record age? *Mar. Freshw. Res.* 69, 1440–1452. doi: 10.1071/mf17279

Natanson, L., Kohler, N., Ardizzone, D., Cailliet, G., Wintner, S., and Mollet, S. (2006). Validated age andgrowth estimates for the shortfin mako, *Isurus oxyrinchus*, in the North Atlantic Ocean. *Env. Biol.Fish.* 77, 367–383. doi: 10.1007/S10641-006-9127-Z

Olsson, I. U. (1970). "The use of oxalic acid as a standard," in *'Radiocarbon Variations and AbsoluteChronology. Proceedings of the 12th Nobel Symposium.'*, ed. I. U. Olsson (New York, NY: John Wiley &Sons), 17.

Passerotti, M. S., Andrews, A. H., Carlson, J. K., Wintner, S. P., Goldman, K. J., and Natanson, L. J. (2014). Maximum age and missing time in the vertebrae of sand tiger shark (*Carcharias taurus*):validated lifespan frombomb radiocarbon dating in the western North Atlantic andsouthwestern Indian Oceans. *Mar. Freshw. Res.* 65, 1131–1140. doi: 10.1071/MF13214

Papastamatiou, Y. P., Verbeck, D., Hutchinson, M., Bracken-Grissom, H. D., and Chapman, D. (2020). An encounter between a pelagic shark and giant cephalopod. *J. Fish Biol.* 97, 588–589. doi: 10.1111/jfb.14415

Reimer, P. J., Brown, T. A., and Reimer, R. W. (2004). Discussion: reporting and calibration of post-bomb 14C data. *Radiocarbon* 46, 1299–1304.

Rigby, C. L., Barreto, R., Carlson, J., Fernando, D., Fordham, S., Francis, M. P., et al. (2019). *Carcharhinus longimanus. The IUCN Red List of Threatened Species 2019: e.T39374A2911619*. Available online at: https://dx.doi.org/10.2305/IUCN.UK.2019-3.RLTS.T39374A2911619.en (accessed May 26, 2020).

Seki, T., Taniuchi, T., Nakano, H., and Shimizu, M. (1998). Age, growth and reproduction of the oceanicwhitetip shark from the Pacific Ocean. *Fish. Sci.* 64, 14–20. doi: 10.2331/fishsci.64.14

Stewart, R. E. A., Campana, S. E., Jones, C. M., and Stewart, B. E. (2006). Bomb radiocarbon datingcalibrates beluga (*Delphinapterus leucas*) age estimates. *Can. J. Zool.* 84, 1840–1852. doi: 10.1139/z06-182

Stuiver, M., and Polach, H. A. (1977). Reporting of C-14 data. *Radiocarbon* 19, 355–363.

Tolotti, M. T., Bach, P., Romanov, E., and Dagorn, L. (2015). *Interactions of oceanic whitetip sharks with the tuna purse seine fishery in the Indian Ocean. IOTC-2015-WPEB11-29*. Italy, RM: Food and Agriculture Organization of the United Nations.

Tolotti, M., Bauer, R., Forget, F., Bach, P., Dagorn, L., and Travassos, P. (2017). Fine-scale vertical movementsof oceanic whitetip sharks (*Carcharhinus longimanus*). *Fish. Bull.* 115, 380–395. doi: 10.7755/FB.115.3.8

Young, C. N., and Carlson, J. K. (2020). The biology and conservation status of the oceanic whitetip shark(*Carcharhinus longimanus*) and future directions for recovery. *Rev. Fish Biol. Fisheries* 30, 293–312. doi: 10.1007/s11160-020-09601-3

Young, C. N., Carlson, J. K., Hutchinson, M., Hutt, C., Kobayashi, D., McCandless, C. T., et al. (2017). *Status review report: oceanic whitetip shark (Carcharhinius longimanus)*. Final Report to the National Marine Fisheries Service, Office of Protected Resources. December 2017. Silver Spring: National Marine Fisheries Service.

Conflict of Interest: The authors declare that the research was conducted in the absence of any commercial or financial relationships that could be construed as a potential conflict of interest.

frontiers
in Marine Science

ORIGINAL RESEARCH
published: 03 December 2020
doi: 10.3389/fmars.2020.594636

Predicting Geographic Ranges of Marine Animal Populations Using Stable Isotopes: A Case Study of Great Hammerhead Sharks in Eastern Australia

Vincent Raoult[1]*, Clive N. Trueman[2], Kelsey M. Kingsbury[3], Bronwyn M. Gillanders[3], Matt K. Broadhurst[4], Jane E. Williamson[5], Ivan Nagelkerken[3], David J. Booth[6], Victor Peddemors[7], Lydie I. E. Couturier[8] and Troy F. Gaston[1]

[1] School of Environmental and Life Sciences, University of Newcastle, Ourimbah, NSW, Australia, [2] Ocean and Earth Science, University of Southampton, Southampton, United Kingdom, [3] Southern Seas Ecology Laboratories, School of Biological Sciences and The Environment Institute, The University of Adelaide, Adelaide, SA, Australia, [4] Fisheries Conservation Technology Unit, National Marine Science Centre, New South Wales Department of Primary Industries, Southern Cross University, Coffs Harbour, NSW, Australia, [5] Department of Biological Sciences, Macquarie University, Sydney, NSW, Australia, [6] School of Life Sciences, University of Technology Sydney, Sydney, NSW, Australia, [7] New South Wales Department of Primary Industries, Sydney Institute of Marine Science, Mosman, NSW, Australia, [8] Univ Brest, IRD, Ifremer, CNRS, LEMAR, Plouzané, France

OPEN ACCESS

Edited by:
Alastair Martin Mitri Baylis,
South Atlantic Environmental Research Institute, Falkland Islands

Reviewed by:
Aaron Carlisle,
University of Delaware, United States
Luciana C. Ferreira,
Australian Institute of Marine Science (AIMS), Australia
Daniel James Madigan,
University of Windsor, Canada

***Correspondence:**
Vincent Raoult
Vincent.raoult@newcastle.edu.au

Specialty section:
This article was submitted to Marine Megafauna, a section of the journal Frontiers in Marine Science

Received: *13 August 2020*
Accepted: *12 November 2020*
Published: *03 December 2020*

Citation:
Raoult V, Trueman CN, Kingsbury KM, Gillanders BM, Broadhurst MK, Williamson JE, Nagelkerken I, Booth DJ, Peddemors V, Couturier LIE and Gaston TF (2020) Predicting Geographic Ranges of Marine Animal Populations Using Stable Isotopes: A Case Study of Great Hammerhead Sharks in Eastern Australia. Front. Mar. Sci. 7:594636. doi: 10.3389/fmars.2020.594636

Determining the geographic range of widely dispersed or migratory marine organisms is notoriously difficult, often requiring considerable costs and typically extensive tagging or exploration programs. While these approaches are accurate and can reveal important information on the species, they are usually conducted on only a small number of individuals and can take years to produce relevant results, so alternative approaches may be preferable. The presence of latitudinal gradients in stable carbon isotope compositions of marine phytoplankton offers a means to quickly determine likely geographic population ranges of species that rely on productivity from these resources. Across sufficiently large spatial and temporal scales, the stable carbon isotopes of large coastal or pelagic marine species should reflect broad geographic patterns of resource use, and could be used to infer geographic ranges of marine populations. Using two methods, one based on a global mechanistic model and the other on targeted low-cost latitudinal sampling of fishes, we demonstrate and compare these stable isotope approaches to determine the core population geography of an apex predator, the great hammerhead (*Sphyrna mokarran*). Both methods indicated similar geographic ranges and suggested that *S. mokarran* recorded in south-eastern Australia are likely to be from more northern Australian waters. These approaches could be replicated in other areas where coastlines span predictable geographic gradients in isotope values and be used to determine the core population geography of highly mobile species to inform management decisions.

Keywords: habitat range population distributions, movement, species distribution model, sharks, manta rays, stable isotopes, tracking, isoscape

INTRODUCTION

Determining the habitat ranges of mobile species is a key precursor for their effective population management (Hobday et al., 2011). For marine species that migrate across large distances, tagging approaches (photo-identification, passive or active tags) are the most widespread methods used to determine geographic ranges (Queiroz et al., 2019). However, while tagging can provide important spatial information (Queiroz et al., 2019) telemetry tags are expensive and satellite tags can have failure rates approaching 50% (Hofman et al., 2019). Also, tags are not always appropriate for smaller species or those that occur in deeper water. Further, tags usually provide few data points that, while informative for certain applications (e.g., determining if individuals use particular habitats, Barnes et al., 2019) have only recently reached population scales > 1,000 for a few commercially important species, such as Atlantic bluefin tuna (*Thunnus thynnus)* (Block, 2019). Inter-jurisdictional collaborations can alleviate some of these restrictions for producing population-scale tagging outputs on less valuable species, but for regionally isolated work the approach remains challenging (Sequeira et al., 2019). In addition, because tagging relies on collecting data over long periods (i.e., up to 13 years, Holmes et al., 2014), there are inherent delays in subsequent management applications.

An alternative method that provides information on the past geography of migratory species without the logistical and temporal costs described above involves stable isotope analysis, which can be derived from non-lethal tissue sampling. Specifically, the relative abundance of stable isotopes of carbon and nitrogen in marine animal tissues have been used extensively to infer resource use and to examine trophic interactions (Post, 2002). More recently, stable isotope compositions of tissues have been used to address spatial questions such as identifying ocean basin-scale patterns of resource use (Bird et al., 2018), and even reconstructing individual migration histories from archived samples (Trueman et al., 2019). Stable isotope methods offer a means to determine the geographic ranges of migratory marine organisms over large temporal scales (annual to decadal, depending on preserved tissue types) at relatively low costs ($10s USD per sample compared to $100s to 1000s per acoustic or satellite tag, respectively). Nevertheless, there are some caveats that have hindered wider use of this approach.

Spatial applications of stable isotope tracers require *a priori* knowledge of the spatial distribution of stable isotope ratios (frequently presented as a spatial model or 'isoscape,' West et al., 2009). Constructing isoscape models from geographically referenced samples is logistically challenging, especially in offshore marine environments, and relatively few sample-based, marine isoscape models have been constructed (Revill et al., 2009; St. John Glew et al., 2019). Moreover, isotopic compositions of baseline organisms in marine systems are likely to be spatio-temporally dynamic, especially in temperate regions with broad temperature shifts. Therefore, isoscapes created from single sampling events may not describe isotopic gradients expressed in consumer organisms across seasons.

In pelagic marine environments, phytoplankton δ^{13}C values are primarily influenced by the concentration and isotopic composition of dissolved inorganic carbon, and phytoplankton taxonomy and growth (Rau et al., 1982), which strongly covary with temperature and thus latitude. The isotopic fractionation of carbon during photosynthetic fixation by phytoplankton facilitates developing mechanistic biogeochemical models that predict spatio-temporal variations in oceanic phytoplankton δ^{13}C values with reasonable accuracy and precision (e.g., Magozzi et al., 2017). Mechanistic models predicting δ^{15}N values have also been developed (Somes et al., 2010), and regional foraging models have been designed around this isotope (Madigan et al., 2016). However, there is some uncertainty around trophic correction factors of δ^{15}N values for higher-order predators (Olin et al., 2013). This means that the decision to use either δ^{15}N or δ^{13}C models to construct isoscapes will be system or species dependent. Extending mechanistic models predicting isotopic compositions of primary production to observed isotopic compositions of higher trophic level animals is complex. Such models require assumptions of the isotopic effects associated with trophic discrimination factors and food web structure (Bird et al., 2018).

Consequently, while stable isotope methods are an attractive tool for inferring the spatial ecology of marine consumers, as for all ecological modeling, the confidence placed in any inferences depends on the quality of the reference dataset. The relative differences in reference isotope data produced by mechanistic or sample-driven approaches are not well understood, with both methods suffering from either logistical or theoretical limitations. Mechanistic approaches often target low trophic level organisms (plankton or planktivores) (Magozzi et al., 2017) while sample-driven approaches typically capture higher-order predators (Logan et al., 2020), making the two approaches difficult to compare.

Sample-driven isoscape approaches require relatively intensive sampling efforts and are typically only feasible for studying commercially important taxa such as tunas (e.g., Logan et al., 2020). Species that are only sporadically caught or have low commercial value will rarely justify the sampling efforts needed to construct reliable two-dimensional spatial isotope models. For these species, alternative sample-driven approaches, relying on more easily sampled indicator species to construct a reference dataset may be more appropriate, although creating bespoke isoscape models can be logistically challenging (St. John Glew et al., 2019). Nevertheless, where spatial variation in one or more stable isotopes is largely defined by latitudinal gradients, one-dimensional linear models may be sufficient to identify likely latitudinal foraging. However, it is important to acknowledge that in coastal or neritic waters, latitudinal variation of δ^{13}C values may be overpowered by broader isotopic signatures from sources of productivity like macrophytes or marine plants (Hill et al., 2006; Raoult et al., 2018) and from inshore-offshore gradients (Kopp et al., 2015). This could mean latitudinal influences on δ^{13}C values of coastal organisms are more difficult to detect than in pelagic environments—without extensive sampling to account for the range of coastal influences.

Assuming trophic enrichment of stable isotopes can be corrected mathematically, any relatively sedentary species can be used to construct sample-driven, latitudinal models provided they are collected in large enough numbers from a range of habitats and locations that account for the possible range in coastal influences. In parallel, using a global oceanic biogeochemical reference model grounded with localized regional targeted sampling could help extrapolate patterns to broader areas while validating the accuracy of the mechanistic model, and incorporate some of the uncertainty surrounding coastal influences on marine δ^{13}C values. The result would potentially greatly reduce the cost of creating isoscapes while providing justification for using mechanistic approaches that extend beyond sampling areas.

Here we draw on both sample-driven and mechanistic approaches to generate reference isoscapes to infer regional geographic ranges in a high-trophic level and globally threatened (listed as Critically Endangered; Rigby et al., 2019) migratory marine consumer: the great hammerhead (*Sphyrna mokarran*). Genetic studies on *S. mokarran* indicate they perform widespread migrations across territorial waters (Guttridge et al., 2017), which makes identifying their geographic range necessary to prioritize effective conservation areas. Off eastern Australia, *S. mokarran* is caught by bather-protection gillnets (Sumpton et al., 2011; Broadhurst and Cullis, 2020) and fisheries (Roff et al., 2018) in diminishing relative abundances from Cairns, North Queensland (∼17°S) to Woolongong, New South Wales (NSW) (∼34°S) (Raoult et al., 2019). Their apparent rarity off NSW has led to *S. mokarran* being regionally listed as Vulnerable (Rigby et al., 2019). However, there is a possibility that NSW waters are not part of the core geographic range for this species, and that much of the population spends most of their lives in more northern waters. Deciphering the predominant habitat range and migration of *S. mokarran* off south-eastern Australia may facilitate more precise conservation-status assessments. The paucity of catches in NSW waters along with a very high discard mortality (Broadhurst and Cullis, 2020) complicates tagging studies that can address this lack of data, although collections of tissue samples obtained from bather-protection programs are available.

Our objective was to determine the geographic range of *S. mokarran* off NSW, Australia, using stable isotope data obtained from specimens caught in bather-protection gillnets. We assessed whether captured specimens were residents to this area, or whether their core geographic range was more northern than NSW. Our specific aims were to create and compare isoscapes using (i) a sample-driven approach that relied on targeted fish sampling from local commercial fisheries and on zooplanktivore sampling from coastal reefs and could only examine latitudinal patterns, and (ii) a mechanistic approach using a global biogeochemical model that could examine both longitudinal and latitudinal patterns. As a synthesis, we provide a framework for using similar approaches to determine the geographic ranges of other wide-ranging species.

MATERIALS AND METHODS

Sampling

Muscle tissue samples were collected from 27 *S. mokarran* caught as bycatch in bather-protection gillnets deployed off Ballina/Evans Head (28.77° S, 153.60° E to 29.10° S; 153.44° E, *n* = 25) and Newcastle (31.25° S, 146.92° E, *n* = 2), NSW during summer and autumn, 2018 (see Broadhurst and Cullis, 2020 for a description of the gear; **Figure 1**). These muscle samples were the same as those used and described in Raoult et al. (2019).

Geo-located reference isoscape fish samples were used to constrain latitudinal gradients in consumer δ^{13}C values and were obtained from various sources during austral summers between 2011 and 2018. Fisheries-caught species mostly consisting of fishes but including some cephalopods were purchased directly from fishing co-operatives in January 2018, and only locally landed species (waters adjacent to the fishing co-operative) were included. All operational NSW co-operatives were sampled between Ballina (28.87° S, 153.58° E) and the New South Wales – Victoria border (37.07° S, 149.89° E). Research trawl samples were also obtained off eastern Tasmania (41.25° S, 148.34° E) from the University of Tasmania's *FV Bluefin* using a demersal trawl at depths of ∼80 m on the continental shelf in 2016. Reef manta ray (*Mobula alfredi*) stable isotope values from muscle tissues were obtained from North Stradbroke (27.40° S, 153.53° E) and Lady Elliot islands (24.11° S, 152.71° E) in southern Queensland from Couturier et al. (2013), sampled in 2011 and 2012. Planktivorous reef fishes were captured in a separate juvenile fish survey in 2017 and 2018 from the southern end of the Great Barrier Reef to the New South Wales – Victoria border (Kingsbury et al., 2020). In general, the fishes selected to create the isoscape were considered likely to be feeding from pelagic food webs and were unlikely to be undertaking large annual north/south migrations. Relatively few species were available that fit both criteria, and to create a suitable reference dataset, we sampled across a wide latitudinal range and included a broad range of species at different life history stages. We corrected for potential trophic enrichment effects on δ^{13}C values using the approach outlined below.

Stable Isotope Analysis

Approximately 1-g samples of muscle tissue indicative of yearly resource use (Malpica-Cruz et al., 2013) were extracted from *S. mokarran* and the fishes obtained from fishing co-operatives and placed onto individual HCl-cleaned glass petri dishes. Samples were dried at 60°C for at least 48 h, then ground into a fine powder using a Retsch MM200 ball mill[1]. *Sphyrna mokarran* samples were lipid- and urea-extracted to prevent those components from affecting stable isotope values (Carlisle et al., 2016), as per the methods described in Raoult et al. (2019).

Adjusting Stable Isotope Values for Trophic Enrichment and Lipid Content

High lipid content in muscle tissues can affect δ^{13}C values (Shipley et al., 2017). As a result, all fish samples, excluding lipid

---

[1] www.retsch.com

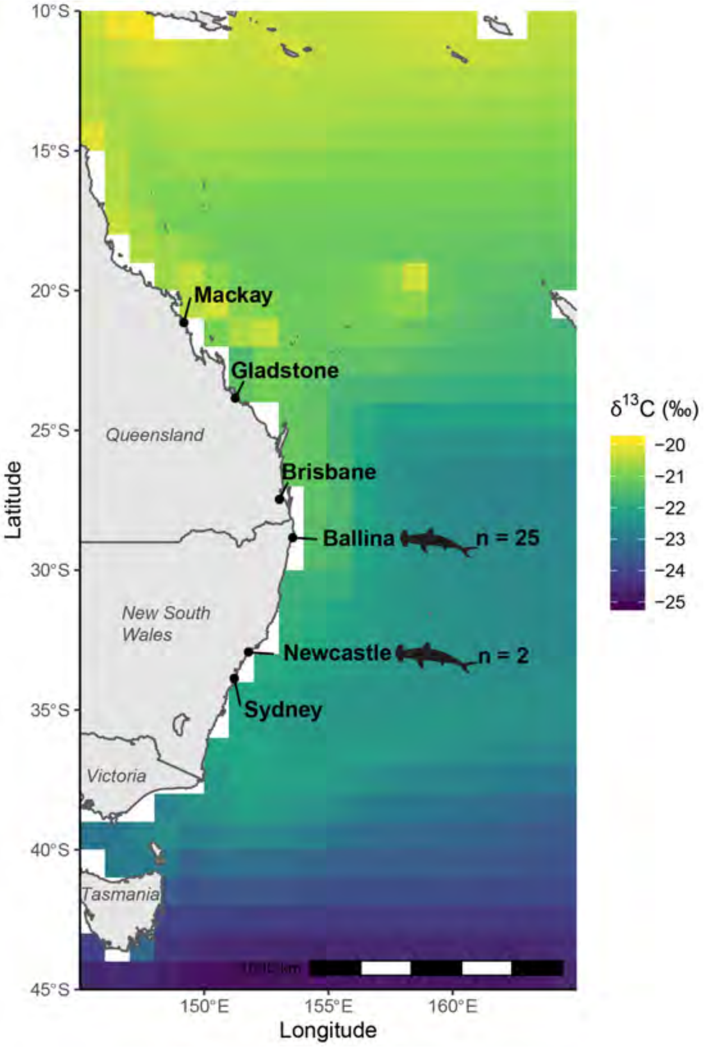

FIGURE 1 | Modeled, biomass-weighted annual median $\delta^{13}C$ values of oceanic phytoplankton off eastern Australia per degree of latitude extracted from NEMO-MEDUSA framework, which predicts stable isotope values from modeled sea surface temperature, dissolved inorganic carbon content and isotopic composition and phytoplankton biomass and growth rates. Locations where great hammerhead shark (*Sphyrna mokarran*) samples were collected are indicated by shark outlines.

and urea-extracted *S. mokarran* tissues with C:N ratios > 3.5 (indicative of high lipid content), were mathematically corrected using the equation from Post et al. (2007).

Stable isotopes of carbon are typically enriched at higher trophic levels. Since our data comprised various species that were likely feeding at different trophic levels, it was first necessary to correct for confounding effects. To achieve this, we constructed the formula using the widely accepted relationship of enrichment of $\delta^{13}C$ values with $\delta^{15}N$ values (Caut et al., 2009):

$$\delta^{13}C_{corrected} = \delta^{13}C_{measured} - \left(\frac{\delta^{15}N_{measured} - \delta^{15}N_{min}}{\Delta^{15}N}\right) \times \Delta^{13}C$$

Where $\delta^{13}C_{corrected}$ is the $\delta^{13}C$ value adjusted for trophic enrichment, $\delta^{13}C_{measured}$ is the $\delta^{13}C$ value from the muscle sample of a fish, $\delta^{15}N_{measured}$ is the $\delta^{15}N$ value of the same sample, $\delta^{15}N_{min}$ the lowest $\delta^{15}N$ value across all samples in the data set, $\Delta^{15}N$ is the ^{15}N diet-tissue discrimination factor for that type of fish, and $\Delta^{13}C$ is the ^{13}C the diet-tissue discrimination factor for that same fish. For fishes in this data set, a mean (±SD) $\Delta^{15}N$ of 2.5 ± 1.1‰ $\Delta^{13}C$ of 1.8 ± 1.2‰ was used (Caut et al., 2009). Squid $\Delta^{13}C$ of mantle tissue is approximately 0‰ (Hobson and Cherel, 2006), so no transformations were applied. Transformed values that had $\delta^{13}C$ values more enriched than −18‰ could indicate possible feeding on benthic algae (Fry et al., 1983; Frédérich et al., 2009; Greenwood et al., 2010; Eurich et al., 2019), however, removing extremes of values would create bias in the following model. To adjust for this, we pre-emptively removed highly enriched $\delta^{13}C$ values > −14‰ before analyses.

The $\delta^{13}C_{corrected}$ values were corrected to the trophic level of a coral reef planktivore, which meant these were still enriched relative to true phytoplankton isotopic values. The difference between exclusive zoo- and phyto-planktivore δ^{13}C values and particulate organic matter (POM) is typically ~1–2‰ according to planktivore-specific studies (Frédérich et al., 2009; Greenwood et al., 2010). To allow comparison of these results with modeled NEMO-MEDUSA values (see below), all sample-driven $\delta^{13}C_{corrected}$ values had 1.5‰ subtracted to reflect this plankton-planktivore enrichment.

For *S. mokarran*, elasmobranch-specific discrimination factors for lipid-extracted muscle were used with a mean (±SD) $\Delta^{15}N$ of 2.8 ± 0.3‰ and $\Delta^{13}C$ of 1.2 ± 0.4‰ (Hussey et al., 2010). However, there is uncertainty in these values, and diet-tissue discrimination factors are known to affect stable isotope models (Bond and Diamond, 2011). Further, while the sample size of *S. mokarran* (n = 27) was relatively large for elasmobranch studies, our sampling distribution may not reflect the true distribution of the population. To account for both uncertainty in diet-tissue discrimination factors and population size, we employed a Monte Carlo Markov Chain (MCMC) approach incorporating the variability of the discrimination factors as in Hussey et al. (2010) (0.3‰ for $\Delta^{15}N$ and 0.4‰ for $\Delta^{13}C$) to calculate the $\delta^{13}C_{corrected}$ in the formula above. The distributions of each discrimination factor were modeled assuming a normal distribution with 1,000 samples, and we ran 10,000 simulations. Resulting δ^{13}C values had 1.5‰ subtracted from them to align with the sample-driven data. The result should provide a broad, conservative estimate of the distribution of the δ^{13}C values in the sampled population of *S. mokarran*.

Modeling Relationships Between Reference δ^{13}C Values and Latitude

We used a general additive model (GAM) framework using the package mgcv (Wood and Wood, 2015) in *R* to model the relationship between trophic enrichment and lipid-corrected δ^{13}C values in referenced fish and squid data ($\delta^{13}C_{fish}$) and latitude. We fitted corrected $\delta^{13}C_{fish}$ values as the response variable using a smoothing term with latitude as the predictor and five nodes. This number of nodes was chosen because increases did not significantly improve model fit (R^2 increase < 0.05), while creating apparent overfit with nodes at each location where samples were collected. While we did not achieve an empirically ideal model using diagnostic criteria such as estimated degrees of frequency relative to k-values, we are confident that the number of nodes chosen was high enough to detect major trends without over-fitting the model.

Median, biomass-weighted annual modeled phytoplankton δ^{13}C values ($\delta^{13}C_{plk}$) were generated from NEMO-MEDUSA biogeochemical model output as described in Magozzi et al. (2017), extracting $\delta^{13}C_{plk}$ values from the three degrees of longitude closest to the Australian coastline. Modeled $\delta^{13}C_{plk}$ values were used in a similar fashion as the measured fish and squid reference data. A GAM was used to assess the relationship between modeled $\delta^{13}C_{plk}$ values and latitude. The aim was not only to determine the core geographic range of *S. mokarran* across a greater latitudinal and longitudinal range, but also to determine whether the mechanistic model aligned with patterns detected in the field-sampled data. Incorporating uncertainty into latitude and longitude bins produced by the mechanistic approach is important to align with the sample-driven technique, however, global models typically have no reliable way of estimating uncertainty (Cooter and Schwede, 2000). To provide a more conservative estimate, we used the mean residual distance of the NEMO-MEDUSA data from the mechanistic GAM for each longitude and latitude bin. Larger confidence intervals would likely only extend the possible area where these sharks would occur, rather than change the geographic center of the area, so this approach is largely insensitive to the chosen confidence interval for this step.

Predicting *Sphyrna mokarran* Latitudinal Range From Reference Data

Latitudes corresponding to the 1,000 MCMC modeled *S. mokarran* δ^{13}C values were estimated using the two GAM models linking latitude to $\delta^{13}C_{fish}$ and $\delta^{13}C_{plk}$ values. We partitioned the simulated $\delta^{13}C_{shark}$ data into bins corresponding to 1° latitudinal ranges, where the minimum and maximum δ^{13}C values corresponded to the lower and higher 95% confidence intervals of the GAM produced from the sample-driven reference isoscape ($\delta^{13}C_{fish}$). The partitioning was such that any given modeled *S. mokarran*δ^{13}C value could have multiple 'bins' where it could occur due to the bin width, thus producing a 'range' of possible geographic locations for a single datum. The resulting cumulative counts of the number of modeled sharks assigned to each specific latitude were then transformed into proportions relative to our modeled population. We assumed that likely modeled population peak areas that made up ~50% of the total population comprised the core habitat for the sampled population.

For both GAM models, multimodal distributions that may occur are assumed to be an artifact of the GAM pattern that can create two or more solutions for one sample depending on the number of nodes. A solution to this problem is to assume the modal peak furthest from the site the animals were caught is the least likely to be the 'true' habitat, and to ignore that distribution. Where prior data are available on habitat use of the species (i.e., no use of open ocean/pelagic only and tropical/temperate preference) these can also be used to inform on the validity of the model outputs. These are, of course, open to interpretation, which is why we present the raw model outputs here to highlight that the results of this approach need to be transparent to inspire confidence in the implications.

Cross-Checking of Validity of Models

A risk when producing models on a single study species is that the observed and apparently valid model patterns may be a coincidence brought on by the selected parameters. To determine whether our method could be applied more broadly to other species, we then followed the pattern identical to the above but using data from sharks with habitat distributions inferred from catch data: the southern sawshark (*Pristiophorus nudipinnis*) and common sawshark (*P. cirratus*). Both species were combined as '*Pristiophorus* spp.' because their fisheries data are not reliably differentiated. These mesopredators are primarily found in south-eastern Australia near Bass Strait (Raoult et al., 2020) and on the coastal shelf and slope. Data from Raoult et al. (2015) ($n = 49$) were supplemented with other samples obtained from the same trawls used for sample-driven samples ($n = 9$). For these species we used the diet-tissue discrimination factor of muscle from leopard sharks (*Triakis semifasciata*), which have a benthic lifestyle similar to *Pristiophorus* spp., on a fish-based diet from Kim et al. (2012) ($\Delta^{15}N$ of 5.5 ± 0.4‰ and $\Delta^{13}C$ of 3.5 ± 0.6‰). Low C:N ratios (<2.5) suggest possible urea impacts. Since urea was not extracted from these tissues, urea is likely depleting δ^{15}N values by ∼0.8‰ (Carlisle et al., 2016). We therefore added 0.8 ± 0.2‰ to δ^{15}N values to compensate and included this uncertainty within the MCMC framework described above. We expected that the core latitude range identified using this approach should broadly align with known habitat distributions, which would provide some clarity as to the ubiquity of the approach.

RESULTS

In total, 681 specimens were used to constrain reference consumer $\delta^{13}C_{fish}$ values and produce a latitudinal relationship (**Supplementary Table 1**). Modeled $\delta^{13}C_{plk}$ values increased from the south to the north off eastern Australia, with higher values associated with coastal regions north of the New South Wales – Queensland border (**Figure 1**). This pattern was followed by consistent δ^{13}C values along the NSW coastline, before values rapidly depleted south of the New South Wales – Victoria border.

Descriptive Models of Field-Sampled and Modeled δ^{13}C Values

General additive models summarizing the spatial variation in $\delta^{13}C_{fish}$ values detected a significant effect for the smoothed latitude term (edf = 3.99, $F = 2302$, $p < 0.001$) corresponding to higher $\delta^{13}C_{fish}$ values toward the equator. Across the latitudinal gradient, the GAM predicted a break in the positive relationship between latitude and $\delta^{13}C_{fish}$ values between ∼37 and ∼32°S (**Figure 2**). The deviance explained for this GAM was 29.4%, reflecting the broad distributions of points. The GAM for the mechanistic model $\delta^{13}C_{plk}$ data detected similar effects for the latitudinal smoothing term (edf = 3.98, $F = 744$, $p < 0.001$) and the broad pattern agreed approximately with the GAM informed from independent field-sampled consumer $\delta^{13}C_{fish}$ values, with differences in δ^{13}C values generally < 1, and no greater than 1.5 (**Supplementary Figure 1**). The main differences between the two models was that $\delta^{13}C_{fish}$ values increased dramatically north of 30°S. As expected for outputs from a relatively simple mechanistic model, the GAM explained a high proportion (96.8%) of the deviance in $\delta^{13}C_{plk}$ values with a low mean residual distance of 0.2‰.

Predicted Habitat Range of *Sphyrna mokarran*

The likely latitude of foraging estimated for the modeled population for *S. mokarran* using field sampled $\delta^{13}C_{fish}$ values as the reference had a normal distribution, with nearly 80% of the population situated between 26°S and 18°S, which was the northern-most extent of where sample-driven data were collected. The highest proportion of the population was near Gladstone, Queensland (**Figure 3**). In comparison, while the mechanistic model also suggests the *S. mokarran* geographic range was north of capture locations, the core geographic range was concentrated north of 15°S (**Figure 3**).

The likely latitude of foraging estimated for the modeled population for *S. mokarran* using mechanistically modeled $\delta^{13}C_{plk}$ values as the reference was concentrated north of the NSW/Queensland border and probably extended further north than 10°S (**Figure 4**). The largest proportion of the population was measured along the coast of Queensland, and at 12°S, which broadly extended east and west at those latitudes and decreased north of this. It also extended east from 20°S with a relatively high proportion near the Des Belona plateau west of New Caledonia.

Cross-Checking of Validity of Models

Previous work (Raoult et al., 2020) indicated that core *Pristiophorus* spp. habitat (where highest abundances and records are recorded) is on the north-east side of Bass Strait near the Victoria – New South Wales border (∼37°S) (**Supplementary Figure 2**). The field sampled model suggested a concentration around Bass Strait (40°S), providing the second peak more north than 30°S is ignored (**Supplementary Figure 3**). The NEMO-MEDUSA modeling agreed with the sample-based approach, with the highest proportion of modeled population at 40°S and decreasing rapidly north of 37°S (**Supplementary Figure 4**).

DISCUSSION

Both the sampling-based and mechanistic (NEMO-MEDUSA) approaches used in this study support a hypothesis that the sampled *S. mokarran* caught in NSW bather-protection gillnets off in south-eastern Australia relied on food resources obtained further north off eastern Australia. And the species is likely only present in south-eastern Australian waters during the warmer summer/autumn months. If so, there may be no permanent resident population of *S. mokarran* in NSW waters, and any *S. mokarran* observed in this area are likely to be seasonal vagrants that fed primarily in Queensland waters.

Such wide latitudinal movements among *S. mokarran* support known migrations across other areas of the species distribution (especially in the Atlantic Ocean), and are similar to those recorded for regional carcharhinids such as the bull shark (*Carcharhinus leucas*) (Lee et al., 2019), and for the reef manta ray (*M. alfredi*) (Couturier et al., 2011). These movements may reflect physiologically driven preferences for sub-tropical and tropical water temperatures, which in the austral summer come with abundant inshore food sources such as schooling Australian cownose rays (*Rhinoptera neglecta*) (Tagliafico et al., 2020). This hypothesis aligns with the mechanistic model for Australian *S. mokarran*, which suggests a geographic range as far north as 10°S. Certainly the species is occasionally recorded

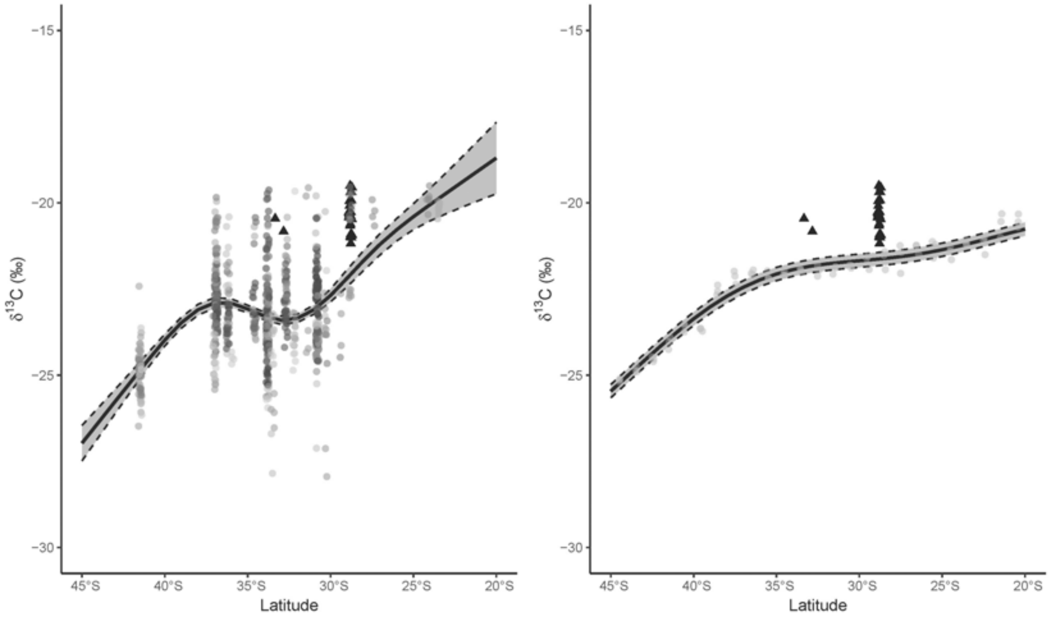

FIGURE 2 | Relationship between latitude and δ^{13}C values calculated from (left) trophic enrichment-adjusted values of fishes and cephalopods (only mean individual values displayed, species in colors) collected along the east coast of Australia (black dashed lines indicate 95% confidence interval around the model), and (right) the comparable range of yearly mean coastal $\delta^{13}C_{plk}$ values from the NEMO-MEDUSA data. Different species used to calculate the relationship indicated in different colored circles, and great hammerhead shark (*Sphyrna mokarran*) mean individual trophic enrichment-adjusted values are indicated in black triangles along with their associated latitude at capture.

in catches of baited drumlines off Cairns (17°S) (QLD shark control data, 2020[2]).

While it is possible that some of the geographic range determined here could be at least be partially affected by prey species feeding at a higher latitude, the sporadic records of *S. mokarran* during the austral summer in NSW suggest the observed patterns are real. Targeted sampling of *S. mokarran* within the northern end of the geographic range near Cairns, QLD (identified as 'core' here) should help validate whether the inferences drawn are correct. Given the ongoing fisheries pressures on this species in this population's eastern Australian core geographic range off Queensland (Roff et al., 2018), we suggest inter-state cooperation is necessary to address the above shortfalls and to collaboratively protect *S. mokarran* throughout its eastern Australian distribution.

Methodological Considerations

The outputs of the two methods produced different patterns, but both suggested that south-eastern Australia was not a core habitat for *S. mokarran*. The sample-driven approach implied a more constrained range, while the mechanistic approach suggested a range that started at a similar latitude, but extended further north, with peak density distributions of the populations that were ∼6° different. When applying the approaches to more southerly *Pristiophorus* spp., both aligned well with the known distributions of the species—provided open-ocean patterns that extend north and east of 30°S and 155°E, respectively, are ignored, since *Pristiophorus* spp. only occur in south-eastern Australia on the continental shelf or slope.

One possible common factor precluding the complete alignment of methods for both *S. mokarran* and *Pristiophorus* spp. was the low number of baseline samples at the extreme distributions of the models (north and south), which would increase sensitivity for error. In such cases, the outputs from the mechanistic model may be more reliable until broader datasets are obtained.

Notwithstanding the above, either the mechanistic or sample-driven approaches could be used to determine the broad geographic range of captured populations of both species. Using a single-axis (i.e., latitudinal), sample-driven approach that does not account for longitudinal variation was sufficiently informative and able to answer the research question with a coastline that aligns with latitudinal change in δ^{13}C values, while costing considerably less to produce than an approach that would include longitudinal data.

Despite the utility of our approach, there are several assumptions that need to be considered when interpreting the results and extending to other species. In particular, ^{13}C stable isotope ratios are primarily driven by diet rather than geographic location, with terrestrial, coastal, and neritic (macrophyte, phytoplankton, saltmarsh, and seagrass) sources all having distinct carbon values as a result of different photosynthetic pathways (Raoult et al., 2018) across a greater isotopic range (∼20‰) than other factors such as depth and latitude (McMahon et al., 2013). This means that for studies aiming to extract a

---

[2] https://www.daf.qld.gov.au/__data/assets/excel_doc/0013/300064/shark-catch-stats-2001-to-dec2016.xls

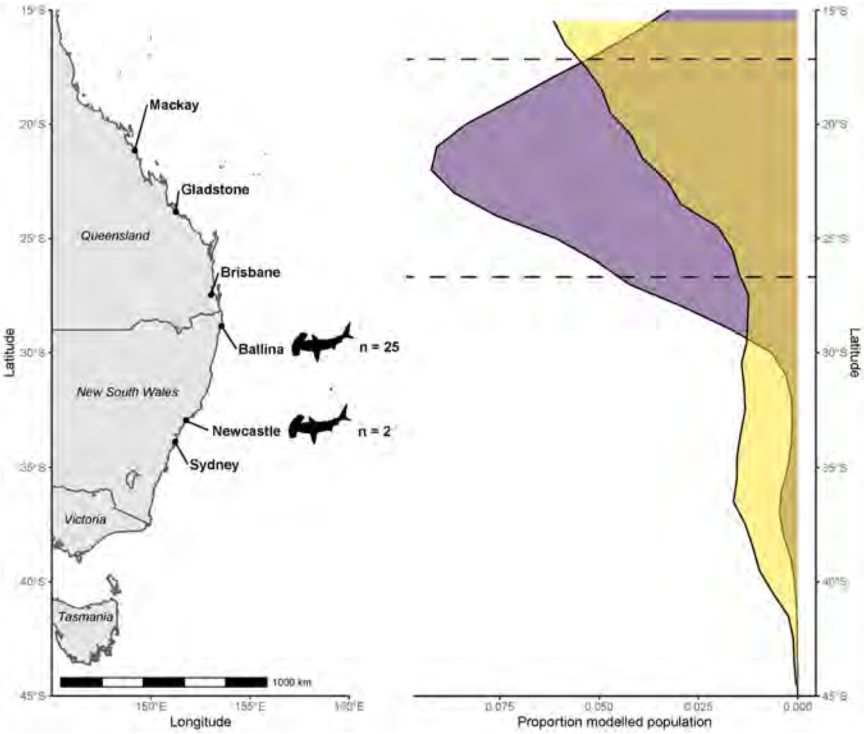

FIGURE 3 | Modeled population geographic range of coastal great hammerhead sharks (*Sphyrna mokarran*) inferred from $\delta^{13}C$ stable isotope values of their muscle tissues, and those from the various marine fish species, used to produce a latitude - $\delta^{13}C_{fish}$ value relationship (purple). Corresponding modeled population density from the mechanistic NEMO-MEDUSA data shown for comparison (yellow). Dashed lines indicate latitudes that contained nearly 80% of the modeled population from the sample-driven model. Locations where great hammerhead shark samples were collected are indicated by shark outlines.

geographic signal from stable isotope values, data will inherently have wide variability because of individual patterns in diet and space use, especially for species that occupy coastal areas. The variability of the sample-driven data for a single species at a single latitude are evidence of these effects. However, by incorporating large data sets as in the present study and others (Bird et al., 2018; Logan et al., 2020), it is possible to decipher the underlying geographic patterns at useful levels of spatial resolution, especially on a continental-scale latitudinal plane where the spatial variation of ^{13}C stable isotope ratios is more easily detected.

Studies seeking to use this model in Australia or replicate the approach elsewhere should consider that species relying on estuarine or terrestrial productivity (like *C. leucas*) might not be appropriate focal subjects. For such species that rely on estuarine productivity, it is likely that localized primary producers will have a greater influence on $\delta^{13}C$ values than phytoplankton-derived productivity and their latitudinal patterns. Where coastal species are the focus (as in this case), larger sampling populations for both the focal species and the sampling-based model should be obtained to ensure that coastal variability is adequately assessed. The similarity of the sample-driven model we produced from coastal species to those produced from pelagic sources obtained previously in the same area (Revill et al., 2009) provides evidence that latitudinal coastal stable isotope patterns are not dissimilar from pelagic ones, and that latitudinal variation can be measured from coastal species on sufficiently large scales. We also draw on results of Bird et al. (2018) who showed (using a global compilation of $\delta^{13}C$ data from sharks tissues) that the $\delta^{13}C$ values of muscle tissues in coastal and neritic sharks do indeed follow latitudinal gradients predicted and measured in phytoplankton, implying that overall, phytoplankton provide the majority of carbon fueling food webs leading to coastal shark production. Thus, while coastal productivity likely influences $\delta^{13}C$ values of study species as well as species used for sample-driven models, it should still be possible to infer data from phytoplankton-based models if researchers are aware of these possible influences.

The eastern coastline of Australia is a challenging geographic area in which to apply this approach because the poleward-flowing East Australian Current strongly impacts annual patterns in $\delta^{13}C$ values. Consequently, the presence of detectable patterns implies that our approach should be even more successful in other parts of the world with less dynamic circulation. More specifically, the patterns for both our mechanistic and sample-driven approaches were similar to previous attempts at sample-driven approaches obtained from a broad suite of consumers collected further offshore (Revill et al., 2009), indicating that such an approach would be repeatable and reusable on decadal scales. Similarly, the use of diet-tissue discrimination factors to correct for isotopic enrichment with trophic level has uncertainty, which we addressed using MCMC simulations. Due to the low relative difference between low and high latitude $\delta^{13}C$ values (7‰ across

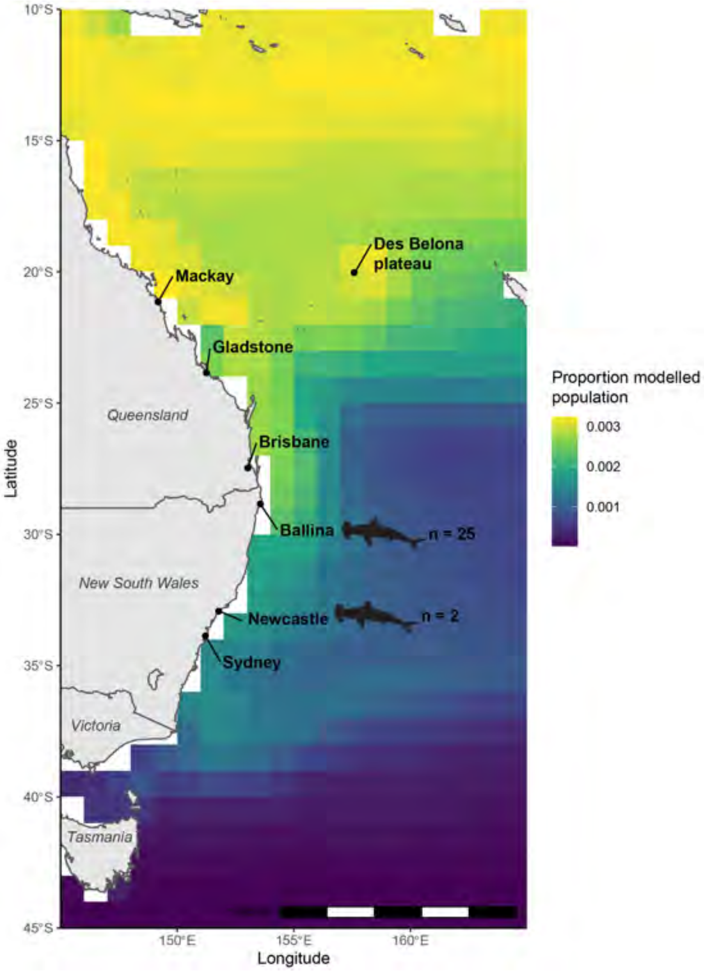

FIGURE 4 | Modeled population geographic range of great hammerhead sharks (*Sphyrna mokarran*) inferred from $\delta^{13}C$ stable isotope values of muscle tissues of great hammerhead sharks and biomass-weighted annual median $\delta^{13}C_{plk}$ values of oceanic phytoplankton extracted from NEMO-MEDUSA framework. Locations where great hammerhead shark samples were collected are indicated by shark outlines.

25° of latitude or approximately 2700 km), we also reiterate that this approach cannot be used to infer fine-scale (<1° of latitude) geographic location. Rather, as in this study, interpretations are limited to answering questions on broad geographic ranges such as the direction (north, south, east, west) of the habitat relative to capture point.

Multimodality of modeled geographic ranges can occur as indicated here, implying the possibility of more than one geographic habitat for one sample population. Multimodality could be driven by individual preferences in diet, which has been identified in *S. mokarran* and other elasmobranchs (Matich et al., 2011; Raoult et al., 2019)—although larger sampling sizes should reduce the likelihood of multimodality with this approach. We suggest assuming core habitat ranges should be connected to the nearest identified core habitat, and to discount other detected habitats as possible artifacts. If biological information is available for the species (i.e., limits of thermal tolerances or bathymetry links) these data can be used to refine the modeled outputs. For example, in our case it is unlikely that some of the population extends southeast into the Pacific Ocean as the model suggests since those water temperatures are likely outside of physical tolerances for this species, although *S. lewini* has been known to dive periodically to waters at ~5°C (Jorgensen et al., 2009). For species for which there is little biological information available, outputs may be less reliable if multimodal distributions are apparent. If researchers using this approach are aware of such limitations, then this method is robust for determining core geographic range on a broad scale for many wide-ranging marine organisms.

Beyond methodological considerations, projects attempting to use similar approaches to examine the geographic patterns of other species should be aware of some of the broader issues we encountered. For example, extrapolating geographic ranges for species that may occur beyond the sample-driven latitudinal range (further north of 20°S in our case) can lead to greater uncertainty. In those instances, we recommend researchers compare their sample-driven patterns to those from the NEMO-MEDUSA data or source samples from latitudinal extremes in the published literature. The model presented here does not account for known habitat preference (like bathymetry) that would otherwise be constraining, and the results should be interpreted accordingly. Ideally, those replicating the approach would incorporate known habitat ranges into the model to constrain results more appropriately. We highlight that the strength of our approach is the ability to use bulk muscle stable isotope values to populate the sampling-based relationship from various species of sources, provided individual sample %C and %N (to correct for lipids) data are available. In our instance there were very few usable data from north of Gladstone, Queensland, which led to a steep extrapolation of $\delta^{13}C$ values that might not be valid. Other studies conducted in areas that have been more broadly sampled historically (i.e., the north Atlantic) may be able to rely on previous work more readily (Le Loc'h et al., 2008).

Appropriate thought needs to be given to the temporal scale being studied, as marine productivity varies seasonally, interannually, and gradually with climate (Gonzalez-Rodriguez, 1994; San Martin et al., 2006; Shen et al., 2015). The use of higher trophic level animals should result in long temporal averaging of signals through food chains associated with addition of turnover rates. Any seasonal variability in carbon source $\delta^{13}C$ values will thus be strongly attenuated through food chains and in animals with slow isotopic assimilation rates. Tissue selection for both target species and sample-driven isoscape creation will also relate directly to the interpretations that can be extracted from this approach. The isoscape designed here used muscle primarily because it has approximately annual turnover rates, depending on the age class of the sampled animals (Kim et al., 2012). Since the objective here was to determine long-term geographic range, tissues with longer turnover like muscle or cartilage (Malpica-Cruz et al., 2012) were preferable. Turnover rates of the mechanistic and sampling-based isoscapes also need to be examined across similar temporal scales as the target population. In our case, we examined annual means in the mechanistic model to align with muscle tissue selection. If researchers wanted to study short-term patterns, they could sample tissues that turn over rapidly like blood or liver, and adjust mechanistic models accordingly. However, we recommend longer turnover tissues like muscle may provide more robust results that will average localized changes in productivity that would otherwise affect results.

Appropriate consumer tissue preparation prior to these approaches is critical. Urea and lipids affect $\delta^{15}N$ and $\delta^{13}C$ values (Carlisle et al., 2016), and these patterns are difficult to accurately correct for using mathematical approaches (Shipley et al., 2017). Incorporating uncertainty (e.g., with MCMC approach) in diet-tissue discrimination factors that account for lipid and urea effects helps alleviate this issue, but results would still be centered based on the mean of these values, which may not be appropriate for the study species. We strongly suggest that lipid and urea extractions are conducted on all bulk tissues used for geographic range calculations to reduce the uncertainty that can result from these effects.

When selecting species to target for sampling-based reference isoscape creation, we initially assumed that juvenile zooplanktivorous fishes (e.g., *Abudefduf* spp.) would provide a more reliable signal than fishes at higher trophic levels. However, after examining the stable isotope values from multiple local studies it was apparent that some of the northernmost values from the southern Great Barrier Reef were likely feeding on turf algae rather than plankton, and these data were excluded from the analyses. We therefore recommend comparing corrected $\delta^{13}C_{fish}$ values to geographically similar turf algae and plankton values where possible to help inform the sampling-based data in this way. Signal noise in juvenile planktivorous fishes could also be caused by rapid (<20 days) tissue turnover (Weidel et al., 2011), which could reflect seasonal stable isotope values rather than the yearly values recorded in larger, slower growing fishes. Of note, even tertiary predators like flathead *Platycephalus* spp. and pink snapper *Pagrus auratus* provided useful reference information, which suggests that targeted species can be from broad trophic ranges, provided these species have relatively constrained geographic ranges. Validating the outputs from this approach would, however, strengthen its reliability for management, and this could be done by consistently sampling species with known restricted habitat ranges along the coast.

Notwithstanding the stated caveats, clearly mechanistic isoscape models such as the NEMO-MEDUSA isotope extension (Magozzi *et al.,* 2017) can be used to infer spatial influences on isotopic variation in measured samples and therefore geographic distributions (e.g., Bird et al., 2018; Trueman et al., 2019). To use this approach, calibration is crucial between the mechanistic isoscape and the study samples. This calibration must consider isotopic effects associated with trophic enrichment, tissue composition, and time averaging. Accounting for these issues is not trivial, and we recommend that mechanistic models are not used in isolation to infer geographic assignments. Rather, the isotopic composition of geo-referenced field samples (using the broad reference species approach outlined here) should be used to first determine appropriate calibrations. Such an approach would still be comparatively low-cost relative to large tagging programs, especially since the data can be re-used for different species.

DATA AVAILABILITY STATEMENT

The original contributions presented in the study are included in the article/**Supplementary Material**, further inquiries can be directed to the corresponding author/s.

ETHICS STATEMENT

The animal study was reviewed and approved by the New South Wales Animal Care and Ethics Committee (NSW ACEC ref. no. 06/08).

AUTHOR CONTRIBUTIONS

VR, CT, VP, MB, JW, and TG conceived the study. VR conducted the fieldwork and sample analysis. KK, BG, DB, IN, and LC provided the additional data and advice on analyses. VR and CT analyzed the results and wrote the initial draft. VR, CT, VP, MB, JW, TG, KK, BG, DB, IN, and LC wrote the follow up draft, provided feedback for additional analyses, and general improvements. All the authors contributed to the article and approved the submitted version.

FUNDING

This research was part-funded through a grant from the Sea World Research and Rescue Foundation (SWRRFI) to VR, VP, TG, and JW, and from the NSW Department of Primary Industries. The sampling and stable isotope analysis of the zooplanktivorous fish samples was supported by an Australian Research Council Discovery grant (DP170101722) to IN, DB, and BG. Manta ray sampling and isotopic analyses were funded by the Australian Research Council Linkage Grant (LP110100712), Earthwatch Institute Australia, Sea World Research and Rescue Foundation Inc., Lady Elliot Island Eco Resort and Manta Lodge and Scuba Centre in Australia.

ACKNOWLEDGMENTS

We thank the skippers and crews of the various NSW bather-protection gillnet contractors for their assistance at sea, and NSW DPI Fisheries staff for logistic support. Many thanks to Chris Brown who provided feedback on the approach. Thanks to Louise Tosetto for her assistance during sampling.

SUPPLEMENTARY MATERIAL

The Supplementary Material for this article can be found online at: https://www.frontiersin.org/articles/10.3389/fmars.2020.594636/full#supplementary-material

REFERENCES

Barnes, T. C., Rogers, P. J., Wolf, Y., Madonna, A., Holman, D., Ferguson, G. J., et al. (2019). Dispersal of an exploited demersal fish species (*Argyrosomus japonicus*, Sciaenidae) inferred from satellite telemetry. *Mar. Biol.* 166:125.

Bird, C. S., Veríssimo, A., Magozzi, S., Abrantes, K. G., Aguilar, A., Al-Reasi, H., et al. (2018). A global perspective on the trophic geography of sharks. *Nat. Ecol. Evol.* 2, 299–305.

Block, B. A. (2019). "Use of electronic tags to reveal migrations of atlantic Bluefin Tunas," in *The Future of Bluefin Tunas: Ecology, Fisheries Management, and Conservation*, ed. B. A. Block (JHU Press), 94.

Bond, A. L., and Diamond, A. W. (2011). Recent Bayesian stable-isotope mixing models are highly sensitive to variation in discrimination factors. *Ecol. Appl.* 21, 1017–1023. doi: 10.1890/09-2409.1

Broadhurst, M. K., and Cullis, B. R. (2020). Mitigating the discard mortality of non-target, threatened elasmobranchs in bather-protection gillnets. *Fish. Res.* 222:105435. doi: 10.1016/j.fishres.2019.105435

Carlisle, A. B., Litvin, S. Y., Madigan, D. J., Lyons, K., Bigman, J. S., Ibarra, M., et al. (2016). Interactive effects of urea and lipid content confound stable isotope analysis in elasmobranch fishes. *Can. J. Fish. Aquat. Sci.* 74, 419–428. doi: 10.1139/cjfas-2015-0584

Caut, S., Angulo, E., and Courchamp, F. (2009). Variation in discrimination factors (Δ15N and Δ13C): the effect of diet isotopic values and applications for diet reconstruction. *J. Appl. Ecol.* 46, 443–453. doi: 10.1111/j.1365-2664.2009.01620.x

Cooter, E. J., and Schwede, D. B. (2000). Sensitivity of the national oceanic and atmospheric administration multilayer model to instrument error and parameterization uncertainty. *J. Geophys. Res. Atmos.* 105, 6695–6707. doi: 10.1029/1999jd901080

Couturier, L. I., Jaine, F. R., Townsend, K. A., Weeks, S. J., Richardson, A. J., and Bennett, M. B. (2011). Distribution, site affinity and regional movements of the manta ray, *Manta alfredi* (Krefft, 1868), along the east coast of Australia. *Mar. Freshw. Res.* 62, 628–637. doi: 10.1071/mf10148

Couturier, L. I., Rohner, C. A., Richardson, A. J., Marshall, A. D., Jaine, F. R., Bennett, M. B., et al. (2013). Stable isotope and signature fatty acid analyses suggest reef manta rays feed on demersal zooplankton. *PLoS One* 8:e77152. doi: 10.1371/journal.pone.0077152

Eurich, J., Matley, J., Baker, R., Mccormick, M., and Jones, G. (2019). Stable isotope analysis reveals trophic diversity and partitioning in territorial damselfishes on a low-latitude coral reef. *Mar. Biol.* 166:17.

Frédérich, B., Fabri, G., Lepoint, G., Vandewalle, P., and Parmentier, E. (2009). Trophic niches of thirteen damselfishes (Pomacentridae) at the Grand Récif of Toliara, Madagascar. *Ichthyol. Res.* 56, 10–17. doi: 10.1007/s10228-008-0053-2

Fry, B., Scalan, R., and Parker, P. (1983). 13C/12C ratios in marine food webs of the Torres Strait, Queensland. *Mar. Freshw. Res.* 34, 707–715. doi: 10.1071/mf9830707

Gonzalez-Rodriguez, E. (1994). Yearly variation in primary productivity of marine phytoplankton from Cabo Frio (RJ, Brazil) region. *Hydrobiologia* 294, 145–156. doi: 10.1007/bf00016855

Greenwood, N., Sweeting, C., and Polunin, N. (2010). Elucidating the trophodynamics of four coral reef fishes of the Solomon Islands using δ 15 N and δ 13 C. *Coral Reefs* 29, 785–792. doi: 10.1007/s00338-010-0626-1

Guttridge, T., Van Zinnicq Bergmann, M., Bolte, C., Howey, L., Finger, J., Kessel, S., et al. (2017). Philopatry and regional connectivity of the great hammerhead shark, *Sphyrna mokarran* in the US and Bahamas. *Front. Mar. Sci.* 4:3. doi: 10.3389/fmars.2017.00003

Hill, J., Mcquaid, C., and Kaehler, S. (2006). Biogeographic and nearshore-offshore trends in isotope ratios of intertidal mussels and their food sources around the coast of southern Africa. *Mar. Ecol. Prog. Ser.* 318, 63–73. doi: 10.3354/meps318063

Hobday, A. J., Hartog, J. R., Spillman, C. M., and Alves, O. (2011). Seasonal forecasting of tuna habitat for dynamic spatial management. *Can. J. Fish. Aquat. Sci.* 68, 898–911. doi: 10.1139/f2011-031

Hobson, K. A., and Cherel, Y. (2006). Isotopic reconstruction of marine food webs using cephalopod beaks: new insight from captively raised *Sepia officinalis*. *Can. J. Zool.* 84, 766–770. doi: 10.1139/z06-049

Hofman, M., Hayward, M., Heim, M., Marchand, P., Rolandsen, C. M., Mattisson, J., et al. (2019). Right on track? Performance of satellite telemetry in terrestrial wildlife research. *PLoS One* 14:e0216223. doi: 10.1371/journal.pone.0216223

Holmes, B. J., Pepperell, J. G., Griffiths, S. P., Jaine, F. R., Tibbetts, I. R., and Bennett, M. B. (2014). Tiger shark (*Galeocerdo cuvier*) movement patterns and habitat use determined by satellite tagging in eastern Australian waters. *Mar. Biol.* 161, 2645–2658. doi: 10.1007/s00227-014-2536-1

Hussey, N. E., Brush, J., Mccarthy, I. D., and Fisk, A. T. (2010). δ 15 N and δ 13 C diet-tissue discrimination factors for large sharks under semi-controlled conditions. *Compar. Biochem. Physiol. Part A Mol. Integrat. Physiol.* 155, 445–453. doi: 10.1016/j.cbpa.2009.09.023

Jorgensen, S., Klimley, A., and Muhlia-Melo, A. (2009). Scalloped hammerhead shark *Sphyrna lewini*, utilizes deep-water, hypoxic zone in the Gulf of California. *J. Fish Biol.* 74, 1682–1687. doi: 10.1111/j.1095-8649.2009.02230.x

Kim, S. L., Del Rio, C. M., Casper, D., and Koch, P. L. (2012). Isotopic incorporation rates for shark tissues from a long-term captive feeding study. *J. Exper. Biol.* 215, 2495–2500. doi: 10.1242/jeb.070656

Kingsbury, K. M., Gillanders, B. M., Booth, D. J., Coni, E. O., and Nagelkerken, I. (2020). Range-extending coral reef fishes trade-off growth for maintenance of body condition in cooler waters. *Sci. Total Environ.* 703:134598. doi: 10.1016/j.scitotenv.2019.134598

Kopp, D., Lefebvre, S., Cachera, M., Villanueva, M. C., and Ernande, B. (2015). Reorganization of a marine trophic network along an inshore-offshore gradient due to stronger pelagic-benthic coupling in coastal areas. *Prog. Oceanogr.* 130, 157–171. doi: 10.1016/j.pocean.2014.11.001

Le Loc'h, F., Hily, C., and Grall, J. (2008). Benthic community and food web structure on the continental shelf of the Bay of Biscay (North Eastern Atlantic) revealed by stable isotopes analysis. *J. Mar. Syst.* 72, 17–34. doi: 10.1016/j.jmarsys.2007.05.011

Lee, K., Smoothey, A., Harcourt, R., Roughan, M., Butcher, P., and Peddemors, V. (2019). Environmental drivers of abundance and residency of a large migratory shark, *Carcharhinus leucas*, inshore of a dynamic western boundary current. *Mar. Ecol. Prog. Ser.* 622, 121–137. doi: 10.3354/meps13052

Logan, J., Pethybridge, H., Lorrain, A., Somes, C., Allain, V., Bodin, N., et al. (2020). Global patterns and inferences of tuna movements and trophodynamics. *Deep Sea Res. Part II Top. Stud. Oceanogr.* 175:104775. doi: 10.1016/j.dsr2.2020.104775

Madigan, D. J., Chiang, W.-C., Wallsgrove, N. J., Popp, B. N., Kitagawa, T., Choy, C. A., et al. (2016). Intrinsic tracers reveal recent foraging ecology of giant Pacific bluefin tuna at their primary spawning grounds. *Mar. Ecol. Prog. Ser.* 553, 253–266. doi: 10.3354/meps11782

Magozzi, S., Yool, A., Vander Zanden, H., Wunder, M., and Trueman, C. (2017). Using ocean models to predict spatial and temporal variation in marine carbon isotopes. *Ecosphere* 8:e01763. doi: 10.1002/ecs2.1763

Malpica-Cruz, L., Herzka, S. Z., Sosa-Nishizaki, O., and Escobedo-Olvera, M. A. (2013). Tissue-specific stable isotope ratios of shortfin mako (*Isurus oxyrinchus*) and white (*Carcharodon carcharias*) sharks as indicators of size-based differences in foraging habitat and trophic level. *Fish. Oceanogr.* 22, 429–445. doi: 10.1111/fog.12034

Malpica-Cruz, L., Herzka, S. Z., Sosa-Nishizaki, O., and Lazo, J. P. (2012). Tissue-specific isotope trophic discrimination factors and turnover rates in a marine elasmobranch: empirical and modeling results. *Can. J. Fish. Aquat. Sci.* 69, 551–564. doi: 10.1139/f2011-172

Matich, P., Heithaus, M. R., and Layman, C. A. (2011). Contrasting patterns of individual specialization and trophic coupling in two marine apex predators. *J. Anim. Ecol.* 80, 294–305. doi: 10.1111/j.1365-2656.2010.01753.x

McMahon, K. W., Hamady, L. L., and Thorrold, S. R. (2013). A review of ecogeochemistry approaches to estimating movements of marine animals. *Limnol. Oceanogr.* 58, 697–714. doi: 10.4319/lo.2013.58.2.0697

Olin, J. A., Hussey, N. E., Grgicak-Mannion, A., Fritts, M. W., Wintner, S. P., and Fisk, A. T. (2013). Variable δ15N diet-tissue discrimination factors among sharks: implications for trophic position, diet and food web models. *PLoS One* 8:e77567. doi: 10.1371/journal.pone.0077567

Post, D. M. (2002). Using stable isotopes to estimate trophic position: models, methods, and assumptions. *Ecology* 83, 703–718. doi: 10.1890/0012-9658(2002)083[0703:usitet]2.0.co;2

Post, D. M., Layman, C. A., Arrington, D. A., Takimoto, G., Quattrochi, J., and Montaña, C. G. (2007). Getting to the fat of the matter: models, methods and assumptions for dealing with lipids in stable isotope analyses. *Oecologia* 152, 179–189. doi: 10.1007/s00442-006-0630-x

Queiroz, N., Humphries, N. E., Couto, A., Vedor, M., Da Costa, I., Sequeira, A. M., et al. (2019). Global spatial risk assessment of sharks under the footprint of fisheries. *Nature* 572, 461–466.

Raoult, V., Broadhurst, M. K., Peddemors, M., Williamson, M., and Gaston, M. (2019). Resource use of great hammerhead sharks *Sphyrna mokarran* off eastern Australia. *J. Fish Biol.* 95, 1430–1440. doi: 10.1111/jfb.14160

Raoult, V., Gaston, T. F., and Taylor, M. D. (2018). Habitat-fishery linkages in two major south-eastern Australian estuaries show that the C4 saltmarsh plant *Sporobolus virginicus* is a significant contributor to fisheries productivity. *Hydrobiologia* 811, 221–238. doi: 10.1007/s10750-017-3490-y

Raoult, V., Gaston, T. F., and Williamson, J. E. (2015). Not all sawsharks are equal: species of co-existing sawsharks show plasticity in trophic consumption both within and between species. *Can. J. Fish. Aquat. Sci.* 72, 1769–1775. doi: 10.1139/cjfas-2015-0307

Raoult, V., Peddemors, V., Rowling, K., and Williamson, J. E. (2020). Spatiotemporal distributions of two sympatric sawsharks (*Pristiophorus cirratus* and *P. nudipinnis*) in south-eastern Australian waters. *Mar. Freshw. Res.* 71, 1342–1354. doi: 10.1071/MF19277

Rau, G., Sweeney, R., and Kaplan, I. (1982). Plankton 13C: 12C ratio changes with latitude: differences between northern and southern oceans. *Deep Sea Res. Part A Oceanogr. Res. Pap.* 29, 1035–1039. doi: 10.1016/0198-0149(82)90026-7

Revill, A. T., Young, J. W., and Lansdell, M. (2009). Stable isotopic evidence for trophic groupings and bio-regionalization of predators and their prey in oceanic waters off eastern Australia. *Mar. Biol.* 156, 1241–1253. doi: 10.1007/s00227-009-1166-5

Rigby, C., Dulvy, N., Barreto, R., Carlson, J., Fernando, D., Fordham, S., et al. (2019). *Sphyrna mokarran. IUCN Red List Threat. Spec.* 2019:e.T39385A2918526.

Roff, G., Brown, C. J., Priest, M. A., and Mumby, P. J. (2018). Decline of coastal apex shark populations over the past half century. *Commun. Biol.* 1:223.

San Martin, E., Irigoien, X., Roger, P. H., Urrutia, ÂL., Zubkov, M. V., and Heywood, J. L. (2006). Variation in the transfer of energy in marine plankton along a productivity gradient in the Atlantic Ocean. *Limnol. Oceanogr.* 51, 2084–2091. doi: 10.4319/lo.2006.51.5.2084

Sequeira, A., Heupel, M., Lea, M. A., Eguíluz, V. M., Duarte, C. M., Meekan, M., et al. (2019). The importance of sample size in marine megafauna tagging studies. *Ecol. Appl.* 29:e01947.

Shen, J., Schoepfer, S. D., Feng, Q., Zhou, L., Yu, J., Song, H., et al. (2015). Marine productivity changes during the end-Permian crisis and Early Triassic recovery. *Earth Sci. Rev.* 149, 136–162. doi: 10.1016/j.earscirev.2014.11.002

Shipley, O. N., Olin, J. A., Polunin, N. V., Sweeting, C. J., Newman, S. P., Brooks, E. J., et al. (2017). Polar compounds preclude mathematical lipid correction of carbon stable isotopes in deep-water sharks. *J. Exper. Mar. Biol. Ecol.* 494, 69–74. doi: 10.1016/j.jembe.2017.05.002

Somes, C. J., Schmittner, A., Galbraith, E. D., Lehmann, M. F., Altabet, M. A., Montoya, J. P., et al. (2010). Simulating the global distribution of nitrogen isotopes in the ocean. *Glob. Biogeochem. Cycles* 24:GB4019. doi: 10.1029/2009GB003767

St. John Glew, K., Graham, L. J., Mcgill, R. A., and Trueman, C. N. (2019). Spatial models of carbon, nitrogen and sulphur stable isotope distributions (isoscapes) across a shelf sea: an INLA approach. *Methods Ecol. Evol.* 10, 518–531. doi: 10.1111/2041-210x.13138

Sumpton, W., Taylor, S., Gribble, N., Mcpherson, G., and Ham, T. (2011). Gear selectivity of large-mesh nets and drumlines used to catch sharks in the Queensland Shark Control Program. *Afr. J. Mar. Sci.* 33, 37–43. doi: 10.2989/1814232x.2011.572335

Tagliafico, A., Butcher, P. A., Colefax, A. P., Clark, G. F., and Kelaher, B. P. (2020). Variation in cownose ray *Rhinoptera neglecta* abundance and group size on the central east coast of Australia. *J. Fish Biol.* 96, 427–433. doi: 10.1111/jfb.14219

Trueman, C. N., Jackson, A. L., Chadwick, K. S., Coombs, E. J., Feyrer, L. J., Magozzi, S., et al. (2019). Combining simulation modeling and stable isotope analyses to reconstruct the last known movements of one of Nature's giants. *PeerJ* 7:e7912. doi: 10.7717/peerj.7912

Weidel, B. C., Carpenter, S. R., Kitchell, J. F., and Vander Zanden, M. J. (2011). Rates and components of carbon turnover in fish muscle: insights from bioenergetics models and a whole-lake 13C addition. *Can. J. Fish. Aquat. Sci.* 68, 387–399. doi: 10.1139/f10-158

West, J. B., Bowen, G. J., Dawson, T. E., and Tu, K. P. (2009). *Isoscapes: Understanding Movement, Pattern, and Process on Earth Through Isotope Mapping*. Berlin: Springer.

Wood, S., and Wood, M. S. (2015). *Package 'mgcv'. R Package Version 1, 29.*

Conflict of Interest: The authors declare that data from a previous study used here was funded partly by Sibelco Pty Ltd. This funder was not involved in the study design, collection, analysis, interpretation of data, the writing of this article or the decision to submit for publication. The authors declare that the research was conducted in the absence of any commercial or financial relationships that could be construed as a potential conflict of interest.

frontiers in Marine Science

ORIGINAL RESEARCH
published: 16 December 2020
doi: 10.3389/fmars.2020.596619

Behavior and Ecology of Silky Sharks Around the Chagos Archipelago and Evidence of Indian Ocean Wide Movement

David J. Curnick[1,2]*, Samantha Andrzejaczek[3], David M. P. Jacoby[1], Daniel M. Coffey[4], Aaron B. Carlisle[5], Taylor K. Chapple[3,6], Francesco Ferretti[7], Robert J. Schallert[3], Timothy White[3,8], Barbara A. Block[3], Heather J. Koldewey[9,10] and Ben Collen[2†]

[1] Institue of Zoology, Zoological Society of London, London, United Kingdom, [2] Department of Genetics, Evolution and Environment, Centre for Biodiversity and Environment Research, University College London, London, United Kingdom, [3] Hopkins Marine Station, Stanford University, Pacific Grove, CA, United States, [4] Harte Research Institute for Gulf of Mexico Studies, Texas A&M University-Corpus Christi, Corpus Christi, TX, United States, [5] School of Marine Science and Policy, University of Delaware, Lewes, DE, United States, [6] Oregon State University, Hatfield Marine Science Center, Newport, OR, United States, [7] Department of Fish and Wildlife Conservation, Virginia Tech, Blacksburg, VA, United States, [8] Global Fishing Watch, Washington, DC, United States, [9] Zoological Society of London, London, United Kingdom, [10] Centre for Ecology and Conservation, University of Exeter, Cornwall, United Kingdom

Edited by:
Mourier Johann,
Institut de Recherche Pour le Développement (IRD), France

Reviewed by:
John David Filmalter,
South African Institute for Aquatic Biodiversity, South Africa
Paul Brickle,
South Atlantic Environmental Research Institute, Falkland Islands
Marc Soria,
Institut de Recherche Pour le Développement (IRD), France

***Correspondence:**
David J. Curnick
david.curnick@zsl.org

†Deceased

Specialty section:
This article was submitted to Marine Megafauna, a section of the journal Frontiers in Marine Science

Received: 19 August 2020
Accepted: 10 November 2020
Published: 16 December 2020

Citation:
Curnick DJ, Andrzejaczek S, Jacoby DMP, Coffey DM, Carlisle AB, Chapple TK, Ferretti F, Schallert RJ, White T, Block BA, Koldewey HJ and Collen B (2020) Behavior and Ecology of Silky Sharks Around the Chagos Archipelago and Evidence of Indian Ocean Wide Movement. Front. Mar. Sci. 7:596619. doi: 10.3389/fmars.2020.596619

Silky sharks (*Carcharhinus falciformis*) represent a major component of global shark catch, both directly and as bycatch, and populations are declining as a result. An improved understanding of their movement ecology is needed to support conservation efforts. We deployed satellite and acoustic tags (2013–2018) and analyzed historical fisheries records (1997–2009), to investigate the spatial ecology of silky sharks in the central Indian Ocean and a large Marine Protected Area (MPA; 640,000 km^2) around the Chagos Archipelago. We observed high fidelity to the MPA, and a sustained diurnal association with a seamount complex, with individuals moving off at night and returning at sunrise. Yet, we also observed large-scale divergent movements in two satellite tagged individuals and documented the furthest recorded displacement distance for a satellite tagged silky shark to date, with one individual moving from the MPA to the Kenyan coast—a displacement distance of 3,549 km (track distance ~4,782 km). Silky sharks undertook diel vertical migrations and oscillatory diving behavior, spending > 99% of their time in the top 100 m, and diving to depths of greater than 300 m, overlapping directly with typical deployments of purse seine and longline sets in the Indian Ocean. One individual was recorded to a depth of 1,112 m, the deepest recorded silky shark dive to date. Individuals spent 96% of their time at liberty within water temperatures between 24 and 30°C. Historic fisheries data revealed that silky sharks were a major component of the shark community around the archipelago, representing 13.69% of all sharks caught by longlines before the fishery closed in 2010. Over half (55.88%) of all individuals caught by longlines and purse seiners were juveniles. The large proportion of juveniles, coupled with the high site fidelity and residence observed in some individuals, suggests that the MPA could provide considerable conservation benefits for silky sharks, particularly during early life-history stages. However, their high mobility potential necessitates that large MPAs need to be considered in conjunction with fisheries regulations and conservation measures in adjacent EEZs and in areas beyond national jurisdiction.

Keywords: fisheries, seamount, *Carcharhinus falciformis*, habitat use, biotelemetry, residency, migration, marine protected area

INTRODUCTION

Significant historical declines have been observed in pelagic shark populations (Baum et al., 2003; Ferretti et al., 2010; Dulvy et al., 2014). This has largely been driven by high spatial overlap with industrial fishing activities (Queiroz et al., 2016, 2019), where pelagic sharks account for over half of shark catch globally (Worm et al., 2013). Central to developing the effective conservation and management strategies urgently needed for these species is a firm understanding of their spatial ecology (Boerder et al., 2019).

Pelagic sharks spend considerable periods of time on the high seas, in areas beyond national jurisdiction (Queiroz et al., 2019), where there are limited legal frameworks to protect them (Wright et al., 2019). However, electronic tagging indicates some pelagic shark species exploit their environment in predictable ways (Block et al., 2011; Lea et al., 2015; Doherty et al., 2017) or show residency to certain sites or features (e.g., Jorgensen et al., 2010; Queiroz et al., 2016; Carlisle et al., 2019; Aldana-Moreno et al., 2020) providing target areas for effective management. Yet, existing studies into pelagic shark spatial ecology are taxonomically and geographically biased. In a recent analysis of pelagic shark tagging data, nearly 77% of pelagic sharks tagged were from just six species (blue shark *Prionace glauca*, shortfin mako *Isurus oxyrinchus*, tiger shark *Galeocerdo cuvier*, salmon shark *Lamna ditropis*, whale shark *Rhincodon typus*, and white shark *Carcharodon carcharias*) and highlighted that the Indian Ocean was generally data-poor compared to the Pacific and Atlantic Oceans (Queiroz et al., 2019). As such, there is a pressing need to broaden our understanding of pelagic shark ecology to understudied species and underrepresented regions.

Silky sharks (*Carcharhinus falciformis*) are important, yet relatively understudied, pelagic predators that inhabit continental shelves, slopes, and offshore waters from the surface down to 500 m (Compagno, 1984; Bonfil, 2008). Adult silky sharks are primarily piscivorous (Compagno, 1984), with juveniles also feeding on pelagic crustaceans (Filmalter et al., 2017), and they form large feeding aggregations when food is plentiful (Bonfil, 2008). In the Gulf of Mexico, neonates and young juveniles have been shown to live a more coastal, demersal lifestyle than adults (Branstetter, 1987; Bonfil, 1997). However, elsewhere, juveniles have been regularly reported in open ocean environments (e.g., Filmalter et al., 2015; Hutchinson et al., 2019; Bonnin et al., 2020), often joining schools of large pelagic fishes, such as tuna (Camhi, 2009; Sánchez-De Ita et al., 2011). Silky sharks grow up to 330 cm in length (Camhi, 2009), and can be highly mobile, with maximum recorded displacement distances of over 3,000 km (Schaefer et al., 2019). Biotelemetry devices have been deployed in the West Indian Ocean and Pacific Ocean to explore the movement and mortality rates of these sharks in response to fisheries' bycatch (Musyl et al., 2003, 2011a; Filmalter et al., 2011; Poisson et al., 2011, 2014; Hutchinson et al., 2015; Musyl and Gilman, 2018), and to quantify associations with fishing gear, such as fish aggregation devices (FADs) (Filmalter et al., 2010, 2015; Muir et al., 2012). A few tagging studies have also evaluated key behaviors such as residency patterns or habitat utilization, but these have been focused in the Pacific Ocean (Musyl et al., 2011b; Hutchinson et al., 2019) and the Red Sea (Clarke et al., 2011a), covering just a fraction of their circumtropical range.

Silky sharks are one of the most heavily exploited elasmobranch species, targeted by both artisanal and industrial longline shark fisheries (Hazin et al., 2007; Bonfil, 2008; Henderson et al., 2009). Their tendency to associate with schools of tuna also results in them representing a major component of bycatch in tropical longline and purse seine fisheries (Román-Verdesoto and Orozco-Zöller, 2005; Bonfil, 2008; Watson et al., 2009; Clarke et al., 2011b; Gilman, 2011). Furthermore, their propensity to associate with floating objects, especially as juveniles (Romanov, 2002; Amandè et al., 2008), makes them particularly vulnerable to FAD fishing (Filmalter et al., 2011), where they can comprise up to 95% of the total elasmobranch bycatch (Román-Verdesoto and Orozco-Zöller, 2005; Gilman, 2011; Lawson, 2011), with a high proportion being juveniles (Amandè et al., 2008, 2010). Mortality rates of sharks caught by purse seiners is also high, with less than 20% of released individuals thought to survive (Poisson et al., 2014; Hutchinson et al., 2015). As a result, the silky shark population in the Atlantic Ocean is declining (Rigby et al., 2017) and stocks in the Western and Central Pacific (WCPFC, 2018) and Indian Ocean are "subject to overfishing" (Urbina et al., 2018). A number of conservation and management actions have been initiated to address perceived declines, such as the listing of silky sharks on[1] of the Convention on the Conservation of Migratory Species of Wild Animals (CMS) and see footnote[1] of the Convention on International Trade in Endangered Species of Wild Fauna & Flora (CITES), or the prohibition of all vessels from retaining or landing any silky shark in the Western and Central Pacific Region (CMM 2013–08). Yet, these measures alone have not reversed population declines, and the status of silky sharks globally was recently uplisted from "Near Threatened" to "Vulnerable" on The IUCN Red List of Threatened Species (Rigby et al., 2017).

No-take marine protected areas (MPAs), also known as marine reserves, have been proposed as effective shark

---

[1] CITES (https://cites.org/eng/app/index.php) and of the CMS (https://www.cms.int/en/species/appendix-i-ii-cms#: :text=Appendix%20II%20covers%20migratory%20species,could%20be%20achieved%20by%20an).

conservation strategies within exclusive economic zones (EEZ) (Baum et al., 2003; Robbins et al., 2006; Watson et al., 2009). However, the success of small-scale no-take MPAs in protecting sharks can be limited (Robbins et al., 2006), as even reef sharks can range beyond the limits of small MPAs (Chapman et al., 2005). Large no-take MPAs that encompass vast swathes of open ocean could be part of the solution for the conservation of sharks (Wood et al., 2008; Game et al., 2009; Koldewey et al., 2010). Yet there is limited evidence that large no-take MPAs can protect mobile pelagic species such as sharks or tunas, with protected areas potentially displacing fishing effort to other areas (De Santo et al., 2011; Kaplan et al., 2014; Curnick et al., 2020). Therefore, the efficacy of MPAs for pelagic sharks will be dependent on the spatial relationship between the habitats of sharks and protected area coverage.

In this study, we investigate movement behaviors of silky sharks in the central Indian Ocean and consider the role of the Chagos Archipelago, and the British Indian Ocean Territory (BIOT) MPA that surrounds it, in their spatial ecology. It has been previously hypothesized that this MPA's large size and habitat heterogeneity could provide conservation benefits for pelagic sharks (Koldewey et al., 2010). However, important knowledge of the spatial ecology and habitat use of pelagic sharks within the central Indian Ocean is sparse. Using a combination of biotelemetry tags (both satellite and acoustic) and historical fisheries data, we aimed to (i) understand the horizontal movement patterns, habitat use and site fidelity of silky sharks within the MPA and how they are connected to the wider Indian Ocean, (ii) quantify the vertical and thermal habitat use by silky sharks, and (iii) assess the relative abundance and population demographics of silky sharks around the Chagos Archipelago. This study contributes to the understanding of silky shark ecology with several novel insights gained into their movement behavior.

MATERIALS AND METHODS

Study Site

The Chagos Archipelago is situated 500 km south of the Maldives and is a group of 55 islands, submerged banks (Sheppard et al., 2012), and 73 seamounts (Yesson et al., 2020). Extending out to the full EEZ, the BIOT MPA covers 640,000 km^2 of ocean, with the vast majority being deep oceanic water with maximum depths of over 5,000 m. The BIOT MPA was declared a no-take protected area in 2010 with the exclusion of all industrial fishing practices. Prior to the establishment of the MPA, the main licensed commercial fishery was for tunas and billfishes, using both longline and purse seine methods (Dunn and Curnick, 2019; Curnick et al., 2020), with considerable shark bycatch (Koldewey et al., 2010).

Telemetry

Shark Capture and Tagging

Silky sharks were caught around the Chagos Archipelago in February and March of 2013 and 2018 using baited handlines with barbless circle hooks. Once hooked, sharks were brought alongside the tagging platform, tail-roped and inverted to initiate tonic immobility (Kessel and Hussey, 2015). Once secured, total length, sex, tagging location (latitude and longitude) and date were recorded for each individual (except for one shark where sex was not recorded). Silky sharks were tagged with either pop-up archival transmitting satellite tags (MiniPATs models 247 and 386; Wildlife Computers, Redmond, WA, United States), Smart Position or Temperature Transmitting tags (SPOT5; Wildlife Computers, Redmond, WA, United States), acoustic tags (V16, 69 kHz, transmission interval 30–90 s or 125–175 s; Vemco, Halifax, Nova Scotia, Canada), or 'double tagged' with a combination of satellite and acoustic tags (**Table 1**).

MiniPATs (n = 6) were leadered with 15 cm of 180 kg monofilament (Moimoi, Kobe, Japan), covered with a single layer of aramide braided cord, two layers of shrink wrap (thermoplastic), and attached to a custom titanium dart (Wilson et al., 2015). MiniPATs were embedded with a stainless-steel tip into the muscle tissue at the base of the dorsal fin through a small incision made with a sterile scalpel blade. Tags were set to activate upon entering the water and record ambient light, temperature and depth and were programmed to detach from tagged sharks after 100–300 days (see **Table 1**). Depth and temperature data were summarized into 24 h bins, and for two individuals, transmitted time series at 2.5- or 10-min intervals when available. At the end of the deployment period, or after a premature release, MiniPATs surfaced and relayed the data via the Argos satellite system[2]. Data messages were then viewed, processed and downloaded through the Wildlife Computers Data Portal[3]. A premature release procedure, whereby the tag would detach from the tether if the tag recorded a constant depth (±3 m) for a period greater than 3 days, was programmed to ensure tag retrieval in the case of shark mortality.

SPOT tags (n = 2) were attached to the top of the first dorsal fin of two sharks using a two-bolt attachment following Weng et al. (2005). SPOT tags were cleaned with alcohol prior to attachment and had a thin rubber pad to limit abrasion with the shark fin. Tags transmitted location data to Argos satellites whenever the shark's fin broke the surface of the water long enough for the tag to send a message (∼15–30 s). The accuracy of position estimates, referred to as location class (LC), was variable and depended on the number and time between transmissions received during a satellite pass. Position accuracy records are classified as either LC 3 (<250 m), 2 (250–500 m), 1 (500–1,500 m), 0 (>1,500 m), A or B (no estimate of spatial accuracy), or Z (invalid) as determined by the Argos system (see Witt et al., 2010)[2]. Only Argos-derived locations with LC 1, 2, or 3 were used in this study.

To explore potential residency to geographic features within the MPA, four sharks were tagged at the Sandes-Swart seamount complex in the south of the archipelago with long-term (VEMCO V16) acoustic transmitters in March 2018. Acoustic tags were soaked in betadine and implanted intraperitoneally through a small incision created with a sterile blade (∼2–3 cm) just off the midline of their abdomen. A single suture (Ethilon, United States) was then used to close the incision. Acoustic tags transmit a unique identification code at regular intervals with a nominal

---

[2] www.argos-system.org

[3] www.wildlifecomputers.com

TABLE 1 | Tag deployments on silky sharks (*Carcharhinus falciformis)* around the Chagos Archipelago between 2013 and 2018.

Shark ID	Deployment date	Deployment latitude	Deployment longitude	Sex	TL	FL	PCL	MiniPAT	Programmed MiniPAT deployment duration (days)	SPOT	V16
1	12/02/2013	−5.259	71.978	U	194	–	–	TS	180	–	–
2	21/03/2013	−6.841	71.202	F	195	–	–	PDT	270	Yes	–
3	22/03/2013	−5.261	71.681	F	225	–	–	NDR	180	Yes	–
4	17/03/2018	−7.138	72.197	M	148	117	105	PDT	300	–	Yes
5	17/03/2018	−7.138	72.197	F	159	131	118	NDR	240	–	Yes
6	17/03/2018	−7.138	72.197	F	169	134	121	TS	100	–	Yes
7	17/03/2018	−7.138	72.197	F	162	128	118	–	–	–	Yes

Location data represented in decimal degrees. For sex, U, unknown; F, female; and M, male. TL, Total length (cm); FL, Fork length (cm); and PCL, Precaudal length (cm). The MiniPAT (Wildlife Computers) column indicates depth and temperature data used in analysis: PDT, summary profiles of depth and temperature data collected; TS, time-series of depth and temperature collected; and NDR, No data reported (tag failed). V16, acoustic tags (Vemco); SPOT, Smart Position or Temperature Transmitting tags (Wildlife Computers).

delay of either 30–90 (Sharks 4 and 5) or 125–175 s (Sharks 6 and 7), for the duration of their battery life (up to 10 years). This code is detected and recorded by a receiver when the shark swims within ∼500 m (Jacoby et al., 2020). Sharks were acoustically tracked as part of a broader tagging program (including both reef-associated and pelagic species) between March 2013 and March 2020 around the Chagos Archipelago (see Carlisle et al., 2019; Andrzejaczek et al., 2020; Jacoby et al., 2020). In March 2019, data (corresponding to March 2018 to March 2019) were downloaded from 47 acoustic receivers [VR2Ws, VR2W-ARs (AR—Acoustic Release), VR2W-UWMs, and VR4Gs; Vemco, Nova Scotia, Canada] located across Peros Banhos atoll (n = 25), Salomon Atoll (n = 7), Great Chagos Bank (n = 3), Nelson Island (n = 1), Egmont Atoll (n = 4), Speakers Bank (n = 3), Benares Shoal (n = 2), Blenheim Reef (n = 1), and Victory Bank (n = 1) (see Carlisle et al., 2019; Jacoby et al., 2020; **Figure 1**). Receivers were deployed on or adjacent to reefs on the ocean-side of geographic features (atoll, shore, or bank) and at depths between 20 and 30 m (**Figure 1**). Across the same monitoring period, three VR2W-ARs were deployed linearly east-to-west on the Sandes-Swart seamount complex (SS01 72.225, −7.146; SS03 72.192, −7.137; and SS04 72.133, −7.149). These summits each reach a depth of ∼70m and rise from depths of more than 600m (for full description, see Hosegood et al., 2019). Receivers were deployed at depths between ∼95 and 350 m (**Figure 1**) and the distances between SS01 and SS03 was ∼3.8 km and between SS03 and SS04 was ∼6.6 km.

All procedures were approved by the Stanford University Administrative Panel on Laboratory Animal Care (APLAC) under permit APLAC-10765 and by the Zoological Society of London's Ethics Committee under permit 186-BME-0652.

Horizontal Movement Patterns

Satellite Tracking

For individuals tagged with MiniPATs, location estimates were processed using the manufacturer's software, Geolocation Processing Estimator 3 (GPE3; Wildlife Computers Inc., Redmond, WA, United States), which has been used widely to process elasmobranch tracking data (e.g., Skomal et al., 2017; Hutchinson et al., 2019; Peel et al., 2020). GPE3 generates two maximum likelihood position estimates per day using a hidden Markov model (Patterson et al., 2009) with a 0.25° × 0.25° grid spacing, and position estimates (two per day) interpolated and smoothed with a cubic spline. Program parameters were defined for silky sharks to generate maximum likelihood position estimates and maximum likelihood tracks (MLT). These included animal speed (representing the standard deviation of a normal distribution of the diffusion rate for the animal), model domain (using only the marine domain to exclude points on land), sea surface temperature (referencing position estimates against known environmental conditions; NOAA High Resolution SST data provided by the NOAA/OAR/ESRL PSD, Boulder, Colorado, United States, from their website at http://www.esrl.noaa.gov/psd/); underlying bathymetry (referencing position estimates against known depths; Amante and Eakins, 2009); and by comparing observed twilight light readings with expected twilight data. GPE3 model runs were further constrained by the inclusion of known positions from SPOT fixes (using only positions of LC 1, 2, and 3), and acoustic tag detections (limited to two locations per 24 h, with the middle detection of the sequence taken on occasions that sharks were detected multiple times on the same receiver on the same day) during the period that the animal was tagged with a MiniPAT. Input data to the model also included the deployment location recorded with GPS and the endpoint tag pop-up location from Argos. Speed filters were applied iteratively to the longest track by distance (Shark 4), with GPE3 model runs examined every 0.25 m/s, from 0.5 to 3.0 m/s. Outputs were compared using the GPE3 quality score provided, with 1.5 m/s producing the most likely track (**Supplementary Table 1**). For consistency, this speed filter was then applied to the tracks of the other three sharks. MLTs were plotted in R (R Development Core Team, 2018) using the "ggplot2" and "marmap" packages over a bathymetry layer obtained from the ETOPO1 database hosted on the NOAA website at 4 min resolution through the "marmap" package in R. As Shark 3's MiniPAT did not report, its track was generated only using SPOT fixes of LC 1, 2, and 3. Total track length (km) and displacement distance (kilometers between tagging location and pop-off location, km) were calculated within the "move" package (Kranstauber and Smolla, 2015). We then averaged the GPE3 generated 12-h probability density surfaces for each tag and resampled the 0.25° GPE3 grid at a resolution of 0.0125° using bilinear interpolation using the R package "raster"

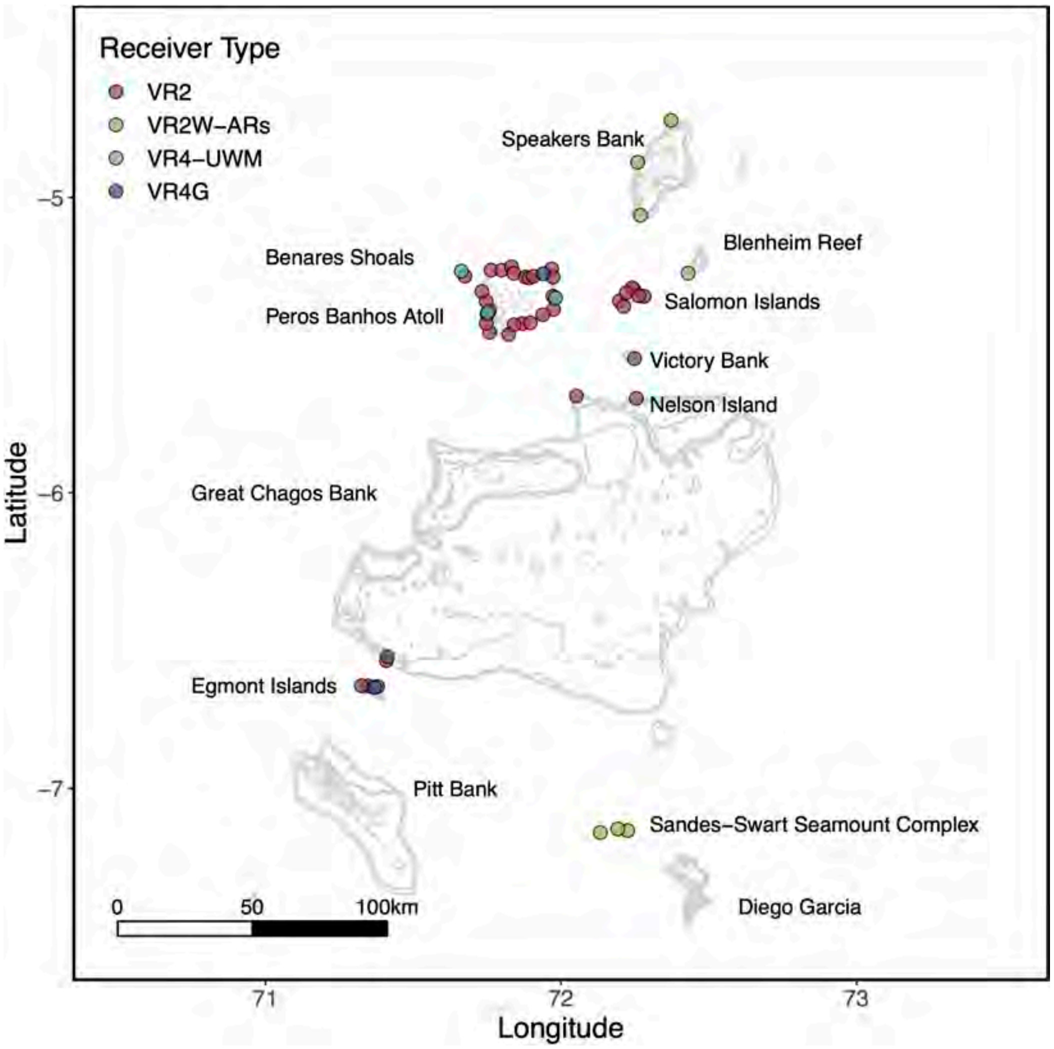

FIGURE 1 | The location of Vemco acoustic receivers across the Chagos Archipelago between March 2018 and March 2019. Colors represent receiver type. Labels depict the location of major island groups, atolls and submerged banks referred to in this study.

(sensu Stewart et al., 2016). From these, we calculated the 50, 75, and 95% polygons as a metric for each animal's activity space from the merged probability surfaces and estimated their size (km^2) and overlap (proportion of full probability surface) with the BIOT MPA.

Acoustic Tracking

For those individuals carrying acoustic tags, we first defined the "monitoring period" as the number of days between the tagging date (17/03/2018, the same for all tagged individuals) and when the receivers were downloaded at the end of the study (23/03/2019). Second, we defined 'detection period' as the number of days between the tagging date and the last detection by an individual on any one of the acoustic receivers around the archipelago. False detections caused by tag clashes or ambient noise (69 kHz) were removed (as per Jacoby et al., 2020). Two measures of residency were then calculated as per Cochran et al. (2019). First, we calculated the minimum residency index (R_{min}) as the proportion of unique days detected across the monitoring period for each shark. However, R_{min} is conservative and is sensitive to fieldwork schedules and assumes the animal is alive and the tag is functioning across the full monitoring period, potentially underrepresenting true residency. We therefore also calculated the maximum residency index (R_{max}) as the proportion of unique days detected across the detection period. In conjunction, these metrics represent the upper and lower bounds for each animal's true residency behavior (Cochran et al., 2019). Visit characteristics (duration and frequency of visits to receiver locations) were calculated for each individual following Meyer et al. (2009, 2018). A visit started and ended when either the location changed, or the transmitter was not detected for 30 min. Visits consisting of single transmitter detections were considered to last 5.9 min (equivalent to the transmitter pulse train duration of 3.6 s, preceded and followed by listening periods equivalent to the maximum nominal delay of

175 s) (**Supplementary Table 3**). We examined temporal overlap of individuals visiting the same receiver station. Detection time was converted to local time (Indian Chagos Time, UTC+6 h) and rounded to the nearest hour to explore diel patterns in occurrence at the seamounts. We then calculated the average hourly presence rates for each individual on any of the receivers from the hour of their first detection through to the hour of their last detection. For example, if shark "x" was detected at 06:00:00 14 times across a full 50-day detection period, the presence rate at 06:00:00 would be 0.28.

Vertical Habitat Utilization

Depth and temperature data from MiniPATs were either summarized into daily (24 h) bins (Sharks 2 and 4) or transmitted as time series at 150 s (Shark 6) or 600 s (Shark 1) intervals (**Table 1**). All values are expressed as the daily mean ± standard deviation. For the summarized data, the temperature bins were: $< 5°C$; $5 \leq 10°C$; $10 \leq 14°C$; $14 \leq 18°C$; $18 \leq 20°C$; $20 \leq 22°C$; $22 \leq 24°C$; $24 \leq 26°C$; $26 \leq 28°C$; $28 \leq 30°C$; $30 \leq 32°C$ and $> 32°C$. For depth, these bins were: < 5 m; $5 \leq 10$ m; $10 \leq 25$ m; $25 \leq 50$ m; $50 \leq 75$ m; $75 \leq 100$ m; $100 \leq 150$ m; $150 \leq 200$ m; $200 \leq 250$ m; $250 \leq 300$ m; $300 \leq 600$ m and > 600 m. Time series data were split into diel phases using the R package "suncalc" (Thieurmel and Elmarhraoui, 2019) in combination with estimated daily locations, and mean depths occupied during the day and night were compared using a Wilcoxon signed rank test for each individual. Dives beyond 140 m depths were quantified, with dive duration estimated as the period of time between leaving and returning to the top 100 m. To minimize the influence of the capture process on shark behavior, we removed the first 24 h post-tagging from our analyses (Cliff and Thurman, 1984).

Relative Abundance and Population Demographics

We obtained fisheries observer data from around the Chagos Archipelago from the Marine Resources Assessment Group (MRAG) who managed fishing licences in the area prior to the MPA's establishment (Mees et al., 2009).

To assess the relative abundance of silky sharks around the Chagos Archipelago, we calculated mean nominal catch per unit effort (CPUE—number of sharks caught divided by the number of hooks deployed, multiplied by 1,000) for silky sharks from longline hook survey data ($n = 41$ sets) between November 2000–January 2003 (equating to ∼1.3% of all longlines set during this period). Equivalent data for purse seine fishing were not available. To quantify the relative contribution of silky sharks to the total catch and total shark catch, the CPUEs of all other major species caught were also calculated.

To characterize silky shark population demographics within the BIOT, we analyzed the fishery observer reports from 116 fishing events between November 1997 to November 2009 (equating to ∼0.7% of all logged longline and purse seine events during this period). For each observed fishing event, data on the sex, weight and fork lengths (FL) of individuals caught were recorded, along with the gear used ("Longline," "Purse Seine," or "Unknown"). In order to easily compare these data with published length-at-maturity studies, we converted FL to total length (TL), using the relationship published by Joung et al. (2008) ($TL = 1.21 * FL + 2.36$). Following a Shapiro-Wilk test for normality, a two-sample t-test was used to compare the sizes of sharks caught by longline and purse seine vessels. Silky sharks were deemed as sexually mature if their TL exceeded 210.0 cm for females and 212.5 cm for males (Joung et al., 2008). A two-proportions Z-test was then carried out to assess whether there was a significant difference in the proportion of immature individuals caught by each gear type (longline versus purse seine).

RESULTS

Horizontal Movement Patterns

Six silky sharks (four female, one male and one of unknown sex) were satellite tagged with MiniPATs in the BIOT MPA in February and March 2013 and March 2018 (**Table 1**). All individuals were immature, except for Shark 3. Four sharks were successfully tracked for durations that ranged from 15 to 270 days with a mean duration of 154 days. These silky sharks showed high variability in individual movement behaviors (**Table 2** and **Figure 2**). We estimate that 77% of Shark 1's 50% polygon (70,540 km^2) and 37% of its 95% polygon (265,391 km^2) overlapped with the BIOT MPA. By comparison, 29% of Shark 4's 50% polygon (155,082 km^2) and 12% of its 95% polygon (416,723 km^2) overlapped with the BIOT MPA (**Supplementary Table 2**). Shark 1 headed predominately due east, with the tag popping off in the high-seas, 1,150 km away from the tagging location (**Figure 2A**). Shark 4 headed predominantly due west, with the tag popping off along the coast of Kenya, 3,549 km away from the tagging location, and having crossed four different EEZs (BIOT, Mauritius, Seychelles and Kenya) (**Figure 2A**). Conversely, Shark 2 was tracked for 270 days, had an estimated track length of over 3,000 km, yet its total 95% probability surface (53,082 km^2) was entirely within the MPA boundary (**Table 2**, **Figure 2B**, and **Supplementary Table 2**). The 95% probability surfaces of Shark 3 and 6 were also entirely within the MPA boundary, but with considerably shorter track durations (**Table 2**, **Figure 2C**, and **Supplementary Table 2**).

Acoustically tagged silky sharks were only detected on the three receivers deployed on the Sandes-Swart seamount complex (SS01, SS03 and SS04). All sharks were detected on all three seamount receivers, although principally on receivers SS03 and SS04, that were furthest west (**Figures 3A,B**). Sharks 4, 5, and 6 were not detected on any receiver after 29, 11, and 23 days, respectively, with R_{min} ranging from 0.01 to 0.07 and R_{max} ranging from 0.17 to 0.91 (**Table 3** and **Figure 3A**). Shark 7 was at liberty for 326 days, with a R_{min} of 0.57 and a R_{max} of 0.65 (**Table 3**). Across the four individuals, average presence rates on any of the seamount receivers peaked at dawn (0.36, 06:30–07:30) and was lowest around midnight (0.002, **Supplementary Figure 1**). Diel detections varied by receiver. Detections on the receivers SS04 and SS03 predominately occurred during daylight hours, with a drop-off in detections after 19:00 and increasing again after 06:00. Detections on SS01 primarily occurred at night, between 19:00 and 07:00 (**Figure 3B**). Shark 7 was detected at SS03 on 130 unique

TABLE 2 | Satellite tag (MiniPATs, Wildlife Computers) deployments on silky sharks (*Carcharhinus falciformis)* around the Chagos Archipelago between 2013 and 2018.

Shark ID	MiniPAT pop-up date	Days at liberty	MiniPAT pop-up latitude	MiniPAT pop-up longitude	Number of known locations	Displacement distance (km)	Track distance (km)	Proportion overlap between track and the BIOT MPA	Max depth (m)	TS daytime mean depth (m)	TS night-time mean depth (m)
1	09/05/2013	87	−5.375	82.369	0	1150.08	2519.35	0.77	400	21.98 ± 11.76	14.21 ± 13.38
2	15/12/2013	270	−6.455	71.219	16	49.84	3032.03	1.00	1112	–	–
4	17/11/2018	245	−3.303	40.256	33	3548.87	4782.66	0.29	392	–	–
6	27/04/2018	15	−7.131	72.124	5	2.76	149.53	1.00	314.5	33.86 ± 14.34	22.41 ± 17.79

Location data represented in decimal degrees. Track duration is the number of days between tagging date and MiniPAT pop-off date. Displacement distance is the linear distance between tag deployment and tag pop-off locations. Known locations are acoustic detections or SPOT tag position estimates used to constrain the state space model within Global Position Estimator 3 (GPE3, Wildlife Computers). Track distance is calculated as the total distance of the maximum likelihood track generated from GPE3. Mean daytime and night-time depths are from tags generating time-series data only. Overlap was calculated as the proportion of the 50% likelihood polygons from the GPE3 probability surfaces that intersected with the BIOT MPA boundary. Overlap scores relating to the 75 and 95% likelihood polygons are presented in ***Supplementary Table 2****.*

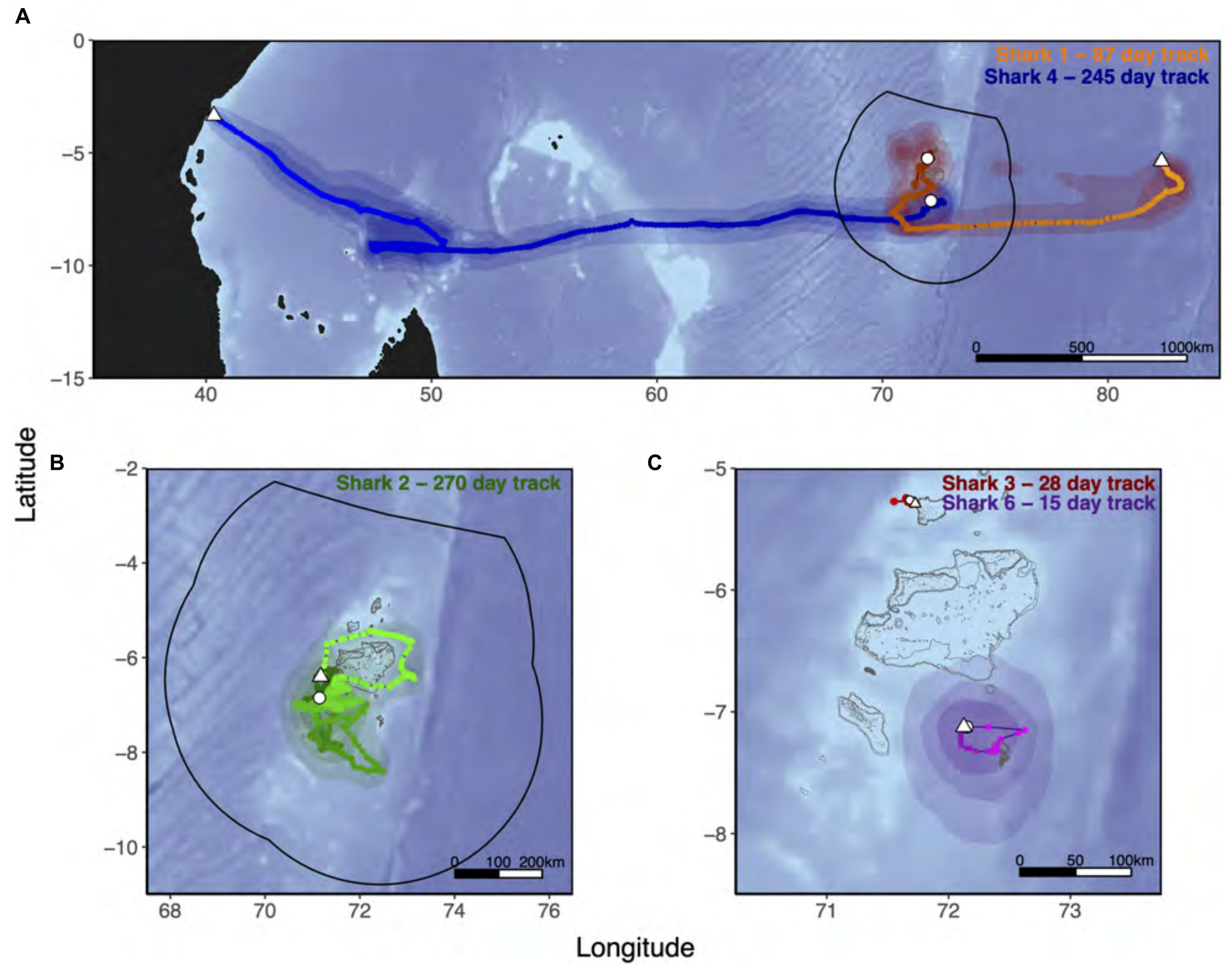

FIGURE 2 | Tracks of five silky sharks (*Carcharhinus falciformis*) tagged around the Chagos Archipelago between 2013 and 2018. Sharks 1, 2, 4, and 6 were tagged with MiniPATs and MLTs were derived using manufacturers geolocation software (GPE3; Wildlife Computers Inc., Redmond, WA, United States), with position estimates interpolated to a 0.025° × 0.025° grid spacing and smoothed with a cubic spline. Speed filters were set to 1.5 m/s for all MLTs. As Shark 3's MiniPAT did not report, its track was reconstructed from SPOT fixes only. MLTs are those of Shark 1 (Orange) and Shark 4 (Blue) (both **A**), Shark 2 (Green, **B**), Shark 3 (Red), and Shark 6 (Purple) (both **C**). Tagging location is indicated with a white circle, tag pop-up position with a white triangle. Shark 5 (satellite tag did not report) and Shark 7 (acoustic tag only) were tagged at the same location as Sharks 4 and 6. Track color lightens as the track progresses. Polygons represent the merged probability density surfaces for each MiniPAT, with light to dark shades representing 95, 75, and 50% probability contours. The boundary of the British Indian Ocean Territory (BIOT) Marine Protected Area (MPA) is shown with the solid black line. The gray outline depicts islands, atolls and submerged reefs. Underlying bathymetry was obtained from the ETOPO1 database hosted on the NOAA website at 4 min resolution through the 'marmap' package in R (R Core Team, 2020).

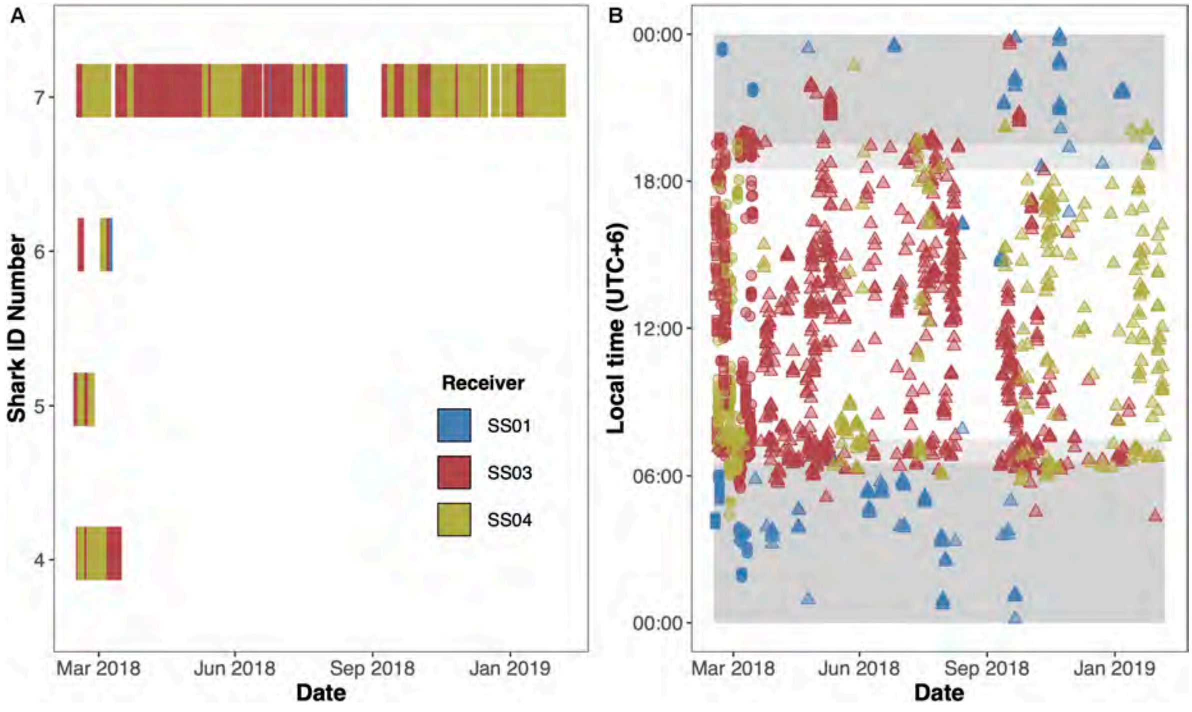

FIGURE 3 | Acoustic detections of four silky sharks (*Carcharhinus falciformis*) at the Sandes-Swart seamount complex in the Chagos Archipelago in March 2018. **(A)** Detections over time for all four individuals. **(B)** Diel detections for individuals (circle = Shark 4, square = Shark 5, diamond = Shark 6, and triangles = Shark 7) across the full time series. Dark gray shaded areas represent night-time (19:30–06:30), and lighter gray shaded areas represent dawn (06:30–07:30) and dusk (18:30–19:30). Colors represent the receivers the shark was detected on with blue = SS01; red = SS03; and yellow = SS04.

TABLE 3 | Acoustic tag deployments on silky sharks (*Carcharhinus falciformis)* around the Chagos Archipelago between 2013 and 2018.

Shark ID	V16 code	Sex	TL	Tagging date	Last date detected	Monitoring period (days)	Detection period (days)	Number of unique days detected	Number of detections	R_{min}	R_{max}
4	28613	M	148	17/03/2018	15/04/2018	371	29	26	452	0.07	0.90
5	28616	F	159	17/03/2018	28/03/2018	371	11	10	140	0.03	0.91
6	19509	F	169	17/03/2018	09/04/2018	371	23	4	11	0.01	0.17
7	19511	F	162	17/03/2018	06/02/2019	371	326	213	987	0.57	0.65

F, female; and M, male; TL, Total length (cm); V16, acoustic tags (Vemco). Monitoring period represents the number of days between the tagging date and when the receivers were downloaded at the end of the study (23/03/2019). Detection period is the number of days between first and last detection. Minimum residency index (R_{min}) equates to the number of unique days a proportion of the monitoring period. Maximum residency index (R_{max}) equates to the number of unique days a proportion of the detection period.

days—equivalent to this individual visiting at least once every 2–3 days—suggesting a core use area. The total number of visits to each receiver by each individual ranged from 1 (Shark 6 at SS04) to 270 (Shark 7 at SS03), with a maximum of eight visits to a receiver by an individual within a single day (**Supplementary Table 3**). With the exception of Shark 6 (lowest residency), the mean time elapsed between consecutive visits (i.e., absence period) by each individual to their most frequented receiver station (SS03) was relatively brief (Shark 4: 0.55 days; Shark 5: 0.28 days; Shark 7: 1.17 days). Mean visit durations at each receiver station were typically brief (overall mean of 16.5 min), and varied by individual, ranging from 5.89 min (Shark 6 on receivers SS03 and SS04) to 30.17 min (Shark 5 on SS04) (**Supplementary Table 3**). Maximum visit duration was 148.67 min (Shark 4 on receiver SS04); however, visits exceeding 1 h at any receiver station were relatively uncommon, accounting for only 3.90% of all visits. The maximum number of individuals simultaneously visiting the same receiver station was two, and only occurred on six and five occasions at SS03 and SS04, respectively, and lasted between 1.69 to 48.35 min (overall mean 10.49 min).

Vertical Habitat Utilization

Depth and temperature data were recorded by MiniPATs deployed on four sharks (Sharks 1, 2, 4, and 6; **Table 1**). Tagged individuals spent 99.41 ± 0.20% of their time in the top 100 m of the water column, with the largest proportion of time in depths of 25–50 m (31.13 ± 8.57%), followed by depths of 10–25 m (30.55 ± 5.47%; **Figure 4A**). All sharks dived to depths greater than 300 m, with a maximum recorded depth of 1112 m reported

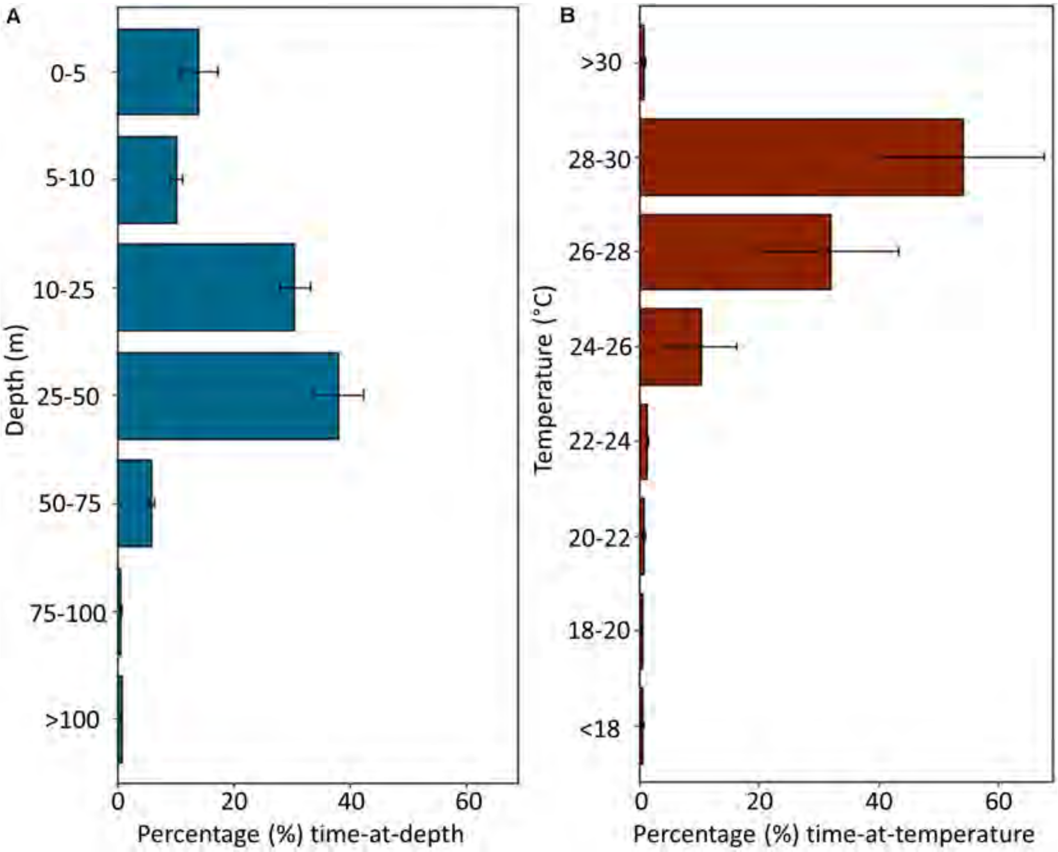

FIGURE 4 | Summarized depth and temperature data recorded by MiniPAT tags deployed on four silky sharks (*Carcharhinus falciformis*) tagged around the Chagos Archipelago. Histograms represent mean percent time spent at **(A)** depth and **(B)** temperature. Error bars indicate ± one standard error.

from Shark 2. Tagged sharks occupied temperatures of 24–30°C for 96.11 ± 1.52% of the deployment period (**Figure 4B**).

Time-series data collected at 10- and 2.5-min intervals from Sharks 1 (n = 8 days) and 6 (n = 16 days), respectively, revealed patterns of diel vertical movement and oscillatory diving (**Figure 5**). Mean depths were significantly deeper in the day than at night (**Table 2**; Wilcoxon signed rank tests: Shark 1: $V = 35$, $p = 0.02$; Shark 6: $V = 133$, $p \leq 0.01$). These two sharks continued to oscillate through the water column between diel phases, spending considerably less time in the surface 5 m during the day and shifting to a shallower distribution at night (**Figure 5** and **Table 2**). We observed seven dives beyond 140 m by Shark 6, with five occurring within an hour of sunrise (~07:00) or sunset (~19:00), one at 04:00 and another at 11:00 local time. The median dive duration was 7.5 min. Shark 1 did not undertake any dives beyond 140 m throughout its time at liberty.

Relative Abundance and Population Estimates

In the months of November to January between 2000 and 2003, the catch of longliners operating around the Chagos Archipelago was dominated by yellowfin *Thunnus albacares* (28.33% of catch by number) and bigeye tuna *Thunnus obesus* (25.91%). Sharks contributed 4.18% of the total catch by number. Furthermore, blue sharks (0.66), pelagic thresher sharks *Alopias pelagicus* (0.44), and silky sharks (0.34) were the most frequently caught per set. Silky sharks accounted for 14.84% of all sharks identified to species level and 13.69% of all sharks caught (**Table 4**). Silky sharks were caught at an average catch rate of 0.20 individuals per thousand hooks set (for comparison, the target species of tuna were caught at roughly 10 individuals per thousand hooks). Pelagic thresher sharks were caught at a rate of 0.25 per thousand hooks and blue sharks at a rate of 0.68 per thousand hooks (**Table 4**).

Silky Shark Size Distributions

Of the 677 sharks reported by fisheries observers between November 1997 and November 2009, 69 were identified as silky sharks and reported as being caught within BIOT. Of all the silky sharks reported, 23 were from longlines (15 female, 7 male and 1 unsexed), 22 from purse seines (12 female and 10 male) and 24 from unrecorded fishing methods (11 female, 8 male and 5 unsexed) (**Figure 6**). The average length of silky sharks caught around the Chagos Archipelago was 211.12 cm (± 8.01 s.e.), with no statistical difference between sex (females 204.49 ± 10.58 cm; males 205.83 ± 12.82 cm), and 55.88% of individuals being

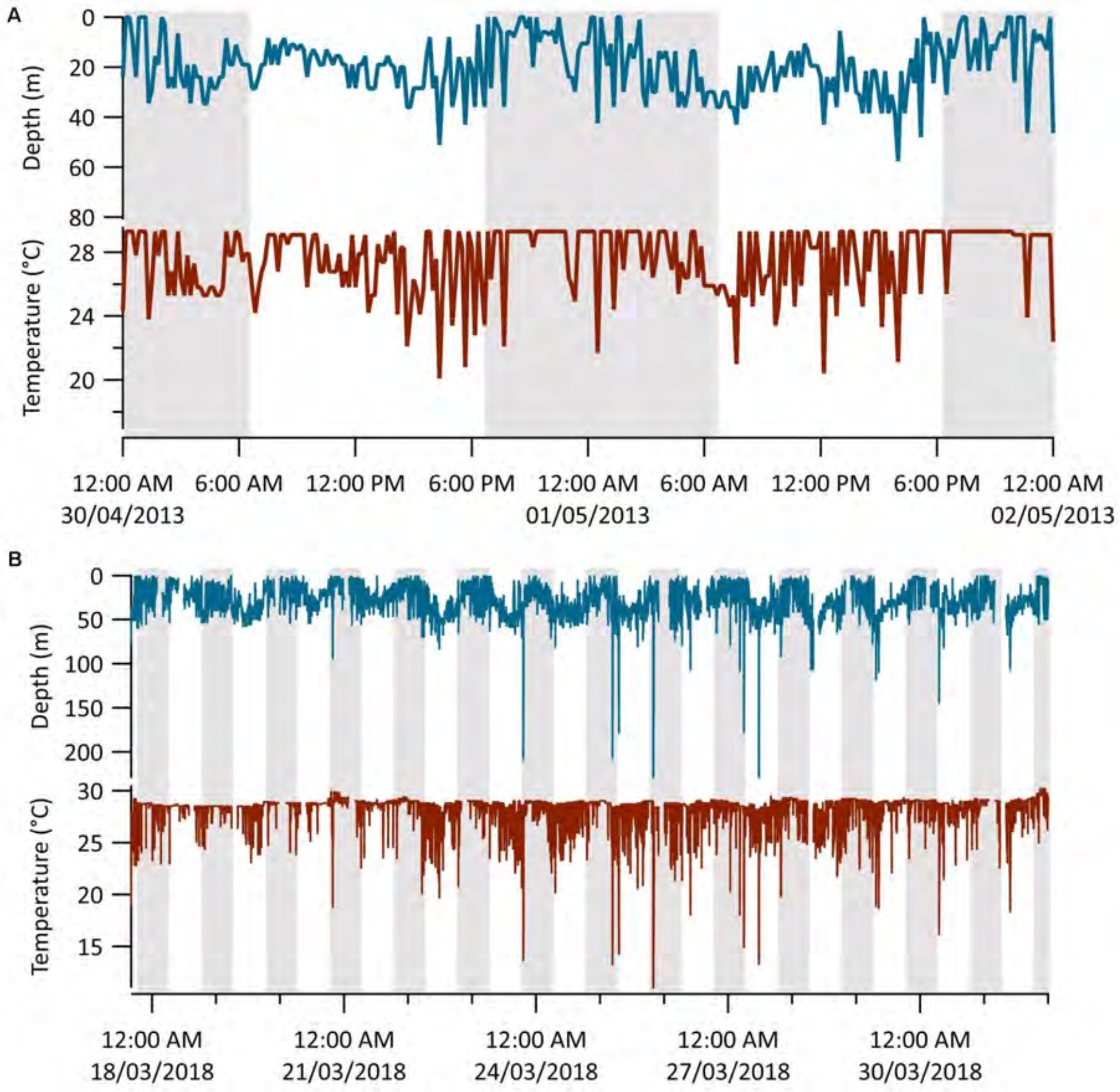

FIGURE 5 | MiniPAT depth (blue) and temperature (red) time-series data from tags deployed on two silky sharks (*Carcharhinus falciformis*) tagged around the Chagos Archipelago. Gray shaded areas represent night-time (19:00–07:00) and white daytime (07:00–19:00). **(A)** Representative diel vertical movements of shark 1 over 2 days. **(B)** The entire transmitted depth and temperature series from shark 6.

immature juveniles. The average length of silky sharks caught by longlines (211.46 ± 8.01 cm) was significantly larger than individuals caught by purse seines (148.55 ± 6.10 cm) (two sample *t*-test: $t = 5.31$, df = 33.96, $p < 0.01$) and purse seines (100%) caught a significantly higher proportion of juveniles than longlines (54.55%) (Chi-squared = 10.48, df = 1, $p < 0.01$). Only 16.67% of sharks from unrecorded fishing methods were immature, and all were female (**Figure 6**).

DISCUSSION

Understanding the movement patterns, depth and thermal preferences of vulnerable pelagic sharks can inform efforts to minimize negative fisheries interactions (Queiroz et al., 2016; Hazen et al., 2018). Through analyses of biotelemetry and fisheries data in the central Indian Ocean, we demonstrate the high variability in horizontal movement behavior of silky sharks in the region and consider the ecological significance of the Chagos Archipelago and the MPA that surrounds it. This study advances our understanding of this relatively understudied species in a region where many fish stocks are already heavily depleted and pressure is expected to increase considerably, with nearly half the world's human population expected to live around the Indian Ocean by 2050 (Doyle, 2018). Our findings contribute toward the understanding and the evaluation of the role that large-scale spatial management strategies, like MPAs, may have in the conservation of mobile pelagic species.

TABLE 4 | Summary table of the frequency (f), CPUE (Number caught per thousand hooks), standard errors (s.e.), and percentage contributions to catches for tunas and sharks from 41 longline sets surveyed as part of an observer run hook survey between November and February in 2000 to 2003 around the Chagos Archipelago.

Species	f	Mean CPUE	s.e.	Percentage of		
				Total catch	Identified sharks	All sharks
Yellowfin tuna *Thunnus albacares*	0.98	10.01	3.66	28.33		
Bigeye tuna *Thunnus obesus*	0.93	9.27	1.54	25.91		
Blue shark *Prionace glauca*	0.66	0.68	0.39	1.82	47.10	43.45
Pelagic thresher shark *Alopias pelagicus*	0.44	0.25	0.22	0.67	17.42	16.07
Silky shark *Carcharhinus falciformis*	0.34	0.20	0.09	0.57	14.84	13.69
All other identified sharks	0.44	0.29	0.10	0.80	20.65	19.05
Unidentified sharks	0.24	0.11	0.07	0.32		7.74
All sharks combined	1.00	1.54	0.16	4.18		

Silky sharks are known to be highly mobile, with previous studies reporting maximum displacement distances of 1,010 km (Hutchinson et al., 2019), 1,339 km (Kohler et al., 1998), 2,200 km (Lara-Lizardi et al., 2020), and even 3,195 km (Schaefer et al., 2019). Two of the sharks tagged within this study exhibited large ranging movements, with Shark 4 (displacement distance 3,549 km, total track distance of 4,782 km) considerably exceeding the published maximum displacement distance for the species. Although both sharks spent considerable periods of time within the BIOT MPA before exiting, such wide-ranging movements suggest large distribution ranges, spanning multiple EEZs and the areas beyond national jurisdiction. This emphasizes the importance of implementing effective fishery management and developing multi-national conservation measures, especially for purse seiners where mortality rates are high, even if sharks are released (Poisson et al., 2014; Hutchinson et al., 2015; Eddy et al., 2016). For example, the use of non-entangling FADs (Franco et al., 2012; Lopez et al., 2017) can reduce the potential of ghost-fishing events (Filmalter et al., 2013) and the introduction of best practice handling and release procedures can reduce post-release mortality (Poisson et al., 2016). Yet, spatial protection can be effective for wide-ranging marine predators even if they do not encapsulate the species' entire home range, if they contain core habitats supporting key life-history stages, such as breeding, feeding or gestation (Hooker et al., 2011).

The distribution and movement of pelagic predators has been shown to correlate with environmental conditions, such as thermal fronts, chlorophyll-*a* concentrations and upwelling events (Block et al., 2011; Lezama-Ochoa et al., 2016; Braun et al., 2019; Lopez et al., 2020). The two silky sharks with the largest displacement distances within this study displayed divergent movement trajectories, with one heading east and the other west. It is important to note that these two individuals were tagged at a similar time of the year, although 5 years apart. As such, inter-annual fluctuations of climate and prevailing oceanic conditions, such as the Indian Ocean Dipole (IOD) (Saji et al., 1999), may have played a factor in the direction and nature of their respective movements. When the IOD is positive, upwelling occurs along coasts of Sumatra and Java, increasing primary productivity in the east and decreasing productivity in the west (Marsac, 2008). Interestingly, Shark 1 headed east during a negative IOD phase and Shark 4 headed west during a positive IOD phase, contrary to our expectation that silky sharks would migrate toward more productive areas. Importantly, given our small sample size, differences observed here could be simply attributable to individual variation, especially as divergent longitudinal movements of silky sharks have been observed in individuals tagged at several other locations (Musyl et al., 2011b; Filmalter et al., 2015; Hutchinson et al., 2019). Alternatively, movement behaviors of individuals may have been artificially impacted by association with drifting FADs (Hutchinson et al., 2019), although a recent study demonstrated that at least 30% of juvenile silky shark movements were not associated with surface currents (Bonnin et al., 2020).

Whilst the aforementioned individuals demonstrate the high mobility potential of silky sharks, the majority of the tagging data available for the species indicate far shorter displacement distances and stronger residency behavior (Kohler et al., 1998; Clarke et al., 2011a; Hutchinson et al., 2019). Shark 2's 270-day maximum likelihood track and 95% probability polygon was entirely within the MPA boundary and around the geographical features of the Chagos Archipelago. Shark 7 also exhibited prolonged residency at the Sandes-Swart seamount complex. The Chagos Archipelago has been previously described as harboring reef fish biomass up to six times higher than elsewhere in the Indian Ocean (Graham et al., 2013) and having high levels of primary production (Hosegood et al., 2019) compared to the surrounding largely oligotrophic ocean (Morel et al., 2010). The archipelago also contains ∼73 seamounts (Yesson et al., 2020) that are hotspots of pelagic biodiversity (Morato et al., 2010; Letessier et al., 2019), and silky sharks are known to frequently use shallow areas adjacent to deep water (Compagno, 1984; Clarke et al., 2011a). As only one adult silky shark was tagged for a limited duration, we cannot rule out that adult sharks may be less resident than the juveniles tracked for longer here. However, the rich resources and varied habitats of the Chagos Archipelago may be providing all the resources required, reducing the need for wide-ranging foraging behavior, especially for juveniles and early life stages. As reducing juvenile mortality has profound positive effects on future population growth (Cortés, 2002; Beerkircher and Shivji, 2003), the exclusion of industrial fisheries, the biggest threat to juvenile silky sharks (Lawson, 2011; Clarke et al., 2018), from the BIOT MPA could be providing considerable benefits for the species. However, this is dependent on effective enforcement and management. The BIOT MPA is threatened by targeted illegal, unreported and unregulated fishing (IUU) vessels, principally from Sri Lanka and India (Clark et al., 2015;

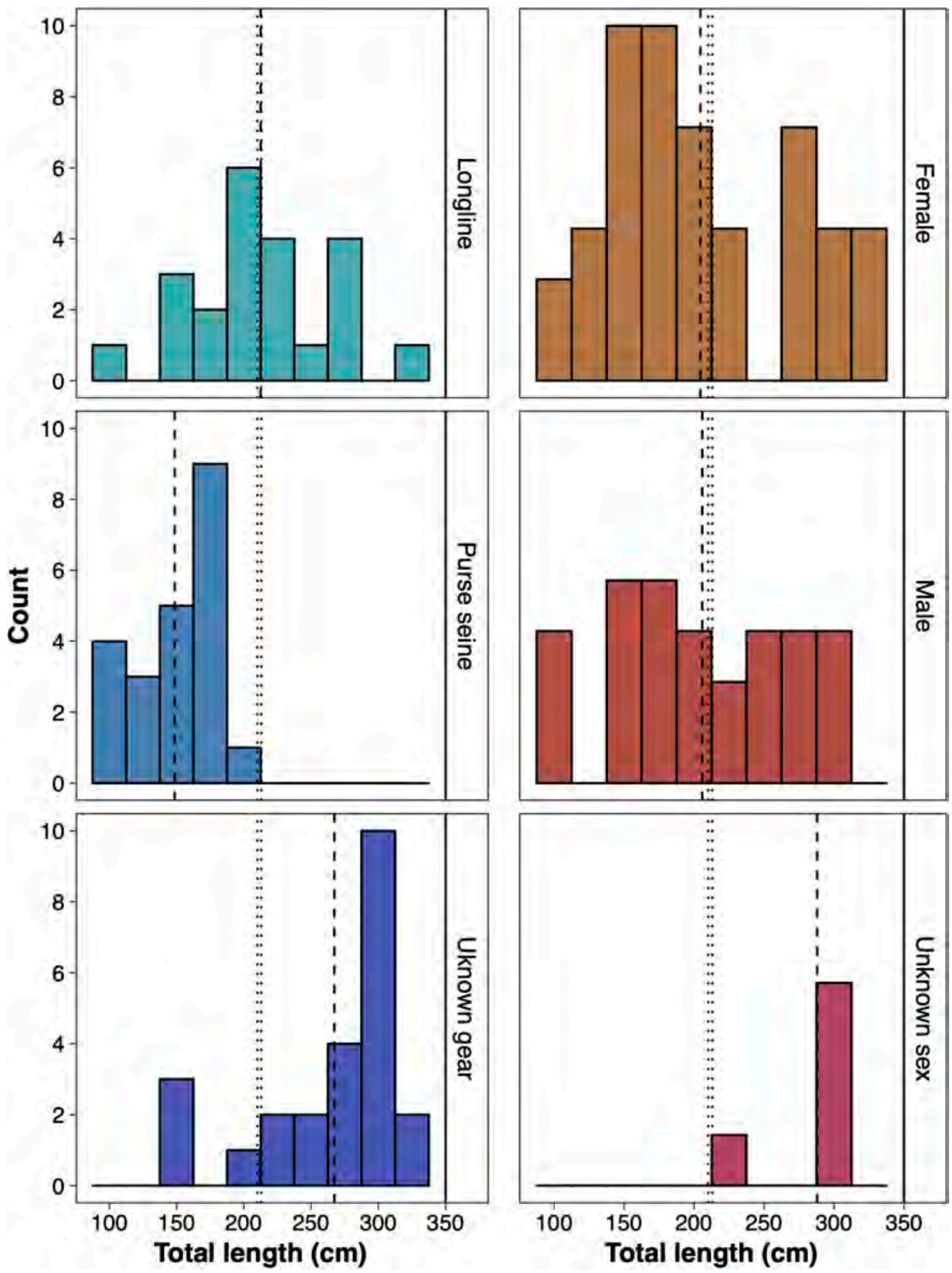

FIGURE 6 | The size distribution of silky sharks (*Carcharhinus falciformis*) caught around the Chagos Archipelago between November 1997 and November 2009 by purse seine, longline and unknown gear (left) and of female, male and individuals of an unknown sex caught by all gear types (right). Vertical dashed lines represent the mean lengths recorded by each respective group. Vertical dotted lines represent the estimated total length of maturity of female (210 cm) and male (212 cm) silky sharks (Joung et al., 2008).

Ferretti et al., 2018; Tickler et al., 2019; Jacoby et al., 2020) and FADs still drift through, potentially aggregating biomass and exporting it outside and into fishable waters.

Notwithstanding some spatial overlap, individuals were temporally separated and visits to receiver stations were typically brief and relatively frequent. We observed considerable differences in detection patterns between individuals, ranging from prolonged occupancy across ∼11 months to repeated detections across a shorter period, 11–29 days. Large variation in residency behavior, including prolonged occupancies, have previously been documented amongst a silky shark population in the Red Sea (Clarke et al., 2011a). Shark 7 remained associated with the seamount for nearly an entire year, suggesting a high degree of fidelity or philopatry to this feature. Seamounts have been previously demonstrated as important sites for pelagic sharks (Morato et al., 2010, 2016; Letessier et al., 2019) and oceanographic observations of the Sandes-Swart seamount complex have attributed the aggregations of predators at its summit to the accumulation of biomass induced by the presence and formation of internal lee waves (Hosegood et al., 2019). Conversely, the relatively high R_{max} and low R_{min} indices in Sharks 4 and 5, suggest intense use of these features during short time periods. Sharks may therefore be utilizing the seamounts as meeting or feeding points intermittently during larger movements. Such association behavior is also consistent with silky shark interactions with FADs, which they typically associate with for between 15 and 30 days (Filmalter et al., 2015; Hutchinson et al., 2019). Importantly, we recognize that tag failure or mortality can also cause the subsequent lack of detections and is a limitation of acoustic data. We also note that, despite acoustic receivers being located throughout the archipelago (Carlisle et al., 2019), silky sharks were only detected on the receivers located on Sandes-Swart seamount complex, close to where they were tagged. However, as the next nearest receivers were located at Egmont Atoll, over 90 km to the north west, we cannot rule out that silky sharks were using other shallow features nearer by, such as Diego Garcia, the Great Chagos Bank or Pitt Bank, that were not monitored by acoustic receivers during this study.

There were clear diel variations in the detections of silky sharks at the seamount. Consistent detections on the seamount during the day and absences at night are in parallel to silky shark behavior observed around FADs, where night-time absences were attributed to feeding excursions (Filmalter et al., 2015). Juvenile silky sharks may therefore be behaving as central place foragers around this feature, as has been demonstrated in reef sharks around Palmyra Atoll in the Pacific (Papastamatiou et al., 2018), during the duration of their association.

We report that tagged silky sharks displayed patterns of diel vertical migration, oscillatory diving behavior and spent > 99% of their time in the top 100 m of the water column, while also diving to depths of greater than 300 m. Our findings are therefore broadly consistent with observations of silky sharks in the Pacific (Musyl et al., 2011b; Hutchinson et al., 2019). Yet, we also observed much deeper dives, with one individual recorded to a depth of 1,112 m, the deepest recorded dive for the species (previously reported at 640 m; Hueter et al., 2018). The vertical distribution and diving behavior of pelagic predatory fishes is typically driven by the need to optimize prey encounter rates and energy expenditure, while remaining within preferred environmental conditions (i.e., temperature, oxygen) (Carey et al., 1990; Klimley et al., 2002; Meyer et al., 2009; Andrzejaczek et al., 2019). Consistent with studies in the Pacific (Hutchinson et al., 2019), Atlantic (Hueter et al., 2018), and western Indian Ocean (Filmalter et al., 2015), silky shark diving depths were, on average, shallower at night than during the day, but deeper dives were generally associated with local dawn and dusk. We interpret this to be foraging behavior, as mesopelagic species are a regular occurrence in the diet of Indian Ocean silky sharks (Filmalter et al., 2017). Overall, the vertical niche occupied by silky sharks in this study overlaps directly with the hanging depth of purse seine nets (up to 200 m) in the Indian Ocean (Kaplan et al., 2014), putting them at high risk of capture should they leave the protection of the MPA. However, typical depths of longline hooks set in the Indian Ocean for yellowfin or bigeye are deeper, between 100–250 m and 100–400 m, respectively (Nishida et al., 2003). As such, there is less direct vertical overlap with longlines, although sharks may undertake deeper vertical movements if attracted to baited hooks, as they are frequently caught by longliners in the Indian Ocean (Huang and Liu, 2010).

It has been hypothesized that pelagic shark species display thermal (Musyl et al., 2011b) and vertical niche partitioning (Choy et al., 2009). Previous studies have shown silky sharks residing in waters within 2°C of the surface water temperature in the Red Sea (Clarke et al., 2011a), but being limited to water temperatures above 23°C (Musyl et al., 2011b) and occupying water temperatures between 24 and 29°C in the Pacific (Hutchinson et al., 2019). Similarly, individuals tagged around the Chagos Archipelago occupied the 24–30°C thermal band for 96% of their time at liberty. Thermal niche is coupled with horizontal and vertical distributions and is temporally and spatially variable (Musyl et al., 2011a). The interannual variability in sea surface temperature driven by climatic oscillations, such as the IOD (Saji et al., 1999), could therefore drive temporal variation in vertical habitat use. This may explain the variation in mean diel depths between the two sharks reporting time-series data tagged in similar months, though 5 years apart, although more tagging data is needed in this area to investigate this hypothesis further.

Analysis of the historical fisheries data indicated that silky sharks were a significant component of the pelagic shark community around the Chagos Archipelago between November 2000 and February 2003, prior to the MPA's establishment. Furthermore, the vast majority of individuals caught were juvenile, indicating that the MPA may be an important area for silky sharks during early life stages. Silky sharks contributed 0.6% of total longline catch. This is broadly consistent with those observed across the Indian Ocean by longlines targeting bigeye tuna, although considerably lower than those targeting yellowfin tuna (7.5%) (Huang and Liu, 2010). This is primarily driven by variations in fishing method, such as hook depth, which is increased when targeting bigeye tuna and can lower silky shark catch by a factor of 6.4 (Gilman et al., 2008). Unfortunately, no data were available on hook depth, nor other fishing method variations, such as bait selection, soak time or deployment time, which are also known to influence catch rates and composition (Romanov, 2002). However, as yellowfin tuna were the dominant catch, we can assume some lines were targeted at this species and therefore silky shark catches were lower than expected. These are likely attributable to the ban on wire leaders in BIOT in 1999 (Dunne et al., 2014), a measure previously shown to reduce the silky shark catch rates by ∼40% (Ward et al., 2008), or the prohibition of fishing within 12 nautical miles of the islands, atolls and reefs of the archipelago (Dunne et al., 2014), as shallow coastal habitats can be an important habitat for juvenile silky sharks (Branstetter, 1987; Bonfil, 1997).

The fisheries observer data represent the best available information on historic pelagic shark communities for the territory, yet there are important considerations when making inferences given their limited coverage. For example, we cannot rule out seasonal variation in silky shark catch rates. The longline hook survey only spanned three years and all sets surveyed were carried out between November and January, the traditional peak fishing season around the Chagos Archipelago (Dunn and Curnick, 2019; Curnick et al., 2020), when migrating tuna are thought to pass through the area (Pearce, 1996). This may in turn lead to increased catch rates of pelagic predators during this time, especially silky sharks who associate with these target species. Species specific shark catches, however, were not routinely recorded in logbooks, despite the IOTC requesting their inclusion in 2005 due to limited shark-specific data (Molina et al., 2005). As such, it is difficult to ascertain whether the patterns seen in the observer data, given the relatively low number of lines surveyed and uneven sampling, were truly representative of catches by the fishery. Further, no quantitative survey data were available for purse seiners in BIOT, where silky shark bycatch is higher (Molina et al., 2005; González et al., 2007), especially for those using FADs (Amandè et al., 2008; Watson et al., 2009; Gilman, 2011).

Within a relatively small sample size, we observed very distinct spatial tracks with a large degree of variation between individuals. Such intra-species variation has been previously noted in silky sharks (Filmalter et al., 2015) and other elasmobranch species, such as the reef manta ray (*Mobula alfredi*) (Andrzejaczek et al., 2020) and Galapagos shark (*Carcharhinus galapagensis*) (Lowe et al., 2006). We advocate that an extensive tagging program with deployments across multiple sexes, life stages, regions and seasons is urgently needed to confirm whether behaviors observed here are consistent through time and ontogeny and are representative of the Indian Ocean population. Such data are crucial to inform future stock assessments for the species that are currently uncertain and data-poor, resulting in management advice being unclear (IOTC, 2017). Further, such data could support the development of adaptive spatial management or dynamic ocean management (Lopez et al., 2020), which are seen as promising tools to improve the conservation and management of these species, and are being considered by several fisheries management organizations (Hobday et al., 2013; Maxwell et al., 2015; Hazen et al., 2018; Welch et al., 2019).

We provide intriguing insights into the behavior of silky sharks in the central Indian Ocean, documenting the furthest displacement distance and deepest dive for the species, yet also demonstrating high site fidelity and prolonged residency. However, given the small number of animals tracked and high variability observed, further investigations are required to confirm how silky sharks found in the MPA are connected to the wider Indian Ocean, whether their behaviors are consistent through time and ontogeny, and what environmental conditions drive these behaviors. We also highlight the value of combining telemetry studies with historical fisheries analyses, and the importance of broadening elasmobranch research to understudied species in data-poor regions. High site fidelity to geographic features and predictable utilization of them by juveniles, as observed here, suggests that well enforced protection in key areas could be an effective conservation strategy for the species. We conclude that spatial protection should be a component of a holistic management strategy for the species, alongside fisheries regulations and conservation measures in adjacent EEZs and in areas beyond national jurisdiction.

DATA AVAILABILITY STATEMENT

The datasets presented in this study can be found in online repositories. The names of the repository/repositories and accession number(s) can be found below: https://www.gtopp.org/ or requested from the corresponding author.

ETHICS STATEMENT

This animal study was reviewed and approved by the Stanford University Administrative Panel on Laboratory Animal Care (APLAC) under permit APLAC-10765 and the Zoological Society of London's ethics committee under permit 186-BME-0652.

AUTHOR CONTRIBUTIONS

DJC, DMPJ, BAB, HJK, and BC secured the funding for the program. DJC and BC conceived the manuscript. DJC, DMPJ, ABC, TKC, FF, RJS, and TW collected the field data. DJC, SA, DMPJ, and DMC analyzed the data and drafted the manuscript, with input from all other co-authors. All authors, except for BC who sadly passed away during the preparation of the manuscript, read and approved the final manuscript.

FUNDING

This work was funded by the Bertarelli Foundation through the Bertarelli Programme in Marine Science, the Zoological Society of London, and a University College London Impact Award. Additional funding for tags was provided by the JSF Pollitzer Charitable Trust, The Rufford Foundation and the Ernest Kleinwort Charitable Trust through the Chagos Conservation Trust.

ACKNOWLEDGMENTS

This manuscript is dedicated to co-author, friend, and mentor Dr. Ben Collen. We would like to thank the MRAG for the provision of the fisheries data used within the study. We would also like to extend our thanks to the various ship captains and crews who supported the deployment and retrieval of our equipment, often in challenging circumstances. We would also like to thank the three reviewers for their thorough and constructive reviews.

SUPPLEMENTARY MATERIAL

The Supplementary Material for this article can be found online at: https://www.frontiersin.org/articles/10.3389/fmars.2020.596619/full#supplementary-material

REFERENCES

Aldana-Moreno, A., Hoyos-Padilla, E. M., González-Armas, R., Galván-Magaña, F., Hearn, A., Klimley, A. P., et al. (2020). Residency and diel movement patterns of the endangered scalloped hammerhead Sphyrna lewini in the Revillagigedo National Park. *J. Fish Biol.* 96, 543–548. doi: 10.1111/jfb.14239

Amandè, M. J., Ariz, J., Chassot, E., de Molina, A. D., Gaertner, D., Murua, H., et al. (2010). Bycatch of the European purse seine tuna fishery in the Atlantic Ocean for the 2003–2007 period. *Aquat. Living Resour.* 23, 353–362. doi: 10.1051/alr/2011003

Amandè, M. J., Chassot, E., Chavance, P., and Pianet, R. (2008). *Silky Shark (Carcharhinus falciformis) Bycatch in the French Tuna Purse-Seine Fishery of the Indian Ocean* (Seychelles: IOTC), 22p.

Amante, C., and Eakins, B. W. (2009). *ETOPO1 1 Arc-Minute Global Relief Model: Procedures, Data Sources and Analysis. NOAA Technical Memorandum NESDIS NGDC-24*. Washington, DC: NOAA, doi: 10.1594/PANGAEA.769615

Andrzejaczek, S., Chapple, T., Curnick, D., Carlisle, A., Castleton, M., Jacoby, D., et al. (2020). Individual variation in residency and regional movements of reef manta rays Mobula alfredi in a large marine protected area. *Mar. Ecol. Prog. Ser.* 639, 137–153. doi: 10.3354/meps13270

Andrzejaczek, S., Gleiss, A. C., Pattiaratchi, C. B., and Meekan, M. G. (2019). Patterns and drivers of vertical movements of the large fishes of the epipelagic. *Rev. Fish Biol. Fish.* 29, 335–354. doi: 10.1007/s11160-019-09555-1

Baum, J. K., Myers, R. A., Kehler, D. G., Worm, B., Harley, S. J., and Doherty, P. A. (2003). Collapse and conservation of shark populations in the Northwest Atlantic. *Science* 299, 389–392. doi: 10.1126/science.1079777

Beerkircher, L., and Shivji, M. S. (2003). A Monte Carlo demographic analysis of the silky shark (Carcharhinus falciformis): implications of gear selectivity. *Fish. Bull.* 101:168.

Block, B., Jonsen, I., Jorgensen, S., Winship, A., Shaffer, S., Bograd, S. J., et al. (2011). Tracking apex marine predator movements in a dynamic ocean. *Nature* 475, 86–90. doi: 10.1038/nature10082

Boerder, K., Schiller, L., and Worm, B. (2019). Not all who wander are lost: improving spatial protection for large pelagic fishes. *Mar. Policy* 105, 80–90. doi: 10.1016/j.marpol.2019.04.013

Bonfil, R. (1997). Status of shark resources in the Southern Gulf of Mexico and Caribbean: implications for management. *Fish. Res.* 29, 101–117. doi: 10.1016/S0165-7836(96)00536-X

Bonfil, R. (2008). "The biology and ecology of the silky shark, Carcharhinus falciformis," in *Sharks of the Open Ocean: Biology, Fisheries and Conservation*, eds M. D. Camhi, E. K. Pikitch, and E. A. Babcock (Hoboken, NJ: Wiey), 114–127. doi: 10.1002/9781444302516.ch10

Bonnin, L., Lett, C., Dagorn, L., Filmalter, J. D., Forget, F., Verley, P., et al. (2020). Can drifting objects drive the movements of a vulnerable pelagic shark? *Aquat. Conserv. Mar. Freshw. Ecosyst.* doi: 10.1002/aqc.3420 [Epub ahead of print].

Branstetter, S. (1987). Age, growth and reproductive biology of the silky shark, Carcharhinus falciformis, and the scalloped hammerhead, *Sphyrna lewini*, from the northwest Gulf of Mexico. *Environ. Biol. Fishes* 19, 161–173. doi: 10.1007/BF00005346

Braun, C. D., Gaube, P., Sinclair-Taylor, T. H., Skomal, G. B., and Thorrold, S. R. (2019). Mesoscale eddies release pelagic sharks from thermal constraints to foraging in the ocean twilight zone. *Proc. Natl. Acad. Sci. U.S.A.* 116, 17187. doi: 10.1073/pnas.1903067116

Camhi, M. (2009). *The Conservation Status of Pelagic Sharks and Rays: Report of the IUCN Shark Specialist Group Pelagic Shark Red List Workshop*. Oxford: University of Oxford.

Carey, F. G., Scharold, J. V., and Kalmijn, A. J. (1990). Movements of blue sharks (*Prionace glauca*) in depth and course. *Mar. Biol.* 106, 329–342. doi: 10.1007/BF01344309

Carlisle, A. B., Tickler, D., Dale, J. J., Ferretti, F., Curnick, D. J., Chapple, T. K., et al. (2019). Estimating space use of mobile fishes in a large marine protected area with methodological considerations in acoustic array design. *Front. Mar. Sci.* 6:256. doi: 10.3389/fmars.2019.00256

Chapman, D. D., Pikitch, E. K., Babcock, E., and Shivji, M. S. (2005). marine reserve design and evaluation using automated acoustic telemetry: a case-study involving coral reef-associated sharks in the mesoamerican caribbean. *Mar. Technol. Soc. J.* 39, 42–55. doi: 10.4031/002533205787521640

Choy, C. A., Popp, B. N., Kaneko, J. J., and Drazen, J. C. (2009). The influence of depth on mercury levels in pelagic fishes and their prey. *Proc. Natl. Acad. Sci. U.S.A.* 106, 13865–13869. doi: 10.1073/pnas.0900711106

Clark, M. J., Duffy, H., Pearce, J., and Mees, C. (2015). *Update on the Catch and Bycatch Composition of Illegal Fishing in the British Indian Ocean Territory (BIOT) and A Summary of Abandoned and Lost Fishing*. London: MRAG Ltd.

Clarke, C., Lea, J. S. E., and Ormond, R. F. G. (2011a). Reef-use and residency patterns of a baited population of silky sharks, *Carcharhinus falciformis*, in the Red Sea. *Mar. Freshw. Res.* 62, 668–675. doi: 10.1071/MF10171

Clarke, S., Harley, S., Hoyle, S., and Rice, J. (2011b). *An Indicator-Based Analysis of Key Shark Species Based on Data Held by SPC-OFP*. Kolonia: Western Central Pacific Fisheries Commission.

Clarke, S., Langley, A., Lennert-Cody, C. E., Aires-da-Silva, A., and Maunder, M. N. (2018). *Pacific-wide Silky Shark (Carcharhinus falciformis) Stock Status Assessment*. Available online at: https://www.wcpfc.int/file/216441/download?token=wBsGzwyd (accessed July 15, 2020).

Cliff, G., and Thurman, G. D. (1984). Pathological and physiological effects of stress during capture and transport in the juvenile dusky shark, *Carcharhinus obscurus*. *Comp. Biochem. Physiol. Part A Physiol.* 78, 167–173. doi: 10.1016/0300-9629(84)90111-7

Cochran, J. E. M., Braun, C. D., Fernando Cagua, E., Campbell, M. F., Hardenstine, R. S., Kattan, A., et al. (2019). Multi-method assessment of whale shark (*Rhincodon typus*) residency, distribution, and dispersal behavior at an aggregation site in the Red Sea. *PLoS One* 14:e0222285. doi: 10.1371/journal.pone.0222285

Compagno, L. J. (1984). Sharks of the world. FAO Species Cat. *Fish. Purp.* 4, 251–255. doi: 10.1016/j.neuropharm.2006.07.020

Cortés, E. (2002). Incorporating uncertainty into demographic modeling: application to shark populations and their conservation. *Conserv. Biol.* 16, 1048–1062. doi: 10.1046/j.1523-1739.2002.00423.x

Curnick, D. J., Collen, B., Koldewey, H. J., Jones, K. E., Kemp, K. M., and Ferretti, F. (2020). Interactions between a large Marine Protected Area, pelagic tuna and associated fisheries. *Front. Mar. Sci.* 7:318. doi: 10.3389/fmars.2020.00318

De Santo, E. M., Jones, P. J. S., and Miller, A. M. M. (2011). Fortress conservation at sea: a commentary on the Chagos marine protected area. *Mar. Policy* 35, 258–260. doi: 10.1016/j.marpol.2010.09.004

Doherty, P. D., Baxter, J. M., Gell, F. R., Godley, B. J., Graham, R. T., Hall, G., et al. (2017). Long-term satellite tracking reveals variable seasonal migration strategies of basking sharks in the north-east Atlantic. *Sci. Rep.* 7:42837. doi: 10.1038/srep42837

Doyle, T. (2018). Blue economy and the Indian Ocean Rim. *J. Indian Ocean Reg.* 14, 1–6. doi: 10.1080/19480881.2018.1421450

Dulvy, N. K., Fowler, S. L., Musick, J. A., Cavanagh, R. D., Kyne, P. M., Harrison, L. R., et al. (2014). Extinction risk and conservation of the world's sharks and rays. *eLife* 3:e00590. doi: 10.7554/eLife.00590

Dunn, N., and Curnick, D. (2019). Using historical fisheries data to predict tuna distribution within the British Indian Ocean Territory Marine Protected Area, and implications for its management. *Aquat. Conserv. Mar. Freshw. Ecosyst.* 29, 2057–2070. doi: 10.1002/aqc.3204

Dunne, R. P., Polunin, N. V. C., Sand, P. H., and Johnson, M. L. (2014). The creation of the Chagos marine protected area: a fisheries perspective. *Adv. Mar. Biol.* 69, 79–127. doi: 10.1016/B978-0-12-800214-8.00003-7

Eddy, C., Brill, R., and Bernal, D. (2016). Rates of at-vessel mortality and post-release survival of pelagic sharks captured with tuna purse seines around drifting fish aggregating devices (FADs) in the equatorial eastern Pacific Ocean. *Fish. Res.* 174, 109–117. doi: 10.1016/j.fishres.2015.09.008

Ferretti, F., Curnick, D., Liu, K., Romanov, E. V., and Block, B. A. (2018). Shark baselines and the conservation role of remote coral reef ecosystems. *Sci. Adv.* 4:eaaq0333. doi: 10.1126/sciadv.aaq0333

Ferretti, F., Worm, B., Britten, G. L., Heithaus, M. R., and Lotze, H. K. (2010). Patterns and ecosystem consequences of shark declines in the ocean. *Ecol. Lett.* 13, 1055–1071. doi: 10.1111/j.1461-0248.2010.01489.x

Filmalter, J., Cowley, P., Forget, F., and Dagorn, L. (2015). Fine-scale 3-dimensional movement behaviour of silky sharks *Carcharhinus falciformis* associated with fish aggregating devices (FADs). *Mar. Ecol. Prog. Ser.* 539, 207–223. doi: 10.3354/meps11514

Filmalter, J. D., Capello, M., Deneubourg, J. L., Cowley, P. D., and Dagorn, L. (2013). Looking behind the curtain: quantifying massive shark mortality in fish aggregating devices. *Front. Ecol. Environ.* 11:291–296. doi: 10.1890/130045

Filmalter, J. D., Cowley, P. D., Potier, M., Ménard, F., Smale, M. J., Cherel, Y., et al. (2017). Feeding ecology of silky sharks *Carcharhinus falciformis* associated with floating objects in the western Indian Ocean. *J. Fish Biol.* 90, 1321–1337. doi: 10.1111/jfb.13241

Filmalter, J. D., Dagorn, L., Cowley, P. D., and Taquet, M. (2011). First descriptions of the behavior of silky sharks, *Carcharhinus falciformis*, around drifting fish aggregating devices in the Indian Ocean. *Bull. Mar. Sci.* 87, 325–337. doi: 10.5343/bms.2010.1057

Filmalter, J. D., Dagorn, L., and Soria, M. (2010). *Double Tagging Juvenile Silky Sharks to Improve Our Understanding of the Behavioural Ecology: Preliminary Results*. Seychelles: Indian Ocean Tuna Commission.

Franco, J., Moreno, G., López, J., and Sancristobal, I. (2012). Testing new designs of drifting fish aggregating device (DFAD) in the Eastern Atlantic to reduce turtle and shark mortality. *Collect. Vol. Sci. Pap. ICCAT* 68, 1754–1762.

Game, E. T., Grantham, H. S., Hobday, A. J., Pressey, R. L., Lombard, A. T., Beckley, L. E., et al. (2009). Pelagic protected areas: the missing dimension in ocean conservation. *Trends Ecol. Evol.* 24, 360–369. doi: 10.1016/j.tree.2009.01.011

Gilman, E., Clarke, S., Brothers, N., Alfaro-Shigueto, J., Mandelman, J., Mangel, J., et al. (2008). Shark interactions in pelagic longline fisheries. *Mar. Policy* 32, 1–18. doi: 10.1016/j.marpol.2007.05.001

Gilman, E. L. (2011). Bycatch governance and best practice mitigation technology in global tuna fisheries. *Mar. Policy* 35, 590–609. doi: 10.1016/j.marpol.2011.01.021

González, I., Ruiz, J., Moreno, G., Murua, H., and Artetxe, I. (2007). *AZTI Discard sampling programme in the spanish purse-seiner fleet in the Western Indian Ocean (2003–2006)*. Seychelles: Indian Ocean Tuna Commission.

Graham, N. A. J., Pratchett, M. S., McClanahan, T. R., and Wilson, S. K. (2013). "The status of coral reef fish assemblages in the chagos archipelago, with implications for protected area management and climate change," in *Coral Reefs of the United Kingdom Overseas Territories*, ed. C. Sheppard (Berlin: Springer), 253–270. doi: 10.1007/978-94-007-5965-7_19

Hazen, E. L., Scales, K. L., Maxwell, S. M., Briscoe, D. K., Welch, H., Bograd, S. J., et al. (2018). A dynamic ocean management tool to reduce bycatch and support sustainable fisheries. *Sci. Adv.* 4, eaar3001. doi: 10.1126/sciadv.aar3001

Hazin, F., Oliveira, P., and Macena, B. (2007). *Aspects of the Reproductive Biology of the Silky Shark, Carcharhinus falciformis (Nardo, 1827), in the vicinity of Archipelago of Saint Peter and Saint Paul, in the equatorial Atlantic Ocean*. Available online at: http://www.iccat.int/documents/cvsp/cv060_2007/no_2%5CCV060020648.pdf (accessed January 11, 2016).

Henderson, A. C., McIlwain, J. L., Al-Oufi, H. S., Al-Sheile, S., and Al-Abri, N. (2009). Size distributions and sex ratios of sharks caught by Oman's artisanal fishery. *Afr. J. Mar. Sci.* 31, 233–239. doi: 10.2989/AJMS.2009.31.2.11.883

Hobday, A. J., Young, J. W., Abe, O., Costa, D. P., Cowen, R. K., Evans, K., et al. (2013). Climate impacts and oceanic top predators: moving from impacts to adaptation in oceanic systems. *Rev. Fish Biol. Fish.* 23, 537–546. doi: 10.1007/s11160-013-9311-0

Hooker, S. K., Cañadas, A., Hyrenbach, K. D., Corrigan, C., Polovina, J. J., and Reeves, R. R. (2011). Making protected area networks effective for marine top predators. *Endanger. Species Res.* 13, 203–218. doi: 10.3354/esr00322

Hosegood, P. J., Nimmo-Smith, W. A. M., Proud, R., Adams, K., and Brierley, A. S. (2019). Internal lee waves and baroclinic bores over a tropical seamount shark 'hot-spot.'. *Prog. Oceanogr.* 172, 34–50. doi: 10.1016/j.pocean.2019.01.010

Huang, H. W., and Liu, K. M. (2010). Bycatch and discards by Taiwanese large-scale tuna longline fleets in the Indian Ocean. *Fish. Res.* 106, 261–270. doi: 10.1016/j.fishres.2010.08.005

Hueter, R. E., Tyminski, J. P., Pina-Amargós, F., Morris, J. J., Abierno, A. R., Valdés, J. A. A., et al. (2018). Movements of three female silky sharks (*Carcharhinus falciformis*) as tracked by satellite-linked tags off the Caribbean coast of Cuba. *Bull. Mar. Sci.* 94, 345–358. doi: 10.5343/bms.2017.1162

Hutchinson, M., Coffey, D. M., Holland, K., Itano, D., Leroy, B., Kohin, S., et al. (2019). Movements and habitat use of juvenile silky sharks in the Pacific Ocean inform conservation strategies. *Fish. Res.* 210, 131–142. doi: 10.1016/j.fishres.2018.10.016

Hutchinson, M., Itano, D., Muir, J., and Holland, K. (2015). Post-release survival of juvenile silky sharks captured in a tropical tuna purse seine fishery. *Mar. Ecol. Prog. Ser.* 521, 143–154. doi: 10.3354/meps11073

IOTC (2017). *Status of the Indian Ocean silky shark (FAL: Carcharhinus falciformis)*. Victoria: IOTC, doi: 10.5281/zenodo.3263244

Jacoby, D. M. P., Ferretti, F., Freeman, R., Carlisle, A. B., Chapple, T. K., Curnick, D. J., et al. (2020). Shark movement strategies influence poaching risk and can guide enforcement decisions in a large, remote marine protected area. *J. Appl. Ecol.* 57, 1782–1792. doi: 10.1111/1365-2664.13654

Jorgensen, S. J., Reeb, C. A., Chapple, T. K., Anderson, S., Perle, C., Van Sommeran, S. R., et al. (2010). Philopatry and migration of Pacific white sharks. *Proc. Biol. Sci.* 277, 679–688. doi: 10.1098/rspb.2009.1155

Joung, S. J., Chen, C. T., Lee, H. H., and Liu, K. M. (2008). Age, growth, and reproduction of silky sharks, *Carcharhinus falciformis*, in northeastern Taiwan waters. *Fish. Res.* 90, 78–85. doi: 10.1016/j.fishres.2007.09.025

Kaplan, D. M., Chassot, E., Amandé, J. M., Dueri, S., Demarcq, H., Dagorn, L., et al. (2014). Spatial management of Indian Ocean tropical tuna fisheries: potential and perspectives. *ICES J. Mar. Sci.* 71, 1728–1749. doi: 10.1093/icesjms/fst233

Kessel, S. T., and Hussey, N. E. (2015). Tonic immobility as an anaesthetic for elasmobranchs during surgical implantation procedures. *Can. J. Fish. Aquat. Sci.* 72, 1287–1291. doi: 10.1139/cjfas-2015-0136

Klimley, P. A., Beavers, S. C., Curtis, T. H., and Jorgensen, S. J. (2002). Movements and swimming behavior of three species of sharks in La Jolla Canyon, California. *Environ. Biol. Fishes* 63, 117–135. doi: 10.1023/A:1014200301213

Kohler, N. E., Casey, J. G., and Turner, P. A. (1998). NMFS cooperative shark tagging program, 1962-93: an atlas of shark tag and recapture data. *Mar. Fish. Rev.* 60, 1–87. doi: 10.7755/mfr.81.2.1

Koldewey, H. J., Curnick, D., Harding, S., Harrison, L. R., and Gollock, M. (2010). Potential benefits to fisheries and biodiversity of the Chagos Archipelago/British Indian Ocean Territory as a no-take marine reserve. *Mar. Pollut. Bull.* 60, 1906–1915. doi: 10.1016/j.marpolbul.2010.10.002

Kranstauber, B., and Smolla, M. (2015). *move: Visualizing and Analyzing Animal Track Data*. Available online at: http://cran.r-project.org/package=move (accessed January 11, 2016).

Lara-Lizardi, F., Hoyos-Padilla, M., Hearn, A., Klimley, A. P., Galván-Magaña, F., Arauz, R., et al. (2020). Shark movements in the Revillagigedo Archipelago and connectivity with the Eastern Tropical Pacific. *bioRxiv[Preprint]* doi: 10.1101/2020.03.02.972844

Lawson, T. (2011). *Estimation of Catch Rates and Catches of Key Shark Species in Tuna Fisheries of the Western and Central Pacific Ocean Using Observer Data. Western and Central Pacific Fisheries Commission (WCPFC)*. Available online at: http://www.wcpfc.int/system/files/EB-IP-02 [Estimation of Catch Rates and Catches of Key Shark Species].pdf (accessed January 11, 2016).

Lea, J. S. E., Wetherbee, B. M., Queiroz, N., Burnie, N., Aming, C., Sousa, L. L., et al. (2015). Repeated, long-distance migrations by a philopatric predator targeting highly contrasting ecosystems. *Sci. Rep.* 5:11202. doi: 10.1038/srep11202

Letessier, T. B., Mouillot, D., Bouchet, P. J., Vigliola, L., Fernandes, M. C., Thompson, C., et al. (2019). Remote reefs and seamounts are the last refuges for marine predators across the IndoPacific. *PLoS Biol.* 17:e3000366. doi: 10.1371/journal.pbio.3000366

Lezama-Ochoa, N., Murua, H., Chust, G., Van Loon, E., Ruiz, J., Hall, M., et al. (2016). Present and future potential habitat distribution of *Carcharhinus falciformis* and *Canthidermis maculata* by-catch species in the tropical tuna purse-seine fishery under climate change. *Front. Mar. Sci.* 3:34. doi: 10.3389/fmars.2016.00034

Lopez, J., Alvarez-Berastegui, D., Soto, M., and Murua, H. (2020). Using fisheries data to model the oceanic habitats of juvenile silky shark (*Carcharhinus falciformis*) in the tropical eastern Atlantic Ocean. *Biodivers. Conserv.* 29, 2377–2397. doi: 10.1007/s10531-020-01979-7

Lopez, J., Goñi, N., Arregi, I., Ruiz, J., Krug, I., Murua, H., et al. (2017). *Main Results of the Spanish Best Practices Program: Evolution of the Use of Non-Entangling FADs, Interaction with Entangled Animals, and Fauna Release Operations. IOTC–2017–WGFAD01–11*. Seychelles: IOTC.

Lowe, C. G., Wetherbee, B. M., and Meyer, C. G. (2006). Using acoustic telemetry monitoring techniques to quantity movement patterns and site fidelity of sharks and giant trevally around French frigate shoals and midway atoll. *Atoll Res. Bull.* 543, 281–303.

Marsac, F. (2008). *Outlook of Ocean Climate Variability in the West tropical Indian Ocean, 1997–2008*. Seychelles: Indian Ocean Tuna Commission.

Maxwell, S. M., Hazen, E. L., Lewison, R. L., Dunn, D. C., Bailey, H., Bograd, S. J., et al. (2015). Dynamic ocean management: defining and conceptualizing real-time management of the ocean. *Mar. Policy* 58, 42–50. doi: 10.1016/j.marpol.2015.03.014

Mees, C., Pearce, J., Clarke, J., and Wilson, O. (2009). *UK (Chagos/BIOT) National Report. IOTC Twelfth Session of the Scientific Committee Mahé*. Seychelles: IOTC.

Meyer, C. G., Anderson, J. M., Coffey, D. M., Hutchinson, M. R., Royer, M. A., and Holland, K. N. (2018). Habitat geography around Hawaii's oceanic islands influences tiger shark (*Galeocerdo cuvier*) spatial behaviour and shark bite risk at ocean recreation sites. *Sci. Rep.* 8, 1–18. doi: 10.1038/s41598-018-23006-0

Meyer, C. G., Clark, T. B., Papastamatiou, Y. P., Whitney, N. M., and Holland, K. N. (2009). Long-term movement patterns of tiger sharks *Galeocerdo cuvier* in Hawaii. *Mar. Ecol. Prog. Ser.* 381, 223–235. doi: 10.3354/meps07951

Molina, A. D. D., Ariz, J., Sarralde, R., de Molina, A. D., Pallarés, P., and Santana, J. C. (2005). *Activity of the Spanish Purse Seine Fleet in the Indian Ocean and by-Catch Data Obtained from Observer Programmes Conducted in 2003 and 2004.* Seychelles: IOTC.

Morato, T., Hoyle, S. D., Allain, V., and Nicol, S. J. (2010). Seamounts are hotspots of pelagic biodiversity in the open ocean. *Proc. Natl. Acad. Sci. U.S.A.* 107, 9707–9711. doi: 10.1073/pnas.0910290107

Morato, T., Miller, P. I., Dunn, D. C., Nicol, S. J., Bowcott, J., and Halpin, P. N. (2016). A perspective on the importance of oceanic fronts in promoting aggregation of visitors to seamounts. *Fish Fish.* 17, 1227–1233. doi: 10.1111/faf.12126

Morel, A., Claustre, H., and Gentili, B. (2010). The most oligotrophic subtropical zones of the global ocean: similarities and differences in terms of chlorophyll and yellow substance. *Biogeosciences* 7:3139. doi: 10.5194/bg-7-3139-2010

Muir, J., Itano, D., Hutchinson, M., Leroy, B., and Holland, K. (2012). *Behavior of Target and Non-Target Species on Drifting FADs and When Encircled by Purse Seine Gear*. Busan: Western and Central Pacific Fisheries Commission-Scientific Committee.

Musyl, M. K., Brill, R. W., Boggs, C. H., Curran, D. S., Kazama, T. K., and Seki, M. P. (2003). Vertical movements of bigeye tuna (*Thunnus obesus*) associated with islands, buoys, and seamounts near the main Hawaiian Islands from archival tagging data. *Fish. Oceanogr.* 12, 152–169. doi: 10.1046/j.1365-2419.2003.00229.x

Musyl, M. K., Brill, R. W., Curran, D. S., Fragoso, N. M., McNaughton, L. M., Nielsen, A., et al. (2011a). Postrelease survival, vertical and horizontal movements, and thermal habitats of five species of pelagic sharks in the central Pacific Ocean. *Fish. Bull.* 109, 341–368. doi: 10.1186/1471-2199-9-107

Musyl, M. K., Domeier, M. L., Nasby-Lucas, N., Brill, R. W., McNaughton, L. M., Swimmer, J. Y., et al. (2011b). Performance of pop-up satellite archival tags. *Mar. Ecol. Prog. Ser.* 433, 1–28. doi: 10.3354/meps09202

Musyl, M. K., and Gilman, E. L. (2018). Post-release fishing mortality of blue (*Prionace glauca*) and silky shark (*Carcharhinus falciformis*) from a Palauan-based commercial longline fishery. *Rev. Fish Biol. Fish.* 28, 567–586. doi: 10.1007/s11160-018-9517-2

Nishida, T., Bigelow, K., Mohri, M., and Marsac, F. (2003). *Comparative Study on Japanese Tuna Longline Cpue Standardization of Yellowfin Tuna (Thunnus Albacares) in the Indian Ocean Based on Two Methods: - General Linear Model (Glm) and Habitat-Based Model (Hbm)/Glm Combined* (Seychelles: IOTC), 6, 48–69.

Papastamatiou, Y. P., Watanabe, Y. Y., Demšar, U., Leos-Barajas, V., Bradley, D., Langrock, R., et al. (2018). Activity seascapes highlight central place foraging strategies in marine predators that never stop swimming. *Mov. Ecol.* 6, 9. doi: 10.1186/s40462-018-0127-3

Patterson, T. A., Basson, M., Bravington, M. V., and Gunn, J. S. (2009). Classifying movement behaviour in relation to environmental conditions using hidden Markov models. *J. Anim. Ecol.* 78, 1113–1123. doi: 10.1111/j.1365-2656.2009.01583.x

Pearce, J. (1996). *A review of the British Indian Ocean Territory fisheries conservation and management zone tuna fishery, 1991 – 1995*. Available online at: http://www.oceandocs.org/bitstream/handle/1834/497/EC601-17.pdf?sequence=1 (accessed January 11, 2016).

Peel, L. R., Stevens, G. M. W., Daly, R., Daly, C. A. K., Collin, S. P., Nogués, J., et al. (2020). Regional movements of reef manta rays (*Mobula alfredi*) in Seychelles Waters. *Front. Mar. Sci.* 7:558. doi: 10.3389/fmars.2020.00558

Poisson, F., Crespo, F. A., Ellis, J. R., Chavance, P., Pascal, B., Santos, M. N., et al. (2016). Technical mitigation measures for sharks and rays in fisheries for tuna and tuna-like species: turning possibility into reality. *Aquat. Living Resour.* 29:402. doi: 10.1051/alr/2016030

Poisson, F., Filmalter, J. D., Vernet, A., and Dagorn, L. (2014). Mortality rate of silky sharks (*Carcharhinus falciformis*) caught in the tropical tuna purse seine fishery in the Indian Ocean. *Can. J. Fish. Aquat. Sci.* 71, 795–798. doi: 10.1139/cjfas-2013-0561

Poisson, F., Vernet, A. L., Filmalter, J. D., Goujon, M., and Dagorn, L. (2011). *Survival Rate of Silky Sharks (Carcharhinus falciformis) Caught Incidentally Onboard French Tropical Purse Seiners* (Seychelles: IOTC), 6.

Queiroz, N., Humphries, N. E., Couto, A., Vedor, M., da Costa, I., Sequeira, A. M. M., et al. (2019). Global spatial risk assessment of sharks under the footprint of fisheries. *Nature* 572, 461–466. doi: 10.1038/s41586-019-1444-4

Queiroz, N., Humphries, N. E., Mucientes, G., Hammerschlag, N., Lima, F. P., Scales, K. L., et al. (2016). Ocean-wide tracking of pelagic sharks reveals extent of overlap with longline fishing hotspots. *Proc. Natl. Acad. Sci. U.S.A.* 113, 1582–1587. doi: 10.1073/pnas.1510090113

R Development Core Team (2018). *R: A Language and Environment for Statistical Computing*. Vienna: R Foundation Statistical Computing.

Rigby, C. L., Sherman, C. S., Chin, A. and Simpfendorfer, C. (2017). *Carcharhinus falciformis. The IUCN Red List of Threatened Species*, e.T39370A117721799. doi: 10.2305/IUCN.UK.2017-3.RLTS.T39370A117721799.en

Robbins, W. D., Hisano, M., Connolly, S. R., and Choat, J. H. (2006). Ongoing collapse of coral-reef shark populations. *Curr. Biol.* 16, 2314–2319. doi: 10.1016/j.cub.2006.09.044

Romanov, E. V. (2002). Bycatch in the tuna purse-seine fisheries of the western Indian Ocean. *Fish. Bull.* 100, 90–105.

Román-Verdesoto, M., and Orozco-Zöller, M. (2005). *Bycatches of Sharks in the Tuna Purse-Seine Fishery of the Eastern Pacific Ocean Reported by Observers of the Inter-American Tropical Tuna Commission, 1993–2004* (San Diego, CA: IATTC).

Saji, N. H., Goswami, B. N., Vinayachandran, P. N., and Yamagata, T. (1999). A dipole mode in the tropical Indian Ocean. *Nature* 401, 360–363. doi: 10.1038/43854

Sánchez-De Ita, J. A., Quiñónez-Velázquez, C., Galván-magaña, F., Bocanegra-Castillo, N., and Félix-Uraga, R. (2011). Age and growth of the silky shark Carcharhinus falciformis from the west coast of Baja California Sur, Mexico. *J. Appl. Ichthyol.* 27, 20–24. doi: 10.1111/j.1439-0426.2010.01569.x

Schaefer, K. M., Fuller, D. W., Aires-Da-Silva, A., Carvajal, J. M., Martínez-Ortiz, J., and Hutchinson, M. R. (2019). Postrelease survival of silky sharks (*Carcharhinus falciformis*) following capture by longline fishing vessels in the equatorial eastern Pacific Ocean. *Bull. Mar. Sci.* 95, 355–369. doi: 10.5343/bms.2018.0052

Sheppard, C. R. C., Ateweberhan, M., Bowen, B. W., Carr, P., Chen, C. A., Clubbe, C., et al. (2012). Reefs and islands of the Chagos Archipelago, Indian Ocean: why it is the world's largest no-take marine protected area. *Aquat. Conserv. Mar. Freshw. Ecosyst.* 22, 232–261. doi: 10.1002/aqc.1248

Skomal, G. B., Braun, C. D., Chisholm, J. H., and Thorrold, S. R. (2017). Movements of the white shark Carcharodon carcharias in the North Atlantic Ocean. *Mar. Ecol. Prog. Ser.* 580, 1–16. doi: 10.3354/meps12306

Stewart, J. D., Beale, C. S., Fernando, D., Sianipar, A. B., Burton, R. S., Semmens, B. X., et al. (2016). Spatial ecology and conservation of Manta birostris in the Indo-Pacific. *Biol. Conserv.* 200, 178–183. doi: 10.1016/j.biocon.2016.05.016

Thieurmel, B., and Elmarhraoui, A. (2019). *suncalc: Compute Sun Position, Sunlight Phases, Moon Position and Lunar Phase*. Available online at: https://CRAN.R-project.org/package=suncalc (accessed October 1, 2020).

Tickler, D. M., Carlisle, A. B., Chapple, T. K., Curnick, D. J., Dale, J. J., Schallert, R. J., et al. (2019). Potential detection of illegal fishing by passive acoustic telemetry. *Anim. Biotelemetry* 7:1. doi: 10.1186/s40317-019-0163-9

Urbina, J. O. D., Brunel, T., Coelho, R., Merino, G., Daniela, R., Santos, C., et al. (2018). *A Preliminary Stock Assessment for the Silky Shark in the Indian Ocean Using a Data-Limited Approach*. Seychelles: IOTC.

Ward, P., Lawrence, E., Darbyshire, R., and Hindmarsh, S. (2008). Large-scale experiment shows that nylon leaders reduce shark bycatch and benefit pelagic longline fishers. *Fish. Res.* 90, 100–108. doi: 10.1016/j.fishres.2007.09.034

Watson, J. T., Essington, T. E., Lennert-Cody, C. E., and Hall, M. A. (2009). Trade-offs in the design of fishery closures: management of silky shark bycatch in the Eastern Pacific Ocean Tuna fishery. *Conserv. Biol.* 23, 626–635. doi: 10.1111/j.1523-1739.2008.01121.x

WCPFC (2018). *SC14 - Summary Report - 11August2019*. Busan: WCPFC.

Welch, H., Hazen, E. L., Bograd, S. J., Jacox, M. G., Brodie, S., Robinson, D., et al. (2019). Practical considerations for operationalizing dynamic management tools. *J. Appl. Ecol.* 56, 459–469. doi: 10.1111/1365-2664.13281

Weng, K. C., Castilho, P. C., Morrissette, J. M., Landeira-Fernandez, A. M., Holts, D. B., Schallert, R. J., et al. (2005). Satellite tagging and cardiac physiology reveal niche expansion in salmon sharks. *Science* 310, 104–106. doi: 10.1126/science.1114616

Wilson, S. G., Jonsen, I. D., Schallert, R. J., Ganong, J. E., Castleton, M. R., Spares, A. D., et al. (2015). Tracking the fidelity of Atlantic bluefin tuna released in Canadian waters to the Gulf of Mexico spawning grounds. *Can. J. Fish. Aquat. Sci.* 72, 1700–1717. doi: 10.1139/cjfas-2015-0110

Witt, M. J., Åkesson, S., Broderick, A. C., Coyne, M. S., Ellick, J., Formia, A., et al. (2010). Assessing accuracy and utility of satellite-tracking data using Argos-linked Fastloc-GPS. *Anim. Behav.* 80, 571–581. doi: 10.1016/j.anbehav.2010.05.022

Wood, L. J., Fish, L., Laughren, J., and Pauly, D. (2008). Assessing progress towards global marine protection targets: shortfalls in information and action. *Oryx* 42, 340–351. doi: 10.1017/S003060530800046X

Worm, B., Davis, B., Kettemer, L., Ward-Paige, C. A., Chapman, D., Heithaus, M. R., et al. (2013). Global catches, exploitation rates, and rebuilding options for sharks. *Mar. Policy* 40, 194–204. doi: 10.1016/j.marpol.2012.12.034

Wright, G., Gjerde, K. M., Johnson, D. E., Finkelstein, A., Ferreira, M. A., Dunn, D. C., et al. (2019). Marine spatial planning in areas beyond national jurisdiction. *Mar. Policy* doi: 10.1016/j.marpol.2018.12.003 [Epub ahead of print].

Yesson, C., Letessier, T. B., Nimmo-Smith, A., Hosegood, P. J., Brierley, A. S., Harouin, M., et al. (2020). Improved bathymetry leads to 4000 new seamount predictions in the global ocean. *UCL Open Environ.* doi: 10.14324/111.444/000044.v1 [Epub ahead of print].

Conflict of Interest: The authors declare that the research was conducted in the absence of any commercial or financial relationships that could be construed as a potential conflict of interest.

frontiers
in Marine Science

ORIGINAL RESEARCH
published: 07 January 2021
doi: 10.3389/fmars.2020.598515

Seasonal Occurrence, Horizontal Movements, and Habitat Use Patterns of Whale Sharks (*Rhincodon typus*) in the Gulf of Mexico

Eric R. Hoffmayer[1]*, Jennifer A. McKinney[2], James S. Franks[3], Jill M. Hendon[3], William B. Driggers III[1], Brett J. Falterman[2], Benjamin Galuardi[4] and Michael E. Byrne[5]

[1] Mississippi Laboratories, Southeast Fisheries Science Center, National Marine Fisheries Service, National Oceanic and Atmospheric Administration, Pascagoula, MS, United States, [2] Louisiana Department of Wildlife and Fisheries, New Orleans, LA, United States, [3] Center for Fisheries Research and Development, Gulf Coast Research Laboratory, The University of Southern Mississippi, Ocean Springs, MS, United States, [4] Greater Atlantic Regional Fishery Office, National Marine Fisheries Service, National Oceanic and Atmospheric Administration, Gloucester, MA, United States, [5] School of Natural Resources, University of Missouri, Columbia, MO, United States

OPEN ACCESS

Edited by:
Mark Meekan,
Australian Institute of Marine Science (AIMS), Australia

Reviewed by:
Adrian C. Gleiss,
Murdoch University, Australia
Philip D. Doherty,
University of Exeter, United Kingdom
Jesse Cochran,
King Abdullah University of Science and Technology, Saudi Arabia

***Correspondence:**
Eric R. Hoffmayer
Eric.hoffmayer@noaa.gov

Specialty section:
This article was submitted to Marine Megafauna, a section of the journal Frontiers in Marine Science

Received: *24 August 2020*
Accepted: *16 November 2020*
Published: *07 January 2021*

Citation:
Hoffmayer ER, McKinney JA, Franks JS, Hendon JM, Driggers WB III, Falterman BJ, Galuardi B and Byrne ME (2021) Seasonal Occurrence, Horizontal Movements, and Habitat Use Patterns of Whale Sharks (Rhincodon typus) in the Gulf of Mexico. Front. Mar. Sci. 7:598515. doi: 10.3389/fmars.2020.598515

In the northern Gulf of Mexico (GOM), whale sharks (*Rhincodon typus*) form large aggregations at continental shelf-edge banks during summer; however, knowledge of movements once they leave aggregation sites is limited. Here we report on the seasonal occurrence of whale sharks in the northern GOM based on over 800 whale shark sightings from 1989 to 2016, as well as the movements of 42 whale sharks tagged with satellite-linked and popup satellite archival transmitting tags from 2008 to 2015. Sightings data were most numerous during summer and fall often with aggregations of individuals reported along the continental shelf break. Most sharks (66%) were tagged during this time at Ewing Bank, a known aggregation site off the coast of Louisiana. Whale shark track duration ranged from three to 366 days and all tagged individuals, which ranged from 4.5 to 12.0 m in total length, remained within the GOM. Sightings data revealed that whale sharks occurred primarily in continental shelf and shelf-edge waters (81%) whereas tag data revealed the sharks primarily inhabited continental slope and open ocean waters (91%) of the GOM. Much of their time spent in open ocean waters was associated with the edge of the Loop Current and associated mesoscale eddies. During cooler months, there was a net movement southward, corresponding with the time of reduced sighting reports. Several sharks migrated to the southwest GOM during fall and winter, suggesting this region could be important overwintering habitat and possibly represents another seasonal aggregation site. The three long-term tracked whale sharks exhibited interannual site fidelity, returning one year later to the vicinity where they were originally tagged. The increased habitat use of north central GOM waters by whale sharks as summer foraging grounds and potential interannual site fidelity to Ewing Bank demonstrate the importance of this region for this species.

Keywords: sightings, elasmobranch, satellite tags, hidden Markov model, Rhincodontidae

INTRODUCTION

Our understanding of the ecology of large marine vertebrates has increased significantly in recent years due to advances in bio-logging technology to study their movements, behavior, physiology and habitat preferences (Hart and Hyrenbach, 2009; Jaine et al., 2014; Chmura et al., 2018; Whitford and Klimley, 2019). Highly migratory fishes, such as pelagic sharks, have been particularly difficult to study due to the complexity of their ecology and the concealing nature and remoteness of their environment. Satellite transmitters have successfully been used to track movements of pelagic sharks across ocean basins and has become a common tool for researchers (Hammerschlag et al., 2011; Hussey et al., 2015). Moreover, this technology has been widely used to monitor habitat use patterns (Hussey et al., 2015), as well as address inter-disciplinary ecological and resource management questions involving foraging ecology (Papastamatiou et al., 2010; Hammerschlag et al., 2011; Jaine et al., 2014), migratory behavior (Lea et al., 2015; Doherty et al., 2017a; Skomal et al., 2017) and overlap in species distribution and fishery exploitation areas (Graham et al., 2016; Queiroz et al., 2016; Calich et al., 2018).

The whale shark, *Rhincodon typus* (Smith, 1828), is a large-bodied, filter feeding species with a circumglobal distribution in warm temperate and tropical marine waters (Compagno, 2001; Jaffa and Taher, 2007). Although whale sharks are known to use the entire water column, from the surface down to over 2000 m (Tyminski et al., 2015), they are thought to spend most of their time in the top 100 m (Wilson et al., 2006; Rowat and Gore, 2007; Tyminski et al., 2015). This primarily epipelagic behavior has allowed for observations by commercial mariners, offshore industry employees, and recreational boaters providing much of the occurrence and distribution data for whale sharks worldwide (Gudger, 1934; Silas, 1986; Taylor, 1996; Colman, 1997; Stevens, 2007). Whale shark occurrence has been correlated with high abundance of prey in coastal areas (Heyman et al., 2001; Rohner et al., 2015, 2018) and productive frontal zones and large-scale spawning events in offshore waters (Hoffmayer et al., 2005; de la Parra Venegas et al., 2011; Ryan et al., 2017).

The majority of whale shark sightings are of solitary individuals (Colman, 1997; Hoffmayer et al., 2005; Rowat and Brooks, 2012); however, whale sharks can also be found in aggregations in certain regions (e.g., Rowat and Brooks, 2012). By studying whale shark occurrence reports, scientists have been able to identify relatively predictable spatiotemporal aggregation patterns at 12 locations, worldwide (Graham and Roberts, 2007; Rowat and Brooks, 2012; Sequeira et al., 2013; Berumen et al., 2014). The purpose of these aggregations is not completely understood, but they typically occur in areas of high localized productivity (Stevens, 2007; Sequeira et al., 2013) and are generally dominated by juvenile males (Rowat et al., 2009; Rowat and Brooks, 2012; Norman et al., 2017a). This high predictability of occurrences has led to commercial whale shark ecotourism in several of these locations, including waters off Australia, the Philippines, Mozambique, Seychelles, Djibouti, Belize, Gulf of California, Holbox, Bay Islands of Honduras, the Red Sea, and the Arabian Gulf (Rowat and Brooks, 2012; Fox et al., 2013; Robinson et al., 2013; Berumen et al., 2014; Rohner et al., 2015), and has allowed access for researchers to study this enigmatic species.

Knowledge on movement and habitat use patterns for whale sharks remains fragmented despite the growing number of tagging studies in recent years. Only a limited number of tagging studies have been performed in regions outside known aggregation sites (Rowat and Brooks, 2012; Sequeira et al., 2013), typically due to the prohibitive costs of vessel operations and spotter planes, which are critical to locating these animals due to sporadic sightings and their epipelagic nature (Colman, 1997). Most studies to date described short-term movements with mean track durations of ∼ 90 days (e.g., Sequeira et al., 2013), and only a few recent studies investigated seasonal changes in habitat use (Berumen et al., 2014; Robinson et al., 2017; Diamant et al., 2018; Cochran et al., 2019). Due to their migratory nature and longevity, there remains a need for long-term studies documenting connectivity into other areas (Sequeira et al., 2013; Andrzejaczek et al., 2016; McKinney et al., 2017; Norman et al., 2017a; Araujo et al., 2019) in order to facilitate international management on this species.

Several molecular studies have revealed that whale sharks form a single global population, however, there is evidence suggesting the Atlantic Ocean population is genetically different from the Indo-Pacific Ocean populations (Castro et al., 2007; Schmidt et al., 2009; Vignaud et al., 2014). Early whale shark reports from the western Atlantic Ocean primarily focused on their occurrence (Gudger, 1918, 1934; Bigelow and Schroeder, 1948; Baughman and Springer, 1950; Breuer, 1954); however, more recent studies have documented aggregations (Graham and Roberts, 2007; de la Parra Venegas et al., 2011; Fox et al., 2013; Cárdenas-Palomo et al., 2014) and connectivity between the Gulf of Mexico (GOM) and Caribbean Sea (Hueter et al., 2013; McKinney et al., 2017; Norman et al., 2017a; Rooker et al., 2019). McKinney et al. (2017) utilizing photo-identification to document whale shark connectivity in the western central Atlantic Ocean, and reported movements between Honduras, Belize, and Mexico with limited connectivity between these regions and the northern GOM. In the largest whale shark satellite tagging study to date in the Atlantic Ocean, Hueter et al. (2013) deployed 35 satellite tags on sharks off the Yucatan Peninsula and documented movement into the northern GOM, the Caribbean Sea, and one shark moving into the South Atlantic Ocean. Additional tagging studies in this region should help to further define whale shark movement patterns and connectivity to other regions.

Unlike other locations throughout the world, the northern GOM is one of the few areas where whale sharks rarely occur in coastal waters, but rather form aggregations along the continental shelf edge (Hoffmayer et al., 2005, 2007; Burks et al., 2006; McKinney et al., 2012, 2017). The nearly exclusive pelagic nature of whale sharks in this region has made it difficult to gather information on their occurrence, and much of the existing information was collected opportunistically (Springer, 1957; Hoffman et al., 1981; Hoffmayer et al., 2005). Beginning in 2003, researchers at The University of Southern Mississippi developed the Northern Gulf of Mexico Whale Shark Sightings Survey (NGWSSS) to gain a better understanding of whale shark occurrence and distribution patterns in the northern

GOM (Hoffmayer et al., 2005). This effort has resulted in the long-term monitoring of a predictable, seasonal whale shark aggregation site in the GOM, which facilitated the deployment of satellite tags to track their movements. This study combines multiple tag technologies along with sightings data to further elucidate whale shark movements and habitat use patterns in the GOM.

MATERIALS AND METHODS

Whale Shark Sightings Data

Details of whale shark sightings reported (2003–2016) to the NGWSSS were obtained from research trips, aerial surveys, recreational and commercial fishers, recreational divers, and various sources within the oil and gas industry (e.g., platform personnel, helicopter pilots) (Hoffmayer et al., 2005)[1]. Information requested from individuals who encountered whale sharks included date, location, direction and distance from a coastal landmark, or identifier number of specific offshore petroleum platforms, number of individuals, estimated total length (TL) of observed sharks, and observed behavior (e.g., swimming, feeding). Follow-up emails and phone calls were conducted to determine the validity of the reports and to request video and photos. Additional sightings data from National Marine Fisheries Service (NMFS) aerial surveys (1989–1998; *n* = 81 sightings) and the Wildbook for Whale Shark Photo-Identification Database[2] from the northern GOM (area 2e; 1999–2016; *n* = 104) were included. Since the majority of the sightings had no associated effort data, we utilized these data as presence only.

All sightings data were combined and plotted in Quantum GIS 2.18 (QGIS Developmental Team 2016) using the global WGS 1984 PDC Mercator projection to investigate seasonal patterns of occurrence and distribution. Seasons were defined using the meteorological definition as spring (March–May), summer (June–August), fall (September–November), and winter (December–February). Seasonal utilization distributions (UDs) were calculated using a fixed kernel density estimator, which was weighted based on the number of sharks reported at each encounter, and analyses were conducted using the KS package (Duong, 2007) in R statistical software (R Core Team, 2016). Total usage space (95%), representing the entire activity space (Burt, 1943), and core usage (50%), representing concentrated use (Worton, 1989), were calculated from the UDs. Any duplication of a single sighting event (i.e., more than one report of the same shark at the same place and time) was removed from the dataset so that the weighing reflected the number of individuals during a sighting event and was not impacted by the number of people observing the sharks.

Satellite Tagging

Satellite tags were opportunistically deployed on whale sharks from 2008 to 2014 in the northern GOM from the DeSoto Canyon to the Flower Gardens Banks National Marine Sanctuary. The primary site for tag deployment was Ewing Bank, a topographic feature ∼130 km south of Cocodrie, Louisiana (**Figure 1**). A spotter plane provided aerial support for the at-sea research team by covering a 52 km^2 radius around the targeted search area. Divers and vessel crew estimated the total length (TL) of the individual whale sharks to the nearest 0.5 m and sex was determined visually by the presence or absence of claspers. Satellite tags tethered to a titanium anchor dart (64 mm long × 16 mm wide × 1 mm thick) were implanted at the base of the dorsal fin using a 2-m pole spear (Ray Odor, Lutz, FL, United States) with a modified tagging tip. A rubber stopper was used on the tagging tip to ensure the tag anchor would not penetrate the skin deeper than 10 cm. The GPS location and time of tag deployment were recorded.

Two different satellite tag types were deployed in this study: satellite-linked towable Smart Position and Temperature Transmitting (SPOT; model SPOT-253, Wildlife Computers, Inc.) and popup satellite archival transmitting (PSAT; model X-Tag, Microwave Telemetry, Inc.; model MK10-PAT, Wildlife Computers, Inc.) tags. A Wildlife Computers, Inc. titanium anchor dart was used with each tag type, however, the tether setup was different for each tag type. We used a 1.5 m of 1.9 mm braided Honeywell Spectra fiber line tied to the tag and the titanium dart using a Palomar knot that was sealed with Krazy Glue instant adhesive (High Point, NC, United States). For the PAT tags, a 15 cm segment of heat shrink-wrapped (3.2 mm Ancor Marine grade heat shrink tubing, Marinco, Menomonee Falls, WI, United States) 1.8 mm monofilament line (136 kg test extra hard Hi-Catch Momoi Fishing Net, Mfg. Co., Ltd., Ako City, Hyogo prefecture, Japan) was attached to the tag and the anchor using stainless steel sleeves (168-2-VB4, Nicopress Products, Cleveland, OH, United States). In addition, the Wildlife Computers, Inc. RD1800 release device was attached to the MK10-PAT tags to sever the monofilament if the whale shark swam below 1800 m depth to prevent the tag from being crushed at extreme depth. The PSATs were attached with a 15 cm length of 2.0 mm 7 × 7 stainless steel cable/1.8 mm monofilament line connected with a stainless steel sleeve and coated in 3.2 mm heat shrink tubing. The monofilament end of the tag and the stainless steel cable was affixed to the titanium anchor using Nicopress stainless steel sleeves. On the PSAT tags, a constant pressure release mechanism was enabled to trigger tag detachment from sharks if depth variations <2 m were maintained for a period of 96 h. All tags were painted with antifouling paint; the X-Tags were treated by the manufacturer, while the MK10-PAT and SPOT tags were painted with gray transducer paint (Pettit Marine Paint, Kop-Coat Marine Group, Rockaway, NJ, United States) to deter growth of epibionts and to minimize attempted predation on the tag (Robinson et al., 2017). For analysis, sharks were separated by sex and categorized immature (<8.0 m TL) or mature (>8.0 m TL) following Norman and Stevens (2007).

---

[1] http://gcrl.usm.edu/whaleshark/whaleshark_survey.php

[2] www.whaleshark.org

FIGURE 1 | Map of the Gulf of Mexico study area.

Geolocation and Behavior Estimation

PSAT Tags

We used a hidden Markov model (HMM), to generate daily location and behavioral state estimates from PSAT data using the R package HMMoce[3], following methods by Braun et al. (2018a; 2018b). The HMM uses a two-step Bayesian state-space approach to estimate the joint probability distribution of location and behavior at each daily point. First, the model estimates daily observation-based location likelihoods generated by matching of *in situ* light-based longitude, sea surface temperature (SST), depth-temperature profiles, and ocean heat content (OHC) data collected from the tags to available time-synoptic oceanographic data. Daily location likelihood surfaces are generated across standard depth levels associated with each oceanographic product, and an overall likelihood is generated by combining the individual profile likelihoods for each depth level. Light-based longitude likelihoods were derived using longitude estimates provided from manufacturer-specific post-processing software (e.g., GPE2 software, Wildlife Computers, Inc.). Daily *in situ* SST estimates were compared to remotely sensed SST from daily, optimally—interpolated SST fields (OI—SST, 0.25° resolution; Reynolds et al., 2007; Banzon et al., 2016) to generate SST likelihoods. Modeled depth-temperature products from the HYbrid Coordinate Ocean Model (HYCOM, 0.08° resolution; Chassignet et al., 2007) at standard depth levels were compared to daily depth-temperature bins from tag data to estimate depth-temperature likelihoods. While Wildlife Computers tags provided binned temperature and depth data, which could be used in the HMMoce Package directly, temperature and depth time series data provided by Microwave Telemetry tags were first converted to depth-temperature bins using the R package RchivalTag (Bauer et al., 2015). Ocean heat content (OHC) was calculated by integrating the heat content of the water column above the minimum daily temperature recorded by the tag (Luo et al., 2015), and HYCOM fields, and these were used to generate an OHC likelihood. Start and end locations were considered known in all cases and model runs.

Next, the model infers the probability density of daily locations and behaviors by fitting an underlying Brownian movement model to the daily likelihood surfaces. The model allows for switching between two behavioral states, nominally migratory and resident, which are characterized by high and low rates of diffusion, respectively (Braun et al., 2018a). Daily model outputs included a daily location estimate, hereafter referred to as most probable track (MPT) locations, and the probability of a whale

---

[3] https://github.com/camrinbraun/HMMoce

shark being in the resident behavioral state. Behavioral state probabilities range from 0 to 1, and we considered a whale shark resident when resident behavior probability was ≥ 0.7, and migratory when resident probability was ≤ 0.3. Behavioral state was defined as unknown if resident probabilities were between 0.3 and 0.7. Once MPTs were generated, cumulative track distances (km) were calculated using great circle distance (km) between MPT daily locations using the Fields package (Nychka et al., 2015) in R. Daily rates of movement were calculated for each track day by calculating the great circle distance between locations.

Towed SPOT Tags

The towed SPOT tags used standard Doppler-based geolocation to track the position of tagged whale sharks. For a detailed description of location estimate accuracy, see Hearn et al. (2013). Position estimates were filtered using a Douglas Filter applied in Movebank[4]. This tool is based on a maximum redundant distance (MRD) filter and removes unrealistic locations. The MRD radius was set to 200 km. Although SPOT tags can provide multiple locations per day, a single location was selected for each track day for these tag types to be consistent with data derived from other tag types used in the study. If multiple locations were available in a given track day, the location with the best location class was selected. If more than one location of a similar class was present within a day, the initial location for that class was selected. We attempted to apply a hierarchical behavioral state switching state-space model based on the first-difference correlated random walk model of Jonsen et al. (2005) and Jonsen (2016) to SPOT tag data to reconstruct tracks and identify behavioral states using the bsam package (Jonsen et al., 2020) in R. However, due to low sample size ($n < 200$ daily locations), short track durations and large temporal gaps between locations, we were not able to get models to converge or to return reasonable model outputs.

Seasonal Distribution and Habitat Use

To make inferences on seasonal distribution of whale sharks in the GOM, the HMM model output was used to generate a seasonal residency distribution (RD) for each PSAT-tagged shark. A RD is conceptually similar to a UD, and represents the expected residence time of an animal within each grid cell over a given time interval based on the posterior distribution of location estimates within that period (Pedersen et al., 2011). Because the models for each animal were fit over the same spatial grid, we integrated RDs for all sharks to develop population-level RDs. The advantage of calculating RDs based on modeled location estimates was that, unlike kernel UD estimates of space use based on MPT locations alone, it implicitly accounts for location uncertainty and correlation to adjacent time periods (Braun et al., 2018b). To illustrate whale shark use of continental shelf (0–200 m), slope (201–2500 m), and open ocean (>2500 m) regions (Wicksten and Packard, 2005) throughout the annual cycle, we extracted the depth from the General Bathymetric Chart of the Oceans (GEBCO) gridded bathymetry data (Gebco Compilation Group, 2020) at each estimated MPT location and at each daily SPOT tag location. We then created monthly kernel density plots of whale shark depth distributions.

Behavioral Analysis

We used results of the HMM to assess how whale shark movement behavior changed seasonally and as a function of water depth. For these analyses we considered days in which the HMM was able to confidently assign a movement state as either resident or migratory. To model seasonal changes in behavior we used logistic regression to model the probability of resident behavior as a function of two harmonic variables that allowed behavior to change in a non-linear fashion;

$$V_1 = \frac{\sin(2\pi \times m)}{12}$$

$$V_2 = \frac{\cos(2\pi \times m)}{12}$$

where m = month (1–12; Byrne et al., 2019). To account for individual variation, we included shark ID as a random effect. To evaluate support for seasonal variation we calculated Akaike's Information Criterion (AIC) for this model and compared it to AIC of an intercept-only model, which would represent constant behavior. We considered a seasonal change in behavior to be supported if the AIC of the seasonal model was >2 AIC units less than the intercept-only model (Burnham and Anderson, 2002).

We predicted that resident behavior was more likely when whale sharks were in shallow waters associated with the continental shelf and shelf-edge. We assessed the effect of depth on resident behavior using mixed-effects logistic regression, with water depth included as a fixed effect and whale shark ID as a random effect to account for individual variation. We used a multiple imputation approach to account for location uncertainty in whale shark daily locations. To accomplish this, we sampled 50 locations (with replacement) from the daily RD of each shark, and extracted the depth at each sampled location. This provided us with 50 data sets of whale shark depth and behavior, where each data set represented a different realization of whale shark daily locations pulled from the probability distribution of a shark's daily location as determined by the HMM. We applied the mixed-effects logistic regression model to each of the 50 imputed data sets and pooled results across models using functions in the mice package (van Buuren and Groothuis-Oudshoorn, 2011) in R. We examined the pooled fixed-effects parameter estimates and considered depth to have a significant effect on behavior if the 95% confidence interval for the estimated effect of depth did not cross 0. Because of the large depth range used by whale sharks, we rescaled depth by dividing all values by 100 to assure model convergence.

Association With Oceanographic Features

Since many whale sharks used open ocean waters of the GOM, we used plots of remotely sensed sea surface height (SSH) to potentially identify localized productivity features such as currents, fronts, and eddies. Whale shark track locations

---

[4] https://www.movebank.org

were overlaid onto maps of SSH during July, September, and October 2014, and February 2015 to gain a better understanding of why they were utilizing these areas. These months and years were chosen to due to the high number of track locations during this time and variability in the position of the Loop Current and associated mesoscale features. To visualize SSH, we used gridded daily absolute dynamic topography (ADT) data from June 2009 to August 2015 provided by the Copernicus Marine and Environment Monitoring Service (CMEMS)[5] and were used to form daily SSH maps for the GOM. Anti-cyclonic eddies (ACE, warm core) and cyclonic eddies (CE, cold core) were identified based on SSH; ACE were defined by having higher SSH than surrounding waters, whereas CEs were defined by having lower SSH values than the surrounding water (Faghmous et al., 2012). Since we were dealing with daily SSH maps, we selected the mid-point of the month (e.g., 15th) to be the best presentation for that month. This allowed us to investigate whether open ocean whale shark movements were associated with the Loop Current and associated mesoscale features.

RESULTS

Sightings Data

The combination of the NMFS (n = 81), Wildbook for Whale Shark (n = 104), and NGWSSS (n = 637) datasets resulted in 822 whale shark sightings entries from 1989 to 2016, with the vast majority of the sightings (82%) occurring from 2007 to 2016. As various sources contributed to the database (e.g., aerial surveys, recreational and commercial fishers, recreational divers, and petroleum industry personnel), no effort data were recorded with the sightings and no density or abundance estimates could be generated. Overall, whale sharks were reported from continental shelf and slope waters throughout the northern GOM with most reported observations occurring from the DeSoto Canyon to waters off Corpus Christi, TX, with some of the highest concentrations occurring in areas in the north central (NC) GOM, in waters surrounding Ewing Bank, and offshore of Tampa Bay. Eighty-one percent of the sightings locations occurred in continental shelf and shelf edge waters with only 19% of the sightings occurring over continental slope and open ocean waters.

Most whale shark sightings (94%) occurred from May to November, with peak sightings in August (**Figure 2**). During spring, the largest core use area occurred in continental slope waters of the NC GOM, with smaller core use areas off the central Florida coast and shelf edge waters off central Texas (**Figure 3A**). During summer there was a relatively tight core use area found along the continental shelf edge near Ewing Bank, with smaller concentrations occurring off northwest Florida (**Figure 3B**). During fall, the majority of the core use areas occurred in continental shelf edge waters extending from the Mississippi River Delta eastward to the DeSoto Canyon (**Figure 3C**). Only 18 (2.2%) whale shark sightings were reported during winter with almost the entire core use areas during this season in continental edge/slope waters of the NC GOM (**Figure 3D**).

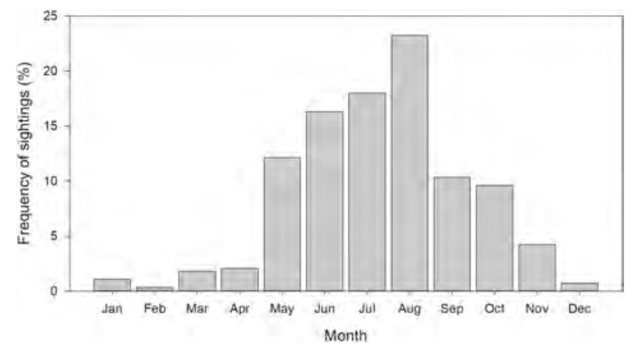

FIGURE 2 | Monthly distribution of whale shark, *Rhincodon typus*, sightings reported in the northern Gulf of Mexico from 1989 to 2016. n = 822.

Satellite Tags

From 2008 to 2014, 50 satellite tags were deployed on 48 individual whale sharks, including two individuals that were double tagged with SPOT and PSAT tags (**Supplementary Tables 1, 2**). The majority of the tags (33 of 50) were deployed on individuals near Ewing Bank (**Figure 1**), while another 15 individuals were tagged in waters south of the Mississippi Canyon, and two individuals were tagged in waters surrounding the DeSoto Canyon (**Figure 1**). Thirty-five tags were deployed during summer (70%) and 15 tags were deployed during fall (30%). Estimated sizes of tagged sharks ranged from 4.5 to 12.0 m TL (mean 7.8 ± 0.3 m). Seven females (range 6.0 to 11.0 m TL, mean 8.8 ± 0.6 m TL) and 35 males (range 4.5 to 12.0 m TL, mean 7.7 ± 0.3 m TL) were tagged, while sex was unable to be confidently assigned for eight sharks (range 6.0 to 9.0 m TL, mean 7.0 ± 0.6 m TL).

Thirty-two PSAT tags were deployed: 14 MK10-PAT (range 9 to 150 days, mean: 83.2 ± 15.0 days, 5 failures) and 18 X-Tag (range 6 to 366 days, mean: 144.6 ± 31.4 days, 1 failure, **Supplementary Table 1**). Typically, light-based longitude and HYCOM likelihoods were used in HMM geolocation models, however, if the modeled track possessed large gaps then SST or OHC likelihoods were used in combination with light-based longitude to produce the MPT (**Supplementary Table 1**). Behavioral states were assigned for 3,124 whale shark MPT locations from 23 sharks using the HMM, with resident, migratory, and unknown behavior assigned for 15.3, 12.4, and 72.4% of the locations, respectively. We suspect that difficulties in confidently assigning behavioral states as resident or migratory were a result of large location uncertainty relative to whale shark movement capacity. In addition to the PSAT tags, 18 SPOT tags (range 3 to 250 days, mean: 58.8 ± 15.6 days 0 failures, **Supplementary Table 2**) were deployed on whale sharks. Overall, location data were received from 44 of the 50 tags with a mean tag duration of 97.0 ± 15.0 days (**Supplementary Tables 1, 2**).

---

[5] http://www.marine.copernicus.eu

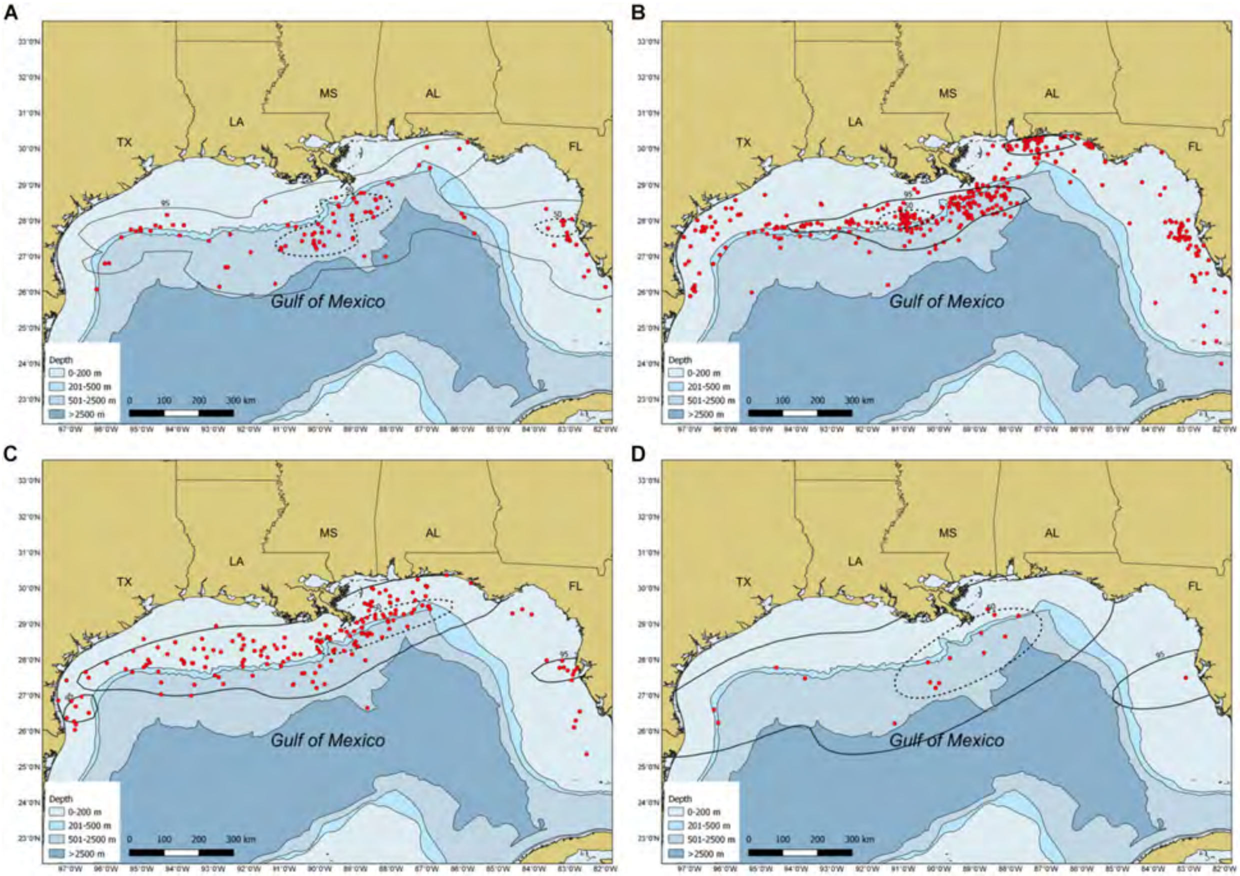

FIGURE 3 | Maps depicting sighting locations (red circles) and weighed kernel utilization distributions of whale sharks, *Rhincodon typus*, in the Gulf of Mexico by season: **(A)** spring, **(B)** summer, **(C)** fall, and **(D)** winter from 1989 to 2016. The 95% (solid black line) and 50% (dashed black line) contours are presented. Circles represent both individual and aggregation sightings.

The 44 tags were deployed for a total of 4,266 days and reported 3,334 days (78.2%) of geolocation data.

Seasonal Residency Distribution

All sharks remained in the GOM with the majority of the locations (~91%) occurring over continental slope and open ocean waters (**Figure 4**). Mean daily rates of individual whale shark movements ranged from 3.8 to 52.3 km/day, with an overall mean rate of 20.5 ± 1.6 km/d (**Supplementary Tables 1, 2**). Seasonal RDs indicate a summer core use area along the continental shelf edge, slope, and open ocean waters from the DeSoto Canyon region west to Ewing Bank, with 88.1% of the locations occurring in the northern GOM (**Figure 5A**). During fall, the 23 tagged sharks exhibited no clear pattern in habitat use areas with most sharks widely distributed throughout the GOM (**Figure 5B**). There was a general southern shift in whale shark distribution in late fall and winter (November–January), corresponding to the greatest observations of tagged whale sharks in the southern GOM (**Figure 5E**). In fact, about 29% of the MPT locations occurred in the southern GOM, with ~90% occurring during late fall. During winter, the largest proportion of MPT locations occurred in the southern GOM, and less than five locations occurred in continental shelf waters of the northern GOM (**Figure 5C**). The 14 tagged sharks during winter exhibited core use areas in the central and SW GOM over continental slope and open ocean waters (**Figure 5C**). During spring, MPT locations were only provided from seven tagged sharks and over 94% of the locations occurred over slope and open ocean waters of the GOM, with the core use area in the central GOM (**Figure 5D**). Roughly 20% of the MPT locations occurred in the southern GOM with most of those locations (~60%) occurring in early spring. In addition to the seasonal residency distribution, the latitudinal density plot of all shark locations revealed a similar movement pattern into the southern GOM from September to March, with an uncharacteristic peak in locations at 23°N in April. However, it should be noted that a single shark heavily influenced this peak (**Figure 5E**).

When investigating regional use of the GOM (e.g., shelf, slope, and open ocean waters) by sex and maturity state by month, females used continental slope and open ocean waters almost exclusively, whereas some mature males occurred over continental shelf and slope waters during summer and fall, while other mature males remained in slope and open ocean waters throughout the year (**Figure 6**). Conversely, immature

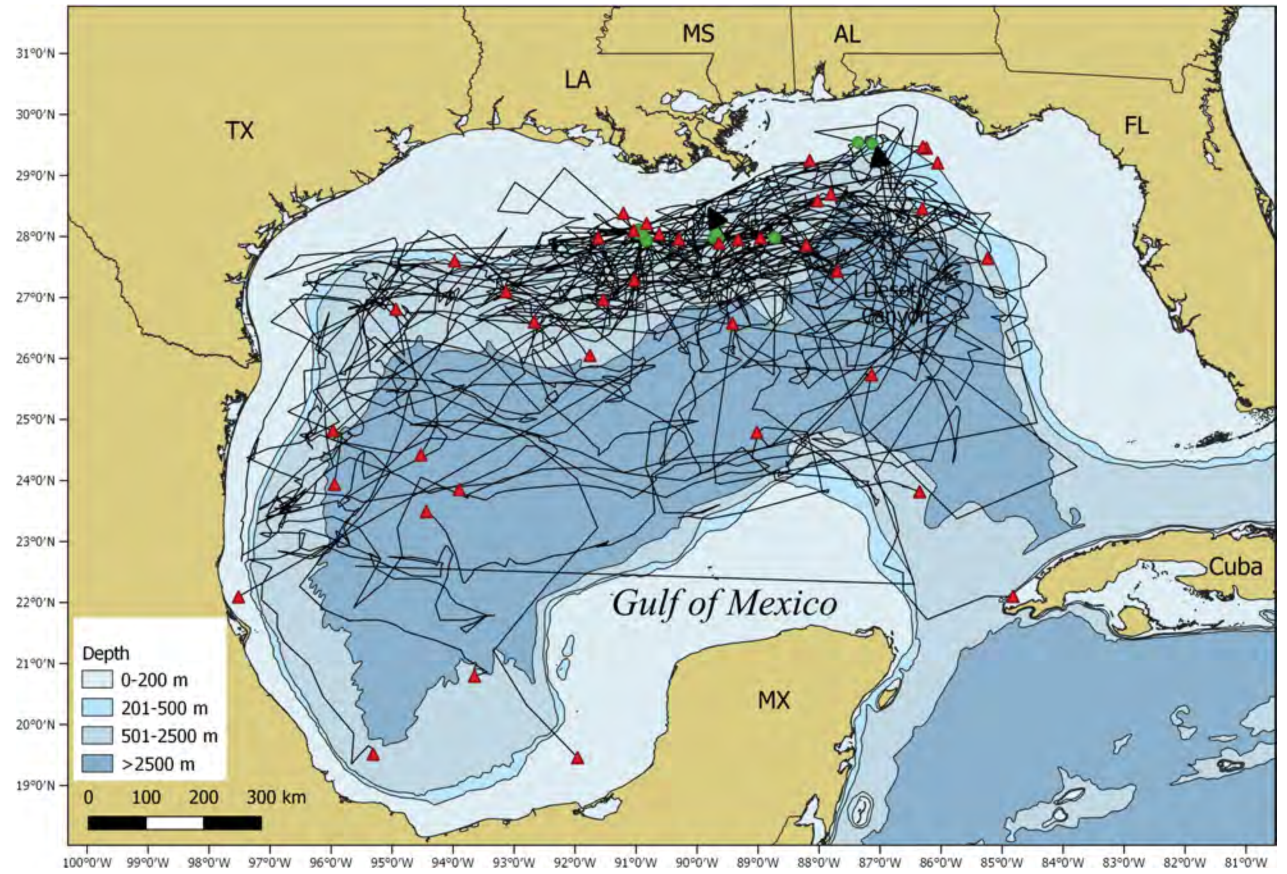

FIGURE 4 | Map of the Gulf of Mexico showing satellite tag based movement trajectories (black lines) of all individual tagged whale sharks, *Rhincodon typus*, along with the tagging (green circles) and popup (red triangles) locations.

males spent the majority of their time in continental shelf and slope waters, only occurring in a few locations over open ocean waters (**Figure 6**).

Short-Term Deployments (<30 Days)

Short-term tracking data ranging from three to 29 days (mean = 15.2 ± 2.2 days) were reported from 14 of the 42-tagged sharks (33.3%), with nine of the 14 tags (64.3%) being towed SPOT tags (**Supplementary Tables 1, 2**). The corresponding distance traveled over this time ranged from 33 to 836 km (mean = 225 ± 63.3 km). All but two of the 14 sharks were tagged at Ewing Bank (85.7%) during summer, and the majority of the movements were within 140 km of the tagging locations (**Supplementary Figure 1A**).

Long-Term Deployments (<30 Days)

The duration of the 28 remaining satellite tagged sharks ranged from 30 to 366 days and their movements occurred throughout the GOM (**Supplementary Figures 1–3**). As such, we grouped their subsequent movements into two broad categories: short (remaining in northern GOM) and long (leaving northern GOM) distance movements. The short distance movements describe the individuals that exhibited residency to the northern GOM; whereas the long distance movements were further subdivided into movements to the southeast (SE) and southwest (SW) GOM.

Residency to the Northern GOM

Seven of the 42-tagged sharks (16.7%) remained in the northern GOM throughout their tracks, which ranged in duration from 41 to 81 days (mean 61.3 ± 5.6 days; **Supplementary Tables 1, 2**). All of these sharks were tagged at Ewing Bank during summer, and all ventured less than 600 km from their tagging location (**Supplementary Figure 1B**). Six sharks exhibited a net eastward movement with tracks terminating from 162 to 558 km east of Ewing Bank (**Supplementary Figure 1B**).

Movements to the Southeastern GOM

Six of the 42-tagged sharks (14.3%) moved into the SW GOM but never left the GOM during the duration of their tracks (**Supplementary Figure 2**), which ranged from 52 to 253 days (mean 130.7 ± 29.3 days; **Supplementary Tables 1, 2**) and covered distances that ranged from 637 to 6,029 km (mean 2,466.2 ± 857.5 km; **Supplementary Tables 1, 2**). The majority of the tags (66.7%) popped up over continental slope waters of the GOM, however, one track ended over continental shelf waters of the northeast GOM

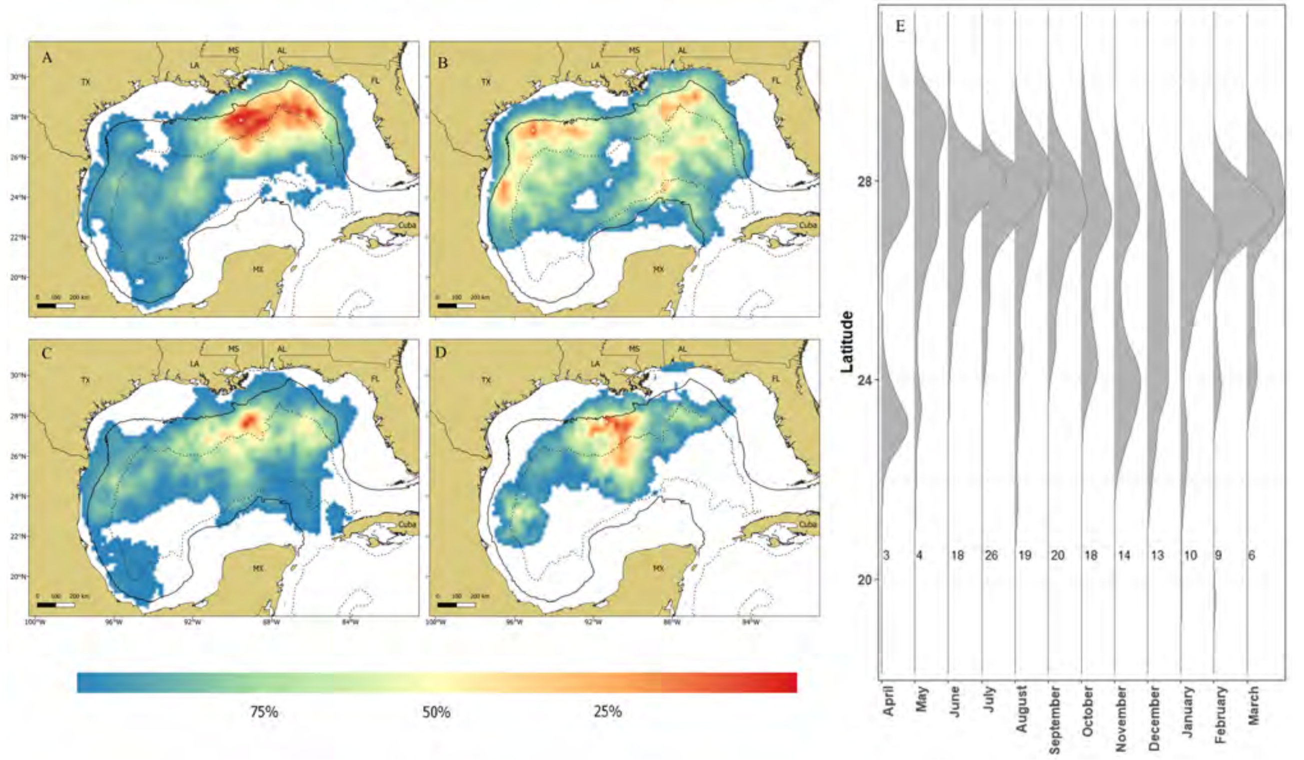

FIGURE 5 | Maps depicting residency distributions of whale sharks, *Rhincodon typus*, based on most probable track locations in the Gulf of Mexico by season; **(A)** summer, **(B)** fall, **(C)** winter, and **(D)** spring. The black solid line represents the 200m isobaths and the black dashed line represents the 2,500 isobath, separating the continental shelf, slope, and open ocean water of the Gulf of Mexico. The latitudinal density plot **(E)** shows the latitudinal distribution of PSAT tagged whale sharks in the northern Gulf of Mexico from 2008–2014. Each vertical line represents a month of the year and the numbers to the right of each line indicate the number of individuals tracked during that month.

and one track terminated over coastal waters of western Cuba in the Golfo de Guanahacabibes, (**Supplementary Figure 2**). Several sharks used the shelf edge/slope waters of the eastern GOM, in the DeSoto Canyon region, before moving south (**Supplementary Figure 2**).

Movements to the Southwestern GOM

Fifteen of the 42 tagged sharks (35.7%) moved into the SW GOM, but never left the GOM during the duration of their tracks (**Supplementary Figure 3**), which ranged from 38 to 367 days (mean 176.8 ± 30.1 days; **Supplementary Tables 1, 2**), and covered from 1,192 to 11,057 km (mean 4,502.1 ± 888.1 km; **Supplementary Tables 1, 2**). Similar to the sharks that moved to the SE GOM, most of the tracks (80.0%) terminated over continental slope and open ocean waters of the GOM (**Supplementary Figure 3**). Seven sharks spent the majority of their time in northern GOM waters but did spend some time in the northern portion of the SW GOM (**Supplementary Figure 3A**). The eight other tagged sharks spent limited time in the northern GOM and made directed movements into the SW GOM (**Supplementary Figure 3B**). Two different movement patterns were observed with four sharks moving east initially in late summer/early fall before moving to the SW GOM, whereas the other four sharks began their southwest movement from the tagging sites in late summer/early fall and followed a path along the continental shelf edge/slope into the SW GOM (**Supplementary Figure 3B**).

Seasonal Movements

During this study, we were able to tag 11 whale sharks on a single day, 10 July 2014 (**Figure 7**), where six tags remained deployed longer than 7 months, and three that were retained for the full one-year duration (**Supplementary Table 1**). This situation provided a unique subset of tagging data to examine individual variation in seasonal movements. During summer, nine sharks remained in the northern GOM, with seven of the sharks using similar areas throughout this time period (**Figure 7A**). During this time, two sharks moved southwest to continental slope waters near the Mexico-Texas border and continental slope/open ocean waters of the SW GOM, respectively (**Figure 7A**). Three tags popped off during summer. During fall, all eight sharks remained initially in the eastern GOM, and three sharks moved to the west, following the shelf edge and over open ocean waters (**Figure 7B**). The remaining sharks moved south with one shark moving the farthest south before the track terminated near the western tip of Cuba (**Figure 7B**). During winter, five of the six-tagged sharks associated with continental slope and open ocean waters of the NC GOM (**Figures 7C,D**). One shark remained

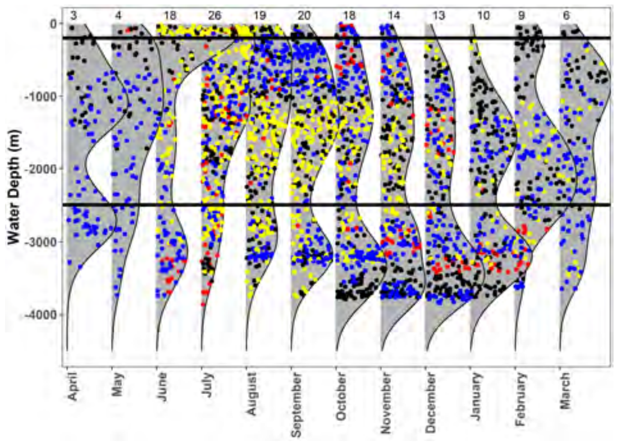

FIGURE 6 | Monthly kernel density plots of water depth at the most probable location estimates for whale sharks, *Rhincodon typus*, in the Gulf of Mexico. Immature males (yellow), adult males (blue), and females (red) are represented. The black horizontal lines designate the separation between the three regions: shelf (0–200 m), slope (200–2500 m), and open ocean (>2500 m). Sample size of tagged sharks is shown at the top of the plot for each month.

exclusively in the southern GOM during this time. During spring, there was a high degree of overlap among sharks in the NC GOM (**Figure 7E**). One shark moved from the southern GOM toward the NC GOM to an area utilized by three other sharks (**Figure 7E**). One shark moved southeast toward northwestern Cuba, where the track terminated (**Figure 7E**). All three tagged sharks that were tracked into the following summer spent time near Ewing Bank (**Figure 7F**), where they had been initially tagged one year earlier.

Behavioral Analyses

A total of 477 and 387 daily locations confidently classified as resident or migratory behavior, respectively, were used to model whale shark behavior. The model that allowed behavior to change seasonally was well supported relative to the model of constant behavior (ΔAIC = 7.86). Model results suggest the probability of resident behavior peaked during late spring and early summer and that whale sharks were less likely to engage in resident behavior during late fall and early winter (**Figure 8**). There was a negative effect of water depth on probability of resident behavior ($\beta = -0.04$, 95% CI: $-0.06 - -0.03$, **Table 1**). Probability of resident behavior was greatest in continental shelf and shelf-edge waters and decreased as depth increased with the lowest probabilities occurring in the open ocean waters of the GOM (**Figure 8**).

Association With Oceanographic Features

During July 2014, data from 10 PSAT tags provided 220 MPT locations (**Figure 9A**), with most of these locations appearing to be associated with a recently formed Loop Current eddy and two smaller anti-cyclonic, warm core eddies to the east and west (**Figure 9A**). PSAT data from eight whale sharks tracked during September 2014 resulted in 227 MPT locations. The majority of these locations occurred on the eastern edge of the Loop Current and an anti-cyclonic, warm core eddy just off the continental shelf edge in the western GOM (**Figure 9B**). Similar to September 2014, many of the 203 MPT locations available for October 2014 were on the periphery of the Loop Current and anti-cyclonic warm core eddies in the western GOM (**Figure 9C**). Only five whale sharks provided 143 MPT locations during February 2015, however, most of those locations were in proximity to the northern and western edge of the Loop Current (**Figure 9D**). In total, many of the MPT locations in these four examples were associated with the Loop Current and associated anti-cyclonic, warm core eddies (**Figure 9**).

DISCUSSION

Seasonal Occurrence, Distribution and Movements

This study represents the largest whale shark movement study to date in the Atlantic Ocean, with data collected from 42-tagged sharks and two decades of sightings reports. It was apparent from the temporal periodicity of sightings and MPT locations that continental shelf edge/slope and open ocean waters in the northern GOM were important habitats for whale sharks year-round. However, the highest use of northern GOM waters coincided with the warmest time of year in this region (i.e., summer and early fall). This increased habitat use of northern GOM water during summer was supported by the behavioral state models as well, which revealed that resident/foraging behavior was more likely occurring during summer over shallower continental shelf waters (**Figure 8**). The increased probability of foraging behavior in continental shelf waters of the NC GOM during summer was most likely related to the increased localized productivity during this time. Certain features, such as the Mississippi River Plume, upwelling along continental shelf edges, and convergence zones, occur in this region during summer and are conducive environments for plankton, a main prey source for whale sharks (Le Fevre, 1986; Richards et al., 1993; Ryan et al., 1999; Wilson et al., 2001; Hoffmayer et al., 2005; McKinney et al., 2012). These findings are consistent with other studies that have documented whale sharks association with areas of high productivity and abundant prey (Colman, 1997; Brunnschweiler et al., 2009; de la Parra Venegas et al., 2011; Berumen et al., 2014; Robinson et al., 2017). The environmental and biological conditions in the NC GOM during summer appear to allow for the occurrence of a large number of whale sharks, including the presence of a seasonal whale shark large aggregation site at Ewing Bank. Outside of this time of increased habitat use of the NC GOM, whale sharks tended to redistribute themselves throughout the GOM. The overall trend in habitat use was characterized by southerly movements into offshore waters of the central and southern GOM during late fall and early winter, and northerly movements back to the northern GOM during late winter and spring (**Figure 5**). These offshore movements likely explain the reduced number of sightings data during the winter and spring months (~10% of sightings occur during this time). In addition, the behavioral state models revealed a higher

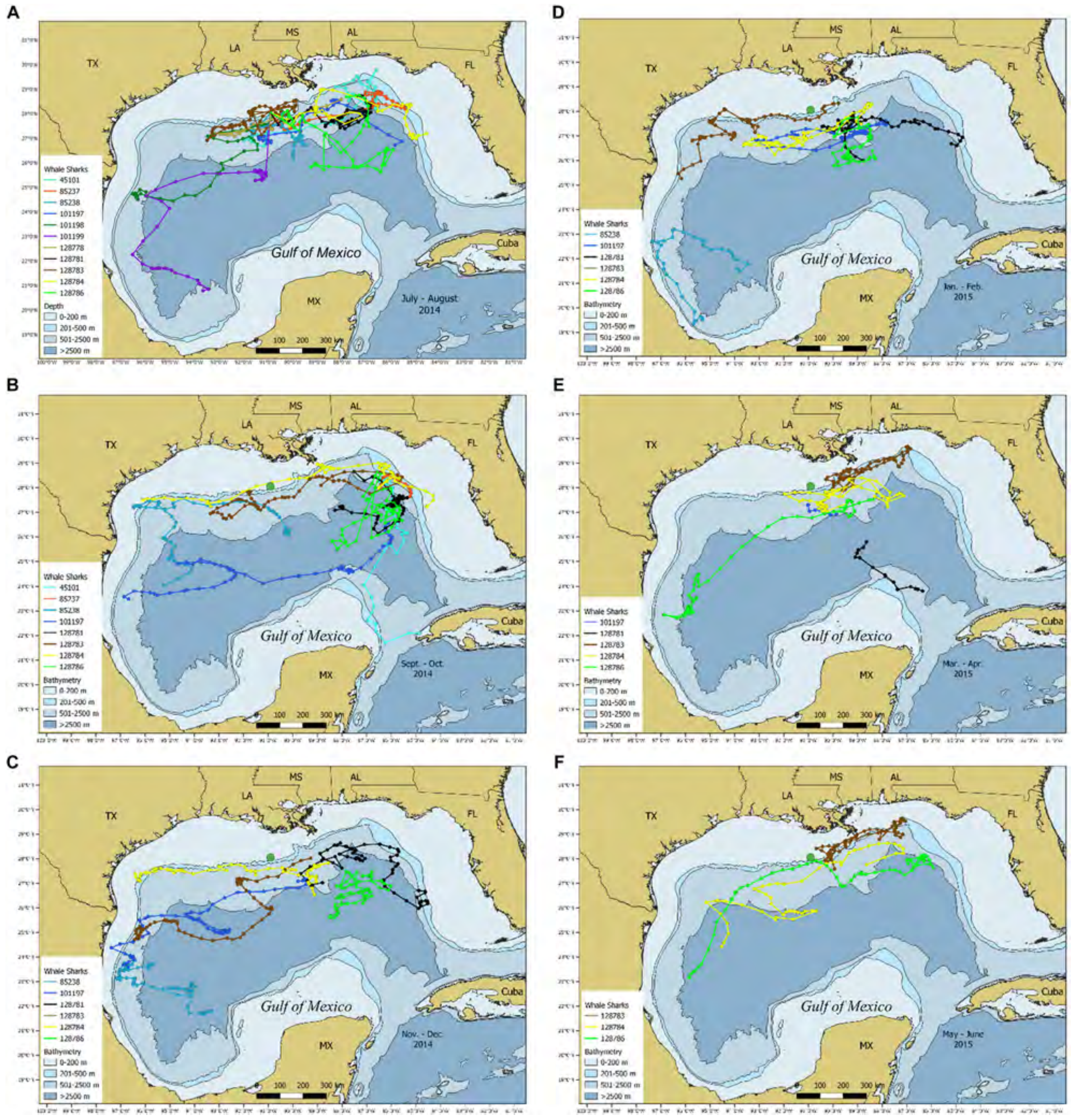

FIGURE 7 | Maps depicting temporal changes in the most probable tracks for whale sharks, *Rhincodon typus*, tagged on 10 July 2014. Tracks range from **(A)** July–August 2014, **(B)** September–October 2014, **(C)** November–December 2015, **(D)** January–February 2015, **(E)** March–April 2015, and **(F)** May–June 2015. Large green circle indicates tagging location of Ewing Bank.

probability of migratory behavior during fall, winter and early spring while individuals primarily inhabited deeper continental slope and open ocean waters of the GOM (**Figure 8**). These seasonal offshore movements away from known foraging areas is supported by the other whale shark tagging study in the region by Hueter et al. (2013), who reported whale shark movements from the southern GOM, with similar timings of movements away from the summer aggregation site during fall. Further supporting this is that as prey abundance at localized seasonal aggregation sites wanes, whale sharks leave these areas to undergo broad scale movements in search of other foraging opportunities (de la Parra Venegas et al., 2011; Hueter et al., 2013; Araujo et al., 2018). The ultimate purpose of the movements away from the northern GOM during fall and

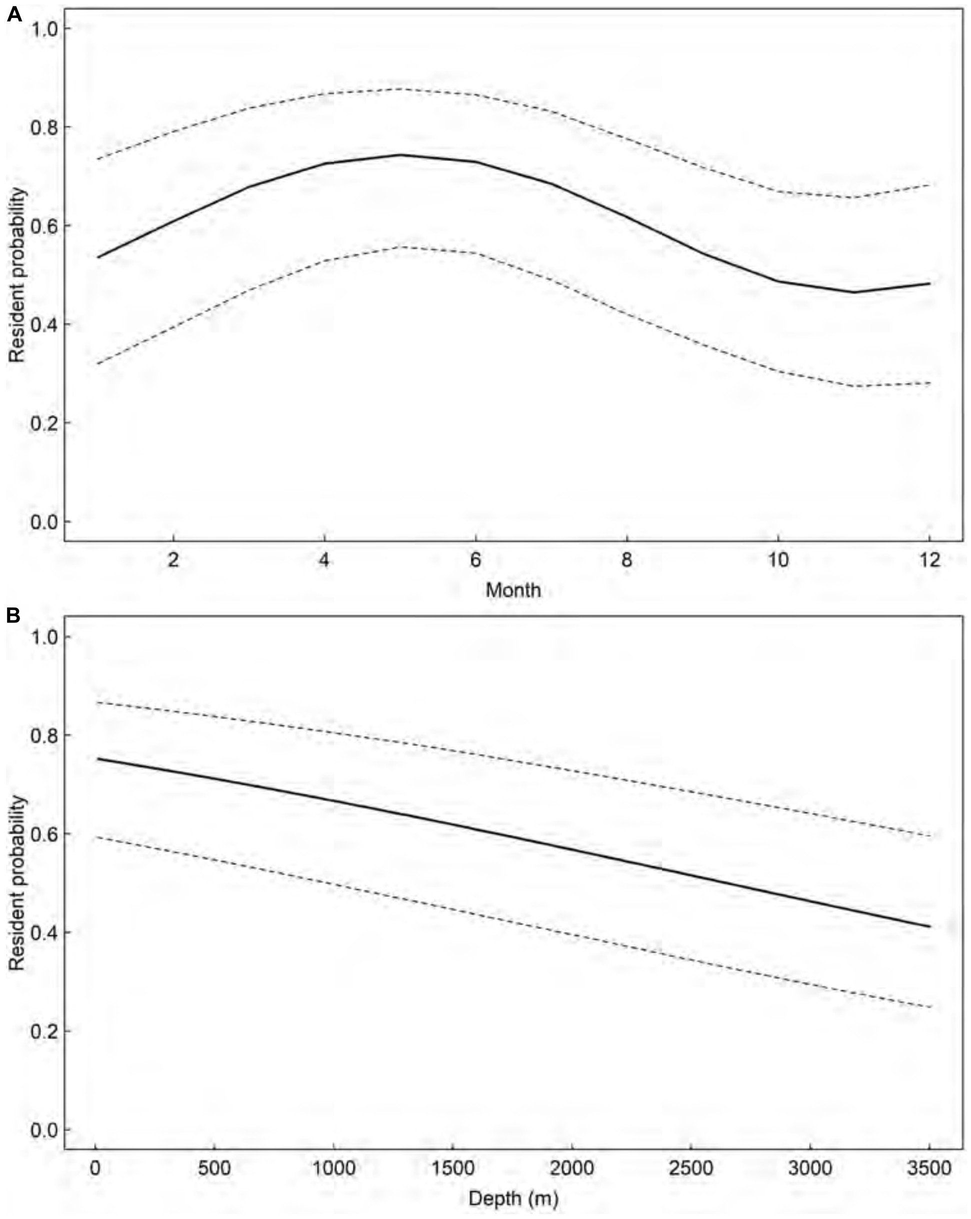

FIGURE 8 | Predicted probability, and associated 95% confidence intervals, of whale shark, *Rhincodon typus*, resident state probability in the Gulf of Mexico seasonally **(A)** and as a function of water depth **(B)** based on mixed-effects logistic regression models.

winter is unknown, however, as observed in other regions these movements could represent searching for additional foraging opportunities and possibly movements to more productive overwintering grounds in the GOM.

Overwintering Habitat

Interestingly, 11 of the 20 (55%) sharks tagged during fall and 11 of the 14 (79%) tagged sharks during winter spent time in the southern GOM in the current study (**Supplementary Figures 2, 3**), with 12 of the 17 (71%) sharks spending time in the SW GOM. This corresponded to a lack of sightings in the northern GOM during those seasons. Similarly, several tagged whale sharks from the Hueter et al. (2013) study moved from the Yucatan Peninsula into the SW GOM during fall and winter. Taken together, these data suggest the southern GOM, and more specifically SW GOM, may be suitable overwintering habitat and possibly indicate an unknown seasonal aggregation site during this time. Other large pelagic fishes, such as blue marlin, *Makaira nigricans*, Atlantic Bluefin tuna, *Thunnus thynnus*, and dusky sharks, *Carcharhinus obscurus*, have been shown to use the SW GOM as overwintering grounds (Kraus et al., 2011; Hoffmayer et al., 2014; Rooker et al., 2019) in the same vicinity where some whale sharks tagged in this study overwintered. Since little effort has been invested in studying whale sharks in the southern

TABLE 1 | Fixed-effects parameter estimates (β) and 95% confidence intervals from mixed-effects logistic regression models of the effects of seasonality and water depth on the probability of PSAT tagged whale sharks, *Rhincodon typus* (n = 22), exhibiting resident behavior in the Gulf of Mexico.

Model	Parameter	β	95% Confidence Interval
Seasonal Model			
	Intercept	0.46	−0.32–1.28
	sin(2π × month)/12	0.29	−0.04–0.61
	cos(2π × month)/12	−0.53	−0.87– −0.20
Depth			
	Intercept	1.12	0.35–1.88
	Depth/100	−0.04	−0.06– −0.03

GOM, outside the Yucatan Peninsula aggregation site, future work should focus on identifying other areas in the region, such as the SW GOM, as potentially important seasonal habitat for the GOM population.

The seasonal decline in sightings during winter and early spring could have also been related to changes in whale shark behavior, with the sharks moving to deeper waters farther offshore, but not necessarily leaving the northern GOM. Cagua et al. (2015) and Norman et al. (2017b) both used acoustic telemetry to monitor fine-scale habitat use patterns and revealed whale sharks were year-round residents off Mafia Island, Tanzania and Ningaloo Reef, Australia, yet there were no sightings outside the peak tourist season at both locations. Those authors determined sharks were using deeper, offshore waters during the time of no sightings, most likely in response to changes in prey distributions. Another possible explanation for the limited number of sightings reported during winter and spring could be the result of seasonally adverse weather conditions in the GOM, which typically result in a reduced number of boaters on the water during this time. However, we relied heavily on the offshore oil and gas industry for sightings throughout the year whose presence is not affected by weather conditions during this time. Over the course of this study, the oil and gas industry provided 127 whale shark sightings, with the lowest number of sightings occurring during winter (n = 4, 3%) and spring (n = 25, 20%), despite no reduction in the number of personnel on the water (Hoffmayer, unpub. data). Not all whale sharks overwintered in the southern GOM as three of the 14 tagged sharks moved to offshore waters but never left the northern GOM, suggesting that a portion of the population overwinters in the northern GOM. Since long-term tag retention can be challenging (i.e., minimal long-term tag

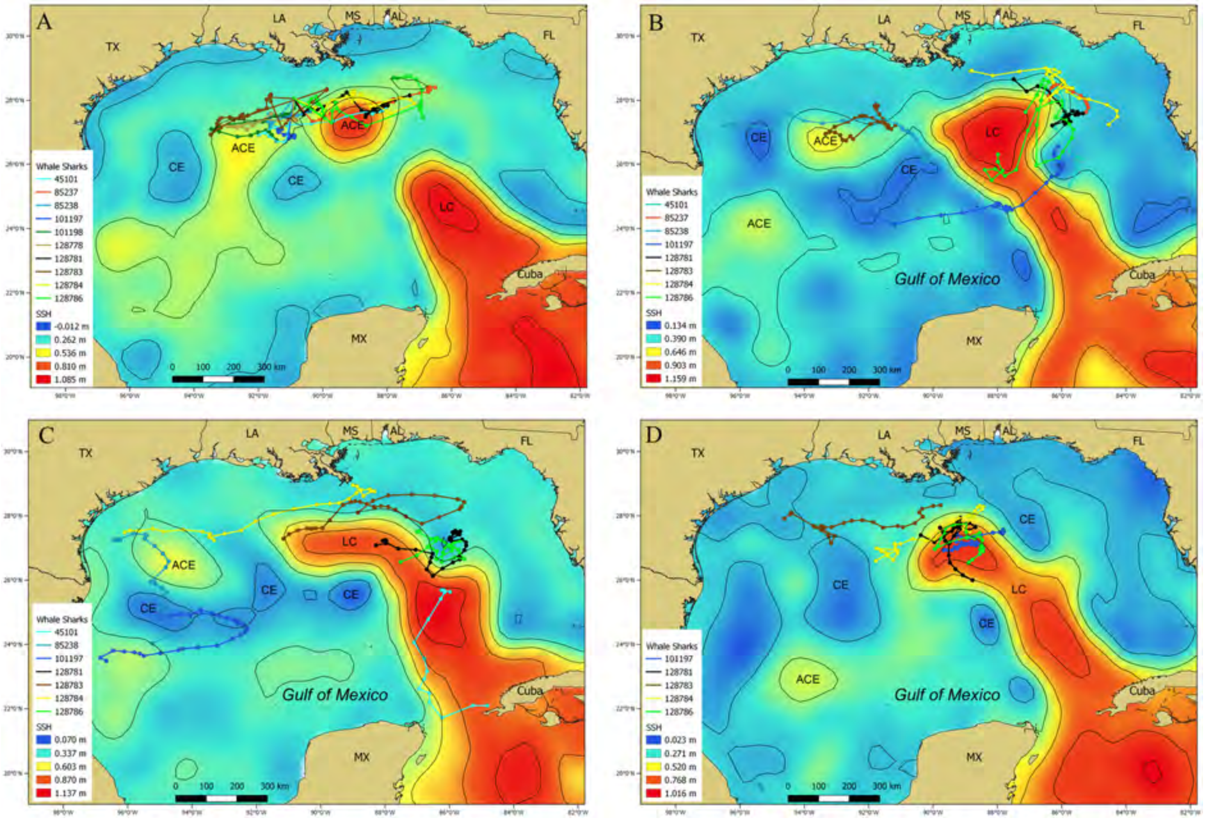

FIGURE 9 | Maps depicting sea surface height (m) showing the Loop Current and warm core and cold core eddies in the Gulf of Mexico with whale shark, *Rhincodon typus*, most probable track locations overlaid during **(A)** July 2014, **(B)** September 2014, **(C)** October 2014, and **(D)** February 2015. Most of the locations from multiple individuals are associated with the Loop Current or other warm core eddies. Contour lines (black lines) are depicted at 0.2 m height increments. The Loop Current (LC), anti-cyclonic eddies (ACE), and cyclonic eddies (CE) are indicated on the map.

retention), future work combining the use of acoustic and fin-mounted satellite-linked tags deployed on whale sharks during late fall in the northern GOM would provide additional insight into overwintering habitat for this species.

GOM Residency

The long-term tracked whale sharks exhibited interannual residency, returning to the vicinity of the Ewing Bank aggregation site one year later after demonstrating a total track displacement distance of 9,305–11,057 km. In addition to the satellite tracking data, photo identification data has revealed five individuals that have shown interannual residency to Ewing Bank, ranging anywhere between one and 4 years later (Hoffmayer, unpublished data). This movement back to the summer aggregation site demonstrates a high level of site fidelity to Ewing Bank and the importance of this area to the biology and ecology of this species in the GOM. Reynolds et al. (2017) studying the movements of whale sharks off Ningaloo Reef, Australia were the first to document homing movements with some sharks moving long distances away from Ningaloo Reef, then returning interannually. Cochran et al. (2019) also reported homing migratory movement of whale sharks to and from known aggregation sites in the Red Sea, using a variety of methods, including visual surveys, passive acoustics and satellite telemetry. Additionally, McKinney et al. (2017), using photo-ID reported 90% of the re-sighted whale sharks were individuals observed at least one year later at the same aggregation site in the western Central Atlantic Ocean where they were originally identified. Thus, it has been documented that although whale sharks may move away from seasonal aggregation sites, they have a high affinity to return to those areas.

Even though several of the tagged sharks were tracked longer than 6 months, there was no evidence of departure from the GOM; however, multiple seasonal cross-basin movements were observed. Considering the large number of tagged individuals and the fact that some whale sharks have been shown to make large-scale seasonal movements (Hueter et al., 2013; Hearn et al., 2016; Araujo et al., 2018; Diamant et al., 2018), it was surprising that no individuals made movements outside the GOM. One possible explanation for this residency to the GOM could be related to tagging location. Coastal pelagic and highly migratory fishes tagged near the Yucatan Channel or Straits of Florida (the two immigration/emigration points for the GOM) show highly variable movements, whereas species tagged in the NC and NW GOM appear to have movements restricted to the GOM. For example, Luo et al. (2020) studying movements of tarpon, *Megalops atlanticus*, in the GOM, reported that individuals tagged in the SE GOM near the Straits of Florida showed variable movements between the GOM and United States east coast; whereas other individuals tagged in the western GOM primarily remained in the GOM. Similarly, Hueter et al. (2013) tagged 35 whale sharks in waters surrounding the Yucatan Peninsula and reported a variety of movements into the GOM, Caribbean Sea, Straits of Florida, and South Atlantic Ocean. Tagging studies of other large pelagic fishes including blue marlin, and dusky, bull, *Carcharhinus leucas*, scalloped hammerhead, *Sphyrna lewini*, and tiger, *Galeocerdo cuvier*, sharks exhibited similar patterns of residency in the GOM (Carlson et al., 2010; Kraus et al., 2011; Hoffmayer et al., 2014; Wells et al., 2018; Ajemian et al., 2020). Therefore, the tagging location may influence whether an individual whale shark migrates out of the GOM and into other adjacent regions.

The high level of residency in the GOM observed in this study corresponded to the lack of connectivity observed between the Ewing Bank and the Yucatan Peninsula aggregation sites. Evidence of whale shark population connectivity between the known large aggregation sites (e.g., northern GOM and Honduras, Seychelles and Tanzania, etc.) is limited. Regional comparisons of spot patterns on whale sharks within the western Indian Ocean indicated no movements among Seychelles, Djibouti, Mozambique and Tanzania, suggesting that major "known" aggregation sites in the region do not have individuals transiting among them (Brooks et al., 2010). Based on over 16 years of whale shark photo identification data, McKinney et al. (2017) revealed connectivity among individuals from aggregations in Honduras, Belize, and Mexico, however, this was likely the direct result of the close proximity of the aggregation locations. Connectivity between the United States and other regions had a lag time between sightings of greater than one year. The lack of connectivity in the present study could be because whale shark migratory patterns occur over a multi-year scale. Sequeira et al. (2013) reviewed available whale shark movement studies and presented a conceptual movement model suggesting a possible 2 to 4 year migration cycle. Wilson et al. (2006) also suggested that whale shark movements were most likely multi-year as data were not consistent with the hypothesis of sharks returning to Ningaloo Reef after a single year. The current maximum duration of one year for PSAT tags used in the current study may not be adequate to record certain aspects of whale shark migratory behavior.

Size Distribution

In this study, both juvenile and adult whale sharks were found to use open ocean habitat, however, adult males and females used deeper, offshore waters compared to the immature males. Whale sharks have been reported to show an ontogenetic shift in habitat use, with juveniles primarily utilizing nearshore, shallow, continental shelf waters, while adults tend to use deeper, offshore, open ocean waters (Rowat and Brooks, 2012; Sequeira et al., 2013; Ramírez-Macías et al., 2017). In a tagging study conducted in the southern GOM, Hueter et al. (2013) reported similar habitat use patterns with juvenile sharks using shallower waters than larger females that utilized more offshore waters. Ketchum et al. (2013) and Ramírez-Macías et al. (2017) reported whale shark size segregation in the Gulf of California, where smaller juveniles tended to aggregate in coastal waters and adults, occurred almost exclusively in oceanic waters and suggested that juveniles were foraging on abundant prey resource found in coastal waters. There are several possible explanations for ontogenetic shifts in habitat use, including thermoregulatory behavior, reproductive requirements in females, and changes in diet (Hueter et al., 2013). Hearn et al. (2016) observed a similar pattern in habitat use and suggested an ontogenetic dietary shift in adult whale sharks results in a closer association with offshore frontal zones. Since most whale shark aggregations occur in coastal waters (Rowat and Brooks, 2012) this use of more offshore waters by adults would explain why immature sharks dominate the aggregations. This use of shallower continental shelf habitat for juvenile whale sharks is not exclusive as several studies, including the current study, have reported juveniles to use offshore waters as well (Hsu et al., 2007; Araujo et al., 2018; Diamant et al., 2018). Additional tracking and dietary studies on juvenile and adult whale sharks will be instrumental in better describing stage-specific movement patterns.

Association With Oceanographic Features

Using sightings reports, satellite telemetry and spatial analyses, our study revealed that whale sharks not only occupy continental shelf and slope waters, but also used open ocean waters of the GOM. In fact, the majority (∼90%) of the MPT locations occurred over continental slope and open ocean waters. This increased use of open ocean waters was presumably related to broad scale movements to other regions of the GOM and exploitation of ephemeral hotspots of productivity, such as convergence zones, the edge of the Loop Current, and associated ACE, for foraging opportunities. During 2014–2015, an average of 80% of the MPT locations in open ocean GOM waters occurred in proximity to these features (**Figure 9**). Although the location of the Loop Current can vary on short time scales (e.g., days to weeks), it represents a relatively consistent area of productivity in the GOM, whereas mesoscale ACEs typically split from the Loop Current at irregular intervals and slowly move toward the western GOM (Chen et al., 2015; Dufois et al., 2016).

Even though ACEs are often associated with low productivity (i.e., low chlorophyll-a concentrations), studies have shown the eddies can have large concentrations of diatoms and other phytoplankton, resulting in enhanced epipelagic productivity as well as increased mesopelagic community biomass (McGillicuddy et al., 2007; Gaube et al., 2014; Fennell and Rose, 2015; Pascual et al., 2015). While our understanding of the influence of ACEs on whale sharks is limited, these features appear to provide enhanced foraging opportunities in the otherwise oligotrophic open ocean environment for at least two species: the blue shark, *Prionace glauca*, and the white shark, *Carcharodon carcharias* (Gaube et al., 2018; Braun et al., 2019). Additionally, reef manta rays, *Manta alfredi*, have been shown to exploit mesoscale eddies in offshore waters of the Great Barrier Reef for foraging purposes and further corroborate the importance of these spatially explicit features to highly migratory species (Jaine et al., 2014). Another large filter feeding elasmobranch, the basking shark, *Cetorhinus maximus*, is known to forage along thermal fronts and actively select the most profitable plankton patches (Sims and Quayle, 1998) and make large horizontal movements to discrete productivity hotspots along shelf edge habitats (Sims et al., 2003; Doherty et al., 2017a,b; Braun et al., 2018b). There are also several examples of whale sharks using mesoscale features for foraging while in the offshore environment, including boundary currents in the northern Pacific Ocean (Hsu et al., 2007), frontal zones in the Gulf of California (Ramírez-Macías et al., 2017), and continental shelf edge upwellings in the northern GOM (McKinney et al., 2012; Hueter et al., 2013). These mesoscale features, like convergence zones and ACEs, could prove to be critical habitat for whale sharks in offshore waters of the GOM. Further study of this association with open ocean mesoscale features is warranted, specifically using habitat modeling to explore the relationship between environmental variables and more accurate tracking locations using satellite-linked tags (i.e., fin-mounted SPOT tags).

CONCLUSION AND RECOMMENDATIONS

Prior to this study, whale sharks were known to form large aggregations at continental shelf edge banks during summer in the northern GOM (Hoffmayer et al., 2005, 2007; McKinney et al., 2012), however, knowledge of their movements and habitat use patterns outside this region was limited. The sightings, satellite tracking and behavioral state model data presented in the current study further supports the fact that the continental shelf/slope waters of the NC GOM are an important foraging habitat for whale sharks during summer. During other seasons, the overall trend in habitat use was characterized by southerly movements into offshore waters of the central and southern GOM during late fall and early winter, and northerly movements back to the northern GOM during late winter and spring. It was also evident from the satellite tracking data that a large portion of the sharks tagged during fall and winter (75–80%) were over wintering in the southern GOM, with most individuals utilizing western waters. Similarly, Hueter et al. (2013) reported that whale sharks move from the Yucatan Peninsula aggregation site to the SW GOM during this same time, which further suggests this region could be an important overwintering habitat and possibly represents another seasonal aggregation site in the region. Sightings data revealed that whale sharks occurred primarily in continental shelf and shelf-edge waters (81%) whereas tag data revealed the sharks primarily inhabit continental slope and open ocean waters (91%) of the GOM. Much of their time spent in open ocean waters was linked to the edge of the Loop Current and associated mesoscale features for foraging opportunities. Although several long-term satellite tracks were presented in the study, there was no evidence of any individual leaving the GOM or visiting the Yucatan Peninsula aggregation site. However, the three long-term tracked whale sharks exhibited interannual site fidelity, returning to the vicinity of the Ewing Bank aggregation site one year after tagging.

The increased habitat use of north central GOM waters by whale sharks as summer foraging grounds and potential interannual site fidelity to Ewing Bank demonstrate the importance of this region for this species. This combined with their tendency to spend a significant amount of time in surface waters makes whale sharks susceptible to ship strikes and gear entanglement from commercial shipping traffic and energy and mineral development in the region. In addition, the impacts from the Deepwater Horizon oil spill to the GOM whale shark population remain largely unknown. Therefore, establishing protections for whale sharks in the GOM and greater Atlantic region would be beneficial to their population. Additionally, the broad-scale GOM-wide movements observed in this study demonstrate multi-national, cooperative efforts are required to properly manage whale sharks in the region. Longer-term satellite telemetry and multi-year tracking data are needed to further our understanding of whale shark movement ecology in the region and will provide the foundation for future management practices.

DATA AVAILABILITY STATEMENT

The datasets presented in this study can be found in online repositories. The names of the repository/repositories and accession number(s) can be found below: Movebank (https://www.movebank.org/cms/webapp?gwt_fragment=page=studies,path=study1153270750).

ETHICS STATEMENT

The animal study was reviewed and approved by the University of Southern Mississippi Institutional Animal Care and Use Committee (09031204 and 11092203), and under National Marine Fisheries Service Highly Migratory Division Exempted Fishing permits SHK-EFP-09-03, SHK-EFP-11-07, SHK-SRP-12-03, SHK-SRP-13-01, SHK-SRP-14-01, and SHK-SRP-15-01.

AUTHOR CONTRIBUTIONS

EH, JF, JM, WD, and JH conceived the study. EH, JM, JH, WD, and BF performed the fieldwork and data collection. EH, BG, and MB analyzed and interpreted the data. EH led the writing of the manuscript. All authors read and approved the final manuscript.

FUNDING

Funding for this research was provided to by the International Fund for Animal Welfare, World Wildlife Fund, Defenders of Wildlife, Shared Earth Foundation, Nature Conservancy Texas Chapter, and Louisiana Department of Wildlife and Fisheries (LDWF).

ACKNOWLEDGMENTS

We wish to thank B. Schumaker of *On Wings of Care* for endless hours searching for whale sharks over the Gulf of Mexico and the associated group of experienced spotters, including T. Collins, D. Abrams, M. Sturdivant, J. Moran, G. Gray, and J. Green. We would also like to thank volunteers from the USM-Gulf Coast Research Laboratory, including W. Dempster, J. Higgs, A. Fogg, S. Ashworth, and C. Butler, the Louisiana Department of Wildlife and Fisheries, including P. Sweat, P. Kent, and C. Marshall, and colleagues E. Hickerson, M. Nuttall, and G. P. Schmahl from the Flower Gardens Banks National Marine Sanctuary. Finally, we are indebted to the following individuals who were instrumental in supporting this research including J. Levenson, S. Earle, R. Nixon, B. Groark, J. Brenner, and captains R. Underwood, W. Delabar, and K. Beach.

SUPPLEMENTARY MATERIAL

The Supplementary Material for this article can be found online at: https://www.frontiersin.org/articles/10.3389/fmars.2020.598515/full#supplementary-material

REFERENCES

Ajemian, M. J., Marcus Drymon, J., Hammerschlag, N., David Wells, R. J., Street, G., Falterman, B., et al. (2020). Movement patterns and habitat use of tiger sharks (*Galeocerdo cuvier*) across ontogeny in the Gulf of Mexico. *PLoS ONE* 15:e0234868. doi: 10.1371/journal.pone.0234868

Andrzejaczek, S., Meeuwig, J., Pierce, S., Davies, T., Fisher, R., and Meekan, M. (2016). The ecological connectivity of whale shark aggregations in the Indian Ocean: a photoidentification approach. *R. Soc. Open Sci.* 3:160455. doi: 10.1098/rsos.160455

Araujo, G., Agustines, A., Tracey, B., Snow, S., Labaja, J., and Ponzo, A. (2019). Photo-ID and telemetry highlight a global whale shark hotspot in Palawan, Philippines. *Sci. Rep.* 9:17209. doi: 10.1038/s41598-019-53718-w

Araujo, G., Rohner, C. A., Labaja, J., Conales, S. J., Snow, S. J., Murray, R., et al. (2018). Satellite tracking of juvenile whale sharks in the Sulu and Bohol seas, Philippines. *PeerJ* 6:e5231. doi: 10.7717/peerj.5231

Banzon, V., Smith, T. M., Chin, T. M., Liu, C. Y., and Hankins, W. (2016). A long-term record of blended satellite and in situ sea-surface temperature for climate monitoring, modeling and environmental studies. *Earth Syst. Sci. Data* 8, 165–176. doi: 10.5194/essd-2015-44

Bauer, R. K., Forget, F., and Fromentin, J. M. (2015). Optimizing PAT data transmission: assessing the accuracy of temperature summary data to estimate environmental conditions. *Fish. Ocean.* 24, 533–539. doi: 10.1111/fog.12127

Baughman, J. T., and Springer, S. (1950). Biological and economic notes on the sharks of the Gulf of Mexico, with special reference to those of Texas, and with a key for their identification. *Am. Midl. Nat.* 44, 96–152. doi: 10.2307/2421758

Berumen, M. L., Braun, C. D., Cochran, J. E. M., Skomal, G. B., and Thorrold, S. R. (2014). Movement patterns of juvenile whale sharks tagged at an aggregation site in the Red Sea. *PLoS One* 9:e103536. doi: 10.1371/journal.pone.0103536

Bigelow, H. B., and Schroeder, W. C. (1948). Fishes of the western North Atlantic, Part I: lancelets, cyclostomes, sharks. *Mem. Sears Found. Mar. Res.* 1, 559–576.

Braun, C. D., Galuardi, B., and Thorrold, S. R. (2018a). HMMoce: an R package for improved geolocation of archival-tagged fishes using a hidden Markov method. *Methods Ecol. Evol.* 9, 1212–1220. doi: 10.1111/2041-210X.12959

Braun, C. D., Gaube, P., Sinclair-Taylor, T. H., Skomal, G. B., and Thorrold, S. R. (2019). Mesoscale eddies release pelagic sharks from thermal constraints to foraging in the ocean twilight zone. *Proc. Natl. Acad. Sci. U.S.A.* 116, 17187–17192. doi: 10.1073/pnas.1903067116

Braun, C. D., Skomal, G. B., and Thorrold, S. R. (2018b). Integrating archival tag data and a high-resolution oceanographic model to estimate basking shark (Cetorhinus maximus) movements in the western Atlantic. *Front. Mar. Sci.* 5:25. doi: 10.3389/fmars.2018.00025

Breuer, J. P. (1954). The littlest biggest fish. *Texas Game Fish* 12, 29.

Brooks, K., Rowat, D., Pierce, S. J., Jouannet, D., and Vely, M. (2010). Seeing spots: photo-identification as a regional tool for whale shark identification. *West. Indian Ocean J. Mar. Sci.* 9, 185–194.

Brunnschweiler, J. M., Baensch, H., Pierce, S. J., and Sims, D. W. (2009). Deep-diving behavior of a whale shark *Rhincodon typus* during long-distance movement in the western Indian Ocean. *J. Fish Biol.* 74, 706–714. doi: 10.1111/j.1095-8649.2008.02155.x

Burks, C. M., Driggers, W. B. I. I. I., and Mullin, K. D. (2006). Abundance and distribution of whale sharks (Rhincodon typus) in the northern Gulf of Mexico. *Fish. Bull.* 104, 579–584.

Burnham, K. P., and Anderson, D. R. (2002). *Model Selection and Multimodel Inference: A Practical Information-Theoretic Approach*, 2nd Edn. New York, NY: Springer.

Burt, W. H. (1943). Territoriality and home range concepts as applied to mammals. *J. Mamm.* 24, 346–352. doi: 10.2307/1374834

Byrne, M. E., Vaudo, J. J., Harvey, G. C. M., Johnston, M. W., Wetherbee, B. M., and Shivji, M. (2019). Behavioral response of a mobile marine predator to environmental variables differs across ecoregion. *Ecography* 42, 1569–1578. doi: 10.1111/ecog.04463

Cagua, E. F., Cochran, J. E. M., Rohner, C. A., Prebble, C. E. M., Sinclair-Taylor, T. H., Pierce, S. J., et al. (2015). Acoustic telemetry reveals cryptic residency of whale sharks. *Biol. Lett.* 11:20150092. doi: 10.1098/rsbl.2015.0092

Calich, H., Estevanez, M., and Hammerschlag, N. (2018). Overlap between highly suitable habitats and longline gear management areas reveals vulnerable and protected regions for highly migratory sharks. *Mar. Ecol. Prog. Ser.* 602, 183–195. doi: 10.3354/meps12671

Cárdenas-Palomo, N., Herrera-Silveira, J., Velázquez-Abunader, I., Reyes, O., and Ordoñez, U. (2014). Distribution and feeding habitat characterization of whale sharks Rhincodon typus in a protected area in the north Caribbean Sea. *J. Fish Biol.* 86, 668–686. doi: 10.1111/jfb.12589

Carlson, J. K., Ribera, M. M., Conrath, C. L., Heupel, M. R., and Burgess, G. H. (2010). Habitat use and movement patterns of bull sharks Carcharhinus leucas determined using pop-up satellite archival tags. *J. Fish Biol.* 77, 661–675. doi: 10.1111/j.1095-8649.2010.02707.x

Castro, A. L. F., Stewart, B. S., Wilson, S. G., Hueter, R. E., Meekan, M. G., Motta, P. J., et al. (2007). Population genetic structure of Earth's largest fish, the whale shark (Rhincodon typus). *Mol. Ecol.* 16, 5183–5192. doi: 10.1111/j.1365-294X.2007.03597.x

Chassignet, E. P., Hurlburt, H. E., Smedstad, O. M., Halliwell, G. R., Hogan, P. J., Wallcraft, A. J., et al. (2007). The HYCOM (HYbrid Coordinate Ocean Model) data assimilative system. *J. Mar. Sys.* 65, 60–83. doi: 10.1016/j.jmarsys.2005.09.016

Chen, Y. L., Chen, H. Y., Jan, S., Lin, Y. H., Kuo, T. H., and Hung, J. J. (2015). Biologically active warm-core anticyclonic eddies in the marginal seas of the western Pacific Ocean. *Deep-Sea Res. I* 106, 68–84. doi: 10.1016/j.dsr.2015.10.006

Chmura, H. E., Glass, T. W., and Williams, C. T. (2018). Biologging physiological and ecological responses to climatic variation: new tools for the climate change era. *Front. Ecol. Evol.* 6:92. doi: 10.3389/fevo.2018.00092

Cochran, J. E. M., Braun, C. D., Cagua, E. F., Campbell, M. F., Hardenstine, R. S., Kattan, A., et al. (2019). Multi-method assessment of whale shark (Rhincodon typus) residency, distribution, and dispersal behavior at an aggregation site in the Red Sea. *PLoS One* 14:e0222285. doi: 10.1371/journal.pone.0222285

Colman, J. G. (1997). A review of the biology and ecology of the whale shark. *J. Fish. Biol.* 51, 1219–1234. doi: 10.1111/j.1095-8649.1997.tb01138.x

Compagno, L. J. V. (2001). *Sharks of the World: an Annotated and Illustrated Catalogue of Shark Species Known to date: Heterodontiformes, Lamniformes, Orectolobiformes*. Rome: FAO Species Catalogue for Fishery.

de la Parra Venegas, R., Hueter, R., González Cano, J., Tyminski, J., Gregorio Remolina, J., Maslanka, M., et al. (2011). An unprecedented aggregation of whale sharks, Rhincodon typus, in Mexican coastal waters of the Caribbean Sea. *PLoS One* 6:e18994. doi: 10.1371/journal.pone.0018994

Diamant, S., Rohner, C. A., Kiszka, J. J., Guillemain, d'Echon, A., Guillemain d'Echon, T., et al. (2018). Movements and habitat use of satellite-tagged whale sharks off western Madagascar. *Endanger. Species Res.* 36, 49–58. doi: 10.3354/esr00889

Doherty, P. D., Baxter, J. M., Gell, F. R., Godley, B. J., Graham Hall, G., Hall, J., et al. (2017a). Long-term satellite tracking reveals variable seasonal migration strategies of basking sharks in the northeast Atlantic. *Nat. Sci. Rep.* 7:42837. doi: 10.1038/srep42837

Doherty, P. D., Baxter, J. M., Godley, B. J., Graham, R. T., Hall, G., Hall, J., et al. (2017b). Testing the boundaries: seasonal residency and inter-annual site fidelity of basking sharks in a proposed Marine Protected Area. *Biol. Conserv.* 209, 68–75. doi: 10.1016/j.biocon.2017.01.018

Dufois, F., Hardman-Mountford, N. J., Greenwood, J., Richardson, A. J., Feng, M., and Matear, R. J. (2016). Anticyclonic eddies are more productive than cyclonic eddies in subtropical gyres because of winter mixing. *Sci. Adv.* 2:e16000282. doi: 10.1126/sciadv.1600282

Duong, T. (2007). Ks: kernel density estimation and kernel discriminant analysis for multivariate data in R. *J. Stat. Software* 21, 1–16. doi: 10.18637/jss.v021.i07

Faghmous, J. H., Chamber, Y., Boriah, S., Liess, S., and Kumar, V. (2012). "A novel and scalable spatio-temporal technique for ocean eddy monitoring," in *Proceedings of the Twenty-Sixth AAAI Conference on Artificial Intelligence*, (Toronto, ON: AAAI), 281–287.

Fennell, S., and Rose, G. (2015). Oceanographic influences on deep scattering layers across the North Atlantic. *Deep Sea Res. I* 105, 132–141. doi: 10.1016/j.dsr.2015.09.002

Fox, S., Foisy, I., de la Parra-Venegas, R., Galvan-Pastoriza, B., Graham, R. T., Hoffmayer, E. R., et al. (2013). Population structure and residency of whale sharks Rhincodon typus at Utila, Bay Islands, Honduras. *J. Fish Biol.* 83, 574–587. doi: 10.1111/jfb.12195

Gaube, P., Braun, C. D., Lawson, G. L., McGillicuddy, D. J. Jr., Penna, A. D., Skomal, G. B., et al. (2018). Mesoscale eddies influence the movements of mature female white sharks in the Gulf Stream and Sargasso Sea. *Sci. Rep.* 8:7363. doi: 10.1038/s41598-018-25565-8

Gaube, P., McGillicuddy, D. J. Jr., Chelton, D. B., Behrenfeld, M. J., and Strutton, P. G. (2014). Regional variations in the influence of mesoscale eddies on near-surface chlorophyll. *J. Geophys. Res. Oceans* 119, 8195–8220. doi: 10.1002/2014JC010111

Gebco Compilation Group (2020). *The GEBCO_2020 Grid - A Continuous Terrain Model of the Global Oceans and Land*. Atlanta: National Oceanography Centre, NERC, doi: 10.5285/a29c5465-b138-234d-e053-6c86abc040b9

Graham, F., Rynne, P., Estevanez, M., Luo, J., Ault, J. S., and Hammerschlag, N. (2016). Use of marine protected areas and exclusive economic zones in the subtropical western North Atlantic Ocean by large highly mobile sharks. *Divers. Distrib.* 22, 534–546. doi: 10.1111/ddi.12425

Graham, R. T., and Roberts, C. M. (2007). Assessing the size, growth rate and structure of a seasonal population of whale sharks (Rhincodon typus Smith 1828) using conventional tagging and photo identification. *Fish. Res.* 84, 71–80. doi: 10.1016/j.fishres.2006.11.026

Gudger, E. (1918). Rhineodon typus, the whale shark – Further notes on its habits and distribution. *Science* 48, 622–627. doi: 10.1126/science.48.1251.622-a

Gudger, E. (1934). The geographical distribution of the whale shark (Rhineodon typus). *Proc. Zool. Soc.* 4, 863–894. doi: 10.1111/j.1096-3642.1934.tb01670.x

Hammerschlag, N., Gallagher, A. J., and Lazarre, D. M. (2011). A review of shark satellite tagging studies. *J. Exp. Mar. Biol. Ecol.* 398, 1–8. doi: 10.1016/j.jembe.2010.12.012

Hart, K. M., and Hyrenbach, K. D. (2009). Satellite telemetry of marine megavertebrates: the coming of age of an experimental science. *Endanger. Species Res.* 10, 9–20. doi: 10.3354/esr00238

Hearn, A. R., Green, J., Roman, M. H., Acuña-Marrero, D., Espinoza, E., and Klimley, A. P. (2016). Adult female whale sharks make long-distance movements past Darwin Island (Galapagos, Ecuador) in the Eastern Tropical Pacific. *Mar. Biol.* 163:214. doi: 10.1007/s00227-016-2991-y

Hearn, A. R., Green, J. R., Espinoza, E., Peñeherrera, C., Acuña, D., and Klimley, A. P. (2013). Simple criteria to determine detachment point of towed satellite tags provide first evidence of return migrations of whale sharks (Rhincodon typus) at the Galapagos Islands. *Ecuador. Anim. Biotelemetry* 1:11. doi: 10.1186/2050-3385-1-11

Heyman, W., Graham, R., Kjerfve, B., and Johannes, R. E. (2001). Whale sharks Rhincodon typus aggregate to feed on fish spawn in Belize. *Mar. Ecol. Prog. Ser.* 251, 275–282. doi: 10.3354/meps215275

Hoffman, W., Fritts, T. H., and Reynolds, R. P. (1981). Whale sharks associated with fish schools off south Texas. *Northeast Gulf Sci.* 5, 55–57. doi: 10.18785/negs.0501.08

Hoffmayer, E. R., Franks, J. S., Driggers, W. B. I. I. I., McKinney, J. A., Hendon, J. M., and Quattro, J. M. (2014). Habitat, movement and environmental preferences of dusky sharks, Carcharhinus obscurus, in the northern Gulf of Mexico. *Mar. Biol.* 161, 911–924. doi: 10.1007/s00227-014-2391-0

Hoffmayer, E. R., Franks, J. S., Driggers, W. B. I. I. I., Oswald, K. J., and Quattro, J. M. (2007). Observations of a feeding aggregation of whale sharks, Rhincodon typus, in the north central Gulf of Mexico. *Gulf Carib. Res.* 19, 69–73. doi: 10.18785/gcr.1902.08

Hoffmayer, E. R., Franks, J. S., and Shelley, J. P. (2005). Recent observations of the whale shark (Rhincodon typus) in the northcentral Gulf of Mexico. *Gulf Caribb. Res.* 17, 117–120. doi: 10.18785/gcr.1701.11

Hsu, H. H., Joung, S. J., Liao, Y. Y., and Liu, K. M. (2007). Satellite tracking of juvenile whale sharks, Rhincodon typus, in the northwestern Pacific. *Fish. Res.* 84, 25–31. doi: 10.1016/j.fishres.2006.11.030

Hueter, R. E., Tyminski, J. P., and de la Parra, R. (2013). Horizontal movements, migration patterns, and population structure of whale sharks in the Gulf of Mexico and northwestern Caribbean Sea. *PLoS One* 8:e71883. doi: 10.1371/journal.pone.0071883

Hussey, N. E., Kessel, S. T., Aarestrup, K., Cooke, S. J., Cowley, P. D., Fisk, A. T., et al. (2015). Aquatic animal telemetry: a panoramic window into the underwater world. *Science* 348:1255642. doi: 10.1126/science.1255642

Jaffa, K. S., and Taher, N. A. B. A. (2007). Whale sharks in Palestinian waters: a whale shark (*Rhincodon typus* Smith 1828) rescued near the Tantura Beach, Carmel Coast, North Palestine. The first record from the Palestinian Mediterranean Coast. *Gazelle: Palestinian. Biol. Bull.* 71, 22–23. doi: 10.1007/s00227-016-2991-y

Jaine, F. R. A., Rohner, C. A., Weeks, S. J., Couturier, L. I. E., Bennett, M. B., Townsend, K. A., et al. (2014). Movements and habitat use of reef manta rays off eastern Australia: offshore excursions, deep diving and eddy affinity revealed by satellite telemetry. *Mar. Eco. Prog. Ser.* 510, 73–86. doi: 10.3354/meps10910

Jonsen, I. D. (2016). Joint estimation over multiple individuals improves behavioural state inference from animal movement data. *Sci. Rep.* 6:20625. doi: 10.1038/srep20625

Jonsen, I. D., Bestley, S., Wotherspoon, S., Sumner, M., and Flemming, J. M. (2020). *bsam: Bayesian State-Space Models for Animal Movement. R Package* 1.1.3. https://github.com/ianjonsen/bsam (accessed January 9, 2020).

Jonsen, I. D., Flemming, J. M., and Myers, R. A. (2005). Robust state-space modeling of animal movement data. *Ecol.* 86, 2874–2880. doi: 10.1890/04-1852

Ketchum, J. T., Galván-Magaña, F., and Klimley, A. P. (2013). Segregation and foraging ecology of whale sharks, Rhincodon typus, in the southwestern Gulf of California. *Environ. Biol. Fish* 96, 779–795. doi: 10.1007/s10641-012-0071-9

Kraus, R. T., Wells, R. J. D., and Rooker, J. R. (2011). Horizontal movements of Atlantic blue marlin (Makaira nigricans) in the Gulf of Mexico. *Mar. Biol.* 158, 699–713. doi: 10.1007/s00227-010-1593-3

Le Fevre, J. (1986). Aspects of the biology of frontal systems. *Adv. Mar. Biol.* 23, 163–299. doi: 10.1016/S0065-2881(08)60109-1

Lea, J. S. E., Wetherbee, B. M., Quieroz, N., Burnie, N., Aming, C., Sousa, L. L., et al. (2015). Repeated, long-distance migrations by a philopatric predator targeting highly contrasting ecosystems. *Nat. Sci. Rep.* 5:11202. doi: 10.1038/srep11202

Luo, J., Ault, J. A., Ungar, B. T., Smith, S. G., Larkin, M. F., Davidson, T. N., et al. (2020). Migrations and movements of Atlantic tarpon revealed by two decades of satellite tagging. *Fish Fish.* 21, 290–318. doi: 10.1111/faf.12430

Luo, J., Ault, J. S., Shay, L. K., Hoolihan, J. P., Prince, E. D., Brown, C. A., et al. (2015). Ocean heat content reveals secrets of fish migrations. *PLoS One* 10:e0141101. doi: 10.1371/journal.pone.0141101

McGillicuddy, D. J., Anderson, L. A., Bates, N. R., Bibby, T., Buesseler, K. O., Carlson, C. A., et al. (2007). Eddy/wind interactions stimulate extraordinary mid-ocean plankton blooms. *Science* 316, 1021–1026. doi: 10.1126/science.1136256

McKinney, J. A., Hoffmayer, E. R., Holmberg, J., Graham, R. T., Driggers, W. B. I. I. I., de la Parra-Venegas, R., et al. (2017). Long-term assessment of whale shark population demography and connectivity using photo-identification in the western Atlantic Ocean. *PLoS One* 12:e0180495. doi: 10.1371/journal.pone.0180495

McKinney, J. A., Hoffmayer, E. R., Wu, W., Fulford, R., and Hendon, J. M. (2012). Feeding habitat of the whale shark Rhincodon typus in the northern Gulf of Mexico determined using species distribution modelling. *Mar. Eco. Prog. Ser.* 458, 199–211. doi: 10.3354/meps09777

Norman, B. M., Holmberg, J. A., Arzoumanian, Z., Reynolds, S. D., Wilson, R. P., Rob, D., et al. (2017a). Undersea constellations: the global biology of an endangered marine megavertebrate further informed through citizen science. *Bioscience* 67, 1029–1043. doi: 10.1093/biosci/bix127

Norman, B. M., and Stevens, J. D. (2007). Size and maturity status of the whale shark (*Rhincodon typus*) at Ningaloo Reef in Western Australia. *Fish. Res.* 84, 81–86. doi: 10.1016/j.fishres.2006.11.015

Norman, B. M., Whitty, J. M., Beatty, S. J., Reynolds, S. D., and Morgan, D. L. (2017b). Do they stay or do they go? Acoustic monitoring of whale sharks at Ningaloo Marine Park, Western Australia. *J. Fish Biol.* 91, 1713–1720. doi: 10.1111/jfb.13461

Nychka, D., Furrer, R., Paige, J., and Sain, S. (2015). *Fields: Tools for Spatial Data. R package version 9.0*. Boulder, CO: University Corporation for Atmospheric Research.

Papastamatiou, Y. P., Friedlander, A. M., Caselle, J. E., and Lowe, C. G. (2010). Long-term movement patterns and trophic ecology of blacktip reef sharks (Carcharhinus melanopterus) at Palmyra Atoll. *J. Exp. Mar. Biol. Ecol.* 386, 94–102. doi: 10.1016/j.jembe.2010.02.009

Pascual, A., Ruiz, S., Buongiorno Nardelli, B., Guinehut, S., Iudicone, D., and Tintoré, J. (2015). Net primary production in the Gulf Stream sustained by quasi-geostrophic vertical exchanges. *Geophys. Res. Lett.* 42, 441–449. doi: 10.1002/2014GL062569

Pedersen, M., Berg, C., Thygesen, U., Nielsen, A., and Madsen, H. (2011). Estimation methods for nonlinear state-space models in ecology. *Ecol. Model.* 222, 1394–1400. doi: 10.1016/j.ecolmodel.2011.01.007

Queiroz, N., Humphries, N. E., Mucientes, G., Hammerschlag, N., Lima, F. P., Scales, K. L., et al. (2016). Ocean-wide tracking of pelagic sharks reveals extent of overlap with longline fishing hotspots. *Proc. Natl. Acad. Sci. U.S.A.* 113, 1582–1587. doi: 10.1073/pnas.1510090113

R Core Team (2016). *R: A Language and Environment for Statistical Computing*. Vienna: R Foundation for Statistical Computing.

Ramírez-Macías, D., Queiroz, N., Pierce, S. J., Humphries, N. E., Sims, D. W., and Brunnschweiler, J. M. (2017). Oceanic adults, coastal juveniles: tracking the habitat use of whale sharks off the Pacific coast of Mexico. *PeerJ* 5:e3271. doi: 10.7717/peerj.3271

Reynolds, R. W., Smith, T. M., Liu, C., Chelton, D. B., Casey, K. S., and Schlax, M. G. (2007). Daily high-resolution-blended analyses for sea surface temperature. *J. Clim.* 20, 5473–5496. doi: 10.1175/2007JCLI1824.1

Reynolds, S. D., Norman, B. M., Beger, M., Franklin, C. E., and Dwyer, R. G. (2017). Movement, distribution and marine reserve use by an endangered migratory giant. *Divers. Distrib.* 23, 1268–1279. doi: 10.1111/ddi.12618

Richards, W. J., McGowen, M. F., Leming, T., Lamkin, J. T., and Kelly, S. (1993). Larval fish assemblages at the Loop Current boundary in the Gulf of Mexico. *Bull. Mar. Sci.* 53, 475–537.

Robinson, D. P., Jaidah, M. Y., Bach, S. S., Rohner, C. A., Jabado, R. W., Ormond, R., et al. (2017). Some like it hot: repeat migration and residency of whale sharks within an extreme natural environment. *PLoS One* 12:e0185360. doi: 10.1371/journal.pone.0185360

Robinson, D. P., Jaidah, M. Y., Jabado, R. W., Lee-Brooks, K., Nour El-Din, N. M., Al Malki, A. A., et al. (2013). Whale sharks, Rhincodon typus, aggregate around offshore platforms in Qatari waters of the Arabian Gulf to feed on fish spawn. *PLoS One* 8:e58255. doi: 10.1371/journal.pone.0058255

Rohner, C. A., Armstrong, A. J., Pierce, S. J., Prebble, C. E. M., Cagua, E. F., Cochran, J. E. M., et al. (2015). Whale sharks target dense prey patches of sergestid shrimp off Tanzania. *J. Plankt. Res.* 37, 352–362. doi: 10.1093/plankt/fbv010

Rohner, C. A., Richardson, A. J., Jaine, F. R. A., Bennett, M. B., Weeks, S. J., Cliff, G., et al. (2018). Satellite tagging highlights the importance of productive Mozambican coastal waters to the ecology and conservation of whale sharks. *Peer J.* 6:e4161. doi: 10.7717/peerj.4161

Rooker, J. R., Dance, M. A., Wells, R. J. D., Ajemian, M. J., Block, B. A., Castleton, M. R., et al. (2019). Population connectivity of pelagic megafauna in the Cuba-Mexico-United States triangle. *Sci. Rep.* 9:1663. doi: 10.1038/s41598-018-38144-8

Rowat, D., and Brooks, K. S. (2012). A review of the biology, fisheries and conservation of the whale shark Rhincodon typus. *J. Fish Biol.* 80, 1019–1056. doi: 10.1111/j.1095-8649.2012.03252.x

Rowat, D., and Gore, M. (2007). Regional scale horizontal and local scale vertical movements of whale sharks in the Indian Ocean off Seychelles. *Fish. Res.* 84, 32–40. doi: 10.1016/j.fishres.2006.11.009

Rowat, D., Speed, C. W., Meekan, M. G., and Gore, M. A. (2009). Population abundance and apparent survival of the vulnerable whale shark Rhincodon typus in the Seychelles aggregation. *Oryx* 43, 591–598. doi: 10.1017/s0030605309990408

Ryan, J. P., Green, J. R., Espinoza, E., and Hearn, A. R. (2017). Association of whale sharks (Rhincodon typus) with thermos-biological frontal systems of the eastern tropical Pacific. *PLoS One* 12:e0182599. doi: 10.1371/journal.pone.0182599

Ryan, J. P., Yoder, J. A., and Cornillon, P. C. (1999). Enhanced chlorophyll at the shelfbreak of the Mid-Atlantic Bight and Georges Bank during the spring transition. *Limnol. Oceanogr.* 44, 1–11. doi: 10.4319/lo.1999.44.1.0001

Schmidt, J. V., Schmidt, C. L., Ozer, F., Ernst, R. E., Feldheim, K. A., Ashley, M. V., et al. (2009). Low genetic differentiation across three major ocean populations of the whale shark. *Rhincodon typus*. *PLoS One* 4:e4988. doi: 10.1371/journal.pone.0004988

Sequeira, A. M. M., Mellin, C., Meekan, M. G., Sims, D. W., and Bradshaw, C. J. A. (2013). Inferred global connectivity of whale shark Rhincodon typus populations. *J. Fish. Biol.* 82, 367–389. doi: 10.1111/jfb.12017

Silas, E. G. (1986). The whale shark (Rhiniodon typus Smith) in Indian coastal waters: is the species endangered or vulnerable? *Mar. Fish. Infor. Serv. T E Ser.* 66, 1–19.

Sims, D., and Quayle, V. (1998). Selective foraging behaviour of basking sharks on zooplankton in a small-scale front. *Nature* 393, 460–464. doi: 10.1038/30959

Sims, D. W., Southall, E. J., Richardson, A. J., Reid, P. C., and Metcalfe, J. D. (2003). Seasonal movements and behaviour of basking sharks from archival tagging: no evidence of winter hibernation. *Mar. Ecol. Prog. Ser.* 248, 187–196. doi: 10.3354/meps248187

Skomal, G. B., Braun, C. D., Chisholm, J. H., and Thorrold, S. R. (2017). Movement of the white shark Carcharodon carcharias in the North Atlantic Ocean. *Mar. Ecol. Prog. Ser.* 580, 1–16. doi: 10.3354/meps12306

Springer, S. (1957). Some observations on the behavior of schools of fishes in the Gulf of Mexico and adjacent waters. *Ecology* 38, 166–171. doi: 10.2307/1932154

Stevens, J. D. (2007). Whale shark (Rhincodon typus) biology and ecology: a review of the primary literature. *Fish. Res.* 84, 4–9. doi: 10.1016/j.fishres.2006.11.008

Taylor, J. G. (1996). Seasonal occurrence, distribution and movements of the whale shark. Rhincodon typus, at Ningaloo Reef, Western Australia. *Mar. Freshw. Res.* 47, 637–642. doi: 10.1071/MF9960637

Tyminski, J. P., de la Parra-Venegas, R., González Cano, J., and Hueter, R. E. (2015). Vertical movements and patterns of diving behavior of whale sharks as revealed by pop-up satellite tags in the eastern Gulf of Mexico. *PLoS One* 10:e0142156. doi: 10.1371/journal.pone.0142156

van Buuren, S., and Groothuis-Oudshoorn, K. (2011). mice: multivariate imputation by chained equations in R. *J. Stat. Softw.* 45, 1–67. doi: 10.18637/jss.v045.i03

Vignaud, T. M., Maynard, J. A., Leblois, R., Meekan, M. G., Vázquez-Juárez, R., and Ramírez-Macías, D. (2014). Genetic structure of populations of whale sharks among ocean basins and evidence for their historic rise and recent decline. *Mol. Ecol.* 23, 2590–2601. doi: 10.1111/mec.12754

Wells, R. J. D., Tin-Han, T. C., Dance, M. A., Drymon, J. M., Falterman, B., Ajemian, M. J., et al. (2018). Movement, behavior, and habitat use of a marine apex predator, the scalloped hammerhead. *Front. Mar. Sci.* 5:321. doi: 10.3389/fmars.2018.00321

Whitford, M., and Klimley, A. P. (2019). An overview of behavioral, physiological, and environmental sensors used in animal biotelemetry and biologging studies. *Anim. Biotelemetry* 7:26. doi: 10.1186/s40317-019-0189-z

Wicksten, M. K., and Packard, J. M. (2005). A qualitative zoogeographic analysis of decapod crustaceans of the continental slopes and abyssal plain of the Gulf of Mexico. *Deep Sea Res. Part I Oceanogr. Res. Pap.* 52, 1745–1765. doi: 10.1016/j.dsr.2005.04.006

Wilson, S. G., Pauly, T., and Meekan, M. G. (2001). Daytime surface swarming by Pseudeuphausia latifrons (Crustacea, Euphausiacea) off Ningaloo Reef, Western Australia. *Bull. Mar. Sci.* 68, 157–162.

Wilson, S. G., Polovina, J. J., and Stewart, B. S. (2006). Movement of whale sharks (Rhincodon typus) tagged at Ningaloo Reef, Western Australia. *Mar. Biol.* 128, 1157–1166. doi: 10.1007/s00227-005-0153-8

Worton, B. J. (1989). Kernel methods for estimating the utilization distribution in home-range studies. *Ecology* 70, 164–168. doi: 10.2307/1938423

Conflict of Interest: The authors declare that the research was conducted in the absence of any commercial or financial relationships that could be construed as a potential conflict of interest.

frontiers
in Marine Science

ORIGINAL RESEARCH
published: 26 January 2021
doi: 10.3389/fmars.2021.623104

New Insights Into the Seasonal Movement Patterns of Shortfin Mako Sharks in the Gulf of Mexico

Kesley J. Gibson*, Matthew K. Streich, Tara S. Topping and Gregory W. Stunz

Harte Research Institute for Gulf of Mexico Studies, Texas A&M University – Corpus Christi, Corpus Christi, TX, United States

Highly mobile apex predators such as the shortfin mako shark (mako shark; *Isurus oxyrinchus*) serve an important role in the marine ecosystem, and despite their declining populations and vulnerability to overexploitation, this species is frequently harvested in high abundance in both commercial and recreational fisheries. In 2017, the North Atlantic stock was deemed overfished and to be undergoing overfishing and was recently listed in CITES Appendix II. Effective management of this species can benefit from detailed information on their movements and habitat use, which is lacking, especially in the Gulf of Mexico, a potential mating and parturition ground. In this study, we used satellite telemetry to track the movements of mako sharks in the western Gulf of Mexico between 2016 and 2020. In contrast to previous studies that have primarily tagged juvenile mako sharks (>80% juveniles), ∼80% of sharks tagged in this study (7 of 9) were presumed to be mature based on published size-at-maturity data. Sharks were tracked for durations ranging from 10 to 887 days (mean = 359 days; median = 239 days) with three mature individuals tracked for >2 years. Mako sharks tagged in this study used more of the northwestern Gulf of Mexico than reported in previous movement studies on juveniles, suggesting potential evidence of size segregation. While one mature female remained in the Gulf of Mexico over a >2-year period, predominantly on the continental shelf, two mature males demonstrated seasonal migrations ∼2,500 km from the tagging location off the Texas coast to the Caribbean Sea and northeastern United States Atlantic coast, respectively. During these migrations, mako sharks traversed at least 12 jurisdictional boundaries, which also exposed individuals to varying levels of fishing pressure and harvest regulations. Movement ecology of this species, especially for mature individuals in the western North Atlantic, has been largely unknown until recently. These data included here supplement existing information on mako shark movement ecology and potential stock structure that could help improve management of the species.

Keywords: shortfin mako, population connectivity, Gulf of Mexico, sharks, migration

Edited by:
Yannis Peter Papastamatiou,
Florida International University,
United States

Reviewed by:
Neil Hammerschlag,
University of Miami, United States
Tobey H. Curtis,
National Oceanic and Atmospheric
Administration (NOAA), United States

****Correspondence:***
Kesley J. Gibson
Kesley.Gibson@tamucc.edu

Specialty section:
This article was submitted to
Marine Megafauna,
a section of the journal
Frontiers in Marine Science

Received: *29 October 2020*
Accepted: *04 January 2021*
Published: *26 January 2021*

Citation:
Gibson KJ, Streich MK,
Topping TS and Stunz GW (2021)
New Insights Into the Seasonal
Movement Patterns of Shortfin Mako
Sharks in the Gulf of Mexico.
Front. Mar. Sci. 8:623104.
doi: 10.3389/fmars.2021.623104

INTRODUCTION

Highly migratory species often fill the role of apex predator in marine ecosystems, but many populations are declining globally which can have cascading effects on lower trophic levels (Estes et al., 2011; Dulvy et al., 2014; Hammerschlag et al., 2019). These highly mobile species create a unique management problem given their wide movement ranges, as they often cross many jurisdictional boundaries, exposing them to varying degrees of protection (Rooker et al., 2019). Given their high potential for movement over very large spatial scales, identifying their particular habitat requirements can be very challenging. Furthermore, highly migratory species, including oceanic sharks, are often caught in commercial and recreational fisheries (Block et al., 2011; Francis et al., 2019) and are vulnerable to overexploitation due to their life history characteristics, which include long lifespans, late maturity, and long reproductive cycles (Pratt and Casey, 1983; Mollet et al., 2000; Cortés et al., 2010). Conservation and rebuilding of these declining species can benefit from species-specific knowledge on movements and habitats needed to complete their life cycles (Hays et al., 2019).

One such species is the shortfin mako (*Isurus oxyrinchus*; hereafter mako shark), which are pelagic, fast-swimming, sharks found in tropical and temperate waters circumglobally. Mako sharks are valued catches in both commercial and recreational fisheries (Campana et al., 2005), and while some directed fisheries exist, mako sharks are often caught as bycatch in commercially important fisheries due to their overlapping habitat with these species (e.g., billfish, tuna; Queiroz et al., 2016). Although 60–80% of longline-hooked mako sharks are alive at haul back (Campana, 2016; Campana et al., 2016; Queiroz et al., 2016), they are typically harvested because of their high-quality meat and valuable fins (Clarke et al., 2006; International Commission for the Conservation of Atlantic Tunas [ICCAT], 2013). In the Atlantic Ocean, Byrne et al. (2017) reported that 30% of their tagged juvenile mako sharks were captured in fisheries suggesting that mako sharks were likely being overexploited, and in 2017, the International Commission for the Conservation of Atlantic Tunas (ICCAT) confirmed that the North Atlantic stock was overfished and undergoing overfishing (International Commission for the Conservation of Atlantic Tunas [ICCAT], 2017, 2019). In 2018, the Shortfin mako was listed as endangered globally on the International Union for Conservation of Nature (IUCN) Red List due to their declining populations (Rigby et al., 2018).

Management of mako sharks is hindered by sparse biological information, including data on movements and habitat ecology (Sippel et al., 2015; Braccini et al., 2016). Until recently, such data for the western North Atlantic (WNA) had been primarily informed by fisheries landings and conventional tag-recapture studies (Casey and Kohler, 1992; Kohler et al., 2002; International Commission for the Conservation of Atlantic Tunas [ICCAT], 2017). While providing valuable information, these fisheries-dependent studies have limitations including low recovery rates, sampling efforts biased by the spatiotemporal distribution of fishing effort, and lack of movement information between capture and recapture events (Vaudo et al., 2017). Casey and Kohler (1992) hypothesized that mako shark movements were largely influenced by sea surface temperature which explained why they moved upward along the northeast coast of the United States and Canadian Grand Banks in the summer and early fall months before moving to the Sargasso Sea for the winter where more favorable thermal conditions were present. Vaudo et al. (2017) found that while mako sharks traveled through the Sargasso Sea, they did not reside there for any length of time. Additionally, their thermal range has been reported to vary more widely than previously thought with individuals inhabiting temperatures ranging from 5.2 to 31.7°C, but mainly frequenting temperatures between 22 and 27°C (Vaudo et al., 2016).

More recently, satellite tracking of mako sharks in the WNA has begun to provide fisheries-independent observations, but these studies have been limited to short tracking periods or smaller size classes (Vaudo et al., 2017; Santos et al., 2018). Additionally, these studies have not included mako sharks that frequent the United States Gulf of Mexico (GOM), yet they do occur in the region (Baughman and Springer, 1950; Ajemian et al., 2016). Stock structure is largely unknown in the GOM and the lack of locations detected in this region in previous studies suggest possible metapopulation structure. Thus, the goal of this study was to provide new information on the movement ecology of shortfin mako sharks in the northwest Atlantic Ocean from animals tagged in the Gulf of Mexico. The specific objectives were to (1) identify mako shark seasonal movement and habitat use patterns and (2) estimate residency in the GOM.

MATERIALS AND METHODS

Study Site and Tagging Procedure

Shark handling and tagging was conducted in accordance with approved guidelines of Texas A&M University-Corpus Christi (Institutional Animal Care and Use Committee-Animal Use Protocol #08-18). Mako sharks were captured via hook and line $\geq$40 nautical miles out of Port Aransas, Texas, or from shore along the Padre Island National Seashore. In these rare events, sharks were landed in the surf with their gills remaining submerged in water. Sharks captured offshore were either secured alongside the vessel or brought onboard via a cradle with a saltwater hose placed in the mouth to irrigate the gills. All sharks were tagged at their capture location. During the tagging procedure, individuals were sexed, measured [fork length (FL); cm], and externally tagged. Each individual was tagged with a smart position or temperature tag (SPOT5 or SPOT6; Wildlife Computers, Redmond, WA, United States) for satellite tracking and a conventional dart tag (Floy©, Seattle, WA, United States), which included a phone number, email address, unique identification number, and "REWARD" for reporting recaptures. For SPOT tag attachment, four small holes were drilled into the distal portion of the leading edge of the dorsal fin, and stainless-steel hardware was used to secure the tag. Prior to deployment, SPOT tags were coated in anti-fouling paint to prevent excessive biofouling that can inhibit communication with satellites. SPOT tags were programmed with a maximum of 70 transmissions per day and had an estimated battery life of 2 + years. The Argos system assigned locations to one of seven accuracy classes, each with an associated error estimate. In decreasing order, the accuracy location classes (with estimated error) were: 3 (<250 m), 2 (250–500 m), 1 (500–1500 m), 0 (>1500 m), with unbounded accuracy for location classes A, and B. Class Z locations were considered poor location estimates (ARGOS, 2016) and, therefore, were omitted from further analyses. All other location classes were included in analyses.

Data Analysis

To provide new information on the seasonal movement ecology of mako sharks, statistical analyses were completed in *R* version 3.5.2 (R Core Team, 2014). Mako shark tracks derived from tag location estimates were first filtered using a speed filter to remove travel speeds >4.5 m/s (Vaudo et al., 2017). Additionally, the first 11-days of the tracks were omitted to allow for dispersal from the tagging location and potential delayed mortality (Vaudo et al., 2017). Seasons were defined as follows: winter: December–February, spring: March–May, summer: June–August, and fall: September–November.

A first-difference correlated random walk switching (DCRWS) model from the *bsam* package was used to characterize movement behaviors of individual sharks with at least 50 location estimates. This model allows for estimation of discrete behavioral modes at regular intervals during irregular time-series data, like satellite telemetry data (Jonsen et al., 2007). The resulting continuous random walk index estimates, which ranged from 1 (transiting behavior) to 2 (area-restricted behavior), were used to classify discrete behavioral modes with values >1.75 classified as area-restricted behavior and values <1.25 classified as transiting behavior (Jonsen et al., 2007). Values between 1.25 and 1.75 were considered unclassified behavior. Duration of transiting behavior was then calculated, and the start and end dates for each excursion were estimated.

To account for autocorrelation and irregularity of positions from SPOT-derived data, the estimated positions from the DCRWS (Jonsen et al., 2005) were used in further analyses. Seasonal kernel utilization distributions (KUD) were calculated using the *adehabitatHR* package with "href" as the smoothing parameter (h) (Calenge, 2015). Home range was calculated at 95% KUD and core area was calculated at 50% KUD (Simpfendorfer et al., 2012). Distance from each estimated position from the tagging location was calculated for each shark, and subsequently, plotted against days at liberty to visualize any patterns by size or sex (Lea et al., 2015).

Ambient depth, or the depth of ocean floor over which the shark was positioned, was extracted for analysis using the *marmap* package (Pante and Simon-Bouhet, 2013) because tags were not equipped with depth sensors. Sea surface temperatures were obtained from the JPL OurOcean Project (2010) using the Marine Geospatial Ecology Toolbox in ArcMap (version 10.6, ESRI, Redlands, CA, United States). Differences in seasonal ambient depth, distance from tagging location, and sea surface temperature were evaluated using a 2-way analysis of variance (ANOVA) with season as a fixed factor and individual as the random factor. If differences were detected, then Welch's *t*-test was used to parse out those differences. All tests were assumed significant at an α = 0.05 significance level.

RESULTS

From 2016 to 2020, nine shortfin mako sharks were tagged with SPOT tags off the coast of Texas (5 M, 4 F; **Table 1**). Eight of the mako sharks were tagged >40 nautical miles offshore from Port Aransas, and one was tagged from shore along the Padre Island National Seashore, Texas. The five males (167–218 cm FL) were mature or nearing maturity, and all four females (282–361 cm FL) were classified as mature based on published 50% size-at-maturity data (males: 182 cm, females: 280 cm; Natanson et al., 2020). Two females had recent (i.e., fresh with no healing or scarring) bite marks anterior to the dorsal fin at capture which could suggest mating or fighting behaviors were occurring (**Figure 1**). One female was recaptured 3 h after being released post-tagging in the same location; this individual was subsequently re-released. Tracking duration varied widely from 10 to 887 days (mean = 359 days; median = 239 days), with four mako sharks tracked for >100 days. At the conclusion of this study (April 2020), one male mako shark (Shark 5) was reporting.

To allow for dispersion from the tagging site, the first 11-days of the tracks were omitted from movement analyses (Vaudo et al., 2017), which excluded the only female tagged from shore (Shark 2). Seasonal population level KUD analysis demonstrated year-round space use in the GOM, but a second area of use

TABLE 1 | Tagging information for shortfin makos tagged in the northwestern Gulf of Mexico, including size at tagging, tracking duration, days with usable detections, and status of SPOT tag at the conclusion of the study.

Shark	Sex	Fork Length (cm)	Deployment Date	Days at Liberty	Days with Usable Positions	Still Reporting
1	M	168	25-February-2016	62	45	No
2*	F	290	26-March-2016	10	10	No
3	M	210	8-April-2016	707	409	No
4	F	353	21-March-2017	887	482	No
5	M	196	13-March-2018	697	536	Yes
6	M	218	18-March-2018	70	60	No
7	F	361	19-March-2018	25	24	No
8	F	282	19-March-2018	16	11	No
9	M	167	28-February-2019	408	235	No

**denotes the female that was recaptured, but due to a short track duration was excluded from further analysis.*

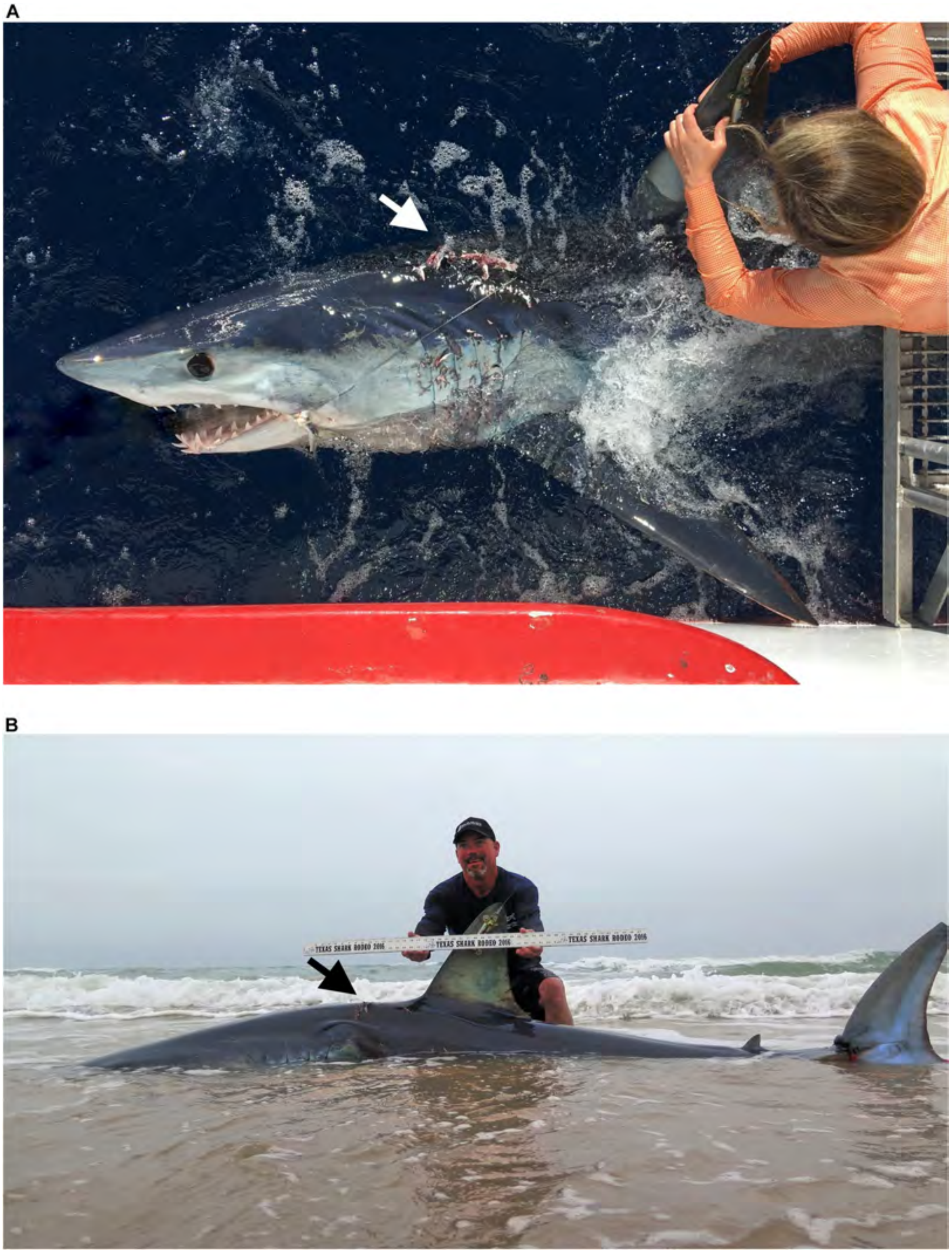

FIGURE 1 | Bite marks (arrows) observed on female shortfin makos, suggesting potential mating or fighting behaviors in the Gulf of Mexico. **(A)** Shark 6 was tagged offshore in 2017. **(B)** Shark 1 was tagged in 2016 from Padre Island National Seashore and was recaptured and released 3 h later in the same location.

appeared in the summer and fall months in the WNA (**Figure 2**). Two mature males that were tracked for multiple years exited the GOM during the summer months and returned to the northwestern GOM in the winter months (**Figure 3**). Shark 3 traveled to the Caribbean Sea in two consecutive summers and returned to the Texas coast in late fall each year. Shark 5 traveled through the Straits of Florida and up the Atlantic coast to the northeast United States in two consecutive summers, returning the first year during winter. As of the conclusion of data collection for this study (April 2020), Shark 5 was still reporting off the Texas coast in the GOM, consistent with the previous year's movement patterns.

For both of these male sharks (Sharks 3 and 5), these long excursions were characterized by directionally persistent

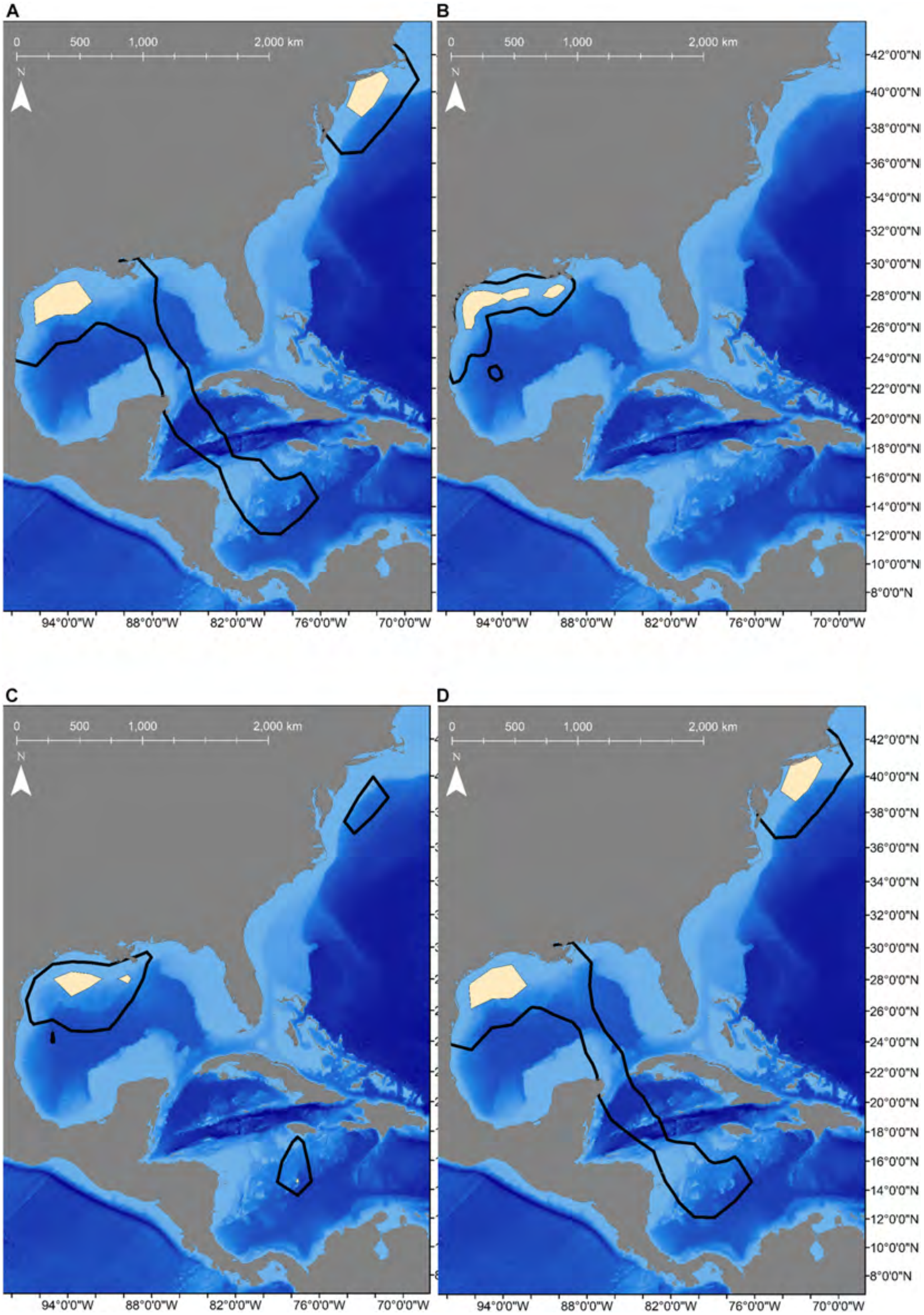

FIGURE 2 | Seasonal population-level Kernel Utilization Distributions (KUD) calculated from satellite-tracked shortfin makos tagged off the Texas coast showing space use changed with the seasons. Black lines represent home range (95% KUD) and tan shaded areas are core area (50% KUD). **(A)** KUDs calculated for winter (*n* = 5 sharks) shows core areas in the northwestern Gulf of Mexico (GOM), but areas off the eastern United States coast was used as well. **(B)** KUDs for spring (*n* = 9 sharks) shows that makos remained in the GOM extensively along the continental shelf and slope. **(C)** KUDs calculated for summer (*n* = 5 sharks) showed more area off the shelf was used in the GOM as well as in the Caribbean Sea and off the northeast coast of the United States. **(D)** KUDs for fall (*n* = 4 sharks) showed two core areas were used in the North Atlantic, including in the northwestern GOM and off the northeastern United States coast.

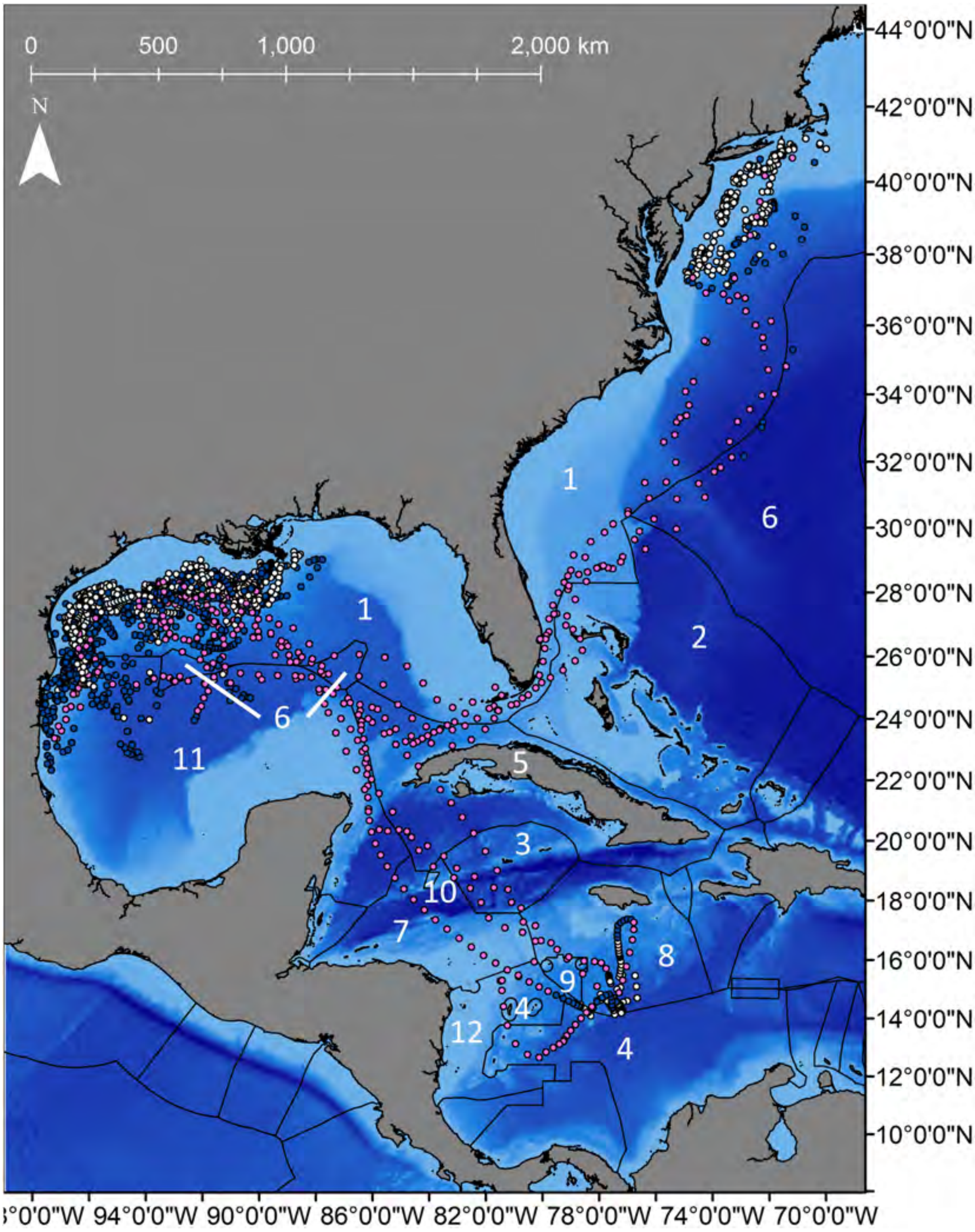

FIGURE 3 | Daily locations for 8 shortfin makos tagged in the northwestern Gulf of Mexico with Exclusive Economic Zones (EEZ) for each country. Navy dots represent resident behavior based on the first-difference correlated random walk switching model, while pink dots represent transiting behavior. Gray dots represent unclassified behavior. EEZs that sharks transited through are represented by numbers that correspond countries listed in **Table 2**.

migration followed by a long seasonal residency period before returning to the GOM. Based on the DCWRS model behavioral mode classifications, excursion durations varied with Shark 3 (227 days) spending more time in the western GOM than Shark 5 (100 days), which returned to the northwestern GOM about 3 months after Shark 3; however, transit time to (Shark 3: 32–40 days; Shark 5: 34–44 days) and from (Shark 3: 40–58 days; Shark 5: 60–70 days) their respective destinations was comparable (**Figures 4**, **5**). Both Shark 3 and Shark 5 each traveled about 2500 km to their respective destinations (**Figure 6**). Conversely, Shark 9, an immature male, did not exit the western GOM, but rather moved into the southwestern GOM near the Mexican shoreline before moving into deeper water and returning northward toward the continental shelf off the Texas

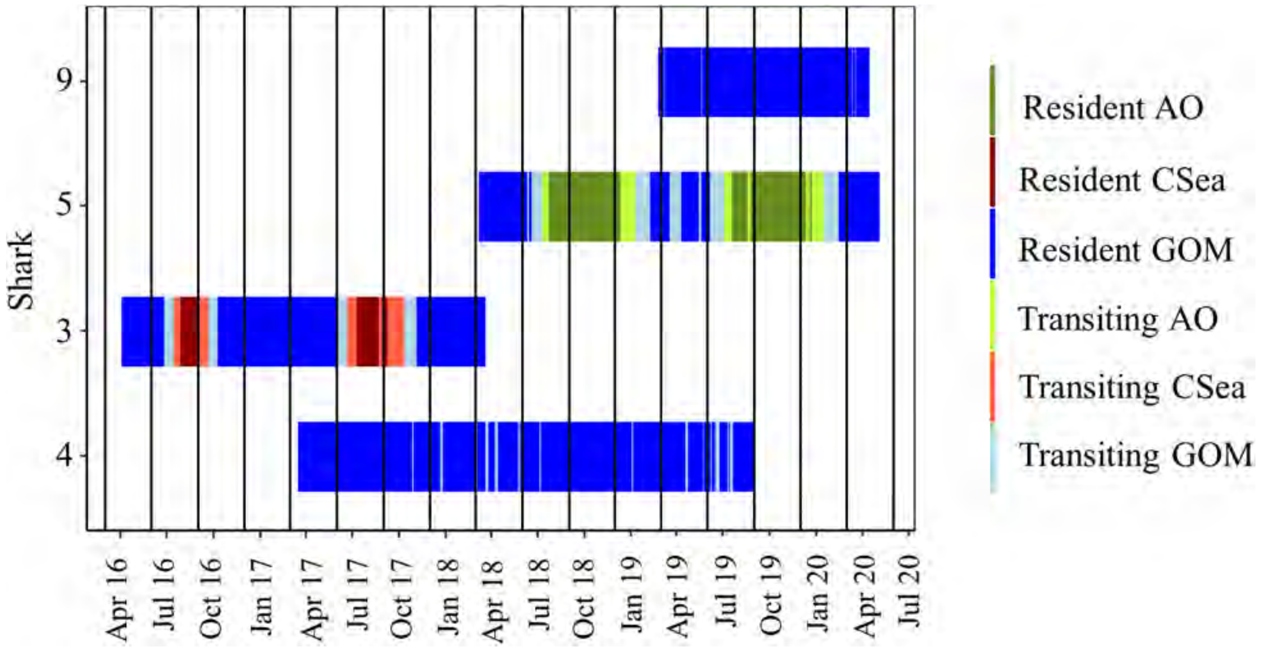

FIGURE 4 | Movement behavior of shortfin makos tracked >100 days over the study period. Sharks demonstrated transiting behavior (light colors) and resident behavior (dark colors) based on the first-difference correlated random walk switching model. Shades of blue represents periods within the Gulf of Mexico (GOM), green represents periods within the Atlantic Ocean (AO), and red represents periods within the Caribbean Sea (CSea). Sharks 5 and 3 were mature males tracked through multiple migrations. Shark 4 was the only female tracked >100 days. Shark 9 was the only immature male tracked >100 days.

coast. However, these movements were classified as unknown behavioral modes by the DCWRS model. Shark 4, a female, similarly remained in the GOM, but after 827 days of transiting between the Flower Garden Banks National Marine Sanctuary (FGBNMS) and north central GOM near the Mississippi River Delta, she moved off the continental shelf into deeper water for the first-time (early summer) where she remained for 30 days before returning to the continental shelf near the FGBNMS. These movements were classified as both transiting and resident behavioral modes by the model (**Figure 5**).

Mako sharks traversed a geographical area of 12.8°–41.2° N latitude and 69.8°–97.7° W longitude, which included the Atlantic Ocean, GOM, Caribbean Sea, and the management jurisdictions for at least 12 nations and international waters (**Table 2**). Tagged mako sharks frequented a wide range of sea surface temperatures ranging from 10.0°–31.0°C (**Figure 7**), although no significant differences were detected among seasons ($F_{1,2969} = 0.65$, $p = 0.58$; **Table 3**). Despite the long-distance excursions by two males, mean monthly distance traveled was not significantly different by sex [$F_{1,3} = 0.89$, $p = 0.99$; mean ± standard deviation (SD): male: 1,958 ± 1,035 km/month, females: 1,836 ± 875 km/month]. For ambient depth, there were no significant differences among seasons ($F_{3,2969} = 0.23$, $p = 0.87$), although males were tracked over deeper depths than females in all seasons except spring (**Table 3** and **Figure 8**). These tracks over deeper ambient depths aligned with observed transiting behaviors (**Figure 5**).

DISCUSSION

During the study period, mako sharks demonstrated varied movement patterns which included both coastal and oceanic habitats. Most mako sharks tagged in this study were mature based on size-at-age information with females in this study representing some of the largest females reported in satellite telemetry studies to date (e.g., Loefer et al., 2005; Abascal et al., 2011; Musyl et al., 2011; Rogers et al., 2015; Campana et al., 2016; Byrne et al., 2017; Vaudo et al., 2017; Francis et al., 2019; Nasby-Lucas et al., 2019). Although sample size was limited, the multi-year movement patterns observed for males differed from the lone female tracked multiple years. The female demonstrated high fidelity to the GOM along the continental shelf for most of the year, while mature males made extensive large-scale migrations that crossed multiple management jurisdictions, demonstrating the need for cooperative international management to conserve and rebuild the declining WNA stock.

Multi-year tracks from the three mature individuals showed fidelity to the GOM varying by season and sex. While the mature female remained in the northwestern GOM year-round, the mature males demonstrated seasonal excursions with individuals exiting the GOM beginning in the late summer-early fall and returning in late fall-early winter each year. While the timing of these directed migrations showed a pattern, the destination of these excursions and residency time at each destination varied individually. For all mako sharks tracked during the study, home

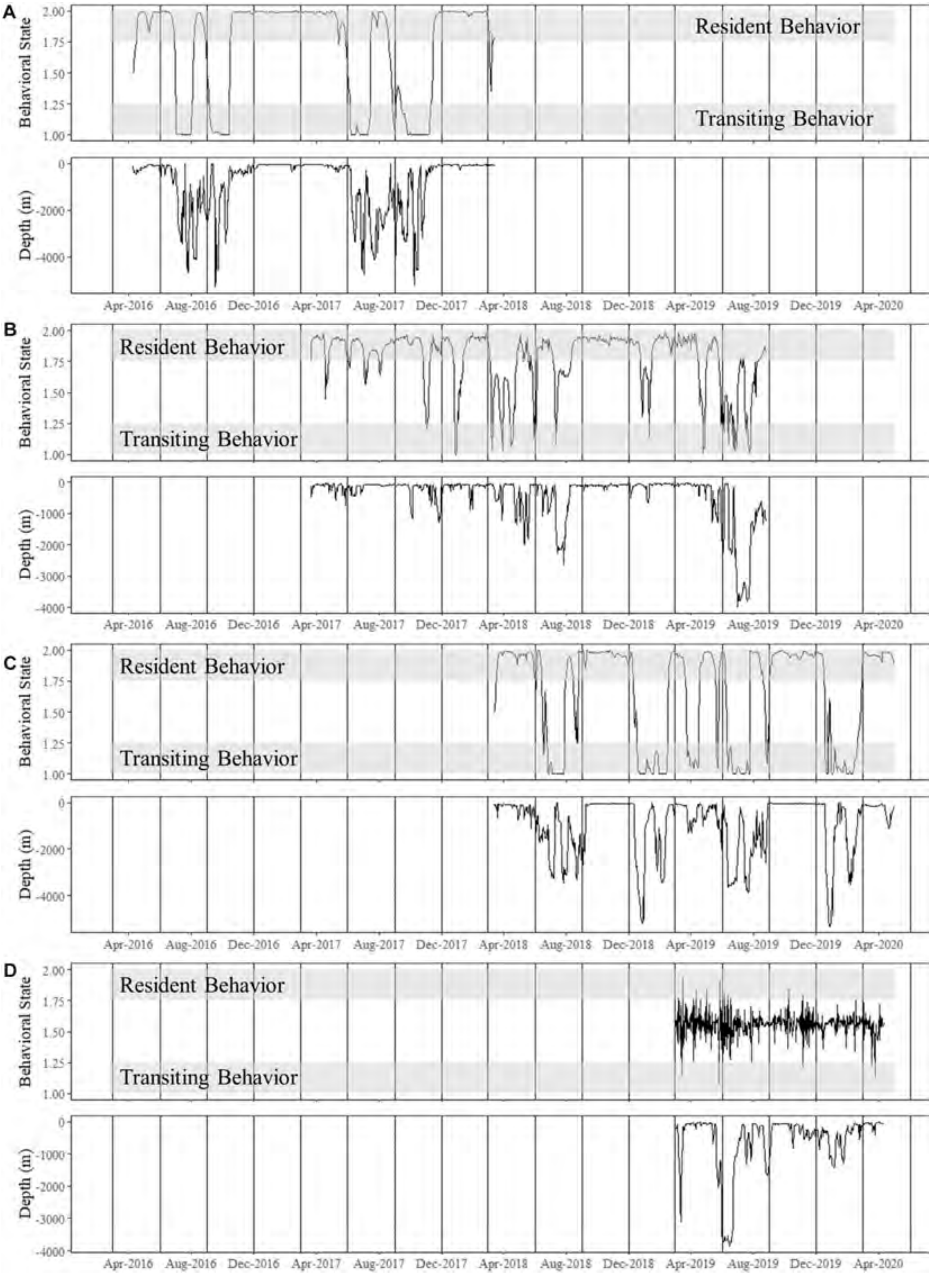

FIGURE 5 | Time series of estimated behavioral state for shortfin makos tracked for multiple years compared to ambient depth use (m), or depth of ocean floor over which the shark was positioned. Note that deeper ambient depths were observed when sharks were transiting. Vertical lines represent the start of each season: summer (June–August), fall (September–November), winter (December–February), and spring (March–May). **(A)** Shark 4, a mature female, spent all her time in the Gulf of Mexico with transiting behavior matching movements to and from the Mississippi River Delta and the Flower Gardens National Marine Sanctuary. Until June–July 2019, Shark 4 remained predominantly on the continental shelf or slope. **(B)** Shark 3, a mature male, made two consecutive excursions to the Caribbean Sea over largely open ocean and deeper water. **(C)** Shark 5, a mature male, made an excursion to the northeast United States during the first year of tracking and was on his second excursion at the conclusion of this study. This male traveled over deeper water exiting the Gulf of Mexico before predominately following the continental shelf up the eastern coast. **(D)** Shark 9 was an immature male that was only tracked within the western Gulf of Mexico.

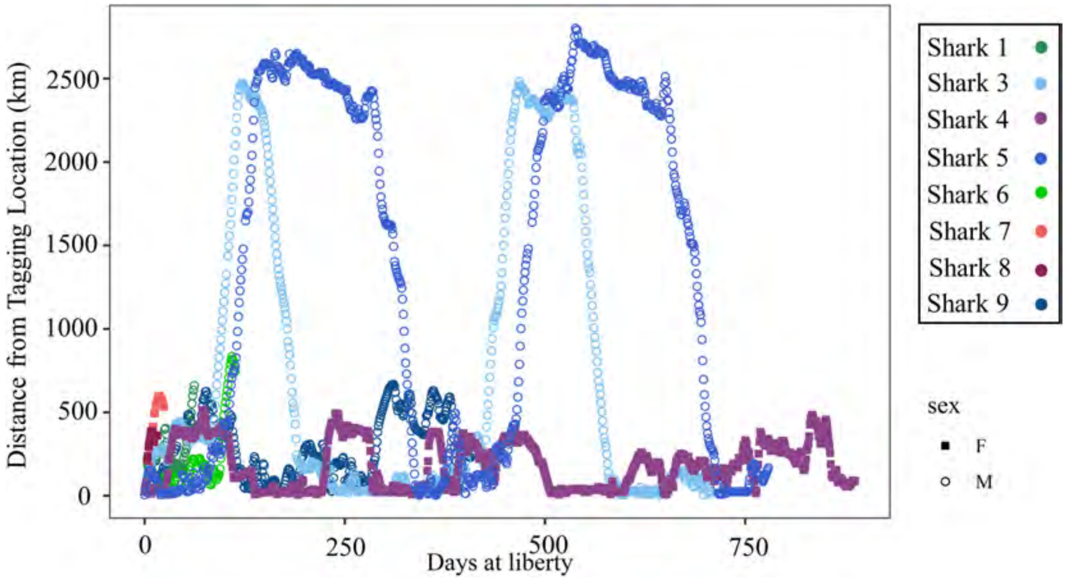

FIGURE 6 | Distance (km) of daily locations from the tagging location plotted by days at liberty since the tagging date for 8 shortfin makos tagged in the northwestern Gulf of Mexico. Females are represented by closed squares and males by open circles. Individual sharks are represented by unique colors.

range during the spring was limited to the GOM when both sexes were present in the northwestern GOM. During the other seasons, home range included additional areas outside the GOM. Home range calculated for mature mako sharks overlapped with the home range reported for juvenile mako sharks for both the GOM and WNA in each season, except for spring, when home range overlapped only in the GOM. This overlap in home range predominately occurred during transiting behavior by mature individuals in this study. Core areas (e.g., more resident behavior) of individuals in this study overlapped previously reported core areas of juveniles only during summer and fall months in the WNA but never in the GOM (see Vaudo et al., 2017 for comparison).

Temperature has been suggested to be a physiological constraint on movements of juvenile mako sharks within the GOM (Vaudo et al., 2016, 2017). However, no differences in sea surface temperatures were detected in this study, despite movements to more southern and northern areas. This finding may be related to the size of mako sharks tagged in this study (mostly mature individuals) versus previous studies that have tagged mostly juveniles. Vaudo et al. (2016) reported that their juvenile mako sharks tagged off the WNA showed southerly directional movements in November and December as sea surface temperatures dropped. These directional movements have also been reported in other studies in the Pacific Ocean (Abascal et al., 2011; Block et al., 2011). Juveniles tagged off the Yucatan Peninsula showed no clear directional patterns (Vaudo et al., 2016). This lack of pattern was attributed to the steady sea surface temperatures reported for this area and the GOM (Longhurst, 2007). Thus, while sharks may be selectively remaining within a preferred temperature, the lack of difference in frequented sea surface temperatures and the directional movements by mature males in this study suggest the minimal overlap in home range may be influenced by other reasons, such as size segregation (Sippel et al., 2015; Nasby-Lucas et al., 2019).

Mako sharks have been shown to use a variety of habitats during their long-distance excursions, including open-ocean and more shallow waters along the continental shelf. This pattern was demonstrated in the current study with individuals occurring over deeper depths (i.e., open ocean) during transiting periods and in shallower ambient depths (i.e., continental shelf) during periods of residency, a phenomenon observed for many marine megafauna (Sequeira et al., 2018). Although rare, recreational anglers have reported catching large, mature mako sharks from shore (Gibson et al., 2019, Stunz *unpublished data*). This coastal, nearshore habitat use, which has also been reported in previous studies (Francis et al., 2019), exposes this generally pelagic species to shore-based fisheries. While most individuals in this study were mature, previous studies on juveniles have also reported similar habitat use patterns between open-ocean and continental shelf use (Rogers et al., 2015; Vaudo et al., 2017; Byrne et al., 2019). Juveniles tagged off the Yucatan Peninsula demonstrated high residency to the eastern edge of the Campeche Bank (Vaudo et al., 2017; Byrne et al., 2019), and juveniles tagged off the coast of Australia exhibited high site fidelity to the mid-outer continental shelf near the Great Australian Bight (Rogers et al., 2015). This shallower, continental shelf habitat is likely attractive due to the abundance and variety of prey available compared to open-ocean habitats (Byrne et al., 2019). Nevertheless, mako sharks often occur as bycatch in pelagic longline fisheries in open-ocean waters (Campana et al., 2005). Extensive seasonal offshore movements and pelagic bycatch occurrences suggests that mako movements may be linked to foraging behavior following a selected food source (Nasby-Lucas et al., 2019). Diet

TABLE 2 | Regulations for each of the management jurisdictions that tagged mako sharks passed through during their excursions from the tagging region in the northwestern GOM.

EEZ	Regulations	References
United States (1)	Amendment 11: Minimum size: 71 in FL for males; 83 in FL for females Non-off, corrodible circle hooks must be used when targeting sharks in the recreational fishery, except when using artificial lures or flies. (1) For all commercial vessels: (a) Mako sharks may be retained if reporting requirements (e.g., observer or electronic monitoring system which can identify if the shark is alive or not) are met. (b) Mako shark is dead at haul back (c) Data on the number of individuals hooked, body length, sex, condition, maturity (whether the individual is pregnant and its litter size) and weight of products for each shortfin mako caught as well as fishing effort (d) When mako sharks are not retained, the number of dead discards and live releases shall be recorded by the observer or estimated from the records of the electronic monitoring system	International Commission for the Conservation of Atlantic Tunas [ICCAT], 2020
Bahamas (2)	Shark sanctuary	https://www.dcnanature.org/wp-content/uploads/2015/06/Pew-Protecting-Sharks-Caribbean-FactSheet.pdf
Cayman Islands (3)	National Conservation Law (2013): No take	http://doe.ky/marine/sharks/
Colombia (4)	Sharks must be landed with fins naturally attached to their bodies	https://awionline.org/content/international-shark-finning-bans-and-policies
Cuba (5)	All sharks caught be landed whole with fins attached	http://blogs.edf.org/edfish/2015/07/02/cubas-plan-for-shark-conservation/
High Seas (6)		
Honduras (7)	No take	https://www.dcnanature.org/wp-content/uploads/2015/06/Pew-Protecting-Sharks-Caribbean-FactSheet.pdf
Jamaica (8)		
Joint: Colombia/Jamaica (9)		
Joint: Honduras/Cayman Islands (10)	No take	http://doe.ky/marine/sharks/ https://www.dcnanature.org/wp-content/uploads/2015/06/Pew-Protecting-Sharks-Caribbean-FactSheet.pdf
Mexico (11)	NORMA Oficial Mexicana NOM-029-PESC-2006 and NORMA Oficial Mexicana NOM-023-SAG/PESC-2014: Minimum size: 71 in FL for males; 83 in FL for females (1) For commercial vessels whose length is greater than 12 m: (a) Mako sharks may be retained if reporting requirements (e.g., observer or electronic monitoring system which can identify if the shark is alive or not) are met. (b) Mako shark is dead at haul back (c) Data on the number of individuals hooked, body length, sex, condition, maturity (whether the individual is pregnant and its litter size) and weight of products for each shortfin mako caught as well as fishing effort (d) When mako sharks are not retained, the number of dead discards and live releases shall be recorded by the observer or estimated from the records of the electronic monitoring system (2) For vessels whose length is equal or smaller than 12 m: (a) Mako sharks may be retained if dead when brought along side for taking on board the vessel	International Commission for the Conservation of Atlantic Tunas [ICCAT], 2020
Nicaragua (12)	No fin exports without proof that the meat was sold	https://awionline.org/content/international-shark-finning-bans-and-policies

*For Exclusive Economic Zones (EEZ) where regulations are known, the listed law or regulation number is listed for reference. For EEZs where regulations could not be found, it is assumed no regulations exists for mako sharks and the regulations were left blank. Numbers in parentheses represent EEZs in **Figure 3**.*

and stable isotope studies suggested that mako sharks prey on a variety of nearshore and offshore fish species like bluefish (*Pomatomus saltatrix*), tuna (*Thunnus* spp.), and swordfish, as well as cephalopods and other sharks (e.g., blue shark, *Prionace glauca*; Stillwell and Kohler, 1982; Compagno, 2001; Estrada et al., 2003; Campana et al., 2005; Wood et al., 2009). While exact drivers for long-distance movements are still unclear, similar offshore patterns for other apex species, like white

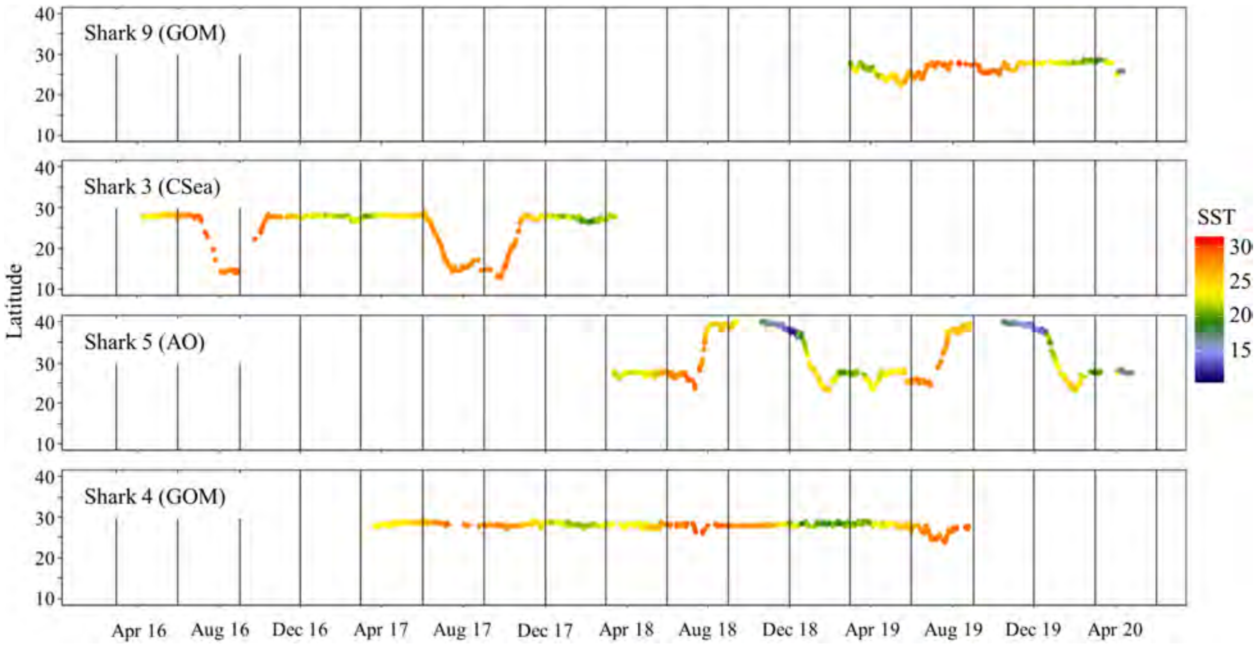

FIGURE 7 | Daily latitude estimates and associated sea surface temperature (from satellite remote-sensing data; °C) for four shortfin makos tracked for >1 year in the western North Atlantic Ocean. Sharks 4 and 9 remained in the Gulf of Mexico while sharks 3 and 5 migrated out of the Gulf of Mexico. Destinations (GOM, Gulf of Mexico; AO, Atlantic Ocean; and CSea, Caribbean Sea) of mako sharks after migration are in parentheses. Vertical lines represent the start of each season: summer (June–August), fall (September–November), winter (December–February), and spring (March–May).

TABLE 3 | Mean sea surface temperature (°C) and ambient depth (m) with standard deviations for mako sharks tracked in this study.

	SST		Depth	
Season	**Male**	**Female**	**Male**	**Female**
Winter (*n* = 5)	21.2 ± 3.1 (19, 24)	20.9 ± 1.4 (10, 26)	−668 ± 1241 (−5336, −5)	−103 ± 149 (−1009, −22)
Spring (*n* = 9)	23.4 ± 2.1 (20, 29)	23.8 ± 1.9 (20, 29)	−405 ± 448 (−3819, −14)	−450 ± 1000 (−3442, −12)
Summer (*n* = 5)	28.0 ± 1.4 (25, 31)	29.0 ± 1 (25, 31)	−1827 ± 1232 (−4682, −31)	−1026 ± 1118 (−3788, −57)
Fall (*n* = 4)	21.4 ± 5.5 (12, 31)	27.6 ± 1.9 (23, 30)	−307 ± 1084 (−4579, −1)	−181 ± 252 (−1552, −65)

Minimum and maximum sea surface temperatures and ambient depths are represented in parenthesis below the means. Sample size of sharks tracked in each season is in parentheses below the season. Males traversed over waters with deeper depths during the winter, summer, and fall seasons.

sharks (*Carcharodon carcharias*), blue sharks, and salmon sharks (*Lamna ditropis*; Holts et al., 1998) have been reported, as well as for their prey items (Block et al., 2005; Hoolihan et al., 2014; Rooker et al., 2019). However, that does not explain the sex-specific differences in movement patterns for mature sharks tagged in this study. Although inferences are limited based on the low sample size in this study, we hypothesize that these differences may be driven by reproduction.

The locations of mating grounds are not yet known for mako sharks; however, two of the four females in this study had fresh bite marks present at time of tagging (late March), while mature males were also present in the tagging region at this time with no bite marks observed. Although these bites could be the result of fighting behavior, the bites may also be the result of mating behaviors, suggesting the GOM may serve as a mating ground. Mating is generally thought to occur during late fall/winter in both hemispheres (Mollet et al., 2000). Male mako sharks in this study were transiting during summer (leaving the GOM) and early winter (returning to the GOM) months, suggesting that mako sharks in the GOM might be mating slightly later in the year than in other regions or that some males may leave the GOM to reproduce elsewhere. This supports the possibility of multiple reproductive stocks as suggested by Schrey and Heist (2003) who proposed that seasonality of mating may be shifted by male sharks to accommodate the availability of fertile females. Sex-biased dispersal has been previously reported in mako sharks in the Pacific Ocean (Mucientes et al., 2009) and Indian Ocean

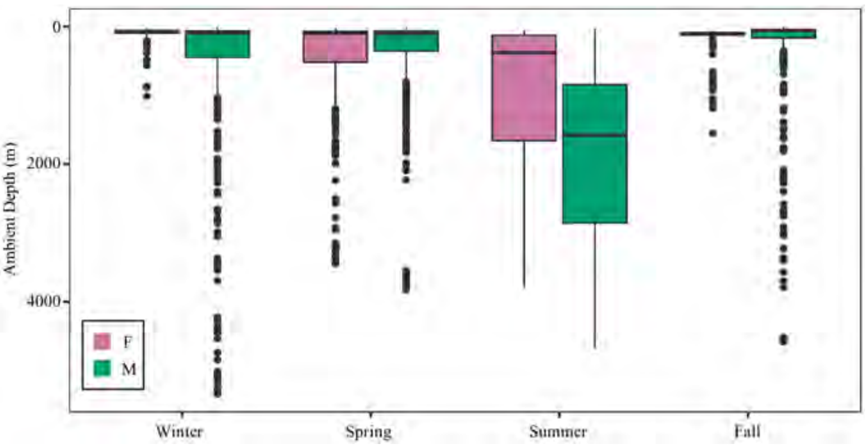

FIGURE 8 | Seasonal ambient water depth (m) by sex. Males frequented a wider range of ambient depths except during the spring, which was the only season when both sexes were located in the Gulf of Mexico during the entire season.

(Corrigan et al., 2018), with males making large movements while females were philopatric (Mollet et al., 2000; Schrey and Heist, 2003). Differences in movement patterns may be a result of sexual segregation (Mucientes et al., 2009). Females may also be avoiding highly aggressive mating behaviors which often result in serious bite wounds that could result in decreased fitness of females (Stevens, 1974; Magurran and Seghers, 1994). Sexual segregation has been reported in the White Shark, a species also in the family Lamnidae, that has seasonal site fidelity to potential breeding and pupping grounds (Bonfil et al., 2005; Jorgensen et al., 2010; Anderson et al., 2011; Domeier and Nasby-Lucas, 2013).

Although little is known about exact pupping grounds, Casey and Kohler (1992) observed young-of-the-year offshore in the Gulf of Mexico and hypothesized that mako sharks in the WNA are born far offshore, likely to protect the pups from predation. One female mature mako in this study was tracked >2.5 years during which time she remained on the continental shelf and slope for >2 years until early summer when she moved further offshore for 30 days before returning to the continental shelf. Although pregnancy cannot be confirmed, this change in behavior is consistent with the hypothesis put forth by Casey and Kohler (1992). Additional tagging should bolster sample size and aid in the identification of any differences in habitat utilization while both sexes are present in the GOM.

Tagging studies including ours and others (e.g., Vaudo et al., 2017) suggest spatial substructure within the North Atlantic stock and warrant possible consideration of more regional management strategies as the failure to accurately identify and manage sub-stocks could result in overfishing and depletion of less productive sub-stocks (Ricker, 1981; Smith et al., 1991). While genetic analyses do not support the presence of genetically distinct stocks for mako sharks in the WNA, they do suggest multiple reproductive stocks may exist with considerable male-mediated gene flow (Heist et al., 1996; Schrey and Heist, 2003). These genetic analyses should be interpreted with caution when proposing a single stock management approach, as a large number of migrants per-generation are required to replenish overfished stocks and can be difficult to demonstrate using genetic studies alone (Waples, 1998; Schrey and Heist, 2003). The movements we observed for mature mako sharks in this study generally support the possibility of distinct reproductive stocks proposed by Schrey and Heist (2003); however, the number of mako sharks tracked for more than one season was limited in this study, so there is a need for additional tagging studies of mature mako sharks to validate current knowledge of movement ecology and test the hypothesis of multiple reproductive stocks.

Management of highly migratory shark species, such as mako sharks, is complicated because they cross multiple management jurisdictions and long-term movement data remains limited. Mako sharks in this study passed through at least 12 management jurisdictions subjecting them to varying levels of fishing pressure and regulations (**Table 2**). This means that they may be protected or managed in some jurisdictions and not in others, highlighting the need for coordinated management. For example, Byrne et al. (2017) reported that 12 of 40 (30%) satellite-tagged juvenile mako sharks tracked in the WNA were harvested by vessels from five countries, including the United States, Canada, Mexico, Spain, and Cuba. Just within the GOM, mako sharks were subject to regulations enforced by the United States and Mexico or lack thereof in Cuba and the High Seas. While the United States and Mexico are members of ICCAT, Cuba ceased participation in 1991 (Kraus et al., 2011). Further complicating management, even members of ICCAT do not agree on steps needed to protect the WNA mako shark population and provide spatial refuge from fishing effort, which is currently lacking even in the High Seas (Sims et al., 2018; Queiroz et al., 2019). Cooperative international management, though complicated and complex, is needed to reduce fishing mortality and rebuild the declining North Atlantic stock. Results from this study demonstrate that mako sharks in the GOM can undertake large-scale movements and may exhibit sex-specific movement patterns. The mature female tracked over multiple years showed high fidelity to the GOM, which may serve as potential mating and parturition grounds. Females in this study were some of the largest reported in satellite telemetry studies, providing data on a size class and breeding stock that has largely been unavailable until now. If mature female mako sharks show philopatry to relatively small areas within national EEZs that adopt and enforce current management recommendations, these regions may have a disproportionate impact on rebuilding and emphasize the need for national management. Correspondingly, large-scale movements across multiple jurisdictional boundaries observed for mature males in this study emphasize the need for international cooperative management to conserve this species. Recent tagging studies like ours and others suggest migratory variations and potential sex- and size-based segregation within the North Atlantic stock that may warrant consideration in future management strategies. Thus, while our study provides new information on the movement ecology for mako sharks in the WNA, especially for mature individuals that have been underrepresented in previous scientific efforts, additional tagging efforts focused on mature individuals are needed to identify mating and parturition grounds and better assess the patterns observed here. These studies will allow a robust evaluation of the possibility of multiple reproductive stocks, leading to more management confidence and aid rebuilding efforts.

DATA AVAILABILITY STATEMENT

The datasets presented in this study can be found in online repositories. The names of the repository/repositories and accession number(s) can be found below: Integrated Ocean Observing System: Animal Telemetry Network (https://portal.atn.ioos.us/?ls=948413b4-471b-b5e6-6f19-c4b6d6fdfb06#metadata/e3849570-c263-4e3b-8a51-31ff672a90b4/project).

ETHICS STATEMENT

Written informed consent was obtained from the individual for the publication of any potentially identifiable images or data included in this article. The animal study was reviewed and approved by the Texas A&M University–Corpus Christi's Institutional Animal Care and Use Committee.

AUTHOR CONTRIBUTIONS

KG conducted the research and wrote the manuscript. MS assisted in data analyses and writing the manuscript. TT conducted the research and assisted in writing the manuscript. GS acquired funding, conducted the research, and assisted in the data analyses and writing the manuscript. All authors gave authorization for submission.

FUNDING

Funding for the field studies and data analysis was provided in part by the Harte Research Institute for Gulf of Mexico Studies, the Texas State Aquarium, the John M. O'Quinn Foundation, and the Coastal Conservation Association – Texas.

ACKNOWLEDGMENTS

We would like to thank the staff and students of the Center for Sportfish Science and Conservation at the Harte Research Institute for Gulf of Mexico Studies for their assistance in the field, and Dr. Brandt Gibson for his help troubleshooting with R code, Eric Ozolins, Dwade Hickey, Ricky Torres, Captain Chad Banks, Captain "Jx" Yeaney, Captain Fred Mallett, and the crew of the Fisherman's Wharf for their help in the field. Considerable logistical support was provided by the Harte Research Institute and Texas A&M University-Corpus Christi. We would also like to thank OCEARCH for their support and display of our tagged sharks on their Global Shark Tracker website.

REFERENCES

Abascal, F. J., Quintans, M., Ramos-Cartelle, A., and Mejuto, J. (2011). Movements and environmental preferences of the shortfin mako, Isurus oxyrinchus, in the southeastern Pacific Ocean. *Mar Biol.* 158, 1175–1184. doi: 10.1007/s00227-011-1639-1

Ajemian, M. J., Jose, P. D., Froeschke, J. T., Wildhaber, M. L., and Stunz, G. W. (2016). Was everything bigger in Texas? Characterization and trends of a land-based recreational shark fishery. *Mar. Coast. Fish.* 8, 553–566. doi: 10.1080/19425120.2016.1227404

Anderson, S. D., Chapple, T. K., Jorgensen, S. J., Klimley, A. P., and Block, B. A. (2011). Long-term individual identification and site fidelity of white sharks, Carcharodon carcharias, of California. *Mar. Biol.* 158, 1233–1237. doi: 10.1007/s00227-011-1643-5

ARGOS (2016). *Argos User's Manual*. Toulouse: CLS/Service Argos.

Baughman, J. L., and Springer, S. (1950). Biological and economic notes on the sharks of the Gulf of Mexico, with especial reference to those of Texas, and with a key for their identification. *Am. Midl. Nat.* 44, 96–152. doi: 10.2307/2421758

Block, B. A., Jonsen, I. D., Jorgensen, S. J., Winship, A. J., Shaffer, S. A., Bograd, S. J., et al. (2011). Tracking apex marine predator movements in a dynamic ocean. *Nature* 475, 86–90. doi: 10.1038/nature10082

Block, B. A., Teo, S. L. H., Walli, A., Boustany, A., Stokesbury, M. J. W., Farwell, C. J., et al. (2005). Electronic tagging and population structure of Atlantic Bluefin Tuna. *Nature* 434, 1121–1127. doi: 10.1038/nature03463

Bonfil, R., Meyer, M., Scholl, M. C., Johnson, R., O'Brien, S., Oosthuizen, H., et al. (2005). Transoceanic migration, spatial dynamics, and population linkages of white sharks. *Science* 310, 100–103. doi: 10.1126/science.1114898

Braccini, M., Aires-da-Silva, A., and Taylor, I. (2016). Incorporating movement in the modelling of shark and ray populations dynamics: approaches and management implications. *Rev. Fish Biol. Fish.* 26, 13–24. doi: 10.1007/s11160-015-9406-x

Byrne, M. E., Cortés, E., Vaudo, J. J., Harvey, G. C. M. C. N., Sampson, M., Wetherbee, B. M., et al. (2017). Satellite telemetry reveals higher fishing mortality rates than previously estimated, suggesting overfishing of an apex marine predator. *Proc. R. Soc. B* 284:20170658. doi: 10.1098/rspb.2017.0658

Byrne, M. E., Vaudo, J. J., Harvey, G. C., Johnston, M. W., Wetherbee, B. M., and Shivji, M. (2019). Behavioral response of a mobile marine predator to environmental variables differs across ecoregions. *Ecography* 42, 1569–1578. doi: 10.1111/ecog.04463

Calenge, C. (2015). *Home Range Estimation in R: The adehabitatHR Package. R Package Version 0.3.23.*

Campana, S. E. (2016). Transboundary movements, unmonitored fishing mortality, and ineffective international fisheries management pose risks for pelagic sharks in the Northwest Atlantic. *Can. J. Aquat. Sci.* 73:1599. doi: 10.1139/cjfas-2015-0502

Campana, S. E., Joyce, W., Fowler, M., and Showell, M. (2016). Discards, hooking, and post-release mortality of the porbeagle (Lamna nasus), shortfin mako (Isurus oxyrinchus), and blue shark (*Prionace glauca*) in the Canadian pelagic longline fishery. *ICES J. Mar. Sci.* 73, 165–181. doi: 10.1093/icesjms/fsv234

Campana, S. E., Marks, L., and Joyce, W. (2005). The biology and fishery of shortfin mako sharks (*Isurus oxyrinchus*) in Atlantic Canadian waters. *Fish. Res.* 73, 341–352. doi: 10.1016/j.fishres.2005.01.009

Casey, J. G., and Kohler, N. E. (1992). Tagging studies on the shortfin mako shark (*Isurus oxyrinchus*) in the western North Atlantic. *Mar. Freshw. Res.* 43, 45–60. doi: 10.1071/mf9920045

Clarke, S. C., McAllister, M. K., Milner-Gulland, E. J., Kirkwood, G. P., Michielsens, C. G. J., Agnew, D. J., et al. (2006). Global estimates of shark catches using trade records from commercial markets. *Ecol. Lett.* 9, 1115–1126. doi: 10.1111/j.1461-0248.2006.00968.x

Compagno, L. J. V. (2001). *Sharks of the World. An Annotated and Illustrated Catalogue of Shark Species Known to Date. Volume 2: Bullhead, Mackerel and Carpet Sharks (Heterodontiformes, Lamniformes and Orectolobiformes). FAO Species Catalogue for Fisheries Purposes No. 1, vol. 2.* Rome: Food and Agriculture Organization of the United Nations.

Corrigan, S., Lowther, A. D., Beheregaray, L. B., and Bruce, B. D. (2018). Population connectivity of the mighly migratory Shortfin Mako (*Isurus oxyrinchus* Rafinesque 1810) and implications for management in the southern hemisphere. *Front. Ecol. Evol.* 6:187. doi: 10.3389/fevo.2018.00187

Cortés, E., Arocha, F., Beerkircher, L., Carvalho, F., Domingo, A., Heupel, M., et al. (2010). Ecological risk assessment of pelagic sharks caught in Atlantic pelagic longline fisheries. *Aquat. Living Resour.* 23, 402–410. doi: 10.1002/mcf2.10029

Domeier, M. L., and Nasby-Lucas, N. (2013). Two-year migration of adult female white sharks (Carcharodon carcharias) reveals widely separated nursery areas and conservation concerns. *Anim. Biotelemetry* 1:2. doi: 10.1186/2050-3385-1-2

Dulvy, N. K., Fowler, S. L., Musick, J. A., Cavanagh, R. D., Kyne, P. M., Harrison, L. R., et al. (2014). Extinction risk and conservation of the world's sharks and rays. *eLife* 3:e00590. doi: 10.7554/eLife.00590

Estes, J. A., Terborg, J., Brashares, J. S., Power, M. E., Berger, J., Bond, W. J., et al. (2011). Trophic downgrading of Plant Earth. *Science* 333, 301–306.

Estrada, J. A., Rice, A. N., Lutcavage, M. E., and Skomal, G. B. (2003). Predicting trophic position in sharks of the north-west Atlantic Ocean using stable isotope analysis. *J. Mar. Biol. Assoc. U.K.* 83, 1947–1350.

Francis, M. P., Shivji, M. S., Duffy, C. A., Rogers, P. J., Byrne, M. E., Wetherbee, B. M., et al. (2019). Oceanic nomad or coastal resident? Behavioural switching in the shortfin mako shark (*Isurus oxyrinchus*). *Mar. Biol.* 166, 1–16. doi: 10.1007/s00227-018-3453-5

Gibson, K. J., Streich, M. K., Topping, T. S., and Stunz, G. W. (2019). Utility of citizen science data: a case study in land-based shark fishing. *PLoS One* 14:e0226782. doi: 10.1371/journal.pone.0226782

Hammerschlag, N., Schmitz, O. J., Flecker, A. S., Lafferty, K. D., Sih, A., Atwood, T. B., et al. (2019). Ecosystem function and services of aquatic predators in the Anthropocene. *Trends Ecol. Evol.* 34, 369–383. doi: 10.1016/j.tree.2019.01.005

Hays, G. C., Bailey, H., Bograd, S. J., Bowen, W. D., Campagna, C., Carmichael, R. H., et al. (2019). Translating marine animal tracking data into conservation policy and management. *Trends Ecol. Evol.* 34, 459–473.

Heist, E. J., Musick, J. A., and Graves, J. E. (1996). Genetic population structure of the shortfin mako (Isurus oxyrinchus) inferred from restriction fragment length polymorphism analysis of mitochondrial DNA. *Can. J. Aquat. Sci.* 53, 583–588. doi: 10.1139/f95-245

Holts, D. B., Julian, A., Sosa-Nishizaki, O., and Bartoo, N. W. (1998). "Pelagic shark fisheries along the west coast of the United States and Baja California, Mexico," in *Proceedings of an International Symposium Held at the 125th Annual Meeting of the American Fisheries Society*, ed. R. E. Hueter (Tampa, FL: Fish. Res.), 115–125. doi: 10.1016/s0165-7836(98)00178-7

Hoolihan, J. P., Wells, R. J. D., Luo, J., Faltherman, B., Prince, E. D., and Rooker, J. R. (2014). Vertical and horizontal movements of yellowfin tuna in the Gulf of Mexico. *Mar. Coast. Fish.* 6:211. doi: 10.1080/19425120.2014.935900

International Commission for the Conservation of Atlantic Tunas [ICCAT] (2013). *Report of the 2012 shortfin mako stock assessment and ecological risk assessment meeting. Collective Volume of Scientific Papers ICCAT*. Madrid: ICCAT, 1427–1570.

International Commission for the Conservation of Atlantic Tunas [ICCAT] (2017). *Report of the Standing Committee on Research and Statistics (SCRS). 2017 SCRS Report ICCAT*. Madrid: ICCAT.

International Commission for the Conservation of Atlantic Tunas [ICCAT] (2019). "Report of the 2019 shortfin mako sharks stock assessment update meeting," in *Proceedings of the SMA SHRK SA Intersessional Meeting*, Madrid.

International Commission for the Conservation of Atlantic Tunas [ICCAT] (2020). *Shark Check Sheets Received in Accordance with REC. 18-06. COC_314/2020.* Madrid: ICCAT.

Jonsen, I. D., Flemming, J. M., and Myers, R. A. (2005). Robust state-space modeling of animal movement data. *Ecology* 86, 2874–2880. doi: 10.1890/04-1852

Jonsen, I. D., Myers, R. A., and James, M. C. (2007). Identifying leatherback turtle foraging behavior from satellite telemetry using a switching state-space model. *Mar. Ecol.* 337, 255–264. doi: 10.3354/meps337255

Jorgensen, S. J., Reeb, C. A., Chapple, T. K., Anderson, S., Perle, C., Van Sommeran, S. R., et al. (2010). Philopatry and migration of Pacific white sharks. *Proc. R. Soc. B* 277, 679–688. doi: 10.1098/rspb.2009.1155

JPL OurOcean Project (2010). *G1SST L4 SST Analysis. Ver. 1. PO.DAAC, CA, USA*. Available online at: https://doi.org/10.5067/GHG1S-4FP01 (accessed December 01, 2020).

Kohler, N. E., Turner, P. A., Hoey, J. J., Natanson, L. J., and Briggs, R. (2002). Tag and recapture data for three pelagic shark species: blue shark (*Prionace glauca*), shortfin mako (*Isurus oxyrinchus*), and porbeagle (*Lamna nasus*) in the North Atlantic Ocean. *Collect. Volumes Sci. Pap. ICCAT* 54, 1231–1260.

Kraus, R. T., Wells, R. J. D., and Rooker, J. R. (2011). Horizontal movements of Atlantic blue marlin (*Makaira nigricans*) in the Gulf of Mexico. *Mar. Biol.* 158, 699–713. doi: 10.1007/s00227-010-1593-3

Lea, J. S. E., Wetherbee, B. M., Queiroz, N., Burnie, N., Aming, C., Sousa, L. L., et al. (2015). Repeated, long-distance migrations by a philopatric predator targeting highly contrasting ecosystems. *Sci. Rep.* 5:11202. doi: 10.1038/srep11202

Loefer, J. K., Sedberry, G. R., and McGovern, J. C. (2005). Vertical movement of a shortfin mako in the western North Atlantic as determined by pop-up satellite tagging. *Southeast. Nat.* 4, 237–246. doi: 10.1656/1528-7092(2005)004[0237:vmoasm]2.0.co;2

Longhurst, A. (2007). *Ecological Geography of the Sea*, 2nd Edn. Burlington, MA: Academic Press.

Magurran, A. E., and Seghers, B. H. (1994). A cost of sexual harassment in the guppy, *Poecilia reticulata*. *Proc. R. Soc. B* 258, 89–92. doi: 10.1098/rspb.1994.0147

Mollet, H. F., Cliff, G., Pratt, H. L. Jr., and Stevens, J. D. (2000). Reproductive biology of the female shortfin mako, Isurus oxyrinchus Rafinesque, 1810, with comments on the embryonic development of lamnoids. *Fish. Bull.* 98, 299–318.

Mucientes, G. R., Queiroz, N., Sousa, L. L., Tarroso, P., and Sims, D. W. (2009). Sexual segregation of pelagic sharks and the potential threat from fisheries. *Biol. Lett.* 5, 156–159. doi: 10.1098/rsbl.2008.0761

Musyl, M. K., Brill, R. W., Curran, D. S., Fragoso, N. M., McNaughton, L. M., Nielsen, A., et al. (2011). Post-release survival, vertical and horizontal movements, and thermal habitats of five species of pelagic sharks in the central Pacific Ocean. *Fish. Bull.* 109, 341–368.

Nasby-Lucas, N., Dewar, H., Sosa-Nishizaki, C., Wilson, C., Hyde, J. R., Vetter, R. D., et al. (2019). Movements of electronically tagged shortfin mako sharks (*Isurus oxyrinchus*) in the eastern North Pacific Ocean. *Anim. Biotelemetry* 7:12. doi: 10.1186/s40317-019-0147-6

Natanson, L. J., Winton, M., Bowlby, H., Joyce, W., Deacy, B., Coelho, R., et al. (2020). Updated reproductive parameters for the shortfin mako (*Isurus oxyrinchus*) in the North Atlantic Ocean with inferences of distribution by sex and reproductive stage. *Fish. Bull.* 118, 21–36. doi: 10.7755/FB.118.1.3

Pante, E., and Simon-Bouhet, B. (2013). Marmap: a package for importing, plotting and analyzing bathymetric and topographic data in R. *PLoS One* 8:e0073051. doi: 10.1371/journal.pone.0073051

Pratt, H. L. Jr., and Casey, J. G. (1983). Age and growth of the shortfin mako, Isurus oxyrinchus, using four methods. *Can. J. Aquat. Sci.* 40, 1944–1957. doi: 10.1139/f83-224

Queiroz, N., Humphries, N. E., Mucientes, G., Hammerschlag, N., Lima, F. P., Scales, K. L., et al. (2016). Ocean-wide tracking of pelagic sharks reveals extent of overlap with longline fishing hotspots. *PNAS* 113, 1582–1587. doi: 10.1073/pnas.1510090113

Queiroz, N., Humphries, N. E., Couto, A., Vedor, M., da Costa, I., and Sequeira, A. M. M. (2019). Global spatial risk assessment of sharks under the footprint of fisheries. *Nature* 572, 461–466. doi: 10.1038/s41586-019-1444-4

R Core Team (2014). *R: A Language and Environment for Statistical Computing*. Vienna: R foundation for statistical computing.

Ricker, W. E. (1981). Changes in the average size and age of Pacific Salmon. *Can. J. Aquat. Sci.* 38, 1636–1656. doi: 10.1139/f81-213

Rigby, C. L., Barreto, R., Carlson, J., Fernando, D., Fordham, S., Francis, M. P., et al. (2018). *Isurus Oxyrinchus. The IUCN Red List of Threatened Species 2019*. Available online at: http://dx.doi.org/10.2305/IUCN.UK.2019-1.RLTS.T39341A2903170.en (accessed September 06, 2019).

Rogers, P. J., Huveneers, C., Page, B., Goldsworthy, S. D., Coyne, M., Lowther, A. D., et al. (2015). Living on the continental shelf edge: habitat use of juvenile shortfin mako sharks Isurus oxyrinchus in the Great Australian Bight, southern Australia. *Fish. Oceanogr.* 24, 205–218. doi: 10.1111/fog.12103

Rooker, J. R., Dance, M. A., Wells, R. J. D., Ajemian, M. J., Block, B. A., Castleton, M. R., et al. (2019). Population connectivity of pelagic megafauna in the Cuba-Mexico-United States triangle. *Sci. Rep.* 9:1663. doi: 10.1038/s41598-018-38144-8

Santos, C. C., Domingo, A., Carlson, J., Natanson, L. J., Cortés, E., Miller, P., et al. (2018). Habitat use and migrations of shortfin mako in the Atlantic using satellite telemetry. *Collect. Volumes Sci. Pap. ICCAT* 73, 445–456.

Schrey, A. W., and Heist, E. J. (2003). Microsatellite analysis of population structure in the shortfin mako (*Isurus oxyrinchus*). *Can. J. Aquat. Sci.* 60, 670–675. doi: 10.1137/F03-064

Sequeira, A. M. M., Rodriguez, J. P., Eguiluz, V. M., Harcourt, R., Hindell, M., Sims, D. W., et al. (2018). Convergence of marine megafauna movement patterns in coastal and open oceans. *Proc. Natl. Acad. Sci. U.S.A.* 115, 3072–3077. doi: 10.1073/pnas.1716137115

Simpfendorfer, C. A., Olsen, E. M., Heupel, M. R., and Moland, E. (2012). Three-dimensional kernel utilization distributions improve estimates of space use in aquatic animals. *Can. J. Aquat. Sci.* 69, 1660–1680. doi: 10.1139/f2011-179

Sims, D. W., Mucientes, G., and Queiroz, N. (2018). Shortfin mako sharks threatened by inaction. *Science* 359:1342.

Sippel, T., Ohshimo, S., Yokawa, K., Kai, M., Carvalho, F., Liu, K. M., et al. (2015). *Spatial and Temporal Patterns of Shortfin Mako Shark Size and Sex in the North Pacific Ocean*. ISC/15/SHARKWG-1/04. Copenhagen: ICES.

Smith, P. J., Francis, R. I. C. C., and McVeagh, M. (1991). Loss of genetic diversity due to fishing pressure. *Fish. Res.* 10, 309–316. doi: 10.1016/0165-7836(91)90082-q

Stevens, J. D. (1974). The occurrence and significance of tooth cuts on the blue shark (*Prionace glauca* L.) from British waters. *J. Mar. Biol. Assoc. U.K.* 54, 373–378. doi: 10.1017/S0025315400058604

Stillwell, C. E., and Kohler, N. E. (1982). Food, feeding habits, and estimates of daily ration of the shortfin mako (*Isurus oxyrinchus*) in the northwest Atlantic. *Can. J. Aquat. Sci.* 39, 407–414. doi: 10.1139/f82-058

Vaudo, J. J., Byrne, M. E., Wetherbee, B. M., Harvey, G. M., and Shivji, M. S. (2017). Long-term satellite tracking reveals region-specific movements of a large pelagic predator, the shortfin mako shark, in the western North Atlantic Ocean. *J. Appl. Ecol.* 54, 1765–1775. doi: 10.1111/1365-2664.12852

Vaudo, J. J., Wetherbee, B. M., Wood, A. D., Weng, K., Howey-Jordan, L. A., Harvey, G. M., et al. (2016). Vertical movements of shortfin mako sharks Isurus oxyrinchus in the western North Atlantic Ocean are strongly influenced by temperature. *Mar. Ecol. Prog. Ser.* 547, 163–175. doi: 10.3354/meps11646

Waples, R. S. (1998). Separating the wheat from the chaff – patterns of genetic differentiation in high gene flow species. *J. Hered.* 89, 438–450. doi: 10.1093/jhered/89.5.438

Wood, A. D., Wetherbee, B. M., Juanes, F., Kohler, N. E., and Wilga, C. (2009). Recalculated diet and daily ration of the shortfin mako (*Isurus oxyrinchus*), with a focus on quantifying predation on bluefish (*Pomatomus saltatrix*) in the northwest Atlantic Ocean. *Fish. Bull.* 107, 76–88.

Conflict of Interest: The authors declare that the research was conducted in the absence of any commercial or financial relationships that could be construed as a potential conflict of interest.

frontiers in Marine Science

ORIGINAL RESEARCH
published: 01 February 2021
doi: 10.3389/fmars.2021.624158

Horizontal and Vertical Movement Patterns and Habitat Use of Juvenile Porbeagles (*Lamna nasus*) in the Western North Atlantic

Gregory Skomal[1]*, Heather Marshall[2,3], Benjamin Galuardi[4,5], Lisa Natanson[6], Camrin D. Braun[7,8] and Diego Bernal[2]

[1] Massachusetts Division of Marine Fisheries, New Bedford, MA, United States, [2] Biology Department, University of Massachusetts Dartmouth, North Dartmouth, MA, United States, [3] State College of Florida, Bradenton, FL, United States, [4] School for Marine Science and Technology, University of Massachusetts Dartmouth, New Bedford, MA, United States, [5] Greater Atlantic Regional Fisheries Office, NOAA Fisheries, Gloucester, MA, United States, [6] Apex Predators Program, NOAA Fisheries, Narragansett, RI, United States, [7] School of Aquatic and Fishery Sciences, University of Washington, Seattle, WA, United States, [8] Biology Department, Woods Hole Oceanographic Institution, Woods Hole, MA, United States

OPEN ACCESS

Edited by:
David Wells,
Texas A&M University at Galveston,
United States

Reviewed by:
Brittany Finucci,
National Institute of Water and
Atmospheric Research (NIWA),
New Zealand
Nuno Queiroz,
Centro de Investigacao em
Biodiversidade e Recursos Geneticos
(CIBIO-InBIO), Portugal

***Correspondence:**
Gregory Skomal
gregory.skomal@mass.gov

Specialty section:
This article was submitted to
Marine Megafauna,
a section of the journal
Frontiers in Marine Science

Received: *30 October 2020*
Accepted: *06 January 2021*
Published: *01 February 2021*

Citation:
Skomal G, Marshall H, Galuardi B,
Natanson L, Braun CD and Bernal D
(2021) Horizontal and Vertical
Movement Patterns and Habitat Use
of Juvenile Porbeagles (Lamna nasus)
in the Western North Atlantic.
Front. Mar. Sci. 8:624158.
doi: 10.3389/fmars.2021.624158

The porbeagle (Lamna nasus) is a large, highly migratory endothermic shark broadly distributed in the higher latitudes of the Atlantic, South Pacific, and Indian Oceans. In the North Atlantic, the porbeagle has a long history of fisheries exploitation and current assessments indicate that this stock is severely overfished. Although much is known of the life history of this species, there is little fisheries-independent information about habitat preferences and ecology. To examine migratory routes, vertical behavior, and environmental associations in the western North Atlantic, we deployed pop-up satellite archival transmitting tags on 20 porbeagles in late November, 2006. The sharks, ten males and ten females ranging from 128 to 154 cm fork length, were tagged and released from a commercial longline fishing vessel on the northwestern edge of Georges Bank, about 150 km east of Cape Cod, MA. The tags were programmed to release in March ($n = 7$), July ($n = 7$), and November ($n = 6$) of 2007, and 17 (85%) successfully reported. Based on known and derived geopositions, the porbeagles exhibited broad seasonally-dependent horizontal and vertical movements ranging from minimum linear distances of 937 to 3,310 km and from the surface to 1,300 m, respectively. All of the sharks remained in the western North Atlantic from the Gulf of Maine, the Scotian Shelf, on George's Bank, and in the deep, oceanic waters off the continental shelf along the edge of, and within, the Gulf Stream. In general, the population appears to be shelf-oriented during the summer and early fall with more expansive offshore radiation in the winter and spring. Although sharks moved through temperatures ranging from 2 to 26°C, the bulk of their time (97%) was spent in 6-20°C. In the summer months, most of the sharks were associated with the continental shelf moving between the surface and the bottom and remaining < 200 m deep. In the late fall and winter months, the porbeagles moved into pelagic habitat and exhibited two behavioral patterns linked with the thermal features of the Gulf Stream: "non-divers" ($n = 7$) largely remained at epipelagic depths and "divers" ($n = 10$) made frequent dives into and remained at mesopelagic depths (200–1000 m). These data demonstrate that juvenile porbeagles are physiologically capable of exploiting the cool temperate waters of the western North Atlantic as well as the mesopelagic depths of the Gulf Stream, possibly allowing exploitation of prey not available to other predators.

Keywords: porbeagle movements, diving behavior, Western North Atlantic Ocean, Gulf Stream, endothermy

INTRODUCTION

The porbeagle, *Lamna nasus*, is a large, highly migratory pelagic shark broadly distributed in the temperate latitudes of the Atlantic, South Pacific, and South Indian Oceans (Compagno, 2002). Historically, the species has been subjected to both commercial and recreational fisheries throughout its range (Curtis et al., 2016; Haugen, 2020). In the North Atlantic, the porbeagle is currently managed as two stocks (i.e., east and west) and the most recent stock assessment indicates that both are heavily overfished (ICCAT, 2009; Curtis et al., 2016). As a result, the IUCN Red List of Threatened Species assessed the species as Vulnerable in 2018 (Rigby et al., 2018). The porbeagle is also currently listed on Annex I of the United Nations Convention on Law of the Sea, Appendix II of the Convention for the Conservation of Migratory Species (CMS, 2008), and, since 2014, Appendix II of the Convention on International Trade in Endangered Species of Wild Fauna and Flora (www.cites.org; Curtis et al., 2016). In 2015, the International Commission for the Conservation of Atlantic Tunas (ICCAT) passed a recommendation requiring contracting and cooperating parties to release unharmed porbeagles caught in association with ICCAT fisheries. In 2016, the porbeagle was proposed to be listed for protection under the U.S. Endangered Species Act, but an evaluation of all available information determined that the listing was not warranted due to a low risk of extinction in the foreseeable future (Curtis et al., 2016). Although major harvesters of porbeagle have either stopped (European Union, Canada) or capped landings (USA) in an effort to allow for the rebuilding of stocks (Campana et al., 2015; reviewed by Haugen, 2020), this species occurs in the highest bycatch risk zone in the North Atlantic (Queiroz et al., 2019) and mortality associated with bycatch may be high (Haugen, 2020). The most optimistic projections predict that stock recovery on both sides of the Atlantic will require decades (ICCAT, 2009). Given the current status of porbeagle stocks, the Standing Committee on Research and Statistics in ICCAT proffered a suite of research recommendations that included a better understanding of stock structure, vertical and migratory movements, and habitat associations with oceanographic features (ICCAT, 2009). Such information on the temporal and spatial distribution of porbeagles in relation to environmental/ecosystem features would not only facilitate a better understanding of catch trends, but also spatial management to reduce potential fishing mortality (ICCAT, 2009).

Although the life history of the porbeagle has been well-studied (Jensen et al., 2002; Joyce et al., 2002; Natanson et al., 2019), much of what is known about stock structure, movements, habitat use, and spatial ecology has come from fisheries-dependent data (Campana and Joyce, 2004; Kohler and Turner, 2019). These studies (using conventional tags and commercial catch data) suggest that porbeagles exhibit seasonal shifts in abundance and are highly migratory in the western North Atlantic (WNA). However, relatively little is known about the three-dimensional movements and habitat use of these fish as well as the biotic and abiotic factors (e.g., ambient temperature, oceanic fronts, prey availability, and reproductive behaviors) that may influence their movements.

While fisheries-dependent data suggest that porbeagles do indeed have a wide thermal distribution (i.e., captured in waters with a sea surface temperature [SST] ranging from 2 to 23°C), most catches near the continental shelves are associated with the thermocline and with oceanographic frontal zones in a relatively narrow temperature range between 5 and 10°C (Campana and Joyce, 2004). Based on these data, Campana and Joyce (2004) suggested that the vertical distribution of the porbeagle in the WNA is relatively narrow (<200 m), although they did not rule out the possibility of vertical migrations to greater depths.

During the last two decades, the advent of electronic tagging technologies has allowed researchers to gain a more holistic, fisheries-independent understanding of the temporal and spatial movement patterns and stock structure of highly migratory fishes (reviewed by Costa et al., 2012). In addition, these new technologies allow for the correlation of movement patterns with oceanographic features (Braun et al., 2019) and, therefore, provide a more robust understanding of habitat use. The most commonly used technology to study the three-dimensional movement ecology in commercially important teleosts and elasmobranchs is the pop-up satellite archival transmitting (PSAT) tag (e.g., Block, 2005; Skomal et al., 2009, 2017; Campana et al., 2010; Galuardi et al., 2010; Musyl et al., 2011). To date, several studies have deployed PSAT tags to examine porbeagle movements in the Atlantic (Pade et al., 2009; Campana et al., 2010; Saunders et al., 2011; Biais et al., 2017). Work in the eastern North Atlantic (ENA) off the coast of the United Kingdom showed that porbeagles appear to exhibit deep (>300 m) and, in some cases, diel diving behavior and highly variable horizontal movements (Pade et al., 2009; Saunders et al., 2011). However, conclusions from those studies were based on relatively low sample sizes (total $n = 7$) and short track durations (22-122 days). In the WNA, the tracks of 21 porbeagles showed deep diving (up to 1,360 m) and broad horizontal movements as far as the Sargasso Sea (Campana et al., 2010). Although track durations spanned almost a year (60–348 days), the porbeagle sample in that study was dominated by large, sexually mature females.

Based on those data, Campana et al. (2010) hypothesized that the Sargasso Sea may be an important parturition area for porbeagles in the WNA. Most recently, Biais et al. (2017) deployed PSAT tags on nine subadult/adult porbeagles in the Bay of Biscay for up to a year, and showed broad migrations to the Arctic Circle, Madeira, and the mid-Atlantic Ridge, as well as site fidelity to the tagging location. However, the lack of juveniles from both sexes in these studies limits the extent to which these findings are applicable to all age classes.

The porbeagle and other members of the family Lamnidae are unique among sharks in having the capacity to retain metabolically produced heat to significantly elevate tissue (i.e., eyes, brain, viscera and swimming muscle) temperatures above ambient (i.e., regional endothermy, Carey and Teal, 1969a; Goldman, 1997; Bernal et al., 2001; Goldman et al., 2004; Sepulveda et al., 2004). Among lamnids, the porbeagle and its congener the salmon shark (*Lamna ditropis*) are able to maintain their eyes, brain, viscera, and swimming muscles up to 20°C above ambient (Goldman et al., 2004; Bernal et al., 2005), resulting in a relatively stable elevated tissue operating temperature. This may allow lamnid sharks to make long duration or more frequent dives below the thermocline or to inhabit very cold, highly productive, subpolar waters (2–10°C) for prolonged periods (i.e., numerous months) of time without compromising locomotor, sensory, and digestive function. In the porbeagle, regional endothermy may allow them to expand their thermal niche to forage in cooler, more productive waters at greater depths and/or higher latitudes (Block and Carey, 1985; Carey et al., 1985; Bernal et al., 2001; Dickson and Graham, 2004). While the vertical movement patterns of large, sexually mature females support a wide thermal (i.e., depth and latitude) distribution (Campana et al., 2010), the vertical movement patterns of juvenile porbeagles remain unknown.

Information on porbeagle movement ecology, habitat use, and stock structure as it relates to juveniles is warranted given relatively little is known about the three-dimensional movements of these fish. As this stock is highly overexploited, fishery managers need more empirical data for the development of enhanced conservation measures to facilitate the restoration of porbeagle populations in the Atlantic. In this study, we used PSAT technology to examine long-term, three-dimensional movements and to characterize habitat use by juvenile porbeagles in the WNA.

MATERIALS AND METHODS

All methods associated with the capture and handling of sharks were conducted in accordance to standards from the Institutional Animal Care and Use Committee of the University of Massachusetts, Dartmouth (Protocol #05-07).

Tagging

During this study, 20 porbeagles were captured and tagged in the western North Atlantic Ocean east of Cape Cod, MA near Cultivator Shoal, George's Bank (41.844°N, 68.095°W) in November, 2006 aboard the *F/V* Eagle Eye II. Sharks were caught on pelagic longline fishing gear comprised of monofilament gangions (9.1 m; 180 kg test) with 18/0 circle hooks (Mustad Corp., Miami, FL, USA) baited with whole Atlantic mackerel (*Scomber scombrus*). Two longline sets of 210 and 315 hooks were allowed to soak for 3 and 5 h, respectively, before hauling. During each set, a temperature profile of the water column was obtained using a conductivity-temperature-depth meter (model SBE911, Sea-Bird Electronics, Bellevue, WA, USA).

All hooked sharks were brought alongside the vessel and inspected for physical trauma (e.g., hook damage); only healthy, actively swimming, mouth-hooked specimens that showed little or no bleeding were selected for this study. Each shark was guided by the monofilament leader into a mesh-lined cradle and quickly lifted to the deck for sex determination, accurate length (over the body fork length, FL) measurement, and PSAT tag attachment ($n = 20$, Model Mk10-PAT, Wildlife Computers Inc., Redmond, WA, USA). Each PSAT tag was tethered to an intramuscular nylon umbrella dart, which was implanted into the musculature and through the cartilaginous supports of the dorsal fin (Kohler and Turner, 2001). All PSAT tags were programmed to release if the shark showed no significant vertical movement (± 1 m) for 96 continuous hours.

Data Analyses

Tags were programmed to collect depth (minimum resolution: 0.5 m), ambient temperature (minimum resolution: 0.05°C), and light intensity (measured as irradiance at 550 nm wavelength) every 10 s for the duration of each deployment. Three subsets of deployed tags were programmed to detach from the sharks after 120 days ($n = 7$; T_{120}; March, 2007), 240 days ($n = 7$; T_{240}; July, 2007), and 360 days ($n = 6$; T_{360}; November, 2007). Upon release, pre-processed binned data (summarized every 6 h [120 and 240 day deployments] or 12 h [360 day deployments]; proportion of time spent at depth [m]: <5, 10, 25, 50, 75, 100, 150, 200, 300, 400, 500, 600, 800, >800; proportion of time spent at ambient temperature: 2–26°C at 2°C intervals) were transmitted through the Argos satellite system over a period of 6–10 days. Each tag also transmitted a temperature-depth profile of the water column inhabited by the shark during each 6- or 12-h interval. This comprised minimum and maximum water temperatures in eight depth bins, ranging from the shallowest to the deepest swimming depths for that time interval. Finally, the tag processed the light level data onboard to correct for depth and subsequently estimated times of dawn, dusk, and midnight or midday.

Temperature profiles of the water column and each shark's possible association with a thermocline, were assessed by plotting depth vs. temperature for discrete periods of time when diving behavior indicated repeated use of a consistent depth range. Given our findings that porbeagles exhibited two distinct diving behaviors [i.e., epipelagic (0–200 m) and mesopelagic (200–1000 m)], we grouped them as "non-divers" and "divers," respectively. This allowed the examination of depth associations, averaged across individuals within each behavior group, using contoured probability plots generated with the ffgrid package in MATLAB (version R2010a).

To estimate the horizontal movements of each shark, we then used the HMMoce package (Braun et al., 2018), which uses light-based position estimates (from the tag), sea surface temperature (SST), and depth-temperature profiles, to construct gridded likelihoods of occupancy using a state space hidden Markov model framework. Observation-based likelihoods were derived from remotely-sensed SST, light-based longitude, and depth-temperature profile data collected by the tags, using four separate likelihood calculations: (1) an SST likelihood was generated for tag-based SST values integrated according to an error term (+/- 1%) and compared to remotely-sensed SST from the Multi-scale Ultra-high Resolution (MUR) sea surface temperature analysis (MUR-SST, 0.01° resolution) (NASA JPL, 2015); (2) light-based longitudinal likelihood was derived using estimates of longitude from GPE2 software (Wildlife Computers, Inc., Redmond, WA, USA) that allowed visual checking of light curves; (3) depth-temperature profile summaries recorded by the tag were compared to daily reanalysis model depth-temperature products from the HYbrid Coordinate Ocean Model (Bleck, 2002; Chassignet et al., 2007; HYCOM, 0.08° resolution) at the standard depth levels available in the model and individual likelihood surfaces for each depth level were then multiplied together for an overall profile likelihood at that time point; and (4) Ocean Heat Content (OHC) was obtained by integrating the heat content of the water column above the minimum daily tag-measured temperature to the most shallow depth recorded by the PSAT and included in the HYCOM fields (Luo et al., 2015). Start and end locations were fixed in all model runs.

The resulting observation likelihoods, in all reasonable pairwise and triplicate combinations, were convolved with a diffusive movement kernel that allowed swim speeds up to 2 m/s (see Braun et al., 2018 for full details of the convolution, filtering, and smoothing components of the model). Model selection comparing different combinations of observation likelihoods used Akaike Information Criterion (AIC). Results from the final smoothing step of the selected model represent the posterior distribution of each state (position) over time. The spatial means of the daily posterior distributions were used to calculate a most probable track.

Residency distribution (RD) plots were generated using the posterior likelihood surfaces from the position estimates. RDs were determined by aggregating the daily posterior probabilities across all tagged sharks, seasonally. Gridded probabilities were calculated with a 0.1° resolution and seasons were based on the lunar calendar: fall, September 20–December 19; winter, December 20–March 19; spring, March 20–June 19; summer, June 20–September 19.

RESULTS

A total of 88 juvenile porbeagles ranging from 90 to 174 cm FL were caught on two pelagic longline sets in November, 2006 on George's Bank (41°N, 68°W) with sea surface temperatures of 12.8–13.0°C and water depths of 90-140 m. A subset of 20 sharks (128–154 cm FL), 10 males (mean ± SE: 133 ± 2.5 cm FL) and 10 females (141 ± 2.3 cm FL) were selected for tagging (**Table 1**). We received data from 17 PSAT tags (7 males, 10 females, T_{120} $n = 5$, T_{240} $n = 7$, and T_{360} $n = 5$) resulting in 4,050 days of total tracking time (**Table 1**). Four tags released prior to their programmed date (T_{240} $n = 2$:185 and 221 days; T_{360} $n = 2$: 307 and 311 days) and three did not report (T_{120} $n = 2$ and T_{360} $n = 1$).

Horizontal Movements

The total minimum straight-line distance traveled by each of the tagged sharks ranged from 937 to 1,903 km for T_{120}, 1,579 to 2,857 km for T_{240}, and 2,517 to 3,310 km for T_{360} (**Table 1**). The porbeagles largely remained in the temperate WNA year-round, occurring in the Gulf of Maine, the Scotian Shelf, on George's Bank, and in the deep, oceanic waters off the continental shelf along the edge of, and within, the Gulf Stream (**Figure 1**). Geoposition estimates of latitude ranged from 35°N (off the Outer Banks, North Carolina, USA) to 45°N; longitude ranged from shelf waters east to 55°W (**Figure 1**). Residency distribution plots show that tagged porbeagles exhibited seasonal changes in distribution (**Figure 2**). During the fall, the sharks were broadly distributed from the Gulf of Maine to oceanic areas, but largely concentrated in deeper regions of the former. In the late fall and winter, porbeagles moved out of the Gulf and off the shelf into oceanic habitat along the northern edge of and within the Gulf Stream (**Figure 2**). In the spring, the porbeagles remained in oceanic habitat along the shelf edge prior to returning to the Gulf of Maine and Scotian Shelf in the summer (**Figure 2**).

Vertical Movements

For all sharks combined, ambient water temperature and swimming depth ranged from 2 to 24°C and from the surface to 1,304 m, respectively. During the late fall and winter months, two general patterns of vertical behavior were observed: (1) "non-divers" (2 females and 5 males) largely remained at shallow depths and rarely penetrated depths >600 m (**Figure 3**); and (2) "divers" (8 females and 2 males) made frequent dives into and remained at mesopelagic depths (200-1000 m) for 38–109 days (average 71 ± 26 days from fall into winter), rarely moving into the upper epipelagic zone (**Figure 4**). Overall, these two distinct dive patterns did not appear to be influenced by the broad-scale horizontal (coastal to offshore) movements of these fish as there were no significant differences in total minimum straight-line distances traveled between divers (2,450 ± 659 km) and non-divers (2,288 ± 715 km; $p > 0.05$, Student's paired T-test). When stratified by dive behavior, the estimated geopositions of the porbeagles during the late fall and winter indicate that non-divers were almost exclusively associated with the cold side of the northern edge of the Gulf Stream, while divers primarily occupied the warm side of this edge, within the Gulf Stream, or in warm water south of the Gulf Stream (**Figure 5**).

When analyzed together, all fish, regardless of season, spent 75% and 50% of their time at depths of <200 m and 75-200 m, respectively, and 97% of their time in temperatures of 6–20°C. In general, porbeagles occupied similar depth and temperature distributions, but divers and non-divers diverged during the fall and winter months as they moved off the shelf (**Figures 6**, **7**). In the fall, divers occupied a broad range of depths from 5 to 800 meters, spending 31% of their time >200 m (**Figure 6**), and 68% of the time in water temperatures ranging from 8 to

TABLE 1 | Tagging information for 17 juvenile porbeagles tagged in the WNA on George's Bank.

Shark	Tag PTT	FL (cm)	Sex	Date tagged	Tag latitude	Tag longitude	At liberty (days)	Behavior	Pop-up latitude	Pop-up longitude	Min. dist. (km)	Obs. like.
1	67814	133.0	F	11/20/06	41.84	−68.10	120	Diver	42.1	−60.88	1553	LSO
2	67815	145.8	F	11/20/06	41.84	−68.10	120	Diver	41.06	−66.30	1887	LO
3	67829	154.0	F	11/20/06	41.84	−68.09	240	Diver	44.22	−62.32	1579	LSO
4	67828	139.7	M	11/21/06	41.84	−68.09	240	Non-diver	44.57	−62.03	2678	LSO
5	67835	140.0	F	11/21/06	41.82	−68.17	311**	Diver	43.31	−61.63	3077	LSO
6	67825	129.0	M	11/21/06	41.82	−68.18	120	Non-diver	40.16	−69.09	937	LSO
7	67827	128.0	M	11/21/06	41.82	−68.21	240	Non-diver	42.17	−65.33	2530	LO
8	67826	135.0	F	11/21/06	41.82	−68.22	240	Non-diver	44.78	−60.94	1939	LSO
9	67832	130.0	M	11/21/06	41.82	−68.24	307**	Diver	44.25	−62.34	3310	LSO
10	67831	136.0	F	11/21/06	41.82	−68.24	360	Diver	44.19	−61.45	2517	LO
11	67819	134.5	F	11/21/06	41.88	−67.91	120	Diver	41.74	−62.92	1903	LO
12	67821	132.0	M	11/21/06	41.89	−67.96	221*	Non-diver	41.22	−67.99	2639	LSO
13	67824	149.5	F	11/21/06	41.85	−67.99	240	Diver	42.24	−66.61	2857	LO
14	67834	144.8	M	11/21/06	41.84	−68.00	360	Diver	41.88	−69.67	2965	LO
15	67833	136.8	F	11/21/06	41.83	−68.01	360	Non-diver	42.58	−65.36	3163	LO
16	67837	141.5	F	11/21/06	41.83	−68.02	120	Diver	40.32	−67.78	1579	LSO
17	67836	127.8	M	11/21/06	41.82	−68.03	185*	Non-diver	35.94	−74.66	2130	SO

Min. dist., Minimum linear distance (km) calculated as sum of daily track segments; Obs. like., Observation likelihood, which indicates observations used in HMMoce to construct the most probable track: L, light-based longitude; S, sea surface temperature; O, integrated ocean heat content. Asterisks indicate premature release of tags programmed for 240 (*) and 360 (**) days.

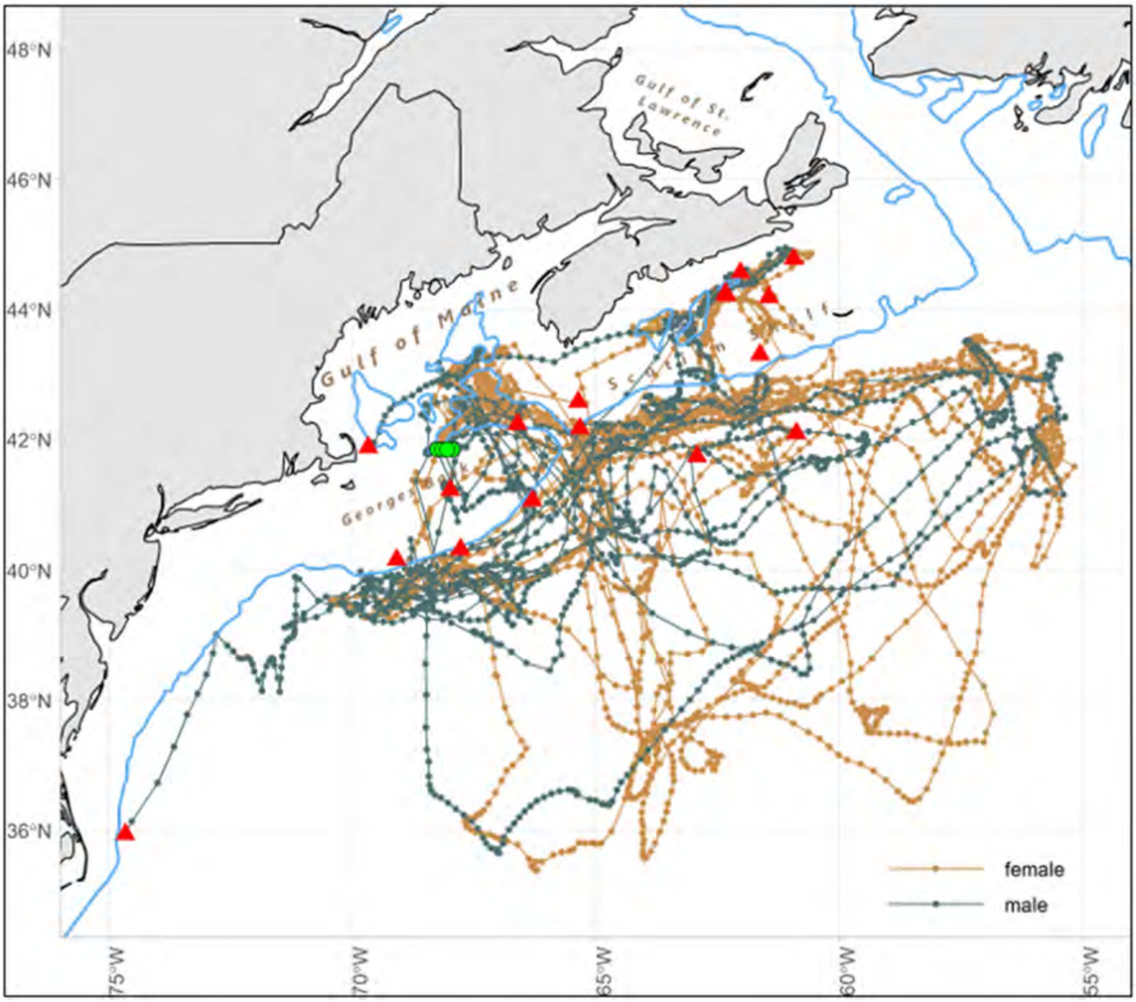

FIGURE 1 | Most probable tracks for 17 juvenile porbeagle sharks, stratified by sex, tagged in the western North Atlantic with tagging (green points) and pop-up (red triangle) locations, and shelf edge (200 m isobath, blue line).

14°C (**Figure 7**). In contrast, non-divers did not move frequently to mesopelagic depths in the fall spending only 11% of the time >200 m, but in a similar temperature range (79% at 8–14°C) when compared to divers. During the winter months, divers exhibited a bimodal depth and temperature distribution comprised of a shallow (40% at 75–200 m), warm (17% at 18–20°C) component and a deep (43% at 300–800 m), cool (22% at 12–14°C) component (**Figures 6**, **7**). However, non-divers remained at shallow depths in the winter (89% <200 m), yet occupied a similar temperature range to that of the divers (**Figure 7**). In addition, these fish were not associated with the warmer (18–20°C) waters encountered by the divers during the same time period. In the spring, both groups returned to epipelagic depths along the edge of the continental shelf with 70% and 92% of the time between 75 and 200 m and in an ambient temperature range of 6–14°C, respectively (**Figures 3**, **4**, **6**, **7**). In the summer, all fish were <200 m (99% of the time) experiencing a wider range of ambient temperatures (from 4 to 18°C) for 97% of the time, but showed a bimodal depth distribution with shallow (59% <25 m) and deeper (25% at 100–200 m) components (**Figures 3**, **4**, **6**, **7**).

DISCUSSION

Based on fisheries-independent data derived from 17 PSAT tags, we show that juvenile porbeagles tagged in the western North Atlantic exhibited broad, seasonally-dependent horizontal and vertical movements, including movement into the Gulf Stream. In the fall, juvenile porbeagles were associated with shelf waters in the Gulf of Maine and George's Bank (**Figure 2**). The sharks tagged in this study were captured on the northern side of Georges Bank in 90–140 m of water as part of 88 juveniles hooked on only two longline sets in this area—this was clearly indicative of high abundance in the area. As fall transitions to winter, juvenile porbeagles moved out of the Gulf of Maine, off the shelf, and into the oceanic waters of the WNA for the winter months, during which some of the sharks moved into the Gulf Stream and exhibited mesopelagic residence. As northeastern shelf waters

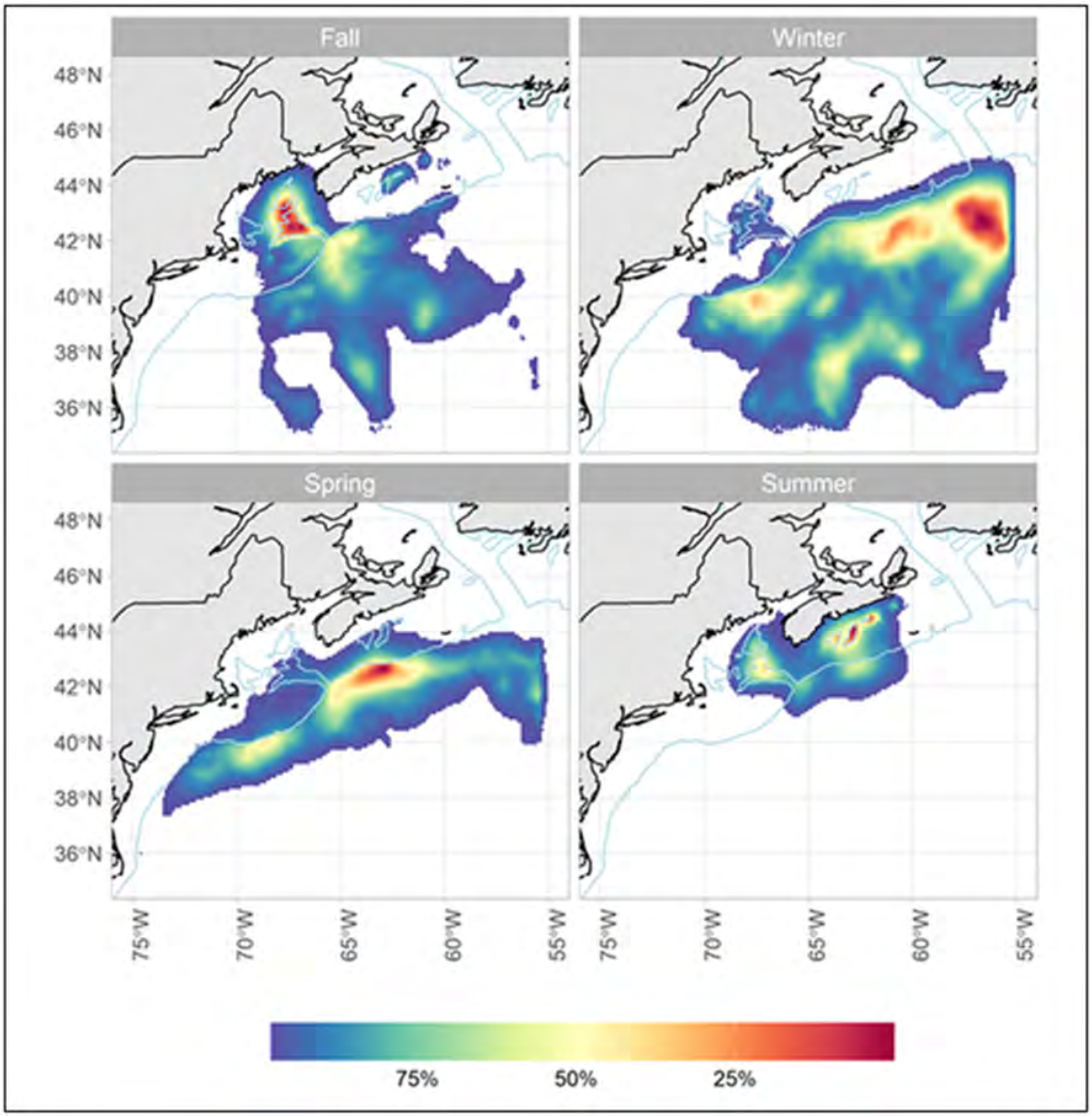

FIGURE 2 | Residency density plots showing seasonal distribution of juvenile porbeagles tagged in the western North Atlantic; seasons are based on the lunar calendar (mo/d: Fall, 9/20–12/19; Winter, 12/20–3/19; Spring, 3/20–6/19; Summer, 6/20–9/19).

warm during the spring months, these sharks transitioned back to the shelf where they spent the summer in the Gulf of Maine and on the Scotian Shelf moving between the surface and the bottom. Although some of these results are consistent with historical fisheries-dependent conventional tagging data (Kohler and Turner, 2019), this study provided evidence of more expansive offshore movement in the WNA. All the porbeagles tagged in this study remained in temperate waters north of 35°N, which differs from other pelagic shark species that seasonally move into more southerly latitudes, including the blue shark (*Prionace glauca*; Kohler and Turner, 2019), the basking shark (*Cetorhinus maximus*; Skomal et al., 2009), and endothermic lamnid sharks (e.g., white shark *Carcharodon carcharias*, Skomal et al., 2017; shortfin mako, *Isurus oxyrinchus*; Vaudo et al., 2017; Kohler and Turner, 2019).

These results are in sharp contrast to previous findings for juvenile porbeagles tagged with this technology in the WNA. Campana et al. (2010) concluded that males and juvenile sharks of both sexes remained primarily in cool temperate waters on the continental shelf, always north of latitude 38°N, for periods of up to 348 days after tagging. However, their findings are likely linked to sample size and composition. Of the 21 sharks tagged in that study, 52% were adult females, two were adult males, and the remaining eight were juvenile females. Most of the tracks of the latter were relatively short (<76 days) and did not span the winter months during which our tagged juveniles moved

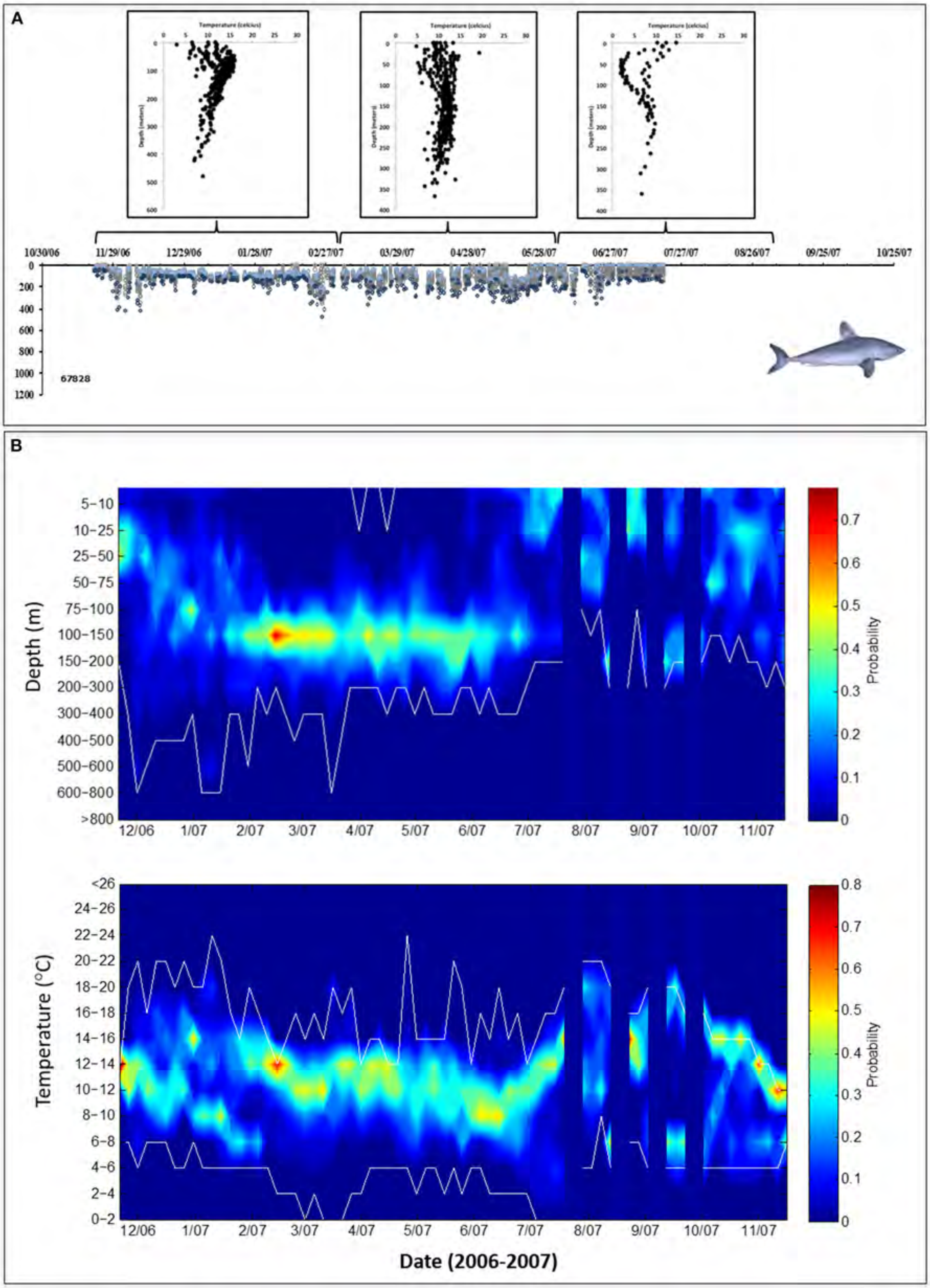

FIGURE 3 | (A) Vertical behavior of a representative "non-diver" porbeagle (Shark 4, PTT 67828) showing depth-temperature profiles at 3-month intervals (upper) corresponding to daily depth observations (lower) comprised of minimum (light blue circles), maximum (dark blue circles), and intermediate (gray circles) depths. **(B)** Contoured probability plots of all depth (upper) and water temperature (lower) data collected from porbeagles classified as non-divers (*n* = 7); white lines indicate upper and lower limits of the data and blue vertical bars indicate areas of missing data.

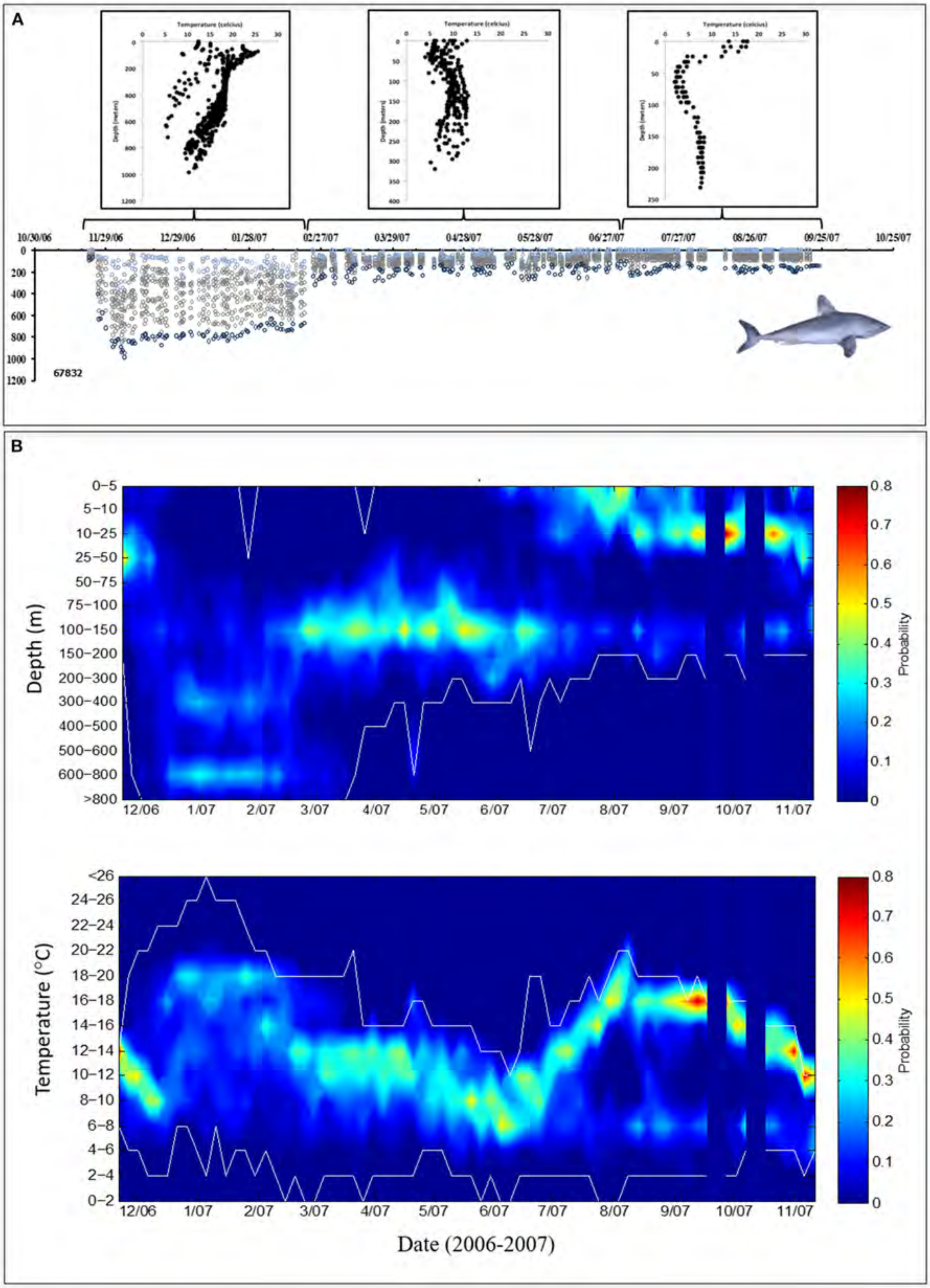

FIGURE 4 | (A) Vertical behavior of a representative "diver" porbeagle (Shark 9, PTT 67832) showing depth-temperature profiles at 3-month intervals (upper) corresponding to daily depth observations (lower) comprised of minimum (light blue circles), maximum (dark blue circles), and intermediate (gray circles) depths. **(B)** Contoured probability plots of all depth (upper) and water temperature (lower) data collected from porbeagles classified as divers ($n = 10$); white lines indicate upper and lower limits of the data and blue vertical bars indicate areas of missing data.

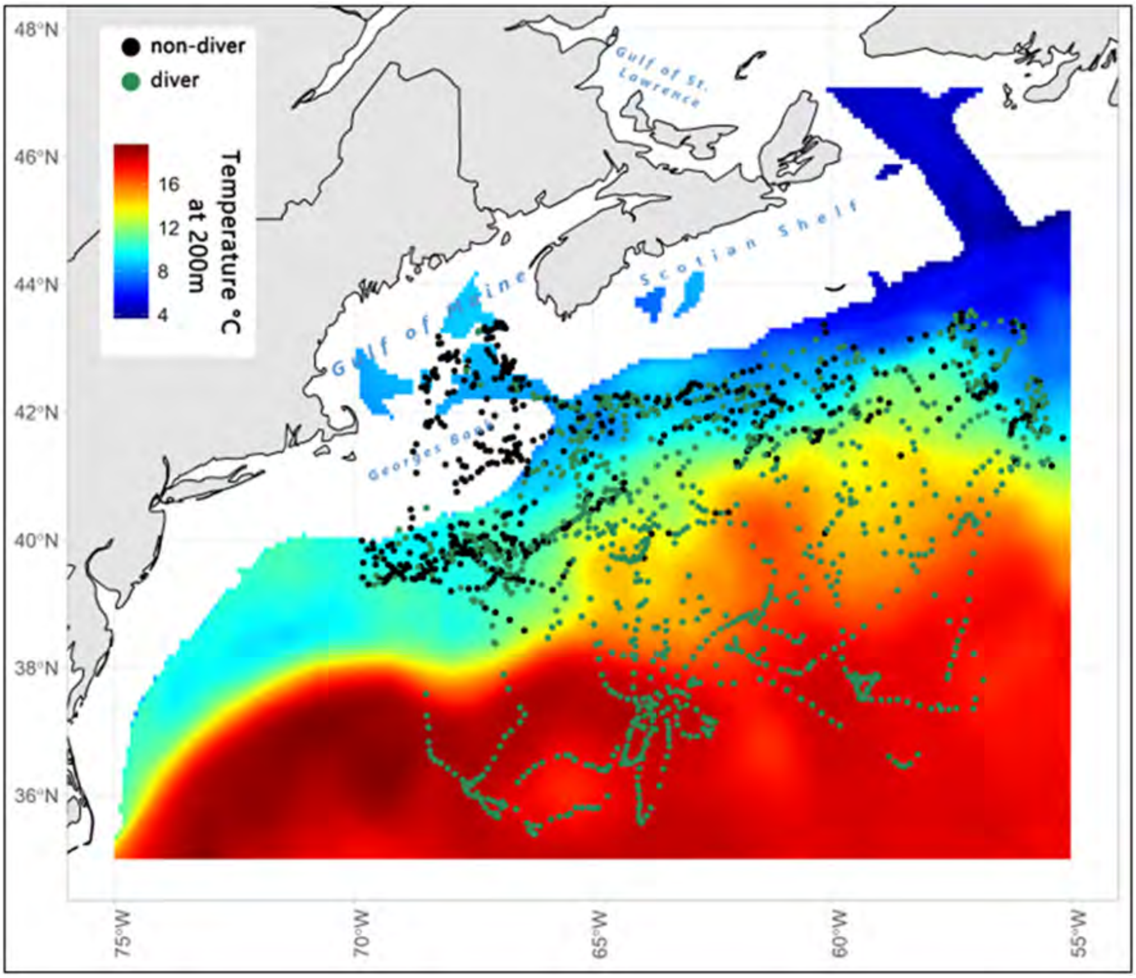

FIGURE 5 | Estimated geopositions for porbeagle divers and non-divers, overlaid on a composite of temperature (°C) at 200 m (HYCOM, 0.08° resolution) for December 2006–March 2007.

offshore. Campana et al. (2010) did show that adult females move into the Gulf Stream and as far as the Sargasso Sea. Our findings demonstrate that juveniles also move into and south of the Gulf Stream, but not as far south as adult females (∼20°N).

To date, three PSAT tagging studies have been conducted on porbeagles in the ENA: Pade et al. (2009; $n = 4$; UK), Saunders et al. (2011; $n = 3$; Ireland), and Biais et al. (2017; $n = 9$; Bay of Biscay). Although samples sizes were relatively low, collectively these studies show that porbeagles are associated with relatively shallow shelf waters during the spring and summer months and move to offshore, deeper waters in the fall and winter months. Most recently, Biais et al. (2017) found that porbeagles tagged in the Bay of Biscay moved extensively (up to 2,000 km) in the ENA as far as north as the Arctic Circle, west to the mid-Atlantic Ridge, and south to Madeira in late summer and returned to the Bay of Biscay in spring of the following year. However, like those tagged by Campana et al. (2010), these fish were primarily sub-adult and adult females, which appear to migrate more extensively than juveniles.

Diving Behavior and Water Temperature

As porbeagles migrated seasonally from shelf to offshore habitat, the juveniles tracked during this study also exhibited seasonal changes in their vertical and thermal distribution (**Figures 6**, **7**). Not surprisingly, other pelagic fish have been shown to exhibit similar seasonal shifts in their depth distribution, which are associated with foraging behavior. For example, the movement of blue sharks from shallow to deep habitat is thought to be correlated with prey availability (Queiroz et al., 2010). Similarly, the movements of juvenile porbeagles that we observed are likely linked to foraging behavior mediated by temperature.

In the WNA, Joyce et al. (2002) examined the stomach contents of 1,022 porbeagles and concluded that this species is an opportunistic feeder on a diverse assemblage of pelagic, epipelagic, and benthic fish species, as well as cephalopods, depending on availability. In juveniles (<150 cm), they found that a variety of fishes and cephalopods constituted major portions of the diet. They also observed a strong seasonal diet shift linked to spatial changes in shark distribution, although they

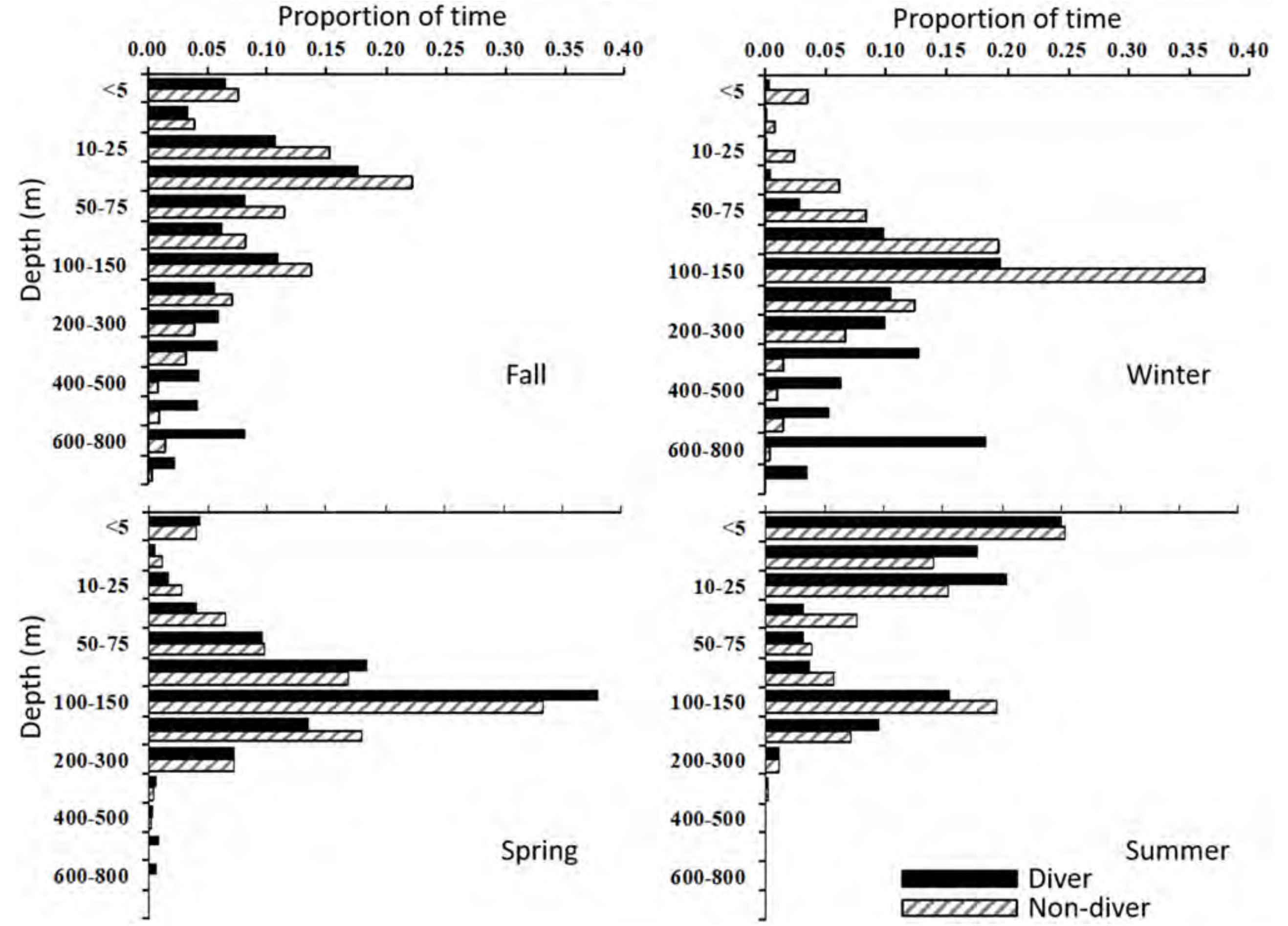

FIGURE 6 | Seasonal time-at-depth histograms for porbeagle divers (solid bar; $n = 10$) and non-divers (hatched bar, $n = 7$) tagged in the western North Atlantic.

grouped the stomach samples coarsely into spring (January-June) and fall (July-December) "seasons" and, hence, do not coincide with true seasons. Regardless, there are some indications that the movements observed in our study are associated with feeding behavior. In stomachs sampled during the months of January to June, Joyce et al. (2002) found a high proportion of cephalopods and pelagic teleosts (e.g., lancetfish, *Alepisaurus ferox*; Atlantic herring, *Clupea harengus*). In our study, this roughly coincides with offshore foraging behavior at epipelagic and mesopelagic depths during the winter. With progression into the autumn months, juvenile porbeagles transitioned off the shelf (**Figure 2**), expanding their vertical behavior. During the late fall and winter, they were broadly distributed along the shelf edge and in offshore regions of the WNA, including the Gulf Stream. Those that we qualify as non-divers remained north of the Gulf Stream or along its northern edge and moved through epipelagic depths (<200 m), spending 84% of the time in a temperature range of 8–16°C. Those juveniles that migrated further offshore into the warm waters of the Gulf Stream and beyond (i.e., divers, **Figure 5**) shifted from epipelagic to mesopelagic habitat and exhibited a bimodal temperature distribution reflective of warm, shallow water and cooler waters at depth. This suggests that, in a manner similar to blue sharks (Carey et al., 1990; Braun et al., 2019) and white sharks (Gaube et al., 2018), these juvenile sharks may potentially dive deep within the Gulf Stream and associated features (i.e., fronts, eddies) in order to exploit more abundant food resources, including pelagic teleosts and cephalopods.

The importance of cephalopods in the diets of large pelagic fishes is well documented in the world's oceans (Smale, 1996). Off the coast of New Zealand, cephalopods were found to be a major component of the porbeagle's diet (Horn et al., 2013). In the offshore waters of the Gulf Stream and Central North Atlantic, Logan et al. (2013) examined stomach samples from nine species of large pelagic tunas, swordfish, and sharks and found that ommastrephid squids were the most common prey group across predator species. Other important prey included octopod, histioteuthid, and architeuthid cephalopods, as well as mesopelagic fishes. Although porbeagle sharks were not sampled by that study, the predominance and abundance of cephalopod species in the region, and reflected in the diets of other pelagic predators, make them a probable component of the porbeagle's diet. During the late fall and winter months, some of the juvenile

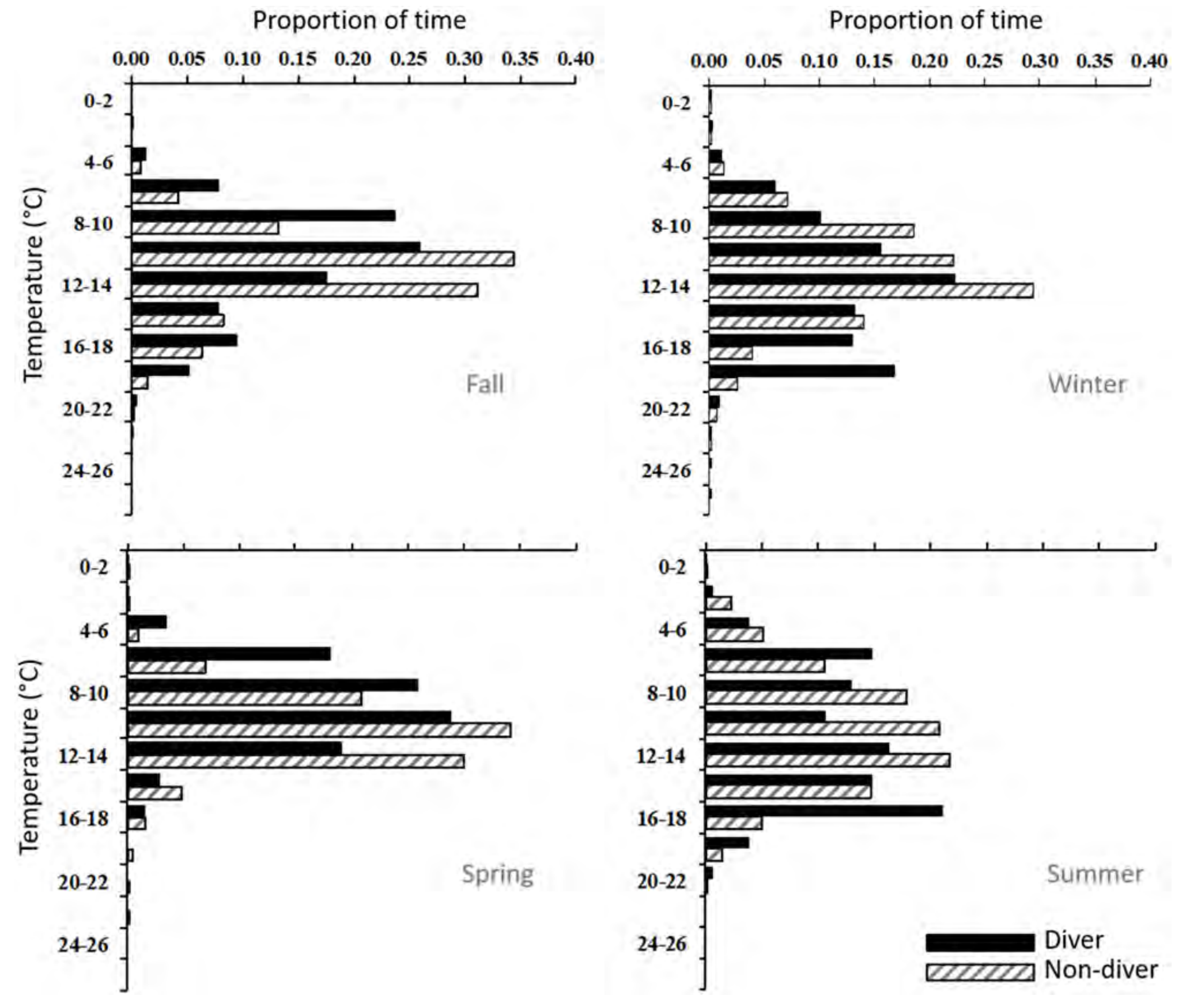

FIGURE 7 | Seasonal time-at-temperature histograms for porbeagle divers (solid bar; $n = 10$) and non-divers (hatched bar, $n = 7$) tagged in the western North Atlantic.

porbeagles tagged in this study moved into these offshore areas (**Figure 5**), which are dominated by cephalopod prey (Logan et al., 2013). Thus, the temporal and spatial distribution of these key prey species may be driving the seasonal differences in depth distribution observed in juvenile porbeagle sharks in this study.

During the spring months, when the porbeagles moved back to the shelf edge and George's Bank (**Figure 2**), they all inhabited epipelagic depths and a predominant temperature range of 6–14°C. During the summer, the porbeagles were shelf-oriented (**Figure 2**), spending all of their time <200 m and 59% of the time in the top 25 m (**Figure 6**). Moving from the surface to the bottom through a well-stratified water column, these sharks spent 97% of the time in the temperature range of 4–18°C (**Figures 3A**, **4A**). In those fish sampled from July to December, Joyce et al. (2002) found a greater proportion of benthic teleosts (groundfish) and fewer pelagics in their stomachs. This reflects summer movement onto the Northeast Shelf Ecosystem, which includes the Gulf of Maine and Georges Bank, and is historically one of the most productive ecosystems in the world, supporting large numbers of fish, invertebrate, and cetacean species (Bigelow and Schroeder, 1953: Kenney and Winn, 1986; German, 1987; Sherman et al., 1988; Fogarty and Murawski, 1998).

The seasonal depth distribution that we observed in porbeagle sharks differs markedly from those previously described in the WNA based on fisheries-dependent catch data (Campana and Joyce, 2004) and PSAT tags (Campana et al., 2010), which suggested that juvenile sharks do not commonly dive >200 m. However, such behavior was observed in the large adult females tagged by Campana et al. (2010). In a pattern remarkably similar to what we observed in our "divers," these mature females encountered the Gulf Stream between 22 December and 9 March, which resulted in an "almost instantaneous initiation of deep diving behavior (daily maximum depth of <248 m before entry and a mean of 845 m after entry)" (Campana et al., 2010). These authors suggested that the porbeagles were migrating beneath the main flow of the Gulf Stream to maximize their net swimming speed, to minimize their ambient temperature, and to ultimately reach the Sargasso Sea for parturition (Campana et al., 2010). Our findings that juvenile porbeagles also exhibit this behavior suggest that foraging, and not reproduction, is likely a key driver of this behavior. As noted by Pade et al. (2009), it is becoming increasingly apparent that the porbeagle exhibits considerable plasticity in horizontal and vertical habitat use and the variable behaviors likely reflect the need for different search strategies depending on habitat and prey types encountered.

Collectively, the results presented in this and previous studies indicate that while porbeagles have broad thermal tolerance, their vertical and horizontal movements are driven by an optimal temperature range. Although the juvenile porbeagles tagged in this study exhibited extensive seasonal shifts in habitat use, both vertically and horizontally, and occupied a broad temperature range of 2–24°C, they spent 97% of the time at 6–20°C. The lower limits reported herein are colder than previous findings using PSAT technology in the WNA (8.0°C, Campana et al., 2010), ENA (9°C, Saunders et al., 2011), and Southern Hemisphere (4.6°C, Francis et al., 2015), but it should be noted that our tagged fish spent only 2% of the time in water <6°C. The sharks in this study also moved into water that was warmer than the maximum reported in the ENA (18.5°C, Pade et al., 2009), but similar to that reported by Campana et al. (2010; 25.4°C). This is associated with movement into the Gulf Stream, yet temperatures in excess of 20°C constituted <1% of the observations. Campana et al. (2010) suggested that the deep diving behavior observed in adult females while in Gulf Stream and Sargasso Sea was driven by water temperature because the surface waters (>22°C) were uninhabitable. Our findings also suggest that the surface waters (<200 m) of the Gulf Stream and temperatures in excess of 20°C represent a thermal barrier that influence the vertical behavior of juvenile porbeagles.

It is important to consider the extent to which, if any, the depth and temperature distribution of porbeagles are influenced (or limited) by their unique thermal physiology. While the body temperature of most sharks closely matches ambient water temperature (i.e., ectothermy) due to loss of all metabolically produced heat via conductive and convective transfer to the surrounding water (Brill et al., 1994), a few sharks (i.e., lamnids and one alopiid) have evolved a suite of morphological adaptations that allow certain regions of their body (i.e., eye, brain, viscera, aerobic swimming muscles) to be maintained warmer relative to ambient temperature (i.e., regional endothermy; Carey and Teal, 1966, 1969a,b; Carey et al., 1971, 1985; Block and Carey, 1985). Regional endothermy may allow these sharks to maintain a more thermally stable internal operating environment during their forays across thermal fronts (Bernal et al., 2001, 2018). Thus, the selective advantages of regional endothermy may have allowed these species, including porbeagles, to expand their thermal niche and make accessible the additional food resources of the cooler, more productive waters at both a greater depth and at higher latitudes (Block and Carey, 1985; Carey et al., 1985; Bernal et al., 2001; Dickson and Graham, 2004).

Carey et al. (1985) compiled *in vivo* muscle and visceral temperatures and compared a suite of anatomical attributes associated with metabolic heat production and conservation (e.g., relative heart size, the amount and distribution of red muscle, the number of vessels in the lateral cutaneous rete) in lamnid sharks and ranked each species by its capacity to elevate its temperature. These endothermic rankings of Carey et al. (1985) are now being validated by PSAT technology, which is generating new horizontal and vertical data about habitat use by these species. For example, it has now been demonstrated that the Pacific salmon shark, ranked first, occupies subarctic winter habitat and demonstrates the greatest tolerance of cold waters, spending 68% of its time in waters cooler than 10°C (Weng et al., 2005). The endothermic capacity of the porbeagle, ranked second by Carey et al. (1985) likely allows this species to remain in northern latitudes year-round in the North Atlantic, spending 46% of the time in waters <12°C based on our findings. In sharp contrast, the white shark (ranked third by Carey et al., 1985) migrates seasonally into temperate latitudes of the WNA, including the Gulf of Maine and the Scotian Shelf, but returns south as water temperatures cool in the late fall; it spends 95% of its time at temperatures >12°C (Skomal et al., 2017). Similarly, the shortfin mako (ranked fifth by Carey et al., 1985), migrates seasonally to northeastern latitudes (59°N) in the WNA (Vaudo et al., 2016; Kohler and Turner, 2019), but habitat use is strongly associated with warmer features and water temperatures between 10 and 15°C represent the lower limit for this species, thereby constraining them horizontally and vertically over the course of the year (Vaudo et al., 2016).

Management

Although juvenile, subadult, and adult porbeagles have been PSAT-tagged on both sides of the Atlantic, none, including the juveniles tagged in this study, have provided evidence of trans-Atlantic movement. The juvenile porbeagle sharks tagged in this study demonstrated an inshore-offshore movement pattern consistent with fidelity to the WNA. Similarly, Biais et al. (2017) found evidence for porbeagle site fidelity and consistent return migrations to and from the Bay of Biscay in the ENA. These porbeagles exhibited migrations as far west as the Mid-Atlantic Ridge, with subsequent movements back to the Bay of Biscay, thereby supporting the idea of a separate ENA stock (Biais et al., 2017). Collectively, these findings support the two stock hypotheses put forth by Pade et al. (2009) and Saunders et al. (2011), and are consistent with conventional tagging data (Kohler and Turner, 2019), in which there is only one documented instance of an immature female porbeagle moving 4,260 km during a trans-Atlantic crossing from Ireland to Canada (Cameron et al., 2018). Nonetheless, molecular analyses have found that porbeagles sampled in the WNA and ENA are not genetically distinct, suggesting some level of migration and mixing (Testerman, 2014). Most recently, Haugen (2020) conducted an interdisciplinary review of all available information (i.e., life history, genetics, and movement) to evaluate North Atlantic stock structure in this species and concluded that geographic variation in life-history traits and movement patterns indicate one phenotypic stock in the WNA and another in the ENA, despite genetic analyses indicating gene flow and genetic homogeneity between the two regions. Based on our findings, coupled with this information, management of the porbeagle should be based on two stocks.

In the North Atlantic, major harvesters of porbeagle have either ceased landing (European Union, Canada) or capped landings (USA) in an effort to allow for the rebuilding of stocks (Campana et al., 2015; reviewed by Haugen, 2020). However, porbeagle bycatch occurs in several fisheries including pelagic longlines, gillnets, and trawls (Curtis et al., 2016; Haugen, 2020). In this study, we found that juvenile porbeagles ranged from shelf waters to the Gulf Stream and are, therefore, susceptible to these fisheries. A recent analysis of the overlap of shark distribution and pelagic longline fishing effort concluded that porbeagle occur in the highest-risk zone in the North Atlantic with high potential for mortality as a result of incidental bycatch (Queiroz et al., 2019). Although the ICCAT (2009) assessment concluded that longline bycatch on the high seas is minor and does not pose a significant threat to the species, at-vessel and post-release mortality is thought to be high (average = 47%; reviewed by Curtis et al., 2016). In the current study, we captured 88 juvenile porbeagles on two pelagic longline sets (525 hooks total) with relatively short soak times (3–5 h) and 21 (24%) sharks were dead at haulback. This not only indicates that porbeagle catch rates can be high on pelagic longlines when these sharks are associated with the shelf, but could lead to significant at-vessel mortality.

In addition to pelagic longline gear, porbeagles are also taken by trawl and gillnet fisheries while in shelf waters. A recent analysis of observer data collected from US gillnet and trawl fisheries indicated that annual bycatch and discards of porbeagles can be on the order of several hundred metric tons in recent years (Haugen, 2020). Unfortunately, these estimates have not been incorporated into stock assessments for this species. Clearly, bycatch mortality might be more substantial than previously thought and all sources need to be taken into consideration in future stock assessments. Our findings show a relatively high risk for juveniles in multiple fisheries across the distribution of this species and highlight the need for continued protection for stock rebuilding.

In this study, we demonstrate that juvenile porbeagles are more broadly distributed in the WNA using near-coastal, shelf habitat during the warm months and migrating to pelagic habitat from the shelf edge to the Gulf Stream during the winter. When in the latter, these sharks exhibited mesopelagic foraging behavior likely driven by cephalopod prey abundance and water temperature. The residency of juvenile porbeagles in temperate latitudes throughout the year is likely facilitated by its endothermic capacity. Additional studies that link these movements with the foraging ecology and physiology of this species are warranted.

DATA AVAILABILITY STATEMENT

The raw data supporting the conclusions of this article will be made available by the authors, without undue reservation.

ETHICS STATEMENT

All methods associated with the capture and handling of sharks were reviewed and approved by Institutional Animal Care and Use Committee of the University of Massachusetts, Dartmouth (Protocol #05-07).

AUTHOR CONTRIBUTIONS

GS and DB conceived the study. GS, HM, and LN performed the field work. GS, HM, BG, and CB conducted the data analyses. GS, HM, and DB wrote the initial draft and all authors provided edits and approval. All authors contributed to the article and approved the submitted version.

FUNDING

This research was funded by the Large Pelagics Research Center (Grant 06-125).

ACKNOWLEDGMENTS

This research was carried out under Exempted Fishing Permit SHK-EFP-06-05 issued by the NMFS Highly Migratory Species Management Division. Special thanks to the crew of F/V Eagle Eye II for working with us to find and tag porbeagles. This research was funded by the Large Pelagics Research Center (Grant 06-125) and Federal Aid in Sport Fish Restoration. This is Massachusetts Division of Marine Fisheries Contribution No. 118.

REFERENCES

Bernal, D., Dickson, K. A., Shadwick, R. E., and Graham, J. B. (2001). Review: analysis of the evolutionary convergence for high performance swimming in lamnid sharks and tunas. *Comp. Biochem. Physiol. A* 129, 695–726. doi: 10.1016/S1095-6433(01)00333-6

Bernal, D., Donley, J. M., Shadwick, R. E., and Syme, D. A. (2005). Mammal-like muscles power swimming in a cold-water shark. *Nature* 437, 1349–1352. doi: 10.1038/nature04007

Bernal, D., Reid, J. P., Roessig, J. M., Matsumoto, S., Sepulveda, C. A., Cech, J. J., et al. (2018). Temperature effects on the blood oxygen affinity in sharks. *Fish Physiol. Biochem*. 44, 949–967. doi: 10.1007/s10695-018-0484-2

Biais, G., Coupeau, Y., Séret, B., Calmettes, B., Lopez, R., Hetherington, S., et al. (2017). Return migration patterns of porbeagle shark (Lamna nasus) in the Northeast Atlantic: implications for stock range and structure. *ICES J. Mar. Sci.* 74, 1268–1276. doi: 10.1093/icesjms/fsw233

Bigelow, H. B., and Schroeder, W. C. (1953). *Fishes of the Gulf of Maine (No. 592).* Washington, DC: US Government Printing Office.

Bleck, R. (2002). An oceanic general circulation model framed in hybrid isopycnic-Cartesian coordinates. *Ocean Model* 4, 55–88. doi: 10.1016/S1463-5003(01)00012-9

Block, B. A. (2005). Physiological ecology in the 21st century: Advancements in biologging science. *Integr. Comp. Biol.* 45, 305–320. doi: 10.1093/icb/45.2.305

Block, B. A., and Carey, F. G. (1985). Warm brain and eye temperatures in sharks. *J. Comp. Physiol. B* 156, 229–236. doi: 10.1007/BF00695777

Braun, C. D., Galuardi, B., and Thorrold, S. R. (2018). HMMoce: An R package for improved geolocation of archival-tagged fishes using a hidden Markov method. *Meth. Ecol. Evol*. 9, 1212–1220. doi: 10.1111/2041-210X.12959

Braun, C. D., Gaube, P., Sinclair-Taylor, T. H., Skomal, G. B., and Thorrold, S. R. (2019). Mesoscale eddies release pelagic sharks from thermal constraints to foraging in the ocean twilight zone. *Proc. Natl. Acad. Sci. U.S.A.* 116, 17187–17192. doi: 10.1073/pnas.1903067116

Brill, R. W., Dewar, H., and Graham, J. B. (1994). Basic concepts relevant to heat transfer in fishes, and their use in measuring the physiological thermoregulatory abilities of tunas. *Environ. Biol. Fish*. 40, 109–124. doi: 10.1007/BF00002538

Cameron, L. W. J., Roche, W., Green, P., Houghton, J. D. R., and Mensink, P. J. (2018). Transatlantic movement in porbeagle sharks (Lamna nasus). *Fish. Res*. 207, 25–27. doi: 10.1016/j.fishres.2018.05.014

Campana, S. E., Fowler, M., Houlihan, D., Joyce, W. N., Showell, M., Simpson, M., et al. (2015). Recovery potential assessment for porbeagle (*Lamna nasus*) in Atlantic Canada. *DFO Can. Sci. Advis. Sec. Res. Doc*. 41:45.

Campana, S. E., Joyce, W., and Fowler, M. (2010). Subtropical pupping ground for a cold-water shark. *Can. J. Fish. Aquat. Sci*. 67, 769–773. doi: 10.1139/F10-020

Campana, S. E., and Joyce, W. N. (2004). Temperature and depth associations of the porbeagle shark (*Lamna nasus*) in the northwest Atlantic. *Fish. Oceanog*. 13, 52–64. doi: 10.1111/j.1365-2419.2004.00236.x

Carey, F. G., Casey, J. G., Pratt, H., Urquhart, D., and McCosker, J. E. (1985). Temperature, heat production, and heat exchange in lamnid sharks. *Mem. S. Cal. Acad. Sci*. 9, 92–108.

Carey, F. G., Scharold, J. V., and Kalmijn, A. J. (1990). Movements of blue sharks (Prionace glauca) in depth and course. *Mar. Biol*. 106, 329–342. doi: 10.1007/BF01344309

Carey, F. G., and Teal, J. M. (1966). Heat conservation in tuna fish muscle. *Proc.Nat. Acad. Sci. U.S.A.* 56:1464. doi: 10.1073/pnas.56.5.1464

Carey, F. G., and Teal, J. M. (1969a). Regulation of body temperature by the bluefin tuna. *Comp. Biochem. Physiol*. 28, 205–213. doi: 10.1016/0010-406X(69)91336-X

Carey, F. G., and Teal, J. M. (1969b). Mako and porbeagle: warm-bodied sharks. *Comp. Biochem. Physiol*. 28, 199–204. doi: 10.1016/0010-406X(69)91335-8

Carey, F. G., Teal, J. M., Kanwisher, J. W., Lawson, K. D., and Beckett, J. S. (1971). Warm-bodied fish. *Amer. Zool*. 11, 137–143. doi: 10.1093/icb/11.1.137

Chassignet, E. P., Hurlburt, H. E., Smedstad, O. M., Halliwell, G. R., Hogan, P. J., Wallcraft, A. J., et al. (2007). The HYCOM (HYbrid Coordinate Ocean Model) data assimilative system. *J. Mar. Syst*. 65, 60–83. doi: 10.1016/j.jmarsys.2005.09.016

CMS (2008). *Proposal for Inclusion of Species on the Appendices of the Convention on the Conservation of Migratory Species of Wild Animals*. Proposal II /10/Rev.1. 16pp.

Compagno, L. J. V. (2002). *FAO Species Catalogues. Sharks of the World. An Annotated and Illustrated Catalogue of the Shark Species Known to Date, parts 1 and 2*. Rome: FAO Fish.

Costa, D. P., Breed, G. A., and Robinson, P. W. (2012). New insights into pelagic migrations: implications for ecology and conservation. *Annu. Rev. Ecol. Evol. Syst*. 43, 73–96. doi: 10.1146/annurev-ecolsys-102710-145045

Curtis, T. H., Laporte, S., Cortes, E., DuBeck, G., and McCandless, C. (2016). *Status Review Report: Porbeagle Shark (Lamna nasus)*. Final Report to National Marine Fisheries Service, Office of Protected Resources.

Dickson, K. A., and Graham, J. B. (2004). Evolution and consequences of endothermy in fishes. *Physiol. Biochem. Zool*. 77, 998–1018. doi: 10.1086/423743

Fogarty, M. J., and Murawski,. S. A. (1998). Large-scale disturbance and the structure of marine systems: fishery impacts on Georges Bank. *Ecol. Appl*. 8, S6–S22. doi: 10.1890/1051-0761(1998)8[S6:LDATSO]2.0.CO;2

Francis, M. P., Holdsworth, J. C., and Block, B. A. (2015). Life in the open ocean: seasonal migration and diel diving behaviour of Southern Hemisphere porbeagle sharks (Lamna nasus). *Mar. Biol*. 162, 2305–2323. doi: 10.1007/s00227-015-2756-z

Galuardi, B., Royer, F., Golet, W., Logan, J., Nielson, J., and Lutcavage, M. (2010). Complex migration routes of Atlantic Bluefin tuna question current population structure paradigm. *Can J. Fish. Aquat. Sci*. 67, 966–976. doi: 10.1139/F10-033

Gaube, P., Braun, C. D., Lawson, G. L., McGillicuddy, D. J., Penna, A., Della, S.komal, G. B., et al. (2018). Mesoscale eddies influence the movements of mature female white sharks in the Gulf Stream and Sargasso Sea. *Sci. Rep*. 8:7363. doi: 10.1038/s41598-018-25565-8

German, A. W. (1987). "History of the early fisheries: 1720–1930," *Georges Bank,* R. Backus ed (Cambridge, MA, Massachusetts Institute of Technology), 409–424.

Goldman, K. J. (1997). Regulation of body temperature in the white shark, Carcharadon carcharias. *J. Comp. Physiol. B* 167, 423–429. doi: 10.1007/s003600050092

Goldman, K. J., Anderson, S. D., Latour, R. J., and Musick, J. A. (2004). Homeothermy in adult salmon sharks, Lamna ditropis. *Env. Biol. Fish*. 71, 403–411. doi: 10.1007/s10641-004-6588-9

Haugen, J. B. (2020). *Fishery Management*, *Conservation, and Bycatch of North Atlantic Porbeagle*. [dissertation] University of Massachusetts Dartmouth, Dartmouth, MA, United States.

Horn, P. L., Ballara, S. L., Sutton, P., and Griggs, L. H. (2013). *Evaluation of the Diets of Highly Migratory Species in New Zealand waters*. Wellington: Ministry for Primary Industries.

ICCAT (2009). *Report of the 2009 Porbeagle Stock Assessment Meeting*. Madrid: SCRS/2009/014.

Jensen, C. F., Natanson, L. J., Pratt Jr, H. L., Kohler, N. E., and Campana, S. E. (2002). The reproductive biology of the porbeagle shark (*Lamna nasus*) in the western North Atlantic Ocean. *Fish. Bull*. 100, 727–738.

Joyce, W. N., Campana, S. E., Natanson, L. J., Kohler, N. E., Pratt Jr, H. L., and Jensen, C. F. (2002). Analysis of stomach contents of the porbeagle shark (*Lamna nasus* Bonaterre) in the northwest Atlantic. *ICES J. Mar. Sci*. 59, 1263–1269. doi: 10.1006/jmsc.2002.1286

Kenney, R. D., and Winn, H. E. (1986). Cetacean high-use habitats of the northeast United States continental shelf. *Fish. Bull*. 84, 345–357.

Kohler, N. E., and Turner, P. A. (2001). Shark tagging: a review of conventional methods and studies. *Env. Biol. Fish*. 60, 191–223. doi: 10.1007/978-94-017-3245-1_12

Kohler, N. E., and Turner, P. A. (2019). Distributions and movements of Atlantic shark species: a 52-year retrospective atlas of mark and recapture data. *Mar. Fish. Rev*. 81, 1–93. doi: 10.7755/MFR.81.2.1

Logan, J. M., Toppin, R., Smith, S., Galuardi, B., Porter, J., and M., Lutcavage (2013). Contribution of cephalopod prey to the diet of large pelagic fish predators in the central North Atlantic Ocean. *Deep Sea Res. II* 95, 74–82. doi: 10.1016/j.dsr2.2012.06.003

Luo, J., Ault, J. S., Shay, L. K., Hoolihan, J. P., Prince, E. D., Brown, C., et al. (2015). Ocean heat content reveals secrets of fish migrations. *PLoS ONE* 10:e0141101. doi: 10.1371/journal.pone.0141101

Musyl, M., Brill, R., McNaughton, L., Swimmer, Y., Domeier, M., Nasby-Lucas, N., et al. (2011). Performance of pop-up satellite archival tags. *Fish. Ocean*. 433, 1–28. doi: 10.3354/meps09202

NASA JPL (2015). *GHRSST Level 4 MUR Global Foundation Sea Surface Temperature Analysis* (v4.1). Pasadena.

Natanson, L. J., Deacy, B. M., Joyce, W., and Sulikowski, J. (2019). Presence of a resting population of female porbeagles (*Lamna nasus*), indicating a biennial reproductive cycle, in the western North Atlantic Ocean. *Fish. Bull*. 117:8. doi: 10.7755/FB.117.1-2.8s

Pade, N. G., Queiroz, N., Humphries, N. E., Witt, M. J., Jones, C. S., Noble, L. R., et al. (2009). First results from satellite-linked archival tagging of porbeagle shark, Lamna nasus: area fidelity, wiser-scale movements and plasticity in diel depth changes. *J. Exp. Mar. Biol. Ecol*. 370, 64–74. doi: 10.1016/j.jembe.2008.12.002

Queiroz, N., Humphries, N. E., Couto, A., Vedor, M., Da Costa, I., Sequeira, A., et al. (2019). Global spatial risk assessment of sharks under the footprint of fisheries. *Nature* 572, 461–466. doi: 10.1038/s41586-019-1444-4

Queiroz, N., Humphries, N. E., Noble, L. R., Santos, A. M., and Sims, D. W. (2010). Short-term movements and diving behavior of satellite-tracked blue sharks *Prionace glauca* in the northeastern Atlantic Ocean. *Mar. Ecol. Prog. Ser*. 406, 265–279. doi: 10.3354/meps08500

Rigby, C. L., Barreto, R., Carlson, J., Fernando, D., Fordham, S. V., Francis, M. P., et al. (2018). *Lamna nasus: The IUCN Red List of Threatened*

Species 2019 Global. International Union for Conservation of Nature. Available online at: https://www.iucnredlist.org/species/11200/500969 (accessed 17 February 2020).

Saunders, R. A., Royer, F., and Clarke, M. W. (2011). Winter migration and diving behaviour of porbeagle shark, Lamna nasus, in the Northeast Atlantic. *ICES J. Mar. Sci*. 68, 166–174. doi: 10.1093/icesjms/fsq145

Sepulveda, C. A., Kohin, S., Chan, C., Vetter, R., and Graham, J. B. (2004). Movement patterns, depth preferences, and stomach temperatures of free-swimming juvenile mako sharks, Isurus oxyrinchus, in the Southern California Bight. *Mar. Biol*. 145, 191–199. doi: 10.1007/s00227-004-1356-0

Sherman, K., Grosslein, M., Mountain, D., Busch, D., O'Reilly, J., and Theroux, R. (1988). "The continental shelf ecosystem off the northeast coast of the United States," in *Ecosystems of the World 27: Continental Shelves,* H. Postema, and J. J. Zijlstra, eds (Amsterdam: Elsevier Press), 279–337.

Skomal, G. B., Braun, C. D., Chisholm, J. H., and Thorrold, S. R. (2017). Movements of the white shark *Carcharodon carcharias* in the North Atlantic Ocean. *Mar. Ecol. Prog. Ser*. 580, 1–16. doi: 10.3354/meps12306

Skomal, G. B., Zeeman, S. I., Chisholm, J. H., Summers, E. L., Walsh, H. J., McMahon, K. W., et al. (2009). Transequatorial migrations by basking sharks in the western Atlantic Ocean. *Cur. Biol*. 19, 1019–1022. doi: 10.1016/j.cub.2009.04.019

Smale, M. J. (1996). Cephalopods as prey. IV. Fishes. *Philos. Trans. R. Soc. London B Biol. Sci*. 351, 1067–1081. doi: 10.1098/rstb.1996.0094

Testerman, C. B. (2014). *Molecular Ecology of Globally Distributed Sharks*. [dissertation] Nova Southeastern University, Fort Lauderdale, FL, United States.

Vaudo, J. J., Byrne, M. E., Wetherbee, B. M., Harvey, G. M., and Shivji, M. S. (2017). Long-term satellite tracking reveals region-specific movements of a large pelagic predator, the shortfin mako shark, in the western North Atlantic Ocean. *J. App. Ecol*. 54,1765–1775. doi: 10.1111/1365-2664.12852

Vaudo, J. J., Wetherbee, B. M., Wood, A. D., Weng, K., Howey-Jordan, L. A., Harvey, G. M., et al. (2016). Vertical movements of shortfin mako sharks Isurus oxyrinchus in the western North Atlantic Ocean are strongly influenced by temperature. *Mar. Ecol. Prog. Ser*. 547, 163–175. doi: 10.3354/meps11646

Weng, K. C., Castilho, P. C., Morrissette, J. M., Landeira-Fernandez, A. M., Holts, D. B., Schallert, R. J., et al. (2005). Satellite tagging and cardiac physiology reveal niche expansion in salmon sharks. *Science*. 310, 104–106. doi: 10.1126/science.1114616

Conflict of Interest: The authors declare that the research was conducted in the absence of any commercial or financial relationships that could be construed as a potential conflict of interest.

frontiers in Marine Science

ORIGINAL RESEARCH
published: 16 March 2021
doi: 10.3389/fmars.2021.645142

Interannual Nearshore Habitat Use of Young of the Year White Sharks Off Southern California

James M. Anderson[1]*, Echelle S. Burns[2,3,4], Emily N. Meese[5], Thomas J. Farrugia[1,6], Brian S. Stirling[1], Connor F. White[7], Ryan K. Logan[8], John O'Sullivan[9], Chuck Winkler[10] and Christopher G. Lowe[1]

[1] Department of Biological Sciences, California State University, Long Beach, CA, United States, [2] Marine Science Institute, University of California, Santa Barbara, Santa Barbara, CA, United States, [3] Bren School of Environmental Science & Management, University of California, Santa Barbara, Santa Barbara CA, United States, [4] Environmental Market Solutions Lab, University of California, Santa Barbara, Santa Barbara, CA, United States, [5] Department of Marine Biology, Texas A&M University at Galveston, Galveston, TX, United States, [6] Alaska Ocean Observing System, Anchorage, AK, United States, [7] Department of Organismic and Evolutionary Biology, Harvard University, Cambridge, MA, United States, [8] Guy Harvey Research Institute, Nova Southeastern University, Dania Beach, FL, United States, [9] Monterey Bay Aquarium, Monterey, CA, United States, [10] Aquatic Research Consultants, San Pedro, CA, United States

OPEN ACCESS

Edited by:
J. Marcus Drymon,
Mississippi State University,
United States

Reviewed by:
Matthew Ajemian,
Florida Atlantic University,
United States
Charlie Huveneers,
Flinders University, Australia

***Correspondence:**
James M. Anderson
james.anderson@csulb.edu

Specialty section:
This article was submitted to
Marine Megafauna,
a section of the journal
Frontiers in Marine Science

Received: *22 December 2020*
Accepted: *23 February 2021*
Published: *16 March 2021*

Citation:
Anderson JM, Burns ES, Meese EN, Farrugia TJ, Stirling BS, White CF, Logan RK, O'Sullivan J, Winkler C and Lowe CG (2021) Interannual Nearshore Habitat Use of Young of the Year White Sharks Off Southern California.
Front. Mar. Sci. 8:645142.
doi: 10.3389/fmars.2021.645142

Young-of-the-year (YOY) and juvenile-stage white sharks may use southern California nearshore beach habitats more extensively than previously known, within meters of some of the most heavily used beaches in the world. Such knowledge forms a critical component of species management and conservation plans, in addition to public safety and risk mitigation planning. We used data derived from a combination of satellite tag locations (13 animals over 3 years) and passive acoustic monitoring (34 animals over 8 years) to examine the occurrence, relative abundance, and residency patterns of YOY white sharks in southern California waters. Our results suggest that southern California contains spatiotemporally dynamic centers of primary nursery habitat. Tagged YOY white sharks formed loose aggregations at "hotspot" locations that were interannually variable, where individuals exhibited temporal fidelity, higher levels of residency, and spatially restricted movements, with multiple YOY individuals simultaneously displaying this behavior. While models of biotic and abiotic variables suggested relative abundance of tagged sharks may be predicted by sea surface temperature, salinity and productivity (chlorophyll-A), these predictors were not consistent across all years of the study. Thus, novel approaches that incorporate technologies to derive high resolution environmental data, paired with more comprehensive telemetry datasets are therefore required to better understand the extrinsic factors that drive habitat selection and residency patterns in juvenile white sharks.

Keywords: ***Carcharodon carcharias*, nursery habitat dynamics, residency, young-of-the-year, space use**

INTRODUCTION

Many coastal shark species are known to select nearshore habitats (e.g., bays, lagoons, and estuaries) during early life stages with neonates and young-of-the-year (YOY) exhibiting reduced space use within these areas (Heupel et al., 2004, 2007; Hueter et al., 2005; Speed et al., 2010; Oh et al., 2017). In some cases, pregnant females give birth in these habitats, while other species may give birth elsewhere and YOY individuals find their way into these areas (Chapman et al., 2015). These protected, shallow, nearshore habitats are thought to offer protection from predation, enhanced prey availability, and typically warm temperatures to allow for faster growth and higher survivorship (Heupel et al., 2004; Hueter et al., 2005; Speed et al., 2012). For most temperate and subtropical species, parturition is seasonal, usually associated with periods of increased temperature, daylength, and primary productivity. Some oceanic species [e.g., shortfin mako (*Isurus oxyrinchus*), salmon sharks (*Lamna ditropis*), and blue sharks (*Prionace glauca*)] are known to use less discrete areas as nursery habitats in open water, that are selected for their warmer conditions and higher productivity (Bustamante and Bennett, 2013; Carlisle et al., 2015; Logan et al., 2020). Neonates and YOYs of oceanic species are considered to be more wide ranging, and their distributions may be more vertically limited compared to adults (Afonso and Hazin, 2015; Carlisle et al., 2015; Hoyos-Padilla et al., 2016; Vandeperre et al., 2016; Coffey et al., 2017). However, while white sharks exhibit an offshore, oceanic phase as adults, YOY individuals [<175 cm total length (TL)] are predominantly found in coastal habitats, which suggests that although birthing in white sharks has not been observed and parturition habitats are unknown, parturition may occur proximally to the nearshore environment (Dewar et al., 2004; Weng et al., 2007a,b; Jorgensen et al., 2012; Domeier and Nasby-Lucas, 2013; Lyons et al., 2013; Harasti et al., 2017; Curtis et al., 2018; Logan et al., 2018; Bruce et al., 2019; White et al., 2019; Bradford et al., 2020; Spaet et al., 2020b).

The Southern California Bight (SCB) extends from Point Conception, CA, United States (34.4° N) to Cabo Banda, Baja California, MX, United States (31.7° N) (Schiff et al., 2016), encompassing a coastline that stretches approximately 560 km. Fisheries catch records of juvenile white sharks (123–300 cm TL) in the SCB suggest this area (Klimley, 1985; Domeier, 2012; Lowe et al., 2012) and Baja, Mexico (Santana-Morales et al., 2012; Oñate-González et al., 2017) serves as a nursery for the Northeast Pacific population. Catch locations of juvenile white sharks in southern California typically occurred less than 20 km from shore and in water depths less than 100 m, and seem to be aggregated at particular locations along the coastline (Lowe et al., 2012; Lyons et al., 2013). While capture locations were fishery dependent, most individuals were captured as bycatch in fisheries targeting nearshore fishes such as California halibut (*Paralichthys californicus*) and white seabass (*Atractoscion nobilis*), species typically associated with sand substratum or ecotone to rocky reefs. YOY white sharks previously fitted with satellite transmitters in southern California have been shown to remain in southern California waters during summer months, but exhibit southerly migrations to the coastal waters of Baja, Mexico during winter months (Weng et al., 2012; White et al., 2019). Estimated daily positions and tracks from juvenile white sharks tagged with pop-up archival tags (PAT tags) indicate individuals spent substantial time in offshore areas (Weng et al., 2007b). This apparent westward distribution of sharks from the coast is likely attributed to the poor spatial resolution of this technology (Dewar et al., 2004; Weng et al., 2012). Conversely, Smart Position Or Temperature Transmitter (SPOT) tagged YOY and juvenile white sharks have consistently displayed nearshore habitat use (Lyons et al., 2013; Weng et al., 2007b; White et al., 2019; Spaet et al., 2020b).

In addition to historic fishery catch location data and SPOT tag geo-position data, there has been considerable anecdotal visual observations of YOY and juvenile white sharks using beach habitat (<200 m from the shoreline) throughout southern California (Lowe et al., unpublished data). These observations are in contrast to the resolution of SPOT tags, which showed tagged individuals displaying surface-oriented behaviors within approximately 7 km of the shore (White et al., 2019) and suggest juvenile and YOY white sharks may use nearshore beach habitats (<200 m from the shoreline) more extensively than previously documented. Such actualities are likely to be an important consideration in management and conservation initiatives for the species, at both the state and federal level. For example, while white shark capture is prohibited in California fisheries, YOY white shark mortality may be increased via bycatch in shore-based recreational fisheries (Benson et al., 2018), potentially inhibiting recovery for this protected species. Additionally, contaminant exposure may be increased for this important age class of white sharks if they are spending considerable time in waters with high amounts of runoff from the densely populated southern California coastline (Lyons and Wynne-Edwards, 2021), with potential long-term ramifications to the population. To address the question of nearshore habitat use, we employed a large, nearshore passive acoustic receiver array, spanning the southern California coastline and offshore islands to quantify interannual distribution and shifts in nearshore beach habitat use of YOY white sharks fitted with coded acoustic transmitters, and examined the extent of pelagic and non-acoustically monitored habitat via YOY white sharks fitted with SPOT tags.

MATERIALS AND METHODS

Study Location and Monitoring Area

The area acoustically monitored spanned from Santa Barbara County to San Diego County, with additional acoustic receivers around the northern Channel Islands and Santa Catalina Island (**Figure 1**). For the purposes of these analyses, the southern California coastline was considered as the area between Point Conception (34.442° N, 120.453° W) and San Diego (32.751° N, 117.161° W). Acoustic receiver coverage increased in southern California over the study period (2010–2018; **Table 1**).

Tag Models and Procedures

Acoustic Tags

A total of 44 YOY white sharks were tagged with coded acoustic transmitters between January 2010 and December 2018. Sharks were tagged with Vemco V16 or V13 coded acoustic transmitters (Vemco|Innovasea, NS, Canada; transmitter family V13-1x-069k, V13-2x-069k, V16-4x-069k, V16-5x-069k, and V16-6x-069k) via one of three ways.

(i) Incidental catch: In collaboration with local commercial gillnet fishers, incidentally captured YOY white sharks

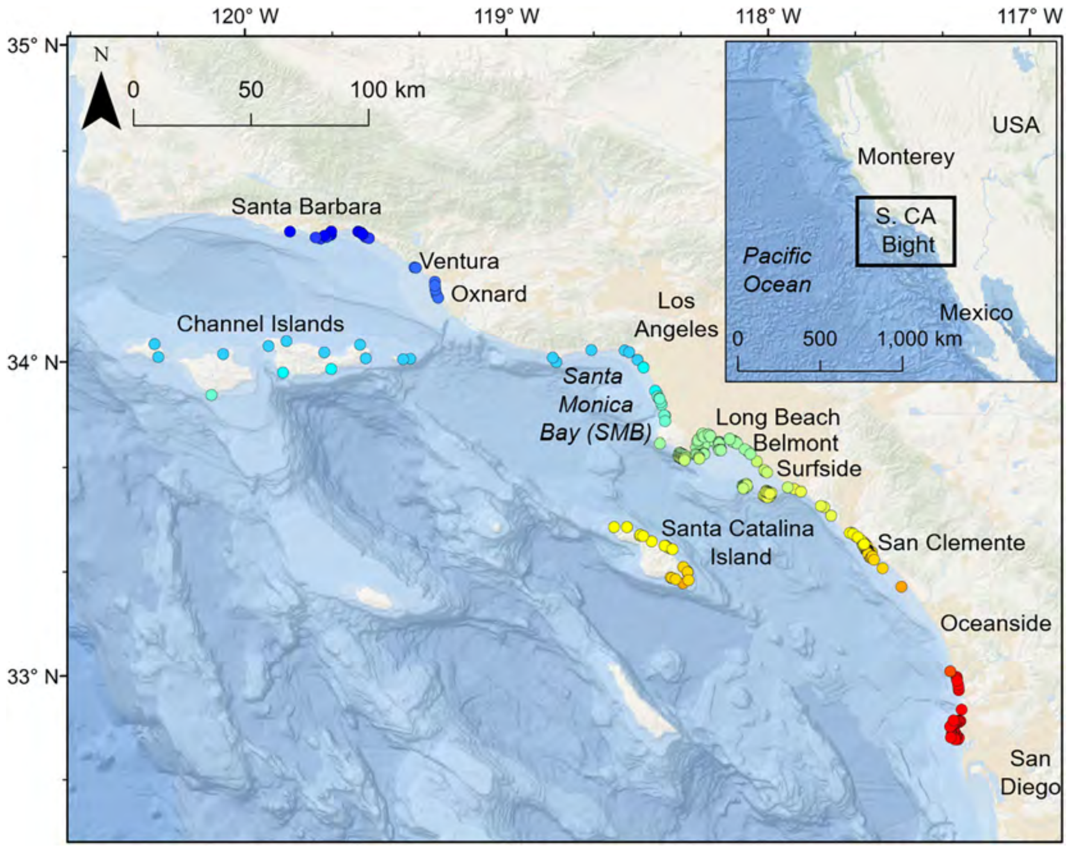

FIGURE 1 | Study area and locations of all receivers used in the study (2014–2018). Receiver locations are color coded according to latitude.

TABLE 1 | Receiver and tag deployment details across all years included in the study.

Year	Total unique receivers	Total unique zones covered	Mean unique receivers per zone	Tags deployed (year^{-1})	Principle tagging location(s)	Total YOY's tagged
2010	39	17	2.3529412	2	SMB	2
2011	46	27	1.7037037	1	Ventura	3
2012	86	44	1.9772727	4	Ventura, SMB	7
2013	99	56	1.7857143	1	SMB	8
2014	162	89	1.9213483	0	NA	8
2015	163	78	2.1794872	14	Surfside, Ventura	22
2017	148	93	1.7526882	5	Long Beach, Ventura	27
2018	153	100	1.94	7	Santa Barbara, Oxnard	34

were brought to the nearest port in a large fish tote (1.2 × 1.2 × 1.2 m) with flowing seawater. Researchers met fishers to physically assess, measure, and surgically implant a plasma-sterilized V16 transmitter into the shark into the abdominal cavity of the shark through a small incision (5 cm). The wound was closed with 2–3 interrupted sutures. Tagged YOY white sharks were then transported approximately 2 km offshore and released. Approximate elapsed times from researchers taking possession of the shark to offshore release were <30 min.

(ii) Targeted catch: YOY white sharks were caught in shallow inshore waters either via a purse-seine, or via targeted quick-extraction with a gillnet. Once restrained by the net, YOY sharks were transferred to a custom-made staging tank and ventilated, before being sexed, sized, and outfitted with a surgically implanted V16 transmitter as described in (i). Approximate handling times in all instances were <20 min.

(iii) Dart tagging: YOY white sharks swimming close to, or at the surface (at least 2 m visibility) were approached by either a small boat or jet-ski from behind, with the aim of minimizing stress and flight response from the targeted animal. When possible, sex of individual was determined using a pole-mounted dip camera. As physical measurement of animals was not possible via this tagging method, shark size (TL, cm) was estimated by comparison to an object of known size (the watercraft) from orthogonal aerial drone footage. Comparative methods such these have been shown to produce valid estimates of size (May et al., 2019). YOY sharks were tagged with either a V13 or V16 using a 3 m long pole, or with a modified pole-spear fitted with a tag applicator. Tags were inserted into the dorsal musculature at the base of the first dorsal fin using a titanium dart tethered to the tag. Approximate time from first sighting of an animal to tag deployment was <5 min. Minimum expected tag-retention for transmitters deployed in this manner was 1 year (Lowe et al., unpublished data).

Satellite Tags

Thirteen YOY white sharks caught via incidental or targeted efforts (see above), tagged between 2006 and 2009, were outfitted with SPOT tags (position only), mounted to the dorsal fin (mini SPOT 5AM-S182C and AM-S183E; Wildlife Computers, WA, United States) to allow real-time monitoring of tagged sharks' geographic position whenever the tag was able to transmit a signal to the ARGOS satellite network. These data were included to facilitate analysis of YOY movement and habitat use patterns when not in acoustically monitored locations.

All capture and tagging procedures were carried out in accordance with State and Federal permits. All experimental protocols were approved under CSULB IACUC protocol #364.

Data Analysis

To spatially examine tagged shark occurrence, relative abundance and residency patterns at monitored locations, a fishnet shapefile with a grid size of 0.01 by 0.01 degrees (generating grid cells approximately 1.2 km^2 in area), including all monitored nearshore and offshore locations in southern California was generated in ArcMap (version 10.5.1). Each grid cell was assigned a zone ID (hereby "zone") value which allowed for the direct comparison of shark presence both within and across monitored areas due to heterogeneous distribution and density of receivers throughout the study area.

Satellite Data

A total of 997 ARGOS locations were obtained from the 13 deployed SPOT tags. To minimize uncertainty in the location estimates, ARGOS locations were filtered to include only location quality classes 1, 2, and 3, which have estimated errors of less than 1500 m (Costa et al., 2010). As we were only interested in the geographic location of position estimates derived from SPOT tags, and the proximity of these location estimates to nearshore habitat, as well as acoustically monitored zones, we did not attempt to interpolate movement paths (tracks) of SPOT tagged YOY white sharks (e.g., through Hidden Markov or State-Space models). SPOT locations were also limited (filtered) to southern California, and locations from the same shark that were less than 1 min apart were removed, resulting in 337 high quality locations. Bathymetric maps from NOAA were used to extract underlying depth at each SPOT location using the "marmap" package in R (Pante et al., 2019). A shapefile of shore types from the California Department of Fish and Wildlife was used to determine the distance from shore and the nearest shore habitat type (beach, hardened shore, or rocky shore) associated with each location using the "rgeos" package in R. Additionally, SPOT locations were aggregated by grid cell zones described above. All analyses of the satellite tag data were carried out in R (version 3.6.0).

Acoustic Monitoring

We determined seasonal and annual occurrence, relative abundance, and residency patterns of tagged YOY white sharks in nearshore southern California waters and associated offshore islands using passive acoustic telemetry for all tagged sharks detected between January 1, 2010 and December 31, 2018. Acoustic detection data were acquired from a wide-spread acoustic receiver array (up to 75 receivers) comprised of Vemco VR2 and VR2W receivers, deployed between Goleta/Santa Barbara and San Diego, spanning a linear distance of 450 km (**Figure 1**), but also included offshore island monitoring sites. From north to south, these included locations proximal to the following locations/landmarks: Santa Barbara, Ventura, and Offshore Islands [San Miguel, Santa Rosa, Santa Cruz, Anacapa (collectively referred to as CINMS hereafter), and Santa Catalina Island), Santa Monica Bay (SMB), Long Beach – Huntington Beach (LB-HB), Newport Beach – Laguna (NBL), Dana Point – San Clemente (DP-SC), Oceanside, and San Diego (**Figure 1**). Receivers were largely installed and maintained by CSULB, but also included receivers of collaborators [University of California San Diego (UCSD), Channel Islands National Marine Sanctuary (CINMS)].

Acoustic receivers were deployed in shallow ($\sim$ 3–40 m depth) coastal waters within 1000 m of the shoreline (50% within 400 m), across a range of environments, including calm protected habitats (e.g., embayments and harbors), exposed high energy sand substrata (beach habitat), and both rocky reef and kelp forest habitats. Receiver detection range varied by site and habitat. Based on the acoustic transmitter and types used, and empirical testing of receiver performance (Stirling et al., unpublished data), a nominal detection range of 500 m was estimated for all receivers in the array.

As receivers used in this study were deployed for other projects (e.g., Wolfe and Lowe, 2015; Logan and Lowe, 2018; Burns et al., 2019; Clevenstine and Lowe, 2021) and there was increased effort in tagging effort over time, receiver deployments varied by location and number over the course of this study, with a general increase in the total number deployed over the study period (**Table 1**).

Acoustic Data Acquisition and Processing

For tagged shark relative abundance and residency, raw receiver data were filtered to include only individuals that were detected more than two times per day, per zone. While it was not possible to precisely determine the age of tagged sharks, we were only interested in the presence or absence of YOY (<175 cm TL) sharks. Thus, detection data were filtered to only include detections of YOY sharks within 365 days of individual tagging dates (i.e., sharks detected >365 days from tagging were no longer YOYs).

Tagged Shark Relative Abundance

To standardize shark relative abundance metrics, relative abundance (shark density) was calculated as the number of unique tagged sharks that were detected in each zone each day, and receiver density was calculated as the number of receivers deployed in a particular zone each day.

From this dataset, several Generalized Additive Models (GAMs) were run using the "mgcv" package (Wood, 2011) in R to examine the relationship of shark relative abundance patterns to biotic and abiotic variables. Information pertaining to acquisition of environmental data used is supplied as **Supplementary Material**. Models were run separately for each year, as opposed to running a single large model with year interactions, to ensure that the models had a reasonable number of predictors to achieve most accurate interpretation of model results. All models were run using a Poisson family distribution and a log-link function.

For each model, tagged shark relative abundance was the response variable. Predictor variables included zone (categorical), receiver density (numeric), season (categorical; where December to February were considered Winter, March to May were considered Spring, June to August were considered Summer, and September to November were considered Fall), sea surface temperature (smoothed, numeric in °C), depth gradient (numeric in meters), sea surface salinity (smoothed, numeric in psu), and chlorophyll-A (smoothed, numeric in mg/m^3). Sea surface temperature, sea surface salinity and chlorophyll-A were allowed to vary nonlinearly within the GAMs (with 10 maximum nodes to prevent overfitting), due to the seasonality of each predictor. A total of five models were run per year:

(1) Relative abundance ~ zone + receiver density + season + s(temperature) + depth gradient + s(sea surface salinity) + s(chlorophyll-A)
(2) Relative abundance ~ zone + receiver density + season + s(temperature)
(3) Relative abundance ~ zone + receiver density + season + depth gradient
(4) Relative abundance ~ zone + receiver density + season + s(sea surface salinity)
(5) Relative abundance ~ zone + receiver density + season + s(chlorophyll-A).

Variables were assessed for covariance and models 2–5 were run to ensure that no single environmental predictor was driving significant results. After models were run, results were checked using *gam.check()* to ensure that the models met the assumptions required of GAMs, and that models did not overfit or underfit the data. Visual assessment of the GAM results was also used to ensure overfitting did not occur.

Shark Residency

A Residency Index (RI) with values ranging from 0 (no residency) to 1 (high residency), was used to examine individual shark presence within each zone following the method from Kessel et al. (2014):

$$\mathrm{RI} = \frac{\mathrm{S}}{\mathrm{T}}$$

Where, RI, Residence Index; S, distinct number of days detected in the zone; T, distinct number of days detected in any zone, within 365 days from individual tagging date.

Following Kessel et al. (2014) animals with less than 20 residence events (residence event considered to be any day a shark was present in a zone) across the entire array in any given year were excluded from the analyses. This approach allows for a degree of standardization where detection days (days where a shark can feasibly be detected) and monitoring days (days a transmitter can be "listened" for) are variable across a study population and array, respectively. Following Oh et al. (2017), individual sharks with RI values <6% were considered non-resident in that zone, while individual sharks with RI values >6% were considered to display resident behaviors within that zone.

Generalized Linear Mixed Models (GLMMs) were used ["lme4" package in R (Bates et al., 2011)] to examine drivers of YOY white shark resident behaviors. GLMMs were chosen because a nonlinear relationship was not expected, and to include both fixed and random factors under a Gaussian distribution. RI values of individual sharks at each zone were modeled as the response variable, and AICc was used to assess the best fitting model. Fixed effects included mean zone depth (calculated using the "marmap" package in R), total length (categorical), the distance from tagging site to the zone, and region. Random effects included tagging year, and shark ID. *p*-Values of fixed effects were obtained using the Anova function in the "car" package in R, with Type II Wald Chi-square tests (Kuznetsova et al., 2017; Fox and Weisberg, 2019). To calculate the deviance explained for each random effect, we used the following equation: [(variation of random effect)/(variation of random effect + total residual variation of the model)] (Bates et al., 2014).

Activity Space Estimation at Residency Hot Spots

Due to the linear expanse over which the receiver array was spread (linear distance ~ 450 km), the variability of receiver coverage across zones, and the variability in receiver distribution and density, common approaches to analyzing space use (such as Minimum Convex Polygons and Kernel Utilization Distribution models) are likely to yield over-estimated areas of core space use (Silva et al., 2018).

To estimate core activity space of sharks at nearshore residency hotspots, we used receiver detection data to calculate centers of activity (COA) (Simpfendorfer et al., 2002), via the COA function from the Animal Tracking Toolbox (ATT) in the "VTrack" package (Udyawer et al., 2018) in R for all tagged sharks that were resident in a zone, for each individual year of the study. Position estimates weighted by the number of detections within the residency hotspot location within a 12-h time frame were calculated for each individual shark. Sharks with less than 5 relocations (COA locations) were not included in the analyses.

Core (50%) activity spaces for YOY white sharks were calculated within VTrack (both individually and pooled) using Brownian Bridge Kernel Utilization Distributions (BBKUD). COA estimation prior to kernel probability distribution allows spatial biases that are inherent in passive acoustic telemetry derived from fixed receiver stations to be accounted for Udyawer et al. (2018). BBKUD estimation was used as it incorporates estimated rates of movement of tagged animals (analogous to the smoother sig1 in the "ADEHabitat" R package). Thus, variation in movement patterns and behavior within an array are accounted for with a flexible, rather than fixed approach, ultimately aimed at reducing Type I and Type II errors. Imprecision of locations (h) was set at 200 m as a conservative estimate of potential COA location error.

RESULTS

Satellite Data

Smart Position Or Temperature Transmitter tag track durations ranged from 10 to 142 days (median = 48 days, mean = 65 days, SD = 48 days), with SPOT tags providing locations on 2–47 of those days (median = 13, mean = 18 days, SD = 16 days). YOY white sharks fitted with SPOT tags yielded ARGOS locations in 287 individual zones. Forty-three zones had two or more ARGOS locations, 27 of which were locations for the same sharks, and 16 of which had locations from two sharks. Broadly, SPOT tag locations showed similar spatial distributions to that seen from the acoustic data, such as a high density of locations surrounding SMB and nearshore areas in southern California. Additionally, SPOT tag locations were also recorded in nearshore areas not monitored by the acoustic receiver array, as well as areas further from the shore (**Figure 2**).

Smart Position Or Temperature Transmitter tag data indicated that tagged sharks used shallow, nearshore environments often. SPOT tag location distribution peaked $\sim$ 2–3 km from shore, with $>$85% of SPOT tag locations occurring in waters $<$200 m deep, and 64% in waters less than 100 m deep. Analysis of shoreline habitat type indicated that across the study area (including offshore islands), available habitat was comprised of coastal marsh (33%), hardened shores (14%), beaches (31%), and rocky shores (22%). Sixty three percent of SPOT tag locations were associated with sandy beach habitats. There was evidence of site fidelity, as 18 zones contained multiple locations (where the same shark was detected more than once on the same day) from individual sharks. Time elapsed between such ARGOS positions ranged between 2 and 100 min. Of these 18 zones, 11 were in SMB, and all were within 10 km of shore. We also observed spatial overlap among individuals, as multiple zones contained detections from multiple sharks. Sixteen zones were used by more than one shark and five zones were visited by three different sharks (Shark IDs: 08_02, 08_04, and 08_09, see **Supplementary Table 1**). While no zones had SPOT tag locations from more than one transmitter on the same day, we did see evidence of spatiotemporal overlap between individuals' area use (**Figure 2**). Six zones had SPOT tag locations from two different animals within the same year, with one zone having SPOT tag locations from two different animals within the same month.

Acoustic Data

Acoustically tagged sharks ranged from 128 to 175 cm TL (**Supplementary Table 2**).

Sharks were detected in monitored zones from San Diego County (32° N) to Santa Barbara County (34° N), as well as in monitored zones at offshore islands (CINMS, Santa Catalina) (**Figure 3**). Thirty-four (77%) of the 44 YOY white sharks outfitted with acoustic transmitters were considered in our analyses (10 tagged sharks were not detected twice on any receiver within a 24-h period). Of these sharks 50% were caught (netted) and outfitted with internal transmitters, while 50% were outfitted with an external (darted) transmitter. Four YOY white sharks were detected on a single day, while 13 were detected across fewer than 20 days in the calendar year from their respective date of tagging (**Supplementary Table 1**).

The majority (99%) of acoustic detections from 2010 to 2018 were along southern California beaches (as opposed to offshore islands), with the bulk of detections (85%) between Long Beach and Huntington Beach (LB-HB). Acoustic detection patterns of individuals varied widely with the number of zones visited ranging between 1 and 26 (mean $\pm$ SD = 6 $\pm$ 6 zones). The number of days a shark was detected within a year from tagging was highly variable among individuals (median: 35 days, range: 1–219 days). Mean number of days detected for all tagged sharks was 50.9 $\pm$ 56.8 days. Across all receivers, YOY white sharks were detected in monitored nearshore beach habitat $\sim$ 9.5–14% of monitored days in each year of the study. Positive relationships were seen between the number of days an animal was detected and total detections of that animal (r^2 = 0.49), as well as between the number of days an animal was detected and the number of zones it visited (r^2 = 0.53; **Supplementary Figure 1**). Ninety-four percent of detections were from YOY sharks outfitted with external transmitters (n = 17) (**Supplementary Figure 1C**).

Shark Relative Abundance

Shark relative abundance was variable across each year of the study (**Figure 4**), and was strongly correlated with the number of YOY sharks tagged that year (r^2 = 0.794: Pearson's product-moment correlation; t = 5.196, p = 0.0013: **Supplementary Figure 2**). The best fitting GAM (in terms of AIC score) varied across years, but the all-inclusive model (model 1) was most consistent, with showing the lowest AIC score across 4 of the 9 years for which models were run [years: 2011, 2015, 2016, and 2018 (**Supplementary Table 3**)]. In addition, all models run for a particular year showed similar trends in terms of the statistical significance of the parameters modeled. Therefore, to increase interpretability and consistency, we report the results from the all-inclusive model only (refer to **Supplementary Table 4** for all models run). Generally, tagged YOY relative abundance patterns were not explained consistently by any predictor variable included across all years (**Supplementary Figures 3–6** and **Supplementary Table 4**). Significant effects of environmental variables upon YOY shark density were largely observed in concert with limited sample sizes and large confidence intervals, further impacting interpretability of the influence of environmental conditions.

Season was found to have a significant effect upon shark relative abundance in 5 of the 9 years of data included in the study. 2011, 2013, 2014, and 2016 were years where season was not a significant predictor of shark relative

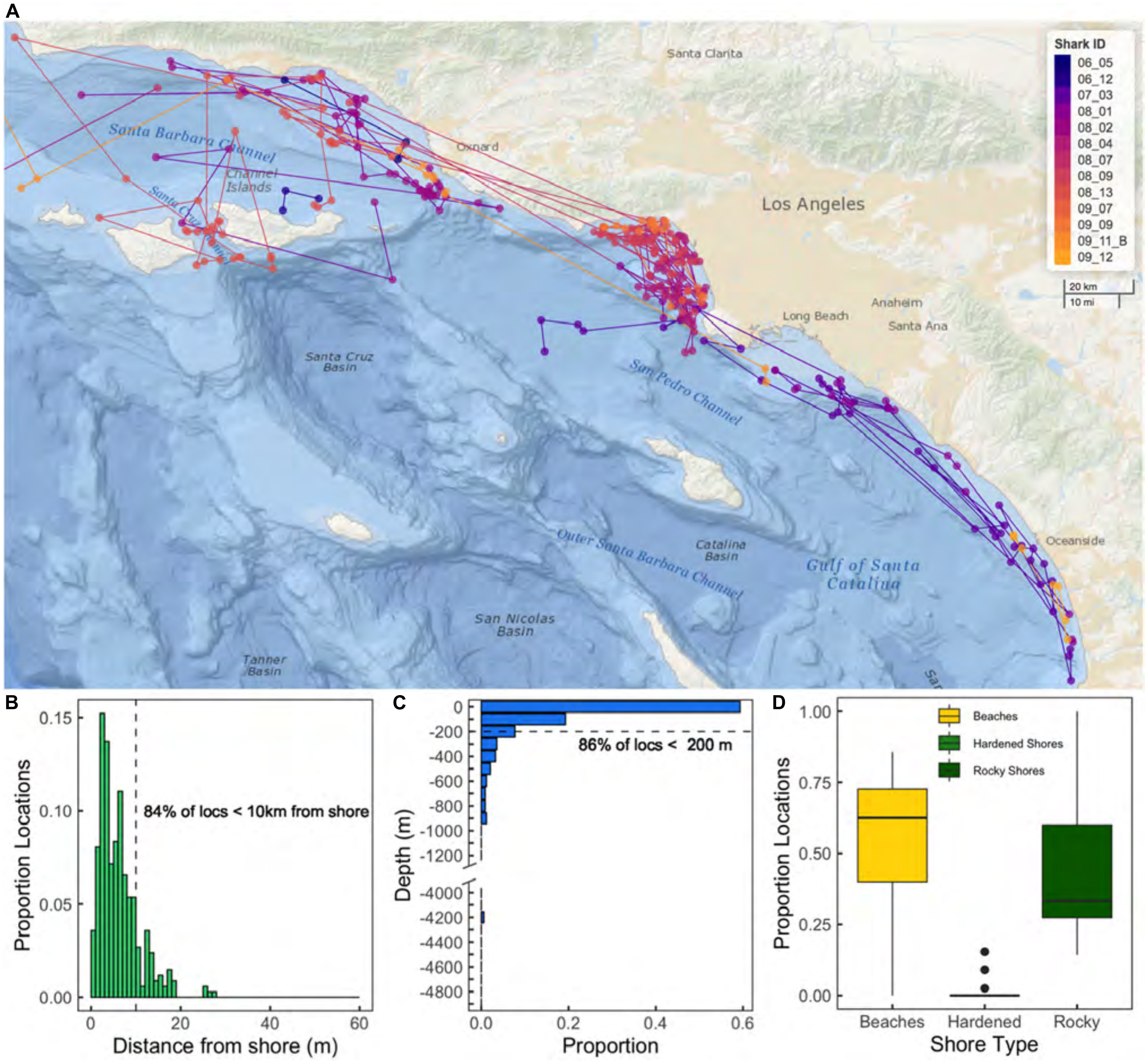

FIGURE 2 | (A) Map of SPOT tag (ARGOS) locations colored by the individual shark ID. Lines represent the shortest path between subsequent locations for an individual shark. **(B)** Histogram showing proportion of ARGOS locations with respect to distance from shore. **(C)** Histogram of proportion of ARGOS locations with respect to underlying water column depth. N.b. the break in the *y*-axis after 1200 m, as there were no locations with associated depth between 1500 and 4000 m. **(D)** Box plot showing proportion of ARGOS locations with respect to shore habitat type. Box extents show interquartile range of proportions. Solid lines show median values.

abundance, but no clear trend between season and shark relative abundance was present.

Temperature had a significant effect on YOY density in four different years (2011, 2015, 2016, and 2018). Shark relative abundance tended to be lower in relation to broader temperature extremes (below 12–15°C and above 20–23°C). Notably, in 2015, shark relative abundance was greatest above 25°C (**Supplementary Figure 3**).

Receiver density varied across years and was highest during years where VPS (Vemco Positioning System) arrays were deployed in specific locations, for example, in 2011 and 2016 (see methods for applicable references). However, no consistent relationship between probability of occurrence and receiver density was evident from year to year. In 2018, receiver density appeared to have a positive effect upon shark relative abundance at receiver densities of one and two receiver per zone.

Depth gradient displayed a negative relationship with shark relative abundance in two different years (2014 and 2016; p = 0.019 and 0.009, respectively), and, shark relative abundance appeared higher when depth gradient was between

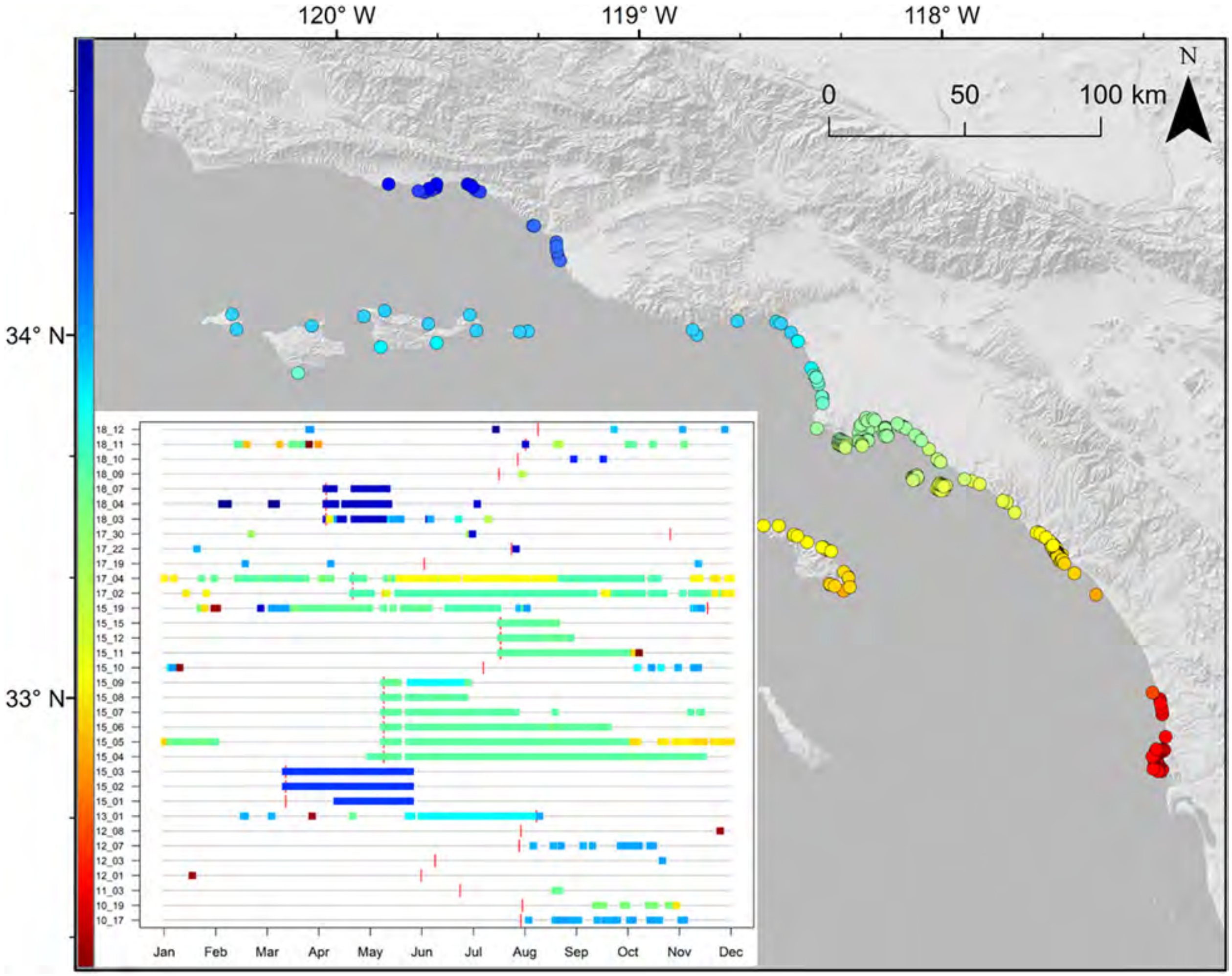

FIGURE 3 | Map of receiver station locations in southern California, with presence-absence plot inset of YOY white sharks acoustically detected during the study period, where each individual is centered on a generic year, and the vertical red bar denotes tagging date of that year, rather than chronologically (2010–2018). Shading indicates latitude of receiver(s) a shark was detected on. The first two digits for each individual in this inset plot indicate tagging year (e.g., 10_17 and 18_12 indicate these two individuals were tagged in 2010 and 2018, respectively).

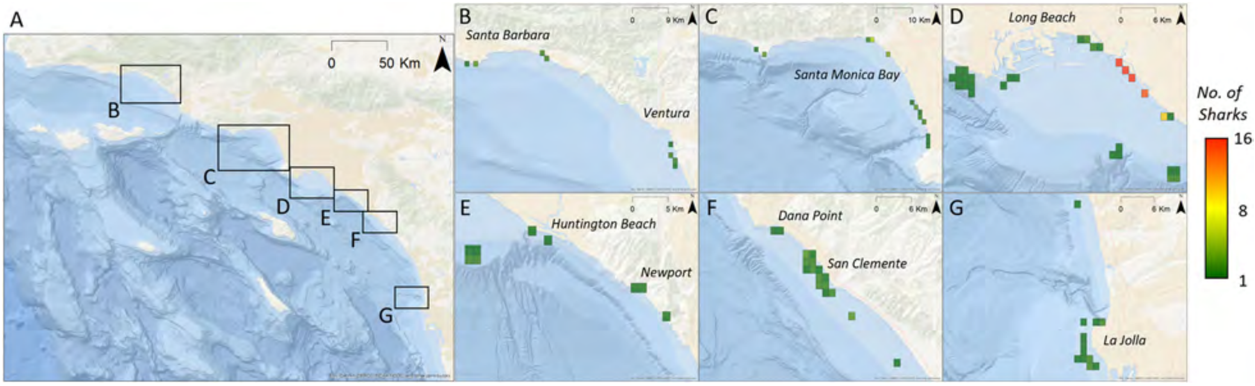

FIGURE 4 | Relative abundance of tagged YOY white sharks (calculated as the total number of sharks per zone per day) across southern California. Regions of importance have been enlarged to view detail. Grid cells are approximately 1.2 km^2 (all years – by location). **(A)** Base-map of broader study area. Black boxes indicate spatially distinct areas where YOY sharks were detected. **(B–G)** Indicate location of zones where YOY sharks were detected. Zones are colored according to cumulative relative abundance.

0.0025 m/depth gradient grid cell (0.017° resolution) and <0.01 m/depth gradient grid cell (0.017° resolution).

Chlorophyll a (Chl*a*) was included as a predictor variable as a proxy for local environmental productivity. Chl*a* appeared to be a significant predictor of shark relative abundance in only 2015 ($p = 0.005$), and shark relative abundance appeared to decrease with higher Chl*a* levels (**Supplementary Figure 5**).

Residency Analyses

Young-of-the-year white sharks exhibited resident events at a total of 99 (out of 156) monitored zones across all years of the study. Zones with greatest residency were variable from year to year (**Figure 5**) and in general, reflect the geographic areas with the greatest acoustic detections. Maximum RI for a zone in an individual year (all sharks for that year combined) ranged from 0.23 to 0.44 (**Figure 5**). Mean (±SE) zone RI, across all zones and across all years, was 0.01 ± 0.004 (median = 0.0005, mode = 0.0001). Within the LB-HB region, Sunset, Surfside, and Bolsa Chica beach areas (latitude = ∼ 33.5° N; **Figure 5G**) had the highest mean overall residency across the study period (RI's = 0.28, 0.23, and 0.09, respectively). Overall RI's for all other zones, averaged across all years, were ≤0.05. While habitat in these areas supported resident YOY sharks across multiple years (**Figures 5D–F**), the high overall RI values for these zones is also likely influenced by comparatively strong resident behaviors seen in 2015, which were in the order of three times greater than any other year in the study (**Supplementary Figure 7**).

Twenty-one animals were considered in residency analyses, of which only four were outfitted with internal transmitters. Maximum RI value (highest residency within a given zone) for an individual shark ranged from 0.55 (37 days detected) to 0.18 (118 days detected) (**Supplementary Table 2**). For all animals combined, overall RI values and number of days detected were weakly related ($r^2 = 0.0321$). By comparison, overall RI and the number of zones visited showed a stronger relationship ($r^2 = 0.433$), indicating that affinity to specific areas (from observed residency values) are unlikely an artifact of the number of days detected (**Figure 5**). Mean RI for individual sharks across all zones visited ranged from 0.5 (±0.014) to 0.04 (±0.009). Ten YOYs (45%) exhibited mean RI's > 0.2.

Residency events were seasonally variable across study years with peak resident days in the late summer through the fall in 2010–2013 (August – late October), while peak resident days occur in early to mid-summer in 2015–2018 (May – July) (**Supplementary Figure 7**).

Total resident events (summed number of resident days recorded in each zone) within the array for sharks with mean RI > 0.2 ranged from 128 (shark ID 15_06) to 38 (shark ID 18_04) (**Figure 6**). Greatest mean RI (0.5) was attributed to a 2015 (externally) tagged shark (shark ID 15_01) with 103 resident events within the array. Lowest mean RI (0.04) was attributed to a 2015 (internally) tagged shark (shark ID 15_19) with 118 resident events within the array.

The best fitting GLMM according to AICc retained all fixed and random factors in the model. As a result, water temperature significantly increased residency time within a zone [$X^2 = 17.33$, $p < 0.001$ (**Supplementary Figure 8**)]. Prior to 2015, the fall and winter months (September – December) significantly increased residency time within a zone, whereas after 2015 residency times began to increase earlier in the year (February – April) ($X^2 = 83.46$, $p < 0.001$). Additionally, both random effects (SharkID and Year), accounted for approximately 46.5 and 42.7% of the overall model variability, respectively (**Supplementary Figure 8**).

Activity Space Estimates

Activity space estimates were calculated for a total of 23 sharks (**Table 2**). Sharks with less than five relocations were not included in these analyses. Two of these 23 sharks were not sharks included in the residency analyses, as they were resident for less than 20 days in their respective years (**Table 2**). The number of resident days for animals included in activity space estimates ranged from 3 to 209 days (median = 46). For all sharks across all years, mean (±SE) estimated 50% core activity space was 30.79 ± 19.32 km^2. This estimate is likely increased by the influence of two individuals that exhibited markedly larger activity spaces (**Table 2**). Notably, these two individuals (shark ID's 15_10 and 18_11) were bycaught sharks, outfitted with internal tags. Resident YOY white sharks were largely found to exhibit relatively small core activity spaces in nearshore beach environments, as calculated using BBKUDs (**Figure 7** and **Table 2**). Combined core activity spaces generally aligned with the areas of peak residency within a given year (**Figure 7**). Individual truncated core activity space (space-use estimates adjusted for terrestrial overlap) ranged from 401.4 to 0.7 km^2. COA position estimates were on average less than 100 m apart. Tight clustering of COA's suggests strongly resident behaviors, concentrated in relatively small areas, with limited dispersal. Core activity space within residency regions was found to vary by individual, as well as by year (**Table 2**).

DISCUSSION

This study presents the first quantification of interannual residency patterns of YOY white sharks from this Northeast Pacific population, in southern California waters. More specifically, this study is the first to qualify and quantify habitat use preferences, and patterns of space use of YOY white sharks while resident in southern California. The present study utilizes comparatively high resolution spatial and temporal analyses derived from 10 years of acoustic monitoring, as well as satellite telemetry, to characterize YOY white shark habitat use and its possible drivers across southern California. Our results indicate that the relationship between shark presence and ocean temperatures may not be as static or as simple as previously hypothesized.

Previous studies that have addressed YOY white sharks from this Northeast Pacific population have identified the SCB as an important resource that provides nursery habitat for these sharks, and that habitat selection is driven by temperature, depth, and distance to shore (Klimley, 1985; Dewar et al., 2004; Weng et al., 2007b; Lowe et al., 2012; Lyons et al., 2013; White et al., 2019). However, the geographic range of YOYs

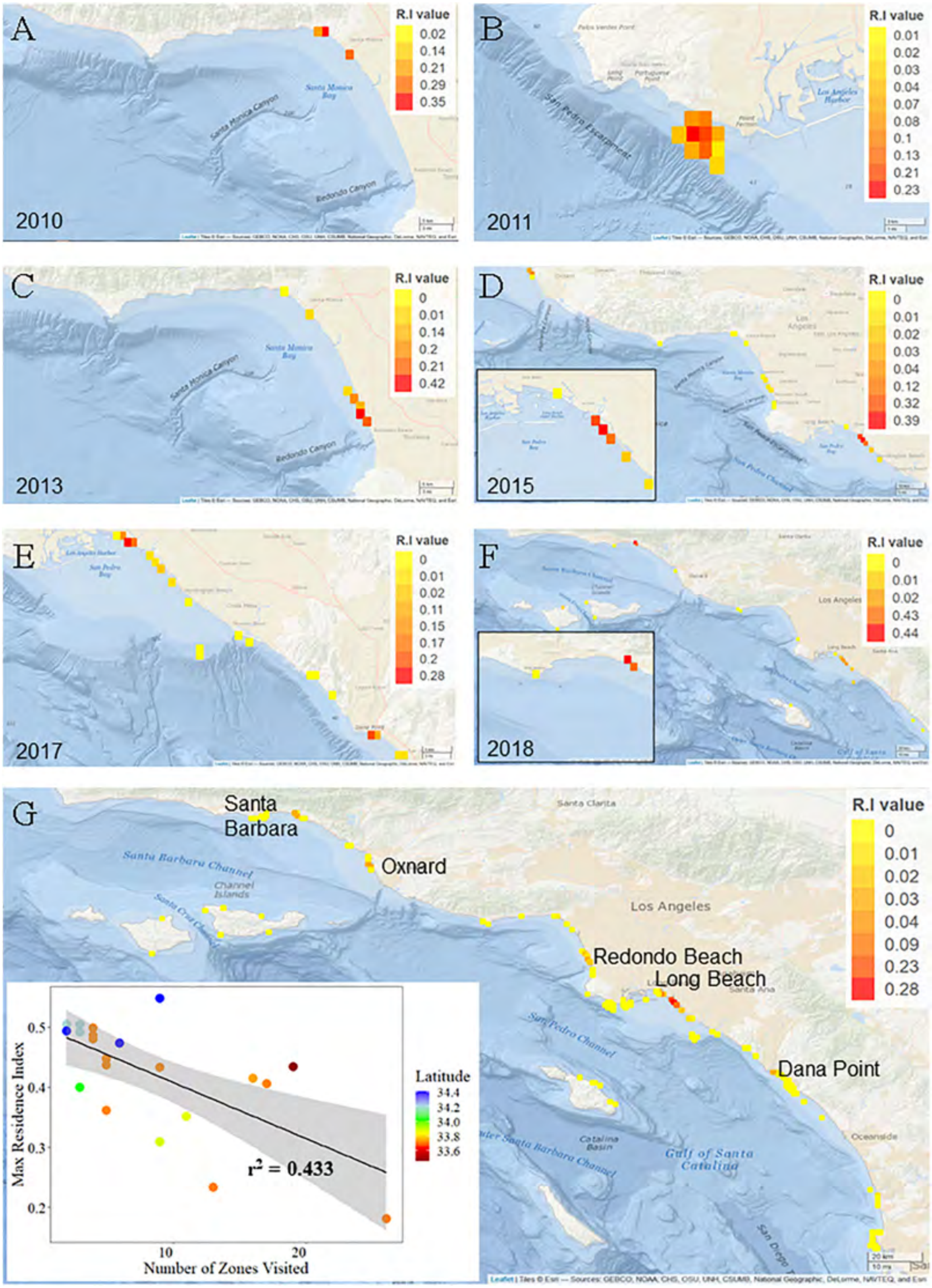

FIGURE 5 | Residency indices for young of the year white sharks in southern California. Grid cells are approximately 1.2 km^2. Note the scale bar for residency values changes across years. **(A–F)** Indicate location of zones of highest YOY white shark residency for each year of the study, colored by RI value. **(G)** Base-map showing cumulative residency values for all zones across all years. Inset scatter plot shows approximate latitude of the zone of highest residency for each YOY white shark included in residency analyses.

and juveniles of this population extends to at least the southern tip of Baja California ~1200 km (Weng et al., 2012), with specific nursery habitat identified toward the southern extent of the latitudinal range of this population, in Bahía de Sebastián Vizcaíno, Mexico (Oñate-González et al., 2017; Tamburin et al., 2019; García-Rodríguez and Sosa-Nishizaki, 2020). These studies,

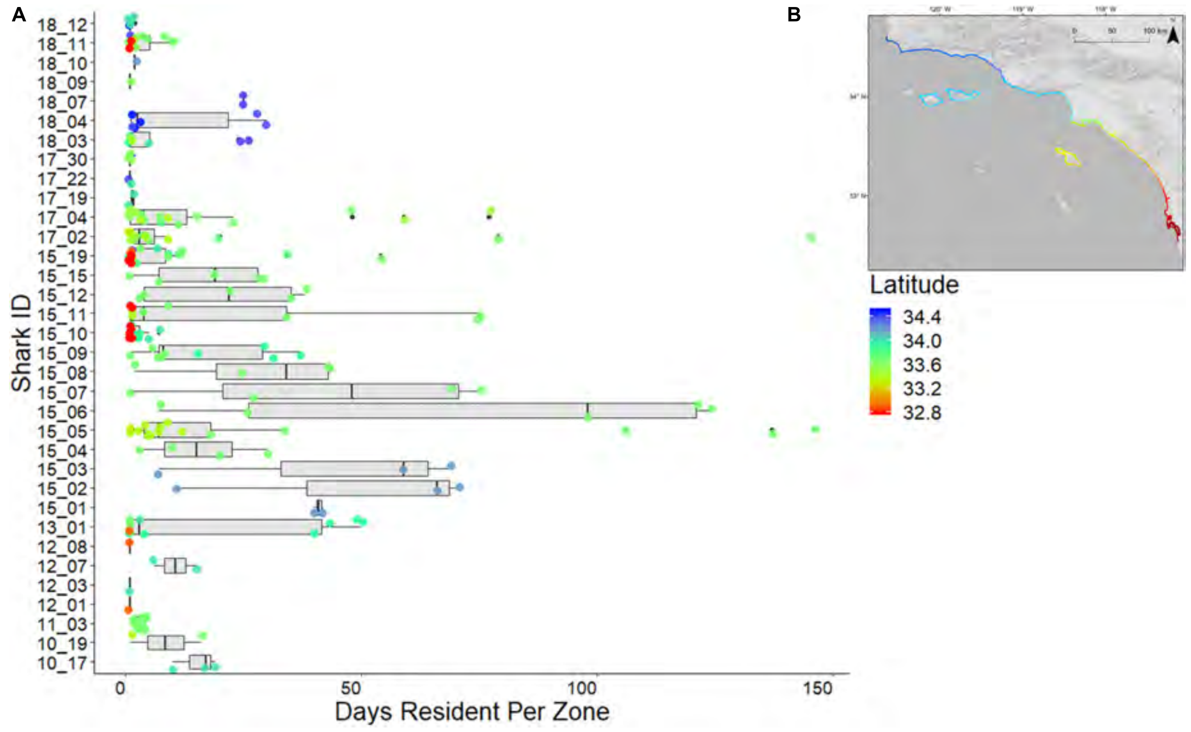

FIGURE 6 | (A) Resident days per zone per individual shark. Boxes indicate interquartile range of residency values of individual sharks, box lines indicate medians, whiskers indicate minimum, and maximum residency values (excluding outliers). Colored circles represent latitude for each zone resident by a shark, referenced by inset map **(B)**.

based upon data derived from satellite telemetry, remote sensing, and fisheries interactions, have been restricted to broad-scale observations of environmental drivers of habitat use and selection.

Our analyses of broad-scale movements using satellite telemetry data, and shark relative abundance and residency patterns from acoustic data, showed that YOY white sharks use shallow, nearshore habitats (within <500 m of the shoreline) at numerous locations across southern California. Often, these locations were beach environments, situated alongside some of the most densely populated and heavily urbanized areas on the United States Pacific west coast (**Figures 2**, **4**, **5**). Although our acoustic array was deployed across a variety of environments that included beach habitat, calm protected habitats, exposed high energy habitats, and both rocky reef and kelp forest habitats (**Figure 1**), >90% of monitored locations were associated with beach habitat, despite the fact that these habitats comprised only 31% of the available shoreline (including offshore islands) throughout the study area. Thus, a caveat of acoustic data is that it is limited to presence (or absence) of tagged animals at monitored locations, as associated habitat use patterns can only reflect observations within the extent of monitored habitat. Even with an acoustic array distributed across a large geographic area, acoustic analyses alone have the potential to under-represent movement patterns and habitats selected. Thus, we incorporated satellite (SPOT tag) telemetered data into our analyses to account for this potential bias, and examine the extent to which SPOT tag-derived ARGOS locations occurred within nearshore vs offshore environments, as well as habitat type associated with ARGOS locations.

The mean duration of SPOT tag transmissions (65 days) was notably short. While we can only speculate as to why this may be, one possibility is that damage to small, thin dorsal fins of YOY white sharks caused by SPOT tag attachments may have inhibited tag performance and transmission capability (Jewell et al., 2011). One SPOT tagged shark was recaptured approximately 1 year after tagging, and its dorsal fin was severely deformed from the weight of the SPOT tag, with the tag bent at a 95° angle from upright.

ARGOS locations (classes 1–3) revealed that although there was some utilization of habitat at offshore islands (CINMS) and some utilization of offshore waters, tagged YOY white sharks were largely observed in relatively shallow coastal locations (largest proportion of locations ∼ 2–3 km from shore, 64% of locations in waters less than 100 m deep) associated with expanses of insular shelf (**Figure 2**). Of all ARGOS locations, 63% were also associated with beach habitat shorelines (**Figure 2D** and **Supplementary Figure 9**). A previous study using SPOT tag data in juvenile white sharks (including YOYs) established that the likelihood of an ARGOS location (i.e., surface swimming behavior) from a tagged shark is not influenced by the local depth of the water column (Lyons et al., 2013). Thus, apparent YOY white shark propensity toward shallow coastal habitat, and

TABLE 2 | Individual core activity space estimates derived from Brownian Bridge Kernel Utilization Densities and clipped (adjusted for terrestrial overlap) estimates.

Shark ID	Tag year	Core activity region (county)	Mean core activity space (50% contour) (km^2)	Clipped core activity space (50% contour) (km^2)	Mean (core)	SE (core)	Days	Mean RI value (all zones)	Tag type
10_17	2010	Los Angeles	69.97	30.74	30.74	NA	29	0.33	Internal
11_03	2011	Los Angeles	2.22	2.22	2.22	NA	3	0.05*	Internal
13_01	2013	Los Angeles	1.96	1.13	1.13	NA	74	0.08	Internal
15_01	2015	Ventura	1.47	1.47			45	0.5	External
15_02	2015	Ventura	1.54	1.54			80	0.33	External
15_03	2015	Ventura	1.63	1.63			77	0.33	External
15_04	2015	Los Angeles	0.7	0.7			34	0.25	External
15_05	2015	Los Angeles/Orange	5.2	2.61			209	0.03	External
15_06	2015	Los Angeles	1.75	1.75			133	0.2	External
15_07	2015	Los Angeles	1	1			82	0.25	External
15_08	2015	Los Angeles	1.34	1.34			47	0.25	External
15_09	2015	Los Angeles	5.55	4.23			47	0.1	External
15_10	2015	Los Angeles	593.93	219.59			15	0.07*	Internal
15_11	2015	Los Angeles	1.4	1.4			89	0.11	External
15_12	2015	Los Angeles	2.35	2.35			45	0.2	External
15_15	2015	Los Angeles	2.12	1.34			35	0.2	External
15_19	2015	Los Angeles/Orange	5.61	3.1	18.66	16.75	118	0.04	Internal
17_02	2017	Los Angeles/Orange	2.14	0.9			183	0.06	Internal
17_04	2017	Los Angeles/Orange	17.1	11.16	6.03	5.13	185	0.05	Internal
18_03	2018	Santa Barbara	21.26	14.45			37	0.1	External
18_04	2018	Santa Barbara	0.94	0.94			36	0.14	External
18_07	2018	Santa Barbara	1.1	1.1			26	0.33	External
18_11	2018	Los Angeles/Orange	821.42	401.44	104.48	99.04	22	0.08	Internal

N.b.; YOY sharks with activity space estimates that were not included in residency calculations are marked with an asterisk next to their respective mean RI value. Mean and SE values correspond to all sharks within a year group.

in particular beach habitat, as indicated by SPOT tag ARGOS locations, is not explained by an increased likelihood for surface swimming in such environments.

YOY Relative Abundance

Tagged shark relative abundance (number of tagged sharks detected in a given zone) was interannually variable (range: 0–9 sharks per receiver per zone; **Supplementary Figure 6**). Across all years, relative abundance of tagged sharks correlated with the number of sharks tagged in each respective year. Similarly, the observed annual locations of zones displaying peak relative abundance largely reflected geographic concentration of tagging effort that year, where YOY white sharks formed loose aggregations. Tagging effort was in-turn largely concentrated in areas where juvenile white sharks had been sighted, and throughout the study, many of the sharks tagged within a given year were tagged within the same general vicinity, over a period of a few days to a few weeks. Thus, the geographic location of zones with peak densities showed broad, spatial interannual variability (see **Figures 4**, **8** and **Supplementary Figure 6**).

Peak relative abundance locations did not display the same temporal and spatial stability as has been described for primary nursery habitat elsewhere in this species' range. Juvenile white sharks (*n.b.* not YOY) from the east Australia population have been documented to use two geographically separated areas in Port Stephens, New South Wales, and Corner Inlet, Victoria (~852 km linear distance separation) as primary nursery habitat, with a possible third location further north in Queensland (Bruce and Bradford, 2012; Werry et al., 2012; Bruce et al., 2019). This, in itself, bears a resemblance to the broad patterns already described for the Northeast Pacific YOY and juvenile white shark population, with the highlighted importance of the SCB, and the identified specific nursery habitat in Bahía de Sebastián Vizcaíno separated by a similar linear distance. The locations of the Australia white shark primary nursery habitat were found to be temporally stable (showed interannual consistency), with juvenile white sharks utilizing the New South Wales habitat from September to January (spring to mid-summer), and the Victoria habitat from January to May (summer through the fall). A more recent analysis (although only one of the included animals was a YOY) further supported the finding that these same

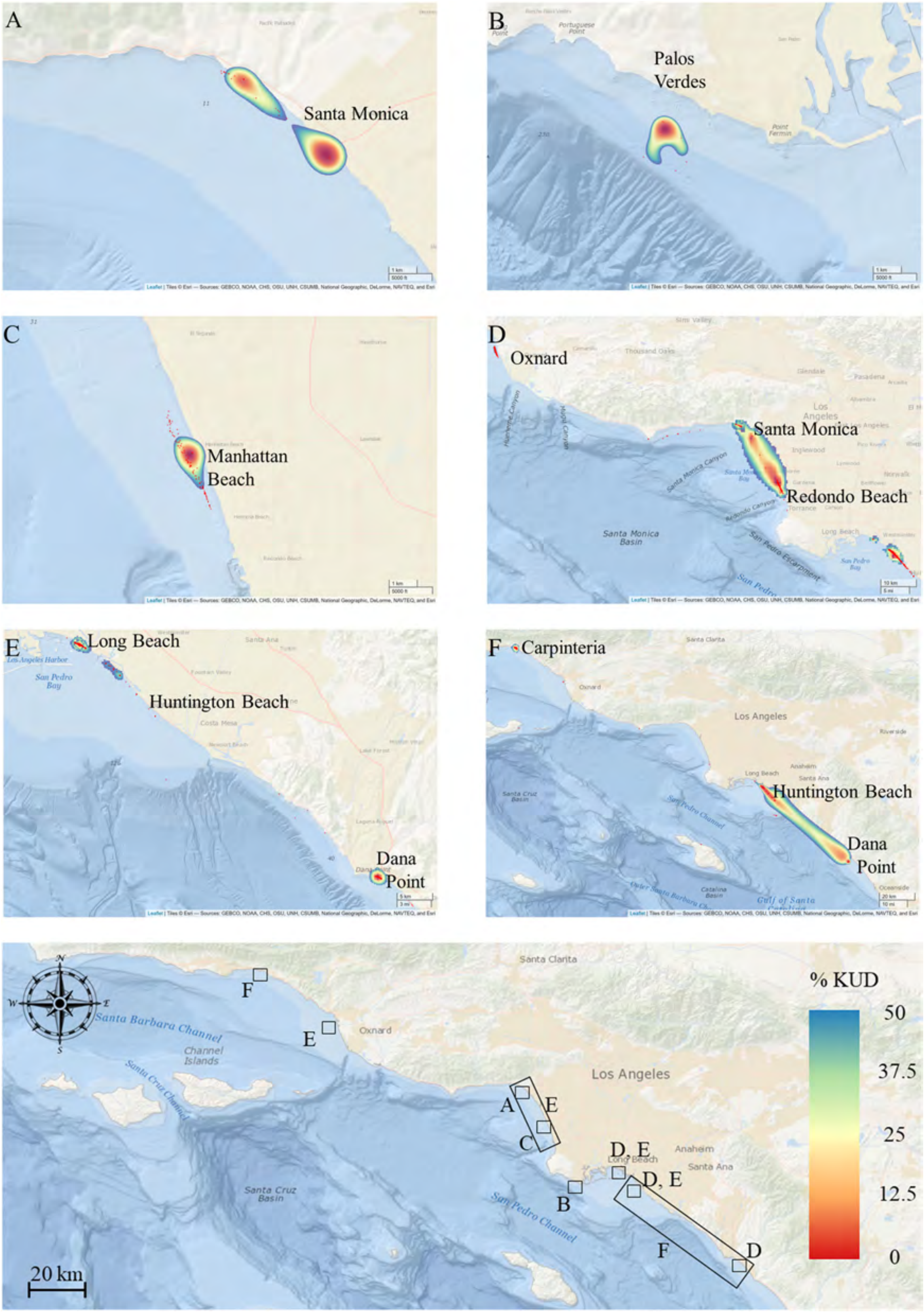

FIGURE 7 | Activity space estimates for animals, overlaid for each year [**(A)** 2010, **(B)** 2011, **(C)** 2013, **(D)** 2015, **(E)** 2017, **(F)** 2018]. Base map shows the locations of BBKUD plots for each panel with reference to the southern California coastline and wider study area. Geographic locations of core activity in each year reflect areas of peak shark density and residency.

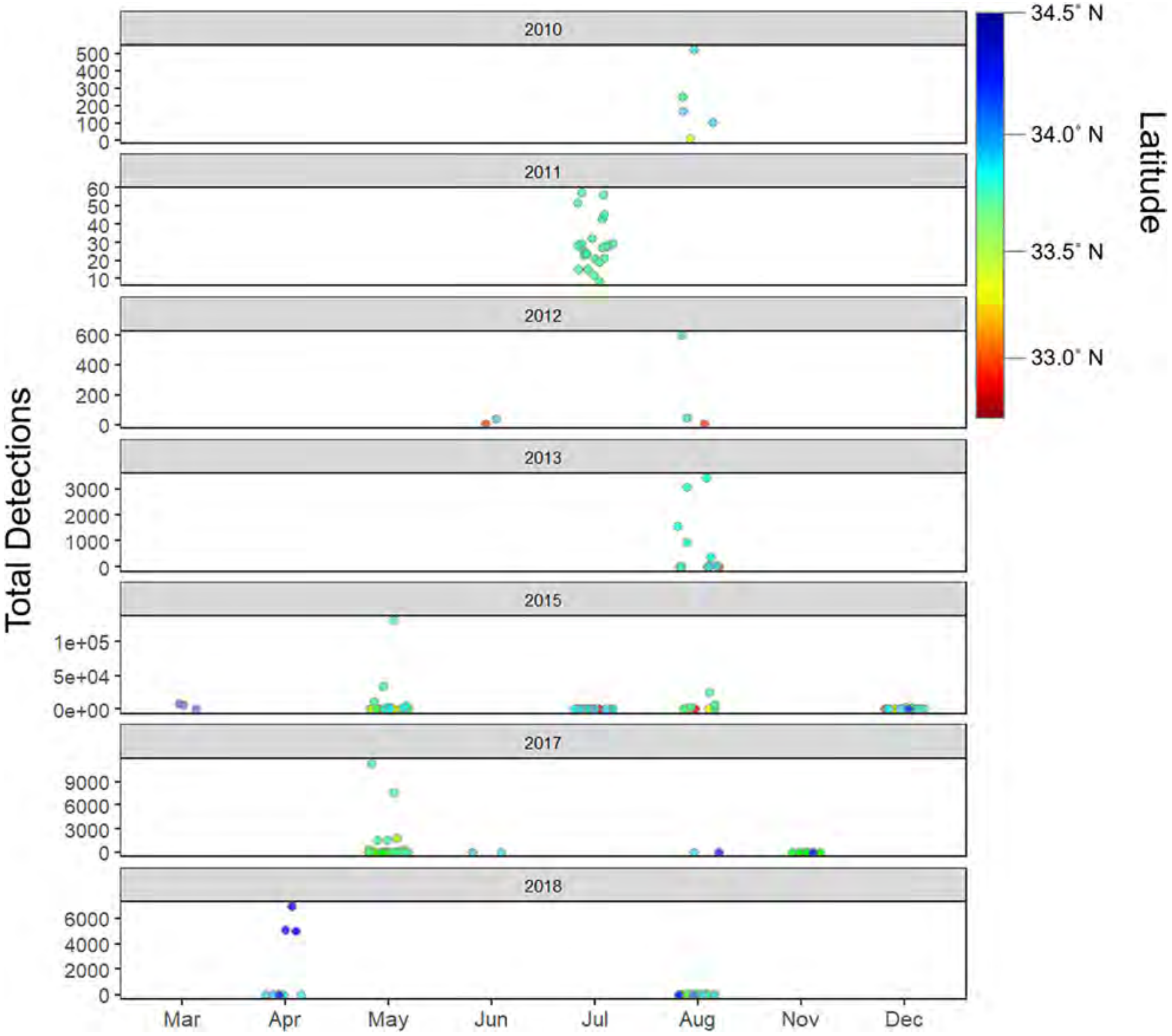

FIGURE 8 | Total detections by year, latitude and month (seasons) – detection patterns show seasonality, and interannual latitudinal variability, with August serving as the month with peak overall detections across all years combined.

two geographic areas functioned as nursery habitat (Spaet et al., 2020b). However, Spaet et al. (2020b) found the geographic extent of each nursery area to be considerably larger, and the seasonality of habitat use in each location showed a shift from December to March, and November to February, respectively. This difference may be explained by sample size in the two studies (n = 22 vs n = 103) and size-class included [175–260 cm (median = 215 cm) vs 147–350 cm (median = 220 cm)], as well as interannual differences (biotic and abiotic) in each of the nursery areas.

YOY Residency

By definition (Heupel et al., 2007), neonate or YOY sharks utilizing nursery habitat display above average residency (site fidelity) to a specific area or location. The geographic extent of such an area may be species or population specific. In concert with YOY relative abundance, residency patterns were spatiotemporally variable at an annual level, with resident days peaking in the summer (May to August), but often with animals continuing to display residency throughout the fall. This temporal pattern differs to that previously reported in YOY white sharks (Weng et al., 2007b), in that peak residency shifted to earlier in the year in the second half of our study period. The seasonal timing of peak residency is likely influenced by plasticity of extrinsic variables [e.g., temperature, prey availability, atmospheric anomalies such as El Niño Southern Oscillations (ENSOs)], as well as the individual intrinsic factors that determine when an individual may arrive at a location (White et al., 2019). From 2010 through 2018 we observed zones of high residency in eight different broad geographic locations in southern California, with multiple YOY sharks displaying concurrent, comparatively high residency at these locations. In general (with exception of 2010, where receiver coverage was limited) RI values in zones of peak residency were an order of magnitude greater than the mean RI value for the respective year, and several orders of magnitude greater than the modal RI value (0.0002). This seasonal YOY residency in nearshore habitats, is not unique, rather it falls in line with descriptions of juvenile white sharks from elsewhere in the species range, including Australia, South Africa, as well as the northwest Atlantic (Bruce and Bradford, 2012; Werry et al., 2012; Dicken and Booth, 2013; Skomal et al., 2017; Curtis et al., 2018; Spaet et al., 2020b).

Peak Residency Locations and Space Use

What is perhaps more novel, and of importance from this study, is the proximity of many of these high YOY white shark residency zones to some of the most (human) frequented and densely populated beach areas within the species' geographical range, and in the world (Tobler et al., 1995). While the two primary nursery habitat areas described in eastern Australia are also in close proximity to towns and cities (Bruce and Bradford, 2012; Werry et al., 2012), the extent of urbanization and the population density of these towns and cities compared to the southern California urban conurbation are strongly divergent. For example, 2010 census data for Redondo Beach, California (administrative area 16.09 km^2), which was the approximate location for peak density and residency in 2012, reported a population density of 4156 people per km^2 (United States Census Bureau, 2012). In contrast, Port Stephens (administrative area 979 km^2) has a population density of 72 people per km^2 (Australian Bureau of Statistics, 2016).

Fifty-two percent of calculated COA's were situated within 200 m of the shoreline, and 82% within 300 m. With a (conservative) COA positional error 200 m used in core activity space estimations, our data show that when utilizing nearshore habitat, tagged YOY white sharks spend extended periods time in waters anywhere from the shore-break to 500 m offshore (**Figure 7**) and reflects spatially restricted residency in most individuals (range = 0.7–401.44 km^2, mode = 1.34 km^2). The comparatively high mean ($\pm$SE) activity space estimates for all animals combined (30.8 $\pm$ 19.3 km^2) was likely driven by two more widely ranging individuals, that showed limited residency across more than one geographically separate area (**Table 2**). These two YOYs were sharks caught in gillnet fisheries ($>$5.5 km offshore), as opposed to being targeted and tagged (whether internally or externally) at an inshore location. Both were resident within monitored zones less than the median number of days for all animals included in activity space estimate analyses (43 days). The large activity space estimates of these two individuals are reflected in the large kernel utilization density plots (see **Figures 7D,F**), and are most likely representative of animals exhibiting transient or partial migratory behaviors, rather than resident, site affiliated behaviors generally displayed by YOY sharks tagged at inshore locations. Nonetheless, mean core activity space for all sharks combined is markedly smaller than that reported in western North Atlantic YOYs (Curtis et al., 2018). This disparity may reflect the availability and distribution of shallower shelf habitat. If YOY white sharks seek and select for such habitat type, there are simply more suitable habitat possibilities within the range of the North Atlantic YOYs, compared to that available in Northeast Pacific YOYs in southern California waters.

Environmental Drivers of YOY Relative Abundance and Residency

Juvenile white shark presence and residency has been shown to be significantly influenced by a range of biotic and abiotic variables across the species' range, including temperature, depth, barometric pressure, and season (Weng et al., 2007b; Bruce and Bradford, 2012; Dicken and Booth, 2013; Skomal et al., 2017; Curtis et al., 2018; White et al., 2019; Spaet et al., 2020b). However, a recent analysis determined environmental factors to be poor predictors of juvenile white shark presence in eastern Australian beach habitat (Spaet et al., 2020a).

In the present study, none of the abiotic variables examined were found to have a consistent relationship with YOY relative abundance across years. However, of the variables examined, temperature and sea surface salinity were the most consistently identified drivers of shark presence, though the direction (positive or negative) and magnitude of the relationships varied. In the case of temperature, YOY densities were generally lower in conjunction with temperature extremes, with the exception of 2015 (an El Niño year – see **Supplementary Figure 3**). The resolution of remote sensing derived SST and salinity data do not show large temporal variation (i.e., monthly and seasonally) across southern California at a geographic meso-scale (for example across the expanse of SMB, or the LB-HB region; for reference see **Figures 1**, **7**). It follows therefore that no discernable change could be observed at an individual zone level. Finer, micro-scale changes in temperature may be an important factor in the selection of specific habitat where sharks show residency, as YOY white sharks display limited endothermic capability, and may be sensitive to fractional changes in °C across the body (Domeier, 2012; White et al., 2019; Anderson et al., 2021). Our model results show that even with our inclusion of higher resolution point temperature data (where available), there are likely aspects of temperature that we were unable to quantify in our analyses.

Perhaps unsurprisingly, our models of environmental drivers of residency pointed to both temperature and month (*ergo* season) significantly influencing residence event duration. Our results are consistent with reported seasonal fishery captures in southern California (Lowe et al., 2012; Lyons et al., 2013), but also suggest that residence event duration was greatly subject to interannual variability, as well as intrinsic plasticity in individual animals.

CONCLUSION

A 2018 review of research priorities for white sharks highlighted the identification of critical habitats for the species and their changes across ontogeny as being of high importance (Huveneers et al., 2018). Our results demonstrate that unlike the spatiotemporally stable primary nursery habitat described for other populations globally, southern California presents a broader habitat resource that supports spatiotemporally *dynamic* primary nursery habitat. It is unknown where parturition occurs in the Northeast Pacific white shark population, but it is generally regarded to likely take place offshore or in deeper water, after which neonates make their way to more sheltered inshore environments (Klimley, 1985; Domeier, 2012). The data presented here demonstrate that in each year, YOY white sharks arrive at these nearshore (beach) locations, remaining within them for extensive periods (days to months), and that these locations can vary, or may be used repeatedly across years. Thus, they are not areas of temporary residency outside of primary habitat areas (Werry et al., 2012), but are in-fact dynamic primary nursery habitat in their own right. This dynamism appears to be a feature unique to Northeast Pacific YOY and juvenile white sharks utilizing the broader southern California nearshore habitats, as it has yet to be described elsewhere.

As with other stages of ontogeny, YOY white sharks likely exhibit behavioral patterns of temporary residency and traveling (Bruce and Bradford, 2008), moving between and stopping at discrete resource patches. It is likely these discrete patches form aggregation and residency "hotspots" for juvenile white sharks, including YOY sharks. Ninety-five percent of tagged YOY sharks exhibiting resident behavior were animals tagged as part of loose aggregations at inshore locations, while only 4 of the 14 fisheries-bycaught animals (29%) were included in our residency analyses. Sharks caught in offshore fisheries were likely in a transient or migratory behavioral state, at the time of capture, which appeared to largely continue post-release. While fisheries-caught sharks were detected in monitored zones, they largely did not display the site-fidelity and restricted activity spaces of YOY sharks tagged at inshore locations.

Standard approaches to discerning the resource qualities that drive nursery habitat selection can only arrive at broad scale parameters, that inadequately address these questions. It is clear that broad, meso-scale approaches to analyzing the environmental correlates of shark occurrence are insufficient. This conclusion is supported by recent analyses that found environmental conditions to be poor predictors of juvenile white shark occurrence in eastern Australia (Spaet et al., 2020a). Thus, novel approaches that incorporate technologies to derive high resolution environmental data (Lowe et al., 2018), paired with more comprehensive telemetry datasets (acoustic and satellite) are therefore required to facilitate accurate predictive modeling of white shark occurrence. Such data are vital for informing both conservation and management policy, at all administrative levels.

DATA AVAILABILITY STATEMENT

The raw data supporting the conclusions of this article will be made available by the authors, without undue reservation.

ETHICS STATEMENT

The animal study was reviewed and approved by the CSU Long Beach Institutional Animal Care and Use Committee #364.

AUTHOR CONTRIBUTIONS

CL, JA, and EB conceived the study. CL, EB, EM, TF, CW, RL, and CW tagged the sharks, collected the satellite and acoustic data. JA, EB, BS, EM, and TF organized and analyzed the data. JA, EB, EM, RL, TF, and CW created the main figures. JA drafted the manuscript. All authors contributed equally to manuscript revisions.

FUNDING

Funding for tagging and acoustic monitoring was provided by Monterey Bay Aquarium and AltaSea. Funding for data maintenance and analysis was provided by State of California. In kind support for tagging and monitoring was provided by Los Angeles and Orange County Lifeguards, Cities of Huntington Beach, Seal Beach, Ventura, Santa Barbara, Newport Beach, Laguna, Long Beach, and San Clemente. The authors declare that this study received funding from Alta Sea. The funder was not involved in the study design, collection, analysis, interpretation of data, the writing of this article or the decision to submit it for publication.

SUPPLEMENTARY MATERIAL

The Supplementary Material for this article can be found online at: https://www.frontiersin.org/articles/10.3389/fmars.2021.645142/full#supplementary-material

REFERENCES

Afonso, A. S., and Hazin, F. H. V. (2015). Vertical movement patterns and ontogenetic niche expansion in the tiger shark, *Galeocerdo cuvier*. *PLoS One* 10:e0116720. doi: 10.1371/journal.pone.0116720

Anderson, J. M., Spurgeon, E. A., Stirling, B. S., May, J. I., Rex, P. T., Hyla, B., et al. (2021). High resolution acoustic telemetry reveals swim speeds and inferred field metabolic rates in juvenile white sharks (Carcharadon carcharias). *Commun. Biol.* (in review).

Australian Bureau of Statistics (2016). *2016 Census Quick Stats. 2016 Census*. Available online at: https://quickstats.censusdata.abs.gov.au/census_services/getproduct/census/2016/quickstat/LGA16400?opendocument (accessed October 30, 2020).

Bates, D., Mächler, M., and Bolker, B. (2011). *lme4: Linear Mixed-Effects Models Using S4 Classes*.

Bates, D., Mächler, M., Bolker, B., and Walker, S. (2011). *lme4: Linear Mixed-Effects Models Using Eigen and S4. R Package Version* 1.1-7.

Benson, J. F., Jorgensen, S. J., O'Sullivan, J. B., Winkler, C., White, C. F., Garcia−Rodriguez, E., et al. (2018). Juvenile survival, competing risks, and spatial variation in mortality risk of a marine apex predator. *J. Appl. Ecol.* 55, 2888–2897. doi: 10.1111/1365-2664.13158

Bradford, R., Patterson, T. A., Rogers, P. J., McAuley, R., Mountford, S., Huveneers, C., et al. (2020). Evidence of diverse movement strategies and habitat use by white sharks, Carcharodon carcharias, off southern Australia. *Mar. Biol.* 167, 96. doi: 10.1007/s00227-020-03712-y

Bruce, B. D., and Bradford, R. W. (2008). *Spatial Dynamics and Habitat Preferences of Juvenile White Sharks – Identifying Critical Habitat and Options for Monitoring Recruitment. Final Report to the Department of the Environment, Water, Heritage and the Arts*. Hobart, TAS: CSIRO Marine and Atmospheric Research.

Bruce, B. D., and Bradford, R. W. (2012). "Habitat use & spatial dynamics of juvenile white sharks, carcharadon carcharias, Eastern Australia," in *Global Perspectives on the Biology and Life History of the White Shark*, ed. M. L. Domeier (New York, NY: CRC Press), 225–254.

Bruce, B. D., Harasti, D., Lee, K., Gallen, C., and Bradford, R. (2019). Broad-scale movements of juvenile white sharks Carcharodon carcharias in eastern Australia from acoustic and satellite telemetry. *Mar. Ecol. Prog. Ser.* 619, 1–15. doi: 10.3354/meps12969

Burns, E. S., Armstrong, J., Tang, D., Sakamoto, K., and Lowe, C. G. (2019). The residency, movement patterns and habitat association of several demersal fish species to the Orange County Sanitation District wastewater outfall. *Mar. Pollut. Bull.* 149:110638.

Bustamante, C., and Bennett, M. B. (2013). Insights into the reproductive biology and fisheries of two commercially exploited species, shortfin mako (Isurus oxyrinchus) and blue shark (*Prionace glauca*), in the south-east Pacific Ocean. *Fish. Res.* 143, 174–183.

Carlisle, A., Litvin, S., Hazen, E., Madigan, D., Goldman, K., Lea, R., et al. (2015). Reconstructing habitat use by juvenile salmon sharks links upwelling to strandings in the California Current. *Mar. Ecol. Prog. Ser.* 525, 217–228. doi: 10.3354/meps11183

Chapman, D. D., Feldheim, K. A., Papastamatiou, Y. P., and Hueter, R. E. (2015). There and Back Again: a review of residency and return migrations in sharks, with implications for population structure and management. *Ann. Rev. Mar. Sci.* 7, 547–570. doi: 10.1146/annurev-marine-010814-015730

Clevenstine, A. J., and Lowe, C. G. (2021). Aggregation site fidelity and movement patterns of the protected marine predator giant sea bass (*Stereolepis gigas*). *Environ. Biol. Fishes* (in press). doi: 10.1007/s10641-021-01057-z

Coffey, D. M., Carlisle, A. B., Hazen, E. L., and Block, B. A. (2017). Oceanographic drivers of the vertical distribution of a highly migratory, endothermic shark. *Sci. Rep.* 7:10434. doi: 10.1038/s41598-017-11059-6

Costa, D. P., Robinson, P. W., Arnould, J. P. Y., Harrison, A.-L., Simmons, S. E., Hassrick, J. L., et al. (2010). Accuracy of ARGOS locations of pinnipeds at-sea estimated using fastloc GPS. *PLoS One* 5:e8677. doi: 10.1371/journal.pone.0008677

Curtis, T. H., Metzger, G., Fischer, C., McBride, B., McCallister, M., Winn, L. J., et al. (2018). First insights into the movements of young-of-the-year white sharks (*Carcharodon carcharias*) in the western North Atlantic Ocean. *Sci. Rep.* 8:10794. doi: 10.1038/s41598-018-29180-5

Dewar, H., Domeier, M., and Nasby-Lucas, N. (2004). Insights into young of the year white shark, carcharodon carcharias, behavior in the southern california bight. *Environ. Biol. Fishes* 70, 133–143. doi: 10.1023/B:EBFI.0000029343.54027.6a

Dicken, M. L., and Booth, A. J. (2013). Surveys of white sharks (C*archarodon carcharias*) off bathing beaches in Algoa Bay, South Africa. *Mar. Freshw. Res.* 64:530. doi: 10.1071/MF12336

Domeier, M. (2012). ""A new Life-History Hypothesis for White Sharks, Carcharodon carcharias, in the Northeastern Pacific," in *Global Perspectives on the Biology and Life History of the White Shark*, ed. M. L. Domeier (Boca Raton, FL: CRC Press), 199–224. doi: 10.1201/b11532-19

Domeier, M. L., and Nasby-Lucas, N. (2013). Two-year migration of adult female white sharks (*Carcharodon carcharias*) reveals widely separated nursery areas and conservation concerns. *Anim. Biotelem.* 1:2. doi: 10.1186/2050-3385-1-2

Fox, J., and Weisberg, S. (2019). *An R Companion to Applied Regression, 3rd edn,* Thousand Oaks, CA: Sage Publications.

García-Rodríguez, E., and Sosa-Nishizaki, O. (2020). Artisanal fishing activities and their documented interactions with juvenile white sharks inside a nursery area. *Aquat. Conserv. Mar. Freshw. Ecosyst.* 2:aqc.3300. doi: 10.1002/aqc.3300

Harasti, D., Lee, K., Bruce, B., Gallen, C., and Bradford, R. (2017). Juvenile white sharks Carcharodon carcharias use estuarine environments in south-eastern Australia. *Mar. Biol.* 164:58. doi: 10.1007/s00227-017-3087-z

Heupel, M. R., Carlson, J. K., and Simpfendorfer, C. A. (2007). Shark nursery areas: Concepts, definition, characterization and assumptions. *Mar. Ecol. Prog. Ser.* 337, 287–297. doi: 10.3354/meps337287

Heupel, M. R., Simpfendorfer, C. A., and Hueter, R. E. (2004). Estimation of shark home ranges using passive monitoring techniques. *Environ. Biol. Fishes* 71, 135–142.

Hoyos-Padilla, E. M., Klimley, A. P., Galván-Magaña, F., and Antoniou, A. (2016). Contrasts in the movements and habitat use of juvenile and adult white sharks (*Carcharodon carcharias*) at Guadalupe Island, Mexico. *Anim. Biotelem.* 4:14. doi: 10.1186/s40317-016-0106-7

Hueter, R. E., Heupel, M. R., Heist, E. J., and Keeney, D. B. (2005). Evidence of philopatry in sharks and implications for the management of shark fisheries. *J. Northwest Atl. Fish. Sci.* 35, 239–247. doi: 10.2960/j.v35.m493

Huveneers, C., Apps, K., Becceri—Garcia, E. E., Bruce, B., Butcher, P. A., Carlisle, A., et al. (2018). Future research directions on the 'elusive' white shark. *Front. Mar. Sci.* 5:455. doi: 10.3389/fmars.2018.00455

Jewell, O. J. D., Wcisel, M. A., Gennari, E., Towner, A. V., Bester, M. N., Johnson, R. L., et al. (2011). Effects of smart position only (SPOT) tag deployment on white sharks carcharodon carcharias in south Africa. *PLoS One* 6:e27242. doi: 10.1371/journal.pone.0027242

Jorgensen, S., Chapple, T., Anderson, S., Hoyos, M., Reeb, C., and Block, B. (2012). "Connectivity among White shark coastal aggregation areas in the Northeastern pacific," in *Global Perspectives on the Biology and Life History of the White Shark*, ed. M. Domeier (Boca Raton, FL: CRC Press), 159–167.

Kessel, S., Chapman, D., Franks, B., Gedamke, T., Gruber, S., Newman, J., et al. (2014). Predictable temperature-regulated residency, movement and migration in a large, highly mobile marine predator (*Negaprion brevirostris*). *Mar. Ecol. Prog. Ser.* 514, 175–190. doi: 10.3354/meps10966

Klimley, P. (1985). The aerial distribution and autoecology of the white shark, Carcharodon carcharias, off the west coast of North America. *Mem. Calif. Acad. Sci.* 9, 15–40.

Kuznetsova, A., Brockhoff, P. B., and Christensen, R. H. B. (2017). lmerTest Package: tests in linear mixed effects models. *J. Stat. Softw.* 82, 1–26. doi: 10.18637/jss.v082.i13

Logan, R., and Lowe, C. (2018). Residency and inter-reef connectivity of three gamefishes between natural reefs and a large mitigation artificial reef. *Mar. Ecol. Prog. Ser.* 593, 111–126. doi: 10.3354/meps12527

Logan, R. K., Vaudo, J. J., Sousa, L. L., Sampson, M., Wetherbee, B. M., and Shivji, M. S. (2020). Seasonal movements and habitat use of juvenile smooth hammerhead sharks in the western north atlantic ocean and significance for management. *Front. Mar. Sci.* 7:566364. doi: 10.3389/fmars.2020.566364

Logan, R. K., White, C. F., Winkler, C., Jorgensen, S. J., O'Sullivan, J. B., Lowe, C. G., et al. (2018). An evaluation of body condition and morphometric relationships within southern California juvenile white sharks Carcharodon carcharias. *J. Fish Biol.* 93, 842–849. doi: 10.1111/jfb.13785

Lowe, C., Blasius, M., Jarvis, E., Mason, T., Goodmanlowe, G., and O'Sullivan, J. (2012). "Historic Fishery interactions with white sharks in the southern california bight," in *Global Perspectives on the Biology and Life History of the White Shark*, ed. M. Domeier (Boca Raton, FL: CRC Press), 169–186. doi: 10.1201/b11532-17

Lowe, C., White, C., and Clark, C. (2018). "Use of autonomous vehicles for tracking and surveying of acoustically tagged elasmobranchs," in *Shark Research. Emerging Technologies and Applications for the Field and Laboratory*, eds J. Carrier, M. Heithaus, and C. Simpfendorfer (Boca Raton, FL: CRC Press).

Lyons, K., Jarvis, E. T., Jorgensen, S. J., Weng, K., O'sullivan, J., Winkler, C., et al. (2013). The degree and result of gillnet fishery interactions with juvenile white sharks in southern California assessed by fishery-independent and-dependent methods. *Fish. Res.* 147, 370–380. doi: 10.1016/j.fishres.2013.07.009

Lyons, K., and Wynne-Edwards, K. E. (2021). Sublethal, sex-specific, osmotic, and metabolic impairments in embryonic and adult round stingrays from a location exposed to environmental contamination in southern California, USA. *Environ. Sci. Pollut. Res.* doi: 10.1007/s11356-021-12546-0 [Epub ahead of print].

May, C., Meyer, L., Whitmarsh, S., and Huveneers, C. (2019). Eyes on the size: accuracy of visual length estimates of white sharks, *Carcharodon carcharias*. *R. Soc. Open. Sci.* 6:190456. doi: 10.1098/rsos.190456

Oh, B. Z. L., Thums, M., Babcock, R. C., Meeuwig, J. J., Pillans, R. D., Speed, C., et al. (2017). Contrasting patterns of residency and space use of coastal sharks within a communal shark nursery. *Mar. Freshw. Res.* 68:1501. doi: 10.1071/MF16131

Oñate-González, E. C., Sosa-Nishizaki, O., Herzka, S. Z., Lowe, C. G., Lyons, K., Santana-Morales, O., et al. (2017). Importance of bahia sebastian vizcaino as a nursery area for white sharks (*Carcharodon carcharias*) in the northeastern pacific: a fishery dependent analysis. *Fish. Res.* 188, 125–137. doi: 10.1016/j.fishres.2016.12.014

Pante, E., Benoit, S., and Irisson, J. (2019). *marmap: Import, Plot and Analyze Bathymetric and Topographic Data*.

Santana-Morales, O., Sosa—Nishizaki, O., Escobedo-Olvera, M., Onate-Gonzalez, E. C., O'Sullivan, J. B., and Cartamil, D. P. (2012). "Incidental catch and ecological observations of juvenile white sharks, carcharodon carcharias in Western Baja California, Mexico. Conservation implications," in *Global Perspectives on the Biology and Life History of the Great White Shark Research (Carcharodon carcharias)*, ed. M. L. Domeier (Boca Raton, FL: CRC Press), 187–198.

Schiff, K., Greenstein, D., Dodder, N., and Gillett, D. J. (2016). Southern California bight regional monitoring. *Reg. Stud. Mar. Sci.* 4, 34–46. doi: 10.1016/j.rsma.2015.09.003

Silva, I., Crane, M., Suwanwaree, P., Strine, C., and Goode, M. (2018). Using dynamic Brownian bridge movement models to identify home range size and movement patterns in king cobras. *PLoS One* 13:e0203449. doi: 10.1371/journal.pone.0203449

Simpfendorfer, C. A., Heupel, M. R., and Hueter, R. E. (2002). Estimation of short-term centers of activity from an array of omnidirectional hydrophones and its use in studying animal movements. *Can. J. Fish. Aquat. Sci.* 59, 23–32. doi: 10.1139/f01-191

Skomal, G., Braun, C., Chisholm, J., and Thorrold, S. (2017). Movements of the white shark Carcharodon carcharias in the North Atlantic Ocean. *Mar. Ecol. Prog. Ser.* 580, 1–16. doi: 10.3354/meps12306

Spaet, J. L. Y., Manica, A., Brand, C., Gallen, C., and Butcher, P. (2020a). Environmental conditions are poor predictors of immature white shark Carcharodon carcharias occurrences on coastal beaches of eastern Australia. *Mar. Ecol. Prog. Ser.* 653, 167–179. doi: 10.3354/meps13488

Spaet, J. L. Y., Patterson, T. A., Bradford, R. W., and Butcher, P. A. (2020b). Spatiotemporal distribution patterns of immature Australasian white sharks (*Carcharodon carcharias*). *Sci. Rep.* 10, 1–13. doi: 10.1038/s41598-020-66876-z

Speed, C., Field, I., Meekan, M., and Bradshaw, C. (2010). Complexities of coastal shark movements and their implications for management. *Mar. Ecol. Prog. Ser.* 408, 275–293. doi: 10.3354/meps08581

Speed, C. W., Meekan, M. G., and McMahon, C. R. (2012). Heat-seeking sharks: support for behaviouralthermoregulation in reef sharks. *Mar. Ecol. Prog. Ser.* 463, 231–245. doi: 10.3354/meps09864

Tamburin, E., Hoyos-Padilla, M., Sánchez-González, A., Hernández-Herrera, A., Elorriaga-Verplancken, F. R., and Galván-Magaña, F. (2019). New nursery area for white sharks (*Carcharodon carcharias*) in the Eastern Pacific Ocean. *Turkish J. Fish. Aquat. Sci.* 20, 325–329. doi: 10.4194/1303-2712-v20_4_08

Tobler, W., Deichmann, U., Gottsegen, J., and Maloy, K. (1995). *The Global Demography Project (Natl. Center for Geographic Information and Analysis, Univ. California, Santa Barbara).* Technical Report: 95-96.

Udyawer, V., Dwyer, R. G., Hoenner, X., Babcock, R. C., Brodie, S., Campbell, H. A., et al. (2018). A standardised framework for analysing animal detections from automated tracking arrays. *Anim. Biotelem.* 6:17. doi: 10.1186/s40317-018-0162-2

United States Census Bureau (2012). *2010 Census of Population & Housing. Redon. Beach (city), Calif.* Available online at: http://quickfacts.census.gov/qfd/states/06/0660018.html (accessed October 30, 2020).

Vandeperre, F., Aires-da-Silva, A., Lennert-Cody, C., Serrão Santos, R., and Afonso, P. (2016). Essential pelagic habitat of juvenile blue shark (*Prionace glauca*) inferred from telemetry data. *Limnol. Oceanogr.* 61, 1605–1625. doi: 10.1002/lno.10321

Weng, K., O'Sullivan, J., Lowe, C., Winkler, C., Blasius, M., Loke-Smith, K., et al. (2012). "Back to the wild," in *Global Perspectives on the Biology and Life History of the White Shark*, ed. M. Domeier (Boca Raton, FL: CRC Press), 419–446. doi: 10.1201/b11532-32

Weng, K. C., Boustany, A. M., Pyle, P., Anderson, S. D., Brown, A., and Block, B. A. (2007a). Migration and habitat of white sharks (*Carcharodon carcharias*) in the eastern Pacific Ocean. *Mar. Biol.* 152, 877–894. doi: 10.1007/s00227-007-0739-4

Weng, K. C., O'Sullivan, J. B., Lowe, C. G., Dewar, H., Winkler, C., and Block, B. A. (2007b). Movements, behavior and habitat preferences of juvenile white sharks *Carcharodon carcharias* in the eastern Pacific. *Mar. Ecol. Prog. Ser.* 338, 211–224. doi: 10.3354/meps338211

Werry, J., Bruce, B., Sumpton, W., Reid, D., and Mayer, D. (2012). "Beach areas used by juvenile white shark, carcharodon carcharias, in Eastern Australia," in *Global Perspectives on the Biology and Life History of the White Shark*, ed. M. L. Domeier (Boca Raton, FL: CRC Press), 271–286. doi: 10.1201/b11532-22

White, C. F., Lyons, K., Jorgensen, S. J., O'Sullivan, J., Winkler, C., Weng, K. C., et al. (2019). Quantifying habitat selection and variability in habitat suitability for juvenile white sharks. *PLoS One* 14:e0214642. doi: 10.1371/journal.pone.0214642

Wolfe, B. W., and Lowe, C. G. (2015). Movement patterns, habitat use and site fidelity of the white croaker (*Genyonemus lineatus*) in the Palos Verdes Superfund Site, Los Angeles, California. *Mar. Environ. Res.* 109, 69–80. doi: 10.1016/j.marenvres.2015.06.002

Wood, S. N. (2011). Fast stable restricted maximum likelihood and marginal likelihood estimation of semiparametric generalized linear models. *J. R. Stat. Soc. B* 73, 3–36. doi: 10.1111/j.1467-9868.2010.00749.x

Conflict of Interest: CW was the Principal of the company Aquatic Research Consultants.

The remaining authors declare that the research was conducted in the absence of any commercial or financial relationships that could be construed as a potential conflict of interest.

frontiers in Marine Science

ORIGINAL RESEARCH
published: 22 March 2021
doi: 10.3389/fmars.2021.643831

Three-Dimensional Movements and Habitat Selection of Young White Sharks (*Carcharodon carcharias*) Across a Temperate Continental Shelf Ecosystem

Rachel L. Shaw[1], Tobey H. Curtis[2], Gregory Metzger[3], Michael P. McCallister[1], Alisa Newton[4], G. Christopher Fischer[5] and Matthew J. Ajemian[1]*

[1] *Fisheries Ecology and Conservation Laboratory, Harbor Branch Oceanographic Institute, Florida Atlantic University, Fort Pierce, FL, United States,* [2] *Atlantic Highly Migratory Species Management Division, National Oceanic and Atmospheric Administration (NOAA) National Marine Fisheries Service, Gloucester, MA, United States,* [3] *South Fork Natural History Museum, Bridgehampton, NY, United States,* [4] *Wildlife Conservation Society, Bronx, NY, United States,* [5] *OCEARCH, Park City, UT, United States*

Edited by:
David Wells,
Texas A&M University at Galveston,
United States

Reviewed by:
Daniel M. Coffey,
Texas A&M University Corpus Christi,
United States
Samantha Andrzejaczek,
Stanford University, United States

***Correspondence:**
Matthew J. Ajemian
majemian@fau.edu

Specialty section:
This article was submitted to
Frontiers in Marine Science,
Marine Megafauna,
a section of the journal
Frontiers in Marine Science

Received: *18 December 2020*
Accepted: *05 February 2021*
Published: *22 March 2021*

Citation:
Shaw RL, Curtis TH, Metzger G, McCallister MP, Newton A, Fischer GC and Ajemian MJ (2021) Three-Dimensional Movements and Habitat Selection of Young White Sharks (Carcharodon carcharias) Across a Temperate Continental Shelf Ecosystem.
Front. Mar. Sci. 8:643831.
doi: 10.3389/fmars.2021.643831

As highly mobile predators with extensive home ranges, some shark species often utilize a continuum of habitats across the continental shelf ranging from the surf zone to the open ocean. For many species, these cross-shelf distributions can change depending on ontogeny or seasonal conditions. Recent research has confirmed a white shark (*Carcharodon carcharias*) summer nursery off Long Island, New York; however, habitat characterization of this nursery has not yet been conducted nor has fine-scale analysis of vertical behavior. Between 2016 and 2019, 21 young-of-the-year and juvenile white sharks were fitted with satellite and acoustic tags to examine distribution and selection for a suite of oceanographic variables during their late summertime (i.e., August to October) residence in the New York Bight. Horizontal position estimates were used to extract a suite of environmental measurements via remote sensing platforms and were linked with vertical profiles to produce three-dimensional movements for a subset of individuals also fitted with pop-up satellite archival tags (n = 7). Sharks exhibited horizontal movements parallel to Long Island's southern shoreline and coastal New Jersey, with distances from 0.1 to 131.5 km from shore. Log-likelihood chi-square analyses determined selection for waters with underlying bathymetry of 20–30 m, sea surface temperatures between 20.0 and 22.0°C, sea surface salinities between 31.0 and 32.0 ppt, and chlorophyll-a concentrations between 2.0 and 8.0 mg·m^{-3}. Multiple individuals also traversed the mid- to outer shelf region after leaving the Montauk tagging area. Vertical depth profiles illustrated oscillations between the surface and 199 m of water, with an average swimming depth of 9.2 ± 8.9 m. Water column temperatures during these oscillations ranged between 7.9 and 26.2°C (mean = 19.5 ± 2.0°C) with several individuals traversing highly stratified regions presumably associated with a mid-shelf cold pool adjacent to the Hudson Shelf Valley. These results suggest young white sharks exhibit connectivity between the immediate shoreline and mid-continental shelf region, where they play important ecological roles as predators on a variety of species. Our study improves characterization of essential fish habitat for young white sharks and provides new insights into their reliance on this productive continental shelf ecosystem.

Keywords: white shark (*Carcharodon carcharias*), Atlantic Ocean (North), New York Bight, telemetry, habitat use, diving behavior

INTRODUCTION

Shark nursery habitats are areas that can disproportionately contribute to the productivity of a population (Beck et al., 2001; Heupel et al., 2007). These areas typically provide an appropriate food supply (both quality and quantity), ideal physical conditions (temperature, salinity, etc.), and reduced biological interactions (predation, competition, etc.) for immature individuals thereby increasing survival rates compared to other habitats (Heupel et al., 2007; Parsons et al., 2008). Coastal shark nursery habitats may include habitat types such as mud flats, coral reefs, mangrove forests, and seagrass beds that are found in enclosed embayments or nearshore areas (Heupel et al., 2018). These habitats perform a nursery role as they limit entry of large predators (as a result of the shallow depth), and offer abundant food resources critical to rapid growth during early life stages (Heupel et al., 2018). However, the current definition is somewhat biased due to a historical focus on tropical and subtropical regions where nurseries are primarily located within semi-enclosed estuaries and lagoons (Heupel et al., 2018). There is considerably less information on coastal and offshore nursery areas (Knip et al., 2010; Heupel et al., 2018).

Temperate continental shelves are among some of the most dynamic and productive marine ecosystems in the world, particularly during spring and summertime when primary and secondary production is at its highest (Friedland et al., 2015). For example, the mid-Atlantic Bight, located within the NE shelf large marine ecosystem of the US, seasonally supports large mobile predators such as sea turtles (Murray and Orphanides, 2013; Dodge et al., 2014), marine mammals (Stepanuk et al., 2018), and sharks (Simpfendorfer et al., 2002; Kohler and Turner, 2019; Latour and Gartland, 2020). While the importance of these areas to sharks has been known for some time, the finer-scale use of shelf systems by these animals has been limited, and impacts our understanding of potential shark "hotspots" within these large ecosystems (Bangley et al., 2020a). The mid-Atlantic Bight has characteristic habitat heterogeneity and dynamic features that arise from the immediate shoreline out to the shelf-edge. These include Gulf Stream eddies (Churchill et al., 1993), bathymetric breaks, valleys, and canyons (Knebel, 1979), as well as major riverine discharges (Hossler and Bauer, 2013). Should sharks exhibit preferences for or aggregate in any of these ephemeral or spatially restricted habitats, these can increase their vulnerability to overexploitation or other anthropogenic disturbances in these regions. As such, understanding the use of these shelf ecosystems by predators is important for species conservation and identifying potential threats to sustainability. This is particularly relevant in the mid-Atlantic Bight where numerous shark species are exposed to commercial and recreational fisheries (Kohler and Turner, 2019; NMFS, 2020), expanding offshore wind energy infrastructure (Methratta, 2020), and climate change (Saba et al., 2016). This region is among the most rapidly warming large marine ecosystems in the world (Saba et al., 2016), with variable consequences likely for species that rely on its habitats including potential distribution shifts and declines in productivity (Hare et al., 2016; Kleisner et al., 2016).

Habitat use and movement dynamics of sharks along and across shelf habitats has been historically challenging to study, although research on young shark movements is growing in such areas (Curtis et al., 2018; White et al., 2019; Bangley et al., 2020a; Logan et al., 2020). This is particularly true for most pelagic shark species, which remain offshore for much of their life history and rarely captured in fishery-independent surveys. These characteristics have limited horizontal and vertical habitat data for these widely ranging species. Fortunately, such information can be revealed using individual-based biotelemetry (i.e., electronic tagging) techniques. For example, through the use of active acoustic tracking along with depth-sensing transmitters, Klimley et al. (2002) and Cartamil et al. (2010) characterized both horizontal and vertical movement patterns of young shortfin mako (*Isurus oxyrinchus*), blue (*Prionace glauca*), white (*Carcharodon carcharias*), and common thresher sharks (*Alopias vulpinus*) in the southern California Bight. However, due to the limitations of acoustic tracking, which requires being within the detection range of the receiver, tracks only lasted maximally 3.1 days and thus were both temporally and spatially restricted. While passive acoustic receiver networks can facilitate extended tracking of movements (Bangley et al., 2020b), these aren't always feasible in exploratory studies of offshore animal movement and behavior around short-lived features. More recently, researchers have begun combining archival and satellite-transmitting tag technologies to support horizontal and vertical tracking of free-ranging individuals and the dynamic habitats they experience. Combined with other remote sensing environmental observations, this approach has been recently utilized to explore how temperate shark species such as basking sharks (*Cetorhinus maximus*), adult white sharks, and blue sharks use ephemeral features such as primary production hotspots along the continental shelf and mesoscale eddies in the open ocean (Curtis et al., 2014; Gaube et al., 2018; Braun et al., 2019). Such coupled information permits analyses of how individual sharks interact with oceanography, transfer nutrients across ecosystem gradients, and advance our understanding of the overall movement dynamics of these highly mobile species.

Here, we utilize a similar three-dimensional approach to examine young-of-the-year (YOY) and young juvenile (age 1–2) white shark habitat use and cross-shelf connectivity in the New York Bight, an established white shark nursery (Curtis et al., 2018). The summer distribution of large juvenile and adult white sharks in the northwest Atlantic generally ranges from New Jersey to Nova Scotia, with aggregations occurring adjacent to burgeoning pinniped colonies (Casey and Pratt, 1985; Curtis et al., 2014; Skomal et al., 2017), but there is still little data on the movements and habitat of YOY and small juvenile sharks (Curtis et al., 2018). All life stages migrate out of northern latitudes during the fall and overwinter off the southeastern U.S. (Curtis et al., 2014, 2018; Skomal et al., 2017). While the northwest Atlantic white shark population appears to be recovering from historical overfishing (Curtis et al., 2014), there remains considerable uncertainty in their population dynamics, seasonal habitat preferences, ecological roles, and exposure to anthropogenic impacts (Skomal et al., 2017; Curtis et al., 2018; Bastien et al., 2020; Bowlby and Gibson, 2020). Improved understanding of habitat selection within the only known northwest Atlantic nursery area will inform ongoing conservation strategies for this vulnerable white shark population.

MATERIALS AND METHODS

Study Location, Animal Collection, and Tagging

This study was conducted in the New York Bight between 2016 and 2019. The New York Bight is the coastal region between Montauk, New York and Cape May, New Jersey. Sharks were collected, sampled, tagged, and released following methods described by Curtis et al. (2018). Briefly, sharks were caught via hook and line using live baitfish. In 2016 and 2017, sharks were tagged using a boatlift platform on the 42 m long M/V OCEARCH, whereas in 2018 and 2019, sharks were tagged in the water while being secured alongside a 7 m fishing vessel.

Sharks were fitted with either a FastGPS Argos transmitter (Sirtrack F6F) alone, or a combination of a Smart Position or Temperature transmitting (SPOT) tag (Wildlife Computers SPOT-258A) and an acoustic transmitter (Vemco V16-6H). The SPOT tags started uplinks after being dry for <0.25 s and sent 10 uplinks per message. Minimum uplink interval was 45 s with a maximum of 160 transmissions per day. The tags were fitted onto the first dorsal fin using nylon bolts and transmitted when the fin was above the sea surface as described by Curtis et al. (2018).

FastGPS Argos transmitters were fitted using the same procedure as the SPOT tags. These tags are designed to transmit to the Argos Satellite System similarly to SPOT tags, but with additional capabilities to also receive radio signals from a GPS satellite when the tag is above the surface for a sufficient period of time. After the transmitter retrieved the signal from the GPS satellite, it then transmitted the retrieved location to the Argos Satellite System. In general, FastGPS tags are capable of producing positions with a lower estimated error (<100 m) than SPOT tags (Dujon et al., 2014). For the first 28 days of deployment, FastGPS transmitters were programmed to transmit to the Argos Satellite System every 45 s, with a GPS fix interval every 120 min. After 28 days, the transmitters were then programmed to continue transmitting to the Argos Satellite System every 45 s, but to increase the GPS fix interval to 180 min to balance battery life throughout the duration of the study. With these settings, tags were expected to receive an average of 35 messages per day and have an expected battery life of 472 days. For both SPOT and FastGPS tags, all Argos position estimates classified as Class Z were removed from the analysis due to the large estimated error associated with that location class (Boyd and Brightsmith, 2013).

Acoustic transmitters (Vemco V16-6H) were cold sterilized with benzalkonium chloride (Benz-all), and surgically placed into the coelomic cavity of each shark and the 4 cm incision was closed in a simple interrupted pattern with 2-O polydioxinone suture (Ethicon PDS II). The implanted acoustic transmitters randomly transmitted a unique signal every 60–90 s, and had a battery life of approximately 10 years. These tags were detected by Vemco acoustic receivers from collaborative acoustic monitoring arrays distributed across the Atlantic coast prior to this study (refer to Bangley et al., 2020b for an explanation of receiver coverage). Given the uncertainty in reporting across the collaborative networks, all acoustic telemetry-based position estimates were considered presence-only data (no absences).

During 2017–2019, a subset of white sharks were also fitted with high-rate pop-up satellite archival tags (Model PSAT LIFE, Lotek Wireless, Inc.). These tags archived light level, temperature, and pressure measurements at 10 s intervals for up to 28 days post-release after which they detached from the shark, floated to the surface, and transmitted data to the Argos satellite system. The transmitted data were aggregated into 5 min bins, with the full 10 s resolution data available only if the tag was physically recovered. Temperature-depth time-series were generated for each tag and summary statistics were compiled.

Movements and Habitat Selection

Horizontal movements were analyzed by downsampling the position estimates from the satellite tags (location classes A, B, 0, 1, 2, and 3) and acoustic transmitters to find daily mean position estimates for each of the 20 individuals with SPOT/FastGPS tags. No horizontal positions were estimated from PSAT data. Following Curtis et al. (2018), gaps between days were linearly estimated and these daily position estimates were then plotted in ArcGIS (version 10.3) and movements faster than 10 $km \cdot h^{-1}$ were filtered out using Movement Ecology Tools for ArcGIS (ArcMET version 10.2.2 v3; Wall, 2014). Any position estimates found on land were also removed.

Environmental data (sea surface temperature, sea surface salinity, chlorophyll a) located at the horizontal position estimates were extracted from NOAA's ERDDAP server using the Xtractomatic and rerddapXtracto packages in R (version 3.6.0) to characterize habitat use. The resolution of the environmental data was coarser than the expected accuracy of most tag positions (<5 km), so horizontal positions were only matched to a single underlying environmental grid cell. Sea surface temperature (SST) was gathered from the GHRSST Level 4 MUR Global Foundation Sea Surface Temperature Analysis dataset (v4.1), which provided daily SSTs with a resolution of 0.1°. The Sea Surface Salinity, Near Real Time, Soil Moisture Active Passive (SMAP) Daily Composite dataset was used to compile daily sea surface salinity with a resolution of 0.25°. Chlorophyll a was used as a proxy for productivity, or areas with high amounts of phytoplankton (Trujillo and Thurman, 2016), as satellites are able to calculate the color of the water to determine relative amounts of phytoplankton on the surface of the ocean (National Aeronautics and Space Administration (NASA), 2019). Daily chlorophyll-a amounts were collected from the Chlorophyll-a Aqua MODIS dataset (0.05° resolution).

A gridded bathymetric dataset (global 30 arc-s interval grid) from the General Bathymetric Chart of the Oceans (GEBCO) was used to analyze the bottom depth and features of the benthos below horizontal position estimates [General Bathymetric Chart of the Oceans (GEBCO), 2019]. Additionally, a 1 km by 1 km grid was calculated in ArcGIS. The corresponding latitudes and longitudes were imported into R Studio in order to identify the available environmental variables throughout the entire New York Bight (coastal waters bound between 41.367°N, 70.296°W and 37.902°N, 75.327°W). The Xtractomatic and rerddapXtracto packages were used to find available environmental data located at the 1 km by 1 km intervals for the entire New York Bight. Environmental data that coincided with the time frame of each individual's track was collected.

A log-likelihood chi-squared test was then conducted to assess habitat preferences of tagged individuals. A log-likelihood chi-squared test compares the goodness-of-fit of the hypothesized model against the observed model and can be used to compute a p-value. For this exercise we assumed all habitat data extracted from the continental shelf of the New York Bight were "available" to sharks. Following Rogers and White (2007), three log-likelihood chi-square statistics were calculated. The first chi-square statistic was used to determine if the sharks were using the various habitats in a similar fashion. The null hypothesis states that all sampled individuals are using the habitats in the same proportions as each other. The following bin widths (i.e., categories) were created for each parameter based on the distribution of the data and to facilitate interpretation: 10 m (bathymetry), 2°C (temperature), 2 mg·m^{-3} (chlorophyll a), and 1 ppt (salinity). A $p < 0.05$ indicates evidence for heterogeneity, signifying individuals were using the various habitats in different proportions. A second chi-square statistic was calculated to examine if selection was occurring for individual habitat types (i.e., particular ranges) by some of the sharks. The null hypothesis states selection is not occurring in at least some of the sharks. The final chi-square statistic was calculated by taking the difference between the first two. This statistic describes whether, on average, sharks were using the various habitat types in proportion to their availability, regardless of which ones were selected. A $p < 0.05$ indicates strong selection for certain habitat types.

In order to determine if there was a preference for specific habitats or environmental variable ranges, selection ratios were calculated. A selection ratio greater than one indicates preference for that habitat, with a selection ratio less than one indicating avoidance for that particular habitat. All statistical tests were conducted in R Studio (version 1.1.453). Selection ratios were plotted for all four parameters to assess which had mean and confidence intervals that were clearly above or below one, indicating habitat selection or avoidance, respectively.

Vertical Activity and Three-Dimensional Movement

For double-tagged sharks (i.e., SPOT/FastGPS + PSAT), the PSAT temperature and depth logs were chronologically integrated with the geopositional data from the SPOT/FastGPS and acoustic transmitters. The horizontal position estimates were then filtered to meet the PSAT time frame of approximately 28 days. With the aim of matching the horizontal position estimates to the vertical log provided by the PSAT, the horizontal position estimates were linearly interpolated to match the interval of the PSAT log at 5 min or 10 s intervals, depending on whether or not the individual's PSAT had been physically recovered. The resulting three-dimensional tracks were plotted in ArcScene 10.3 and overlaid onto bathymetry for visualization of movements with respect to bottom features, and reflect the best possible tracks given the availability of horizontal positions.

RESULTS

Horizontal Movements and Habitat Selection

Movement data from 21 white sharks (11 males, 10 females) were collected between 2016 and 2019. A total of 880 positions were received from SPOT/FastGPS transmitters and 4,478 detections were received from 49 unique ACT acoustic receivers, which were subsequently downsampled to daily positions. Individual sizes ranged from 138.0 to 166.4 cm total length (TL; **Table 1**). Horizontal position estimates from the satellite tags and acoustic detections demonstrated movement parallel to Long Island's southern shoreline and along the New Jersey coastline (**Figure 1**). During this time frame, individuals traveled 0.1 to 131.5 km away from shore, with an average (±1 *SD*) distance from shore of 12.7 ± 0.2 km. Total track distances between 57.4 and 2,089.0 km were observed, with an average of 616.1 ± 126.7 km. Individual track durations during the study period ranged from 8 to 170 days, with an average track duration of 58 ± 10 days. All daily position estimates were located along the continental shelf except one; WS-11 had one daily position estimate on the continental slope.

Bathymetry

The average available bathymetry in the New York Bight was 52.1 ± 33.3 m, with a maximum depth of 294.3 m. The average underlying bathymetry (i.e., depths that tagged individuals swam over) was 27.7 ± 13.4 m, with a maximum depth of 338.2 m, and a minimum depth of 7.2 m. While the most commonly available bathymetry bin in the New York Bight was 30–40 m (available in 15% of the area), individuals were most frequently observed in shallower areas, between 20 and 30 m (48% of the time). Individuals only swam over depths between 30.0 and 40.0 m 27% of the time. Chi-square statistical results confirmed heterogeneity in underlying bathymetry use among sampled sharks (χ_{L12} = 852.1356, df = 551, P = 0.00001; **Table 2**), and that some individuals were selective in underlying bathymetry (χ_{L22} = 2,743.34, df = 580, P = 0.00001). On average,

TABLE 1 | Biological information of tagged sharks in the study.

Individual	Sex	Total length (cm)	Date of capture	Tag type	SPOT/ACT/GPS duration (days)	PSAT duration (days)
WS-1	F	142.0	2016-08-19	SPOT/ACT	64	NA
WS-2	M	158.0	2016-08-20	SPOT/ACT	62	NA
WS-3	M	138.0	2016-08-21	SPOT/ACT	31	NA
WS-4	M	166.0	2016-08-21	SPOT/ACT	8	NA
WS-5	M	158.0	2016-08-22	SPOT/ACT	15	NA
WS-6	F	155.0	2016-08-23	SPOT/ACT	44	NA
WS-7	F	161.8	2016-08-23	SPOT/ACT	44	NA
WS-8	M	162.0	2016-08-23	SPOT/ACT	67	NA
WS-9	M	150.0	2017-08-11	SPOT/ACT	151	NA
WS-10	F	151.1	2017-08-12	SPOT/ACT	48	NA
WS-11	M	166.4	2017-08-12	SPOT/ACT/PSAT	170	27
WS-12	M	165.0	2017-08-14	SPOT/ACT/PSAT	58	28
WS-13	M	147.0	2017-08-17	SPOT/ACT/PSAT	64	28**
WS-14	F	165.0	2017-08-20	SPOT/ACT/PSAT	66*	28**
WS-15	F	165.4	2017-08-20	SPOT/ACT/PSAT	97	27
WS-16	F	154.4	2017-08-21	SPOT/ACT	120	NA
WS-17	F	152.0	2017-08-22	SPOT/ACT	1*	NA
WS-18	F	156.0	2017-08-24	SPOT/ACT	10	NA
WS-19	M	182.9	2018-07-19	PSAT	NA	28
WS-20	M	152.0	2019-08-11	FastGPS/PSAT	15	28**
WS-21	F	155.5	2019-08-12	FastGPS/PSAT	27	28

*Eighteen of the twenty-one individuals were tagged with a satellite tag and an acoustic tag, while two individuals were tagged with a FastGPS tag. Eight of these individuals were also tagged with a PSAT. ACT signifies an acoustic tag. *Did not receive transmissions from SPOT tag. **PSAT recovered; data available in 10 s intervals.*

individuals were not using the bathymetry in proportion to its availability, regardless of which depths were selected ($\chi_{L22} - \chi_{L12} = 1{,}891.201$, df = 29, $P = 0.00001$). Selection ratio results showed a preference for underlying depths between 20 and 30 m, avoidance of depths shallower than 10 m and deeper than 40 m (**Figure 2A**). Mean selection ratios were above 1 for the 10–20 and 30–40 m intervals; however, confidence intervals were below the threshold value. As such, these habitats were considered to be neither selected nor avoided.

Sea Surface Temperature

Throughout the study period SST in the New York Bight ranged from 12.4 to 29.4°C (mean = 21.9 ± 2.8°C). Individuals swam in mean SSTs of 21.3 ± 2.0°C, with a maximum SST of 26.4°C, and a minimum SST of 15.7°C. All three chi-square statistics for SST analysis were found to be significant ($P < 0.0001$; **Table 2**), suggesting tagged individuals were using the SSTs differently and selecting for specific ranges of temperature. Chi-square results show sampled sharks exhibited heterogeneous use of available SSTs ($\chi_{L12} = 603.08$, df = 152, $P < 0.0001$), and individuals were demonstrating selection ($\chi_{L22} = 961.379$, df = 160, $P < 0.0001$). Additionally, there was evidence that the average selection was not in proportion to the availability of resources ($\chi_{L22} - \chi_{L12} = 358.299$, df = 8, $P < 0.0001$). Selection ratios results suggested a preference for SST between 20.0 and 22.0°C, and potentially between 18.0 and 20.0°C; confidence intervals extended slightly below the selection ratio threshold, so preference at the latter range was unclear (**Figure 2B**). Results also showed an avoidance of SSTs below 18.0°C and above 24.0°C, with no evidence of selection or avoidance for the 22.0–24.0°C temperature bin.

Chlorophyll-a

The mean chlorophyll-a concentration in the New York Bight ranged from 0.1 to 20.0 mg·m^{-3} (mean = 1.7 ± 2.3 mg·m^{-3}). Individuals swam in an average of 3.6 mg·m^{-3} (±3.2 mg·m^{-3}), with a maximum of 19.6 mg·m^{-3}, and a minimum of 0.3 mg·m^{-3}. Chlorophyll-a was used heterogeneously ($\chi_{L12} = 264.0624$, df = 170, $P = < 0.00001$; **Table 2**). At least some of the sharks were selective in the chlorophyll-a concentrations that were swam in compared to that chlorophyll-a concentration's availability ($\chi_{L22} = 730.8104$, df = 180, $P = 0.00001$). On average, the sampled sharks were not using chlorophyll-a concentrations in proportion to their availability, regardless of which concentrations that were being selected for ($\chi_{L22} - \chi_{L12} = 466.748$, df = 9, $P = 0.00001$). Selection ratio results found avoidance for lower concentrations of chlorophyll a between 0.0 and 2.0 mg·m^{-3}, and preference for concentrations between 2.0 and 8.0 mg·m^{-3} (**Figure 2C**). There was also potential for preference above concentrations of 8.0 mg·m^{-3}; however, confidence intervals extended below the selection ratio threshold. Due to this, a preference for concentrations greater than 8.0 mg·m^{-3} was unresolved.

Sea Surface Salinity

The average available sea surface salinity in the New York Bight was 32.8 ± 1.2 ppt, with a maximum of 37.5 ppt, and a minimum of 30.0 ppt. The average sea surface salinity that individuals

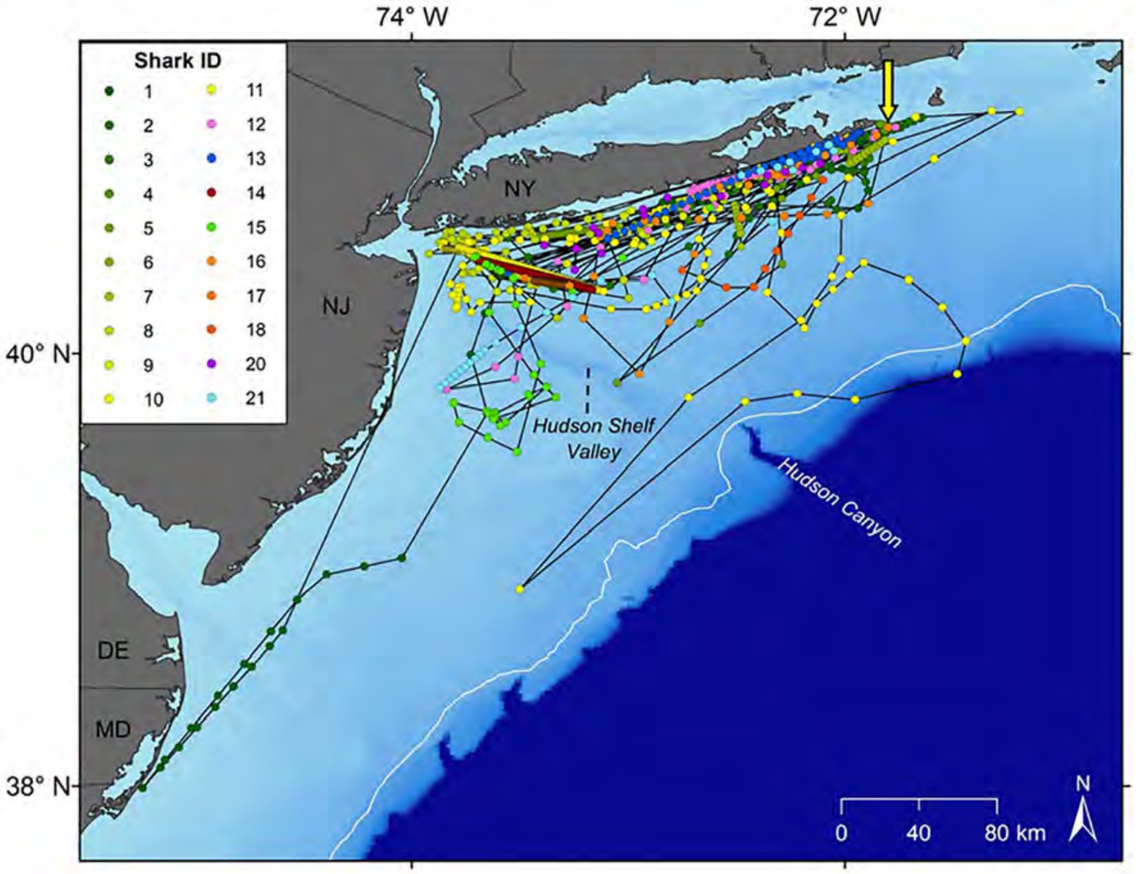

FIGURE 1 | Horizontal tracks of the 21 white sharks tagged in the study. Yellow arrow depicts capture and release site off Montauk, NY. Dots represent daily locations via downsampling of Smart Position or Temperature (SPOT) transmitting tags, FastGPS, and/or acoustic detections.

TABLE 2 | Table of chi-square test statistics and associated values for each of the parameters analyzed in with respect to habitat preferences.

Parameter	Chi-square Statistic	Value	df	*P*
Bathymetry	$\chi_{L1}{}^2$	852.1	551	<0.00001
	$\chi_{L2}{}^2$	2743.3	580	<0.00001
	$\chi_{L2}{}^2 - \chi_{L1}{}^2$	1891.2	29	<0.00001
SST	$\chi_{L1}{}^2$	603.1	152	<0.00001
	$\chi_{L2}{}^2$	961.4	160	<0.00001
	$\chi_{L2}{}^2 - \chi_{L1}{}^2$	358.3	8	<0.00001
SSS	$\chi_{L1}{}^2$	68.9	133	0.99999
	$\chi_{L2}{}^2$	131.1	140	0.69292
	$\chi_{L2}{}^2 - \chi_{L1}{}^2$	62.2	7	<0.00001
Chl-a	$\chi_{L1}{}^2$	264.1	171	<0.00001
	$\chi_{L2}{}^2$	730.8	180	<0.00001
	$\chi_{L2}{}^2 - \chi_{L1}{}^2$	466.7	9	<0.00001

Abbreviations are as follows; SST, sea surface temperature; SSS, sea surface salinity; Chl-a, Chlorophyll-a.

swam in was 32.3 ppt (±0.9), with a maximum of 35.7 ppt, and a minimum of 30.5 ppt. The first chi-square statistic was not significant ($\chi_{L12} = 68.897$, df = 133, $P = 0.99$), which suggests all sampled sharks were using sea surface salinities in the same proportions as the other sampled sharks (**Table 2**). Selection was not occurring in at least some of the sharks; some of the sharks were using the sea surface salinities in proportion to their availability ($\chi_{L22} = 131.0885$, df = 140, $P = 0.69$). On average, there was strong selection for certain sea surface salinities ($\chi_{L22} - \chi_{L12} = 62.19167$, df = 7, $P = 0.00001$), as was demonstrated on an individual basis. For example, WS-3, WS-10, and WS-12 had a strong selection for sea surface salinities between 31.0 and 32.0 ppt, while WS-7 selected for 32.0–33.0 ppt, and WS-21 had a strong selection for 30.0–32.0 ppt. Overall, selection ratio results illustrated a preference for sea surface salinities between 31.0 and 32.0 ppt, with neutral responses to salinity ranges of 30.0–31.0 and 32.0–34.0 and avoidance for anything >34.0 (**Figure 2D**).

Vertical Movements

White shark depth ranges from the 8 individuals fitted with PSAT tags spanned the surface to 199 m, with individual means between 6.6 and 11.7 m (**Table 3**). These mean depths were positioned at roughly half of the available water column based on underlying bathymetry estimated from horizontal positions. Temperatures recorded by PSAT tags ranged from 7.9 to 26.2°C with individual means from 19.2 to 20.7°C (**Table 3**). Mean temperatures recorded by PSAT tags approximated those

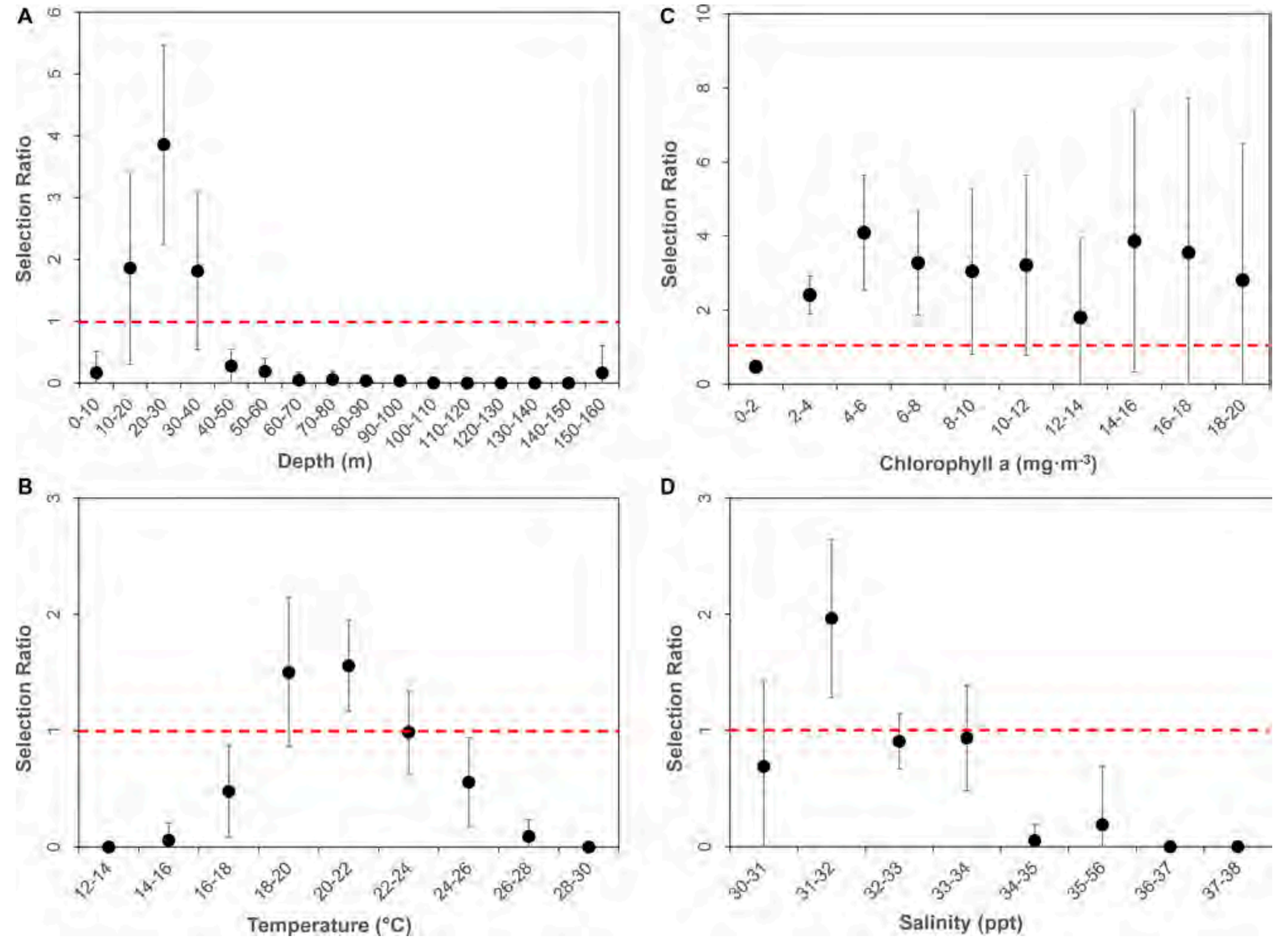

FIGURE 2 | Dot plot of mean selection ratios (and confidence intervals) for various environmental parameters by bins: **(A)** Bathymetry, **(B)** Sea Surface Temperature, **(C)** Chlorophyll-a, and **(D)** Sea Surface Salinity. All environmental data were derived from remote sensing at daily horizontal position estimates of tagged animals. Dashed horizontal red line represents selection ratio of 1, above which values are "selected" for, and below which are considered "avoided."

extracted from remote sensing of SSTs (i.e., within 1°C) based on horizontal positions, although the latter recorded warmer temperatures. The smallest individual tagged with a PSAT (WS-13) exhibited the shallowest max depth (24.3 m) and warmest minimum temperature (17.3°C), as well as the narrowest depth and temperature ranges (**Table 3**).

Three-dimensional interpolation of vertical and horizontal positions was possible for 7 individuals. Analyses of these data found that individuals swam over benthos between 4 and 424 m deep, mainly on the continental shelf, with one dive recorded off the continental slope (**Figures 3**, **4**). There were multiple instances of sharks traversing and presumably interacting with large bathymetric and/or oceanographic features as they moved across the continental shelf, although this varied across individuals (**Supplementary Figures 1–7**). For example, several individuals (WS-11, WS-12, WS-15, and WS-21) crossed the Hudson Shelf Valley during southward movements across the New York Bight (**Figure 4A**; S1, S2, S5, S7). One individual, WS-15, also appeared to interact with relatively cold water (<10°C) when traversing the Hudson Shelf Valley (S5), which was apparent from 20 to 80 m depth and in stark contrast with surface water that approached 25°C during this period in late August 2017 (**Figures 3F**, **4B**). Other instances of considerable thermal stratification (i.e., 10°C difference between surface water and deepest dives) were evident in dive profiles of WS-14 (**Figure 3D**), WS-19 (**Figure 3G**), WS-20 (**Figure 3H**), and WS-21 (**Figure 3I**). Unfortunately, WS-14 had limited horizontal position estimates due to a lack of transmissions from its SPOT tag (S4). However, the depth profiles from this recovered tag showed extensive oscillations between the surface and depth (i.e., 30–50 m) (**Figure 3E**). Other portions of temperature-depth profiles for these individuals were more homogeneous, with temperatures around 20°C and more limited depths <30 m. For example, WS-13 stayed close to Montauk, NY (**Figure 4A**; S3) and did not travel as far south as the other tagged sharks during the 28 days period.

TABLE 3 | Descriptive statistics for temperature and depth from the eight individuals fitted with pop-off satellite archival tags.

				Depth (m)			Temperature (°C)		
Individual	**Sex**	**Total length (cm)**	**Date of capture**	**Min**	**Mean ± *SD***	**Max**	**Min**	**Mean ± *SD***	**Max**
WS-11	M	166.4	2017-08-12	0.0	9.0 ± 13.9	199.4	7.9	19.9 ± 2.8	24.2
WS-12	M	165.0	2017-08-14	0.0	11.7 ± 8.7	411	10.7	19.4 ± 1.7	24.7
WS-13	M	147.0	2017-08-17	0.3	8.9 ± 4.4	24.3	17.3	19.3 ± 0.6	22.0
WS-14	F	165.0	2017-08-20	0.0	9.3 ± 6.1	48.5	9.4	19.2 ± 1.4	23.7
WS-15	F	165.4	2017-08-20	0.0	8.7 ± 11.6	77.2	8.7	19.4 ± 3.2	24.5
WS-19	M	182.9	2018-07-19	0.0	8.3 ± 9.0	43.1	9.0	20.7 ± 3.3	26.2
WS-20	M	152.0	2019-08-11	0.0	9.9 ± 7.0	41.6	9.5	19.3 ± 1.7	24.6
WS-21	F	155.5	2019-08-12	0.0	6.6 ± 8.1	46.5	8.5	20.5 ± 1.9	24.2

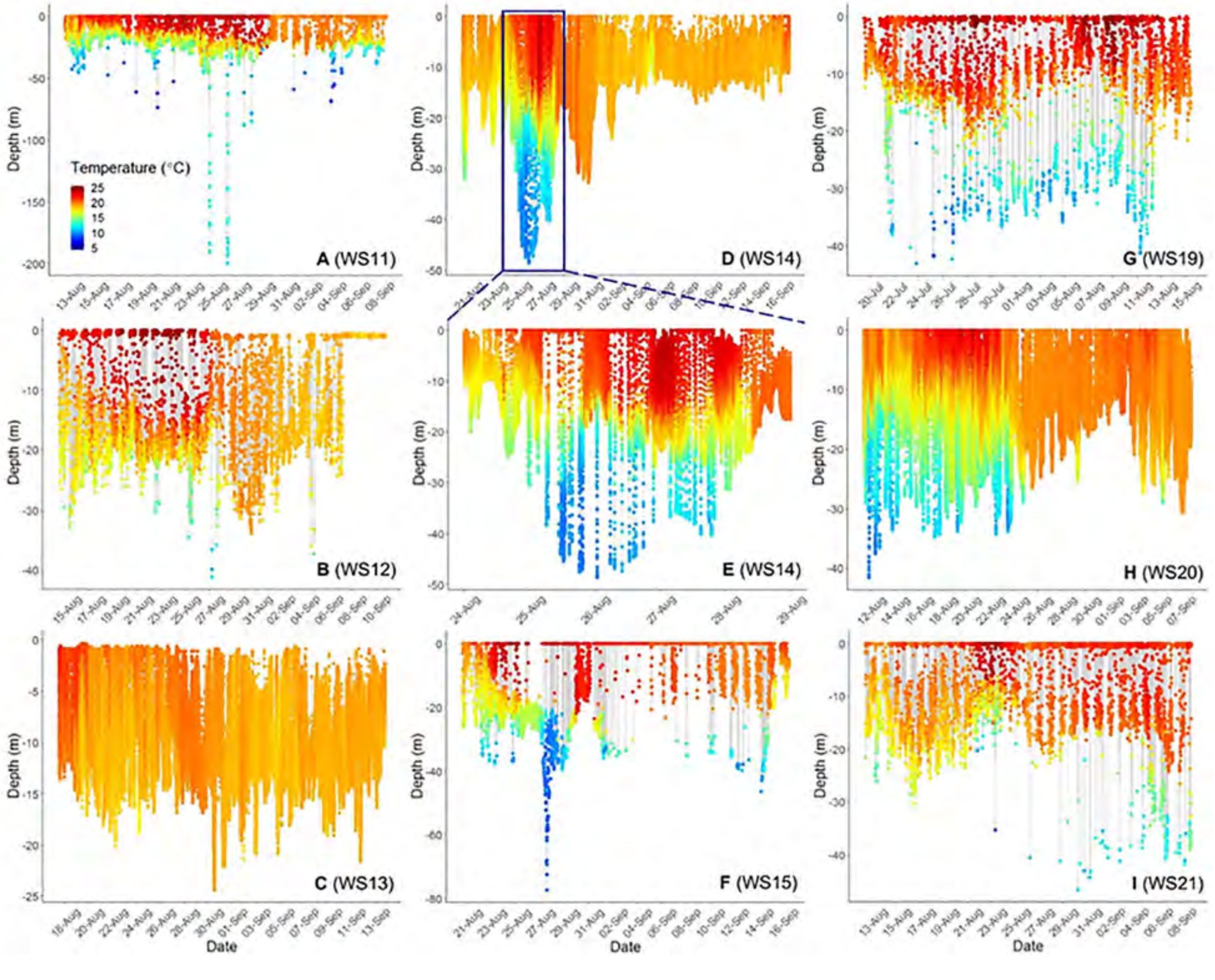

FIGURE 3 | Time-series scatterplots of vertical depth and temperature profiles (color bar on bottom left of first plot) for 8. White Sharks 11–15 **(A–F)** were tagged in 2017, whereas 19 was tagged in 2018 **(G)** and 20 and 21 **(H,I)** are from 2019. **(E)** Represents an expansion of the blue box in **(D)** to demonstrate diel patterns in depth and temperature use. **(C,D,H)** Represent complete dive profiles from recovered PSAT tags.

DISCUSSION

This study significantly expands our understanding of fine-scale vertical movement patterns and habitat selection of YOY and small juvenile white sharks in the New York Bight, the only confirmed nursery area for the northwest Atlantic white shark population (Curtis et al., 2018). Furthermore, it contributes to the growing body of information on the general life history

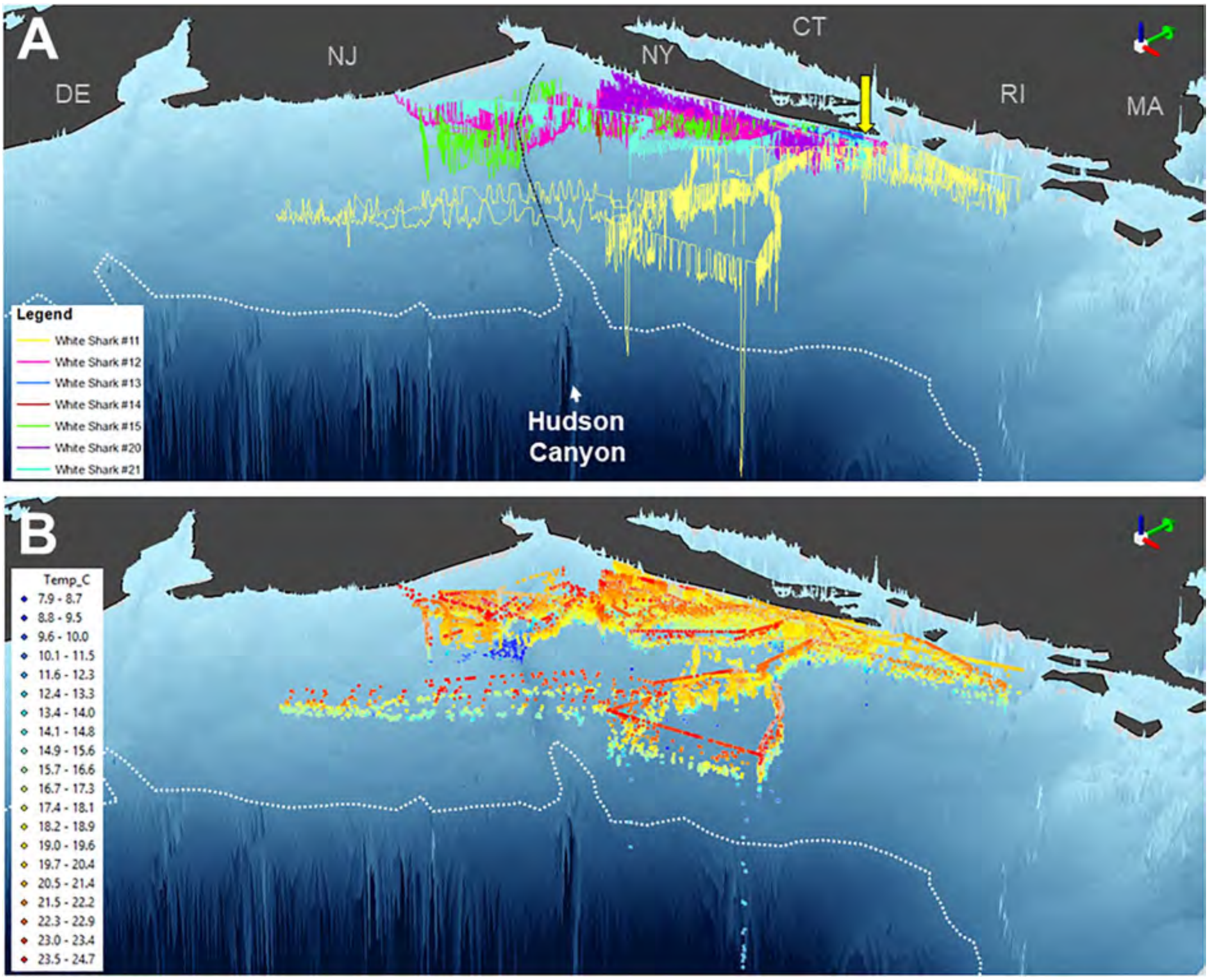

FIGURE 4 | Three-dimensional position estimates for 7 double or triple-tagged sharks in the New York Bight region. Positions are colored by individual shark in **(A)** (as per **Figure 1**) and temperature in **(B)**. Bathymetry is presented based on GEBCO data, with the continental shelf break (i.e., 200 m isobath) indicated by a white dotted line and the Hudson Shelf Valley identified by black dashed line. Green 3D arrows (top right of panels) point north. Yellow arrow depicts capture and release site off Montauk, NY.

and ecology of white sharks in this comparatively understudied region (Curtis et al., 2014, 2018; Skomal et al., 2017; Huveneers et al., 2018; Bastien et al., 2020). The residency and consistent selection of continental shelf habitat in the New York Bight by young white sharks results in a striking size-based segregation of the population during summer and autumn months (July through November) when larger white sharks (>2.5 m) mainly occupy more northern waters from Massachusetts to Newfoundland, Canada (Casey and Pratt, 1985; Curtis et al., 2014; Skomal et al., 2017; Bastien et al., 2020). The relative scarcity of large white sharks in the nursery area during this period provides young sharks a refuge from natural mortality and risk effects associated with predation, and permits them to play a role as apex predators in the system. Thus, their habitat selection patterns can result in important direct and indirect effects on ecosystem structure and nutrient pathways from the coastal zone to offshore habitats.

Habitat Selection

Across the multiple years examined in this study, tagged individuals consistently displayed horizontal movements parallel to Long Island's southern shoreline and the New Jersey coast. Consistent with the preliminary observations of Curtis et al. (2018), horizontal movements ranged from the surf zone to over 130 km from shore; however, over 90% of the horizontal movements were within 20 km of Long Island's southern shoreline. Juvenile white sharks in the Southern California Bight were also found to stay close to shore, with an average distance of 7.2 ± 5.7 km (White et al., 2019). White et al. (2019) attempted to model suitable juvenile white shark habitat along the U.S. Atlantic coast using observations from the U.S. Pacific coast, including distance from shore as a key variable. Our results suggest that distance from shore may not be as important as bathymetry, given the sharks in the present study occupied waters further from shore than predicted by White et al. (2019), and tended to select waters >10 km from shore overlying bottom depths from 20 to 30 m. This is likely due to significant differences in the width of the continental shelf in southern California compared to the New York Bight (<10 vs. >100 km, respectively). The reasons for the apparent avoidance of nearshore shallow waters (<10 m deep) by young white sharks tracked in this study requires further exploration, but could be due to lower prey availability, higher wave energy and related higher turbidity, and/or competition from other co-occurring predators (e.g., sand tiger shark *Carcharias taurus*, sandbar shark *Carcharhinus plumbeus*, or dusky shark *C. obscurus*). Based on the available observations globally, YOY and juvenile white sharks appear to be primarily coastal and shelf-oriented, consistently occurring over depths of less than 200 m, but utilizing habitats across the breadth of the shelf (Weng et al., 2007; Bruce and Bradford, 2012; White et al., 2019; Spaet et al., 2020). Occasional forays beyond the shelf edge, particularly in the northeastern Pacific where the continental shelf is very narrow, results in juvenile white sharks displaying epipelagic behaviors (Dewar et al., 2004; Weng et al., 2007, 2012). Selection of focal areas within shelf ecosystems are likely influenced by other environmental conditions including temperature, productivity, and prey availability.

The sharks in this study selected waters with SSTs between 18.0 and 22.0°C. Juvenile white sharks in the northeastern Pacific Ocean were found in similar temperatures between 14.0 and 24.0°C (White et al., 2019). The highest catch rates of juveniles in eastern Australia occurred in SSTs between 17.0 and 18.0°C (Bruce et al., 2019). White sharks exhibit regional endothermy, and as such, are able to tolerate a wider range of temperatures than most ectothermic fish providing a variety of predatory advantages (Carey et al., 1982; Watanabe et al., 2019). Summer-autumn water temperatures in the New York Bight may span the optimal physiological temperatures for young white sharks, making the region ideal from a thermal perspective. However, YOY and juvenile white sharks appear to occupy a narrower range of temperatures than larger individuals (Curtis et al., 2014; Skomal et al., 2017), and the most restricted temperature range recorded from PSATs was from the smallest individual tagged in the study. These ontogenetic differences could be due to the smaller body mass, less developed heat exchange mechanisms (i.e., less red muscle, smaller retia), and higher surface area to volume ratios of young sharks, making it more physiologically costly to defend an elevated core temperature over as wide a range of temperatures as adults. This has important implications for the future of young white shark habitats given the effects of climate change and variability, especially in the mid-Atlantic Bight which is warming at a much faster rate than most of the global ocean (Saba et al., 2016; Huveneers et al., 2018).

Young white sharks in the New York Bight also selected areas with relatively high levels of productivity (i.e., mesotrophic waters) as reflected by salinity and chlorophyll-a concentration. Tagged individuals selected sea surface salinities between 31.0 and 32.0 ppt (i.e., slightly less saline than oceanic waters), and chlorophyll-a concentrations >2.0 mg m^{-3}. White sharks are not considered euryhaline, although they do occasionally occur within estuarine water bodies (Harasti et al., 2017). Sea surface salinity preferences have not been studied previously for white sharks, but are commonly used in habitat suitability models for other species. Shallow areas close to land tend to have lower salinities due to proximity to coastal runoff and freshwater flow, and may contribute to a decreased predation risk to young sharks as larger individuals avoid these areas (Simpfendorfer et al., 2005; Wetherbee et al., 2007; Knip et al., 2011; Trujillo and Thurman, 2016). Freshwater inputs and longshore currents also contribute to increased primary productivity and phytoplankton blooms nearshore, as indicated by the shoreward increase in chlorophyll-a concentrations in this region (Xu et al., 2011). Phytoplankton make up the base of the food web, and as such, high concentrations in an area can support an abundance of life, including higher-order predators like sharks (Trujillo and Thurman, 2016). Due to upwelling (the flow of deep nutrient rich water to the surface), coastal areas are generally high in nutrients and phytoplankton (Trujillo and Thurman, 2016). Similarly, phytoplankton concentrations along Long Island's southern shoreline are affected by groundwater upwelling, which is the occurrence of groundwater high in nutrients seeping through sediment on the seafloor (Gobler and Sañudo-Wilhelmy, 2001). Additionally, this area is home to several rivers, including the Hudson River, and as such, nutrient runoff may cause an increase of primary productivity. Thus, it is not unexpected that YOY and juvenile white sharks select areas with high productivity to be used as a foraging ground where they prey on a variety of fishes and invertebrates (Casey and Pratt, 1985). Our results differ from those found in the northeastern Pacific Ocean as White et al. (2019) noted chlorophyll-a was found to not be a significant variable in habitat selection for juvenile white sharks in the Southern California Bight. However, in the Mediterranean Sea, studies have suggested high productivity in the Adriatic Sea and the Sicilian Channel may be the reason behind the higher occurrence of white sharks in the area (Coll et al., 2007; Boldrocchi et al., 2017). In nursery areas off eastern Australia, seasonal upwelling and therefore, nutrient enrichment, are believed to coincide with suitable prey aggregations of various teleosts, providing the nurseries with an abundance of prey for immature white sharks (Bruce and Bradford, 2012).

Three-Dimensional Movements

Few studies have explored vertical behavior of YOY or juvenile white sharks (Klimley et al., 2002; Dewar et al., 2004; Weng et al., 2007, 2012), and this is the first such study in the Atlantic Ocean basin. Vertical behavior of the PSAT-tagged sharks varied between individuals and locations within the New York Bight. The drivers of shark vertical behavior have long been a subject of inquiry, with a variety of physical and biological variables suggested to hold influence (e.g., Carey et al., 1990; Klimley et al., 2002; Gaube et al., 2018). While SSTs ranging between 15.7 and 26.4°C were found at the locations of the tagged individuals, further research is needed to determine if vertical behavior is influenced by SST (e.g., Andrzejaczek et al., 2018).

The vertical diving behavior and accompanying measurements of temperature identified several areas across the shelf with thermally stratified water column structure. This was most evident around the Hudson Shelf Valley region where some of the coldest temperatures were recorded (<10°C) during the summertime tracking period from WS-14 and WS-15. Interestingly, these 50–80 m waters were colder than those recorded during the deepest dives of WS-11 to 200 m, which occurred seaward of this region off the continental shelf. Previous physical measurements in the mid-Atlantic Bight have shown that a "cold pool" of water commonly develops along the bottom of the mid-shelf region through the summertime (Houghton et al., 1982; Falkowski et al., 1983; Rona et al., 2015). Although primary production decreases at the surface of this region relative to the coastline, chlorophyll-a levels at depth (i.e., 20–40 m) approximate those measured nearshore (Falkowski et al., 1983). The presence of multiple white sharks in these areas for several days suggests that the edge of the mid-Atlantic Cold Pool may provide suitable subsurface habitat for these predators, as has been recently suggested for juvenile dusky sharks (Bangley et al., 2020a). Indeed, the waters surrounding the Hudson Shelf Valley as well as shelf-edge waters of the mid-Atlantic Bight are targeted by several fisheries (Rona et al., 2015), and have high levels of habitat and biological diversity (Pierdomenico et al., 2015, 2017). Young white sharks may therefore be exploiting more abundant food resources that accompany this unique subsurface feature, which apparently facilitates oceanographic conditions that support high levels of prey productivity. Additional tagging, including high-resolution biologging, accelerometry, and animal-borne video systems, to observe young white shark behavior is needed from this area. Further, what drives these individuals to move offshore from protected and productive waters along Long Island's southern shorelines is still uncertain and should be explored.

Prey availability also likely influences young white shark vertical activity. Juvenile white sharks are documented to feed mainly on smaller demersal elasmobranchs (*Hypanus* spp., *Myliobatis* spp., *Leucoraja* spp., *Mustelus canis*), and teleosts such as searobins (*Prionotus* spp.), hakes (*Urophycis* spp.), and flounders (Pleuronectidae and Paralichthyidae), which may influence bottom-oriented behavior (Casey and Pratt, 1985; Santana-Morales et al., 2012; Onate-Gonzalez et al., 2017). Likewise, locally abundant pelagic prey species including squids (*Illex* spp. and *Doryteuthis* spp.), mackerel (*Scomber* spp.), and menhaden (*Brevoortia tyrannus*) may drive surface-oriented or diel vertical migration behaviors in certain locations. In the New York Bight, demersal species increase in abundance from the continental shelf edge shoreward (National Oceanic and Atmospheric Administration (NOAA), 2018), and the highly productive nearshore waters are vastly diverse and home to over 300 species of fish (Briggs and Waldman, 2002). However, pelagic prey may also become locally aggregated, particularly in thermally stratified waters where we observed extensive diving in upper layers (Gaube et al., 2018).

Undoubtedly, our work shows that young white sharks traverse variable oceanographic features across the continental shelf in the New York Bight, and these may be influenced by the underlying bathymetry. Further efforts to integrate multiple complementary tag technologies on each tagged individual will provide more complete characterizations of movements and the drivers of habitat selection in an inherently three-dimensional environment.

Implications for Management

There is growing recognition of the importance of nursery areas to the overall sustainability of shark populations (Heupel et al., 2007, 2018). In order to inform conservation and management efforts in these areas, however, they must first be accurately characterized with an understanding of where, when, and how a given species uses the habitat. The study of juvenile white shark habitats and potential anthropogenic impacts on those areas was recently considered to be a high research priority amongst white shark scientists around the world (Huveneers et al., 2018). As the New York Bight, a relatively small and discrete region, remains the only confirmed white shark nursery area in the entire North Atlantic Ocean, it may be of critical importance to the long-term maintenance of the regional white shark population. The results from this study may help improve the characterization of Essential Fish Habitat (EFH) for YOY and juvenile white sharks for NOAA National Marine Fisheries Service (NMFS) fishery management plans (e.g., National Oceanic and Atmospheric Administration (NOAA), 2017a). NMFS has considered designating a Habitat Area of Particular Concern (HAPC) in the northern mid-Atlantic Bight and the shoreline off southern New England for YOY and juvenile white sharks; however, the agency determined that an insufficient amount of data was available at the time to support this (National Oceanic and Atmospheric Administration (NOAA), 2017a,b). The improvement of EFH characterization and the potential designation of HAPCs for young white sharks using the data presented herein could benefit the ongoing assessment and mitigation of habitat impacts from fisheries, offshore energy development, habitat degradation, and other human activities.

Fisheries bycatch remains a primary threat to white sharks in the northwest Atlantic (Curtis et al., 2014; Huveneers et al., 2018; Bowlby and Gibson, 2020) and tracking data from the present study can also be used to assess bycatch susceptibility and potentially inform spatial management by NMFS (Lyons et al., 2013; Queiroz et al., 2019). Finally, understanding species-habitat relationships are critical for predicting the potential impacts of long-term environmental changes including climate change (e.g., Kleisner et al., 2017; Crear et al., 2020). White shark coastal nursery areas may be comparatively vulnerable to the effects of global warming (Huveneers et al., 2018) and given the importance of water temperature in habitat selection and seasonal movements of young white sharks (Weng et al., 2007; Curtis et al., 2018; this study), climate change impacts on the mid-Atlantic continental shelf ecosystem (Saba et al., 2016) could pose viable threats to the survival of juveniles, negatively affecting sustained recruitment to the adult population. Telemetry and biologging tools continue to provide the information necessary to simultaneously address numerous questions on the ecology, behavior, and conservation of highly mobile marine species that have traditionally been challenging to explore.

DATA AVAILABILITY STATEMENT

The raw data supporting the conclusions of this article will be made available by the authors, without undue reservation.

ETHICS STATEMENT

The animal study was reviewed and approved by Florida Atlantic University. All individuals collected in this animal study were collected and tagged using university-approved animal use protocols (FAU AUP# 16-07, 19-19). All activities were undertaken with permits or letters of acknowledgment from both state (New York State Department of Environmental Conservation LPSCI-1634) and federal (NMFS SHK-EFP-16-04, SHKLOA-17-02, SHK-LOA-18-11, SHK-LOA-19-06) agencies. All efforts were made to minimize animal pain and suffering during capture and handling procedures. All surgeries were overseen by a licensed veterinarian specializing in aquatic veterinary medicine.

AUTHOR CONTRIBUTIONS

RS, TC, and MA designed the study. TC, GM, GF, and MA secured funding for the project. RS led the data analysis with assistance from TC and MA and led the writing of manuscript with assistance from all authors. All authors participated in fieldwork.

FUNDING

Funding and support was provided by the OCEARCH, Harbor Branch Oceanographic Institute Foundation, Florida Atlantic University Foundation, South Fork Natural History Museum, Andrew F. Sabin Family Foundation, NMFS Atlantic Highly Migratory Species Management Division, Southampton Public Schools, and a number of private donors.

ACKNOWLEDGMENTS

We are grateful to all of the organizations and individuals that contributed to the field work and data collection associated with this study including OCEARCH, South Fork Natural History Museum, Reel Science Charters, Harbor Branch Oceanographic Institute, Wildlife Conservation Society, and the New York Aquarium, with special thanks to B. McBride, B. Eyre, D. J. Lettieri, T. Goggins, A. Meite, R. Hueter, L. Winn, J. Quinlan, M. Hyatt, H. Walters, J. Labelle, M. Camhi, C. Eddy, M. Drymon, G. Roskar, L. Hoopes, F. Quevedo, C. Paparo, W. Zublionis, J. Metzger, and M. Berkhout. We thank M. Frisk and his lab at Stony Brook University, Wildlife Conservation Society, and other members of the ACT Network for providing acoustic tag detections in the New York Bight. For analytical assistance we also thank C. Bangley, B. Galuardi, D. Crear, B. DeGroot, and L. Brewster. The views or opinions expressed herein are those of the authors and do not necessarily reflect those of NOAA, the Department of Commerce, or any other institution.

SUPPLEMENTARY MATERIAL

The Supplementary Material for this article can be found online at: https://www.frontiersin.org/articles/10.3389/fmars.2021.643831/full#supplementary-material

Supplementary Figure 1 | Three-dimensional position estimates for WS-11 in the New York Bight region. Positions are colored by individual shark in **(A)** (as per **Figure 1**) and temperature in **(B)**. Bathymetry is presented based on GEBCO data, with the continental shelf break (i.e., 200 m isobath) indicated by a white dotted line and the Hudson Shelf Valley identified by black dashed line. Green 3D arrows (top right of panels) point north. Yellow arrow depicts capture and release site off Montauk, NY.

Supplementary Figure 2 | Three-dimensional position estimates for WS-12 in the New York Bight region. Positions are colored by individual shark in **(A)** (as per **Figure 1**) and temperature in **(B)**. Bathymetry is presented based on GEBCO data, with the continental shelf break (i.e., 200 m isobath) indicated by a white dotted line and the Hudson Shelf Valley identified by black dashed line. Green 3D arrows (top right of panels) point north. Yellow arrow depicts capture and release site off Montauk, NY.

Supplementary Figure 3 | Three-dimensional position estimates for WS-13 in the New York Bight region. Positions are colored by individual shark in **(A)** (as per **Figure 1**) and temperature in **(B)**. Bathymetry is presented based on GEBCO data, with the continental shelf break (i.e., 200 m isobath) indicated by a white dotted line and the Hudson Shelf Valley identified by black dashed line. Green 3D arrows (top right of panels) point north. Yellow arrow depicts capture and release site off Montauk, NY.

Supplementary Figure 4 | Three-dimensional position estimates for WS-14 in the New York Bight region. Positions are colored by individual shark in **(A)** (as per **Figure 1**) and temperature in **(B)**. Bathymetry is presented based on GEBCO data, with the continental shelf break (i.e., 200 m isobath) indicated by a white dotted line and the Hudson Shelf Valley identified by black dashed line. Green 3D arrows (top right of panels) point north. Yellow arrow depicts capture and release site off Montauk, NY.

Supplementary Figure 5 | Three-dimensional position estimates for WS-15 in the New York Bight region. Positions are colored by individual shark in **(A)** (as per **Figure 1**) and temperature in **(B)**. Bathymetry is presented based on GEBCO data, with the continental shelf break (i.e., 200 m isobath) indicated by a white dotted line and the Hudson Shelf Valley identified by black dashed line. Green 3D arrows (top right of panels) point north. Yellow arrow depicts capture and release site off Montauk, NY.

Supplementary Figure 6 | Three-dimensional position estimates for WS-20 in the New York Bight region. Positions are colored by individual shark in **(A)** (as per **Figure 1**) and temperature in **(B)**. Bathymetry is presented based on GEBCO data, with the continental shelf break (i.e., 200 m isobath) indicated by a white dotted line and the Hudson Shelf Valley identified by black dashed line. Green 3D arrows (top right of panels) point north. Yellow arrow depicts capture and release site off Montauk, NY.

Supplementary Figure 7 | Three-dimensional position estimates for WS-21 in the New York Bight region. Positions are colored by individual shark in **(A)** (as per **Figure 1**) and temperature in **(B)**. Bathymetry is presented based on GEBCO data, with the continental shelf break (i.e., 200 m isobath) indicated by a white dotted line and the Hudson Shelf Valley identified by black dashed line. Green 3D arrows (top right of panels) point north. Yellow arrow depicts capture and release site off Montauk, NY.

REFERENCES

Andrzejaczek, S., Gleiss, A. C., Jordan, L. K. B., Pattiaratchi, C. B., Howey, L. A., Brooks, E. J., et al. (2018). Temperature and the vertical movements of oceanic whitetip sharks, *Carcharhinus longimanus*. *Sci. Rep.* 8:8351. doi: 10.1038/s41598-018-26485-3

Bangley, C. W., Curtis, T. H., Secor, D. H., Latour, R. J., and Ogburn, M. B. (2020a). Identifying important juvenile Dusky Shark habitat in the northwest Atlantic Ocean using acoustic telemetry and spatial modeling. *Mar. Coast. Fish.* 12, 348–363. doi: 10.1002/mcf2.10120

Bangley, C. W., Whoriskey, F. G., Young, J. M., and Ogburn, M. B. (2020b). Networked animal telemetry in the Northwest Atlantic and Caribbean Waters. *Mar. Coast. Fish.* 12, 339–347. doi: 10.1002/mcf2.10128

Bastien, G., Barkley, A., Chappus, J., Heath, V., Popov, S., Smith, R., et al. (2020). Inconspicuous, recovering, or northward shift: status and management of the white shark (*Carcharodon carcharias*) in Atlantic Canada. *Can. J. Fish. Aquat. Sci*. 77, 1666–1677. doi: 10.1139/cjfas-2020-0055

Beck, M. W., Heck, K. L., Able, K. W., Childers, D. L., Eggleston, D. B., Gillanders, B. M., et al. (2001). The identification, conservation, and management of estuarine and marine nurseries for fish and invertebrates: a better understanding of the habitats that serve as nurseries for marine species and the factors that create site-specific variability in nursery quality will improve conservation and management of these areas. *Bioscience* 51, 633–641. doi: 10.1641/0006-3568(2001)051[0633:ticamo]2.0.co;2

Boldrocchi, G., Kiszka, J., Purkis, S., Storai, T., Zinzula, L., and Burkholder, D. (2017). Distribution, ecology, and status of the white shark, *Carcharodon carcharias*, in the Mediterranean Sea. *Rev. Fish Biol. Fish.* 27, 515–534. doi: 10.1007/s11160-017-9470-5

Bowlby, H. D., and Gibson, A. J. F. (2020). Implications of life history uncertainty when evaluating status in the Northwest Atlantic population of white shark (*Carcharodon carcharias*). *Ecol. Evol.* 10, 4990–5000. doi: 10.1002/ece3.6252

Boyd, J. D., and Brightsmith, D. J. (2013). Error properties of Argos satellite telemetry locations using least squares and Kalman filtering. *PLoS One* 8:e63051. doi: 10.1371/journal.pone.0063051

Braun, C. D., Gaube, P., Sinclair-Taylor, T. H., Skomal, G. B., and Thorrold, S. R. (2019). Mesoscale eddies release pelagic sharks from thermal constraints to foraging in the ocean twilight zone. *Proc. Natl. Acad. Sci.* 116, 17187–17192. doi: 10.1073/pnas.1903067116

Briggs, P. T., and Waldman, J. R. (2002). Annotated list of fishes reported from the marine waters of New York. *Northeastern Nat.* 9:35.

Bruce, B., Harasti, D., Lee, K., Gallen, C., and Bradford, R. (2019). Broad-scale movements of juvenile white sharks *Carcharodon carcharias* in eastern Australia from acoustic and satellite telemetry. *Mar. Ecol. Prog. Ser.* 619, 1–15. doi: 10.3354/meps12969

Bruce, B. D., and Bradford, R. W. (2012). "Habitat use and spatial dynamics of juvenile white sharks, *Carcharodon carcharias*, in eastern Australia," in *Global Perspectives on the Biology and life History of the White Shark*, ed. M. L. Domeier, (Boca Raton, FL: CRC Press), 225–254.

Carey, F. G., Kanwisher, J. W., Brazier, O., Gabrielson, G., Casey, J. G., and Pratt, H. L. Jr. (1982). Temperature and activities of a white shark. *Carcharodon carcharias*. *Copeia* 2, 254–260. doi: 10.2307/1444603

Carey, F. G., Scharold, J. V., and Kalmijn, Ad. J (1990). Movements of blue sharks (*Prionace glauca*) in depth and course. *Mar. Biol.* 106, 329–342. doi: 10.1007/BF01344309

Cartamil, D., Wegner, N. C., Aalbers, S., Sepulveda, C. A., Baquero, A., and Graham, J. B. (2010). Diel movement patterns and habitat preferences of the common thresher shark (*Alopias vulpinus*) in the Southern California Bight. *Mar. Freshw. Res.* 61:596. doi: 10.1071/MF09153

Casey, J. G., and Pratt, H. P. (1985). Distribution of the white shark, *Carcharodon carcharias*, in the Western North Atlantic. *Mem. South. Calif. Acad. Sci.* 9, 2–14.

Churchill, J. H., Levine, E. R., Connors, D. N., and Cornillon, P. C. (1993). Mixing of shelf, slope and Gulf Stream water over the continental slope of the Middle Atlantic Bight. *Deep Sea Res. I Oceanogr. Res. Pap.* 40, 1063–1085. doi: 10.1016/0967-0637(93)90090-p

Coll, M., Santojanni, A., Palomera, I., Tudela, S., and Arneri, E. (2007). An ecosystem model of the Northern and Central Adriatic Sea: analysis of ecosystem structure and fishing impacts. *J. Mar. Syst.* 67, 119–154. doi: 10.1016/j.jmarsys.2006.10.002

Crear, D. P., Latour, R. J., Friedrichs, M. A., St-Laurent, P., and Weng, K. C. (2020). Sensitivity of a shark nursery habitat to a changing climate. *Mar. Ecol. Prog. Ser.* 652, 123–136. doi: 10.3354/meps13483

Curtis, T. H., McCandless, C. T., Carlson, J. K., Skomal, G. B., Kohler, N. E., Natanson, L. J., et al. (2014). Seasonal distribution and historic trends in abundance of white sharks, *Carcharodon carcharias*, in the western North Atlantic Ocean. *PLoS One* 9:e99240. doi: 10.1371/journal.pone.0099240

Curtis, T. H., Metzger, G., Fischer, C., McBride, B., McCallister, M., Winn, L. J., et al. (2018). First insights into the movements of young-of-the-year white sharks (*Carcharodon carcharias*) in the western North Atlantic Ocean. *Sci. Rep.* 8:10794.

Dewar, H., Domeier, M., and Nasby-Lucas, N. (2004). Insights into young of the year white shark, *Carcharodon carcharias*, behavior in the Southern California Bight. *Environ. Biol. Fish.* 70, 133–143. doi: 10.1023/b:ebfi.0000029343.54027.6a

Dodge, K. L., Galuardi, B., Miller, T. J., and Lutcavage, M. E. (2014). Leatherback turtle movements, dive behavior, and habitat characteristics in ecoregions of the Northwest Atlantic Ocean. *PLoS One* 9:e91726. doi: 10.1371/journal.pone.0091726

Dujon, A. M., Lindstrom, R. T., and Hays, G. C. (2014). The accuracy of Fastloc-GPS locations and implications for animal tracking. *Methods Ecol. Evol.* 5, 1162–1169. doi: 10.1111/2041-210x.12286

Falkowski, P. G., Vidal, J., Hopkins, T. S., Rowe, G. T., Whitledge, T. E., and Harrison, W. G. (1983). Summer nutrient dynamics in the Middle Atlantic Bight: primary production and utilization of phytoplankton carbon. *J. Plankton Res.* 5, 515–537.

Friedland, K. D., Leaf, R. T., Kane, J., Tommasi, D., Asch, R. G., Rebuck, N., et al. (2015). Spring bloom dynamics and zooplankton biomass response on the US Northeast Continental Shelf. *Cont. Shelf Res.* 102, 47–61. doi: 10.1016/j.csr.2015.04.005

Gaube, P., Braun, C. D., Lawson, G. L., McGillicuddy, D. J., Della Penna, A., Skomal, G. B., et al. (2018). Mesoscale eddies influence the movements of mature female white sharks in the Gulf Stream and Sargasso Sea. *Sci. Rep.* 8, 1–8. doi: 10.1016/j.dsr.2017.02.006

General Bathymetric Chart of the Oceans (GEBCO), (2019). *Global Ocean & Land Terrain Models*. Available online at: https://www.gebco.net/data_and_products/gridded_bathymetry_data/#a1 (accessed December 1, 2020).

Gobler, C., and Sañudo-Wilhelmy, S. (2001). Temporal variability of groundwater seepage and brown tide blooms in a Long Island embayment. *Mar. Ecol. Prog. Ser.* 217, 299–309. doi: 10.3354/meps217299

Harasti, D., Lee, K., Bruce, B., Gallen, C., and Bradford, R. (2017). Juvenile white sharks *Carcharodon carcharias* use estuarine environments in south-eastern Australia. *Mar. Biol.* 164:58.

Hare, J. A., Morrison, W. E., Nelson, M. W., Stachura, M. M., Teeters, E. J., Griffis, R. B., et al. (2016). A vulnerability assessment of fish and invertebrates to climate change on the Northeast US Continental Shelf. *PLoS One* 11:e0146756. doi: 10.1371/journal.pone.0146756

Heupel, M. R., Carlson, J. K., and Simpiendorfer, C. A. (2007). Shark nursery areas: concepts, definition, characterization and assumptions. *Mar. Ecol. Prog. Ser.* 337, 287–297. doi: 10.3354/meps337287

Heupel, M. R., Kanno, S., Martins, A. P. B., and Simpfendorfer, C. A. (2018). Advances in understanding the roles and benefits of nursery areas for elasmobranch populations. *Mar. Freshw. Res.* 70, 897–907. doi: 10.1071/MF18081

Hossler, K., and Bauer, J. E. (2013). Amounts, isotopic character, and ages of organic and inorganic carbon exported from rivers to ocean margins: 1. Estimates of terrestrial losses and inputs to the Middle Atlantic Bight. *Glob. Biogeochem. Cycles* 27, 331–346. doi: 10.1002/gbc.20033

Houghton, R. W., Schlitz, R., Beardsley, R. C., Butman, B., and Chamberlin, J. L. (1982). The Middle Atlantic Bight cold pool: evolution of the temperature structure during summer 1979. *J. Phys. Oceanogr.* 12, 1019–1029. doi: 10.1175/1520-0485(1982)012<1019:tmabcp>2.0.co;2

Huveneers, C., Apps, K., Becerril-García, E. E., Bruce, B., Butcher, P. A., Carlisle, A. B., et al. (2018). Future research directions on the "Elusive" White Shark. *Front. Mar. Sci.* 5:455. doi: 10.3389/fmars.2018.00455

Kleisner, K. M., Fogarty, M. J., McGee, S., Barnett, A., Fratantoni, P., Greene, J., et al. (2016). The effects of sub-regional climate velocity on the distribution and spatial extent of marine species assemblages. *PLoS one* 11:e0149220. doi: 10.1371/journal.pone.0149220

Kleisner, K. M., Fogarty, M. J., McGee, S., Hare, J. A., Moret, S., Perretti, C. T., et al. (2017). Marine species distribution shifts on the US Northeast Continental Shelf under continued ocean warming. *Prog. Oceanogr.* 153, 24–36. doi: 10.1016/j.pocean.2017.04.001

Klimley, A. P., Beavers, S. C., Curtis, T. H., and Jorgensen, S. J. (2002). Movements and swimming behavior of three species of sharks in La Jolla Canyon, California. *Environ. Biol. Fish.* 63, 117–135. doi: 10.1023/a:1014200301213

Knebel, H. J. (1979). Anomalous topography on the continental shelf around Hudson Canyon. *Mar. Geol.* 33, 67–75. doi: 10.1016/0025-3227(79)90074-4

Knip, D. M., Heupel, M. R., and Simpfendorfer, C. A. (2010). Sharks in nearshore environments: models, importance, and consequences. *Mar. Ecology Prog. Ser.* 402, 1–11. doi: 10.3354/meps08498

Knip, D. M., Heupel, M. R., Simpfendorfer, C. A., Tobin, A. J., and Moloney, J. (2011). Ontogenetic shifts in movement and habitat use of juvenile pigeye sharks *Carcharhinus amboinensis* in a tropical nearshore region. *Mar. Ecology Prog. Ser.* 425, 233–246. doi: 10.3354/meps09006

Kohler, N. E., and Turner, P. A. (2019). Distributions and movements of atlantic shark species: A 52-year retrospective atlas of mark and recapture data. *Mar. Fish. Rev.* 81, 1–94. doi: 10.7755/mfr.81.2.1

Latour, R. J., and Gartland, J. (2020). Dynamics of the shark community in the Mid-Atlantic Bight. *Mar. Biol.* 16:100.

Logan, R. K., Vaudo, J. J., Sousa, L. L., Sampson, M., Wetherbee, B. M., and Shivji, M. S. (2020). Seasonal movements and habitat use of juvenile smooth hammerhead sharks in the western North Atlantic Ocean and significance for management. *Front. Mar. Sci.* 7:731. doi: 10.3389/fmars.2020.566364

Lyons, K., Jarvis, E. T., Jorgensen, S. J., Weng, K., O'Sullivan, J., Winkler, C., et al. (2013). The degree and result of gillnet fishery interactions with juvenile white sharks in southern California assessed by fisheries-independent and -dependent methods. *Fish. Res.* 147, 370–380. doi: 10.1016/j.fishres.2013.07.009

Methratta, E. T. (2020). Monitoring fisheries resources at offshore wind farms: BACI vs. BAG designs. *ICES J. Mar. Sci.* 77, 890–900. doi: 10.1093/icesjms/fsaa026

Murray, K. T., and Orphanides, C. D. (2013). Estimating the risk of loggerhead turtle Caretta caretta bycatch in the US mid-Atlantic using fishery-independent and-dependent data. *Mar. Ecol. Prog. Ser.* 477, 259–270. doi: 10.3354/meps10173

National Aeronautics and Space Administration (NASA), (2019). *Chlorophyll*. Available online at: https://earthobservatory.nasa.gov/global-maps/MY1DMM_CHLORA (accessed December 1, 2020).

National Oceanic and Atmospheric Administration (NOAA), (2017a). *Atlantic Highly Migratory Species; Essential Fish Habitat*. Available online at: https://www.federalregister.gov/documents/2017/09/07/2017-18961/atlantic-highly-migratory-species-essential-fish-habitat (accessed December 1, 2020).

National Oceanic and Atmospheric Administration (NOAA), (2017b). *Final Amendment 10 to the 2006 Consolidated Atlantic Highly Migratory Species Fishery Management Plan: Essential Fish Habitat and Environmental Assessment*. Available online at: https://www.habitat.noaa.gov/application/efhinventory/docs/a10_hms_efh.pdf#page=419 (accessed December 1, 2020).

National Oceanic and Atmospheric Administration (NOAA), (2018). *Ecology of the Northeast US Continental Shelf*. Available online at: https://www.nefsc.noaa.gov/ecosys/ecosystem-ecology/fish-squid.html (accessed December 1, 2020).

Onate-Gonzalez, E. C., Sosa-Nishizaki, O., Herska, S. Z., Lowe, C. G., Lyons, K., Santana-Morales, O., et al. (2017). Importance of Bahia Sebastian Vizcaino of a nursery area for white sharks (*Carcharodon carcharias*) in the Northeastern Pacific: a fishery dependent analysis. *Fish. Res.* 188, 125–137. doi: 10.1016/j.fishres.2016.12.014

Parsons, G. R., Hoffmayer, E. R., Frank, J., and Bet-Sayed, W. (2008). "A review of shark reproductive ecology: life history and evolutionary implications," in *Fish Reproduction*, Edn. 1 Edn, eds M. J. Rocha, A. Aruke, and B. G. Kapoor, (Abingdon: Taylor and Francis), 435–469.

Pierdomenico, M., Gori, A., Guida, V. G., and Gili, J. M. (2017). Megabenthic assemblages at the Hudson Canyon head (NW Atlantic margin): Habitat-faunal relationships. *Prog. Oceanogr.* 157, 12–26. doi: 10.1016/j.pocean.2017.08.001

Pierdomenico, M., Guida, V. G., Macelloni, L., Chiocci, F. L., Rona, P. A., Scranton, M. I., et al. (2015). Sedimentary facies, geomorphic features and habitat distribution at the Hudson Canyon head from AUV multibeam data. *Deep Sea Res. II Top. Stud. Oceanogr.* 121, 112–125. doi: 10.1016/j.dsr2.2015.04.016

Queiroz, N., Humphries, N. E., Couto, A., Vedor, M., da Costa, I., Sequeira, A. M. M., et al. (2019). Global spatial risk assessment of sharks under the footprint of fisheries. *Nature* 572, 461–466. doi: 10.1038/s41586-019-1444-4

Rogers, K. B., and White, G. C. (2007). "Analysis of movement and habitat use from telemetry data," in *Analysis and Interpretation of Freshwater Fisheries Data*, eds C. S. Guy, and M. L. Brown, (Bethesda, MA: American Fisheries Society), 625–676.

Rona, P., Guida, V., Scranton, M., Gong, D., Macelloni, L., Pierdomenico, M., et al. (2015). Hudson submarine canyon head offshore New York and New Jersey: a physical and geochemical investigation. *Deep Sea Res. II Top. Stud. Oceanogr.* 121, 213–232. doi: 10.1016/j.dsr2.2015.07.019

Saba, V. S., Griffies, S. M., Winton, M., Anderson, W., Alexander, M. A., Hare, J. A., et al. (2016). Enhanced warming of the US Northeast Continental Shelf under climate change: implications for fisheries. *AGUOS* 2016: PC14B-2067.

Santana-Morales, O., Sosa-Nishizaki, O., Escobedo-Olvera, M. A., Onate-González, E. C., O'Sullivan, J. B., and Cartamil, D. (2012). "Incidental catch and ecological observations of juvenile white sharks, *Carcharodon carcharias,* in western Baja California, Mexico. Conservation implications," in *Global Perspectives on the Biology and Life History of the White Shark*, ed. M. L. Domeier, (New York, NY: CRC Press), 187–198.

Simpfendorfer, C. A., Freitas, G. G., Wiley, T. R., and Heupel, M. R. (2005). Distribution and habitat partitioning of immature bull sharks (*Carcharhinus leucas*) in a southwest Florida estuary. *Estuaries* 28, 78–85. doi: 10.1007/bf02732755

Simpfendorfer, C. A., Hueter, R. E., Bergman, U., and Connett, S. M. (2002). Results of a fishery-independent survey for pelagic sharks in the western North Atlantic, 1977–1994. *Fish. Res.* 55, 175–192. doi: 10.1016/s0165-7836(01)00288-0

Skomal, G. B., Braun, C. D., Chisholm, J. H., and Thorrold, S. R. (2017). Movement of the white shark *Carcharodon carcharias* in the North Atlantic Ocean. *Mar. Ecol. Prog. Ser*. 580, 1–16. doi: 10.3354/meps12306

Spaet, J. L., Patterson, T. A., Bradford, R. W., and Butcher, P. A. (2020). Spatiotemporal distribution patterns of immature Australasian white sharks (*Carcharodon carcharias*). *Sci. Rep.* 10, 1–13.

Stepanuk, J. E., Read, A. J., Baird, R. W., Webster, D. L., and Thorne, L. H. (2018). Spatiotemporal patterns of overlap between short-finned pilot whales and the US pelagic longline fishery in the Mid-Atlantic Bight: An assessment to inform the management of fisheries bycatch. *Fish. Res.* 208, 309–320. doi: 10.1016/j.fishres.2018.07.008

Trujillo, A. P., and Thurman, H. V. (2016). "Biological productivity and energy transfer," in *Essentials of Oceanography: Twelfth Edition*, (Boston, MA: Pearson), 403–441.

Wall, J. (2014). *Movement Ecology Tools for ArcGIS (ArcMET)*. Available online at: http://www.movementecology.net/arcmet_manual.html (accessed December 1, 2020).

Watanabe, Y. Y., Payne, N. L., Semmens, J. M., Fox, A., and Huveneers, C. (2019). Swimming strategies and energetics of endothermic white sharks during foraging. *J. Exp. Biol.* 222:jeb185603. doi: 10.1242/jeb.185603

Weng, K. C., O'Sullivan, J. B., Lowe, C. G., Winker, C. E., Blasius, M. E., Loke-Smith, K. A., et al. (2012). "Back to the Wild: release of juvenile white sharks from the Monterey Bay Aquarium," in *Global Perspectives on the Biology and Life History of the White Shark*, ed. M. L. Domeier, (Boca Raton, FL: CRC Press), 419–446.

Weng, K. C., O'Sullivan, J. B., Lowe, C. G., Winkler, C. E., Dewar, H., and Block, B. A. (2007). Movements, behavior and habitat preferences of juvenile white sharks *Carcharodon carcharias* in the eastern Pacific. *Mar. Ecol. Prog. Ser*. 338, 211–224. doi: 10.3354/meps338211

Wetherbee, B., Gruber, S., and Rosa, R. (2007). Movement patterns of juvenile lemon sharks *Negaprion brevirostris* within Atol das Rocas, Brazil: a nursery characterized by tidal extremes. *Mar. Ecol. Prog. Ser.* 343, 283–293. doi: 10.3354/meps06920

White, C. F., Lyons, K., Jorgensen, S. J., O'Sullivan, J., Winkler, C., Weng, K. C., et al. (2019). Quantifying habitat selection and variability in habitat suitability for juvenile white sharks. *PLoS One* 14:e0214642. doi: 10.1371/journal.pone

Xu, Y., Chant, R., Gong, D., Castelao, R., Glenn, S., and Schofield, O. (2011). Seasonal variability of chlorophyll a in the Mid-Atlantic Bight. *Cont. Shelf Res.* 31, 1640–1650. doi: 10.1016/j.csr.2011.05.019

Conflict of Interest: The authors declare that the research was conducted in the absence of any commercial or financial relationships that could be construed as a potential conflict of interest.

frontiers in Marine Science

ORIGINAL RESEARCH
published: 26 May 2021
doi: 10.3389/fmars.2021.653606

Isotopic Tracers Suggest Limited *Trans*-Oceanic Movements and Regional Residency in North Pacific Blue Sharks (*Prionace glauca*)

Daniel J. Madigan[1]*, Oliver N. Shipley[2], Aaron B. Carlisle[3], Heidi Dewar[4], Owyn E. Snodgrass[4] and Nigel E. Hussey[1]

[1] Department of Integrative Biology, University of Windsor, Windsor, ON, Canada, [2] Department of Biology, University of New Mexico, Albuquerque, NM, United States, [3] School of Marine Science and Policy, University of Delaware, Lewes, DE, United States, [4] Fisheries Resources Division, Southwest Fisheries Science Center, National Marine Fisheries Service (NMFS), National Oceanic and Atmospheric Administration (NOAA), La Jolla, CA, United States

Edited by:
Mourier Johann,
Institut de Recherche Pour le Développement (IRD), France

Reviewed by:
Vincent Raoult,
The University of Newcastle, Australia
Mario Espinoza,
Universidad Creativa de Costa Rica,
Costa Rica
Boris Espinasse,
UiT The Arctic University of Norway,
Norway

***Correspondence:**
Daniel J. Madigan
daniel.madigan@stonybrook.edu

Specialty section:
This article was submitted to
Marine Megafauna,
a section of the journal
Frontiers in Marine Science

Received: 14 January 2021
Accepted: 12 April 2021
Published: 26 May 2021

Citation:
Madigan DJ, Shipley ON,
Carlisle AB, Dewar H, Snodgrass OE
and Hussey NE (2021) Isotopic
Tracers Suggest Limited
Trans-Oceanic Movements
and Regional Residency in North
Pacific Blue Sharks (Prionace glauca).
Front. Mar. Sci. 8:653606.
doi: 10.3389/fmars.2021.653606

Blue sharks (*Prionace glauca*) are globally distributed, large-bodied pelagic sharks that make extensive migrations throughout their range. In the North Pacific, mark-recapture studies have shown *trans*-Pacific migrations, but knowledge gaps in migration frequency hinder understanding of regional connectivity and assessments of regional demography for stock assessments. Here, we use oceanographic gradients of stable isotope ratios (i.e., regional isoscapes) to determine exchange rates of blue sharks between the East and West North Pacific Ocean (EPO and WPO). We generated regional $\delta^{13}C$ and $\delta^{15}N$ distributions for blue sharks from published values in the North Pacific (n = 180; both sexes, juveniles and adults combined). Discriminant analysis suggested low *trans*-Pacific exchange, categorizing all western (100%) and most eastern (95.3%) blue sharks as resident to their sampling region, with isotopic niche overlap of WPO and EPO highly distinct (0.01–5.6% overlap). Limited *trans*-Pacific movements suggest that other mechanisms maintain genetic mixing of the North Pacific blue shark population. Potential finer scale movement structure was indicated by isotopic differences in sub-regions of the eastern and western Pacific, though application of mixing models are currently limited by aberrantly low blue shark $\delta^{13}C$ values across studies. Our results suggest that blue shark population dynamics may be effectively assessed on a regional basis (i.e., WPO and EPO). We recommend further studies to provide size- and sex-specific movement patterns based on empirical isotopic values with large sample sizes from targeted regions. Strategically applied stable isotope approaches can continue to elucidate migration dynamics of mobile marine predators, complementing traditional approaches to fisheries biology and ecology.

Keywords: stable isotope, isoscape, pelagic ecology, isoclock, trophic ecology, migration

INTRODUCTION

Blue sharks (*Prionace glauca*) are large-bodied, highly migratory sharks with a global distribution extending throughout temperate and subtropical waters (Nakano and Stevens, 2008; Coelho et al., 2018). Blue shark populations have declined broadly, with high longline bycatch and mortality rates due to extensive overlap with commercial fisheries across much of their global range (Queiroz et al., 2016, 2019). This is true for the North Atlantic (50–79% decline over 30 years; ICCAT, 2015) and Mediterranean (96.5–99.8% decline since the early 19th century; Ferretti et al., 2008) populations as a result of both targeted fisheries (i.e., for fins, meat, squalene) and bycatch (Clarke et al., 2006a,b; Cardeñosa et al., 2020), though the North Pacific population has recently been assessed as not overfished (ISC, 2017). While studies have challenged model-based inferences of shark population declines (Burgess et al., 2005), blue sharks are the major bycatch species in high-seas fisheries regionally (McKinnell and Seki, 1998; Francis et al., 2001) and perhaps globally (Clarke et al., 2006b; Campana et al., 2009). Limited genetic structure has been observed across populations sampled from disparate oceanic regions (King et al., 2015; Taguchi et al., 2015; Veríssimo et al., 2017; Bailleul et al., 2018), though regional populations are managed separately. Mechanisms for high genetic homogeneity across global blue shark populations remain mostly speculative, mainly because studies are lacking in adequate sample sizes and sufficient demographic coverage to allow for robust conclusions to be made (Veríssimo et al., 2017). This limitation spans not only genetic information, but also a robust understanding of other aspects of the species' life history, particularly movements and migrations in relation to proposed mating and parturition grounds.

In the North Pacific Ocean, data suggest that mature blue sharks migrate to a latitudinal band spanning ∼20–30°N for mating during the early summer months, with pupping typically occurring the following summer after a ∼12-month gestation. Gravid females are believed to move further north to parturition grounds located in sub-arctic waters between 35 and 45°N (Nakano, 1994). Males and females typically segregate spatially prior to mating events, but some overlap between immature and mature individuals of opposite sexes can occur (Maxwell et al., 2019). Broadscale movements in the Pacific have been described with conventional and electronic tagging studies (Musyl et al., 2011; Maxwell et al., 2019), and although some blue sharks exhibit long-distance migrations over thousands of kilometers (Maxwell et al., 2019), most tracking data shows predominately latitudinal movements. However, recent conventional mark-recapture information has shown that some individuals migrate across the northern Pacific Ocean from the western Pacific Ocean (WPO) into the eastern Pacific Ocean (EPO) and vice versa (Sippel et al., 2011), a behavior that also has been observed in the North Atlantic (Howey et al., 2017). The extent of connectivity between North Pacific sub-populations (e.g., WPO and EPO), however, remains unquantified. For example, it remains unclear whether genetic mixing and homogeneity (King et al., 2015) is maintained by *trans*-Pacific migrations of juveniles or adults, or by some other mechanism such as pupping and recruitment dynamics. Thus, the proportion of blue sharks performing *trans*-Pacific migrations warrants investigation, as quantifying movement connectivity can clarify regional source-sink dynamics, inform spatial scales of management, and help explain the mechanisms that facilitate genetic homogeneity.

While electronic and conventional tagging approaches have provided useful information on blue shark movement and migration dynamics, studies are limited by high cost (for electronic tagging) and often require high sample sizes and protracted study duration to yield necessary ecological information (Sequeira et al., 2019). Consequently, complementary approaches are required for rapid assessment of blue shark migration and movement connectivity. Intrinsic chemical tracers measured in animal tissues, such as stable isotope (SI) ratios, are useful for reconstructing prior animal migrations (Graham et al., 2010; Trueman et al., 2019; Madigan et al., 2021). Stable isotope analysis (SIA)-based movement studies utilize the distinct isotopic composition of prey baselines (i.e., regional isoscapes) across oceanic sub-regions, driven by local oceanographic and biogeochemical regimes (McMahon et al., 2013; Brault et al., 2018; Espinasse et al., 2020). In the North Pacific Ocean, pelagic prey fields in the EPO and WPO are isotopically distinct, particularly for nitrogen isotope ratios ($\delta^{15}N$) (Matsubayashi et al., 2020). In the EPO, upwelling of nutrient-rich water in the California Current promotes larger nitrate metabolizing primary producers such as diatoms, which creates a ^{15}N-enriched isotopic composition of regional prey (Altabet et al., 1999; Montoya, 2007; Madigan et al., 2012a, 2017). Comparatively, WPO waters are nutrient-poor, which promotes dominance of nitrogen-fixing picophytoplankton at the base of the food web and lower (i.e., ^{15}N depleted) $\delta^{15}N$ composition of regional prey pools (Takai et al., 2007; Fujinami et al., 2018; Ohshimo et al., 2019).

Knowledge of regional isotopic baseline variation can be combined with measured predator stable isotope ratios and tissue-specific incorporation rates to identify individuals that have recently migrated from one system into another (Madigan et al., 2021; Shipley et al., 2021). Tissues of recent migrants will reflect an isotopic mix of prey baselines from the prior and current regions, provided that sampling has occurred prior to the consumer reaching isotopic steady-state with prey from their current region (Heady and Moore, 2013; Moore et al., 2016; Madigan et al., 2021). Residents are then defined as those individuals that are at isotopic steady-state with prey baselines in their current region (Madigan et al., 2014). This technique has been applied to characterize *trans*-Pacific migrations of Pacific bluefin tuna (*Thunnus orientalis*), using machine learning algorithms to define migrants vs. residents, and thus predicting the extent of mixing between WPO and EPO populations (Madigan et al., 2014). More recently, SIA approaches have been used to determine movement transitions across systems spanning marine, brackish, and freshwater habitats (Moore et al., 2016; Shipley et al., 2021), and have proven to be a robust and insightful approach for clarifying aspects of animal migration.

In the current study, we use regional $\delta^{13}C$ and $\delta^{15}N$ values from sampled sharks and prey to quantify potential *trans*-Pacific exchange rates of blue sharks between the WPO and EPO. We use multiple analytical methods with isotopic data to examine the extent of regional residency and foraging connectivity between oceanic sub-regions. This approach provides a tracer-based assessment of habitat use that is complementary to traditional tagging approaches and provides a framework than can be adopted across other study taxa and ecosystems. Inferred movements from isotopic signatures aid in constraining the extent of blue shark movements in the North Pacific basin, clarify the migratory mechanisms that may drive a mixed genetic stock, and can inform appropriate multi-national or regional management strategies for North Pacific blue sharks.

MATERIALS AND METHODS

Data Compilation

Blue Shark SI Data

A literature search was performed to obtain all SI data to-date for blue sharks in the North Pacific. Based on conventional tagging data and available SI data, we categorized North Pacific data into the WPO and EPO. From all studies, mean, reported error (SD or SE), and minimum and maximum values (when reported) of blue shark $\delta^{13}C$ and $\delta^{15}N$ values were tabulated. The literature search showed studies in four discrete regions of the EPO, so EPO blue sharks were further categorized into these four EPO sub-regions: Northern California Current (NCC), Southern California Bight (SCB), southern Baja (SBaja), and the eastern Tropical Pacific (ETP) (see section "Results"). We only used studies that accounted for lipid and urea effects on $\delta^{13}C$ and $\delta^{15}N$ through either chemical extraction or arithmetic correction and DI rinsing. While we recognize that different treatments can affect isotopic values, lipid content in most shark species is low (Hussey et al., 2012) and correction for urea in available data was not feasible. As a result, values were used as reported in published studies. Blue shark $\delta^{13}C$ and $\delta^{15}N$ values were estimated to represent their past foraging behavior for ~0.5–1.5 years before sampling, based on published turnover rate estimates (Madigan et al., 2012b) and blue shark body size ranges across published studies (Thomas and Crowther, 2015; Vander Zanden et al., 2015).

Estimating Population-Wide Blue Shark SI Values

We used an iterative bootstrapping approach to resample each published $\delta^{13}C$ and^{15}N data distribution (n = 5 studies) to generate estimates of population-wide blue shark SI values for each ocean region. Blue shark $\delta^{13}C$ and^{15}N estimates were bootstrapped (1000×) by randomly sampling from mean (±SD) values published for each study region. This resulted in 1×10^3 estimates for the WPO (n = 1 study) and 4×10^3 estimates for the EPO (n = 4 studies), with separate, region-specific resampled populations for sub-regions of the EPO.

Prey SI Data

We searched the literature for published studies reporting SI values of epi- and mesopelagic prey in the WPO and EPO, based on known regional blue shark diets of epi- and mesopelagic forage fish, cephalopods, and crustaceans (Preti et al., 2012; Fujinami et al., 2018). Across relevant studies, prey-specific $\delta^{13}C$ and $\delta^{15}N$ means (±SD) were tabulated for subsequent analyses. As with blue sharks above, prey values were also obtained and regional means (±SD) calculated for the four defined sub-regions of the EPO (NCC, SCB, SBaja, and ETP). As with blue shark data, we only used studies that accounted for lipid effects on $\delta^{13}C$ through chemical extraction or arithmetic correction, and values were used as they were reported in published studies.

Prey $\delta^{13}C$ and $\delta^{15}N$ values were used to generate regional mean diet $\delta^{13}C$ and $\delta^{15}N$ values in the EPO and WPO for subsequent analyses (see sections "Discriminant Analysis" and Isotopic Mixing Models"). For prey data in each region, we accounted for associated error of each prey mean $\delta^{13}C$ and $\delta^{15}N$ values by bootstrapping 1000 values from reported means (±SD) for each prey item. We then randomly selected from these prey distributions (1000×) to generate a mean blue shark diet value for the WPO (n = 145 prey species) and EPO (n = 75 prey species). Each prey item was weighed equally based on demonstrably broad and opportunistic blue shark diets. This resulted in 1×10^3 estimated mean (±SD) diet $\delta^{15}N$ values for both the WPO and EPO. We also used the above approach to generate mean $\delta^{13}C$ and $\delta^{15}N$ diet estimates in the four EPO sub-regions. Combining data from studies that span different time periods accepts potential temporal variation in isotopic baselines and consumers, but given the observed distinction between isotope values between the WPO and EPO (see section "Results"), we deemed it unlikely that this would significantly impact overall results.

Data Analyses

Three analytical approaches were applied to blue shark and prey SI data to characterize blue shark movements (explained in detail below). Isotopic niche overlap of blue shark values was used to obtain general, quantitative metrics of likely blue shark exchange between sub-regions. We then used discriminant analysis to explicitly categorize individual shark isotope values as indicative of prior use of WPO or EPO waters. Finally, mixing models were used to estimate blue shark use of region-specific prey based on the isotopic composition of sharks and prey in each region.

Regional Variability and Overlap of Blue Shark SI Values

For the WPO and four EPO sub-regions (NCC, SCB, SBaja, ETP), integrated $\delta^{13}C$ and $\delta^{15}N$ niche areas (Bayesian ellipses: SEA_B) were determined, generating ellipses for each sub-region that incorporate 40% of the available data (Jackson et al., 2011). Isotopic overlap between each sub-region was then inferred using a Bayesian approach implemented in the R package "nicheROVER." Overlap estimates were generated from 1000 posterior draws based on 95% probabilistic niche regions (Swanson et al., 2015).

Diet-Dependent Diet-Tissue Discrimination Factors (DTDFs)

Discriminant analysis and isotopic mixing models required application of blue shark $\delta^{15}N$ and $\delta^{13}C$ diet-tissue discrimination factors (DTDFs). Because trophic discrimination factors can vary due to a suite of environmental and physiological processes (Hussey et al., 2012; Shipley and Matich, 2020) and have been shown to co-vary with diet δ^{15}N and δ^{13}C values (Caut et al., 2009; Hussey et al., 2014), we calculated diet-specific DTDFs for blue sharks within each region. For each calculated prey mean, we calculated mean DTDFs from algorithms reported in two studies: (1) Caut et al. (2009):

$$\Delta^{15}\mathrm{N} = -0.281(\delta^{15}\mathrm{N}_{\mathrm{diet}}) + 5.879 \tag{1}$$

$$\Delta^{13}\mathrm{C} = -0.213(\delta^{13}\mathrm{C}_{\mathrm{diet}}) - 2.848 \tag{2}$$

and (2) Hussey et al. (2014):

$$\Delta^{15}\mathrm{N} = -0.27(\delta^{15}\mathrm{N}_{\mathrm{diet}}) + 5.92 \tag{3}$$

where Δ^{15}N and Δ^{13}C represent diet-derived DTDFs for δ^{15}N and δ^{13}C, and $\delta^{15}\mathrm{N}_{\mathrm{diet}}$ and $\delta^{13}\mathrm{C}_{\mathrm{diet}}$ represent mean diet δ^{15}N and δ^{13}C values, respectively. For each regional diet δ^{15}N mean, we calculated two DTDF values following Eqs 1, 2 and used the mean of both DTDF values (i.e., estimated DTDF values from equations) for applied diet-based blue shark Δ^{15}N and Δ^{13}C values for each sub-region.

Discriminant Analysis

Only δ^{15}N values were used in discriminant analysis due to non-differentiation of WPO and EPO δ^{13}C values (see sections "Results" and "Discussion"), following methods in Madigan et al. (2014). We generated training data for discriminant analysis using regional prey means and regional prey-based DTDFs. Specifically, regional DTDFs were added to regional prey means to generate 1×10^3 estimated blue shark δ^{15}N values for the WPO, EPO, and EPO sub-regions. We then applied these training data to discriminant analysis of WPO and EPO blue shark δ^{15}N data to classify individual sharks as recent migrants or long-term ($\geq$1 year, based on ectotherm isotopic turnover rates; Thomas and Crowther, 2015; Vander Zanden et al., 2015) residents to the region in which they were sampled. Discriminant analysis reported an error value for the classification of unknown data, which estimates the percentage of individuals that were classified incorrectly (Klecka, 1980).

Isotopic Mixing Models

We applied isotopic mixing models to assess their efficacy for describing foraging across sub-regions in both the EPO and WPO. Bayesian isotope mixing models (R package "simmr"; Parnell, 2020) were used to estimate regional prey inputs to EPO and WPO blue sharks, providing estimates of regional connectivity. For the WPO, mixing models were run for a single blue shark population (due to n = 1 study in the WPO) and regional prey were based on reported prey values for four WPO sub-regions (Eastern Japan, Kuroshio-Oyashio, Sea of Japan, and offshore Taiwan) in Madigan et al. (2015), with additional prey data from Ohshimo et al. (2019). For the EPO, mixing models were run for regional blue shark populations and the pooled EPO population; regional prey endmembers were the NCC, SCB, SBaja, ETP, and the WPO. Endmember values and DTDFs were based on compilations of regional prey fields (**Table 1**).

We estimated the accuracy of regional endmembers (n = 4 for WPO, n = 5 for EPO) by simulating 10,000 prey mixing polygons (Smith et al., 2013) and quantifying the probability of each individual consumer falling outside of the 95% prey mixing space. A relatively high proportion of blue sharks had >95% probability of falling outside the mixing space due to low δ^{13}C values (see section "Results"), as has been observed in other studies (Rabehagasoa et al., 2012; Li et al., 2014; Kiszka et al., 2015). We consequently evaluated the two-isotope mixing model results to assess the effects of potential bias toward low δ^{13}C diet inputs. We also performed a single isotope (δ^{15}N

TABLE 1 | δ^{13}C and δ^{15}N values (mean ± 1 SD) of published prey items by North Pacific Ocean sub-region, and calculated diet-dependent diet-tissue discrimination factors (DTDFs; Δ^{13}C and Δ^{15}N) estimated for blue sharks (*Prionace glauca*).

Region in North Pacific	Sub-regions[a]	n[b]	Years of collection	δ^{13}C ‰	δ^{15}N ‰	References	DTDFs ‰	
							Δ^{13}C	Δ^{15}N
WPO	East Japan	11,24,7,15	2002–2017	−18.4 (0.8)	11.1 (1.2)	Takai et al., 2007 Madigan et al., 2016 Fujinami et al., 2018 Ohshimo et al., 2019	1.1 (0.3)	2.8 (0.4)
	Kuroshio-Oyashio	7,22	1990–2014	−18.7 (0.7)	10.7 (1.0)	Madigan et al., 2016 Ohshimo et al., 2019	1.1 (0.2)	2.9 (0.3)
	Sea of Japan	4,23	1990–2014	−17.3 (1.2)	11.0 (1.1)	Madigan et al., 2016 Ohshimo et al., 2019	0.8 (0.4)	2.8 (0.4)
	Taiwan	9,21	1990–2014	−17.7 (0.4)	8.8 (1.1)	Madigan et al., 2016 Ohshimo et al., 2019	0.9 (0.1)	3.4 (0.4)
EPO	NCC	27	2000–2002	−18.6 (1.2)	13.5 (1.5)	Miller et al., 2013	1.1 (0.4)	2.1 (0.5)
	SCB	16	2007–2010	−19.0 (0.6)	14.1 (0.8)	Madigan et al., 2012a	1.2 (0.2)	1.9 (0.3)
	SBaja	6 13	2001–2006, 2015–2016	−17.7 (1.4)	15 (2.8)	Hernández-Aguilar et al., 2015 Tamburin et al., 2019	0.9 (0.5)	1.7 (0.9)
	ETP	13	2009–2011	−17.7 (0.8)	7.2 (1.4)	Choy et al., 2015	0.9 (0.3)	3.9 (0.5)

DTDFs were calculated from each region's mean δ^{13}C and δ^{15}N values, based on published diet-based estimates for ectothermic fish (Caut et al., 2009; Hussey et al., 2014).

[a] *WPO: Western Pacific Ocean; EPO: Eastern Pacific Ocean; NCC: Northern California Current; SCB: Southern California Bight; SBaja: Southern Baja; ETP: Eastern Tropical Pacific.*

[b] *Sample size refers to n means reported in studies for a species/prey group, not individual samples within studies.*

only) mixing model for both the WPO and EPO to compare to the two-isotope model results. The probable contributions of regional prey endmembers to blue shark diet were inferred from 10,000 model iterations, with a burn-in period of 1000 and a thinning interval of 100. Model convergence was evaluated based on inspection of Gelman-Rubin diagnostics, where values for each parameter should equal ∼1.0 (Phillips et al., 2014; Parnell, 2020).

RESULTS

Data Compilation

Blue Shark SI Data

We obtained δ^{13}C and δ^{15}N values for blue shark muscle from one WPO study (Fujinami et al., 2018) (total $n = 120$ individuals) and four EPO studies (Miller et al., 2010; Madigan et al., 2012a; Li et al., 2014; Hernández-Aguilar et al., 2015) (total $n = 60$) from different regions of the EPO (NCC, SCB, SBaja, and ETP) (**Figure 1**). All studies included male and female sharks across juvenile and adult size ranges, though reporting of size and sex metadata did not allow for this information to be associated with individual δ^{13}C and δ^{15}N values.

We assumed that published blue shark δ^{13}C and δ^{15}N values were generally normally distributed, based on reporting of mean ± SD or SE. Blue shark δ^{13}C values showed high overlap between the WPO and EPO, with the majority of data in both regions falling between −20.0 and −17.0‰ (**Figure 2**); this was also observed in WPO and EPO prey that were used to calculate isoscape "baselines" for both regions (see **Figure 2** and section below). In contrast, blue shark δ^{15}N values were distinct between the WPO and EPO (**Figure 2**).

Consistent with previous studies, mean blue shark δ^{15}N values were consistently lower in the WPO (12.1‰; Fujinami et al., 2018) than in the EPO (14.7, 15.2, 15.8, and 16.5‰; Miller et al., 2010; Madigan et al., 2012a; Li et al., 2014; Hernández-Aguilar et al., 2015; **Figures 2**, **3**). The range of δ^{15}N values was relatively small in all regions, with minimal outliers (i.e., high values in WPO, low values in EPO) reported in any studies. Based on studies that reported δ^{15}N minima and maxima, these values were (WPO) 10.3–14.0‰ and (EPO) 13.8–18.8‰.

Prey SI Data

We obtained δ^{13}C and δ^{15}N data for WPO prey (muscle tissue) from five studies (Takai et al., 2007; Madigan et al., 2016; Ohshimo et al., 2016, 2019; Fujinami et al., 2018) for a total of 145 prey species, and obtained data for EPO prey from five studies (Madigan et al., 2012a; Miller et al., 2013; Choy et al., 2015; Hernández-Aguilar et al., 2015; Tamburin et al., 2019) for a total of 75 prey species. Prey species included the most commonly observed species in WPO and EPO blue shark diet (Preti et al., 2012; Hernández-Aguilar et al., 2015; Fujinami et al., 2018), including forage fish (anchovy *Engraulis* spp., sardine *Sardinops* spp., scombrids), squids (Ommastrephidae, Gonatidae, Oegopsidae), and crustaceans (red crab *Pleuroncodes planipes*), as well as other epi- and mesopelagic fish, squids, and crustaceans that have also been observed in blue shark diet (Preti et al., 2012; Hernández-Aguilar et al., 2015; Fujinami et al., 2018).

As with WPO and EPO blue shark data, prey δ^{13}C values showed high overlap while prey δ^{15}N values were discrete between the WPO and EPO (**Table 1** and **Figure 2**). For this reason, we used only δ^{15}N values for discriminant analysis, consistent with previous studies that used δ^{15}N to quantify exchange rates of WPO and EPO Pacific bluefin tuna (Madigan et al., 2017; Tawa et al., 2017). Overall WPO prey δ^{13}C

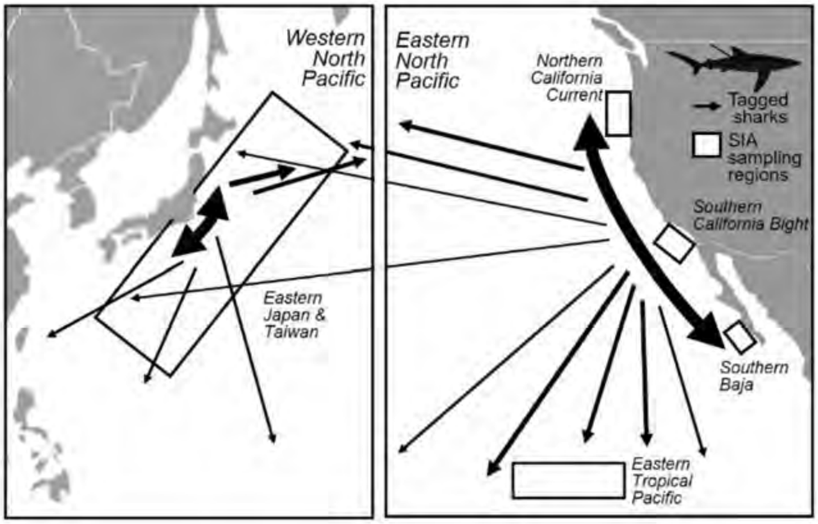

FIGURE 1 | Map of summarized blue shark (*Prionace glauca*) movements and sampling locations for isotopic studies in the North Pacific Ocean. Movements (black arrows) are based on conventional tagging data in the western and eastern Pacific Ocean (WPO and EPO), with arrow size scaled to relative proportion of observed movements. Boxes show regions of blue shark tissue sampling for stable isotope analysis (SIA). Tagging data are summarized from Sippel et al. (2011); SIA sampling locations from Miller et al. (2010), Madigan et al. (2012a), Li et al. (2014), Hernández-Aguilar et al. (2015), Fujinami et al. (2018).

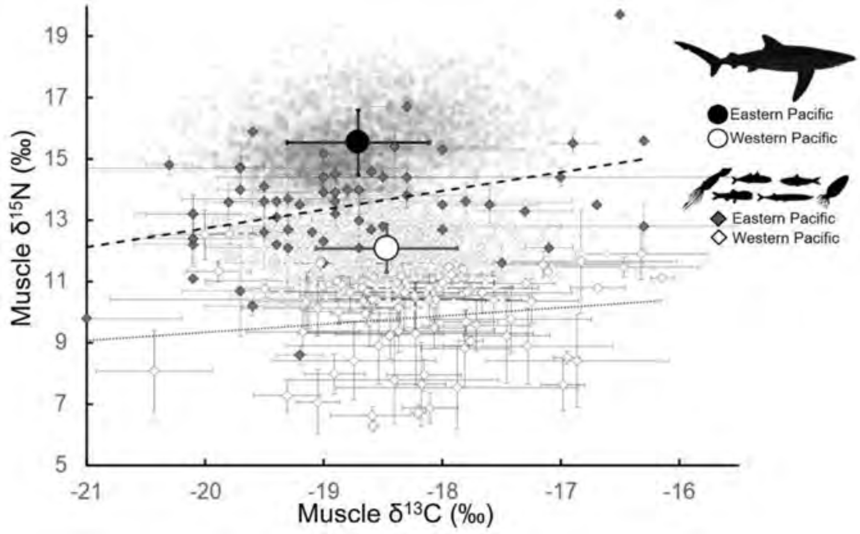

FIGURE 2 | Stable isotope values of blue sharks (*Prionace glauca*) and prey in the western and eastern North Pacific Ocean. Blue shark values in the eastern (dark circles) and western (open circles) were estimated from published distributions of blue shark values in each ocean basin, with means shown (large filled and open circles; ± SD). Prey data (diamonds; species mean ± SD) were selected based on general prey groups (e.g., mesopelagic squids, forage fish) reported in published diet studies, and include epi- and mesopelagic forage fish, squids, and crustaceans. Lines represent linear fits to eastern (dashed line) and western (solid line) prey data.

values were −18.2 ± 0.9‰; range −21.5 to −16.1‰, and δ^{15}N values were 9.9 ± 1.6‰; range 4.3–12.6‰. EPO prey SI values were (δ^{13}C) −18.6 ± 1.0‰; range −20.1 to −16.3‰, and (δ^{15}N) 14.1 ± 1.0‰; range 12.3–15.9‰. Prey δ^{13}C and δ^{15}N differences were variable across sub-regions (**Table 1**). Total diet estimates based on bootstrapped prey SI values were highly variable across regions (**Table 1**). Diet estimates were used in discriminant analysis and mixing models (below).

Data Analyses

Regional Variability and Overlap of Blue Shark SI Values

Across the five sub-regions, isotopic variability measured in terms of niche space (which was uniform across SEA and $\mathrm{SEA_B}$ estimates) was greatest for individuals captured in the ETP (1.8‰^{2}), and lowest in the NCC (0.6‰^{2}). SCB, SBaja, and WPO individuals exhibited intermediate variability (1.1‰^{2}–1.2‰^{2}, **Table 2** and **Figure 4**).

Isotopic niche overlap was extremely low between all possible combinations of EPO sub-regions and WPO blue sharks (<6%, **Table 2** and **Figure 4**). Overlap between sub-regions of the EPO was substantial, but highly variable, with overlap estimates ranging from 12 to 94% (**Table 2** and **Figure 4**). Blue sharks sampled in the NCC and SCB generally overlapped significantly with the isotopic niches of those from the ETP (>70%), but there was less overlap with SBaja (<48%). SBaja blue sharks overlapped minimally with NCC and SCB sharks (<39%), but overlapped highly with ETP sharks (94%, **Table 2** and **Figures 4**, **5**). Overlap of ETP sharks was relatively high with SCB and SBaja sharks (61 and 75%, respectively), but lower with the NCC (30%, **Table 2** and **Figures 4**, **5**). Overall, bilateral isotopic niche overlap (see **Table 2**) suggested that the highest level of WPO↔EPO connectivity was in the NCC (12%, 28%; **Table 2**), and the lowest level of WPO↔EPO connectivity in SBaja (<1%; **Table 2** and **Figure 5**). Within the EPO, the highest δ^{15}N-inferred connectivity of blue sharks was between the NCC and SCB (72%, 94%; **Table 2**) and SBaja and the ETP (94%, 75%; **Table 2**), and the lowest connectivity between SBaja and the NCC (12%, 28%; **Table 2** and **Figure 5**).

Diet-Dependent DTDFs

Across all regions (i.e., EPO and WPO values, including all sub-regions), calculated blue shark Δ^{13}C values ranged from 0.8 to 1.2‰ and for Δ^{15}N from 1.7 to 3.9‰. Due to substantial variation in WPO diet δ^{15}N values, overall WPO DTDFs generated in bootstrapped estimates ranged from 1.8 to 4.8‰ (3.1 ± 0.5‰), and EPO DTDFs from 1.4 to 1.9‰ (1.5 ± 0.1‰) (see **Table 1** for all regional DTDFs). Sub-region diet-dependent DTDFs varied substantially within both the EPO and WPO, based on differences in sub-region prey baselines (**Table 1**).

Discriminant Analysis

Discriminant analysis classified all WPO blue sharks as residents to the WPO (0% EPO migrants). In the EPO, 95.3% of blue sharks were categorized as residents to the EPO (∼5% WPO migrants), which varied by EPO sub-region: NCC (11% migrants), ETP (5% migrants), SCB (2% migrants), and SBaja (0% migrants), with <1% classification error across all regional discriminant analyses. The value representing the cutoff point in discriminant analyses (threshold δ^{15}N value between WPO- and EPO-classified sharks) was similar across all analyses conducted, at ∼14.0‰. Most δ^{15}N values of WPO migrants in the EPO (δ^{15}N < 14.0‰) were in the tails of bootstrapped population δ^{15}N values, though one

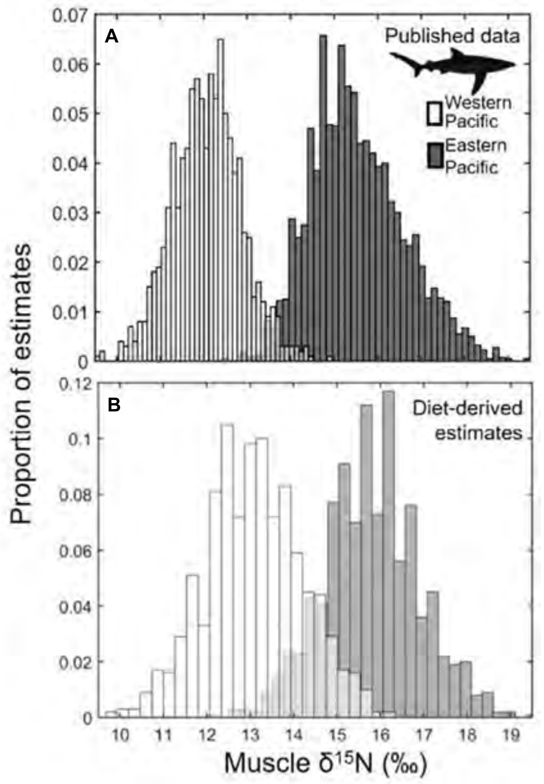

FIGURE 3 | Distributions of bootstrapped blue shark (*Prionace glauca*) δ^{15}N values from the North Pacific Ocean. **(A)** Blue shark muscle δ^{15}N values were taken from the published literature from sampling regions off Japan and Taiwan (western Pacific Ocean; open bars) and the California Current and the Eastern Tropical Pacific (eastern Pacific Ocean; gray bars). **(B)** Blue shark diet-derived δ^{15}N values were estimated by calculating regional prey baselines, based on published data, and adding resampled blue shark diet-dependent DTDF estimates for each region.

empirical EPO value (δ^{15}N = 13.8‰; minimum reported in ETP) was classified as a WPO migrant.

Training data for discriminant analysis (estimated blue shark δ^{15}N values from WPO and EPO prey, calculated from region-specific diet estimates and DTDFs), were (WPO) 13.1 ± 1.1‰ and (EPO) 15.8 ± 1.1‰. WPO and EPO training data were highly discrete between the two regions (13% overlap; **Figure 3**) and highly coherent with bootstrapped blue shark δ^{15}N distributions (**Figure 3**).

Isotopic Mixing Models

Substantial blue shark SI data (9–32%) fell outside of the prey mixing space due to low shark δ^{13}C values (**Supplementary Figure 1** and **Supplementary Table 2**), leading to unreliable mixing model results. There were large discrepancies between dual (δ^{13}C and δ^{15}N) and single (δ^{15}N) isotope mixing models in both the EPO and WPO (**Supplementary Figures 2, 3** and **Supplementary Tables 2, 3**). In the EPO, the dual isotope model suggested high SCB inputs to all regions (66–100%), likely biased by the SCB having the lowest prey δ^{13}C values (**Supplementary Figure 2**). Results suggested low contributions from the WPO (i.e., *trans*-Pacific migrants) in the NCC (15%) and SCB (12%), and minimal inputs from the NCC and SBaja (0–5%) (**Supplementary Figure 2** and **Supplementary Table 2**). The single isotope model indicated higher contributions from all EPO sub-regions, though SCB inputs were still important to all sub-regions (**Supplementary Figure 2** and **Supplementary Table 2**).

TABLE 2 | Bayesian inferred probabilistic niche overlap of blue sharks (*Prionace glauca*) captured from five sub-regions.

	Sub-region (ii)				
Sub-region (i)	**Northern California Current**	**Southern California Bight**	**Southern Baja**	**Eastern Tropical Pacific**	**WPO**
Northern California Current	–	93.9	28.4	90.5	5.6
Southern California Bight	72.4	–	47.3	83.3	0.8
Southern Baja	12.4	38.3	–	93.9	<0.1
Eastern Tropical Pacific	30.1	61.3	74.7	–	2.7
WPO	2.6	0.9	<0.1	4.0	–

Table is interpreted as the probabilistic niche overlap between sub-region (i) and sub-region (ii) and vice versa. Values show % overlap of 95% probabilistic niche regions.
WPO: Western Pacific Ocean.

In the WPO, a similarly high proportion of blue shark SI data (55%) fell outside of prey mixing space due to low shark δ^{13}C values (**Supplementary Figure 1** and **Supplementary Table 2**). The dual isotope model suggested blue sharks foraged most on prey from Kuroshio-Oyashio (65%), though model results were likely biased by that region's relatively low prey δ^{13}C values (**Supplementary Figure 3**). When δ^{13}C values were excluded from mixing models, the single-isotope δ^{15}N model suggested greater contributions to blue shark diet from all sub-regions, with the southern region (offshore Taiwan) contributing the most (56%; **Supplementary Figure 3** and **Supplementary Table 3**). The 95% credible intervals for all mixing models results are shown in **Supplementary Tables 2, 3**.

DISCUSSION

Region-specific stable isotope values of blue sharks and prey allowed for inferences of prior movement patterns and regional connectivity in the North Pacific Ocean, quantifying dynamics that have been observed (e.g., *trans*-Pacific migrations), but for which frequency and exchange rates are unknown. Our results suggest minimal *trans*-Pacific movements and indicate potential finer-scale movement and residency dynamics within sub-regions of the EPO and WPO, though key caveats were evident in estimates of finer scale movements. High coherence of prey-estimated blue shark δ^{15}N values with empirical SI values demonstrated the effectiveness and predictive value of North Pacific isoscapes. Overall, our results demonstrate the efficacy of our multi-analytical stable isotope approach to identify movements of a highly migratory pelagic species in the North Pacific, and the potential for future analyses with consideration

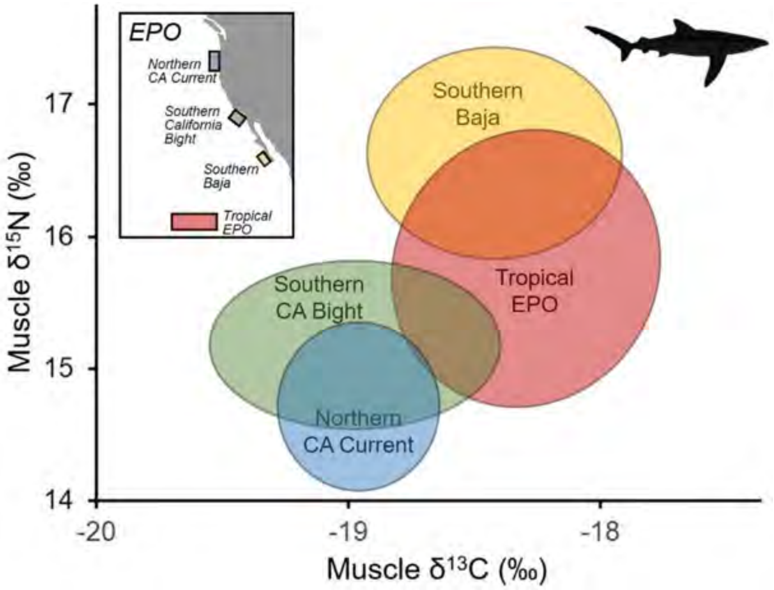

FIGURE 4 | Differences in isotopic niches of blue shark (*Prionace glauca*) across discrete regions within the eastern North Pacific Ocean. Map (upper left) shows regions where blue sharks were sampled and subsequently analyzed for $\delta^{13}C$ and $\delta^{15}N$ values. Ellipses represent 95% of blue shark $\delta^{13}C$ and $\delta^{15}N$ values following Swanson et al. (2015).

of sample treatment and quantification of crucial species-specific isotopic parameters.

Trans-Pacific migrations in North Pacific blue sharks were first demonstrated by conventional tagging efforts in the eastern Pacific (Sippel et al., 2011), and we used SI data to assess the frequency of EPO↔WPO movements. In the WPO, SI datasets revealed no evidence of migrations from the EPO, compared to conventional tagging studies that reported 4 of 205 (~2%) EPO-tagged (NCC, SCB, and SBaja) blue sharks migrating to the WPO (Sippel et al., 2011). In the EPO, discriminant analysis indicated *trans*-Pacific migration from the WPO in low proportions (~5%) of our EPO bootstrapped population estimates, including at least one empirical migrant value ($\delta^{15}N$ = 13.8‰; ETP). However, conventional tagging found no *trans*-Pacific migration to the EPO from the WPO (*n* = 207) (Sippel et al., 2011), and more recent satellite tagging in the EPO (*n* = 47) and WPO (*n* = 21) showed movements only within those respective ocean regions (Maxwell et al., 2019; Fujinami et al., 2021). While tagging studies have thus provided quantitative metrics of *trans*-Pacific migrations, tag-inferred movements have limitations, including simplistic movement information and potential non-reporting of tag recovery (conventional tags), limited sample size (electronic tags), and short-term tracks that do not capture long-distance movements (both tag types) (Siskey et al., 2019). Tagging data is also prospective, capturing future rather than prior movements that are potentially biased by tagging location. In contrast, isotopic measurements coupled with isotopic turnover rates and DTDFs can provide retrospective, quantifiable timeframes of prior movements. While SI-inferred movements are limited by isotopic turnover rates of analyzed tissue, prior movements can be characterized due to mobile predators integrating prey isotopic signatures during movements through isotopically distinct regions (Graham et al., 2010; MacKenzie et al., 2012; Carlisle et al., 2015; Madigan, 2015; Trueman and Glew, 2019). As such, isotope- and tag-inferred migration patterns are effective complementary techniques (Carlisle et al., 2012, 2015; Madigan et al., 2015, 2018; Shipley et al., 2021). Here, comparing isotopic estimates to past conventional tagging suggests that blue sharks make both eastward and westward *trans*-Pacific migrations, though the number of sharks that make these migrations appears to be low (<5%).

The low *trans*-Pacific exchange inferred here improve understanding of blue shark population dynamics in the North Pacific. Genetic analyses have shown global panmixia across regional blue shark populations, with minimal evidence of regional population structure (Taguchi et al., 2015; Veríssimo et al., 2017; Bailleul et al., 2018). This lack of observed population structure requires some mechanism of regional population mixing, and while maintenance of population genetic homogeneity does not necessarily require high mixing (Bremer et al., 2005; Waples and Gaggiotti, 2006), the minimal *trans*-Pacific exchange we observed here is unlikely to be the primary driver. Current understanding of blue shark life history provides several alternative scenarios for mixing of EPO and WPO populations. If WPO and EPO sharks mate (central-southern waters; ~20–30°N) and pup (northern waters; ~35–45°N) (Nakano, 1994; Nakano and Stevens, 2008) in their respective ocean basins, EPO- and WPO-origin young-of-the-year (YOYs) could subsequently recruit to either the WPO or EPO. In addition, the Central Pacific Ocean (CPO) (i.e., waters around Hawaii) could serve as a mixing region for WPO and EPO sharks, as some exchange of blue sharks in this region has

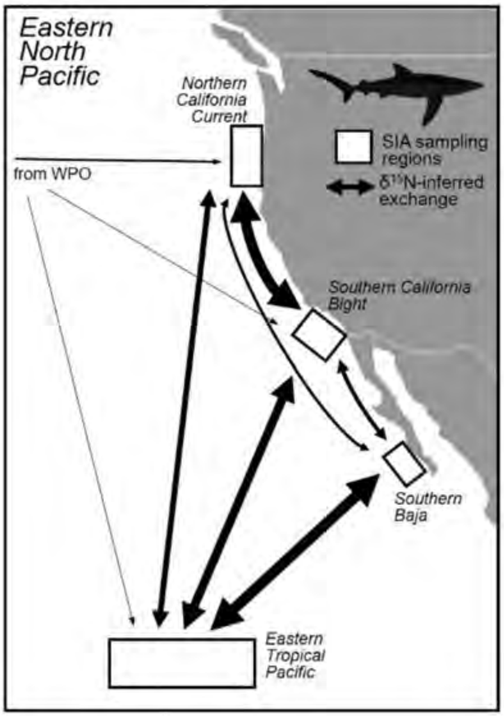

FIGURE 5 | Summarized estimates of blue shark (*Prionace glauca*) migratory exchange between eastern North Pacific Ocean regions, inferred from niche overlap of regional $\delta^{13}C$ and $\delta^{15}N$ values. Migratory exchange was inferred quantitatively by calculating overlap between 95% probabilistic isotopic niches of each sub-region, using a Bayesian approach ("nicheROVER"; Swanson et al., 2015). Arrows are scaled to the degree of isotopic niche overlap between regions; note that exchange rates are relative and approximate.

been observed previously (Sippel et al., 2011). Consequently, dispersive YOY recruitment and/or partial, temporary mixing of adults in the CPO (if for mating or parturition) could drive genetic mixing while maintaining regional WPO and EPO isotopic signatures that indicate regional residency of juveniles and adults. Alternatively, genetic analysis has demonstrated the possibility of "genetic time-lag" effects in blue sharks (Bailleul et al., 2018), with the possibility of discrete sub-populations despite genetic homogeneity; thus, WPO and EPO separation observed here could indicate discrete, minimally mixed sub-populations. As such, the degree to which YOY recruitment and adult mixing contribute to North Pacific blue shark population dynamics warrants further study.

Comparison of blue shark and prey values between the WPO and EPO demonstrated that $\delta^{15}N$, and not $\delta^{13}C$, serves as a regional diagnostic tracer in the North Pacific Ocean as has been previously observed in Pacific bluefin tuna (Madigan et al., 2017). We observed high overlap of WPO and EPO prey $\delta^{13}C$ values, but almost no overlap of prey $\delta^{15}N$ values (**Figure 2**). Mechanisms for this have been demonstrated, with photosynthetic pathways in pelagic primary producers (C_3 photosynthesis) varying more with latitude (i.e., due to variable productivity, temperature, and seawater pCO_2 regimes), rather than longitude (Bowen, 2010; Magozzi et al., 2017; Brault et al., 2018; Ohshimo et al., 2019). Coherence of prey-based estimated $\delta^{15}N$ blue shark values with shark-derived values (**Figure 3**) further supports both the robustness of the $\delta^{15}N$ isoscape approach and the marked separation between $\delta^{15}N$ values of WPO and EPO sharks. Similar patterns of distinct EPO and WPO isotopic signatures have been found in Pacific bluefin tuna, a large-bodied pelagic teleost in the WPO and EPO that makes seasonal migrations through the same WPO and EPO regions (Boustany et al., 2010; Madigan et al., 2017; Tawa et al., 2017). In Pacific bluefin tuna, $\delta^{15}N$-based estimates of *trans*-Pacific migration were demonstrably effective based on coherence with other chemical tracers, while non-differentiation of tuna $\delta^{13}C$ made it an ineffective migration tracer (Madigan et al., 2017). This differs from more typical isotopic applications to ecology, which generally use $\delta^{15}N$ to estimate trophic dynamics and $\delta^{13}C$ to trace energy source and foraging location(s), due to lower trophic fractionation of $\delta^{13}C$ than of $\delta^{15}N$ (Post, 2002). However, more recent studies have demonstrated that in some systems and for certain predators, baseline $\delta^{15}N$ values across ecoregions can result in predators acquiring regional $\delta^{15}N$ signatures that outweigh trophic effects (Graham et al., 2010; Hobson et al., 2010; Madigan et al., 2017; Shipley et al., 2021). Isoscapes will be basin- and ecosystem-dependent. In the North Pacific, the $\delta^{15}N$ gradient is caused by upwelling-driven enrichment of ^{15}N in the EPO and low $\delta^{15}N$ values due to oligotrophic N-fixation in the WPO (Takai et al., 2007; Madigan et al., 2012a, 2017; Fujinami et al., 2018; Ohshimo et al., 2019). The finer scale structure of $\delta^{13}C$ and $\delta^{15}N$ values in the WPO and EPO shown here demonstrate the utility of SIA in these ecosystems to track inter- and intra-basin predator movements.

We used niche overlap of blue shark $\delta^{13}C$ and $\delta^{15}N$ values to quantify finer scale connectivity dynamics within EPO and WPO sub-regions. In the EPO, isotopic niche overlap suggested variable mixing between the NCC, SCB, SBaja, and ETP (**Figure 5**). High exchange was suggested between the NCC and SCB; this is supported by conventional (Sippel et al., 2011) and electronic tag studies, which also found sexual segregation between these two regions (Maxwell et al., 2019). Lower overlap between SBaja and the NCC/SCB suggests that sharks may be more resident to this region. Regional proximity likely plays a role in exchange dynamics, as in general, more proximate regions showed greater migratory exchange (**Figure 5**). Collectively, estimated connectivity in the ETP and SBaja supports the premise that coastal and pelagic waters off SBaja may serve as both an overwintering ground for juveniles and a potential reproductive function for adults (Vögler et al., 2012), with isotopic overlap suggesting migration from SBaja to the ETP (**Figure 5**). Importantly, movement dynamics related to size and sex structure have been observed across these regions (Nakano and Stevens, 2008; Vögler et al., 2012; Maxwell et al., 2019), which we could not evaluate here due to a lack of size- and sex-specific information to match with blue shark isotopic values. Improved insight into size- and sex-specific movement dynamics could be accomplished with robust sampling of blue sharks for empirical isotopic measurements, coupled with size and sex metadata across the defined study regions. This could easily be achieved through sampling of fisheries [by]catch, potentially incorporating tissues of different turnover rates (i.e., fast [plasma, liver]; slow [muscle]; Thomas and Crowther, 2015; Vander Zanden et al., 2015).

While mixing models provided exploratory and potentially informative estimates of regional connectivity, results of finer scale sub-regional movements appeared biased and thus unreliable. Although the δ^{15}N values of sharks and DTDF-corrected prey highly overlapped, shark δ^{13}C values were low relative to prey in both the EPO and WPO (**Supplementary Figures 2, 3**). Furthermore, prey mixing polygons (Smith et al., 2013) showed up to 32% and 55% of blue shark values falling outside of the simulated prey mixing space, due to these low shark δ^{13}C values (**Supplementary Figure 1** and **Supplementary Tables 2, 3**). This likely biased mixing model estimates toward the lowest δ^{13}C prey input(s); this confounding factor was observed in the two-isotope mixing models in both the WPO (high input of Kuroshio-Oyashio) and EPO (high input of SCB) (**Supplementary Figures 2, 3**). A similar effect of low blue shark δ^{13}C values was observed in a previously published estimate of diet based on isotope mixing models in the SBaja sub-region, in which low blue shark δ^{13}C values relative to prey resulted in the two lowest δ^{13}C prey items (pelagic octopus *Argonauta* spp. and pelagic red crab *P. planipes*) dominating diet estimates (Hernández-Aguilar et al., 2015). Consequently, mixing model results here demonstrate that biased results will likely occur when predator SI values are substantially offset from prey inputs. While this is unsurprising and has previously been identified in the literature, studies continue to adopt this approach and report findings without identifying potential bias. It is imperative that investigators use appropriate diagnostic tools (i.e., quantitative assessment of prey vs. predator data following Smith et al., 2013) to ensure results are accurate or that potential bias is reported. For blue sharks, low δ^{13}C values that are irreconcilable with local prey is consistent across studies and requires clarification.

There are three possible explanations for the consistently low δ^{13}C values observed in blue sharks: (i) feeding in a region, within timeframes, or on prey not represented in regional studies; (ii) estimated Δ^{13}C values for blue sharks are too high, and fractionation between prey and blue shark muscle is lower than our estimated DTDF values; or (iii) shark sample preparation for SIA resulted in artificially low δ^{13}C values across studies. Missing or isotopically misrepresented prey sources (scenario [i]) is a common issue across studies (Smith et al., 2013); here, sampling too close to coastlines could result in unrealistically high prey δ^{13}C and/or δ^{15}N values for a pelagic shark. However, most studies used in these analyses explicitly sampled in offshore epi- and mesopelagic zones. In addition, prey data are available for two offshore regions that were not included here, the TZCF and CPO, and prey δ^{13}C values from those regions (-18.2 ± 0.8‰ and -17.7 ± 0.8‰, respectively) (Gould et al., 1997; Choy et al., 2015) are also not low enough to explain the observed shark δ^{13}C values. Temporal variability in isotopic values, while possibly influential, is also an unlikely explanation here, as studies spanned multiple seasons and years and different EPO and WPO values are driven by coarsely consistent oceanographic conditions (Madigan et al., 2017). It is possible that our DTDF estimates are imprecise (scenario [ii]), as they were calculated as diet-based DTDFs following Caut et al. (2009) and Hussey et al. (2014), rather than empirically derived from laboratory experiments. Differential amino acid composition and subsequent ^{13}C fractionation in blue sharks could drive atypical DTDFs (McMahon et al., 2010). Laboratory-derived Δ^{13}C DTDFs available for other elasmobranch species (Hussey et al., 2010; Logan and Lutcavage, 2010; Kim et al., 2012) are rarely <1.0‰ (the mean DTDF applied here), and a DTDF of ≤ 0‰ would be necessary for blue shark values to be highly coherent with prey. Negative Δ^{13}C values for sharks are rare in available studies, though one negative value (-0.5‰) has been estimated for one prey type (of 8 total diet items in natural diet) in the catshark *Scyliorhinus canicula*, so this DTDF in wild blue sharks cannot be ruled out (Caut et al., 2013). Similar observations in other ocean basins of low blue shark δ^{13}C values relative to prey and/or other sharks (Rabehagasoa et al., 2012; Li et al., 2014; Kiszka et al., 2015) support the possibility that a unique aspect of blue shark muscle composition or physiology could drive atypically low Δ^{13}C, but this likely can only be validated with captive studies. Finally, it is possible that sample preparation partially contributed to low δ^{13}C values in at least some studies (scenario [iii]). Studies included here performed lipid and/or urea extraction, but not always both (Madigan et al., 2012a; Li et al., 2014; Hernández-Aguilar et al., 2015; Fujinami et al., 2018), or mathematically corrected for lipids (Miller, 2006). Many of these studies preceded thorough published analyses demonstrating the importance of both lipid and urea extraction in elasmobranch tissues, which prevents artificially low δ^{13}C and/or δ^{15}N values (Carlisle et al., 2016; Li et al., 2016; Arostegui et al., 2019); recent work has also shown that water rinses for urea extraction may actually increase δ^{13}C values (Carlisle et al., 2016). Our analyses, which draw upon published studies, underscore the need for standardized, consistent sample treatment in ongoing and future isotopic studies (Wolf et al., 2009; Shipley and Matich, 2020), while also noting the value of large archival datasets to address questions at an ocean basin scale. While laboratory-derived DTDFs will be difficult to obtain directly for blue sharks in captivity, improved understanding of ^{13}C dynamics in this species will be necessary to refine the accuracy of mixing model results, an issue that may also be applicable across other elasmobranch species.

While the data used here came from known high-use regions for blue sharks in the North Pacific, there are other relevant regions that could not be included in our analyses. In particular, the North Pacific Transition Zone (NPTZ) (also referred to as the Transition Zone Chlorophyll Front) has been shown as a region of high blue shark abundance (Pearcy, 1991; Polovina et al., 2001; Kubodera et al., 2007; Vögler et al., 2012). Recently, the NPTZ has been demonstrated as a migratory corridor for pregnant females that were satellite tagged in the WPO (Fujinami et al., 2021), has been suggested as a nursery ground for young sharks (Nakano and Stevens, 2008), and may be a migratory corridor for other blue shark life stages/sexes as well as tunas, swordfish, and turtles (Block et al., 2011). While blue shark isotope data were not available from the NPTZ, prey δ^{13}C and δ^{15}N appear to be similar to the WPO (Gould et al., 1997). As such, blue sharks with long-term residency in the NPTZ may be isotopically indistinguishable from WPO residents. It is currently unknown whether blue sharks in the NPTZ are residential to the frontal region for adequate timeframes (i.e., months to >1 yr) to acquire the NPTZ isotopic signal or whether they use the region temporarily during inter-region migrations; the WPO migrants we observed here in the NCC could reasonably be entering the California Current via the NPTZ. Isotopic sampling of NPTZ sharks, likely accessible from bycatch in offshore fisheries, could ascertain migration dynamics in NPTZ sharks. Similarly, blue sharks are common in the Central Pacific (i.e., waters around Hawaii; CPO), where conventional tagging suggests mixing with both the EPO and CPO (Sippel et al., 2011). With no isotopic characterizations of blue sharks in the CPO, we could not include this region here; however, isotopic analysis of CPO sharks could reveal the extent to which these sharks are residential to the region, as local prey seem to be distinctive from other regions, particularly prey $\delta^{15}N$ values (Choy et al., 2015). Collecting samples across the spatial range of North Pacific fisheries is tractable, especially since a small biopsy sample from a subsequently released, live shark is sufficient for SIA.

This study was limited to the use of bootstrap-estimated blue shark $\delta^{13}C$ and $\delta^{15}N$ values rather than using direct empirical measurements. While our approach allowed for population-wide estimates based on empirically derived data distributions, some regional blue shark studies had relatively low sample sizes (e.g., $n = 9$ in SCB, $n = 10$ in NCC), and in this context, the "tails" of bootstrapped distributions likely lead to unrealistically high and low SI values (Madigan et al., 2017). Bootstrapped estimates can also lead to de-coupled shark $\delta^{13}C$ and $\delta^{15}N$ values (see shark data ellipses in **Figures 2**, **4** and **Supplementary Figure 2**), when empirical $\delta^{13}C$ and $\delta^{15}N$ values are often positively correlated. This could affect mixing model estimates of prey/regional contributions to blue shark diet. The lack of size and sex data also limited our ability to undertake more detailed reconstruction of blue shark residency and movement dynamics across life history. Finally, isotopic identification of migrants is dictated by tissue turnover to steady-state conditions (here, likely ∼0.5 to 1.5 year before sampling), precluding identification of long-distance migrations that occurred prior to these timeframes. As such, results here should be taken in the context of these limitations and be viewed as a preliminary framework for regionally focused, empirical investigation.

CONCLUSION

Our results, drawing upon published $\delta^{13}C$ and $\delta^{15}N$ data for blue sharks and prey sampled at multiple locations in the EPO and WPO, provide a new and replicable means to assess blue shark residency and migration dynamics in the North Pacific. The analyzed data provide strong evidence for limited direct migrations between the WPO and EPO and reiterate the utility of $\delta^{15}N$ isoscapes for the reconstruction of migratory predator movements in the North Pacific Ocean. Limited *trans*-Pacific migrations suggest that other mechanisms maintain genetic homogeneity of the North Pacific blue shark population, including YOY movements and/or partial mixing of adults in the Central Pacific. Regional structure in $\delta^{13}C$ and $\delta^{15}N$ data have promise for further quantification of finer-scale blue shark movements, increasing the resolutions of movement patterns suggested here, but consideration of isotopic parameters (e.g., accurate species-specific DTDFs), appropriate sample preparation of shark tissues, and length/sex metadata of sampled sharks are necessary. With emerging research showing varying residency and *trans*-regional movements in migratory predators, isoscapes can employ high sample sizes across a breadth of animal life stages, regions, and timeframes to reconstruct habitat use of highly mobile marine animals. Through these isotopic approaches, population-level estimates of movement dynamics are feasible on scales that may not be readily available from conventional tagging or telemetry studies.

DATA AVAILABILITY STATEMENT

The data analyzed in this study is subject to the following licenses/restrictions: Data came from published manuscripts, which are only publicly available through purchase of publications. Requests to access these datasets should be directed to daniel.madigan@stonybrook.edu.

AUTHOR CONTRIBUTIONS

DJM, ONS, NEH, and ABC conceived the study. DJM, ONS, and ABC performed the analyses. DJM and ONS wrote the manuscript, with input from all authors. All authors interpreted results and refined analyses.

FUNDING

This project was supported by WWF Canada and an NSERC Discovery Grant (#04922-2017) to NEH.

ACKNOWLEDGMENTS

Information and comments regarding conventional tagging data were generously provided by T. Sippel, and K. James provided valuable comments on the manuscript.

SUPPLEMENTARY MATERIAL

The Supplementary Material for this article can be found online at: https://www.frontiersin.org/articles/10.3389/fmars.2021.653606/full#supplementary-material

Supplementary Figure 1 | Comparisons of blue shark (*Prionace glauca*) $\delta^{13}C$ and $\delta^{15}N$ values to regional prey. Prey fields (filled gray forms) were generated by simulating 10,000 polygons using prey $\delta^{13}C$ and $\delta^{15}N$ values, following Smith et al. (2013). All prey values are adjusted by the addition of calculated diet-based DTDFs to allow quantification of overlap with blue shark $\delta^{13}C$ and $\delta^{15}N$ values (black circles). Proportion of blue shark values falling outside prey polygons, mostly due to low shark $\delta^{13}C$ values, were 55% in the WPO (upper left panel) and 9–32% in regions of the EPO (other panels). These data highlight the importance of quantitatively assessing prey/predator isotope dynamics to ensure accurate interpretation of mixing models results and/or to determine (and report) the level of potential bias.

Supplementary Figure 2 | Isotopic overlap of regional blue shark (*Prionace glauca*) data with regional prey, and exploratory mixing model estimates of regional prey contributions, in sub-regions of the eastern Pacific Ocean. **(A)** Bootstrapped blue shark δ^{13}C and δ^{15}N values (small circles, colored by EPO sampling sub-region) and regional prey means (large circles; error bars ± SD), from the western (WPO) and eastern (EPO) Pacific Ocean. Mean prey δ^{13}C and δ^{15}N values are adjusted by the addition of calculated diet-dependent diet-tissue discrimination factors (DTDFs) (Caut et al., 2009; Hussey et al., 2014). After prey mean adjustment for DTDF, most blue shark δ^{13}C values were left-shifted (lower δ^{13}C) relative to prey δ^{13}C values. **(B)** Estimated regional prey inputs to EPO blue shark diet from Bayesian mixing models. Left panel shows results from the dual isotope model (δ^{13}C and δ^{15}N), which were biased toward the regional prey with lowest δ^{13}C values, and right panel the single isotope (δ^{15}N) model.

Supplementary Figure 3 | Isotopic overlap of blue shark (*Prionace glauca*) data with regional prey, and exploratory mixing model estimates of regional prey contributions, in the western Pacific Ocean. **(A)** Bootstrapped blue shark δ^{15}N values (small gray circles) and regional prey means (large circles, colored by WPO sub-region) from the western Pacific Ocean (WPO). Mean prey δ^{13}C and δ^{15}N values are adjusted by the addition of calculated diet-dependent diet-tissue discrimination factors (DTDFs) (Caut et al., 2009; Hussey et al., 2014). After prey mean adjustment for DTDF, most blue shark δ^{13}C values were left-shifted (lower δ^{13}C) from expected prey-based values. **(B)** Estimated regional prey inputs to WPO blue shark diet from Bayesian mixing models. Left panel shows results from two isotope model (^{13}C and δ^{15}N), which were biased toward the regional prey with lowest δ^{13}C values, and right panel shows a single isotope (δ^{15}N) model.

Supplementary Table 1 | Isotopic niche metrics generated from carbon and nitrogen stable isotope values of blue sharks (*Prionace glauca*). Standard ellipse (SEA) areas (‰^{2}) are derived from Northern California Current, Southern California Bight, Southern Baja, Eastern Tropical Pacific, and West Pacific Ocean (WPO). SEA estimates represent maximum likelihood (SEA) and Bayesian (SEA$_B$; [75% Cis]) derived estimates based on 40% of the data.

Supplementary Table 2 | Reliance of EPO blue shark populations on regional prey groups as inferred from Bayesian isotope mixing models. Results are median estimates (95% credible intervals [CIs]) derived from the posterior distributions of dual (δ^{13}C and δ^{15}N) and single (δ^{15}N) isotope models. For dual isotope models, the percentage of individuals with >95% probability of falling outside of the simulated prey mixing space is shown.

Supplementary Table 3 | Reliance of WPO blue shark populations on regional prey groups as inferred from Bayesian isotope mixing models. Results are median estimates (95% credible intervals [CIs]) derived from the posterior distributions of dual (δ^{13}C and δ^{15}N) and single (δ^{15}N) isotope models. For dual isotope models the percentage of individuals that had a >95% probability of falling outside of the simulated prey mixing space is indicated.

REFERENCES

Altabet, M. A., Pilskaln, C., Thunell, R., Pride, C., Sigman, D., Chavez, F., et al. (1999). The nitrogen isotope biogeochemistry of sinking particles from the margin of the Eastern North Pacific. *Deep Sea Res. Part I Oceanogr. Res. Pap.* 46, 655–679. doi: 10.1016/s0967-0637(98)00084-3

Arostegui, M. C., Schindler, D. E., and Holtgrieve, G. W. (2019). Does lipid-correction introduce biases into isotopic mixing models? Implications for diet reconstruction studies. *Oecologia* 191, 745–755. doi: 10.1007/s00442-019-04525-7

Bailleul, D., Mackenzie, A., Sacchi, O., Poisson, F., Bierne, N., and Arnaud-Haond, S. (2018). Large-scale genetic panmixia in the blue shark (*Prionace glauca*): a single worldwide population, or a genetic lag-time effect of the “grey zone” of differentiation? *Evol. Appl.* 11, 614–630. doi: 10.1111/eva.12591

Block, B. A. I, Jonsen, D., Jorgensen, S. J., Winship, A. J., Shaffer, S. A., Bograd, S. J., et al. (2011). Tracking apex marine predator movements in a dynamic ocean. *Nature* 475, 86–90. doi: 10.1038/nature10082

Boustany, A. M., Matteson, R., Castleton, M., Farwell, C., and Block, B. A. (2010). Movements of Pacific bluefin tuna (*Thunnus orientalis*) in the Eastern North Pacific revealed with archival tags. *Prog. Oceanogr.* 86, 94–104. doi: 10.1016/j.pocean.2010.04.015

Bowen, G. J. (2010). Isoscapes: spatial pattern in isotopic biogeochemistry. *Annu. Rev. Earth Planet. Sci.* 38, 161–187. doi: 10.1146/annurev-earth-040809-152429

Brault, E. K., Koch, P. L., McMahon, K. W., Broach, K. H., Rosenfield, A. P., Sauthoff, W., et al. (2018). Carbon and nitrogen zooplankton isoscapes in West Antarctica reflect oceanographic transitions. *Mar. Ecol. Prog. Ser.* 593, 29–45. doi: 10.3354/meps12524

Bremer, J. R. A., Viñas, J., Mejuto, J., Ely, B., and Pla, C. (2005). Comparative phylogeography of Atlantic bluefin tuna and swordfish: the combined effects of vicariance, secondary contact, introgression, and population expansion on the regional phylogenies of two highly migratory pelagic fishes. *Mol. Phylogenet. Evol.* 36, 169–187. doi: 10.1016/j.ympev.2004.12.011

Burgess, G. H., Beerkircher, L. R., Cailliet, G. M., Carlson, J. K., Cortés, E., Goldman, K. J., et al. (2005). Is the collapse of shark populations in the Northwest Atlantic Ocean and Gulf of Mexico real? *Fisheries* 30, 19–26. doi: 10.1577/1548-8446(2005)30[19:itcosp]2.0.co;2

Campana, S. E., Joyce, W., and Manning, M. J. (2009). Bycatch and discard mortality in commercially caught blue sharks *Prionace glauca* assessed using archival satellite pop-up tags. *Mar. Ecol. Prog. Ser.* 387, 241–253. doi: 10.3354/meps08109

Cardeñosa, D., Fields, A. T., Babcock, E. A., Shea, S. K., Feldheim, K. A., and Chapman, D. D. (2020). Species composition of the largest shark fin retail-market in mainland China. *Sci. Rep.* 10, 1–10.

Carlisle, A. B., Goldman, K. J., Litvin, S. Y., Madigan, D. J., Bigman, J. S., Swithenbank, A. M., et al. (2015). Stable isotope analysis of vertebrae reveals ontogenetic changes in habitat in an endothermic pelagic shark. *Proc. R. Soc. Lond. B Biol. Sci.* 282:20141446. doi: 10.1098/rspb.2014.1446

Carlisle, A. B., Kim, S. L., Semmens, B. X., Madigan, D. J., Jorgensen, S. J., Perle, C. R., et al. (2012). Using stable isotope analysis to understand migration and trophic ecology of northeastern Pacific white sharks (*Carcharodon carcharias*). *PLoS One* 7:e30492. doi: 10.1371/journal.pone.0030492

Carlisle, A. B., Litvin, S. Y., Madigan, D. J., Lyons, K., Bigman, J. S., Ibarra, M., et al. (2016). Interactive effects of urea and lipid content confound stable isotope analysis in elasmobranch fishes. *Can. J. Fish. Aquat. Sci.* 99, 1–10.

Caut, S., Angulo, E., and Courchamp, F. (2009). Variation in discrimination factors (Δ^{15}N and Δ^{13}C): the effect of diet isotopic values and applications for diet reconstruction. *J. Appl. Ecol.* 46, 443–453. doi: 10.1111/j.1365-2664.2009.01620.x

Caut, S., Jowers, M. J., Michel, L., Lepoint, G., and Fisk, A. T. (2013). Diet-and tissue-specific incorporation of isotopes in the shark *Scyliorhinus stellaris*, a North Sea mesopredator. *Mar. Ecol. Prog. Ser.* 492, 185–198. doi: 10.3354/meps10478

Choy, C. A., Popp, B. N., Hannides, C. C. S., and Drazen, J. C. (2015). Trophic structure and food resources of epipelagic and mesopelagic fishes in the North Pacific Subtropical Gyre ecosystem inferred from nitrogen isotopic compositions. *Limnol. Oceanogr.* 60, 1156–1171. doi: 10.1002/lno.10085

Clarke, S. C., Magnussen, J. E., Abercrombie, D. L., McAllister, M. K., and Shivji, M. S. (2006a). Identification of shark species composition and proportion in the Hong Kong shark fin market based on molecular genetics and trade records. *Conserv. Biol.* 20, 201–211. doi: 10.1111/j.1523-1739.2005.00247.x

Clarke, S. C., McAllister, M. K., Milner-Gulland, E. J., Kirkwood, G., Michielsens, C. G., Agnew, D. J., et al. (2006b). Global estimates of shark catches using trade records from commercial markets. *Ecol. Lett.* 9, 1115–1126. doi: 10.1111/j.1461-0248.2006.00968.x

Coelho, R., Mejuto, J., Domingo, A., Yokawa, K., Liu, K. M., Cortés, E., et al. (2018). Distribution patterns and population structure of the blue shark (*Prionace glauca*) in the Atlantic and Indian Oceans. *Fish Fish.* 19, 90–106.

Espinasse, B., Hunt, B. P., Batten, S. D., and Pakhomov, E. A. (2020). Defining isoscapes in the Northeast Pacific as an index of ocean productivity. *Glob. Ecol. Biogeogr.* 29, 246–261. doi: 10.1111/geb.13022

Ferretti, F., Myers, R. A., Serena, F., and Lotze, H. K. (2008). Loss of large predatory sharks from the Mediterranean Sea. *Conserv. Biol.* 22, 952–964. doi: 10.1111/j.1523-1739.2008.00938.x

Francis, M. P., Griggs, L. H., and Baird, S. J. (2001). Pelagic shark bycatch in the New Zealand tuna longline fishery. *Mar. Freshw. Res.* 52, 165–178. doi: 10.1071/mf00086

Fujinami, Y., Nakatsuka, S., and Ohshimo, S. (2018). Feeding habits of the blue shark (*Prionace glauca*) in the Northwestern Pacific based on stomach contents and stable isotope ratios. *Pacif. Sci.* 72, 21–39. doi: 10.2984/72.1.2

Fujinami, Y., Shiozaki, K., Hiraoka, Y., Semba, Y., Ohshimo, S., and Kai, M. (2021). Seasonal migrations of pregnant blue sharks *Prionace glauca* in the northwestern Pacific. *Mar. Ecol. Prog. Ser.* 658, 163–179. doi: 10.3354/meps13557

Gould, P., Ostrom, P., and Walker, W. (1997). Trophic relationships of albatrosses associated with squid and large-mesh drift-net fisheries in the North Pacific Ocean. *Can. J. Zool.* 75, 549–562. doi: 10.1139/z97-068

Graham, B. S., Koch, P. L., Newsome, S. D., McMahon, K. W., and Aurioles, D. (2010). "Using isoscapes to trace the movements and foraging behavior of top predators in oceanic ecosystems," in *Isoscapes*, eds J. B. West, G. J. Bowen, T. E. Dawson, and K. P. Tu (Netherlands: Springer), 299–318. doi: 10.1007/978-90-481-3354-3_14

Heady, W. N., and Moore, J. W. (2013). Tissue turnover and stable isotope clocks to quantify resource shifts in anadromous rainbow trout. *Oecologia* 172, 21–34. doi: 10.1007/s00442-012-2483-9

Hernández-Aguilar, S. B., Escobar-Sánchez, O., Galván-Magaña, F., and Abitia-Cárdenas, L. A. (2015). Trophic ecology of the blue shark (*Prionace glauca*) based on stable isotopes (δ^{13}C and δ^{15}N) and stomach content. *J. Mar. Biol. Assoc.U. K.* 96:1403. doi: 10.1017/S002531541500139

Hobson, K. A., Barnett-Johnson, R., and Cerling, T. (2010). "Using isoscapes to track animal migration," in *Isoscapes: Understanding Movement, Pattern, and Process on Earth Through Isotope Mapping*, eds B. J. West, J. G. Bowen, E. T. Dawson, and P. K. Tu (Dordrecht: Springer), 273–298. doi: 10.1007/978-90-481-3354-3_13

Howey, L. A., Wetherbee, B. M., Tolentino, E. R., and Shivji, M. S. (2017). Biogeophysical and physiological processes drive movement patterns in a marine predator. *Mov. Ecol.* 5:16.

Hussey, N. E., Brush, J. I, McCarthy, D., and Fisk, A. T. (2010). δ^{15}N and δ^{13}C diet-tissue discrimination factors for large sharks under semi-controlled conditions. *Comparat. Biochem. Physiol. Part A Mol. Integrat. Physiol.* 155, 445–453. doi: 10.1016/j.cbpa.2009.09.023

Hussey, N. E., MacNeil, M. A., McMeans, B. C., Olin, J. A., Dudley, S. F. J., Cliff, G., et al. (2014). Rescaling the trophic structure of marine food webs. *Ecol. Lett.* 17, 239–250.

Hussey, N. E., MacNeil, M. A., Olin, J. A., McMeans, B. C., Kinney, M. J., Chapman, D. D., et al. (2012). Stable isotopes and elasmobranchs: tissue types, methods, applications and assumptions. *J. Fish Biol.* 80, 1449–1484. doi: 10.1111/j.1095-8649.2012.03251.x

ICCAT (2015). *Report of the 2015 ICCAT Blue Shark Stock Assessment Session*. Madrid: ICCAT.

ISC (2017). "Stock assessment and future projections of blue shark in the North Pacific Ocean through 2015," in *Proceedings of the 17th Meeting of the International Scientific committee on Tuna and Tuna-like Species in the North Pacific Ocean (ISC)*, Vancouver.

Jackson, A. L., Inger, R., Parnell, A. C., and Bearhop, S. (2011). Comparing isotopic niche widths among and within communities: SIBER-stable isotope Bayesian Ellipses in R. *J. Anim. Ecol.* 80, 595–602. doi: 10.1111/j.1365-2656.2011.01806.x

Kim, S. L., Casper, D. R., Galván-Magaña, F., Ochoa-Díaz, R., Hernández-Aguilar, S. B., and Koch, P. L. (2012). Carbon and nitrogen discrimination factors for elasmobranch soft tissues based on a long-term controlled feeding study. *Environ. Biol. Fish.* 95, 37–52. doi: 10.1007/s10641-011-9919-7

King, J., Wetklo, M., Supernault, J., Taguchi, M., Yokawa, K., Sosa-Nishizaki, O., et al. (2015). Genetic analysis of stock structure of blue shark (*Prionace glauca*) in the north Pacific ocean. *Fish. Res.* 172, 181–189. doi: 10.1016/j.fishres.2015.06.029

Kiszka, J., Aubail, A., Hussey, N., Heithaus, M., Caurant, F., and Bustamante, P. (2015). Plasticity of trophic interactions among sharks from the oceanic south-western Indian Ocean revealed by stable isotope and mercury analyses. *Deep Sea Res. Part I Oceanogr. Res. Pap.* 96, 49–58. doi: 10.1016/j.dsr.2014.11.006

Klecka, W. R. (1980). *Discriminant Analysis*. Newbury Park, CA: Sage Publications, Inc.

Kubodera, T., Watanabe, H., and Ichii, T. (2007). Feeding habits of the blue shark, *Prionace glauca*, and salmon shark, Lamna ditropis, in the transition region of the Western North Pacific. *Rev. Fish Biol. Fish.* 17:111. doi: 10.1007/s11160-006-9020-z

Li, Y., Gong, Y., Chen, X., Dai, X., and Zhu, J. (2014). Trophic ecology of sharks in the mid-east Pacific ocean inferred from stable isotopes. *J. Ocean Univ. China* 13, 278–282. doi: 10.1007/s11802-014-2071-1

Li, Y., Zhang, Y., Hussey, N. E., and Dai, X. (2016). Urea and lipid extraction treatment effects on δ^{15}N and δ^{13}C values in pelagic sharks. *Rapid Commun. Mass Spectrom.* 30, 1–8. doi: 10.1002/rcm.7396

Logan, J., and Lutcavage, M. (2010). Stable isotope dynamics in elasmobranch fishes. *Hydrobiologia* 644, 231–244. doi: 10.1007/s10750-010-0120-3

MacKenzie, K. M., Trueman, C. N., Palmer, M. R., Moore, A., Ibbotson, A. T., Beaumont, W. R., et al. (2012). Stable isotopes reveal age-dependent trophic level and spatial segregation during adult marine feeding in populations of salmon. *ICES J. Mar. Sci.* 69, 1637–1645. doi: 10.1093/icesjms/fss074

Madigan, D. J. (2015). "Understanding bluefin migration using intrinsic tracers in tissues," in *Biology and Ecology of Bluefin Tuna*, eds T. Kitagawa and S. Kimura (Boca Raton, FL: CRC Press), 211–224.

Madigan, D. J., Baumann, Z., Carlisle, A. B., Hoen, D. K., Popp, B. N., Dewar, H., et al. (2014). Reconstructing trans-oceanic migration patterns of Pacific bluefin tuna using a chemical tracer toolbox. *Ecology* 95, 1674–1683. doi: 10.1890/13-1467.1

Madigan, D. J., Baumann, Z., Carlisle, A. B., Snodgrass, O., Dewar, H., and Fisher, N. S. (2017). Isotopic insights into migration patterns of Pacific bluefin tuna in the eastern Pacific Ocean. *Can. J. Fish. Aquat. Sci.* 75, 260–270. doi: 10.1139/cjfas-2016-0504

Madigan, D. J., Brooks, E. J., Bond, M. E., Gelsleichter, J., Howey, L. A., Abercrombie, D. L., et al. (2015). Diet shift and site-fidelity of oceanic whitetip sharks *Carcharhinus longimanus* along the Great Bahama Bank. *Mar. Ecol. Prog. Ser.* 529, 185–197. doi: 10.3354/meps11302

Madigan, D. J., Carlisle, A. B., Dewar, H., Snodgrass, O. E., Litvin, S. Y., Micheli, F., et al. (2012a). Stable isotope analysis challenges wasp-waist food web assumptions in an upwelling pelagic food web. *Sci. Rep.* 2:e654.

Madigan, D. J., Litvin, S. Y., Popp, B. N., Carlisle, A. B., Farwell, C. J., and Block, B. A. (2012b). Tissue turnover rates and isotopic trophic discrimination factors in the endothermic teleost, Pacific bluefin tuna (*Thunnus orientalis*). *PLoS One* 7:e49220. doi: 10.1371/journal.pone.0049220

Madigan, D. J., Chiang, W.-C., Wallsgrove, N. J., Popp, B. N., Kitagawa, T., Choy, C. A., et al. (2016). Intrinsic tracers reveal recent foraging ecology of giant Pacific bluefin tuna at their primary spawning grounds. *Mar. Ecol. Prog. Ser.* 553, 253–266. doi: 10.3354/meps11782

Madigan, D. J., Shipley, O. N., and Hussey, N. E. (2021). "Applying isotopic clocks to identify prior migration patterns and critical habitats in mobile marine predators," in *Conservation Physiology: Applications for Wildlife Conservation and Management*, eds C. L. Madliger, C. E. Franklin, O. P. Love, and S. J. Cooke (Oxford: Oxford University Press), 69–85. doi: 10.1093/oso/9780198843610.003.0005

Madigan, D. J., Snodgrass, O. E., and Fisher, N. S. (2018). From migrants to mossbacks: tracer- and tag-inferred habitat shifts in the California yellowtail *Seriola dorsalis*. *Mar. Ecol. Prog. Ser.* 597, 221–230. doi: 10.3354/meps12593

Magozzi, S., Yool, A., Vander Zanden, H., Wunder, M., and Trueman, C. (2017). Using ocean models to predict spatial and temporal variation in marine carbon isotopes. *Ecosphere* 8:e01763. doi: 10.1002/ecs2.1763

Matsubayashi, J., Osada, Y., Tadokoro, K., Abe, Y., Yamaguchi, A., Shirai, K., et al. (2020). Tracking long-distance migration of marine fishes using compound-specific stable isotope analysis of amino acids. *Ecol. Lett.* 23, 881–890. doi: 10.1111/ele.13496

Maxwell, S. M., Scales, K. L., Bograd, S. J., Briscoe, D. K., Dewar, H., Hazen, E. L., et al. (2019). Seasonal spatial segregation in blue sharks (*Prionace glauca*) by sex and size class in the Northeast Pacific Ocean. *Diver. Distribut.* 25, 1304–1317.

McKinnell, S., and Seki, M. P. (1998). Shark bycatch in the Japanese high seas squid driftnet fishery in the North Pacific Ocean. *Fish. Res.* 39, 127–138. doi: 10.1016/s0165-7836(98)00179-9

McMahon, K. W., Fogel, M. L., Elsdon, T. S., and Thorrold, S. R. (2010). Carbon isotope fractionation of amino acids in fish muscle reflects biosynthesis and isotopic routing from dietary protein. *J. Anim. Ecol.* 79, 1132–1141. doi: 10.1111/j.1365-2656.2010.01722.x

McMahon, K. W., Hamady, L. L., and Thorrold, S. R. (2013). A review of ecogeochemistry approaches to estimating movements of marine animals. *Limnol. Oceanogr.* 58, 697–714. doi: 10.4319/lo.2013.58.2.0697

Miller, T. W. (2006). *Trophic Dynamics of Marine Nekton and Zooplankton in the Northern California Current Pelagic Ecosystem*. Corvallis: Oregon State University.

Miller, T. W., Bosley, K. L., Shibata, J., Brodeur, R. D., Omori, K., and Emmett, R. (2013). Contribution of prey to Humboldt squid Dosidicus gigas in the northern California Current, revealed by stable isotope analyses. *Mar. Ecol. Prog. Ser.* 477, 123–134. doi: 10.3354/meps10133

Miller, T. W., Brodeur, R. D., Rau, G., and Omori, K. (2010). Prey dominance shapes trophic structure of the northern California Current pelagic food web: evidence from stable isotopes and diet analysis. *Mar. Ecol. Prog. Ser.* 420, 15–26. doi: 10.3354/meps08876

Montoya, J. P. (2007). "Natural abundance of ^{15}N in marine planktonic ecosystems," in *Stable Isotopes in Ecology and Environmental Science*, eds R. Michener and K. Lajtha (Boston, FL: Blackwell), 176–201. doi: 10.1002/9780470691854.ch7

Moore, J. W., Gordon, J., Carr-Harris, C., Gottesfeld, A. S., Wilson, S. M., and Russell, J. H. (2016). Assessing estuaries as stopover habitats for juvenile Pacific salmon. *Mar. Ecol. Prog. Ser.* 559, 201–215. doi: 10.3354/meps11933

Musyl, M. K., Brill, R. W., Curran, D. S., Fragoso, N. M., McNaughton, L. M., Nielsen, A., et al. (2011). Postrelease survival, vertical and horizontal movements, and thermal habitats of five species of pelagic sharks in the central Pacific Ocean. *Fish. Bull.* 109, 341–368.

Nakano, H. (1994). Age, reproduction and migration of blue shark in the North Pacific Ocean. *Bull. Natl. Res. Insti. Far Seas Fish.* 31, 141–256.

Nakano, H., and Stevens, J. D. (2008). "The biology and ecology of the blue shark, *Prionace glauca*," in *Sharks of the Open Ocean: Biology, Fisheries and Conservation*, eds M. D. Canhi, E. K. Pikitch, and E. A. Babcock (Hoboken, NJ: Wiley Online Library), 140–151. doi: 10.1002/9781444302516.ch12

Ohshimo, S., Madigan, D. J., Kodama, T., Tanaka, H., Komoto, K., Suyama, S., et al. (2019). Isoscapes reveal patterns of δ^{13}C and δ^{15}N of pelagic forage fish and squid in the Northwest Pacific Ocean. *Prog. Oceanogr.* 175, 124–138. doi: 10.1016/j.pocean.2019.04.003

Ohshimo, S., Tanaka, H., Nishiuchi, K., and Yasuda, T. (2016). Trophic positions and predator-prey mass ratio of the pelagic food web in the East China Sea and Sea of Japan. *Mar. Freshw. Res.* 67, 1692–1699. doi: 10.1071/mf15115

Parnell, A. (2020). *simmr: A Stable Isotope Mixing Model. R Package*.

Pearcy, W. G. (1991). Biology of the transition region. *NOAA Techn. Rep. NMFS* 105, 39–55.

Phillips, D. L., Inger, R., Bearhop, S., Jackson, A. L., Moore, J. W., Parnell, A. C., et al. (2014). Best practices for use of stable isotope mixing models in food-web studies. *Can. J. Zool.* 92, 823–835. doi: 10.1139/cjz-2014-0127

Polovina, J. J., Howell, E., Kobayashi, D. R., and Seki, M. P. (2001). The transition zone chlorophyll front, a dynamic global feature defining migration and forage habitat for marine resources. *Prog. Oceanogr.* 49, 469–483. doi: 10.1016/s0079-6611(01)00036-2

Post, D. M. (2002). Using stable isotopes to estimate trophic position: models, methods, and assumptions. *Ecology* 83, 703–718. doi: 10.1890/0012-9658(2002)083[0703:usitet]2.0.co;2

Preti, A., Soykan, C., Dewar, H., Wells, R., Spear, N., and Kohin, S. (2012). Comparative feeding ecology of shortfin mako, blue and thresher sharks in the California Current. *Environ. Biol. Fish.* 95, 127–146. doi: 10.1007/s10641-012-9980-x

Queiroz, N., Humphries, N. E., Couto, A., Vedor, M., Costa, I. Da, Sequeira, A. M., et al. (2019). Global spatial risk assessment of sharks under the footprint of fisheries. *Nature* 572, 461–466.

Queiroz, N., Humphries, N. E., Mucientes, G., Hammerschlag, N., Lima, F. P., Scales, K. L., et al. (2016). Ocean-wide tracking of pelagic sharks reveals extent of overlap with longline fishing hotspots. *Proc. Natl. Acad. Sci. U.S.A.* 113, 1582–1587. doi: 10.1073/pnas.1510090113

Rabehagasoa, N., Lorrain, A., Bach, P., Potier, M., Jaquemet, S., Richard, P., et al. (2012). Isotopic niches of the blue shark *Prionace glauca* and the silky shark *Carcharhinus falciformis* in the southwestern Indian Ocean. *Endang. Spec. Res.* 17, 83–92. doi: 10.3354/esr00418

Sequeira, A., Heupel, M., Lea, M. A., Eguíluz, V. M., Duarte, C. M., Meekan, M., et al. (2019). The importance of sample size in marine megafauna tagging studies. *Ecol. Appl.* 29:e01947.

Shipley, O. N., and Matich, P. (2020). Studying animal niches using bulk stable isotope ratios: an updated synthesis. *Oecologia* 193, 27–51. doi: 10.1007/s00442-020-04654-4

Shipley, O. N., Newton, A. H., Frisk, M. G., Henkes, G. A., Walters, H., LaBelle, J., et al. (2021). Telemetry validated nitrogen stable isotope clocks identify ocean-to-estuarine habitat shifts in mobile organisms. *Methods Ecol. Evol.* 12, 897–908. doi: 10.1111/2041-210X.13567

Sippel, T., Wraith, J., Kohin, S., Taylor, V., Holdsworth, J., Taguchi, M., et al. (2011). "A summary of blue shark (*Prionace glauca*) and shortfin mako shark (*Isurus oxyrinchus*) tagging data available from the North and Southwest Pacific Ocean," in *Proceedings of the California: Working Document Submitted to the ISCShark Working Group Workshop*, La Jolla, CA.

Siskey, M. R., Shipley, O. N., and Frisk, M. G. (2019). Skating on thin ice: Identifying the need for species-specific data and defined migration ecology of *Rajidae* spp. *Fish Fish.* 20, 286–302. doi: 10.1111/faf.12340

Smith, J. A., Mazumder, D., Suthers, I. M., and Taylor, M. D. (2013). To fit or not to fit: evaluating stable isotope mixing models using simulated mixing polygons. *Methods Ecol. Evol.* 4, 612–618. doi: 10.1111/2041-210x.12048

Swanson, H. K., Lysy, M., Power, M., Stasko, A. D., Johnson, J. D., and Reist, J. D. (2015). A new probabilistic method for quantifying n-dimensional ecological niches and niche overlap. *Ecology* 96, 318–324. doi: 10.1890/14-0235.1

Taguchi, M., King, J. R., Wetklo, M., Withler, R. E., and Yokawa, K. (2015). Population genetic structure and demographic history of Pacific blue sharks (*Prionace glauca*) inferred from mitochondrial DNA analysis. *Mar. Freshw. Res.* 66, 267–275. doi: 10.1071/mf14075

Takai, N., Hirose, N., Osawa, T., Hagiwara, K., Kojima, T., Okazaki, Y., et al. (2007). Carbon source and trophic position of pelagic fish in coastal waters of south-eastern Izu Peninsula, Japan, identified by stable isotope analysis. *Fish. Sci.* 73, 593–608. doi: 10.1111/j.1444-2906.2007.01372.x

Tamburin, E., Kim, S. L., Elorriaga-Verplancken, F. R., Madigan, D. J., Hoyos-Padilla, M., ánchez-González, A. S., et al. (2019). Isotopic niche and resource sharing among young sharks (*Carcharodon carcharias* and *Isurus oxyrinchus*) in Baja California, Mexico. *Mar. Ecol. Prog. Ser.* 613, 107–124. doi: 10.3354/meps12884

Tawa, A., Ishihara, T., Uematsu, Y., Ono, T., and Ohshimo, S. (2017). Evidence of westward transoceanic migration of Pacific bluefin tuna in the Sea of Japan based on stable isotope analysis. *Mar. Biol.* 4:94.

Thomas, S. M., and Crowther, T. W. (2015). Predicting rates of isotopic turnover across the animal kingdom: a synthesis of existing data. *J. Anim. Ecol.* 84, 861–870. doi: 10.1111/1365-2656.12326

Trueman, C. N., and Glew, K. S. J. (2019). "Isotopic tracking of marine animal movement," in *Tracking animal Migration with Stable Isotopes*, eds C. N. Trueman and K. S. J. Glew (Amsterdam: Elsevier), 137–172. doi: 10.1016/b978-0-12-814723-8.00006-4

Trueman, C. N., Jackson, A. L., Chadwick, K. S., Coombs, E. J., Feyrer, L. J., Magozzi, S., et al. (2019). Combining simulation modeling and stable isotope analyses to reconstruct the last known movements of one of Nature's giants. *PeerJ* 7:e7912. doi: 10.7717/peerj.7912

Vander Zanden, M. J., Clayton, M. K., Moody, E. K., Solomon, C. T., and Weidel, B. C. (2015). Stable isotope turnover and half-life in animal tissues: a literature synthesis. *PLoS One* 10:e0116182. doi: 10.1371/journal.pone.0116182

Veríssimo, A. Í, Sampaio, J. R., Alexandrino, M. P., Mucientes, G., Queiroz, N., da Silva, C., et al. (2017). World without borders—genetic population structure of a highly migratory marine predator, the blue shark (*Prionace glauca*). *Ecol. Evol.* 7, 4768–4781. doi: 10.1002/ece3.2987

Vögler, R., Beier, E., Ortega-García, S., Santana-Hernández, H., and Valdez-Flores, J. J. (2012). Ecological patterns, distribution and population structure of *Prionace glauca* (Chondrichthyes: Carcharhinidae) in the tropical-subtropical transition zone of the north-eastern Pacific. *Mar. Environ. Res.* 73, 37–52.

Waples, R. S., and Gaggiotti, O. (2006). INVITED REVIEW: what is a population? An empirical evaluation of some genetic methods for identifying the number of gene pools and their degree of connectivity. *Mol. Ecol.* 15, 1419–1439. doi: 10.1111/j.1365-294x.2006.02890.x

Wolf, N., Carleton, S. A., and del Rio, C. M. (2009). Ten years of experimental animal isotopic ecology. *Funct. Ecol.* 23, 17–26. doi: 10.1111/j.1365-2435.2009.01529.x

Conflict of Interest: The authors declare that the research was conducted in the absence of any commercial or financial relationships that could be construed as a potential conflict of interest.

frontiers
in Marine Science

ORIGINAL RESEARCH
published: 06 July 2021
doi: 10.3389/fmars.2021.682730

First Insights Into the Horizontal Movements of Whale Sharks (*Rhincodon typus*) in the Northern Arabian Sea

Lucy M. Arrowsmith[1*†], **Charan Kumar Paidi**[2†], **Farukhkha Husenkha Bloch**[2†], **Sajan John**[2†], **Binod Chandra Choudhury**[2†], **Rahul Kaul**[2†], **Ana M. M. Sequeira**[3†], **Charitha B. Pattiaratchi**[1†] and **Mark G. Meekan**[4†]

[1] Oceans Graduate School, The UWA Oceans Institute, The University of Western Australia, Crawley, WA, Australia, [2] Wildlife Trust of India, Noida, India, [3] School of Biological Sciences, The UWA Oceans Institute, The University of Western Australia, Crawley, WA, Australia, [4] Australian Institute of Marine Science, Indian Ocean Marine Research Centre, The University of Western Australia, Crawley, WA, Australia

Edited by:
Nuno Queiroz,
Centro de Investigacao em Biodiversidade e Recursos Geneticos (CIBIO-InBIO), Portugal

Reviewed by:
Marisa Vedor,
Centro de Investigacao em Biodiversidade e Recursos Geneticos (CIBIO-InBIO), Portugal
Ornella Céline Weideli,
Labormedizinische Zentrum Dr. Risch, Liechtenstein
Ginevra Boldrocchi,
University of Insubria, Italy

***Correspondence:**
Lucy M. Arrowsmith
lucy.arrowsmith@research.uwa.edu.au

†ORCID:
Lucy M. Arrowsmith
orcid.org/0000-0003-4558-6650
Charan Kumar Paidi
orcid.org/0000-0001-8608-5022
Farukhkha Husenkha Bloch
orcid.org/0000-0002-5062-6605
Sajan John
orcid.org/0000-0001-8885-6222
Binod Chandra Choudhury
orcid.org/0000-0001-5959-1261
Rahul Kaul
orcid.org/0000-0001-9930-7309
Ana M. M. Sequeira
orcid.org/0000-0001-6906-799X
Charitha B. Pattiaratchi
orcid.org/0000-0003-2229-6183
Mark G. Meekan
orcid.org/0000-0002-3067-9427

Specialty section:
This article was submitted to Marine Megafauna, a section of the journal Frontiers in Marine Science

Received: 19 March 2021
Accepted: 10 June 2021
Published: 06 July 2021

Whale sharks off the western coast of India have suffered high levels of fishing pressure in the past, and today continue to be caught in small-scale fisheries as by-catch. Additionally, coastlines in this region host very large and growing human populations that are undergoing rapid development. This exacerbates ongoing anthropogenic threats to this species such as pollution, habitat loss, and ship traffic. For these reasons, there is an urgent need for data on movement patterns of whale sharks in this region of the Indian Ocean. Here, we address this issue by providing the first data on the horizontal movements of whale sharks tagged in the northern Arabian Sea off the western coast of the Indian state of Gujarat. From 2011 to 2017, eight individuals, ranging from 5.4 to 8 m were tagged and monitored using satellite telemetry. Tag retention varied from 1 to 137 days, with the sharks traveling distances of 34 – ∼2,230 km. Six of the eight individuals remained close to their tagging locations, although two sharks displayed wide ranging movements into the Arabian Sea, following frontal zones between water masses of different sea surface temperatures. We explore the relationship between the movement patterns of these whale sharks and the physical and biological processes of the region.

Keywords: satellite tags, migration, movement ecology, tagging, oceanography

INTRODUCTION

The whale shark (*Rhincodon typus*, Smith 1828) is found in shallow and open ocean locations throughout the world's tropical and subtropical environments, with known aggregations occurring from the Gulf of Mexico (Hueter et al., 2013) to Ningaloo Reef, Western Australia (Norman et al., 2016). Although there are predictable coastal occurrences of these sharks, they often transit large (1000s km) distances, spending most of their time in surface waters (<20 m depth), with regular dives to depths of 300–500 m (Brunnschweiler et al., 2009). Advances in satellite telemetry techniques have expanded our knowledge of the migratory movements of the species and assisted in identifying key drivers of these complex movements. Of these drivers, water temperatures

(Sequeira et al., 2012; Meekan et al., 2015), frontal systems (Ryan et al., 2017), bathymetry and continental reef slopes (Copping et al., 2018), have been predicted to have the highest influence on the spatial use patterns of this species by contributing to enhanced primary productivity (Sleeman et al., 2010a).

The migratory behavior of whale sharks, in combination with their slow growth rates (Meekan et al., 2020) and K-selected life history, make populations highly vulnerable to anthropogenic pressures, such as ship strikes (Speed et al., 2008; Lester et al., 2020), bycatch and targeted fishing (Capietto et al., 2014) and pollution (Boldrocchi et al., 2020). These threats are of particular concern as the species is classified as "Endangered" on the IUCN Red List (Pearce and Norman, 2016). Ultimately, this has motivated satellite tagging programs that seek to identify movement patterns and assist in identifying areas of potential threats to the species (Reynolds et al., 2017; Robinson et al., 2017; Araujo et al., 2018; Rohner et al., 2020) in order to target effective conservation planning (Sequeira et al., 2019).

Several programs have deployed tags on sharks at various aggregation sites in the Indian Ocean, including Ningaloo, Madagascar, Mozambique and Seychelles (**Supplementary Table 1**). Despite this sampling effort, there have been no tagging studies of populations of whale sharks along the Indian coast in the northern Arabian Sea. This is important because the western coast of India has been predicted to be a location where a high probability of whale sharks occur (Sequeira et al., 2014) and a key aggregation site (Pravin, 2000; Bloch et al., 2018). Prior to 2001, whale sharks in the Arabian Sea were the subject of a targeted fishery that hunted these animals for their fins, skin and meat (Kumari and Raman, 2010). This fishery largely ceased operation after May 2001 following the inclusion of whale sharks into the Schedule I of the Indian Wildlife (Protection) Act, 1972. However, accidental entanglements during fishing and unintentional landings are common along the Indian coastline (Akhilesh et al., 2013; Retheesh et al., 2020) and whale sharks in this region may also face pressures from increased levels of pollution in nearby waters (Jabado et al., 2018). Data on the movement patterns of whale sharks along this coastline is now required to understand patterns of residency, identify the range of the population for conservation planning and document and aid any population recovery.

Here, we report the results of a satellite tagging study of whale sharks in the northern Arabian Sea along the coast of Gujarat, India. We describe horizontal patterns of movement of these animals in relation to remote sensing data of water temperature and sea surface colour (Chl-*a*) to identify key drivers of this species' movement patterns in this region.

MATERIALS AND METHODS

Whale sharks caught as by-catch in purse seine fishing nets were tagged in the northern Arabian Sea off the fishing town of Veraval (**Figure 1a**) from April 2011 to November 2017 using Smart Positioning Tags (SPOT tags; Wildlife Computers). Shark size was estimated using a tape measure and sex was determined based on the presence or absence of claspers (Norman and Stevens, 2007). Eight satellite tags were deployed, with two being fin-mounted (WS-1 and WS-2) and six tags tethered to the dorsal fins of sharks (WS-3–WS-8). Transmitted locations of each of the eight sharks tagged were obtained through the ARGOS satellite tracking system. To maximize battery life, tags transmitted every day for the first week and then every second day after that. Tags only transmit when the tag clears the surface long enough to locate and transmit to an ARGOS satellite. The transmitted positions were determined by Doppler-estimated calculations and assigned quality numbers or letters depending on associated errors (3, 2, 1, 0, A, B, and Z), which range inaccuracy from <250 m to >5 km. Locations with "Z" classes are considered unreliable (Argos, 2011), and they were removed from the datasets before analysis.

We analyzed the tracks in R (R Core Team, 2013) to produce histograms of the quality of transmissions of each day. We removed duplicated messages and applied a 2 ms^{-1} speed filter to remove inaccurate locations based on the maximum speeds of whale sharks (Rowat and Gore, 2007; Rohner et al., 2018). Once filtered, tracks with alternating days missing satellite positions were interpolated to give estimated locations. When points in the tracks had greater gaps, they were fitted with a state-space model with the "*bsam*" package (Jonsen et al., 2005) in R to model the movement process. To determine if some of the tags detached before they ceased reporting, we analyzed the timing between points, the quality of the message and oceanographic data. We then assumed tags had detached from sharks when the following characteristics were observed: (i) speed increased to average current flows, (ii) direction of travel followed current patterns, and (iii) contact with satellites became regular and predictable (Hearn et al., 2013).

We obtained sea surface temperature (SST) data from the HYCOM + NCODA Global $1/12^0$ analysis and the reanalysis database (Chassignet et al., 2007). Using MATLAB (2010), we extracted daily water temperature, salinity, surface elevation and water velocity data in the vicinity of each track. The daily SST were averaged to produce a single SST plot overlaid on the satellite track. We did not include the longest track (WS-7) in this part of the analysis, as the fine-scale resolution of the oceanographic features might have been lost, instead, we analyzed each daily plot for this track. The SST plots were visually examined to identify links between movements and features of physical (fronts etc.) or biological (phytoplankton etc.) oceanography. The daily SST plots were also used to produce animated movies showing the changes in water temperature in relation to the track for all sharks (see **Supplementary Materials**). Daily chlorophyll-*a* (Chl-*a*) concentrations were derived from the MODIS-Aqua, a product of the NASA satellite system[1] at a 4.6 km resolution through ArcGIS (ESRI, 2011). Records for day and night were merged into a 24-h time series of the average concentration of Chl-*a* and overlaid over each track. Bathymetry data were obtained from the 2015 General Bathymetric Charts of the Oceans (GEBCO, 2015), at a resolution of 30 arc-s interval grids and analyzed in ArcGIS.

---

[1] http://oceancolor.gsfc.nasa.gov

RESULTS

Of the eight sharks tagged with SPOT tags from 2011 to 2017, the seven tags that transmitted locations (WS-1–WS-7; **Table 1**) are reported here. Two tags started transmitting the day of tagging, with the rest transmitting 1–8 days after tagging. Tags remained on the sharks from 6 to 137 days, however, transmissions from two tags (WS-6 and WS-7) continued for several months after detachment. Sharks traveled a mean distance of 29.45 km day^{-1} (0.34 ms^{-1}; 1.46–60 km day^{-1} = 0.02–0.69 ms^{-1}), covering distances of 33–2,229 km (**Figure 1a**). Five of the sharks tagged were females, whereas the remaining two were immature males (**Table 1**). The smallest shark tagged was a 5.8 m female and the largest an 8 m female.

Six sharks had tag retentions of ≤40 days, and of these, five (WS-1–WS-5) mostly stayed on the continental shelf off the coast of Gujarat and Maharashtra (**Figure 1a**). WS-1 was tagged in the coastal waters off Veraval and traveled 2,136 km over 40 days, initially moving approximately 270 km south, then traveling north-east, coming within 40 km of the Maharashtra coastline, before heading back toward Gujarat. The tag attached to WS-2 transmitted for only six days during which time the shark covered a distance of 147 km. WS-3 was tagged off the northern coastline of Gujarat and over 15 days while the tag was attached moved north traveling ∼490 km to the Indus Canyon. WS-4 traveled 34 km in the 23 days of tag transmissions, remaining close to the Gujarat coast. WS-5 remained in close proximity (<20 km) to the coastline, moving 468 km before the tag stopped transmitting after 26 days. In contrast to the other sharks, WS-6 moved south into the Arabian Sea toward the latitudes of the Lakshadweep Islands approximately 370 km from the coast until the tag detached on the 2nd February 2017 (**Figure 1b**).

A 6.8 m female (WS-7) provided the longest track, traveling 2,229 km over 137 days (**Figure 1c**). This shark was tagged off the coast of Veraval and moved east, staying in shelf waters and coming within ∼20 km of the Daman and Diu coastline before heading west toward the middle of the Arabian Sea, inhabiting oceanic waters for the rest of the track. The shark stayed in SSTs ranging from 22 to 29°C while following frontal systems between water masses and cold-water eddies (**Supplementary Video 7**) until the tag probably detached on the 31st March 2018.

Sea surface temperatures through the area of the tracks ranged from 18.4 to 33.4°C, with a mean of 26.4 ± 4.77°C. The mean water temperature each shark experienced range from 27.32 to 29.91 (WS-1: 28.74 ± 1.13°C; WS-2: 27.32 ± 1.35°C; WS-3: 29.91 ± 0.55°C; WS-4: 29.37 ± 0.33°C; WS-5: 27.49 ± 1.69°C; WS-6: 27.35 ± 1.25°C; WS-7: 27.33 ± 1.28°C), with sharks spending most time within a SST range of 24–31°C (**Figures 2a–f**). Four of the seven sharks stayed close to the Gujarat coastline, where water temperatures of <27°C were observed in most years except for 2015 when temperatures were between 29 and 33°C (**Figures 2c,d**). WS-7 showed the greatest spatial extent of movements remaining in a temperature band of 24–28°C and close to frontal systems, a prominent oceanographic feature in the Arabian Sea (Madhupratap et al., 2001; **Supplementary Video 7**). Movements of the sharks remained in moderate to high levels of Chl-*a* ranging from 0.5 to 4.47 mg/m^2, with the

TABLE 1 | Whale shark tagging information equipped with SPOT tags, with track number, shark ID, sex, estimated total length [TL (m)], tagging date, first transmission, estimated pop-up date, last transmission, track duration (starting from the first transmission date to estimated pop-up date), track distance (km), and speed (km day^{-1}).

#	ID	Sex	Est. TL (m)	Start date		End date		Days	Track distance (km) (up to est. detachment)	Speed (km day^{-1})
				Tagged	First transmission	Est. detachment date	Last transmission			
WS-1	102679	M	–	13-Mar-2011	15-Mar-2011	24-Apr-2011	24-Apr-2011	40	2,136.78	53.42
WS-2	102680	F	–	27-Dec-2013	28-Dec-2013	03-Jan-2014	03-Jan-2014	06	146.86	24.48
WS-3	123179	F	5.4	09-May-2015	10-May-2015	25-May-2015	25-May-2015	15	488.20	32.55
WS-4	123182	F	6	07-Oct-2015	07-Oct-2015	30-Oct-2015	30-Oct-2015	23	33.50	1.46
WS-5	123178	F	8	23-Dec-2016	23-Dec-2016	18-Jan-2017	18-Jan-2017	26	468.11	18
WS-6	123181	F	6.3	30-Dec-2016	07-Jan-2017	02-Feb-2017	13-Dec-2017	26	1,560.25	60
WS-7	123180	M	6.8	11-Nov-2017	13-Nov-2017	30-Mar-2018	03-Oct-2018	137	2,229.09	16.27
WS-8	123177	F	8	01-Apr-2015	01-Apr-2015	02-Apr-2015	02-Apr-2015	01	Failed to report	–

Track distance was measured as the sum of straight-line distances between adjacent locations in ArcGIS.

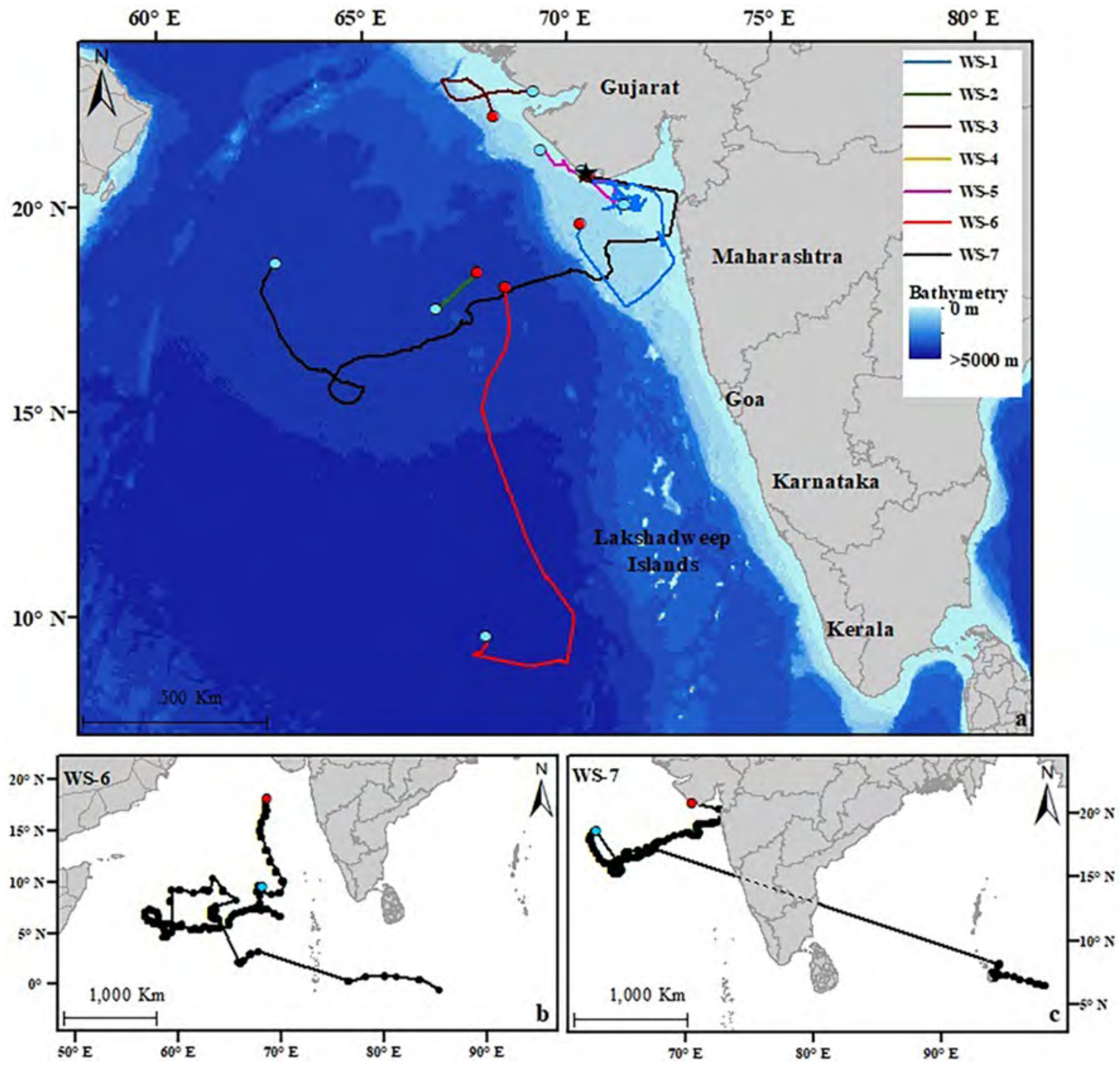

FIGURE 1 | (a) Study area for the tagged whale sharks in the Arabian Sea. The star indicates the fishing town of Veraval, the port of tagging operations. Colored tracks show the estimated track lengths of the seven whale shark tracks (WS-1–WS-7). WS-8 was excluded from analysis as the tag failed to report. Red dots show the first geolocation and the blue dots show the estimated point of detachment. **(b,c)** The full length of transmissions for WS-6 and WS-7. Red dots show the first location and the blue dots show the estimated point of detachment.

highest levels observed close to Veraval (WS-1: 1.82 ± 1.1 mg/m^2; WS-2: 1.67 ± 0.1 mg/m^2; WS-3: 1.63 ± 1.09 mg/m^2; WS-5: 1.81 ± 0.27 mg/m^2; WS-6: 1.53 ± 1.12 mg/m^2; and WS-7: 1.64 ± 1 mg/m^2). Due to the location of WS-4 being too close to the coastline, Chl-*a* data were unavailable for the geolocations of this shark (**Figures 3a–g**).

DISCUSSION

Our tagging resulted in tracks of different durations, with most lasting <40 days, however, one tag remained successfully attached to a whale shark for up to 137 days allowing a more detailed examination of the oceanographic context of their movement patterns in this region. The path of this longer track was consistent with suggestions that whale sharks tend to occupy water masses with temperatures in the range of 24–29°C and are associated with frontal zones (Sequeira et al., 2012; Ryan et al., 2017). When the tracks were relatively short, due to tag retention times, whale sharks tended to remain close to the coast where the coolest waters in the region were found, although this result may have also reflected the tagging location, especially for sharks with less than 1-week tagging duration.

Filter feeding on nekton and plankton provides access to food that is abundant and very widely distributed, but such prey is also patchy in pelagic environments. In the warm, oligotrophic tropical ocean, the need to search and locate prey requires strategies for cost-efficient foraging (Gleiss et al., 2013; Meekan et al., 2015). The focus of whale shark movements on frontal zones is consistent with cost-effective foraging behaviors

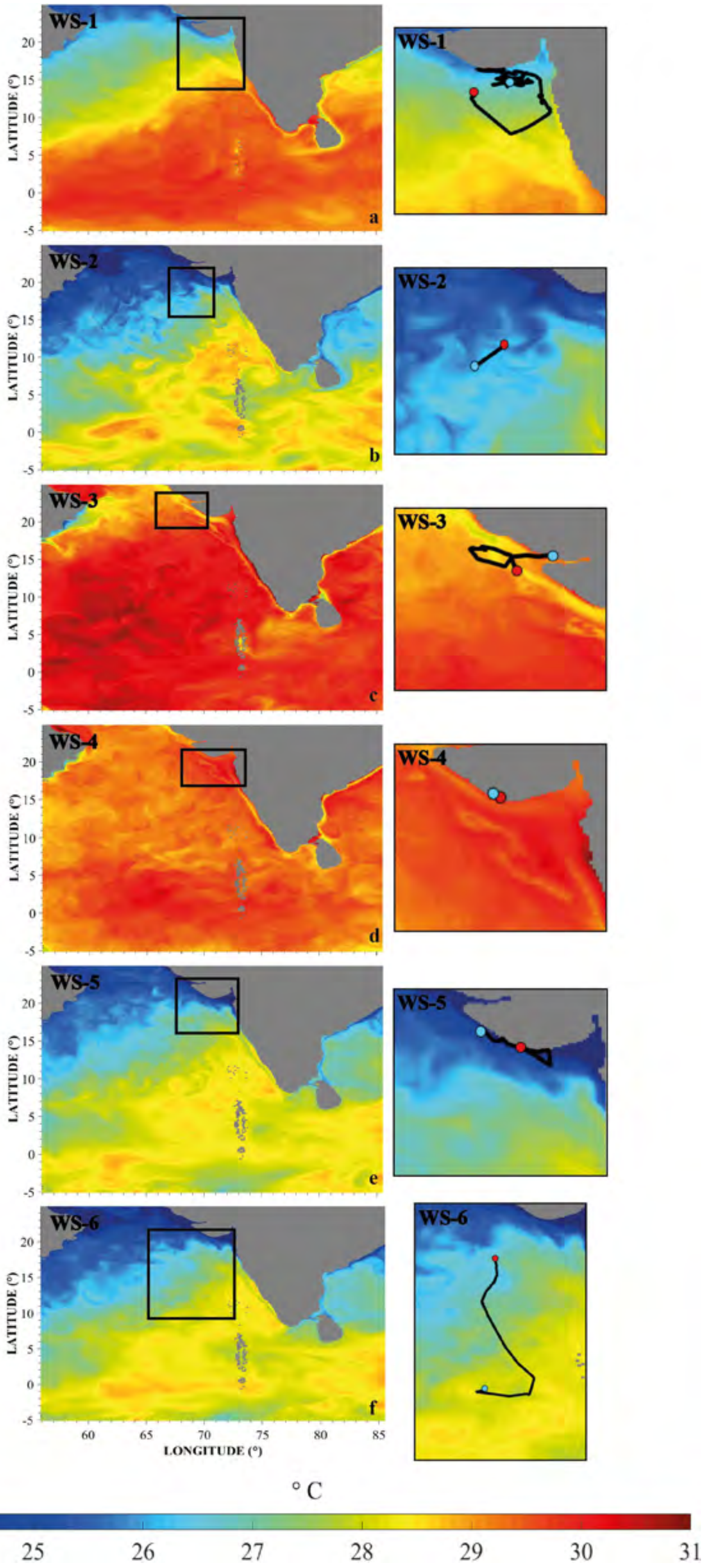

FIGURE 2 | (a–f) Daily mean sea surface temperature plots in the Arabian Sea and northeastern Indian Ocean for WS-1–WS-6. Figures on the left-hand side show the overview of the area during the tagging period of each shark. Black boxes correspond to the right-hand plots, illustrating a subsection of the area where the whale shark tracks are shown. SST range from 24 to 31°C. The SST plot for WS-7 is not included here as it was analyzed separately and can be found in the **Supplementary Materials** (**Supplementary Video 7**).

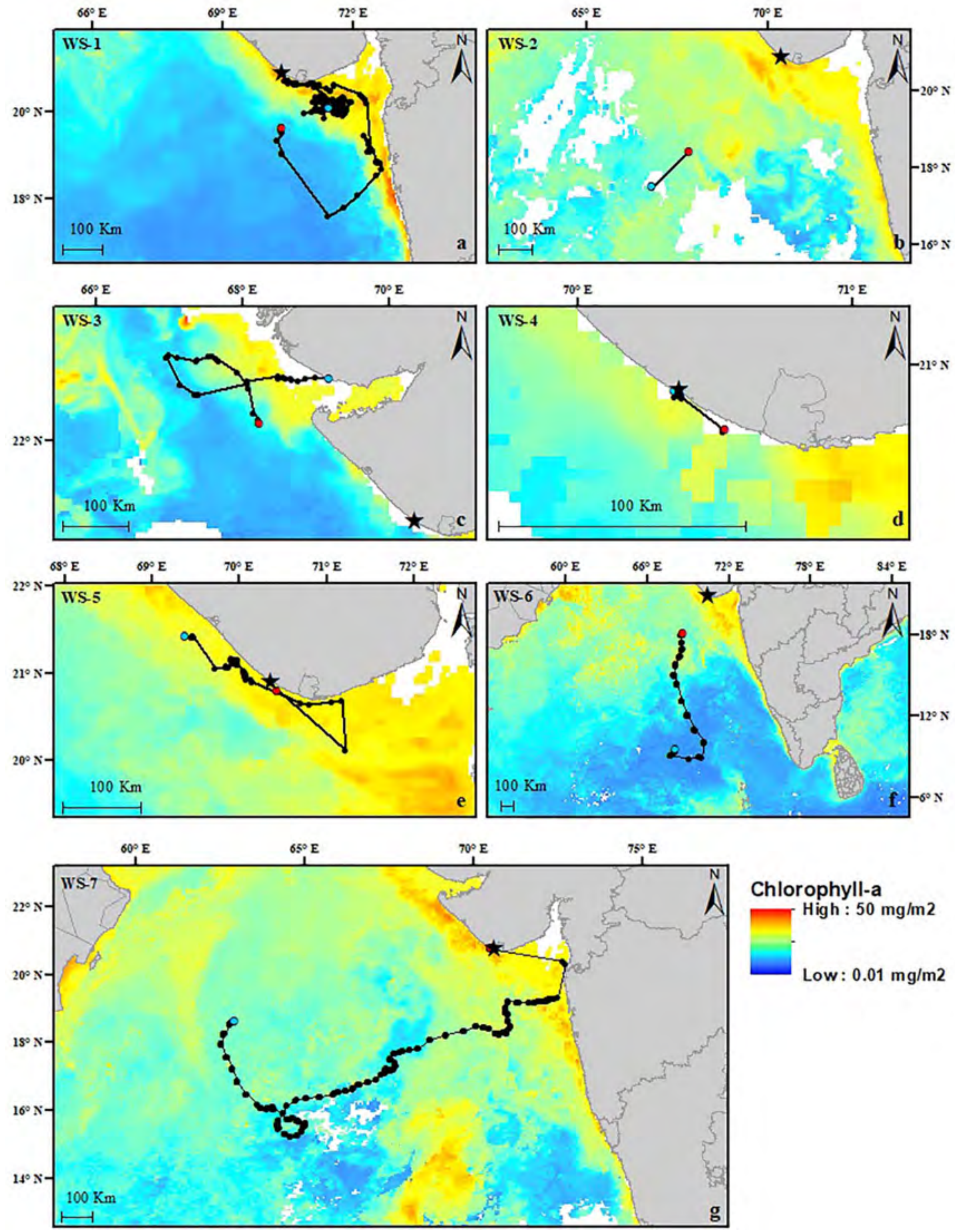

FIGURE 3 | (a–g) Daily mean chlorophyll-*a* (Chl-*a*) plots from 2011–2018 corresponding to each whale shark track, shown in black. Red dots show the first locations, and the blue dots show the last locations, either from the tag ceasing reporting locations or determined by possible tag detachment locations. The star shows the location of the fishing town of Veraval, India. Chl-*a* ranged from 0.01 to 50 mg/m^2.

since these oceanographic features in those locations lead to the accumulation of planktonic and small nektonic prey (Ramirez-Macias et al., 2017; Ryan et al., 2017). This minimizes the cost of foraging for this filter-feeder, which tends to have an energetic budget that is very finely balanced (Meekan et al., 2015), similar to basking sharks (Sims and Quayle, 1998). The association of whale sharks with frontal zones is consistent across various locations. For example, tagging studies in the Galapagos found that these sharks inhabited boundary systems between warm and cool water currents (Ryan et al., 2017). Indeed, selective foraging within such oceanographic features is a behavior common to a very wide range of oceanic taxa, including other sharks (Sims and Quayle, 1998; Queiroz et al., 2017; Andrzejaczek et al., 2018), turtles (Polovina et al., 2003), birds (Shaffer et al., 2009), and teleost fishes (Fiedler and Bernard, 1987). In addition to frontal zones, whale sharks have also been observed in areas of higher Chl-*a* levels (Sleeman et al., 2007; Rohner et al., 2018). When data were available, we found that the sharks in our study all remained in areas of relatively moderate to high Chl-*a* levels. Here, we suggest that the whale sharks may stay close to the coastline and on the shelf to take advantage of possible higher food availability than elsewhere in the northern Arabian Sea. This phenomenon is also thought to occur for juvenile whale sharks in Mozambique, where the coast has similar oceanographic characteristics (Rohner et al., 2018). Although Chl-*a* has been used as a proxy for zooplankton biomasses (Jaine et al., 2012), previous studies have suggested it to be poor for such observations (Sleeman et al., 2010b; Lyngsgaard et al., 2017), thus using sonar tags to detect prey fields (Goulet et al., 2019) might be a more appropriate method in investigating the foraging preferences of this species in the northern Arabian Sea.

Recent studies show that frontal systems between warm and cold-water masses may also offer the opportunity for ectothermic sharks to extend feeding opportunities while maintaining metabolic efficiency. Braun et al. (2019) showed that blue sharks (*Prionace glauca*) used warm core eddies to feed on otherwise inaccessible prey in the cool waters of the mesopelagic. By descending at frontal zones, whale sharks may be using a similar mechanism to forage on prey in the deep scattering layer (Ryan et al., 2017). Our study also shows that whale sharks tended to avoid waters that were too warm, with our tagged sharks moving to cooler waters when SSTs increased in this region. Higher SSTs were observed during 2015 (WS-3 and WS-4), at a time when the El Nino Southern Oscillation (ENSO) phenomenon was one of the strongest for the past four decades (Vidya and Kurian, 2018), resulting in higher SSTs in comparison to other years. Despite this, we observed these sharks remaining in cooler water temperatures for the duration of the track. Avoidance of very warm surface waters may be necessary to maintain optimal metabolic rates and limit energetic demands in an oligotrophic tropical ocean. Studies have shown that whale sharks spend a considerable amount of time in a preferred temperature range (24–29°C) (Wilson et al., 2006; Sequeira et al., 2012; Tyminski et al., 2015; Diamant et al., 2018), potentially using water temperatures to thermoregulate their bodies (Thums et al., 2013; Meekan et al., 2015). Here, we also observed a higher occurrence of sharks in a narrow band of SSTs, supporting the literature on the habitat preferences of this species. Identifying the key drivers of these movement patterns will require studies that deploy tags that provide high resolution and accurate records of temperature and depth use by whale sharks.

Our study provides some of the first information on the movement patterns of whale sharks in the eastern part of the northern Arabian Sea. Subpopulations of whale sharks in the southern and central-western Indian Ocean have been suggested to be separated from the northwestern Indian Ocean and Arabian Sea region based on photo identification and isotopic studies (Prebble et al., 2018; Boldrocchi et al., 2020). Additionally, Sequeira et al. (2013) hypothesized that whale sharks could potentially travel between Gujarat and the Maldives, indicating the connectivity between a subpopulation. In our study, WS-6 moved south toward the latitudes of Lakshadweep Islands, a pattern of movement consistent with the possibility some whale sharks migrate from Gujarat toward the Maldives. Additionally, the migration of this shark toward the Southern Equatorial Counter Current before traveling westward could support the theory that the current may form a southern boundary for Indian whale shark populations. One of the tracks of the sharks we tagged (WS-7) showed the animal crossing two-thirds of the northern Arabian Sea, heading toward Oman before the tag detached. Tagging of whale sharks in the Red Sea has shown some animals exiting the Gulf of Aden into the Arabian Sea (Berumen et al., 2014), whereas tagging of sharks in the Persian Gulf has recorded sharks exiting the Gulf of Oman and traveling southward toward the Gulf of Aden (Robinson et al., 2017). Furthermore, whale sharks have also been found along neighbouring coasts of the Persian Gulf, suggesting a wide distribution of these animals in this area (Gore et al., 2019). Given these long-distance movements of sharks in the northern Arabian Sea and the lack of major oceanographic boundaries in this region, there is little evidence (for the moment) to suggest that the populations of whale sharks off the coast of India are likely to form a separate subpopulation from those in other parts of the Arabian Sea. More tagging combined with high resolution genetic studies will be required to resolve this issue.

Sharks are under considerable threats from fishing (Queiroz et al., 2019) and ship strikes in the Indian Ocean (Speed et al., 2008; Lester et al., 2020). For whale sharks, fishing poses by-catch and ship strike threats as they spend a large part of daylight hours basking on the surface of the ocean (Thums et al., 2013; Meekan et al., 2015). On the shelf and close to the Gujarat coast, mechanized fishing vessels account for 89% of all fishing boats (CMFRI, 2019), and based on AIS data, there is intense fishing activity off the coast of Maharashtra (Murua et al., 2019). For this reason, it seems likely that there would be considerable overlap in distributions of fishing vessels and whale sharks in this region. In the northern Arabian Sea, tuna fishing is a major industry (Varghese et al., 2014; CMFRI, 2019) and higher catches have been reported in the vicinity of frontal zones (Anand et al., 2005). We showed that whale sharks moved into the open ocean of the Arabian Sea and given that some of these sharks focused their movements on frontal zones, that are often associated with tuna schools, an interaction between tuna fishers and whale sharks seems likely. Despite the prohibition of the intentional setting of seine nets on whale sharks in 2013 by regional fisheries management organisations (RMFOs) (e.g., Indian Ocean Tuna Commission; IOTC, 2013), and bycatch of whale sharks in purse seine nets being relatively low (Fontes et al., 2020), further work, particularly with juvenile animals, is required to identify the level of risk of mortality of whale sharks following interactions with fishing vessels.

Our study provides the first data on whale shark movements in the eastern part of the northern Arabian Sea and highlights movements linked to frontal systems and narrow temperature bands. We provide baseline information regarding the movements of this species, put in the context of potential threats that these animals face in this area. However, due to limited tag retention times and lack of environmental data recorded by the tags, our results require further validation through more deployments of satellite tags, to gain a better understanding of the behavior and oceanographic context of movements of the species. The deployment of tags that have capabilities to record temperature and depth to describe both horizontal and vertical axes of movement will be essential to optimize and implement effective conservation strategies for whale sharks in the Arabian Sea.

DATA AVAILABILITY STATEMENT

The raw data supporting the conclusions of this article will be made available by the authors, without undue reservation.

ETHICS STATEMENT

The animal study was reviewed and approved by the Forest Department, Government of Gujarat (GFD).

AUTHOR CONTRIBUTIONS

BC, RK, and MM conceived the study. CKP, FB, and SJ collected the data. LA analyzed the data. LA and MM wrote the manuscript with critical input from all authors.

FUNDING

The fieldwork funding for this study was from TATA Chemicals Limited. Tags and tagging equipment were provided by the Forest Department, Government of Gujarat (GFD). LA was supported by the Research Training Scholarship (RTP) at UWA. AS was funded by a 2020 Pew Fellowship in Marine Conservation and an Australian Research Council Discovery Early Career Research Award (Grant DE170100841).

ACKNOWLEDGMENTS

We would like to thank the Government of Gujarat Forest Department (GFD) for the necessary permissions to tag the whale sharks and to TATA Chemicals Limited for funding the study. We would like to thank Diresh Joshi, Prem Jothi, Gautham Sambath, and Prakash Doriva for their support in the field. We are also grateful to the fishermen for reporting the accidental captures of these animals and for assisting their release after tagging occurred.

SUPPLEMENTARY MATERIAL

The Supplementary Material for this article can be found online at: https://www.frontiersin.org/articles/10.3389/fmars.2021.682730/full#supplementary-material

Supplementary Table 1 | List of published *Rhincodon typus* studies using tagging technologies in the Indian Ocean. Table shows the years data were collected; the types of tags and the number (*n*) used in the study; the number (*n*) of individuals and sex of individuals ("M" represent males, "F" represents females, and "U" represents unidentified); size (m); the track duration in days; the track distance (km), and speed (km day^{-1}).

Supplementary Video 1 | Animation of the changes in sea surface temperatures of WS-1. Black "X" indicates the daily whale shark locations, using a combination of recorded positions from the tag and locations from the state-space model when geolocations were unavailable. Sea surface temperatures were set to range from 24 to 31°C.

Supplementary Video 2 | Animation of the changes in sea surface temperatures of WS-2. Black "X" indicates the daily whale shark locations, using a combination of recorded positions from the tag and locations from the state-space model when geolocations were unavailable. Sea surface temperatures were set to range from 24 to 31°C.

Supplementary Video 3 | Animation of the changes in sea surface temperatures of WS-3. Black "X" indicates the daily whale shark locations, using a combination of recorded positions from the tag and locations from the state-space model when geolocations were unavailable. Sea surface temperatures were set to range from 24 to 31°C.

Supplementary Video 4 | Animation of the changes in sea surface temperatures of WS-4. Black "X" indicates the daily whale shark locations, using a combination of recorded positions from the tag and locations from the state-space model when geolocations were unavailable. Sea surface temperatures were set to range from 24 to 31°C.

Supplementary Video 5 | Animation of the changes in sea surface temperatures of WS-5. Black "X" indicates the daily whale shark locations, using a combination of recorded positions from the tag and locations from the state-space model when geolocations were unavailable. Sea surface temperatures were set to range from 24 to 31°C.

Supplementary Video 6 | Animation of the changes in sea surface temperatures of WS-6. Black "X" indicates the daily whale shark locations, using a combination of recorded positions from the tag and locations from the state-space model when geolocations were unavailable. Sea surface temperatures were set to range from 24 to 31°C.

Supplementary Video 7 | Animation of the changes in sea surface temperatures of WS-7. Black "X" indicates the daily whale shark locations, using a combination of recorded positions from the tag and locations from the state-space model when geolocations were unavailable. Sea surface temperatures were set to range from 24 to 31°C.

REFERENCES

Akhilesh, K. V., Shanis, C. P. R., White, W. T., Manjebrayakath, H., Bineesh, K. K., Ganga, U., et al. (2013). Landings of whale sharks rhincodon typus smith, 1828 in Indian waters since protection in 2001 through the Indian Wildlife (Protection) Act, 1972. *Environ. Biol. Fishes* 96, 713–722. doi: 10.1007/s10641-012-0063-9

Anand, A., Kumari, B., Nayak, S. R., and Krishnamurthy, Y. V. N. (2005). Locating oceanic tuna resources in the eastern arabian sea using remote sensing. *J. Indian Soc. Remote Sensing* 33, 511–520. doi: 10.1007/BF02990736

Andrzejaczek, S., Gleiss, A., Jordan, L., Pattiaratchi, C., Howey, L., Brooks, E., et al. (2018). Temperature and the vertical movements of oceanic whitetip sharks, Carcharhinus longimanus. *Sci. Rep.* 8:8351. doi: 10.1038/s41598-018-26485-3

Araujo, G., Rohner, C. A., Labaja, J., Conales, S. J., Snow, S. J., Murray, R., et al. (2018). Satellite tracking of juvenile whale sharks in the Sulu and Bohol Seas, Philippines. *PeerJ* 6:18. doi: 10.7717/peerj.5231

Argos, C. (2011). *ARGOS User's Manual: Worldwide Tracking and Environmental Monitoring by Satellite*. France: Argos/CLS.

Berumen, M., Braun, C., Cochran, J., Skomal, G., and Thorrold, S. (2014). Movement patterns of juvenile whale sharks tagged at an aggregation site in the red sea. *PLoS One* 9:e103536. doi: 10.1371/journal.pone.0103536

Bloch, F. H., Premjothi, P. V. R., Choudury, B. C., Kaul, R., and John, S. (2018). An assessment of the past and present distribution status of the Whale Shark (*Rhincodon typus*) along the west coast of India based on traditional ecological knowledge (TEK). *Perspect. Biodiveristy India* 400. *page,

Boldrocchi, G., Omar, M., Azzola, A., and Bettinetti, R. (2020). The ecology of the whale shark in Djibouti. *Aquat. Ecol.* 54, 535–551. doi: 10.1007/s10452-020-09758-w

Braun, C. D., Gaube, P., Sinclair-Taylor, T. H., Skomal, G. B., and Thorrold, S. R. (2019). Mesoscale eddies release pelagic sharks from thermal constraints to foraging in the ocean twilight zone. *Proc. Natl. Acad. Sci. U.S.A.* 116, 17187–17192. doi: 10.1073/pnas.1903067116

Brunnschweiler, J., Baensch, H., Pierce, S., and Sims, D. (2009). Deep-diving behaviour of a whale shark *Rhincodon typus* during long-distance movement in the western Indian Ocean. *J. Fish Biol.* 74, 706–714. doi: 10.1111/j.1095-8649.2008.02155.x

Capietto, A., Escalle, L., Chavance, P., Dubroca, L., Delgado de Molina, A., Murua, H., et al. (2014). Mortality of marine megafauna induced by fisheries: insights from the whale shark, the world's largest fish. *Biol. Conservation* 174, 147–151. doi: 10.1016/j.biocon.2014.03.024

Chassignet, E. P., Hurlburt, H. E., Smedstad, O. M., Halliwell, G. R., Hogan, P. J., Wallcraft, A. J., et al. (2007). The hycom (hybrid coordinate ocean model) data assimilative system. *J. Mari. Syst.* 65, 60–83. doi: 10.1016/j.jmarsys.2005.09.016

CMFRI. (2019). *CMFRI Annual Report 2019*. Kerala: Central Marine Fisheries Research Institute.

Copping, J., Stewart, B., Mcclean, C., Hancock, J., and Rees, R. (2018). Does bathymetry drive coastal whale shark (*Rhincodon typus*) aggregations? *PeerJ* 6:e4904. doi: 10.7717/peerj.4904

Diamant, S., Rohner, C. A., Kiszka, J. J., Guillemain d'echon, A., Guillemain, d'echon, T., et al. (2018). Movements and habitat use of satellite-tagged whale sharks off western Madagascar. *Endangered Spec. Res.* 36, 49–58. doi: 10.3354/esr00889

ESRI. (2011). *ArcGIS Desktop: Release 10*. Redlands, CA: Environmental Systems Research Institute.

Fiedler, P. C., and Bernard, H. J. (1987). Tuna aggregation and feeding near fronts observed in satellite imagery. *Continental Shelf Res.* 7, 871–881. doi: 10.1016/0278-4343(87)90003-3

Fontes, J., Mcginty, N., Machete, M., and Afonso, P. (2020). Whale shark-tuna associations, insights from a small pole-and-line fishery from the mid-north Atlantic. *Fish. Res.* 229:105598. doi: 10.1016/j.fishres.2020.105598

GEBCO. (2015). *General Bathymetric Chart of the Oceans, Version 20141103.*

Gleiss, A., Wright, S., Liebsch, N., Wilson, R., and Norman, B. (2013). Contrasting diel patterns in vertical movement and locomotor activity of whale sharks at ningaloo reef. *Mari. Biol.* 160, 2981–2992. doi: 10.1007/s00227-013-2288-3

Gore, M., Waqas, U., Khan, M. M., Ahmad, E., Baloch, A. S., and Baloch, A. R. (2019). A first account of the elasmobranch fishery of Balochistan, south-west Pakistan. *Western Indian Ocean J. Mari. Sci.* 18, 95–105. doi: 10.4314/wiojms.v18i1.9

Goulet, P., Guinet, C., Swift, R., Madsen, P. T., and Johnson, M. (2019). A miniature biomimetic sonar and movement tag to study the biotic environment and predator-prey interactions in aquatic animals. *Deep Sea Res. Part I Ocean. Res. Papers* 148, 1–11. doi: 10.1016/j.dsr.2019.04.007

Hearn, A. R., Green, J. R., Espinoza, E., Peñaherrera, C., Acuña, D., and Klimley, A. P. (2013). Simple criteria to determine detachment point of towed satellite tags provide first evidence of return migrations of whale sharks (*Rhincodon typus*) at the galapagos islands, ecuador. *Animal Biotelemetry* 1:11. doi: 10.1186/2050-3385-1-11

Hueter, R., Tyminski, J., and de la Parra, R. (2013). Horizontal movements, migration patterns, and population structure of whale sharks in the gulf of mexico and northwestern caribbean sea. *PLoS One* 8:e71883. doi: 10.1371/annotation/491b9b6c-7f77-4fb0-b336-572078aec830

IOTC (2013). *Resolution 13/05 on the Conservation of Whale Sharks (Rhincodon typus)*. Seychelles: IOTC.

Jabado, R. W., Kyne, P. M., Pollom, R. A., Ebert, D. A., Simpfendorfer, C. A., Ralph, G. M., et al. (2018). Troubled waters: threats and extinction risk of the sharks, rays and chimaeras of the Arabian sea and adjacent waters. *Fish and Fisheries* 19, 1043–1062. doi: 10.1111/faf.12311

Jaine, F. R. A., Couturier, L. I. E., Weeks, S. J., Townsend, K. A., Bennett, M. B., Fiora, K., et al. (2012). When giants turn up: sighting trends, environmental influences and habitat use of the manta ray manta alfredi at a coral reef. *PLoS One* 7:e46170. doi: 10.1371/journal.pone.0046170

Jonsen, I. D., Flemming, J. M., and Myers, R. A. (2005). Robust state–space modeling of animal movement data. *Ecology* 86, 2874–2880. doi: 10.1890/04-1852

Kumari, B., and Raman, M. (2010). Whale shark habitat assessments in the northeastern Arabian Sea using satellite remote sensing. *Int. J. Remote Sensing* 31, 379–389. doi: 10.1080/01431160902893444

Lester, E., Meekan, M. G., Barnes, P., Raudino, H., Rob, D., Waples, K., et al. (2020). Multi-year patterns in scarring, survival and residency of whale sharks in ningaloo marine park, Western Australia. *Mari. Ecol. Prog. Series* 634, 115–125. doi: 10.3354/meps13173

Lyngsgaard, M. M., Markager, S., Richardson, K., Møller, E. F., and Jakobsen, H. H. (2017). How well does chlorophyll explain the seasonal variation in phytoplankton activity? *Estuar. Coasts* 40, 1263–1275. doi: 10.1007/s12237-017-0215-4

Madhupratap, M., Nair, K. N. V., Gopalakrishnan, T. C., Haridas, P., Nair, K. K. C., Venugopal, P., et al. (2001). Arabian Sea oceanography and fisheries of the west coast of India. *Curr. Sci.* 81, 355–361.

MATLAB. (2010). *MATLAB and Statistics Toolbox Release*. Natick: The MathWorks Inc.

Meekan, M., Fuiman, L., Davis, R., Berger, Y., and Thums, M. (2015). Swimming strategy and body plan of the world's largest fish: implications for foraging efficiency and thermoregulation. *Front. Mari. Sci.* 2:64. doi: 10.3389/fmars.2015.00064

Meekan, M. G., Taylor, B. M., Lester, E., Ferreira, L. C., Sequeira, A. M. M., Dove, A. D. M., et al. (2020). Asymptotic growth of whale sharks suggests sex-specific life-history strategies. *Front. Mari. Sci.* 7:575683. doi: 10.3389/fmars.2020.575683

Murua, H., Granado, I., Gee, J., Kroodsma, D., Miller, N., Taconet, M., et al. (2019). *FAO Area 51 - AIS-Based Fishing Activity in the Western Indian Ocean*. *city pub.

Norman, B., Reynolds, S., and Morgan, D. (2016). Does the whale shark aggregate along the Western Australian coastline beyond Ningaloo reef? *Pacific Conservation Biol.* 22, 72–80. doi: 10.1071/PC15045

Norman, B. M., and Stevens, J. D. (2007). Size and maturity status of the whale shark (*Rhincodon typus*) at ningaloo reef in Western Australia. *Fisheries Research* 84, 81–86. doi: 10.1016/j.fishres.2006.11.015

Pearce, S., and Norman, B. (2016). *Rhincodon typus. The IUCN Red List of Threatened Species 2016 [Online]*. Available online at: http://dx.doi.org/10.2305/IUCN.UK.2016-1.RLTS.T19488A2365291.en (accessed 01/08/2018)

Polovina, J., Balazs, G., Howell, E., Parker, D., Seki, M., and Dutton, P. (2003). Foraging and migration habitat of loggerhead (*Caretta caretta*) and olive ridley (*Lepidochelys olivacea*) sea turtles in the central north pacific ocean. *Fish. Oceanogr.* 13, 36–51. doi: 10.1046/j.1365-2419.2003.00270.x

Pravin, P. C. F. P. D. A. (2000). Whale shark in the Indian coastneed for conservation. *Curr. Sci.* 79, 310–315.

Prebble, C. E. M., Rohner, C. A., Pierce, S. J., Robinson, D. P., Jaidah, M. Y., Bach, S. S., et al. (2018). Limited latitudinal ranging of juvenile whale sharks in the western indian ocean suggests the existence of regional management units. *Mari. Ecol. Prog. Series* 601, 167–183. doi: 10.3354/meps12667

Queiroz, N., Humphries, N. E., Couto, A., Vedor, M., da Costa, I., Sequeira, A. M. M., et al. (2019). Global spatial risk assessment of sharks under the footprint of fisheries. *Nature* 572, 461–466. doi: 10.1038/s41586-019-1444-4

Queiroz, N., Vila-Pouca, C., Couto, A., Southall, E., Mucientes, G., Humphries, N., et al. (2017). Convergent foraging tactics of marine predators with different feeding strategies across heterogeneous ocean environments. *Front. Mari. Sci.* 4:239. doi: 10.3389/fmars.2017.00239

R Core Team. (2013). *R: A Language and Environment for Statisitcal Computing*. Vienna: R Core, Team.

Ramirez-Macias, D., Queiroz, N., Pierce, S., Humphries, N., Sims, D., and Brunnschweiler, J. (2017). Oceanic adults, coastal juveniles: tracking the habitat use of whale sharks off the Pacific coast of Mexico. *PeerJ* 5, 32–71. doi: 10.7717/peerj.3271

Retheesh, T., Jacob Peter, P., and Kishore, T. G. (2020). Whale shark landed in sakthikulangara fisheries harbour. *Mari. Fish. Inform. Service Technical Extens. Series* 2020, 37–37.

Reynolds, S., Norman, B., Beger, M., and Franklin, C. (2017). Movement, distribution and marine reserve use by an endangered migratory giant. *J. Conservation Biogeog.* 23, 1268–1279. doi: 10.1111/ddi.12618

Robinson, D., Jaidah, M., Bach, S., Rohner, C., Jabado, R., Ormond, R., et al. (2017). Some like it hot: repeat migration and residency of whale sharks within an extreme natural environment. *PLoS One* 12:e0185360. doi: 10.1371/journal.pone.0185360

Rohner, C., Richardson, A., Jaine, F., Bennett, M., Weeks, S., Cliff, G., et al. (2018). Satellite tagging highlights the importance of productive *Mozambican coastal* waters to the ecology and conservation of whale sharks. *PeerJ* 6, 41–61. doi: 10.7717/peerj.4161

Rohner, C. A., Cochran, J. E. M., Cagua, E. F., Prebble, C. E. M., Venables, S. K., Berumen, M. L., et al. (2020). No place like home? High residency and predictable seasonal movement of whale sharks off tanzania. *Front. Mari. Sci.* 7:2296–7745. doi: 10.3389/fmars.2020.00423

Rowat, D., and Gore, M. (2007). Regional scale horizontal and local scale vertical movements of whale sharks in the Indian Ocean off Seychelles. *Fish. Res.* 84, 32–40. doi: 10.1016/j.fishres.2006.11.009

Ryan, J., Green, J., Espinoza, E., and Hearn, A. (2017). Association of whale sharks (*Rhincodon typus*) with thermo-biological frontal systems of the eastern tropical Pacific. *PLoS One* 12:e0182599. doi: 10.1371/journal.pone.0182599.g002

Sequeira, A., Mellin, C., Fordham, D., Meekan, M., and Bradshaw, C. (2014). Predicting current and future global distributionsof whale sharks. *Global Change Biol.* 20, 778–789. doi: 10.1111/gcb.12343

Sequeira, A., Mellin, C., Meekan, M., Sims, D., and Bradshaw, C. (2013). Inferred global connectivity of whale shark, *Rhincodon typus*, populations. *J. Fish Biol.* 82, 367–389. doi: 10.1111/jfb.12017

Sequeira, A., Mellin, C., Rowat, D., Meekan, M., and Bradshaw, C. (2012). Ocean-scale prediction of whale shark distribution. *Diversity Distribut.* 18, 504–518. doi: 10.1111/j.1472-4642.2011.00853.x

Sequeira, A. M. M., Hays, G. C., Sims, D. W., Eguíluz, V. M., Rodríguez, J. P., Heupel, M. R., et al. (2019). Overhauling ocean spatial planning to improve marine megafauna conservation. *Front. Mari. Sci.* 6:639. doi: 10.3389/fmars.2019.00639

Shaffer, S. A., Weimerskirch, H., Scott, D., Pinaud, D., Thompson, D. R., Sagar, P. M., et al. (2009). Spatiotemporal habitat use by breeding sooty shearwaters *Puffinus griseus*. *Mari. Ecol. Prog. Series* 391, 209–220. doi: 10.3354/meps07932

Sims, D. W., and Quayle, V. A. (1998). Selective foraging behaviour of basking sharks on zooplankton in a small-scale front. *Nature* 393, 460–464. doi: 10.1038/30959

Sleeman, J., Meekan, M., Fitzpatrick, B., Steinberg, C., Ancel, R., and Bradshaw, C. (2010a). Oceanographic and atmospheric phenomena influence the abundance of whale sharks at Ningaloo Reef, Western Australia. *J. Exp. Mari. Biol. Ecol.* 382, 77–81. doi: 10.1016/j.jembe.2009.10.015

Sleeman, J., Meekan, M., Wilson, S., Jenner, C., Jenner, M., Boggs, G., et al. (2007). Biophysical correlates of relative abundances of marine megafauna at Ningaloo Reef, Western Australia. *Mari. Fresh. Res.* 58, 608–623. doi: 10.1071/MF06213

Sleeman, J., Meekan, M., Wilson, S., Polovina, J., Stevens, J., Boggs, G., et al. (2010b). To go or not to go with the flow: environmental influences on whale shark movement patterns. *J. Exp. Mari. Biol. Ecol.* 390, 84–98. doi: 10.1016/j.jembe.2010.05.009

Speed, C. W., Meekan, M. G., Rowat, D., Pierce, S. J., Marshall, A. D., and Bradshaw, C. J. A. (2008). Scarring patterns and relative mortality rates of Indian Ocean whale sharks. *J. Fish Biol.* 72, 1488–1503. doi: 10.1111/j.1095-8649.2008.01810.x

Thums, M., Meekan, M., Stevens, J., Wilson, S., and Polovina, J. (2013). Evidence for behavioural thermoregulation by the world's largest fish. *J. R. Soc. Int.* 10, 1–5. doi: 10.1098/rsif.2012.0477

Tyminski, J., Parra-Venegas, R., Cano, J., and Hueter, R. (2015). Vertical movements and patterns in diving behaviour in whale sharks as revealed by pop-up satellite tags in the Eastern Gulf of Mexico. *PLoS One* 10:142–156. doi: 10.1371/journal.pone.0142156

Varghese, S. P., Somvanshi, V. S., and Dalvi, R. S. (2014). Diet composition, feeding niche partitioning and trophic organisation of large pelagic predatory fishes in the eastern Arabian Sea. *Hydrobiologia* 736, 99–114. doi: 10.1007/s10750-014-1895-4

Vidya, P. J., and Kurian, S. (2018). Impact of 2015–2016 ENSO on the winter bloom and associated phytoplankton community shift in the northeastern Arabian Sea. *J. Mari. Syst.* 186, 96–104. doi: 10.1016/j.jmarsys.2018.06.005

Wilson, S., Polovina, J., Stewart, B., and Meekan, M. (2006). Movements of whale sharks *(Rhincodon typus)* tagged at Ningaloo Reef, Western Australia. *Mari. Biol.* 148, 1157–1166. doi: 10.1007/s00227-005-0153-8

Conflict of Interest: The authors declare that this study received funding from TATA Chemicals Limited. The funder was not involved in the study design, collection, analysis, interpretation of the data, the writing of this article or the decision to submit it for publication.

Citation: Arrowsmith LM, Paidi CK, Bloch FH, John S, Choudhury BC, Kaul R, Sequeira AMM, Pattiaratchi CB and Meekan MG (2021) First Insights Into the Horizontal Movements of Whale Sharks (Rhincodon typus) in the Northern Arabian Sea. Front. Mar. Sci. 8:682730. doi: 10.3389/fmars.2021.682730

frontiers in Marine Science

ORIGINAL RESEARCH
published: 09 July 2021
doi: 10.3389/fmars.2021.688076

Oceanic Diel Vertical Movement Patterns of Blue Sharks Vary With Water Temperature and Productivity to Change Vulnerability to Fishing

Marisa Vedor[1,2], Gonzalo Mucientes[1,3], Sofia Hernández-Chan[1], Rui Rosa[2], Nick Humphries[4], David W. Sims[4,5,6] and Nuno Queiroz[1,4]*

[1] Centro de Investigação em Biodiversidade e Recursos Genéticos/Rede de Investigação em Biodiversidade e Biologia Evolutiva (CIBIO/InBIO), Universidade do Porto, Vairão, Portugal, [2] Laboratório Marítimo da Guia, Marine and Environmental Sciences Centre (MARE), Faculdade de Ciências, Universidade de Lisboa, Cascais, Portugal, [3] Instituto de Investigaciones Marinas, Consejo Superior de Investigaciones Científicas (IIM-CSIC), Vigo, Spain, [4] Marine Biological Association of the United Kingdom, Plymouth, United Kingdom, [5] Ocean and Earth Science, National Oceanography Centre Southampton, University of Southampton, Southampton, United Kingdom, [6] Centre for Biological Sciences, University of Southampton, Southampton, United Kingdom

OPEN ACCESS

Edited by:
*Mourier Johann,
Institut de Recherche Pour le Développement (IRD), France*

Reviewed by:
*Daniel M. Coffey,
Texas A&M University–Corpus Christi, United States
Yuuki Watanabe,
National Institute of Polar Research, Japan*

***Correspondence:**
*Nuno Queiroz
nuno.queiroz@cibio.up.pt*

Specialty section:
This article was submitted to Marine Megafauna, a section of the journal Frontiers in Marine Science

Received: *30 March 2021*
Accepted: *18 June 2021*
Published: *09 July 2021*

Citation:
Vedor M, Mucientes G, Hernández-Chan S, Rosa R, Humphries N, Sims DW and Queiroz N (2021) Oceanic Diel Vertical Movement Patterns of Blue Sharks Vary With Water Temperature and Productivity to Change Vulnerability to Fishing. Front. Mar. Sci. 8:688076. doi: 10.3389/fmars.2021.688076

In the pelagic environment diel vertical movements (DVM) are widespread across taxa, from zooplankton ascending from day-time depths into surface layers at night to avoid visual predators, to apex predators following prey movements to maximise foraging opportunities. The drivers of DVM in large predators such as pelagic sharks have only recently begun to be investigated in detail with the advent of sophisticated archival tags and high-resolution oceanographic datasets. In this study, we satellite tagged adult [>180 cm fork length, (FL)] blue sharks (*Prionace glauca*) in the North Atlantic Ocean to examine behavioural changes in response to the encountered environment, and therefore, to determine potential risks of capture using pelagic longline fisheries data. Although blue sharks recurrently use surface waters, cyclic diel behaviours were observed, with >95% of night-time spent above 250 m depth and variable day-time depth use. Hence, three different diel behaviours were identified during the tracking period: (i) regular normal DVM (nDVM) (dawn descent – dusk ascent, with over 90% of nighttime spent above 250 m, and between 5 and 50% of the day below this threshold); (ii) surface-oriented behaviour (occupation of surface waters both day and night), and (iii) deep depth-oriented nDVM [dawn descent – dusk ascent, with the majority (>50%) of daytime spent at depth]. Importantly, diel behaviours generally occurred in different ocean regions with nDVM frequently observed in high latitudes, associated with cold, highly productive waters (e.g., North Atlantic Current/Labrador Current convergence zone, West African upwelling area), while depth-oriented nDVM was observed in warm, oligotrophic areas. Thus, day-time occupation of shallow waters significantly increased with lower water temperature at depth (100 m), and with increasing concentration (and decreasing depth) of the chlorophyll a maximum. During nights of full moon blue sharks spent significantly more time in the depth range of longline hooks, while fishing effort and catches were also higher. We demonstrate that increased occupancy of surface layers driven by highly productive, cold waters and greater lunar illumination lead to higher capture risk. Understanding habitat-specific vulnerability to fishing in a commercially important pelagic shark species is essential for improving management and conservation measures.

Keywords: diel vertical movement, longline fisheries, fishing risk, environment, lunar phase

INTRODUCTION

Apex pelagic predators, given their extensive movements and wide distributions, play an important role shaping the ecological structure and habitat use of oceanic communities (Sims, 2003; Campana, 2016; Boerder et al., 2019). Yet, over the past decades, populations of commercially important species have been declining due to overexploitation (Baum et al., 2003; Pacoureau et al., 2021). This has been partially fuelled by a lack of knowledge on the movement and habitat use patterns, and where and when fish interact with fishing vessels, which in turn hinder stock assessment models (Mejuto and García-Cortés, 2005; Queiroz et al., 2019). While original stock assessments assumed fish populations were evenly distributed at an ocean-basin scale, recent approaches that include a spatial structure have shown a largely improved estimation performance (Punt, 2019). However, most current stock assessments still account for catchability as a measure of spatial distribution (Punt, 2019), raising the need for movement-based stock assessments as opposed to fisheries-based (Baum et al., 2003; Dunn et al., 2019). Advances in satellite telemetry and the increasing availability of remotely sensed environmental data have, however, allowed the coupling of recorded behavioural data with aspects of the encountered environment (Whitford and Klimley, 2019; Francisco et al., 2020). This has permitted studies that describe habitat preferences of migratory marine vertebrates even in remote areas, such as the open ocean (Humphries et al., 2010; Guzman et al., 2018; Sequeira et al., 2018). In addition, understanding how environmental changes affect the movements and behaviour of pelagic fish has also enabled the identification of areas and periods of higher vulnerability to fisheries (Song et al., 2009; Queiroz et al., 2016, 2019; Hays et al., 2019). Taken together, this spatial and behavioural information is therefore essential to the development of more effective conservation measures (Hammerschlag et al., 2016; Sequeira et al., 2019; Hindell et al., 2020).

Besides wide-ranging distributions, pelagic predators such as sharks and tunas (*Thunnus spp.*) are also efficient divers, exploring a multitude of vertical habitats from the surface to the bathyal (Schaefer and Fuller, 2002; Wilson et al., 2005; Howey-Jordan et al., 2013). A particularly distinctive cyclic behaviour has been described for a wide range of pelagic species, from zooplankton to apex predators – diel vertical movements (DVM) (e.g., Weng et al., 2009; Coffey et al., 2017; Hafker et al., 2017). DVM in zooplankton is characterised by occupation of surface waters at nighttime and, as a phototaxic response, diving into deeper waters during daytime where light levels are lower (Lampert, 1989). These cyclic movements have been primarily associated with zooplankton avoidance of visual predators, which are then mimicked throughout the food chain to optimise prey encounter success (Hays, 2003). However, drivers of DVM for pelagic predators have generally been associated with thermoregulation and/or foraging (Pade et al., 2009; Campana et al., 2011; Queiroz et al., 2012; Andrzejaczek et al., 2019). For example, Atlantic bluefin tunas in the Gulf Stream reduced time spent in shallow warm waters and exhibited deeper DVMs possibly as a behavioural mechanism to maintain optimal body temperature (Teo et al., 2006). However, DVM in ectothermic fish may also represent a behavioural mechanism that balances the higher energy costs associated with night-time foraging activity in shallow, warm waters, with reduced activity in deep cold waters during daytime that lowers metabolic rate (Sims et al., 2006).

DVM associated with predator avoidance is particularly important for species at lower trophic levels, where day-time occupation of aphotic layers and night-time shoaling in the darkness decreases the predation success of visual predators, consequently increasing the chances of prey survival (Wirsing et al., 2011). However, for pelagic top predators, DVM has been mostly associated with foraging behaviour (Carey et al., 1990; Andrzejaczek et al., 2019). By following prey diel rhythms, predators increase the spatial and temporal overlap with prey distribution, increasing the success of prey encounter (Sims et al., 2005). Several species of marine megafauna are diel vertical migrators, and some of the most important components of their diet include mesopelagic fish and diel vertically migrating species, supporting the notion that DVM increases foraging success (Sims et al., 2005; Pade et al., 2009; Duffy et al., 2017; Braun et al., 2019a). Shifts in diel behavioural patterns have been linked to variations in the thermal profile of the water column and to the distribution and timing of peak productivity. For instance, both blue and salmon sharks have shown an increased surface occupancy in highly productive frontal regions, associated with cold surface temperatures and sharp water-column stratification (Queiroz et al., 2012; Coffey et al., 2017). Besides diel differences in vertical space-use, activity rates also follow a diel cycle, being generally higher at night than during the day (Andrews et al., 2009; Papastamatiou et al., 2018). For example, increased night-time activity of sharks was linked to high food abundance (Sims et al., 2006). Hence, this increased nocturnal activity has been associated with foraging on prey aggregations occurring in warm surface waters during this period (Sims et al., 2006; Papastamatiou et al., 2018).

Although changes in vertical behaviour are strongly linked to the physical and biological environment, they can also vary in response to the illuminated lunar fraction. Distributions of plankton on nights of full moon are generally deeper than on nights of new moon which manifests as a phototaxic response for predator avoidance (Tarling, 1999; Last et al., 2016). This behaviour is driven by a similar light-avoidance mechanism to the one observed for DVM, but here deepening occurs at night in response to moonlight. This behaviour cascades through trophic levels, from mesopelagic fish (Olivar et al., 2017) up to top predators (e.g., tunas and swordfish *Xiphias gladius*) where deeper movements on nights of full moon have been hypothesised to improve foraging success within prey aggregated at deeper depths (Musyl et al., 2003; Dewar et al., 2011; Abascal et al., 2015). Furthermore, behavioural variations linked to the lunar phase affect the capture risk of pelagic predators by commercial fisheries. For example, catches of commercial species such as yellowfin and blackfin tuna, and blue sharks were higher in nights of full moon (Curran, 2014; Orbesen et al., 2017), while catch rates for swordfish were highest during both new and full moon phases (Poisson et al., 2010; Lerner et al., 2013; Orbesen et al., 2017). The vertical behaviour of blue sharks has been the subject of a large number of studies (e.g., Carey et al., 1990; Campana et al., 2011; Queiroz et al., 2012; Braun et al., 2019b), but knowledge of the fine-scale behaviour of oceanic adult blue sharks and their vulnerability to fishing as a consequence is scarce. Blue sharks are one of the most exploited species by pelagic longline fisheries, with populations declining by ∼40% since the 1970s (Baum et al., 2003; Pacoureau et al., 2021) largely as a result of high mortality risk from fishing (Queiroz et al., 2016, 2019). Despite recently established fishing quotas for blue sharks in some regions, the uncertainty in current stock assessments make understanding shark fine-scale behaviour a priority for effective conservation management (Hammerschlag et al., 2016; Robinson et al., 2017; Boerder et al., 2019). To address these knowledge gaps, we used pop-off satellite-linked archival transmitters (PSATs) attached to adult blue sharks in the North Atlantic Ocean, to investigate potential coupling between open-ocean shark DVM with environmental fields and to identify both the spatial and temporal risks posed by longline fishing in the region.

MATERIALS AND METHODS

Shark Tagging

A total of 22 adult blue sharks (*Prionace glauca*) were tagged in two general oceanic locations (in the mid-Atlantic and the north-western Atlantic regions) between June 2010 and August 2011. Sharks were captured on commercial baited surface longlines and brought alongside the vessel in the gear-hauling phase and tagged. Pop-off satellite-linked archival transmitter tags (PSATs; Mk-10 model, Wildlife Computers, Redmond, WA, United States) were rigged with a monofilament tether covered with silicone tubing and looped through a small hole made in the base of the first dorsal fin. Depth, external temperature, and light-level parameters were archived at 1 s intervals and stored as summary data over set intervals of 6 h (00:00, 06:00, 12:00, and 18:00). For each period, time-at-depth histograms (TAD; aggregated in eight depth bins, 50, 100, 150, 200, 250, 400, 600, >600 m), minimum and maximum depth and temperature, as well as profiles of water temperature at depth were available. All shark tagging procedures undertaken in this study were approved by institutional ethical review committees and completed by licenced, trained, and experienced personnel.

Track Processing

The movement of PSAT-tagged sharks was estimated using either satellite relayed data from each tag or from archival data after the tags were physically recovered. Positions of each shark between attachment and tag pop-up were reconstructed using software provided by the manufacturer (WC-GPE, global position estimator programme suite), where daily maximal rate-of-change in light intensity was used to estimate local time of midnight or midday for longitude calculations, and day-length estimation for determining latitude. Anomalous longitude estimates resulting from dive-induced shifts in the estimated timings of dawn and dusk from light curves were automatically discarded from the dataset using software provided by the manufacturer (WC-GPE); latitude estimates were subsequently iterated for the previously obtained longitudes. An integrated state-space model [unscented Kalman filter – UKFSST (Lam et al., 2008); using spatially complete NOAA Optimum Interpolation Quarter Degree Daily SST Analysis data] was then applied to correct the raw geolocation estimates and obtain the most probable track. A regular time-series of locations was then estimated using a continuous-time correlated random walk Kalman filter, CTCRW (Jonsen et al., 2005) performed in R [*crawl* package (Johnson et al., 2008)]. Subsequently, the CTCRW state-space model was applied to each individual track, producing a single position estimate per day. Argos positions were parameterised with the K error model parameters for longitude and latitude implemented in the crawl package (Jonsen et al., 2005). To obtain unbiased estimates of shark space use, gaps between consecutive dates in the raw tracking data were interpolated to one position per day. However, any tracks with gaps exceeding 20 days were split into segments prior to interpolation, thus avoiding the inclusion of unrepresentative location estimates (Queiroz et al., 2016, 2019).

Diel Diving Behaviour

To detect cyclical patterns in the behaviour of the sharks, maximum depths for each 6 h interval were analysed with a Lomb-Scargle (LS) periodogram (Lomb, 1976; Scargle, 1982), using a detection range between 10 and 30 h in R package *lomb* (Ruf, 2010; Azzurro et al., 2012). The maximum percentage of total data variance fitted by the corresponding periodicity was chosen as the peak value (Campbell et al., 2010; Azzurro et al., 2012).

To analyse diel differences in the behaviour of blue sharks, the time between 12:00 GMT and 18:00 GMT (6 h period) was considered daytime, while night-time was considered between 00:00 GMT and 06:00 GMT (6 h period). Time bins which encompassed sunset and sunrise times (between 06:00–12:00 GMT and 18:00–00:00 GMT, respectively; **Supplementary Figure 1**) were excluded from the analyses (Dewar et al., 2011; Abecassis et al., 2012). Following previous studies on the diel behaviour of blue sharks, three classes were defined based on individual TAD and maximum depth for each daytime and night-time period over 5-day periods (Campana et al., 2011; Queiroz et al., 2012). A 5-day period was classified as (i) depth-oriented nDVM if a shark spent more than 90% of the night-time above 250 m and 50% of the daytime below this depth; (ii) regular nDVM was characterised by over 90% of the night above 250 m, and between 5 and 50% of the day below the threshold. Finally, (iii) surface-oriented behaviour was characterised by over 90% of both day and night-time above 250 m. This depth threshold was used because it corresponds to the depth above which >95% of night-time occupancy for tracked blue sharks occurs (**Supplementary Figure 1**). Lastly, periods without clear day and night TAD patterns were classified as "other" and excluded from further analyses (corresponding to 4.0% of the total analysed periods). Subsequently, time-weighted depth and temperature were calculated for each 6 h day- and night-time bins using the function *weighted.mean* in R software, using the middle point of the bins defined for TAD data and the maximum depth/temperature. Pairwise Wilcoxon Rank Sum tests were used to statistically compare day and night-time weighted values, within each diel class. To further explore the behavioural thermoregulation hypothesis, a Pearson correlation was used to test the relationship between time-weighted temperatures during the day and the consecutive night. Moreover, individual dives were identified using the *diveMove* R package for high-resolution archival dive data available for three sharks (S3, S11, and S15), following Queiroz et al. (2017). For each dive, we assessed its duration and respective time-weighted temperatures. A Spearman correlation was used to compare the average time-weighted temperatures between day- and night-time dives.

Monthly mean modelled environmental data (0.25° × 0.25°) were acquired from Copernicus Marine Environment Monitoring Service (CMEMS) global ocean biogeochemistry non-assimilative hindcast (PISCES 1998–2011) for chlorophyll *a* (mg m^{-3}) and global ocean physics reanalysis (GLORYS2V3 1993–2012) for temperature (°C) products for the North Atlantic Ocean. Environmental data was extracted from the surface to 1,750 m depth, and to account for the spatial error around real individual geolocations, data was averaged for 1.25° in latitude and 0.75° in longitude (using a 5 × 3 grid cell) around each position. The relationship between day-time occupation of shallow waters (TAD above 250 m depth) and environmental variables, (i) sea surface temperature (SST), (ii) temperature at depth 100 m, (iii) maximum concentration of chlorophyll *a* in the water column, and (iv) depth of the chlorophyll *a* maximum, was investigated using a general linear mixed model (GLMM) with binomial distribution and cauchit link function. Data exploration techniques were used to identify potential outliers and assess collinearity among independent variables. Hence, chlorophyll *a* concentrations above 1 mg m^{-3} were considered outliers and discarded from further analysis (corresponding to 2.56% of data); in addition, the depth of the chlorophyll *a* maximum showed a high collinearity with concentration – variance inflation factor (VIF) higher than three (Zuur et al., 2009) – and was removed from the model selection process. Individual sharks were considered an independent sampling unit and were included as random effects; however, individuals with less than 10 data points were discarded from the analyses [resulting in the exclusion of S12; (Zuur et al., 2009)]. General mixed models were constructed by backward selection of individual terms to allow for testing of biologically meaningful interactions. The selected terms were: (i) sea surface temperature (SST), (ii) temperature at depth 100 m, and (iii) maximum concentration of chlorophyll *a* in the water column. The model was trained with 75% of data ($n = 456$) and the optimal selection was based on Akaike Information Criterion (AIC). At each stage of the selection process, fitted models were compared to the null model. Consequently, the fitted model with the lowest AIC was chosen as an optimal structure, with which a GLMM was built using *MASS* R package. Normal quantile–quantile plots of deviance residuals were assessed for normality of residuals and fit, while homoscedasticity, model misspecification, and residual spatial autocorrelation were evaluated by inspecting plots of response residuals against fitted values and candidate explanatory variables, respectively. Spatial and temporal residual autocorrelation was further assessed by including respective covariate structures and comparing model performance. This resulted in the inclusion of an autocorrelation structure of order 1 *corAR1* (*nmle* R package) in the model.

Lunar Phase and Hook Encounter Risk

Lunar phase (visible fraction of the disc, a continuous variable where 0 is dark moon and 1 corresponds to full moon) was extracted for each estimated shark geolocation. To account for the spatial error around individual geolocations, visible fraction of the disc data was averaged for 1.25° in latitude and 0.75° in longitude around each shark position. Data was obtained using the function *moonAngle* in the *oce* R package. To analyse shark night-time depth occupation in relation to the moon phase, the illuminated lunar fraction was divided into four 0.25 bins representative of the four lunar phases: (i) new moon, (ii) first and (iii) third quarter, and (iv) full moon.

Drifting pelagic longline fishing effort data at 0.01° × 0.01° grid resolution were obtained from Global Fishing Watch (GFW) and subsequently gridded using the same spatial resolution as the environmental data (0.25 × 0.25° grid cells) and between the years 2012 to 2016. The number of fishing days in each month within each grid cell was summed and then averaged across years (Queiroz et al., 2019). Geo-referenced catch data for blue shark were also obtained from logbooks of Spanish commercial longliners between 2013 and 2017. Similarly, monthly catch per unit of effort (CPUE) was summed within each 0.25 × 0.25° grid cells and averaged across years. GFW and CPUE analyses also considered the spatial error around individual geolocations. Despite the lack of fishing data for the same period sharks were tracked (2010–2011), fishing patterns and the associated capture risk are consistent across years (Kroodsma et al., 2018; Queiroz et al., 2019). Hence, by averaging fishing effort and CPUE across multiple years, interannual variation was considered when calculating the mean vulnerability of tracked sharks. Since longlines are deployed at night at depths between 100 and 300 m (Domingo et al., 2016), the TAD between 100 and 250 m was also calculated (TAD_{hook}) for each shark location. This percentage of time at hook depth was initially compared between nights of new and full moon; GFW fishing effort and CPUE were also analysed

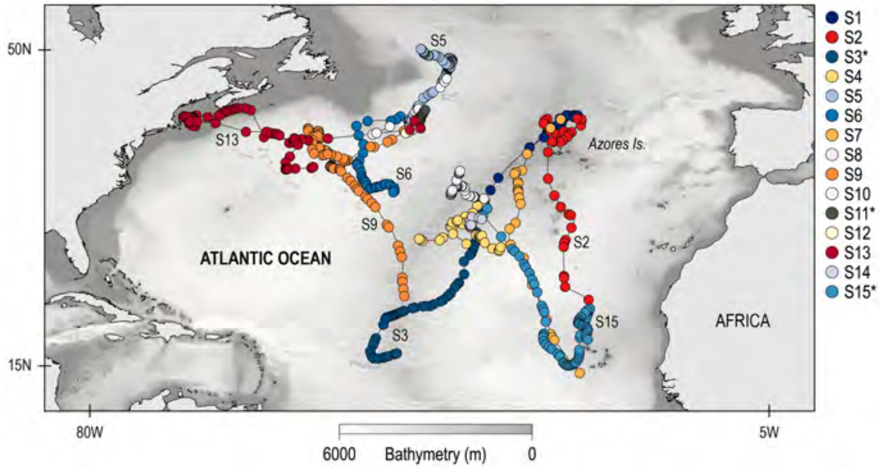

FIGURE 1 | Individual geolocations for 15 blue sharks tracked in the North Atlantic Ocean between 2010 and 2011.

in relation to the lunar phase using an independent-sample Wilcoxon rank sum test.

RESULTS

Between 2010 and 2011, a total of 15 blue sharks were successfully tracked in the North Atlantic for a total of 1,325 cumulative days (**Figure 1** and **Table 1**). Sharks tagged in the mid-Atlantic either remained in the same general area for the tracking duration (between 90 and 120 days; S1, S4, S8, and S14) or moved southward (S2, S3, S7, and S15; these sharks were tracked between 78 and 120 days). Of these, S2, S7, and S15 moved south/south-east into the Cape Verde islands area, while S3 moved south-west into oligotrophic waters (**Figure 1**). The spatial distribution pattern for sharks tagged in the West Atlantic was more complex. Of the seven individuals tagged, four blue sharks (S5, S10, S11, and S12) remained in the overall area associated with the Gulf Stream (the North Atlantic Current/Labrador Current convergence zone) generally moving north along the edges of the frontal area, for periods ranging from seven to 89 days (**Figure 1**). Two sharks (S6 and S9) moved south into warmer waters (for 56 and 120 days, respectively) and one shark (S13) moved west into the shelf area off the American east coast, south of Nova Scotia. This shark was tracked for 180 days and was the only to have moved into cold surface waters (**Supplementary Figure 2**).

Diel Diving Behaviour

Periodograms of individual maximum dive depth for each 6 h bin showed a significant cyclic behaviour for 12 (out of 15) sharks, of which 11 individuals peaked significantly within the 23–25 h range, which was considered to represent a diel rhythm (Shepard et al., 2006; Campbell et al., 2010). The periodogram of S3 peaked significantly at 12 h, while the analysis was non-significant for sharks S8, S11, and S12 (**Table 1**).

Regular nDVM was the most observed behaviour (55.7% of the time; **Figure 2A**), followed by surface-oriented (22.8% of the time; **Figure 2C**) and finally, depth-oriented nDVM (17.5% of the time; **Figure 2B**). Overall, the time-weighted depth of blue sharks was significantly deeper during daytime and shallower during nighttime (pairwise Wilcoxon signed rank test, $V = 27243$, $\alpha = 0.05$, $p < 0.001$, $n = 236$), with an average day-time depth of 175 ± 99 m and an average night-time depth of 59 ± 46 m. The same pattern was observed for each diel behaviour; while performing regular nDVM, the average day-time depth of tracked blue sharks was 146 ± 95 m and average night-time was 45 ± 38 m (median: 147 m and 33 m, respectively), whereas in depth-oriented nDVM behaviour, average day-time depth was 246 ± 74 m and night-time 92 ± 42 m (median: 244 m and 95 m, respectively). For surface-oriented behaviour, a shallower average depth was observed, with an average depth of 101 ± 49 m during the day and 19 ± 12 m during the night (median: 116 m and 21 m, respectively). Hence, the median day and night-time depth for each diel behaviour was different (Kruskal–Wallis rank sum test, daytime: chi-squared = 77.276, $\alpha = 0.05$, $p < 0.001$, $n = 236$; night-time: chi-squared = 73.78, $\alpha = 0.05$, $p < 0.001$, $n = 236$). Moreover, during the day, time-weighted water temperature was significantly colder (19.34 ± 3.16°C) than at night (23.26 ± 2.99°C; pairwise Wilcoxon signed rank test, $V = 29306$, $\alpha = 0.05$, $p < 0.001$, $n = 259$). This general pattern was consistent across diel behaviours; during nDVM, average day-time temperature was 20.83 ± 3.10°C and average night-time temperature was 23.39 ± 3.33°C (paired Wilcoxon signed rank exact test, $V = 3125$, $\alpha = 0.05$, $p < 0.001$, $n = 88$); while sharks were performing depth-oriented nDVM, the average temperature was 17.53 ± 2.66°C and 23.02 ± 2.50°C for day- and night-time, respectively (paired Wilcoxon signed rank exact test, $V = 2065$, $\alpha = 0.05$, $p < 0.001$, $n = 64$). Finally, for surface-oriented behaviour, average day-time temperature was 18.85 ± 2.42°C and 23.28 ± 3.11°C at night (paired Wilcoxon signed rank exact test, $V = 611$, $\alpha = 0.05$, $p < 0.001$, $n = 35$). However, time weighted temperatures during the day were positively correlated with the time-weighted temperatures experienced in consecutive nights (Pearson correlation = 0.49, $t = 8.66$, $\alpha = 0.05$, $p < 0.001$, $n = 244$).

TABLE 1 | Summary data for satellite-tagged blue sharks.

Shark ID	Fork length (cm)	Sex	Tag type	Location tagged	Tagging date	Days-at-liberty	Pop-up date	%DVM	Periodogram
Shark 1	260	M	PAT-Mk10	Mid-Atlantic	21/08/2011	90	30/12/2011	93.75	24
Shark 2	250	M	PAT-Mk10	Mid-Atlantic	22/08/2011	120	20/12/2011	94.74	24.02
Shark 3*	240	M	PAT-Mk10	Mid-Atlantic	26/08/2011	78	24/12/2011	68.75	12
Shark 4	200	M	PAT-Mk10	Mid-Atlantic	26/08/2011	120	24/12/2011	95.83	24.02
Shark 5	185	M	PAT-Mk10	West Atlantic	26/06/2010	89	23/09/2010	100	23.99
Shark 6	192	F	PAT-Mk10	West Atlantic	27/06/2010	56	25/09/2010	100	23.94
Shark 7	240	F	PAT-Mk10	Mid-Atlantic	21/08/2011	90	19/11/2011	100	24.02
Shark 8	240	F	PAT-Mk10	Mid-Atlantic	26/08/2011	120	25/12/2011	78.57	ns
Shark 9	260	F	PAT-Mk10	West Atlantic	29/06/2010	120	27/10/2010	70.83	24.01
Shark 10	240	F	PAT-Mk10	West Atlantic	30/06/2010	27	27/12/2010	100	24.09
Shark 11*	200	M	PAT-Mk10	West Atlantic	25/06/2010	14	23/10/2010	100	ns
Shark 12	210	M	PAT-Mk10	West Atlantic	25/06/2010	7	23/10/2010	100	ns
Shark 13	235	M	PAT-Mk10	West Atlantic	25/06/2010	180	22/12/2010	58.82	23.99
Shark 14	220	F	PAT-Mk10	Mid-Atlantic	27/08/2011	120	25/12/2011	95.45	24.06
Shark 15*	220	F	PAT-Mk10	Mid-Atlantic	28/08/2011	94	30/11/2011	100	23.97
DNR 1	165	F	PAT-Mk10	West Atlantic	25/06/2010	120	23/10/2010	–	–
DNR 2	170	F	PAT-Mk10	West Atlantic	30/06/2010	Failed	–	–	–
DNR 3	185	M	PAT-Mk10	West Atlantic	25/06/2010	Failed	–	–	–
DNR 4	230	F	PAT-Mk10	Mid-Atlantic	28/08/2011	180	24/02/2012	–	–
DNR 5	220	F	PAT-Mk10	Mid-Atlantic	29/08/2011	180	25/02/2012	–	–
DNR 6	240	M	PAT-Mk10	Mid-Atlantic	27/08/2011	180	23/02/2012	–	–
DNR 7	245	M	PAT-Mk10	Mid-Atlantic	27/08/2011	180	23/02/2012	–	–

F, female; M, male; Ns, non-significant periodogram.
Starred individuals indicate archival data was retrieved from the tag.

Similarly, for a subset of archival data, average time-weighted temperatures during day-time dives were positively correlated with night-time dives (Spearman correlation = 0.18, S = 848744, α = 0.05, $p < 0.05$, $n = 184$).

Environmental-Linked Behavioural Changes

The vertical behaviour of the sharks changed throughout the tracking period in relation to both encountered temperature and chlorophyll *a* concentration in the water column, with regular nDVM (and surface-oriented) behaviour generally associated with colder, more productive waters (**Figure 3**). In contrast, depth-oriented diel behaviour was commonly observed in regions with less productive, warmer surface waters, but, strikingly, with deep chlorophyll *a* maxima layers (**Figure 3**). Similar patterns were evident from high-resolution archival data (**Figure 4**). Regular nDVM was generally characterised by shallower day-time dives, colder surface waters ($23.55 \pm 3.76°C$) and higher chlorophyll *a* concentrations near the surface (**Figures 4A,C**), while depth-oriented nDVM was performed in regions of warmer ($27.35 \pm 0.80°C$), oligotrophic surface waters, and lower, deeper maximum concentrations of chlorophyll *a* (**Figures 4B,D**). Differences in habitat use were also clear between the two diel behaviours over 24 h periods (**Figure 5**). During both normal diel patterns, sharks showed greater night-time occupation of waters above *ca.* 25°C (**Figures 5A,B**), however, during nighttime, a consistent occupation in lower temperatures ($<17°C$) was evident during depth-oriented nDVM (**Figure 5D**). Similarly, blue sharks maximised time at medium to high ($>4.5 \times 10^{-2}$ mg m^{-3}) chlorophyll *a* concentrations during nighttime (**Figures 5C,D**), although time spent at these concentrations was greater during regular nDVM (**Figure 5C**). Importantly, in depth-oriented nDVM, a peak in the amount of time spent in layers of low chlorophyll *a* concentrations (*ca.*$<1.4 \times 10^{-2}$ mg m^{-3}) was also observed during daytime (**Figure 5D**).

The GLMM analysis revealed that day-time occupancy in shallow water (i.e., TAD above 250 m) significantly increased with decreasing (i) water temperature at depth (100 m), and (ii) with increasing concentration of chlorophyll *a* (**Table 2**, **Figure 6**, and **Supplementary Figure 3**). The depth of the maximum concentration of chlorophyll *a* was inversely correlated with the concentration (Spearman's rank correlation: rho = −0.92, $S = 30395248$, p-value < 0.001, $n = 456$); hence, the observed increased shark day-time occupancy in shallow water was also linked to the shoaling depth of the chlorophyll *a* maximum. Therefore, regular nDVM was predominantly observed associated with the Gulf Stream and the North Atlantic Current-Labrador Current convergence zone (NAC-LCCZ), but also in mid-Atlantic regions and in the proximity of archipelagos, such as the Azores and Cape Verde (**Figure 7A**). Surface-oriented behaviour was almost exclusively observed off the American east coast, in the vicinity of the Gulf Stream and in the mid-Atlantic (**Supplementary Figure 4**), whereas depth-oriented nDVM was generally observed during southward movements in mid-Atlantic regions (**Figure 7B**). Interestingly, almost no spatial overlap was observed between the two nDVM behaviours.

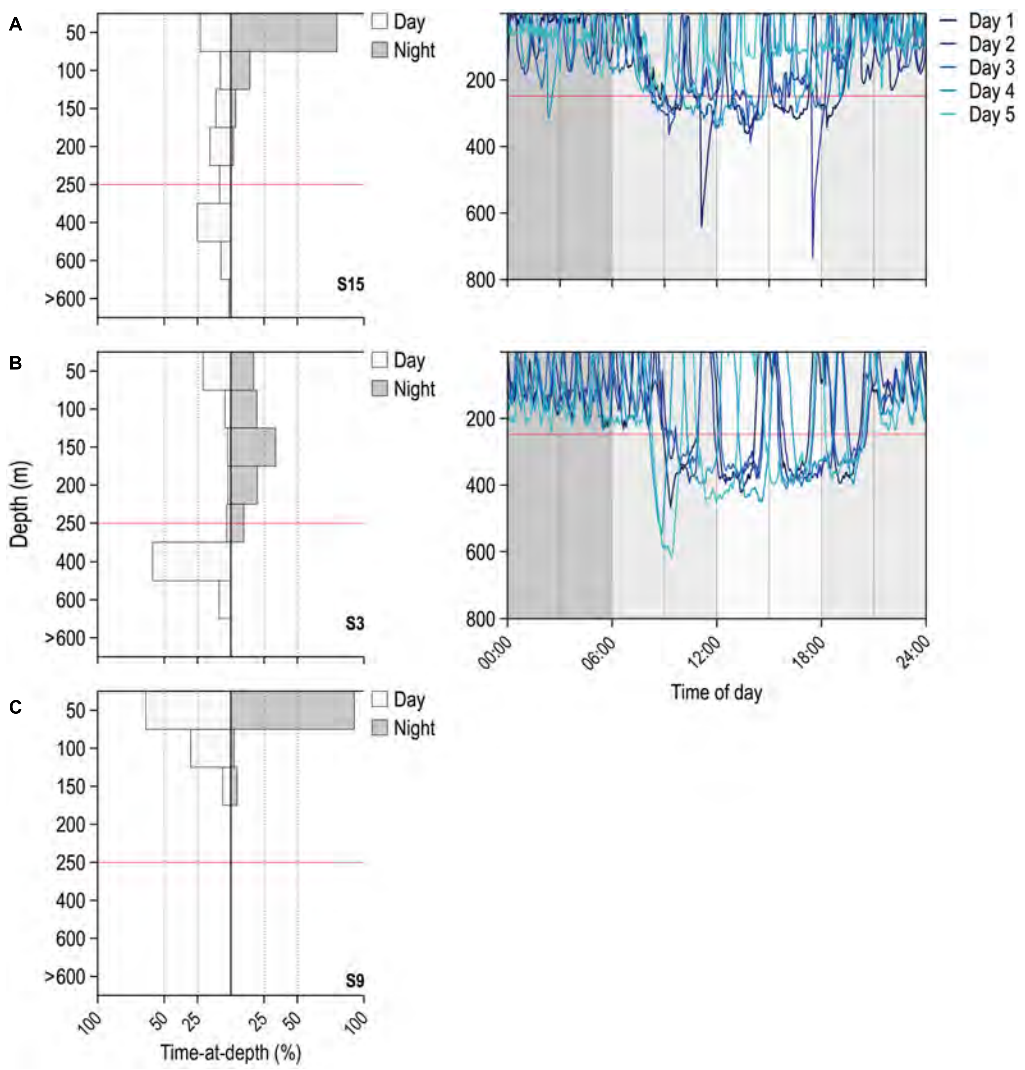

FIGURE 2 | Diel behaviour of blue sharks. Left panel shows the percentage of time-at-depth for day- (white) and night-time (grey) for **(A)** nDVM (day-time occupancy above 250 m: 66.0%), **(B)** depth-oriented nDVM (32.7%), and **(C)** surface-oriented (100%) diel diving behaviours; Right panels show the correspondent 5-day archival depth use. Horizontal red lines denote the depth threshold considered to define each diel class (250 m depth).

This resulted in a latitudinal pattern, with surface-oriented and regular nDVM commonly observed in high latitudes of colder, productive waters (**Figure 8**). Regular nDVM was also frequent in low latitudes but only associated with cold, productive waters of frontal regions (in the western Africa upwelling region) (**Figures 7A**, **8**). The depth-oriented nDVM more frequently observed in lower latitudes of warmer, deep chlorophyll *a* maxima and oligotrophic waters (**Figure 8**).

Lunar Phase and Overlap With Surface Longlining Hooks

During nights of new moon, occupation of surface waters (less than 100 m; average: 81.9% ± 22.4) was higher than in nights of full moon (70.6% ± 25.5; Wilcoxon rank sum test, $W = 15862$, $\alpha = 0.05$, $p < 0.001$, $n = 424$). However, TAD_{hook} was significantly greater on nights of full moon when compared to nights of new moon (15.55% ± 22.28 and 9.37% ± 18.06, respectively; Wilcoxon rank sum test, $W = 25475$, $\alpha = 0.05$, $p < 0.01$, $n = 424$). In fact, along shark geolocations, both fishing effort (890 ± 611 fishing days) as well as CPUE were also highest on nights of full moon (278 ± 144 kg grid cell^{-1} set^{-1}) when compared to nights of new moon (687 ± 443 days and 253 ± 192 kg grid cell^{-1} set^{-1}, respectively; Wilcoxon rank sum test, fishing effort: $W = 25475$, $\alpha = 0.05$, $p < 0.01$, $n = 284$; CPUE: $W = 5777$, $\alpha = 0.05$, $p < 0.01$, $n = 194$).

DISCUSSION

Blue sharks performed extensive movements covering a large area of the North Atlantic, with results showing that diel

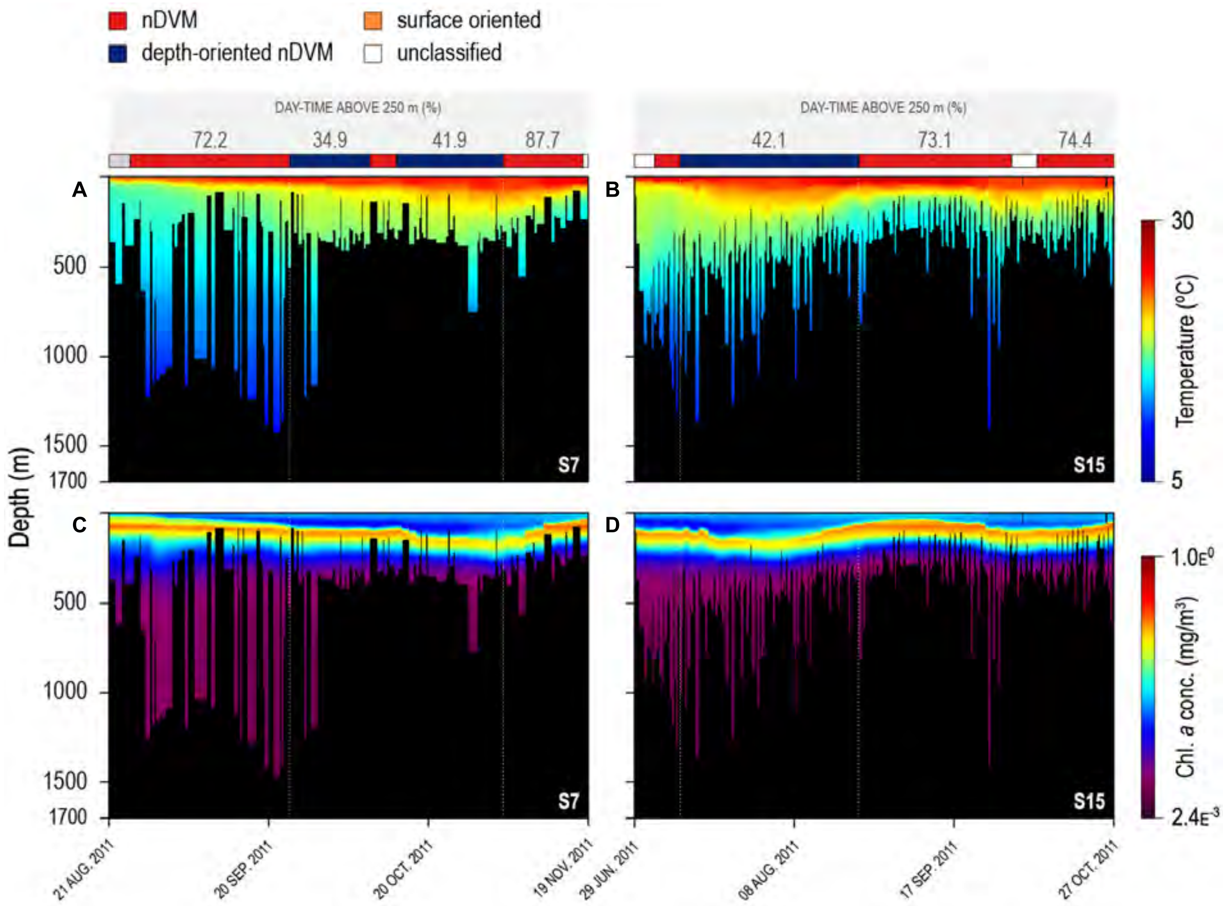

FIGURE 3 | Maximum daily dive depths for two individual blue sharks, shark #7 on the left **(A,C)** and #15 on the right **(B,D)**. Dive series are overlaid on water temperature **(A,B)** and chlorophyll *a* concentration **(C,D)**. Coloured bar above represent the identified diel behaviour.

behaviours shifted in response to environmental changes. Specifically, sharks (i) spent more time at depth in less productive, warmer, and deep chlorophyll *a* maximum regions, and (ii) performed behavioural patterns linked with surface occupancy in colder, more productive waters. The latter was also associated with a higher spatio-temporal overlap with hook depths and thus, higher fishing risk in these areas, particularly on nights of full moon.

Horizontal Movements

Tracked sharks performed typical, extensive movements in the open ocean of the North Atlantic and also into shelf waters. Such movements are generally thought to be part of long-distance, seasonal migrations linked with foraging and/or reproduction (Queiroz et al., 2005; Nakano and Stevens, 2008; Stevens, 2010). During summer, blue sharks typically migrate north following the warming of surface waters at higher latitudes (Queiroz et al., 2010), exemplified by known movements into productive waters of the northern Gulf Stream and North Atlantic Current (Queiroz et al., 2019). Movements into shelf waters also occur, which allows sharks to forage on shelf-associated seasonal schools of small pelagic fish and tuna (Henderson et al., 2001; Southward et al., 2004). Hence, the summer diet of blue sharks in northern latitudes has been described to shift from being typically comprised of cephalopods to a preference for teleosts (Stevens, 1973).

Besides performing extensive horizontal movements, blue sharks we tracked also displayed high residency in specific regions, broadly associated with mesoscale oceanic features, such as thermal fronts and upwelling regions. For example, individuals tracked in the West Atlantic showed greater occupation of the Gulf Stream and the NAC-LCCZ, both frontal regions of high primary productivity and forage accumulation, where megafauna is known to aggregate (Campana et al., 2011; Scales et al., 2014; Braun et al., 2019b). Similarly, sharks tagged in the mid-Atlantic, near the Azores archipelago showed a longer residence within this area, which has been previously described as a preferred wintering ground for this species (Vandeperre et al., 2014). Three sharks displayed southward movements during the winter into the tropical Atlantic likely following warm SST isotherms toward southern waters (Queiroz et al., 2012). Female blue sharks S7 and S14 moved into the Eastern Tropical Atlantic (ETA), a highly productive area associated with the strong West African

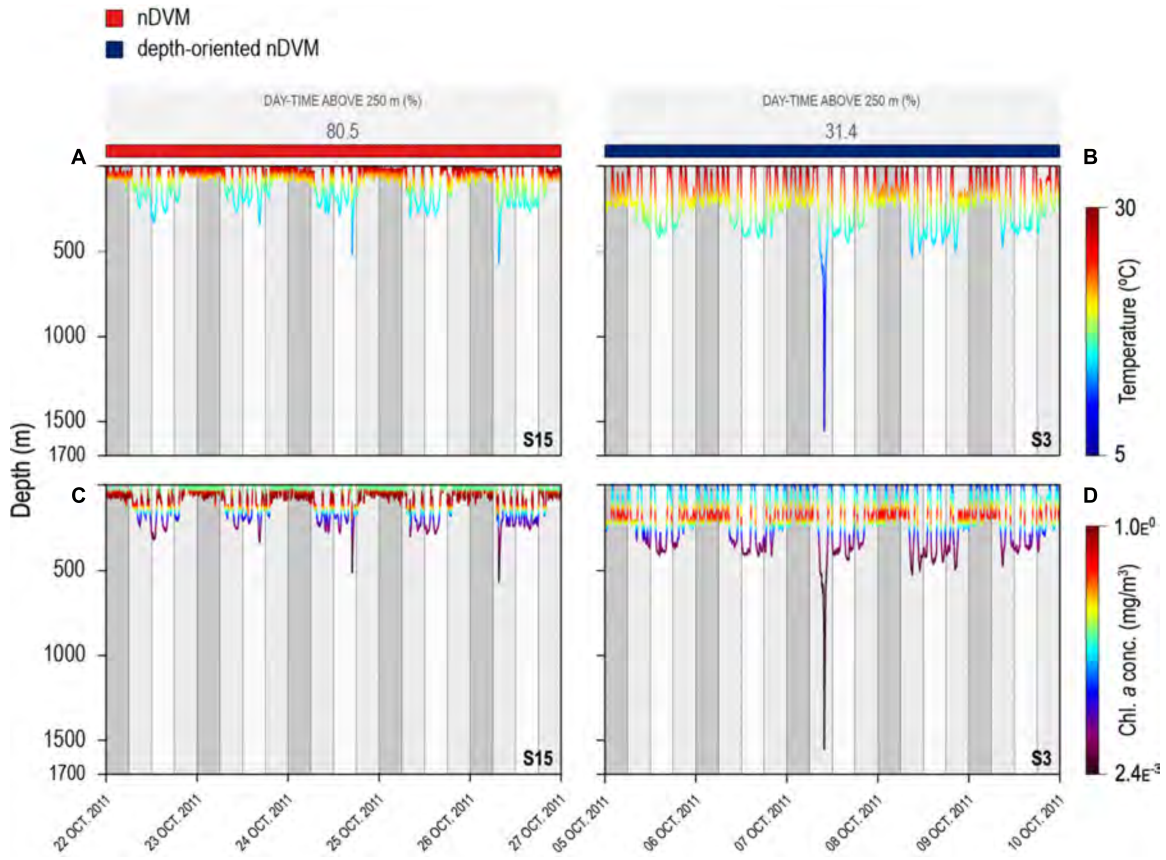

FIGURE 4 | Archival 5-day period depth series for two individual blue sharks, during nDVM for shark #15 on the left **(A,C)** and depth-oriented nDVM for shark #3 on the right **(B,D)**. Shark depth is overlaid with water temperature **(A,B)** and chlorophyll *a* concentration **(C,D)**. Coloured bar above represent the identified diel behaviour.

upwelling regime (Karstensen et al., 2008; Stramma et al., 2010; Gilly et al., 2013).

Diel Vertical Movements

The majority of tracked sharks in this study displayed a cyclical behaviour, with 11 out of 15 individuals showing a diel rhythm [peak within 23–25 h range; (Campbell et al., 2010)]. The vertical movements for one individual were cyclic at 12 h (semi-diel rhythm; S3) indicating circatidal movements (Shepard et al., 2006). However, no diel behaviour was detected (i.e., the periodogram was non-significant) for three individuals. These were either tracked for short periods of time (seven to 14 days, for S12 and S11, respectively) or were frequently recorded diving to extreme depths (S8). In this last case, the irregularity of deep dives along the tracking period could have reduced the chance of detecting cyclical patterns in the maximum depth, and thus a significant diel pattern. Nonetheless, using Lomb-Scargle periodograms we were able to identify cyclical rhythms for the majority of the tracked sharks, likely because it is robust to the presence of non-regular and zero-inflated data, both of which are usually considered to be typical disadvantages of satellite relayed telemetry data (Ruf, 2010; Schaffeld et al., 2016).

Interestingly, this study observed for the first time, to our knowledge, semi-diel movements for pelagic sharks in the open ocean. Instead, these have been often described for sharks associated with coastal and shelf areas, where the cyclical tidal transport of zooplankton influences the behaviour of predators in higher trophic levels (Shepard et al., 2006; Rodríguez-Cabello et al., 2016). Nonetheless, shark S3 was tracked moving exclusively in the open ocean, with frequent excursions into the bathyal (maximum dive depth of 1,704 m), possibly associated with deep-water foraging on organisms influenced by semi-diel patterns in deep-water currents. Indeed, semi-diel vertical migrations have also been observed in open-ocean deep-sea communities at over 1,000 m depth (Aguzzi et al., 2010, 2018), where tidal effects propagate throughout the water column from changes in strength and direction of deep-water currents (Uiblein et al., 2002; Trenkel et al., 2004; Lorance and Trenkel, 2006; Aguzzi et al., 2010) and by variations in temperature and salinity (Ratsimandresy et al., 2017). Furthermore, bathymetric features, such as deep-sea banks or ridges, create a displacement in the water column structure and on deep-water currents (Genin, 2004; Cotté and Simard, 2005), potentially favouring plankton advection from the bathyal to shallower depths, thereby acting as an upwelling area highly attractive for pelagic

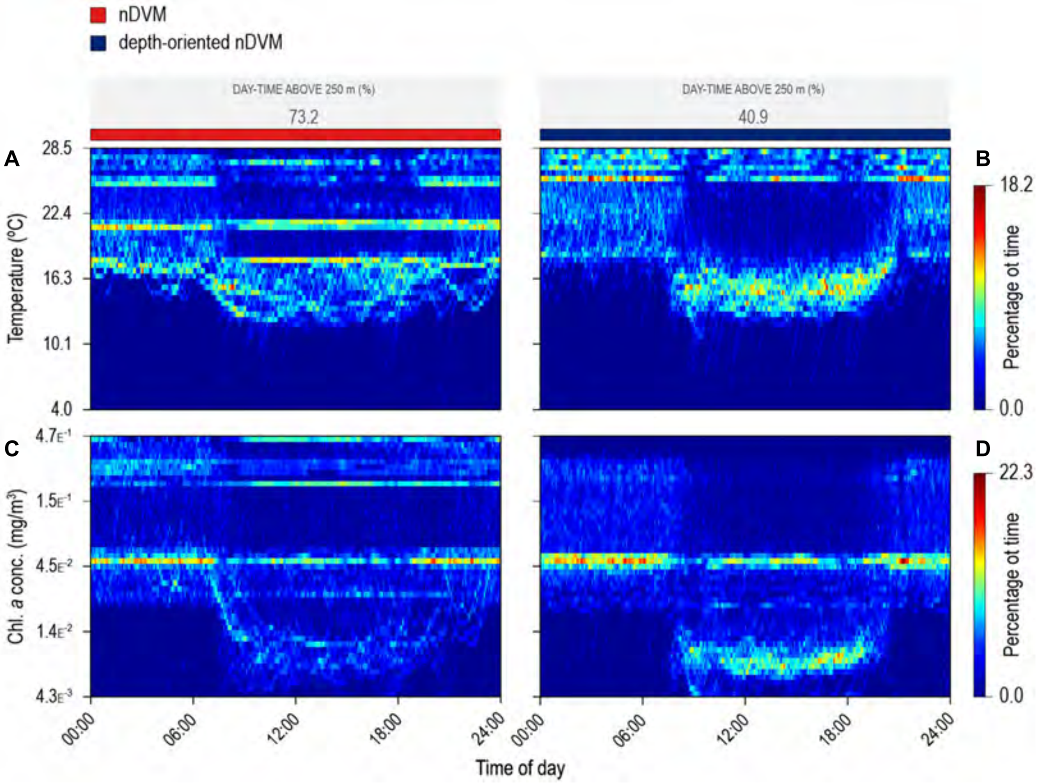

FIGURE 5 | Blue shark habitat-use for a 24 h period, during nDVM on the left **(A,C)** and depth-oriented nDVM on the right **(B,D)**. Time-at-temperature **(A,B)**; and time-at-chlorophyll *a* **(C,D)**. Coloured bar above represents the identified diel behaviour.

predators (Genin, 2004). Despite this, a semi-diel rhythm was only observed for one of the tracked individuals, with most sharks performing cyclic diel behaviour.

DVM can be observed at a global scale, from plankton to top predators (Longhurst and Harrison, 1989; Zhang and Dam, 1997), being possibly associated with thermoregulatory movements and/or as an optimisation of foraging (e.g., Sims et al., 2006; Last et al., 2016; Hafker et al., 2017). For example, by reducing day-time activity in deep, cold waters and foraging at night in shallow, warm waters, catsharks enhance energetic efficiency by conserving metabolic expenditure (Sims et al., 2006). Similarly, the blue sharks we tracked experienced significantly lower temperatures during the day than at night. This pattern was consistent for the three identified diel behaviours. Hence, we cannot exclude that blue sharks benefit from energy conservation by occupying colder waters during the day; however, our findings show no evidence that sharks re-surface at night to recover from heat loss, since day-time mean temperatures were positively correlated with the successive night (both using histogram or archival data) which does not support the behavioural thermoregulation hypothesis from the data we collected. If blue sharks were thermoregulating on a diel basis a negative relationship between daytime temperatures and consecutive nighttime temperatures is expected, where the colder the time-weighted temperatures experienced during the day were, the warmer the temperatures at night were expected to be (Thums et al., 2013); however, this was not the pattern we observed. It is possible that deep dives undertaken during the night would have been observed if sharks were diving to reduce internal temperature (Campana et al., 2011), however, during this period, the blue sharks we tracked remained largely in shallow waters above 250 m. Hence, our collective results indicate that the vertical patterns we recorded were most likely linked to prey aggregations and associated depth changes. The occupation of near-surface depths at night together with day-time mesopelagic dives were indicative of tracked blue sharks maximising the day/night spatial overlap with aggregations of diel vertically migrating prey, potentially increasing foraging success (Campana et al., 2011; Queiroz et al., 2012; Hammerschlag et al., 2016). Furthermore, regular nDVM and surface-oriented behaviour of sharks in this study were frequently observed associated with

TABLE 2 | Summary of the generalised linear mixed model (GLMM) comparing shark day-time occupancy in shallow water (i.e., TAD above 250 m) in response to water temperature at depth (100 m) and concentration of the chlorophyll *a* maximum ($n = 456$; *p*-value: ***<0.001; **<0.01).

	Value	Std. Error	DF	*t*-value	*p*-value
(Intercept)	1.140	0.195	440	5.850	<0.001***
Scaled maximum concentration of chlorophyll *a*	0.364	0.126	440	2.895	<0.01**
Scaled temperature at depth	−0.415	0.132	440	−3.142	<0.01**

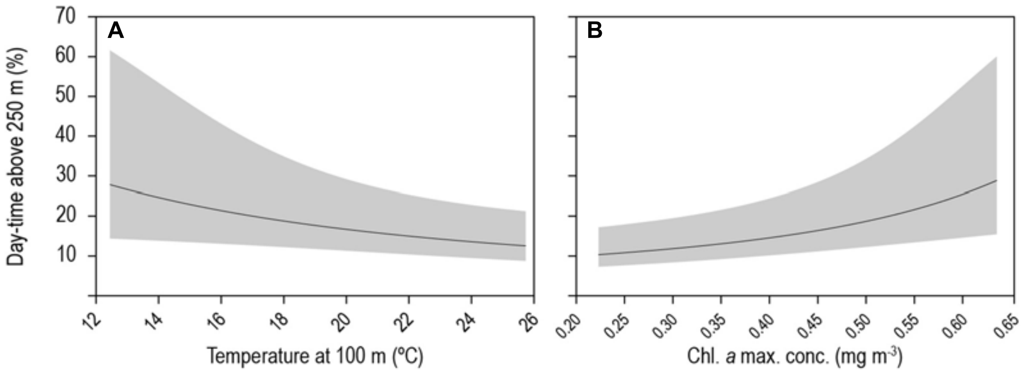

FIGURE 6 | Generalised linear mixed model (GLMM) relationships between blue shark day-time occupancy above 250 m depth and environmental variables. GLMM predicted probabilities of depth-use along **(A)** temperature at depth (100 m) and **(B)** concentration of the chlorophyll *a* maximum. Continuous lines represent mean predicted values for the species and shaded areas represent the 95% confidence intervals.

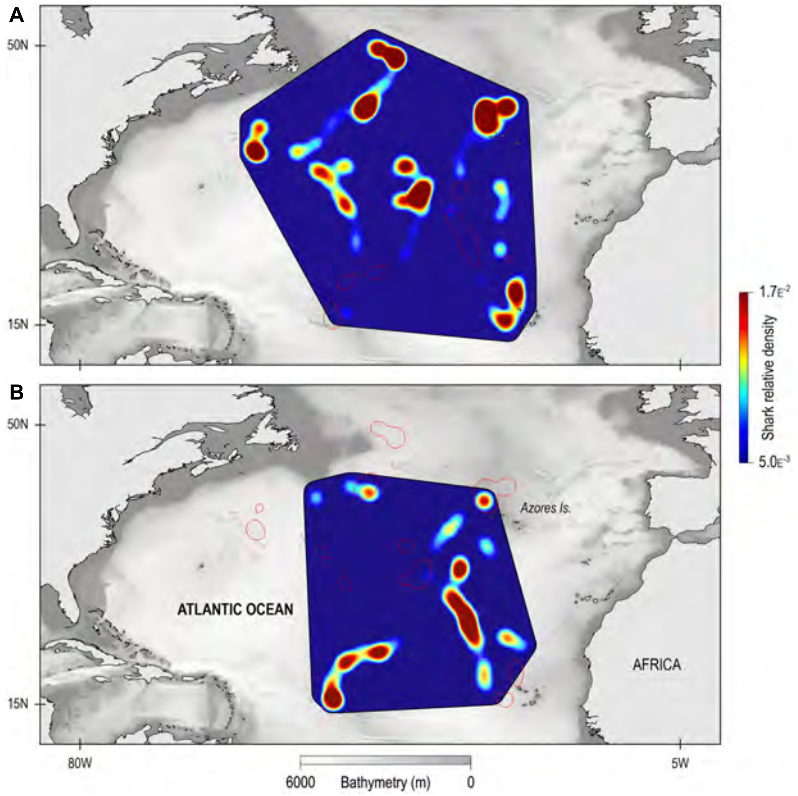

FIGURE 7 | Kernel density estimates of space-use of tracked blue sharks, for **(A)** nDVM and **(B)** depth-oriented nDVM. The red dashed line denotes the 90th percentile for depth-oriented nDVM (top) and nDVM (bottom) shown to exemplify the mismatch in hotspot location of the different behaviours.

areas where prey typically aggregates near the surface, such as frontal regions, e.g., the NAC-LCCZ and the western Africa upwelling region (Sims et al., 2006; Campana et al., 2011). In these areas, sharks also maximised time in shallow layers with high chlorophyll *a* concentration, where prey densities are putatively higher (Ainley et al., 2005).

Vertical movements largely driven by tracking prey aggregations could also explain our observation of depth-oriented nDVM occurring in warm, oligotrophic surface waters in the mid-Atlantic region, where tracked blue sharks spent a larger proportion of the daytime targetting layers of maximum productivity at depth. The increased vertical overlap with layers of chlorophyll *a* maxima suggests blue sharks were targetting prey aggregations at depth (Bianchi et al., 2013), such as energetically profitable squid (Clarke et al., 1996; Galván-Magaña et al., 2013). Shifts in diel behaviours (for example,

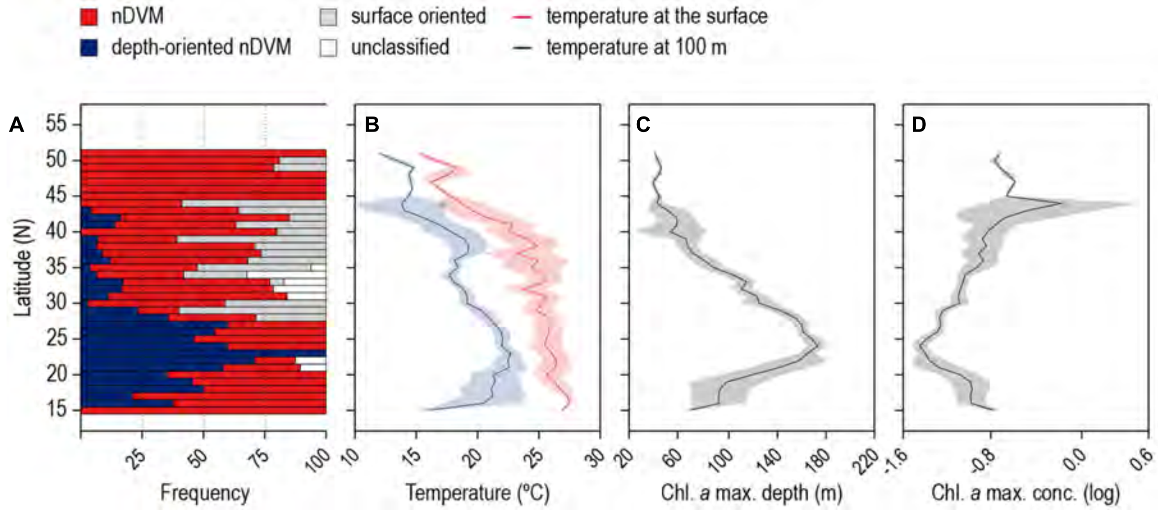

FIGURE 8 | Latitudinal variation between 15 and 51°N for the **(A)** frequency of classified diel behaviours, **(B)** average temperature at the surface (red) and at 100 m depth (blue), **(C)** depth and **(D)** concentration of the chlorophyll *a* maximum in the water column.

from regular nDVM to a distinctive depth-oriented nDVM) in response to increases in the abundance of deep-water prey, such as cephalopods or mesopelagic fish, were previously observed for blue sharks in the North Atlantic (Campana et al., 2011; Queiroz et al., 2012). Moreover, other top predators that feed on similar vertically migrating prey, such as tuna and swordfish, also displayed consistent cyclical tracking of the deep scattering layer (DSL), likely to maximise foraging success (Schaefer et al., 2009; Dewar et al., 2011; Sepulveda et al., 2018). Finally, our results demonstrate that the frequency of diel diving patterns showed a latitudinal gradient, with regular and depth-oriented nDVM generally observed in non-overlapping regions of the North Atlantic at higher latitudes, and higher day-time occupation of deep waters occurring toward lower latitudes. Taken together, our results suggest that the vertical movements of blue sharks were intricately linked to the water column profile, and consequently, to prey distribution patterns.

Lunar Phase and Overlap With Surface Longlining Hooks

During nights of new moon blue shark dives were generally restricted to shallow waters (between the surface and 100 m depth), while on nights of full moon, sharks displayed an increased occupation of depths between 100 and 250 m. Although several studies have related fish vertical movement shifts to the lunar phase (e.g., Bestley et al., 2009; Abascal et al., 2010; Eveson et al., 2018), few studies have described this behaviour for elasmobranchs (Graham et al., 2006; Shepard et al., 2006; Hammerschlag et al., 2016). For example, planktivorous basking sharks showed cyclical lunar activity, with an increased diving frequency fortnightly (Shepard et al., 2006), while the depth of whale sharks varied with lunar illumination, with shallower dives during snapper spawning events in full moon, likely to maximise foraging on fish eggs (Graham et al., 2006). Hence, occupation of deeper waters by blue sharks during nights of full moon may be driven by the phototaxic response of prey to higher luminosity near the surface (identical to the predator avoidance mechanisms triggering DVM) and, thus, prey species are found in deeper layers than on dark new moon nights (Lerner et al., 2013).

Catches of surface longliners targetting swordfish, tunas and sharks are generally higher in periods of increased lunar illumination (Podesta et al., 1993; Curran, 2014; Orbesen et al., 2017). In our study, an increased occupation of deeper depth layers during nights of full moon led to higher overlap with longline hooks [which are generally set 100–300 m depth (Domingo et al., 2016)], which is especially relevant since blue sharks are a commercially important species. We showed that fishing effort (i.e., number of fishing vessels per grid cell) and blue shark catches (CPUE from logbook catch data) were also higher during nights of full moon at the locations where blue sharks were tracked. Therefore, during this period blue sharks were more vulnerable to fishing activity, not only vertically (higher likelihood of hook encounter), but also geographically due to higher fishing pressure occurring in the region.

CONCLUSION

In summary, we found that the diel diving behaviours of blue sharks in relation to environmental fields and lunar illumination act to change the sharks' vulnerability to fishing effort. Greater occupancy of cold, highly productive shallow waters was observed, where susceptibility to hook encounter was also high. Previous studies have linked an increased space-use of highly productive frontal areas by pelagic sharks (including blue sharks) to a higher exposure risk to fishing (Queiroz et al., 2016, 2019). However, despite the large decline of shark populations and the high extinction risk (Baum et al., 2003; Pacoureau et al., 2021), exploitation of the stocks of oceanic sharks has only recently been regulated in the North Atlantic (International Commission for the Conservation of Atlantic Tunas [ICCAT], 2020). Nonetheless, management measures of longline fisheries could be further improved by minimising shark mortality, for example, by implementing spatial management such as seasonal closures and marine protected areas (MPAs), enforcing adaptations to depth of hook deployment, and stronger selectivity of target species by fishing gear to reduce bycatch (Queiroz et al., 2016, 2019; Morgan et al., 2020; Pacoureau et al., 2021). Knowing where and when sharks are more vulnerable to fishing, such as we show here for adult blue sharks, will be important for the implementation of novel dynamic approaches for assessing the status of threatened oceanic sharks (Hays et al., 2019).

DATA AVAILABILITY STATEMENT

The raw data supporting the conclusions of this article will be made available by the authors, without undue reservation.

ETHICS STATEMENT

The animal study was reviewed and approved by the Marine Biological Association of the United Kingdom (MBA) Animal Welfare Ethical Review Body (AWERB).

AUTHOR CONTRIBUTIONS

NQ and DWS planned the data analysis. NQ led the data analysis with contributions from MV and DWS. MV led the manuscript writing with contributions from NQ, DWS, and all other authors. All authors approved the work for publication.

FUNDING

Funding was provided by the Save Our Seas Foundation (DWS and NQ), Fundação para a Ciência e a Tecnologia (FCT) under the grants PTDC/MAR/100345/2008 and COMPETE FCOMP-01-0124-FEDER-010580 and PTDC/BIA-COM/28855/2017 and COMPETE POCI-01–0145-FEDER-028855 (NQ and DWS), Natural Environment Research Council (NERC), United Kingdom (NE/R00997/X/1), European Research Council (ERC-AdG-2019 883583 OCEAN DEOXYFISH), NERC Oceans 2025 Strategic Programme (all to DWS), MARINFO–NORTE-01–0145-FEDER-000031 [funded by Norte Portugal Regional Operational Programme (NORTE2020), under the PORTUGAL 2020 Partnership Agreement, through the European Regional Development Fund (ERDF) to NQ], European Maritime and Fisheries Fund MAR-01.04.02-FEAMP-0006 (RR and NQ), and Xunta de Galicia, Spain, under the Isabel Barreto Programme 2009–2012 (GM). FCT supported NQ (CEECIND/02857/2018), MV (PTDC/BIA-COM/28855/2017), and GM (PTDC/MAR-BIO/4458/2012). DWS was supported by a Marine Biological Association Senior Research Fellowship.

ACKNOWLEDGMENTS

This research is part of the Global Shark Movement Project (globalsharkmovement.org).

SUPPLEMENTARY MATERIAL

The Supplementary Material for this article can be found online at: https://www.frontiersin.org/articles/10.3389/fmars.2021.688076/full#supplementary-material

Supplementary Figure 1 | Archival blue shark depth use **(A)** for a 24 h period, and **(B)** during night-time. Panel above represents the mean light-level for a 24 h period. Shaded red areas represent the twilight periods (time bins between 06:00–12:00 and 18:00–00:00) that were excluded from the analyses. Red line denotes the depth threshold used to classify differences in diel behaviour (i.e., 250 m depth). Notice in **(B)**, that 97.5% of night-time occupancy occurred above this depth threshold."

Supplementary Figure 2 | Tracks for 15 blue sharks overlaid on the average 2010/2011 sea surface temperature.

Supplementary Figure 3 | Pearson residuals from GLMM between blue shark day-time occupancy above 250 m depth and environmental variables. Pearson residuals along **(A)** fitted values; **(B)** concentration of the chlorophyll *a* maximum and **(C)** temperature at depth (100 m). **(D)** Quantile-quantile plot for the Pearson residuals.

Supplementary Figure 4 | Kernel density estimates of space-use of tracked blue sharks for the surface-oriented behaviour. The red dashed line represents the 90th percentile for depth-oriented nDVM shown to exemplify the mismatch in hotspot location of the different behaviours.

REFERENCES

Abascal, F. J., Mejuto, J., Quintans, M., and Ramos-Cartelle, A. (2010). Horizontal and vertical movements of swordfish in the Southeast Pacific. *ICES J. Mar. Sci.* 67, 466–474. doi: 10.1093/icesjms/fsp252

Abascal, F. J., Mejuto, J., Quintans, M., García-Cortés, B., and Ramos-Cartelle, A. (2015). Tracking of the broadbill swordfish, Xiphias gladius, in the central and eastern North Atlantic. *Fish. Res.* 162, 20–28. doi: 10.1016/j.fishres.2014.09.011

Abecassis, M., Dewar, H., Hawn, D., and Polovina, J. (2012). Modeling swordfish daytime vertical habitat in the North Pacific Ocean from pop-up archival tags. *Mar. Ecol. Prog. Ser.* 452, 219–236. doi: 10.3354/meps09583

Aguzzi, J., Costa, C., Furushima, Y., Chiesa, J. J., Company, J. B., Menesatti, P., et al. (2010). Behavioral rhythms of hydrocarbon seep fauna in relation to internal tides. *Mar. Ecol. Prog. Ser.* 418, 47–56. doi: 10.3354/meps08835

Aguzzi, J., Fanelli, E., Ciuffardi, T., Schirone, A., De Leo, F. C., Doya, C., et al. (2018). Faunal activity rhythms influencing early community succession of an implanted whale carcass offshore Sagami Bay, Japan. *Sci. Rep.* 8:11163. doi: 10.1038/s41598-018-29431-5

Ainley, D. G., Spear, L. B., Tynan, C. T., Barth, J. A., Pierce, S. D., Glenn Ford, R., et al. (2005). Physical and biological variables affecting seabird distributions during the upwelling season of the northern California Current. *Deep Sea Res. II Top. Stud. Oceanogr.* 52, 123–143. doi: 10.1016/j.dsr2.2004.08.016

Andrews, K. S., Williams, G. D., Farrer, D., Tolimieri, N., Harvey, C. J., Bargmann, G., et al. (2009). Diel activity patterns of sixgill sharks, *Hexanchus griseus*: the ups and downs of an apex predator. *Anim. Behav.* 78, 525–536. doi: 10.1016/j.anbehav.2009.05.027

Andrzejaczek, S., Gleiss, A. C., Pattiaratchi, C. B., and Meekan, M. G. (2019). Patterns and drivers of vertical movements of the large fishes of the epipelagic. *Rev. Fish Biol. Fish.* 29, 335–354. doi: 10.1007/s11160-019-09555-1

Azzurro, E., Aguzzi, J., Maynou, F., José Chiesa, J., and Savini, D. (2012). Diel rhythms in shallow Mediterranean rocky-reef fishes: a chronobiological approach with the help of trained volunteers. *J. Mar. Biol. Assoc. U.K.* 93, 461–470. doi: 10.1017/s0025315412001166

Baum, J. K., Myers, R. A., Kehler, D. G., Worm, B., Harley, S. J., and Doherty, P. A. (2003). Collapse and conservation of shark populations in the Northwest Atlantic. *Science* 299, 389–392. doi: 10.1126/science.1079777

Bestley, S., Gunn, J. S., and Hindell, M. A. (2009). Plasticity in vertical behaviour of migrating juvenile southern bluefin tuna (*Thunnus maccoyii*) in relation to oceanography of the south Indian Ocean. *Fish. Oceanogr.* 18, 237–254. doi: 10.1111/j.1365-2419.2009.00509.x

Bianchi, D., Galbraith, E. D., Carozza, D. A., Mislan, K. A. S., and Stock, C. A. (2013). Intensification of open-ocean oxygen depletion by vertically migrating animals. *Nat. Geosci.* 6, 545–548. doi: 10.1038/ngeo1837

Boerder, K., Schiller, L., and Worm, B. (2019). Not all who wander are lost: improving spatial protection for large pelagic fishes. *Mar. Policy* 105, 80–90. doi: 10.1016/j.marpol.2019.04.013

Braun, C. D., Gaube, P., Afonso, P., Fontes, J., Skomal, G. B., and Thorrold, S. R. (2019a). Assimilating electronic tagging, oceanographic modelling, and fisheries data to estimate movements and connectivity of swordfish in the North Atlantic. *ICES J. Mar. Sci.* 76, 2305–2317.

Braun, C. D., Gaube, P., Sinclair-Taylor, T. H., Skomal, G. B., and Thorrold, S. R. (2019b). Mesoscale eddies release pelagic sharks from thermal constraints to foraging in the ocean twilight zone. *Proc. Natl. Acad. Sci. U.S.A.* 116, 17187–17192. doi: 10.1073/pnas.1903067116

Campana, S. E. (2016). Transboundary movements, unmonitored fishing mortality, and ineffective international fisheries management pose risks for pelagic sharks in the Northwest Atlantic. *Can. J. Fish. Aquat. Sci.* 73, 1599–1607. doi: 10.1139/cjfas-2015-0502

Campana, S. E., Dorey, A., Fowler, M., Joyce, W., Wang, Z., Wright, D., et al. (2011). Migration pathways, behavioural thermoregulation and overwintering grounds of blue sharks in the Northwest Atlantic. *PLoS One* 6:e16854. doi: 10.1371/journal.pone.0016854

Campbell, H. A., Sullivan, S., Read, M. A., Gordos, M. A., and Franklin, C. E. (2010). Ecological and physiological determinants of dive duration in the freshwater crocodile. *Funct. Ecol.* 24, 103–111. doi: 10.1111/j.1365-2435.2009.01599.x

Carey, F. G., Scharold, J. V., and Kalmijn, A. J. (1990). Movements of blue sharks (*Prionace glauca*) in depth and course. *Mar. Biol.* 106, 329–342. doi: 10.1007/bf01344309

Clarke, M. R., Clarke, D. C., Martins, H. R., and Silva, H. M. (1996). The diet of the blue shark (*Prionace glauca* L.) in Azorean waters." Arquipélago. *Life Mar. Sci.* 14, 41–56.

Coffey, D. M., Carlisle, A. B., Hazen, E. L., and Block, B. A. (2017). Oceanographic drivers of the vertical distribution of a highly migratory, endothermic shark. *Sci. Rep.* 7:10434. doi: 10.1038/s41598-017-11059-6

Cotté, C., and Simard, Y. (2005). Formation of dense krill patches under tidal forcing at whale feeding hot spots in the St. Lawrence estuary. *Mar. Ecol. Prog. Ser.* 288, 199–210. doi: 10.3354/meps288199

Curran, D. S. (2014). "Shark catch in pelagic longline fisheries: a review of mitigation measures," in *Proceedings of the WCPFC Scientific Committee 10th Regular Session. WCPFC SC10-2014/EB-IP-11, Majuro, Republic of the Marshall Islands*, (kolonia: WCPFC), 16.

Dewar, H., Prince, E. D., Musyl, M. K., Brill, R. W., Sepulveda, C., Luo, J., et al. (2011). Movements and behaviors of swordfish in the Atlantic and Pacific Oceans examined using pop-up satellite archival tags. *Fish. Oceanogr.* 20, 219–241. doi: 10.1111/j.1365-2419.2011.00581.x

Domingo, A., Forselledo, R., Miller, P., Jiménez, S., Mas, F., and Pons, M. (2016). *General Description of Longline Fisheries. ICCAT Manual*, 312. Madrid: ICCAT.

Duffy, L. M., Kuhnert, P. M., Pethybridge, H. R., Young, J. W., Olson, R. J., Logan, J. M., et al. (2017). Global trophic ecology of yellowfin, bigeye, and albacore tunas: understanding predation on micronekton communities at ocean-basin scales. *Deep Sea Res. II Top. Stud. Oceanogr.* 140, 55–73. doi: 10.1016/j.dsr2.2017.03.003

Dunn, D. C., Harrison, A. L., Curtice, C., DeLand, S., Donnelly, B., Fujioka, E., et al. (2019). The importance of migratory connectivity for global ocean policy. *Proc. R. Soc. B Biol. Sci.* 286:20191472. doi: 10.1098/rspb.2019.1472

Eveson, J. P., Patterson, T. A., Hartog, J. R., and Evans, K. (2018). Modelling surfacing behaviour of southern bluefin tuna in the great Australian bight. *Deep Sea Res. II Top. Stud. Oceanogr.* 157-158, 179–189. doi: 10.1016/j.dsr2.2018.03.007

Francisco, F. A., Nuhrenberg, P., and Jordan, A. (2020). High-resolution, non-invasive animal tracking and reconstruction of local environment in aquatic ecosystems. *Mov. Ecol.* 8:27. doi: 10.1186/s40462-020-00214-w

Galván-Magaña, F., Polo-Silva, C., Hernández-Aguilar, S. B., Sandoval-Londoño, A., Ochoa-Díaz, M. R., Aguilar-Castro, N., et al. (2013). Shark predation on cephalopods in the Mexican and Ecuadorian Pacific Ocean. *Deep Sea Res. II Top. Stud. Oceanogr.* 95, 52–62. doi: 10.1016/j.dsr2.2013.04.002

Genin, A. (2004). Bio-physical coupling in the formation of zooplankton and fish aggregations over abrupt topographies. *J. Mar. Syst.* 50, 3–20. doi: 10.1016/j.jmarsys.2003.10.008

Gilly, W. F., Beman, J. M., Litvin, S. Y., and Robison, B. H. (2013). Oceanographic and biological effects of shoaling of the oxygen minimum zone. *Ann. Rev. Mar. Sci.* 5, 393–420. doi: 10.1146/annurev-marine-120710-100849

Graham, R. T., Roberts, C. M., and Smart, J. C. (2006). Diving behaviour of whale sharks in relation to a predictable food pulse. *J. R. Soc. Interface* 3, 109–116. doi: 10.1098/rsif.2005.0082

Guzman, H. M., Gomez, C. G., Hearn, A., and Eckert, S. A. (2018). Longest recorded trans-Pacific migration of a whale shark (*Rhincodon typus*). *Mar. Biodivers. Rec.* 11:8. doi: 10.1186/s41200-018-0143-4

Hafker, N. S., Meyer, B., Last, K. S., Pond, D. W., Huppe, L., and Teschke, M. (2017). Circadian clock involvement in zooplankton diel vertical migration. *Curr. Biol.* 27 2194–2201.e3. doi: 10.1016/j.cub.2017.06.025

Hammerschlag, N., Skubel, R. A., Calich, H., Nelson, E. R., Shiffman, D. S., Wester, J., et al. (2016). Nocturnal and crepuscular behavior in elasmobranchs: a review of movement, habitat use, foraging, and reproduction in the dark. *Bull. Mar. Sci.* 93, 355–374. doi: 10.5343/bms.2016.1046

Hays, G. C. (2003). A review of the adaptive significance and ecosystem consequences of zooplankton diel vertical migrations. *Hydrobiologia* 503, 163–170. doi: 10.1023/B:HYDR.0000008476.23617.b0

Hays, G. C., Bailey, H., Bograd, S. J., Bowen, W. D., Campagna, C., Carmichael, R. H., et al. (2019). Translating marine animal tracking data into conservation policy and management. *Trends Ecol. Evol.* 34, 459–473. doi: 10.1016/j.tree.2019.01.009

Henderson, A. C., Flannery, K., and Dunne, J. (2001). Observations on the biology and ecology of the blue shark in the North-east Atlantic. *J. Fish Biol.* 58, 1347–1358. doi: 10.1111/j.1095-8649.2001.tb02291.x

Hindell, M. A., Reisinger, R. R., Ropert-Coudert, Y., Hückstädt, L. A., Trathan, P. N., Bornemann, H., et al. (2020). Tracking of marine predators to protect Southern Ocean ecosystems. *Nature* 580, 87–92. doi: 10.1038/s41586-020-2126-y

Howey-Jordan, L. A., Brooks, E. J., Abercrombie, D. L., Jordan, L. K., Brooks, A., Williams, S., et al. (2013). Complex movements, philopatry and expanded depth range of a severely threatened pelagic shark, the oceanic whitetip (*Carcharhinus longimanus*) in the western North Atlantic. *PLoS One* 8:e56588. doi: 10.1371/journal.pone.0056588

Humphries, N. E., Queiroz, N., Dyer, J. R., Pade, N. G., Musyl, M. K., Schaefer, K. M., et al. (2010). Environmental context explains levy and brownian movement patterns of marine predators. *Nature* 465, 1066–1069. doi: 10.1038/nature09116

International Commission for the Conservation of Atlantic Tunas [ICCAT] (2020). *International Commission for The Conservation of Atlantic Tunas Report for biennial period, 2018-19 PART II (2019)*. Madrid: ICCAT.

Johnson, D. S., London, J. M., Lea, M. A., and Durban, J. W. (2008). Continuous-time correlated random walk model for animal telemetry data. *Ecology* 89, 1208–1215. doi: 10.1890/07-1032.1

Jonsen, I. D., Flemming, J. M., and Myers, R. A. (2005). Robust state–space modeling of animal movement data. *Ecology* 86, 2874–2880. doi: 10.1890/04-1852

Karstensen, J., Stramma, L., and Visbeck, M. (2008). Oxygen minimum zones in the eastern tropical Atlantic and Pacific oceans. *Prog. Oceanogr.* 77, 331–350. doi: 10.1016/j.pocean.2007.05.009

Kroodsma, D. A., Mayorga, J., Hochberg, T., Miller, N. A., Boerder, K., Ferretti, F., et al. (2018). Tracking the global footprint of fisheries. *Science* 359, 904–908. doi: 10.1126/science.aao5646

Lam, C. H., Nielsen, A., and Sibert, J. R. (2008). Improving light and temperature based geolocation by unscented Kalman filtering. *Fish. Res.* 91, 15–25. doi: 10.1016/j.fishres.2007.11.002

Lampert, W. (1989). The adaptive significance of diel vertical migration of zooplankton. *Funct. Ecol.* 3, 21–27. doi: 10.2307/2389671

Last, K. S., Hobbs, L., Berge, J., Brierley, A. S., and Cottier, F. (2016). Moonlight drives ocean-scale mass vertical migration of zooplankton during the Arctic winter. *Curr. Biol.* 26, 244–251. doi: 10.1016/j.cub.2015.11.038

Lerner, J. D., Kerstetter, D. W., Prince, E. D., Talaue-McManus, L., Orbesen, E. S., Mariano, A., et al. (2013). Swordfish vertical distribution and habitat use in relation to diel and lunar cycles in the Western North Atlantic. *Trans. Am. Fish. Soc.* 142, 95–104. doi: 10.1080/00028487.2012.720629

Lomb, N. R. (1976). Least-squares frequency analysis of unequally spaced data. *Astrophys. Space Sci.* 39, 447–462. doi: 10.1007/bf00648343

Longhurst, A. R., and Harrison, W. G. (1989). The biological pump: profiles of plankton production and consumption in the upper ocean. *Prog. Oceanogr.* 22, 47–123. doi: 10.1016/0079-6611(89)90010-4

Lorance, P., and Trenkel, V. M. (2006). Variability in natural behaviour, and observed reactions to an ROV, by mid-slope fish species. *J. Exp. Mar. Biol. Ecol.* 332, 106–119. doi: 10.1016/j.jembe.2005.11.007

Mejuto, J., and García-Cortés, B. (2005). Reproductive and distribution parameters of the blue shark *Prionace glauca*, on the basis of on-board observations at sea in the Atlantic, Indian and Pacific Oceans. *Collect. Vol. Sci. Pap. ICCAT* 58, 974–1000.

Morgan, A., Calich, H., Sulikowski, J., Hammerschlag, N., and Yates, K. (2020). Evaluating spatial management options for tiger shark (*Galeocerdo cuvier*) conservation in US Atlantic Waters. *ICES J. Mar. Sci.* 77, 3095–3109. doi: 10.1093/icesjms/fsaa193

Musyl, M. K., Brill, R. W., Boggs, C. H., Curran, D. S., Kazama, T. K., and Seki, M. P. (2003). Vertical movements of bigeye tuna (*Thunnus obesus*) associated with islands, buoys, and seamounts near the main Hawaiian Islands from archival tagging data. *Fish. Oceanogr.* 12, 152–169. doi: 10.1046/j.1365-2419.2003.00229.x

Nakano, H., and Stevens, J. D. (2008). "The biology and ecology of the blue shark, *Prionace glauca*," in *Sharks of the Open Ocean: Biology, Fisheries and Conservation*, eds M. D. Camhi, E. K. Pikitch, and E. A. Babcock (Oxford: Blackwell Scientific), 140–151.

Olivar, M., Pilar, P., Hulley, A., Castellón, A., Emelianov, M., López, C., et al. (2017). Mesopelagic fishes across the tropical and equatorial Atlantic: biogeographical and vertical patterns. *Prog. Oceanogr.* 151, 116–137. doi: 10.1016/j.pocean.2016.12.001

Orbesen, E. S., Snodgrass, D., Shideler, G. S., Brown, C. A., and Walter, J. F. (2017). Diurnal patterns in Gulf of Mexico epipelagic predator interactions with pelagic longline gear: implications for target species catch rates and bycatch mitigation. *Bull. Mar. Sci.* 93, 573–589. doi: 10.5343/bms.2016.1008

Pacoureau, N., Rigby, C. L., Kyne, P. M., Sherley, R. B., Winker, H., Carlson, J. K., et al. (2021). Half a century of global decline in oceanic sharks and rays. *Nature* 589, 567–571. doi: 10.1038/s41586-020-03173-9

Pade, N. G., Queiroz, N., Humphries, N. E., Witt, M. J., Jones, C. S., Noble, L. R., et al. (2009). First results from satellite-linked archival tagging of porbeagle shark, *Lamna nasus*: area fidelity, wider-scale movements and plasticity in diel depth changes. *J. Exp. Mar. Biol. Ecol.* 370, 64–74. doi: 10.1016/j.jembe.2008.12.002

Papastamatiou, Y. P., Watanabe, Y. Y., Demsar, U., Leos-Barajas, V., Bradley, D., Langrock, R., et al. (2018). Activity seascapes highlight central place foraging strategies in marine predators that never stop swimming. *Mov. Ecol.* 6:9. doi: 10.1186/s40462-018-0127-3

Podesta, G. P., Browder, J. A., and Hoey, J. J. (1993). Exploring the association between swordfish catch rates and thermal fronts on US longline grounds in the western North Atlantic. *Cont. Shelf Res.* 13, 253–277.

Poisson, F., Gaertner, J. C., Taquet, M., Durbec, J. P., and Bigelow, K. (2010). Effects of lunar cycle and fishing operations on longline-caught pelagic fish: fishing performance, capture time, and survival of fish. *Fish. Bull.* 108, 268–281.

Punt, A. E. (2019). Spatial stock assessment methods: a viewpoint on current issues and assumptions. *Fish. Res.* 213, 132–143. doi: 10.1016/j.fishres.2019.01.014

Queiroz, N., Humphries, N. E., Couto, A., Vedor, M., da Costa, I., Sequeira, A. M. M., et al. (2019). Global spatial risk assessment of sharks under the footprint of fisheries. *Nature* 572, 461–466. doi: 10.1038/s41586-019-1444-4

Queiroz, N., Humphries, N. E., Mucientes, G., Hammerschlag, N., Lima, F. P., Scales, K. L., et al. (2016). Ocean-wide tracking of pelagic sharks reveals extent of overlap with longline fishing hotspots. *Proc. Natl. Acad. Sci. U.S.A.* 113, 1582–1587. doi: 10.1073/pnas.1510090113

Queiroz, N., Humphries, N. E., Noble, L. R., Santos, A. M., and Sims, D. W. (2010). Short-term movements and diving behaviour of satellite-tracked blue sharks *Prionace glauca* in the northeastern Atlantic Ocean. *Mar. Ecol. Prog. Ser.* 406, 265–279. doi: 10.3354/meps08500

Queiroz, N., Humphries, N. E., Noble, L. R., Santos, A. M., and Sims, D. W. (2012). Spatial dynamics and expanded vertical niche of blue sharks in oceanographic fronts reveal habitat targets for conservation. *PLoS One* 7:e32374. doi: 10.1371/journal.pone.0032374

Queiroz, N., Lima, F. P., Maia, A., Ribeiro, P. A., Correia, J. P., and Santos, A. M. (2005). Movement of Blue Shark, *Prionace glauca*, in the North-East Atlantic based on mark - recapture data. *J. Mar. Biol. Assoc. U.K.* 85, 1107–1112. doi: 10.1017/s0025315405012154

Queiroz, N., Vila-Pouca, C., Couto, A., Southall, E. J., Mucientes, G., Humphries, N. E., et al. (2017). Convergent foraging tactics of marine predators with different feeding strategies across heterogeneous ocean environments. *Front.Mar. Sci.* 4:239. doi: 10.3389/fmars.2017.00239

Ratsimandresy, A., Hamoutene, D., Lang, C., MacSween, C., Marshall, K., Kenny, S., et al. (2017). *Arctic Charr (Salvelinus Alpinus) Distribution in Seawater Cages in Relation to Environmental Conditions: Fisheries and Oceans Canada= Pêches et océans Canada*. Canadian Technical Report of Fisheries and Aquatic Sciences. Fs97-6/3203E-PDF: vi + 20 p. St. John's, NL: Fisheries and Oceans Canada.

Robinson, N. M., Nelson, W. A., Costello, M. J., Sutherland, J. E., and Lundquist, C. J. (2017). A systematic review of marine-based Species Distribution Models (SDMs) with recommendations for best practice. *Front. Mar. Sci.* 4:421. doi: 10.3389/fmars.2017.00421

Rodríguez-Cabello, C., González-Pola, C., and Sánchez, F. (2016). Migration and diving behavior of Centrophorus squamosus in the NE Atlantic. combining electronic tagging and Argo hydrography to infer deep ocean trajectories. *Deep Sea Res. I Oceanogr. Res. Pap.* 115, 48–62. doi: 10.1016/j.dsr.2016.05.009

Ruf, T. (2010). The lomb-scargle periodogram in biological rhythm research: analysis of incomplete and unequally spaced time-series. *Biol. Rhythm Res.* 30, 178–201. doi: 10.1076/brhm.30.2.178.1422

Scales, K. L., Miller, P. I., Hawkes, L. A., Ingram, S. N., Sims, D. W., Votier, S. C., et al. (2014). Review: on the front line: frontal zones as priority at-sea conservation areas for mobile marine vertebrates. *J. Appl. Ecol.* 51, 1575–1583. doi: 10.1111/1365-2664.12330

Scargle, J. D. (1982). Studies in astronomical time series analysis. II-statistical aspects of spectral analysis of unevenly spaced data. *Astrophys. J.* 263, 835–853.

Schaefer, K. M., and Fuller, D. W. (2002). Movements, behavior, and habitat selection of bigeye tuna (*Thunnus obesus*) in the eastern equatorial Pacific, ascertained through archival tags. *Fish. Bull.* 100, 765–788.

Schaefer, K. M., Fuller, D. W., and Block, B. A. (2009). "Vertical movements and habitat utilization of skipjack (*Katsuwonus pelamis*), yellowfin (*Thunnus albacares*), and bigeye (*Thunnus obesus*) tunas in the equatorial Eastern Pacific Ocean, ascertained through archival tag data," in *Tagging and Tracking of Marine Animals with Electronic Devices*, eds J. L. Nielsen, H. Arrizabalaga, N. Fragoso, A. Hobday, M. Lutcavage, and J. Sibert (Dordrecht: Springer Netherlands), 121–144.

Schaffeld, T., Bräger, S., Gallus, A., Dähne, M., Krügel, K., Herrmann, A., et al. (2016). Diel and seasonal patterns in acoustic presence and foraging behaviour of free-ranging harbour porpoises. *Mar. Ecol. Prog. Ser.* 547, 257–272. doi: 10.3354/meps11627

Sepulveda, C. A., Aalbers, S. A., Heberer, C., Kohin, S., and Dewar, H. (2018). Movements and behaviors of swordfishXiphias gladiusin the United States Pacific leatherback conservation area. *Fish. Oceanogr.* 27, 381–394. doi: 10.1111/fog.12261

Sequeira, A. M. M., Hays, G. C., Sims, D. W., Eguíluz, V. M., Rodríguez, J. P., Heupel, M. R., et al. (2019). Overhauling ocean spatial planning to improve marine megafauna conservation. *Front. Mar. Sci.* 6:639. doi: 10.3389/fmars.2019.00639

Sequeira, A. M. M., Rodriguez, J. P., Eguiluz, V. M., Harcourt, R., Hindell, M., Sims, D. W., et al. (2018). Convergence of marine megafauna movement patterns in coastal and open oceans. *Proc. Natl. Acad. Sci. U.S.A.* 115, 3072–3077. doi: 10.1073/pnas.1716137115

Shepard, E. L. C., Ahmed, M. Z., Southall, E. J., Witt, M. J., Metcalfe, J. D., and Sims, D. W. (2006). Diel and tidal rhythms in diving behaviour of pelagic sharks identified by signal processing of archival tagging data. *Mar. Ecol. Prog. Ser.* 328, 205–213. doi: 10.3354/meps328205

Sims, D. W. (2003). Tractable models for testing theories about natural strategies: foraging behaviour and habitat selection of free-ranging sharks. *J. Fish Biol.* 63, 53–73. doi: 10.1111/j.1095-8649.2003.00207.x

Sims, D. W., Southall, E. J., Tarling, G. A., and Metcalfe, J. D. (2005). Habitat-specific normal and reverse diel vertical migration in the plankton-feeding basking shark. *J. Anim. Ecol.* 74, 755–761. doi: 10.1111/j.1365-2656.2005.00971.x

Sims, D. W., Wearmouth, V. J., Southall, E. J., Hill, J. M., Moore, P., Rawlinson, K., et al. (2006). Hunt warm, rest cool: bioenergetic strategy underlying diel vertical migration of a benthic shark. *J. Anim. Ecol.* 75, 176–190. doi: 10.1111/j.1365-2656.2005.01033.x

Song, L., Zhou, J., Zhou, Y., Nishida, T., Jiang, W., and Wang, J. (2009). Environmental preferences of bigeye tuna, *Thunnus obesus*, in the Indian Ocean: an application to a longline fishery. *Environ. Biol. Fish.* 85, 153–171. doi: 10.1007/s10641-009-9474-7

Southward, A. J., Langmead, O., Hardman-Mountford, N. J., Aiken, J., Boalch, G. T., Dando, P. R., et al. (2004). Long-term biological and environmental researches in the western English Channel. *Adv. Mar. Biol* 47, 1–105.

Stevens, J. D. (1973). Stomach contents of the blue shark (*Prionace glauca* L.) off south-west England. *J. Mar. Biol. Assoc. U.K.* 53, 357–361.

Stevens, J. D. (2010). "Epipelagic oceanic elasmobranchs," in *Sharks and Their Relatives II: Biodiversity, Adaptive Physiology and Conservation*, eds J. C. Carrier, J. A. Musick, and M. R. Heithaus (Boca Raton, FL: CRC Press), 3–35.

Stramma, L., Schmidtko, S., Levin, L. A., and Johnson, G. C. (2010). Ocean oxygen minima expansions and their biological impacts. *Deep Sea Res. I Oceanogr. Res. Pap.* 57, 587–595. doi: 10.1016/j.dsr.2010.01.005

Tarling, G. (1999). The effect of lunar eclipse on the vertical migration behaviour of Meganyctiphanes norvegica (Crustacea: Euphausiacea) in the Ligurian Sea. *J. Plankton Res.* 21, 1475–1488. doi: 10.1093/plankt/21.8.1475

Teo, S. L. H., Boustany, A., Dewar, H., Stokesbury, M. J. W., Weng, K. C., Beemer, S., et al. (2006). Annual migrations, diving behavior, and thermal biology of Atlantic bluefin tuna, *Thunnus thynnus*, on their Gulf of Mexico breeding grounds. *Mar. Biol.* 151, 1–18. doi: 10.1007/s00227-006-0447-5

Thums, M., Meekan, M., Stevens, J., Wilson, S., and Polovina, J. (2013). Evidence for behavioural thermoregulation by the world's largest fish. *J. R. Soc. Interface* 10:20120477. doi: 10.1098/rsif.2012.0477

Trenkel, V. M., Lorance, P., and Mahévas, S. (2004). Do visual transects provide true population density estimates for deepwater fish? *ICES J. Mar. Sci.* 61, 1050–1056.

Uiblein, F., Lorance, P., and Latrouite, D. (2002). Variation in locomotion behaviour in northern cutthroat eel (Synaphobranchus kaupi) on the Bay of Biscay continental slope. *Deep Sea Res. I Oceanogr. Res. Pap.* 49, 1689–1703. doi: 10.1016/s0967-0637(02)00065-1

Vandeperre, F., Aires-da-Silva, A., Fontes, J., Santos, M., Serrao Santos, R., and Afonso, P. (2014). Movements of blue sharks (*Prionace glauca*) across their life history. *PLoS One* 9:e103538. doi: 10.1371/journal.pone.0103538

Weng, K. C., Stokesbury, M. J., Boustany, A. M., Seitz, A. C., Teo, S. L., Miller, S. K., et al. (2009). Habitat and behaviour of yellowfin tuna *Thunnus albacares* in the Gulf of Mexico determined using pop-up satellite archival tags. *J. Fish Biol.* 74, 1434–1449. doi: 10.1111/j.1095-8649.2009.02209.x

Whitford, M., and Klimley, A. P. (2019). An overview of behavioral, physiological, and environmental sensors used in animal biotelemetry and biologging studies. *Anim. Biotelem.* 7:26. doi: 10.1186/s40317-019-0189-z

Wilson, S. G., Polovina, J. J., Stewart, B. S., and Meekan, M. G. (2005). Movements of whale sharks (*Rhincodon typus*) tagged at Ningaloo Reef, Western Australia. *Mar. Biol.* 148, 1157–1166. doi: 10.1007/s00227-005-0153-8

Wirsing, A. J., Heithaus, M. R., and Dill, L. (2011). Predator-induced modifications to diving behavior vary with foraging mode. *Oikos* 120, 1005–1012. doi: 10.1111/j.1600-0706.2010.18844.x

Zhang, X., and Dam, H. G. (1997). Downward export of carbon by diel migrant mesozooplankton in the central equatorial Pacific. *Deep Sea Res. II Top. Stud. Oceanogr.* 44, 2191–2202. doi: 10.1016/s0967-0645(97)00060-x

Zuur, A. F., Ieno, E. N., Walker, N., Saveliev, A. A., and Smith, G. M. (2009). *Mixed Effects Models and Extensions in Ecology with R, Statistics for Biology and Health*. New York, NY: Springer-Verlag.

Conflict of Interest: The authors declare that the research was conducted in the absence of any commercial or financial relationships that could be construed as a potential conflict of interest.

frontiers in Marine Science

ORIGINAL RESEARCH
published: 28 July 2021
doi: 10.3389/fmars.2021.686343

Movements, Habitat Use, and Diving Behavior of Shortfin Mako in the Atlantic Ocean

Catarina C. Santos[1,2]*, Andrés Domingo[3], John Carlson[4], Lisa J. Natanson[5], Paulo Travassos[6], David Macías[7], Enric Cortés[4], Philip Miller[8], Fábio Hazin[6†], Federico Mas[8], Josetxu Ortiz de Urbina[7], Pedro G. Lino[1] and Rui Coelho[1,2]

[1] IPMA – Portuguese Institute for Sea and Atmosphere, Olhão, Portugal, [2] CCMAR – Centre of Marine Sciences, University of Algarve, Faro, Portugal, [3] DINARA – Dirección Nacional de Recursos Acuáticos, Laboratorio de Recursos Pelágicos, Montevideo, Uruguay, [4] National Marine Fisheries Service, Southeast Fisheries Science Center, Panama City, FL, United States, [5] National Marine Fisheries Service, Northeast Fisheries Science Center, Narragansett Laboratory, RI, United States, [6] Departamento de Pesca e Aquicultura, Universidade Federal Rural de Pernambuco, Recife, Brazil, [7] Instituto Español de Oceanografía, Fuengirola, Spain, [8] CICMAR – Centro de Investigación y Conservación Marina, Canelones, Uruguay

Edited by:
David Wells,
Texas A&M University at Galveston,
United States

Reviewed by:
Christopher G. Lowe,
California State University,
Long Beach, United States
Kesley Gibson Banks,
Texas A&M University Corpus Christi,
United States

***Correspondence:**
Catarina C. Santos
catarina.santos@ipma.pt

†Deceased

Specialty section:
This article was submitted to
Marine Megafauna,
a section of the journal
Frontiers in Marine Science

Received: *26 March 2021*
Accepted: *06 July 2021*
Published: *28 July 2021*

Citation:
Santos CC, Domingo A, Carlson J, Natanson LJ, Travassos P, Macías D, Cortés E, Miller P, Hazin F, Mas F, Ortiz de Urbina J, Lino PG and Coelho R (2021) Movements, Habitat Use, and Diving Behavior of Shortfin Mako in the Atlantic Ocean. Front. Mar. Sci. 8:686343. doi: 10.3389/fmars.2021.686343

The shortfin mako is one of the most important shark species caught in Atlantic Ocean pelagic fisheries. Given increasing concerns for the stock status of the species, the present study was designed to fill gaps in the knowledge of habitat use and movement patterns of shortfin mako in the Atlantic Ocean. From 2015 to 2019, 53 shortfin makos were tagged with pop-up satellite archival tags within the North, Central, and Southwest Atlantic Ocean, with successful transmissions received from 34 tags. Generally, sharks tagged in the Northwest and Central Atlantic moved away from tagging sites showing low to no apparent residency patterns, whereas sharks tagged in the Northeast and Southwest Atlantic spent large periods of time near the Canary Archipelago and Northwest Africa, and over shelf and oceanic waters off southern Brazil and Uruguay, respectively. These areas showed evidence of site fidelity and were identified as possible key areas for shortfin mako. Sharks spent most of their time in temperate waters (18–22°C) above 90 m; however, data indicated the depth range extended from the surface down to 979 m, in water temperatures ranging between 7.4 and 29.9°C. Vertical behavior of sharks seemed to be influenced by oceanographic features, and ranged from marked diel vertical movements, characterized by shallower mean depths during the night, to yo-yo diving behavior with no clear diel pattern observed. These results may aid in the development of more informed and efficient management measures for this species.

Keywords: fisheries, shortfin mako, Atlantic Ocean, animal behavior, satellite telemetry, shark, pelagic longline

INTRODUCTION

The shortfin mako, *Isurus oxyrinchus*, is a pelagic shark with a circum-global distribution. It occurs from the surface down to at least 1,064 m depth and is occasionally found in coastal waters where the continental shelf is narrow (Compagno, 2001; Stevens, 2008; Abascal et al., 2011; Mucientes-Sandoval et al., 2012; Rogers et al., 2015; Vaudo et al., 2017; Francis et al., 2019). It is among the fastest fishes of the sea and is an ambush predator that feeds on pelagic prey such as cephalopods and teleosts (Stillwell and Kohler, 1982; Compagno, 2001; Maia et al., 2006; Díez et al., 2015). The shortfin mako is one of the most important shark species caught by pelagic longline and gillnet fisheries targeting mainly swordfish and tunas in the Atlantic Ocean, second only to blue shark, *Prionace glauca*, in terms of catches (Campana et al., 2005; Camhi et al., 2008; Mejuto et al., 2009; Coelho et al., 2012). Although they are usually captured as bycatch, shortfin makos were nearly always retained because of their highly prized meat and fins (Camhi et al., 2008; Dulvy et al., 2008; Stevens, 2008; Rigby et al., 2019). The species aggressiveness and power made it one of the most desirable game fishes in the world for recreational anglers (Stevens, 2008). Since their inclusion in 2019 on CITES Appendix II it is possible that discards have increased. However, like many other pelagic sharks, populations of shortfin mako have a limited capacity to resist, and rebound from, high fishing pressure on account of their life history characteristics (Barker and Schluessel, 2005; Dulvy et al., 2008). In all, the shortfin mako is considered one of the shark species at greatest risk of overexploitation in the Atlantic Ocean owing to its low productivity and high susceptibility to pelagic fisheries (Simpfendorfer et al., 2008; Cortés et al., 2010, 2015).

Recent findings indicate that increasing fishing pressure in recent decades has seriously impacted the shortfin mako populations in the Atlantic Ocean. The latest stock assessment carried out in 2017 by the International Commission for the Conservation of Atlantic Tunas (ICCAT, the inter-governmental organization responsible for the management and conservation of pelagic sharks in the Atlantic) showed that the South Atlantic stock had a 32% probability of being overfished and a 42% probability of experiencing overfishing, while for the North Atlantic stock there was a combined 90% probability of the stock being in an overfished state and experiencing overfishing (Anon, 2017). Given the increasing concerns for its stock status, the shortfin mako was recently declared globally Endangered by the IUCN Red List of Threatened Species (Rigby et al., 2019) and also included in 2019 in the CITES Appendix II list, which bans international trade unless proven to be legal and sustainable (CITES, 2019). The current unsustainable fishing mortality levels and population declines bring to light the importance of focusing research efforts on ecological and biological aspects of this species. Animal tracking has become one of the major tools used to understand the ecology and behavior of a variety of marine species, providing essential information for management planning (e.g., Shillinger et al., 2008; Stevens et al., 2010; Graham et al., 2012; Wilson et al., 2015; Ketchum et al., 2020).

Shifts in oceanographic conditions and seasonal variations of highly productive areas are believed to lead large oceanic fishes like sharks to undertake long-distance migrations in search of food and mating grounds (e.g., Weng et al., 2007; Skomal et al., 2009; Francis et al., 2015). Elucidating these movements (i.e., use of space and activity patterns) is therefore fundamental to understand the behavior of a species and its population structure, as well as to define essential habitats, with an aim to implement effective management measures (Camhi et al., 2008; Rogers et al., 2015; Vaudo et al., 2016). Considering the likely possibility of sharks as key-elements in oceanic ecosystems, knowledge of whether they are moving within regions that might be undergoing different types and levels of fishing activity is essential to predict fishing impacts on their populations and throughout the food web. However, even though these issues are of great importance, studying long-term movements of pelagic sharks can be challenging mostly because of the highly migratory nature of the species and the complex logistics involved in this type of studies (Vaudo et al., 2016).

In recent years, satellite tagging has been increasingly used to study a wide range of marine species, including large pelagic fishes (Hammerschlag et al., 2011; Abascal et al., 2015; Wilson et al., 2015; Santos and Coelho, 2018). For the Atlantic Ocean, these studies have provided important information on spatial ecology of several pelagic shark species including Lamniform sharks such as the porbeagle, *Lamna nasus* (e.g., Pade et al., 2009; Saunders et al., 2011; Biais et al., 2017; Skomal et al., 2021) and the basking shark, *Cetorhinus maximus* (e.g., Skomal et al., 2009; Doherty et al., 2017; Braun et al., 2018). In contrast, and despite its historical importance for commercial and recreational fisheries, studies on movement patterns and habitat use of shortfin mako in the Atlantic Ocean are still scarce. In the Atlantic Ocean, satellite tagging data come almost exclusively from shortfin makos tagged in the northwestern area. The most comprehensive study to date was carried out by Vaudo et al. (2017), in which long-term horizontal movements and seasonal distributions were analyzed for 26 shortfin makos. This study reported region-specific movements as well as the species capacity for making long-distance and highly directional excursions. In an earlier study, Vaudo et al. (2016) investigated the vertical movements of eight shortfin makos which occupied a wide range of temperatures and depths, although movements seemed to be highly influenced by ocean temperature. Additionally, a study by Loefer et al. (2005) analyzed data from only one adult male that revealed a diel pattern of vertical movement defined by greater mean depths and larger depth ranges during daytime. Again, vertical movements seemed to be influenced by sea-surface temperatures. More recently, a study by Gibson et al. (2021) reported movement patterns of mostly mature shortfin makos tagged in the northwestern Gulf of Mexico, which seemed to differ by sex. Males made extensive migrations toward the Caribbean Sea and the northeastern United States Atlantic coast, while the lone female demonstrated high fidelity to the Gulf of Mexico coastal shelf. Additionally, a study by Coelho et al. (2020) reported movements of two shortfin makos tagged outside of the northwestern area. These sharks, tagged in the tropical Northeast Atlantic in the Cabo Verde islands region, used areas along the western African continental shelf. In Queiroz et al. (2016, 2019), the Gulf Stream, the North Atlantic Current/Labrador Current convergence zone, the Azores islands, the mid-Atlantic Ridge area, and the upwelling zone off Northwest Africa were identified as high use areas for the shortfin mako.

Here we address these information gaps by presenting the most extensive study to date on habitat use and movements of shortfin mako tagged with PSATs in the Atlantic Ocean. By joining efforts with various research teams working in the Atlantic, we were able to tag a large set of specimens across a wide area. Specific objectives of this study include (1) analyzing horizontal movements and spatial distribution of shortfin mako in the Atlantic Ocean, (2) investigating vertical habitat utilization, and (3) discussing the use of oceanic vs. continental shelf and slope areas by this species in the Atlantic Ocean.

MATERIALS AND METHODS

Tagging Procedure

Tagging took place across a wide area of the Atlantic Ocean, between 2015 and 2019, integrated within the ICCAT Shark Research and Data Collection Programme (SRDCP). The main tagging areas were the Northwest, Northeast, Central, and Southwest Atlantic, with the tagging conducted onboard Uruguayan research vessels, and vessels from the Portuguese, Brazilian, Spanish, and United States pelagic longline fleets (**Figure 1**). The tag deployment was opportunistic when sharks were captured during regular fishing operations and was carried out by scientific fisheries observers and scientists. Sharks were either hoisted alongside the vessel or brought on board for tagging. An umbrella-type nylon dart (Domeier dart) was used to insert the tag laterally to the dorsal musculature below the first dorsal fin base, using the methodology described by Howey-Jordan et al. (2013). Sharks were tagged and released immediately upon capture, without anesthesia, by cutting the gangion line as close as possible to the mouth or removing the hook when possible. Before tag attachment, tags were tested and programmed to record information for periods between 30 and 180 days (see **Supplementary Material**). In addition, during the tagging operation, animals were sexed, and measurements in fork length (FL) taken to the nearest cm. Date and time were recorded for each individual release, and the geographic tagging location (latitude and longitude) was determined by global positioning system (GPS). All shortfin mako tagging was performed in accordance with protocols approved by the ICCAT Standing Committee on Research and Statistics. A total of 53 tags were deployed and two models of PSATs were used: MiniPAT (39) and sPAT tags (14) (see **Supplementary Material**) built by Wildlife Computers.

Data Analysis

Geographic positions at tagging were determined by GPS, while the pop-up locations of transmitting tags were established as the first point of transmission with an Argos satellite. In order to investigate movement patterns, the most probable tracks between tagging and pop-up locations were calculated from miniPATs light level data using astronomical algorithms provided by the tag manufacturer (Pedersen et al., 2011; Wildlife Computers, 2018). For the miniPATs, the daily locations were calculated based on the light levels recorded and using state-space statistical models (GPE3 software, processed through the tag manufacturer web portal). The miniPATs provide observations on twilight, temperature and dive depth, and the state-space modeling approach uses those observations and the corresponding reference data, along with a simple diffusion-based movement model, to generate time-discrete gridded probability surfaces throughout the deployment. The corresponding oceanographic reference data used were from the NOAA Optimum Interpolation SST V2 High Resolution Dataset for the sea surface temperature provided by NOAA/OAR/ESRL PSD, Boulder, CO, United States, from their web site at http://www.esrl.noaa.gov/psd/, and from the NOAA ETOP01 Global Relief Model, "Bedrock" version, for bathymetry (Amante and Eakins, 2009). The grids used were 0.25 × 0.25° of latitude × longitude. From those probability surfaces, the most likely animal locations for a given day/time were derived. In the case of sPATs, light sensors are not optimized for geolocation. Therefore, the distances traveled by the sharks tagged with sPATs were measured in straight lines between the tagging and the pop-up locations.

In order to assess the habitat use among different bathymetric areas, two main areas were considered, namely the continental margins vs. oceanic areas. The continental margins include both the shelf and slope areas, with the shelf defined as the areas where bottom depth is less than 140 m, and the slope defined as the areas wherever bottom depth ranges between 140 and 3,500 m. The oceanic area was considered as that where bottom depths exceed 3,500 m (IFREMER, 2009). The habitat use was then calculated as the number of occurrences recorded within each of those bathymetric areas. Additionally, the time spent within national EEZs vs. international waters was calculated by considering the number of recordings obtained for each area. The time spent within each bathymetric area (continental margins vs. oceanic area) was also calculated for the different size classes (110–140, 141–175, and 176–220 cm FL).

For sharks tagged with miniPATs, vertical habitat use was investigated by calculating the percentage of time-at-depth and time-at-temperature, separately for daytime and night-time. Sunset and sunrise were calculated using the library "RAtmosphere" in R, and took into account the date (Julian day), latitude and longitude (Teets, 2003). Time-at-depth and time-at-temperature data were aggregated into 30 m and 2°C bins, respectively, based on the above analyses. These data were subsequently expressed as a fraction of the total time of observation for each shark, and the fractional data bins averaged across all sharks within each category.

Mortality events were assigned in cases where depth profiles showed individuals rapidly sinking through the water column to depths greater than 1,700 m, thus initiating the tag safety release mechanism, earlier than 30 days after release. Depredation events were assigned in cases where no light changes were detected during a period of several days, with temperature profiles showing sudden increase in temperature that remained above the temperature values measured before ingestion, regardless of depth, until the tag was expelled/regurgitated (see **Supplementary Material**). In these cases, the tracks were estimated excluding all data collected after the depredation event, and the subsequent depth and temperature data were not considered in the habitat use analyses.

Depth and temperature data were tested for normality with Kolmogorov–Smirnov tests with Lilliefors correction and for homogeneity of variances with Levene tests. Given the lack of normality in the data and the heterogeneity of variances, time-at-depth and time-at-temperature were compared between the daily period (daytime vs. night-time), and bathymetric areas

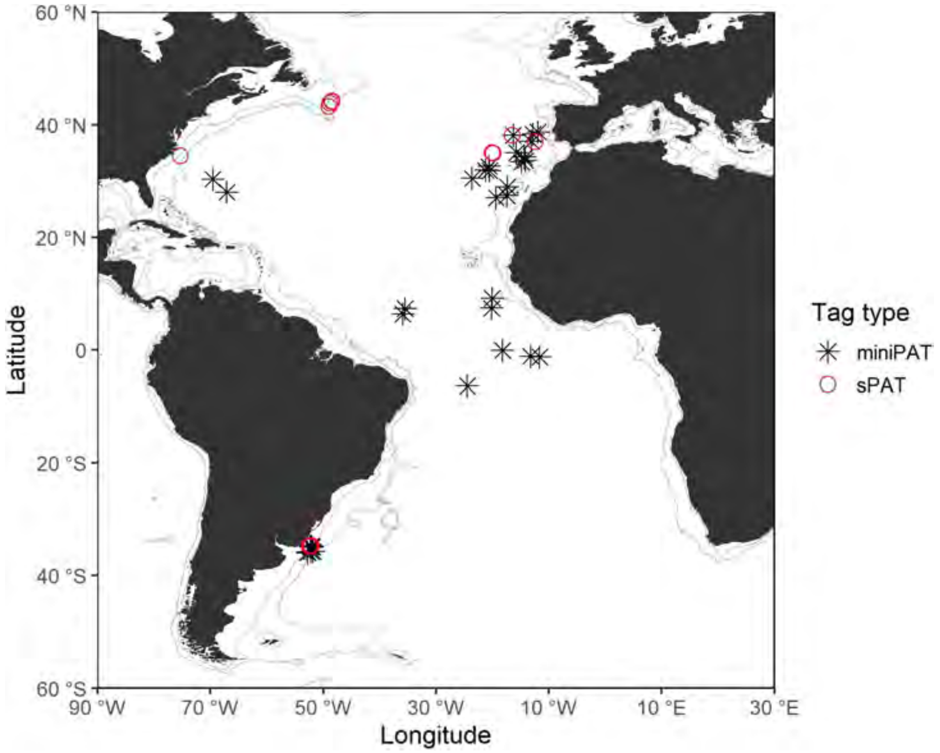

FIGURE 1 | Tagging locations of shortfin makos tagged with PSATs in the Atlantic Ocean during this study. Gray lines represent the boundaries of continental and insular margins (140–3,500 m depth).

(continental margins vs. oceanic area) with non-parametric *k*-sample permutation tests. For this, a Monte Carlo approach was used with the data randomized and re-sampled 9,999 times to build the expected distribution of the differences under a random distribution, which was then used to determine the significance of the differences in the time-at-depth and time-at-temperature for the sample. Time-at-depth and time-at-temperature were also compared among size classes (110–140, 141–175, and 176–220 cm FL) with non-parametric Kruskal–Wallis tests.

Statistical analyses for this paper were carried out using the R language (R Core Team, 2020), with the following additional libraries: "car" (Fox and Weisberg, 2019), "ggplot2" (Wickham, 2016), "grid" (R Core Team, 2020), "maps" (Becker et al., 2013), "maptools" (Bivand and Lewin-Koh, 2020), "ncdf4" (Pierce, 2019), "nortest" (Gross and Ligges, 2015), "perm" (Fay and Shaw, 2010), "plotrix" (Lemon, 2006), "raster" (Hijmans, 2020), "scales" (Wickham and Seidel, 2020), "RColorBrewer" (Neuwirth, 2014), and "shapefiles" (Stabler, 2013). The analysis of habitat use among different bathymetric areas and distances traveled was carried out using QGIS 3.10.14 (QGIS.org, 2021).

RESULTS

PSAT Tagging

Of the 53 tags deployed, only 16 tags detached on their scheduled pop-up date, which represented a premature release rate of ≈70%. Three tags failed to transmit any kind of data and 16 tags detached from the shark earlier than 20 days after being deployed. Premature release of these tags resulted largely from mortality events (14) but also from unknown causes (2). Additionally, two tags suffered early tag detachment (37 and 58 days after tag deployment) and were determined to be ingested by other fish, most probably as a result of a depredation attempt on the tagged sharks. Data collected with the 16 tags that suffered premature release earlier than 20 days after being deployed were excluded from the analysis. For the remaining 34 tags, a total of 1,877 tracking days was registered (1,578 tracking days for miniPATs and 299 tracking days for sPATs, with mean tracking duration of 66 and 30 days for miniPATs and sPATs, respectively) (see **Supplementary Material**).

Horizontal Movements and Spatial Distribution

The estimated most likely tracks of the 34 sharks monitored showed that shortfin makos ranged widely between 77°W–13°E and 44°N–41°S, and traveled approximate distances ranging from 19 to 8,931 km (see **Figures 2**, **3** and **Supplementary Material**).

Shortfin makos tagged with sPATs in the temperate Northwest Atlantic followed general southern trajectories (**Figure 2**). Distances traveled by these specimens were measured in straight lines between the tagging and pop-up locations and ranged from 278 to 1,191 km. The two shortfin makos

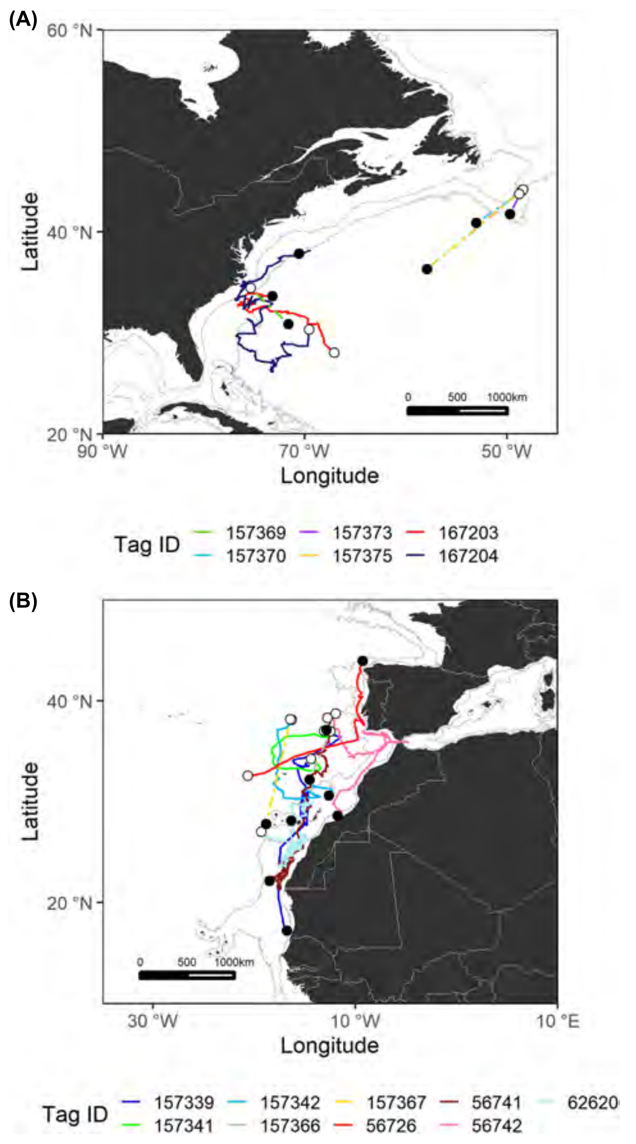

FIGURE 2 | Estimated most likely tracks for each shortfin mako tagged in the Northwest Atlantic **(A)** and Northeast Atlantic **(B)** regions. The tagging locations are represented with open circles and the pop-up locations with black circles. Note that for sPATs only straight line tracks are shown (dashed lines). Gray lines represent the boundaries of continental and insular margins (140–3,500 m depth).

tagged with miniPATs followed distinct paths. The shortfin mako with tag ID 167203 traveled more than 2,400 km, swam westward toward the shelf and slope waters off the northeastern United States and subsequently turned east into oceanic waters. Shark 167204 initially swam southward and then shifted its course moving north to continental shelf areas and approaching the United States eastern coast for a total of 5,684 km traveled.

In the Northeast Atlantic, the movement patterns recorded were diverse (**Figure 2**). Most shortfin makos tagged in the temperate Northeast Atlantic swam to southern tropical areas, while two of them (tag IDs 157341 and 56726) remained in temperate waters, moving toward higher latitudes. Shark 56726 was tagged in open waters and subsequently directed its movement toward the southwestern Portuguese coast, moving north afterwards, in an excursion that seemed to be oriented toward the Gulf of Biscay. Shark 157341 traveled about 1,500 km in offshore waters, following a general northward direction. The remaining shortfin makos made extensive journeys toward the shelf and slope waters of the Canary archipelago and the West African coast. Through the entire tracks, these sharks covered total distances ranging from 561 to 5,315 km.

In the Southwest Atlantic, sharks were tagged within the continental slope off Uruguay and subsequently tended to stay in the same general area, except for one specimen (tag ID 62566) that ventured east toward international waters after spending an initial period moving around within the same area (**Figure 3**). Shortfin makos tagged in this region appeared to reveal site fidelity and periods of residency concentrated near and within the continental margin. Specifically, these residency periods occurred over the continental shelf, slope, and adjacent waters off southern Brazil, Uruguay, and northern Argentina. Generally, resident behavior was followed and/or preceded by oscillatory patterns of movements parallel to the continent.

In general, sharks tagged in the central region of the Atlantic Ocean made long-distance movements from oceanic waters toward continental areas (**Figure 3**). Two of the longest movements recorded in this study were made by shortfin makos tagged in the central region, over a 4-month period. Shark 167208 swam south, crossing the Gulf of Guinea and reaching the Namibian EEZ where it remained for 4 weeks until the tag popped-up. This shark crossed hemispheres, in a trans-equatorial highly directional movement covering a total distance of more than 8,900 km. Shark 169528 swam 6,780 km, moving west and nearing the continental slope off northern Brazil.

The vast majority of analyzed tracks belong to juvenile sharks of both sexes; only two mature sharks were monitored. These sharks were presumed to be mature based on published 50% size-at-maturity data (males: 182 cm FL, females: 280 cm FL; Natanson et al., 2020). Both were male, tagged in the Southwest (tag ID 157376) and Central (tag ID 167207) Atlantic regions and followed the general trend to move within/toward the continental shelf.

Generally, sharks tagged in this study spent most of their time (≈56%) swimming within the shelf and slope areas. They spent more than 80% of their time inside national waters, crossing 17 different EEZs. In terms of high-use areas, probabilities of distribution of tagged shortfin makos were higher closer to the West African continental shelf and around the Canary archipelago and the south coastal region of the Iberian Peninsula. Similarly, the continental shelf and adjacent waters off Uruguay and south Brazil were also highly used areas where sharks tended to stay for longer periods (**Figures 4**, **5**). This contrasts with oceanic waters of the Central Atlantic Ocean, where shortfin makos were also present but seemed to be mostly traveling and not staying for longer periods in any specific areas. The use of oceanic vs. continental shelf and slope areas varied among sharks of different size classes. Smaller sharks (110–140 cm FL)

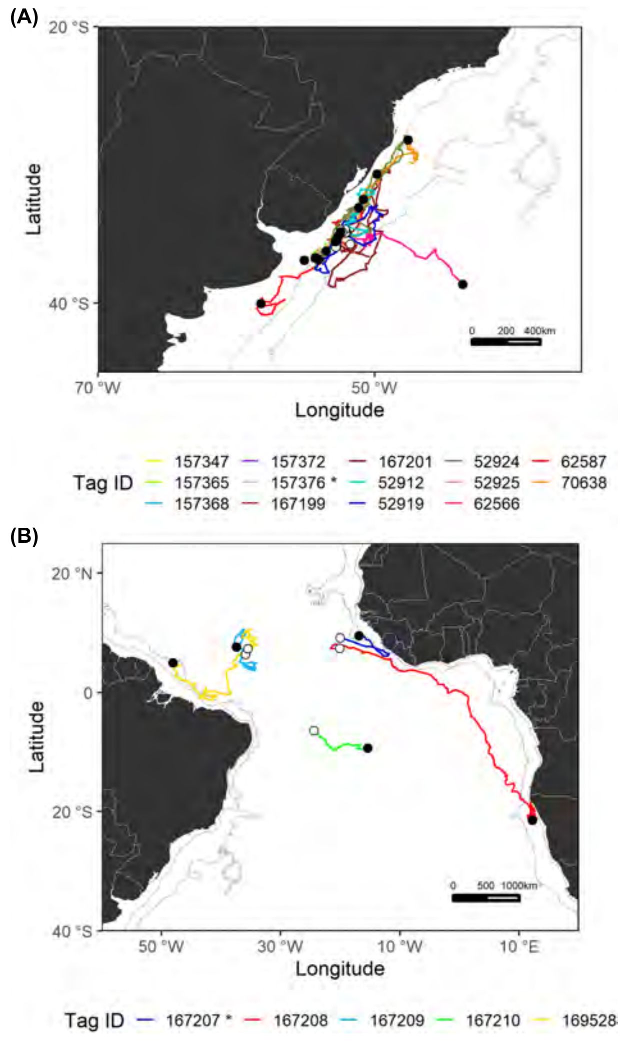

FIGURE 3 | Estimated most likely tracks for each shortfin mako tagged in the Southwest Atlantic **(A)** and Central Atlantic **(B)** regions. The tagging locations are represented with open circles and the pop-up locations with black circles. The asterisk (*) in the legend indicates mature sharks. Note that for sPATs only straight line tracks are shown (dashed lines). Gray lines represent the boundaries of continental and insular margins (140–3,500 m depth).

spent $\approx$56% of their time within shelf/slope areas, while medium-sized sharks (141–175 cm FL) spent $\approx$80% of their time within shelf/slope areas, and larger sharks (176–220 cm FL) swam mostly in oceanic waters, spending $\approx$28% of their time within shelf/slope areas. However, these differences may be related to the tagging locations of sharks.

Vertical Habitat Use

The tagged shortfin makos swam through a depth range from the surface down to 979.5 m, in water temperatures that ranged between 7.4 and 29.9°C. However, sharks spent the largest proportion of their time in depths above 90 m, in water temperatures ranging from 18 to 22°C (mean depth = 68.5 m, SD = 78.1 m; mean temperature = 19.4°C, SD = 3.1°C) (**Figure 6**). These vertical habitat preferences were displayed during both day and night-time, although significant differences were found when comparing habitat use between day and night (depth: permutation test differences = 21.7 m, p-value < 0.001; temperature: permutation test differences = −1.1°C, p-value < 0.001). Differences in vertical habitat use between day and night were less notable when sharks swam in shelf and slope areas (daytime: mean depth = 63.6 m, SD = 87.8 m; night-time: mean depth = 49.1 m, SD = 41.1 m) compared to when they used oceanic waters, where they occupied greater mean depths during daytime and night-time (daytime: mean depth = 121.1 m, SD = 97.5 m; night-time: mean depth = 72.3 m, SD = 65.4 m) (**Figure 7**). Vertical habitat use varied among sharks of different size classes (Kruskal–Wallis tests, p-value < 0.001). Smaller sharks ($\leq$140 cm FL) spent more time in slightly cooler waters than larger individuals (110–140 cm FL: mean temperature = 19.0°C, min = 7.4°C, max = 28.1°C; 141–175 cm FL: mean temperature = 19.7°C, min = 7.5°C, max = 25.2°C; 176–220 cm FL: mean temperature = 19.7°C, min = 8.1°C, max = 29.9°C) (**Figures 8–10**). Larger shortfin makos ($\geq$176 cm FL) occupied greater mean depths (110–140 cm FL: mean depth = 83.1 m, min = 0.5 m, max = 490.5 m; 141–175 cm FL: mean depth = 58.7 m, min = 0 m, max = 979 m; 176–220 cm FL: mean depth = 90.4 m, min = 0 m, max = 740 m) compared to smaller- and especially medium-sized specimens (**Figures 8–10**). These differences may be related to the tagging locations of sharks.

Diel behavior varied considerably among sharks. While some individuals exhibited a clear diel cyclicity defined by shallower mean depths during the night and greater mean depths during daily hours, most sharks showed an oscillatory swimming behavior characterized by continuous movements up and down the water column (yo-yo diving) with some occasional deep dives followed by rapid ascents (**Figure 11**). Diel vertical movements were exhibited by sharks that spent greater periods of time in oceanic waters, namely those tagged in the Central and Northwest Atlantic. Sharks that mostly swam in shelf and slope waters, like the shortfin makos tagged in the Southwest and Northeast regions of the Atlantic, tended to demonstrate oscillatory swimming behavior.

DISCUSSION

Worldwide, overfishing has had severe effects on marine ecosystems (Stevens et al., 2000; Myers et al., 2007; Ferretti et al., 2010; Pershing et al., 2010). Direct targeting and incidental bycatch of apex fish predators by commercial fishing fleets has negatively impacted their stocks, including those of pelagic sharks, in most regions of the world (Dulvy et al., 2008; Pacoureau et al., 2021). Due to their life history traits that result in low intrinsic rates of population increase, poor management, and low conservation priority, pelagic sharks are among the most vulnerable species to overexploitation (Camhi et al., 2008; Dulvy et al., 2008; Cortés et al., 2010). Increasing fishing pressure on shortfin makos in recent decades has raised concerns over their conservation, with the latest projections indicating alarming

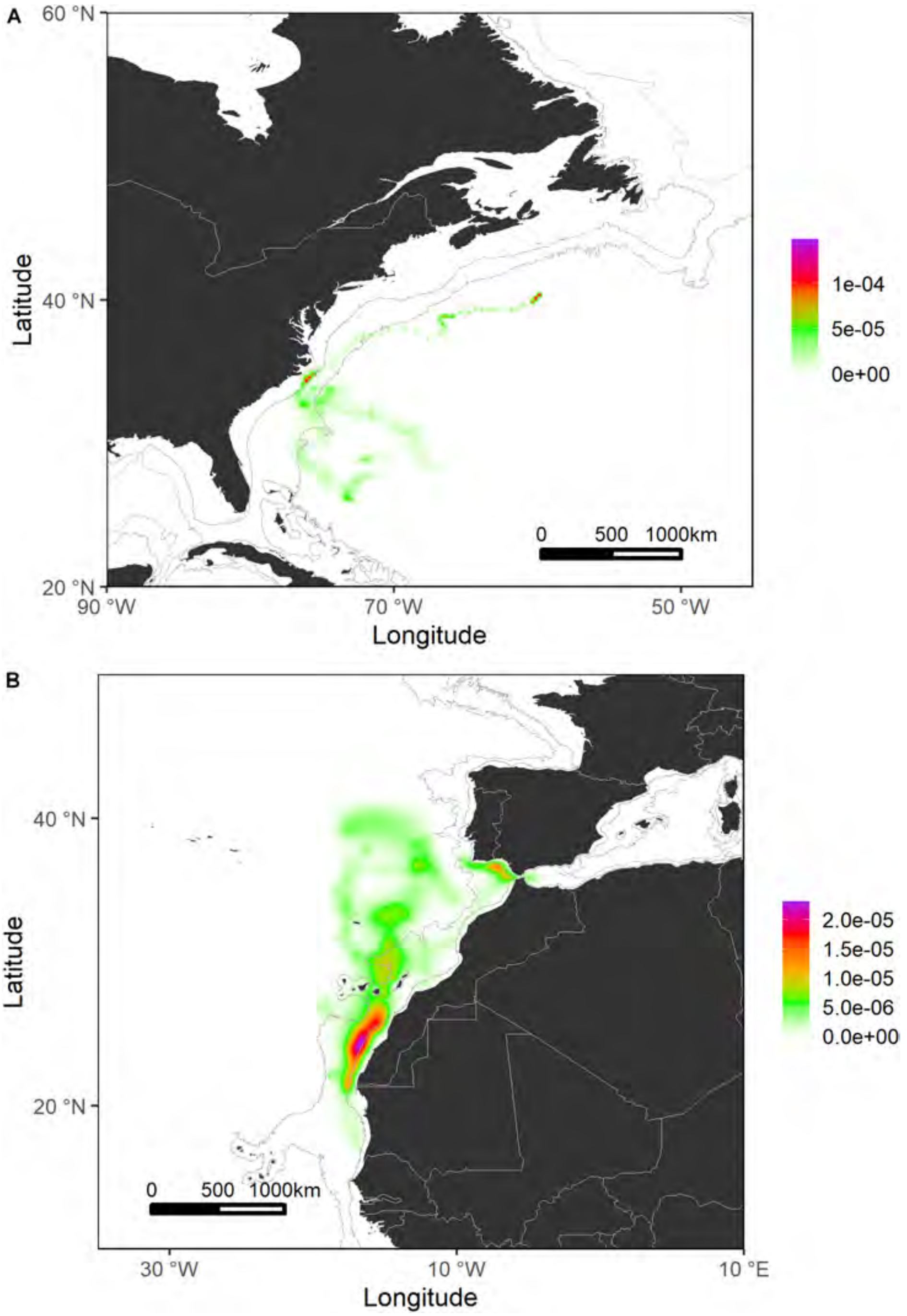

FIGURE 4 | Probability surfaces of the spatial distribution of shortfin makos tagged in the Northwest Atlantic **(A)** and Northeast Atlantic **(B)** regions. Gray lines represent the boundaries of continental and insular margins (140–3,500 m depth).

signs of population depletion in the North Atlantic Ocean (Anon, 2017). For this reason, understanding habitat preferences and identifying migratory routes that might provide insight on the existence of possible critical habitats, such as mating grounds and nursery areas, or areas that may be considered as separate fisheries management units, is crucial to ensure effective management measures and successful conservation strategies.

Here we present the most extensive record of movements of shortfin makos tagged with PSATs in the Atlantic Ocean to date, by tagging juvenile specimens of both sexes and two mature males. No mature females were tagged, and sex was undetermined for seven specimens. The main constraint in the present study was the premature detachment of PSATs. Of the 53 tags deployed, only 16 detached on their scheduled pop-up date,

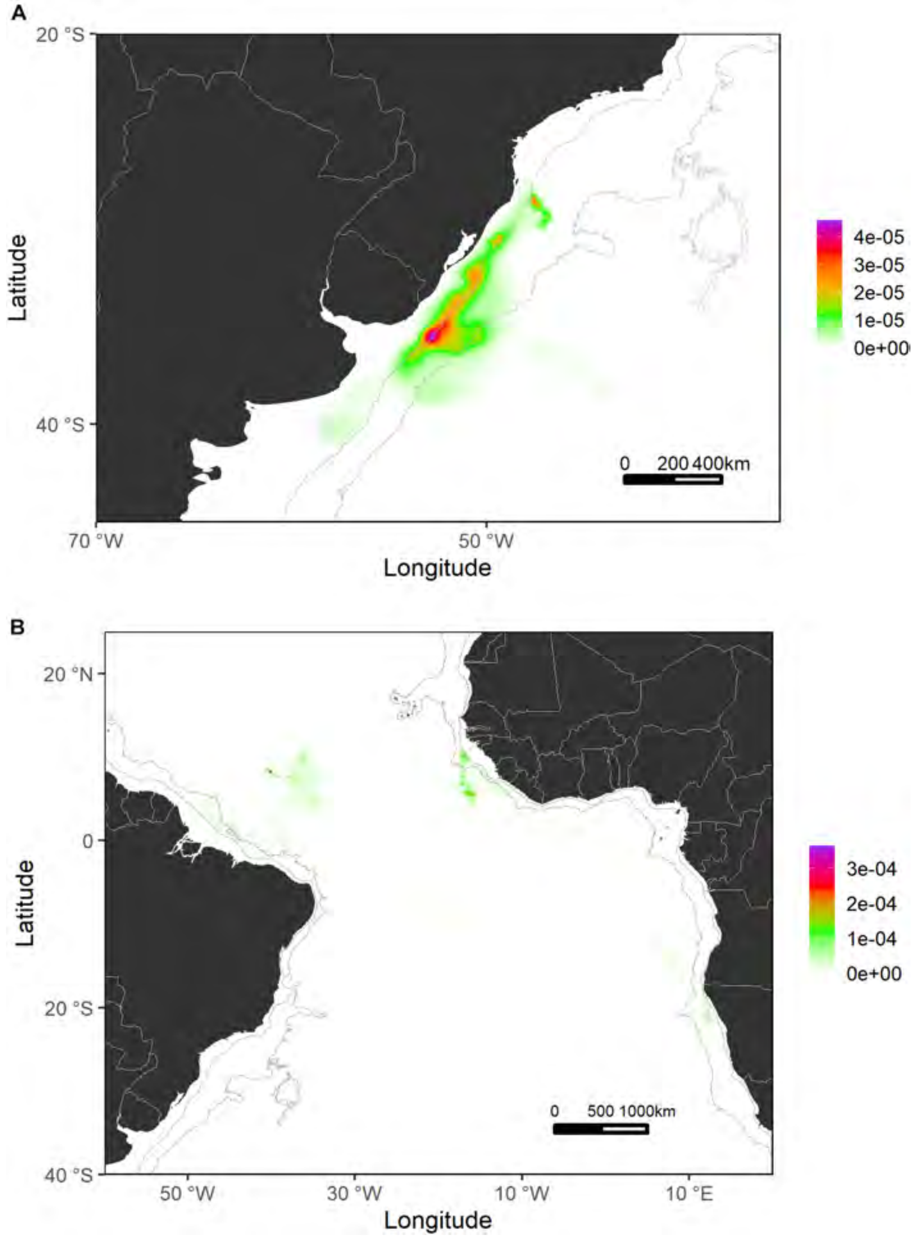

FIGURE 5 | Probability surfaces of the spatial distribution of shortfin makos tagged in the Southwest Atlantic **(A)** and Central Atlantic **(B)** regions. Gray lines represent the boundaries of continental and insular margins (140–3,500 m depth).

representing a premature release rate of ≈70%. This percentage is close to the average rate of 66% found in a review of shark satellite tagging studies by Hammerschlag et al. (2011). The causes of early tag detachment and tag failure are still not well understood and there may be several explanations including biofouling, mechanical failure of critical tag components, human error, battery failure, and tag damage (Hays et al., 2007; Musyl et al., 2011). Additionally, as one of the fastest sharks, premature release in shortfin mako may be caused by high-burst swimming events that could weaken the anchorage and cause early detachment of the tag. Hammerschlag et al. (2011) stated that the method used for PSAT deployment, which consists of inserting the tag in the shark skin using a dart anchor, is highly conducive to tag shedding, which may explain the high premature release rate of this type of tags. By contrast, SPOT tags (smart position and temperature tags) have demonstrated the capacity to stay attached to sharks for much longer periods. These tags are usually mounted to the dorsal fin of sharks using bolts and nuts, and as such are less conducive to rapid shedding. When comparing studies on shortfin mako movements, studies that used SPOT tags (e.g., Vaudo et al., 2017; Francis et al., 2019; Gibson et al., 2021) generally reported much longer tracks than studies using PSATs

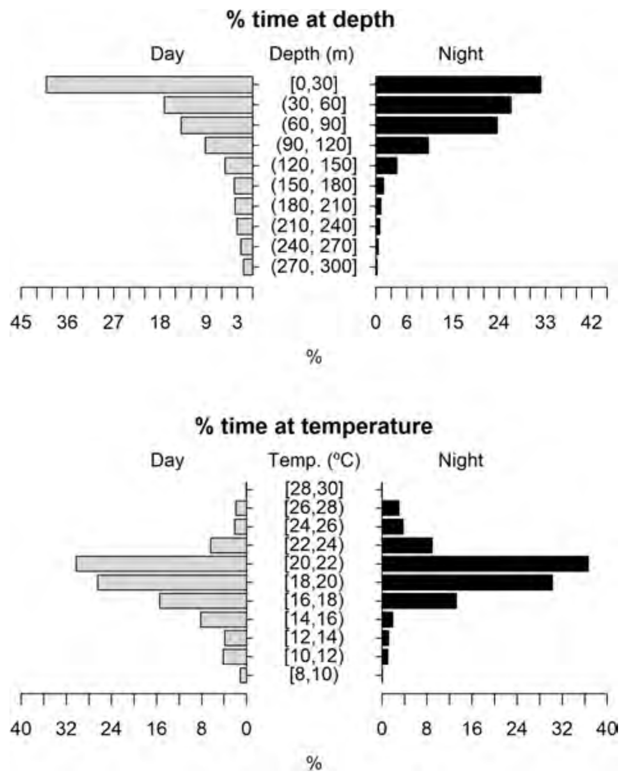

FIGURE 6 | Vertical habitat use of shortfin makos for daytime and night-time in terms of depth and temperature. Depth classes are categorized in 30 m intervals and temperature classes in 2°C intervals.

(e.g., Stevens et al., 2010; Abascal et al., 2011; Vaudo et al., 2016). Here we used the same Domeier umbrella anchor used in some of the tags deployed in Vaudo et al. (2016). In that study, two out of four tags suffered premature release, although mean tracking days (132 days) was higher than that reported in our study (30–66 days). In Vaudo et al. (2016), the remaining tags were attached using a stainless-steel M dart and all suffered premature release (mean tracking days = 15). Abascal et al. (2011), which used the same stainless-steel M dart, stated that premature detachment of tags was found to be the main problem in the study (premature release rate of 87.5%; mean tracking days = 53). In Stevens et al. (2010), of seven PSATs deployed either on blue, shortfin mako, thresher, or bigeye thresher sharks, only one reached its pop-off date (mean tracking days = 58). Those tags were attached using a stainless-steel Floy tag-anchor. High premature release rates of PSAT tags and consequent short tracking periods limit the ability to determine seasonal patterns of habitat use, contrary to SPOT tags which frequently report tracking periods of >1 year and therefore can be used to assess movement seasonality. However, since SPOT tags are not equipped with depth sensors, they are not suitable for examining vertical behavior of fish. Similarly to what was reported for several large pelagic species (Kerstetter et al., 2004; Hoolihan et al., 2014; Cosgrove et al., 2015), two early tag detachments detected in this study were probably the result of depredation events by other sharks, as indicated by sudden increases in temperature which remained stable regardless of depth, and low light level values which demonstrate that the tag was in darkness.

Our data confirmed the wide geographic distribution of shortfin mako in the Atlantic Ocean (Compagno, 2001; Cortés et al., 2010). Shortfin makos tagged in this study moved in multiple directions, usually traveling long distances between oceanic waters and waters within the continental shelf and slope. These extensive movements are consistent with previous studies that also demonstrated the highly migratory nature of this species (Casey and Kohler, 1992; Abascal et al., 2011; Vaudo et al., 2017; Queiroz et al., 2019; Coelho et al., 2020; Gibson et al., 2021). A previous conventional tag-and-recapture study by Casey and Kohler (1992) suggested that movements of shortfin mako in the Northwest Atlantic Ocean were seasonal and largely influenced by sea surface temperature. In Vaudo et al. (2017) shortfin makos displayed considerable variability in movements, with seven sharks tagged off the United States making long-distance, highly directional southern excursions into less productive subtropical/tropical waters before returning north. More recently, Gibson et al. (2021) reported high use of the Gulf of Mexico area and extensive seasonal migrations of mature male shortfin makos toward the Caribbean Sea and the northeastern United States Atlantic coast beginning in the late summer-early fall. These movements differed from those undertaken by the two shortfin makos in our study tagged with miniPATs in the Northwest Atlantic (tag IDs 167203 and 167204), which did not approach the Gulf of Mexico region and followed general north-oriented movements toward shelf and slope waters off eastern United States starting in late winter. Our data revealed that for shortfin makos tagged in the Northeast and Central Atlantic regions, except for a couple of sharks, horizontal movements tended to be oriented toward shelf and slope waters. Coelho et al. (2020) obtained similar results, with most shortfin makos tagged in the Cabo Verde EEZ traveling toward areas closer to the African shelf. Finally, sharks tagged in the Southwest area off Uruguay appeared to demonstrate fidelity to the more nutrient-rich waters of the Subtropical Convergence Zone. This area is characterized by the confluence of two water masses with contrasting features: the warm Brazil Current and the cold Malvinas/Falkland Current. In addition to this water-mixing process, discharges from the Rio de la Plata make the Subtropical Convergence Zone a highly productive ecosystem with capacity to sustain high trophic levels (sharks, tunas, seabirds, sea turtles, and marine mammals) (Acha et al., 2004; Domingo et al., 2009; Jiménez et al., 2011; Pons and Domingo, 2013; Passadore et al., 2014; Gaube et al., 2017). The reasons for these horizontal movements are not entirely known but may suggest an ability to discriminate among areas of particular significance for foraging or reproduction purposes (Heupel et al., 2007; Petersen et al., 2007; Block et al., 2011).

Generally, shortfin makos tracked in the present study made excursions toward the continental shelf and slope. The shelf and slope waters of the Subtropical Convergence Zone, the Canary archipelago and the northwestern African continental shelf seemed to be areas of particular importance for the species. Previous studies reported the aggregation of immature sharks

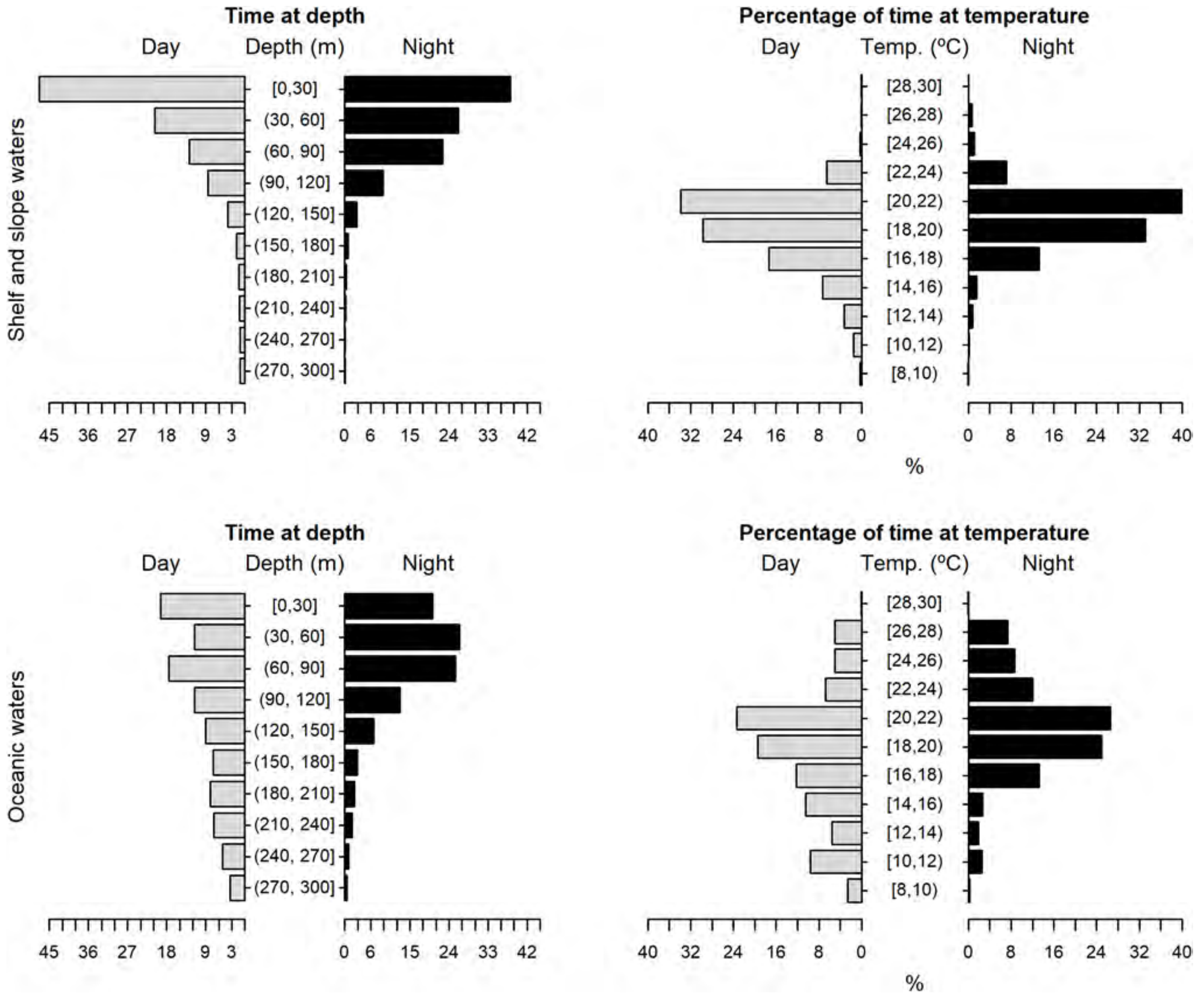

FIGURE 7 | Vertical habitat use of shortfin makos when using shelf and slope waters **(top plots)** vs. oceanic waters **(bottom plots)**, for daytime and night-time in terms of depth and temperature. Depth classes are categorized in 30 m intervals and temperature classes in 2°C intervals.

around these areas, suggesting that they may serve as nursery grounds. Coelho et al. (2018) documented high density of smaller-sized blue sharks in temperate Southwest waters off southern Brazil and Uruguay, which would represent one of the main nursery grounds for that species in the South Atlantic Ocean. For shortfin mako, Vooren et al. (2005) and Costa et al. (2002) reported the presence of neonates and pregnant females off southern Brazil. Moreover, the hypothesis of a nursery ground off Northwest Africa and Portugal is supported by the occurrence of neonate and young-of-the-year shortfin makos reported in Maia et al. (2007) and Natanson et al. (2020). Here, the presence of two neonates tagged off the Canary archipelago (tag IDs 62420 and 62621) reinforces the importance of this region for parturition. Additionally, horizontal movements might be driven by feeding events. For instance, the shortfin mako with tag ID 167208 swam for more than 8,900 km from the Central Atlantic Ocean toward shelf and slope waters off northern Namibia, remaining in the area for nearly 1 month until tag detachment. This region is included within the Benguela marine ecosystem, one of the most productive marine systems in the world, which attracts many top predators seeking food (Petersen et al., 2007; Santos and Coelho, 2018). Interestingly, this shark moved from northern to southern hemisphere, which may question the current North–South Atlantic (separated by the 5°N) division of stocks used for all pelagic sharks by ICCAT.

Tagged shortfin makos spent their time from the surface down to 979.5 m depth, in temperature ranges of 7.4–29.9°C, although most of the time they were in depths above 90 m, in water temperatures ranging from 18 to 22°C. When sharks used oceanic environments they occupied greater mean depths during daytime and night-time. Information on habitat preference of shortfin mako in the Atlantic Ocean is limited; however, our

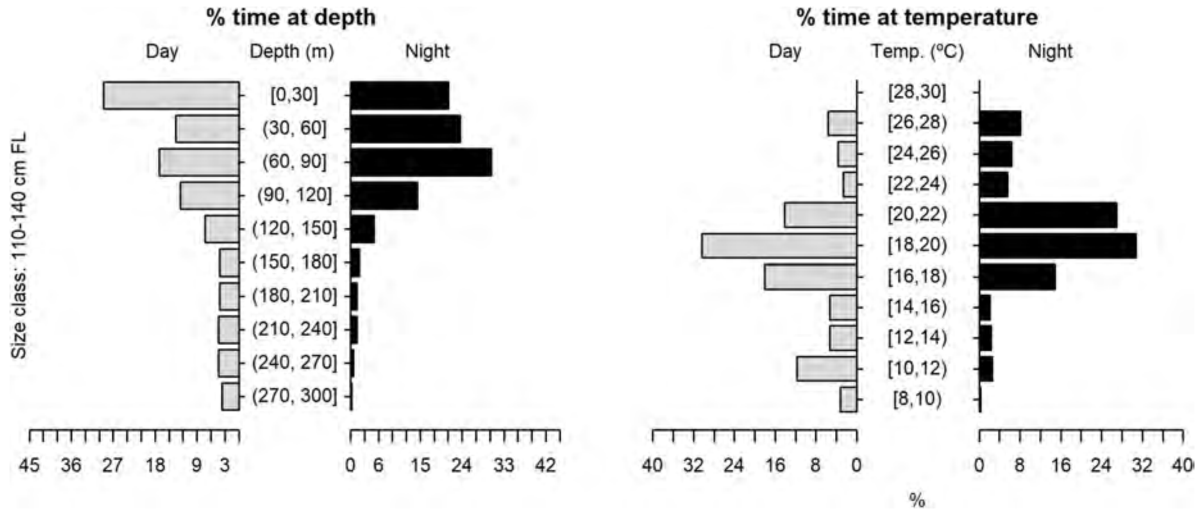

FIGURE 8 | Vertical habitat use of shortfin makos ranging in size from 110 to 140 cm FL, for daytime and night-time in terms of depth and temperature. Depth classes are categorized in 30 m intervals and temperature classes in 2°C intervals.

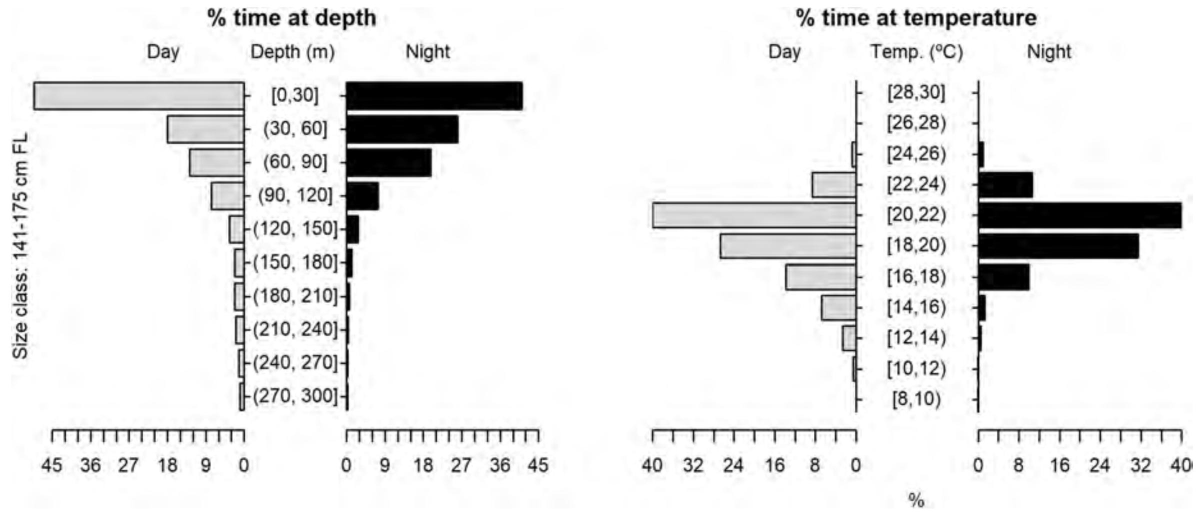

FIGURE 9 | Vertical habitat use of shortfin makos ranging in size from 141 to 175 cm FL, for daytime and night-time in terms of depth and temperature. Depth classes are categorized in 30 m intervals and temperature classes in 2°C intervals.

results are consistent with those previously reported for this species. In Loefer et al. (2005), tag data of one specimen captured off the southeastern United States indicated a depth range of 0–556 m in temperatures between 10.4 and 28.6°C. Vaudo et al. (2016) reported that shortfin makos tagged off the northeastern United States and Gulf of Mexico experienced temperatures between 5.2 and 31.1°C, swimming through a depth range from near the surface down to 866 m. In Gibson et al. (2021) shortfin makos frequented a wide range of sea surface temperatures ranging from 10.0 to 31.0°C. Casey and Kohler (1992) indicated that in the North Atlantic the preferred surface water temperature of shortfin mako appeared to lie in a narrow range between 17 and 22°C. Body size has been suggested to influence the vertical distribution of shortfin mako, with larger sharks showing a greater tolerance to cooler waters than smaller individuals (Vaudo et al., 2016). In this study, mean temperature recorded for smaller individuals was slightly lower than those recorded for medium- and larger-sized sharks. Moreover, smaller individuals spent more time in cooler waters compared to medium and larger-sized sharks, revealing they are able to occupy a broad range of thermal habitats.

In terms of diel movement patterns, we found that swimming behavior differed among sharks. Sharks tagged in open waters of the Central and Northwest regions tended to exhibit diel vertical movements, characterized by shallower mean depths during the night and greater mean depths during daytime. Vaudo et al. (2016) obtained similar results, with sharks showing diel diving

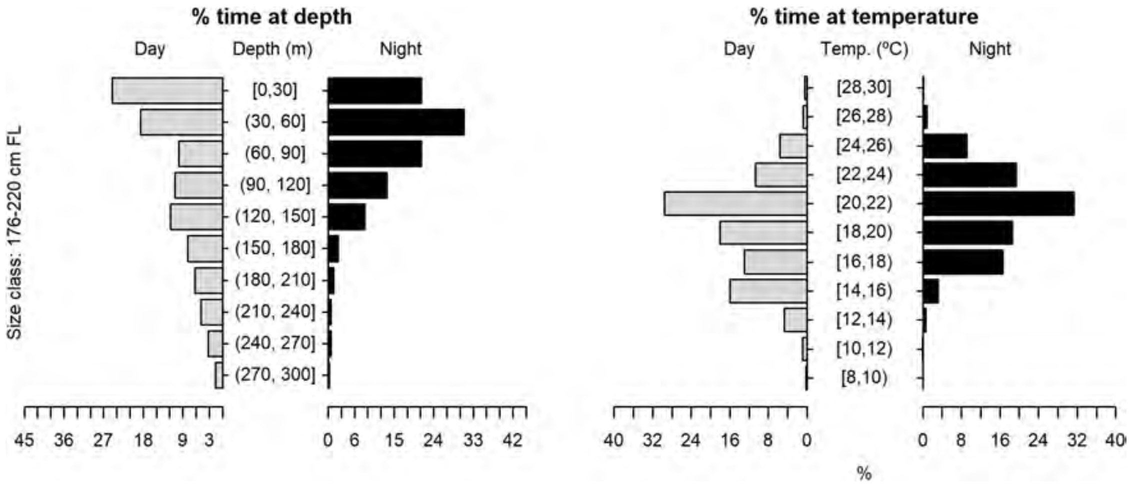

FIGURE 10 | Vertical habitat use of shortfin makos ranging in size from 176 to 220 cm FL, for daytime and night-time in terms of depth and temperature. Depth classes are categorized in 30 m intervals and temperature classes in 2°C intervals.

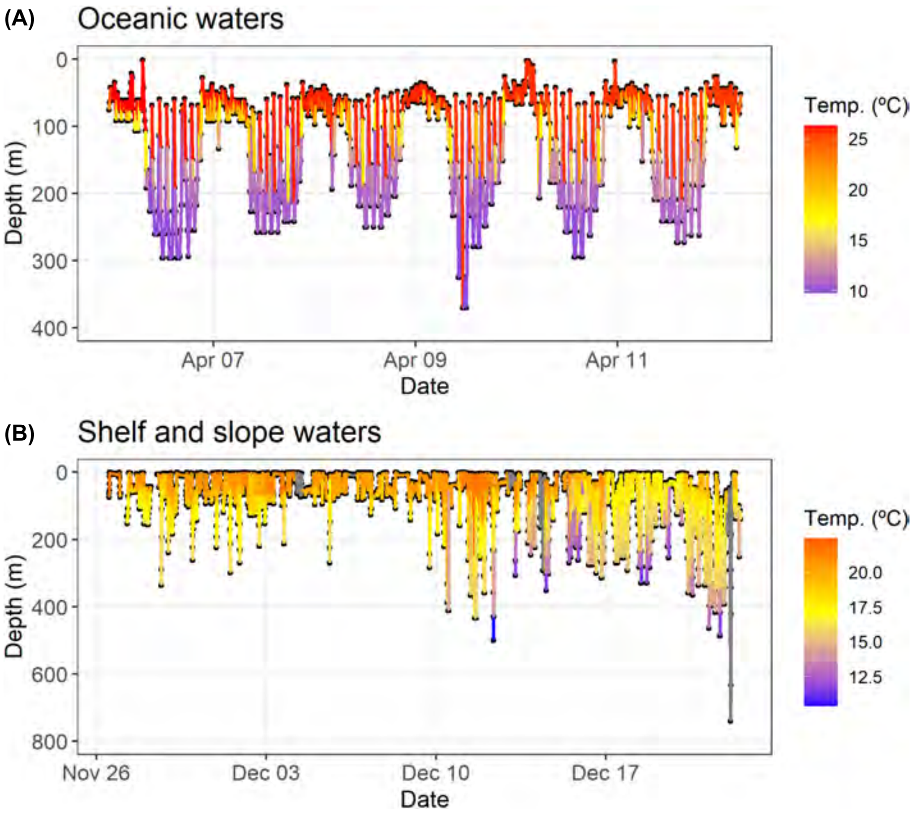

FIGURE 11 | Details of diving behavior profiles of shortfin makos. The plot on the top **(A)** (shark with tag ID 169528) represents the diel vertical behavior. The plot on the bottom **(B)** (shark with tag ID 52925) shows the oscillatory diving (yo-yo diving) behavior, with occasional deep dives.

behavior with deeper dives occurring primarily during daytime. In Loefer et al. (2005), the specimen tagged also demonstrated a diel pattern of vertical movement defined by greater mean depths and larger depth ranges during daylight hours. The results of both studies suggested that vertical movements of shortfin mako were strongly influenced by water temperatures, which appeared to be the major influence on the movement ecology of the species. The differences between day and night behavior have also been described as a foraging strategy to locate and remain near prey (Sepulveda et al., 2004; Vetter et al., 2008).

Most sharks tagged in the present study, namely those tagged in the Southwest and Northeast Atlantic regions which mostly used shelf and slope waters, showed a vertical oscillatory swimming behavior. These sharks constantly moved up and down in the water column, with some occasional deep dives followed by rapid ascents. In the Southeastern Pacific Ocean, a study on environmental preferences of shortfin mako by Abascal et al. (2011) reported that sharks did not exhibit any clear diel cyclicity, but mean vertical distribution was deeper during daytime. These sharks also displayed bounce dives, which the authors associated with feeding events. Deep diving behavior has been suggested to be related with foraging ecology of other pelagic sharks, including blue shark, tiger shark, *Galeocerdo cuvier*, scalloped hammerhead, *Sphyrna lewini*, bigeye thresher, *Alopias superciliosus*, and oceanic whitetip, *Carcharhinus longimanus* (Stevens et al., 2010; Nakamura et al., 2011; Hoffmayer et al., 2013; Howey-Jordan et al., 2013; Coelho et al., 2015). Additionally, the most widely proposed reason for this behavior has been attributed to warming the body after heat loss during descents into cooler water (Klimley et al., 2002). However, like other lamnid sharks, the shortfin mako is an endothermic species that is able to maintain body temperatures above the surrounding seawater temperature (Carey et al., 1981). Other functions proposed for yo-yo diving are related to energy conservation through a fly-glide swimming strategy, orientation, and the use of chemical and magnetic information to guide migrations (Klimley et al., 2002; Iosilevskii et al., 2012).

Conclusion

Overall, our findings for the shortfin mako confirmed its capacity to inhabit temperate and tropical waters, over broad depth and temperature ranges. Nevertheless, sharks spent most of their time in depths above 90 m, in water temperatures ranging from 18 to 22°C. Our results suggested two different patterns of diving activity which seemed to be influenced by the proximity to the continents. Individuals that spent greater periods of time in oceanic waters demonstrated diel cyclicity, staying in shallower waters during the night, while sharks that swam in shelf and slope waters tended to display yo-yo diving behavior with some occasional deep dives. Furthermore, satellite-tagged shortfin makos showed considerable variability in horizontal movements, but generally tended to move toward or remain over shelf and slope waters of the Southwest Atlantic Subtropical Convergence Zone, the Canary archipelago and West Africa. These movements challenge the typical view of shortfin makos being mostly oceanic nomads and hint at the importance of these continental margin areas for the species. Despite the existing relationship between habitat use and tagging locations, it is interesting to highlight that sharks spent most of their time in national EEZ waters moving across the jurisdictional management borders of several nations and the high seas, which emphasizes the necessity for international coordination efforts to effectively apply the required management actions. Moreover, the evidence of shark movements across hemispheres may question the current north–south division of stocks in the Atlantic. Finally, the apparent residency of those sharks in some areas, such as in the Southwest Atlantic, might help to better delineate and refine management unit areas for the species. This should be done in tandem with ongoing population genetic studies being carried out within ICCAT, whose preliminary results have suggested, for example, a unique genetic structure of shortfin makos off Uruguay in the Southwest Atlantic (ICCAT, 2018).

The results of this study provide a better understanding of shortfin mako movements and activity patterns in the Atlantic Ocean and confirm that satellite tagging is an important tool that can provide valuable information on spatial ecology of data-limited species. We expect that similar studies will continue to be carried out to elucidate ecological aspects and determine the drivers of movement patterns of these animals, as well as to provide insight on movement differences between sexes and/or maturity stages, ultimately contributing to the provision of sustainable management and conservation measures.

DATA AVAILABILITY STATEMENT

Data from ICCAT tags used in the paper can be made available upon request to ICCAT Secretariat, following the rules and procedures for the protection, access to, and dissemination of data compiled by ICCAT. Data from other tags used in the paper can be made available upon reasonable request to the authors.

ETHICS STATEMENT

The animal study was reviewed and approved by ICCAT Standing Committee on Research and Statistics.

AUTHOR CONTRIBUTIONS

AD, EC, and RC contributed to the conception and design of the study. AD, JC, LN, PT, DM, PM, FH, FM, JO, and RC organized and led the fieldwork, and undertook data collection. CS, RC, PM, and PL undertook analyses. CS led the writing of the manuscript with revisions and assistance from all other authors. All authors contributed to the final article and approved the submitted version.

FUNDING

This study was carried out as a part of a collaborative work conducted by the ICCAT Shark Species Group integrated in the ICCAT Shark Research and Data Collection Program (SRDCP). This work was funded by ICCAT as a part of the regular budget and by contributions from individual Contracting Parties, particularly the European Union through the EU Grant Agreements with ICCAT on "Strengthening the scientific basis for decision-making in ICCAT" and the "ICCAT Science envelope." Additional satellite tags were acquired by Project "MAKOWIDE – A wide scale inter-hemispheric and inter-disciplinary study aiming the conservation of the shortfin mako shark in the Atlantic Ocean (Ref: FAPESP/19740/2014)," funded by FCT (Portuguese Foundation for Science and

Technology), and there was also support from FCT through project UIDB/04326/2020. CS was supported by an FCT Doctoral grant (Ref: SFRH/BD/139187/2018). The authors thank NOAA/NMFS/SEFSC for providing funds to publish this article as open access.

ACKNOWLEDGMENTS

We are grateful to all fishery observers and longline skippers from the Nations involved in this study. We would like to dedicate this study to FH, who passed away during the late stage revision process of this manuscript. The premature departure of our colleague FH leaves the fisheries and marine biology and ecology community poorer. His legacy and dedication to research will always be remembered.

SUPPLEMENTARY MATERIAL

The Supplementary Material for this article can be found online at: https://www.frontiersin.org/articles/10.3389/fmars.2021.686343/full#supplementary-material

REFERENCES

Abascal, F. J., Mejuto, J., Quintans, M., García-Cortés, B., and Ramos-Cartelle, A. (2015). Tracking of the broadbill swordfish, *Xiphias gladius*, in the central and eastern North Atlantic. *Fish. Res.* 162, 20–28. doi: 10.1016/j.fishres.2014.09.011

Abascal, F. J., Quintans, M., Ramos-Cartelle, A., and Mejuto, J. (2011). Movements and environmental preferences of the shortfin mako, *Isurus oxyrinchus*, in the southeastern Pacific Ocean. *Mar. Biol.* 158, 1175–1184. doi: 10.1007/s00227-011-1639-1

Acha, E. M., Mianzan, H. W., Guerrero, R. A., Favero, M., and Bava, J. (2004). Marine fronts at the continental shelves of austral South America. Physical and ecological processes. *J. Mar. Syst.* 44, 83–105. doi: 10.1016/j.jmarsys.2003.09.005

Amante, C., and Eakins, B. W. (2009). *ETOPO1 1 Arc-Minute Global Relief Model: Procedures, Data Sources and Analysis. NOAA Technical Memorandum NESDIS NGDC-24*. Washington, D.C: NOAA National Geophysical Data Center. doi: 10.7289/V5C8276M

Anon (2017). *Report of the 2017 ICCAT Shortfin mako assessment meeting*. Madrid: International Commission for the Conservation of Atlantic Tunas.

Barker, M. J., and Schluessel, V. (2005). Managing global shark fisheries: suggestions for prioritizing management strategies. *Aquat. Conserv. Mar. Freshwater Ecosyst.* 15, 325–347. doi: 10.1002/aqc.660

Becker, R. A., Wilks, A. R., Brownrigg, R., and Minka, T. P. (2013). *Maps: Draw Geographical Maps, R Package Version 2.3-6*. Available online at: http://CRAN.R-project.org/package=maps (accessed February 26, 2021)

Biais, G., Coupeau, Y., Séret, B., Calmettes, B., Lopez, R., Hetherington, S., et al. (2017). Return migration patterns of porbeagle shark (*Lamna nasus*) in the Northeast Atlantic: implications for stock range and structure. *ICES J. Mar. Sci.* 74, 1268–1276. doi: 10.1093/icesjms/fsw233

Bivand, R., and Lewin-Koh, N. (2020). *Maptools: Tools for Handling Spatial Objects. R package version 1.0-2*. Available online at: https://CRAN.R-project.org/package=maptools (accessed February 26, 2021).

Block, B. A., Jonsen, I. D., Jorgensen, S. J., Winship, A. J., Shaffer, S. A., Bograd, S. J., et al. (2011). Tracking apex marine predator movements in a dynamic ocean. *Nature* 475, 86–90. doi: 10.1038/nature10082

Braun, C. D., Skomal, G. B., and Thorrold, S. R. (2018). Integrating archival tag data and a high-resolution oceanographic model to estimate basking shark (*Cetorhinus maximus*) movements in the Western Atlantic. *Front. Mar. Sci.* 5:25. doi: 10.3389/fmars.2018.00025

Camhi, M., Pikitch, E. K., and Babcock, E. A. (2008). *Sharks of the Open Ocean: Biology, Fisheries and Conservation*. Oxford: Blackwell Publishing.

Campana, S. E., Marks, L., and Joyce, W. (2005). The biology and fishery of shortfin mako sharks (*Isurus oxyrinchus*) in Atlantic Canadian waters. *Fish. Res.* 73, 341–352. doi: 10.1016/j.fishres.2005.01.009

Carey, F. G., Teal, J. M., and Kanwisher, J. W. (1981). The visceral temperature of mackerel sharks (Lamnidae). *Physiol. Zool.* 54, 334–344.

Casey, J. G., and Kohler, N. E. (1992). Tagging studies on the shortfin mako shark (Isurus oxyrinchus) in the western North Atlantic. *Aust. J. Mar. Freshwater Res.* 43, 45–60. doi: 10.1071/MF9920045

CITES (2019). *Summary Record of the Twelfth Session for Committee I*. Available online at: https://cites.org/sites/default/files/eng/cop/18/Com_I/SR/E-CoP18-Com-I-Rec-12-R1.pdf (accessed October 25, 2020).

Coelho, R., Fernandez-Carvalho, J., Lino, P. G., and Santos, M. N. (2012). An overview of the hooking mortality of elasmobranchs caught in a swordfish pelagic longline fishery in the Atlantic Ocean. *Aquat. Living Resour.* 25, 311–319. doi: 10.1051/alr/2012030

Coelho, R., Fernandez-Carvalho, J., and Santos, M. N. (2015). Habitat use and diel vertical migration of bigeye thresher shark: overlap with pelagic longline fishing gear. *Mar. Environ. Res.* 112, 91–99. doi: 10.1016/j.marenvres.2015.10.009

Coelho, R., Macías, D., de Urbina, J. O., Martins, A., Monteiro, C., Lino, P. G., et al. (2020). Local indicators for global species: pelagic sharks in the tropical northeast Atlantic, Cabo Verde islands region. *Ecol. Indic.* 110:105942. doi: 10.1016/j.ecolind.2019.105942

Coelho, R., Mejuto, J., Domingo, A., Yokawa, K., Liu, K. M., Cortés, E., et al. (2018). Distribution patterns and population structure of the blue shark (*Prionace glauca*) in the Atlantic and Indian Oceans. *Fish. Fish.* 19, 90–106. doi: 10.1111/faf.12238

Compagno, L. J. V. (2001). *Sharks of the World. An annotated and Illustrated Catalogue of Shark Species Known to Date. Bullhead, Mackerel and Carpet Sharks (Heterodontiformes, Lamniformes and Orectolobiformes)*, Vol. 2. Rome: FAO, 109–115.

Cortés, E., Arocha, F., Beerkircher, L., Carvalho, F., Domingo, A., Heupel, M., et al. (2010). Ecological risk assessment of pelagic sharks caught in Atlantic pelagic longline fisheries. *Aquat. Living Resour.* 23, 25–34. doi: 10.1051/alr/2009044

Cortés, E., Domingo, A., Miller, P., Forselledo, R., Mas, F., Arocha, F., et al. (2015). Expanded ecological risk assessment of pelagic sharks caught in Atlantic pelagic longline fisheries. *Collect. Vol. Sci. Pap. ICCAT* 71, 2637–2688.

Cosgrove, R., Arregui, I., Arrizabalaga, H., Goni, N., and Neilson, J. D. (2015). Predation of pop-up satellite archival tagged albacore (*Thunnus alalunga*). *Fish. Res.* 162, 48–52. doi: 10.1016/j.fishres.2014.09.003

Costa, F. E. S., Braga, F. M. S., Arfelli, C. A., and Amorim, A. F. (2002). Aspects of the reproductive biology of the Shortfin mako, *Isurus oxyrinchus* (elasmobranchii Lamnidae), in the southeastern region of Brazil. *Braz. J. Biol.* 62, 239–248. doi: 10.1590/S1519-69842002000200007

Díez, G., Soto, M., and Blanco, J. M. (2015). Biological characterization of the skin of shortfin mako shark *Isurus oxyrinchus* and preliminary study of the hydrodynamic behaviour through computational fluid dynamics. *J. Fish. Biol.* 87, 123–137. doi: 10.1111/jfb.12705

Doherty, P. D., Baxter, J. M., Gell, F. R., Godley, B. J., Graham, R. T., Hall, G., et al. (2017). Long-term satellite tracking reveals variable seasonal migration strategies of basking sharks in the north-east Atlantic. *Sci. Rep.* 7:42837. doi: 10.1038/srep42837

Domingo, A., Rios, M., and Pons, M. (2009). Distribucion espacio temporal, composición de tallas y relaciones ambientales del atún Aleta Amarilla (*Thunnus albacares*) en el Atlántico SW. *Col. Vol. Sci. Pap. ICCAT* 64, 999–1010.

Dulvy, N. K., Baum, J. K., Clarke, S., Compagno, L. J., Cortés, E., Domingo, A., et al. (2008). You can swim but you can't hide: the global status and conservation of oceanic pelagic sharks and rays. *Aquat. Conserv. Mar. Freshwater Ecosyst.* 18, 459–482. doi: 10.1002/aqc.975

Fay, M. P., and Shaw, P. A. (2010). Exact and asymptotic weighted logrank tests for interval censored data: the interval R package. *J. Stat. Softw.* 36, 1–34.

Ferretti, F., Worm, B., Britten, G. L., Heithaus, M. R., and Lotze, H. K. (2010). Patterns and ecosystem consequences of shark declines in the ocean. *Ecol. Lett.* 13, 1055–1071. doi: 10.1111/j.1461-0248.2010.01489.x

Fox, J., and Weisberg, S. (2019). *An {R} Companion to Applied Regression*, 3rd Edn. Thousand Oaks, CA: Sage.

Francis, M. P., Holdsworth, J. C., and Block, B. A. (2015). Life in the open ocean: seasonal migration and diel diving behaviour of Southern Hemisphere porbeagle sharks (*Lamna nasus*). *Mar. Biol.* 162, 2305–2323. doi: 10.1007/s00227-015-2756-z

Francis, M. P., Shivji, M. S., Duffy, C. A., Rogers, P. J., Byrne, M. E., Wetherbee, B. M., et al. (2019). Oceanic nomad or coastal resident? Behavioural switching in the shortfin mako shark (*Isurus oxyrinchus*). *Mar. Bio.* 166, 1–16. doi: 10.1007/s00227-018-3453-5

Gaube, P., Barceló, C., McGillicuddy, D. J. Jr., Domingo, A., Miller, P., Giffoni, B., et al. (2017). The use of mesoscale eddies by juvenile loggerhead sea turtles (Caretta caretta) in the southwestern Atlantic. *PLoS One* 12:e0172839. doi: 10.1371/journal.pone.0172839

Gibson, K. J., Streich, M. K., Topping, T. S., and Stunz, G. W. (2021). New insights into the seasonal movement patterns of Shortfin Mako sharks in the Gulf of Mexico. *Front. Mar. Sci.* 8:5. doi: 10.3389/fmars.2021.623104

Graham, R. T., Witt, M. J., Castellanos, D. W., Remolina, F., Maxwell, S., Godley, B. J., et al. (2012). Satellite tracking of manta rays highlights challenges to their conservation. *PloS One* 7:e36834. doi: 10.1371/journal.pone.0036834

Gross, J., and Ligges, U. (2015). *nortest: Tests for Normality. R Package Version 1.0-4*. Available online at: https://CRAN.R-project.org/package=nortest (accessed February 26, 2021).

Hammerschlag, N., Gallagher, A. J., and Lazarre, D. M. (2011). A review of shark satellite tagging studies. *J. Exp. Mar. Biol. Ecol.* 398, 1–8. doi: 10.1016/j.jembe.2010.12.012

Hays, G. C., Bradshaw, C. J. A., James, M. C., Lovell, P., and Sims, D. W. (2007). Why do Argos satellite tags deployed on marine animals stop transmitting? *J. Exp. Mar. Bio. Ecol.* 349, 52–60. doi: 10.1016/j.jembe.2007.04.016

Heupel, M. R., Carlson, J. K., and Simpfendorfer, C. A. (2007). Shark nursery areas: concepts, definition, characterization and assumptions. *Mar. Ecol. Prog. Ser.* 337, 287–297. doi: 10.3354/meps337287

Hijmans, R. J. (2020). *raster: Geographic Data Analysis and Modeling. R package version 3.4-5*. Available online at: https://CRAN.R-project.org/package=raster (accessed February 26, 2021).

Hoffmayer, E. R., Franks, J. S., Driggers, W. B., and Howey, P. W. (2013). Diel vertical movements of a scalloped hammerhead, *Sphyrna lewini*, in the northern Gulf of Mexico. *B. Mar. Sci.* 89, 551–557. doi: 10.5343/bms.2012.1048

Hoolihan, J. P., Wells, R. J. D., Luo, J., Falterman, B., Prince, E. D., and Rooker, J. R. (2014). Vertical and horizontal movements of yellowfin tuna in the Gulf of Mexico. *Mar. Coast. Fish.* 6, 211–222. doi: 10.1080/19425120.2014.935900

Howey-Jordan, L. A., Brooks, E. J., Abercrombie, D. L., Jordan, L. K., Brooks, A., Williams, S., et al. (2013). Complex movements, philopatry and expanded depth range of a severely threatened pelagic shark, the oceanic whitetip (*Carcharhinus longimanus*) in the western North Atlantic. *PloS One* 8:e56588. doi: 10.1371/journal.pone.0056588

ICCAT (2018). *Report of the 2018 ICCAT Intersessional Meeting of the Shark Species Group*. Madrid: ICCAT–International Commission for the Conservation of Atlantic Tunas.

IFREMER (2009). *Continental Margins Between 140m and 3500m Depth*. Available online at: https://www.marineregions.org/ (accessed February 22, 2021)

Iosilevskii, G., Papastamatiou, Y. P., Meyer, C. G., and Holland, K. N. (2012). Energetics of the yo-yo dives of predatory sharks. *J. Theor. Biol.* 294, 172–181. doi: 10.1016/j.jtbi.2011.11.008

Jiménez, S., Domingo, A., Abreu, M., and Brazeiro, A. (2011). Structure of the seabird assemblage associated with pelagic longline vessels in the southwestern Atlantic: implications for bycatch. *Endang. Species Res.* 15, 241–254. doi: 10.3354/esr00378

Kerstetter, D. W., Polovina, J., and Graves, J. E. (2004). Evidence of shark predation and scavenging on fishes equipped with pop-up satellite archival tags. *Fish. Bull.* 102:750.

Ketchum, J. T., Hoyos-Padilla, M., Aldana-Moreno, A., Ayres, K., Galván-Magaña, F., Hearn, A., et al. (2020). Shark movement patterns in the Mexican Pacific: a conservation and management perspective. *Adv. Mar. Biol.* 85, 1–37. doi: 10.1016/bs.amb.2020.03.002

Klimley, A. P., Beavers, S. C., Curtis, T. H., and Jorgensen, S. J. (2002). Movements and swimming behavior of three species of sharks in La Jolla Canyon. *California. Environ. Biol. Fishes* 63, 117–135. doi: 10.1023/A:1014200301213

Lemon, J. (2006). Plotrix: a package in the red light district of R. *R News* 6, 8–12.

Loefer, J. K., Sedberry, G. R., and McGovern, J. C. (2005). Vertical movements of a shortfin mako in the western North Atlantic as determined by pop-up satellite tagging. *Southeast. Nat.* 4, 237–246.

Maia, A., Queiroz, N., Cabral, H. N., Santos, A. M., and Correia, J. P. (2007). Reproductive biology and population dynamics of the shortfin mako, *Isurus oxyrinchus* Rafinesque, 1810, off the southwest Portuguese coast, eastern North Atlantic. *J. Appl. Ichthyol* 23, 246–251. doi: 10.1111/j.1439-0426.2007.00849.x

Maia, A., Queiroz, N., Correia, J. P., and Cabral, H. (2006). Food habits of the shortfin mako, *Isurus oxyrinchus*, off the southwest coast of Portugal. *Environ. Biol. Fish.* 77, 157–167. doi: 10.1007/s10641-006-9067-7

Mejuto, J., García-Cortés, B., Ramos-Cartelle, A., De la Serna, J. M., González-González, I., and Fernández-Costa, L. (2009). Standardized catch rates for the blue shark (*Prionace glauca*) and shortfin mako (*Isurus oxyrinchus*) caught by the Spanish surface longline fleet in the Atlantic Ocean during the period 1990-2007. *Collect. Vol. Sci. Pap. ICCAT* 64, 1509–1521.

Mucientes-Sandoval, G., Queiroz, N., Humphries, N. E., Saborido, F., and Sims, D. W. (2012). *Movements, Behaviour And Habitat Preferences of Pop-Up Satellite Tracked Shortfin Mako Sharks (Isurus oxyrinchus) in the North Atlantic*. Vancouver, CA: World Congress of Herpetology, 497–498.

Musyl, M. K., Domeier, M. L., Nasby-Lucas, N., Brill, R. W., McNaughton, L. M., Swimmer, J. Y., et al. (2011). Performance of pop-up satellite archival tags. *Mar. Ecol. Prog. Ser.* 433, 1–28. doi: 10.3354/meps09202

Myers, R. A., Baum, J. K., Shepherd, T. D., Powers, S. P., and Peterson, C. H. (2007). Cascading effects of the loss of apex predatory sharks from a coastal ocean. *Science* 315, 1846–1850. doi: 10.1126/science.1138657

Nakamura, I., Watanabe, Y. Y., Papastamatiou, Y. P., Sato, K., and Meyer, C. G. (2011). Yo-yo vertical movements suggest a foraging strategy for tiger sharks *Galeocerdo cuvier*. *Mar. Ecol. Prog. Ser.* 424, 237–246. doi: 10.3354/meps08980

Natanson, L. J., Winton, M., Bowlby, H., Joyce, W., Deacy, B., Coelho, R., et al. (2020). Updated reproductive parameters for the shortfin mako (*Isurus oxyrinchus*) in the North Atlantic Ocean with inferences of distribution by sex and reproductive stage. *Fish. Bull* 118, 21–36.

Neuwirth, E. (2014). *RColorBrewer: Color Brewer Palettes. R package version 1.1-2*. Available online at: https://CRAN.R-project.org/package=RColorBrewer (accessed February 26, 2021).

Pacoureau, N., Rigby, C. L., Kyne, P. M., Sherley, R. B., Winker, H., Carlson, J. K., et al. (2021). Half a century of global decline in oceanic sharks and rays. *Nature* 589, 567–571. doi: 10.1038/s41586-020-03173-9

Pade, N. G., Queiroz, N., Humphries, N. E., Witt, M. J., Jones, C. S., Noble, L. R., et al. (2009). First results from satellite-linked archival tagging of porbeagle shark, *Lamna nasus*: area fidelity, wider-scale movements and plasticity in diel depth changes. *J. Exp. Mar. Biol. Ecol.* 370, 64–74. doi: 10.1016/j.jembe.2008.12.002

Passadore, C., Domingo, A., Szephegyi, M., and Secchi, E. R. (2014). Influence of environmental and longline fishing operational variables on the presence of killer whales (*Orcinus orca*) in south-western Atlantic. *J. Mar. Biol. Assoc. U.K.* 94:1267. doi: 10.1017/S002531541200166X

Pedersen, M. W., Patterson, T. A., Thygesen, U. H., and Madsen, H. (2011). Estimating animal behavior and residency from movement data. *Oikos* 120, 1281–1290. doi: 10.1111/j.1600-0706.2011.19044.x

Pershing, A. J., Christensen, L. B., Record, N. R., Sherwood, G. D., and Stetson, P. B. (2010). The impact of whaling on the ocean carbon cycle: why bigger was better. *PloS One* 5:e12444. doi: 10.1371/journal.pone.0012444

Petersen, S., Nel, D., and Omardien, A. (2007). *Towards an Ecosystem Approach to Longline Fisheries in the Benguela: An Assessment of Impacts on Seabirds, Sea Turtles and Sharks. WWF Report Series–2007/Marine/001*. Cape Town: World Wild Fund.

Pierce, D. (2019). *ncdf4: Interface to Unidata netCDF (Version 4 or Earlier) Format Data Files. R Package Version 1.17*. Available online at: https://CRAN.R-project.org/package=ncdf4 (accessed February 26, 2021).

Pons, M., and Domingo, A. (2013). Update of standardized catch rates of shortfin mako, *Isurus oxyrinchus*, caught by the Uruguayan longline fleet (1982-2010). *Collect. Vol. Sci. Pap. ICCAT* 69, 1630–1638.

QGIS.org (2021). *QGIS Geographic Information System*. Available online at: https://qgis.org/en/site/ (accessed February 27, 2021).

Queiroz, N., Humphries, N. E., Couto, A., Vedor, M., da Costa, I., Sequeira, A. M. M., et al. (2019). Global spatial risk assessment of sharks under the footprint of fisheries. *Nature* 572, 461–466. doi: 10.1038/s41586-019-1444-4

Queiroz, N., Humphries, N. E., Mucientes, G., Hammerschlag, N., Lima, F. P., Scales, K. L., et al. (2016). Ocean-wide tracking of pelagic sharks reveals extent of overlap with longline fishing hotspots. *P. Natl. Acad. Sci.U.S.A.* 113, 1582–1587. doi: 10.1073/pnas.1510090113

R Core Team (2020). *R: A Language and Environment for Statistical Computing*. Vienna: R Foundation for Statistical Computing.

Rigby, C. L., Barreto, R., Carlson, J., Fernando, D., Fordham, S., Francis, M. P., et al. (2019). *Isurus oxyrinchus. The IUCN Red List of Threatened Species 2019:e.T39341A2903170*. Available online at: http://dx.doi.org/10.2305/IUCN.UK.2019-1.RLTS.T39341A2903170.en (accessed October 25, 2020).

Rogers, P. J., Huveneers, C., Page, B., Goldsworthy, S. D., Coyne, M., Lowther, A. D., et al. (2015). Living on the continental shelf edge: habitat use of juvenile shortfin makos *Isurus oxyrinchus* in the Great Australian Bight, southern Australia. *Fish. Oceanogr.* 24, 205–218. doi: 10.1111/fog.12103

Santos, C. C., and Coelho, R. (2018). Migrations and habitat use of the smooth hammerhead shark (*Sphyrna zygaena*) in the Atlantic Ocean. *PloS One* 13:e0198664. doi: 10.1371/journal.pone.0198664

Saunders, R. A., Royer, F., and Clarke, M. W. (2011). Winter migration and diving behaviour of porbeagle shark, *Lamna nasus*, in the Northeast Atlantic. *ICES J. Mar. Sci.* 68, 166–174. doi: 10.1093/icesjms/fsq145

Sepulveda, C. A., Kohin, S., Chan, C., Vetter, R., and Graham, J. B. (2004). Movement patterns, depth preferences, and stomach temperatures of free-swimming juvenile mako sharks, *Isurus oxyrinchus*, in the Southern California. *Bight. Mar. Biol.* 145, 191–199. doi: 10.1007/s00227-004-1356-0

Shillinger, G. L., Palacios, D. M., Bailey, H., Bograd, S. J., Swithenbank, A. M., Gaspar, P., et al. (2008). Persistent leatherback turtle migrations present opportunities for conservation. *PLoS Biol.* 6:e171. doi: 10.1371/journal.pbio.0060171

Simpfendorfer, C., Cortés, E., Heupel, M., Brooks, E., Babcock, E., Baum, J., et al. (2008). *An Integrated Approach to Determining the Risk of Overexploitation for Data-Poor Pelagic Atlantic sharks. ICCAT SCRS/2008/140*. Madrid: International Commission for the Conservation of Atlantic Tunas.

Skomal, G., Marshall, H., Galuardi, B., Natanson, L., Braun, C. D., and Bernal, D. (2021). Horizontal and vertical movement patterns and habitat use of juvenile porbeagles (*Lamna nasus*) in the western north Atlantic. *Front. Mar. Sci.* 8:624158. doi: 10.3389/fmars.2021.624158

Skomal, G. B., Zeeman, S. I., Chisholm, J. H., Summers, E. L., Walsh, H. J., McMahon, K. W., et al. (2009). Transequatorial migrations by basking sharks in the western Atlantic Ocean. *Curr. Biol.* 19, 1019–1022. doi: 10.1016/j.cub.2009.04.019

Stabler, B. (2013). *Shapefiles: Read and Write ESRI Shapefiles. R Package Version 0.7.* Available online at: https://CRAN.R-project.org/package=shapefiles (accessed February 26, 2021).

Stevens, J. D. (2008). "The biology and ecology of the shortfin mako shark, *Isurus oxyrinchus*," in *Sharks of the Open Ocean: Biology, Fisheries and Conservation*, eds M. D. Camhi, E. K. Pikitch, and E. A. Babcock (Oxford: Blackwell Publishing), 87–94.

Stevens, J. D., Bonfil, R., Dulvy, N. K., and Walker, P. A. (2000). The effects of fishing on sharks, rays, and chimaeras (chondrichthyans), and the implications for marine ecosystems. *ICES J. Mar. Sci.* 57, 476–494. doi: 10.1006/jmsc.2000.0724

Stevens, J. D., Bradford, R. W., and West, G. J. (2010). Satellite tagging of blue sharks (*Prionace glauca*) and other pelagic sharks off eastern Australia: depth behaviour, temperature experience and movements. *Mar. Biol.* 157, 575–591. doi: 10.1007/s00227-009-1343-6

Stillwell, C. E., and Kohler, N. E. (1982). Food, feeding habits, and estimates of daily ration of the shortfin mako (*Isurus oxyrinchus*) in the Northwest Atlantic. *Can. J. Fish. Aquat. Sci.* 39, 407–414. doi: 10.1139/f82-058

Teets, D. A. (2003). Predicting sunrise and sunset times. *Coll. Math. J.* 34, 317–321.

Vaudo, J. J., Byrne, M. E., Wetherbee, B. M., Harvey, G. M., and Shivji, M. S. (2017). Long-term satellite tracking reveals region-specific movements of a large pelagic predator, the shortfin mako shark, in the western North Atlantic Ocean. *J. Appl. Ecol.* 54, 1765–1775. doi: 10.1111/1365-2664.12852

Vaudo, J. J., Wetherbee, B. M., Wood, A. D., Weng, K., Howey-Jordan, L. A., Harvey, G. M., et al. (2016). Vertical movements of shortfin mako sharks *Isurus oxyrinchus* in the western North Atlantic Ocean are strongly influenced by temperature. *Mar. Ecol. Prog. Ser.* 547, 163–175. doi: 10.3354/meps11646

Vetter, R., Kohin, S., Preti, A., Mcclatchie, S. A. M., and Dewar, H. (2008). Predatory interactions and niche overlap between mako shark, *Isurus oxyrinchus*, and jumbo squid, *Dosidicus gigas*, in the California Current. *CalCOFI Rep.* 49, 142–156.

Vooren, C. M., Klippel, S., and Galina, A. B. (2005). "Elasmobrânquios das águas costeiras da Plataforma Sul," in *Ações Para a Conservação de Tubarões e Raias no Sul do Brasil*, eds C. M. Vooren and S. Klippel (Porto Alegre: Igaré), 113–120.

Weng, K. C., Boustany, A. M., Pyle, P., Anderson, S. D., Brown, A., and Block, B. A. (2007). Migration and habitat of white sharks (*Carcharodon carcharias*) in the eastern Pacific Ocean. *Mar. Biol.* 152, 877–894. doi: 10.1007/s00227-007-0739-4

Wickham, H. (2016). *ggplot2: Elegant Graphics for Data Analysis*. New York, NY: Springer-Verlag.

Wickham, H., and Seidel, D. (2020). *scales: Scale Functions for Visualization. R package version 1.1.1*. Available online at: https://CRAN.R-project.org/package=scales (accessed February 26, 2021).

Wildlife Computers (2018). *Location Processing (GPE3 & Fastloc) in the Wildlife Computers Data Portal User Guide*. Available online at: https://static.wildlifecomputers.com/Location-Processing-UserGuide.pdf (accessed November 22, 2019).

Wilson, S. G., Jonsen, I. D., Schallert, R. J., Ganong, J. E., Castleton, M. R., Spares, A. D., et al. (2015). Tracking the fidelity of Atlantic bluefin tuna released in Canadian waters to the Gulf of Mexico spawning grounds. *Can. J. Fish. Aquat. Sci.* 72, 1700–1717. doi: 10.1139/cjfas-2015-0110

Conflict of Interest: The authors declare that the research was conducted in the absence of any commercial or financial relationships that could be construed as a potential conflict of interest.

frontiers in Marine Science

ORIGINAL RESEARCH
published: 06 August 2021
doi: 10.3389/fmars.2021.704134

Ontogenetic Patterns of Elemental Tracers in the Vertebrae Cartilage of Coastal and Oceanic Sharks

Mariah C. Livernois[1]*, John A. Mohan[2], Thomas C. TinHan[1], Travis M. Richards[1], Brett J. Falterman[3], Nathan R. Miller[4] and R. J. David Wells[1,5]

[1] Department of Marine Biology, Texas A&M University at Galveston, Galveston, TX, United States, [2] School of Marine and Environmental Programs, University of New England, Biddeford, ME, United States, [3] Fisheries Research Support, L.L.C., Mandeville, LA, United States, [4] Jackson School of Geosciences, The University of Texas at Austin, Austin, TX, United States, [5] Department of Ecology and Conservation Biology, Texas A&M University, College Station, TX, United States

As predators, coastal and oceanic sharks play critical roles in shaping ecosystem structure and function, but most shark species are highly susceptible to population declines. Effective management of vulnerable shark populations requires knowledge of species-specific movement and habitat use patterns. Since sharks are often highly mobile and long-lived, tracking their habitat use patterns over large spatiotemporal scales is challenging. However, the analysis of elemental tracers in vertebral cartilage can describe a continuous record of the life history of an individual from birth to death. This study examined trace elements (Li, Mg, Mn, Zn, Sr, and Ba) along vertebral transects of five shark species with unique life histories. From most freshwater-associated to most oceanic, these species include Bull Sharks (*Carcharhinus leucas*), Bonnethead Sharks (*Sphyrna tiburo*), Blacktip Sharks (*Carcharhinus limbatus*), Spinner Sharks (*Carcharhinus brevipinna*), and Shortfin Mako Sharks (*Isurus oxyrinchus*). Element concentrations were compared across life stages (young-of-the-year, early juvenile, late juvenile, and adult) to infer species-specific ontogenetic patterns of habitat use and movement. Many of the observed elemental patterns could be explained by known life history traits: *C. leucas* exhibited clear ontogenetic changes in elemental composition matching expected changes in their use of freshwater habitats over time. *S. tiburo* elemental composition did not differ across ontogeny, suggesting residence in estuarine/coastal regions. The patterns of elemental composition were strikingly similar between *C. brevipinna* and *C. limbatus*, suggesting they co-occur in similar habitats across ontogeny. *I. oxyrinchus* elemental composition was stable over time, but some ontogenetic shifts occurred that may be due to changes in migration patterns with maturation. The results presented in this study enhance our understanding of the habitat use and movement patterns of coastal and oceanic sharks, and highlights the applicability of vertebral chemistry as a tool for characterizing shark life history traits.

Keywords: trace elements, vertebrae, ontogeny, sharks, habitat use, movement

Edited by:
Clive N. Trueman,
University of Southampton,
United Kingdom

Reviewed by:
Susanne Eva Tanner,
University of Lisbon, Portugal
Ming-Tsung Chung,
The University of Tokyo, Japan

****Correspondence:***
Mariah C. Livernois
mlivernois@tamu.edu

Specialty section:
This article was submitted to
Marine Megafauna,
a section of the journal
Frontiers in Marine Science

Received: *01 May 2021*
Accepted: *13 July 2021*
Published: *06 August 2021*

Citation:
Livernois MC, Mohan JA, TinHan TC, Richards TM, Falterman BJ, Miller NR and Wells RJD (2021) Ontogenetic Patterns of Elemental Tracers in the Vertebrae Cartilage of Coastal and Oceanic Sharks. Front. Mar. Sci. 8:704134. doi: 10.3389/fmars.2021.704134

INTRODUCTION

Marine predators, including coastal and oceanic sharks, play critical roles in shaping ecosystem structure and function, primarily through direct (predation) and indirect (risk/behavior) effects on prey populations (Heithaus et al., 2008). Most shark species demonstrate longer lifespans, slower reproductive development, and lower fecundity than most exploited teleost fishes (Hoenig and Gruber, 1990). These traits enhance their susceptibility to population declines due to stressors such as habitat loss, climate change, and fishing pressure (Worm et al., 2013). The decline and loss of sharks in coastal waters can have profound effects on local ecological dynamics (Myers et al., 2007; Ferretti et al., 2010), so it is essential to understand the unique life history characteristics of these species to build effective management and conservation strategies. Central to this effort will be increasing our knowledge of species- and population-specific movement and habitat use patterns, migration routes, degrees of site fidelity, and population connectivity (Speed et al., 2011; Chapman et al., 2015).

Most estuarine and coastal environments are highly productive and diverse, and many shark species use these regions for reproduction, feeding, and as juvenile nursery grounds (Knip et al., 2010; Bethea et al., 2015). The reliance on nearshore habitats by a variety of shark species means that interspecific co-occurrence is likely, along with potential ecological interactions (Matich et al., 2017a; Heupel et al., 2019). The implications of multiple-predator co-occurrence can be widespread, including altered predation pressure for shared prey populations (Sih et al., 1998). However, some degree of differentiation in life history among sympatric predator species is expected, since resource partitioning often occurs to diminish potential competitive interactions (Papastamatiou et al., 2006). Therefore, examining the life history patterns of multiple shark species simultaneously can provide a far more informative view of ecosystem function than single-species studies alone.

Since large predators are often highly mobile and long-lived, tracking their movements and habitat use over extended periods of time and space can be prohibitively challenging (e.g., Block et al., 2011). One method for examining shark life history that has been developed in recent years is the analysis of natural biogeochemical tracers in vertebrae. Elements that are present in the environment are incorporated into the vertebral hydroxyapatite matrix during the biomineralization process, as the vertebrae grow concentrically over time. Although studies validating elemental uptake pathways into elasmobranch vertebrae are currently limited, concentrations of certain elements are thought to be associated with environmental variables such as salinity (Sr, Ba; Tillett et al., 2011) and temperature (Ba, Mg; Smith et al., 2013), dietary intake (Zn, Mn; Mathews and Fisher, 2009), maternal loading (Zn; Raoult et al., 2018), and unresolved physiological controls (McMillan et al., 2017). Consequently, chemical analysis of vertebrae sampled continuously along their radial growth axis may proxy how environmental conditions changed throughout an individual's life (Scharer et al., 2012; Smith et al., 2013). This method has been used on sharks to retrospectively determine natal origin (Lewis et al., 2016; Smith et al., 2016; TinHan et al., 2020), movements across salinity gradients that correspond with ontogeny and reproduction (Tillett et al., 2011), and lifetime interactions with oceanographic features (Mohan et al., 2018).

This study focused on an assemblage of coastal and oceanic shark species in the northwestern Gulf of Mexico (nwGOM), from Galveston, TX, United States to the Mississippi River Delta, LA, United States (**Figure 1**). The biological diversity and habitat heterogeneity created by estuarine-oceanic gradients in the nwGOM makes it a particularly interesting area to examine the life histories of sharks. The selected species inhabit a gradient of habitats from freshwater-influenced estuaries to the open ocean, and experience varying degrees of potential co-occurrence and overlap. In approximate order of most estuarine to most oceanic, the species of interest in this study are Bull Sharks (*Carcharhinus leucas*), Bonnethead Sharks (*Sphyrna tiburo*), Blacktip Sharks (*Carcharhinus limbatus*), Spinner Sharks (*Carcharhinus brevipinna*), and Shortfin Mako Sharks (*Isurus oxyrinchus*). Using elemental tracers in vertebrae, the objectives of this study are to identify patterns in the elemental signatures of vertebral cartilage of five shark species across ontogeny, and to use the observed patterns to infer aspects of each species' life history, such as movements and habitat use patterns.

MATERIALS AND METHODS

Study Area and Species

Sharks used for this study were collected from the nwGOM, specifically near Galveston, Texas and the Mississippi River Delta, Louisiana (**Figure 1**). This region hosts a wide range of environmental conditions due to coastal and oceanic currents and freshwater input from estuaries. Bathymetry varies across the nwGOM; the continental shelf (to 200 m depth) extends far offshore (up to ∼100 nautical miles) in the western part of this region, but the shelf break is closer to shore (∼10 nautical miles) near the Mississippi River Delta (Bryant et al., 1990). The largest ocean circulation system in the GOM, the Loop Current and associated eddies, can extend into the study area near the Mississippi River Delta (Weisberg and Liu, 2017), but seasonal wind patterns and large riverine inputs generally drive nearshore currents throughout the region (Smith and Jacobs, 2005). Individuals of each shark species collected from Galveston and Louisiana were pooled for analyses, despite some differences in habitats and environmental conditions between those sampling regions. Our study aimed to describe movement and habitat use patterns across a larger spatial scale (the nwGOM), as opposed to comparing smaller regional patterns.

The species included in this study exemplify the diversity of sharks in the nwGOM. *C. leucas* are euryhaline, and juveniles utilize low salinity habitats as nursery grounds (Froeschke et al., 2010a; Heupel et al., 2010; Matich and Heithaus, 2015). Late juveniles and adults generally inhabit coastal and offshore waters, but adult females return to estuaries to give birth (Tillett et al., 2012). *S. tiburo* inhabit estuarine and coastal environments, generally exhibiting residency within a home estuary but using a variety of habitats within coastal and estuarine zones throughout

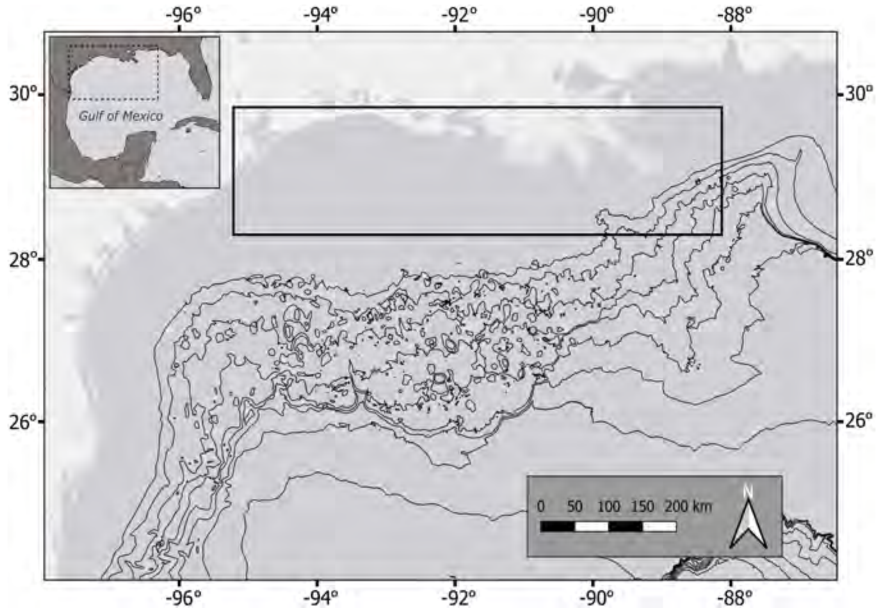

FIGURE 1 | Study area in the northwestern Gulf of Mexico (area within dashed square). The region where all sharks were collected is within the solid black square. Black contour lines begin at the continental shelf break (200 m depth).

their lifetime (Heupel et al., 2006). In the nwGOM, *S. tiburo* are found primarily in moderate to high-salinity waters (20–40 ppt) and near tidal inlets (Froeschke et al., 2010b; Plumlee et al., 2018). *C. limbatus* and *C. brevipinna* both inhabit bays and coastal estuaries as juveniles, where they prefer moderate to high salinities, warm temperatures, and moderate to deep depths (Ward-Paige et al., 2015; Plumlee et al., 2018). Both species are known to travel long distances within coastal waters (Kohler et al., 1998), and *C. limbatus* exhibit evidence of reproductive philopatry (Hueter et al., 2005; Keeney et al., 2005). *I. oxyrinchus* are pelagic and highly migratory, making large-scale movements across ocean basins. *I. oxyrinchus* mating and pupping ground locations in the GOM are not well understood, but there is some evidence to suggest females give birth offshore (Casey and Kohler, 1992; Gibson et al., 2021).

Vertebrae Collection

Individuals from each species were opportunistically collected in the study region between 2014 and 2017. Depending on the number and quality of samples available, 9–12 individuals per species were chosen for analysis. The selected samples, representing the largest individuals in the collection, were evenly distributed between males and females, and were collected during similar time periods (**Table 1**). At least five thoracic vertebrae were removed from each individual, and all vertebrae were frozen at −20°C for storage and were thawed prior to processing.

Once thawed, vertebral columns were submerged for 20–30 s in boiling water to aid in removing excess muscle and connective tissue. Individual vertebral centra were then separated, cleaned, and dried for at least 24 h. A single cleaned vertebral centrum per individual was then cut along its longitudinal axis using an IsoMet low-speed diamond blade saw (Buehler, Illinois Tool Works Inc.), removing a 2 mm cross-section from the center. The two sides of a sectioned centrum are essentially identical, since the vertebrae grow concentrically outward over time. Cross sections from each sample were thus cut in half to isolate one side of the centrum and were mounted on a glass petrographic slide using Crystalbond thermoplastic cement adhesive (**Figure 2**).

Trace Element Sampling

Vertebrae elemental concentrations were measured from sectioned vertebral centra in the direction of radial (outward) growth using an Elemental Scientific NWR193UC (193 nm wavelength, <4 ns pulse width) laser system coupled to an Agilent 7500ce inductively coupled mass spectrometer (LA-ICP-MS) at The University of Texas at Austin. The laser system is equipped with a large format two-volume laser cell with fast washout (<1 s), which accommodated all vertebrae samples and standards in a single loading. Laser ablation parameters were optimized for sensitivity and signal stability from test ablations on representative unknowns: 60% laser power, 10 Hz repetition rate, 25 × 100 μm aperture, 15 μm/s scan rate, He flow of 850 mL/min, and Ar flow of 800 mL/min. Prior to analysis, samples and standards were pre-ablated to remove potential surface contamination. Laser analyses of unknowns were bracketed hourly by standard measurements (USGS MAPS-4, MACS-3 and NIST 612, typically measured in triplicate for 60 s). Baselines were determined from 60-s gas blank intervals measured while the laser was off and all masses were scanned by the quadrupole. USGS MAPS-3 (synthetic bone) was used as the primary reference standard and accuracy and precision were proxied from 39 replicates of NIST 612 and USGS MACS-3

TABLE 1 | Sample sizes (Count) of individuals analyzed with LA-ICP-MS by species and sex, with years of collection, average fork length (FL) ± 1 SD in cm, and range of ages in years (sexes pooled).

Species	Sex	Count	Years	FL	Age range	Total count
C. leucas	Male	5	2015–2016	136.1 ± 39.5	1–16	10
	Female	5	2014–2016	103.8 ± 15.8		
S. tiburo	Male	6	2014–2016	83.4 ± 4.6	2–10	12
	Female	6	2014–2016	94.7 ± 7.3		
C. limbatus	Male	6	2015–2017	122.7 ± 8.9	3–15	12
	Female	6	2015–2017	133.6 ± 15.2		
C. brevipinna	Male	5	2015–2016	146.5 ± 7.0	3–17	10
	Female	5	2015–2016	152.9 ± 39.0		
I. oxyrinchus	Male	7	2014–2015	199.2 ± 25.1	5–16	9
	Female	3	2015	217.5 ± 25.3		

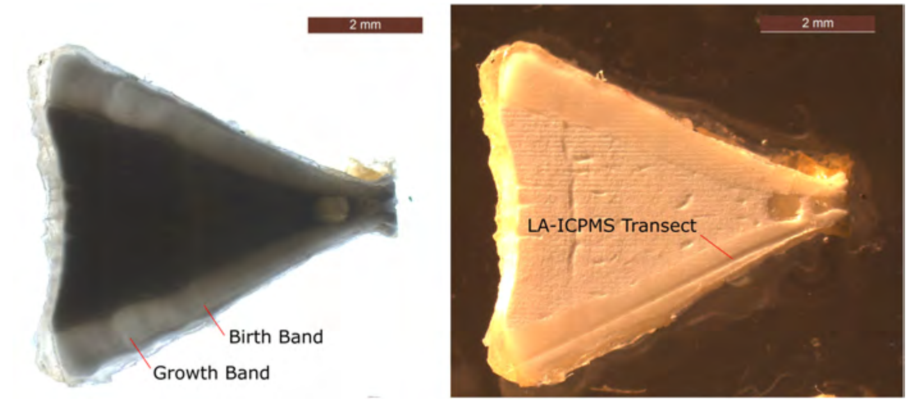

FIGURE 2 | Example of a sectioned *C. leucas* vertebral centrum, shown with transmitted light **(left)** for viewing growth bands (birth band and first growth band shown with red lines), and reflected light **(right)** for viewing LA-ICP-MS transect path.

(synthetic aragonite) analyzed as unknowns. Analyte recoveries for NIST 612 and USGS MACS-3 were typically within 5% of GeoREM preferred values. Oxide production rates, as monitored by ThO/Th on NIST 612, averaged 0.34% over the analysis periods. Laser energy densities over the analytical sessions averaged 3.70 ± 0.04 J/cm^2 for line traverses. The quadrupole time-resolved method measured 11 masses using integration times of 10 ms ($^{24-25}$Mg, ^{43}Ca, ^{55}Mn, ^{88}Sr), 20 ms (^{7}Li, $^{66-68}$Zn, ^{138}Ba), 25 ms (^{137}Ba). The sampling period of 0.24 s corresponds to 89% quadrupole measurement time, with data reporting every 3.63 μm at the scanning rate of 15 μm/s. Time-resolved intensities were converted to concentration (ppm) equivalents using Iolite software (Hellstrom et al., 2008), with ^{43}Ca as the internal standard and a Ca index value of 35 weight% (Mohan et al., 2018). Specifically, the counts-per-second (CPS) of each element were ratioed to the ^{43}Ca CPS at each time point along the transects, which was compared to the known element:Ca ratio in the reference standard. Many studies of otolith and vertebrae chemistry have converted ppm to element:Ca molar ratios, but this was not conducted for these element concentrations since the ppm units were already standardized to ^{43}Ca. Assuming a constant index value of Ca (35 weight%) may influence the reliability of the calculated element concentrations, given there is the potential for variability in Ca within and among vertebrae. However, an examination of Ca CPS along a transect in this study revealed limited Ca variability, which was unlikely to drastically affect element concentration estimates. Future studies of the variation in Ca weight% within and among shark vertebrae would enhance the precision of LA-ICP-MS results.

Aging and Life Stage Determination

Following LA-ICP-MS analysis, digital images of vertebral centra were obtained using transmitted light on a dissecting microscope mounted with a camera to visualize the opaque bands in the corpus calcareum that correspond to growth (growth bands, **Figure 2**). The age of each shark was determined by counting the visible growth bands, with four independent readers conducting blind counts and subsequently resolving any discrepancies. The birth band was identified as the first growth band accompanied by a change in the growth axis angle. Each individual growth band after the birth band was also identified and marked during the aging process. For all species but *I. oxyrinchus*, annual deposition of growth bands (one growth band per year) was assumed (McMillan et al., 2017). For *I. oxyrinchus*, we assumed a deposition rate of two growth bands per year for the first 5 years of life, then annual deposition for the remaining years (Wells et al., 2013; Kinney et al., 2016). The distance (μm) from the start of the LA-ICP-MS laser transect path to the birth band was measured for each transect using ImageJ v1.53a (Schneider et al., 2012), and any prenatal trace element data were excluded from further analyses. The birth band was thus used as the starting point of each transect. Distances (μm) from the birth band to each growth band were then measured, which provided an age (in years) at each measurement along a given transect. Finally, the distance (μm) from the birth band to the visible edge of the corpus calcareum was measured to determine the end of the transect, and all data beyond that point were excluded from analyses.

To examine ontogenetic patterns of elemental signatures, life stages were determined for each shark species based on literature-derived values of age at 50% sexual maturity (**Table 2**). Age at maturity is sex-specific for *C. limbatus*, *C. brevipinna*, and *I. oxyrinchus*, but not for *C. leucas* or *S. tiburo*, which was reflected in life stage determination. We isolated four distinct life stages: young-of-the-year (YOY), early juvenile (EJ), late juvenile (LJ), and adult (AD). The juvenile stage, after surviving as a YOY but before reaching maturity, is prolonged for many of the study species, and can include periods of ontogenetic shifts in habitat use and feeding. To examine this period in greater detail, we partitioned it into EJ (first half of juvenile stage) and LJ (second half) for all species but *S. tiburo*. Since *S. tiburo* mature quickly (age 2), the juvenile stage was not partitioned and did not include an EJ stage. Life stage designations were then added to the trace element transect data to align with the distance at each age based on growth band measurements. Since not all individuals of a given species were the same age, the number of individuals within each life stage differed (i.e., some sharks were captured prior to reaching maturity). Sample sizes for each life stage per species are listed in **Table 2**.

Statistical Analyses

Six elements were used for statistical analysis: Li, Mg, Mn, Zn, Sr, and Ba. Because we obtained comparable profiles for elements measured with different isotopes, for plotting and statistical analyses we selected the isotope with highest natural abundance (^{24}Mg, ^{66}Zn, ^{138}Ba). Element concentration values were smoothed to remove the effect of outliers by conducting a 15-point rolling median followed by a 15-point rolling mean along the time-series of each transect, a filter length corresponding to approximately 50 μm of vertebrae material (1–2 months of growth). Smoothed trace element concentration means and 95% confidence intervals were plotted against distance (increasing age) from the birth band to visually and qualitatively compare elemental patterns within and among species.

Prior to statistical analyses of life stages, one mean value was calculated per element per life stage for each individual shark. While this reduces the amount of information provided by the transects, it is necessary to avoid issues with autocorrelation and lack of independence among data points. Since the original data are in the form of a time series (i.e., highly autocorrelated and thus each observation is not independent from the others), using multiple data points within each individual's life stage would be inappropriate for most statistical tests. A multi-element principal component analysis (PCA) was conducted for each species, with life stage as the grouping variable. This provides a visualization of how vertebrae elemental composition differs among life stages within each species by reducing the multidimensional dataset to two dimensions; namely, by plotting the principal components that explain the most variability in the data (Hotelling, 1933). One PCA was conducted per species using the "prcomp" function in the "stats" package in R version 3.5.1 (R Core Team, 2019), with data points being zero-centered and scaled to unit variance prior to analysis. Although PCAs are valuable for examining overall elemental composition of vertebrae across ontogeny, an Analysis of Variance (ANOVA) framework was also employed to determine differences in individual elements across life stages. A series of ANOVA tests were conducted for each species to determine which elements differed across life stages (n = 6 tests per species, one per element). All models were checked for the assumptions of homoscedasticity and normality of residuals using Levene's test and Shapiro–Wilks test, respectively. Most models fit these assumptions.

RESULTS

Plots of the mean concentration along the LA-ICP-MS transects revealed species-specific elemental patterns through life (**Figure 3**). We use distance from the birth band to approximate time from birth to death of each individual. Li concentrations generally decreased over time for all species except *C. leucas*, which increased over time (from ∼1 to 1.5 ppm, **Figure 3A**). *S. tiburo* consistently had the highest Li concentrations of all species (∼2.5 to 2 ppm), followed by *C. brevipinna* (∼2 to 1.5 ppm), then *C. limbatus* and *I. oxyrinchus* (both ∼1.5 to 1 ppm, **Figure 3A**). Mg concentrations were very similar among species, and generally exhibited a declining trend over time (from ∼4000 to ∼3500 ppm) but with high variability (**Figure 3B**). Mn concentrations were similar for all species except *S. tiburo*, which exhibited much higher concentrations that increased throughout life (from ∼75 to ∼200 ppm, **Figure 3C**). For *C. leucas*, *C. limbatus*, and *C. brevipinna*, Mn concentrations peaked early in life (∼50 ppm), then declined and stabilized for the remainder of life (∼25 ppm, **Figure 3C**). *I. oxyrinchus* had the lowest Mn concentrations of all species, which were stable over time (∼10 ppm, **Figure 3C**). Zn concentrations were also similar among species, and were generally high early in life (∼30 ppm) followed by a gradual decline, ultimately stabilizing late in life (∼20 ppm, **Figure 3D**). A notable exception was *I. oxyrinchus*, which had consistently higher Zn concentrations than the other species (from ∼45 to ∼30 ppm) and exhibited large oscillations in Zn late in life (**Figure 3D**). Sr concentrations were generally stable over time for all species except *C. leucas*, which exhibited increasing Sr concentration over time (from ∼1750 to ∼2300 ppm, **Figure 3E**). *S. tiburo* had the highest Sr concentrations (∼2250 ppm) until the end of life, when *C. leucas* surpassed them (∼2300 ppm, **Figure 3E**). The lowest Sr values were seen in both *C. limbatus* and *C. brevipinna* (∼1600 ppm), with *I. oxyrinchus* in the middle (∼1900 ppm, **Figure 3E**). Finally, Ba concentrations were low and stable for *C. limbatus*, *C. brevipinna,* and *I. oxyrinchus* over time (all ∼10 ppm, **Figure 3F**). For *C. leucas*, Ba remained stable and higher than all

TABLE 2 | Life stage classifications for each shark species by sex: young-of-the-year (YOY), early juvenile (EJ), late juvenile (LJ), and adult (AD).

Species	Sex	YOY	EJ	LJ	AD	References
C. leucas	M	0	1–4	5–9	10+	Cruz-Martinez et al., 2005
	F	0	1–4	5–9	10+	
	Count	10	10	5	4	
S. tiburo	M	0	NA	1	2+	Parsons, 1993; Carlson and Parsons, 1997
	F	0	NA	1	2+	
	Count	12	NA	12	12	
C. limbatus	M	0	1–2	3–4	5+	Branstetter, 1987; Carlson et al., 2006
	F	0	1–3	4–6	7+	
	Count	12	12	11	11	
C. brevipinna	M	0	1–3	4–6	7+	Branstetter, 1987; Carlson and Baremore, 2005
	F	0	1–3	4–7	8+	
	Count	10	10	9	8	
I. oxyrinchus	M	0	1–3	4–7	8+	Natanson et al., 2006, 2020
	F	0	1–8	9–17	18+	
	Count	9	9	7	5	

Total sample sizes of each life stage per species are listed (Count), with males and females combined. Age at maturity values were obtained from previous studies (References).

other species throughout early life (~30 ppm), then gradually decreased over time (to ~10 ppm, **Figure 3F**). The opposite was true for *S. tiburo*, whose Ba concentrations increased over time and became much higher than all other species late in life (from ~25 to ~150 ppm, **Figure 3F**).

Differences emerged among the study species in terms of the overall elemental composition of vertebrae among life stages based on PCA (**Figure 4**). *C. leucas* life stages separated into two distinct groups: YOY/EJ and LJ/AD (**Figure 4A**). Principal component 1 (PC1) explained the majority (65.2%) of the variation among data points, while PC2 explained much less variation (14.8%). The elements with the most influence along PC1 were Sr and Li (positive loadings), while Mn, Ba, Mg, and Zn had negative loadings for that axis. *S. tiburo* had almost no separation among life stages along either PC axis (**Figure 4B**). PC1 explained 47.5% of the variation among data points, while PC2 explained 23.8%. Loadings were negative along PC1 for all elements. *C. limbatus* exhibited distinct separation of the YOY life stage, while LJ and AD overlapped nearly completely (**Figure 4C**). The EJ ellipse fell between YOY and the LJ/AD grouping. PC1 explained 40.1% of the variation among data points, while PC2 explained 21.8%. The elements with the most influence along PC1 were Ba (positive loading), and Zn and Li (negative loading), which appeared to explain much of the variation among life stages in contract to values of Mg and Sr, whose vectors aligned with variation within each life stage. *C. brevipinna* exhibited a similar pattern to *C. limbatus*, with YOY separating from the other life stages, LJ and AD overlapping, and EJ in the middle (**Figure 4D**). However, the separation between these groupings was less defined, with EJ overlapping more with the LJ/AD group. PC1 explained 34.7% of the variation among data points, and PC2 explained 28.5%. The most influential elements along PC1 were Ba (positive loading), and Mn and Li (negative loadings). Along PC2, Mg and Zn exhibited positive loadings while Sr was negative. For *I. oxyrinchus*, the YOY and EJ ellipses overlapped, and the LJ overlapped slightly with all four life stages (**Figure 4E**). AD was separate from YOY and EJ. PC1 explained 46.6% of the variation among data points, while PC2 explained 19.4%. All elements besides Ba influenced PC1 (negative loadings), while Ba exhibited a negative loading along PC2.

Analysis of individual element concentrations revealed species-specific ontogenetic patterns across life stages (**Figure 5**). Statistically significant results are reported here, while a full summary of results can be found in **Table 3**. For *C. leucas*, five elements differed significantly among life stages: Mg ($p = 0.035$), Mn ($p < 0.001$), Zn ($p = 0.022$), Sr ($p < 0.001$), and Ba ($p < 0.001$, **Table 3** and **Figures 5B–F**). For *S. tiburo*, no elements differed significantly among life stages (**Table 3** and **Figures 5A–F**). The mean concentrations of four elements differed significantly among life stages for *C. limbatus*: Li ($p < 0.001$), Mn ($p < 0.001$), Zn ($p < 0.001$), and Ba ($p < 0.001$, **Table 3** and **Figures 5A,C,D,F**). The mean concentrations of three elements differed significantly among life stages for *C. brevipinna*: Li ($p < 0.001$), Mn ($p < 0.001$), and Ba ($p < 0.001$, **Table 3** and **Figures 5A,C,F**). For *I. oxyrinchus*, four elements differed significantly among life stages: Li ($p < 0.001$), Mg ($p = 0.025$), Mn ($p < 0.001$), and Zn ($p = 0.011$, **Table 3** and **Figures 5A–D**).

DISCUSSION

Patterns of element concentrations in the vertebral cartilage of five shark species may be linked to their movement and habitat use patterns through life. The documented ontogenetic patterns of vertebral element composition can be partly explained by known life history traits. However, some unexpected species-specific elemental concentration patterns may be linked to physiological and biological controls, as opposed to purely reflecting ambient environmental conditions. While much is left to learn regarding the pathways and rates of element uptake in elasmobranch vertebrae, the results presented here highlight the

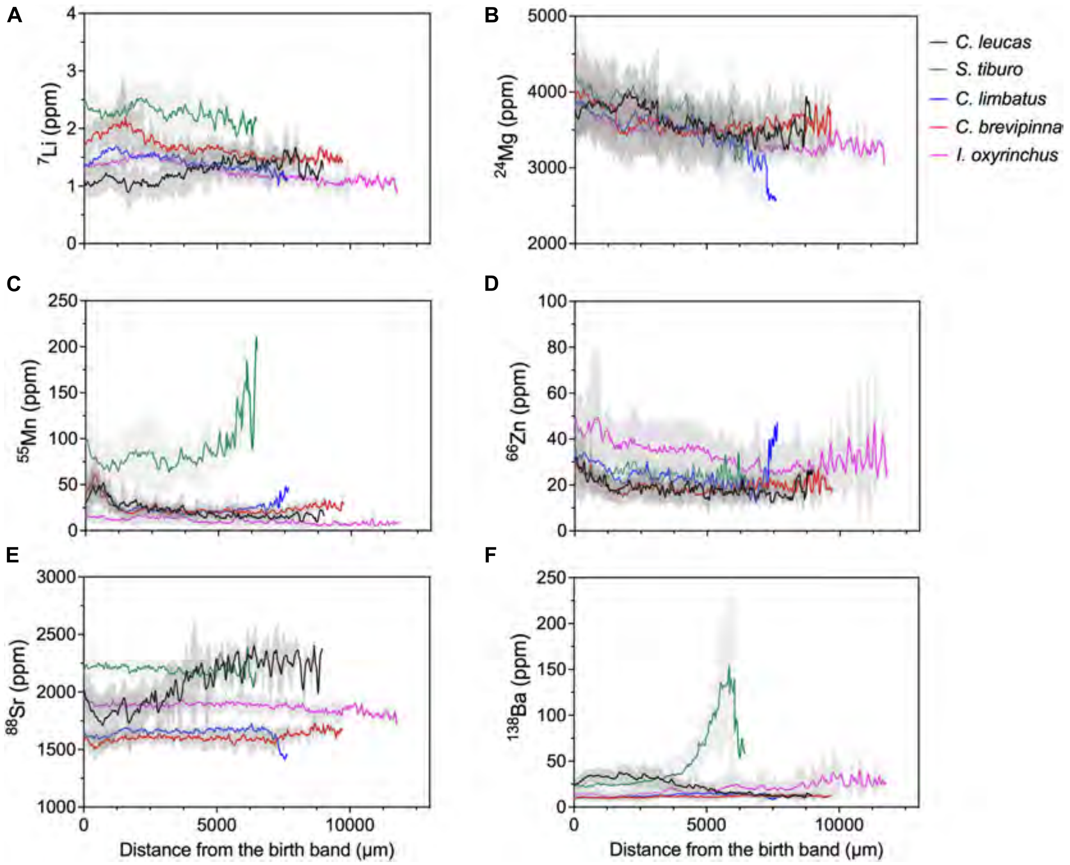

FIGURE 3 | LA-ICP-MS transects for each individual element, with species represented by color. Solid lines represent the mean value of the element from the birth band (distance = 0) to capture for each species individually. Shaded areas represent 95% confidence intervals around the mean.

applicability of this technique as a method for understanding the life histories of estuarine, coastal, and oceanic sharks.

The most euryhaline of the study species, *C. leucas* exhibit a complex life history that was reflected in ontogenetic patterns of vertebral element concentrations. A clear difference in overall element composition was observed between early life (YOY and EJ) and later life (LJ and AD), and all but one of the elements (Li) differed significantly across life stages. Since *C. leucas* are known to use freshwater regions in estuaries as nursery grounds early in life (Heupel et al., 2010), many of the observed patterns of element composition in their vertebrae can be explained by changes in their exposure to freshwater as they age. Sr and Ba generally increase and decrease, respectively, with increasing salinity (Dorval et al., 2005), and are considered fairly reliable proxies for salinity history in elasmobranch vertebrae (McMillan et al., 2017). Our results suggest that *C. leucas* inhabit low-salinity estuarine regions throughout the first 4–5 years of life, followed by increasing use of marine habitats as they transition to adulthood. Similar elemental patterns have been observed in the vertebrae of *C. leucas* in Australian coastal waters, including evidence suggesting periodic returns to freshwater habitats for pupping in adult females (Tillett et al., 2011; Werry et al., 2011). The consistent ontogenetic shift in Sr and Ba concentrations in *C. leucas* vertebrae within multiple ocean basins lends support to the use of this method as a tracer of salinity history in euryhaline elasmobranchs. Additionally, since *C. leucas* exhibit movements between vastly different water types with different trace element composition (fresh, brackish, and seawater), they are an ideal species for vertebral chemistry due to the relative clarity of trends across ontogeny.

In contrast to the clear ontogenetic patterns of element composition in *C. leucas* vertebrae, *S. tiburo* exhibited very little change in elemental signatures throughout their lifetime. Two elements, Mn and Ba, increased near the end of the *S. tiburo* life history transects, but this trend was inconsistent among individuals and not supported by statistical comparisons among life stages. *S. tiburo* occupy estuarine and coastal habitats and are thought to be resident within a home estuarine/coastal region (Heupel et al., 2006). While there is evidence that adult *S. tiburo* migrate seasonally along the United States. East Coast (Driggers et al., 2014), this is unresolved in the nwGOM. Furthermore, *S. tiburo* distribution does not appear to differ between seasons (spring and fall) along the Texas coast (Froeschke et al., 2010b), suggesting long-distance migration may not occur in this region. The lack of clear ontogenetic changes in vertebrae element composition may indicate that *S. tiburo* in the nwGOM

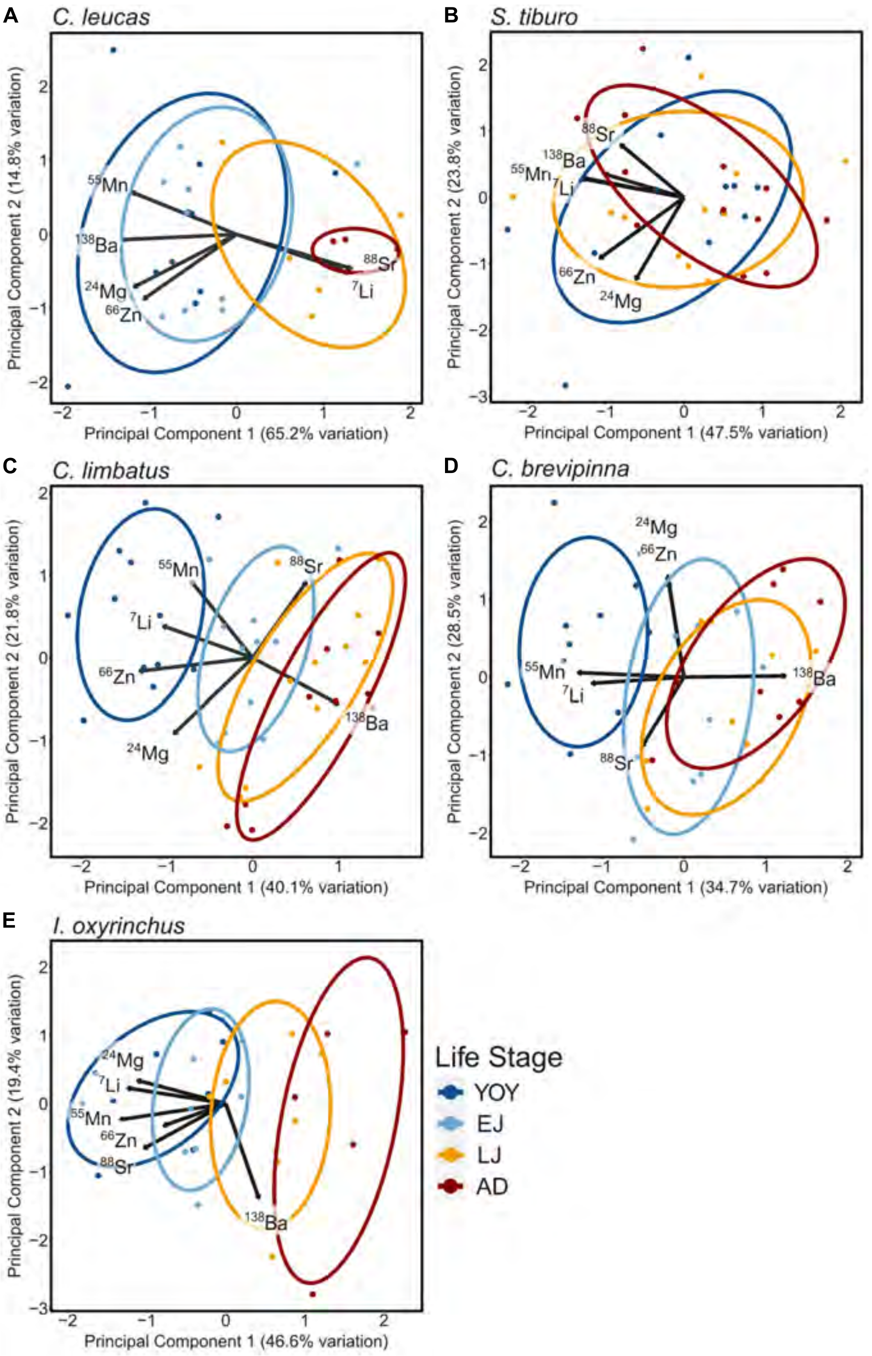

FIGURE 4 | Visualized principal component analysis for each species, with life stage (YOY, young-of-the-year; EJ, early juvenile; LJ, late juvenile; AD, adult) as the grouping factor (represented by color). Principal components 1 and 2 are represented as the *x* and *y* axis, respectively, and the percent of total variation explained by each PC is listed. Loadings for each element are represented by black arrows, and are labeled per element.

mainly reside in specific estuarine and coastal regions, and their habitat use does not change dramatically across ontogeny. Comparing ontogenetic changes in vertebrae trace elements of *S. tiburo* from multiple locations throughout the GOM and western Atlantic may help to characterize regional differences in migration patterns. *S. tiburo* also exhibit natal philopatry, meaning adults return to regions near their own birthplace, and their population is highly structured in the western Atlantic and GOM based on genetic markers (Escatel-Luna et al., 2015; Portnoy et al., 2015; Gonzalez et al., 2019). Collectively, the apparent limited movement and dispersal patterns of *S. tiburo* in the nwGOM could mean that they are prone to localized

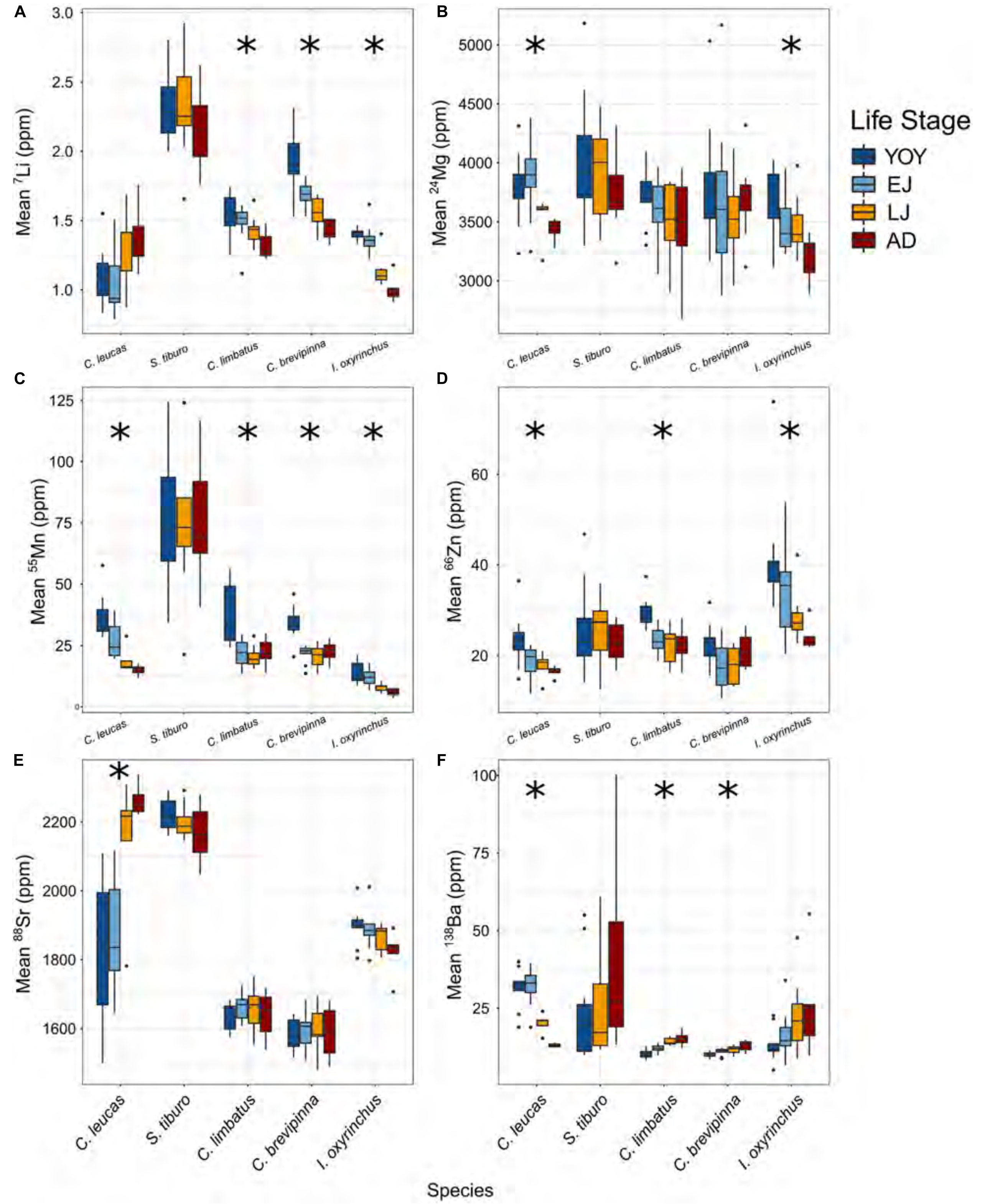

FIGURE 5 | Boxplots visualizing differences among life stages for each element and species, with life stage represented by color. Boxes show the 25th percentile, median, and 75th percentile, with whiskers representing 1.5 times the interquartile range. Outliers (data points that fall outside the range of the whiskers) are represented by black circles. Asterisks represent species with statistically significant differences among life stages (ANOVA). The asterisks (*) indicate statistical significance.

depletion via anthropogenic impacts (Walker, 1998; Hueter et al., 2005). Vertebral chemistry may be a useful tool in identifying species and populations that are prone to similar risks.

Carcharhinus brevipinna and *C. limbatus* exhibited similar life history concentration patterns for most elements examined, suggesting their habitat use patterns likely overlap throughout ontogeny. Both species use coastal bays and estuaries as nursery grounds, and they often co-occur in the same habitats (Castro, 1993; Hueter and Manire, 1994; Parsons and Hoffmayer, 2007). In coastal environments, juveniles and subadults of both species exhibit preferences for moderate to high salinities (20–30 ppt), warm temperatures (>25–30°C), and close proximity to tidal inlets (Ward-Paige et al., 2015; Plumlee et al., 2018). Stable post-YOY elemental concentration patterns for both species suggest preferences for specific environmental conditions that do not change drastically with ontogeny. However, the notable observed shift in elemental concentrations following the YOY life stage for both species may indicate movement away from nursery areas after their first year of life. Adult *C. limbatus* and *C. brevipinna* are known to be highly mobile, traveling long distances along coastlines in the GOM and western Atlantic (Castro, 1993; Kohler et al., 1998; Kajiura and Tellman, 2016), which may explain the changes in trace element profiles following their YOY stage. Considering the clear similarities in vertebral chemistry between *C. limbatus* and *C. brevipinna* in this study, the likelihood of these two species sharing the same habitats throughout ontogeny is high, which may influence their ecological roles in their shared habitats (Matich et al., 2017b). Further study of the overlap patterns between them, including habitat use and diet, would enhance our understanding of how these similar species coexist.

Similar to *C. limbatus* and *C. brevipinna*, *I. oxyrinchus* life history transects were generally stable over time, but ontogenetic shifts in element composition and concentrations emerged when comparing life stages. The two elements most closely linked with salinity, Sr and Ba, did not differ across life stages, suggesting that *I. oxyrinchus* do not inhabit estuarine or low-salinity regions like river plumes. This result is consistent with currently known habitat use patterns of this species: They generally inhabit coastal and pelagic zones, which have low environmental variability compared to highly dynamic estuaries. The general stability of element concentrations along *I. oxyrinchus* life history transects may reflect a relatively narrow range of suitable environmental conditions, such as temperature and salinity (Vaudo et al., 2016). It is also important to note that *I. oxyrinchus* are the only lamnid shark capable of regional endothermy examined in this study (Wolf et al., 1988). The relative stability of temperature within the bodies of *I. oxyrinchus* may contribute to stability in elemental concentrations if temperature exerts control over element uptake into vertebrae. Tagging studies have provided some clarity on the movement and habitat use patterns of *I. oxyrinchus* in the GOM, which may explain the observed differences in vertebrae elemental composition across life stages. For example, juvenile *I. oxyrinchus* tagged off the coast of Mexico appear to remain in the GOM year-round, largely within continental shelf habitats (Vaudo et al., 2017). Conversely, sexually mature adult *I. oxyrinchus* in the GOM are documented making long-distance migrations, as far as northeastern United States. Atlantic coastal waters in the summer and returning to the GOM in the winter (Gibson et al., 2021). Differences in migration patterns between juvenile and adult *I. oxyrinchus* in the GOM may have contributed to the differences in elemental signatures observed between life stages.

Although many of the observed differences in trace element concentrations among these five species could be explained by differences in life history and habitat use, some elements showed unexpected patterns. For example, Sr concentrations are thought to be associated with salinity history, but were only moderate for *I. oxyrinchus* which are the most oceanic of the study species. We would expect their Sr concentrations to be the highest of all the study species, since seawater generally holds higher Sr concentrations than fresh or estuarine waters (Dorval et al., 2005). Similarly, *S. tiburo* vertebrae had elevated concentrations of specific elements (Li, Mn, Sr, Ba) compared to other study species that reside in similar coastal and estuarine regions. Element uptake in these sharks may therefore be influenced by species-specific physiological and biological mechanisms in addition to reflecting ambient water concentrations and environmental history. In the case of *S. tiburo*, we hypothesize that the elevated concentrations of Li, Mn, Sr, Ba may be related to the difference in diet between *S. tiburo* and the other study species. *S. tiburo* consume primarily benthic prey such as crabs and shrimp (Bethea et al., 2007; Plumlee and Wells, 2016; Kroetz et al., 2017), while the other study species consume fish and other pelagic prey (Stillwell and Kohler, 1982; Bethea et al., 2004; Plumlee and Wells, 2016; TinHan, 2020). Trace element uptake in elasmobranch vertebrae is thought to be at least in part driven by dietary sources (Mathews and Fisher, 2009), so differences in diet and water column position (benthic vs. pelagic) could potentially influence differences in vertebral chemistry among species. Elucidating the species-specific mechanisms that influence the concentrations of trace elements would enhance the utility of vertebral chemistry as a method for direct comparisons of habitat use patterns among species.

Another element with an unexpected pattern was Mg, as concentrations were very similar and exhibited similar patterns of decreasing concentration over time for all species regardless of differences in known habitat use patterns among them. One experimental validation study using Round Stingrays (*Urobatis halleri*) concluded that Mg concentrations in vertebrae decreased with increasing temperature, and that uptake was not mediated by somatic growth rates or vertebral accretion rates which also increase with temperature (Smith et al., 2013). The maximum age of the sharks in this study was 17 years (*C. brevipinna*), and water temperatures in the nwGOM have increased over that timescale (by approximately 0.05°C per year from 1963 to 2015, Turner et al., 2017). It is therefore possible that the consistent decrease in Mg in the vertebrae of these coastal and oceanic sharks is reflecting temperature increases due to global climate change. The relationship between Mg uptake and environmental conditions requires further study, but these results represent the possibility of reconstructing water temperature changes over time in long-lived elasmobranchs.

Similarities also emerged among most of the species in their patterns of Mn and Zn concentrations, with both elements being

TABLE 3 | Results from ANOVA tests comparing mean elemental values among life stages for each species and element independently.

		Element					
Species	**Test statistic**	**^{7}Li**	**^{24}Mg**	**^{55}Mn**	**^{66}Zn**	**^{88}Sr**	**^{138}Ba**
C. leucas	*F*	2.84	3.36	12.63	3.82	8.28	16.34
	df	3, 25	3, 25	3, 25	3, 25	3, 25	3, 25
	p-value	0.058	**0.035**	**<0.001**	**0.022**	**<0.001**	**<0.001**
S. tiburo	*F*	1.54	1.72	0.002	0.58	2.68	2.03
	df	2, 33	2, 33	2, 33	2, 33	2, 33	2, 33
	p-value	0.229	0.194	0.998	0.564	0.083	0.148
C. limbatus	*F*	7.68	1.67	13.04	11.71	0.93	28.77
	df	3, 42	3, 42	3, 42	3, 42	3, 42	3, 42
	p-value	**<0.001**	0.189	**<0.001**	**<0.001**	0.437	**<0.001**
C. brevipinna	*F*	16.58	0.63	15.94	2.91	0.07	8.12
	df	3, 33	3, 33	3, 33	3, 33	3, 33	3, 33
	p-value	**<0.001**	0.603	**<0.001**	0.049	0.975	**<0.001**
I. oxyrinchus	*F*	24.84	3.67	7.70	4.58	2.35	1.93
	df	3, 26	3, 26	3, 26	3, 26	3, 26	3, 26
	p-value	**<0.001**	**0.023**	**<0.001**	**0.011**	0.096	0.149

Statistically significant results are represented by bolded p-values (<0.05).

elevated early in life followed by a decline. A similar pattern was observed for multiple shark species from Australia, including *C. brevipinna*, where Zn concentrations were very high pre-birth and declined post-birth (Raoult et al., 2018). The elevated Zn concentrations observed in the early life of all species in this study match the post-birth pattern observed by Raoult et al. (2018), and we hypothesize that this may be the result of maternal loading. Maternal loading is the process by which pregnant females transfer elements and molecules to their embryos via lipid mobilization (Addison and Brodie, 1987). This process is known to occur in sharks with regard to trophically derived contaminants in liver and muscle tissue (Lyons et al., 2013; Mull et al., 2013), and trace elements in the vertebrae of shark embryos (Coiraton and Amezuca, 2020). Both Zn and Mn are thought to be primarily incorporated into elasmobranch vertebrae via dietary sources as opposed to ambient environmental conditions (Mathews and Fisher, 2009), so it is reasonably likely that these trophically derived elements would undergo maternal loading during embryonic development. Additionally, Mn has been linked to dissolved oxygen levels in the otoliths of teleost fish (Limburg and Casini, 2019) and bivalve shells (Schöne et al., 2021). It is therefore possible that exposure to hypoxia may have influenced elemental concentrations in the vertebrae of the sharks in this study. Hypoxic conditions are widespread and highly variable in the nwGOM (Rabalais and Turner, 2019), but the influence of hypoxia exposure on shark vertebrae chemistry remains unresolved.

The use of vertebral chemistry can enhance our understanding of habitat use patterns through ontogeny in elasmobranchs, but interpretation of element concentrations would benefit from experimental validation of uptake routes and rates among taxa. We are aware of only two published experimental studies to date that have examined the effects of environmental conditions (temperature, pH, water chemistry) on element uptake in elasmobranch vertebrae, including one stingray and one oviparous shark (Smith et al., 2013; Pistevos et al., 2019). The lack of information regarding the complexities of environmental, physiological, and biological controls of trace element uptake limits our ability to make inferences about habitat use and movement. Experimental validation is likely hindered in part by the difficulties inherent to husbandry and maintenance of animals that are as slow-growing, long-lived, and large as many of the shark species in the nwGOM. *S. tiburo* are relatively small sharks with rapid time to maturity, which makes them an ideal candidate for experimental validation of the effects of extrinsic (environmental conditions) and intrinsic (physiological and biological) factors on trace element incorporation in shark vertebrae. An alternative to controlled tank studies is mark-recapture approaches that have been applied to sharks in the eastern Pacific (e.g., Mohan et al., 2018). Future validation studies would strengthen our ability to interpret the life history transects presented here, which would lead to a better understanding of the movements and habitat use patterns of coastal and oceanic sharks.

The results of this study exemplify the diversity of habitat use, movement, and migration patterns of sharks in the nwGOM, and provide evidence that vertebral chemistry is a promising method for reconstructing aspects of shark life history. Examining the movements of large, long-lived animals is extraordinarily challenging (Block et al., 2011), but chemical analysis of vertebrae eliminates the issues of long-term tracking (as with telemetry studies) or high recapture rates (as with conventional tagging). There is still considerable work to be done to validate the mechanisms of trace element uptake into elasmobranch vertebrae, but those studies would allow us to revisit our results and shed new light on the life histories of these sharks. Anthropogenic impacts including fishing mortality and habitat loss have resulted in declining populations of many shark species in the GOM (Baum and Myers, 2004), and the IUCN lists all of the species in this study as either near threatened (*C. leucas* and *C. limbatus*, Burgess and Branstetter, 2009; Simpfendorfer and Burgess, 2009), vulnerable (*C. brevipinna*, Rigby et al., 2020), or endangered (*I. oxyrinchus* and *S. tiburo,* Rigby et al., 2019; Pollom et al., 2020). Conservation and management of these species will require understanding the intricacies of their habitat requirements and movement patterns, especially for those that migrate through multiple jurisdictions (Rooker et al., 2019). Trace elements in vertebral cartilage, especially following validation studies, may prove to be instrumental in conserving populations of threatened elasmobranchs.

DATA AVAILABILITY STATEMENT

The raw data supporting the conclusions of this article will be made available by the authors, without undue reservation.

ETHICS STATEMENT

Ethical review and approval was not required for the animal study because this study used pre-existing samples. No animals were handled during the course of this study.

AUTHOR CONTRIBUTIONS

ML and RW conceived the study. BF collected and provided shark samples. ML, JM, and NM conducted LA-ICP-MS sampling. ML led the statistical analyses with assistance from TT, JM, TR, and RW and drafted the manuscript. JM, TT, and TR created the figures. All authors contributed equally to manuscript revisions.

FUNDING

This work was supported by a grant to ML by Texas Sea Grant Grants-in-Aid of Graduate Research (GIA-2019-2021).

ACKNOWLEDGMENTS

We thank the many volunteers at Texas A&M University at Galveston who helped to collect shark samples from Galveston docks, and Louisiana Department of Wildlife and Fisheries employees C. Marshall and P. Kent who helped to collect shark samples from Louisiana docks. Special thanks to E. Gutierrez and M. Curtis for assisting with sample collection and processing, and to R. Ware (NSF Research Experience for Undergraduate Students 2019) for helping with vertebrae aging.

REFERENCES

Addison, R. F., and Brodie, P. F. (1987). Transfer of Organochlorine Residues from Blubber through the Circulatory System to Milk in the Lactating Grey Seal *Halichoerus grypus*. *Can. J. Fish. Aquat. Sci.* 44, 782–786. doi: 10.1139/f87-095

Baum, J. K., and Myers, R. A. (2004). Shifting baselines and the decline of pelagic sharks in the Gulf of Mexico. *Ecol. Lett.* 7, 135–145. doi: 10.1111/j.1461-0248.2003.00564.x

Bethea, D. M., Buckel, J. A., and Carlson, J. K. (2004). Foraging ecology of the early life stages of four sympatric shark species. *Mar. Ecol. Prog. Ser.* 268, 245–264. doi: 10.3354/meps268245

Bethea, D. M., Hale, L., Carlson, J. K., Cortés, E., Manire, C. A., and Gelsleichter, J. (2007). Geographic and ontogenetic variation in the diet and daily ration of the bonnethead shark, *Sphyrna tiburo*, from the eastern Gulf of Mexico. *Mar. Biol.* 152, 1009–1020. doi: 10.1007/s00227-007-0728-7

Bethea, D. M., Ajemian, M. J., Carlson, J. K., Hoffmayer, E. R., Imhoff, J. L., Grubbs, D., et al. (2015). Distribution and community structure of coastal sharks in the northeastern Gulf of Mexico. *Environ. Biol. Fish.* 98, 1233–1254. doi: 10.1007/s10641-014-0355-3

Block, B. A., Jonsen, I. D., Jorgensen, S. J., Winship, A. J., Shaffer, S. A., Bograd, S. J., et al. (2011). Tracking apex marine predator movements in a dynamic ocean. *Nature* 475, 86–90. doi: 10.1038/nature10082

Branstetter, S. (1987). Age and Growth Estimates for Blacktip, *Carcharhinus limbatus*, and Spinner, *C. brevipinna*, Sharks from the Northwestern Gulf of Mexico. *Copeia* 1987, 964–974. doi: 10.2307/1445560

Bryant, W. R., Bryant, J. R., Feeley, M. H., and Simmons, G. R. (1990). Physiographic and Bathymetric Characteristics of the Continental Slope, Northwest Gulf of Mexico. *Geo-Mar. Lett.* 10, 182–199. doi: 10.1007/BF02431065

Burgess, H. G., and Branstetter, S. (2009). *Carcharhinus limbatus*. The IUCN Red List of Threatened Species. London: IUCN Red List. doi: 10.2305/IUCN.UK.2009-2.RLTS.T3851A10124862

Carlson, J. K., and Baremore, I. E. (2005). Growth dynamics of the spinner shark (*Carcharhinus brevipinna)* off the United States southeast and Gulf of Mexico coasts: a comparison of methods. *Fish. Bull.* 103, 280–291.

Carlson, J. K., and Parsons, G. R. (1997). Age and growth of the bonnethead shark, *Sphyrna tiburo*, from northwest Florida, with comments on clinal variation. *Environ. Biol. Fish.* 50, 331–341. doi: 10.1023/A:1007342203214

Carlson, J. K., Sulikowski, J. R., and Baremore, I. E. (2006). Do differences in life history exist for blacktip sharks, *Carcharhinus limbatus*, from the United States South Atlantic Bight and Eastern Gulf of Mexico? *Environ. Biol. Fish.* 77, 279–292. doi: 10.1007/s10641-006-9129-x

Casey, J. G., and Kohler, N. E. (1992). Tagging studies on the Shortfin Mako Shark (*Isurus oxyrinchus*) in the Western North Atlantic. *Aust. J. Mar. Freshw. Res.* 43, 45–60. doi: 10.1071/MF9920045

Castro, J. I. (1993). The shark nursery of Bulls Bay, South Carolina, with a review of shark nurseries of the southeastern coast of the United States. *Environ. Biol. Fish.* 38, 37–48. doi: 10.1007/BF00842902

Chapman, D. D., Feldheim, K. A., Papastamatiou, Y. P., and Hueter, R. E. (2015). There and Back Again: A Review of Residency and Return Migrations in Sharks, with Implications for Population Structure and Management. *Ann. Rev. Mar. Sci.* 7, 547–570. doi: 10.1146/annurev-marine-010814-015730

Coiraton, C., and Amezuca, F. (2020). *In utero* elemental tags in vertebrae of the scalloped hammerhead shark *Sphyrna lewini* reveal migration patterns of pregnant females. *Sci. Rep.* 10:1799. doi: 10.1038/s41598-020-58735-8

Cruz-Martinez, A., Chiappa-Carrara, X., and Arenas-Fuentes, V. (2005). Age and Growth of the Bull Shark, *Carcharhinus leucas*, from Southern Gulf of Mexico. *J. Northw. Atl. Fish. Sci.* 35, 367–374. doi: 10.2960/J.v35.m481

Dorval, E., Jones, C. M., and Hannigan, R. (2005). Chemistry of surface waters: Distinguishing fine-scale differences in sea grass habitats of Chesapeake Bay. *Limnol. Oceanogr.* 50, 1073–1083. doi: 10.4319/lo.2005.50.4.1073

Driggers, W. B. III, Frazier, B. S., Adams, D. H., Ulrich, G. F., Jones, C. M., Hoffmayer, E. R., et al. (2014). Site fidelity of migratory bonnethead sharks *Sphyrna tiburo* (L. 1758) to specific estuaries in South Carolina. *USA. J. Exp. Mar. Biol. Ecol.* 459, 61–69. doi: 10.1016/j.jembe.2014.05.006

Escatel-Luna, E., Adams, D. H., Uribe-Alcocer, M., Islas-Villaneuva, V., and Diaz-Jaimes, P. (2015). Population Genetic Structure of the Bonnethead Shark, *Sphyrna tiburo,* from the Western North Atlantic Ocean Based on mtDNA Sequences. *J. Hered.* 106, 355–365. doi: 10.1093/jhered/esv030

Ferretti, F., Worm, B., Britten, G. L., Heithaus, M. R., and Lotze, H. K. (2010). Patterns and ecosystem consequences of shark declines in the ocean. *Ecol. Lett.* 13, 1055–1071. doi: 10.1111/j.1461-0248.2010.01489.x

Froeschke, J., Stunz, G. W., Sterba-Boatwright, B., and Wildhaber, M. L. (2010a). An empirical test of the 'shark nursery area concept' in Texas bays using a long-term fisheries-independent data set. *Aquat. Biol.* 11, 65–76. doi: 10.3354/ab00290

Froeschke, J., Stunz, G. W., and Wildhaber, M. L. (2010b). Environmental influences on the occurrence of coastal sharks in estuarine waters. *Mar. Ecol. Prog. Ser.* 407, 279–292. doi: 10.3354/meps08546

Gibson, K. J., Streich, M. K., Topping, T. S., and Stunz, G. W. (2021). New Insights Into the Seasonal Movement Patterns of Shortfin Mako Sharks in the Gulf of Mexico. *Front. Mar. Sci.* 8:623104. doi: 10.3389/fmars.2021.623104

Gonzalez, C., Gallagher, A. J., and Caballero, S. (2019). Conservation genetics of the bonnethead shark *Sphyrna tiburo* in Bocas del Toro, Panama: Preliminary evidence of a unique stock. *PLoS One* 14:e0220737. doi: 10.1371/journal.pone.0220737

Heithaus, M. R., Frid, A., Wirsing, A. J., and Worm, B. (2008). Predicting ecological consequencesof marine top predator declines. *Trends Ecol. Evol.* 23, 202–210. doi: 10.1016/j.tree.2008.01.003

Hellstrom, J. C., Paton, C., Woodhead, J. D., and Hergt, J. (2008). Iolite: software for spatially resolved LA-(quad and MC) ICPMS analysis. *Mineralog. Assoc. Can. Short Cour.* 40, 343-348.

Heupel, M. R., Munroe, S. E. M., Lédée, E. J. I., Chin, A., and Simpfendorfer, C. A. (2019). Interspecifc interactions, movement patterns and habitat use in a diverse coastal shark assemblage. *Mar. Biol.* 166:68. doi: 10.1007/s00227-019-3511-7

Heupel, M. R., Simpfendorfer, C. A., Collins, A. B., and Tyminski, J. P. (2006). Residency and movement patterns of bonnethead sharks, *Sphyrna tiburo*, in a large Florida estuary. *Environ. Biol. Fish.* 76, 47–67. doi: 10.1007/s10641-006-9007-6

Heupel, M. R., Yeiser, B. G., Collins, A. B., Ortega, L., and Simpfendorfer, C. A. (2010). Long-term presence and movement patterns of juvenile bull sharks, *Carcharhinus leucas*, in an estuarine river system. *Mar. Freshwater Res.* 61, 1–10. doi: 10.1071/MF09019

Hoenig, J. M., and Gruber, S. H. (1990). Life-history patterns in the elasmobranchs: implications for fisheries management. *NOAA Tech. Rep.* 90:16.

Hotelling, H. (1933). Analysis of a complex of statistical variables into principal components. *J. Educ. Psychol.* 24, 417–441. doi: 10.1037/h0071325

Hueter, R. E., Heupel, M. R., Heist, E. J., and Keeney, D. B. (2005). Evidence of Philopatry in Sharks and Implications for the Management of Shark Fisheries. *Northw. Atl. Fish. Sci.* 35, 239–247. doi: 10.2960/J.v35.m493

Hueter, R. E., and Manire, C. A. (1994). *Bycatch and catch-release mortality of small sharks in the Gulf coast nursery grounds of Tampa Bay and Charlotte Harbor*. Mote Marine Technical Report No. 368. Silver Spring: NOAA, 183.

Kajiura, S. M., and Tellman, S. L. (2016). Quantification of Massive Seasonal Aggregations of Blacktip Sharks (*Carcharhinus limbatus*) in Southeast Florida. *PLoS One* 11:e0150911. doi: 10.1371/journal.pone.0150911

Keeney, D. B., Heupel, M. R., Hueter, R. E., and Heist, E. J. (2005). Microsatellite and mitochondrial DNA analyses of the genetic structure of blacktip shark (*Carcharhinus limbatus*) nurseries in the northwestern Atlantic, Gulf of Mexico, and Caribbean Sea. *Mol. Ecol.* 14, 1911–1923. doi: 10.1111/j.1365-294X.2005.02549.x

Kinney, M. J., Wells, R. J. D., and Kohin, S. (2016). Oxytetracycline age validation of an adult shortfin mako shark *Isurus oxyrinchus* after 6 years at liberty. *J. Fish Biol.* 89, 1828–1833. doi: 10.1111/jfb.13044

Knip, D. M., Heupel, M. R., and Simpfendorfer, C. A. (2010). Sharks in nearshore environments: models, importance, and consequences. *Mar. Ecol. Prog. Ser.* 402, 1–11. doi: 10.3354/meps08498

Kohler, N. E., Casey, J. G., and Turner, P. A. (1998). NMFS Cooperative Shark Tagging Program, 1962-93: An Atlas of Shark Tag and Recapture Data. *Mar. Fish. Rev.* 60, 1–87.

Kroetz, A. M., Drymon, J. M., and Powers, S. P. (2017). Comparative Dietary Diversity and Trophic Ecology of Two Estuarine Mesopredators. *Estuaries Coast.* 40, 1171–1182. doi: 10.1007/s12237-016-0188-8

Lewis, J. P., Patterson, W. F., Carlson, J. K., and McLachlin, K. (2016). Do vertebral chemical signatures distinguish juvenile blacktip shark (*Carcharhinus limbatus*) nursery regions in the northern Gulf of Mexico? *Mar. Freshw. Res.* 67, 1014–1022. doi: 10.1071/MF15088

Limburg, K. E., and Casini, M. (2019). Otolith chemistry indicates recent worsened Baltic cod condition is linked to hypoxia exposure. *Biol. Lett.* 15:20190352. doi: 10.1098/rsbl.2019.0352

Lyons, K., Carlisle, A., Preti, A., Mull, C., Blasius, M., O'Sullivan, J., et al. (2013). Effects of trophic ecology and habitat use of maternal transfer of contaminants in four species of young of the year lamniform sharks. *Mar. Environ. Res.* 90, 27–38. doi: 10.1016/j.marenvres.2013.05.009

Mathews, T., and Fisher, M. S. (2009). Dominance of dietary intake of metals in marine elasmobranch and teleost fish. *Sci. Total Environ.* 407, 5156–5161. doi: 10.1016/j.scitotenv.2009.06.003

Matich, P., and Heithaus, M. R. (2015). Individual variation in ontogenetic niche shifts in habitat use and movement patterns of a large estuarine predator (*Carcharhinus leucas*). *Oecologia* 178, 347–359. doi: 10.1007/s00442-015-3253-2

Matich, P., Kizka, J. J., Mourier, J., Planes, S., and Heithaus, M. R. (2017b). Species co-occurrence affects the trophic interactions of two juvenile reef shark species in tropical lagoon nurseries in Moorea (French Polynesia). *Mar. Environ. Res.* 127, 84–91. doi: 10.1016/j.marenvres.2017.03.010

Matich, P., Mohan, J. A., Plumlee, J. D., TinHan, T., Wells, R. J. D., and Fisher, M. (2017a). Factors shaping the co-occurrence of two juvenile shark species along the Texas Gulf Coast. *Mar. Biol.* 164:141. doi: 10.1007/s00227-017-3173-2

McMillan, M. N., Izzo, C., Wade, B., and Gillanders, B. M. (2017). Elements and elasmobranchs: hypotheses, assumptions, and limitations of elemental analysis. *J. Fish. Biol.* 90, 559–594. doi: 10.1111/jfb.13189

Mohan, J. A., Miller, N. R., Herzka, S. S., Sosa-Nishizaki, O., Kohin, S., Dewar, H., et al. (2018). Elements of time and place: manganese and barium in shark vertebrae reflect age and upwelling histories. *Proc. R. Soc. B* 285:20181760. doi: 10.1098/rspb.2018.1760

Mull, C. G., Lyons, K., Blasius, M. E., Winkler, C., O'Sullivan, J. B., and Lowe, C. G. (2013). Evidence of Maternal Offloading of Organic Contaminants in White Sharks (*Carcharodon carcharias*). *PLoS One* 8:e62886. doi: 10.1371/journal.pone.0062886

Myers, R. A., Baum, J. K., Shepherd, T. D., Powers, S. P., and Peterson, C. H. (2007). Cascading Effects of the Loss of Apex Predatory Sharks from a Coastal Ocean. *Science* 315, 1846–1850. doi: 10.1126/science.1138657

Natanson, L. J., Kohler, N. E., Ardizzone, D., Cailliet, G. M., Wintner, S. P., and Mollet, H. F. (2006). Validated age and growth estimates for the shortfin mako, *Isurus oxyrinchus*, in the North Atlantic Ocean. *Environ. Biol. Fish.* 77, 367–383. doi: 10.1007/s10641-006-9127-z

Natanson, L. J., Winton, M., Bowlby, H., Joyce, W., Deacy, B., Coelho, R., et al. (2020). Updated reproductive parameters for the shortfin mako (Isurus oxyrinchus) in the North Atlantic Ocean with inferences of distribution by sex and reproductive stage. *Fish. Bull.* 118, 21–36. doi: 10.7755/FB.118.1.3

Papastamatiou, Y. P., Wetherbee, B. M., Lowe, C. G., and Crow, G. L. (2006). Distribution and diet of four species of carcharhinid shark in the Hawaiian Islands: evidence for resource partitioning and competitive exclusion. *Mar. Ecol. Prog. Ser.* 320, 239–251. doi: 10.3354/meps320239

Parsons, G. R. (1993). Age determination and growth of the bonnethead shark *Sphyrna tiburo*: a comparison of two populations. *Mar. Biol.* 117, 23–31. doi: 10.1007/BF00346422

Parsons, G. R., and Hoffmayer, E. R. (2007). Identification and Characterization of Shark Nursery Grounds along the Mississippi and Alabama Gulf Coasts. *Am. Fish. Soc. Symp.* 50, 301–316.

Pistevos, J. C. A., Reis-Santos, P., Izzo, C., and Gillanders, B. M. (2019). Element composition of shark vertebrae shows promise as a natural tag. *Mar. Freshw. Res.* 70, 1722–1733. doi: 10.1071/MF18423

Plumlee, J. D., Dance, K. M., Matich, P., Mohan, J. A., Richards, T. M., TinHan, T. C., et al. (2018). Community structure of elasmobranchs in estuaries along the northwest Gulf of Mexico. *Estuar. Coast. Shelf Sci.* 204, 103–113. doi: 10.1016/j.ecss.2018.02.023

Plumlee, J. D., and Wells, R. J. D. (2016). Feeding ecology of three coastal shark species in the northwest Gulf of Mexico. *Mar. Ecol. Prog. Ser.* 550, 163–174. doi: 10.3354/meps11723

Pollom, R., Carlson, J., Charvet, P., Avalos, C., Bizzarro, J., Blanco-Parra, M. P., et al. (2020). *Sphyrna tiburo*. The IUCN Red List of Threatened

Species 2020. London: IUCN Red List. doi: 10.2305/IUCN.UK.2020-3.RLTS.T39387A124409680

Portnoy, D. S., Puritz, J. B., Hollenbeck, C. M., Gelsleichter, J., Chapman, D., and Gold, J. R. (2015). Selection and sex-biased dispersal in a coastal shark: the influence of philopatry on adaptive variation. *Mol. Ecol.* 24, 5877–5885. doi: 10.1111/mec.13441

R Core Team (2019). *R: A language and environment for statistical computing. R Foundation for Statistical Computing*. Vienna: R Core Team.

Rabalais, N. N., and Turner, R. E. (2019). Gulf of Mexico Hypoxia: Past, Present, and Future. *Limnol. Oceanogr. Bull.* 28, 117–124. doi: 10.1002/lob.10351

Raoult, V., Howell, N., Zahra, D., Peddemors, V. M., Howard, D. L., de Jonge, M. D., et al. (2018). Localized zinc distribution in shark vertebrae suggests differential deposition during ontogeny and across vertebral structures. *PLoS One* 13:e0190927. doi: 10.1371/journal.pone.0190927

Rigby, C. L., Barreto, R., Carlson, J., Fernando, D., Fordham, S., Francis, M. P., et al. (2019). *Isurus oxyrinchus.* The IUCN Red List of Threatened Species 2019. London: IUCN Red List. doi: 10.2305/IUCN.UK.2019-1.RLTS.T39341A2903170

Rigby, C. L., Carlson, J., Smart, J. J., Pacoureau, N., Herman, K., Derrick, D., et al. (2020). *Carcharhinus brevipinna*. The IUCN Red List of Threatened Species 2020. London: IUCN Red List. doi: 10.2305/IUCN.UK.2020-3.RLTS.T39368A2908817

Rooker, J. R., Dance, M. A., Wells, R. J. D., Ajemian, M. J., Block, B. A., Castleton, M. R., et al. (2019). Population connectivity of pelagic megafauna in the Cuba-Mexico-United States triangle. *Sci. Rep.* 9:1663. doi: 10.1038/s41598-018-38144-8

Scharer, R. M., Patterson, W. F. III, Carlson, J. K., and Poulakis, G. R. (2012). Age and Growth ofEndangered Smalltooth Sawfish (*Pristis pectinata*) Verified with LA-ICP-MS Analysis of Vertebrae. *PLoS One* 7:e47850. doi: 10.1371/journal.pone.0047850

Schneider, C. A., Rasband, W. S., and Eliceiri, K. W. (2012). NIH Image to ImageJ: 25 years of image analysis. *Nat. Methods* 9, 671–675. doi: 10.1038/nmeth.2089

Schöne, B. R., Huang, X., Zettler, M. L., Zhao, L., Mertz-Kraus, R., Jochum, K. P., et al. (2021). Mn/Ca in shells of *Arctica islandica* (Baltic Sea) – A potential proxy for ocean hypoxia? *Estuar. Coast. Shelf Sci.* 251:107257. doi: 10.1016/j.ecss.2021.107257

Sih, A., Englund, G., and Wooster, D. (1998). Emergent impacts of multiple predators on prey.*Trends. Ecol. Evol.* 13, 350–355. doi: 10.1016/S0169-5347(98)01437-2

Simpfendorfer, C., and Burgess, G. H. (2009). *Carcharhinus leucas.* The IUCN Red List of Threatened Species 2009. London: IUCN Red List. doi: 10.2305/IUCN.UK.2009-2.RLTS.T39372A10187195

Smith, S. R., and Jacobs, G. A. (2005). Seasonal circulation fields in the northern Gulf of Mexico calculated by assimilating current meter, shipboard ADCP, and drifter data simultaneously with the shallow water equations. *Cont. Shelf Res.* 25, 157–183. doi: 10.1016/j.csr.2004.09.010

Smith, W. D., Miller, J. A., and Heppel, S. S. (2013). Elemental Markers in Elasmobranchs: Effects of Environmental History and Growth on Vertebral Chemistry. *PLoS One* 8:e62423. doi: 10.1371/journal.pone.0062423

Smith, W. D., Miller, J. A., Márquez-Farías, J. F., and Heppell, S. S. (2016). Elemental signatures reveal the geographic origins of a highly migratory shark: prospects for measuring population connectivity. *Mar. Ecol. Prog. Ser.* 556, 173–193. doi: 10.3354/meps11844

Speed, C. W., Meekan, M. G., Field, I. C., McMahon, C. R., Stevens, J. D., McGregor, F., et al. (2011). Spatial and temporal movement patterns of a multi-species coastal reef shark aggregation. *Mar. Ecol. Prog. Ser.* 429, 261–275. doi: 10.3354/meps09080

Stillwell, C. E., and Kohler, N. E. (1982). Food, feeding habits, and daily ration of the shortfin mako (*Isurus oxyrinchus*) in the Northwest Atlantic. *Can. J. Fish. Aquat. Sci.* 39, 407–414. doi: 10.1139/f82-058

Tillett, B. J., Meekan, M. G., Field, I. C., Thorburn, D. C., and Ovenden, J. R. (2012). Evidence for reproductive philopatry in the bull shark *Carcharhinus leucas*. *J. Fish. Biol.* 80, 2140–2158. doi: 10.1111/j.1095-8649.2012.03228.x

Tillett, B. J., Meekan, M. G., Parry, D., Munksgaard, N., Field, I. C., Thorburn, D., et al. (2011). Decoding fingerprints: elemental composition of vertebrae correlates to age-related habitat use in two morphologically similar sharks. *Mar. Ecol. Prog. Ser.* 434, 133–142. doi: 10.3354/meps09222

TinHan, T. C. (2020). *Population and Trophic Connectivity of Bull Sharks in the Northwestern Gulf of Mexico*. Doctoral dissertation, Texas: Texas A&M University.

TinHan, T. C., O'Leary, S. J., Portnoy, D. S., Rooker, J. R., Gelpi, C. G., and Wells, R. J. D. (2020). Natural tags identify nursery origin of a coastal elasmobranch *Carcharhinus leucas*. *J. Appl. Ecol.* 57, 1222–1232. doi: 10.1111/1365-2664.13627

Turner, R. E., Rabalais, N. N., and Justić, D. (2017). Trends in summer bottom-water temperatures on the northern Gulf of Mexico continental shelf from 1985 to 2015. *PLoS One* 12:e0184350. doi: 10.1371/journal.pone.0184350

Vaudo, J. J., Byrne, M. E., Wetherbee, B. M., Harvey, G. M., and Shivji, M. S. (2017). Long-term satellite tracking reveals region-specific movements of a large pelagic predator, the shortfin mako shark, in the western North Atlantic Ocean. *J. Appl. Ecol.* 54, 1765–1775. doi: 10.1111/1365-2664.12852

Vaudo, J. J., Wetherbee, B. M., Wood, A. D., Weng, K., Howey-Jordan, L. A., Harvey, G. M., et al. (2016). Vertical movements of shortfin mako sharks *Isurus oxyrinchus* in the western North Atlantic Ocean are strongly influenced by temperature. *Mar. Ecol. Prog. Ser.* 547, 163–175. doi: 10.3354/meps11646

Walker, T. I. (1998). Can shark resources be harvested sustainably? A question revisited with a review of shark fisheries. *Mar. Freshw. Res.* 49, 553–572. doi: 10.1071/MF98017

Ward-Paige, C. A., Britten, G. L., Bethea, D. M., and Carlson, J. K. (2015). Characterizing and predicting essential habitat features for juvenile coastal sharks. *Mar. Ecol.* 36, 419–431. doi: 10.1111/maec.12151

Weisberg, R. H., and Liu, Y. (2017). On the Loop Current Penetration into the Gulf of Mexico. *J. Geophys. Res. Oceans* 122, 9679–9694. doi: 10.1002/2017JC013330

Wells, R. J. D., Smith, S. E., Kohin, S., Freund, E., Spear, N., and Ramon, D. A. (2013). Age validation of juvenile Shortfin Mako (*Isurus oxyrinchus*) tagged and marked with oxytetracycline off southern California. *Fish. Bull.* 111, 147–160. doi: 10.7755/FB.111.2.3

Werry, J. M., Lee, S. Y., Otway, N. M., Hu, Y., and Sumpton, W. (2011). A multi-faceted approach for quantifying the estuarine-nearshore transition in the life cycle of the bull shark. *Carcharhinus leucas*. *Mar. Freshw. Res.* 62, 1421–1431. doi: 10.1071/MF11136

Wolf, N. G., Swift, P. R., and Carey, F. G. (1988). Swimming muscle helps warm the brain of lamnid sharks. *J. Comp. Physiol. B* 157, 709–715. doi: 10.1007/BF00691001

Worm, B., Davis, B., Kettemer, L., Ward-Paige, C. A., Chapman, D., Kessel, S. T., et al. (2013). Global catches, exploitation rates, and rebuilding options for sharks. *Mar. Policy* 40, 194–204. doi: 10.1016/j.marpol.2012.12.034

Conflict of Interest: BF was employed by Fisheries Research Support, L.L.C.

The remaining authors declare that the research was conducted in the absence of any commercial or financial relationships that could be construed as a potential conflict of interest.

frontiers in Marine Science

ORIGINAL RESEARCH
published: 10 August 2021
doi: 10.3389/fmars.2021.687738

Stable Isotope Analysis of Juvenile White Sharks Inside a Nursery Area Reveals Foraging in Demersal-Inshore Habitats and Trophic Overlap With Sympatric Sharks

Emiliano García-Rodríguez[1†], *Sharon Z. Herzka*[1*†], *Oscar Sosa-Nishizaki*[1*†], *Christopher G. Lowe*[2] *and John B. O'Sullivan*[3]

[1] Department of Biological Oceanography, Center for Scientific Research and Higher Education of Ensenada (CICESE), Ensenada, Mexico, [2] Department of Biological Sciences, California State University, Long Beach, CA, United States, [3] Monterey Bay Aquarium, Monterey, CA, United States

OPEN ACCESS

Edited by:
J. Marcus Drymon,
Mississippi State University,
United States

Reviewed by:
Simona Alessandra Ceriani,
Florida Fish and Wildlife Research Institute, United States
Richard Reina,
Monash University, Australia

***Correspondence:**
Sharon Z. Herzka
sherzka@cicese.mx
Oscar Sosa-Nishizaki
ososa@cicese.mx

†ORCID:
Emiliano García-Rodríguez
orcid.org/0000-0002-9078-1300
Sharon Z. Herzka
orcid.org/0000-0001-7091-7656
Oscar Sosa-Nishizaki
orcid.org/0000-0002-3043-768X

Specialty section:
This article was submitted to Marine Megafauna, a section of the journal Frontiers in Marine Science

Received: *30 March 2021*
Accepted: *28 May 2021*
Published: *10 August 2021*

Citation:
García-Rodríguez E, Herzka SZ, Sosa-Nishizaki O, Lowe CG and O'Sullivan JB (2021) Stable Isotope Analysis of Juvenile White Sharks Inside a Nursery Area Reveals Foraging in Demersal-Inshore Habitats and Trophic Overlap With Sympatric Sharks. Front. Mar. Sci. 8:687738. doi: 10.3389/fmars.2021.687738

Knowledge about top predators' trophic ecology is crucial for defining their role in ecosystems, understanding habitat preferences, characterizing life stage-specific feeding habits, and evaluating their interaction with fisheries. In the northeastern Pacific, white sharks (*Carcharodon carcharias*) occupy coastal habitats during the early life stages, including Bahía Sebastián Vizcaíno (BSV) in Mexico, which is a known nursery area. Although BSV presumably provides high prey abundance, the trophic ecology of immature white sharks is poorly understood. Carbon and nitrogen bulk stable isotope analyses (SIA) were used to explore the trophic relationship of early life stages with their potential prey and to infer dietary overlap with sympatric sharks, while SIA of amino acids were used to estimate trophic position. Muscle samples from young white sharks and inshore demersal prey commonly found in their stomach contents were sampled. Demersal prey and literature-derived isotope ratios for pelagic and offshore species were incorporated into mixing models with a Bayesian framework to estimate their contribution to white shark tissues. Nearshore demersal prey had the highest contribution for all life stages (between 35 and 47%), consistent with previous reports based on gut content analysis. The contribution of pelagic (between 26 and 37%) and offshore (between 14 and 32%) prey was smaller and suggests potential periodic changes in foraging grounds and the presence of a maternal-derived isotopic signature. A high contribution of demersal prey indicates a high level of interaction with local fisheries that target those species and catch white sharks incidentally and is consistent with immature shark movement patterns. Isotope ratios of two sympatric sharks, smooth hammerhead *Sphyrna zygaena* and copper sharks *Carcharhinus brachyurus*, were used to estimate the overlap in isotopic niche space. Immature white sharks had the smallest isotopic niche, while the highest was for copper sharks. Overlap was greatest between white sharks and hammerheads (∼45%), while overlap with copper sharks was limited (<20%), suggesting less potential for competition. Trophic position estimates were similar to those previously reported for the species. These results highlight the importance of coastal demersal prey heavily targeted by local fisheries for the diet of young white sharks and support the importance of BSV as a nursery habitat.

Keywords: white shark, trophic ecology, stable isotope analyses, nursery area, demersal foraging, amino acids

INTRODUCTION

Most shark species are considered top predators occupying high trophic levels and their presence or absence influences food web structure (Cortés, 1999; Ferretti et al., 2010; Heupel et al., 2014). Some species are highly migratory and move between coastal and pelagic habitats, that are used throughout ontogeny for nursery, feeding, mating, or parturition (Heupel et al., 2007; Block et al., 2011; Domeier and Nasby-Lucas, 2013; Carlisle et al., 2015a; Nasby-Lucas et al., 2019; Nosal et al., 2019). Ontogenetic habitat changes are commonly accompanied by switches in their diet (Malpica-Cruz et al., 2013; Carlisle et al., 2015b; Estupiñán-Montaño et al., 2019; Matich et al., 2019). So, characterizing the trophic relationships of sharks throughout their life cycle is needed for understanding their ecological role in each ecosystem they inhabit.

Adult white sharks (*Carcharodon carcharias)* are distributed mostly in offshore pelagic waters, including oceanic islands (Klimley et al., 1992; Domeier and Nasby-Lucas, 2007; Jorgensen et al., 2010; Francis et al., 2015; Boldrocchi et al., 2017; Skomal et al., 2017; Moro et al., 2020), while juveniles occupy coastal areas as nurseries (Bruce and Bradford, 2012; Harasti et al., 2017; Curtis et al., 2018; Bruce et al., 2019). In the northeast Pacific, newborn, young of the year, and juvenile white shark occupy coastal areas until they become sub-adults and can migrate between spatially separate nurseries (Klimley et al., 1992; Dewar et al., 2004; Weng et al., 2007, 2012; Lowe et al., 2012; Oñate-González et al., 2017; White et al., 2019). Coastal nurseries harbor high food abundance and provide shelter from predators, allowing young white sharks to grow faster, which is crucial for their juvenile survival and recruitment to adult population growth (Mollet and Cailliet, 2002; Heupel et al., 2007).

The white shark is a top predator that exhibits ontogenetic changes in its feeding habits and habitat use (Estrada et al., 2006; Carlisle et al., 2012; Kim et al., 2012; French et al., 2018). Whereas the feeding preferences of adults have been more widely studied (Estrada et al., 2006; Hussey et al., 2012), dietary information for the early life stages is more limited and suggest a more benthic-oriented foraging (Santana-Morales et al., 2012; Grainger et al., 2020). Juveniles shift their diet from feeding on smaller bony fishes and elasmobranchs (mainly rays) to larger fishes as they grow. After becoming sub-adults, white sharks start to expand their diet to include marine mammals (Tricas and McCosker, 1984; Estrada et al., 2006; Hussey et al., 2012; Malpica-Cruz et al., 2013). In the northeast Pacific, adult white sharks spend between six and eight months of the year in offshore areas (Domeier and Nasby-Lucas, 2008; Jorgensen et al., 2010) where their feeding habits are poorly understood.

Bahía Sebastián Vizcaíno (BSV) bay is located on the western coast of the Baja California Peninsula, Mexico. BSV is a natal nursery area for white sharks born locally as well as young sharks born in the Southern California Bight, United States, that migrate south covering approximately 600 km (Oñate-González et al., 2017; White et al., 2019). In Mexican waters, the species has been under protection since 2007 and the targeted catch is prohibited (DOF, 2007, 2010, 2014). However, they are caught incidentally in the nearshore areas of BSV as well as within Ojo de Liebre Lagoon (OLL), a semi-enclosed hypersaline shallow estuary located within the bay system (García-Rodríguez and Sosa-Nishizaki, 2020). These catches occur when local artisanal fishers target high-value species that are part of the white shark's diet (Santana-Morales et al., 2012; García-Rodríguez and Sosa-Nishizaki, 2020).

In addition to the direct mortality caused by incidental catches, the potential competition between artisanal fisheries and young white sharks (and other shark species) for prey could have a negative effect on regional conservation efforts. For top predators like turtles, birds, and marine mammals, it has been well documented that competition could have adverse effects on their abundance by limiting prey's spatial availability (Huss et al., 2014; Hilborn et al., 2017; Hansson et al., 2018). For example, a switch in the diet resulting from prey overfishing has been reported for the spiny dogfish *Squalus acanthias* (Koen Alonso et al., 2002). Also, high overlap between target fishery species and shark prey has been documented for the spiny dogfish (Lucifora et al., 2009). In sand tiger sharks (*Carcharias taurus*), spatial overlap between prey and fisheries increased their vulnerability to overfishing (Gračan et al., 2017). Changes in prey availability due to spatial overlap with fisheries in nursery areas could decrease the benefits these provide for the early life stages of sharks, potentially changing their diets, limiting their growth, and affecting juvenile survival.

Limitation in prey availability due to fisheries could increase the competition between shark species with similar dietary preferences. Interspecific competition between young white sharks and sympatric shark species that inhabit BSV, like smooth hammerheads (*Sphyrna zygaena*) or Carcharhinids, is possible. Previous studies have reported resource partitioning in communal areas to reduce interspecific competition, which could be associated with changes in the distribution and habitat use of sympatric shark species with high dietary overlap (Bethea et al., 2004; Papastamatiou et al., 2006; Kinney et al., 2011). The description of the trophic relationships between immature white sharks, their prey, and the level of dietary overlap with sympatric species that may compete for feeding resources lend insight into their ecological role in the nursery habitat provided by BSV.

Quantitative diet composition estimates are based on stomach content analysis, providing a basis for understanding a species' prey spectrum and its overall trophic ecology, including trophic level (Cortés, 1999; Bizzarro et al., 2017). While it can provide a snapshot of what a shark has eaten most recently, stomach content analysis has several constraints, including that it is labor-intensive and highly invasive or lethal, soft-bodied prey can be under-represented in the analysis due to the digestive process, and the results can have limited spatial resolution unless extensive sampling efforts are implemented. It can, however, provide a snapshot of what a shark has eaten most recently. This approach often requires a very high sample size to quantify diet variation across a population and still can lead to a limited interpretation of their trophic ecology (Hussey et al., 2012; Munroe et al., 2018).

Bulk stable isotope analysis (SIA) of soft tissues provides information that complements that obtained through stomach content analysis by providing integrated spatial-temporal insight into trophic relationships and energy fluxes in marine ecosystems (Michener and Kaufman, 2007; Boecklen et al., 2011). Isotopic ratios can also be used to characterize the isotopic niche, which is reflective of a consumer's trophic niche and can be used to estimate the overlap in prey resources between populations, life stages, or species (Jackson et al., 2011; Hette-Tronquart, 2019; Marshall et al., 2019).

Isotope turnover rates should be considered when interpreting SIA ratios in sharks (Kim et al., 2012; Malpica-Cruz et al., 2012). Soft, metabolically active tissues reflect the isotopic composition of the prey consumed over time; tissues with higher isotope turnover rates (i.e., blood) reflect a shorter feeding period than those with lower turnover rates (i.e., muscle) (Logan and Lutcavage, 2010; Hussey et al., 2012; Malpica-Cruz et al., 2012). Isotopic equilibrium between the isotopic composition of muscle tissue in sharks is reached after several months or even years, with younger, faster growing individuals reaching equilibrium faster, after about a threefold biomass gain (Logan and Lutcavage, 2010; Kim et al., 2012; Malpica-Cruz et al., 2012).δ^{13}C values provide information regarding the dominant sources of primary production, which vary among habitat types, for example between benthic and pelagic food webs. Thus, they can be used to trace shark habitat shifts, particularly between coastal and oceanic ecosystems, as well as to distinguish between benthic vs. pelagic feeding (Finlay and Kendall, 2007; Munroe et al., 2018). Due to a consistent enrichment in ^{15}N between a consumer and its assimilated diet, δ^{15}N values have been used to characterize ontogenetic shifts in trophic level (Peterson and Fry, 1987; Post, 2002). Given prior knowledge regarding a consumer's feeding habits and adequate characterization of the spatial and temporal variability in the isotopic baseline (Phillips et al., 2014), SIA are also useful for estimating the contribution of different sources to a consumer's diet (Parnell et al., 2013). However, characterization of the isotopic baseline can be challenging, particularly for highly migratory species.

Recently, the use of compound-specific stable isotope analysis of amino acids (CSIA-AA) has been proposed as a complementary method to bulk SIA. "Source" AAs do not exhibit a substantial enrichment in ^{15}N between consumers and their foods, and thus reflect the isotopic baseline, while "trophic" AA exhibit a high and consistent enrichment that is conductive to estimate trophic level (Chikaraishi et al., 2009; O'Connell, 2017). CSIA-AA are advantageous because a single tissue contains both kinds of AA, allowing for the calculation of trophic position and inferring of foraging patterns without the need for an independent characterization of an isotopic baseline (Chikaraishi et al., 2010; Hoen et al., 2014; Munroe et al., 2018). The canonical source and trophic AAs are phenylalanine (Phe) and glutamic acid (Glu), respectively (McMahon and McCarthy, 2016).

To understand the trophic ecology of the early life stages of white sharks in the BSV-OLL nursery, we used bulk SIA of shark muscle and putative prey items to estimate the contribution of different prey groups to their diet and assess ontogenetic dietary shifts related to movements between habitats. CSIA of the canonical source and trophic AA were used to estimate trophic level. We also evaluate the level of dietary overlap with sympatric shark species that feed within the system, which provides insight into the potential for competition with local fisheries and sympatric species for local prey. The study provides information that can improve the environmentally sound management and conservation strategies in the area.

METHODS

Sample Collection

Muscle samples (1 cm^3) from the dorsal area of white sharks were collected between 2013 to 2017, either within BSV or off the northwestern coast of the Baja California peninsula, termed outside of BSV (OBSV) hereafter (**Figure 1**, **Table 1** and **Supplementary Material**). Samples were obtained opportunistically from white sharks caught incidentally by artisanal fisheries and from individuals tagged within BSV. Artisanal fisheries operate in coastal areas, so incidental catches of white sharks occur near landing sites (**Figure 1**). Individuals tagged within BSV were sampled along the southern coast of the Bay and near the mouth of the Ojo de Liebre lagoon (**Figure 1**). For all sharks sampled inside BSV, total length (TL) and sex were recorded. Based on their size, sharks were divided into three life stages: newborn (NB; less than 150 cm TL), young of the year (YOY; between 151 and 175 cm TL), and juveniles (JUV; larger than 175 cm TL). Although sharks sampled OBSV were not measured because local fishers provided samples, they estimated their size >200 cm TL and were therefore categorized as juveniles.

Based on the analysis of small white sharks captured incidentally in BSV, Malpica-Cruz et al. (2013) inferred that blood and muscle tissues were in isotopic equilibrium with local prey given the similarity in isotope ratios between tissues. Our interpretation of the stable isotope ratios of immature white sharks sampled in BSV is based on this assumption. Larger sharks sampled outside BSV move along the west coast of the Baja California peninsula (Weng et al., 2012), and may exhibit a different isotopic composition than those from BSV, reflecting distinct food sources or isotopic baselines.

Muscle tissue (1 cm^3) from demersal fish and rays (n = 72) previously reported as prey for juvenile white sharks in BSV by Santana-Morales et al. (2012) were collected from fishing

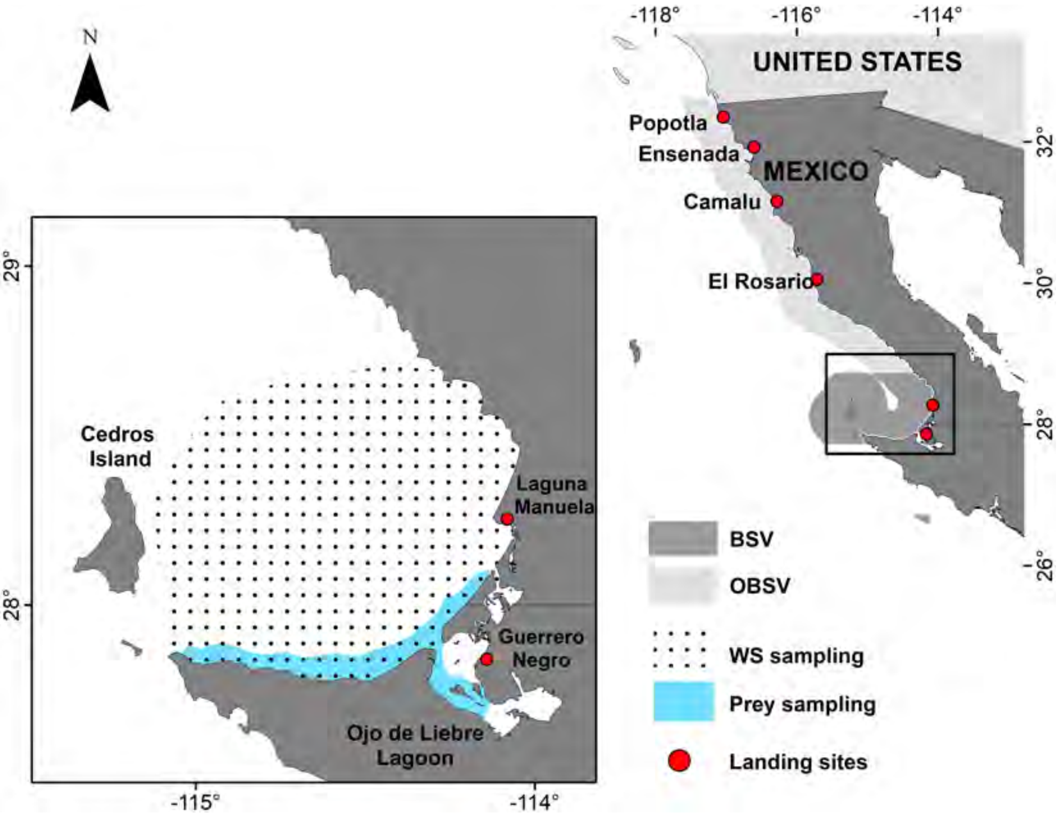

FIGURE 1 | Areas of the Baja California peninsula where white shark muscle samples were collected. BSV, Bahía Sebastián Vizcaíno; OBSV, Outside Bahía Sebastián Vizcaíno. Red points indicate landing sites where white sharks incidentally caught were sampled. Pointed area refers to the places where white sharks were collected inside BSV. The blue area indicates regions where prey inside BSV were collected. Prey samples from Tamburin et al. (2019, 2020) where collected in the pointed area.

activities during the summer of 2016. Potential prey were caught near the mouth of OLL and along BSVs southern coast (**Figure 1**), and included white seabass (*Atractoscion nobilis*), California halibut (*Paralichthys californicus*), California bat ray (*Myliobatis californica*), California butterfly ray (*Gymnura marmorata*), diamond stingray (*Hypanus dipterururs*), and shovelnose guitarfish (*Pseudobatos productus*) (**Table 2**). Shovelnose guitarfish was selected because it is the most abundant demersal elasmobranch in the area, as well as potential prey for white sharks. Muscle tissue from smooth hammerheads (*S. zygaena*) and copper sharks (*Carcharhinus brachyurus*) was also collected opportunistically in BSV during the summer of 2016 to examine the level of niche overlap with white sharks.

TABLE 1 | Isotopic values for different life stages of immature white sharks collected in Bahía Sebastián Vizcaíno and the northern part of the Baja California peninsula (OBSV: Outside Bahía Sebastián Vizcaíno).

Life stage	*n*	Total length (cm)	δ^{13}C (‰)		δ^{15}N (‰)	
			Mean	SD	Mean	SD
Newborn	12	138–150	−17.1*	0.6	17.3*	0.3
Young of the year	13	152–170	−16.6	0.7	17.4*	0.7
Juvenile	6	173–201	−16.2	0.2	18.1	0.3
Juvenile OBSV	8	176–300	−16.5	0.6	17.9	1.1

**Indicates significant differences between life stages tested with one-way ANOVA and Tukey post hoc test. Differences between juveniles inside BSV and OBSV were tested with the Kruskal-Wallis test. The significance level is 0.01.*

Sample Preparation for Bulk Isotope and CSIA-AA Analysis

All samples were lipid and urea extracted (white seabass and halibut were only lipid extracted) as previously recommended for bulk SIA (Li et al., 2016; Carlisle et al., 2017) by following the methods of Kim and Koch (2012) and Carlisle et al. (2017). Briefly, tissue samples were soaked in petroleum ether and mixed with a vortex mixer. After letting the samples dry uncapped for 8 h, they were centrifuged for 10 min, rinsed in 10 ml of DIW and mixed again. Samples were then centrifuged after 30 min and were dried in an oven at 60°C for 24 h. Subsequently, 0.8–1.2 mg were ground to a fine powder and placed in tin capsules for shipment to the Stable Isotope Facility at the University of California Davis (SIA-UCD) using a PDZ Europa ANCA-GSL elemental analyzer interfaced to a PDZ Europa 20-20 isotope ratio mass spectrometer (Sercon Ltd., Cheshire, United Kingdom). Analytical precision for laboratory internal standards, bovine liver, glutamic acid, enriched alanine and nylon 6, was 0.06, 0.06, 0.06, and 0.05‰ for $\delta^{15}N$, respectively, and 0.06, 0.10, 0.07, and 0.08‰ for $\delta^{13}C$, respectively.

For CSIA-AA analysis, white shark samples were dried in an oven for 24 h at 60° as recommended by Hoen et al. (2014). Between 7 and 10 mg of ground dry sample was weighed and stored in pre-combusted 5 ml glass vials. Samples were analyzed at SIF-UCD with a Trace Ultra GC gas chromatography coupled to Thermo Delta V Plus through a GC IsoLink, following protocols described by Yarnes and Herszage (2017). Each sample was analyzed in triplicate. Precision for Phe and Glu were 0.30 and 0.40‰ respectively.

Stable isotope values are expressed in standard delta notation (δ). For $\delta^{15}N$ values, atmospheric nitrogen was used as a standard, while the Vienna Pee Dee Belemnite (VPDB) standard was used for $\delta^{13}C$. Units are in parts per thousand (‰):

$$\delta 15N\ (‰)\ =\ \left(\left[R_{sample} -\ R_{standard}\right] - 1\right) \times 10^3$$

where R is the isotope ratio (^{15}N:^{14}N or ^{13}C:^{12}C).

Differences in mean $\delta^{15}N$ and $\delta^{13}C$ between life stages (NB vs. YOY vs. Juveniles) were tested using one-way ANOVA analysis with a Tukey *post-hoc* test, the data met the assumptions of normality and homogeneity of variances Differences in isotopic composition of juvenile white sharks sampled inside and outside of BSV were examined using a Kruskal-Wallis test because the assumption of normality was not met, as determined with a Shapiro-Wilk test.

Trophic Relationships Between White Sharks and Potential Prey

To estimate the relative contribution of potential prey caught inside BSV to the diet of immature white sharks sampled within the system, prey were categorized into three groups of species depending on their predominant habitat: *demersal*, *pelagic*, *and offshore*. The potential prey sampled in this study (see Section "Sample Collection") were categorized to a *demersal* habitat (**Table 2**). All these species are caught with bottom-set gillnets in BSV, supporting their use of demersal habitats in the region (García-Rodríguez and Sosa-Nishizaki, 2020). In addition, the

TABLE 2 | Isotope ratios of potential prey of immature white sharks.

Habitat	Common name	Species	*n*	TL (cm)	$\delta^{13}C$ (SD)	$\delta^{15}N$ (SD)
Demersal	Bat ray	*Myliobatis californica*	10	56–74**	−16.4 (0.7)	14.4 (2.8)
	Butterfly ray	*Gymnura marmorata*	10	76–94**	−15.4 (0.6)	14.7 (1.7)
	Diamond stingray	*Hypanus dipterururs*	10	66–78**	−16.2 (1.1)	16.1 (1.6)
	Shovelnose guitarfish	*Pseudobatos productus*	22	76–96	−16.6 (1.3)	15.3 (2.0)
	California halibut	*Paralichthys californicus*	10	53–78	−15.2 (2.2)	13.6 (2.1)
	White seabass	*Atractoscion nobilis*	10	49–85	−16.6 (0.6)	16.5 (1.9)
	Average of demersal prey				−16.8 (0.8)	15.8 (0.8)
Pelagic	Pacific mackerel*	*Scomber japonicus*	n/a		−17.8 (0.6)	15.7 (0.9)
	Corvinas*	*Cynoscion* spp.	n/a		−16.3 (0.7)	16.3 (1.0)
	Needlefish*	*Tylosurus* spp.	n/a		−18.0 (0.1)	18.3 (0.1)
	Sea robins*	*Prionotus* spp.	n/a		−18.0 (1.5)	15.5 (0.8)
	Dolphinfishes*	*Coryphaena* spp.	n/a		−18.6 (0)	13.4 (0)
	Squid*	Unid. spp.	n/a		−17.7 (1.3)	12.7 (2.5)
	Average of pelagic prey				−17.6 (0.3)	16.0 (0.7)
Offshore	Pacific saury*	*Cololabis saira*	n/a		−19.7 (0.5)	10.7 (1.5)
	Lanternfish*	Myctophidae	n/a		−20.1 (0.5)	12.2 (0.7)
	Pacific mackerel*	*Scomber japonicus*	n/a		−18.6 (0.1)	14.6 (0.2)
	Jack mackerel*	*Trachurus symmetricus*	n/a		−19.4 (0)	12.2 (0)
	Halfbeak*	*Hyporhampus naos*	n/a		−19.2 (0.2)	8.6 (0.3)
	Pelagic triggerfish*	*Canthidermis* spp.	n/a		−20.1 (0)	11.1 (0)
	Flyingfish*	Exocoetidae	n/a		−20.1 (0)	12.4 (0)
	Humboldt squid*	*Dosidicus gigas*	n/a		−19.4 (0.2)	13.1 (0.6)
	Pelagic octopus*	*Ocythoe tuberculata*	n/a		−19.3 (0.9)	13.7 (1.9)
	Pelagic red crab*	*Pleuroncodes planipes*	n/a		−19.0 (0.9)	11.6 (0.9)
	Sardine*	*Sardinops sagax*	n/a		−19.8 (0.2)	13.6 (0.6)
	Average of offshore prey				−19.3 (0.7)	12.1 (1.5)

Prey were grouped based on their habitat type and used as endpoints in mixing models.
Values are means ± one standard deviation (SD).
n/a, not available.
**Values taken from Tamburin et al. (2019, 2020).*
***Disc width (cm).*
All isotopic values are in ‰.

stable isotope ratios of the six species were very similar, and thus similar prey were grouped for mixing models, as recommended by Parnell et al. (2013) and Phillips et al. (2014). For the *pelagic* and *offshore* habitats, we used the δ^{13}C and δ^{15}N values published by Tamburin et al. (2019, 2020) for potential prey of immature white sharks sampled in the BSV region (**Table 2**). White shark samples from Tamburin et al. (2019, 2020) were collected between 2015 and 2017, and we assume their prey samples were also collected during those years. Overall means ± standard deviation (SD) for each habitat category were used as inputs for the isotope mixing models.

Bayesian mixing models (Parnell et al., 2013) were used to estimate the contribution of each prey category to the diet of immature white sharks. Analyses were performed using the *simmr* package (Parnell, 2016) in R. Models were run with uninformed priors, four Markov Chain Monte Carlo (MCMC) chains, with 1,000 burn-in and 10,000 iterations. We used the empirically derived trophic enrichment factors (TEF) reported for shark muscle estimated in controlled feeding experiments by Kim et al. (2012) and Malpica-Cruz et al. (2012). TEF values from those studies were averaged for their use in mixing models ($\Delta\ \delta^{13}C = 1.3 \pm 0.5‰$; $\Delta\ \delta^{15}N = 3.0 \pm 0.9‰$). Prey contributions were estimated separately for each life stage (newborns, young of the year, and juveniles). Results are reported as the percent contribution of each prey group with 97.5% credibility intervals.

Isotopic Niche Overlap With Sympatric Species

The isotopic niche was estimated as the standard ellipse area (SEAc; Jackson et al., 2011). Smooth hammerheads were categorized based on their size (**Table 3**). Size categories were selected to match the sizes of the immature white sharks: newborns (60–85 cm TL), small juvenile (103–147 cm TL) that have similar sizes to newborn white sharks, and large juveniles (151–183 cm TL), which overlap with YOY white sharks. The isotopic niche overlap between the life stages of white sharks (newborn, YOY, and juvenile caught inside and outside BSV) and between sympatric shark species was estimated using the *SIBER* package in R.

Estimates of Trophic Position

Trophic position was estimated using CSIA-AA and the equation proposed by Hoen et al. (2014). This equation uses a trophic enrichment factor (TEF, the trophic discrimination per trophic level between trophic and source AA calculated based on the isotope discrimination of Glu and Phe) that accounts for differences in AA isotope discrimination between grazers and carnivores, which is relevant for high trophic level sharks:

$$TP = \frac{\left(\delta^{15}N_{glu} - \delta^{15}N_{phe}\right) - \beta - TEF_{herbivore}}{TEF_{carnivore}} + 2$$

Where $\delta^{15}N_{glu}$ (the canonical trophic AA) and $\delta^{15}N_{phe}$ (the canonical source AA) are the isotopic compositions of Glu and Phe in the consumer tissues. β is the difference between the δ^{15}N values of trophic and source AAs in primary producers (3.4 ± 0.9‰, Chikaraishi et al., 2009), $TEF_{herbivore}$ is equal to 7.6‰ and the $TEF_{carnivore}$ is equal to 2.8‰, as reported for sharks in controlled experiments (Hoen et al., 2014).

TABLE 3 | Mean isotopic values for size classes of hammerheads and copper sharks on Bahía Sebastián Vizcaíno.

Species	*n*	Total length (cm)	^{13}C (‰)		^{15}N (‰)	
			Mean	**SD**	**Mean**	**SD**
Newborn hammerhead	13	60–85	−16.3	0.7	17.2	0.4
Small juvenile hammerhead	29	103–147	−16.9	0.8	17.4	0.8
Large juvenile hammerhead	21	151–183	−17.3	0.3	18.9	0.9
Copper shark	17	102–304	−15.2	0.8	18.3	1.0

RESULTS

Muscle tissue samples from 31 immature white sharks were collected inside BSV. Based on their size, 12 were categorized as newborns, 13 as YOY, and six as juveniles. Eight additional samples were collected from juveniles outside BSV. Isotope ratios for white sharks sampled in BSV ranged from −17.8 to −15.5‰ for δ^{13}C (−16.7 ± 0.6‰ mean ± SD) and from 16.4 to 18.7‰ for δ^{15}N (17.5 ± 0.6‰). Muscle samples from YOY and juveniles had slightly higher δ^{13}C (0.5 and 0.8‰) and δ^{15}N values (0.2 and 0.8‰) compared with those of NB (**Figure 2** and **Table 1**). There were significant differences in mean δ^{15}N values between NB and YOY compared with juveniles (one-way ANOVA, $p = 0.02$, and $p = 0.03$) but not between NB and YOY ($p = 0.91$). There were significant differences in mean δ^{13}C values between NB and the other life stages ($p = 0.01$). We did not find significant differences in the mean C or N isotopic composition for juveniles caught within and outside BSV (Kruskal-Wallis, $p = 0.2$ and $p = 0.7$, respectively).

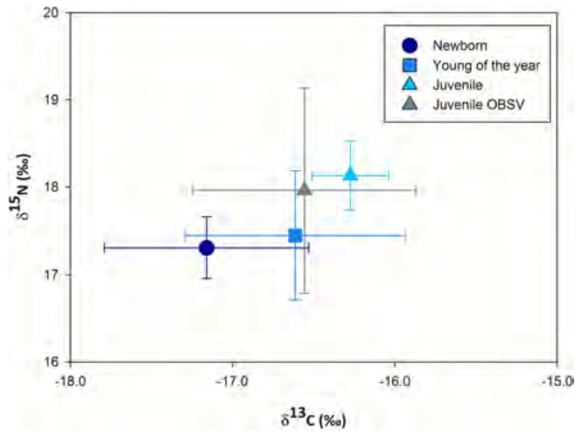

FIGURE 2 | Mean carbon and nitrogen stable isotope ratios (±SD) measured in the muscle tissues of immature white sharks sampled in Bahía Sebastián Vizcaíno and the northern part of the Baja California peninsula. Isotopic values are reported as a function of life stage: newborn (<150 cm TL), young of the year (between 151 and 170 cm TL), and juveniles (<171 cm TL). TL, total length.

The overall variability in prey from the *demersal* habitat was small (SD = 0.8‰ for both δ^{15}N and δ^{13}C); **Table 2**). Muscle tissue from demersal prey showed intraspecific variability in δ^{15}N and δ^{13}C values. White seabass and diamond stingray had higher δ^{15}N values (0.3 and 2.9‰ more enriched in ^{15}N) than the other demersal species sampled (**Table 2**). The mean isotopic composition of the prey from the *demersal* habitat was enriched in ^{13}C (0.8‰) compared with those from the *pelagic* habitat. However, prey from the *pelagic* habitat were slightly enriched in ^{15}N compared with *demersal* prey (0.2‰). Compared to prey from the *offshore* habitat, *demersal* species were enriched in both ^{13}C and ^{15}N (2.46 and 3.75‰; **Table 2**).

Bayesian mixing models indicate that *demersal* prey species provide the highest percentage contribution to muscle in NB (35.2%; CI: 7.0–64.7%), YOY (47.1%; CI: 10.1–75.15%), and juvenile white sharks (47.5%; CI: 10.8–81.0%) (**Figure 3**), followed by prey from *offshore* habitat in NB (32.6%; CI: 5.9–62.6%) and YOY (26.7%; CI: 9.6–41.9%) and by the *pelagic* habitat in juveniles (37.8%; CI: 6.7–75.3%).

Isotopic niche analysis showed that juveniles from OBSV had the broadest isotopic niche (SEAc = 2.45) of all white shark groups, followed by BSV YOY (SEAc = 1.51), NB (SEAc = 0.65), and juveniles (SEAc = 0.38; **Figure 4**). The highest overlap between isotopic niches was between YOY and juveniles OBSV (57.4%), while juveniles sampled in BSV had the smallest overlap with the other groups (<25%) (**Figure 4**).

Regarding sympatric shark species, in smooth hammerheads, δ^{15}N values ranged from 14.9 to 20.1‰ and δ^{13}C values from −14.2 to −18.0‰ (**Table 3**). Mean δ^{15}N values from larger hammerheads were higher compared with conspecific newborns (1.7‰) and small juveniles (1.5‰). For δ^{13}C, mean values from larger hammerheads were slightly lower than for the other groups (1.0‰ and 0.4‰) (**Figure 5** and **Table 3**). For copper sharks, δ^{15}N values ranged from 16.5 to 20.4‰ and δ^{13}C between −17.1 to −14.4‰ (**Table 3**). Muscle tissue from copper sharks had higher δ^{13}C values compared with hammerheads (by 1.1 to 2.1‰). For δ^{15}N values, copper sharks also had higher values, except for large hammerheads that were slightly higher (0.6‰) than copper sharks.

SIBER results showed that immature white sharks had the smallest isotopic niche of all sympatric shark species, while copper sharks had the largest. The overlap between immature white sharks and hammerheads was higher (45.27%) than with copper sharks (15.92%). A higher overlap was found when comparing life stages. The most extensive overlap was estimated between YOY and newborn hammerheads (55.17%), followed by the overlap between YOY and small juvenile hammerheads (54.69%) and the overlap between NB and newborn hammerheads (48.48%). The overlap with copper sharks was higher for YOY (27.55%) than for NB and juveniles from BSV (8.92 and 12.03%, respectively) (**Figure 6**).

Ten sharks were sampled for CSIA-AA of δ^{15}N inside ($n = 7$) and outside ($n = 3$) of BSV. Glutamic acid values ranged from 25.5 to 31.0‰, and phenylalanine ranged from 9.2 to 12.8‰ (**Table 4**). The trophic position estimated was higher for sharks outside BSV (5.3) than for the ones sampled within the Bay (4.3; **Table 4**).

DISCUSSION

Differences in δ^{15}N values found between immature white shark life stages indicate a size-based shift in feeding, and the and δ^{13}C values of NB likely reflect the maternal contribution. In the northeastern Pacific, adult white sharks are known to feed in offshore areas, including oceanic islands like Guadalupe island (Jorgensen et al., 2010; Hoyos-Padilla et al., 2016), where the isotopic baseline is depleted in ^{13}C relative to coastal and benthic habitats (Carlisle et al., 2012; Malpica-Cruz et al., 2013). Pregnant females move from these offshore areas to parturition grounds in coastal areas in Mexico and the US (Domeier and Nasby-Lucas, 2013; Oñate-González et al., 2015), which are enriched in ^{13}C due to the predominance of benthic production (Carlisle et al., 2012; Allen et al., 2013; Tamburin et al., 2020) and higher δ^{13}C phytoplankton in coastal areas compared to offshore waters (Vokhshoori et al., 2014). Our results show that newborn shark muscle tissue was depleted in ^{13}C compared with the following life stages. Given that very young white sharks are known to feed on benthic prey (Tricas and McCosker, 1984; Grainger et al., 2020), these results suggest the prevalence of ^{13}C-depleted maternal signature transferred to embryos during their gestation, as reported for other shark species with matrotrophic reproductive strategies (Estrada et al., 2006; McMeans et al., 2009; Olin et al., 2011, 2018). By the time sharks reached the YOY stage in our study, this maternal influence seems to have been diluted through the incorporation of new tissues during growth, leading to isotopic values similar to those of juveniles (Malpica-Cruz et al., 2013; Tamburin et al., 2020). For tissues of rapidly growing young sharks, exogenous feeding is reflected faster than in older sharks due to rapid growth and a threefold gain in mass (Malpica-Cruz et al., 2012). In immature white sharks, the change in isotopic composition that reflects active foraging has been reported to occur, for muscle tissue, at sizes between 150 and 170 cm TL (Malpica-Cruz et al., 2013), like our data indicate.

Immature white sharks are known to primarily use coastal habitats, sometimes covering long distances (hundreds of kilometers) between nurseries (Dewar et al., 2004; Harasti et al., 2017; Curtis et al., 2018; Bruce et al., 2019; Anderson et al., 2021). We did not find significant differences in the mean δ^{13}C or δ^{15}N between juvenile sharks caught inside and outside BSV. These results suggest that immature white sharks, born in BSV or migrating from southern California, United States toward BSV (Weng et al., 2007, 2012; White et al., 2019), are feeding on prey with similar isotopic values along the western coast of the Baja California peninsula. However, considerable variability in δ^{15}N was observed for sharks outside BSV. This variability is due to an enrichment in ^{15}N in larger juveniles (around 300 cm TL), which could be related to a shift in diet to feed on larger prey in coastal areas, like large bony fishes and marine mammals, as has been previously reported for the species (Carlisle et al., 2012; Hussey et al., 2012).

Results from mixing models indicated that white shark muscle reflected demersal prey as the main contributor for all life stages. These results are similar to what has been reported for the diet of juvenile white sharks based on stomach contents analysis (Tricas and McCosker, 1984; Grainger et al., 2020), including samples

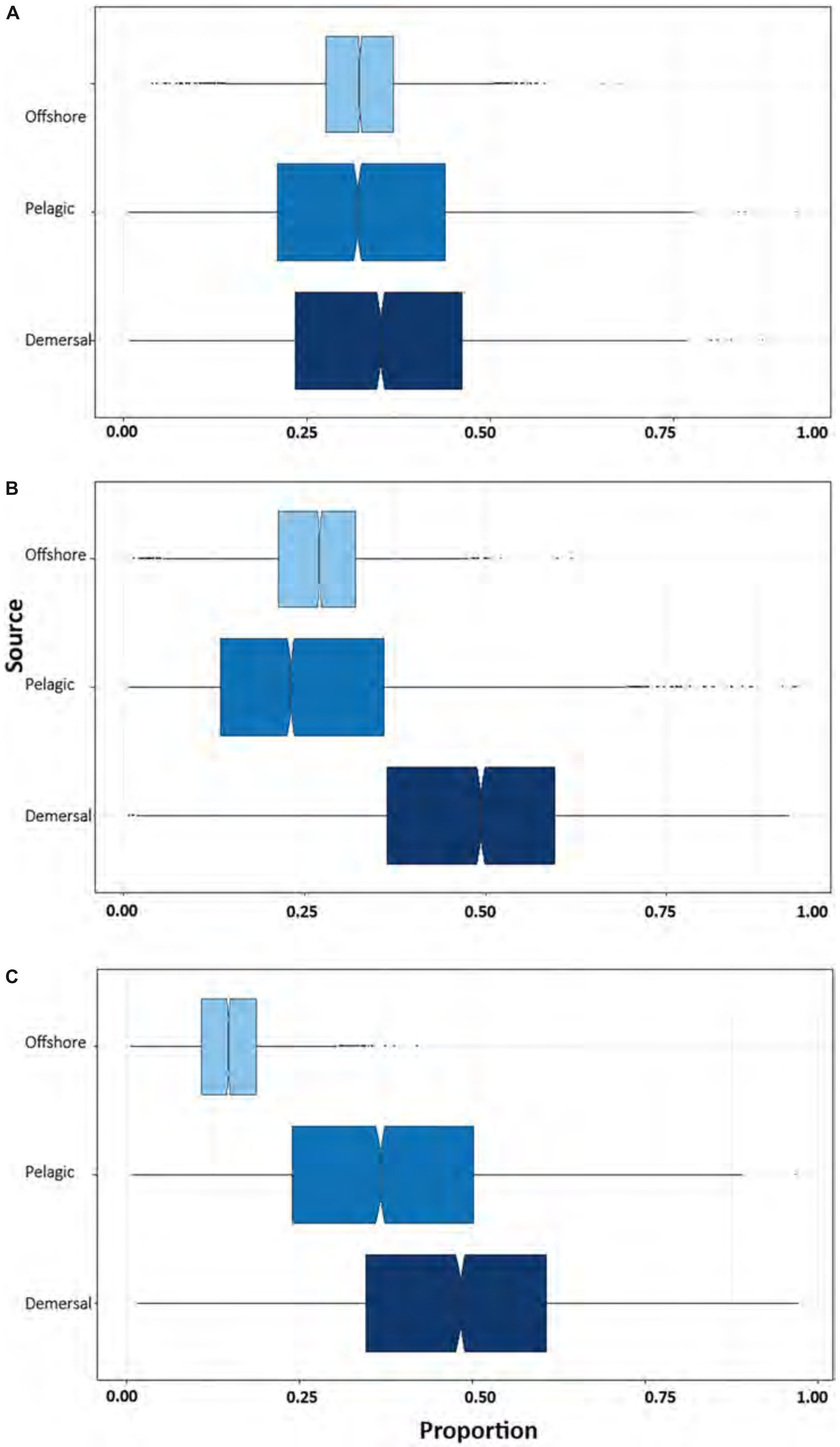

FIGURE 3 | Contribution of prey from different habitats to the isotopic composition of the muscle tissue of immature white sharks sampled in Bahía Sebastián Vizcaíno. **(A)** Newborn, **(B)** young of the year **(C)** juvenile white sharks.

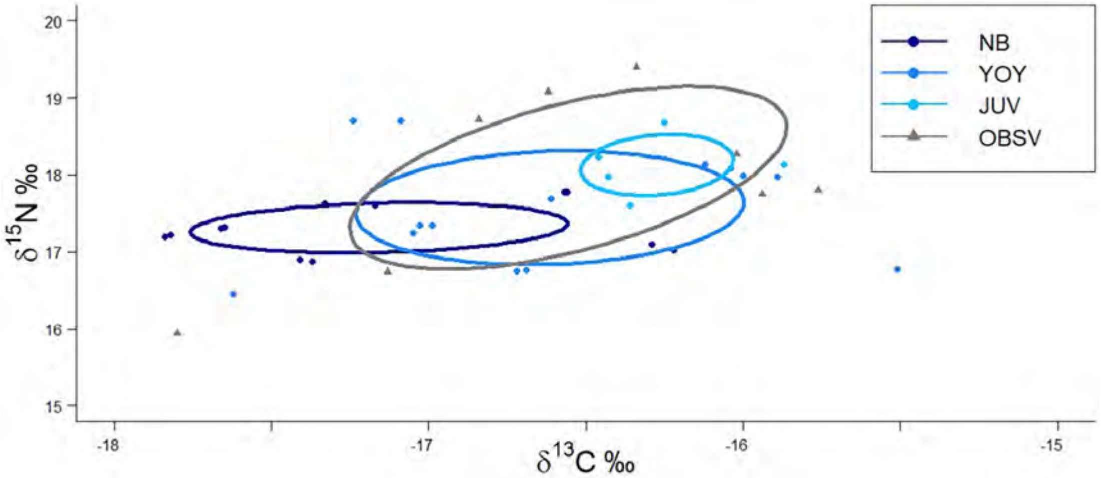

FIGURE 4 | Standardized ellipse of isotopic niches of immature white sharks sampled along the western coast of the Baja California peninsula. NB, newborn; YOY, young of the year; JUV, juvenile collected within Bahía Sebastián Vizcaíno; OBSV, juveniles outside Bahía Sebastián Vizcaíno. Points indicate individual values from immature white sharks sampled.

from BSV where the most common items usually found are rays (mostly bat rays; Santana-Morales et al., 2012; pers. obs.). However, the relative contribution of demersal prey changed between life stages.

For juvenile white sharks, the contribution of pelagic prey (37.8%) was higher than for newborns and YOY (32.2 and 26.2%, respectively). Although previous feeding studies of immature white sharks report a diet dominated by demersal species, they also report the presence of pelagic prey like sardines, mackerel, pelagic sharks, and cephalopods, which become more important in juveniles larger than 185 cm TL (Tricas and McCosker, 1984; Hussey et al., 2012). In BSV, pelagic prey like mackerel *Scomber japonicus* and squid (order Teuthoidea) have been found in the stomach contents of immature white sharks (Santana-Morales et al., 2012).

BSV is a critical feeding and nursery region for a large variety of pelagic and demersal species (Hernández-Rivas et al., 2000), suggesting that it could sustain high prey availability for immature white sharks. Preliminary tagging results in BSV show that immature white sharks move from very nearshore areas (including the Ojo de Liebre Lagoon) to areas farther from the coastline but still within BSV, where they might feed on those pelagic species (García-Rodíguez, 2020). In addition, pelagic prey could move to inshore areas seasonally, where their availability to immature white sharks may be higher. The higher contribution of demersal and pelagic prey to the isotopic composition of immature white sharks confirms the function of BSV as a nursery for this species, which provides important feeding grounds.

A higher contribution of prey from *offshore* habitats for neonates (32.6%) and YOY (26.2%) than for juveniles (14.9%) was also estimated, suggesting that the maternal isotopic composition may still have been detectable in some of these smaller sharks but diluted by the time sharks are juveniles, as biomass gain dilutes the maternal signature present at birth and metabolic turnover accelerates the rate at which isotopic equilibrium is reached (Herzka, 2005). Based on mass-length relationships reported for immature white sharks (Logan et al., 2018), immature white sharks born at 138 cm TL double their mass by the time they reach 160–165 cm TL. Previous studies have reported that immature white sharks in the region reflect exogenous feeding in muscle tissues between 150 and 170 cm TL (Malpica-Cruz et al., 2013). A three-fold increase in weight, which is necessary for approximating equilibrium following a dietary shift, would be reached at 190 cm. Hence, juveniles should reflect little or none of the maternally derived isotopic composition.

This smaller contribution of offshore prey estimated for juveniles could be related to movements and foraging in offshore areas. According to satellite telemetry, in the Northeast Pacific, juvenile white sharks commonly select very nearshore habitats (<30 km from the coast; White et al., 2019); however, a few individuals have been shown to move occasionally to offshore areas as far as 1,350 km from the mainland coast in the United States and Mexico (Weng et al., 2012; White et al., 2019).

Although mixing models provide insight into feeding habitats and ontogenetic shifts in feeding, in our study SIA was not useful for discriminating between specific prey that contribute to the diet of immature white sharks. Given the protected status of this species, direct sampling of sharks for stomach contents is

TABLE 4 | Trophic position (TP) for immature white sharks from Bahía Sebastián Vizcaíno and the northern part of the Baja California peninsula.

Area	δ^{15}N Glx (‰)	δ^{15}N Phe (‰)	TP	± SD
BSV	27.2 ± 1.2 SD	10.8 ± 1.2 SD	4.3	0.6
OBSV	29.6 ± 2.3 SD	10.9 ± 0.6 SD	5.3	0.8

TEF, trophic enrichment factors; SD, standard deviation.

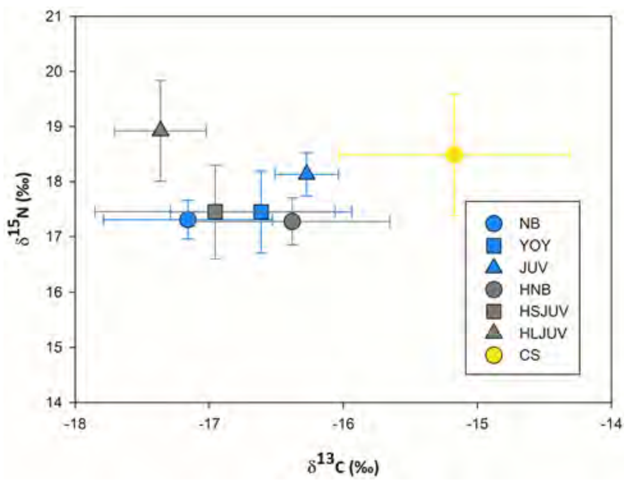

FIGURE 5 | Mean carbon and nitrogen stable isotope ratios (±SD) measured in the muscle of immature white sharks, smooth hammerheads and copper sharks from Bahía Sebastián Vizcaíno and the northern part of the Baja California peninsula. NB = newborn white sharks, YOY = young of the year white sharks, JUV = juvenile white sharks, HNB = newborn hammerheads, HSJUV = small juvenile hammerheads, HLJUV = large juvenile hammerheads and CS = copper shark.

not feasible, although gut content analysis of incidental captures could provide some insight into their feeding preferences, as it has in the past (Santana-Morales et al., 2012).

One caveat in our study is the temporal mismatch between white shark and prey samples. Ideally, consumer and sources should be collected at the same time to limit temporal variability (Phillips et al., 2014). As is the case for other top predators, white sharks are not abundant (Huveneers et al., 2018), so sample collection is mostly opportunistic. Due to the small sample size, we could not control for year and life stage in our statistical analyses. However, isotopic values for white sharks were similar to those previously reported for the species within BSV (Malpica-Cruz et al., 2013), suggesting that temporal variability is limited in younger sharks.

Tamburin et al. (2020) sampled muscle tissue (n = 12) for bulk SIA from immature white sharks in OLL and other areas inside BSV between 2015 and 2018. They also sampled potential prey representing different habitats where these sharks could be foraging (including prey from Guadalupe Island). These authors found a higher contribution of offshore prey to the isotopic muscle composition from neonates and YOY. They associate it with the prevalence of a maternally derived isotopic signature. They also estimated higher proportional contribution of inshore pelagic species to tissues of juvenile white sharks, and suggested that these prey were a more important dietary component than reported in previous studies (Santana-Morales et al., 2012; Malpica-Cruz et al., 2013). In contrast, we found a higher contribution from demersal prey to the isotopic composition of immature white sharks, consistent with the more benthic foraging previously reported (Tricas and McCosker, 1984; Hussey et al., 2012; Grainger et al., 2020). Their demersal prey species differed from those analyzed in our study. They did not include batoids other than the bat ray, nor demersal bony fishes like white seabass and halibut, which are the target species of fisheries where immature white sharks are incidentally caught and which have been reported in

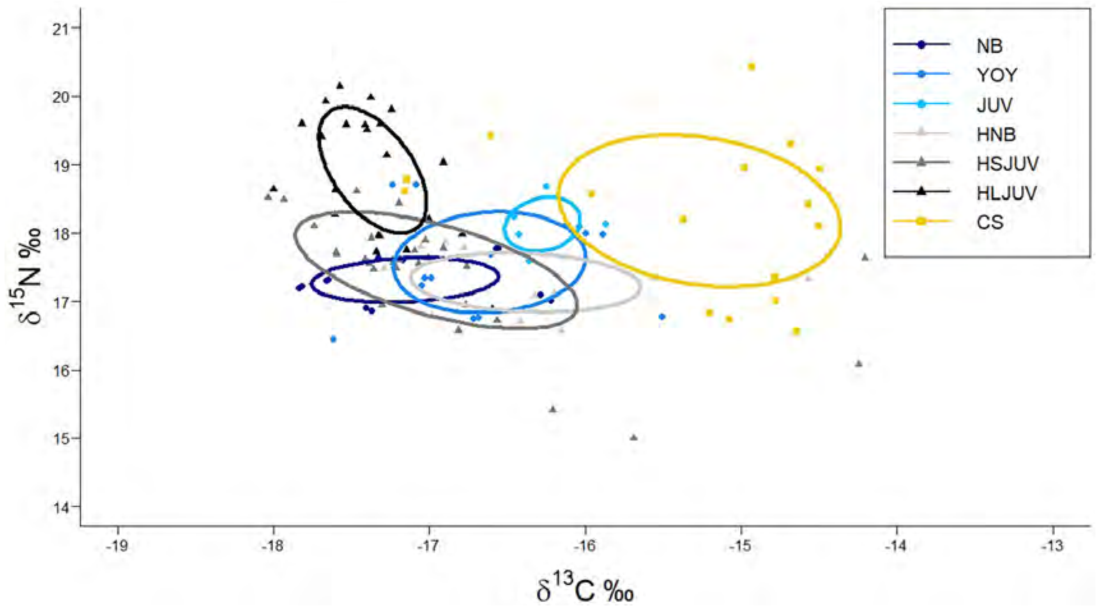

FIGURE 6 | Isotopic niches of different life stages of different size classes of immature white sharks, smooth hammerhead sharks and copper sharks sampled in Bahía Sebastián Vizcaíno. NB, newborn white sharks; YOY, young of the year white sharks; JUV, juvenile white sharks; HNB, newborn hammerheads; HSJUV, small juvenile hammerheads; HLJUV, large juvenile hammerheads; CS, copper shark.

their stomach contents (Santana-Morales et al., 2012; García-Rodríguez and Sosa-Nishizaki, 2020). Hence, demersal prey may not have been fully representative of the shark's food sources. Also, differences in the trophic discrimination factors could contribute to the differences between studies (Phillips et al., 2014). Tamburin et al. (2020) used the values reported by Kim et al. (Δ δ^{13}C = 1.7 ± 0.5‰; Δ δ^{15}N = 3.7 ± 0.4‰; 2012) while we averaged those values with the ones reported by Malpica-Cruz et al. (Δ δ^{13}C = 1.0‰; Δ δ^{15}N = 2.3‰; 2012). The TDFs from both studies are based on controlled feeding experiments on young leopard sharks and should be considered valid. In addition, many of the samples collected by Tamburin et al. (2020) were from white sharks sampled inside the Ojo de Liebre lagoon during March. According to preliminary acoustic telemetry data, March is when juveniles (larger than 175 cm TL) enter into this habitat (García-Rodíguez, 2020). These juvenile white sharks could be migrating between the Southern California Bight and BSV and could be feeding on coastal pelagic species with different isotopic compositions during these habitat transitions, as the higher variability in the isotopic composition of sharks caught outside of BSV suggests.

In our study, all of the demersal prey samples were collected near the Ojo de Liebre Lagoon's mouth, which is a high-intensity fishing area where most of the incidental catches of immature white sharks occur (García-Rodríguez and Sosa-Nishizaki, 2020). Based on information from satellite transmitters, White et al. (2019) predicted that juvenile individuals select shallow areas ($>$1,000 m deep), close to the shore ($<$30 km from the coast) and surface waters between 14 and 24°C. Based on their characterization of the habitat characteristics suitable for juveniles, BSV, including the Ojo de Liebre lagoon, is suitable year-round for immature white sharks. Other coastal areas along the western coast of the Baja California peninsula also appear to provide suitable habitats during parts of the year. Coastal habitats near lagoons like San Ignacio and San Quintin Bay are suitable mostly during summer and summer-fall, respectively (White et al., 2019), and incidental catches of immature white sharks have been reported. Rochín-Alamillo (2011) documented incidental catches during summer in San Ignacio lagoon, and a juvenile white shark tagged in BSV with a satellite transmitter moved near the San Quintin Bay, where it was incidentally caught during summer (Benson et al., 2018). Some immature white sharks seem to enter these lagoon and estuary habitats to take advantage of seasonal prey availability (Harasti et al., 2017). Coastal lagoons along the Baja California peninsula and their inlet areas present a high abundance of known prey (Danemann and de la Cruz-Agüero, 1993; De la Cruz-Agüero et al., 1994; Rosales-Casián, 1996) and seasonal environmental suitability (White et al., 2019) for immature white sharks. This suitability and the confirmed presence of white sharks incidentally caught when fishers target their prey (Rochín-Alamillo, 2011), suggest that these coastal lagoons and their inlet areas could provide benefits commonly associated with the known nursery areas from the Southern California Bight and BSV.

Anecdotal knowledge gathered from artisanal fishers indicates that demersal prey sampled in this study, like shovelnose guitarfishes and diamond stingray, are found in BSV waters throughout the year, while California bat rays, butterfly rays, and demersal bony fishes like California halibut and white seabass are present seasonally (García-Rodríguez and Sosa-Nishizaki, 2020). The availability of potential prey throughout the year supports the importance of BSV as a nursery habitat.

Some of the demersal prey species are targeted by the local artisanal fishery in BSV during summer, when most immature white sharks are caught (Santana-Morales et al., 2012; Oñate-González et al., 2017; García-Rodríguez and Sosa-Nishizaki, 2020). Landings of California halibut, white seabass, and rays represent around 30% of the total yearly landings from bony fishes in the area (CONAPESCA, 2018), and are therefore an important component of local fisheries. Changes in fishing effort directed at these demersal species might change the white shark's susceptibility to being incidentally caught. In addition, intense fishing activities could influence immature white sharks behavior, such as their feeding habits, movement patterns, and habitat shifts. Hence, future studies should monitor potential prey distribution, fishing effort, and white sharks.

The comparison of SEAc between life stages showed that juveniles outside BSV have a broader isotopic niche, which is likely due to feeding during their movements between California and Baja California (Weng et al., 2007, 2012; White et al., 2019). YOY and NB likely have smaller isotopic niches because their activities are restricted to BSV. Surprisingly, juveniles inside BSV had the narrowest isotopic niche, although this could be due to the small sample size (*n* = 6; Jackson et al., 2011), which may not be sufficiently representative of this life stage. The smaller sample size we obtained from juvenile white sharks is mostly due to the lower susceptibility of this life stage to be incidentally caught in demersal bottom nets compared with newborns and YOYs (Oñate-González et al., 2017; García-Rodríguez and Sosa-Nishizaki, 2020). While there was partial overlap in the isotopic niche between all life stages, the highest was between juveniles caught OBSV and YOY from BSV. Sharks sampled outside BSV could have been born in BSV or in the Southern California Bight. However, as they increase in size, they can move between nurseries and spend some months of the year in BSV, where they could feed on similar habitats or on resources with similar isotopic composition of the YOY.

Comparisons of the isotopic niches between sympatric species showed that immature white sharks and smooth hammerheads had a 45% overlap. This overlap was higher for YOY white sharks and small juvenile hammerheads (103–147 cm), suggesting they feed on prey with similar isotopic composition. Juvenile smooth hammerheads feed mostly on squid, small pelagic fishes like scombrids and benthic bony fishes (Smale, 1991; Ochoa-Díaz, 2009), which are also prey for juvenile white sharks collected in BSV (Santana-Morales et al., 2012).

In contrast, there was a limited (15%) isotopic niche overlap between white sharks and copper sharks. Based on what has been reported for other regions, copper sharks in BSV may be feeding on many of the same pelagic species consumed by white sharks, like sardines, mackerels, skipjacks, and tunas (Smale, 1991; Santana-Morales et al., 2012). However, copper sharks are only caught in late spring and summer, when immature white sharks are caught incidentally (Oñate-González et al., 2017; García-Rodríguez and Sosa-Nishizaki, 2020). The temporal overlap between species is thus limited. In addition, copper sharks have a more tropical distribution than white sharks. Some of the copper sharks we sampled were also larger than white sharks and spanned the adult stages, which could contribute to a broader isotopic niche.

A partial overlap in the isotopic niche was reported between juvenile white sharks and juvenile shortfin makos *Isurus oxyrinchus* in BSV (Tamburin et al., 2019). However, makos have been reported to feed on more pelagic prey like Pacific saury *Cololabis saira* and jumbo squid *Dosidicus gigas* off the California coast (Preti et al., 2012). The partial overlap with makos and the higher overlap between the smaller life stages of immature white sharks and juvenile smooth hammerheads found in this study does not necessarily mean that they are competing for resources, since resource partitioning and spatial segregation could avoid competition (Bethea et al., 2004; Kinney et al., 2011). The potential for competition for resources among sympatric species highlights the importance of monitoring the population trends of prey in addition to those of sympatric sharks.

The trophic position calculated for sharks sampled in BSV (4.3) was similar to those previously reported for white sharks of similar sizes based on stomach content or bulk stable isotope analysis (Cortés, 1999; Estrada et al., 2006; Hussey et al., 2012). The trophic position estimated for white sharks caught OBSV was higher than that for BSV (5.3 vs 4.3), and higher than reported previously for the species. White sharks caught OBSV are likely moving between different habitats and could be feeding on prey with a higher TP than those in BSV, or on a different isotopic baseline. Alternatively, this could indicate that Hoen et al.'s (2014) TEF is unsuitable for large sharks due to size-related changes in the nutritional characteristics of the prey (such as protein or lipid content and quality; Nuche-Pascual et al., 2021). Some of the OBSV sharks were large juveniles (∼300 cm TL), and nearing the size when a shift in diet occurs and individuals start feeding on bigger prey, like marine mammals. These results highlight the importance of empirical studies examining the factors influencing AA TEFs for shark tissues.

CONCLUSION

Stable isotope analysis provided new information about the trophic ecology and complexity of immature white sharks in the northeastern Pacific and new insights into how their trophic habits are related to habitat shifts through their ontogeny. Our results support the importance of BSV as a nursery and foraging ground for sharks born within BSV and California and indicate that they may be sharing prey with sympatric species. We found that the most important prey for white sharks caught within BSV are those heavily targeted by coastal fisheries, which likely increases their susceptibility to being incidentally caught. However, SIA could not reveal the specific prey that white sharks are feeding in the region, so complementary methods should be used in the future. Also, research should focus on comprehending predator-prey relationships between white sharks and their prey to understand how changes in prey abundance and distribution could influence the early life stages of white sharks.

DATA AVAILABILITY STATEMENT

The raw data supporting the conclusions of this article will be made available by the authors, without undue reservation.

ETHICS STATEMENT

Ethical review and approval was not required for the animal study because Animals were sampled under permits SGPS/DGVS/04180/13, SGPS/DGVS/06243/14, SGPS/DGVS/06777/15, SGPS/DGVS/06294/16, SGPS/DGVS /07290/17, issued by the General Direction of WIldlife from the National Ministry of Environment and Natural Resources.

AUTHOR CONTRIBUTIONS

EG-R, SH, OS-N, and CL conceived the study and designed the study. EG-R collected and processed samples, analyzed the data, wrote the original draft, and prepared figures. All authors contributed equally to manuscript revisions and approved the final draft.

FUNDING

This research was funded by the Monterey Bay Aquarium, the Alliance WWF- Fundación Carlos Slim and the National Commission of Natural Protected Areas (CONANP) through the Conservation Program for Threatened Species (PROCER). EG-R held a scholarship (#237075) from CONACYT. The funder was not involved in the study design, collection, analysis, interpretation of data, the writing of this article or the decision to submit it for publication.

ACKNOWLEDGMENTS

We thank the members of the Fisheries Ecology Laboratory from CICESE that took part in the sampling collection; Beatriz Cordero and Abelardo Campos from CICESE's Aquaculture Department and Carmen Rodriguez from the CICESE's Biological Oceanography Department for helping in sample preparation; the Biosphere Reserve of El Vizcaíno for the support with permits. Many thanks to all the fishermen from the Baja California peninsula that supported the sampling collection, especially Edgar Zepeda and Rodrigo Guzmán.

SUPPLEMENTARY MATERIAL

The Supplementary Material for this article can be found online at: https://www.frontiersin.org/articles/10.3389/fmars.2021.687738/full#supplementary-material

REFERENCES

Allen, C. D., Lemons, G. E., Eguchi, T., LeRoux, R. A., Fahy, C. C., Dutton, P. H., et al. (2013). Stable isotope analysis reveals migratory origin of loggerhead turtles in the southern California bight. *Mar. Ecol. Prog. Ser.* 472, 275–285. doi: 10.3354/meps10023

Anderson, J. M., Burns, E. S., Meese, E. N., Farrugia, T. J., Stirling, B. S., White, C. F., et al. (2021). Interannual nearshore habitat use of young of the year white sharks off southern California. *Front. Mar. Sci.* 8:645142. doi: 10.3389/fmars.2021.645142

Benson, J. F., Jorgensen, S. J., O'Sullivan, J. B., Winkler, C., White, C. F., Garcia-Rodriguez, E., et al. (2018). Juvenile survival, competing risks, and spatial variation in mortality risk of a marine apex predator. *J. Appl. Ecol.* 55, 2888–2897. doi: 10.1111/1365-2664.13158

Bethea, D. M., Buckel, J. A., and Carlson, J. K. (2004). Foraging ecology of the early life stages of four sympatric shark species. *Mar. Ecol. Prog. Ser.* 268, 245–264. doi: 10.3354/meps268245

Bizzarro, J. J., Carlisle, A. B., Smith, W. D., and Cortés, E. (2017). "Diet composition and trophic ecology of northeast Pacific ocean sharks," in *Northeast Pacific Shark Biology, Research and Conservation (Part A), Adv. Mar. Biol*, Vol. 77, eds S. E. Larson and D. Lowry (London: Academic Press), 111–148. doi: 10.1016/bs.amb.2017.06.001

Block, B. A., Jonsen, I. D., Jorgensen, S. J., Winship, A. J., Shaffer, S. A., Bograd, S. J., et al. (2011). Tracking apex marine predator movements in a dynamic ocean. *Nature* 475, 86–90. doi: 10.1038/nature10082

Boecklen, W. J., Yarnes, C. T., Cook, B. A., and James, A. C. (2011). On the use of stable isotopes in trophic ecology. *Annu. Rev. Ecol. Evol. Syst.* 42, 411–440. doi: 10.1146/annurev-ecolsys-102209-144726

Boldrocchi, G., Kiszka, J., Purkis, S., Storai, T., Zinzula, L., and Burkholder, D. (2017). Distribution, ecology, and status of the white shark, *Carcharodon carcharias*, in the Mediterranean Sea. *Rev. Fish Biol. Fish.* 27, 515–534. doi: 10.1007/s11160-017-9470-5

Bruce, B., Harasti, D., Lee, K., Gallen, C., and Bradford, R. (2019). Broad-scale movements of juvenile white sharks *Carcharodon carcharias* in eastern Australia from acoustic and satellite telemetry. *Mar. Ecol. Prog. Ser.* 619, 1–15. doi: 10.3354/meps12969

Bruce, B. D., and Bradford, R. W. (2012). "Habitat use and spatial dynamics of juvenile white sharks, *Carcharodon carcharias*, in eastern Australia," in *Global Perspectives on the Biology and Life History of White Shark*, ed. M. L. Domeier (Boca Raton,FL: CRC Press), 225–254.

Carlisle, A. B., Goldman, K. J., Litvin, S. Y., Madigan, D. J., Bigman, J. S., Swithenbank, A. M., et al. (2015a). Stable isotope analysis of vertebrae reveals ontogenetic changes in habitat in an endothermic pelagic shark. *Proc. R. Soc. B Biol. Sci.* 282:20141446. doi: 10.1098/rspb.2014.1446

Carlisle, A. B., Kim, S. L., Semmens, B. X., Madigan, D. J., Jorgensen, S. J., Perle, C. R., et al. (2012). Using stable isotope analysis to understand the migration and trophic ecology of northeastern pacific white sharks (Carcharodon carcharias). *PLoS One* 7, e30492. doi: 10.1371/journal.pone.0030492

Carlisle, A. B., Litvin, S. Y., Hazen, E. L., Madigan, D. J., Goldman, K. J., Lea, R. N., et al. (2015b). Reconstructing habitat use by juvenile salmon sharks links upwelling to strandings in the California Current. *Mar. Ecol. Prog. Ser.* 525, 217–228. doi: 10.3354/meps11183

Carlisle, A. B., Litvin, S. Y., Madigan, D. J., Lyons, K., Bigman, J. S., Ibarra, M., et al. (2017). Interactive effects of urea and lipid content confound stable isotope analysis in elasmobranch fishes. *Can. J. Fish. Aquat. Sci.* 74, 419–428. doi: 10.1139/cjfas-2015-0584

Chikaraishi, Y., Ogawa, N. O., Kashiyama, Y., Takano, Y., Suga, H., Tomitani, A., et al. (2009). Determination of aquatic food-web structure based on compound-specific nitrogen isotopic composition of amino acids. *Limnol. Oceanogr. Methods* 7, 740–750. doi: 10.4319/lom.2009.7.740

Chikaraishi, Y., Ogawa, N. O., and Ohkouchi, N. (2010). "Further evaluation of the trophic level estimation based on nitrogen isotopic composition of amino acids," in *Earth, Life, and Isotopes,* eds. N. Ohokouchi, I. Tayasu, K. Koba (Kyoto: Kyoto University Press), 37–51.

CONAPESCA (2018). *Base De Datos De Avisos De Arribo Pesqueros*. Available online at: https://www.plataformadetransparencia.org.mx [accessed June 20, 2019]

Cortés, E. (1999). Standardized diet compositions and trophic levels of sharks. *ICES J. Mar. Sci.* 56, 707–717. doi: 10.1006/jmsc.1999.0489

Curtis, T. H., Metzger, G., Fischer, C., Mcbride, B., Mccallister, M., and Winn, L. J. (2018). First insights into the movements of young-of-the-year white sharks (*Carcharodon carcharias*) in the western north Atlantic ocean. *Sci. Rep.* 8, 1–8. doi: 10.1038/s41598-018-29180-5

Danemann, G. D., and de la Cruz-Agüero, J. (1993). Ictiofauna de laguna San Ignacio, Baja California sur, México. *Cienc. Mar.* 19, 333–341. doi: 10.7773/cm.v19i3.936

De la Cruz-Agüero, J., Galván-Magaña, F., Abitia-Cárdenas, L. A., Rodríguez-Romero, J., and Gutiérrez-Sánchez, F. J. (1994). Lista sistematica de los peces marinos de Bahía Magdalena, Baja California sur (México). *Cienc. Mar.* 20, 17–31.

Dewar, H., Domeier, M., and Nasby-Lucas, N. (2004). Insights into young of the year white shark, *Carcharodon carcharias*, behavior in the Southern California Bight. *Environ. Biol. Fishes* 70, 133–143. doi: 10.1023/B:EBFI.0000029343.54027.6a

DOF (2007). Norma Oficial Mexicana NOM-029-PESC-2006: pesca responsable de tiburónes y rayas. especificaciones para su aprovechamiento. *Diario Oficial Federación* 1, 60–102.

DOF (2010). Norma Oficial Mexicana NOM-059-ECOL-2001:protección ambiental-especies nativas de México de flora y fauna silvestres-categorías de riesgo y especificaciones para su inclusión, exclusión o cambio-Lista de especies en riesgo. *Diario Oficial Federación* 1, 1–77.

DOF (2014). Acuerdo por el que se establece veda permanente para la pesca de tiburón blanco (*Carcharodon carcharias*) en aguas de jurisdicción federal de los Estados Unidos Mexicanos. *Diario Oficial Federación* 1, 14–16.

Domeier, M. L., and Nasby-Lucas, N. (2007). Annual re-sightings of photographically identified white sharks (*Carcharodon carcharias*) at an eastern Pacific aggregation site (Guadalupe Island, Mexico). *Mar. Biol.* 150, 977–984. doi: 10.1007/s00227-006-0380-7

Domeier, M. L., and Nasby-Lucas, N. (2008). Migration patterns of white sharks *Carcharodon carcharias* tagged at Guadalupe Island, Mexico, and identification of an eastern Pacific shared offshore foraging area. *Mar. Ecol. Prog. Ser.* 370, 221–237. doi: 10.3354/meps07628

Domeier, M. L., and Nasby-Lucas, N. (2013). Two-year migration of adult female white sharks (*Carcharodon carcharias*) reveals widely separated nursery areas and conservation concerns. *Anim. Biotelemetry* 1:2. doi: 10.1186/2050-3385-1-2

Estrada, J. A., Rice, A. N., Natanson, L. J., and Skomal, G. B. (2006). Use of isotopic analysis of vertebrae in reconstructiong ontogenetic feeding ecology in white sharks. *Ecology* 87, 829–834. doi: 10.1890/0012-9658(2006)87[829:uoiaov]2.0.co;2

Estupiñán-Montaño, C., Galván-Magaña, F., Sánchez-González, A., Elorriaga-Verplancken, F. R., Delgado-Huertas, A., and Páez-Rosas, D. (2019). Dietary ontogeny of the blue shark, *Prionace glauca*, based on the analysis of δ13C and δ15N in vertebrae. *Mar. Biol.* 166:101. doi: 10.1007/s00227-019-3550-0

Ferretti, F., Worm, B., Britten, G. L., Heithaus, M. R., and Lotze, H. K. (2010). Patterns and ecosystem consequences of shark declines in the ocean. *Ecol. Lett.* 13, 1055–1071. doi: 10.1111/j.1461-0248.2010.01489.x

Finlay, J. C., and Kendall, C. (2007). "Stable isotope tracing of temporal and spatial variability in organic matter sources to freshwater ecosystems," in *Stable Isotopes in Ecology and Environmental Science*, eds R. H. Michener and K. Lajtha (Oxford, UK: Blackwell Publishing Ltd), 283–333. doi: 10.1002/9780470691854.ch10

Francis, M. P., Duffy, C., and Lyon, W. (2015). Spatial and temporal habitat use by white sharks (*Carcharodon carcharias*) at an aggregation site in southern New Zealand. *Mar. Freshw. Res.* 66, 900–918. doi: 10.1071/MF14186

French, G. C. A., Rizzuto, S., Stürup, M., Inger, R., Barker, S., van Wyk, J. H., et al. (2018). Sex, size and isotopes: cryptic trophic ecology of an apex predator, the white shark *Carcharodon carcharias*. *Mar. Biol.* 165:102. doi: 10.1007/s00227-018-3343-x

García-Rodíguez, E. (2020). *Importance of Ojo de Liebre lagoon and Vizcaino Bay in the Early Life Stages of White Sharks:Ecological and Fishery Issues*. Doctoral thesis. Ensenada, BC: Centro de Investigación Científica y de Educación Superior de Ensenada, Baja California.

García-Rodríguez, E., and Sosa-Nishizaki, O. (2020). Artisanal fishing activities and their documented interactions with juvenile white sharks inside a nursery area. *Aquat. Conserv. Mar. Freshw. Ecosyst.* 30, 903–914. doi: 10.1002/aqc.3300

Gračan, R., Zavodnik, D., Krstinić, P., Dragičević, B., and Lazar, B. (2017). Feeding ecology and trophic segregation of two sympatric mesopredatory sharks in the heavily exploited coastal ecosystem of the Adriatic Sea. *J. Fish Biol.* 90, 167–184. doi: 10.1111/jfb.13158

Grainger, R., Peddemors, V. M., Raubenheimer, D., and Machovsky-capuska, G. E. (2020). Diet composition and nutritional niche breadth variability in juvenile white sharks (*Carcharodon carcharias*). *Front. Mar. Sci.* 7:422. doi: 10.3389/fmars.2020.00422

Hansson, S., Bergström, U., Bonsdorff, E., Härkönen, T., Jepsen, N., Kautsky, L., et al. (2018). Competition for the fish – fish extraction from the Baltic Sea by humans, aquatic mammals, and birds. *ICES J. Mar. Sci.* 75, 999–1008. doi: 10.1093/icesjms/fsx207

Harasti, D., Lee, K., Bruce, B., Gallen, C., and Bradford, R. (2017). Juvenile white sharks *Carcharodon carcharias* use estuarine environments in south-eastern Australia. *Mar. Biol.* 164:58. doi: 10.1007/s00227-017-3087-z

Hernández-Rivas, M., Jimenez-Rosenberg, S. P., Funes-Rodríguez, R., and Saldierna-Martinez, R. (2000). "El centro de actividad biológica de la bahía de Sebastián Vizcaíno, una primera aproximación," in *BAC: Centros De Actividad Biológica Del Pacífico Mexicano*, eds D. Lluch-Belda, J. F. Elorduy-Garay, S. Lluch-Cota, and G. Ponce Diaz (La Paz: Centro de Investigaciones Biológicas del Noroeste), 65–68.

Herzka, S. Z. (2005). Assessing connectivity of estuarine fishes based on stable isotope ratio analysis. *Estuar. Coast. Shelf Sci.* 64, 58–69. doi: 10.1016/j.ecss.2005.02.006

Hette-Tronquart, N. (2019). Isotopic niche is not equal to trophic niche. *Ecol. Lett.* 22, 1987–1989. doi: 10.1111/ele.13218

Heupel, M., Knip, D., Simpfendorfer, C., and Dulvy, N. (2014). Sizing up the ecological role of sharks as predators. *Mar. Ecol. Prog. Ser.* 495, 291–298. doi: 10.3354/meps10597

Heupel, M. R., Carlson, J. K., and Simpfendorfer, C. A. (2007). Shark nursery areas: concepts, definition, characterization and assumptions. *Mar. Ecol. Prog. Ser.* 337, 287–297. doi: 10.3354/meps337287

Hilborn, R., Amoroso, R. O., Bogazzi, E., Jensen, O. P., Parma, A. M., Szuwalski, C., et al. (2017). When does fishing forage species affect their predators? *Fish. Res.* 191, 211–221. doi: 10.1016/j.fishres.2017.01.008

Hoen, D. K., Kim, S. L., Hussey, N. E., Wallsgrove, N. J., Drazen, J. C., and Popp, B. N. (2014). Amino acid 15N trophic enrichment factors of four large carnivorous fishes. *J. Exp. Mar. Bio. Ecol.* 453, 76–83. doi: 10.1016/j.jembe.2014.01.006

Hoyos-Padilla, E. M., Klimley, A. P., Galván-Magaña, F., and Antoniou, A. (2016). Contrasts in the movements and habitat use of juvenile and adult white sharks (*Carcharodon carcharias*) at Guadalupe Island, Mexico. *Anim. Biotelemetry* 4, 1–14. doi: 10.1186/s40317-016-0106-7

Huss, M., de Roos, A. M., Van Leeuwen, A., and Gårdmark, A. (2014). Facilitation of fisheries by natural predators depends on life history of shared prey. *Oikos* 123, 1071–1080. doi: 10.1111/oik.00839

Hussey, N. E., MacNeil, M. A., Olin, J. A., McMeans, B. C., Kinney, M. J., Chapman, D. D., et al. (2012). Stable isotopes and elasmobranchs: tissue types, methods, applications and assumptions. *J. Fish Biol.* 80, 1449–1484. doi: 10.1111/j.1095-8649.2012.03251.x

Huveneers, C., Apps, K., Becerril-García, E. E., Bruce, B., Butcher, P. A., Carlisle, A. B., et al. (2018). Future research directions on the "elusive"white shark. *Front. Mar. Sci.* 5:455. doi: 10.3389/fmars.2018.00455

Jackson, A. L., Inger, R., Parnell, A. C., and Bearhop, S. (2011). Comparing isotopic niche widths among and within communities: SIBER - stable isotope Bayesian Ellipses in R. *J. Anim. Ecol.* 80, 595–602. doi: 10.1111/j.1365-2656.2011.01806.x

Jorgensen, S. J., Reeb, C. A., Chapple, T. K., Anderson, S., Perle, C., Van Sommeran, S. R., et al. (2010). Philopatry and migration of Pacific white sharks. *Proc. R. Soc. B Biol. Sci.* 277, 679–688. doi: 10.1098/rspb.2009.1155

Kim, S. L., del Rio, C. M., Casper, D., and Koch, P. L. (2012). Isotopic incorporation rates for shark tissues from a long-term captive feeding study. *J. Exp. Biol.* 215, 2495–2500. doi: 10.1242/jeb.070656

Kim, S. L., and Koch, P. L. (2012). Methods to collect, preserve, and prepare elasmobranch tissues for stable isotope analysis. *Environ. Biol. Fishes* 95, 53–63. doi: 10.1007/s10641-011-9860-9

Kinney, M. J., Hussey, N. E., Fisk, A. T., Tobin, A. J., and Simpfendorfer, C. A. (2011). Communal or competitive? Stable isotope analysis provides evidence of resource partitioning within a communal shark nursery. *Mar. Ecol. Prog. Ser.* 439, 263–276. doi: 10.3354/meps09327

Klimley, A. P., Anderson, S. D., Pyle, P., and Henderson, R. P. (1992). Spatiotemporal patterns of white shark (Carcharodon carcharias) predation at the south Farallon Islands, California. *Copeia* 1992, 680–690. doi: 10.2307/1446143

Koen Alonso, M., Alberto Crespo, E., Aníbal García, N., Noemí Pedraza, S., Ariel Mariotti, P., and Judith Mora, N. (2002). Fishery and ontogenetic driven changes in the diet of the spiny dogfish, *Squalus acanthias*, in Patagonian waters, Argentina. *Environ. Biol. Fishes* 63, 193–202. doi: 10.1023/A:1014229432375

Li, Y., Zhang, Y., Hussey, N. E., and Dai, X. (2016). Urea and lipid extraction treatment effects on δ^{15}N and δ^{13}C values in pelagic sharks. *Rapid Commun. Mass Spectrom.* 30, 1–8. doi: 10.1002/rcm.7396

Logan, J. M., and Lutcavage, M. E. (2010). Stable isotope dynamics in elasmobranch fishes. *Hydrobiologia* 644, 231–244. doi: 10.1007/s10750-010-0120-3

Logan, R. K., White, C. F., Winkler, C., Jorgensen, S. J., O'Sullivan, J. B., Lowe, C. G., et al. (2018). An evaluation of body condition and morphometric relationships within southern California juvenile white sharks *Carcharodon carcharias*. *J. Fish Biol.* 93, 842–849. doi: 10.1111/jfb.13785

Lowe, C. G., Blasius, M. E., Jarvis, E. T., Mason, T. J., Goodmanlowe, G. D., and O'Sullivan, J. B. (2012). "Historic fisheries interactions with white sharks in the southern California Bigh," in *Global Perspectives on the Biology and Life History of the White Shark*, ed. M. L. Domeier (Boca Raton, FL: CRC Press), 169–186.

Lucifora, L. O., García, V. B., and Escalante, A. H. (2009). How can the feeding habits of the sand tiger shark influence the success of conservation programs? *Anim. Conserv.* 12, 291–301. doi: 10.1111/j.1469-1795.2009.00247.x

Malpica-Cruz, L., Herzka, S. Z., Sosa-Nishizaki, O., and Escobedo-Olvera, M. A. (2013). Tissue-specific stable isotope ratios of shortfin mako (*Isurus oxyrinchus*) and white (*Carcharodon carcharias*) sharks as indicators of size-based differences in foraging habitat and trophic level. *Fish. Oceanogr.* 22, 429–445. doi: 10.1111/fog.12034

Malpica-Cruz, L., Herzka, S. Z., Sosa-Nishizaki, O., Lazo, J. P., and Trudel, M. (2012). Tissue-specific isotope trophic discrimination factors and turnover rates in a marine elasmobranch: empirical and modeling results. *Can. J. Fish. Aquat. Sci.* 69, 551–564. doi: 10.1139/f2011-172

Marshall, H. H., Inger, R., Jackson, A. L., McDonald, R. A., Thompson, F. J., and Cant, M. A. (2019). Stable isotopes are quantitative indicators of trophic niche. *Ecol. Lett.* 22, 1990–1992. doi: 10.1111/ele.13374

Matich, P., Kiszka, J. J., Heithaus, M. R., Le Bourg, B., and Mourier, J. (2019). Inter-individual differences in ontogenetic trophic shifts among three marine predators. *Oecologia* 189, 621–636. doi: 10.1007/s00442-019-04357-5

McMahon, K. W., and McCarthy, M. D. (2016). Embracing variability in amino acid δ15N fractionation: mechanisms, implications, and applications for trophic ecology. *Ecosphere* 7, 1–26. doi: 10.1002/ecs2.1511

McMeans, B. C., Olin, J. A., and Benz, G. W. (2009). Stable-isotope comparisons between embryos and mothers of a placentatrophic shark species. *J. Fish Biol.* 75, 2464–2474. doi: 10.1111/j.1095-8649.2009.02402.x

Michener, R. H., and Kaufman, L. (2007). "Stable isotope ratios as tracers in marine food webs: an update," in *Stable Isotopes in Ecology and Environmental Science*, eds R. Michener and K. Lajtha (Oxford, UK: Blackwell Publishing Ltd), 238–282. doi: 10.1002/9780470691854.ch9

Mollet, H. F., and Cailliet, G. M. (2002). Comparative population demography of elasmobranch using life history tables, Leslie matrixes and stage-based models. *Mar. Freshw. Res.* 53, 503–516. doi: 10.1071/MF01083

Moro, S., Jona-Lasinio, G., Block, B., Micheli, F., De Leo, G., Serena, F., et al. (2020). Abundance and distribution of the white shark in the Mediterranean Sea. *Fish Fish.* 21, 338–349. doi: 10.1111/faf.12432

Munroe, S. E. M., Meyer, L., and Heithaus, M. (2018). "Dietary biomarkers in shark foraging and movement ecology," in *Shark Research: Emerging Technologies and Applications for the Field and Laboratory*, eds J. Carrier, M. Heithaus, and C. Simpfendorfer (Boca Raton, FL: CRC Press), 1–24.

Nasby-Lucas, N., Dewar, H., Sosa-Nishizaki, O., Wilson, C., Hyde, J. R., Vetter, R. D., et al. (2019). Movements of electronically tagged shortfin mako sharks (*Isurus oxyrinchus*) in the eastern North Pacific Ocean. *Anim. Biotelemetry* 7, 1–26. doi: 10.1186/s40317-019-0174-6

Nosal, A. P., Cartamil, D. P., Wegner, N. C., Lam, C. H., and Hastings, P. A. (2019). Movement ecology of young-of-the-year blue sharks *Prionace glauca* and shortfin makos *Isurus oxyrinchus* within a putative binational nursery area. *Mar. Ecol. Prog. Ser.* 623, 99–115. doi: 10.3354/meps13021

Nuche-Pascual, M. T., Ruiz-Cooley, R. I., and Herzka, S. (2021). A meta-analysis of amino acid δ15N trophic enrichment factors in fishes relative to nutritional and ecological drivers. *Ecosphere* e03570. doi: 10.1002/ecs2.3570

Ochoa-Díaz, M. R. (2009). *Espectro Trófico Del Tiburón Martillo Sphyrna Zygaena (Linnaeus, 1758) En Baja California Sur: Aplicación De Δ13c Y Δ15n*. Ph.D. thesis. La Paz: Centro Interdisciplinario de Ciencias Marinas.

O'Connell, T. C. (2017). 'Trophic' and 'source' amino acids in trophic estimation: a likely metabolic explanation. *Oecologia* 184, 317–326. doi: 10.1007/s00442-017-3881-9

Olin, J. A., Hussey, N. E., Fritts, M., Heupel, M. R., Simpfendorfer, C. A., Poulakis, G. R., et al. (2011). Maternal meddling in neonatal sharks: implications for interpreting stable isotopes in young animals. *Rapid Commun. Mass Spectrom.* 25, 1008–1016. doi: 10.1002/rcm.4946

Olin, J. A., Shipley, O. N., and McMeans, B. C. (2018). Stable isotope fractionation between maternal and embryo tissues in the bonnethead shark (*Sphyrna tiburo*). *Environ. Biol. Fishes* 101, 489–499. doi: 10.1007/s10641-018-0715-5

Oñate-González, E. C., Rocha-Olivares, A., Saavedra-Sotelo, N. C., and Sosa-Nishizaki, O. (2015). Mitochondrial genetic structure and matrilineal origin of white sharks, *Carcharodon carcharias*, in the northeastern Pacific: implications for their conservation. *J. Hered.* 106, 347–354. doi: 10.1093/jhered/esv034

Oñate-González, E. C., Sosa-Nishizaki, O., Herzka, S. Z., Lowe, C. G., Lyons, K., Santana-Morales, O., et al. (2017). Importance of Bahia Sebastian Vizcaino as a nursery area for white sharks (*Carcharodon carcharias*) in the northeastern Pacific: a fishery dependent analysis. *Fish. Res.* 188, 125–137. doi: 10.1016/j.fishres.2016.12.014

Papastamatiou, Y., Wetherbee, B., Lowe, C., and Crow, G. (2006). Distribution and diet of four species of carcharhinid shark in the Hawaiian Islands: evidence for resource partitioning and competitive exclusion. *Mar. Ecol. Prog. Ser.* 320, 239–251. doi: 10.3354/meps320239

Parnell, A. C. (2016). *simmr: A Stable Isotope Mixing Model*. https://CRAN.R-project.org/package=simmr.

Parnell, A. C., Phillips, D. L., Bearhop, S., Semmens, B. X., Ward, E. J., Moore, J. W., et al. (2013). Bayesian stable isotope mixing models. *Environmetrics* 24, 387–399. doi: 10.1002/env.2221

Peterson, B. J., and Fry, B. (1987). Stable isotopes in ecosystem studies. *Annu. Rev. Ecol. Syst.* 18, 293–320. doi: 10.1016/0198-0254(88)92720-3

Phillips, D. L., Inger, R., Bearhop, S., Jackson, A. L., Moore, J. W., Parnell, A. C., et al. (2014). Best practices for use of stable isotope mixing models in food-web studies. *Can. J. Zool.* 92, 823–835. doi: 10.1139/cjz-2014-0127

Post, D. M. (2002). Using stable isotopes to estimate trophic position: models, methods, and assumptions. *Ecology* 83, 703–718. doi: 10.1890/0012-9658(2002)083[0703:USITET]2.0.CO;2

Preti, A., Soykan, C. U., Dewar, H., Wells, R. J. D., Spear, N., and Kohin, S. (2012). Comparative feeding ecology of shortfin mako, blue and thresher sharks in the California Current. *Environ. Biol. Fishes* 95, 127–146. doi: 10.1007/s10641-012-9980-x

Rochín-Alamillo, A. (2011). *Composición y Abundancia De Elasmobranquios En El Complejo Lagunar San Ignacio, Baja California Sur*. Ph.D. thesis. La Paz: Centro Interdisciplinario de Ciencias Marinas.

Rosales-Casián, J. A. (1996). Ictiofauna de la bahía de San Quintín, Baja California, México, y su costa adyacente. *Cienc. Mar.* 22, 443–458. doi: 10.7773/cm.v22i4.875

Santana-Morales, O., Sosa-Nishizaki, O., Escobedo-Olvera, M., Onate-Gonzalez, E., O'Sullivan, J., and Cartamil, D. (2012). "Incidental catch and ecological observations of juvenile white sharks, *Carcharadon carcharias*, in western Baja california, Mexico. conservation implications," in *Global Perspectives on the Biology and Life History of the White Shark*, ed. M. L. Domeier (Boca Raton, FL: CRC Press), 187–198.

Skomal, G. B., Braun, C. D., Chisholm, J. H., and Thorrold, S. R. (2017). Movements of the white shark *Carcharodon carcharias* in the north Atlantic ocean. *Mar. Ecol. Prog. Ser.* 580, 1–16. doi: 10.3354/meps12306

Smale, M. J. (1991). Occurrence and feeding of three shark species, *Carcharhinus brachyurus*, *Carcharhinus obscurus* and *Sphyrna zygaena*, on the eastern Cape coast of South Africa. *South Afr. J. Mar. Sci.* 11, 31–42. doi: 10.2989/025776191784287808

Tamburin, E., Elorriaga, F. R., Colombo, V., Montaño, E., Madigan, D. J., Sánchez, A., et al. (2020). New insights into the trophic ecology of young white sharks (*Carcharodon carcharias*) in waters off the Baja California Peninsula, Mexico. *Mar. Biol.* 167:55. doi: 10.1007/s00227-020-3660-8

Tamburin, E., Kim, S., Elorriaga-Verplancken, F., Madigan, D., Hoyos-Padilla, M., Sánchez-González, A., et al. (2019). Isotopic niche and resource sharing among young sharks (*Carcharodon carcharias* and *Isurus oxyrinchus*) in Baja California, Mexico. *Mar. Ecol. Prog. Ser.* 613, 107–124. doi: 10.3354/meps12884

Tricas, T. C., and McCosker, J. E. (1984). Predatory behavior of the white shark (*Carcharodon carcharias*), with notes on its biology. *Proc. Calif. Acad. Sci.* 43, 221–238.

Vokhshoori, N. L., Larsen, T., and McCarthy, M. D. (2014). Reconstructing δ13C isoscapes of phytoplankton production in a coastal upwelling system with amino acid isotope values of littoral mussels. *Mar. Ecol. Prog. Ser.* 504, 59–72. doi: 10.3354/meps10746

Weng, K. C., O'Sullivan, J. B., Lowe, C. G., Winkler, C. E., Dewar, H., and Block, B. A. (2007). Movements, behavior and habitat preferences of juvenile white sharks *Carcharodon carcharias* in the eastern Pacific. *Mar. Ecol. Prog. Ser.* 338, 211–224. doi: 10.3354/meps338211

Weng, K. C., Sullivan, J. B. O., Lowe, C. G., Winkler, C. E., Blasius, M. E., Locke-Smith, K. A., et al. (2012). "Back to the wild release of juvenile white sharks from the monterey bay aquarium," in *Global Perspectives on the Biology and Life History of the White Shark*, ed. M. L. Domeier (Boca Raton, FL: CRC Press), 419–446.

White, C. F., Lyons, K., Jorgensen, S. J., O'Sullivan, J., Winkler, C., Weng, K. C., et al. (2019). Quantifying habitat selection and variability in habitat suitability for juvenile white sharks. *PLoS One* 14:e0214642. doi: 10.1371/journal.pone.0214642

Yarnes, C. T., and Herszage, J. (2017). The relative influence of derivatization and normalization procedures on the compound-specific stable isotope analysis of nitrogen in amino acids. *Rapid Commun. Mass Spectrom.* 31, 693–704. doi: 10.1002/rcm.7832

Conflict of Interest: The authors declare that the research was conducted in the absence of any commercial or financial relationships that could be construed as a potential conflict of interest.

frontiers in Marine Science

ORIGINAL RESEARCH
published: 31 August 2021
doi: 10.3389/fmars.2021.697175

Continental-Scale Network Reveals Cross-Jurisdictional Movements of Sympatric Sharks With Implications for Assessment and Management

Charlie Huveneers[1]*, Yuri Niella[2], Michael Drew[1,3], Rory McAuley[4], Paul Butcher[5], Victor Peddemors[6], Daniela Waltrick[7], Chris Dowling[7], Silas Mountford[7], Ian Keay[7] and Matias Braccini[7]

[1] Southern Shark Ecology Group, College of Science and Engineering, Flinders University, Bedford Park, SA, Australia, [2] Department of Biological Sciences, Macquarie University, North Ryde, NSW, Australia, [3] SARDI Aquatic Sciences, West Beach, SA, Australia, [4] School of Biological Sciences, The University of Western Australia, Crawley, WA, Australia, [5] New South Wales Department of Primary Industries, National Marine Science Centre, Coffs Harbour, NSW, Australia, [6] New South Wales Department of Primary Industries, Sydney Institute of Marine Science, Mosman, NSW, Australia, [7] Western Australian Fisheries and Marine Research Laboratories, Department of Primary Industries and Regional Development, Government of Western Australia, North Beach, WA, Australia

OPEN ACCESS

Edited by:
Clive N. Trueman,
University of Southampton,
United Kingdom

Reviewed by:
Nuno Queiroz,
Centro de Investigação em Biodiversidade e Recursos Genéticos (CIBIO-InBIO), Portugal
Karissa Opal Lear,
Murdoch University, Australia

***Correspondence:**
Charlie Huveneers
Charlie.huveneers@flinders.edu.au

Specialty section:
This article was submitted to Marine Megafauna, a section of the journal Frontiers in Marine Science

Received: *19 April 2021*
Accepted: *28 June 2021*
Published: *31 August 2021*

Citation:
Huveneers C, Niella Y, Drew M, McAuley R, Butcher P, Peddemors V, Waltrick D, Dowling C, Mountford S, Keay I and Braccini M (2021) Continental-Scale Network Reveals Cross-Jurisdictional Movements of Sympatric Sharks With Implications for Assessment and Management. Front. Mar. Sci. 8:697175. doi: 10.3389/fmars.2021.697175

Understanding the movement ecology of marine species and connectivity of populations is required for effective fisheries management. This is especially the case for species with wide-ranging distributions for which movement can span across several jurisdictions with different management regulations. We used the Australian national network of acoustic receivers facilitated by the Integrated Marine Observing System (IMOS) to describe the extent and frequency of movements for two large epipelagic shark species, the bronze whaler (*Carcharhinus brachyurus*) and dusky shark (*Carcharhinus obscurus*). A total of 210 sharks (117 bronze whalers and 93 dusky sharks) were tracked for a 10-year period during which 21% and 9% of detected bronze whalers and dusky sharks, respectively, moved between Australian states. Bronze whalers showed more variable inter-state movements, mostly between Western Australia and South Australia but also eastwards to New South Wales (NSW). Although no dusky sharks tagged in Western Australia undertook inter-state movements, ~50% of the sharks tagged in South Australia went to Western Australia. Five of the 14 dusky sharks tagged in NSW (36%) were detected across different states but remained on the east and southeast coasts (Queensland, NSW, Victoria, and Tasmania). The IMOS receivers also detected six bronze whalers in Ningaloo Reef, representing an extension of the previously known Australian distribution. Our findings highlight the value of collaboration between researchers and the value of national infrastructure, by providing a more accurate understanding of inter-state movements. This new information will allow the development of more adequate population dynamic models for stock assessment and management advice, requiring collaboration among state agencies for coordinating research activities, sharing data and resources, and establishing appropriate cross-jurisdictional policies. This is essential to achieve successful management and conservation outcomes for highly migratory species.

Keywords: shark fisheries, acoustic tracking, large-scale movement, dusky shark, bronze whaler, *Carcharhinus obscurus*, *Carcharhinus brachyurus*, fisheries management

INTRODUCTION

Many marine species undertake extensive oceanic and continental-scale movements, which are influenced by a variety of biological and environmental factors, often related to resource needs (e.g., Block et al., 2011; Espinoza et al., 2016). In species exhibiting large-scale movements, local or regional management measures may not provide adequate protection if the species is exploited in other regions. These species are also more likely to move between different jurisdictions, further complicating management and conservation efforts (Heupel et al., 2015). Defining the extent and occurrence of long-range movements is therefore necessary for a comprehensive understanding of a species' spatial ecology and, within a resource management context, for determining the extent of connectivity among stocks and ensuring sustainable resource use (Lascelles et al., 2014). Various approaches have been applied to define movements and connectivity between stocks: genetics (e.g., Junge et al., 2019), body morphology (e.g., Turan, 2004), microchemistry (Izzo et al., 2016; McMillan et al., 2018), parasites (e.g., Barton et al., 2018), and tracking (e.g., Block et al., 2011; Hussey et al., 2015). For fisheries management, there is a need to ensure that stock delineation and connectivity are measured at the same temporal scale at which movements occur, since fisheries management operates at the ecological rather than the evolutionary scale. Genetic methods can struggle to distinguish the degree of connectivity below which separate stock management is required if migration rates are high (Waples et al., 2008), because demographically-independent populations might still be connected genetically over many generations (Ovenden, 2013). Results from tracking studies might therefore be more relevant to fisheries management, in determining whether stocks are demographically-independent units that should be managed separately (Lédée et al., 2021).

There is an increasing number of acoustic tracking networks worldwide, including in North America (Pacific Ocean Shelf Tracking – POST, Florida Acoustic Cooperative Telemetry – FACT, Integrated Tracking of Aquatic Animals – iTag), South Africa (Acoustic Tracking Array Platform – ATAP), and Europe (European Tracking Network – ETN), with most of these large-scale arrays being affiliated to the global Ocean Tracking Network (OTN; O'Dor and Stokesbury, 2009). In Australia, the Integrated Marine Observing System (IMOS) Animal Tracking Facility enables large-scale collaborative animal tracking research through the deployment of continental-scale curtains and grids of IMOS-owned acoustic receivers. The IMOS Animal Tracking Facility network is complemented by a large number of independent, project-based, non-IMOS acoustic receivers that are deployed by individual researchers and research teams to address regional research needs. All IMOS data and the voluntarily supplied detections from non-IMOS receivers are hosted by and publicly accessible through the Australian Ocean Data Network (AODN) and the IMOS Animal Tracking database (Hoenner et al., 2018)[1]. These data enable large-scale studies of animal movements (Heupel et al., 2015), the ability to reveal intra-specific differences in movement profiles and site residency of a wide range of species (Brodie et al., 2018), and to determine how changes in human activity impact animal populations during global disruptions such as the COVID-19 pandemic (Huveneers et al., 2021). The IMOS Animal Tracking Facility provides an opportunity to quantify the extent of movement and connectivity of marine species and determine the most suitable spatial scale for stock assessments and management purposes (Lédée et al., 2021).

The bronze whaler *Carcharhinus brachyurus* and the dusky shark *Carcharhinus obscurus* are globally distributed species which are commercially and recreationally targeted in many parts of their distributions, as well as being taken with other more productive shark species in mixed-species fisheries (see Rogers et al., 2013a; Bradshaw et al., 2018). Bronze whaler and dusky shark have life history traits that make them highly susceptible to overexploitation (e.g., slow growth, late age-at-maturity) (Romine et al., 2009; Rogers et al., 2013a; Drew et al., 2017). At a global level, both species are of conservation concern, with the bronze whaler listed as Vulnerable by the IUCN Red List due to declining population trends over most of its range (Huveneers et al., 2020) and the dusky shark listed as Endangered due to a global population reduction of ∼72% (Rigby et al., 2019; Pacoureau et al., 2021). In Australia, bronze whaler and dusky sharks are commercially targeted in New South Wales (NSW), South Australia (SA), and Western Australia (WA) (Simpfendorfer, 1999; Macbeth et al., 2009; Rogers et al., 2013a). In NSW, mostly adult dusky sharks are caught by longline fisheries (Macbeth et al., 2009; Pleizier et al., 2015; Barnes et al., 2016). Catches in NSW appear to have declined due to management action and reduced fishing effort in recent years. In SA, there are no species-specific regulations managing commercial catches of bronze whalers and dusky sharks. However, these species are managed under input controls, with measures aimed at limiting fishing effort and mortality of large mature individuals. These include limits on the daily number of hooks that can be set (200 hooks), on leader diameter for longlines (2 mm), and mesh size restrictions for demersal gill nets (150 mm). Bronze whalers and dusky sharks (reported

---

[1] animaltracking.aodn.org.au

together as whaler sharks) are considered secondary species, with sustainability of the fishery and stock status assessed using performance indicators. Demographic models suggest that current catch levels of bronze whaler are likely to be sustainable, but that population decline could occur if total catches increase (Bradshaw et al., 2018). However, the need to differentiate the two species remains a key uncertainty in estimating current levels of fishing mortality. The status of the SA whaler shark fishery is therefore classified as undefined (Steer et al., 2020). In WA, due to the rapid increase in shark catches between the mid-1970s and 1990s and other sustainability concerns, a range of management measures have been introduced since the early 1990s (limited entry, effort limits, a maximum size limit, state-wide commercial protection of sharks in most non-target fisheries, prohibition of metal trace wire and large hooks, mesh-size limits in target gillnet fisheries, spatial closures, and recreational bag limits) (Braccini et al., 2021). Weight of evidence assessments are conducted on four indicator species every 5 years, including dusky sharks but not bronze whalers. Stock status of dusky sharks is sustainable – recovering with current management arrangements considered suitable to allow the gradual recovery of the breeding stock from historic overfishing (Braccini et al., 2021). However, dusky shark stock assessment only includes WA catches (Braccini et al., 2021).

Genetic studies have suggested large-scale stock segregation of bronze whalers between Australia–New Zealand, South Africa–Namibia, and Peru (Benavides et al., 2011b), and some delineation within Australia between WA and the rest of the Australian population (Junge et al., 2019). Dusky sharks are currently considered to have an eastern and western stock in Australia, with conventional and electronic tracking showing that dusky sharks move between SA and WA (Rogers et al., 2013b), and genetic analyses suggesting restricted gene flow between eastern and western Australia (Geraghty et al., 2014). However, previous and recent genetic analyses have also proposed panmixia within Australia (Ovenden et al., 2009; Benavides et al., 2011a; Junge et al., 2019). The appropriate spatial scale to assess and manage bronze whaler and dusky shark stocks, and the extent of their movements across each species distribution are still unknown.

We investigated the broad-scale movements and levels of connectivity among bronze whalers and dusky sharks in Australian waters between WA, SA, Victoria (VIC), Tasmania (TAS), NSW, and Queensland (QLD), a spatial scale of 7,300 km, using the network of acoustic receivers facilitated through the IMOS Animal Tracking Facility. We also assessed the benefits of the IMOS Animal Tracking Facility by comparing our ability to detect cross-jurisdictional movements using receivers from the IMOS Animal Tracking Facility (IMOS receivers), community-owned receivers (non-IMOS receivers), or a combination of both. The results from this study provide movement information over spatial and temporal scales relevant to fishery management decisions (Crossin et al., 2017) and insights into the importance of having a continental-scale network of acoustic receivers to support the assessment of species with broad movement patterns for effective fisheries management.

MATERIALS AND METHODS

Shark Tagging and Acoustic Tracking

Sharks were captured using a variety of standard fishing methods including scientific and commercial longlines (NSW, SA, and WA), single hook droplines (WA), and recreational game fishing (SA). Captured individuals were measured to the nearest 1 cm, sexed, and had a V16 acoustic transmitter surgically implanted using established methods. Transmitters were programmed on a pseudo-random repeat rate of 40–80 s (NSW), 50–110 s (SA), or 70–200 s (WA) resulting in battery life ranging 1982–3650 days. Details about fishing and tagging methods can be found in Barnes et al. (2016) for NSW, Drew et al. (2019) for SA, and Braccini et al. (2017, 2018a) for WA.

We examined the broad-scale movements of dusky sharks and bronze whalers through acoustic tracking and the multiple acoustic receiver arrays combined through the IMOS Animal Tracking Facility. To date over 9,735 acoustic receiver deployments have occurred at 1,757 locations around Australia ranging from 113.6°E to 159.3°E and 11.8°S to 43.1°S (Hoenner et al., 2018). Receivers include core IMOS Animal Tracking Facility infrastructure and receiver arrays maintained by independent researchers who contribute data to the IMOS Animal Tracking Facility (**Figure 1**). While the total number of receivers slightly varied across the 10-year study period (2010–2020), receivers were constantly deployed at key locations where bronze whalers and dusky sharks were detected throughout the study period. Further details about the receiver array in SA and WA are provided in Drew et al. (2019) and Braccini et al. (2017, 2018a), respectively.

Data Analysis

The total detection dataset for the two study species was initially filtered to exclude any false detections (Simpfendorfer et al., 2015), identified following the acceptance criteria developed by the manufacturer (Pincock, 2008). All analyses were conducted in the R software (version 4.0.5; R Core Team 2021).

Inter-State Movements, Connectivity, and Seasonality

For each species, we used a Generalized Linear Model (GLM) to assess the effect of tracking time (i.e., number of days from tagging to the last data download) on the likelihood of detecting inter-state movements. We used a binomial distribution to model the presence/absence of inter-state movements as a function of tracking time.

The frequency and directionality of inter-state movements was assessed using connectivity plots. For each shark that undertook at least one inter-state movement, each movement was categorized according to the outgoing (i.e., the last state where a shark was detected previously) and incoming (i.e., the next state where a shark was consecutively detected) nature of the movement. A movement matrix was then created for each species, in which the respective total number of individuals moving from/to each state was included. A circular connectivity

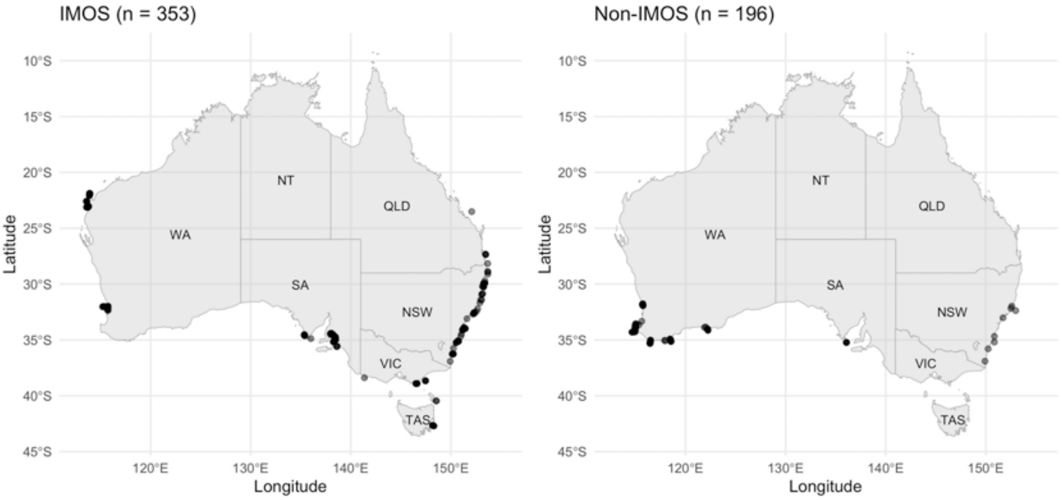

FIGURE 1 | Map of Australia showing the location of **(left)** Integrated Marine Observing System (IMOS) receivers and **(right)** non-IMOS receivers that detected bronze whalers and dusky sharks during the study period.

plot was then used to illustrate the shark species-specific inter-state movements using the circlize R package (Gu et al., 2014).

For each detected individual, the proportion of time spent in each state was calculated by reconstructing trajectories assuming straight line movement between detections. For this, the position between consecutive detections from different receivers was interpolated (avoiding crossing over land) and the amount of time spent between these detections was split proportionally to the distance between the receivers.

Seasonality of inter-state movement was assessed by modeling changes in detection longitude across months, as spatial variation in the study area was mostly longitudinal. The acoustic detection dataset was first standardized to include only a unique daily location per individual, to avoid biases from sharks repeatedly detected by one receiver in a day and to account for differences in detection range between receivers (Huveneers et al., 2016). Generalized Additive Mixed Models (GAMM) were then built for each species using the mgcv R package (Wood and Wood, 2015), including location longitudes as the response variables with Gamma distributions. Model candidate predictors included month as a continuous variable ranging from 1 (January) to 12 (December) with a cyclic-cubic regression spline, and the dimensions of the basis used for the smoothing term (k) kept to a value of five to avoid model overfitting. Shark ID was included as a random effect to account for inter-individual variation. Year was not tested as a candidate variable in the models as most sharks from both species were tracked for a small number of years. The effects of size or maturity on movements were not assessed due to the small size ranges of tagged sharks and insufficient numbers of mature sharks. Final models (Longitude $\sim$ Month $+$ Shark ID) were visually inspected for a normal residual distribution.

Benefits of IMOS Animal Tracking Facility

A randomization test (1,000 random samples simulations) was done to assess the benefits of the IMOS Animal Tracking Facility, by comparing our ability to detect inter-state movements depending on the group of receivers used: (i) exclusively IMOS receivers, (ii) exclusively non-IMOS receivers, and (iii) combining both receiver types. For each tagged individual, inter-state movement was considered to have occurred if the shark was detected for at least 1 day in a different state from where it was tagged. In each iteration, performed with replacement, 50% of all tagged sharks (i.e., including individuals detected only within the state where they were tagged and those detected also in a different state) were selected randomly for bronze whalers (N = 58) and dusky sharks (N = 46), and the percentage of individuals moving inter-state calculated. Analysis of variance (ANOVA) and Tukey *post hoc* tests were used to investigate differences among receiver groups.

RESULTS

A total of 210 sharks (117 bronze whalers and 93 dusky sharks) were tagged between 31 January 2010 and 19 October 2016 in NSW, SA, and WA (**Table 1**) and tracked until 5 November 2020. Based on known size-at-maturity (Last and Stevens, 2009; Drew et al., 2017), most tagged bronze whalers (mean ± standard deviation: 200.9 ± 86.3 cm total length) and dusky sharks (279.9 ± 60.7 cm total length) were immature. Similar numbers of bronze whalers were tagged in WA (51.3%; N = 60) and SA (48.7%; N = 57), whereas most dusky sharks were tagged in WA (75.3%; N = 70) (**Table 1**). From all sharks tagged, 112 (95.7%) bronze whalers and 92 (98.9%) dusky sharks were detected for at least 1 day during the monitoring period. For these sharks, bronze whalers (4,819 ± 19,750 detections/individual) were detected between 3 and 3,127 days (mean = 577.2 ± 801.6 days), whereas dusky sharks (327 ± 551 detections/individual) were detected between 1 and 2,730 days (mean = 539.1 ± 734.9 days).

TABLE 1 | Summary of bronze whalers and dusky sharks tagged in Western Australia (WA) and South Australia (SA), and monitored throughout southern Australia.

Species	Sex	Number tagged in WA	Number tagged in SA	Number tagged in NSW	Total length (cm) ± standard deviation	Mean tracking (days) ± standard deviation
Bronze whaler	Female	44	31	–	213.7 ± 83.3	1227.8 ± 754.5
	Male	16	23	–	175.5 ± 54.4	1049.7 ± 838.3
	Unknown	–	3	–	–	557.0 ± 523.4
	Total	60	57	–	200.9 ± 86.3	1151.5 ± 783.0
Dusky shark	Female	45	4	7	293.4 ± 61.3	953.3 ± 666.7
	Male	24	5	6	266.5 ± 56.1	1247.9 ± 711.5
	Unknown	1	–	1	246.5 ± 125.2	1550.4 ± 1581.8
	Total	70	9	14	279.9 ± 60.7	1075.2 ± 710.6

Tracking days represent period between date of tagging and last detection.

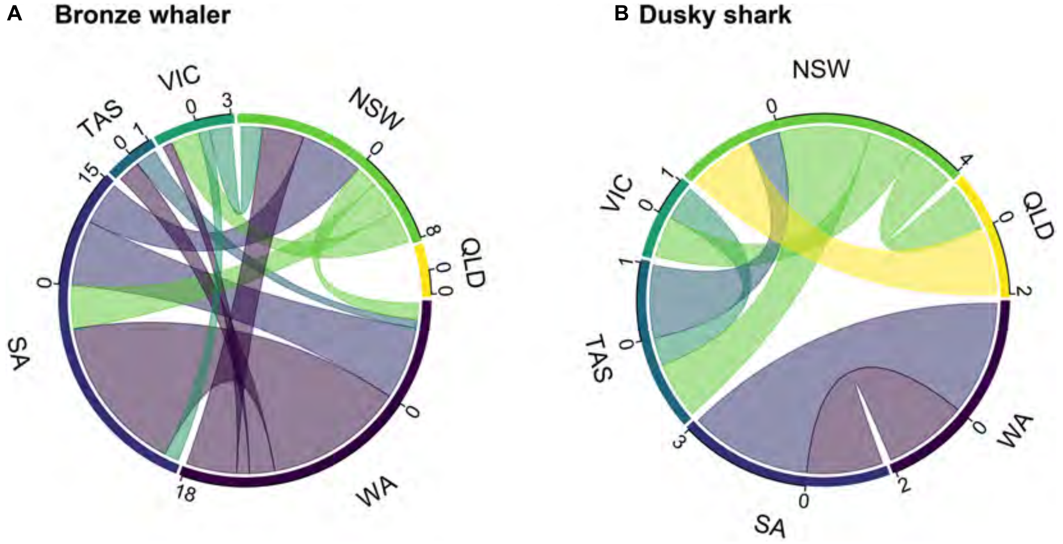

FIGURE 2 | Connectivity plots of **(A)** bronze whalers and **(B)** dusky sharks, showing the number and direction of outgoing movements (numbers = observed inter-state movements) from each state (color scale; WA, Western Australia; SA, South Australia; TAS, Tasmania; VIC, Victoria; NSW, New South Wales; and QLD, Queensland).

Inter-State Movements, Connectivity, and Seasonality

Tracking time had no significant effect on the likelihood of detecting inter-state movements for either dusky sharks (GLM; *p*-value = 0.484) or bronze whalers (GLM; *p*-value = 0.181). Of the 117 bronze whalers and 93 dusky sharks tagged, 25 (21.4%) bronze whalers (seven tagged in SA and 18 in WA) and eight (8.6%) dusky sharks (three tagged in SA and five tagged in NSW) showed inter-state movements. Most of the inter-state movements of the SA-tagged bronze whalers were to the east coast (five out of seven), with only three SA-tagged bronze whalers detected in WA. All but three of the 18 WA-tagged bronze whalers showing inter-state movements were detected in SA, with seven also detected on the east coast (VIC, TAS, NSW; **Figure 2A**). No Bronze whalers were detected in QLD (**Figure 2A**). Dusky shark movements were more clearly limited to southwest (SA, WA) and east/southeast (QLD, NSW, VIC, TAS) coasts (**Figure 2B**). Most bronze whalers tagged in WA spent most of their time within WA, whereas two sharks spent most time in SA and two in NSW (**Figure 3A**). While most individuals tagged in SA (four) resided in SA, two bronze whalers spent most of their time in NSW, and one spent most of its time in WA (**Figure 3A**). All SA-tagged dusky sharks spent >50% of their time in WA (**Figure 3B**). For NSW-tagged dusky sharks, five individuals moved inter-state; two moved northwards to QLD and three moved southwards to TAS (**Figure 3B**).

While the movements of bronze whalers and dusky sharks were influenced by month, there was high inter-individual variation for both species, with Shark ID explaining a great proportion of the deviance (**Table 2**). The relative amount of deviance varied between species, with shark ID explaining more deviance than month for bronze whalers (85.2 vs. 3.4%), but the opposite occurring in dusky sharks (15.0 vs. 62.5%). Trends and seasonality of bronze whaler movements across states were not clear, with bronze whalers being detected for most of the year in WA and SA, and across winter, spring, and summer in VIC and NSW (**Figure 4A**). A slight trend of bronze whalers moving away from WA between February and July was also

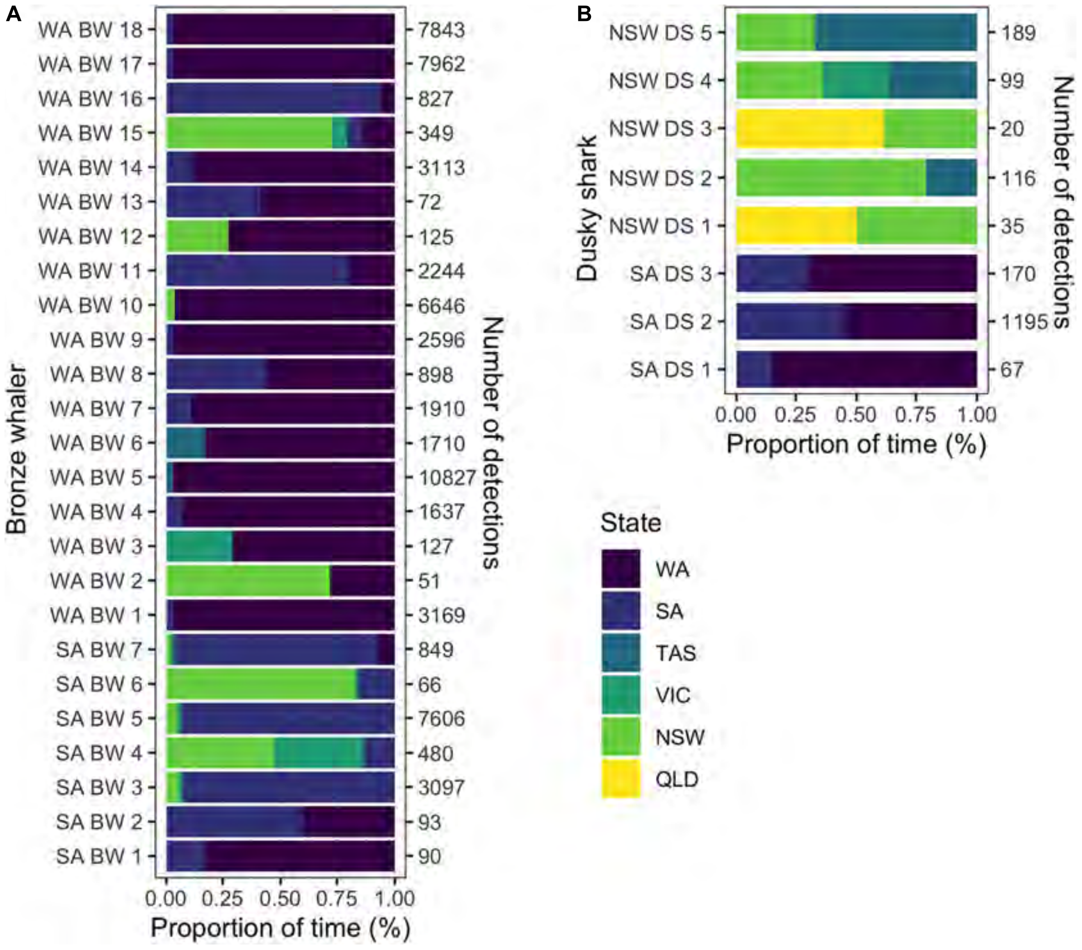

FIGURE 3 | Proportions of time spent by **(A)** bronze whalers and **(B)** dusky sharks in each state (color scale: WA, Western Australia; SA, South Australia; VIC, Victoria; and NSW, New South Wales) for the individuals detected at multiple states. Naming legend is composed by the state where the individual was tagged (SA, South Australia; WA, Western Australia), species (BW, bronze whaler; DS, dusky shark) and shark number.

observed (**Figure 4A** and **Table 2**). A clearer seasonal trend was observed in the movement patterns of dusky sharks, with individuals tending to move into SA waters during the austral summer (December–February) and into WA in winter–spring (July–October) (**Figure 4B** and **Table 2**).

Benefits of IMOS Animal Tracking Facility

The randomization analysis indicated that the number of random sharks to show inter-state movements varied significantly for bronze whalers (ANOVA; F-value = 7038, p-value < 0.001) and dusky sharks (ANOVA; F-value = 3010, p-value < 0.001) depending on what receiver group was used. Significantly lower numbers of bronze whalers undertaking inter-state movements were observed with non-IMOS receivers compared to IMOS receivers alone, while higher numbers of sharks were found to move between states when the two receiver types were combined (**Figure 5A**). For dusky sharks, no inter-state movements were recorded when only non-IMOS receivers were used, whereas the IMOS and all-receiver groups identified similar numbers of sharks moving between states (**Figure 5B**).

DISCUSSION

Our study shows that 25 out of 117 tagged bronze whalers (21.4%) and eight out of 93 tagged dusky sharks (8.6%) showed inter-state movements, with bronze whaler showing more complex and frequent inter-state movements than dusky shark. For bronze whaler, inter-state movements occurred among all five of the southern states, whereas SA- and WA-tagged dusky sharks only moved between WA and SA, and NSW-tagged dusky sharks remained on the east and southeast coasts. While the number of tagged individuals moving among jurisdictions is relatively low, our findings highlight the wide-ranging nature of these two shark species, which needs to be considered in future stock assessments.

For dusky shark, although 8.6% of all tagged individuals undertook inter-state movements, ∼50% of dusky sharks tagged in SA went to WA. Similarly, a previous study found that all satellite-tracked dusky sharks tagged in SA went to WA (Rogers et al., 2013b). While the number of dusky sharks tagged in SA is small (seven dusky sharks tagged with acoustic tags – this study; three dusky sharks tagged with pop-up satellite

TABLE 2 | Generalized Additive Mixed Models (GAMM) of longitude variation as a function of month for bronze whaler and dusky shark including shark identification number (Shark ID) as random effects.

Species	Variable	Edf.	Ref.df.	*F*	*p*	Dev.exp.
Bronze whaler	Month	2.93	3.00	376725	<0.001	3.4%
	Shark ID	19.97	20.00	3114	<0.001	85.2%
Dusky shark	Month	2.66	3.00	1297	<0.001	62.5%
	Shark ID	1.64	2.00	6.22	<0.001	15.0%

Included are the effective degrees of freedom (Edf.), reference degrees of freedom (Ref.df.), F-statistics (F), p-value (p), and percentage of deviance explained (Dev.exp.) of each variable.

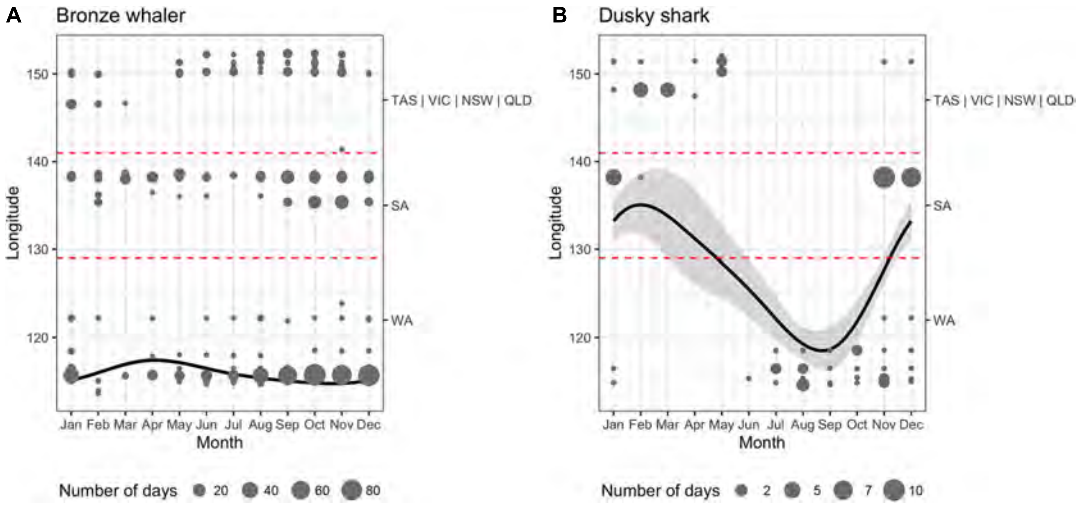

FIGURE 4 | Generalized Additive Mixed Models (GAMM) of longitude variation as a function of month for all tagged **(A)** bronze whaler and **(B)** dusky sharks. Shaded areas, points, and dashed lines, respectively, represent the 95% confidence intervals, the raw location data weighted by the number of days detected in each station (point size), and the longitudinal boundaries between states (WA, Western Australia; SA, South Australia; VIC, Victoria; and NSW, New South Wales).

tags – Rogers et al., 2013b), the high percentage of dusky sharks tagged in SA going to WA [50% of the ten tagged dusky sharks across Rogers et al. (2013b) and our study] provides evidence of connectivity between the two states. Previous studies reporting movements from conventional tags also show that 3% of recaptured dusky sharks tagged in WA (2,470 dusky sharks tagged since 1994 and 473 recaptures) were recaptured in SA (Bartes et al., unpublished data). The low percentage of WA-tagged dusky sharks moving into SA, higher percentage of SA-tagged sharks moving into WA and the species' preference for tropical to warm temperate habitats (Last and Stevens, 2009; Rigby et al., 2019) suggest that dusky shark distribution in this region is likely centered around WA. Small numbers of individuals may occasionally move toward SA when conditions are suitable, such as increased water temperatures during the austral summer (Rogers et al., 2013b). Dusky sharks tagged in NSW showed inter-state movements, but were constrained to eastern Australia, similar to the movements of dusky sharks tagged with pop-up satellite tags in northern NSW (Barnes et al., 2016).

Our findings showing dusky shark movements within, but not between the southwest and east coasts support the separated population structure suggested by Geraghty et al. (2014), with two separated populations in the east and west coasts. These findings challenge the hypothesis of panmixia within Australia proposed by other genetic studies (Ovenden et al., 2009; Benavides et al., 2011a; Junge et al., 2019). While it is possible that some connectivity occurs through northern Australia, this could not be determined in our study due to the limited number of receivers deployed in far north WA and Northern Territory. Bass Strait has previously been identified as a provincial zoogeographic boundary and a region of significant clustering of breaks (Dawson, 2005), with several marine species showing genetic divergences in the vicinity of this region (e.g., white shark, *Carcharodon carcharias*; Blower et al., 2012; sawsharks, *Pristiophorus* spp.; Nevatte et al., 2021). Such divergence is likely related to the historical total barrier to gene flow during the late Pliocene, when periods of cold climate and low sea-level segregated warm temperate organisms east or west of the emergent Bassian Isthmus resulting in population divergence and speciation (Waters, 2008). During subsequent periods of warmer and higher seas, sister taxa expanded into the Bass Strait region leading to weakly correlated phylogeographic and biogeographic patterns, with gene flow across Bass Strait hindered by modern oceanographic conditions creating a barrier to dispersal (Dawson, 2005). The panmixia reported in previous studies might have been facilitated by the movements of a small number of individuals (Lowe and Allendorf, 2010) and reflects

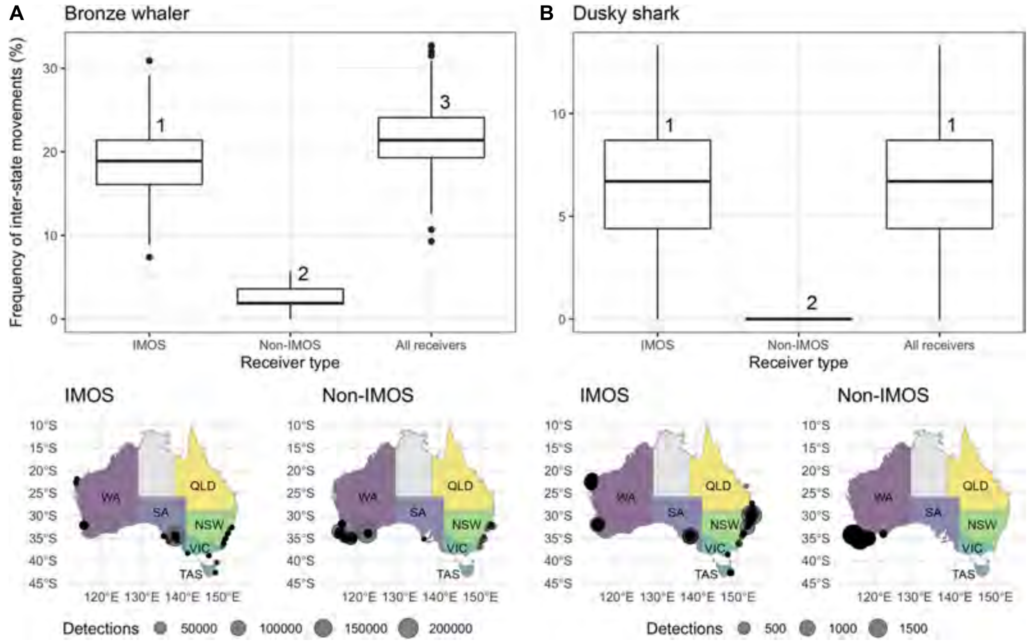

FIGURE 5 | Top panel: Simulation results of frequency distributions of inter-state movements recorded for **(A)** bronze whalers and **(B)** dusky sharks using receivers from IMOS, non-IMOS, and a combination of both (All receivers). Numbers above boxes represent the significantly different groups according to the Tukey *post hoc* test. Bottom panel: Acoustic detections of **(A)** bronze whalers and **(B)** dusky sharks by receiver type (IMOS vs. non-IMOS).

the broad connectivity of populations that might occur over multiple generations (i.e., at the evolutionary scale). While this information is valuable for understanding species behavior and evolution, it is less relevant for stock assessment and management advice (Kerr et al., 2016). In situations when genetic analyses suggest panmixia, demographic independence can still occur, leading to discrete stocks that should be modeled and assessed separately (Braccini et al., 2016).

In the case of bronze whalers, acoustic tracking suggests that bronze whalers in southwest Australia represent a single population with complex movements; a WA component that frequents SA and sometimes venture into NSW and a SA component more likely to move eastwards to NSW through VIC. The SA-tagged sharks were also less likely to spend time in WA. This movement from WA and SA to eastern Australia somewhat contrasts with the movement of dusky shark and other large marine predators, i.e., white sharks, where Bass Strait delineates east and west coast stocks. A separation of the WA bronze whalers from the rest of Australia was suggested by Junge et al. (2019), but is not supported by our findings as 18 of the WA-tagged sharks (23%) moved inter-state, including seven bronze whalers detected in VIC, TAS, and NSW. Overall, bronze whalers show significant connectivity between WA, SA, and NSW. As SA is at the center of the bronze whaler distribution, it is likely playing a central part in this single Australia-wide population.

Seasonal movements varied between species, with dusky sharks showing considerably more defined seasonal inter-state movement patterns than bronze whalers. Dusky shark movements matched the previously identified migration westward and across the Great Australian Bight to WA during autumn (Rogers et al., 2013b). In WA, adult dusky sharks occurring north of Perth have a high chance of moving south during the Austral summer, while dusky sharks south of Perth are more likely to move north during the Austral winter (Braccini et al., 2018a). Similarly, dusky shark movements on the east coast support previously reported short-term movements obtained via pop-up satellite tags (Barnes et al., 2016). Large-scale seasonal migrations of dusky sharks are common globally, including in South Africa (Hussey et al., 2009), Western Atlantic Ocean (Kohler et al., 1998; Bangley et al., 2020), and Gulf of Mexico (Hoffmayer et al., 2014). The long battery life of acoustic tags lasting multiple years, however, enabled us to identify consistent occurrence and timing of inter-state movements between SA and WA from individual dusky sharks not previously recorded. Previous studies have also highlighted a strong seasonal occurrence of bronze whalers in inshore waters and migrations likely driven by water temperature and availability of resources (Lucifora et al., 2005; Dudley and Cliff, 2010; Drew et al., 2019). In southern Australia, bronze whalers migrate inside the South Australian gulfs in spring to early autumn (September–April), which coincides with seasonally warm gulf water temperatures (Drew et al., 2019). Additionally, departure from the gulfs in late autumn (May–June) was observed by all bronze whalers tagged with pop-up tags and tracked for more than 60 days (five out of 10 tagged sharks), coinciding with the cooling off gulf and inshore coastal water temperatures (Drew unpublished data). Yet, bronze whalers can be found in the South Australian gulfs throughout winter (Drew et al., 2019), showing that they can withstand the 11°C water temperature during mid-winter (July–August) (Petrusevics, 1993). The lack of consistency in bronze whaler seasonal migrations between SA and WA observed in this study does not support the seasonal migration of bronze whalers outside the SA gulfs identified previously (Drew et al., 2019). However, the same study also shows that some bronze whalers remain in the gulfs throughout winter, highlighting a considerable degree of individual variation in movement patterns (as shown by Shark ID explaining more deviance than month).

Bronze whalers were previously known to occur throughout southern Australia from Geraldton (WA) across to Coffs Harbour (NSW) (Last and Stevens, 2009; Huveneers et al., 2020). The IMOS receivers detected six bronze whalers in Ningaloo Reef, representing an extension of the known western Australian distribution toward tropical waters and to lower latitudes compared to eastern Australia. While the species is considered to be cosmopolitan in warm temperate and some tropical areas, these detections off Ningaloo Reef are the most northern records of a bronze whaler within tropical waters in Australia.

Implications to Fisheries Management

The spatial extent of stock assessments should reflect biological population distributions, but this is challenging, particularly for marine species that exhibit large-scale movements such as bronze whaler and dusky shark, as individuals can move over large areas not constrained by jurisdictional boundaries. In Australia, despite fisheries agencies recognizing dusky shark as having two separate populations (eastern and western stocks; Woodhams et al., 2021) and bronze whalers as having one Australia-wide stock (Rogers et al., 2021), both species are assessed and managed as single unit stocks within the jurisdictions of each estate (e.g., Braccini et al., 2018b; Bradshaw et al., 2018; Steer et al., 2020). Evidence generated by our study, together with previously collected genetic and movement information, support that bronze whalers form a single biological stock spanning from WA to NSW, whereas dusky sharks form two biological stocks, a western stock (WA–SA) and an eastern stock (VIC–NSW). In WA, demographic analysis has identified the need to protect large juveniles and adults from fishing mortality to ensure population persistence (McAuley et al., 2007). Despite harvesting only small juveniles in WA at levels deemed sustainable, unknown sources of mortality in older sharks such as through the SA fishery (Rogers et al., 2013a) may affect abundance and recruitment in WA. Because there are no restrictions on the age- or size-class of sharks that can be fished in SA, it is probable that the SA whaler shark fishery is contributing to overall mortality of the population. Since our findings provide evidence of movements between SA and WA, it is recommended that SA catches of whaler sharks are reported at the species level and that SA dusky shark catch information is shared with WA so that they can be incorporated in future stock assessments. In the case of bronze whalers, while current catch levels are likely to be sustainable, demographic models suggest that population decline could occur if total catches increase (Bradshaw et al., 2018). It is therefore important for all jurisdictions to share information about bronze whaler catches so that any increase in catches can be identified and that the overall stock status can be monitored and assessed. Our study contributes to improving the delineation of the appropriate spatial scale for assessing and managing the bronze whaler and dusky shark stocks in Australia. This information will allow the development of more adequate population dynamic models for stock assessment and management advice, requiring collaboration among state agencies for coordinating research activities, sharing data and resources, and establishing appropriate cross-jurisdictional policies. This is essential to achieve successful management and conservation outcomes for highly migratory species (Lascelles et al., 2014).

Benefits of IMOS Animal Tracking Facility

The IMOS Animal Tracking Facility enabled a more accurate detection of inter-state movements than receivers deployed by independent research groups in two ways: (1) in the case of dusky shark, the IMOS receivers detected inter-state movements which were not detected by non-IMOS receivers; and (2) in the case of bronze whaler, the use of non-IMOS receivers detected less than half of the inter-state movements compared to both types of receivers combined, underestimating the actual amount of inter-state movements. Such discrepancy between receiver types is likely to be a function of the different receiver array designs, their disparate intended purposes, and the relative location of IMOS and non-IMOS receivers in each jurisdiction. IMOS receivers are mostly deployed as cross-shelf curtains designed to record large-scale movements (Steckenreuter et al., 2017), while non-IMOS receivers are typically deployed as a grid or specific location targeting a small number of species (except for WA, see McAuley et al., 2017). IMOS receivers also have a broad geographic footprint with the only detections in northern WA, TAS, or QLD being on IMOS receivers. While non-IMOS receivers might also be deployed in these areas, they either did not detect the sharks included in this study or detections were not uploaded to the IMOS database. Overall, this analysis highlights the benefits of the IMOS receiver network and importance of a national database, such as the IMOS Animal Tracking database (Hoenner et al., 2018), in providing animal movement data suitable for development of data-driven management scenarios.

There are inherent limitations to using acoustic tracking and receivers to estimate cross-jurisdictional movements. Acoustic receivers can have variable detection ranges, influenced by a variety of factors including transmitter power output, biofouling, ambient noise, and environmental conditions (Kessel et al., 2014; Huveneers et al., 2016). The ability to detect inter-state movement will also be affected by the acoustic coverage as infrastructure deployments vary in space and time, and logistic limitations can restrict deployments of receivers in remote locations. For example, a small number of receivers were deployed in far north WA and Northern Territory (NT) during the study period, with most of these receivers located in rivers or estuarine environments. This limited the ability to record dusky sharks in the northern part of their distribution.

Conclusion

Determining the movement patterns of mobile species and identifying stock delineation at the ecological scale rather than evolutionary scale is critical for adequate fisheries management.

Our findings showed that while a small number of bronze whalers and dusky sharks undertook cross-jurisdictional movements, these are sufficient to refine our understanding of the stock structure of these two species and to challenge some of the previous findings based on genetic analyses. Our study also highlighted the benefit of having a national network of acoustic receivers facilitated by an overarching initiative and revealed that bronze whalers occur further north than previously thought. Further use of the data available through the IMOS Animal Tracking facility will likely enable similar discoveries and will help delineating stock structure in other wide-ranging species (Lédée et al., 2021).

DATA AVAILABILITY STATEMENT

Publicly available datasets were analyzed in this study. This data can be found here: https://animaltracking.aodn.org.au/.

ETHICS STATEMENT

The animal study was reviewed and approved by the Flinders University Animal Ethics Committee (ethics approval #E360) and NSW DPI Animal Care and Ethics Committee (Ref. 12/19).

AUTHOR CONTRIBUTIONS

CH, MD, RM, and MB conceived the study. YN, MB, and CH analyzed the data and wrote the manuscript. All authors contributed to the fieldwork and data management, and edited and approved the manuscript.

FUNDING

Funding was provided through an Australian Research Council Linkage Project grant (LP120100652), the Fisheries Research and Development Corporation (FRDC grant numbers 2010/003, 2010/062, and 2012/020) on behalf of the Australian Government, the Adelaide and Mount Lofty Ranges Natural Resources Management Board, the Neiser Foundation, the Nature Foundation of South Australia Inc., and the Tracking Research for Animal Conservation Society (TRACS). Financial support to YN through an International Macquarie University Research Training Program scholarship is deeply acknowledged.

ACKNOWLEDGMENTS

The data was sourced from the Ocean Tracking Network project (http://oceantrackingnetwork.org) and from Australia's Integrated Marine Observing System (IMOS) – IMOS is enabled by the National Collaborative Research Infrastructure Strategy (NCRIS). It is operated by a consortium of institutions as an unincorporated joint venture, with the University of Tasmania as Lead Agent. We thank scientists for uploading receiver detections on the IMOS acoustic tracking database, enabling to access detections from these sharks beyond our specific projects.

REFERENCES

Bangley, C. W., Curtis, T. H., Secor, D. H., Latour, R. J., and Ogburn, M. B. (2020). Identifying important juvenile Dusky Shark habitat in the northwest Atlantic Ocean using acoustic telemetry and spatial modeling. *Mar. Coastal Fish.* 12, 348–363. doi: 10.1002/mcf2.10120

Barnes, C. J., Butcher, P. A., Macbeth, W. G., Mandelman, J. W., Smith, S. D., and Peddemors, V. M. (2016). Movements and mortality of two commercially exploited carcharhinid sharks following longline capture and release off eastern Australia. *Endang. Species Res.* 30, 193–208. doi: 10.3354/esr00730

Barton, D. P., Taillebois, L., Taylor, J., Crook, D. A., Saunders, T., Hearnden, M., et al. (2018). Stock structure of Lethrinus laticaudis (Lethrinidae) across northern Australia determined using genetics, otolith microchemistry and parasite assemblage composition. *Mar. Freshwater Res.* 69, 487–501. doi: 10.1071/mf17087

Benavides, M. T., Horn, R. L., Feldheim, K. A., Shivji, M. S., Clarke, S. C., Wintner, S., et al. (2011a). Global phylogeography of the dusky shark Carcharhinus obscurus: implications for fisheries management and monitoring the shark fin trade. *Endang. Species Res.* 14, 13–22. doi: 10.3354/esr00337

Benavides, M. T., Feldheim, F., Duffy, C., Wintner, S., Braccini, M., Boomer, J., et al. (2011b). Phylogeography of the copper shark (*Carcharhinus brachyurus*) in the southern hemisphere: implications for the conservation of a coastal apex predator. *Mar. Freshwater Res.* 62, 861–869. doi: 10.1071/mf10236

Block, B. A., Jonsen, I. D., Jorgensen, S. J., Winship, A. J., Shaffer, S. A., Bograd, S. J., et al. (2011). Tracking apex marine predator movements in a dynamic ocean. *Nature* 475, 86–90. doi: 10.1038/nature10082

Blower, D. C., Pandolfi, J. M., Bruce, B. D., Gomez-Cabrera, M. C., and Ovenden, J. R. (2012). Australian white shark population genetics reveals fine scale population structure, transoceanic dispersal events and low effective population sizes. *Mar. Ecol. Prog. Series* 455, 229–244. doi: 10.3354/meps09659

Braccini, M., Aires-da-Silva, A., and Taylor, I. (2016). Incorporating movement in the modelling of shark and ray population dynamics: approaches and management implications. *Rev. Fish Biol. Fish.* 26, 13–24. doi: 10.1007/s11160-015-9406-x

Braccini, M., de Lestang, S., and McAuley, R. (2018a). Dusky sharks (Carcharhinus obscurus) undertake large-scale migrations between tropical and temperate ecosystems. *Can. J. Fish. Aquat. Sci.* 75, 1525–1533. doi: 10.1139/cjfas-2017-0313

Braccini, M., Hesp, A., and Molony, B. (2021). Risk-based weight of evidence assessment of commercial sharks in western Australia. *Ocean Coastal Manag.* 205:105501. doi: 10.1016/j.ocecoaman.2020.105501

Braccini, M., Johnson, G., Woodhams, J., Rogers, P., and Peddemors, P. (2018b). *Dusky shark, Carcharhinus obscurus* in *Status of Australian Fish Stocks Reports*. Canberra: Fisheries Research & Development Corporation.

Braccini, M., Rensing, K., Langlois, T., and McAuley, R. (2017). Acoustic monitoring reveals the broad-scale movements of commercially important sharks. *Mar. Ecol. Prog. Series* 577, 121–129. doi: 10.3354/meps12251

Bradshaw, C., Prowse, T., Drew, M., Gillanders, B., Donnellan, S., and Huveneers, C. (2018). Predicting sustainable shark harvests when stock assessments are lacking. *ICES J. Mar. Sci.* 75, 1591–1601. doi: 10.1093/icesjms/fsy031

Brodie, S., Lédée, E. J. I., Heupel, M. R., Babcock, R. C., Campbell, H. A., Gledhill, D. C., et al. (2018). Continental-scale animal tracking reveals functional movement classes across marine taxa. *Sci. Rep.* 8:3717. doi: 10.1038/s41598-018-21988-5

Crossin, G. T., Heupel, M. R., Holbrook, C. M., Hussey, N. E., Lowerre−Barbieri, S. K., Nguyen, V. M., et al. (2017). Acoustic telemetry and fisheries management. *Ecol. Appl.* 27, 1031–1049.

Dawson, M. N. (2005). Incipient speciation of Catostylus mosaicus (Scyphozoa, Rhizostomeae, Catostylidae), comparative phylogeography and biogeography in south-east Australia. *J. Biogeogr.* 32, 515–533. doi: 10.1111/j.1365-2699.2004.01193.x

Drew, M., Rogers, P., and Huveneers, C. (2017). Slow life-history traits of a neritic predator, the bronze whaler (Carcharhinus brachyurus). *Mar. Freshwater Res.* 68, 461–472. doi: 10.1071/mf15399

Drew, M., Rogers, P., Lloyd, M., and Huveneers, C. (2019). Seasonal occurrence and site fidelity of juvenile bronze whalers (Carcharhinus brachyurus) in a temperate inverse estuary. *Mar. Biol.* 166, 1–17.

Dudley, S. F., and Cliff, G. (2010). Influence of the annual sardine run on catches of large sharks in the protective gillnets off KwaZulu-Natal, South Africa, and the occurrence of sardine in shark diet. *Afr. J. Mar. Sci.* 32, 383–397. doi: 10.2989/1814232x.2010.502641

Espinoza, M., Heupel, M. R., Tobin, A. J., and Simpfendorfer, C. A. (2016). Evidence of partial migration in a large coastal predator: opportunistic foraging and reproduction as key drivers? *PLoS One* 11:e0147608. doi: 10.1371/journal.pone.0147608

Geraghty, P. T., Williamson, J. E., Macbeth, W. G., Blower, D. C., Morgan, J. A., Johnson, G., et al. (2014). Genetic structure and diversity of two highly vulnerable carcharhinids in Australian waters. *Endang. Species Res.* 24, 45–60. doi: 10.3354/esr00580

Gu, Z., Gu, L., Eils, R., Schlesner, M., and Brors, B. (2014). circlize implements and enhances circular visualization in R. *Bioinformatics* 30, 2811–2812. doi: 10.1093/bioinformatics/btu393

Heupel, M. R., Simpfendorfer, C. A., Espinoza, M., Smoothey, A. F., Tobin, A., and Peddemors, V. (2015). Conservation challenges of sharks with continental scale migrations. *Front. Mar. Sci.* 2:12. doi: doi: 10.3389/fmars.2015.00012

Hoenner, X., Huveneers, C., Steckenreuter, A., Simpfendorfer, C., Tattersall, K., Jaine, F., et al. (2018). Australia's continental-scale acoustic tracking database and its automated quality control process. *Sci. Data* 5:170206. doi: 10.1038/sdata.2017.206

Hoffmayer, E. R., Franks, J. S., Driggers, W. B., McKinney, J. A., Hendon, J. M., and Quattro, J. M. (2014). Habitat, movements and environmental preferences of dusky sharks. Carcharhinus obscurus, in the northern Gulf of Mexico. *Mar. Biol.* 161, 911–924. doi: 10.1007/s00227-014-2391-0

Hussey, N. E., Kessel, S. T., Aarestrup, K., Cooke, S. J., Cowley, P. D., Fisk, A. T., et al. (2015). Aquatic animal telemetry: A panoramic window into the underwater world. *Science* 348:1255642. doi: 10.1126/science.1255642

Hussey, N., McCarthy, I., Dudley, S. F. J., and Mann, B. (2009). Nursery grounds, movement patterns and growth rates of dusky sharks. Carcharhinus obscurus: a long-term tag and release study in South African waters. *Mar. Freshwater Res.* 60, 571–583. doi: 10.1071/mf08280

Huveneers, C., Jaine, F. R. A., Barnett, A., Butcher, P. A., Clarke, T. M., Currey-Randall, L. M., et al. (2021). The power of national acoustic tracking networks to assess the impacts of human activity on marine organisms during the COVID-19 pandemic. *Biol. Conservat.* 2021:108995. doi: 10.1016/j.biocon.2021.108995

Huveneers, C., Rigby, C. L., Dicken, M., Pacoureau, N., and Derrick, D. (2020). *Carcharhinus brachyurus. The IUCN Red List of Threatened Species* e.T41741A2954522. Gland: International Union for Conservation of Nature, doi: 10.2305/IUCN.UK.2020-3.RLTS.T41741A2954522.en

Huveneers, C., Simpfendorfer, C. A., Kim, S., Semmens, J. M., Hobday, A. J., Pederson, H., et al. (2016). The influence of environmental parameters on the performance and detection range of acoustic receivers. *Methods Ecol. Evol.* 7, 825–835. doi: 10.1111/2041-210x.12520

Izzo, C., Huveneers, C., Drew, M., Bradshaw, C. J., Donnellan, S. C., and Gillanders, B. M. (2016). Vertebral chemistry demonstrates movement and population structure of bronze whaler. *Mar. Ecol. Prog. Series* 556, 195–207. doi: 10.3354/meps11840

Junge, C., Donnellan, S. C., Huveneers, C., Bradshaw, C. J., Simon, A., Drew, M., et al. (2019). Comparative population genomics confirms little population structure in two commercially targeted carcharhinid sharks. *Mar. Biol.* 166:16.

Kerr, L. A., Hintzen, N. T., Cadrin, S. X., Clausen, L. W., Dickey-Collas, M., Goethel, D. R., et al. (2016). Lessons learned from practical approaches to reconcile mismatches between biological population structure and stock units of marine fish. *ICES J. Mar. Sci.* 74, 1708–1722. doi: 10.1093/icesjms/fsw188

Kessel, S., Cooke, S., Heupel, M., Hussey, N., Simpfendorfer, C., Vagle, S., et al. (2014). A review of detection range testing in aquatic passive acoustic telemetry studies. *Rev. Fish Biol. Fish.* 24, 199–218. doi: 10.1007/s11160-013-9328-4

Kohler, N., Casey, J. G., and Turner, P. A. (1998). NMFS cooperative shark tagging programme, 1962–93: An atlas of shark tag and recapture data. *Mar. Fish. Rev.* 60, 1–87. doi: 10.7755/mfr.81.2.1

Lascelles, B., Notarbartolo Di Sciara, G., Agardy, T., Cuttelod, A., Eckert, S., Glowka, L., et al. (2014). Migratory marine species: their status, threats and conservation management needs. *Aquat. Conserv.* 24, 111–127. doi: 10.1002/aqc.2512

Last, P. R., and Stevens, J. D. (2009). *Sharks and rays of Australia*. Australia: CSIRO Australia.

Lédée, E., Heupel, M., Taylor, M., Harcourt, R., Fabrice, J., Huveneers, C., et al. (2021). National-scale acoustic telemetry and network analysis reveal new insights into stock structure. *Fish Fisheries*. faf.12565.

Lowe, W. H., and Allendorf, F. W. (2010). What can genetics tell us about population connectivity? *Mole. Ecol.* 19, 3038–3051. doi: 10.1111/j.1365-294x.2010.04688.x

Lucifora, L. O., Menni, R. C., and Escalante, A. H. (2005). Reproduction and seasonal occurrence of the copper shark, *Carcharhinus brachyurus*, from north Patagonia, Argentina. *ICES J. Mar. Sci.* 62, 107–115. doi: 10.1016/j.icesjms.2004.09.003

Macbeth, W., Geraghty, P., Peddemors, V. M., and Gray, C. (2009). *Observer-based study of targeted commercial fishing for large shark species in waters off northern New South Wales*. Australia: Final report to the Northern Rivers Catchment Management Authority.

McAuley, R. B., Simpfendorfer, C. A., and Hall, N. G. (2007). A method for evaluating the impacts of fishing mortality and stochastic influences on the demography of two long-lived shark stocks. *ICES J. Mar. Sci.* 64, 1710–1722. doi: 10.1093/icesjms/fsm146

McAuley, R., Bruce, B., Keay, I., Mountford, S., Pinnell, T., and Whoriskey, F. (2017). Broad-scale coastal movements of white sharks off Western Australia described by passive acoustic telemetry data. *Mar. Freshwater Res.* 68, 1518–1531. doi: 10.1071/mf16222

McMillan, M., Huveneers, C., Semmens, J., and Gillanders, B. (2018). Natural tags reveal populations of Conservation Dependent school shark use different pupping areas. *Mar. Ecol. Prog. Series* 599, 147–156. doi: 10.3354/meps12626

Nevatte, R. J., Williamson, J. E., Wueringer, B. E., and Gillings, M. R. (2021). Contrasting patterns of population structure in commercially fished sawsharks from southern Australian waters. *Rev. Fish Biol. Fish.* 2021, 1–21.

O'Dor, R. K., and Stokesbury, M. J. (2009). "The Ocean Tracking Network–Adding Marine Animal Movements to the Global Ocean Observing System," in *Tagging and Tracking of Marine Animals with Electronic Devices*, eds J. L. Nielsen, H. Arrizabalaga, N. Fragoso, A. Hobday, M. Lutcavage, and J. Sibert (Berlin: Springer), 91–100. doi: 10.1007/978-1-4020-9640-2_6

Ovenden, J. R. (2013). Crinkles in connectivity: combining genetics and other types of biological data to estimate movement and interbreeding between populations. *Mar. Freshwater Res.* 64, 201–207. doi: 10.1071/mf12314

Ovenden, J. R., Kashiwagi, T., Broderick, D., Giles, J., and Salini, J. (2009). The extent of population genetic subdivision differs among four co-distributed shark species in the Indo-Australian archipelago. *BMC Evol. Biol.* 9, 1–15. doi: 10.1186/1471-2148-9-40

Pacoureau, N., Rigby, C. L., Kyne, P. M., Sherley, R. B., Winker, H., Carlson, J. K., et al. (2021). Half a century of global decline in oceanic sharks and rays. *Nature* 589, 567–571. doi: 10.1038/s41586-020-03173-9

Petrusevics, P. (1993). SST fronts in inverse estuaries, South Australia-indicators of reduced gulf-shlef exchange. *Mar. Freshwater Res.* 44, 305–323. doi: 10.1071/mf9930305

Pincock, D. (2008). *False Detections: What They Are and How to Remove Them from Detection Data. DOC-004691 Version 01.*

Pleizier, N., Gutowsky, L. F., Peddemors, V. M., Cooke, S. J., and Butcher, P. A. (2015). Variation in whole-, landed-and trimmed-carcass and fin-weight ratios for various sharks captured on demersal set-lines off eastern Australia. *Fish. Res.* 167, 190–198. doi: 10.1016/j.fishres.2015.02.008

Rigby, C. L., Barreto, R., Carlson, J., Fernando, D., Fordham, S., Francis, M. P., et al. (2019). *Carcharhinus obscurus*. *The IUCN Red List of*

Threatened Species e.T3852A2872747. Available online at: https://dx.doi.org/10.2305/IUCN.UK.2019-3.RLTS.T3852A2872747.en (accessed date:28 September 2020).

Rogers, P., Braccini, M., Peddemors, P., Roelofs, A., and Woodhams, J. (2021). "Bronze whaler, *Carcharhinus brachyurus*," in *Status of Australian fish stocks reports 2020*, eds T. Piddocke, C. Ashby, K. Hartmann, A. Hesp, P. Hone, J. Klemke, et al. (Canberra: Fisheries Research and Development Corporation).

Rogers, P., Huveneers, C., Goldsworthy, S. D., Cheung, W. W. L., Jones, K. G., Mitchell, J. G., et al. (2013a). Population metrics and movement of two sympatric carcharhinids: a comparison of the vulnerability of pelagic sharks of the southern Australian gulfs and shelves. *Mar. Freshwater Res.* 64, 20–30. doi: 10.1071/mf11234

Rogers, P., Huveneers, C., Goldsworthy, S. D., Mitchell, J. G., and Seuront, L. (2013b). Broad-scale movements and pelagic habitat of the dusky shark *Carcharhinus obscurus* off Southern Australia determined using pop-up satellite archival tags. *Fish. Oceanogr.* 22, 102–112. doi: 10.1111/fog.12009

Romine, J. G., Musick, J. A., and Burgess, G. H. (2009). Demographic analyses of the dusky shark, *Carcharhinus obscurus*, in the Northwest Atlantic incorporating hooking mortality estimates and revised reproductive parameters. *Env. Biol. Fish.* 84, 277–289. doi: 10.1007/s10641-008-9435-6

Simpfendorfer, C. A. (1999). Demographic analysis of the dusky shark fishery in Southwestern Australia. *Am. Fish. Soc. Symp.* 23, 149–160.

Simpfendorfer, C. A., Huveneers, C., Steckenreuter, A., Tattersall, K., Hoenner, X., Harcourt, R., et al. (2015). Ghosts in the data: false detections in VEMCO pulse position modulation acoustic telemetry monitoring equipment. *Animal Biotelemet.* 3:1.

Steckenreuter, A., Hoenner, X., Huveneers, C., Simpfendorfer, C., Buscot, M. J., Tattersall, K., et al. (2017). Optimising the design of large-scale acoustic telemetry curtains. *Mar. Freshwat. Res.* 68, 1403–1413. doi: 10.1071/MF16126

Steer, M., Fowler, A., Rogers, P., Bailleul, F., Earl, J., Matthews, D., et al. (2020). *Assessment of the South Australian Marine Scalefish Fishery in 2018. SARDI Publication No. F2017/000427-3. SARDI Research Report Series No. 1049*. South Australia: SARDI Aquatics Sciences.

Turan, C. (2004). Stock identification of Mediterranean horse mackerel (Trachurus mediterraneus) using morphometric and meristic characters. *ICES J. Mar. Sci.* 61, 774–781.

Waples, R. S., Punt, A. E., and Cope, J. M. (2008). Integrating genetic data into management of marine resources: how can we do it better? *Fish Fisheries* 9, 423–449.

Waters, J. M. (2008). Marine biogeographical disjunction in temperate Australia: historical landbridge, contemporary currents, or both? *Diver. Distrib.* 14, 692–700.

Wood, S., and Wood, M. S. (2015). *Package 'mgcv'. R package version*, Vol. 1:29.

Woodhams, J., Braccini, M., Peddemors, P., and Rogers, P. (2021). *Dusky shark, Carcharhinus obscurus*," in *Status of Australian fish stocks reports 2020*. Canberra: Fisheries Research and Development Corporation.

Conflict of Interest: The authors declare that the research was conducted in the absence of any commercial or financial relationships that could be construed as a potential conflict of interest.

frontiers in Marine Science

ORIGINAL RESEARCH
published: 01 September 2021
doi: 10.3389/fmars.2021.673016

Compound-Specific Stable Isotope Analysis of Amino Acids in Pelagic Shark Vertebrae Reveals Baseline, Trophic, and Physiological Effects on Bulk Protein Isotope Records

Sarah Magozzi[1,2]*, Simon R. Thorrold[3], Leah Houghton[3], Victoria A. Bendall[4], Stuart Hetherington[4], Gonzalo Mucientes[5,6], Lisa J. Natanson[7], Nuno Queiroz[5], Miguel N. Santos[8,9] and Clive N. Trueman[1]

[1] School of Ocean and Earth Science, University of Southampton, Southampton, United Kingdom, [2] Department of Integrative Marine Ecology, Stazione Zoologica Anton Dohrn, Fano Marine Centre, Fano, Italy, [3] Department of Biology, Woods Hole Oceanographic Institution, Woods Hole, MA, United States, [4] Cefas Laboratory, Lowestoft, United Kingdom, [5] Centro de Investigação em Biodiversidade e Recursos Genéticos, Rede de Investigação em Biodiversidade e Biologia Evolutiva, Universidade do Porto, Porto, Portugal, [6] Instituto de Investigacións Mariñas, Consejo Superior de Investigaciones Científicas (IIM-CSIC), Vigo, Spain, [7] Northeast Fisheries Science Center, National Oceanic and Atmospheric Administration, Narragansett, RI, United States, [8] Instituto Português do Mar e da Atmosfera, Olhão, Portugal, [9] Secretariat of the International Commission for Conservation of Atlantic Tunas, Madrid, Spain

Edited by:
Charlie Huveneers,
Flinders University, Australia

Reviewed by:
Lauren C. Meyer,
Flinders University, Australia
Aaron Carlisle,
University of Delaware, United States

***Correspondence:**
Sarah Magozzi
sarah.magozzi@szn.it

Specialty section:
This article was submitted to
Marine Megafauna,
a section of the journal
Frontiers in Marine Science

Received: 26 February 2021
Accepted: 27 July 2021
Published: 01 September 2021

Citation:
Magozzi S, Thorrold SR, Houghton L, Bendall VA, Hetherington S, Mucientes G, Natanson LJ, Queiroz N, Santos MN and Trueman CN (2021) Compound-Specific Stable Isotope Analysis of Amino Acids in Pelagic Shark Vertebrae Reveals Baseline, Trophic, and Physiological Effects on Bulk Protein Isotope Records. Front. Mar. Sci. 8:673016. doi: 10.3389/fmars.2021.673016

Variations in stable carbon and nitrogen isotope compositions in incremental tissues of pelagic sharks can be used to infer aspects of their spatial and trophic ecology across life-histories. Interpretations from bulk tissue isotopic compositions are complicated, however, because multiple processes influence these values, including variations in primary producer isotope ratios and consumer diets and physiological processing of metabolites. Here we challenge inferences about shark tropho-spatial ecology drawn from bulk tissue isotope data using data for amino acids. Stable isotope compositions of individual amino acids can partition the isotopic variance in bulk tissue into components associated with primary production on the one hand, and diet and physiology on the other. The carbon framework of essential amino acids (EAAs) can be synthesised *de novo* only by plants, fungi and bacteria and must be acquired by consumers through the diet. Consequently, the carbon isotopic composition of EAAs in consumers reflects that of primary producers in the location of feeding, whereas that of non-essential amino acids (non-EAAs) is additionally influenced by trophic fractionation and isotope dynamics of metabolic processing. We determined isotope chronologies from vertebrae of individual blue sharks and porbeagles from the North Atlantic. We measured carbon and nitrogen isotope compositions in bulk collagen and carbon isotope compositions of amino acids. Despite variability among individuals, common ontogenetic patterns in bulk isotope compositions were seen in both species. However, while life-history movement inferences from bulk analyses for blue sharks were supported by carbon isotope data from essential amino acids, inferences for porbeagles were not, implying that the observed trends in bulk protein isotope compositions in porbeagles have a trophic or physiological explanation, or are suprious effects. We explored variations in carbon isotope compositions of non-essential amino acids, searching for systematic variations that might imply ontogenetic changes in physiological processing, but patterns were highly variable and did not explain variance in bulk protein δ^{13}C values. Isotopic effects associated with metabolite processing may overwhelm spatial influences that are weak or inconsistently developed in bulk tissue isotope values, but interpreting mechanisms underpinning isotopic variation in patterns in non-essential amino acids remains challenging.

Keywords: carbon, essential amino acids, non-essential amino acids, migration, diet, routing, blue sharks (*Prionace glauca*), porbeagles (*Lamna nasus*)

INTRODUCTION

Pelagic shark populations have declined regionally by >90% in the past 20 years, largely as a result of overfishing and bycatch (Worm et al., 2013), while the global abundance of oceanic sharks has declined by 70% since 1970 (Pacoureau et al., 2021). The vulnerability of sharks to marine-capture fisheries depends on individual movements and the presence of movement traits across individuals, populations, or species that may suggest a shared vulnerability (Queiroz et al., 2016, 2019; Vandeperre et al., 2016; Coelho et al., 2020). Effective management of the remaining shark populations requires a thorough understanding of their spatial ecology (Costa et al., 2012; Briscoe et al., 2016). Movements of pelagic sharks are, however, difficult to monitor or reconstruct, particularly throughout ontogeny (Graham et al., 2010; Trueman et al., 2012; McMahon et al., 2013). While physical tags have revolutionized our understanding of space use by pelagic fishes, they rarely report over the life-time of a tagged individual, and juvenile animals may be too small to support satellite-linked pop-up tags. Consequently, knowledge of juvenile movements, and connections between juvenile and adult habitats, remain poorly understood for many pelagic shark species.

Stable isotope analysis (SIA) of animal tissues has become a routine tool used in ocean ecology to reconstruct animal movements (e.g., Best and Schell, 1996; Cherel et al., 2009; Carlisle et al., 2015; Bird et al., 2018) and changes in diet and trophic level (e.g., MacNeill et al., 2005; Estrada et al., 2006; Newsome et al., 2009; Pethybridge et al., 2018; Lorrain et al., 2020) (for reviews see Post, 2002; Graham et al., 2010; Boecklen et al., 2011; McMahon et al., 2013; Trueman and St John Glew, 2019). Because the isotopic composition of primary producers varies across space and time (McMahon et al., 2013; Schmittner and Somes, 2016; Magozzi et al., 2017), animal movements can, in theory, be reconstructed retrospectively by relating variation in tissue isotopic composition to variability in isotopic baselines (McMahon et al., 2013; Trueman and St John Glew, 2019). Sequential analysis of tissues that retain a chronological record in the form of periodically deposited increments or growth bands, including shark vertebrae, may further provide movement (and trophic) information throughout life of individuals (Hobson, 1999; Newsome et al., 2010; Trueman et al., 2012; e.g., Estrada et al., 2006; Carlisle et al., 2015).

The underlying premise of the isotope tracer method is that the isotopic composition of animal tissue reflects that of primary producers at the base of the foodweb, overlain by a relatively predictable trophic offset (DeNiro and Epstein, 1978, 1981). However, this premise is a simplification of a complex suite of interacting ecological and biochemical factors. Variance in isotopic compositions from bulk tissue analyses can reflect mixed effects from variation in isotopic compositions of primary producers (baseline effects; Schmittner and Somes, 2016; Magozzi et al., 2017), changes in diet and trophic level (trophic effects), and variation in metabolic routing of dietary macronutrients to tissue synthesis (physiological effects; Trueman et al., 2005; Newsome et al., 2014; Wang et al., 2019). Interactions among these isotope effects significantly complicate the interpretation of bulk tissue isotope data alone to infer movements, diet or trophic level changes (e.g., Newsome et al., 2010; Trueman et al., 2012; e.g., Popp et al., 2007). SIA of specific structural compounds within tissues, such as individual amino acids, has been increasingly employed in animal movement (McMahon et al., 2011a,b; Seminoff et al., 2012) and trophic (Chikaraishi et al., 2009, 2014; Lorrain et al., 2009) studies to reduce uncertainty in estimates of change in location, diet and trophic level and nutrient source (e.g., Larsen et al., 2013; McCarthy et al., 2013; McMahon et al., 2015a).

A number of amino acids critical for life functions can only be synthesized *de novo* by some plants, fungi and bacteria. These essential amino acids are subsequently transferred unaltered through foodwebs (Hare et al., 1991; Reeds, 2000; Jim et al., 2006; McMahon et al., 2010). Consequently, the carbon isotope composition of essential amino acids ($\delta^{13}C_{EAA}$) in consumer tissues retains the isotopic composition fixed during biosynthesis by primary producers (Jim et al., 2006; Popp et al., 2007; McMahon et al., 2010; Wang et al., 2019). Differences in $\delta^{13}C_{EAA}$ values among consumers reflect variations in the isotopic compositions of primary production at the time and place of biosynthesis and can therefore be used to infer movement across spatio-temporal isotope gradients (Schmittner and Somes, 2016; Magozzi et al., 2017) and/or variations in the relative contribution of foodwebs fueled by different carbon sources (e.g., Larsen et al., 2009, 2013). Non-essential amino acids can either be routed directly from dietary sources to tissue or synthesized *de novo* by using metabolites derived from ingested nutrients

(McMahon et al., 2010, 2015b; Newsome et al., 2011; Berg et al., 2015). Carbon isotopes are fractionated during biomolecule degradation and synthesis (Hayes, 2001; Howland et al., 2003; Jim et al., 2006), therefore variability in $\delta^{13}C$ values of non-essential amino acids ($\delta^{13}C_{non-EAA}$) can reflect trophic and physiological effects superimposed on any baseline effects.

Non-essential amino acids can be synthesized from dietary intermediates, whether protein, lipids or carbohydrates (Berg et al., 2015). Marine pelagic predators draw energy and nutrients largely from protein and lipid sources with relatively little energy drawn from carbohydrates (Wang et al., 2019). Lipids are energy dense nutrient sources, and fish nutrition balances protein and lipid (energy) sources (Bowyer et al., 2013). Protein and energy requirements and availability vary in time and space, therefore the proportion of metabolites assimilated from protein compared to lipid precursor molecules is likely to vary considerably in time, space and among individuals depending on their nutritional status. Lipids are typically depleted in ^{13}C relative to protein, therefore the degree to which a particular amino acid is synthesized from lipid compared to protein dietary precursors should be reflected in its ^{13}C content (Wolf et al., 2015; Wang et al., 2018). Controlled-feeding experiments on salmon (Wang et al., 2019) and a study with mammals (Newsome et al., 2014; Wolf et al., 2015) have shown that the $\delta^{13}C$ values of glycolytic amino acids are highly sensitive to the lipid content of diets and lipid utilization for amino acid synthesis whereas values of Krebs cycle amino acids are not (see also Leigh et al., 2018; Wang et al., 2018; Whiteman et al., 2018). These results imply that, where diets contain no carbohydrates, glycolytic amino acids (e.g., glycine, serine, and alanine) are synthesized from glycogen predominantly contributed from the metabolism of fatty acids, whereas amino acids whose synthesis is associated with the Krebs cycle (e.g., glutamic acid, aspartic acid, and proline) draw on carbon provided by processing of both protein and lipid sources (Choy et al., 2010; Fernandes et al., 2012; Newsome et al., 2014). Variability in $\delta^{13}C$ values of glycolytic vs. Krebs cycle amino acids may therefore reflect changes in macronutrient contents of diets and/or shifts in the metabolic allocation of macronutrients for tissue synthesis. However, how carnivorous fish use dietary intermediates to synthesize amino acids is still poorly understood and may ultimately depend on their digestive physiology and nutritional requirements (e.g., Leigh et al., 2018; Whiteman et al., 2018).

The combination of essential and non-essential amino acids, the isotopic compositions of which are influenced differently by contrasting mechanisms, therefore offers an opportunity to differentiate among alternative variables contributing to variance in bulk tissue isotope values. The potential for identifying variations in animal nutrient physiology from variations in $\delta^{13}C_{non-EAA}$ values is particularly attractive but a coherent framework to interpret variability in $\delta^{13}C_{non-EAA}$ data remains elusive. In this study, we present stable carbon ($\delta^{13}C$) and nitrogen ($\delta^{15}N$) isotope chronologies of bulk cartilage collagen from sequential vertebral samples for individual blue sharks (*Prionace glauca*, Linnaeus 1758) and porbeagles (*Lamna nasus*, Bonnaterre 1788) caught across the North Atlantic. In parallel, we present comparable carbon isotope chronologies of individual essential and non-essential amino acids from the same sharks. We quantified variation in $\delta^{13}C$ values of bulk collagen and individual amino acids at multiple levels (between species, among areas and individuals and within-individuals) and tested for common, broad ontogenetic isotope patterns across individual blue sharks and porbeagles. We contrasted patterns in $\delta^{13}C$ values of bulk protein and essential amino acids to disentangle baseline from trophic effects on bulk tissue $\delta^{13}C$ values and test whether observed ontogenetic trends can be best interpreted in terms of movement or diet and trophic level change. Given the small number of individuals examined (nine blue sharks and six porbeagles), we clearly did not aim here to draw inferences about the ecology for species or populations. We argue that, if ontogenetic patterns in bulk protein $\delta^{13}C$ values are matched by variability in $\delta^{13}C$ values of essential amino acids, then at least a component of variance in the bulk protein signal must be associated with movement (in time and/or space) across isotopically distinct baselines. By contrast, if trends in bulk protein $\delta^{13}C$ values are solely associated with a shift in diet or trophic position, they should not be apparent in the $\delta^{13}C$ values of essential amino acids (and should match trends in bulk $\delta^{15}N$ values). We also investigated patterns in $\delta^{13}C$ values of non-essential amino acids, particularly isotopic spacing between glycolytic and Krebs cycle amino acids, to explore whether systematic variations in nutrient physiology could be encoded in the bulk or amino acid isotope values.

MATERIALS AND METHODS

Sample Description

Vertebral samples were collected from nine blue sharks and six porbeagles caught across the North Atlantic. Three blue sharks were captured in offshore waters south of Canary Islands (eastern blue sharks), three in the mid-Atlantic Ridge area northwest of the Azores (central blue sharks), and three in oceanic waters between Cape Hatteras and the Gulf of Maine (western blue sharks; **Figure 1**). Blue sharks were bycaught by pelagic longlines targeting swordfish, tunas and sharks, by research and commercial fishing vessels using pelagic longlines or during shark fishing tournaments using rods and reels. Two porbeagles were bycaught on the continental shelf in the Celtic Sea during commercial gillnet fishery targeting gadiform fish and retained under dispensation as part of a fishery bycatch study (eastern porbeagles; Ellis and Bendall, 2015; Ellis et al., 2015). One porbeagle was bycaught by a fisherman near the Faroe Islands and donated to research. Three porbeagles were caught between Massachusetts and Grand Banks (off southern Newfoundland) by commercial vessels using pelagic longlines (western porbeagles; **Figure 1**; for metadata see **Table 1**).

Sample Preparation for Bulk Tissue Analysis

Trunk vertebrae were excised from above the branchial chamber in porbeagles and western blue sharks, and vertebrae were removed posterior to the skull in central and eastern blue sharks. All vertebrae were immediately frozen after dissection. Vertebral

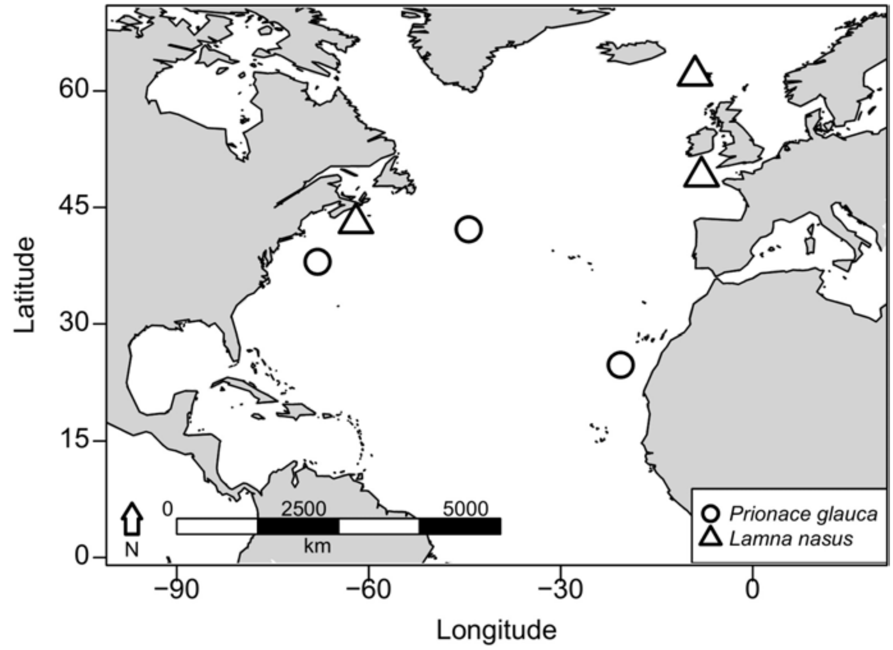

FIGURE 1 | Capture areas for blue sharks (*Prionace glauca*) and porbeagles (*Lamna nasus*) in the North Atlantic.

TABLE 1 | Metadata for individual blue sharks (*Prionace glauca*) and porbeagles (*Lamna nasus*) analyzed for stable isotopes, including individual ID, species, capture area, capture date or year, sex, maturity stage, fork length (FL, cm), vertebral radius (measured: VR, mm; adjusted VR: AdjVR, mm), number of samples collected for each vertebra (N), and (achieved) average interval between adjacent samples (AvgInt, mm).

Individual ID	Species	Capture area	Capture date	Sex	Maturity	FL	VR	AdjVR	*N*	AvgInt
16	*Prionace glauca*	mid-Atlantic Ridge	17/06/2014	Female	Mature	242.0	11.0	11.3	19	0.59
24	*Prionace glauca*	mid-Atlantic Ridge	20/06/2014	Female	Mature	240.0	11.0	11.2	21	0.53
12	*Prionace glauca*	mid-Atlantic Ridge	16/06/2014	Female	Mature	219.0	10.0	10.2	17	0.60
101	*Prionace glauca*	Canary Islands	07/02/2014	Female	Mature	258.0	12.0	12.0	16	0.75
131	*Prionace glauca*	Canary Islands	08/02/2014	Female	Mature	249.0	12.0	11.6	17	0.68
33	*Prionace glauca*	Canary Islands	05/02/2014	Female	Mature	244.0	11.5	11.3	21	0.54
335	*Prionace glauca*	Northwest Atlantic	21/02/1979	Female	Mature	268.0	17.0	16.4	34	0.48
415	*Prionace glauca*	Northwest Atlantic	16/05/1984	Female	Mature	265.0	15.0	16.2	31	0.52
441	*Prionace glauca*	Northwest Atlantic	29/06/1985	Female	Mature	245.0	14.5	14.9	28	0.53
11	*Lamna nasus*	Celtic Sea	2011	Female	Maturing	211.0	15.0	15.2	24	0.63
40	*Lamna nasus*	Celtic Sea	2014	Female	Immature	197.0	12.5	14.0	24	0.58
1000	*Lamna nasus*	Faroe Islands	2014	Female	Maturing	210.0	15.5	15.1	24	0.63
599	*Lamna nasus*	Northwest Atlantic	05/12/1999	Female	Mature	260.0	17.5	19.2	32	0.60
601	*Lamna nasus*	Northwest Atlantic	06/12/1999	Female	Mature	256.5	17.5	18.9	34	0.56
578	*Lamna nasus*	Northwest Atlantic	27/11/1999	Female	Mature	256.0	17.0	18.9	30	0.63

AdjVR is calculated from FL using validated (for blue shark and porbeagle trunk vertebrae) and estimated (for blue shark cervical vertebrae) VR:FL relationships. AvgInt is calculated as AdjVR/N (for details, see ***Supplementary Material****).*

centra were then defrosted, physically cleaned of excess muscle and connective tissue and air-dried for 3–10 days, depending on dimensions (Kim and Koch, 2012). A 6 mm section was cut from each centrum using a low-speed diamond-bladed Isomet® saw. This section was divided in two halves: a thinner (5–5.4 mm) section was cut from one half and used for bulk tissue isotope analysis, the other half was used for amino acid analysis. Approximately equidistant samples (mean ± SD interval between adjacent samples among vertebrae: 0.59 ± 0.07 mm; **Table 1**) were collected along the vertebral radius by manually cutting the thinner half section with a scalpel. Equidistant samples were chosen over sampling growth bands, as growth bands can be difficult to identify, particularly in blue sharks (Magozzi personal observation), and are compressed toward the vertebral edge due to reduced growth/accretion rates with age (Natanson et al., 2002; Skomal and Natanson, 2003), which makes it hard to sample each single growth band and obtain sufficient material for isotopic analysis. For this reason, the temporal resolution of isotope chronologies from equidistant samples was higher (e.g., <1 year) closer to the vertebral centrum and lower toward the edge (e.g., a few years) but sufficient to depict isotopic variation at ecologically relevant time-scales for all specimens and life-history stages.

Vertebral samples were decalcified by exposure to 2 ml of 1 M HCl for 48 h to remove any potential influence of ^{13}C-enriched bioapatite on the δ^{13}C values of bulk cartilage collagen (Hussey et al., 2012; Kim and Koch, 2012; Christiansen et al., 2014; see also Tuross et al., 1988). During treatment samples were kept at a constant temperature of 4°C to reduce decalcification rates and prevent collagen dissolution and damage. Samples were then washed five times with 2 ml of Milli-Q water, frozen and freeze-dried.

Samples weighing <0.5 mg (i.e., the minimum weight required for dual carbon and nitrogen isotope analysis of bulk protein) were combined to the lighter adjacent sample(s) until the combined weight exceeded 0.5 mg. Due to the typical bowtie shape of vertebral sections, more samples generally required to be combined closer to the centrum or even further along the radius in portions of the vertebra characterized by large water or air content. Thus, the combination of samples often resulted in decreased temporal resolution at the core. Single or combined samples with a weight of >1.5 mg were powdered and ∼1.25 mg of material was randomly selected for analysis. Blue shark samples were analyzed at full resolution (i.e., all adjacent samples), porbeagle samples at half resolution (i.e., one every other sample) for distances along the vertebral radius <7 mm and at full resolution afterward. This choice was made to minimize analytical costs, whilst also achieving a sufficient temporal resolution throughout ontogeny in the two species. Evidence from satellite-tagging studies indicates that, while juvenile blue sharks may undergo extensive latitudinal movements (Queiroz et al., 2010; Vandeperre et al., 2014), porbeagles tend to remain on the shelf until they conduct an ontogenetic habitat shift toward offshore waters with the onset of maturity (Biais et al., 2017) and are therefore unlikely to express large isotopic variation during early life-history stages. The vertebral radius at maturity is estimated to be ∼15 mm in porbeagles from age at maturity equal to 13 years (Natanson et al., 2002); a value of 7 mm was selected here as a more conservative cutoff to account for approximations in the sampled interval.

Sample Preparation for Compound-Specific Analysis

The procedures for sample preparation for amino acid isotope analysis were similar to those for bulk tissue analysis except that the half section used for this analysis was 6 mm thick and more adjacent samples required to be combined at the core and along the vertebral radius, as the minimum weight for compound-specific analysis is 4 mg (prior to hydrolysis and derivatization; Houghton personal communication). Vertebral samples were analyzed at full resolution for central and eastern blue sharks, at half resolution for all other specimens to minimize analytical costs. Thus, the temporal resolution of amino acid analysis was generally lower than for bulk tissue analysis but sufficient to identify breakpoints in amino acid isotope chronologies.

For compound-specific analysis, samples were initially acid-hydrolyzed (after combining adjacent samples) in 1 ml 6 N HCl at 110°C (temperature range: 105–115°C) for 20 h to liberate single amino acids from protein. Vials were tightly closed during hydrolysis to prevent sample and acid evaporation. After hydrolysis, samples were dried with a gentle stream of N_2 at 60°C (temperature range: 55–65°C) for 30–60 min, depending on sample weight and excess HCl volume. Samples were then dissolved in 100 μl 0.1 N HCl and preserved at 4°C until derivatization.

A total of 50 μl of the sample+HCl solution were derivatized by adding 35 μl of methanol, 30 μl of pyridine, and 15 μl of methyl chloroformate (MCF); after additions, the mixture was vortexed for 30 s. Amino acid-MCF derivates were separated from the reaction mixture by adding a volume of chloroform that depended on sample original weight: 50 μl for 4–10 mg, 75 μl for 11–22 mg, and 100 μl for >23 mg. After chloroform addition, the mixture was vortexed for another 30 s. At this stage the reaction mixture was stratified and the organic layer of amino acid-MFC derivates was separated from the aqueous layer using electrophoresis pipette tips and used for analysis.

Bulk Tissue Isotope Analysis

Carbon and nitrogen isotopic compositions of bulk cartilage collagen were measured using a PDZ Europa ANCA-GSL elemental analyzer interfaced to a PDZ Europa 20–20 isotope ratio mass spectrometer (Sercon Ltd., Cheshire, United Kingdom) at the UC Davis Stable Isotope Facility. Samples from Northeast Atlantic porbeagles were transported to the United States accompanied by a CITES Export Permit (No. 529713/01). All samples were analyzed in duplicate. Analytical quality-control was assessed through repeated measurement of laboratory-internal reference materials (nylon, glutamic acid, and USGS-41; for details see Magozzi, 2017), which were in turn calibrated to international reference materials. Nylon was used as a drift reference to correct for variation over the course of a run, glutamic acid to calculate the elemental totals and apply a linear correction to the isotope values. The isotope values were then scaled to two reference materials of known isotopic compositions: nylon and USGS-41. Precision was calculated as the standard deviation of isotope values for bovine liver NIST 1577 across runs (i.e., for the time period over which the samples were analyzed), accuracy as the difference between the mean isotope value for bovine liver and its accepted value. Precision was 0.03‰ for δ^{13}C values and 0.10‰ for δ^{15}N values, accuracy 0.01‰ for δ^{13}C values and 0.06‰ for δ^{15}N values. Final δ^{13}C and δ^{15}N values were expressed relative to the international reference materials V-PDB (Vienna PeeDee Belemnite) and Air, respectively. The raw ratio (R) of the heavy (^{13}C, ^{15}N) to the light (^{12}C, ^{14}N) isotope in a sample was converted to a δ-value expressed in ‰ using Eq. (1):

$$\delta X = \left[\left(\frac{R_{sample}}{R_{standard}}\right) - 1\right] \cdot 1000 \qquad (1)$$

where X is the heavier isotope. $R_{standard}$ refers to the raw ratio of an internationally accepted reference gas for the analyzed isotope.

Compound-Specific Isotope Analysis

Derivatized samples were analyzed with gas chromatography-combustion-isotope ratio monitoring mass spectrometry (GC-C-irm-MS) at the Woods Hole Oceanographic Institution. Samples were dissolved in dichloromethane (DCM) and injected on column in splitless mode at 260°C and separated on an Agilent VF-23ms column (length: 30 m, inner diameter: 0.25 mm, film thickness: 0.25 μm; Agilent Technologies, Wilmington, DE, United States) in an Agilent 689N Gas Chromatograph (GC). Sample concentrations were adjusted to achieve a minimum of 2 V output for all amino acids. Gas chromatography conditions were set to optimize peak separation and shape as follows: initial temperature 80°C held for 1 min; ramped to 260°C at 6°C min^{-1}; held for 3 min. The separated amino acid peaks were combusted online in a Finnigan GC-C continuous flow interface at 930°C and then measured as CO_2 on a Thermo Finnigan Mat 253 irm-MS (Agilent Technologies 689N GC). Standardization of runs was achieved using intermittent pulses of a CO_2 reference gas of known isotopic composition. All samples were run in duplicate. Carbon isotopic compositions were recovered for the essential amino acids: valine, isoleucine, leucine, threonine, and phenylalanine; and for the non-essential amino acids: alanine, glycine, proline, aspartic acid, and glutamic acid. A typical chromatogram from the analysis of carbon isotope ratios in amino acid-MCF derivates is displayed in **Supplementary Figure 2**. Values of $\delta^{13}C$ for threonine showed poor chromatography and inconsistencies among replicates, therefore were omitted from data analysis.

Two internal lab reference materials (AA1 and AA2) were created with single amino acids with known $\delta^{13}C$ values. Additionally, 20 mg of lyophilized muscle from Atlantic cod (*Gadus morhua*, Linnaeus 1758) were acid-hydrolyzed and re-dissolved in 100 μl 0.1 N HCl and 50 μl of the solution used as reference material. All reference materials were concurrently derivatized with the samples and dissolved in 100 μl chloroform. Derivatization correction factors were determined for each amino acid based on known $\delta^{13}C$ values of the amino acids in the reference materials prior to derivatization, and applied to each sample to adjust for the introduction of exogenous carbon and kinetic fractionation from derivatization. As no international reference materials are currently available for the analysis of carbon isotope ratios in individual amino acids and no large inter-laboratory calibration has yet come up with consensus $\delta^{13}C$ values, mean values across three laboratories (i.e., the Fish Ecology Laboratory, the Marine Biological Laboratory, and the UC Davis Stable Isotope Facility; **Supplementary Table 1**) were used. Reference materials were interspersed among samples and analyzed 4–6 times. Precision was determined as the standard deviation of the $\delta^{13}C$ values for each amino acid in the cod standard during the time period of sample analysis. Precision was 0.31‰ for valine, 0.34‰ for isoleucine, 0.40‰ for leucine, 0.30‰ for threonine, 0.26‰ for phenylalanine, 0.13‰ for alanine, 0.30‰ for glycine, 0.32‰ for proline, 0.40‰ for aspartic acid, 0.22‰ for glutamic acid.

Data Analysis

To account for differential vertebral growth rates throughout ontogeny, linear distance of samples along the vertebral radius was converted to age using validated (for blue shark and porbeagle trunk vertebrae; Natanson et al., 2002; Skomal and Natanson, 2003) and estimated (for blue shark cervical vertebrae; this study) vertebral width:body size relationships and validated body size:age (Von Bertalanffy) growth curves for blue sharks (Skomal and Natanson, 2003) and porbeagles (Natanson et al., 2002; for details on age estimation see **Supplementary Material**). Clearly, due to reduced growth/accretion rates with age, the same sampled interval corresponded to "less years" integrated at smaller distances along the vertebral radius, "more years" integrated at larger distances along the radius. Thus, conversion of sample distance to age accounted for time-series expansion closer to the vertebral centrum and time-series compression toward the edge. Differences in growth and longevity between blue sharks and porbeagles were accounted for by parameters in vertebral width:body size relationships and Von Bertalanffy growth curves. Age at birth was 0 years and age at maturity was 5 and 13 years in blue sharks and porbeagles, respectively (Natanson et al., 2002; Skomal and Natanson, 2003); these values were used as cutoffs to distinguish between pre-birth, juvenile and adult life-history stages when examining isotope chronologies. Sample age is not displayed in plots for pre-birth samples, as Von Bertalanffy growth curves are not applicable to estimate age during the pre-birth stage. Age classes were determined for each species by subsetting the maximum age range across individuals by 1 year-intervals, and samples were assigned to their age classes based on their estimated age. Age classes were sufficiently small to allow the identification of relatively continuous ontogenetic patterns across individuals.

Principal component analysis (PCA) was applied to the $\delta^{13}C$ values of essential and non-essential amino acids to reduce the data to two dimensions (PC1 and PC2) explaining the majority of variance in $\delta^{13}C$ values of amino acids. For non-essential amino acids, spacing (i.e., difference) in $\delta^{13}C$ values was calculated between independent pairs of glycolytic (lipid-derived) and Krebs cycle (lipid+protein-derived) amino acids (glycine and alanine compared to glutamic acid and proline, respectively) and explored as a potential indicator for shifts in macronutrient contents of diets and/or changes in metabolic routing of macronutrients to amino acid synthesis (Wolf et al., 2015; Wang et al., 2018, 2019).

In order to test for common isotope patterns across individual blue sharks and porbeagles, the values of each variable (i.e., bulk protein $\delta^{13}C$ and $\delta^{15}N$ values, PC1 scores for $\delta^{13}C$ values of essential and non-essential amino acids and spacing in $\delta^{13}C$ values between glycolytic and Krebs cycle amino acids) in each sample were normalized to the individual mean (life history-normalization) to emphasize within-individual variation in ontogenetic profiles, whilst reducing among-individual differences. Ontogenetic patterns in life history-normalized $\delta^{13}C$ and $\delta^{15}N$ values of bulk protein and differences between species and among areas and individuals were tested with generalized additive mixed models (GAMMs). Estimated sample age was added as a smoother, species and area as parametric fixed effects and individuals as a random effect (Pinheiro and Bates, 2000; Zuur et al., 2014). Model fits were calculated for full models and optimal models were selected with Akaike Information Criteria (AIC; Zuur et al., 2014). Generalized additive mixed models were fitted using the *mgcv* R package (Wood, 2006) and all analysis were performed using R v.4.0.2 (R Core Team, 2019).

RESULTS

Bulk Protein

Bulk protein $\delta^{13}C$ values ranged between -16.73 and -13.95‰ (mean ± SD: -15.13 ± 0.65‰) in blue sharks and between -15.80 and -13.71‰ (mean ± SD: -14.55 ± 0.38‰) in porbeagles. Values of $\delta^{15}N$ varied between 9.09 and 14.14‰ (mean ± SD: 11.47 ± 1.11‰) in blue sharks and between 9.42 and 16.29‰ (mean ± SD: 12.84 ± 1.47‰) in porbeagles. The $\delta^{15}N$ range in porbeagles was, however, strongly influenced by ^{15}N-enriched subadult and adult samples from Northwest Atlantic individuals.

Despite high among-individual variability in individual isotopic profiles (**Supplementary Figure 4**), we identified common, broad ontogenetic patterns in life history-normalized $\delta^{13}C$ and $\delta^{15}N$ values ($\delta^{13}C_n$, $\delta^{15}N_n$) of bulk protein across individuals of each species (**Figure 2**). Ontogenetic patterns in $\delta^{13}C_n$ and $\delta^{15}N_n$ values were non-linear (smoother 'estimated sample age': p-value = $2{\cdot}10^{-16}$, $F_{\delta^{13}C} = 26.46$; $F_{\delta^{15}N} = 26.29$) and differed significantly between species (maximum *p*-value = 0.006, *F* = 7.62; **Supplementary Tables 2, 3**). In blue sharks, $\delta^{13}C_n$ values increased progressively during juvenile and early adult growth, reaching a relatively steady state in the adult life stage (**Figure 2A**). Values of $\delta^{15}N_n$ increased during juvenile growth and decreased in adult stages (**Figure 2B**). Both $\delta^{13}C_n$ and $\delta^{15}N_n$ values were higher in the pre-birth stage and decreased around birth ($\delta^{15}N_n$ values to a lesser extent; **Figures 2A,B**). Pre-birth $\delta^{13}C_n$ values were highest across life-history and comparable to adult levels, whereas pre-birth $\delta^{15}N_n$ values were higher than late adult levels. Among-individual variances in both $\delta^{13}C_n$ and $\delta^{15}N_n$ values were relatively high but constant across life-history and lower than in porbeagles (**Figures 2A,B**).

In porbeagles, mean $\delta^{13}C_n$ values increased in the juvenile stage (until an age of ∼7–8 years), then remained relatively constant until capture (**Figure 2C**). Pre-birth $\delta^{13}C_n$ values were higher than post-partum values but generally lower than adult levels. Among-individual variance in $\delta^{13}C_n$ values was markedly higher than in blue sharks, particularly in the pre-birth stage and early juvenile and subadult stages associated with shifts in mean $\delta^{15}N_n$ values (see below). Mean values of $\delta^{15}N_n$ showed two stepwise increases, a small one just after birth and a larger one in the subadult stage (at ∼11–12 years of age), whereas values in intermediate juvenile and adult periods remained relatively constant (**Figure 2D**). The stepwise pattern in the subadult stage was driven by a step increase in $\delta^{15}N_n$ values in individuals from the Northwest Atlantic, and the plateau phase in the adult stage was also only seen in these sharks (**Supplementary Figures 4M–O**). Similar to $\delta^{13}C_n$ values, pre-birth $\delta^{15}N_n$ values were higher than values after birth but lower than values in the adult stage (**Figures 2C,D**). Among-individual variance in $\delta^{15}N_n$ values was broadly consistent with that in $\delta^{13}C_n$ values, peaking in the pre-birth stage and early and late juvenile stages.

Amino Acids

Carbon isotope compositions of individual amino acids were analyzed for 128 blue shark vertebral samples (*n* = 196 bulk collagen samples). For porbeagles, 80 samples were analyzed for carbon isotopes in amino acids (*n* = 133 bulk protein samples). Mean ± SD $\delta^{13}C$ values for each amino acid in blue shark and porbeagle samples are presented in **Supplementary Table 4**. Individual isotope chronologies for $\delta^{13}C$ values in single amino are presented in **Supplementary Figures 5–13**.

Values of $\delta^{13}C$ of non-essential amino acids ($\delta^{13}C_{non-EAA}$) were more positive than values of essential amino acids (**Supplementary Figures 5–13**), and the bulk protein $\delta^{13}C$ value corresponded to the weighted average of $\delta^{13}C_{EAA}$ and $\delta^{13}C_{non-EAA}$ values. Co-variations between bulk protein and single amino acid $\delta^{13}C$ values are shown in **Figures 3**, **4** for essential and non-essential amino acids, respectively. Bulk protein $\delta^{13}C$ values were higher and spanned a smaller range in porbeagles. Individual blue sharks grouped by capture area, implying that spatially determined among-individual variation explained more of the variance than the within-individual term. Within individual sharks, amino acid $\delta^{13}C$ values co-varied more with bulk protein $\delta^{13}C$ values in blue sharks compared to porbeagles, implying a common mechanism influencing multiple amino acids in the same direction and therefore contributing to bulk collagen $\delta^{13}C$ values. This was especially clear for the non-essential glycolytic amino acids alanine and glycine. In porbeagles, there was very weak co-variance between bulk protein $\delta^{13}C$ values and $\delta^{13}C$ values for any single amino acids, implying that mechanisms underpinning variation in bulk protein $\delta^{13}C$ values varied among- and within-individuals, likely complicating efforts to interpret bulk collagen $\delta^{13}C$ values in an ecological or behavioral context. Aspartate/aspartic acid and, to a lesser extent, glutamate/glutamic acid $\delta^{13}C$ values separated blue shark and porbeagle individuals into two clusters but these clusters did not correspond to different capture areas.

Essential Amino Acids

Principal components 1 and 2 explained 72% and 13% of the total variance in the $\delta^{13}C$ values of essential amino acids ($\delta^{13}C_{EAA}$), respectively (**Supplementary Figures 14A,B**). Most positive PC1 scores corresponded to most positive $\delta^{13}C$ values of all essential amino acids. Shark samples laid along a gradient on the PC1 axis: central and eastern North Atlantic blue sharks had most negative PC1 (hence $\delta^{13}C_{EAA}$) values, individuals from the Northwest Atlantic had most positive values (**Supplementary Figure 14A**). Porbeagles had intermediate PC1 scores and also separated, to a lesser extent, by area and individual (**Supplementary Figure 14B**).

Despite high variability in PC1 individual profiles (**Supplementary Figure 15**), broad, common patterns in

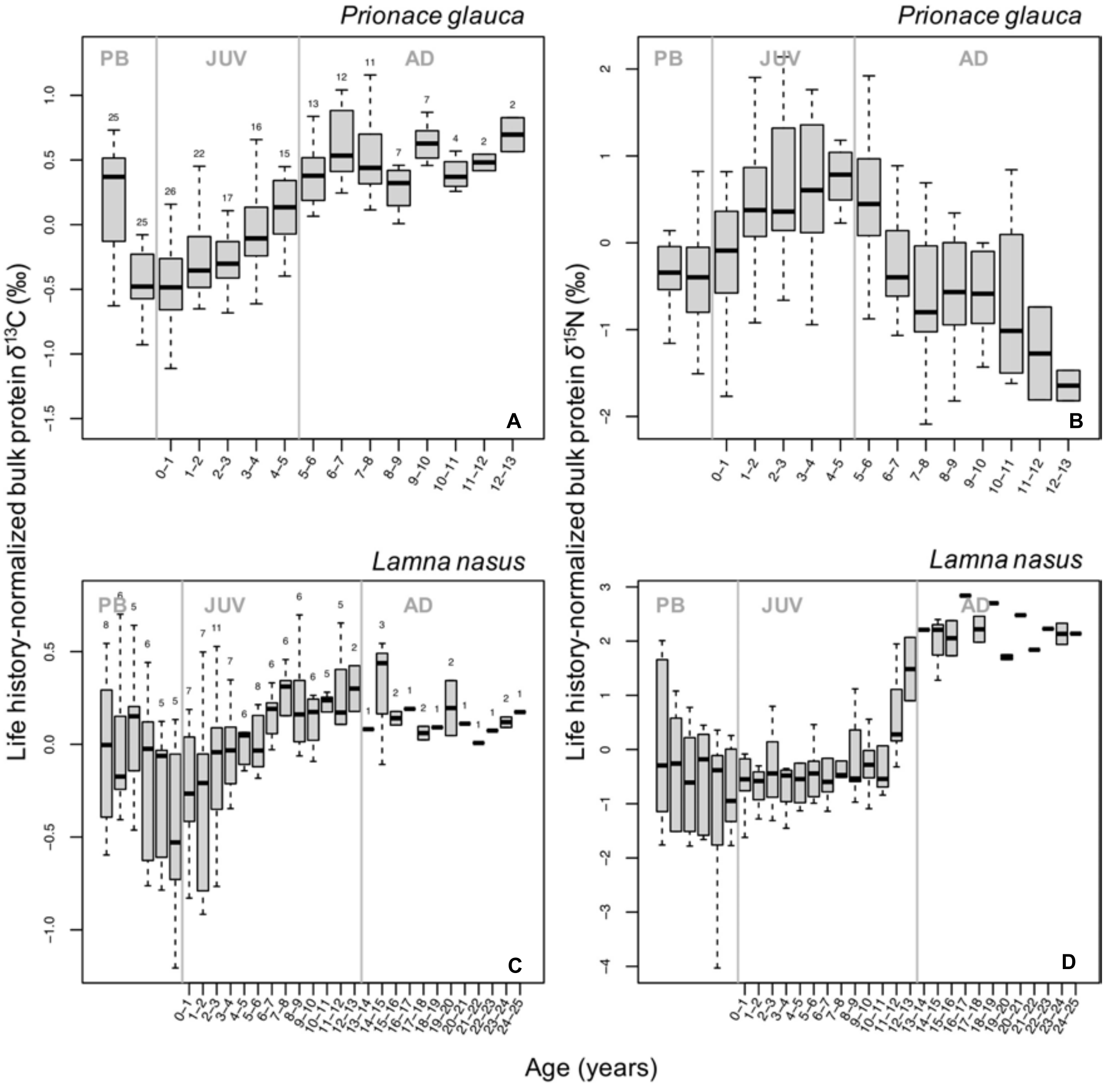

FIGURE 2 | Boxplots of life-history normalized $\delta^{13}C$ **(A,C)** and $\delta^{15}N$ **(B,D)** values of bulk protein by age class in blue sharks **(A,B)** and porbeagles **(C,D)**. Numbers at the top of each boxplot in **(A,C)** indicate the number of samples analyzed $\delta^{13}C$ for each age class; the same numbers were analyzed for $\delta^{15}N$. Gray vertical lines represent age at birth (0 years) and at maturity (5 and 13 years for blue sharks and porbeagles, respectively) and separate pre-birth (PB), juvenile (JUV), and adult (AD) life-history stages. Age classes are not plotted for samples in the PB stage as Von Bertalanffy growth curves are not applicable to back-calculate age during this stage.

life history-normalized PC1 scores for $\delta^{13}C$ values of essential amino acids ($PC1_{n-EAA}$) were observed across blue sharks and porbeagles (**Figure 5**). In blue sharks, $PC1_{n-EAA}$ (hence $\delta^{13}C_{EAA}$) values were highest in the pre-birth stage, decreased sharply around birth and increased progressively during juvenile and early adult growth but did not show any clear trend in the late adult stage (**Figure 5A**). Adult $PC1_{n-EAA}$ values were generally comparable to pre-birth levels, except for some age classes. In porbeagles, $PC1_{n-EAA}$ scores decreased during juvenile growth until an age of ~6–7 years, possibly increased back until 11–12 years of age, but showed no clear patterns in subadult and adult stages (**Figure 5C**). Scores of $PC1_{n-EAA}$ were highest in the pre-birth stage and decreased after birth.

Non-essential Amino Acids

PC1 and PC2 explained 45% and 22% of the total variance in $\delta^{13}C_{non-EAA}$ values, respectively (**Supplementary Figures 14C,D**). Most positive PC1 scores corresponded to most positive $\delta^{13}C$ values of all non-essential amino acids except aspartic acid; most positive PC2 were associated with most positive values of alanine and most negative values of glutamic acid and aspartic acid. Blue sharks had generally more negative PC1 scores for $\delta^{13}C_{non-EAA}$ values than porbeagles but more positive PC2 scores (except individual 1000; **Supplementary Figures 14C,D**). Individuals from the central and eastern North Atlantic had more negative PC1 and PC2 than Northwest Atlantic sharks in both species. Ontogenetic patterns in PC1

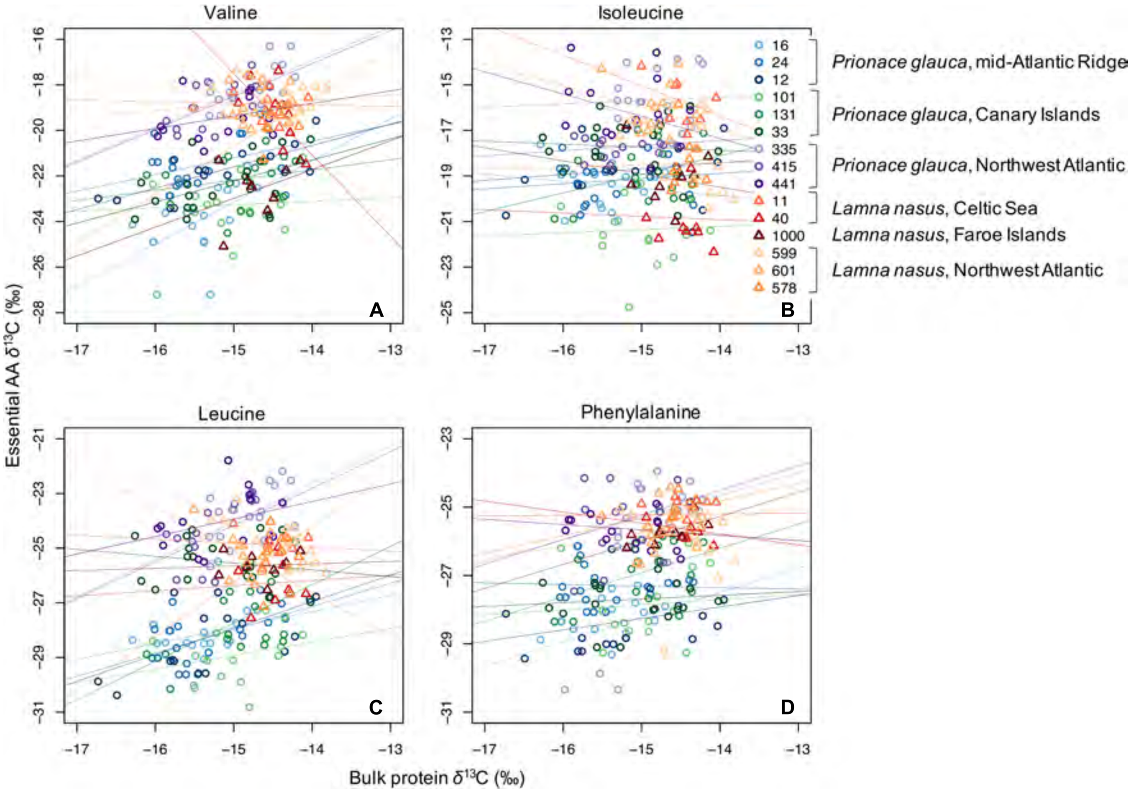

FIGURE 3 | Scatterplots of raw δ^{13}C values of bulk protein vs. single essential amino acids (**A**, valine; **B**, isoleucine; **C**, leucine; and **D**, phenylalanine) in comparable vertebral samples from individual blue sharks and porbeagles caught across the North Atlantic (as in figure legend).

scores for $\delta^{13}C_{non-EAA}$ values were similar to patterns in $\delta^{13}C_{EAA}$ (**Figures 5B–D** and **Supplementary Figure 15**) with additional influences of aspartic acid (**Supplementary Figures 14C,D**; see also **Figure 4D** and **Supplementary Figure 12**).

Spacing Between Glycolytic and Krebs Cycle Amino Acids

In general, broad ontogenetic patterns in life history-normalized values of spacing in δ^{13}C values between pairs of glycolytic and Krebs cycle amino acids (glycine and glutamic acid compared to alanine and proline, respectively) did not match those in bulk protein δ^{13}C values (**Figure 6**). In blue sharks, spacing between both pairs of amino acids decreased slightly around birth and increased during juvenile growth, then remained relatively constant in late juvenile and adult stages (**Figures 6A,B**). In porbeagles, spacing between both amino acid pairs showed systematic patterns, with a sharp increase associated with birth and early juvenile stages, followed by broadly U-shaped profiles before declining in the most recent samples (**Figures 6C,D**). The precise timing of transitions in these profiles differed slightly between the two amino acid pairs. More or less pronounced excursions in spacing between glycolytic and Krebs cycle amino acids were observed through ontogeny in all sharks (**Supplementary Figure 16**). In general, excursions in spacing between independent pairs of amino acids showed relatively strong covariation, with a few exceptions. In many cases, excursions in spacing coincided with those in bulk protein δ^{13}C and/or δ^{15}N values.

DISCUSSION

This study aimed to test inferences about life-history movements drawn from ontogenetic patterns in bulk collagen δ^{13}C and δ^{15}N values in shark vertebrae using complementary data for single amino acid δ^{13}C values. The study is based on a small number of individuals (nine blue sharks and six porbeagles) with highly variable isotope chronologies. We were therefore obviously unable to infer species- or population-level behavioral or ecological patterns from these data. Below we discuss possible interpretations of aspects of shark spatial and trophic ecology based on bulk protein isotopic life-histories and the extent to which these may be supported, contradicted or refined based on amino acid δ^{13}C patterns.

Inferences Based on Patterns in Bulk Protein

Bulk protein δ^{13}C and δ^{15}N values in blue sharks, normalized by life-history, showed a common pattern of increasing values during juvenile growth (**Figures 2A,B**), despite relatively high variation in individual profiles (**Supplementary Figures 4A–I**).

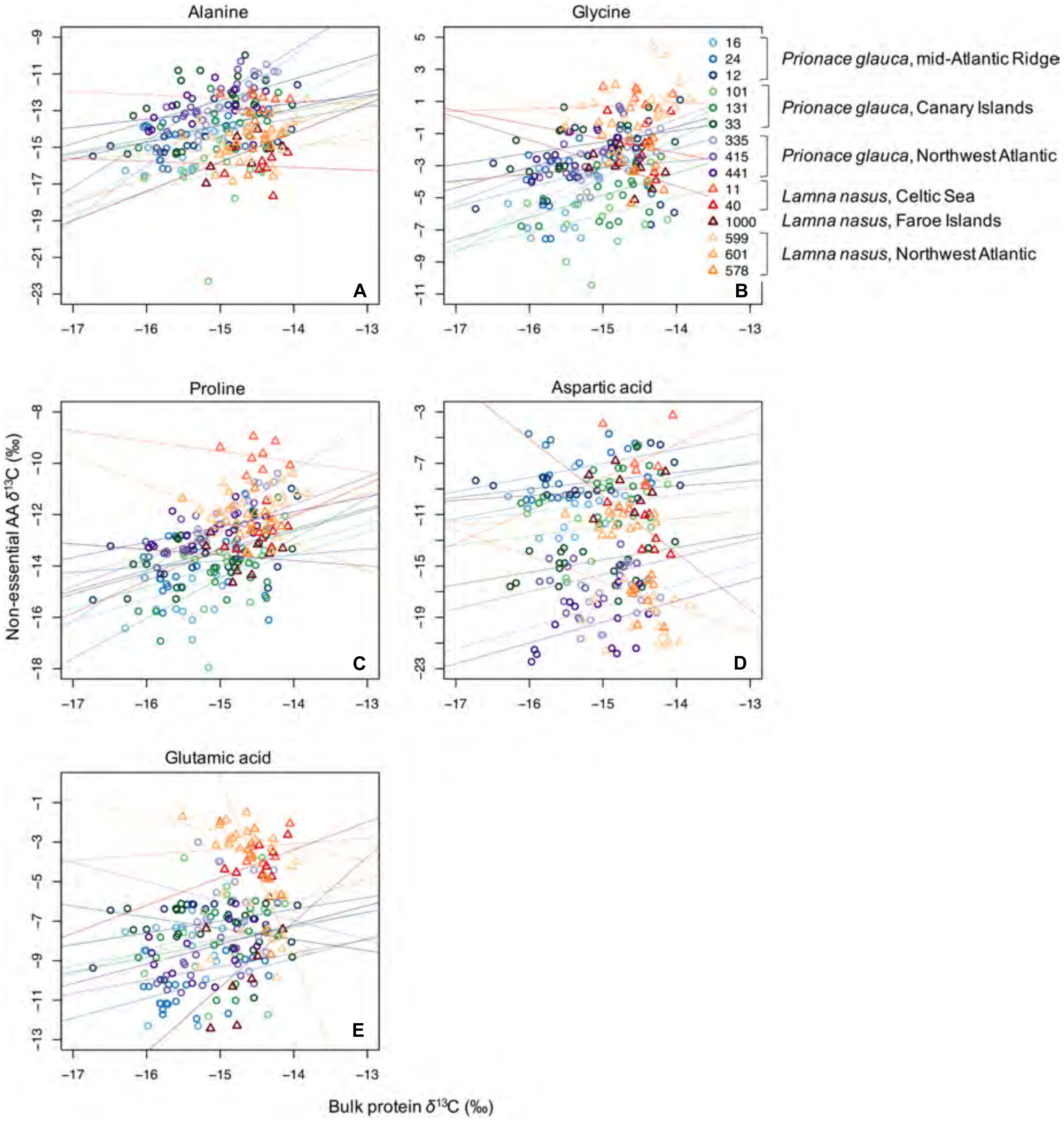

FIGURE 4 | Scatterplots of raw $\delta^{13}C$ values of bulk protein vs. single non-essential amino acids (**A**, alanine; **B**, glycine; **C**, proline; **D**, aspartic acid; and **E**, glutamic acid) in comparable vertebral samples from individual blue sharks and porbeagles caught across the North Atlantic (as in figure legend).

Increases in $\delta^{13}C$ values in marine animals are commonly interpreted as baseline effects resulting from increased use of warmer waters closer to the equator (McMahon et al., 2013; Magozzi et al., 2017) and/or more coastal foodwebs with higher levels of primary production (O'Learly, 1981; Miller et al., 2008). Increases in $\delta^{13}C$ values could also reflect increases in trophic position, however the lack of a corresponding trend in $\delta^{15}N$ values in blue sharks implies that trophic level-change alone could not explain the $\delta^{13}C$ pattern. In the eastern North Atlantic in particular, blue sharks are believed to be primarily oceanic sharks (Vandeperre et al., 2014, 2016; Coelho et al., 2018), therefore ontogenetic trends in bulk protein $\delta^{13}C$ values in blue sharks are likely to be interpreted as reflecting a life-history migration resulting in increased use of resources from relatively warm southern locations through the juvenile and early adult life stages. In the Northwest Atlantic, juveniles are often observed near the shelf, particularly in summer, meaning that isotopic signals in the juvenile stages could as well be influenced by coastal processed. The increase in $\delta^{15}N$ values during juvenile growth and subsequent decrease in the adult stage (**Figure 2B**) is also consistent with baseline effects associated with an increasing dependence on resources living in warmer waters (McMahon et al., 2013; Schmittner and Somes, 2016) rather than a strong ontogenetic trophic shift.

Ontogenetic profiles in bulk protein δ^{13}C and δ^{15}N values in porbeagles are considerably more challenging to interpret compared to blue sharks. Life history-normalized bulk protein δ^{13}C values displayed a minor ontogenetic increase with approximately half of the range seen in blue sharks, and high among-individual variance in both early and late juvenile life stages (**Figure 2C**). Bulk protein δ^{15}N values were relatively flat until the late juvenile stage, when a pronounced step increase was observed (**Figure 2D**). Similar to blue sharks, the ontogenetic profiles in bulk protein δ^{13}C values in porbeagles may imply a gradual increase in reliance on resources with higher δ^{13}C values (e.g., closer to the equator and/or more coastal resources) throughout juvenile growth but with a high degree of among-individual variance. The step increase in δ^{15}N values in late juvenile stages may potentially be linked to a change in diet or trophic level as inferred for other lamnid sharks (Estrada et al., 2006; Kerr et al., 2006), as there is no clear association with δ^{13}C values that might imply a habitat shift. Such a step increase in δ^{15}N values was, however, only observed in individuals from the Northwest Atlantic (**Supplementary Figures 4M–O**), possibly suggesting a delay in trophic shift in the Northeast Atlantic population, movement across larger nitrogen isoscapes in the eastern part of the basin, and/or differences in age estimation models not accounted for here.

In summary, bulk protein profiles in blue sharks may be interpreted as suggesting common ontogenetic changes in space use, toward greater use of oceanic and warmer waters with increasing age. For porbeagle sharks, a lack of clear, consistent, isotopic patterns, and a relatively small increase in δ^{13}C values, would likely imply no strong, common ontogenetic trend in space use, and potentially location- and population-specific variations in life-history movements.

Testing Inferences With Essential Amino Acids

Essential amino acids can only be synthesized by primary producers and bacteria, and must be acquired by consumers directly through the diet. Variations in bulk tissue isotope values reflecting horizontal movements should therefore be replicated consistently in the δ^{13}C values of essential amino acids, without confounding influences from trophic discrimination and physiology (Reeds, 2000; McMahon et al., 2010).

In blue sharks, at least a component of the positive ontogenetic trend in bulk protein δ^{13}C values was matched by a common ontogenetic pattern of increasing δ^{13}C values of essential amino acids (**Figure 5A**). Inferences drawn from bulk protein δ^{13}C values are therefore supported by patterns in δ^{13}C values of essential amino acids. That is, the ontogenetic increase in bulk protein δ^{13}C values observed in these sharks during juvenile and early adult growth can be explained by progressively increased dependence on resources from waters characterized by more positive δ^{13}C baselines (e.g., warmer waters). The interpretation of a life-history migration to southern waters is consistent with results from satellite-tagging studies in the eastern North Atlantic, which indicate that juvenile and subadult blue sharks conduct seasonal movements between temperate and subtropical waters (Queiroz et al., 2010; Vandeperre et al., 2014; see also Campana et al., 2011), whereas adult sharks undertake a directional migration to tropical waters possibly associated with parturition and pupping (Vandeperre et al., 2014, 2016; Coelho et al., 2018).

Maternal δ^{13}C values of essential amino acids were higher than post-partum values and comparable to adult levels (**Figure 5A**) as seen in bulk protein δ^{13}C values, indicating that pupping might occur in isotopically distinct areas with more negative δ^{13}C baselines than those used by the mothers while provisioning eggs and by adult sharks. Adult δ^{13}C values of essential amino acids approached maternal levels by ~5–6 years of age, which approximately corresponds to the onset of maturity in blue sharks (Pratt, 1979; Skomal and Natanson, 2003).

In stark contrast to observations in blue sharks and bulk collagen values, δ^{13}C values of essential amino acids in porbeagles, expressed as life history-normalized $\mathrm{PC1}_{\mathrm{EAA}}$ scores, decreased during juvenile growth until an age of ~6–7 years (**Figure 5C**). Assuming that essential amino acids reflect baseline conditions, this trend implies a common trend of increasing assimilation of carbon from prey with low δ^{13}C values (e.g., resources from offshore and/or colder waters), as the sharks grow. The interpretation of porbeagle isotopic life-histories based on bulk protein and essential amino acid δ^{13}C values are therefore difficult to reconcile. Porbeagles are believed to conduct an ontogenetic habitat shift from shelf to shelf-edge and oceanic environments (Bendall et al., 2013; Ellis and Bendall, 2015; Ellis et al., 2015; Biais et al., 2017), and have been shown to conduct extensive latitudinal migrations (Pade et al., 2009; Saunders et al., 2011; Biais et al., 2017). Contrasting patterns in bulk protein and essential amino acid δ^{13}C values could be possibly reconciled by an increasing trophic level, if trophic level increased sufficiently to raise δ^{13}C values to counteract the decrease in δ^{13}C values of essential amino acids. However, this was not supported by the trend in bulk collagen δ^{15}N values, which would be expected to be more sensitive to changes in trophic level. Satellite-tag data are therefore consistent with the interpretations based on patterns in essential amino acid δ^{13}C values (**Figure 5C**), not with those based on bulk protein δ^{13}C values.

Pre-partum δ^{13}C values reflected carbon assimilation during maternal provision and represented the highest values that were found across life-history (**Figure 5C**). This pattern suggests that pregnant female porbeagles may exploit isotopically distinct (more positive) foraging grounds compared to those used by subadult and adult sharks and is consistent with the observation of a directional movement to subtropical waters by tagged mature (presumably pregnant) females in the Northwest Atlantic (Campana et al., 2010; see also Natanson et al., 2019).

Additional Inferences Drawn From Non-essential Amino Acids

Ontogenetic profiles in PC1 scores for δ^{13}C values of non-essential amino acids in blue sharks also showed a common

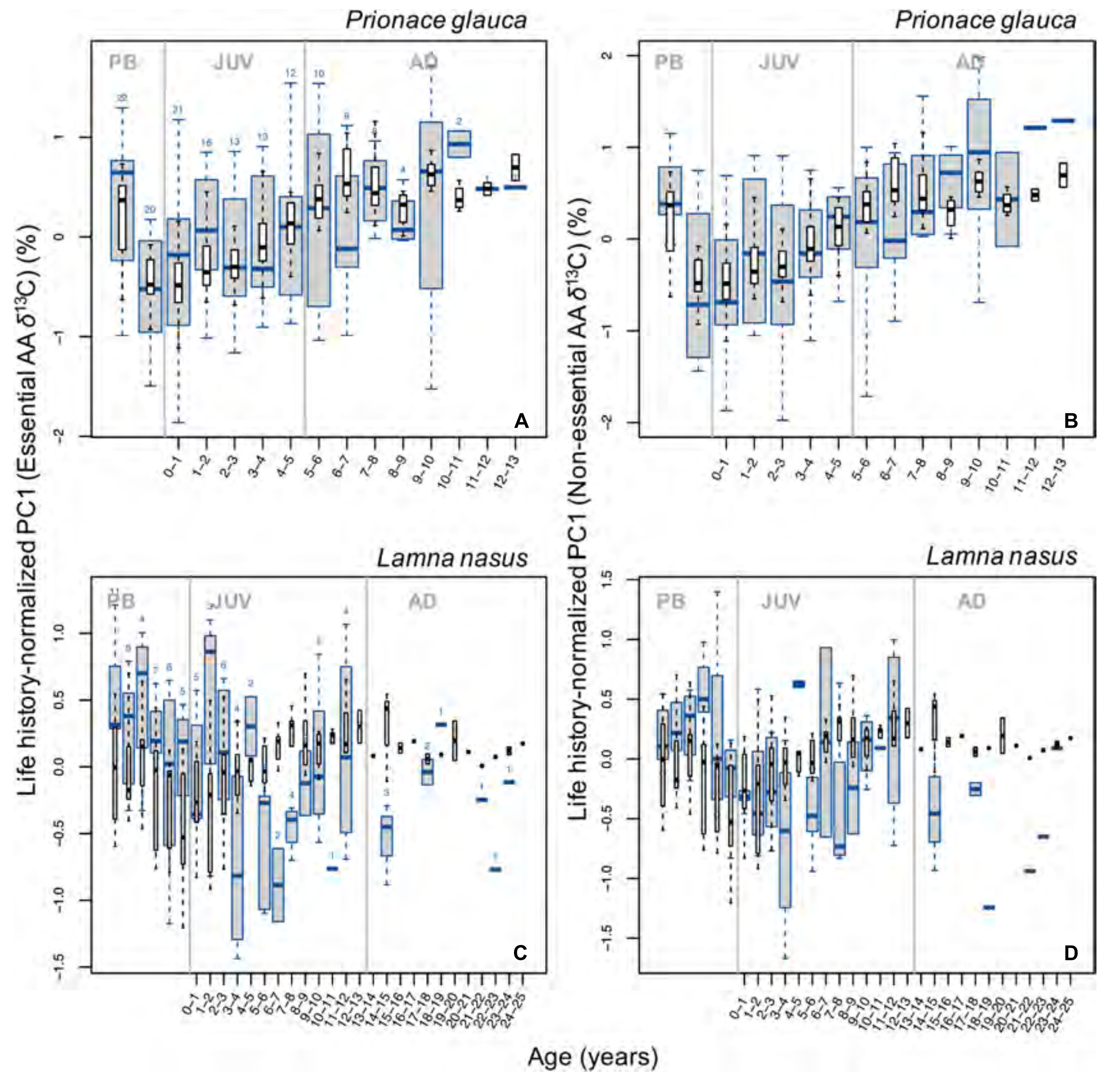

FIGURE 5 | Boxplots (in blue) of life history-normalized PC1 values from PCAs with $\delta^{13}C$ values of essential **(A,C)** and non-essential **(B,D)** amino acids by age class in blue sharks **(A,B)** and porbeagles **(C,D)**. Boxplots (in black) of life history-normalized $\delta^{13}C$ values of bulk protein are overlain for comparison. Figure description is the same as for **Figure 2**.

increase (**Figure 5B**), consistent with a baseline effect expressed in both essential and non-essential amino acids. As all non-essential amino acids are influenced by baseline effects, the isotopic spacing in $\delta^{13}C$ values between glycolytic and Krebs cycle amino acids to some extent controls for the baseline influence (assuming that the rate of incorporation of newly ingested carbon is consistent between the two amino acids). For blue sharks, observed ontogenetic patterns in life history-normalized isotopic spacing varied among individuals resulting in no clear common trend (**Figures 6A,B** and **Supplementary Figures 16A–I**). This pattern also suggests that the common signal seen in bulk protein $\delta^{13}C$ values in blue sharks is largely controlled by baseline spatial influences rather than dietary and/or physiological effects.

Ontogenetic trends in life history-normalized PC1 scores for $\delta^{13}C$ values of non-essential amino acids in porbeagles are unclear (**Figure 6D**) but ontogenetic profiles of normalized spacing in $\delta^{13}C$ values between glycolytic and Krebs cycle amino acids show consistent, systematic trends with a strong increase after birth, followed by U-shaped patterns throughout juvenile growth (**Figures 6C,D** and **Supplementary Figures 16J–O**). The biochemical or nutritional mechanisms underpinning differences in isotopic spacing between non-essential amino acids remain uncertain. However, the presence of systematic trends in isotopic spacing between amino acids assumed to be responsive to differences in macronutrient (lipid and protein) assimilation and use (Wolf et al., 2015; Wang et al., 2018, 2019) implies that amino acid isotope data hold information associated with individual nutrition, and that bulk protein $\delta^{13}C$ values may be very difficult to interpret reliably.

Therefore, we suggest that in porbeagles relatively minor isotopic variability associated with ontogenetic transitions between juvenile foraging in more coastal, shelf waters

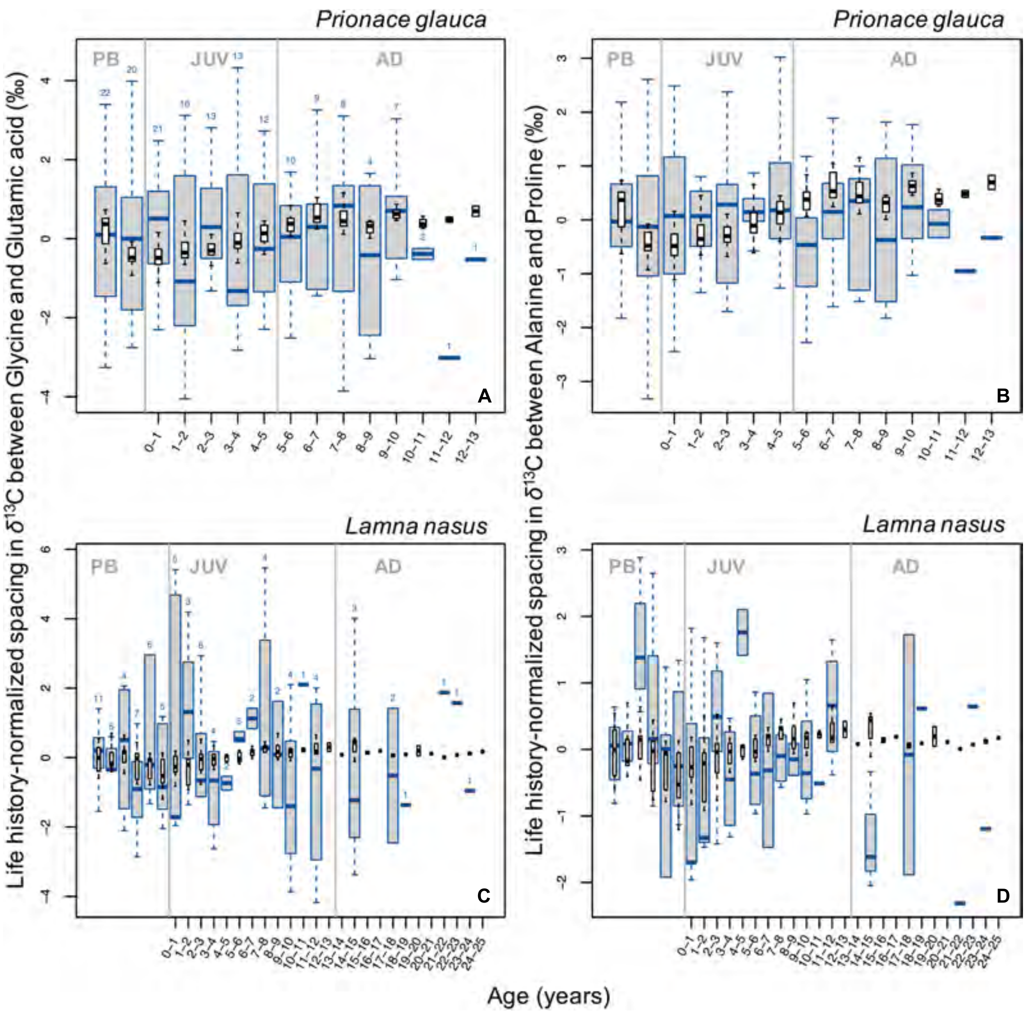

FIGURE 6 | Boxplots (in blue) of life history-normalized spacing in δ^{13}C values between independent pairs of glycolytic (lipid-derived) and Krebs cycle (lipid+protein-derived) amino acids (**A,C,** glycine and glutamic acid; **B,D** alanine and proline) by age class in blue sharks **(A,B)** and porbeagles **(C,D)**. Boxplots (in black) of life history-normalized δ^{13}C values of bulk protein are overlain for comparison. Figure description is the same as for **Figure 2**.

and greater dependence on cooler, offshore and slope environments in adult stages are masked in bulk protein δ^{13}C values by individual variation and by physiological influences potentially associated with differential use of lipid and protein macronutrients. In contrast, common ontogenetic movement transitions across latitudinal gradients in δ^{13}C values in blue sharks are large enough to be clearly expressed in bulk protein δ^{13}C values and overwhelm any shared ontogenetic trends in macronutrient use.

CONCLUSION

SIA can provide a useful complement to satellite archival tags to study the movements of pelagic sharks throughout their lives. However, bulk tissue isotopic signals are often confounded by mixed baseline, trophic and physiological effects. Compound-specific analyses of individual amino acids may be required to disentangle these effects, aiding interpretations of bulk tissue isotope data to infer migration histories.

In this study we analyzed an average of 22 samples from each shark. Assuming that the cost of bulk isotope analysis is $10 per sample, high-resolution analysis of an individual costs $160–280. The cost of compound-specific isotope analysis is approximately 10 times that of traditional bulk analysis, and resources and expertise associated with sample preparation and analysis are significantly greater. Additionally, compound-specific analysis requires more sample material, resulting in decreased temporal resolution for longitudinal ecological information. A cost- and time-effective combination of bulk and compound-specific SIA, whereby individual amino acid analyses are used to test hypotheses generated from high-resolution or multiple-individual studies of bulk tissue analyses, may represent an acceptable compromise to complement tag-derived movement information.

Despite the small number of individuals examined here, and large among-individual variability in isotopic profiles, we found evidence of common, broad ontogenetic isotope patterns in blue sharks. Such isotopic life-histories appeared to be somewhat associated with ontogenetic movement across isotopically distinct baselines, despite additional influences from trophic and physiological effects. Given the large intra- and inter-individual isotopic variability we observed, these findings should, of course, be tested by increasing the sample size but, if verified, could imply a shared vulnerability of each species across life-history to fishery capture. Furthermore, comparisons of maternal and post-partum $\delta^{13}C$ values provided information on transgenerational movements and suggested that blue sharks and porbeagles might adopt different strategies for parturition and pupping, based on the analyzed individuals of each species.

Our study contributes to a growing body of work illustrating the biochemical complexity that can underpin variations in bulk tissue stable isotope compositions. Inferences drawn from bulk tissue isotope data may be relatively robust in situations where the behavior of the animal results in a consistent change in the isotopic composition of all or many macronutrients, such as a directed migration across large spatial isotopic gradients. In such cases, isotopic variation in ingested nutrients is pervasively expressed during metabolic processing, and is likely to overwhelm superimposed isotopic variation associated with more subtle changes in metabolic routing. However, where variance in bulk isotope compositions is more closely related to variations in macronutrient processing and associated biochemical routing of metabolites, high levels of among- and within-individual variation are likely to significantly complicate interpretation of bulk tissue $\delta^{13}C$ values. In the case of porbeagles studied here, it is possible that apparent population-specific trends in bulk collagen $\delta^{13}C$ values were spurious co-incidences. Attempts to interpret such trends to infer aspects of life-history ecology are therefore dangerous. We suggest that single amino acid analyses offers one of the few options to test such inferences independently.

Future research should explore how spatio-temporal variation in isotopic baselines, migration and tissue isotopic discrimination interact to influence tissue isotopic compositions in pelagic sharks. Such space-time isotope dynamics can be explored using a simulation modeling framework combining isoscape models, agent-based models of behavior and movement, and physiology-biochemistry models (e.g., Carpenter-Kling et al., 2019; Trueman et al., 2019; Magozzi et al., 2020). Furthermore, additional controlled-feeding experiments such as those by Wang et al. (2019) are required to better constrain trophic and physiological influences on $\delta^{13}C$ values of non-essential amino acids.

DATA AVAILABILITY STATEMENT

The original contributions presented in the study are included in the article/**Supplementary Material**, further inquiries can be directed to the corresponding author.

ETHICS STATEMENT

Ethical review and approval was not required for the animal study because the study examined vertebral samples from dead sharks that were bycaught by longline fisheries primarily targeting tuna and swordfish.

AUTHOR CONTRIBUTIONS

SM led the research and wrote the manuscript. VB, SH, GM, LN, NQ, and MS provided the shark vertebral samples. LH provided advice on sample preparation and compound-specific isotope analysis. CT and ST advised on data analysis and interpretation. All authors contributed critically to the manuscript drafts and gave final approval for publication.

FUNDING

The internship of SM at the Woods Hole Oceanographic Institution was funded by the School of Ocean and Earth Science at University of Southampton. Stable isotope analyses were paid by CT and ST research budgets and SM Ph.D. and placement funding.

ACKNOWLEDGMENTS

We would like to thank the School of Ocean and Earth Science at University of Southampton for supporting the participation of SM to the Woods Hole Exchange Program; during such exchange program SM prepared and analyzed shark vertebral samples for isotopes in individual amino acids. We would also like to thank Greg Skomal for sharing knowledge on blue shark and porbeagle ecology and providing advice on sample collection.

SUPPLEMENTARY MATERIAL

The Supplementary Material for this article can be found online at: https://www.frontiersin.org/articles/10.3389/fmars.2021.673016/full#supplementary-material

REFERENCES

Bendall, V. J., Ellis, J. R., Hetherington, S. J., McCully, S. R., Righton, D., and Silva, J. F. (2013). Preliminary observations on the biology and movements of porbeagle *Lamna nasus* around the British Isles. *Collect. Vol. Sci. Pap.* 69, 1702–1722.

Berg, J. M., Stryer, L., Tymoczko, J. L., and Gatto, G. J. (2015). *Biochemistry*, 8th Edn. New York, NY: W. H. Freeman and Company.

Best, P. B., and Schell, D. M. (1996). Stable isotopes in southern right whale (*Eubalaena australis*) baleen as indicators of seasonal movements, feeding and growth. *Mar. Biol.* 124, 483–494. doi: 10.1007/bf00351030

Biais, G., Coupeau, Y., Seret, B., Calmettes, B., Lopez, R., Hetherington, S., et al. (2017). Return migration of porbeagle shark (*Lamna nasus*) in the Northeast Atlantic: implications for stock range and structure. *ICES J. Mar. Sci.* 74, 1268–1276. doi: 10.1093/icesjms/fsw233

Bird, C. S., Verissimo, A., Magozzi, S., Abrantes, K. G., Aguilar, A., Al-Reasi, H., et al. (2018). A global perspective on the trophic geography of sharks. *Nat. Ecol. Evol.* 2, 299–305.

Boecklen, W. J., Yarnes, C. T., Cook, B. A., and James, A. C. (2011). On the use of stable isotopes in trophic ecology. *Annu. Rev. Ecol. Evol. Syst.* 42, 411–440.

Bowyer, J. N., Qin, J. G., and Stone, D. A. (2013). Protein, lipid and energy requirements of cultured marine fish in cold, temperate, and warm water. *Rev. Aquacult.* 5, 10–32. doi: 10.1111/j.1753-5131.2012.01078.x

Briscoe, D. K., Maxwell, S. M., Kudela, R., Crowder, L. B., and Croll, D. (2016). Are we missing important areas in pelagic marine conservation? Redefining conservation hotspots in the ocean. *Endanger. Species Res.* 29, 229–237. doi: 10.3354/esr00710

Campana, S. E., Dorey, A., Fowler, M., Joyce, W., Wang, Z., Wright, D., et al. (2011). Migration pathways, behavioural thermoregulation and overwintering grounds of blue sharks in the Northwest Atlantic. *PLoS One* 6:e16854. doi: 10.1371/journal.pone.0016854

Campana, S. E., Joyce, W. N., and Fowler, M. (2010). Subtropical pupping ground for a cold-water shark. *Can. J. Fish. Aquat. Sci.* 67, 769–773. doi: 10.1139/f10-020

Carlisle, A. B., Goldman, K. J., Litvin, S. Y., Madigan, D. J., Bigman, J. S., Switherbank, A. M., et al. (2015). Stable isotope analysis of vertebrae reveals ontogenetic changes in habitat in an endothermic pelagic shark. *Proc. R. Soc. B Biol. Sci.* 282:20141446. doi: 10.1098/rspb.2014.1446

Carpenter-Kling, T., Pistorius, P., Connan, M., Reisinger, R., Magozzi, S., and Trueman, C. N. (2019). Sensitivity of δ13C values of seabird tissues to combined spatial, temporal and ecological drivers: a simulation approach. *J. Exp. Mar. Biol. Ecol.* 512, 12–21. doi: 10.1016/j.jembe.2018.12.007

Cherel, Y., Kernaleguen, L., Richard, P., and Guinet, C. (2009). Whisker isotopic signature depicts migration patterns and multi-year intra- and inter-individual foraging strategies in fur seals. *Biol. Lett.* 5, 830–832. doi: 10.1098/rsbl.2009.0552

Chikaraishi, Y., Ogawa, N. O., Kashiyama, Y., Takano, Y., Suga, H., Tomitani, A., et al. (2009). Determination of aquatic food-web structure based on compound-specific nitrogen isotopic composition of amino acids. *Limnol. Oceanogr.* 7, 740–750. doi: 10.4319/lom.2009.7.740

Chikaraishi, Y., Steffan, S. A., Ogawa, N. O., Ishikawa, N. F., Sasaki, Y., Tsuchiya, M., et al. (2014). High-resolution food webs based on nitrogen isotopic composition of amino acids. *Ecol. Evol.* 4, 2423–2449. doi: 10.1002/ece3.1103

Choy, K., Smith, C. I., Fuller, B. T., and Richards, M. P. (2010). Investigation of amino acid δ13C signatures in bone collagen to reconstruct human palaeodiets using liquid chromatography-isotope ratio mass spectrometry. *Geochim. Cosmochim. Acta* 74, 6093–6111. doi: 10.1016/j.gca.2010.07.025

Christiansen, H. M., Hussey, N. E., Wintner, S. P., Cliff, G., Dudley, S. F. J., and Fisk, A. T. (2014). Effect of sample preparation techniques for carbon and nitrogen stable isotope analysis of hydroxyapatite structures in the form of elasmobranch vertebral centra. *Rapid Commun. Mass Spectrom.* 28, 448–456. doi: 10.1002/rcm.6801

Coelho, R., Macías, D., Ortiz De Urbina, J., Martins, A., Monteiro, C., Lino, P. G., et al. (2020). Local indicators for global species: pelagic sharks in the tropical northeast Atlantic, Cabo Verde islands region. *Ecol. Indic.* 110:105942. doi: 10.1016/j.ecolind.2019.105942

Coelho, R., Mejuto, J., Domingo, A., Yokawa, K., Kwang-Ming, L., Cortés, E., et al. (2018). Distribution patterns and population structure of blue shark (*Prionace glauca*) in the Atlantic and Indian Oceans. *Fish Fish.* 19, 90–106.

Costa, D. P., Breed, G. A., and Robinson, P. W. (2012). New insights into pelagic migrations: implications for ecology and conservation. *Annu. Rev. Ecol. Evol. Syst.* 43, 73–96. doi: 10.1146/annurev-ecolsys-102710-145045

DeNiro, M. J., and Epstein, S. (1978). Influence of diet on distribution of carbon isotopes in animals. *Geochim. Cosmochim. Acta* 42, 495–506. doi: 10.1016/0016-7037(78)90199-0

DeNiro, M. J., and Epstein, S. (1981). Influence of diet on the distribution of nitrogen isotopes in animals. *Geochim. Cosmochim. Acta* 45, 341–351. doi: 10.1016/0016-7037(81)90244-1

Ellis, J. R., and Bendall, V. A. (2015). *Preliminary Estimates of Bycatch Rates of Porbeagle Shark Lamna Nasus in Gillnet Fisheries in the Celtic Sea (ICES Divisions VIIf-h) and Associated Biological Observations*. Lisbon: WGEF.

Ellis, J. R., Bendall, V. J., Hetherington, S. J., Silva, J. F., and McCully Phillips, S. R. (2015). *National Evaluation of Populations of Threatened and Uncertain Elasmobranchs (NEPTUNE)*. Lowestoft: CEFAS.

Estrada, J. A., Rice, A. N., Natanson, L. J., and Skomal, G. B. (2006). Use of isotopic analysis of vertebrae in reconstructing ontogenetic feeding ecology in white sharks. *Ecology* 87, 829–834. doi: 10.1890/0012-9658(2006)87[829:uoiaov]2.0.co;2

Fernandes, R., Nadeau, M.-J., and Grootes, P. M. (2012). Macronutrient-based model for dietary carbon routing in bone collagen and bioapatite. *Archaeol. Anthropol. Sci.* 4, 291–301. doi: 10.1007/s12520-012-0102-7

Graham, B. S., Koch, P. L., Newsome, S. D., McMahon, K. W., and Aurioles, D. (2010). "). Using isoscapes to trace the movements and foraging behavior of top predators in oceanic ecosystems," in *Isoscapes: Understanding Movement, Pattern, and Process on Earth through Isotope Mapping*, eds J. B. West, G. J. Bowen, T. E. Dawson, and K. P. Tu (Berlin: Springer).

Hare, P. E., Fogel, M. L., Stafford, T. W., Mitchell, A. D., and Hoering, T. C. (1991). The isotopic composition of carbon and nitrogen in individual amino acids isolated from modern and fossil proteins. *J. Archaeol. Sci.* 18, 277–292. doi: 10.1016/0305-4403(91)90066-x

Hayes, J. M. (2001). Fractionation of carbon and hydrogen isotopes in biosynthetic processes. *Rev. Mineral. Geochem.* 43, 225–277. doi: 10.1515/9781501508745-006

Hobson, K. A. (1999). Tracing origins and migration of wildlife using stable isotopes: a review. *Oecologia* 120, 314–326. doi: 10.1007/s004420050865

Howland, M. R., Corr, L. T., Young, S. M. M., Jones, V., Jim, S., van der Merwe, N. J., et al. (2003). Expression of the dietary isotope signal in the compound-specific δ13C values of pig bone lipids and amino acids. *Int. J. Osteoarchaeol.* 13, 54–65. doi: 10.1002/oa.658

Hussey, N. E., MacNeil, M. A., Olin, J. A., McMeans, B. C., Kinney, M. J., Chapman, D. D., et al. (2012). Stable isotopes and elasmobranchs: tissue types, methods, applications and assumptions. *J. Fish Biol.* 80, 1449–1484. doi: 10.1111/j.1095-8649.2012.03251.x

Jim, S., Jones, V., Ambrose, S. H., and Evershed, R. P. (2006). Quantifying dietary macronutrient sources of carbon for bone collagen biosynthesis using natural abundance stable carbon isotope analysis. *Br. J. Nutr.* 95, 1055–1062. doi: 10.1079/bjn20051685

Kerr, L. A., Andrews, A. H., Cailliet, G. M., Brown, T. A., and Coale, K. H. (2006). Investigations of Δ14C, δ13C, and δ15N in vertebrae of white shark (*Carcharodon carcharias*) from the eastern North Pacific Ocean. *Environ. Biol. Fishes* 77, 337–353. doi: 10.1007/s10641-006-9125-1

Kim, S. L., and Koch, P. L. (2012). Methods to collect, preserve, and prepare elasmobranch tissues for stable isotope analysis. *Environ. Biol. Fishes* 95, 53–63. doi: 10.1007/s10641-011-9860-9

Larsen, T., Taylor, D. L., Leigh, M. B., and O'Brien, D. M. (2009). Stable isotope fingerprinting: a novel method for identifying plant, fungal, or bacterial origins of amino acids. *Ecology* 90, 3526–3535. doi: 10.1890/08-1695.1

Larsen, T., Ventura, M., Andersen, N., O'Brien, D. M., Piatkowski, U., and McCarthy, M. D. (2013). Tracing carbon sources through aquatic and terrestrial food webs using amino acid stable isotope fingerprinting. *PLoS One* 8:e73441. doi: 10.1371/journal.pone.0073441

Leigh, S. C., Papastamatiou, Y. P., and German, D. P. (2018). Seagrass digestion by a notorious 'carnivore'. *Proc. R. Soc.B Biol. Sci.* 285:20181583. doi: 10.1098/rspb.2018.1583

Lorrain, A., Graham, B., Menard, F., Popp, B., Bouillon, S., van Breugel, P., et al. (2009). Nitrogen and carbon isotope values of individual amino acids: a tool to study foraging ecology of penguins in the Southern Ocean. *Mar. Ecol. Prog. Ser.* 391, 293–306. doi: 10.3354/meps08215

Lorrain, A., Pethybridge, H., Cassar, N., Receveur, A., Allain, V., Bodin, N., et al. (2020). Trends in tuna carbon isotopes suggest global changes in pelagic phytoplankton communities. *Glob. Chang. Biol.* 26, 458–470. doi: 10.1111/gcb.14858

MacNeill, M. A., Skomal, G. B., and Fisk, A. T. (2005). Stable isotopes from multiple tissues reveal diet switching in sharks. *Mar. Ecol. Prog. Ser.* 302, 199–206. doi: 10.3354/meps302199

Magozzi, S. (2017). *Reconstructing Ontogenetic Movements in Pelagic Sharks Coupling Ocean Models and Stable Isotope Data in Incrementally Grown Tissues*. Ph. D. thesis. Southampton: University of Southampton.

Magozzi, S., Vander Zanden, H. B., Wunder, M. B., and Trueman, C. N. (2017). Using ocean models to predict spatial and temporal variation in marine carbon isotopes. *Ecosphere* 8:e01763.

Magozzi, S., Vander Zanden, H. B., Wunder, M. B., Trueman, C. N., Pinney, K., Peers, D., et al. (2020). Combining models of environment, behavior and physiology to predict tissue hydrogen and oxygen isotope variance among individual terrestrial animals. *Front. Ecol. Evol.* 8:536109. doi: 10.3389/fevo.2020.536109

McCarthy, M. D., Lehman, J., and Kudela, R. (2013). Compound-specific amino acid δ15N patterns in marine algae: tracer potential for cyanobacterial vs. eukaryotic organic nitrogen sources in the ocean. *Geochim. Cosmochim. Acta* 103, 104–120. doi: 10.1016/j.gca.2012.10.037

McMahon, K. W., Berumen, M. L., Mateo, I., Elsdon, T. S., and Thorrold, S. R. (2011a). Carbon isotopes in otolith amino acids identify residency of juvenile snapper (Family: Lutjanidae) in coastal nurseries. *Coral Reefs* 30, 1135–1145. doi: 10.1007/s00338-011-0816-5

McMahon, K. W., Fogel, M. L., Elsdon, T. S., and Thorrold, S. R. (2010). Carbon isotope fractionation of amino acids in fish muscle reflects biosynthesis and isotopic routing from dietary protein. *J. Anim. Ecol.* 79, 1132–1141. doi: 10.1111/j.1365-2656.2010.01722.x

McMahon, K. W., Fogel, M. L., Johnson, B. J., Houghton, L. A., and Thorrold, S. R. (2011b). A new method to reconstruct fish diet and movement patterns from δ13C values in otolith amino acids. *Can. J. Fish. Aquat. Sci.* 68, 1330–1340. doi: 10.1139/f2011-070

McMahon, K. W., Hamady, L. L., and Thorrold, S. R. (2013). A review of ecogeochemistry approaches to estimating movements of marine animals. *Limnol. Oceanogr.* 58, 697–714. doi: 10.4319/lo.2013.58.2.0697

McMahon, K. W., McCarthy, M. D., Sherwood, O. A., Larsen, T., and Guilderson, T. P. (2015a). Millennial- scale plankton regime shifts in the subtropical North Pacific Ocean. *Science* 350, 1530–1533. doi: 10.1126/science.aaa9942

McMahon, K. W., Polito, M. J., Abel, S., McCarthy, M. D., and Thorrold, S. R. (2015b). Carbon and nitrogen isotope fractionation of amino acids in an avian marine predator, the gentoo penguin (*Pygoscelis papua*). *Ecol. Evol.* 5, 1278–1290. doi: 10.1002/ece3.1437

Miller, T. W., Brodeur, R. D., and Rau, G. H. (2008). Carbon stable isotopes reveal relative contribution of shelf-slope production to the Northern California Current pelagic community. *Limnol. Oceanogr.* 53, 1493–1503. doi: 10.4319/lo.2008.53.4.1493

Natanson, L. J., Deacy, B. M., Joyce, W., and Sulikowski, J. (2019). Presence of a resting population of female porbeagles (*Lamna nasus*), indicating a biennial reproductive cycle, in the western North Atlantic. *Fish. Bull.* 117, 70–77. doi: 10.7755/fb.117.1-2.8

Natanson, L. J., Mello, J. J., and Campana, S. E. (2002). Validated age and growth of the porbeagle shark, *Lamna nasus*, in the western North Atlantic Ocean. *Collect. Vol. Sci. Pap. ICCAT* 54, 1261–1279.

Newsome, S. D., Clementz, M. T., and Koch, P. L. (2010). Using stable isotope biogeochemistry to study marine mammal ecology. *Mar. Mamm. Sci.* 26, 509–572.

Newsome, S. D., Etnier, M. A., Monson, D. H., and Fogel, M. L. (2009). Retrospective characterization of ontogenetic shifts in killer whale diets via δ13C and δ15N analysis of teeth. *Mar. Ecol. Prog. Ser.* 374, 229–242. doi: 10.3354/meps07747

Newsome, S. D., Fogel, M. L., Kelly, L., and Martinez del Rio, C. (2011). Contribution of direct incorporation from diet and microbial amino acids to protein synthesis in *Nile tilapia*. *Funct. Ecol.* 25, 1051–1062. doi: 10.1111/j.1365-2435.2011.01866.x

Newsome, S. D., Wolf, N., Peters, J., and Fogel, M. L. (2014). Amino acid δ13C analysis shows flexibility in the routing of dietary protein and lipids to the tissue of an omnivore. *Integr. Comp. Biol.* 54, 890–902. doi: 10.1093/icb/icu106

O'Learly, M. H. (1981). Carbon isotope fractionation in plants. *Phytochemistry* 20, 553–567. doi: 10.1016/0031-9422(81)85134-5

Pacoureau, N., Rigby, C. L., Kyne, P. M., Sherley, R. B., Winker, H., Carlson, J. K., et al. (2021). Half a century of global decline in oceanic sharks and rays. *Nature* 598, 567–571. doi: 10.1038/s41586-020-03173-9

Pade, N. G., Queiroz, N., Humphries, N. E., Witt, M. J., Jones, C. S., Noble, L. R., et al. (2009). First results from satellite-linked archival tagging of porbeagle shark, *Lamna nasus*: area fidelity, wider-scale movements and plasticity in diel depth changes. *J. Exp. Mar. Biol. Ecol.* 370, 64–74. doi: 10.1016/j.jembe.2008.12.002

Pethybridge, H., Choy, C. A., Logan, J. M., Allain, V., Lorrain, A., Bodin, N., et al. (2018). A global meta-analysis of marine predator nitrogen stable isotopes: relationships between trophic structure and environmental conditions. *Glob. Ecol. Biogeogr.* 27, 1043–1055. doi: 10.1111/geb.12763

Pinheiro, J. C., and Bates, D. M. (2000). *Mixed Effect Models in S and S-Plus*. New York, NY: Springer.

Popp, B. N., Graham, B. S., Olson, R. J., Hannides, C. C. S., Lott, M. J., Lopez-Ibarra, G. A., et al. (2007). "Insight into the trophic ecology of yellowfin tuna, Thunnus albacares, from compound-specific nitrogen isotope analysis of proteinaceous amino acids," in *Stable Isotopes as Indicators of Ecological Change*, eds T. Dawson and R. Siegwolf (Amsterdam: Elsevier).

Post, D. M. (2002). Using stable isotopes to estimate trophic position: models, methods, and assumptions. *Ecology* 83, 703–718. doi: 10.1890/0012-9658(2002)083[0703:usitet]2.0.co;2

Pratt, H. L. Jr. (1979). Reproduction in the blue shark, *Prionace glauca*. *Fish. Bull.* 77, 445–470.

Queiroz, N., Humphries, N. E., Couto, A., Vedor, M., da Costa, I., Sequeira, A. M. M., et al. (2019). Global spatial risk assessment of sharks under the footprint of fisheries. *Nature* 572, 461–466.

Queiroz, N., Humphries, N. E., Mucientes, G., Hammerschlag, N., Lima, F. P., Scales, K. L., et al. (2016). Ocean-wide tracking of pelagic sharks reveals extent of overlap with longline fishing hotspots. *Proc. Natl. Acad. Sci. U.S.A.* 113, 1582–1587. doi: 10.1073/pnas.1510090113

Queiroz, N., Humphries, N. E., Noble, L. R., Santos, A. M., and Sims, D. W. (2010). Short-term movements and diving behaviour of satellite-tracked blue sharks *Prionace glauca* in the northeastern Atlantic Ocean. *Mar. Ecol. Prog. Ser.* 406, 265–279. doi: 10.3354/meps08500

R Core Team (2019). *R: A Language and Environment for Statistical Computing*. Vienna: R Foundation for Statistical Computing.

Reeds, P. (2000). Dispensable and indispensable amino acids for humans. *J. Nutr.* 130, 1835S–1840S.

Saunders, R. A., Royer, F., and Clarke, M. W. (2011). Winter migration and diving behaviour of porbeagle shark, *Lamna nasus*, in the North East Atlantic. *ICES J. Mar. Sci.* 68, 166–174. doi: 10.1093/icesjms/fsq145

Schmittner, A., and Somes, C. J. (2016). Complementary constraints from carbon (13C) and nitrogen (15N) isotopes on the Glacial Ocean's soft-tissue biological pump. *Paleoceanography* 31, 625–913.

Seminoff, J. A., Benson, S. R., Arthur, K. E., Eguchi, T., Dutton, P. H., Tapilatu, R. F., et al. (2012). Stable isotope tracking of endangered sea turtles: validation with satellite telemetry and δ15N analysis of amino acids. *PLoS One* 7:e37403. doi: 10.1371/journal.pone.0037403

Skomal, G. B., and Natanson, L. J. (2003). Age and growth of the blue shark (*Prionace glauca*) in the North Atlantic Ocean. *Fish. Bull.* 101, 627–639.

Trueman, C. N., Jackson, A. L., Chadwick, K. S., Coombs, E. J., Freyer, L. J., Magozzi, S., et al. (2019). Combining simulation modeling and stable isotope analyses to reconstruct the last known movements of one of Nature's giants. *PeerJ* 7:e7912. doi: 10.7717/peerj.7912

Trueman, C. N., MacKenzie, K. M., and Palmer, M. R. (2012). Identifying migrations in marine fishes through stable isotope analysis. *J. Fish Biol.* 81, 826–847. doi: 10.1111/j.1095-8649.2012.03361.x

Trueman, C. N., McGill, R. A. R., and Guyard, P. H. (2005). The effect of growth rate on tissue-diet isotopic spacing in rapidly growing animals. An experimental study with Atlantic salmon (*Salmo salar*). *Rapid Commun. Mass Spectrom.* 19, 3239–3247. doi: 10.1002/rcm.2199

Trueman, C. N., and St John Glew, K. (2019). "Isotopic tracking of marine animal movement," in *Tracking Animal Migration with Stable Isotopes*, eds K. A. Hobson and L. I. Wassenaar (Cambridge: Academic Press).

Tuross, N., Fogel, M. L., and Hare, P. E. (1988). Variability in the preservation of the isotopic compositions of collagen from fossil bone. *Geochim. Cosmochim. Acta* 52, 929–935. doi: 10.1016/0016-7037(88)90364-x

Vandeperre, F., Aires-da-Silva, A., Fontes, J., Santos, M., Santos, R. S., and Afonso, P. (2014). Movements of blue sharks (*Prionace glauca*) across their life history. *PLoS One* 9:e103538. doi: 10.1371/journal.pone.0103538

Vandeperre, F., Aires-da-Silva, A., Lennert-Cody, C. E., Serrao Santos, R., and Afonso, P. (2016). Essential pelagic habitat of juvenile blue shark (*Prionace glauca*) inferred from telemetry data. *Limnol. Oceanogr.* 61, 1605–1625. doi: 10.1002/lno.10321

Wang, Y. V., Wan, A. H. L., Krogdahl, A., Johnson, M., and Larsen, T. (2019). 13C values of glycolytic amino acids as indicators of carbohydrate utilization in carnivorous fish. *PeerJ* 7:e7701. doi: 10.7717/peerj.7701

Wang, Y. V., Wan, A. H. L., Lock, E.-J., Andersen, N., Winter-Schuh, C., and Larsen, T. (2018). Know your fish: a novel compound-specific isotope approach for tracing wild and farmed salmon. *Food Chem.* 256, 380–389. doi: 10.1016/j.foodchem.2018.02.095

Whiteman, J. P., Kim, S. L., McMahon, K. W., Koch, P. L., and Newsome, S. D. (2018). Amino acid isotope discrimination factors for a carnivore: physiological insights from leopard sharks and their diet. *Oecologia* 188, 977–989. doi: 10.1007/s00442-018-4276-2

Wolf, N., Newsome, S. D., Peters, J., and Fogel, M. L. (2015). Variability in the routing of dietary proteins and lipids to consumer tissues influences tissue-specific isotopic discrimination. *Rapid Commun. Mass Spectrom.* 29, 1448–1456. doi: 10.1002/rcm.7239

Wood, S. N. (2006). *Generalized Additive Models: An Introduction with R*. Boca Raton, FL: Chapman and Hall/CRC Press.

Worm, B., Davis, B., Kettemer, L., Ward-Paige, C. A., Chapman, D., Heithaus, M. R., et al. (2013). Global catches, exploitation rates, and rebuilding options for sharks. *Mar. Policy* 40, 194–204. doi: 10.1016/j.marpol.2012.12.034

Zuur, A. F., Saveliev, A. A., and Ieno, E. N. (2014). *A Beginner's Guide to Generalised Additive Mixed Models with R*. Newburgh, NY: Highland Statistics Ltd.

Conflict of Interest: The authors declare that the research was conducted in the absence of any commercial or financial relationships that could be construed as a potential conflict of interest.

frontiers
in Marine Science

ORIGINAL RESEARCH
published: 18 November 2021
doi: 10.3389/fmars.2021.744202

Spatio-Temporal Variability in White Shark (*Carcharodon carcharias*) Movement Ecology During Residency and Migration Phases in the Western North Atlantic

Bryan R. Franks[1]*, John P. Tyminski[2], Nigel E. Hussey[3], Camrin D. Braun[4,5], Alisa L. Newton[6], Simon R. Thorrold[5], George C. Fischer[7], Brett McBride[7] and Robert E. Hueter[2,7]

[1] Marine Science Research Institute, Department of Biology & Marine Science, Jacksonville University, Jacksonville, FL, United States, [2] Center for Shark Research, Mote Marine Laboratory, Sarasota, FL, United States, [3] Integrative Biology, University of Windsor, Windsor, ON, Canada, [4] School of Aquatic and Fisheries Sciences, University of Washington, Seattle, WA, United States, [5] Biology Department, Woods Hole Oceanographic Institution, Woods Hole, MA, United States, [6] Disney's Animals, Science, and Environment, Bay Lake, FL, United States, [7] OCEARCH, Park City, UT, United States

Edited by:
Yannis Peter Papastamatiou,
Florida International University,
United States

Reviewed by:
Charlie Huveneers,
Flinders University, Australia
Alison Towner,
Rhodes University, South Africa

***Correspondence:**
Bryan R. Franks
bfranks@ju.edu

Specialty section:
This article was submitted to
Marine Megafauna,
a section of the journal
Frontiers in Marine Science

Received: 19 July 2021
Accepted: 13 October 2021
Published: 18 November 2021

Citation:
Franks BR, Tyminski JP,
Hussey NE, Braun CD, Newton AL,
Thorrold SR, Fischer GC, McBride B
and Hueter RE (2021)
Spatio-Temporal Variability in White
Shark (Carcharodon carcharias)
Movement Ecology During Residency
and Migration Phases in the Western
North Atlantic.
Front. Mar. Sci. 8:744202.
doi: 10.3389/fmars.2021.744202

Understanding how mobile, marine predators use three-dimensional space over time is central to inform management and conservation actions. Combining tracking technologies can yield powerful datasets over multiple spatio-temporal scales to provide critical information for these purposes. For the white shark (*Carcharodon carcharias*), detailed movement and migration information over ontogeny, including inter- and intra-annual variation in timing of movement phases, is largely unknown in the western North Atlantic (WNA), a relatively understudied area for this species. To address this need, we tracked 48 large juvenile to adult white sharks between 2012 and 2020, using a combination of satellite-linked and acoustic telemetry. Overall, WNA white sharks showed repeatable and predictable patterns in horizontal movements, although there was variation in these movements related to sex and size. While most sharks undertook an annual migratory cycle with the majority of time spent over the continental shelf, some individuals, particularly adult females, made extensive forays into the open ocean as far east as beyond the Mid-Atlantic Ridge. Moreover, increased off-shelf use occurred with body size even though migration and residency phases were conserved. Summer residency areas included coastal Massachusetts and portions of Atlantic Canada, with individuals showing fidelity to specific regions over multiple years. An autumn/winter migration occurred with sharks moving rapidly south to overwintering residency areas in the southeastern United States Atlantic and Gulf of Mexico, where they remained until the following spring/summer. While broad residency and migration periods were consistent, migratory timing varied among years and among individuals within years. White sharks monitored with pop-up satellite-linked archival tags made extensive use of the water column (0–872 m) and experienced a broad range of temperatures (−0.9 – 30.5°C), with evidence for differential vertical use based on migration and residency phases. Overall, results show dynamic inter- and intra-annual three-dimensional patterns of movements conserved within discrete phases. These results demonstrate the value of using multiple tag types to track long-term movements of large mobile species. Our findings expand knowledge of the movements and migration of the WNA white shark population and comprise critically important information to inform sound management strategies for the species.

Keywords: white shark, western North Atlantic, telemetry, migration, fidelity

INTRODUCTION

The movements of individual animals over time and space have profound impacts on animal ecology at all levels from the individual to the ecosystem (Nathan et al., 2008; Earl and Zollner, 2017). For highly mobile species, horizontal movement patterns can be predictable, composed of residency areas connected by migration corridors, with population-level movements in response to regional biotic and abiotic drivers (Bowlin et al., 2010; Shaw, 2016). Migrations between distant residency regions commonly occur in response to maintaining optimal thermal envelopes (Kessel et al., 2014; Payne et al., 2016, 2018), but are often associated with seeking out highly productive areas (i.e., high prey availability) (e.g., Jorgensen et al., 2010; Barnett et al., 2011) and areas for reproduction (Chapman et al., 2015). While population-level movement may appear predictable, certain species can show variability in migration timing among individuals and across years as a result of the dynamic environment they inhabit and their individual physiological needs (Brodersen et al., 2012; Fraser et al., 2019; Bauer et al., 2020). Defining animal residency and migration routes and variation in timing of movements consequently is essential to accurately delineate core space use for wildlife management. Moreover, vertical movements of susceptible aquatic animals can reveal regions where likelihood of negative interactions can occur, for example, in depths occupied relative to fishing effort and potential for capture (Coelho et al., 2015; Tolotti et al., 2015; Hutchinson et al., 2019). Vertical movements can also be predictable with species exhibiting specific behaviors during residency vs. migration phases (Bonfil et al., 2005; Francis et al., 2012). Gaining a thorough understanding of a species' ecology therefore requires multi-faceted long-term telemetry datasets from individual animals across and within multiple life stages (Speed et al., 2010; Hussey et al., 2015). Importantly, this assessment requires data over multiple years to capture individual and population-level variation in animal movements, to accurately inform measures for spatial and temporal management.

Contemporary research using multiple tag technologies to obtain longer-term datasets has yielded key insights into how aquatic animals interact with their environment (e.g., Vaudo et al., 2017; Braun et al., 2019; Cochran et al., 2019; Hoffmayer et al., 2021), potential drivers of vertical and horizontal movement (e.g., Coffey et al., 2017; Gaube et al., 2018; Lee et al., 2021), and how space use changes through ontogeny (e.g., Skomal et al., 2017; Ajemian et al., 2020), while also providing critical information for the implementation of effective management and conservation strategies (e.g., Acuña-Marrero et al., 2017; White et al., 2017; Bangley et al., 2020). In recent years, studies using pop-up satellite-linked archival tags (PSATs) on sharks have revealed long-term movement and migration routes as well as habitat use patterns (e.g., Weng et al., 2007a,b; Pade et al., 2009; Comfort and Weng, 2015). Additionally, this type of archival tag, if physically recovered, can deliver high resolution time series data on ambient temperature and depth, enhancing our knowledge of the complex temporal and behavioral dynamics of marine predators (Sims, 2010). While PSATs yield important information related to movements and behavior, deployments are usually short-term (<12 months) and light-based geolocations exhibit relatively high uncertainty (root mean square errors within ∼80–150 km; Braun et al., 2018). Incorporating multiple tag types, such as satellite-linked smart position and temperature transmitting (SPOT) and ultrasonic acoustic tags, on individual animals can both substantially increase the temporal scale of tracks (5–10 years) and also can provide increased accuracy of locations [LC = 3 SPOT error <250 m; CLS (Collecte Localisation Satellites), 2016]. Finally, higher-accuracy geolocations derived from SPOT and acoustic detections can be incorporated into PSAT geolocation algorithms to improve track estimation from these tags.

The white shark (*Carcharodon carcharias*) is a wide-ranging, apex predator distributed globally in temperate to sub-tropical waters (Bruce, 2008). The species is described to occur in seven general regions: southern Africa, Australia/New Zealand, the western North Atlantic (WNA), the southwest Atlantic, the Mediterranean, and the northwest and northeast Pacific (NEP) (Compagno et al., 1997). While population structure is not clearly defined within and among all regions, genetically distinct groups exist at the regional level such as in the WNA and southern Africa (O'Leary et al., 2015) and at finer scales such as in southern-western and eastern Australia/New Zealand (Blower et al., 2012; Gubili et al., 2015; Hillary et al., 2018). As a highly migratory species, the white shark has been shown to undertake long-distance movements along continental shelves, forays into pelagic waters, and infrequently across ocean basins (Bonfil et al., 2005; Weng et al., 2007a; Domeier and Nasby-Lucas, 2008; Duffy et al., 2012), with no evidence of trans-equatorial movements (Jorgensen et al., 2010).

Studies from various regions around the world show that most white sharks exhibit migratory and residency behaviors (Bruce et al., 2006; Duffy et al., 2012; Skomal et al., 2017; Lee et al., 2021) and in many instances these movement phases are predictable (Weng et al., 2007a; Jorgensen et al., 2010; Duffy et al., 2012). Drivers of these movements have been suggested to be abiotic factors including temperature or currents as well as biotic factors such as mating, pupping, prey availability, or predation risk (Duffy et al., 2012; Domeier and Nasby-Lucas, 2013; Hoyos-Padilla et al., 2016; Skomal et al., 2017; Jorgensen et al., 2019). White sharks from multiple ocean basins have been shown to spend considerable time in coastal over-shelf waters with regular offshore, pelagic phases (Bonfil et al., 2005; Jorgensen et al., 2010; Domeier, 2012; Duffy et al., 2012; Bradford et al., 2020). At times, these pelagic phases can coincide in latitude or longitude with a typical population-level seasonal migration pattern (Weng et al., 2007a; Domeier and Nasby-Lucas, 2008, 2013) or in contrast to the typical seasonal pattern (Bonfil et al., 2010; Skomal et al., 2017; Bradford et al., 2020; Spaet et al., 2020). Clarifying these movement phases in understudied white shark populations is critical given their designation as 'Vulnerable' by the IUCN (Rigby et al., 2019), their propensity to occupy coastal waters where there is potential for human-shark conflicts, and their naturally low population sizes as apex predators in marine food webs (Huveneers et al., 2018; Kock et al., 2018; Colefax et al., 2020).

Aspects of the biology, ecology, and status of the white shark population in the WNA have been documented in only a handful of studies, beginning with Casey and Pratt (1985), and updated and expanded on in Curtis et al. (2014). The WNA population is considered to have declined in abundance in the 1970s and 1980s, with evidence of a population bottleneck (O'Leary et al., 2015), followed by an apparent recovery beginning in the 1990s and continuing to the present day (Skomal et al., 2012; Curtis et al., 2014). There is a general paucity of data regarding large juvenile to adult white sharks in the WNA compared to other geographical regions (e.g., southern Africa, Australia/New Zealand, northeast Pacific), including limited data regarding their core movement phases. More specifically, information related to the residency, migration, and variation in timing of individuals when in and transitioning between phases is lacking for the WNA. Through a combination of satellite telemetric methods, Skomal et al. (2017) documented more extensive ranges of white sharks in the WNA than previously described, and confirmed a seasonal, predominantly latitudinal migration. In addition, these results demonstrated an ontogenetic shift in horizontal movements from predominantly shelf-oriented to more pelagic with increasing body size. Deep dives to mesopelagic zones during pelagic phases have been proposed as a foraging strategy (Gaube et al., 2018) and/or sexual segregation by pregnant females (Skomal et al., 2017). The New York Bight was proposed (Casey and Pratt, 1985) and subsequently confirmed (Curtis et al., 2018) to be a summer nursery area for the population with young-of-year (YOY) sharks demonstrating relatively narrow depth and temperature preferences (Shaw et al., 2021) while in the region. Additionally, Curtis et al. (2018) demonstrated a similar but much less extensive latitudinal migration for YOY sharks with individuals moving to shelf waters off the Carolinas in autumn/winter before subsequently returning north in late spring/early summer. More recently, Bastien et al. (2020) showed that movements of white sharks into Atlantic Canada were more common than previously thought, potentially as a result of population recovery and/or a northward range expansion. SPOT tags further revealed repeated seasonal movements into the region suggesting evidence for philopatry (Bastien et al., 2020).

Expanding on previous work on white shark movements in the WNA (Skomal et al., 2017; Curtis et al., 2018; Bastien et al., 2020; Winton et al., 2021), the overall objective of the current study was to broadly examine individual- and population-level variation in white shark spatial ecology across the region. Specifically, through the use of long-term SPOTs coupled with PSATs and acoustic telemetry, multi-year data were collected to examine and provide an overview of both inter- and intra-individual variation in movement behaviors in both horizontal and vertical planes. The specific aims of the study were to: (1) quantify residency and migratory phases of WNA white sharks over an annual cycle; (2) compare movement and migration patterns by size and sex while proposing potential drivers of movement; (3) examine variation in individual-level movement patterns across multiple years and determine the extent of fidelity or philopatric behavior to identified residency sites; (4) describe vertical behavior and variation associated with residency and migratory phases; and (5) propose a model of white shark population-level movements in the WNA that is consistent with their life history and accounts for ontogenetic and sex-specific differences in movement. Identifying size-based critical habitat variation in white shark movement behaviors for the WNA population has been identified as a research priority for this species (Huveneers et al., 2018).

MATERIALS AND METHODS

Capture and Tagging

Large juvenile and adult white sharks (n = 48) were captured by the fishing crew of the M/V OCEARCH at multiple locations along the Atlantic coast of the United States and Canada from 2012 to 2020 (**Figures 1**, **2**). Sampling areas included waters around the southeastern United States (South

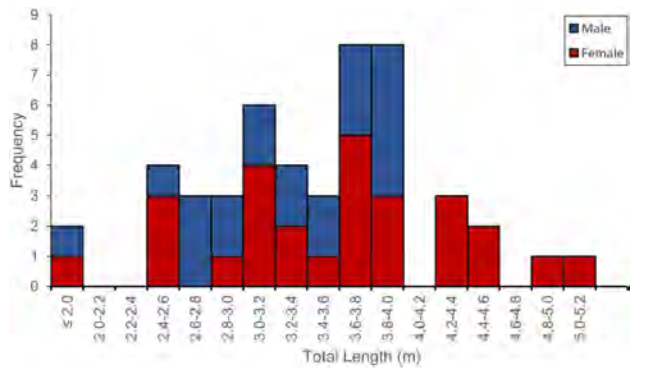

FIGURE 1 | Frequency-size distribution for 48 white sharks caught and tagged in the western North Atlantic between 2012 and 2020.

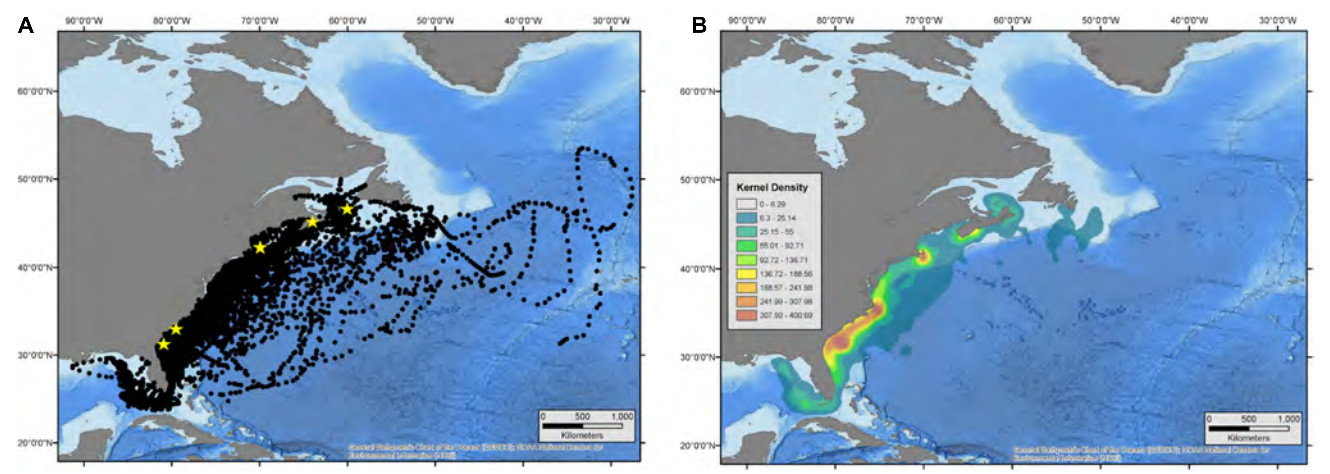

FIGURE 2 | Daily hSSM-derived locations **(A)** and an overall estimated kernel density **(B)** for all white sharks tagged between 2012 and 2020. Yellow stars in panel **(A)** represent general locations of tagging in NE Florida, Georgia/South Carolina, Massachusetts, and two locations in Nova Scotia.

Carolina to Florida), Massachusetts, and Nova Scotia. Methods of shark capture and processing followed procedures described in Domeier and Nasby-Lucas (2012) and Bastien et al. (2020). In brief, sharks were captured using a modified, break-away drumline technique or by rod-and-reel with 20/0 circle hooks deployed from a V-hull center console boat. Drumline leaders were rigged with buoys, weights, and/or bamboo crosses to prevent hook ingestion. Cable leaders were threaded through polypropylene rope to reduce the possibility of wire damaging the animal. If a large shark was sighted (>4 m total length, TL), a 27/0 circle hook was sometimes used to target that specific animal. All fishing lines and gear were monitored continuously while deployed. Once a shark was hooked, the shark was controlled with additional buoys as needed and guided onto the OCEARCH ship's research platform submerged below the water's surface. The platform was then raised, the shark was secured, and sampling and tag attachment procedures were initiated. While the shark was on the platform, the hook was removed, a wet towel was placed over the eyes and gill slits, and a ventilation hose providing free-flowing seawater was placed into the mouth to maintain gas exchange and reduce physiological stress. Ambient seawater was also regularly poured over the shark to keep the skin moist and the animal's temperature stable. Beginning in 2016, an experienced aquatic veterinarian was present on the ship and monitored the health of all animals during capture, handling, and release. As a precautionary measure and in response to a recommendation by permitting agencies, a rating score to assess factors such as handling time and associated physical condition of the animal was introduced in 2019. These scores were assigned prior to bringing sharks to the platform and during work-up procedures to determine the extent of research procedures to be conducted on each animal. The rating score was developed using Hueter et al. (2006) as a framework and modified to account for differences in the species and capture/handling methods used in this study.

While sharks were on the platform, work-ups were completed in a two-stage process with measurements taken, samples collected, examinations performed, and tags attached simultaneously. Sharks were equipped with one (n = 5), two (n = 22), or three (n = 21) types of transmitters, which varied in transmission type, battery longevity, accuracy, and data parameters. These comprised externally attached real-time SPOTs and PSATs (Wildlife Computers Inc., Redmond, WA, United States) and internally implanted coded acoustic tags (Vemco/InnovaSea, Bedford, NS, Canada). Length of time for sharks on the platform ranged 15–25 min ($\bar{x}$ = 17.6; SD = 3.7), after which the platform was lowered allowing the animal to swim off following a brief recovery period of usually 1–2 min. Post-release behavior was monitored visually from a small boat and/or with drone cameras, followed by data received from the tags.

Life Stage Classification

Knowledge of white shark life-stage characteristics, particularly size-at-maturity for both sexes, remains uncertain, particularly in the WNA. Reported or suggested size-at-maturity in the white shark ranges from 3.5 to 3.8 m TL for males and 4.5 to 5.0 m TL for females (Francis, 1996; Pratt, 1996; Compagno, 2001; Tanaka et al., 2011), with more recent studies using a narrower range of >3.5–3.8 m TL for males and >4.5–4.8 m TL for females (Weng et al., 2007a; Bruce and Bradford, 2012; Curtis et al., 2014; Skomal et al., 2017). It has been suggested, however, based on unconfirmed evidence, that maturity may be reached at smaller sizes: 2.7–3.1 m for males and 3.9–4.5 m for females (Francis, 1996; Pratt, 1996; Malcolm et al., 2001). In the current study, maturity was directly (through physical examination and morphometrics) and indirectly (through analyses of ultrasound exams, hormone levels, and sperm collected) assessed for each captured shark. Based on this assessment, male and female sharks in our sample were classified into three and four life stages, respectively. Male groups comprised large juvenile (≤2.80 m

TL), subadult (2.81–3.45 m TL for all but one animal), and adult (≥3.46 m TL for all but one animal). One male shark (3.32 m TL) smaller than 3.46 m TL was classified as an adult based on clasper condition. Female groups comprised large juvenile (≤3.30 m TL), subadult (3.31–3.79 m TL), maturing (3.80–4.19 m TL), and mature (≥4.20 m TL). The distinction of "maturing" and "mature" groups within female sharks was determined based on measured length/girth ratios and estradiol levels measured in blood collected from the sharks during the work-up procedures (Gelsleichter, unpublished data). We acknowledge the term "subadult" is often not well defined with quantitative criteria. Here the terms distinguish the difference between juvenile and subadult stages with subadults being nearer to sexual maturity. This is deemed necessary given the propensity for ontogenetic shifts in movements and diet, whereby white shark behavior and physiology are undergoing change through growth during this life stage transition period. Consequently, we classified juvenile males ≥2.8 m TL but not yet mature as subadult males and juvenile females ≥3.3 m TL but not yet maturing as subadult females.

Tagging Methods

Acoustic Transmitters

The first stage of research procedures on the ship's platform was conducted while the shark was in lateral recumbency to expose the abdomen and one lateral surface. An acoustic transmitter was surgically implanted into the coelomic cavity (Vemco model V16-6x, lifespan = 3,540 days, n = 40; or Vemco model V16-4x, lifespan = 2,435 days, n = 1; 85.4% of total individuals sampled). Acoustic transmitters and surgical tools were sterilized in a bath of benzalkonium chloride prior to use. The surgical procedure consisted of a 4–6 cm incision made with a sterile scalpel blade through the epidermis, muscle wall, and peritoneum using forceps to hold the body wall, to ensure internal organs were protected. Following incision, the transmitter was inserted into the coelomic cavity, and the incision was closed using 2–4 interrupted or cruciate sutures (Ethicon PDS, absorbable monofilament, Ethicon Inc., Somerville, NJ, United States).

Smart Position and Temperature Transmitting Tagging

For the second stage of procedures, sharks were rolled upright to rest on their ventral surface and SPOT tags (Wildlife Computers model SPOT-257 or SPOT-258) were attached to the first dorsal fin. The SPOT tags, which transmit messages via the Argos satellite network when the tag breaks the water–air interface, were attached to the leading edge of the first dorsal fin and located to maximize antenna height while also ensuring secure attachment to the fin. Tags were secured with four surgical-grade nylon bolts, plastic spacers, and stainless-steel locknuts inserted through holes in the fin made with a cordless electric drill. The hardware was designed to fail to allow the tag to detach from the fin after battery life has been expended. Observations from other regions suggest this attachment method results in tag shedding 1–6 years after tag deployment, with little effect on health and vitality of the shark (Jewell et al., 2011). Tags were coated with antifouling paint to reduce interference in tag function by bio-fouling organisms. A total of 44 sharks received the larger SPOT-257 tags with an estimated 5-year battery life, three sharks received a smaller SPOT-258 tag with an estimated 1-year battery life, and one shark did not receive a SPOT tag due to permit restrictions at the time on tag limits related to shark body length. All SPOT tags were programmed to provide horizontal location estimates at a repetition rate of 15 seconds when the upper wet/dry sensor detected the tag had broken the surface of the water.

Pop-Up Satellite-Linked Archival Tagging

For 21 sharks (large juvenile [n = 6], subadult [n = 6], maturing [n = 5], and mature [n = 4]), PSATs (Wildlife Computers MiniPAT) were attached into the dorsal musculature just below the first dorsal fin. Tags were coated with antifouling paint as above. A stainless steel or titanium dart attached to a 15-cm stainless cable tether that was protected with heat-shrink tubing (3M, Two Harbors, MN, United States) was used to anchor the device. Tags were programmed to detach after periods ranging from 180 to 365 days, float to the sea surface, and transmit a summary of their archived data via the Argos satellite system until battery failure. The PSATs archived measurements of ambient light, temperature, and pressure every 5–15 s that were summarized into depth/temperature time series at intervals ranging from 75 to 600 s for satellite transmission. Time-at-depth and time-at-temperature histogram data were summarized into 12- or 24-h periods.

Smart Position and Temperature Transmitting and Acoustic Data Processing and Analyses

All geolocations derived from sharks outfitted with SPOT tags included error estimates in the form of a location class (3,2,1,0,A,B,Z) and/or Kalman-derived error ellipses. While most tags deployed in this study are still active and providing data, a cut-off date of 30 November 2020 was established for all SPOT data used in the analyses here. Data were filtered in three steps to remove spurious locations as follows: (i) locations with no error estimate (i.e., Z class geolocations); (ii) locations on land; and (iii) by applying a speed filter (3 ms^{-1}), unrealistic locations from previous reliable locations based on animal swimming speed. Where available, acoustic detections for each SPOT-tagged shark were included to improve geolocation estimates. While some detections were obtained from our own acoustic receivers deployed in the NE Florida region, the majority were obtained through the major acoustic collaborative networks in the WNA including the Florida Atlantic Coast Telemetry (FACT), the Atlantic Coast Telemetry (ACT), and the Ocean Tracking Network (OTN) nodes. These data-sharing networks include receiver arrays that span coastal waters from Nova Scotia to the Gulf of Mexico (GOM) and detection data are distributed three to four times per year among acoustic telemetry researchers who participate in the networks. For each shark, when consecutive acoustic detections were provided on a single receiver over a day, one random time during that detection block was chosen to incorporate into the dataset for that shark.

Raw, filtered SPOT and acoustic locations were first presented as abacus plots to define broad-scale movements into regions over time and to assess multi-year fidelity to specific residence areas. Regularized tracks were then constructed using combined SPOT and acoustic tag locations. Joint estimation of behavioral state over multiple individual movement datasets is known to improve parameter estimates (Jonsen, 2016), consequently, a hierarchical (i.e., joint) state-space model (hSSM) was fitted to the combined data using the 'bsam' package in the R Statistical Environment (R Core Team, 2020). hSSMs provide both daily regularized locations and an estimate of the behavioral state at each location (Jonsen et al., 2007, 2013; Acuña-Marrero et al., 2017; Bastien et al., 2020). Behavioral states in the model are estimated using a combination of turn angle and move persistence as defined in Jonsen (2016). Resultant behavioral state values ranged from 1 to 2, representing transient (relatively fast and more directional movement paths) to area-restricted (relatively slow and more meandering movement paths) behaviors, respectively (Jonsen et al., 2007). Behaviors were classified as transient when scores were $\leq$1.25 and resident when $\geq$1.75. As SPOT tag transmissions can be irregular in time, complete tracks for individuals were segmented for any time gaps $>$20 days (Bastien et al., 2020) prior to model fitting. Resulting segments of less than 10 locations or shorter than 5 days were not included in subsequent analyses. Daily, regularized locations were then processed for three key analyses. To identify on/off shelf movements, locations were clipped to the continental shelf ($\sim$<200 m depth contour with 50 km buffer) using ArcGIS 10.8 and mapped by individual and defined groups (i.e., maturity state and sex). Using linear regression, ontogenetic differences within sexes were examined to test for increasing use of off-shelf waters by size class. To identify core-area use relative to season and by sex and life stage, kernel density estimates were calculated using the Geostatistical and Spatial Analyst extensions in ArcGIS 10.8. Finally, to examine annual seasonality and inter- and intra-annual variability in residence and migration timing, regularized locations were assessed by plotting latitudinal location over time for all years combined and for each year independently. Visual examination of plots of spatial distributions of sharks during each time period, patterns of latitudinal shifts in movements, and hSSM-derived behavioral scores were used to define behavioral seasons to include the bulk of individuals tracked during each respective time period. Migration corridors were defined using a combination of timing and speed of movements, the behavioral score assigned in the hSSM, along with horizontal locations during each track segment. Migration corridors and timing of migration were only utilized for track segments in which both clear departure/arrival locations and dates to and from residency areas were identifiable.

Pop-Up Satellite-Linked Archival Tag Data Processing and Analyses

Transmitted PSAT data were decoded with manufacturer software (WC-DAP 3.0, Wildlife Computers, Inc.), and light-based geolocations were estimated using GPE3 software (Wildlife Computers, Inc.) with the animal speed parameter set at 2 ms^{-1} (based on empirical data from Watanabe et al., 2019). This speed parameter is used in the geolocation framework to construct a Gaussian kernel that represents allowable daily diffusion over a model grid and thus differed from the 3 ms^{-1} threshold that was used above as a max daily displacement filter for the SPOT-derived data. The GPE3 model is based, in part, on previous work by Pedersen et al. (2008) that used hidden Markov models to geolocate Atlantic cod. The approach uses the archived tag data (light level, depth, and temperature) and corresponding sea surface temperature (SST) and bathymetry reference data in a gridded hidden Markov model to generate a most probable track (MPT) and associated uncertainty. Double tagging of a subset of individual sharks allowed improvement of track estimation through incorporating SPOT locations into the GPE3 processing as "known" locations. Prior to track estimation, the raw SPOT locations were first filtered using the 'foieGras' package in R (Jonsen et al., 2020) with the speed filter set for 3 ms^{-1}. Obvious outliers (e.g., locations on land) were excluded. If available, acoustic detections (maximum of one per day) were similarly used in GPE3 to supplement satellite-transmitted data to further optimize the derived geolocation estimates.

RESULTS

Overall Summary

The 48 large juvenile to adult white sharks were caught and tagged between September 2012 and October 2020 (**Table 1**). Locations of capture/tagging included sites along the coast of the SE United States (n = 7), Massachusetts (n = 15), and Nova Scotia (n = 26). Sharks ranged in size from 2.00 m to 5.01 m TL and comprised 27 females (9 large juvenile, 6 subadult, 5 maturing, and 7 mature) and 21 males (5 large juvenile, 6 subadult, and 10 mature) (**Figure 1**).

Of the 48 sharks, 47 were equipped with SPOT tags, 24 with PSATs, and 41 with acoustic transmitters. Of the 47 SPOT-tagged sharks, all provided locations (mean locations provided = 281; 16–2,791) with track durations ranging from 38 to 2,647 days ($\bar{x}$ = 511) (Table 1). Additionally, 23 of 41 sharks with acoustic transmitters provided 2,837 detections ($\bar{x}$ = 123 per shark) between 2016 and 2020, with the majority received through the regional data-sharing collaborative networks (FACT, ACT, OTN). For the 18 individuals that did not provide acoustic detections, 5 were tagged in autumn 2019 and 12 in autumn 2020, consequently data were not yet available for most of these animals due to the time lag associated with receiver downloads and data sharing. Down-sampling to one location and associated date/time per detection event resulted in the incorporation of 378 acoustic detections into tracking datasets with assigned Argos Location Class = 1 (500–1500 m accuracy) for track modeling. A total of 46 sharks provided at least one track segment for the hSSM analysis based on the predefined criteria (See SPOT Data Processing and Analyses). The total number of daily locations generated with the hSSM model was 10,367 with an average of 225 days per shark that provided at least one segment (15–1,291 d). The resulting percentage of tracking deployment duration with regularized daily locations ranged from 2 to 100% ($\bar{x}$ = 60%).

White sharks in the WNA were tracked over a wide latitudinal and longitudinal range (23.31° to 53.73° N and 91.51° to 27.48°

TABLE 1 | Summary data for tracked sharks.

Shark ID	Tag date	TL (m)	Life stage	Sex	Transmitters	Tag latitude	Tag longitude	Tracking duration (days)	# of daily locations
WS12-16*	13-Sep-12	4.47	A	F	S	41.62	−69.88	987	59
WS12-17*	17-Sep-12	4.88	A	F	S	41.62	−69.88	1734	1291
WS13-01*	3-Mar-13	4.42	A	F	S, P	30.39	−81.38	1473	649
WS13-02*	15-Aug-13	3.83	M	F	S, P	41.61	−69.96	1199	21
WS13-03*	20-Aug-13	4.32	A	F	S, P	41.61	−69.96	2647	1055
ACK2016-01	21-Sep-16	3.79	M	F	S, P, A	41.49	−69.98	830	198
ACK2016-02	22-Sep-16	3.71	SA	F	S, P, A	41.49	−69.98	1429	525
ACK2016-03	22-Sep-16	3.85	M	F	S, P, A	41.49	−69.98	38	69
ACK2016-04	7-Oct-16	3.00	SA	M	S, P, A	41.49	−69.98	668	295
ACK2016-05	7-Oct-16	3.38	SA	F	S, P, A	41.49	−69.98	785	145
ACK2016-06	7-Oct-16	2.63	LJ	M	S, P, A	41.49	−69.98	284	240
LC2017-01	3-Mar-17	3.78	A	M	S, A	32.09	−80.57	739	713
LC2017-03	5-Mar-17	2.60	LJ	F	S, A	32.23	−80.63	486	174
NS2018-01	24-Sep-18	3.41	SA	M	S, P, A	44.23	−64.28	570	191
NS2018-02	24-Sep-18	3.86	A	M	S	44.23	−64.28	786	155
NS2018-03	29-Sep-18	3.90	A	M	S, A	44.23	−64.28	685	323
NS2018-04	30-Sep-18	3.25	SA	M	A	44.23	−64.28	N/A	N/A
NS2018-05	5-Oct-18	2.74	LJ	M	S, A	44.23	−64.28	720	348
NS2018-06	8-Oct-18	2.86	LJ	F	S, P, A	44.23	−64.28	289	177
NS2018-07	8-Oct-18	4.25	A	F	S, A	44.23	−64.28	440	161
SE2019-02	15-Feb-19	3.11	LJ	F	S, P, A	30.36	−80.84	637	311
SE2019-03	22-Feb-19	3.79	M	F	S, P, A	32.06	−80.42	638	192
SE2019-04	26-Feb-19	2.66	LJ	M	S, P, A	32.00	−80.59	631	379
SE2019-05	26-Feb-19	3.88	M	F	S, P, A	32.00	−80.59	639	167
ACK2019-01	12-Aug-19	3.66	SA	F	S	41.42	−69.88	276	0
NS2019-01	15-Sep-19	3.71	A	M	S, A	46.02	−59.68	421	179
NS2019-02	16-Sep-19	3.93	A	M	S, A	46.02	−59.68	74	74
NS2019-03	20-Sep-19	4.33	A	F	S, P, A	46.02	−59.68	437	306
NS2019-04	26-Sep-19	2.50	LJ	F	S, A	46.04	−59.69	385	131
NS2019-05	29-Sep-19	3.53	SA	F	S, A	44.23	−64.28	428	22
NS2019-06	30-Sep-19	3.32	A	M	S, A	44.23	−64.29	205	100
NS2019-07	1-Oct-19	2.88	SA	M	S, A	44.23	−64.28	286	179
NS2019-08	1-Oct-19	3.13	LJ	F	S, A	44.23	−64.29	45	45
NS2019-09	3-Oct-19	3.46	A	M	S, A	44.23	−64.29	418	277
NS2019-10	3-Oct-19	3.13	SA	M	$S^{\#}$, A	44.23	−64.29	413	127
NS2019-11	4-Oct-19	3.63	A	M	S, A	44.23	−64.28	423	367
MA2020-01	9-Aug-20	3.13	LJ	F	S, A	41.48	−69.95	108	107
MA2020-02	11-Aug-20	2.00	LJ	M	$S^{\#}$, A	41.48	−69.95	94	80
MA2020-03	13-Aug-20	2.46	LJ	M	S, A	41.48	−69.95	109	46
MA2020-04	13-Aug-20	2.00	LJ	F	S, A	41.48	−69.95	105	106
NS2020-01	12-Sep-20	3.89	A	M	S, P, A	46.02	−59.68	75	47
NS2020-02	29-Sep-20	3.70	SA	F	S, P, A	44.23	−64.28	51	15
NS2020-03	1-Oct-20	3.15	SA	M	S, P, A	44.24	−64.27	57	58
NS2020-04	1-Oct-20	3.92	A	M	S, P, A	44.24	−64.27	54	53
NS2020-05	1-Oct-20	2.48	LJ	F	S, P, A	44.24	−64.27	50	50
NS2020-06	2-Oct-20	5.01	A	F	S, P, A	44.24	−64.27	52	51
NS2020-07	4-Oct-20	3.04	LJ	F	S, P, A	44.23	−64.27	57	57
NS2020-08	4-Oct-20	3.36	SA	F	$S^{\#}$, P, A	44.23	−64.27	52	52

**Denotes track first published in Skomal et al. (2017).*

LJ, large juvenile; SA, subadult; M, maturing; A, adult; S, 5-year SPOT; $S^{\#}$, 1-year SPOT; P, PSAT; A, acoustic.

Tracking duration = number of days between tagging date and last SPOT location received.

# of daily locations = number of days a location was generated from state space model.

W), from the Straits of Florida to north of Newfoundland and the Grand Banks, and from the central GOM to east of the Mid-Atlantic Ridge (**Figure 2A**). Overall, there were four focal areas used by tagged sharks: (1) a large area on the shelf from the SE United States and into the GOM; (2) the waters off Massachusetts; (3) the waters surrounding Nova Scotia including the Bay of Fundy and into the Gulf of St. Lawrence; and (4) the shelf break around the Grand Banks (**Figure 2B**). Across all sharks, a total of 82% of daily location estimates occurred over the continental shelf in water with a depth of <200 m.

Of 21 PSATs deployed on white sharks between 2016 and 2020, nine reported and transmitted usable data, four failed to report, and eight are still pending following deployments in 2020. For the objectives of this study, we report only the results from PSAT tags programmed with standardized parameters, which comprises tags deployed on animals captured in the SE United States and Nova Scotia in 2018–2019 ($n = 4$). Two of the tags deployed off Nova Scotia in 2018 were physically recovered yielding complete year-long high-resolution datasets (e.g., depth/temp every 15 s). Combined, these PSAT data recorded a maximum dive depth of 872 m and water temperatures ranging from −0.9 to 30.5°C.

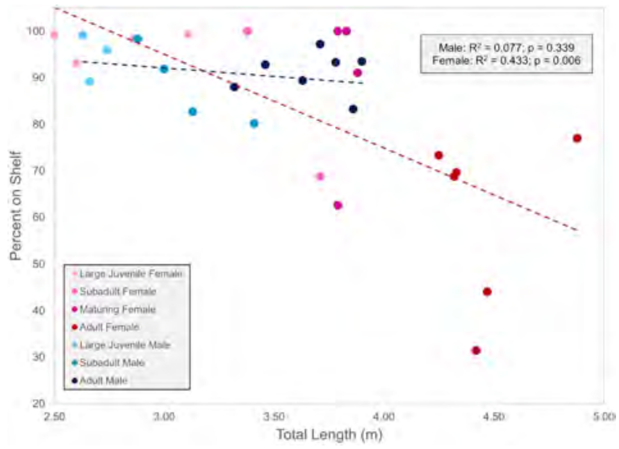

FIGURE 3 | Proportion of on-shelf locations for all white sharks with a tracking duration longer than 200 days based on regularized daily locations provided by the hSSM derived from SPOT and acoustic locations. Size ranges for life stages are found in the Section "Life Stage Classification." Lines are best fit regression lines.

Sex/Life Stage

Larger sharks of both sexes showed a trend of increasing use of pelagic waters with a higher proportion of locations off the continental shelf relative to smaller individuals, although this trend was much stronger and only significant for female sharks ($R^2 = 0.433$, $p = 0.006$) when compared to males ($R^2 = 0.077$, $p = 0.339$) (**Figure 3**). For female sharks, there was a marked difference in the spatial movements of larger (mostly adult; >3.5 m) female sharks versus other life stages (**Figures 3**, **4A,C**). Pooling hSSM-derived daily locations within each age class showed that adult females had a higher proportion of days in off-shelf waters (31–77%; x̄ = 61% of locations on-shelf) compared to juvenile (93–99%; x̄ = 98% of locations on-shelf), subadult (69–100%; x̄ = 90% of locations on-shelf), and maturing (63–100%; x̄ = 91% of locations on-shelf) females (**Figures 3**, **4A,C**). When examining behavioral state for these adult females, a higher proportion of off-shelf daily locations were classified as transient behavior ($b = 1.0–1.25$; 32.5%) compared to on-shelf locations (3.2%) (**Supplementary Figure 1**). This indicated that these animals were predominantly undertaking more directed movements when in offshore habitats versus area-restricted movements. These movements, however, were not uniform in terms of destination, spatial extent, or timing, with forays as far as the Mid-Atlantic Ridge and beyond (**Figure 4C**). Specifically, for three mature females (WS12-17, WS13-01, and WS13-03) with >3 years of SPOT data, forays were generally made in the overwintering period, but consistent periodicity in these offshore, open-ocean forays was not observed. For one female, offshore forays were made in consecutive years (4.4 m TL, WS13-01), for another there was a 2-year interval between forays (4.9 m TL, WS12-17), and for a third there was a 3-year interval (4.3 m TL, WS13-03) (**Supplementary Figures 2–4**). In general, male sharks were more shelf-oriented (80–99% of locations on-shelf) than females (31–99% of locations on-shelf). Within male sharks, subadult (80–98%; x̄ = 88%) and adult (83–97%; x̄ = 91%) groups spent proportionally less time in shelf waters when compared to large juveniles (89–99%; x̄ = 95%; **Figures 3**, **4B,D**).

Residency and Migration Phases

When considering all white sharks with daily location estimates, a clear seasonal cycle in their latitudinal movement patterns was observed. These movements comprised two distinct residency phases and two migratory phases. Residency phases included: (1) an overwintering period (1 December – 15 May) when sharks primarily occupied shelf waters from Cape Hatteras to the GOM; and (2) a late summer/early autumn period (1 July – 15 October), when sharks were generally clustered in northern waters either off Massachusetts (Cape Cod and Nantucket) or Atlantic Canada (Nova Scotia, Prince Edward Island, New Brunswick, and Newfoundland) (**Figures 5**, **6**). The two migration phases were in late spring/early summer (16 May – 30 June) and late autumn (16 October – 30 November), when animals were transiting between their southern overwintering and northern summer regions (**Figures 5A,C**, **6B,D**). Generally, regularized locations in the migration corridor between Long Island, NY and Cape Hatteras, NC yielded a relatively higher proportion of behavioral scores indicating transient or directed movements (<1.25 = 22.1%; >1.74 = 44.3%) while behavioral scores north and south of these regions in the residence areas were more indicative of area-restricted movements (<1.25 = 6.4%; >1.74 = 68.6%) (**Figure 7**). During both northern and southern migration phases, however, some white sharks demonstrated a degree of stop-over behavior in the region around Cape Hatteras, with some individuals remaining in the area between North and South Carolina during their overwintering phase while others moving farther south at varying rates into Georgia/Florida and around the Florida peninsula into the GOM. While most tracked sharks followed this seasonal movement pattern there were exceptions in terms of timing of movements, as well

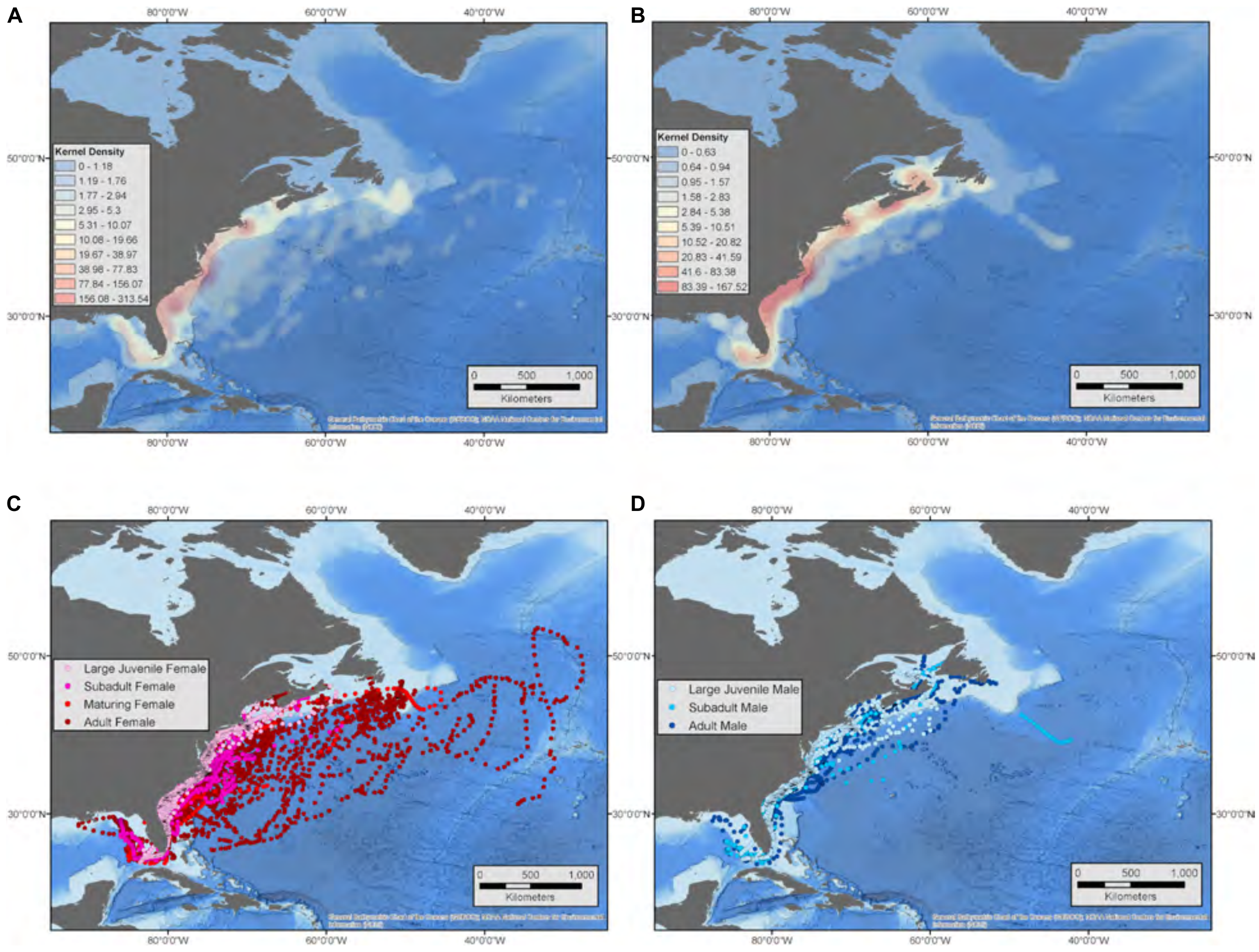

FIGURE 4 | Kernel density plots generated using pooled locations from all female white sharks **(A)** and all male white sharks **(B)**. Underlying daily hSSM-derived locations for each life stage for female **(C)** and male **(D)** sharks with color scaled by life stage from large juvenile to adult.

as differential space use relative to the conserved population pattern detailed above. This was particularly evident in the three large adult females that undertook extensive off-shelf movements in varying years and an inverse latitudinal shift in movements, with higher latitudes occupied in the late summer/early autumn and lower latitudes during warmer months in some years (**Figures 5B,D** and **Supplementary Figures 2–4**). Notably, of the five sharks tagged prior to 2016, these three large females provided most of the locations from that time period.

While a large proportion of WNA white sharks undertook rapid, directed shifts in latitude during the migratory phases, the initiation dates of both northern and southern migrations were variable among individual sharks and within/across years (**Figures 5C–E**). For example, the initiation of northward migrations (defined as movements departing 35.2N following residency behavior off Cape Hatteras; **Figures 5**, **6**) ranged from early May to mid-August ($\bar{x}$ = 66.8 ± 21.6 days) across all sharks and years where data were available (2017–2020). The shortest interval in any year between the day that the first and the last sharks began their northward migration was 33 days (2018) and the longest interval was 92 days (2019). The timing of the initiation of the southward migration was equally variable among individuals within years ranging from mid/late September to early December ($\bar{x}$ = 53.8 ± 8.4 days) for the period 2016–2020. The shortest interval in any year between when the first and last sharks began their southward migrations was 42 days (2017) and the longest was 66 days (2018). Moreover, interannual variability in migration timing was evident (**Figures 5C,D**). White sharks generally arrived at and departed from their northern summer/autumn residence areas slightly earlier in 2019 and 2020 ($\bar{x}$ = 26 June arrived, $\bar{x}$ = 11 September departed; passing 41.6°N [~Nantucket, MA]) when compared to 2017 and 2018 ($\bar{x}$ = 22 July arrived, $\bar{x}$ = 14 October departed; passing 41.6°N) (**Figure 5C**). Model-derived daily locations allowed for migration timespans to be calculated for 48 migration paths (30 southward and 11 northward migrations). While southward migrations were slightly faster on average ($\bar{x}$ = 19.7 d, SD = 11.7) than northward migrations ($\bar{x}$ = 23.1 d, SD = 16.7), there was no significant difference

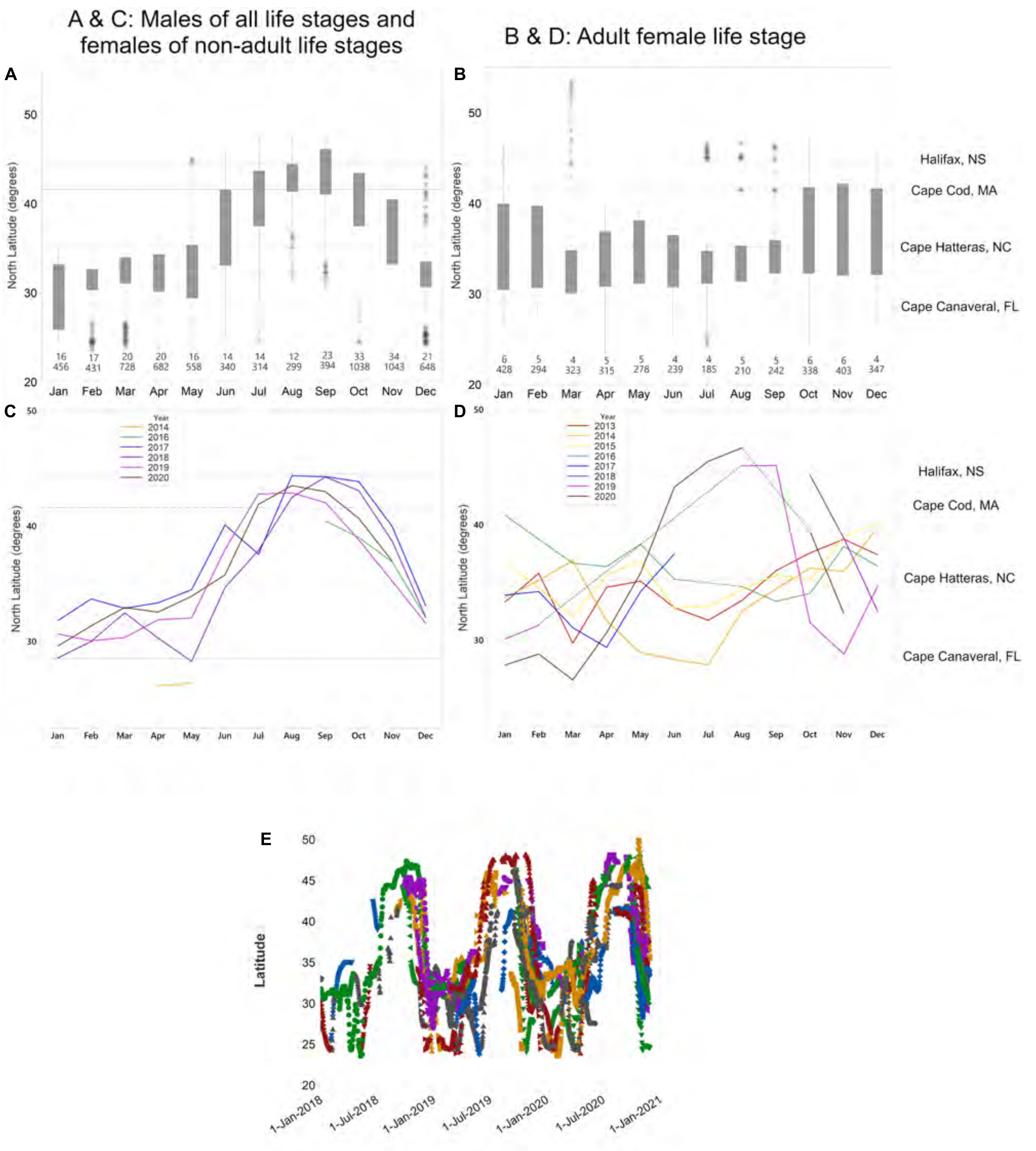

FIGURE 5 | Box-and-whisker plots **(A,B)**, summarized for all years, all sharks; and means of monthly latitude **(C,D)** within each year of all regularized tracks from white sharks tracked between 2013 and 2020 (**A,C** = males of all life stages and females of all non-adult life stages; **B,D** = adult females). Latitudes of regularized daily locations for individual sharks **(E)** tracked over a 2-year period (November 2018 – November 2020) to show individual variability in movements. In panels **(A,B)** boxes represent interquartile range, whiskers are 1.5 × IQR, asterisks are outliers, and numbers above each month represent # of individuals (top number) and total number of locations (bottom number) in each respective month. Lines in panels **(C,D)** represent mean latitude during each month and broken lines in panel **(D)** connect gaps within years with no data during those months. Colors and symbols in panel **(E)** denote individual sharks with locations during that period. Dotted horizontal lines in each figure represent latitudes from north to south of Halifax, Nova Scotia; Cape Cod, Massachusetts; Cape Hatteras, NC, and Cape Canaveral, FL as labeled to the right of figures.

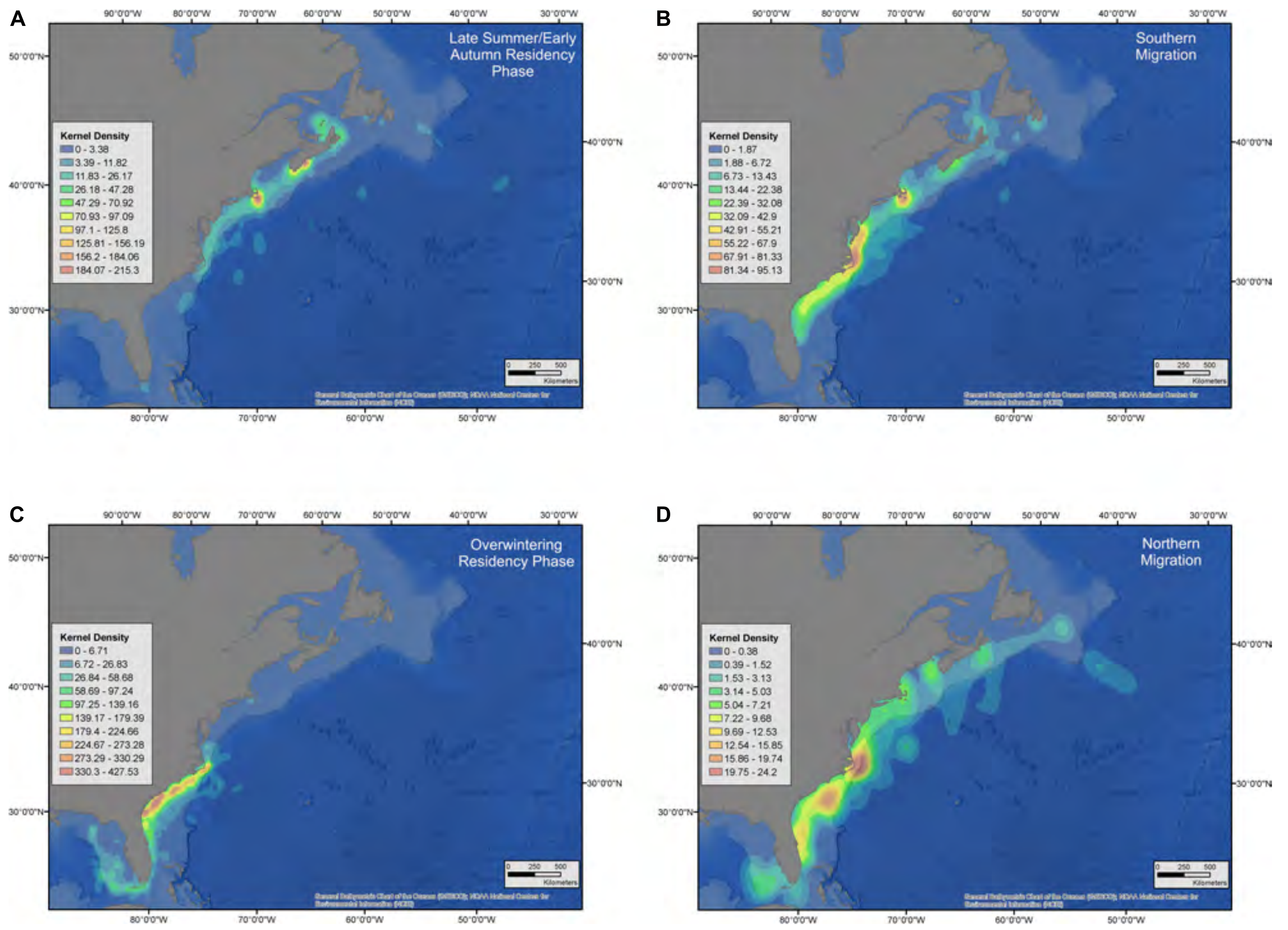

FIGURE 6 | Kernel density distributions by behavioral season of white sharks in the western North Atlantic. Interpolated kernel density distributions are derived from regularized tracks built from SPOT and acoustic locations. Data is pooled among all years, sexes, and age classes except for adult female sharks. Panels are segmented by behavioral state/season: Late summer/early autumn (**A:** 1 July – 15 October), southern migration (**B:** 16 October – 30 November), overwintering (**C:** 1 December – 15 May), northern migration (**D:** 16 May – 30 June).

in the length of time of the migration (Mood's Median Test, $p > 0.1$).

Summarized time-at-temperature data (n = 4 PSATs) indicated that WNA white sharks spent the largest proportion of their time in temperatures ranging between 15–18°C (27.1%) and 78.6% of their time in 12–24°C temperatures (**Figure 8** and **Supplementary Figure S5**). Temperature time series data (n = 4; recorded at 600 s intervals) provided further insight into seasonal differences. Variation in temperatures occupied during the two seasonal residency phases was observed with sharks occupying slightly warmer average temperatures during the overwintering period off the southern United States (19.0°C; SD = 3.84) when compared to the summer residency period off Nova Scotia and Massachusetts (14.7°C; SD = 3.89; **Figures 8A,C** and **Supplementary Figures 5A,C**). During northern and southern migration phases, average temperatures occupied were similar (16.5°C [SD = 5.80] and 16.3°C [SD = 4.18], respectively) (**Figures 8B,D**), but the largest variation recorded occurred during the northern migration period (**Figure 8D** and **Supplementary Figure 5D**). For one 3.8 m TL female (SE2019-03), evidence of occupying extremely cold waters was recorded between mid-July to early August while the animal was near the Southeast Shoal (SES) of the Grand Banks of Newfoundland (**Figure 9B**). On at least four different days, this shark spent periods of time (as much as 2.1% during a single 12-h period [15.1 min]) in water < 0°C (min. −0.9°C). Significant time was also spent in the 0–3°C range during this period (as much as 35.7% during a 12-h period [4.3 h]). These cold temperatures were not associated with extreme depths, but largely occurred at high latitudes in depths of 50–100 m. For example, a minimum temperature of −0.2°C was recorded on 4 August 2019 when the day's maximum depth was 56 m. This tag's temperature thermistor is rated to −40°C and was calibrated down to 2°C by the manufacturer prior to shipping. We assessed the sensor's accuracy post deployment by comparing SST recorded by the tag on the day of release with nearby (<300 m distance) remotely sensed high resolution SST values. There was <0.5°C difference in these values indicating the temperature sensor was functioning within normal parameters during deployment.

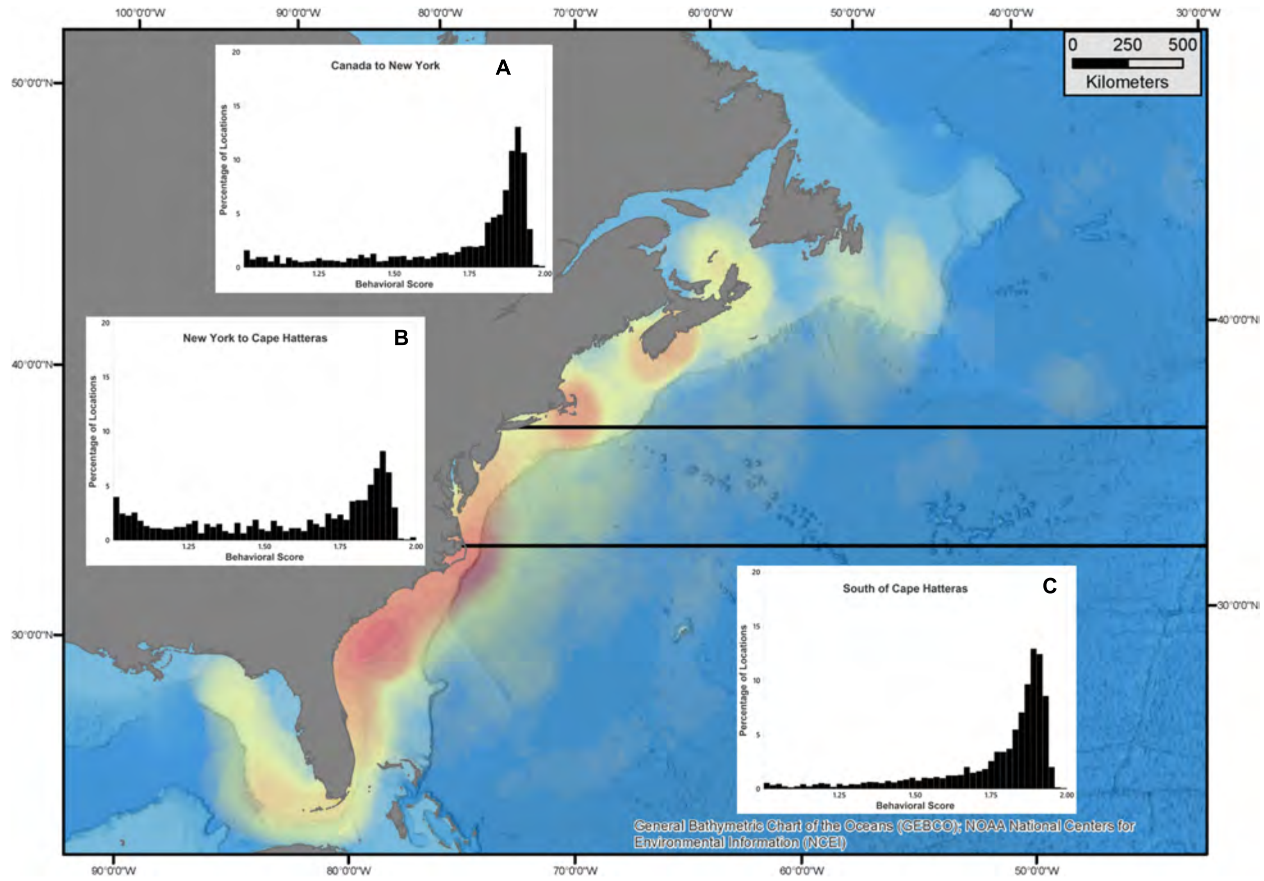

FIGURE 7 | Proportions of white shark locations across range of behavioral scores derived from the hSSM from each of three regions: North of Long Island, NY **(A)**; south of Cape Hatteras, NC including the Gulf of Mexico **(C)**; and the migration corridor between these two **(B)**. Utilizing hSSM-derived behavioral scores, behavior is classified as resident (b = 1.75–2.00), transient (b = 1.00–1.25), or unclassified (b = 1.26–1.74) The basemap represents a simple point density of all daily locations. Three adult, female sharks with significant off-shelf locations were not included.

High resolution data from the two recovered PSATs were used to detect changes in patterns of vertical habitat use dependent on the movement phase of the individual (i.e., transient or resident). During periods of transient or more directed horizontal movements as determined by MPTs, a shift to a larger proportion of near-surface swimming was recorded (**Supplementary Figure 6**). For example, shark NS2018-06 (2.9 m TL female) spent 73.7% of time in sub-surface waters (1–2 m) during the 3-day period of transient behavior compared to 19.6% of time at that depth range in the 3 days prior, when movements were indicative of more resident behavior (29 October – 5 November 2018; **Supplementary Figure 6**). This 3-day period of near-surface time was punctuated by occasional dives to mostly moderate depths (∼10–90 m) and one deep dive to 460 m. These relatively fast-paced dives showed a pattern of faster descents than ascents and minimal time spent at the maximum depth, a pattern consistent with a gliding descent and powered ascent (Gleiss et al., 2011) that commonly correlate with directed movements by marine species. A broader comparison of time-at-depth data from full PSAT tracks (n = 4) showed a similar pattern with 38.0% of time spent in near-surface waters (0–5 m) on days identified as transient (>60 km d^{-1} traveled) compared to 22.8% of time spent near surface during days identified as resident (<60 km d^{-1} traveled).

Fidelity

Overall, sharks showed coarse-scale fidelity to specific regions, most notably during the July–November residency phase at higher latitudes (**Figure 10** and **Supplementary Figure 7**). Of six sharks tagged with SPOT tags in Atlantic Canada in 2018, all individuals returned to Atlantic Canada waters in 2019 (year 2) and three individuals were present in the region in 2020 (**Figure 10B**). Similarly, of 11 SPOT-tagged sharks tagged in Atlantic Canada in 2019, six provided data in the subsequent summer period and five of those six moved back into Atlantic Canada waters (**Figure 10B**). The shark that did not provide data (2.5 m TL male, NS2019-04) was only located during the month of October the following year off Massachusetts heading south. Consequently, its movements in Atlantic Canada may not have been detected. Several sharks tagged in Nova Scotia were tracked near and around the Massachusetts region, but these movements were typically short stop-overs either before entering

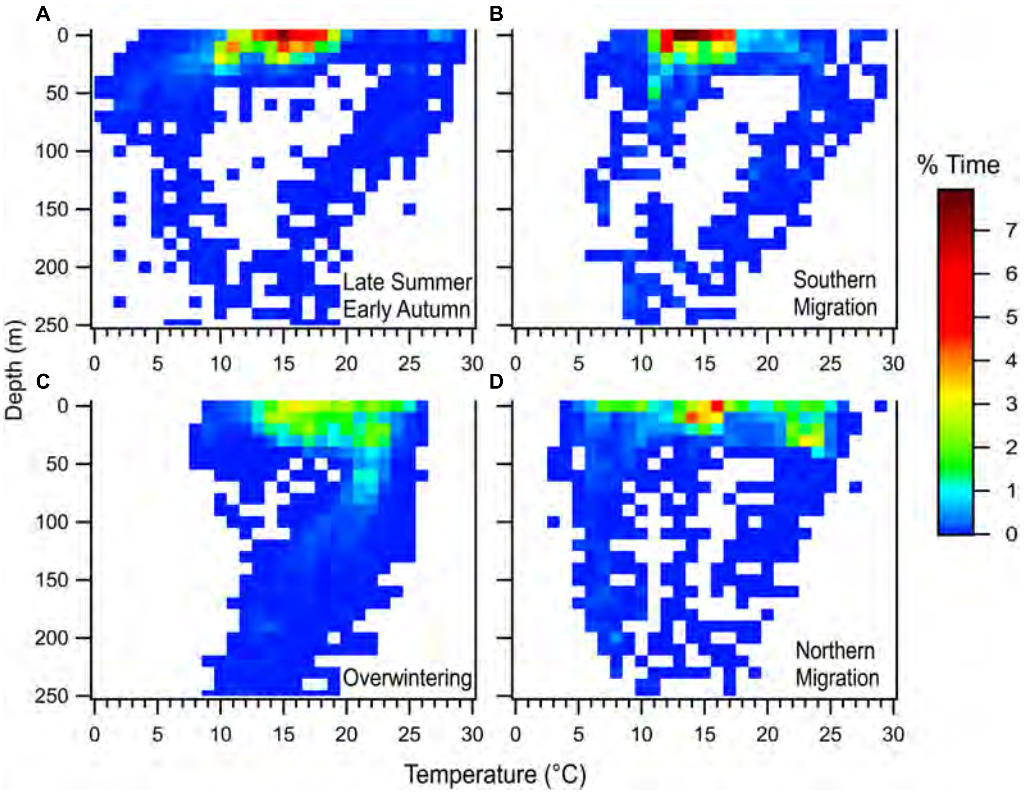

FIGURE 8 | Aggregated temperature-at-depth profile from time series data of four PSAT-tagged white sharks demonstrating vertical habitat utilization across seasons. **(A)** Late summer/early autumn. **(B)** Southern migration. **(C)** Overwintering. **(D)** Northern migration. While depth data did extend below 250 m, this represented <1% of overall time, thus for clarity, *y*-axes represent time between 0 and 250 m depth.

or after leaving Canadian waters, indicating a preference for more northern residency areas (**Figure 10B**). Conversely, of the 11 sharks tagged in waters near Massachusetts in the summer period between 2012 and 2019, eight provided locations in the second summer period, seven in the third summer period, and three in the fourth and fifth summer periods (**Figure 10C**). There was no clear pattern for the subsequent late summer/early autumn period habitat used, but six were detected in Massachusetts waters in following years and only two sharks of the 11 [a 3.0 m TL male (ACK2016-04) and a 3.8 m TL female (WS13-02)] showed movements into Atlantic Canada waters (**Figure 10C**). Of the seven sharks tagged off the SE United States during the overwintering period, six provided locations in their first late summer/early autumn residency period and four in the second residency period (**Figure 10D**). Of these, one shark resided in waters around Massachusetts in the two summer periods it was tracked and was not detected in Atlantic Canada waters; one shark was tracked moving through Massachusetts waters and into Atlantic Canada in the first period, then was located in waters off Newfoundland in the second period; three sharks inhabited Atlantic Canada waters in both subsequent late summer/early autumn periods and were not detected in Massachusetts waters; and one was tracked into Massachusetts waters in 1 year and Atlantic Canada in two other years (**Figure 10D**). Regional fidelity was also observed during the overwintering residency phase. Of the 36 sharks tagged between 2013 and 2019, 14 spent time in waters around the Florida Keys or in the GOM during the overwintering period and nine of those returned to the GOM in subsequent overwintering periods (**Figures 10B–D**).

While there were migrations on- and off-shelf, this varied both among and within individuals. In all sex/size classes except adult females, there were 30 southward migrations where model-derived daily locations generated clear departure and arrival dates from pinniped foraging areas at northern latitudes to the Outer Banks region in North Carolina, the northern limit of the overwintering area. Of these 30 southward migrations, 17 occurred entirely over shelf waters (e.g., Figure 9A), three entirely in offshore waters (e.g., **Figure 9B** and **Supplementary Figure 8A**), and ten in which sharks had portions of their migration in off-shelf waters (i.e., partially off-shelf). Additionally, there were 11 northward migrations where model-derived daily locations generated clear departure and arrival dates from the Outer Banks to pinniped foraging areas. Of these 11 northward migrations, nine were over shelf waters, one was clearly in offshore waters, and one showed the shark moving into off-shelf waters during a portion of the migration. There was no clear pattern of individual sharks showing fidelity to a particular migratory pathway across sex or size (e.g., **Figure 9** and **Supplementary Figure 8**; excluding adult females). In the adult female class, north-south migratory patterns could be resolved

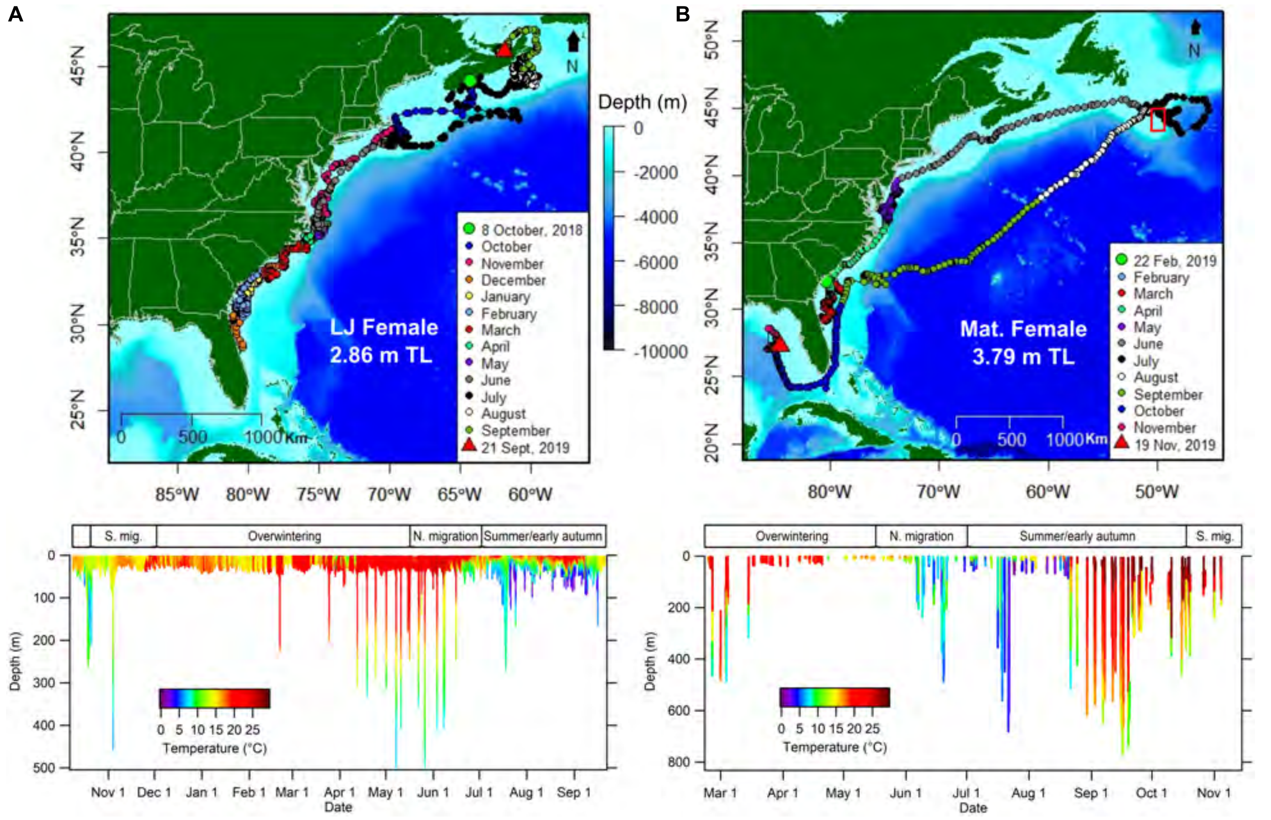

FIGURE 9 | Most probable tracks (MPTs) and depth-temperature profiles derived from PSATs from white sharks NS2018-06 **(A)** and SE2019-03 **(B)**. The MPT is a light-based track that incorporated SST, bathymetry, and known locations from SPOT and acoustic tags into the model. The white sharks were tagged off Nova Scotia **(A)** and South Carolina **(B)**. The approximate location of the Southeast Shoal is shown as a red box on the Grand Banks of Newfoundland.

for four southward migrations (two over-shelf, one offshore, and one partially off-shelf) and three northward migrations (two offshore and one partially off-shelf). While sample size for this group is low, females were more likely to undertake migrations in offshore waters when compared to other groups.

For sharks with multi-year datasets, fine-scale fidelity was evident with multiple sharks returning to specific sites within residency regions in subsequent years (**Figures 10**, **11** and **Supplementary Figures 8B,C**). A 3.9 m TL male shark (NS2018-03), tagged in Nova Scotia in autumn 2018, subsequently returned in 2019 and 2020 to <2 km from the tagging location (**Supplementary Figure 8C**). For the overwintering residency phase, a 4.9 m TL female shark (WS12-17) was tracked during parts of five annual cycles and showed strong fidelity by returning in 4 of 5 years to a site on the shelf off the Georgia coast (**Figure 11**).

DISCUSSION

Through a combination of satellite and acoustic telemetry, our 8 years of data provide the first comprehensive assessment of white shark movement behavior for individuals tagged at multiple locations in the WNA. Using multiple tag types and integrating resulting datasets allowed us to generate robust measures of movements over considerable spatial and temporal scales. Derived data reveal detailed insights into the broad-scale movements of large juvenile to adult life stages of both sexes. White sharks in the WNA are predominantly shelf-oriented with a repeated and conserved seasonal latitudinal migration evident in all size/sex classes except for large mature females. Residency areas of high use in northern latitudes include the waters off Massachusetts, Atlantic Canada, and the Grand Banks. While migration windows for most individuals are within the same 1.5-month period, variation in the timing of migration among individuals within years and across years is evident. Individual white sharks show fidelity to regions across years, revisiting the same general areas of residence over a multi-year period, and fine-scale fidelity is seen in multiple individuals returning to the same locations over 3+ years. Vertical diving behavior is variable but broadly corresponds to shallower occurrence during directed movements and deeper diving when resident. Our data significantly expand current knowledge of the spatio-temporal movements of white sharks to inform transboundary management of this threatened species in the WNA.

Size/Sex Variation in Movement

White sharks in the WNA show variation in movement patterns by both life stage and sex, similar to trends observed for other geographically isolated populations worldwide (Jorgensen

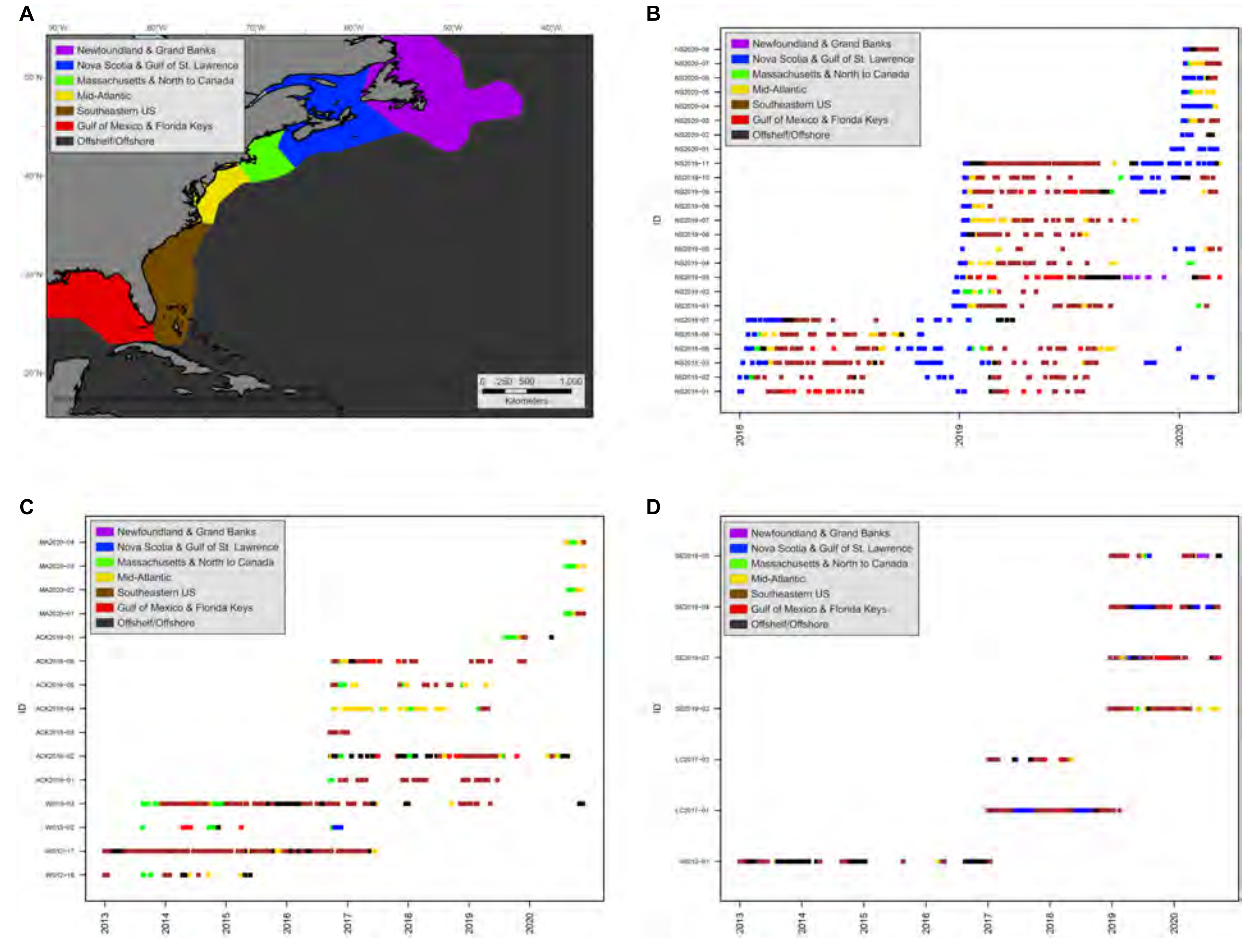

FIGURE 10 | Abacus plots of raw SPOT and acoustic locations of all white sharks colored by region of location or detection (**A:** Map of regions denoting color of region; **B:** Nova Scotia caught sharks; **C:** Massachusetts caught sharks; **D:** SE United States caught sharks). On-shelf regions (all except offshelf/offshore) extend from the shoreline to the shelf break with a 50 km buffer. Regions include: Newfoundland and Grand Banks (purple), Nova Scotia and Gulf of St. Lawrence (blue), Massachusetts and north to Canadian EEZ (green), mid-Atlantic (gold), southeastern United States (brown), Gulf of Mexico and Florida Keys (red), and offshelf/offshore (black). Sharks captured/tagged in Nova Scotia **(B)** were less likely to be detected in subsequent years in waters near Massachusetts (green) and more likely to be detected in Canadian waters (blue or purple). Conversely, sharks captured/tagged in Massachusetts **(C)** were less likely to be detected in subsequent years in Canadian waters (blue or purple) and more likely to be detected back in waters near Massachusetts (green). Of the Southeastern shelf caught sharks **(D)**, there were preferences to utilize one or the other summer/autumn region (blue/purple or green) in subsequent years of tracking but usually not both. During overwintering periods, sharks with detections in the Gulf of Mexico (red) were likely to have detections in the Gulf of Mexico in subsequent overwintering periods.

et al., 2010; Kock et al., 2013; Bruce and Bradford, 2015; Bruce et al., 2019). Large juveniles of both sexes are primarily coastal, occurring on the continental shelf throughout residency and migratory phases. While larger individuals exhibit similar seasonality in migration and residency phases, a trend of greater use of off-shelf waters with increasing body size was found in both sexes, with the ontogenetic shift being considerably more pronounced and statistically significant in female sharks. These findings are in agreement with previous work on WNA white sharks (Skomal et al., 2017) highlighting the proximity of this species to regions of high human activity (Winton et al., 2021), in terms of both recreational water use and fisheries as well as anthropogenic disturbance along the entire Atlantic coast of the United States and Canada. Given YOY white sharks tagged in their primary nursery area in the New York Bight showed more restricted latitudinal movements during 1 and 2 years of age (Curtis et al., 2018; Shaw et al., 2021), it is apparent that expansion of activity space and extension of residency and migration phases occur relatively quickly, likely between ages 3 and 4. The fact that multiple sharks ≤ 2.5 m TL were captured and tagged in Massachusetts and Atlantic Canada supports this rapid range expansion with body size that is conserved through to adulthood, with ontogenetic increases in range being mostly longitudinal off-shelf. Evidence from acoustic telemetry data for individuals captured and tagged as YOY animals also shows movements into Florida and Massachusetts by age 3 and Canada to the GOM by age 4 (Curtis and Franks, unpublished data; Curtis et al., 2018; Shaw et al., 2021). Consequently, white sharks in the WNA are

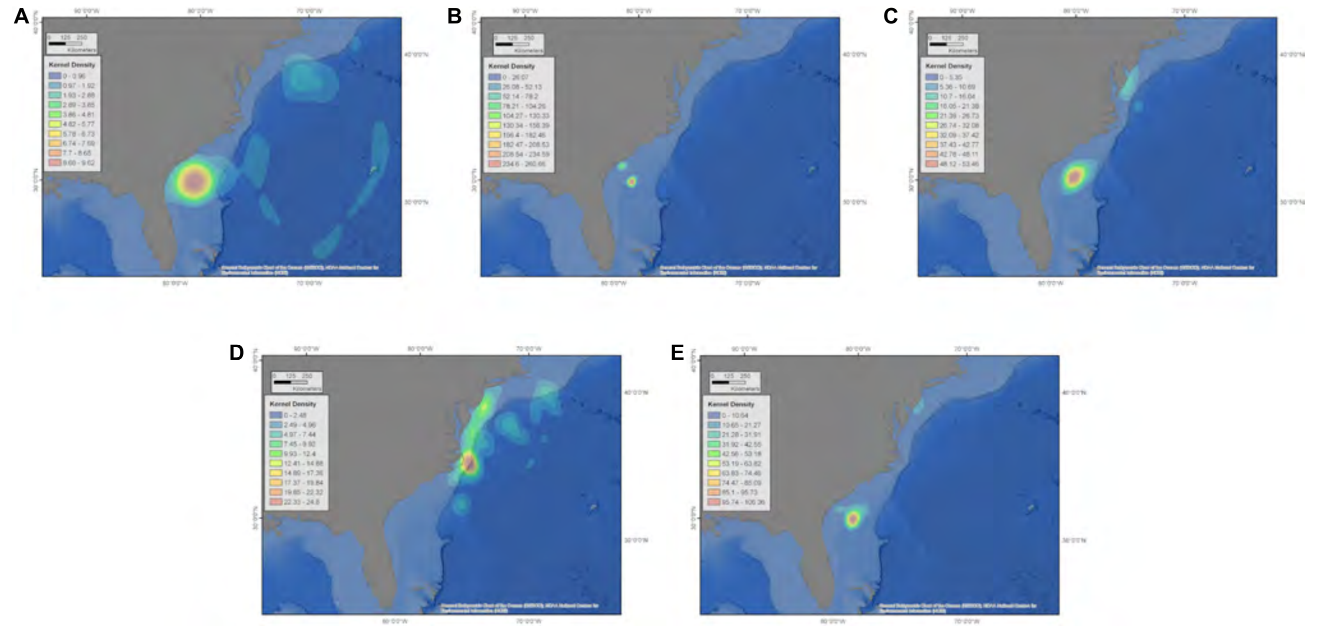

FIGURE 11 | Kernel density distributions of daily locations between October 16 and June 30 for a 4.9 m TL female white shark (WS12-17) for year 1 (**A:** 2012–2013), year 2 (**B:** 2013–2014), year 3 (**C:** 2014–2015), year 4 (**D:** 2015–2016), year 5 (**E:** 2016–2017). This shark showed strong fidelity to an area on the shelf off the coast of Georgia in 4 of 5 years tracked.

utilizing near the maximum latitudinal range (∼25°) observed in the population by approximately age 4 and a size of 2.5 m TL. Range expansion in juvenile white sharks from other regions has been shown (NEP: Weng et al., 2007b; eastern Australia: Spaet et al., 2020) but the age/size and magnitude of expansion differs from our study. This may be due to shorter track durations for other regions (Weng et al., 2007b) or physical and/or biological differences between regions, such as prey availability, predation pressures, or bathymetry (Spaet et al., 2020). In the WNA there is also a consistent shift in increased proportion of time spent in offshore waters (longitudinal expansion) with increasing body size, similar to that observed for the white shark in Australia (Bruce et al., 2019; Lee et al., 2021) and the NEP (Jorgensen et al., 2010; Domeier, 2012; Domeier and Nasby-Lucas, 2012; Hoyos-Padilla et al., 2016). These longitudinal range expansions may reflect a reduction in predation risk after threshold sizes are reached (Skov et al., 2011; Hussey et al., 2017; Stump et al., 2017); improved access to biological or physical features to meet changing physiological demands (food sources, temperature profiles) (Ford, 1983; Breau et al., 2011; Braun et al., 2019); and/or in the case of off-shelf movements, to use alternate migratory pathways that reduce travel time to/from residency areas, or to select or avoid particular features such as the Gulf Stream current or associated habitats (Block et al., 2011; Dodson et al., 2013; Chambault et al., 2017; Gaube et al., 2018).

While adult females in our study did not show a clear cycle (1–3 years) in their extensive offshore movements in the WNA, these movements are potentially linked to reproductive behavior (Skomal et al., 2017; note five sharks included in their study are also incorporated into our dataset, including the three females discussed below), during pregnancy. In the NEP, adult females are thought to be on a biennial cycle in which they move into pelagic waters for periods of up to 16 months, then undertake directed movements to coastal regions where pupping is suspected to occur (i.e., presence of newborn sharks; Domeier and Nasby-Lucas, 2013). Bowlby and Gibson (2020) suggested that the reproductive cycle for white sharks in the WNA is >2 years, which could explain the inconsistent movement cycles observed here. Given the limited data available for adult females (3 individuals), we can neither confirm nor rule out a potential 2-year reproductive cycle as proposed in the NEP (Domeier and Nasby-Lucas, 2013), but the observed inconsistent periodicity of movement patterns may reflect variability in reproductive dynamics among regional white shark populations that requires further investigation. Further data for this life stage in the WNA will provide improved resolution on the timing and duration of this offshore pattern.

The majority of geolocations of white sharks on the Grand Banks southeast of Newfoundland were from adult females, suggesting this area may play an important role for that life-stage. The region of the Grand Banks and Flemish Cap is known to be highly dynamic with the confluence of the Labrador Current and the Gulf Stream/North Atlantic Current driving areas of upwelling along with strong eddy fields (Anderson and Gardner, 1986; Zhao et al., 2013), that results in increased primary and secondary production (Anderson and Gardner, 1986; Pepin et al., 2011). Potentially abundant prey in the region includes large bony fishes, other elasmobranchs, and marine mammals such as harp (*Pagophilus groenlandicus*) and hooded seals (*Cystophora cristata*) that are present in winter to late spring

(Stenson and Sjare, 1997; Coughlan, 2002; Epperly et al., 2012; Andersen et al., 2013). This region may provide high prey abundance and consequently a high-energy foraging refuge, isolated from coastal pinniped colonies, where white shark abundance is higher. Variation in diet between sexes, including adult females having a more generalized diet, has been suggested for white sharks in other regions (French et al., 2018) and may reflect broader niche utilization as a result of expanded space use.

Currently, there is no direct evidence of mating activity when sharks are present in late summer/autumn residency areas in the WNA, similar to other regions (Jorgensen et al., 2012). However, indirect evidence (i.e., location/timing of departures from shelf waters) suggests these adult females undertake protracted off-shelf forays in the WNA in late winter/early spring following mating. The timing of these offshore movements post-mating is supported by an estimated 15–20 months gestation period (Bruce, 2008; Christiansen et al., 2014; Bowlby and Gibson, 2020) and an early summer (May–June) pupping season (Curtis et al., 2018; Santana-Morales et al., 2020). If females in the WNA are gestating during these offshore forays, reasons could include physical and/or thermal refuging, or a foraging habitat geographically separated from male conspecifics, to avoid harassment by males while females are pregnant (Jorgensen et al., 2012; Sulikowski et al., 2016). These results demonstrate the importance of multi-year telemetry datasets to explain the scale and pattern of individual movements during the gestation period for long-lived species (Edwards et al., 2019).

Seasonality and Migration

Similar to several other elasmobranch species (Biais et al., 2017; Nosal et al., 2021; reviewed in Chapman et al., 2015), white sharks undergo predictable migrations and residency periods in the WNA on an annual cycle. For most sharks tracked in the WNA over multiple years, the annual pattern is conserved but with unequal periodicity. While most sharks in our study undertook migrations during similar time periods (May–June and October–November), the timing of migration varied among individuals both within years and across years. Individual intra-annual and inter-annual variation in migration timing leads to questions of cues and triggers of this movement behavior. Observed inter-annual variability suggests flexibility in migration cues where environmental stochasticity likely plays a role. Similar to other migratory species, there are likely multiple interacting factors impacting migration, including static, fixed cues such as photoperiod that may trigger physiological or behavioral changes as an ultimate factor along with more dynamic, local proximal factors such as temperature, or prey distribution/abundance (Bauer et al., 2011; Winkler et al., 2014). Further, intra-annual variation among individuals may reflect inherent variability, i.e., phenotypic plasticity (Pulido, 2007; Hayes et al., 2012) or variability in predation success during the preceding residency period and associated body condition and/or reproductive status.

Evidence suggests that white sharks deplete energy reserves during their migrations (Del Raye et al., 2013) and forage at a lower rate when away from coastal pinniped colonies (Carlisle et al., 2012). Moreover, white sharks are known to demonstrate a shift in diet through ontogeny, with increases in mammal prey and decreases in teleost and elasmobranch prey with increasing size (Hussey et al., 2012; Grainger et al., 2020). In the context of WNA white sharks, the 3–4 month period when sharks are present near pinniped colonies in Massachusetts and Canada likely provides a critical time for energy acquisition, whereby enhanced feeding opportunities may play a key role in the balance of annual energy budgets. Captured sharks off Nova Scotia in 2018–2020 showed direct (substantial amounts of seal fur in fecal samples and fresh seal scratch wounds around the head and mouth) and indirect (large girths and distended abdominal areas) evidence of substantial feeding on seals (Newton and Franks, pers. obs., Fotso Tagne and Hussey, unpublished data). This is further supported by observations of seal corpses bearing bite wounds attributed to white sharks around Sable Island off the coast of Nova Scotia (Lucas and Natanson, 2010). Of these corpses, the vast majority (99%) were observed from July to October and were primarily seal pups (73%) although gray seals of all ages showed evidence of white shark predation (Lucas and Natanson, 2010). Gray seal populations in the waters around Massachusetts (Wood et al., 2020) and Atlantic Canada (Hammill et al., 2017) have increased in recent years with current estimates placing the total population in Atlantic Canada at 400,000–500,000 individuals with pup production increasing at a higher rate in more southern areas of their range (NE United States and SW Nova Scotia) (den Heyer et al., 2021). Given shark foraging activity and movements in this region are likely driven not just by pinniped density but also variation in pinniped behavior through ontogeny (Brodie and Beck, 1983; Moxley et al., 2020), future work should focus on an examination of fine-scale space use by white sharks and how it relates to pinniped size, abundance, reproductive cycles, foraging behavior, and seasonal movements.

In the overwintering residency period, it is thought white sharks may be feeding on whales off the SE United States coast and in the GOM (Skomal et al., 2017) in addition to squids, teleost fishes, and other elasmobranchs. While these feeding opportunities may provide important required energy during this time, they are likely to be sporadic and less reliable, in contrast to the high availability of pinniped prey during summer/autumn. Consequently, behaviors are likely selected for those that will maximize caloric consumption during the late summer/early autumn periods near expanding pinniped colonies, while exploiting sporadic feeding opportunities, such as whale carcasses or transient concentrations of other prey, during the overwintering period. This is evident across species and habitat types, where predator search patterns shift based on prey availability (Sims et al., 2012). White sharks, as endothermic predators, likely feed frequently to maintain energetic needs (Semmens et al., 2013) and energetic costs of migration must be accounted for through gains during time spent in other portions of their range. It is possible that the consistent, energy-rich food source of seal colonies in the northern portion of their range in summer/early autumn may provide a net energy gain during this period, providing an energetic surplus for somatic and reproductive growth. In contrast, in the overwintering areas, more diffuse feeding opportunities may only provide energy to meet metabolic needs for maintenance and migration. Additionally, mean water temperatures experienced in these southern overwintering areas are warmer than that of the northern summer regions, consequently the energetic costs of endothermy may be reduced during winter.

During periods of directed horizontal travel a white shark (2.9 m TL large, juvenile female, NS2018-06) was shown to shift to a pattern of increased near-surface swimming punctuated by occasional deep dives. A number of white shark tracking studies have reported a similar pattern of increased surface swimming (Bonfil et al., 2005; Weng et al., 2007a; Domeier and Nasby-Lucas, 2008) and increased swimming speed (Bonfil and O'Brien, 2015; Watanabe et al., 2019) during traveling or oceanic phases. However, white sharks moving directly at the surface incur wave drag, which is energetically costly (Watanabe et al., 2019). Wave drag can be avoided by swimming deeper than ∼2.5 body diameters (Alexander, 2013), which would be ∼2 m for white sharks (Watanabe et al., 2019). This is consistent with our observations for shark NS2018-06, which displayed surface swimming during the transient phase predominantly in the 1–2 m subsurface range (73.7% of time). The occasional dives during these periods of near-surface swimming could play a navigational (Keller et al., 2021) and/or thermoregulatory role (Domeier and Nasby-Lucas, 2008) or represent energy-efficient foraging forays (Gleiss et al., 2011; Watanabe et al., 2019). Overall, these results suggest that white sharks can select depths and speeds depending on their behavioral state that optimize energy expenditure.

In the WNA and other regions, a combination of thermal regime, foraging opportunities, and reproduction have been proposed as reasons driving white shark seasonal migrations (Casey and Pratt, 1985; Jorgensen et al., 2010; Carlisle et al., 2012; Duffy et al., 2012; Curtis et al., 2014; Bradford et al., 2020). Our data are consistent with these interacting factors driving migration of WNA white sharks, which spend more than 75% of their time in 12–24°C waters and the largest proportion of their time (27%) in the 15–18°C range. The most likely factor driving these sharks to leave late summer/autumn foraging areas in northern latitudes to overwinter in lower latitudes is cooling water temperatures in early winter, as suggested by Casey and Pratt (1985). This is supported by our data as the timing of departure from northern latitudes during late autumn/early winter (October–November) corresponds to average daily water temperatures of ∼9–15°C. Departure from these regions is unlikely to relate to decreased regional prey availability, given that pinniped abundance in Atlantic Canada is higher during winter and spring periods (Hammill et al., 2017). While both depth (0–872 m) and temperature (−0.9 – 30.5°C) ranged considerably for white sharks in this study, sharks spent the majority of time in much narrower ranges, consistent with previous studies within the WNA and other regions.

One PSAT-tagged subadult female in our study, a 3.8 m TL maturing female (SE2019-03), spent portions of four different days in water with subzero temperatures (min. −0.9°C) during the summer (2019 15 July – 4 August) while in continental slope waters east of the Grand Banks of Newfoundland. To our knowledge, this is the coldest temperature on record for a white shark, less than the minimum temperature of 1.6°C reported by Skomal et al. (2017), or for any other lamnid species. Porbeagles (*Lamna nasus*) in the WNA, for example, have been shown to occupy a temperature range of 2–26°C (Pade et al., 2009; Saunders et al., 2011; Skomal et al., 2021), while salmon sharks (*L. ditropis*) in the NEP occur in 2–24°C (Goldman et al., 2004; Weng et al., 2005). Only the non-endothermic Greenland shark (*Somniosus microcephalus*) has been shown to frequent colder waters with temperatures documented as low as −1.7°C (Skomal and Benz, 2004). The subzero temperatures experienced by this female white shark occurred in the vicinity of the SES, an area with the highest benthic biomass on the Grand Banks (Hutcheson et al., 1981) and a known offshore spawning site for capelin (*Mallotus villosus*) (Carscadden et al., 1989). The SES has relatively warm July–August bottom water (∼2–4°C) that is well-suited for the demersal spawning capelin. In contrast, the nearby waters immediately east of the shelf are considerably colder (∼ −1.5 – 0.7°C) as depths exceed 50 m (Templeman, 1975; Whitehead and Glass, 1985; Loder, 1991). During the prespawning period, capelin form relatively large and compact schools that are heavily preyed upon by humpback whales (*Megaptera novaeangliae*) as well as a number of other cetacean species including finback whales (*Balaenoptera physalus*), minke whales (*Balaenoptera acutorostrata*), white-beaked dolphins (*Lagenorhynchus albirostris*), and short-beaked saddleback dolphins (*Delphinus delphis*) (Whitehead and Glass, 1985). The white shark's ability to maintain a warmer-than-ambient body temperature likely enables expansion of its thermal niche and access to habitats largely limited to other top predators, accepting that regional endothermy is more associated with higher swim speeds rather than broader thermal niches (Harding et al., 2021). It is likely the white sharks are drawn to the abundant food supply of the SES during this period and at times may actively hunt or scavenge on cetaceans in the subzero waters just off the slope of the shelf, though we cannot rule out the possibility of white sharks foraging on the spawning capelin while on the shoal.

The durations of residency and migratory periods in WNA white sharks are consistent with sharks tracked in other geographical regions (Francis et al., 2015; Spaet et al., 2020), but the seasonal patterns, irrespective of hemisphere, differ slightly among regions. This is likely due to variations in physical factors such as water temperatures and currents or biological factors such as prey behavior and reproductive cycles. The latitudinal scope of the migration of white sharks in the WNA can be attributed to the type of available winter habitat, the location of productive foraging habitats, and how the sharks move between these two. In New Zealand and the NEP, available winter habitat is mostly oceanic in off-shelf waters whereas productive foraging areas are coastal. In the WNA, Australia, and for the most part southern Africa, both residency phases generally occur in on-shelf habitat. The predominantly longitudinal migration found in NEP white sharks is likely reflective of the eastern boundary current (California Current) in the region, resulting in cooler temperatures and productive foraging habitats (i.e., pinniped colonies) being located nearer to the equator. In other areas where white shark movements and migration have been studied (eastern Australia, New Zealand, and southern Africa), the coasts are generally associated with western boundary currents, where productive foraging habitats are found at higher latitudes and overwintering habitats are nearer to the equator, either on-shelf (southern Africa, and eastern Australia) or oceanic (New Zealand). Although no comprehensive telemetry study of white sharks has been conducted in the northwest Pacific, capture and sighting data have reported that white sharks are present there in northern latitudes in most months except winter and present in southern latitudes in most months except summer (Nakaya, 1994; Christiansen et al., 2014). This trend is consistent with the migration phases observed in the WNA and demonstrates how major surface currents such as western boundary currents and variable thermal conditions interact to shape latitudinal migrations.

The variability in migration seen among individuals and years demonstrates the importance of a thorough, long-term understanding of these movement patterns, to accurately characterize spatial distribution for management and conservation. A changing climate, particularly ocean warming, may not only affect the distribution of marine species such as sharks (Bangley et al., 2018; Tanaka et al., 2021) but may also impact timing of movements and migration. Ongoing, long-term monitoring of the WNA white shark population is essential, therefore, given the observed increase in water temperature of 0.41°C between 1950 and 2009 (IPCC, 2014) in the Atlantic Ocean, the finding that some areas of the WNA white shark range (Gulf of Maine) have warmed at a faster rate than 99% of the world's oceans (Pershing et al., 2015), and projected temperature increases of up to 3°C in the northwest Atlantic Ocean (35–45°N) by the end of this century (Saba et al., 2016).

Fidelity

White sharks tracked in the WNA demonstrate inter-annual fidelity to particular regions both during their overwintering and summer residency phases. In particular, most WNA sharks show a preference for one of the two known late summer/early autumn residency areas, namely Massachusetts and Nova Scotia, with relatively little overlap between the two. Individual sharks also showed fine-scale site fidelity returning to specific areas within these regions over multiple years, in some cases within 1–3 km for up to three consecutive years. Site fidelity, whereby individual animals repeatedly re-use specific areas within their range (Piper, 2011), is part of an overall behavioral pattern of animals returning to specific "homes" within their ranges, termed philopatry (Hueter et al., 2005). Philopatric behavior likely confers multiple benefits to individuals including increased familiarity with the physical and biological parameters in their range, thereby increasing biological and ecological efficiencies of behaviors such as prey capture, movement and migration, mating, and physiology, contributing to increases in fitness (Switzer, 1993; Merkle et al., 2014; Madigan et al., 2015). Similar to the results for the WNA white sharks, site fidelity has been shown for white sharks in the NEP where individuals returned to the same coastal sites over multi-year periods (Jorgensen et al., 2010, 2012; Domeier and Nasby-Lucas, 2012), with little overlap between the two pinniped foraging areas in the NEP (Central California vs. Guadalupe Island; Jorgensen et al., 2012) and evidence of some sharks returning to the same site in 14 of 22 years (Anderson et al., 2011). Major geographical differences between the residency areas in the NEP and the WNA, however, are evident. In the NEP, sharks move eastward from offshore, open-ocean areas to reach coastal sites, whereas in the WNA, sharks move north from southern overwintering regions along the continental shelf. As a result, there is a greater likelihood of WNA sharks visiting both northern latitude regions, particularly for sharks that must transit through Massachusetts waters to reach Atlantic Canada. Despite this, many tracked sharks, particularly those tagged in Canada, show strong fidelity to that region, returning in each subsequent late summer/autumn season. This provides strong evidence that a subset of animals actively selects locations in Atlantic Canada for the residency period. Fidelity to specific foraging sites while migrating through and bypassing potentially suitable forage habitat has been shown in other migratory species (Bonadonna et al., 2001; Shimada et al., 2020) where familiarity likely plays a key role. This fidelity would be enhanced in areas or with species where forage is predictable such as benthic foraging sea turtles (Shimada et al., 2020), herbivorous grazers (Merkle et al., 2015), front-associated predators (Lowther et al., 2011), or, in the case of white sharks, foraging around concentrated pinniped colonies (e.g., Robbins et al., 2015; Hewitt et al., 2018). These data provide evidence that there is delineation of foraging areas within the northern latitude residency phase (Atlantic Canada vs. Massachusetts), suggesting the possibility for subpopulation structure in the WNA, with implications for regional management. Continued long-term tracking coupled with genetics will be required to confirm this.

While there was evidence of site fidelity during the overwintering residency period, including fine-scale fidelity for some sharks (**Figures 10**, **11**), the general pattern was not as clear as compared to the northern late summer/early autumn residency period. For instance, individuals that migrated to the GOM typically returned to that location in subsequent years, but this was not consistent for all sharks tracked over multiple years. One potential reason for this pattern may relate to prey availability as potential prey resources are more diffuse in the southern portions of their annual range during the winter period. If foraging opportunities and ultimately success are more reliable within specific areas, then it follows that fidelity to those regions may be more pronounced. With scant, direct evidence for specific forage in this overwintering region and during migrations, sharks may be foraging opportunistically in more productive regions or potentially exploiting other prey sources that are consistent, e.g., large schooling fishes or invertebrates (Murphy et al., 1998; Galuardi et al., 2010; Braun et al., 2019) or whale calves (Gowan and Ortega-Ortiz, 2014; Kennedy et al., 2014).

Strong, multi-year fidelity to specific regions demonstrates that white sharks are likely using complex navigational cues during both migratory and residency phases to return to preferred areas. White sharks around aggregation sites in California (Goldman and Anderson, 1999) and in South Africa (Jewell et al., 2013) have been shown to become more selective in space use as they increase in size. This suggests a refinement of space use over time, possibly as a result of experience and the building of memory maps (Fagan et al., 2013) that could

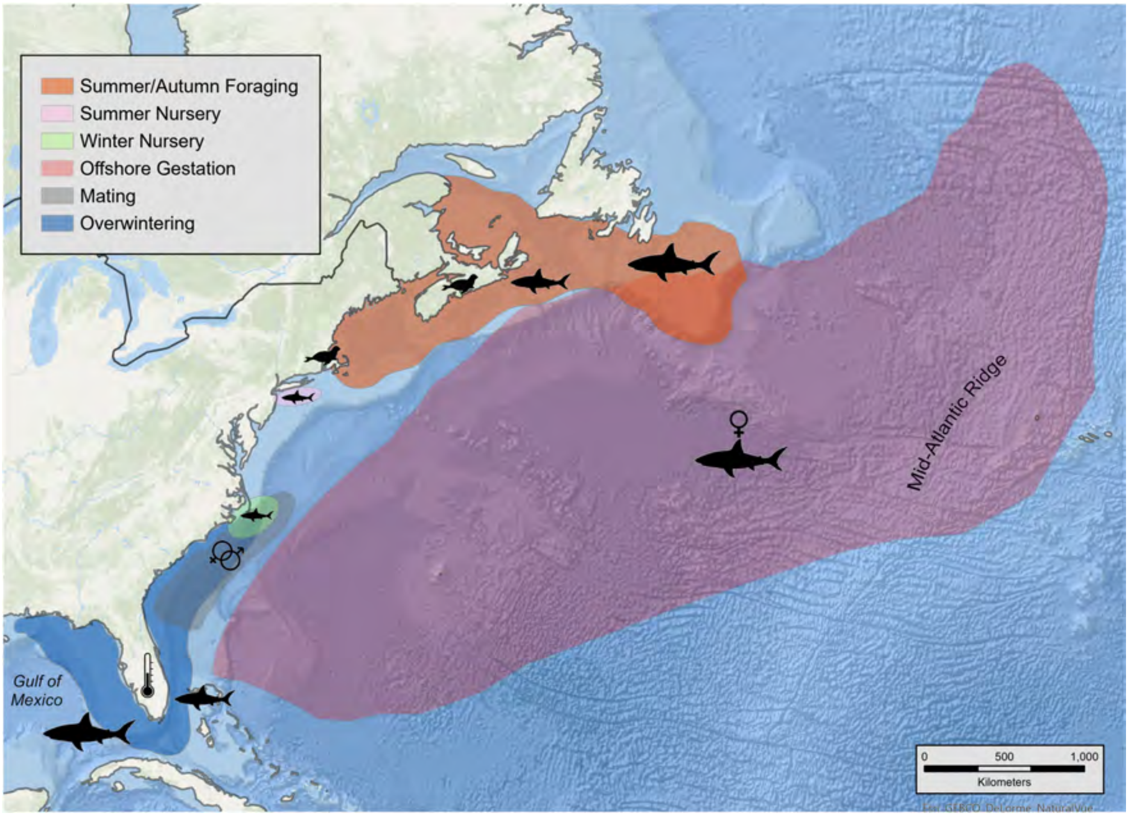

FIGURE 12 | Summary and conceptual framework for general movement patterns by white sharks in the western North Atlantic. Size of shark silhouette corresponds to broad age/size classes while seal silhouettes represent areas of known pinniped foraging areas by white sharks. Areas noted are based on a combination of previously published studies (Casey and Pratt, 1985; Curtis et al., 2014, 2018; Skomal et al., 2017; Gaube et al., 2018; Bastien et al., 2020; Shaw et al., 2021), data from this study, and proposed hypotheses for mating and gestation areas. Proposed mating area was derived from general locations of sharks during the late winter to early summer period of each year with the assumption of a ∼12–18 month gestation period, as well as anecdotal evidence of a large, female white shark observed with mating wounds off the shelf break of the Georgia coast in June of 2018. Proposed gestation area was derived from general locations of adult, female white sharks during these expansive offshore movement periods every 1–3 years.

result in increased foraging efficiency. The late summer/autumn residency phase of white sharks in the WNA is likely a strategy to maximize energy intake during this period potentially through optimal foraging, yielding net-positive energy budgets during this period. Increased familiarity, via fidelity, potentially reduces feeding search times and increases prey capture and handling efficiency, and thus increases energy inputs during this important summer foraging period when prey is abundant, driving overall annual growth. Additionally, with seal colonies relatively diffuse in the WNA region (Massachusetts to Newfoundland) when compared to other areas (Ferreira and Ferreira, 1996; Bradshaw et al., 2000), it may allow for individual sharks to establish specific areas to revisit each year to minimize intraspecific, competitive interactions and thus alleviate density-dependent effects.

While fidelity provides benefits to animals in the form of increased efficiency and fitness, there are potential implications to the animal or population if conditions change. Habitat degradation, climate change, and increased potential for localized depletion can all disproportionately impact species or populations that are philopatric or return to the same areas over time (Hueter et al., 2005). Alternatively, intra- and inter-annual variation in movement dynamics (migration timing and duration of residency phases) observed in sharks tagged for multiple years in the current study suggests a degree of flexibility to change. If true, then white sharks could adapt to modified ecosystems under climate change but may still face the threat of other natural or anthropogenic disturbances.

CONCLUSION

White sharks in the WNA are dynamic in their use of space, yet trends in their space use are consistent across age classes, with a rapid expansion of latitudinal range early in life that is conserved through to adulthood. Although overall migration and residency patterns are consistent, there is considerable variability both among groups, such as life stage and sex, as well as within groups when comparing individual space use over a multi-year period. Generally, WNA white sharks show a series of regular movements and migrations, utilizing three regions in northern latitudes (Massachusetts, Nova Scotia and the Gulf of St. Lawrence, and the Grand Banks) in late summer/early autumn and one expansive shared area along the shelf off the SE United States and in the GOM in winter and spring seasons. These patterns are consistent with the exception of some use of offshore areas, particularly forays into far offshore waters by a subset of large females.

In conclusion, with our findings presented here, we propose the following hypotheses and paradigms explaining the movement ecology of the white shark in the WNA and other regions (**Figure 12**):

(1) Strong site fidelity in WNA white sharks suggests subpopulation structure that may be detectable with additional telemetry data from individuals with 10-year acoustic tags and from parallel genetic analyses, particularly when considering Massachusetts and Atlantic Canada-oriented sharks.

(2) Western North Atlantic white sharks generally show a north-south coastal range that expands rapidly within the first few years of life with consistent seasonal migrations that expand off-shelf with ontogeny. This general pattern is broken by post-mated adult females as they move far offshore during pregnancy, potentially to avoid interactions with other sharks and/or to exploit specific biological or physical features. As we do not see evidence of mating during the late summer/early autumn period around pinniped colonies and adult females initiate offshore forays in late winter and spring, we hypothesize mating is likely occurring offshore from the coast of North Carolina to northern Florida in the late winter to early summer (**Figure 12**).

(3) The world's regional populations of white sharks assort themselves into groupings sharing common patterns of movement ecology and habitat use. These patterns are likely driven by a combination of biological needs such as foraging, reproduction, and temperature constraints along with physical parameters such as shelf structure and width, major current characteristics, and landmass size/orientation. These patterns serve to connect foraging areas to meet energetic requirements for physiological and reproductive needs. With this paradigm, broad-scale movements of populations globally can be classified into general patterns: (1) major migratory routes are in the latitudinal plane (western North Atlantic, New Zealand, eastern Australia, northwest Pacific, southern Africa) or the longitudinal plane (northeast Pacific, southern-western Australia); and (2) overwintering areas are either mostly over-shelf (western North Atlantic, eastern Australia, southern Africa) with some time in oceanic waters or offshore, oceanic (northeast Pacific, New Zealand). Further refinement of this paradigm will be revealed through continued long-term behavioral and ecological research such as multi-year telemetry.

Future research will test these hypotheses and evaluate our paradigms for white shark ecology. Defining the movement patterns of migratory, wide-ranging, long-lived predators such as the white shark presents challenges related to the limitations of current telemetry technology. By deploying multiple tag types that provide data over periods of up to a decade, we can gain deeper insights into their movements and migration over multiple spatial and temporal scales (Edwards et al., 2019). Only through long-term telemetry datasets on individual animals in conjunction with other biological studies will it be possible to resolve critical questions related to the biology, ecology, conservation, and management of the white shark.

DATA AVAILABILITY STATEMENT

Datasets from SPOT tags used in this study are housed in the Movebank.org online repository. Data from all tags can be made available upon reasonable request to the corresponding author.

ETHICS STATEMENT

The animal study was reviewed and approved by Jacksonville University's Institutional Animal Care and Use Committee (IACUC).

AUTHOR CONTRIBUTIONS

GF and BM led the fieldwork. All authors conducted fieldwork and contributed to data collection. BF, JT, CB, NH, and RH conceived the manuscript. BF analyzed the data with assistance from JT and contributions from CB and NH. BF drafted the manuscript with assistance from JT, CB, NH, and RH along with input from all the other co-authors. All authors read and approved the final manuscript.

FUNDING

Primary funding for this work, including research shiptime, fishing operations, and acoustic and SPOT tags, was provided by OCEARCH and its sponsors. Funding for PSATs was provided by the Shark Foundation (Hai Siftung) and the Disney Conservation Fund. PSAT data analysis was supported by a grant from NOAA/National Sea Grant to RH. Support for RH's contributions was provided by the Perry W. Gilbert Chair in Shark Research at Mote Marine Laboratory, NOAA, and OCEARCH.

ACKNOWLEDGMENTS

We are most grateful to the Captain and entire crew and staff of the M/V OCEARCH for their unique skills in capturing and handling white sharks for this study. This work would not have been possible without their expertise and hard work. We also thank all the collaborating scientists associated with the WNA white shark project for their contributions. Special thanks are extended to Mike James of Fisheries and Oceans Canada, for his substantial efforts to recover two of our PSATs on Nova Scotia shores.

SUPPLEMENTARY MATERIAL

The Supplementary Material for this article can be found online at: https://www.frontiersin.org/articles/10.3389/fmars.2021.744202/full#supplementary-material

Supplementary Figure 1 | Proportions of locations across range of behavioral scores from the hSSM from locations over the continental shelf and off-the-shelf. Locations are color coded by behavioral score (1.00–1.25 = transient, 1.25–1.75, 1.75–2.00 = resident).

Supplementary Figure 2 | Daily regularized locations for WS-13-01, a 4.4 m TL adult female white shark tracked for 1,473 days.

Supplementary Figure 3 | Daily regularized locations for WS12-17, a 4.9 m TL adult female white shark tracked for 1,734 days.

Supplementary Figure 4 | Daily regularized locations for WS-13-03, a 4.3 m TL adult female white shark tracked for 2,647 days.

Supplementary Figure 5 | Time-at-temperature for four PSAT-tagged white sharks across behavioral seasons. **(A)** Late summer/early autumn; **(B)** southern migration; **(C)** overwintering; **(D)** northern migration.

Supplementary Figure 6 | Week-long depth profile from recovered PSAT of white shark NS2018-06 demonstrating contrasting vertical movement between resident and transient phases. **(A)** High resolution depth data from October 29 to November 5. Mean daily distance traveled for the resident (red) and transient (green) phases is shown as a colored trace (right axis). **(B)** Inset map of the mid Atlantic coast showing the most probable track (MPT) for this period. **(C)** Time-at-depth for the resident phase. **(D)** Time-at-depth for the transient phase.

Supplementary Figure 7 | Daily regularized locations classified as resident behavior ($b > 1.75$) for sharks captured in Massachusetts and Nova Scotia showing fidelity to summer/early autumn residency areas.

Supplementary Figure 8 | Migration pathways from regularized daily locations for a 3.8 m TL adult male white shark (LC2017-01) **(A)** over a 2-year cycle (2017–2018) demonstrating both on-shelf and off-shelf migrations. Tracks are color-coded by year and season. Northern migrations represented by red hues, southern migrations by green, and residency locations by blue. This shark migrated on-shelf during both northward migrations but migrated off-shelf during one of two southward migrations during its 2-year tracking period. Raw SPOT and acoustic locations for a 3.7 m TL subadult female (ACK2016-02) in the region around Massachusetts over a 5-year period **(B)** and 3.9 m TL adult male (NS2018-03) in the region around Nova Scotia over a 3-year period **(C)** showing fine-scale fidelity to specific areas within the summer/autumn foraging areas. In panels **(B,C)**, common months share symbols and common years share color.

REFERENCES

Acuña-Marrero, D., Smith, A. N. H., Hammerschlag, N., Hearn, A., Anderson, M. J., Calich, H., et al. (2017). Residency and movement patterns of an apex predatory shark (*Galeocerdo cuvier*) at the Galapagos Marine Reserve. *PLoS One* 12:e0183669. doi: 10.1371/journal.pone.0183669

Ajemian, M. J., Drymon, J. M., Hammerschlag, N., Wells, R. J. D., Street, G., Falterman, B., et al. (2020). Movement patterns and habitat use of tiger sharks (*Galeocerdo cuvier*) across ontogeny in the Gulf of Mexico. *PLoS One* 15:e02348680. doi: 10.1371/journal.pone.0234868

Alexander, R. M. (2013). *Principles of Animal Locomotion*. Princeton, NJ: Princeton University Press.

Andersen, J. M., Wiersma, Y. F., Stenson, G. B., Hammill, M. O., Rosing-Asvid, A., and Skern-Maurizen, M. (2013). Habitat selection by hooded seals (*Cystophora cristata*) in the Northwest Atlantic Ocean. *ICES J. Mar. Sci.* 70, 173–185. doi: 10.1093/icesjms/fss133

Anderson, J. T., and Gardner, G. A. (1986). Plankton communities and physical oceanography observed on the Southeast Shoal region, Grand Bank of Newfoundland. *J. Plankton Res.* 8, 1111–1135. doi: 10.1093/plankt/8.6.1111

Anderson, S. D., Chapple, T. K., Jorgensen, S. J., Klimley, A. P., and Block, B. A. (2011). Long-term individual identification and site fidelity of white sharks, *Carcharodon carcharias*, off California using dorsal fins. *Mar. Biol.* 158, 1233–1237. doi: 10.1007/s00227-011-1643-5

Bangley, C. W., Curtis, T. H., Secor, D. H., Latour, R. J., and Ogburn, M. B. (2020). Identifying important juvenile dusky shark habitat in the Northwest Atlantic Ocean using acoustic telemetry and spatial modeling. *Mar. Coast. Fish.* 12, 348–363. doi: 10.1002/mcf2.10120

Bangley, C. W., Paramore, L., Shiffman, D. S., and Rulifson, R. A. (2018). Increased abundance and nursery habitat use of the bull shark (*Carcharhinus leucas*) in response to a changing environment in a warm-temperate estuary. *Sci. Rep.* 8:6018. doi: 10.1038/s41598-018-24510-z

Barnett, A., Abrantes, K. G., Stevens, J. D., and Semmens, J. M. (2011). Site fidelity and sex-specific migration in a mobile apex predator: implications for conservation and ecosystem dynamics. *Anim. Behav.* 81, 1039–1048. doi: 10.1016/j.anbehav.2011.02.011

Bastien, G., Barkley, A., Chappus, J., Heath, V., Popov, S., Smith, R. A., et al. (2020). Inconspicuous, recovering, or northward shift: Status and management of the white shark (*Carcharodon carcharias*) in Atlantic Canada. *Can. J. Fish. Aquat. Sci.* 77, 1666–1677. doi: 10.1139/cjfas-2020-0055

Bauer, S., McNamara, J. M., and Barta, Z. (2020). Environmental variability, reliability of information and the timing of migration. *Proc. R. Soc. B* 287:20200622. doi: 10.1098/rspb.2020.0622

Bauer, S., Nolet, B. A., Giske, J., Chapman, J. W., Åkesson, S., Hedenström, A., et al. (2011). "Cues and decision rules in animal migration," in *Animal Migration: A Synthesis*, eds E. J. Milner-Gulland, J. M. Fryxell, and A. R. E. Sinclair (New York, NY: Oxford University Press), 68–88. doi: 10.1093/acprof:oso/9780199568994.003.0006

Biais, G., Coupeau, Y., Séret, B., Calmettes, B., Lopez, R., Hetherington, S., et al. (2017). Return migration patterns of porbeagle shark (*Lamna nasus*) in the Northeast Atlantic: implications for stock range and structure. *ICES J. Mar. Sci.* 74, 1268–1276. doi: 10.1093/icesjms/fsw233

Block, B. A., Jonsen, I. D., Jorgensen, S. J., Winship, A. J., Shaffer, S. A., Bograd, S. J., et al. (2011). Tracking apex marine predator movements in a dynamic ocean. *Nature* 475, 86–90. doi: 10.1038/nature10082

Blower, D. C., Pandolfi, J. M., Bruce, B. D., Gomez-Cabrera, M. D. C., and Ovenden, J. R. (2012). Population genetics of Australian white sharks reveals fine-scale spatial structure, transoceanic dispersal events and low effective population sizes. *Mar. Ecol. Prog. Ser.* 455, 229–244. doi: 10.3354/meps09659

Bonadonna, F., Lea, M. A., Dehorter, O., and Guinet, C. (2001). Foraging ground fidelity and route-choice tactics of a marine predator: the Antarctic fur seal *Arctocephalus gazella*. *Mar. Ecol. Prog. Ser.* 223, 287–297. doi: 10.3354/meps223287

Bonfil, R., and O'Brien, S. (2015). Strongly directional and differential swimming behavior of an adult female white shark, *Carcharodon carcharias* (Chondrichthyes: Lamnidae) from Guadalupe Island, Mexico. *Lat. Am. J. Aquat. Res.* 43, 267–273. doi: 10.3856/vol43-issue1-fulltext-24

Bonfil, R., Francis, M. P., Duffy, C., Manning, M. J., and O'Brien, S. (2010). Large-scale tropical movements and diving behavior of white sharks *Carcharodon carcharias* tagged off New Zealand. *Aquat. Biol.* 8, 115–123. doi: 10.3354/ab00217

Bonfil, R., Meÿer, M., Scholl, M. C., Johnson, R., O'Brien, S., Oosthuizen, H., et al. (2005). Transoceanic migration, spatial dynamics, and population linkages of white sharks. *Science* 310, 100–103. doi: 10.1126/science.1114898

Bowlby, H. D., and Gibson, A. J. F. (2020). Implications of life history uncertainty when evaluating status in the Northwest Atlantic population of white shark (*Carcharodon carcharias*). *Ecol. Evol.* 10, 4990–5000. doi: 10.1002/ece3.6252

Bowlin, M. S., Bisson, I. A., Shamoun-Baranes, J., Reichard, J. D., Sapir, N., Marra, P. P., et al. (2010). Grand challenges in migration biology. *Integr. Comp. Biol.* 50, 261–279. doi: 10.1093/icb/icq013

Bradford, R., Patterson, T. A., Rogers, P. J., McAuley, R., Mountford, S., Huveneers, C., et al. (2020). Evidence of diverse movement strategies and habitat use by white sharks, *Carcharodon carcharias*, off southern Australia. *Mar. Biol.* 167, 1–12. doi: 10.1007/s00227-020-03712-y

Bradshaw, C. J., Davis, L. S., Lalas, C., and Harcourt, R. G. (2000). Geographic and temporal variation in the condition of pups of the New Zealand fur seal (*Arctocephalus forsteri*): evidence for density dependence and differences in the marine environment. *J. Zool.* 252, 41–51. doi: 10.1111/j.1469-7998.2000.tb00818.x

Braun, C. D., Galuardi, B., and Thorrold, S. R. (2018). HMMoce: an R package for improved geolocation of archival-tagged fishes using a hidden Markov method. *Methods Ecol. Evol.* 9, 1212–1220. doi: 10.1111/2041-210X.12959

Braun, C. D., Gaube, P., Sinclair-Taylor, T. H., Skomal, G. B., and Thorrold, S. R. (2019). Mesoscale eddies release pelagic sharks from thermal constraints to foraging in the ocean twilight zone. *Proc. Natl. Acad. Sci. U.S.A.* 116, 17187–17192. doi: 10.1073/pnas.1903067116

Breau, C., Cunjak, R. A., and Peake, S. J. (2011). Behaviour during elevated water temperatures: can physiology explain movement of juvenile Atlantic salmon to cool water? *J. Anim. Ecol.* 80, 844–853. doi: 10.1111/j.1365-2656.2011.01828.x

Brodersen, J., Nilsson, P. A., Chapman, B. B., Skov, C., Hansson, L. A., and Brönmark, C. (2012). Variable individual consistency in timing and destination of winter migrating fish. *Biol. Lett.* 8, 21–23. doi: 10.1098/rsbl.2011.0634

Brodie, P., and Beck, B. (1983). Predation by sharks on the grey seal (*Haliochoerus grypus*) in Eastern Canada. *Can. J. Fish. Aquat. Sci.* 40, 267–271. doi: 10.1139/f83-040

Bruce, B. D. (2008). "The biology and ecology of the white shark, *Carcharodon carcharias*," in *Sharks of the Open Ocean: Biology, Fisheries, and Conservation*, eds M. D. Camhi, E. K. Pikitch, and E. A. Babcock (Oxford: Blackwell Publishing), 69–81. doi: 10.1002/9781444302516.ch5

Bruce, B. D., and Bradford, R. W. (2012). "Habitat use and spatial dynamics of juvenile white sharks *Carcharodon carcharias*," in *Eastern Australia, in Global Perspectives on the Biology and Life History of the White Shark*, ed. M. L. Domeier (Boca Raton, FL: CRC Press), 225–254.

Bruce, B. D., Harasti, D., Lee, K., Gallen, C., and Bradford, R. (2019). Broad-scale movements of juvenile white sharks *Carcharodon carcharias* in eastern Australia from acoustic and satellite telemetry. *Mar. Ecol. Prog. Ser.* 619, 1–15. doi: 10.3354/meps12969

Bruce, B. D., Stevens, J. D., and Malcolm, H. (2006). Movements and swimming behaviour of white sharks (*Carcharodon carcharias*) in Australian waters. *Mar. Biol.* 150, 161–172. doi: 10.1007/s00227-006-0325-1

Bruce, B., and Bradford, R. (2015). Segregation or aggregation? Sex-specific patterns in the seasonal occurrence of white sharks *Carcharodon carcharias* at the Neptune Islands, South Australia. *J. Fish Biol.* 87, 1355–1370. doi: 10.1111/jfb.12827

Carlisle, A. B., Kim, S. L., Semmens, B. X., Madigan, D. J., Jorgensen, S. J., Perle, C. R., et al. (2012). Using stable isotope analysis to understand the migration and trophic ecology of northeastern Pacific white sharks (*Carcharodon carcharias*). *PLoS One* 7:e30492. doi: 10.1371/journal.pone.0030492

Carscadden, J. E., Frank, K. T., and Miller, D. S. (1989). Capelin (*Mallotus villosus*) spawning on the Southeast Shoal: influence of physical factors past and present. *Can. J. Fish. Aquat. Sci.* 46, 1743–1754. doi: 10.1139/f89-221

Casey, J. G., and Pratt, H. L. Jr. (1985). Distribution of the white shark, *Carcharodon carcharias*, in the Western North Atlantic. *Mem. South. Calif. Acad. Sci.* 9, 2–14.

Chambault, P., Roquet, F., Benhamou, S., Baudena, A., Pauthenet, E., de Thoisy, B., et al. (2017). The Gulf Stream frontal system: a key oceanographic feature in the habitat selection of the leatherback turtle? *Deep Res. Part I Oceanogr. Res. Pap.* 123, 35–47. doi: 10.1016/j.dsr.2017.03.003

Chapman, D. D., Feldheim, K. A., Papastamatiou, Y. P., and Hueter, R. E. (2015). There and back again: a review of residency and return migrations in sharks, with implications for population structure and management. *Annu. Rev. Mar. Sci.* 7, 547–570. doi: 10.1146/annurev-marine-010814-015730

Christiansen, H. M., Lin, V., Tanaka, S., Velikanov, A., Mollet, H. F., Wintner, S. P., et al. (2014). The last frontier: catch records of white sharks (*Carcharodon carcharias*) in the Northwest Pacific Ocean. *PLoS One* 9:e94407. doi: 10.1371/journal.pone.0094407

CLS (Collecte Localisation Satellites) (2016). *Argos User's Manual*. Available online at: http://www.argos-system.org (accessed July 09, 2021)

Cochran, J. E. M., Braun, C. D., Fernando Cagua, E., Campbell, M. F., Hardenstine, R. S., Kattan, A., et al. (2019). Multi-method assessment of whale shark (*Rhincodon typus*) residency, distribution, and dispersal behavior at an aggregation site in the Red Sea. *PLoS One* 4:e0222285. doi: 10.1371/journal.pone.0222285

Coelho, R., Fernandez-Carvalho, J., and Santos, M. N. (2015). Habitat use and diel vertical migration of bigeye thresher shark: overlap with pelagic longline fishing gear. *Mar. Environ. Res.* 112, 91–99. doi: 10.1016/j.marenvres.2015.10.009

Coffey, D. M., Carlisle, A. B., Hazen, E. L., and Block, B. A. (2017). Oceanographic drivers of the vertical distribution of a highly migratory, endothermic shark. *Sci. Rep.* 7:10434. doi: 10.1038/s41598-017-11059-6

Colefax, A. P., Kelaher, B. P., Pagendam, D. E., and Butcher, P. A. (2020). Assessing white shark (*Carcharodon carcharias*) behavior along coastal beaches for conservation-focused shark mitigation. *Front. Mar. Sci.* 7:268. doi: 10.3389/fmars.2020.00268

Comfort, C. M., and Weng, K. C. (2015). Vertical habitat and behaviour of the bluntnose sixgill shark in Hawaii. *Deep Sea Res. Part II* 115, 116–126. doi: 10.1016/j.dsr2.2014.04.005

Compagno, L. J. (2001). *Sharks of the World: An Annotated and Illustrated Catalogue of Shark Species Known to Date (No. 1)*. Rome: Food & Agriculture Organization, 269.

Compagno, L. J. V., Marks, M. A., and Fergusson, I. K. (1997). Threatened fishes of the world: *Carcharodon carcharias* (Linnaeus, 1758) (Lamnidae). *Environ. Biol. Fish.* 50, 61–62. doi: 10.1023/A:1007308406137

Coughlan, G. (2002). *The Southeast Shoal Area of the Grand Banks of Newfoundland Potential as a Marine Protected Area: A Biophysical and Socio-Economic Area Examination.* [Master's thesis]. Calgary, AB: University of Calgary.

Curtis, T. H., McCandless, C. T., Carlson, J. K., Skomal, G. B., Kohler, N. E., Natanson, L. J., et al. (2014). Seasonal distribution and historic trends in abundance of white sharks, *Carcharodon carcharias*, in the western North Atlantic ocean. *PLoS One* 9:e99240. doi: 10.1371/journal.pone.0099240

Curtis, T. H., Metzger, G., Fischer, C., McBride, B., McCallister, M., Winn, L. J., et al. (2018). First insights into the movements of young-of-the-year white sharks (*Carcharodon carcharias*) in the western North Atlantic Ocean. *Sci. Rep.* 8:10794. doi: 10.1038/s41598-018-29180-5

Del Raye, G., Jorgensen, S. J., Krumhansl, K., Ezcurra, J. M., and Block, B. A. (2013). Travelling light: white sharks (*Carcharodon carcharias*) rely on body lipid stores to power ocean-basin scale migration. *Proc. R. Soc. B Biol. Sci.* 280:20130836. doi: 10.1098/rspb.2013.0836

den Heyer, C. E., Don Bowen, W., Dale, J., Gosselin, J., Hammill, M. O., Johnston, D. W., et al. (2021). Contrasting trends in gray seal (*Haliochoerus grypus*) pup production throughout the increasing northwest Atlantic metapopulation. *Mar. Mamm. Sci.* 37, 611–630. doi: 10.1111/mms.12773

Dodson, J. J., Aubin-Horth, N., Thériault, V., and Páez, D. J. (2013). The evolutionary ecology of alternative migratory tactics in salmonid fishes. *Biol. Rev.* 88, 602–625. doi: 10.1111/brv.12019

Domeier, M. L. (2012). "A new life-history hypothesis for white sharks, *Carcharodon carcharias*," in *The Northeastern Pacific, in Global Perspectives on the Biology and Life History of the White Shark*, ed. M. L. Domeier (Boca Raton, FL: CRC Press), 199–224. doi: 10.1201/b11532-21

Domeier, M. L., and Nasby-Lucas, N. (2008). Migration patterns of white sharks *Carcharodon carcharias* tagged at Guadalupe Island, Mexico, and identification of an eastern Pacific shared offshore foraging area. *Mar. Ecol. Prog. Ser.* 370, 221–237. doi: 10.3354/meps07628

Domeier, M. L., and Nasby-Lucas, N. (2012). "Sex-specific migration patterns and sexual segregation of adult white sharks, *Carcharodon carcharias*," in *The Northeastern Pacific, in Global Perspectives on the Biology and Life History of the White Shark*, ed. M. L. Domeier (Boca Raton, FL: CRC Press), 133–146.

Domeier, M. L., and Nasby-Lucas, N. (2013). Two-year migration of adult female white sharks (*Carcharodon carcharias*) reveals widely separated nursery areas and conservation concerns. *Anim. Biotelem.* 1, 1–10. doi: 10.1186/2050-3385-1-2

Duffy, C. A. J., Francis, M. P., Manning, M. J., and Bonfil, R. (2012). "Regional population connectivity, oceanic habitat, and return migration revealed by satellite tagging of white sharks, *Carcharodon carcharias*, at New Zealand aggregation sites," in *Global Perspectives on the Biology and Life History of the White Shark*, ed. M. L. Domeier (Boca Raton, FL: CRC Press), 301–318.

Earl, J. E., and Zollner, P. A. (2017). Advancing research on animal-transported subsidies by integrating animal movement and ecosystem modelling. *J. Anim. Ecol.* 86, 987–997. doi: 10.1111/1365-2656.12711

Edwards, J. E., Hiltz, E., Broell, F., Bushnell, P. G., Campana, S. E., Christiansen, J. S., et al. (2019). Advancing research for the management of long-lived species: a case study on the Greenland shark. *Front. Mar. Sci.* 6:87. doi: 10.3389/fmars.2019.00087

Epperly, S. P., Watson, J. W., Foster, D. G., and Shah, A. K. (2012). Anatomical hooking location and condition of animals captured with pelagic longlines: the Grand Banks experiments 2002–2003. *Bull. Mar. Sci.* 88, 513–527. doi: 10.5343/bms.2011.1083

Fagan, W. F., Lewis, M. A., Auger-Méthé, M., Avgar, T., Benhamou, S., Breed, G., et al. (2013). Spatial memory and animal movement. *Ecol. Lett.* 16, 1316–1329. doi: 10.1111/ele.12165

Ferreira, C. A., and Ferreira, T. P. (1996). "Population dynamics of white sharks in South Africa," in *Great White Sharks: The Biology of Carcharodon carcharias*, eds A. P. Klimley and D. G. Ainley (San Diego, CA: Academic Press), 381–391. doi: 10.1016/B978-012415031-7/50036-7

Ford, R. G. (1983). Home range in a patchy environment: optimal foraging predictions. *Am. Zool.* 23, 315–326. doi: 10.1093/icb/23.2.315

Francis, M. P. (1996). "Observations on a pregnant white shark with a review of reproductive biology," in *Great White Sharks: The Biology of Carcharodon carcharias*, eds A. P. Klimley and D. G. Ainley (San Diego, CA: Academic Press), 0157–172. doi: 10.1016/B978-012415031-7/50016-1

Francis, M. P., Duffy, C. A. J., Bonfil, R., and Manning, M. J. (2012). "The third dimension. Vertical habitat use by white sharks, *Carcharodon carcharias*," in *New Zealand and in Oceanic and Tropical Waters of the Southwest Pacific Ocean, in Global Perspectives on the Biology and Life History of the White Shark*, ed. M. L. Domeier (Boca Raton, FL: CRC Press), 319–342. doi: 10.1201/b11532-25

Francis, M. P., Duffy, C., and Lyon, W. (2015). Spatial and temporal habitat use by white sharks (*Carcharodon carcharias*) at an aggregation site in southern New Zealand. *Mar. Freshw. Res.* 66, 900–918. doi: 10.1071/MF14186

Fraser, K. C., Shave, A., de Greef, E., Siegrist, J., and Garroway, C. J. (2019). Individual variability in migration timing can explain long-term, population-level advances in a songbird. *Front. Ecol. Evol.* 7:324. doi: 10.3389/fevo.2019.00324

French, G. C. A., Rizzuto, S., Stürup, M., Inger, R., Barker, S., van Wyk, J. H., et al. (2018). Sex, size, and isotopes: cryptic trophic ecology of an apex predator, the white shark *Carcharodon carcharias*. *Mar. Biol.* 165, 1–11. doi: 10.1007/s00227-018-3343-x

Galuardi, B., Royer, F., Golet, W., Logan, J., Neilson, J., and Lutcavage, M. (2010). Complex migration routes of Atlantic bluefin tuna (*Thunnus thynnus*) question current population structure paradigm. *Can. J. Fish. Aquat. Sci.* 67, 966–976. doi: 10.1139/F10-033

Gaube, P., Braun, C. D., Lawson, G. L., McGillicuddy, D. J., Della Penna, A., Skomal, G. B., et al. (2018). Mesoscale eddies influence the movements of mature female white sharks in the Gulf Stream and Sargasso Sea. *Sci. Rep.* 8:7363. doi: 10.1038/s41598-018-25565-8

Gleiss, A. C., Jorgensen, S. J., Liebsch, N., Sala, J. E., Norman, B., Hays, G. C., et al. (2011). Convergent evolution in locomotory patterns of flying and swimming animals. *Nat. Commun*. 2:352. doi: 10.1038/ncomms1350

Goldman, K. J., and Anderson, S. D. (1999). Space utilization and swimming depth of white sharks, *Carcharodon carcharias*, at the South Farallon Islands, central California. *Environ. Biol. Fish.* 56, 351–364. doi: 10.1023/A:1007520931105

Goldman, K. J., Anderson, S. D., Latour, R. J., and Musick, J. A. (2004). Homeothermy in adult salmon sharks, *Lamna ditropis*. *Environ. Biol. Fish*. 71, 403–411. doi: 10.1007/s10641-004-6588-9

Gowan, T. A., and Ortega-Ortiz, J. G. (2014). Wintering habitat model for the North Atlantic right whale (*Eubalaena glacialis*) in the southeastern United States. *PLoS One* 9:e95126. doi: 10.1371/journal.pone.0095126

Grainger, R., Peddemors, V. M., Raubenheimer, D., and Machovsky-Capuska, G. E. (2020). Diet composition and nutritional niche breadth variability in juvenile white sharks (*Carcharodon carcharias*). *Front. Mar. Sci.* 7:422. doi: 10.3389/fmars.2020.00422

Gubili, C., Robinson, C. E. C., Cliff, G., Wintner, S. P., de Sabata, E., De Innocentiis, S. D., et al. (2015). DNA from historical and trophy samples provides insights into white shark population origins and genetic diversity. *Endanger. Species Res.* 27, 233–241. doi: 10.3354/esr00665

Hammill, M. O., den Heyer, C. E., Bowen, W. D., and Lang, S. L. C. (2017). Grey seal population trends in canadian waters, 1960–2016 and harvest advice. *DFO Can. Sci. Advis. Sec. Res. Doc. 2017/052.* v + 30 p.

Harding, L., Jackson, A., Barnett, A., Donohue, I., Halsey, L., Huveneers, C., et al. (2021). Endothermy makes fishes faster but does not expand their thermal niche. *Funct. Ecol.* 35, 1951–1959. doi: 10.1111/1365-2435.13869

Hayes, S. A., Hanson, C. V., Pearse, D. E., Bond, M. H., Garza, J. C., and MacFarlane, R. B. (2012). Should I stay or should I go? The influence of genetic origin on emigration behavior and physiology of resident and anadromous juvenile *Oncorhynchus mykiss*. *N. Am. J. Fish. Manag*e. 32, 772–780. doi: 10.1080/02755947.2012.686953

Hewitt, A. M., Kock, A. A., Booth, A. J., and Griffiths, C. L. (2018). Trends in sightings and population structure of white sharks, *Carcharodon carcharias*, at Seal Island, False Bay, South Africa, and the emigration of subadult female sharks approaching maturity. *Environ. Biol. Fish*. 101, 39–54. doi: 10.1007/s10641-017-0679-x

Hillary, R. M., Bravington, M. V., Patterson, T. A., Grewe, P., Bradford, R., Feutry, P., et al. (2018). Genetic relatedness reveals total population size of white sharks in eastern Australia and New Zealand. *Sci. Rep.* 8:2661. doi: 10.1038/s41598-018-20593-w

Hoffmayer, E. R., McKinney, J. A., Franks, J. S., Hendon, J. M., Driggers, W. B., Falterman, B. J., et al. (2021). Seasonal occurrence, horizontal movements, and habitat use patterns of whale sharks (*Rhincodon typus*) in the Gulf of Mexico. *Front. Mar. Sci.* 7:1070. doi: 10.3389/fmars.2020.598515

Hoyos-Padilla, E. M., Klimley, A. P., Galván-Magaña, F., and Antoniou, A. (2016). Contrasts in the movements and habitat use of juvenile and adult white sharks (*Carcharodon carcharias*) at Guadalupe Island, Mexico. *Anim. Biotelem.* 4, 1–14. doi: 10.1186/s40317-016-0106-7

Hueter, R. E., Heupel, M. R., Heist, E. J., and Keeney, D. B. (2005). Evidence of philopatry in sharks and implications for the management of shark fisheries. *J. Northwest Atl. Fish. Sci.* 35, 239–247. doi: 10.2960/J.v35.m493

Hueter, R. E., Manire, C. A., Tyminski, J. P., Hoenig, J. M., and Hepworth, D. A. (2006). Assessing mortality of released or discarded fish using a logistic model of relative survival derived from tagging data. *Trans. Am. Fish. Soc.* 135, 500–508. doi: 10.1577/T05-065.1

Hussey, N. E., DiBattista, J. D., Moore, J. W., Ward, E. J., Fisk, A. T., Kessel, S., et al. (2017). Risky business for a juvenile marine predator? Testing the influence of foraging strategies on size and growth rate under natural conditions. *Proc. R. Soc. B* 284:20170166. doi: 10.1098/rspb.2017.0166

Hussey, N. E., Kessel, S. T., Aarestrup, K., Cooke, S. J., Cowley, P. D., Fisk, A. T., et al. (2015). Aquatic animal telemetry: a panoramic window into the underwater world. *Science* 348:6240. doi: 10.1126/science.1255642

Hussey, N. E., McCann, H. M., Cliff, G., Dudley, S. F. J., Wintner, S. P., and Fisk, A. T. (2012). "Size-based analysis of diet and trophic position of the white shark, *Carcharodon carcharias*," in *South African Waters, in Global Perspectives on the Biology and Life History of the White Shark*, ed. M. L. Domeier (Boca Raton, FL: CRC Press), 27–50. doi: 10.1201/b11532-5

Hutcheson, M. S., Stewart, P. L., and Spry, J. M. (1981). *The Biology of Benthic Communities of the Grand Banks of Newfoundland (Including the Hibernia Area).* Grand Banks Oceanographic Study, Consultants Report to Mobil Oil Canada Limited, Vol. 7. St. John's, NL: MacLaren Plansearch Limited, 138.

Hutchinson, M., Coffey, D. M., Holland, K., Itano, D., Leroy, B., Kohin, S., et al. (2019). Movements and habitat use of juvenile silky sharks in the Pacific Ocean inform conservation strategies. *Fish. Res.* 210, 131–142. doi: 10.1016/j.fishres.2018.10.016

Huveneers, C., Apps, K., Becerril-García, E. E., Bruce, B., Butcher, P. A., Carlisle, A. B., et al. (2018). Future research directions on the "elusive" white shark. *Front. Mar. Sci*. 5:455. doi: 10.3389/fmars.2018.00455

IPCC (2014). *Climate Change 2014 Synthesis Report*. Geneva: IPCC.

Jewell, O. J. D., Wcisel, M. A., Gennari, E., Towner, A. V., Bester, M. N., Johnson, R. L., et al. (2011). Effects of smart position only (SPOT) tag deployment on white sharks *Carcharodon carcharias* in South Africa. *PLoS One* 6:e27242. doi: 10.1371/journal.pone.0027242

Jewell, O. J., Johnson, R. L., Gennari, E., and Bester, M. N. (2013). Fine scale movements and activity areas of white sharks (*Carcharodon carcharias*) in Mossel Bay, South Africa. *Environ. Biol. Fish.* 96, 881–894. doi: 10.1007/s10641-012-0084-4

Jonsen, I. (2016). Joint estimation over multiple individuals improves behavioural state inference from animal movement data. *Sci. Rep.* 6:20625. doi: 10.1038/srep20625

Jonsen, I. D., Basson, M., Bestley, S., Bravington, M. V., Patterson, T. A., Pedersen, M. W., et al. (2013). State-space models for bio-loggers: a methodological road map. *Deep Sea Res. Part II* 88–89, 34–46. doi: 10.1016/j.dsr2.2012.07.008

Jonsen, I. D., Myers, R. A., and James, M. C. (2007). Identifying leatherback turtle foraging behaviour from satellite telemetry using a switching state-space model. *Mar. Ecol. Prog. Ser.* 337, 255–264. doi: 10.3354/meps337255

Jonsen, I. D., Patterson, T. A., Costa, D. P., Doherty, P. D., Godley, B. J., Grecian, W. J., et al. (2020). A continuous-time state-space model for rapid quality-control of Argos locations from animal-borne tags. *Mov. Ecol.* 8, 1–13. doi: 10.1186/s40462-020-00217-7

Jorgensen, S. J., Anderson, S., Ferretti, F., Tietz, J. R., Chapple, T., Kanive, P., et al. (2019). Killer whales redistribute white shark foraging pressure on seals. *Sci. Rep.* 9:6153. doi: 10.1038/s41598-019-39356-2

Jorgensen, S. J., Chapple, T. K., Anderson, S., Hoyos, M., Reeb, C., and Block, B. A. (2012). "Connectivity among white shark coastal aggregation areas in the Northeastern Pacific," in *Global Perspectives on the Biology and Life History of the White Shark*, ed. M. L. Domeier (Boca Raton, FL: CRC Press), 159–168.

Jorgensen, S. J., Reeb, C. A., Chapple, T. K., Anderson, S., Perle, C., Van Sommeran, S. R., et al. (2010). Philopatry and migration of Pacific white sharks. *Proc. R. Soc. B Biol. Sci.* 277, 679–688. doi: 10.1098/rspb.2009.1155

Keller, B. A., Putman, N. F., Grubbs, R. D., Portnoy, D. S., and Murphy, T. P. (2021). Map-like use of Earth's magnetic field in sharks. *Curr. Biol.* 31, 2881–2886. doi: 10.1016/j.cub.2021.03.103

Kennedy, A. S., Zerbini, A. N., Vásquez, O. V., Gandilhon, N., Clapham, P. J., and Adam, O. (2014). Local and migratory movements of humpback whales (*Megaptera novaeangliae*) satellite-tracked in the North Atlantic Ocean. *Can. J. Zool.* 92, 9–18. doi: 10.1139/cjz-2013-0161

Kessel, S. T., Chapman, D. D., Franks, B. R., Gedamke, T., Gruber, S. H., Newman, J. M., et al. (2014). Predictable temperature-regulated residency, movement, and migration in a large, highly mobile marine predator (*Negaprion brevirostris*). *Mar. Ecol. Prog. Ser.* 514, 175–190. doi: 10.3354/meps10966

Kock, A. A., Photopoulou, T., Durbach, I., Mauff, K., Meyer, M., Kotze, D., et al. (2018). Summer at the beach: spatio-temporal patterns of white shark occurrence along the inshore areas of False Bay, South Africa. *Mov. Ecol.* 6:7. doi: 10.1186/s40462-018-0125-5

Kock, A., O'Riain, M. J., Mauff, K., Meÿer, M., Kotze, D., and Griffiths, C. (2013). Residency, habitat use and sexual segregation of white sharks, *Carcharodon carcharias* in False Bay, South Africa. *PLoS One* 8:e55048. doi: 10.1371/journal.pone.0055048

Lee, K., Butcher, P., Harcourt, R., Patterson, T., Peddemors, V., Roughan, M., et al. (2021). Oceanographic conditions associated with white shark (*Carcharodon carcharias*) habitat use along eastern Australia. *Mar. Ecol. Prog. Ser.* 659, 143–159. doi: 10.3354/meps13572

Loder, J. W. (1991). Summertime bottom temperatures on the Southeast Shoal of the Grand Bank, and implications for exchange rates. *Can. J. Fish. Aquat. Sci.* 48, 1316–1325. doi: 10.1139/f91-158

Lowther, A. D., Harcourt, R. G., Hamer, D. J., and Goldsworthy, S. D. (2011). Creatures of habit: foraging habitat fidelity of adult female Australian sea lions. *Mar. Ecol. Prog. Ser.* 443, 249–263. doi: 10.3354/meps09392

Lucas, Z. N., and Natanson, L. J. (2010). Two shark species involved in predation on seals at Sable Island, Nova Scotia, Canada. *Proc. N. S. Inst. Sci.* 45, 64–88.

Madigan, D. J., Brooks, E. J., Bond, M. E., Gelsleichter, J., Howey, L. A., Abercrombie, D. L., et al. (2015). Diet shift and site-fidelity of oceanic whitetip sharks *Carcharhinus longimanus* along the Great Bahama Bank. *Mar. Ecol. Prog. Ser.* 529, 185–197. doi: 10.3354/meps11302

Malcolm, H., Bruce, B. D., and Stevens, J. D. (2001). *A Review of the Biology and Status of White Sharks in Australian Waters. Report to Environment Australia, Marine Species Protection Program*. Hobart, TAS: CSIRO Marine Research, 113.

Merkle, J. A., Cherry, S. G., and Fortin, D. (2015). Bison distribution under conflicting foraging strategies: site fidelity vs. Energy maximization. *Ecology* 96, 1793–1801. doi: 10.1890/14-0805.1

Merkle, J. A., Fortin, D., and Morales, J. M. (2014). A memory-based foraging tactic reveals an adaptive mechanism for restricted space use. *Ecol. Lett.* 17, 924–931. doi: 10.1111/ele.12294

Moxley, J. H., Skomal, G., Chisholm, J., Halpin, P., and Johnston, D. W. (2020). Daily and seasonal movements of Cape Cod gray seals vary with predation risk. *Mar. Ecol. Prog. Ser.* 644, 215–228. doi: 10.3354/meps13346

Murphy, M. D., Adams, D. H., Tremain, D. M., and Winner, B. L. (1998). Direct validation of ages determined for adult black drum, *Pogonias cromis, in east-central Florida, with notes on black drum migration. Fish. Bull.* 96, 382–387.

Nakaya, K. (1994). Distribution of white shark in Japanese waters. *Fish. Sci.* 60, 515–518. doi: 10.2331/fishsci.60.515

Nathan, R., Getz, W. M., Revilla, E., Holyoak, M., Kadmon, R., Saltz, D., et al. (2008). A movement ecology paradigm for unifying organismal movement research. *Proc. Natl. Acad. Sci. U.S.A.* 105, 19052–19059. doi: 10.1073/pnas.0800375105

Nosal, A. P., Cartamil, D. P., Ammann, A. J., Bellquist, L. F., Ben-Aderet, N. J., Blincow, K. M., et al. (2021). Triennial migration and philopatry in the critically endangered soupfin shark *Galeorhinus galeus*. *J. Appl. Ecol.* 58, 1570–1582. doi: 10.1111/1365-2664.13848

O'Leary, S. J., Feldheim, K. A., Fields, A. T., Natanson, L. J., Wintner, S., Hussey, N., et al. (2015). Genetic diversity of white sharks, *Carcharodon carcharias*, in the Northwest Atlantic and Southern Africa. *J. Hered.* 106, 258–265. doi: 10.1093/jhered/esv001

Pade, N. G., Queiroz, N., Humphries, N. E., Witt, M. J., Jones, C. S., Noble, L. R., et al. (2009). First results from satellite-linked archival tagging of porbeagle shark, *Lamna nasus*: area fidelity, wider-scale movements and plasticity in diel depth changes. *J. Exp. Mar. Biol. Ecol.* 370, 64–74. doi: 10.1016/j.jembe.2008.12.002

Payne, N. L., Meyer, C. G., Smith, J. A., Houghton, J. D., Barnett, A., Holmes, B. J., et al. (2018). Combining abundance and performance data reveals how temperature regulates coastal occurrences and activity of a roaming apex predator. *Glob. Change Biol.* 24, 1884–1893. doi: 10.1111/gcb.14088

Payne, N. L., Smith, J. A., van der Meulen, D. E., Taylor, M. D., Watanabe, Y. Y., Takahashi, A., et al. (2016). Temperature dependence of fish performance in the wild: links with species biogeography and physiological thermal tolerance. *Funct. Ecol.* 30, 903–912. doi: 10.1111/1365-2435.12618

Pedersen, M. W., Righton, D., Thygesen, U. H., Andersen, K. H., and Madsen, H. (2008). Geolocation of North Sea cod (*Gadus morhua*) using hidden Markov models and behavioural switching. *Can. J. Fish. Aquat. Sci.* 65, 2367–2377. doi: 10.1139/F08-144

Pepin, P., Colbourne, E., and Maillet, G. (2011). Seasonal patterns in zooplankton community structure on the Newfoundland and Labrador Shelf. *Prog. Oceanogr.* 91, 273–285. doi: 10.1016/j.pocean.2011.01.003

Pershing, A. J., Alexander, M. A., Hernandez, C. M., Kerr, L. A., Le Bris, A., Mills, K. E., et al. (2015). Slow adaptation in the face of rapid warming leads to collapse of the Gulf of Maine cod fishery. *Science* 350, 809–812. doi: 10.1126/science.aac9819

Piper, W. H. (2011). Making habitat selection more "familiar": a review. *Behav. Ecol. Sociobiol.* 65, 1329–1351. doi: 10.1007/s00265-011-1195-1

Pratt, H. L. (1996). "Reproduction in the male white shark," in *Great White Sharks: The Biology of Carcharodon carcharias*, eds A. P. Klimley and D. G. Ainley (San Diego, CA: Academic Press), 131–138. doi: 10.1016/B978-012415031-7/50014-8

Pulido, F. (2007). Phenotypic changes in spring arrival: evolution, phenotypic plasticity, effects of weather and condition. *Clim. Res.* 35, 5–23. doi: 10.3354/cr00711

R Core Team (2020). *R: A Language and Environment for Statistical Computing*. Vienna: R Foundation for Statistical Computing.

Rigby, C. L., Barreto, R., Carlson, J., Fernando, D., Fordham, S., Francis, M., et al. (2019). *Carcharodon carcharias. IUCN Red List Threat. Species* 2019:e.T3855A2878674.

Robbins, R. L., Enarson, M., Bradford, R. W., Robbins, W. D., and Fox, A. G. (2015). Residency and local connectivity of white sharks at Liguanea Island: a second aggregation site in South Australia? *Open Fish Sci. J.* 8, 23–29. doi: 10.2174/1874401X01508010023

Saba, V. S., Griffies, S. M., Anderson, W. G., Winton, M., Alexander, M. A., Delworth, T. L., et al. (2016). Enhanced warming of the Northwest Atlantic Ocean under climate change. *J. Geophys. Res.-Oceans* 121, 118–132. doi: 10.1002/2015JC011346

Santana-Morales, O., Abadía-Cardoso, A., Hoyos-Padilla, M., Naylor, G. J., Corrigan, S., Malpica-Cruz, L., et al. (2020). The smallest known free-living white shark *Carcharodon carcharias* (Lamniformes: Lamnidae): ecological and management implications. *Copeia* 108, 39–46. doi: 10.1643/OT-19-233

Saunders, R. A., Royer, F., and Clarke, M. W. (2011). Winter migration and diving behaviour of porbeagle shark, *Lamna nasus*, in the Northeast Atlantic. *ICES J. Mar. Sci.* 68, 166–174. doi: 10.1093/icesjms/fsq145

Semmens, J. M., Payne, N. L., Huveneers, C., Sims, D. W., and Bruce, B. D. (2013). Feeding requirements of white sharks may be higher than originally thought. *Sci. Rep.* 3:1471. doi: 10.1038/srep01471

Shaw, A. K. (2016). Drivers of animal migration and implications in changing environments. *Evol. Ecol.* 30, 991–1007. doi: 10.1007/s10682-016-9860-5

Shaw, R. L., Curtis, T. H., Metzger, G., McCallister, M. P., Newton, A., Fischer, G. C., et al. (2021). Three-dimensional movements and habitat selection of young white sharks (*Carcharodon carcharias*) across a temperate continental shelf ecosystem. *Front. Mar. Sci.* 8:151. doi: 10.3389/fmars.2021.643831

Shimada, T., Limpus, C. J., Hamann, M., Bell, I., Esteban, N., Groom, R., et al. (2020). Fidelity to foraging sites after long migrations. *J. Anim. Ecol.* 89, 1008–1016. doi: 10.1111/1365-2656.13157

Sims, D. W. (2010). "Tracking and analysis techniques for understanding free-ranging shark movements and behavior," in *Sharks and Their Relatives II: Biodiversity, Adaptive Physiology, and Conservation*, eds J. C. Carrier, J. A. Musick, and M. R. Heithaus (Boca Raton, FL: CRC Press), 351–392. doi: 10.1201/9781420080483-c8

Sims, D. W., Humphries, N. E., Bradford, R. W., and Bruce, B. D. (2012). Lévy flight and Brownian search patterns of a free-ranging predator reflect different prey field characteristics. *J. Anim. Ecol.* 81, 432–442. doi: 10.1111/j.1365-2656.2011.01914.x

Skomal, G. B., and Benz, G. W. (2004). Ultrasonic tracking of Greenland sharks, *Somniosus microcephalus*, under Arctic ice. *Mar. Biol.* 145, 489–498. doi: 10.1007/s00227-004-1332-8

Skomal, G. B., Braun, C. D., Chisholm, J. H., and Thorrold, S. R. (2017). Movements of the white shark *Carcharodon carcharias* in the North Atlantic Ocean. *Mar. Ecol. Prog. Ser.* 580, 1–16. doi: 10.3354/meps12306

Skomal, G. B., Chisholm, J., and Correia, S. J. (2012). "Implications of increasing pinniped populations on the diet and abundance of white sharks off the coast of Massachusetts," in *Global Perspectives on the Biology and Life History of the White Shark*, ed. M. L. Domeier (Boca Raton, FL: CRC Press), 405–418.

Skomal, G., Marshall, H., Galuardi, B., Natanson, L., Braun, C., and Bernal, D. (2021). Horizontal and vertical movements patterns and habitat use of juvenile porbeagles (*Lamna nasus*) in the western north Atlantic. *Front. Mar. Sci.* 8:624158. doi: 10.3389/fmars.2021.624158

Skov, C., Aarestrup, K., Baktoft, H., Brodersen, J., Brönmark, C., Hansson, L. A., et al. (2011). Sizing up your enemy: individual predation vulnerability predicts migratory probability. *Proc. R. Soc. B Biol. Sci.* 278, 1414–1418. doi: 10.1098/rspb.2010.2035

Spaet, J. L. Y., Patterson, T. A., Bradford, R. W., and Butcher, P. A. (2020). Spatiotemporal distribution patterns of immature Australasian white sharks (*Carcharodon carcharias*). *Sci. Rep.* 10:10169. doi: 10.1038/s41598-020-66876-z

Speed, C. W., Field, I. C., Meekan, M. G., and Bradshaw, C. J. (2010). Complexities of coastal shark movements and their implications for management. *Mar. Ecol. Prog. Ser.* 408, 275–293. doi: 10.3354/meps08581

Stenson, G. B., and Sjare, B. (1997). "Seasonal distribution of harp seals, (*Phoca groenlandica*)," in The Northwest Atlantic, 23. *ICES C. M. 1997*/CC 10:23.

Stump, K. L., Crooks, C. J., Fitchett, M. D., Gruber, S. H., and Guttridge, T. L. (2017). Hunted hunters: an experimental test of the effects of predation risk on juvenile lemon shark habitat use. *Mar. Ecol. Prog. Ser.* 574, 85–95. doi: 10.3354/meps12187

Sulikowski, J. A., Wheeler, C. R., Gallagher, A. J., Prohaska, B. K., Langan, J. A., and Hammerschlag, N. (2016). Seasonal and life-stage variation in the reproductive ecology of a marine apex predator, the tiger shark *Galeocerdo cuvier*, at a protected female-dominated site. *Aquat. Biol.* 24, 175–184. doi: 10.3354/ab00648

Switzer, P. V. (1993). Site fidelity in predictable and unpredictable habitats. *Evol. Ecol.* 7, 533–555. doi: 10.1007/BF01237820

Tanaka, K. R., Van Houtan, K. S., Mailander, E., Dias, B. S., Galginaitis, C., O'Sullivan, J., et al. (2021). North Pacific warming shifts the juvenile range of a marine apex predator. *Sci. Rep.* 11:3373. doi: 10.1038/s41598-021-82424-9

Tanaka, S., Kitamura, T., Mochizuki, T., and Kofuji, K. (2011). Age, growth and genetic status of the white shark (*Carcharodon carcharias*) from Kashima-nada, Japan. *Mar. Freshw. Res.* 62, 548–556. doi: 10.1071/MF10130

Templeman, W. (1975). Comparison of temperatures in July-August hydrographic sections of the eastern Newfoundland area in 1972 and 1973 with those from 1951 to 1971. *Int. Comm. Northwest Atl. Fish. Spec. Publ.* 10, 17–31.

Tolotti, M. T., Bach, P., Hazin, F., Travassos, P., and Dagorn, L. (2015). Vulnerability of the oceanic whitetip shark to pelagic longline fisheries. *PLoS One* 10:e0141396. doi: 10.1371/journal.pone.0141396

Vaudo, J. J., Byrne, M. E., Wetherbee, B. M., Harvey, G. M., and Shivji, M. S. (2017). Long-term satellite tracking reveals region-specific movements of a large pelagic predator, the shortfin mako shark, in the western North Atlantic Ocean. *J. Appl. Ecol.* 54, 1765–1775. doi: 10.1111/1365-2664.12852

Watanabe, Y. Y., Payne, N. L., Semmens, J. M., Fox, A., and Huveneers, C. (2019). Swimming strategies and energetics of endothermic white sharks during foraging. *J. Exp. Biol.* 222:jeb185603. doi: 10.1242/jeb.185603

Weng, K. C., Castilho, P. C., Morrissette, J. M., Landeira-Fernandez, A. M., Holts, D. B., Schallert, R. J., et al. (2005). Satellite tagging and cardiac physiology reveal niche expansion in salmon sharks. *Science* 310, 104–106. doi: 10.1126/science.1114616

Weng, K. C., Boustany, A. M., Pyle, P., Anderson, S. D., Brown, A., and Block, B. A. (2007a). Migration and habitat of white sharks (*Carcharodon carcharias*) in the eastern Pacific Ocean. *Mar. Biol.* 152, 877–894. doi: 10.1007/s00227-007-0739-4

Weng, K. C., O'Sullivan, J. B., Lowe, C. G., Winkler, C. E., Dewar, H., and Block, B. A. (2007b). Movements, behavior and habitat preferences of juvenile white sharks *Carcharodon carcharias* in the eastern Pacific. *Mar. Ecol. Prog. Ser.* 338, 211–224. doi: 10.3354/meps338211

White, T. D., Carlisle, A. B., Kroodsma, D. A., Block, B. A., Casagrandi, R., De Leo, G. A., et al. (2017). Assessing the effectiveness of a large marine protected area for reef shark conservation. *Biol. Conserv.* 207, 64–71. doi: 10.1016/j.biocon.2017.01.009

Whitehead, H., and Glass, C. (1985). The significance of the Southeast Shoal of the Grand Bank to humpback whales and other cetacean species. *Can. J. Zool.* 63, 2617–2625. doi: 10.1139/z85-391

Winkler, D. W., Jørgensen, C., Both, C., Houston, A. I., McNamara, J. M., Levey, D. J., et al. (2014). Cues, strategies, and outcomes: how migrating vertebrates track environmental change. *Mov. Ecol.* 2, 1–15. doi: 10.1186/2051-3933-2-10

Winton, M. V., Sulikowski, J., and Skomal, G. B. (2021). Fine-scale vertical habitat use of white sharks at an emerging aggregation site and implications for public safety. *Wildl. Res.* 48, 345–360. doi: 10.1071/WR20029

Wood, S. A., Murray, K. T., Josephson, E., and Gilbert, J. (2020). Rates of increase in gray seal (*Halichoerus grypus atlantica*) pupping at recolonized sites in the United States, 1988–2019. *J. Mammal.* 101, 121–128. doi: 10.1093/jmammal/gyz184

Zhao, H., Han, G., and Wang, D. (2013). Timing and magnitude of spring bloom and effects of physical environments over the Grand Banks of Newfoundland. *J. Geophys. Res.* 118, 1385–1396. doi: 10.1002/jgrg.20102

Conflict of Interest: The authors declare that the research was conducted in the absence of any commercial or financial relationships that could be construed as a potential conflict of interest.

The handling editor declared a past co-authorship with one of the authors CB.

frontiers in Marine Science

ORIGINAL RESEARCH
published: 25 February 2022
doi: 10.3389/fmars.2022.835576

Multi-Decadal High-Resolution Data Reveal the Cryptic Vertical Movement Patterns of a Large Marine Predator Along the Californian Coast

Samantha Andrzejaczek[1]*, Taylor K. Chapple[1,2], Salvador J. Jorgensen[3,4], Scot D. Anderson[3], Michael Castleton[1], Paul E. Kanive[3,5], Timothy D. White[1] and Barbara A. Block[1]

[1] Hopkins Marine Station, Stanford University, Pacific Grove, CA, United States, [2] Coastal Oregon Marine Experiment Station, Oregon State University, Newport, OR, United States, [3] Monterey Bay Aquarium, Monterey, CA, United States, [4] Institute of Marine Sciences, University of California, Santa Cruz, Santa Cruz, CA, United States, [5] Department of Ecology, Montana State University, Bozeman, MT, United States

OPEN ACCESS

Edited by:
David Wells,
Texas A&M University at Galveston,
United States

Reviewed by:
Michael Domeier,
Marine Conservation Science Institute
(MCSI), United States
Luis Cardona,
University of Barcelona, Spain

****Correspondence:***
Samantha Andrzejaczek
sandrzejaczek@gmail.com

Specialty section:
This article was submitted to
Marine Megafauna,
a section of the journal
Frontiers in Marine Science

Received: *14 December 2021*
Accepted: *25 January 2022*
Published: *25 February 2022*

Citation:
Andrzejaczek S, Chapple TK, Jorgensen SJ, Anderson SD, Castleton M, Kanive PE, White TD and Block BA (2022) Multi-Decadal High-Resolution Data Reveal the Cryptic Vertical Movement Patterns of a Large Marine Predator Along the Californian Coast. Front. Mar. Sci. 9:835576. doi: 10.3389/fmars.2022.835576

Over the last two decades, satellite tagging of adult and sub-adult white sharks *Carcharodon carcharias* off the west coast of North America has revealed a predictable onshore-offshore migratory cycle. Our current understanding of the vertical movements exhibited by white sharks while in their coastal foraging phase in the California Current, however, remains limited. Here, we used recovered datasets from 31 archival satellite tags to quantify vertical habitat use. Tags were deployed on individuals between 2000 and 2018 and recorded depth and temperature data at continuous 1–120 s intervals before being recovered up to a year after deployments. Four satellite-tagged individuals were concurrently tagged with acoustic tags, providing precise location data when detected by acoustic receivers that allowed us to explore how reported vertical habitat use varied spatially. While in the coastal shelf waters, white sharks moved at a mean depth ± SD of 14.3 ± 4.0 m and occupied significantly deeper depths during the day than the night. High individual, temporal and spatial variation was evident in vertical movements, while consistent diel and lunar effects emphasized the importance of light-level driving vertical behavior around hunting sites. The vertical movement behaviors reported here provide knowledge of how white sharks may directly and indirectly interact with their mammalian prey in a dynamic three-dimensional system during their capital foraging phase. Temporal patterns in vertical behavior, for instance, indicated that surface waters during early morning hours are the riskiest place for prey. Combining these novel findings with higher-resolution biologging techniques in future studies will allow us to further contextualize fine-scale vertical movement behaviors of white sharks and examine the specific foraging events that could not yet be isolated in the tagging data.

Keywords: biologging, California Current System, diving behavior, marine megafauna, movement ecology, satellite tagging, telemetry, white shark

INTRODUCTION

Electronic tagging has revealed that many species of marine megafauna are migratory and exhibit site fidelity, returning to the same site for foraging and/or reproduction purposes. The California Current System, for instance, is a known biological hotspot where several predatory bird, marine mammal, and fish species return to predictable locations after long-distance (> 1,000 km) migrations (Block et al., 2011). Here, adult and sub-adult white sharks (*Carcharodon carcharias*) forage on marine mammals that aggregate at rookeries within cool, nutrient rich waters during the coastal phase of their annual migration (Ainley et al., 1981; LeBoeuf et al., 1982; Long et al., 1996). This phase typically occurs during autumn and early winter months and represents a period of capital foraging, where sharks bulk up their lipid stores before heading to oligotrophic offshore waters, where they spend the majority of the year (Jorgensen et al., 2009; Del Raye et al., 2013). Alongside direct effects (e.g., bites and/or predation attempts), foraging white sharks may also impact coastal populations of prey species through indirect effects, such as risk effects, whereby prey alter their behavior to reduce the likelihood of direct interactions occurring (Lima and Dill, 1990). In aquatic environments, the risk of predation varies across both horizontal and vertical axes, depending on the respective movement behaviors of the predator, influencing prey behavior across three dimensions (e.g., Lester et al., 2020; Beltran et al., 2021). Despite the decades of field-based research into the movement, life history and predatory behaviors of white sharks in California (e.g., Klimley, 1994; Goldman and Anderson, 1999; Boustany et al., 2002; Weng et al., 2007a; Jorgensen et al., 2009, 2019; Chapple et al., 2016), comprehensive investigation into the fine-scale vertical movement behaviors during their critical coastal foraging phase remains limited.

Fine-scale movements and hunting behaviors of white sharks on the Californian coast have traditionally been explored through discrete observational studies (e.g., Klimley et al., 1992) or active acoustic tracking (e.g., Goldman and Anderson, 1999; Klimley et al., 2001, 2002). These studies have provided insights into how white sharks may hunt around aggregation sites. While searching for prey, white sharks are hypothesized to swim near the bottom of coastal sites to remain concealed from surface-dwelling prey while maintaining vision with surface waters (Strong, 1996; Goldman and Anderson, 1999). During the daytime, it is hypothesized that sharks can maintain visual contact with the surface from depths of at least 30 m, and initiate attacks from such depths. Coastal white sharks have also been recorded swimming in an oscillatory pattern, where they continuously move up and down through the water column, perhaps to search for sensory cues of prey (olfactory, visual, electrosensory), thermoregulate and/or conserve energy (Klimley et al., 2002). The short duration and discontinuous nature of these past studies, however, limits applicability at larger spatial and temporal scales where other variables, such as water temperature (Andrzejaczek et al., 2018a), prey availability (Mourier et al., 2016) and ontogeny (Afonso and Hazin, 2015), are likely to influence movement patterns. This knowledge will not only help us better understand how white sharks may directly and indirectly impact their prey in a dynamic three-dimensional system, but also how white sharks may overlap vertically with human-use activities, such as fishing and recreational ocean users.

Investigating vertical movement patterns at these larger scales requires techniques that can remotely and continuously track movements for longer periods (i.e., months). Satellite tags deployed on white sharks in California over the last two decades may offer insights into cryptic vertical movement behaviors at larger temporal and spatial scales. To date, acoustic tags and pop-up satellite archival transmitting tags (PSATs) have been attached to white sharks for periods of months-years, revealing a highly predictable migratory cycle, where sharks aggregate on the coast near pinniped rookeries from late summer (August in the northern hemisphere) and undergo long-distance migrations to offshore pelagic habitats in winter (Boustany et al., 2002; Weng et al., 2007a; Domeier and Nasby-Lucas, 2008; Jorgensen et al., 2009). PSATs used in these studies transmit a summary of recorded data through satellites following release from a tagged individual, and allow not only the horizontal tracks of individuals to be reconstructed, but also have the capacity to record additional variables, such as pressure and temperature, enabling insight into the sub-surface movement behaviors of sharks (e.g., Jorgensen et al., 2012a; Andrzejaczek et al., 2018a; Braun et al., 2018). In the event where PSATs are physically recovered, a full archival dataset can be downloaded, consisting of continuous time-series of high-resolution depth and temperature data. Although recoveries of these tags are rare, they have provided detailed insights into seasonal patterns of vertical habitat use of other elasmobranch species, such as salmon sharks (*Lamna ditropis*) (Coffey et al., 2017) and oceanic whitetip sharks (*Carcharhinus longimanus*) (Andrzejaczek et al., 2018a) and more recently, have been used to explore vertical movements at hourly-diel scales for oceanic manta rays (*Mobula birostris*) (Andrzejaczek et al., 2021). For white sharks, high-resolution archival data could be leveraged to make new inferences about cryptic movements during their coastal foraging phase, and explore existing hypotheses about their hunting behaviors.

Here, we use archival datasets from recovered PSAT tags deployed on sub-adult and adult white sharks from 2000 to 2018 to investigate high-resolution vertical movement patterns on the central and northern coast of California. We explore vertical movement behaviors that have been associated with hunting behaviors, such as movements associated with seabed depths and oscillatory diving. Specifically, we aim to understand how patterns vary temporally (i.e., among diel phases, lunar phases, and months of the year) and between individuals of different ontogenetic stages, and discuss the processes that may be underlying these patterns. We also supplement the dataset with existing acoustic and photo-ID data to explore how vertical movements vary spatially.

MATERIALS AND METHODS

Data Collection

PSATs (PAT versions 2.0, 3.0, 4.0, MiniPAT and Mk10-PAT; Wildlife Computers, Redmond, Washington, United States) and

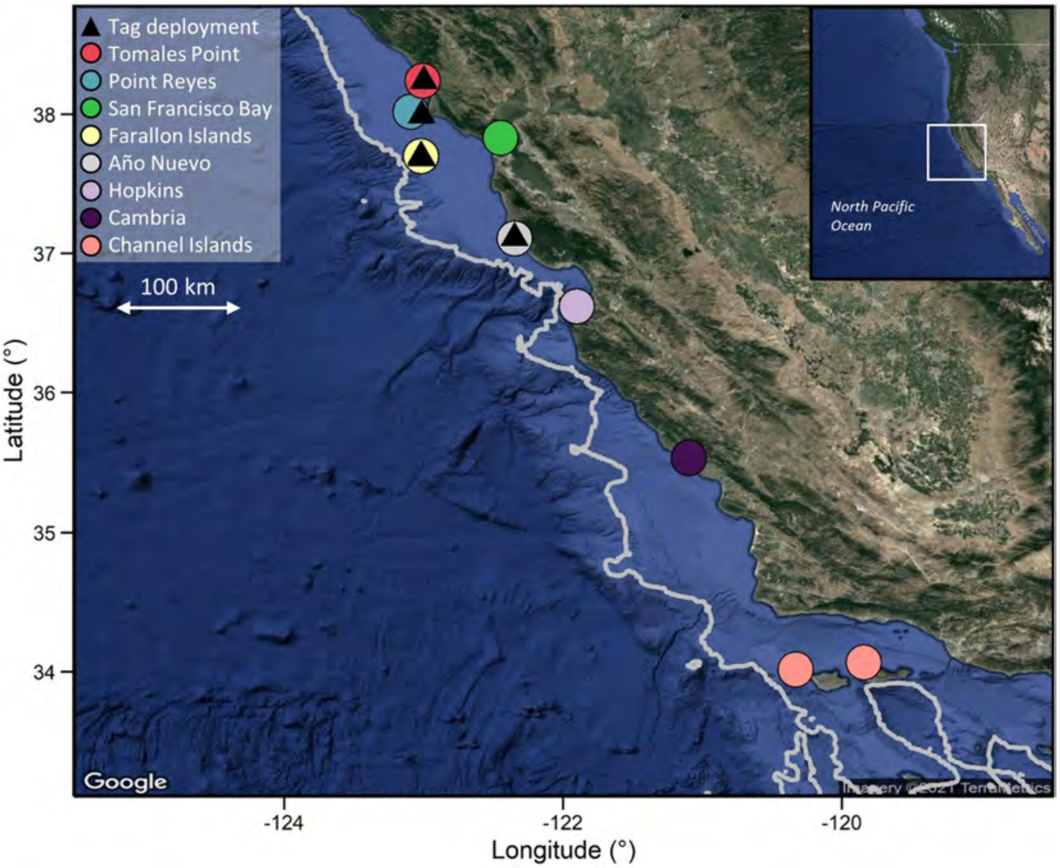

FIGURE 1 | PSAT deployment locations on the Northern Californian coast and locations of acoustic receivers. Depth contour line represents the 1,000 m depth contour. Note that scale varies among maps. Bathymetry data were extracted from the ETOPO1 database using marmap in R.

individually coded acoustic transmitter tags (hereafter "acoustic tags"; V16-4H; Innovasea, Halifax, Nova Scotia) were deployed on white sharks at aggregation sites in central California (Año Nuevo Island, South Farallon Island, Point Reyes and Tomales Point; **Figure 1**) between September and February from 2000 to 2018 (**Table 1**) using previously described methods (Jorgensen et al., 2009). Briefly, free-swimming sharks were attracted to research vessels using a seal-shaped decoy and a small amount of olfactory attractant. Surface photography and underwater footage was used to obtain individual photo-identification images and sex, with sex determined by the absence (female) or presence (male) of claspers (Chapple et al., 2011). Total length was visually estimated as sharks swam alongside a research vessel of known length, and individuals were classified as sub-adults at > 2.4 m total length (TL), and adults at > 4.5 m TL for females (Francis, 1996) and > 3.8 m TL for males (Pratt, 1996). A 3–4 m tagging pole was used to inset a titanium dart tethered tag (see Wilson et al., 2015 for tether information) beneath the shark's dorsal skin. Where possible (given tag supply and favorable shark behavior), both acoustic and satellite tags were deployed on the same individuals (i.e., individuals were double-tagged).

PSAT tags were programmed to sample ambient light levels, ambient temperature and pressure at 1–120 s intervals (**Table 1**) and to detach after periods ranging from 30 to 365 days. Tags would also detach if a constant depth reading (signifying mortality or shedding) was recorded for 3–4 days (depending on the year of deployment). Only tags that were physically recovered following detachment, enabling download of the full archival dataset, were included in this study. Likewise, data from acoustic tags were only used from double-tagged individuals where the PSAT tag was recovered. Detection data from acoustically tagged individuals were downloaded, at a minimum, annually from receivers placed along the California coast between 33.5 and 41.5°N, including at each of the aggregation sites where tags were deployed (Jorgensen et al., 2009; **Figure 1**). The number of receivers at each site was temporally variable, ranging from an average of one receiver per year at Tomales Point to > 20 per year in San Francisco Bay, where receivers are maintained by several other organizations in the case of the latter.

All methods were carried out in accordance with relevant guidelines and regulations, and all experimental protocols were approved under Stanford University animal care protocol 10,765 and under approved permits from the California Department of Fish and Wildlife, National Oceanic and Atmospheric Administration, National Park Service and Monterey Bay National Marine Sanctuary.

TABLE 1 | Recovered tag deployment details for white sharks tagged in northern California from 2000 to 2018.

White shark ID	Tag number	Deploy date	Length (cm)	Sex	Deploy lat (°E)	Deploy long (°W)	Date archive starts	Archive duration (days)	Days in coastal phase	Sample freq (sec)	Date of tag pop-up	Pop-up lat (°E)	Pop-up long (°W)
WS1	00P0291	16-Oct-00	457	M	37.7	−123.0	16-Oct-00	182	35	120	16-Apr-01	20.7	−156.8
WS2	04P0156	5-Nov-04	U	U	37.7	−123.0	5-Nov-04	305	120[r]	60	6-Sep-05	37.1	−122.4
WS3	04P0160	30-Nov-04	396	F	38.2	−123.0	3-Dec-04	192	72	60	NA	NA	NA
WS4	04P0153	3-Dec-04	426	F	38.2	−123.0	5-Dec-04	81	61	60	7-Feb-05	37.8	−122.9
WS5	05P0144	19-Nov-05	488	M	37.7	−123.0	21-Nov-05	278	22[r]	60	26-Aug-06	NA	NA
WS6	05P0133	21-Nov-05	427	M	37.7	−123.0	21-Nov-05	230	69	30	19-Aug-06	38.5	−123.3
WS7	04P0249	15-Dec-05	390	M	37.1	−122.3	18-Dec-05	227	45	60	6-Aug-06	35.6	−121.2
WS8	05P0132	15-Dec-05	480	F	37.1	−122.3	16-Dec-05	299	112[r]	60	11-Oct-06	37.1	−122.3
WS9	05P0059	21-Jan-06	400	F	37.1	−122.3	22-Jan-06	224	93	60	3-Sep-06	NA	NA
WS10	06A0437	2-Oct-06	335	M	37.7	−123.0	2-Oct-06	109	106	15	19-Jan-07	36.7	−122.2
WS11	06A0746	9-Oct-06	488	F	37.7	−123.0	9-Oct-06	360	202[r]	15	6-Oct-07	33.5	−118.5
WS12	06A0555	10-Oct-06	427	U	38.0	−123.0	10-Oct-06	241	83	15	NA	NA	NA
WS13	06A0561	1-Nov-06	427	F	37.1	−122.3	1-Nov-06	8	9	15	13-Nov-06	36.8	−122.0
WS14[a]	08A0624	12-Jan-09	427	F	38.2	−123.0	22-Jan-09	93	94	10	29-Apr-09	37.7	−122.8
WS15[a]	08A0599	19-Jan-09	427	F	38.2	−123.0	19-Jan-09	201	25[r]	10	12-Aug-09	37.0	−122.0
WS16	11A0600	16-Nov-11	488	F	37.1	−122.3	16-Nov-11	164	100	15	2-May-12	21.3	−157.2
WS17[a]	10P0484	8-Dec-11	457	F	37.1	−122.3	8-Dec-11	374	214[r]	15	14-Dec-12	46.9	−124.1
WS18	11A0599	8-Dec-11	244	F	38.2	−123.0	8-Dec-11	64	47[r]	15	NA	NA	NA
WS19	10A0675	14-Dec-12	274	F	38.2	−123.0	14-Dec-12	250	59[r]	15	26-Aug-13	37.9	−122.4
WS20	13P0233	12-Feb-14	274	M	37.1	−122.3	12-Feb-14	286	70[r]	15	28-Nov-14	35.1	−120.6
WS21[d]	L330B-1239	22-Feb-15	259	M	38.2	−123.0	22-Feb-15	40	NA	20	4-Apr-15	38.2	−123.0
WS22	13P0077	7-Nov-17	503	F	37.1	−122.3	10-Nov-17	168	12[r]	15	27-Apr-18	36.8	−121.8
WS23	17P0583	10-Nov-17	396	F	37.1	−122.3	18-Nov-17	163	15	3	1-May-18	22.3	−130.3
WS24[b]	17P0545	11-Nov-17	442	F	37.1	−122.3	11-Nov-17	180	159	3	10-May-18	25.1	−127.2
WS25[b]	17P0600	11-Nov-17	488	F	37.1	−122.3	11-Nov-17	164	82	3	25-Apr-18	22.7	−131.5
WS26[c]	17P0597	11-Nov-17	488	F	37.1	−122.3	11-Nov-17	61	61	1	12-Jan-18	37.1	−122.3
WS27	13P0075	14-Nov-17	457	M	38.2	−123.0	14-Nov-17	162	66	5	26-Apr-18	25.1	−134.1
WS28	17P0391	21-Nov-17	381	M	37.1	−122.3	21-Nov-17	164	74	3	5-May-18	22.7	−126.1
WS29[d]	17P0245	13-Dec-17	411	M	38.2	−123.0	14-Dec-17	NA	NA	3	4-May-18	24.5	−127.3
WS30[a]	17P0715	13-Dec-17	427	M	38.2	−123.0	13-Dec-17	137	35	3	29-Apr-18	23.5	−131.7
WS31	17P0716	18-Dec-17	442	M	37.1	−122.3	18-Dec-17	132	106	3	4-May-18	22.5	−132.9
WS32	17P0570	18-Dec-17	427	M	37.1	−122.3	18-Dec-17	139	51	3	7-May-18	26.8	−133.6
WS33	18P0649	15-Nov-18	442	M	37.1	−122.3	15-Nov-18	259	30[r]	3	2-Aug-19	37.5	−122.5
WS34	18P0676	27-Nov-18	366	M	37.1	−122.3	27-Nov-18	247	3	3	3-Aug-19	33.0	−118.6

[a] *Individuals double-tagged with acoustic tags.* [b] *Individuals re-sighted using photo-ID methods.* [c] *Individual the same as WS25.* [d] *Significant drift in pressure sensor (tag excluded from analysis).* [r] *Tag remained attached after white shark returned from offshore migration.*

Data Processing

R 4.0 (R Core Team, 2020) was used for all data processing and analyses, except where stated otherwise.

Track Reconstruction

PSAT data were decoded using the manufacturer's software (Wildlife Computers DAP Processor 3.0). Data were firstly trimmed to the attachment period, with detachment from an individual identified by the depth time-series recording a constant near-zero depth for > 12 h, shortly followed by the initiation of Argos data transmissions. Most-probable tracks were then estimated using the tag manufacturer's software that utilizes a hidden Markov model (Pedersen et al., 2011; WC-GPE3, Wildlife Computers), and considers transmitted light level, temperature and depth data alongside sea surface temperature (SST; NOAA OI SST V2 High Resolution) and bathymetric constraints (ETOPO1-Bedrock). This method calculates a posterior probability distribution that estimates two maximum likelihood position estimates per day (Skomal et al., 2017). The diffusion parameter was set to 3 ms^{-1} (Block et al., 2011) to govern the allowable distance moved per day.

Processing Depth and Temperature Data

A two-step process using the most-probable tracks and the high-resolution depth data was used to trim the archival time-series to the coastal phase of the white shark migration. To isolate coastal activity, a large geographic boundary was first used to constrain the tracks periods along the California Current System of the NE Pacific coast (**Supplementary Figure 1**), with a large enough boundary to incorporate the errors associated with light-based geolocation (Lisovski et al., 2020). Secondly, to obtain more precise start and end dates of this coastal phase, the time-series data was then queried to find the first date at which white sharks had entered the "travel" phase of their westward migration, indicated by consecutive days with dives to depths > 100 m interspersed with a high proportion of time in surface waters (<5 m) (Jorgensen et al., 2012a). For individuals where tags remained attached following their offshore migration, the query was reversed to find the last date at which the shark was in the "travel" phase. The calculated dates were then used to obtain the final trimmed coastal time-series dataset.

Depth and temperature time-series data were summarized into hourly time windows, with computed variables including median, mean, minimum, maximum and standard deviation. The proportion of time spent in distinct depth ranges each hour was also calculated. For sharks with a sampling frequency of 5 s or faster (n = 11; **Table 1**), vertical velocity (VV) was calculated by taking the difference in depth between successive points, and dividing by the sampling frequency to obtain VV at a 1 s frequency. VV was then used to split the depth record into vertical swimming phases (i.e., < 0 = descending, 0 = level swimming, > 0 = ascending). The proportion of time spent moving vertically (ascending and descending), termed the "diving ratio," was also calculated by determining the percentage of time vertically moving within an hour (Andrzejaczek et al., 2018b).

Double-Tagged Sharks

To investigate site-specific vertical behavior, acoustic and PSAT datasets were paired where deployment periods overlapped (n = 4; **Table 1**). > 1 acoustic detection per 12-h period at a site was used to link a tagged individual with a site, and a continuous span of time spent at a site was defined where this occurred over consecutive 12-h periods. The photo-ID database was also queried to find dates where photo-IDs of tagged sharks overlapped with deployment periods, providing an additional means to link individuals to aggregation sites.

Environmental Parameters

The R package suncalc was used to obtain daily lunar illumination data, and to determine times of sunrise and sunset (Thieurmel and Elmarhraoui, 2019) and subsequently split the data into diel phases. Daily average sea surface temperature (SST) was estimated by averaging the temperature in the uppermost 5 m of the water column for each day (Andrzejaczek et al., 2018a). For days that white sharks did not enter this depth range, the estimate from the previous day was used (n = 47 days). Monthly SST anomaly, an indicator of El Niño, was extracted from https://www.cpc.ncep.noaa.gov/products/analysis_monitoring/ensostuff/detrend.nino34.ascii.txt. Anomalies referenced from a 30-year base period were calculated for the Niño 3.4 region (5°N—5°S, 120°–170°W). Values on this scale range from negative (cooling; La Niña) to positive (warming; El Niño).

Statistical Analyses

Generalized Additive Mixed Models

A suite of Generalized Additive Mixed Models (GAMMs) with Gaussian error distributions were constructed using the mgcv package in R (Wood, 2017) to test the response of biologically relevant vertical movement metrics to temporal and environmental variables. Calculated response metrics were (1) % time in the top 5 m, (2) % time in the 15–30 m depth bin and (3) diving ratio, and were summarized for each hour of data. Response metric (1) was calculated as a metric of surface use, (2) as a rough bin to cover the mean maximum depth of aggregation sites assumed to represent swimming along the seafloor, and (3) as a proxy for vertical or oscillatory activity. Median depth was originally also modeled, however, due to lack of model fit both before and after transformation, was not included in the final analysis. Response metrics (1) and (2) were modeled separately for sex to ease model interpretation, while response metric (3) could not be split due to reduced sample size of individuals with higher resolution tags (n = 3 females and 7 males) and instead included "sex" as a categorical explanatory variable. Response metrics (1) and (2) were both logit transformed prior to analysis so that predicted values were not negative, and did not exceed one, as well as to normalize data. The continuous variables considered for all models were time of day (hour of day), fraction of the moon illuminated (0–1), daily average SST and monthly SST anomaly. Month and age class (adult and sub-adult) were also included as categorical factors. All models included shark ID as a random effect to account for individual variation in movement patterns. Temporal auto-correlation was tested on the initial fit of each model, revealing a steady decline of serial correlation with increasing lag from time t. The correlation at lag = 1 was subsequently used to specify the correlation structure of the data (Zuur et al., 2009) and added as a final term to each model using the corAR1 function in R.

A full subsets approach was used to model every combination of variables possible. Models within 2 AICc units of each other were considered to be equally ranked. When the difference in AICc values (ΔAICc) between top candidate models was < 2, the model containing the lowest number of explanatory variables (i.e., the most parsimonious) was selected as the appropriate model for the data.

Multivariate Analyses

Principal components analysis (PCA) was applied separately to the summarized hourly depth data of two double-tagged sharks who displayed relatively high visitation to sites with acoustic receivers (WS15 and WS17; > 12 days at sites). Scaled values of median depth, maximum depth, interquartile range in depth and proportion of time in the top 5 m were used in the PCA analyses to investigate how vertical movements varied among sites for each of these sharks.

RESULTS

Data Overview

We recovered 34 datasets from PSAT tags deployed on white sharks at aggregation sites on the central coast of California from 2000 to 2019. Tags were retrieved from locations on the US west coast (from Washington to the Channel Islands; n = 21), in Hawaii (n = 4) and in waters offshore (n = 9) (**Table 1**). Tags were either recovered by the research team or were returned after being found by members of the public. A total of 31 individual datasets were used in data processing and analyses, with two not used due to sensor issues, and only one dataset used from a single individual with two satellite tags with overlapping deployment periods (WS25 and WS26; **Table 1**). Of the 31 datasets, 16 were from sharks visually identified as females, 13 from males, and two from sharks of unknown sex (**Table 1**). Sharks ranged in estimated lengths from 2.5 to 5 m (median ∼4.3 m; **Table 1**). The mean total deployment duration of tags was 193 ± 96 days (range 12–391 days), with time in the coastal phase during tag deployment averaging 73 ± 51 days (range 3–214 days; **Table 1**). A majority of the coastal phase occurred over the months of November, December and January (67.4 ± 29.5%; **Supplementary Table 1**).

While in their coastal phase, tagged white sharks occupied a mean depth of 14.3 ± 4.0 m and a median depth ± interquartile range of 11.0 ± 4.5 m, with relatively high variation between individual sharks (**Figures 2**, **3**). Given the non-Gaussian distribution of the data, median depth was used to summarize diel depth use, with sharks occupying a significantly deeper median depth during the day than the night (day: 12.4 ± 5.8 m; night: 10.0 ± 4.7 m; Wilcoxon paired rank sum test: V = 6,50,978, $p < 0.001$, 95% confidence interval: –2.5, –2.0; **Figure 2**). Males also occupied slightly, but significantly, deeper depths than females (male: 11.7 ± 7.7 m; female: 10.6 ± 8.1 m; Wilcoxon rank sum test: W = 3,95,418, $p < 0.001$, 95% confidence interval: –2.6, –1.5; **Figure 3**), and adults occupied slightly, but significantly, deeper depths than subadults (adult: 11.7 ± 9.4 m; subadult: 9.9 ± 5.9 m; Wilcoxon rank sum test: W = 5,85,535, $p < 0.001$, 95% confidence interval: 0.70, 1.7; **Figure 3**). Depth use was skewed to the top 25 m of the water column, with 87.4 ± 7.6% of the time spent in this zone and a majority of this spent in the 10–25 m depth bin for both diel periods (**Figure 2**). White sharks recorded a mean temperature of 12.9 ± 1.2°C, and an average SST of 13.2 ± 1.4°C. Higher resolution data from 10 white sharks revealed individuals were moving vertically for 70.7 ± 3.7% of the time at a mean vertical velocity of 0.1 ± 0.01 ms^{-1} and maximum rates of 4.1 and 6.0 ms^{-1} for descent and ascent, respectively.

Temporal Patterns

GAMMs revealed temporal patterns in all modeled vertical movement metrics (**Table 2** and **Figure 4**). Deviance explained for the selected models ranged from 11 to 22.1%, with the individual ID (the random effect) explaining more than half of this when modeled alone (**Table 2** and **Figure 4**). For a list of all model subsets considered in the selection process see **Supplementary Material**.

% Top 5 m

The probability of being in surface waters (the top 5 m) was highest during the night as well as the new moon period (i.e., lowest lunar illumination) for both females and males (**Figures 4A,B**). The models revealed a decreasing probability of use of the top 5 m toward early morning and with increasing lunar illumination. Females displayed a variable relationship with SST anomaly, with highest probability of surface use during negative anomalies (i.e., La Niña) and lowest during positive anomalies (i.e., El Niño, **Figure 4A**). Surface use was also predicted to be highest for females in August, September and October, and lowest in December and January (**Supplementary Figure 2**). Although selected in the final model, the smoother for average SST was not significant for females. For males, surface use was predicted to increase with increasing SST (**Figure 4B**), and was highest in March and April and lowest in September and October (**Supplementary Figure 2**). We note that only one tagged male (WS31) was present on the coast in March and April.

% 15–30 m

The probability of being in waters 15–30 m deep was highest during the early morning and a full moon for both females and males (**Figures 4C,D**). Probability decreased into nighttime hours and decreasing lunar illumination. Use of the 15–30 m bin also decreased with increasing SST (**Figures 4C,D**). Although selected in the final models, the smoother for SST anomaly was not significant for females or males (**Table 2**). For females, use of the 15–30 m depth bin was lowest in April and highest in June, August, September and December (**Supplementary Figure 2**). For males, lowest use occurred in March and April, and highest in September, October and December (**Supplementary Figure 2**).

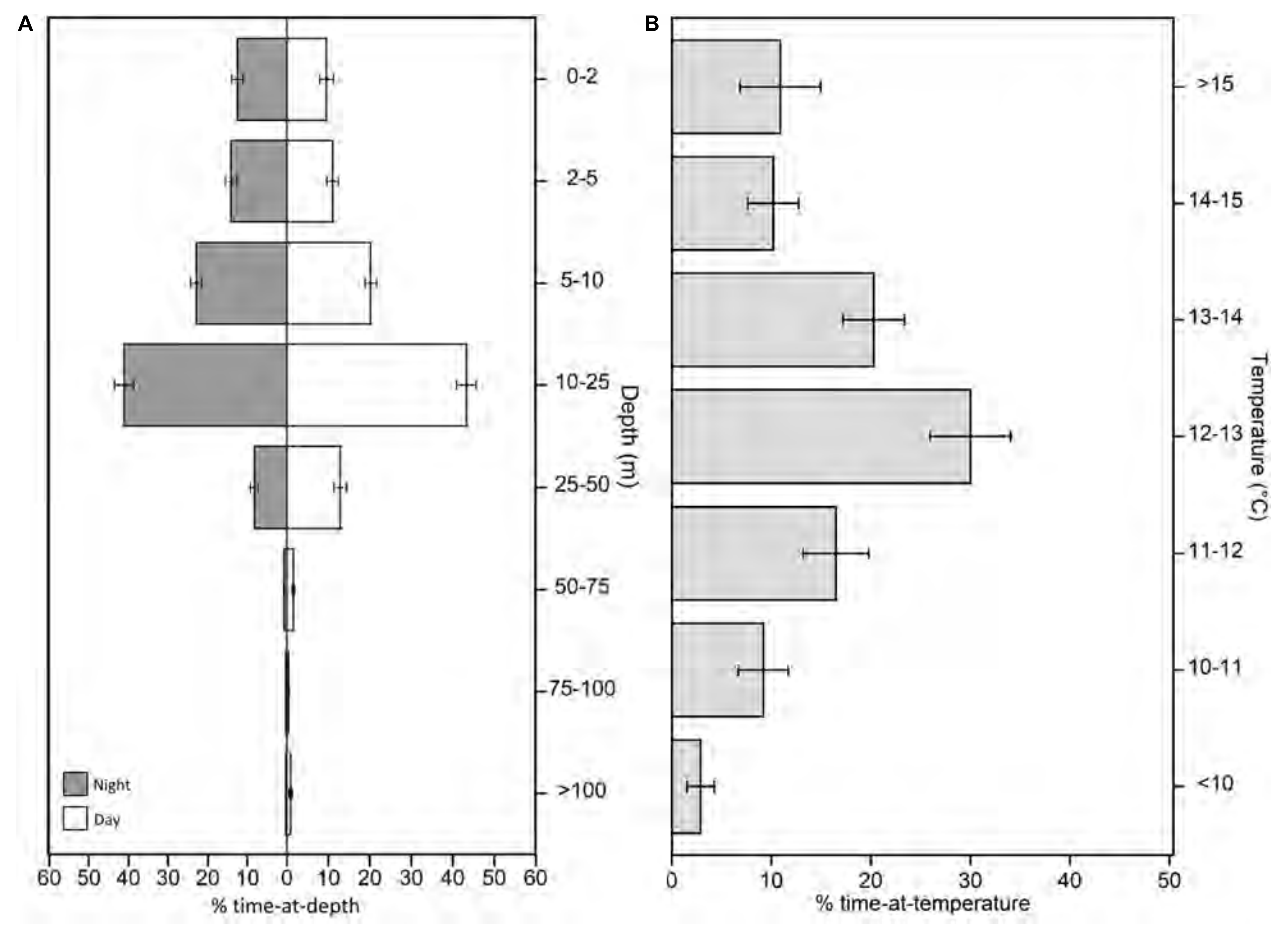

FIGURE 2 | Summarized time-series data from PSATs recovered from 32 individual white sharks *Carcharodon carcharias*. Summaries are from data restricted to the coastal phase of the white shark migration. **(A)** Percent time-at-depth for night and day-time periods. **(B)** Percent time-at-temperature. Note that for **(A)**, bin size is not equal between categories.

Diving Ratio

Hour of the day was the only continuous variable selected in the final model for diving ratio (i.e., vertical activity; **Figure 4E**). Diving ratio was predicted to be highest in the early morning, remaining high throughout the day and dropping before sunset until sunrise. Diving ratio was predicted to be highest in January, July and December and lowest in March, April and August (**Supplementary Figure 2**), though we note only one individual was present on the coast in July.

Site-Specific Vertical Movement Patterns

Double-Tag Data

Four sharks were also acoustically tagged with deployment periods overlapping with recovered PSATs (WS14, WS15, WS17, and WS30; **Table 3**). Fine-scale presence (i.e., minimum two detections within consecutive 12 h periods) were recorded at Tomales, Point Reyes and Año Nuevo, with a maximum consecutive period of 16 days at one site recorded (WS30 at Año Nuevo). WS17, a 4.6 m adult female, was double-tagged at Año Nuevo in December 2011, moved offshore in March, returned via the Channel Islands where it was detected in September, moving back up northward along the coast via Cambria in October before being detected once again at Año Nuevo in October and November 2012. WS15 entered San Francisco Bay for a period of 9 h where it was detected 287 times across 16 different receivers. Detections in San Francisco Bay by WS15 were accompanied by an increase in ambient temperature from 11.4 ± 1.0 to 14.3 ± 0.3°C and an increase in median depth use from 7.4 ± 6.1 to 14.2 ± 10.5 m (**Supplementary Figure 3**). Notably, this shark was acoustically detected in San Francisco Bay in four consecutive years (2007–2010), with the first day of detection in a given year occurring in July or August.

White sharks continued to exhibit oscillatory swimming behavior at all sites at which they were detected (**Supplementary Figure 3**), however, depth distributions varied with site. Relatively shallow distributions were recorded at Tomales (median depth ± IQR = 5.0 ± 3.0 m; **Figure 5A**), deeper distributions in San Francisco Bay (14.7 ± 5.7 m; **Figure 5A**) and Cambria (16.1 ± 8.4 m; **Figure 5A**), shallow but variable distributions at the Channel Islands (9.0 ± 17.9 m; **Figure 5A**, and **Supplementary Figure 4**), and deeper and highly variable

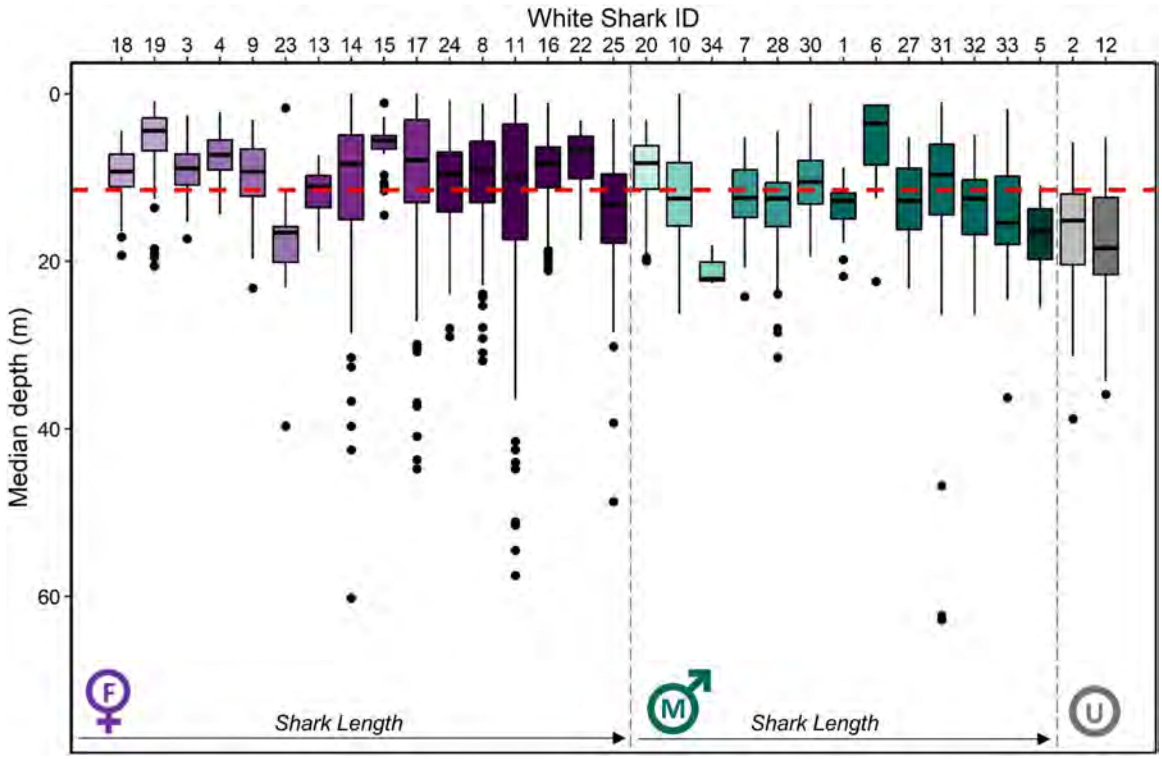

FIGURE 3 | Median depth (m) by individual white shark *Carcharodon carcharias* in the coastal phase of their migration in the NE Pacific. Boxplots are ordered firstly by sex (female = purple, male = green, unknown = gray) then by size (small to large from left to right), with darker shades indicating larger individuals. The red dashed line indicates the average median depth of all individuals (11.7 ± 8.4 m), while the average median depth for female and male individuals is 10.6 ± 9.1 m and 11.7 ± 6.4 m, respectively.

at Point Reyes (12.6 ± 37.1 m) (**Figure 5A**). Median depth use at Año Nuevo was close to that of that of the entire dataset (11.0 ± 8.7 m; **Figure 5A**).

Principal components analysis (PCA) was applied separately to the summarized hourly depth data of two double-tagged sharks which displayed relatively high visitation to sites with acoustic receivers (WS15 and WS17; > 12 days at sites). 94.1 and 85.6% of the variation in vertical movement behaviors could be explained by the first two components for WS15 and WS17, respectively (**Figure 5B**). For both, PC1 had the highest correlation with maximum and median depth (> 50% for each variable) and PC2 with IQR and % time in the top 5 (> 70% for top 5 m, > 50% IQR). Sites came out in relatively clear clusters, with greater median, maximum and IQR in depth characterizing San Francisco Bay (**Figure 5Bi**), greater maximum and IQR in depth Point Reyes, and higher surface use the Channel Islands (**Figure 5Bii**). Año Nuevo was clustered in the middle (∼0,0) for both individuals (**Figure 5B**).

The Channel Islands

The most-probable tracks from WS11 and WS17, both mature female individuals, revealed they returned to the coast from their offshore migrations via the Channel Islands in June 2007 and July 2012, respectively. The tag from WS11 popped off at Santa Catalina Island in October, while WS17 moved north from the Channel Islands in early October as evident from subsequent acoustic detections at Cambria followed by Año Nuevo. For these two sharks, vertical movements at the Channel Islands were characterized by continuous, deep (> 100 m) oscillatory movements interspersed with periods of surface swimming (**Supplementary Figure 4**). Diel periodicity was evident in the time-series data, with the deepest oscillations occurring during the morning, and high surface use at night (**Supplementary Figure 4**). Depth and temperature profiles recorded highly stratified waters, with warm SSTs (> 18°C) and ambient temperatures < 12°C at depths greater than 100 m (**Supplementary Figure 4**).

Photo-ID Data

Two white sharks were identified by the research team using photo-ID at Año Nuevo during their respective PSAT deployments; WS24 was observed on the 12th Dec 2017 and WS25 on the 7th December 2017. The timing of departure and arrival to the aggregation site by the research vessel was matched to the vertical time-series of each shark to examine behaviors when the vessel that uses attractant scent was present (**Supplementary Figure 5**). Sharks initially displayed deeper distributions with dives to and from the surface in the first few hours of boat arrival, followed by continuous periods of surface swimming coinciding with the time of photo-ID. Upon departure of the boat from the site, vertical movements increased in depth, and surface swimming stopped (**Supplementary Figure 5**).

TABLE 2 | Summary of the GAMMs selected by the model selection process (for full set of models included in the model selection process, see **Supplementary File A**).

Selected models	Deviance explained (full model/random effect)		Smoother	Estimated DF smoother	Significance of smoother
	Full model	**Random effect only**			
1a.% top 5 m (F) ∼ Hour + Fraction + Anom + SST + Month + WSID	14.2%	7.3%	Hour	7.7	<0.001*
			Fraction	2.3	0.006*
			Anom	3.6	<0.001*
			SST	2.6	0.23
			WSID	13.7	<0.001*
1b.% top 5 m (M) ∼ Hour + Fraction + SST + Month + WSID	22.1%	13.6%	Hour	7.4	<0.001*
			Fraction	2.4	<0.001*
			SST	1.0	<0.001*
			WSID	10.9	<0.001*
2a.% 15–30 m (F) ∼ Hour + Fraction + Anom + SST + Month + WSID	11%	7.8%	Hour	3.4	<0.001*
			Fraction	2.5	0.02*
			Anom	1.0	0.07
			SST	1.0	<0.001*
			WSID	14.5	<0.001*
2b.% 15–30 m (M) ∼ Hour + Fraction + Anom + SST + Month + WSID	16.6%	11.7%	Hour	6.8	<0.001*
			Fraction	2.5	<0.001*
			Anom	1.0	0.09
			SST	1.0	<0.001*
			WSID	10.8	<0.001*
3. Diving ratio ∼ Hour + Month + WSID	16.6%	8.8%	Hour	7.6	<0.001*
			WSID	9.2	<0.001*

*Models 1 and 2 are separated by (a) females (F) and (b) males (M). Selected explanatory variables include hour of the day (hour), fraction of the moon illuminated (fraction), SST anomaly (Anom), average SST (SST), month of the year (Month) and individual white shark ID (WSID).% time in depth bins were logit transformed prior to use in models. Deviance explained shows that for the full chosen model, and for that when the random effect is modeled alone. * indicates a significant smoother with the p-value set at 0.05. See* ***Supplementary Material*** *for full list of model subsets considered in the selection process.*

DISCUSSION

In this study, we utilized a large, high-resolution dataset obtained from recovered PSAT tags to examine the vertical habitat use of adult and sub-adult white sharks during the capital foraging phase of their annual migration in the California Current System. Our data revealed broad commonalities in vertical patterns associated with diel timing and lunar phase, while exposing differences across sites selected by white sharks, as well as broader individual-level variation. The comprehensive dataset and analyses enabled detailed investigation of white shark vertical and thermal habitat use, as well as exploration of the processes that may be driving these patterns, and assessment of their ecological and anthropogenic implications.

Patterns and Drivers of Vertical Movements

Diel and lunar trends in white shark vertical movement patterns during their coastal phase suggest that ambient light affects the hunting behaviors of these visual predators. Sharks reduced surface water use and increased use of depths that correlate with that of the seabed around aggregation sites during the early morning, a strategy that would help sharks remain cryptic while searching for surface-oriented prey (Strong, 1996; Goldman and Anderson, 1999). Vertical activity (or "oscillatory diving") was also highest during this period, a behavior that could be used to search for prey while reducing the energy costs associated with locomotion (Klimley et al., 2002; Watanabe et al., 2019b; Andrzejaczek et al., 2020). Previous work using tri-axial and swim speed sensors on white sharks at the Neptune Islands found oscillatory dives were characterized by slow swim speeds and drift descents, a pattern thought to be a "sit-and-wait" strategy for this perpetually swimming predator, allowing it to increase encounter rates with fast-swimming pinniped prey while reducing swimming costs (Watanabe et al., 2019b). Conversely, at night, white sharks in this study displayed shallower distributions and reduced vertical movement activity, possibly continuing to hunt under the cover of darkness (Klimley et al., 2001; Francis et al., 2012; Watanabe et al., 2019a), though with reduced vertical scope to search for prey. Deeper distributions were correlated with higher lunar illumination, a pattern previously recorded for white sharks in other regions and for other ontogenetic groups (Weng et al., 2007b; Nasby-Lucas et al., 2009; Winton et al., 2021), and may represent sharks following an optimal isolume near foraging sites. Whether these variable vertical movement modes correspond with foraging success throughout the diel cycle remains unquantified, largely due to the difficulties of observing predation attempts during the night. The deployment of tags with high-resolution sensors, such as accelerometers, may help us to better fill this knowledge gap in the near future (e.g., Jorgensen et al., 2015).

Size class and sex had subtle effects on vertical movement patterns. Adult white sharks displayed slightly deeper

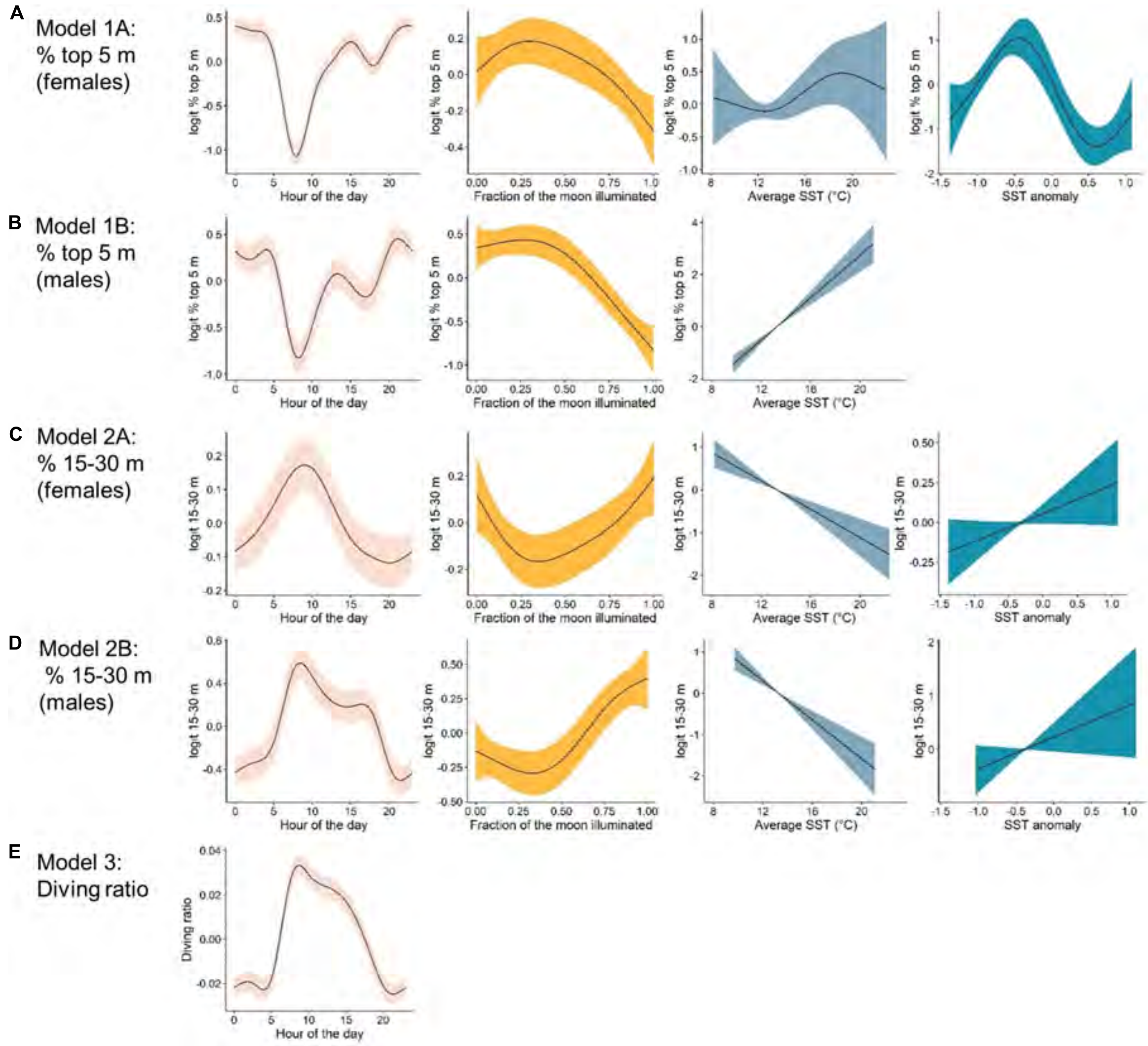

FIGURE 4 | Marginal effects plots from top-ranked generalized additive mixed models indicating the effects, from left to right, of: hour of the day, lunar illumination, average sea surface temperature °C (SST) and SST anomaly, on vertical movement metrics. The response variable for each model are as follows: **(A)** % time in the top 5 m by females. **(B)** % time in the top 5 m by males. **(C)** % time in the 15–30 m depth bin by females. **(D)** % time in the 15–30 m depth bin by males, and **(E)** the diving ratio. Note that scales on the *y*-axes differ between plots.

distributions than sub-adults, however, no other significant trends in vertical movement between these ontogenetic classes were found. As smaller size classes (< 300 cm) have more recently shifted from a predominately piscivorous to marine mammal-based diet, differences in movement patterns may be expected as they adjust to new foraging strategies (Goldman and Anderson, 1999; Domeier et al., 2012). The weak difference here, however, is likely biased by the fact that sub-adult sharks in this study were tagged at marine mammal aggregation sites, and therefore had likely already recruited into the adult population. Lunar and diel effect were consistent among male and female sharks, though the effect of month and average SST varied between sexes, and females had marginally deeper distributions than males. Acoustic data show that males arrive on the coast earlier than females (Chapple et al., 2016), coinciding with the months that recorded the lowest surface use for each group. Notably, differences in vertical habitat use and spatial distribution also vary between

TABLE 3 | Acoustic tag data summary for double-tagged sharks.

WSID	Deploy date	Last detection	Number detections during study period	Number of sites detected at during study period
WS14	20-Jan-2009	27-Aug-2011	182	2
WS15	12-Nov-2007	11-Match-2011	638	3
WS17	8-Dec-2011	24-Nov-2012	663	5
WS30	4-Oct-2017	12-Feb-2019	748	2

Number of detections and sites at which individuals were detected at is for the period for the period overlapping with recovered PSAT deployments only.

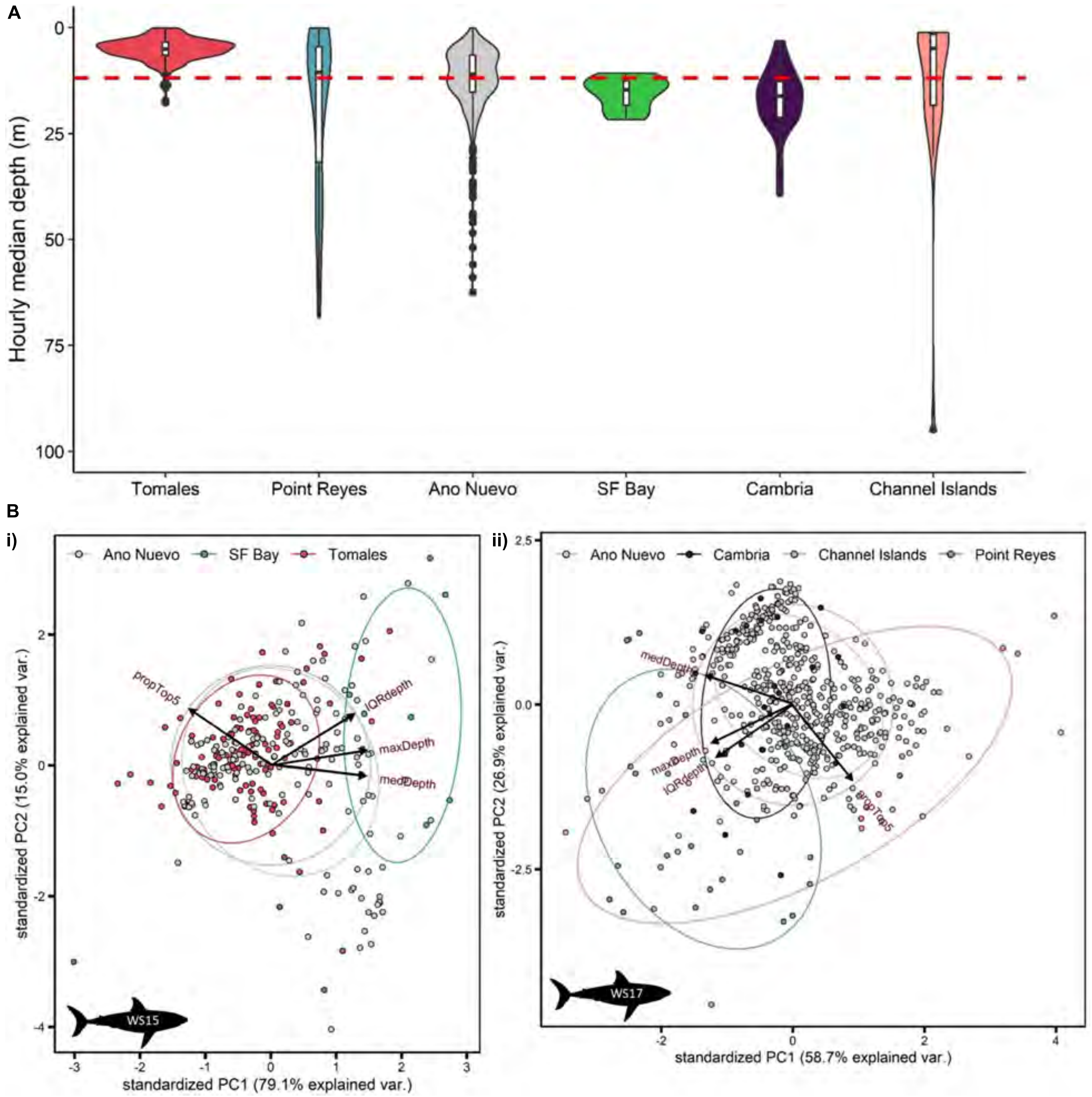

FIGURE 5 | Summarized depth data from PSATS recovered from double-tagged white sharks *Carcharodon carcharias* in the coastal phase of their migration in the NE Pacific. Site-specific vertical behaviors were determined by date-time matching time-series data with acoustic detection data. Individual sharks were matched to a site either by recording > 1 detection per day at a site, or by a photo-identification match. **(A)** Violin plot of hourly median depth by site (n = 84 days). The red dashed line indicates the average median depth of all site-specific data (11.8 ± 11.3 m). **(B)** Principal component analysis of hourly summarized depth data for two sharks (i) WS15 (n = 298 h) and (ii) WS17 (n = 556 h). Input variables were % use top 5 m, maximum depth, median depth and interquartile range in depth. Points are colored by site.

males and females during the offshore phase of their migration (Jorgensen et al., 2012a). Although the processes driving such variation remain cryptic, similar trends with lunar and diel phase while in the coastal phase suggest hunting strategy remains consistent among sexes.

Documented differences in vertical movements between male and female white sharks found here may also be driven by the unique migration patterns of two adults. We had full archival records from two mature females that both displayed unique behaviors from males, spending several months in the vicinity of the Channel Islands in southern California. At this site, average SSTs were approximately 5°C warmer than the overall coastal mean, and tagged sharks displayed higher surface use, as well as deeper diving behavior, than at other coastal sites. Patterns of vertical movement between these two individual sharks were remarkably consistent, despite being 5 years apart, and may be driven by these adults migrating to these warmer waters for parturition (Klimley, 1985; Jorgensen et al., 2012b). This period is consistent with the peak abundance of neonates in the area (late summer-fall; Klimley, 1985), and warmer temperatures may facilitate higher survival of pups (Klimley, 1985), while deep diving behavior by adults may prevent body temperature heating above optimum (Andrzejaczek et al., 2018a). Given the large pinniped populations also present at this locality (Lowry et al., 2020) however, we cannot discount the possibility that white sharks were using the Channel Islands exclusively as a foraging site.

Although consistent trends were reported in the modeling process, it is important to acknowledge that a high amount of variability (>77%) in the recorded vertical movement patterns remained unexplained by the final GAMMS. Such low levels of explained deviance are relatively common in telemetry studies (e.g., Peel et al., 2019; Spaet et al., 2020), and here, are likely due to physical and biological variables that could not be quantified at the appropriate resolution due to the errors associated with light-based geolocation. Errors can be significant (Lisovski et al., 2020) and may prohibit the measurement of environmental data at local scales (e.g., bathymetry, tides, wind, swell, turbidity, chlorophyll, dissolved oxygen content). In eastern Australia, for instance, occurrence models for acoustically tagged juvenile white sharks significantly improved when receiver location was added to the models, likely due to this factor capturing location-specific habitat characteristics that weren't otherwise measured (Spaet et al., 2020). For example, swell height and water clarity have been previously associated with greater attack frequency, perhaps by reducing the available haul-out area for pinniped prey and their detection of stalking white sharks, respectively (Pyle et al., 1996), which may translate into changes in vertical movement patterns. In our study, average SST and monthly SST anomaly were the only environmental variables included in the model and had a weak or no relationship with vertical movements. Reduction in use of depth bins associated with seabed depths of aggregation sites with increased SSTs may be associated with white sharks being in warmer, offshore regions, however, errors in geolocations again prevent us from exploring this pattern in more detail. In addition, white sharks are likely to be switching between different movement states (i.e., resident/foraging and transient) while in their coastal phase and will not always be hunting for prey, resulting in modifications to their vertical movement behaviors.

Data from four double-tagged sharks and photo-ID provided further evidence that site-specific behaviors may be responsible for at least some of the unexplained variation in our study. Bathymetry may be a strong driver of differences between sites, with Tomales having a much shallower seabed than the other sites, limiting median hourly depths to the top 20 m, while steeper and deeper habitat present at the Channel Islands enabled deeper maximum hourly median depths (up to 142 m). Similarly, bathymetry is likely one of the primary factors driving differences among white shark vertical distributions on a more regional scale, such as between aggregations here in central and northern California, and aggregations at Guadalupe Island, where a much greater proportion of time was spent in waters greater than 50 m in the deeper waters of the latter (Domeier et al., 2012). Such differences in available vertical habitat could influence both the way in which sharks hunt for prey, and the strategies taken up by prey to avoid predation (e.g., by diving to much greater depths). Vertical movement metrics recorded at Año Nuevo were consistent with the overall dataset mean, which is to be expected given this is one of the main aggregation sites and where we predict many of the tagged sharks spent considerable amounts of time. At this site, research efforts may have also introduced variability into the data, with vessel presence likely resulting in more surface-oriented behavior than is typical of white sharks here, a phenomenon that we expect will occur in other instances where bait is introduced into white shark habitat, such as through fishing activities or tourism (i.e., cage diving operations). Another notable behavior was from one subadult female shark entering San Francisco Bay for a period of 9 h, a movement that was repeated in four consecutive years at approximately the time sharks are arriving back on the coast following their offshore migrations (July–August). White sharks have relatively large olfactory bulbs (Yopak et al., 2015) that have been hypothesized to aid in navigation (Jacobs, 2012; Yopak et al., 2015), and we therefore speculate that either a unique olfactory or oceanographic signal from the Bay area may act as a "homing signal" for this shark. Other factors that may have influenced differences among sites include site-specific oceanography, prey availability and behavior, and movement state (i.e., resident or transient).

Implications

The potential for white sharks to adjust their vertical behaviors to successfully forage on pinniped prey may have implications at a broader ecosystem level, whereby prey populations aiming to reduce their risk of predation alter their own behavior (Brown et al., 1999). Surface waters (i.e., the top 5 m) around white shark aggregation sites in California during early morning hours were predicted to be the riskiest place for pinniped prey, which may have led to the development of behavioral strategies in pinniped populations (e.g., modified vertical distributions, grouping behavior, and/or the timing of offshore departures) that reduce encounter rates with sharks. Juvenile and adult female northern elephant seals *Mirounga angustirostris*, for example, largely avoid entering the surface zone, and instead use the bathymetry of the seabed to navigate toward the edge of continental shelf when seasonally migrating offshore (Le Boeuf and Crocker, 1996). In contrast, mature male elephant seals enter surface waters repeatedly around aggregation sites during the breeding season, and pups learn to swim in this high-risk zone, which may lead to higher rates of predation for these ontogenetic groups (Le Boeuf and Crocker, 1996). California sea lions *Zalophus californianus* also transit through this hunting zone frequently, moving into continental shelf waters or offshore to forage for days at a time before returning to haul-out onshore (Melin et al., 2000; McHuron et al., 2018). For this latter taxa, groups of individuals have been observed to perform fast and simultaneous proposing movements at the surface on both departure and return movements to coastal aggregation sites, which may reduce individual predation risk following the selfish herd theory (Laroche et al., 2008; De Vos and O'Riain, 2010). We further predict that pinnipeds may vary the timing of movement (i.e., diel and seasonally) through coastal aggregation waters as a response to shark hunting tactics, as has been observed by adult Cape fur seals *Arctocephalus pusillus pusillus* in South Africa (Laroche et al., 2008). A key next step in the California Current system will be to investigate spatial and temporal overlap among these predators (white sharks) and prey (pinniped), especially as such predator-induced shifts in prey movement may impede access to preferred foraging and/or breeding conditions, consequently impacting reproductive opportunities and growth.

From a management context, our understanding of white shark vertical movements will benefit the development of education- and monitoring-based approaches aimed at reducing risk of harmful shark-human interactions (Gibbs and Warren, 2015; Winton et al., 2021), as well as evaluating the susceptibility of white sharks to fishing gears that vary on a vertical gradient (e.g., Wright et al., 2021). Currently, per capita rates of unprovoked bites on humans in the northeastern Pacific Ocean remain relatively low (Curtis et al., 2012; Ferretti et al., 2015). Increasing recreational ocean use (Ferretti et al., 2015) paired with shifts in potential range (Tanaka et al., 2021) and abundance (Kanive et al., 2021) of white sharks, however, may influence these interactions. An understanding of how and when white sharks use surface waters on the coast may improve our ability to proactively develop risk avoidance behaviors and reduce the probability of these rare events occurring (Winton et al., 2021). For example, understanding which hours of the day white sharks are more likely to occupy surface waters may inform swimmers as to the safest times to use the ocean. Similar to white sharks in Cape Cod (Winton et al., 2021), surface use behavior on the California coast was highest at night, a period when beach visitation rates are typically the lowest. However, this may not correlate with periods of active hunting. An important next step in this process will therefore be to confirm how the surface use of white sharks translates to discrete behaviors when foraging and transiting, so that we can further refine our understanding of when and where these predators are likely to be foraging. Aerial monitoring methods (i.e., drones, blimps), previously shown to be effective for real-time shark detection and alerting in Australia (Butcher et al., 2019; Adams et al., 2020), provide one such means to quantify surface-based behaviors by white sharks. However, as median depths reported here for adult and subadults are typically deeper than we expect average detection range of a drone, we predict these aerial methods are unlikely to be as useful in the California region for these larger white sharks. Alternatively, and as discussed above, high-resolution biologging tags that record activity levels of individuals could be used. By describing the coastal behaviors of these animals at this fine-scale, we will be better equipped to manage both human-shark interaction risks and white shark populations in a dynamic, shifting global climate.

DATA AVAILABILITY STATEMENT

Tagging data up until 2009 is a part of the publicly available TOPP dataset. All other raw data supporting the conclusions of this article will be made available by the authors, without undue reservation.

ETHICS STATEMENT

The animal study was reviewed and approved by the Stanford University animal care protocol 10765.

AUTHOR CONTRIBUTIONS

SA and BB conceived the study. SA, TC, SJ, SDA, PK, TW, and BB performed fieldwork and data collection. SA and MC processed and analyzed the data. SA, TC, SJ, PK, and BB interpreted the data. SA led the writing of the manuscript. All authors read and approved the final manuscript.

FUNDING

Funding for this research was provided by the Moore, Packard and Monterey Bay Aquarium Research Foundations. We thank Discovery Communications, NOAA IOOS and CeNCOOS for providing funds for tags in 2017 and 2018. Additional funds were available from Rolex Award for Enterprise and individual philanthropic supporters of the Stanford white shark program. We thank the Schmidt Ocean Institute for providing the research vessel Falkor and enabling recovery of tags offshore.

ACKNOWLEDGMENTS

We thank the white shark research program volunteers as well as Stanford graduate and undergraduate students, postdoctoral researchers, and Block lab staff that provided unwavering support for the program across the two decades of tagging research, including T. Reimer, J. Cornelius, N. Arnoldi, S. Van Sommeran, E. Estess, K. Weng, and A. Boustany. We thank James Ganong and Alan Swithenbank for their efforts in maintaining the TOPP database and processing and archiving of data. We thank M. Goodman for statistical advice. We thank Tom O'Leary for donating time and vessel opportunities for shark observation and electronic tagging at Año Nuevo. We thank the crew and captains of RSV Dereck and M. Bayliss, and S. Rhodes and P. Conroy of the Norcal at the Farallones. We would also like to thank David Wells, Michael Domeier, and Luis Cardona for providing constructive comments that improved the manuscript.

SUPPLEMENTARY MATERIAL

The Supplementary Material for this article can be found online at: https://www.frontiersin.org/articles/10.3389/fmars.2022.835576/full#supplementary-material

Supplementary Data Sheet 2 | Full list of model subsets considered in the model selection process. Each tab includes the subsets considered for each unique model, with 'a' and 'b' being for females and males respectively. The highlighted row indicates the selected model.

REFERENCES

Adams, K. R., Gibbs, L., Knott, N. A., Broad, A., Hing, M., Taylor, M. D., et al. (2020). Coexisting with sharks: a novel, socially acceptable and non-lethal shark mitigation approach. *Sci. Rep.* 10:17497. doi: 10.1038/s41598-020-74270-y

Afonso, A. S., and Hazin, F. H. (2015). Vertical movement patterns and ontogenetic niche expansion in the tiger shark, *Galeocerdo cuvier*. *PLoS One* 10:e116720. doi: 10.1371/journal.pone.0116720

Ainley, A. D., Strong, C. S., Huber, T. J., Lewis, T. J., and Morrell, S. H. (1981). Predation by sharks on pinnipeds at the Farallon Islands. *U.S. Fish Bull.* 78, 941–945.

Andrzejaczek, S., Gleiss, A. C., Jordan, L. K. B., Pattiaratchi, C. B., Howey, L. A., Brooks, E. J., et al. (2018a). Temperature and the vertical movements of oceanic whitetip sharks, *Carcharhinus longimanus*. *Sci. Rep.* 8:8351. doi: 10.1038/s41598-018-26485-3

Andrzejaczek, S., Gleiss, A. C., Pattiaratchi, C. B., and Meekan, M. G. (2018b). First insights into the fine-scale movements of the sandbar shark, *Carcharhinus plumbeus*. *Front. Mar. Sci.* 5:483. doi: 10.3389/fmars.2018.00483

Andrzejaczek, S., Gleiss, A. C., Lear, K. O., Pattiaratchi, C., Chapple, T. K., and Meekan, M. G. (2020). Depth-dependent dive kinematics suggest cost-efficient foraging strategies by tiger sharks. *R. Soc. Open Sci.* 7:200789. doi: 10.1098/rsos.200789

Andrzejaczek, S., Schallert, R. J., Forsberg, K., Arnoldi, N. S., Cabanillas-Torpoco, M., Purizaca, W., et al. (2021). Reverse diel vertical movements of oceanic manta rays off the northern coast of Peru and implications for conservation. *Ecol. Solut. Evid.* 2:e12051. doi: 10.1002/2688-8319.12051

Beltran, R. S., Kendall-Bar, J. M., Pirotta, E., Adachi, T., Naito, Y., Takahashi, A., et al. (2021). Lightscapes of fear: how mesopredators balance starvation and predation in the open ocean. *Sci. Adv.* 7:eabd9818. doi: 10.1126/sciadv.abd9818

Block, B. A., Jonsen, I. D., Jorgensen, S. J., Winship, A. J., Shaffer, S. A., Bograd, S. J., et al. (2011). Tracking apex marine predator movements in a dynamic ocean. *Nature* 475, 86–90. doi: 10.1038/nature10082

Boustany, A. M., Davis, S. F., Pyle, P., Anderson, S. D., Boeuf, B. J., and Block, B. A. (2002). Expanded niche for white sharks. *Nature* 415:415235b. doi: 10.1038/415035b

Braun, C. D., Skomal, G. B., and Thorrold, S. R. (2018). Integrating archival tag data and a high-resolution oceanographic model to estimate basking shark (*Cetorhinus maximus*) movements in the Western Atlantic. *Front. Mar. Sci.* 5:25. doi: 10.3389/fmars.2018.00025

Brown, J. S., Laundré, J. W., and Gurung, M. (1999). The ecology of fear: optimal foraging, game theory, and trophic interactions. *J. Mammal.* 80, 385–399. doi: 10.2307/1383287

Butcher, P. A., Piddocke, T. P., Colefax, A. P., Hoade, B., Peddemors, V. M., Borg, L., et al. (2019). Beach safety: can drones provide a platform for sighting sharks? *Wild. Res.* 46, 701–712. doi: 10.1071/WR18119

Chapple, T. K., Chambert, T., Kanive, P. E., Jorgensen, S. J., Rotella, J. J., Anderson, S. D., et al. (2016). A novel application of multi-event modeling to estimate class segregation in a highly migratory oceanic vertebrate. *Ecology* 97, 3494–3502. doi: 10.1002/ecy.1589

Chapple, T. K., Jorgensen, S. J., Anderson, S. D., Kanive, P. E., Klimley, A. P., Botsford, L. W., et al. (2011). A first estimate of white shark, *Carcharodon carcharias*, abundance off Central California. *Biol. Lett.* 7, 581–583. doi: 10.1098/rsbl.2011.0124

Coffey, D. M., Carlisle, A. B., Hazen, E. L., and Block, B. A. (2017). Oceanographic drivers of the vertical distribution of a highly migratory, endothermic shark. *Sci. Rep.* 7:10434. doi: 10.1038/s41598-017-11059-6

Curtis, T. H., Bruce, B. D., Cliff, G., Dudley, S. F. J., Klimley, A. P., Kock, A., et al. (2012). "Responding to the risk of white shark attack: updated statistics, prevention, control methods, and recommendations," in *Global Perspectives on the Biology and Life History of the White Shark*, ed. M. L. Domeier (Boca Raton, FL: CRC Press), 477–509.

De Vos, A., and O'Riain, M. J. (2010). Sharks shape the geometry of a selfish seal herd: experimental evidence from seal decoys. *Biol. Lett.* 6, 48–50. doi: 10.1098/rsbl.2009.0628

Del Raye, G., Jorgensen, S. J., Krumhansl, K., Ezcurra, J. M., and Block, B. A. (2013). Travelling light: white sharks (*Carcharodon carcharias*) rely on body lipid stores to power ocean-basin scale migration. *Proc. R. Soc. B Biol. Sci.* 280:20130836. doi: 10.1098/rspb.2013.0836

Domeier, M. L., and Nasby-Lucas, N. (2008). Migration patterns of white sharks *Carcharodon carcharias* tagged at Guadalupe Island, Mexico, and identification of an eastern Pacific shared offshore foraging area. *Mar. Ecol. Prog. Ser.* 370, 221–237. doi: 10.3354/meps07628

Domeier, M. L., Nasby-Lucas, N., and Lam, C. H. (2012). "Fine-scale habitat use by white sharks at Guadalupe Island, Mexico," in *Global Perspectives on the Biology and Life History of the White Shark*, ed. M. L. Domeier (Boca Raton, FL: CRC Press), 121–132. doi: 10.1111/jfb.12828

Ferretti, F., Jorgensen, S., Chapple, T. K., De Leo, G., and Micheli, F. (2015). Reconciling predator conservation with public safety. *Front. Ecol. Environ.* 13:412–417. doi: 10.1890/150109

Francis, M. P. (1996). "Observations on a pregnant white shark with a review of reproductive biology," in *Great White Sharks: The Biology of Carcharodon Carcharias*, eds A. P. Klimley and D. G. Ainley (San Diego, CA: Academic Press), 157–172.

Francis, M. P., Duffy, C. A. J., Bonfil, R., and Manning, M. J. (2012). "The third dimension – vertical habitat use by white sharks, *Carcharodon carcharias*, in New Zealand and in oceanic and tropical waters of the southwest Pacific Ocean," in *Global Perspectives on the Biology and Life History of the Great White Shark*, ed. M. L. Domeier (Boca Raton, FL: CRC Press).

Gibbs, L., and Warren, A. (2015). Transforming shark hazard policy: learning from ocean-users and shark encounter in Western Australia. *Mar. Policy* 58, 116–124. doi: 10.1016/j.marpol.2015.04.014

Goldman, K. J., and Anderson, S. D. (1999). Space utilization and swimming depth of white sharks, *Carcharodon carcharias*, at the South Farallon Islands, Central California. *Environ. Biol. Fish.* 56, 351–364. doi: 10.1023/a:1007520931105

Jacobs, L. F. (2012). From chemotaxis to the cognitive map: the function of olfaction. *Proc. Natl. Acad. Sci. U.S.A.* 109(Suppl. 1):10693. doi: 10.1073/pnas.1201880109

Jorgensen, S. J., Anderson, S., Ferretti, F., Tietz, J. R., Chapple, T., Kanive, P., et al. (2019). Killer whales redistribute white shark foraging pressure on seals. *Sci. Rep.* 9:6153. doi: 10.1038/s41598-019-39356-2

Jorgensen, S. J., Arnoldi, N. S., Estess, E. E., Chapple, T. K., Rückert, M., Anderson, S. D., et al. (2012a). Eating or meeting? Cluster analysis reveals intricacies of white shark (*Carcharodon carcharias*) migration and offshore behavior. *PLoS One* 7:e47819. doi: 10.1371/journal.pone.0047819

Jorgensen, S. J., Chapple, T. K., Anderson, S., Hoyos, M., Reeb, C., and Block, B. A. (2012b). "Connectivity among white shark coastal aggregation areas in the northeastern Pacific," in *Global Perspectives on the Biology and Life History of the White Shark*, ed. M. L. Domeier (Boca Raton, FL: CRC Press), 159–168. doi: 10.1093/jhered/esv034

Jorgensen, S. J., Gleiss, A. C., Kanive, P. E., Chapple, T. K., Anderson, S. D., Ezcurra, J. M., et al. (2015). In the belly of the beast: resolving stomach tag data to link temperature, acceleration and feeding in white sharks (*Carcharodon carcharias*). *Anim. Biotelem.* 3, 1–10. doi: 10.1186/s40317-015-0071-6

Jorgensen, S. J., Reeb, C. A., Chapple, T. K., Anderson, S., Perle, C., Van Sommeran, S. R., et al. (2009). Philopatry and migration of Pacific white sharks. *Proc. R. Soc. B Biol. Sci.* 9, 679–688. doi: 10.1098/rspb.2009.1155

Kanive, P. E., Rotella, J. J., Chapple, T. K., Anderson, S. D., White, T. D., Block, B. A., et al. (2021). Estimates of regional annual abundance and population growth rates of white sharks off central California. *Biol. Conserv.* 257:109104. doi: 10.1016/j.biocon.2021.109104

Klimley, A. P. (1985). The areal distribution and autoecology of the white shark, *Carcharodon carcharias*, off the west coast of North America. *Mem. South. Califor. Acad. Sci.* 9, 15–40.

Klimley, A. P. (1994). The predatory behavior of the white shark. *Am. Sci.* 82, 122–133.

Klimley, A. P., Anderson, S. D., Pyle, P., and Henderson, R. P. (1992). Spatiotemporal patterns of white shark (*Carcharodon carcharias*) predation at the south farallon Islands, California. *Copeia* 1992, 680–690. doi: 10.2307/1446143

Klimley, A. P., Beavers, S. C., Curtis, T. H., and Jorgensen, S. J. (2002). Movements and swimming behavior of three species of sharks in La Jolla Canyon, California. *Environ. Biol. Fish.* 63, 117–135. doi: 10.1023/A:1014200301213

Klimley, A. P., Le Boeuf, B. J., Cantara, K. M., Richert, J. E., Davis, S. F., Van Sommeran, S., et al. (2001). The hunting strategy of white sharks (*Carcharodon carcharias*) near a seal colony. *Mar. Biol.* 138, 617–636. doi: 10.1007/s002270000489

Laroche, R. K., Kock, A. A., Dill, L. M., and Oosthuizen, W. H. (2008). Running the gauntlet: a predator–prey game between sharks and two age classes of seals. *Anim. Behav.* 76, 1901–1917. doi: 10.1016/j.anbehav.2008.06.025

Le Boeuf, B. J., and Crocker, D. E. (1996). "Diving behavior of elephant seals: implications for predator avoidance," in *Great White Shark: The Biology of Carcharodon Carcharias*, ed. A. P. Klimley (San Diego, CA: Academic Press).

LeBoeuf, B. J., Riedman, R. M., and Keyes, R. S. (1982). White shark predation on pinnipeds in California coastal waters. *Fish. Bull.* 80, 891–895.

Lester, E. K., Langlois, T. J., Simpson, S. D., McCormick, M. I., and Meekan, M. G. (2020). The hemisphere of fear: the presence of sharks influences the three dimensional behaviour of large mesopredators in a coral reef ecosystem. *Oikos* 129, 731–739. doi: 10.1111/oik.06844

Lima, S. L., and Dill, L. M. (1990). Behavioral decisions made under the risk of predation: a review and prospectus. *Canad. J. Zool.* 68, 619–640. doi: 10.1139/z90-092

Lisovski, S., Bauer, S., Briedis, M., Davidson, S. C., Dhanjal-Adams, K. L., Hallworth, M. T., et al. (2020). Light-level geolocator analyses: a user's guide. *J. Anim. Ecol.* 89, 221–236. doi: 10.1111/1365-2656.13036

Long, D. J., Hanni, K. D., Pyle, P., Roletto, J., Jones, R. E., and Bandar, R. (1996). "White shark predation on four pinniped species in central California waters: Geographic and temporal patterns inferred from wounded carcasses," in *Great White Sharks: The Biology of Carcharodon Carcharias*, eds A. P. Klimley and D. G. Ainley (San Diego, CA: Academic Press).

Lowry, M. S., Jaime, E. M., Nehasil, S. E., Betcher, A., and Condit, R. (2020). *Winter Surveys at the Channel Islands and Point Conception Reveal Population Growth of Northern Elephant Seals and Residence Counts of Other Pinnipeds, NOAA Technical Memorandum NMFS-SWFSC-627.* Washington, DC: U.S. Department of Commerce, National Oceanic and Atmospheric Administration.

McHuron, E. A., Block, B. A., and Costa, D. P. (2018). Movements and dive behavior of juvenile California sea lions from Año Nuevo Island. *Mar. Mam. Sci.* 34, 238–249. doi: 10.1111/mms.12449

Melin, S. R., Delong, R. L., Thomason, J. R., and Vanblaricom, G. R. (2000). Attendance patterns of California sea lion (*Zalophus californianus*) females and pups during the non-breeding season at San Miguel Island. *Mar. Mam. Sci.* 16, 169–185. doi: 10.1111/j.1748-7692.2000.tb00911.x

Mourier, J., Maynard, J., Parravicini, V., Ballesta, L., Clua, E., Domeier, M. L., et al. (2016). Extreme inverted trophic pyramid of reef sharks supported by spawning groupers. *Curr. Biol.* 26, 2011–2016. doi: 10.1016/j.cub.2016.05.058

Nasby-Lucas, N., Dewar, H., Lam, C. H., Goldman, K. J., and Domeier, M. L. (2009). White shark offshore habitat: a behavioral and environmental characterization of the eastern pacific shared offshore foraging area. *PLoS One* 4:e8163. doi: 10.1371/journal.pone.0008163

Pedersen, M. W., Patterson, T. A., Thygesen, U. H., and Madsen, H. (2011). Estimating animal behavior and residency from movement data. *Oikos* 120, 1281–1290. doi: 10.1111/j.1600-0706.2011.19044.x

Peel, L. R., Stevens, G. M. W., Daly, R., Keating Daly, C. A., Lea, J. S. E., Clarke, C. R., et al. (2019). Movement and residency patterns of reef manta rays *Mobula alfredi* in the Amirante Islands, Seychelles. *Mar. Ecol. Progr. Ser.* 621, 169–184. doi: 10.3354/meps12995

Pratt, H. L. (1996). "Reproduction in the male white shark," in *Great White Sharks: The Biology of Carcharodon Carcharias*, eds A. P. Klimley and D. G. Ainley (San Diego, CA: Academic Press), 131–138. doi: 10.1016/b978-012415031-7/50014-8

Pyle, P., Anderson, S. D., Klimley, A. P., and Henderson, R. P. (1996). "Environmental factors affecting the occurrence and behavior of white sharks at the Farallon Islands, California," in *Great White Sharks: The Biology of Carcharodon Carcharias*, eds A. P. Klimley and D. G. Ainley (San Diego, CA: Academic Press), 281–291.

R Core Team (2020). *R: A Language and Environment for Statistical Computing*, ed. R.F.f.S. Computing (Vienna: R Core Team).

Skomal, G. B., Braun, C. D., Chisholm, J. H., and Thorrold, S. R. (2017). Movements of the white shark *Carcharodon carcharias* in the North Atlantic Ocean. *Mar. Ecol. Progr. Ser.* 580, 1–16. doi: 10.3354/meps12306

Spaet, J. L. Y., Manica, A., Brand, C. P., Gallen, C., and Butcher, P. A. (2020). Environmental conditions are poor predictors of immature white shark Carcharodon carcharias occurrences on coastal beaches of eastern Australia. *Mar. Ecol. Progr. Ser.* 653, 167–179. doi: 10.3354/meps13488

Strong, W. R. Jr. (1996). "Shape discrimination and visual predatory tactics in white sharks," in *Great White Sharks: The Biology of Carcharodon Carcharias*, eds A. P. Klimley and A. D. Ainley (New York, NY: Academic Press), 229–240. doi: 10.1016/b978-012415031-7/50022-7

Tanaka, K. R., Van Houtan, K. S., Mailander, E., Dias, B. S., Galginaitis, C., O'Sullivan, J., et al. (2021). North Pacific warming shifts the juvenile range of a marine apex predator. *Sci. Rep.* 11:3373. doi: 10.1038/s41598-021-82424-9

Thieurmel, B., and Elmarhraoui, A. (2019). *suncalc: Compute Sun Position, Sunlight Phases, Moon Position and Lunar Phase [Online]*. Available online at: https://CRAN.R-project.org/package=suncalc (accessed September 10, 2020).

Watanabe, Y. Y., Payne, N. L., Semmens, J. M., Fox, A., and Huveneers, C. (2019b). Swimming strategies and energetics of endothermic white sharks during foraging. *J. Exp. Biol.* 222:jeb185603. doi: 10.1242/jeb.185603

Watanabe, Y. Y., Payne, N. L., Semmens, J. M., Fox, A., and Huveneers, C. (2019a). Hunting behaviour of white sharks recorded by animal-borne accelerometers and cameras. *Mar. Ecol. Progr. Ser.* 621, 221–227. doi: 10.3354/meps12981

Weng, K. C., Boustany, A. M., Pyle, P., Anderson, S. D., Brown, A., and Block, B. A. (2007a). Migration and habitat of white sharks (*Carcharodon carcharias*) in the eastern Pacific Ocean. *Mar. Biol.* 152, 877–894. doi: 10.1007/s00227-007-0739-4

Weng, K. C., O'Sullivan, J. B., Lowe, C. G., Winkler, C. E., Dewar, H., and Block, B. A. (2007b). Movements, behavior and habitat preferences of juvenile white sharks *Carcharodon carcharias* in the eastern Pacific. *Mar. Ecol. Progr. Ser.* 338, 211–224. doi: 10.3354/meps338211

Wilson, S. G., Jonsen, I. D., Schallert, R. J., Ganong, J. E., Castleton, M. R., Spares, A. D., et al. (2015). Tracking the fidelity of Atlantic bluefin tuna released in Canadian waters to the Gulf of Mexico spawning grounds. *Canad. J. Fisher. Aquatic Sci.* 72, 1700–1717. doi: 10.1139/cjfas-2015-0110

Winton, M. V., Sulikowski, J., and Skomal, G. B. (2021). Fine-scale vertical habitat use of white sharks at an emerging aggregation site and implications for public safety. *Wildlife Res.* 48, 345–360. doi: 10.1071/WR20029

Wood, S. N. (2017). *Generalized Additive Models: An Introduction With R*. Boca Raton, Fl: CRC Press.

Wright, S. R., Righton, D., Naulaerts, J., Schallert, R. J., Griffiths, C. A., Chapple, T., et al. (2021). Yellowfin tuna behavioural ecology and catchability in the south atlantic: the right place at the right time (and Depth). *Front. Mar. Sci.* 8:616. doi: 10.3389/fmars.2021.664593

Yopak, K. E., Lisney, T. J., and Collin, S. P. (2015). Not all sharks are "swimming noses": variation in olfactory bulb size in cartilaginous fishes. *Brain Struct. Funct.* 220, 1127–1143. doi: 10.1007/s00429-014-0705-0

Zuur, A., Ieno, E. N., Walker, N., Saveliev, A. A., and Smith, G. M. (2009). *Mixed Effects Models and Extensions in Ecology With R*. Heidelberg: Springer Science & Business Media.

Conflict of Interest: The authors declare that the research was conducted in the absence of any commercial or financial relationships that could be construed as a potential conflict of interest.

frontiers | Frontiers in Marine Science

ORIGINAL RESEARCH
published: 17 June 2022
doi: 10.3389/fmars.2022.779047

Trophic-Mediated Pelagic Habitat Structuring and Partitioning by Sympatric Elasmobranchs

André S. Afonso[1,2†], *Bruno C. L. Macena*[3*†], *Bruno Mourato*[4], *Natalia P. A. Bezerra*[1], *Sibele Mendonça*[1], *Joyce D. G. R. de Queiroz*[1] *and Fábio H. V. Hazin*[1‡]

[1] Departamento de Pesca e Aquicultura, Universidade Federal Rural de Pernambuco, Recife, Brazil, [2] Marine and Environmental Sciences Centre, Polytechnic Institute of Leiria, Peniche, Portugal, [3] Ocean Sciences Institute - Okeanos and Institute of Marine Research, University of the Azores, Horta, Portugal, [4] Instituto do Mar, Universidade Federal de São Paulo, São Paulo, Brazil

OPEN ACCESS

Edited by:
Clive N. Trueman,
University of Southampton,
United Kingdom

Reviewed by:
Víctor Hugo Cruz-Escalona,
Instituto Politécnico Nacional (IPN),
Mexico
Felipe Galván-Magaña,
Centro Interdisciplinario de Ciencias
Marinas (IPN), Mexico

***Correspondence:**
Bruno C. L. Macena
brunomacena@gmail.com

†These authors have contributed equally to this work

‡Deceased

Specialty section:
This article was submitted to Marine Megafauna, a section of the journal Frontiers in Marine Science

Received: *17 September 2021*
Accepted: *16 May 2022*
Published: *17 June 2022*

Citation:
Afonso AS, Macena BCL, Mourato B, Bezerra NPA, Mendonça S, de Queiroz JDGR and Hazin FHV (2022) Trophic-Mediated Pelagic Habitat Structuring and Partitioning by Sympatric Elasmobranchs. Front. Mar. Sci. 9:779047. doi: 10.3389/fmars.2022.779047

Pelagic elasmobranchs are key elements of oceanic ecosystems and must be preserved if marine trophic networks are to be kept in balance. Yet, they face intense fishing pressure that has been threatening their populations worldwide. Ensuring proper conservation management of these taxa depends on a better understanding of the strategies they use to explore the pelagic realm and their contributions to trophic web structuring across the ocean column. This study aimed at examining relationships between vertical habitat use and trophic attributes among six sympatric pelagic elasmobranchs using satellite transmitting tags in the western equatorial South Atlantic Ocean. The vertical movements of 35 elasmobranch individuals were tracked during an overall total of 1911 days. Clear relationships between species' feeding habits, maximum diving depths, and proportion of time spent either in epipelagic or in surface waters were evidenced by Bayesian generalized linear mixed models and multivariate analysis. Filter-feeders made most use of deep waters from the mesopelagic and bathypelagic and shifted their diving depths in phase with diel vertical migrations of the deep scattering layer, i.e., shallower during the night and deeper during the day. Specialists exhibited distinct diving patterns in epipelagic and mesopelagic waters across the diel period which are potentially indicative of habitat partitioning, whereas generalists were more surface-oriented but also explored deeper waters compared to specialists. The trophic level also seemed to influence elasmobranch maximum diving depths, which tended to become shallower as species' trophic level increased. These results corroborate previous evidence of widespread vertical habitat partitioning among sympatric pelagic predators and depict a trophic-mediated structuring of the pelagic environment where top-down control may be exerted at different depths by distinct species. Further research is yet required to understand the role of elasmobranch vertical movements in structuring pelagic habitats as well as to guide ecosystem-based fisheries management aimed at reducing species susceptibility to fishing gear and at preserving the structure and functionality of marine trophic networks.

Keywords: diving behavior, foraging strategy, telemetry, marine predators, mesopelagic, shark, ray

INTRODUCTION

Globally, chondrichthyan fishes face widespread, unsustainable fishing pressure (Davidson et al., 2016; Queiroz et al., 2019) which has resulted in more than one-third of these taxa being currently threatened with extinction (Dulvy et al., 2021). Populations of easily accessible coastal elasmobranchs are known to have already collapsed (Jackson et al., 2001), and modern technology has enabled the exploitation of the oceanic realm by industrial fisheries at alarmingly high rates, so that about half of all oceanic shark species are is now endangered (Pacoureau et al., 2021). Such a reality poses a considerable challenge to researchers and managers because these taxa generally play an important role in balancing and connecting marine ecosystems (Heithaus et al., 2012; Afonso et al., 2017) while being considerably susceptible to overfishing (Dulvy and Forrest, 2010). Hence, serious concerns about the sustainability of elasmobranch fisheries and the ecological consequences of their removal from the marine environment have been raised (Ferretti et al., 2010; Trindade-Santos et al., 2020). Ensuring the health of marine ecosystems may thus depend on the effective conservation of elasmobranch populations. However, essential knowledge about the ecology and behavior of pelagic species is scant due to their remoteness, crypticness, and vagility, ultimately hampering the ability to achieve optimal resource management.

The pelagic oceanic realm comprises the largest ecosystems on the globe (Robison, 2009) and is divided into different depth strata with distinct physicochemical and biological properties. The epipelagic euphotic biome spans from the surface down to 200 m in depth and corresponds to the stratum where sunlight penetration enables primary production by photosynthetic organisms. The mesopelagic dysphotic biome spans between 200 and 1000 m in depth and comprises a major faunal assemblage with one of the greatest biomasses in the biosphere (Irigoien et al., 2014). This assemblage gathers mostly fish and invertebrates within the so-called 'Deep Scattering Layer' (DSL) (Costello and Breyer, 2017) and constitutes a regular source of prey for marine megafauna (Hazen, 2010). The bathypelagic biome spans below 1000 m in depth and is characterized by the total absence of sunlight and by a sharp decrease in fish abundance (Sutton et al., 2010). The vertical distribution of oceanic fauna in the pelagic environment is modulated by abiotic factors including temperature, dissolved oxygen, light level, and pressure (Bianchi et al., 2013; Klevjer et al., 2016; Bernal et al., 2017) which vary considerably across the water column (Costello and Breyer, 2017). Notwithstanding, systematic movements across pelagic biomes by several marine taxa are known to occur on a regular basis, particularly between the epipelagic and mesopelagic strata (Sutton, 2013). This is because, at small spatial scales, the vertical gradient of the oceanic realm renders much higher habitat variability than the horizontal one, a feature that DSL organisms and pelagic fauna explore to improve foraging efficiency and feeding success while reducing predation risk. Diel vertical migrations conducted by nektonic and planktonic fauna from the DSL are among the most massive migratory processes known to date, and epipelagic predators are believed to adapt their movements accordingly to feed directly on DSL prey or on lower order predators that feed on DSL prey (Hays, 2003).

Large-bodied elasmobranchs shape the structure of marine ecosystems *via* trophic-related relationships mediated by direct predation upon lower trophic levels (Hammerschlag, 2019) and intra- or inter-specific competition (Sabando et al., 2020). Competition among predators may lead to fewer feeding opportunities and reduced fitness (Smith et al., 2017; Jorgensen et al., 2019), hence resource partitioning between sympatric elasmobranchs has often evolved (Tillett et al., 2014; Espinoza et al., 2019; Mulas et al., 2019). In the pelagic realm, elasmobranch resource partitioning could be more feasibly achieved on the vertical scale, and there is growing evidence that co-occurring predatory species use different compartments of the depth gradient to forage (Le Croizier et al., 2020b; Besnard et al., 2021; Madigan et al., 2021). An intrinsic relationship between species diving behavior and its trophic attributes might thus be expected among the pelagic elasmobranch community. In accordance, previous simulation-based research highlighted that the vertical distribution of prey could have a greater influence on the diving behavior of pelagic predators than the abiotic gradient by itself (Dagorn et al., 2000). Pelagic habitat partitioning has been identified among other high-level predators such as tuna and seabirds, and prey abundance showed to improve distribution models for these species (Receveur et al., 2021). It is known that anthropogenic disturbances to marine ecosystems such as the ones produced by fisheries tend to propagate across the complexity of food webs (Ferretti et al., 2010), eventually developing into unforeseen ecological damage. Therefore, understanding the vertical structure of pelagic trophic networks and the venues of energy flow within and between oceanic habitats is utterly required to guide fisheries management toward a sustainable use of marine resources.

This study seeks to explore potential relationships between the diving behavior and intrinsic trophic attributes in sympatric, large-bodied pelagic elasmobranchs using biologging data collected in a poorly known region, i.e., the South Atlantic Ocean. With this approach, we aim at finding preliminary evidence of a trophic-mediated, vertical compartmentalization of the pelagic realm shaped by the behaviors of pelagic predators and their prey, as well as at depicting possible pathways for energy transference between different pelagic biomes.

MATERIAL AND METHODS

Ethical Statements

Elasmobranch tagging was conducted with the approval of the Ethics Committee on Research with Animals of the Universidade Federal Rural de Pernambuco (licenses no. #23082.009679/2009, #23082.025519/2014, and #23082.025800/2015).

Study Area

This study was conducted in the western equatorial Atlantic Ocean off Northeast Brazil (**Figure 1**). We focused our elasmobranch tagging efforts on a region spanning between latitudes 1°N and 8°S to preclude potentially confounding effects derived from regional-specific environmental factors. Tagging locations were off the Saint Peter and Saint Paul Archipelago (0.9°N, 29.3°W), off the Fernando de Noronha Archipelago (3.8°S, 32.4°W), and off Recife (8.1°S, 34.5°W).

Data Collection and Tagging Procedure

Elasmobranchs were tagged with pop-up satellite archival tags (MK-10 and miniPAT models; Wildlife Computers, USA), hereafter referred to as PSATs. These tags record a time-series of depth, seawater temperature, and luminosity readings which depict both vertical and horizontal movements performed by free-ranging tagged individuals during a user-programmable deployment span. Then, the tags pop up to the ocean surface and inform their position with high (< 1.5 km) accuracy while transmitting summarized depth (± 4 m) and temperature (± 0.05° C) data through the satellites with a 1- to 24-hour temporal resolution. These summaries include the depth range (i.e., minimum and maximum depths) of PSAT movements along with a vertical profile of seawater temperature (PDT), and histograms of the relative time spent at different depth strata (TAD) within a temporal unit. Luminosity data are also relayed to reconstruct horizontal movements based on the timing of crepuscular events. PSATs can withstand pressure levels as high as 200 atm, thus they are able to track bathypelagic dives up to ~2000 m in depth.

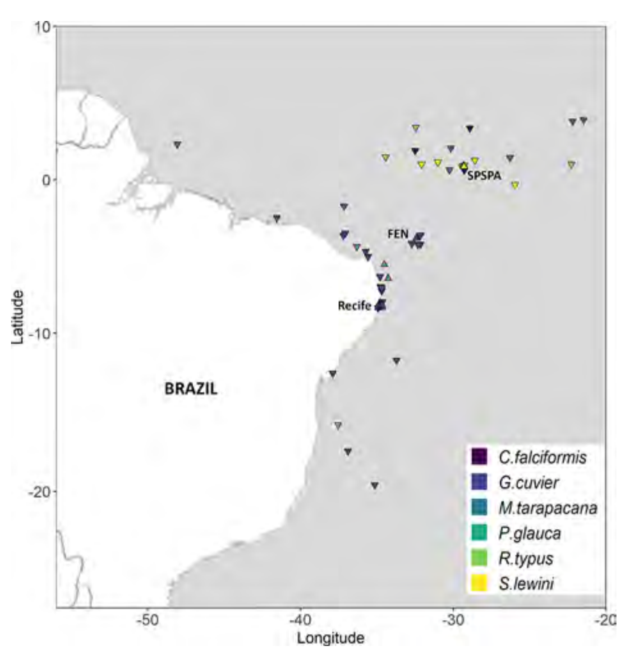

FIGURE 1 | Map of the study area in the western equatorial and tropical South Atlantic Ocean depicting tag deployment locations (triangles) and pop-up locations (inverted triangles). Colors represent different elasmobranch species.

The tagged species included three carcharhinids (tiger shark *Galeocerdo cuvier*, silky shark *Carcharhinus falciformis*, and blue shark *Prionace glauca*), one sphyrnid (scalloped hammerhead shark *Sphyrna lewini*), one rhincodontid (whale shark *Rhincodon typus*), and one mobulid (sicklefin devil ray *Mobula tarapacana*). In general, sharks were caught with longline fishing gear and either brought onboard or restrained underwater alongside the boat. Sharks were identified, sexed, and measured for total length (TL) to the nearest centimeter. A PSAT was then fitted to the first dorsal fin or, alternatively, to the dorsal musculature beneath the first dorsal fin so that it would be towed near the shark's body. Mobulids and whale sharks were tagged while swimming near the surface by an experienced diver, who made use of a 150 cm pole to fit PSATs into the posterior region of the dorsal musculature. Whale shark total length and devil ray disk width (DW) were visually estimated during the tagging procedure. More detailed information about the tagging procedure for the different species can be found in Afonso (2013); Carvalho et al. (2015); Macena (2016); Afonso et al. (2017); Bezerra et al. (2019), and Mendonça et al. (2018).

Data Processing

Satellite-relayed data were decoded using the proprietary manufacturer's DAP® software, and the most likely movements between tag deployment and pop-up locations were estimated using GPE3® software in the Wildlife Computers Data Portal. Elasmobranch maximum diving depths (*maxDepth*, in meters) were filtered from PDT data and ascribed with a diel stage (i.e., day or night), which was defined by applying the *sunriset* function in the maptools R package (Bivand and Lewin-Koh, 2021) to the date, time, and most likely location of each *maxDepth*. Because PSAT data were pooled from different individual studies and presented heterogeneous temporal resolution (i.e., data were summarized in 3-, 4-, 6-, or 12-hour intervals), the maximum depth reading during a single diel stage was used. Moreover, the proportion of time spent by elasmobranchs in epipelagic waters above the 200-m isobath (*T200*) and in surface waters above the 10-m isobath (*T10*) were retrieved from TAD data. These depth strata were selected in order to measure the combined utilization of meso- and bathypelagic waters by these epipelagic species, and also to examine their association with the uppermost layer of the sea column where potential air-breathing prey could be the most available. A diel stage was also ascribed to *T200* and *T10* data as previously described.

Since individual trophic levels were not assessed in this study, shark trophic levels at the species level were obtained from Cortés (1999), whereas the trophic level of the sicklefin devil ray was obtained from FishBase (Froese and Pauly, 2021). Also, species were grouped according to their feeding habits into three categories, namely filter-feeders, generalists, and specialists. Categorizing elasmobranch species as dietary generalists or specialists may be rudimental since these categories often fail to capture the continuum nature of trophic specialization (Compagno, 1990). In fact, elasmobranchs tend to be more or less specialized, but they rarely match with the whole definition of specialist or generalist (Munroe et al., 2014). Insufficient data on elasmobranch diet and prey composition prevent comprehensive assessments of dietary specialization, though. As such, the relative categorization of elasmobranch trophic habits could still provide helpful information about ecosystem structure and species vulnerabilities. Here, we opted for conducting a relative categorization of generalist and specialist species based on the cumulative proportions of prey categories in sharks' diets, as reported by Cortés (1999). For each species, we assessed the number of prey categories (in decreasing order of relevance) required to accumulate at least 90% of the diet composition. Species with fewer or more prey categories at the 90% threshold were categorized as specialists or generalists, respectively. Accordingly, *P. glauca*, *C. falciformis*, and *S. lewini* were all classified as specialists because they required only two to three prey categories to attain the 90% threshold (93%-100% of their diets were composed of teleosts, cephalopods, and crustaceans). On the other hand, *G. cuvier* was classified as a generalist because it required six prey categories to comprise 94% of its diet composition (**Table S1**). Filter-feeders were identified by their widely described feeding strategy.

Data Analysis

All analyses were conducted in R version 4.1.1 (R Core Team, 2021). Because the available data were not balanced across feeding habits, a random filter was applied to the overrepresented generalist dataset using the *sample* R function with no replacements so that the number of both *maxDepth* and TAD samples would amount to 500 in generalists. Vertical profiles of seawater temperature were generated with PDT data to inspect for potential thermal variability between species. Distribution density histograms of *maxDepth* per feeding habit category and per diel stage were generated to visualize patterns in diving behavior across these factors, with *maxDepth* being also discriminated across species. In turn, the relationship between species trophic level and *maxDepth* was visually explored with boxplots, with significant differences between trophic levels being tested with Kruskal-Wallis variance analysis followed by a *post-hoc* multiple comparison Dunn test, which was run with the *kruskal.test* and the *dunnTest* functions in the FSA R package (Ogle et al., 2021). Even though the trophic level is an intrinsically continuous measure, the properties of our dataset precluded an efficient use of parametric regression analysis. Therefore, we opted for interpreting trophic level as an ordered categorical variable to identify any potentially consistent trend in *maxDepth* variation across the trophic level gradient. Additionally, a multivariate cluster analysis was conducted to assess similarities between species in relation to the frequency distribution of *maxDepth* and to determine the most adequate species grouping with no prior assumptions. The NbClust R package (Charrad et al., 2014) was used to ascertain the most adequate number of clusters. The function *NbClust* calculates 23 different types of indexes and proposes the best clustering scheme based on the most common number of clusters given by the indexes (i.e., majority rule). The data was scaled prior to cluster analysis, and the dissimilarity matrix was computed using Euclidean distance with the 'complete' method of cluster analysis. Then, a dendrogram was plotted to examine hierarchical relationships among species and compare the resulting clusters with species trophic attributes. On the other hand, distribution density histograms of *T200* and *T10* per feeding habit and per diel phase were generated to examine trends in the utilization of epipelagic (≤ 200 m in depth) and surface (≤ 10 m in depth) waters by species groups. TAD data for blue sharks were unavailable, hence this species was not included in the analysis.

Bayesian generalized linear mixed models were used to identify statistically significant covariates that could affect the variability in elasmobranch diving behavior and vertical distribution. Three different models were fitted using *maxDepth* (continuous variable ≥ 0), *T200*, and *T10* (both proportions ranging between 0 and 1) as response variables. Preliminary inspection of the distribution of *maxDepth* indicated that these data were highly left-skewed. Hence, we applied a transformation of Tukey's Ladder of Powers to reduce the skewness and produce a more normal distribution of the response variable (lambda = 0.075; W = 0.9846; $p < 0.001$) using the rcompanion R package (Mangiafico, 2015). Therefore, after this transformation, we assumed that the response variable *maxDepth* was a random variable with a normal distribution. *T200* and *T10* proportion data were modeled *via* the beta probability distribution, where the mean of proportions enters the model through the *logit* link function. The beta distribution is defined for any real number between 0 and 1 and therefore it is appropriate for proportional data with asymmetric shapes (Gupta and Nadarajah, 2004). This approach has been successfully applied to regression modeling and brings several advantages over other methods addressing binomial data (Ferrari and Cribari-Neto, 2004; Paradinas et al., 2018). Candidate predictor variables included feeding habit (i.e., generalist, specialist, and filter-feeding), diel phase (i.e., day and night), and the interaction among these factors. Including the interaction of feeding habit with diel phase was deemed necessary because descriptive plots suggested different species might respond differently to the diel cycle, but the independent effect of the diel phase was not explored. Further, due to the nature of the data which comprised multiple observations over time for the same fish, we included each individual elasmobranch as a random factor, thus implying the data are independent, identically, and normally distributed (i.i.d.), with mean 0 and variance σ^2.

Bayesian inference and parameter estimates in the form of marginal posterior distributions were obtained through the Integrated Nested Laplace Approximation (INLA) approach, which is currently implemented in the R environment by the R-INLA package (http://www.r-inla.org). As recommended by Held et al. (2010), we used default priors for all fixed-effect parameters, which were defined by a vague zero-mean Gaussian prior distribution with a variance of 100 (except for the variance of the intercept which has the default value of zero). The selection of predictors and the decision on their entry or exclusion was based on the forward stepwise approach considering the Deviance Information Criterion (DIC). The best model was chosen based on the lowest DIC score and on the visual inspection of the residual distributions following the methodology of standard graphical checks proposed by Ortiz and Arocha (2004). In order to prioritize parsimony over model complexity, simpler models with less predictors were chosen when rounded DIC scores were tied.

RESULTS

Between June 2009 and June 2014, a total of 35 elasmobranchs belonging to six species were tagged with PSAT tags in the western equatorial South Atlantic Ocean between latitudes 0.92° N and 8.36°S (**Figure 1**). These comprised 16 tiger sharks, two blue sharks, three silky sharks, six scalloped hammerhead sharks, three whale sharks, and five sicklefin devil rays (**Table S2**). The size of tagged individuals ranged from 128 to 310 cm TL with a mean ± standard deviation of 195 (± 54) in tiger sharks, 130 to 180 cm TL (mean = 156 ± 25) in silky sharks, 205 to 260 cm TL (mean = 224 ± 25) in scalloped hammerhead sharks, 600 to 900 cm TL (mean = 800 ± 173) in whale sharks, and 245 to 270 cm DW (mean = 255 ± 13; N = 3) in sicklefin devil rays (**Table S2**). No measurements for blue sharks were available. Female-to-male sex ratios equaled 2.2 in tiger sharks, 1.0 in blue sharks and whale sharks, and 4.0 in scalloped hammerhead sharks and sicklefin devil rays, with no female silky sharks being tagged. Species classification per feeding habit (and trophic level) resulted in a filter-feeding group encompassing whale sharks (3.6) and sicklefin devil rays (3.8); a specialist group encompassing silky sharks (4.2), blue sharks (4.1), and scalloped hammerheads (4.1); and a generalist group represented by tiger sharks (4.1).

PSAT deployment duration ranged between 3 and 122 days (mean = 54.6 ± 43.8), rendering a total of 1911 tracking days (**Table S2**). In general, the distance between the tagging and pop-up locations was relatively small and all movements were circumscribed to the western equatorial and tropical South Atlantic (**Figure 1**). Overall, a total of 1783 PDT samples and 2497 TAD samples were collected, with the number of samples per species ranging from 85 to 1052 (mean = 297 ± 373) for PDT data and from 191 to 1361 (mean = 499 ± 485) for TAD data. After applying a random filter to the overrepresented tiger shark, the number of samples across functional groups was reasonably balanced for both PDT ($N_{\text{filter-feeder}}$ = 311, $N_{\text{generalist}}$ = 489, $N_{\text{specialist}}$ = 420) and TAD ($N_{\text{filter-feeder}}$ = 544, $N_{\text{generalist}}$ = 500, $N_{\text{specialist}}$ = 592) data.

Maximum Diving Depth (*maxDepth*)

The maximum diving depth of species grouped by feeding habit (i.e., filter-feeding, generalist, and specialist) exhibited striking differences. Filter-feeders moved mostly within the upper 500 m of the water column and exhibited a bimodal maximum diving depth frequency distribution peaking evenly at about the 100- and 300-m isobaths during the night, contrasting with a unimodal distribution peaking at the ~300-m isobath during the day (**Figure 2**). Notwithstanding, filter-feeders also performed some deeper dives across the mesopelagic and bathypelagic zones up to ~2000 m in depth. Generalists exhibited comparatively shallower diving depths, with most dives occurring around the 50-m isobath and becoming increasingly less frequent with increasing depth (up to ~1100 m) regardless of the diel phase (**Figure 2**). Specialists showed a bimodal diving depth frequency distribution during the day, with the main peak at the ~100 m isobath and a secondary peak at the ~300 m isobath. Yet, a single peak at ~150 m was noticed at night, albeit deeper mesopelagic dives > 500 m in depth were more frequent during this diel stage. Also, specialists performed dives up to ~750 m in depth, which is shallower than the > 1000 m deep dives performed by generalists and filter-feeders.

Additionally, specialist species showed to be highly segregated by depth in terms of their diving behavior. *C. falciformis* consistently performed diurnal shallow dives within the epipelagic at a strikingly preferred depth of about 80 m, but during the night it dove more frequently into deeper waters around the 150-m isobath (**Figure S1**). Likewise, *S. lewini* showed a diurnal preference for epipelagic diving centered around the 100-m isobath, albeit performing frequent dives into mesopelagic waters up to ~400 m in depth (**Figure S1**). However, the frequency of maximum diving depths of this species changed to a relatively uniform distribution across the water column down to the 750-m isobath during nocturnal periods. In turn, *P. glauca* dove to maximum depths of ~600 m but it exhibited a preference for waters from the upper mesopelagic centered around the 300-m isobath during the daytime, and around the 250-m isobath during the night (**Figure S1**). In both diel stages, a secondary peak in diving depth frequency in epipelagic waters between the 50- and 100-m isobaths was observed.

In comparison, filter-feeding species showed more coinciding diving depth distributions, although *R. typus* performed deeper bathypelagic dives than *M. tarapacana* (**Figure S1**). The former species showed a unimodal, mesopelagic-oriented diving pattern centered around the 300-m isobath during the day, but during nocturnal periods it tended to perform more shallow dives into the lower epipelagic (~130 m in depth). In turn, *M. tarapacana* showed a bimodal distribution in maximum diving depth frequency which resembled the distribution of *P. glauca*, with a deeper peak around the 350-m isobath most prominent during the daytime and a shallower peak around the 100-m isobath most prominent during the night (**Figure S1**). The seawater temperature experienced by tagged elasmobranchs ranged between 4 and 31°C, with species' vertical movements being associated with similar thermal profiles of the water column (**Figure S2**).

Elasmobranch maximum diving depths also seemed to correlate negatively with species trophic level, as exploratory boxplots indicated medians and interquartile ranges of diving depth distributions to consistently decrease with increasing trophic level (**Figure 3**). Average maximum diving depths decreased monotonously from 448 m in the lowest trophic level (3.5), to 93 m in the highest trophic level (4.2).

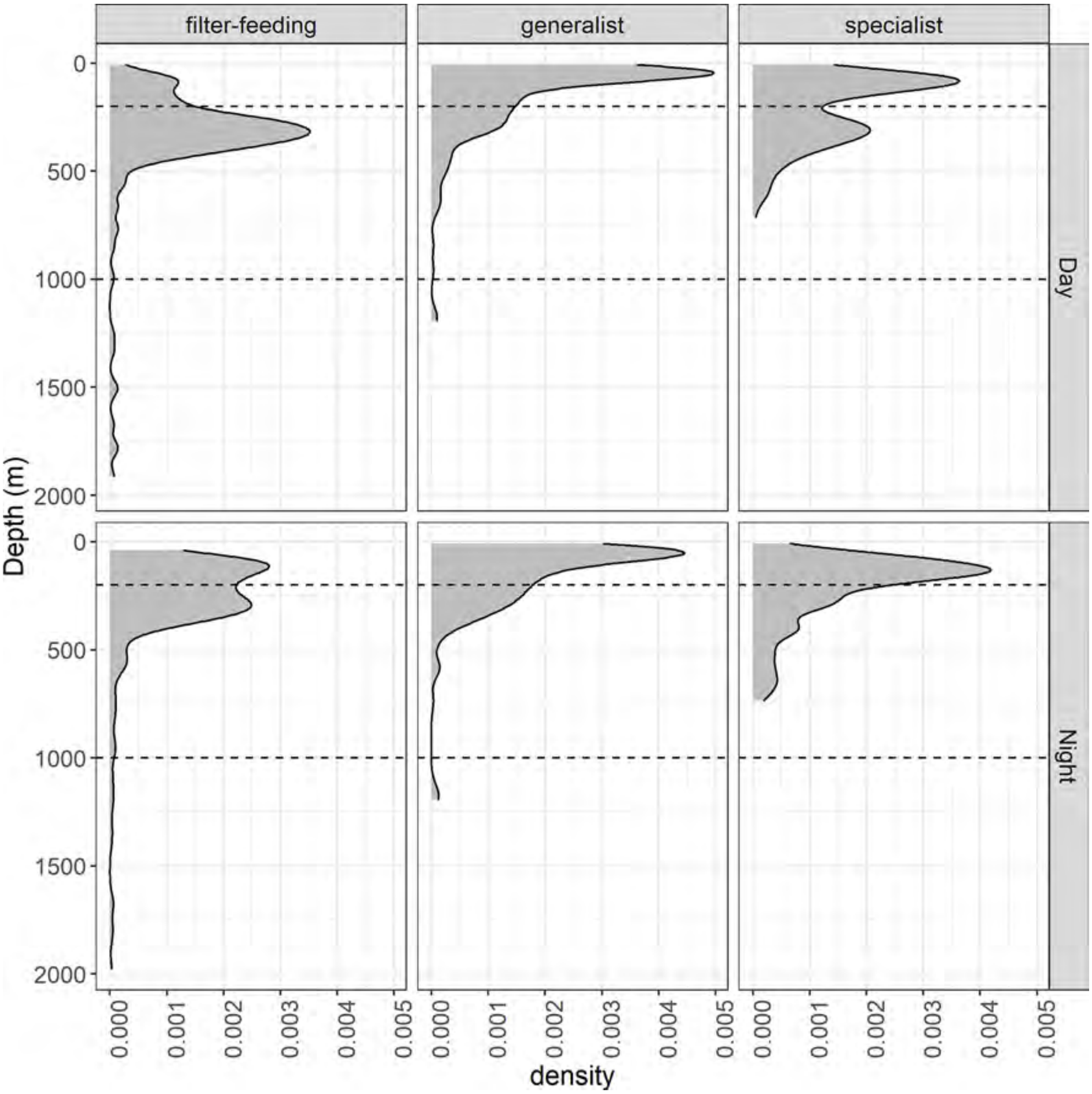

FIGURE 2 | Density plot of the smoothed distribution of pelagic elasmobranch maximum diving depths (*maxDepth*, in meters) grouped by species feeding habit for each diel phase. The upper and lower horizontal dashed lines depict the 200- and 1000-m isobaths, respectively.

AKruskal-Wallis rank sum test showed that these differences in diving depth across trophic levels were statistically significant (χ^2 = 112.37, d.f. = 3, p < 0.001), and a *post-hoc* multiple comparison Dunn test rendered significant differences to all pairwise combinations of trophic level (p ≤ 0.006; **Table S3**). Due to collinearity issues with feeding habitat, we refrained from including trophic levels in the INLA modeling.

The stepwise INLA model selection procedure for the response variable *maxDepth* selected feeding habit and its interaction with the diel cycle as the most relevant predictors of elasmobranch diving depth (**Table S4**). Overall, generalists and specialists performed significantly shallower dives than filter-feeders (**Figure 4**; **Table S5**). Further, filter-feeders tended to dive shallower during the night, contrasting with deeper diving behavior during the night by specialists (**Figure 4**; **Table S5**). Maximum diving depths in generalists proved to be unaffected by the diel stage. The diagnosis of model performance revealed that it conformed reasonably with its assumptions (**Figure S3**).

Multivariate analysis of *maxDepth* was conducted with three clusters because the output of the NbClust R package indicated this number of clusters to have the greatest statistical support (**Figure S4**). Tiger sharks formed a single-species group with the highest dissimilarity from the remainder of the species, while whale sharks formed another single-species group (**Figure 5**). The remainder of the species formed a third group, but sicklefin devil rays were hierarchically closer to whale sharks. The blue, silky, and scalloped hammerhead sharks were all grouped

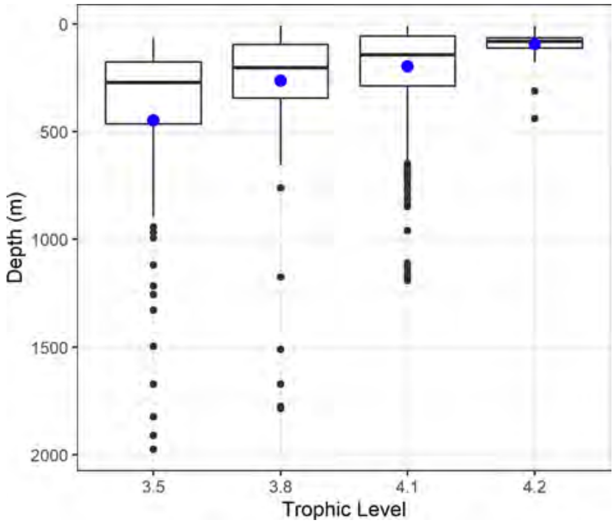

FIGURE 3 | Boxplots of the distribution of maximum diving depths in relation to trophic level in pelagic elasmobranch species. The bold horizontal line depicts the median, the solid horizontal lines in the box depict the interquartile range, the vertical solid lines represent the distribution range, and the solid circles depict potential outliers. The larger, solid, blue circles depict the mean maximum diving depths for each trophic level. Note the decreasing trend in maximum diving depths with increasing trophic levels.

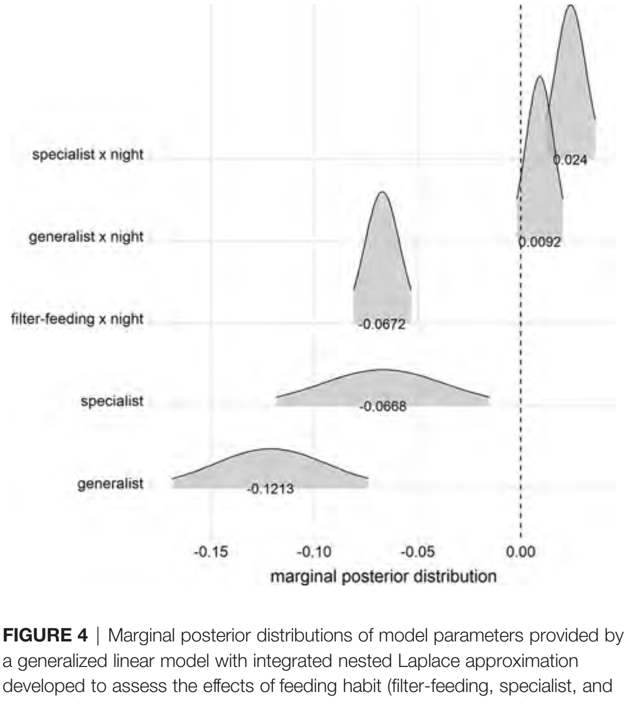

FIGURE 4 | Marginal posterior distributions of model parameters provided by a generalized linear model with integrated nested Laplace approximation developed to assess the effects of feeding habit (filter-feeding, specialist, and generalist) and the interaction of feeding habit with the diel cycle (day vs. night) on pelagic elasmobranch maximum diving depths (*maxDepth*). The vertical dashed line depicts null effects. Note that 2.5% of the distribution in each tail was discarded to provide a confidence level of 95%.

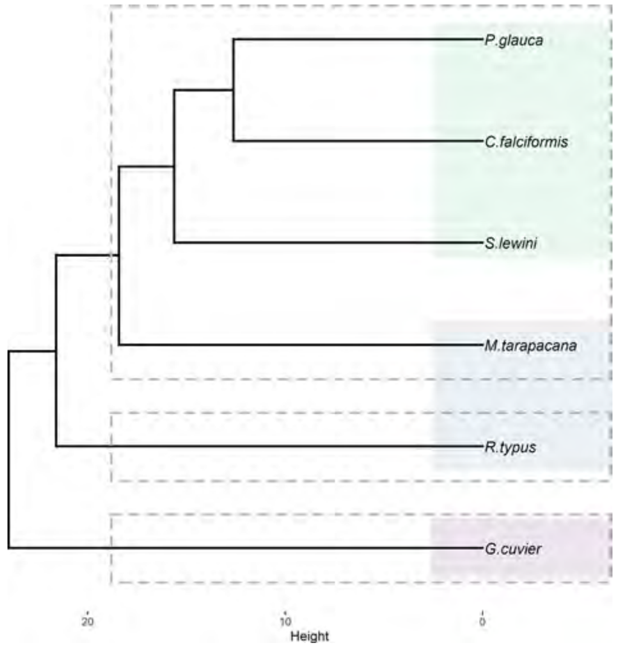

FIGURE 5 | Hierarchical cluster dendrogram depicting three groups of pelagic elasmobranch species (dashed rectangles) ordered by their similarities in relation to maximum diving depths. The shaded, colored rectangles represent groups of species which share the same feeding habit (i.e., filter-feeding, specialist, and generalist).

together, although the latter exhibited higher dissimilarity among these three species (**Figure 5**). The observed clusters and hierarchical arrangement strongly matched species grouping by feeding habits, although filter-feeders turned out to be separated into different clusters.

Time Spent in Epipelagic (*T200*) and Surface (*T10*) Waters

An epipelagic-oriented distribution in the taxa analyzed was clearly evidenced by TAD data, with all functional groups exhibiting a tendency to spend most of their time above the 200-m isobath (**Figure 6**). However, differences in deep (> 200 m) water use were observed across feeding habit categories and across the diel phase. Generalists distinguished from the remaining categories by exhibiting a striking preference for epipelagic waters and spending a nearly negligible proportion of time in mesopelagic or deeper waters during both day and night (**Figure 6**). Specialists tended to make short-lived (< 25% of a time-unit) incursions below the epipelagic, but occasionally they spent the whole time-unit in mesopelagic waters (**Figure 6**). In comparison, filter-feeders showed a higher use of deep (> 200 m) waters but they rarely moved exclusively at such depths during a time-unit. A propensity to spend more time at depths below 200 m during the daytime was observed in this group (**Figure 6**). However, a beta-regression INLA modeling of the *T200* response variable informed that a single-predictor model based on feeding habits would provide the best fit for the data

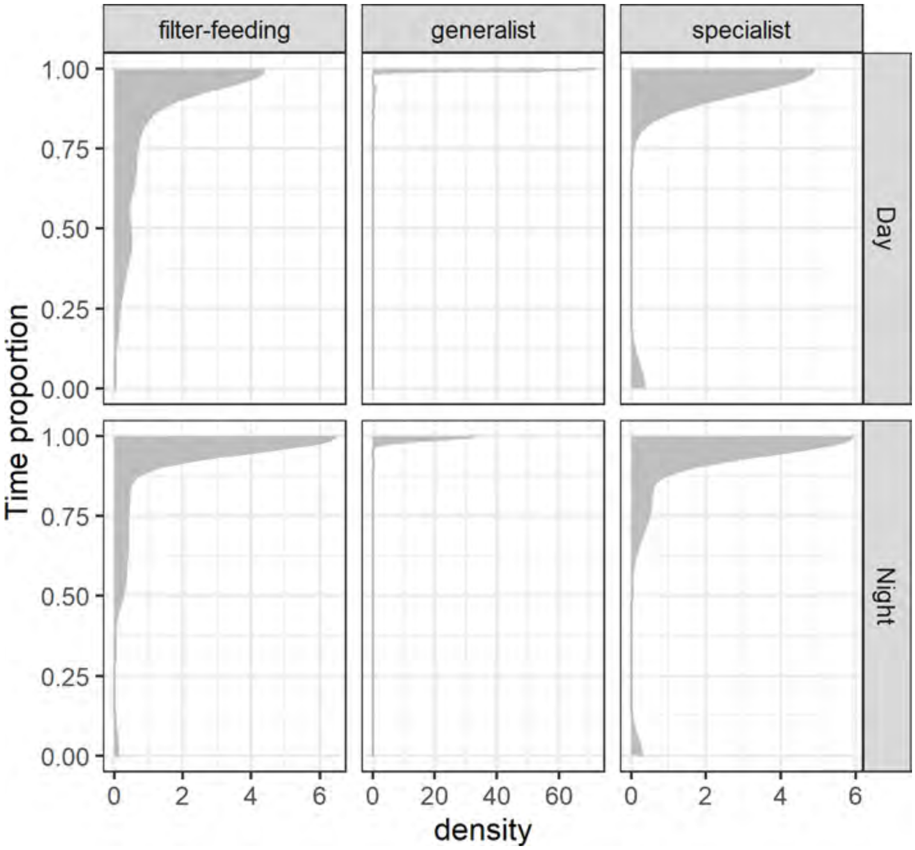

FIGURE 6 | Density plot of the smooth distribution of the proportion of time spent in epipelagic waters (≤ 200 m in depth; *T200*) by pelagic elasmobranchs grouped by their feeding habits (filter-feeding, generalist, specialist) and across the diel cycle (night and day).

(**Table S4**). This implies that the diel cycle did not significantly interact with the time spent by these species below the epipelagic zone. As for feeding habits, both specialists and generalists spent significantly more time in epipelagic waters than filter-feeders, with generalists exhibiting the most striking difference (**Table 1**).

Regarding surface behavior, differences in the proportion of time spent in the uppermost 10-m layer of the water column were best explained by the effects of feeding habits and the interaction of feeding habits with the diel cycle (**Table S4**). Specialists exhibited the lowest association to surface waters among all species groups, but they seemed to respond to the diel cycle by increasing the proportion of time spent above the 10-m isobath during the night (**Figure 7**). Generalists showed a more extensive reliance on surface waters which was most striking also during the night, while filter-feeders exhibited the opposite trend by tending to spend more time in surface waters during the day (**Figure 7**). The INLA modeling of the *T10* response variable revealed that specialists spent significantly less time in surface waters than filter-feeders, but generalists were statistically similar to filter-feeders (**Table 2**). Furthermore, sea surface (≤ 10 m in depth) use was significantly higher during the night for both specialists and generalists, whereas no significant diel differences were detected in filter-feeders.

TABLE 1 | Means and credibility intervals of 95% (Inferior and Superior) for marginal posterior distributions estimated by a beta-regression INLA model to assess the effect of feeding habit (FeedHab; as generalist, specialist, and filter-feeding) on the proportion of time spent in epipelagic (≤ 200 m in depth) waters by pelagic elasmobranchs.

Parameter	Mean	Inferior	Superior
Intercept	2.002	0.183	3.825
FeedHab:Generalist	4.771	1.766	8.575
FeedHab:Specialist	2.244	0.031	4.822
Precision parameter for the beta observations	0.956	0.809	1.120
Precision for random factor	0.250	0.085	0.549

Tag deployment was included as a random factor.

DISCUSSION

This study explores a novel approach to addressing marine habitat structuring by different functional groups within the pelagic elasmobranch assemblage. The dataset used in this study was restricted to sympatric elasmobranchs tagged in the same equatorial region to avoid introducing any potentially-confounding geographical effects into the analysis. This resulted

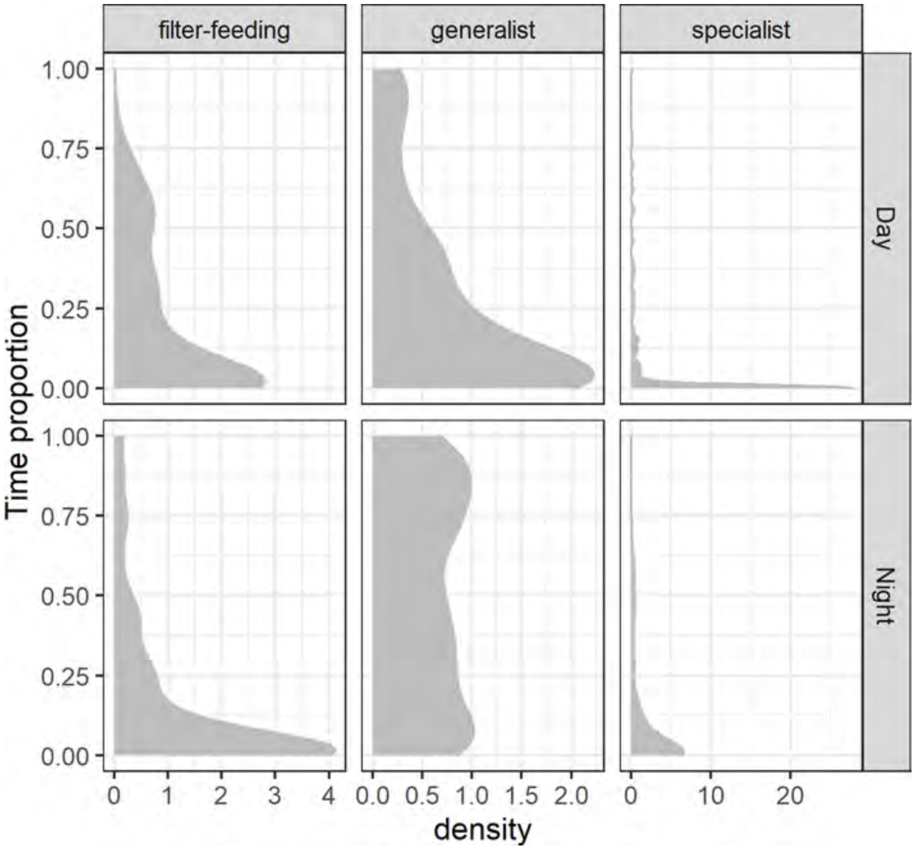

FIGURE 7 | Density plot of the smooth distribution of the proportion of time spent in surface waters (≤ 10 m in depth; *T10*) by pelagic elasmobranchs grouped by their feeding habits (filter-feeding, generalist, specialist) and across the diel cycle (night and day).

in a small number of species being represented in the dataset, raising the possibility that the observed trends may not generalize to the whole pelagic elasmobranch community. Nonetheless, the results herein reported are promising in that they denote a most relevant relationship between species vertical movements and their respective trophic attributes, besides being built upon a sample size that is aligned with recommendations for an exploratory approach such as ours (Sequeira et al., 2019). We thus encourage future research efforts aimed at examining the occurrence of trophic-mediated structuring of pelagic habitats by elasmobranchs with more diversified datasets and in other regions of the globe. The role of deep-water movements in epipelagic fish is likely related to relevant bioecological functions including foraging, thermoregulation, predator avoidance, parasite eviction, and navigation (Carey and Scharold, 1990; Braun et al., 2022). Physiological traits are traditionally regarded as the main modulators of vertical distribution in marine fishes because different species have distinct capacities to cope with depth-related environmental gradients (Horodysky et al., 2016). However, previous research suggests that the preyscape in the pelagic realm may be equally relevant in determining the dynamics in predator vertical movements (Dagorn et al., 2000; Howey et al., 2016). Even though it is widely accepted that foraging plays a central role in shaping deep-diving behavior by pelagic predators, empirical evidence of such a linkage is generally lacking (Braun et al., 2022). On that account, the multivariate approach undertaken in this study suggests that trophic behavior should be closely related to diving behavior in pelagic elasmobranchs since species ended

TABLE 2 | Means and credibility intervals of 95% (Inferior and Superior) for marginal posterior distributions estimated by a beta-regression INLA model to assess the effect of feeding habit (FeedHab; as generalist, specialist, and filter-feeding) and the interaction of FeedHab with the diel period (DielPer) (i.e., day and night) on the proportion of time spent in surface (≤ 10 m in depth) waters by pelagic elasmobranchs.

Parameter	Mean	Inferior	Superior
Intercept	-1.566	-2.209	-0.925
FeedHab:Generalist	0.296	-0.549	1.138
FeedHab:Specialist	-1.069	-1.892	-0.249
FeedHab:Filter-feeding x DielPer:Night	-0.208	-0.473	0.060
FeedHab:Generalist x DielPer:Night	1.007	0.542	1.470
FeedHab:Specialist x DielPer:Night	0.657	0.281	1.031
Precision parameter for the beta observations	2.082	1.924	2.238
Precision for random factor	1.305	0.633	1.937

Tag deployment was included as a random factor.

up being clustered according to their feeding habits. Such an outcome sustains the suitability of the feeding habit classification herein used and corroborates the hypothesis that trophic traits modulate depth use in epipelagic elasmobranchs.

Marine predators play a significant role in structuring and connecting pelagic habitats through complex trophic interactions, and their continued removal by fisheries produces cascading alterations to marine food webs, inclusively in the open ocean (Pauly et al., 1998; Scheffer et al., 2005; Polovina and Woodworth-Jefcoats, 2013). Increasing the knowledge about the trophic structure of pelagic environments is essential to understand the extent of ecological damage produced by fisheries and derive ecosystem-focused management strategies. This study depicts trophic-related trends in diving behavior and depth use within the pelagic elasmobranch assemblage which may contribute to clarifying some of the processes regulating the vertical compartmentalization and connectivity of the pelagic environment by sympatric predators. Vertical movement patterns in large epipelagic predators have been distinguished between single dives, oscillatory swimming, and diel vertical movements, with the latter being the most common pattern detected over a 24-hour period (Andrzejaczek et al., 2019). The temporal resolution provided by our sampling process (i.e., hours) was therefore adequate to capture diel shifts in vertical habitat use, which should more directly depict interspecific differences in trophic behavior compared to other diving patterns of finer (i.e., < 1 hour) resolution.

The INLA modeling showed that depth use was significantly influenced by species' feeding habits, and this relationship was sustained by complementary multivariate analysis. Since functional groups experienced similar rates of temperature decrease while diving, the observed differences should not derive from variability in the thermal properties of the ocean column at different tagging sites. Filter-feeding whale sharks and sicklefin devil rays made most use of deep waters from the mesopelagic and bathypelagic regarding both maximum diving depths and amount of time spent below the 200-m isobath. Both these species are known to be deep divers and evidence suggesting they feed extensively on demersal and deep-water zooplankton has been reported (Couturier et al., 2013; Rohner et al., 2013; Thorrold et al., 2014; Tyminski et al., 2015), although they are often observed while feeding at or near the sea surface (Motta et al., 2010; Mendonça et al., 2018). In the Atlantic Ocean, a relatively high biomass of meso- and macroplanktonic organisms including copepods, chaetognaths, and decapods have been detected across mesopelagic and bathypelagic waters around equatorial latitudes (Vereschchaka et al., 2017), inclusively in Brazilian waters (Cavalcanti & Larrazábal, 2004). Deep-water incursions by epipelagic filter-feeders may thus relate to a trophic strategy relying on feeding grounds located at the epipelagic zone and at greater depths, e.g., in the DSL (Braun et al., 2022). Such a hypothesis is sustained by the diel pattern of depth use observed in this group. Even though the *T200* model did not incorporate the diel cycle as a predictor, likely because all species exhibited a strong affinity for epipelagic waters during the whole diel cycle, significantly shallower diving depths and a greater proportion of time spent in epipelagic waters by filter-feeders during nocturnal periods match the diel vertical migration pattern exhibited by many organisms from the DSL, which ascent during the night and descent during the day (Robinson et al., 2010). Further, since the lower mesopelagic fauna may not undertake significant diel vertical movements (Sutton et al., 2013; Olivar et al., 2017), a substantial source of deep-water prey would still be available during the night, which could explain the maintenance of nocturnal deep-diving behaviors by filter-feeders. During the daytime, filter-feeders tended to dive deeper and spend more time in the mesopelagic, which could relate to significantly greater diurnal utilization of surface (≤ 10 m in depth) waters, e.g., for thermoregulation purposes.

Specialists also showed a response to the diel cycle regarding the utilization of mesopelagic waters. Interspecific variability in vertical habitat use among specialist species was evidenced in both diel stages, with silky sharks assuming a more epipelagic behavior while blue and hammerhead sharks made differential use of mesopelagic waters across the diel cycle. The two latter species are known to make extensive use of deep waters (Bezerra et al., 2019; Vedor et al., 2021) and to feed on mesopelagic and vertical migrant fish and cephalopods from the DSL in the tropical South Atlantic Ocean and elsewhere (Vaske Júnior et al., 2009a; Besnard et al., 2021), but they seem to explore the depth gradient in different ways. Deep-water fishes, particularly gonostomatids and myctophids, are frequently found around this region, with the Cyclothone genus being the most abundant of such taxa off equatorial Brazil (Olivar et al., 2017). These species could potentially provide a reliable prey source to pelagic piscivorous sharks. In turn, silky sharks are generally associated with the surface mixed layer (Curnick et al., 2020; Madigan et al., 2021) and they exhibit highly selective diving depths well above the mesopelagic zone, which likely reflects predatory behavior on epipelagic prey including fish, cephalopods, and crustaceans (Filmalter et al., 2017). Altogether, the three species categorized as specialists showed to follow distinct strategies of depth use which may be indicative of habitat partitioning. The generalist tiger shark did not change its diving behavior across the diel cycle, but it tended to make broader use of the water column than specialist species by exhibiting more surface-oriented behavior while exploring greater depths from the lower mesopelagic and upper bathypelagic zones. Resource partitioning across spatial and temporal gradients has been identified among sympatric coastal sharks (Papastamatiou et al., 2006; Lear et al., 2021) and within pelagic elasmobranch assemblages, where it should be most associated with the vertical dimension of the oceanic realm as different species tend to forage at different depths (Besnard et al., 2021). In fact, the vertical distribution of pelagic oceanic fauna assessed with echosounders revealed a high density of organisms in the epipelagic zone above the 200-m isobath and in the mesopelagic zone, where a primary DSL extending vertically over > 200 m and centered at a mean depth of 525 m precedes a secondary, narrower DSL centered around the 825-m isobath (Proud et al., 2017). Such a prey landscape endows sympatric pelagic elasmobranchs with diverse feeding opportunities across a range of depths, which could favor the emergence of vertical habitat partitioning as a strategy to avoid interspecific competition resulting from a reportedly high degree of trophic overlap among these species (Li et al., 2016; Bornatowski et al., 2017). As for the generalist tiger shark, its diet comprises a multitude of taxa including air-breathing prey (Lowe et al., 1996; Dicken et al., 2017), which could explain the comparatively high association with the top 10 m of the water column. However, it should be acknowledged that the horizontal component of tiger shark movements may have partially amplified this result because this species is also able to explore shallow, coastal habitats.

Regarding the effect of the trophic level, a negative influence on elasmobranch diving depths seems to be present at least to some extent. Although such an inverse relationship was partially shaped by the effect of deep-diving filter-feeders associated with low trophic levels, it still prevailed for the remainder of the species in this study. Hence, generalist and specialist predation upon high-order epipelagic mesopredators should also be contributing to the observed pattern. Tiger sharks are apex predators known to feed on a wide variety of high-level predators including cetaceans, elasmobranchs, and seabirds (Dicken et al., 2017), but since their typical diet also comprises low-order consumers (e.g., chelonians, crustaceans; Lowe et al., 1996) the resulting trophic level turns out to be similar to other more specialist sharks which tend to feed mostly on mesopredator teleosts and cephalopods such as the blue (Kubodera et al., 2007) and scalloped hammerhead (Vaske Júnior et al., 2009b) sharks. If the trophic level ascribed to tiger sharks were to reflect their position as apex predators within the elasmobranch assemblage herein considered, a stronger relationship between trophic level and diving depths might have been found. Albeit a parametric approach was attempted to assess the effect of trophic level on diving depths, it proved ineffective mainly due to a low representativity and coarse resolution of the trophic level variable. Indeed, conspecifics may exhibit a range of different trophic levels which could not be determined because individual trophic levels were not empirically measured, thus all conspecifics were necessarily ascribed with a unique trophic level. Additional variability in a species' trophic level across spatial and temporal scales might be expected since it depends on the prey consumed by individuals, which could change geographically and seasonally. In this study, we opted to use the most cited literature reporting diet-based trophic levels for shark species (i.e., Cortés, 1999), but other authors report different trophic level values and even different feeding habits for the same species. For instance, the silky shark has been ascribed with a generalist feeding habit and a trophic level of 4.4 (Páez-Rosas et al., 2018), although these estimates were built upon stable isotopes rather than stomach content analysis. Further research controlling for potential bias in trophic level assessments and including more pelagic elasmobranch species is required to clarify whether vertical habitat use could be predicted based on species' trophic level. Notwithstanding, a linkage between diving behavior and trophic level may be present in pelagic elasmobranchs and could reflect the vertical distribution of species' preferred prey, assuming that prey trophic levels tend to decrease with increasing depth and that the foraging strategies of these predators rely on a differential consumption of prey, as observed by Páez-Rosas et al. (2018).

Marine habitat partitioning has been reported for several taxonomic groups including batoids (Humphries et al., 2016), teleosts (Fairclough et al., 2008; Young et al., 2010), mammals, and seabirds (Pinela et al., 2010; Receveur et al., 2021), and may as well be a common feature within pelagic elasmobranch assemblages. Different from coastal elasmobranchs, for which a multiplicity of distinct food webs is available in the much-diversified neritic environment, oceanic elasmobranchs tend to rely mostly on latitudinally-restricted phytoplankton-based food webs (Bird et al., 2018). This could translate into a high interspecific competition in the comparatively homogeneous pelagic environment, which would potentially promote habitat partitioning by sympatric predators. Because the variability in preyscape is much higher across the vertical scale of the oceanic realm than along the horizontal plane, a resource partitioning following the depth gradient might be expectable. In accordance, previous research revealed differential mercury uptake among sympatric epipelagic shark species likely indicative of distinct foraging depths (Le Bourg et al., 2019; Besnard et al., 2021), since mercury content in oceanic predators tends to increase with an increased depth distribution of pelagic prey (Blum et al., 2013; Choy et al., 2015; Madigan et al., 2018). Mounting evidence of interspecific variation in vertical habitat use among sympatric pelagic top predators (e.g., Musyl et al., 2011; Madigan et al., 2021) further corroborates the hypothesis of pelagic resource partitioning and highlights the necessity of considering species-specific feeding depths when developing trophodynamic models of the pelagic ecosystem. Several other pelagic elasmobranchs such as the great white, *Carcharodon carcharias*; the shortfin mako, *Isurus oxyrinchus*; the oceanic whitetip, *Carcharhinus longimanus*; and the pelagic thresher, *Alopias pelagicus* sharks display mesopelagic diving patterns suggestive of their reliance on this biome (Howey et al., 2016; Arostegui et al., 2020; Le Croizier et al., 2020a; Santos et al., 2021). Moreover, a comprehensive review on vertical movements by large epipelagic elasmobranchs and teleosts identified diel patterns in depth use in nearly all species examined (Andrzejaczek et al., 2019). Other extrinsic and intrinsic factors not addressed by this study will expectedly modulate elasmobranch depth use in further detail (e.g., ontogenetic stage; Afonso and Hazin, 2015). Since trophic-mediated vertical movements by epipelagic and mesopelagic fauna promote great interconnectivity and interdependence between ocean depth strata (Sutton, 2013), understanding how the depth gradient is compartmentalized by species movements and how such a compartmentalization influences energy flow within the oceanic community is essential to gain a thorough perspective on ecosystem resilience and vulnerabilities. Given the high, three-dimensional complexity of pelagic ecosystems, such a goal may be only achievable through dedicated, global research integrating the multitude of bioecological and environmental processes which regulate trophodynamics in the open ocean.

Pelagic elasmobranchs are unarguably keystone elements in oceanic ecosystems because they regulate the abundance of other marine taxa including high-order predators (Bornatowski et al., 2018) while providing a swift pathway to energy and nutrient transference between vertical pelagic habitats by making use of a wide portion of the ocean column. Therefore, ascertaining depth-explicit trophic linkages in this group could be most useful to build accurate scenarios for the potential effects of overfishing and climate change on marine ecosystems. The fact that the populations of several pelagic shark species from the South Atlantic have low resilience to fishing pressure and have been declining (e.g., the silky shark declined 12.7%$\cdot$y^{-1} according to Santander-Neto et al., 2021; see also Barreto et al., 2016) adds to the growing concerns about a severe, downgrading damage to marine trophic networks potentially produced by ongoing climate change (Nagelkerken et al., 2020), which will expectedly be exacerbated in equatorial latitudes (Chaudhary et al., 2016). Further research on vertical habitat partitioning by pelagic marine predators worldwide is utterly warranted to identify species' essential habitats along the oceanic vertical gradient and to bridge gaps in knowledge about trophic-mediated structuring processes of pelagic food webs where top-down control is exerted at different depths by distinct species. All this information may prove essential toward the effectiveness of pelagic ecosystem-based fisheries management aimed at reducing species susceptibility to fishing gear and at preserving the structure and functionality of marine trophic webs.

DATA AVAILABILITY STATEMENT

The original contributions presented in the study are included in the article/**Supplementary Material**. Further inquiries can be directed to the corresponding author.

AUTHOR CONTRIBUTIONS

BCLM and AA conceived and designed the study. BCLM, AA and NB conducted elasmobranch tagging and data sampling. BM and BCLM performed data analysis with contributions from AA and FHVH. AA wrote the manuscript with contributions from all authors. FH supervised the execution of the project. All authors contributed to the article and approved the submitted version.

FUNDING

Funding provided by the TRIATLAS project through the European Union's Horizon 2020 Research and Innovation Programme (grant No. 817578), the Conselho Nacional de Desenvolvimento Científico e Tecnológico - CNPq (478070/2008-0, 482557/2011-7), the Fundação Grupo Boticário (0760/2007.2), the Save Our Seas Foundation (66/2008), and the Fundação para a Ciência e Tecnologia – FCT (UIDB/04292/2020; UIDP/04292/2020), is deeply acknowledged. Scholarships granted by the FACEPE foundation to NPAB and by CNPq to BCLM (140567/2012-7) are also acknowledged.

ACKNOWLEDGMENTS

We are thankful to all colleagues and interns from Universidade Federal Rural de Pernambuco and to all fishermen who assisted with field work. We acknowledge the Instituto Chico Mendes de Conservação da Biodiversidade (ICMBio), the Brazilian Navy (SECIRM) and the Conselho Nacional de Desenvolvimento Científico e Tecnológico (CNPq) through the Pró-Arquipélago Program (557183/2009-0; 562062/20102-6; 405460/2012-0; 442884/2015-0) for providing precious logistic support.

SUPPLEMENTARY MATERIAL

The Supplementary Material for this article can be found online at: https://www.frontiersin.org/articles/10.3389/fmars.2022.779047/full#supplementary-material

REFERENCES

Afonso, A. S. (2013). *Bioecology and Movement Patterns of Sharks Off Recife, Brazil: Applications in the Mitigation of Shark Attack Hazard* (Portugal: Universidade do Algarve). Available at: http://hdl.handle.net/10400.1/2872.

Afonso, A. S., Garla, R., and Hazin, F. H. V. (2017). Tiger Sharks can Connect Equatorial Habitats and Fisheries Across the Atlantic Ocean Basin. *PLoS One* 12, 1–15. doi: 10.1371/journal.pone.0184763

Afonso, A. S., and Hazin, F. H. V. (2015). Vertical Movement Patterns and Ontogenetic Niche Expansion in the Tiger Shark. *PLoS One* 10, e0116720. doi: 10.1371/journal.pone.0116720

Andrzejaczek, S., Gleiss, A. C., Pattiaratchi, C. B., and Meekan, M. G. (2019). Patterns and Drivers of Vertical Movements of the Large Fishes of the Epipelagic. *Rev. Fish. Biol. Fish.* 29, 335–354. doi: 10.1007/s11160-019-09555-1

Arostegui, M. C., Gaube, P., Berumen, M. L., DiGiulian, A., Jones, B. H., Røstad, A., et al. (2020). Vertical Movements of a Pelagic Thresher Shark (Alopias Pelagicus): Insights Into the Species' Physiological Limitations and Trophic Ecology in the Red Sea. *Endanger. Species Res.* 43, 387–394. doi: 10.3354/ESR01079

Barreto, R., Ferretti, F., Flemming, J. M., Amorim, A., Andrade, H., Worm, B., et al. (2016). Trends in the Exploitation of South Atlantic Shark Populations. *Conserv. Biol.* 30, 792–804. doi: 10.1111/cobi.12663

Bernal, D., Brill, R. W., Dickson, K. A., and Shiels, H. A. (2017). Sharing the Water Column: Physiological Mechanisms Underlying Species-Specific Habitat Use in Tunas. *Rev. Fish. Biol. Fish.* 27, 843–880. doi: 10.1007/s11160-017-9497-7

Besnard, L., Le Croizier, G., Galván-Magaña, F., Point, D., Kraffe, E., Ketchum, J., et al. (2021). Foraging Depth Depicts Resource Partitioning and Contamination Level in a Pelagic Shark Assemblage: Insights From Mercury Stable Isotopes. *Environ. Pollut.* 283, 117066. doi: 10.1016/j.envpol.2021.117066

Bezerra, N. P. A., Macena, B. C. L., Travassos, P., Afonso, P., and Hazin, F. H. V. (2019). Evidence of Site Fidelity and Deep Diving Behaviour of Scalloped Hammerhead Shark (*Sphyrna Lewini*) Around the Saint Peter and Saint Paul Archipelago, in the Equatorial Mid-Atlantic Ridge. *Mar. Freshw. Res* 71, 708–718. doi: 10.1071/MF19029

Bianchi, D., Galbraith, E. D., Carozza, D. A., Mislan, K. A. S., and Stock, C. A. (2013). Intensification of Open-Ocean Oxygen Depletion by Vertically Migrating Animals. *Nat. Geosci.* 6, 545–548. doi: 10.1038/ngeo1837

Bird, C. S., Veríssimo, A., Magozzi, S., Abrantes, K. G., Aguilar, A., Al-Reasi, H., et al. (2018). A Global Perspective on the Trophic Geography of Sharks. *Nat. Ecol. Evol.* 2, 299–305. doi: 10.1038/s41559-017-0432-z

Bivand, R., and Lewin-Koh, N. (2021). Maptools: Tools for Handling Spatial Objects. R package version 1.1-2. Available at: https://CRAN.R-project.org/package=maptools.

Blum, J. D., Popp, B. N., Drazen, J. C., Choy, A. C., and Johnson, M. W. (2013). Methylmercury Production Below the Mixed Layer in the North Pacific Ocean. *Nat. Geosci.* 6, 879–884. doi: 10.1038/ngeo1918

Bornatowski, H., Angelini, R., Coll, M., Barreto, R. R. P., and Amorim, A. F. (2018). Ecological Role and Historical Trends of Large Pelagic Predators in a Subtropical Marine Ecosystem of the South Atlantic. *Rev. Fish. Biol. Fish.* 28, 241–259. doi: 10.1007/s11160-017-9492-z

Bornatowski, H., Barreto, R., Navia, A. F., and de Amorim, A. F. (2017). Topological Redundancy and 'Small-World' Patterns in a Food Web in a Subtropical Ecosystem of Brazil. *Mar Ecol.* 38, e12407. doi: 10.1111/maec.12407

Braun, C. D., Arostegui, M. C., Thorrold, S. R., Papastamatiou, Y. P., Gaube, P., Fontes, J., et al. (2022). The Functional and Ecological Significance of Deep Diving by Large Marine Predators. *Ann. Rev. Mar. Sci.* 14, 7.1–7.31. doi: 10.1146/annurev-marine-032521-103517

Carey, F. G., and Scharold, J. V. (1990). Movements of Blue Sharks (Prionace Glauca) in Depth and Course. *Mar. Biol.* 106, 329–342. doi: 10.1007/BF01344309

Carvalho, F., Ahrens, R., Murie, D., Bigelow, K., Aires-Da-Silva, A., Maunder, M. N., et al. (2015). Using Pop-Up Satellite Archival Tags to Inform Selectivity in Fisheries Stock Assessment Models: A Case Study for the Blue Shark in the South Atlantic Ocean. *ICES J. Mar. Sci.* 72, 1715–1730. doi: 10.1093/icesjms/fsv026

Cavalcanti, E. A. H., and Larrazábal, M. E. L. (2004). Macrozooplâncton Da Zona Econômica Exclusiva do Nordeste do Brasil (Segunda Expedição Oceanográfica – REVIEZEE/NE II) Com Ênfase Em Copepoda (Crustacea). *Ver. Bras. Zool.* 21, 467–475. doi: 10.1590/S0101-81752004000300008

Charrad, M., Ghazzali, N., Boiteau, V., and Niknafs, A. (2014). Nbclust: An R Package for Determining the Relevant Number of Clusters in a Data Set. *J. Stat. Software* 61, 1–36. doi: 10.18637/jss.v061.i06

Chaudhary, C., Saeedi, H., and Costello, M. J. (2016). Bimodality of Latitudinal Gradients in Marine Species Richness. *Trends Ecol. Evol.* 31, 670–676. doi: 10.1016/j.tree.2016.06.001

Choy, C. A., Popp, B. N., Hannides, C. C. S., and Drazen, J. C. (2015). Trophic Structure and Food Resources of Epipelagic and Mesopelagic Fishes in the North Pacific Gyre Ecosystem Inferred From Nitrogen Isotopic Compositions. *Limnol. Oceanogr.* 60, 1156–1171. doi: 10.1002/lno.10085

Compagno, L. V. (1990). Alternative Life-History Styles of Cartilaginous Fishes in Time and Space. *Environ. Biol. Fish.* 28, 33–75. doi: 10.1007/bf00751027

Cortés, E. (1999). Standardized Diet Compositions and Trophic Levels of Sharks. *ICES J. Mar. Sci.* 56, 707–717. doi: 10.1006/jmsc.1999.0489

Costello, M. J., and Breyer, S. (2017). Ocean Depths: The Mesopelagic and Implications for Global Warming. *Curr. Biol.* 27, R36–R38. doi: 10.1016/j.cub.2016.11.042

Couturier, L. I. E., Rohner, C. A., Richardson, A. J., Marshall, A. D., Jaine, F. R. A., Bennett, M. B., et al. (2013). Stable Isotope and Signature Fatty Acid Analyses Suggest Reef Manta Rays Feed on Demersal Zooplankton. *PLoS One* 8(10), e77152. doi: 10.1371/journal.pone.0077152

Curnick, D. J., Andrzejaczek, S., Jacoby, D. M. P., Coffey, D. M., Carlisle, A. B., Chapple, T. K., et al. (2020). Behavior and Ecology of Silky Sharks Around the Chagos Archipelago and Evidence of Indian Ocean Wide Movement. *Front. Mar. Sci.* 7. doi: 10.3389/fmars.2020.596619

Dagorn, L., Menczer, F., Bach, P., and Olson, R. J. (2000). Co-Evolution of Movement Behaviours by Tropical Pelagic Predatory Fishes in Response to Prey Environment: A Simulation Model. *Ecol. Modell.* 134, 325–341. doi: 10.1016/S0304-3800(00)00374-4

Davidson, L. N. K., Krawchuk, M. A., and Dulvy, N. K. (2016). Why Have Global Shark and Ray Landings Declined: Improved Management or Overfishing? *Fish. Fish.* 17, 438–458. doi: 10.1111/faf.12119

Dicken, M. L., Hussey, N. E., Christiansen, H. M., Smale, M. J., Nkabi, N., Cliff, G., et al. (2017). Diet and Trophic Ecology of the Tiger Shark (Galeocerdo Cuvier) From South African Waters. *PLoS One* 12, e0177897. doi: 10.1371/journal.pone.0177897

Dulvy, N. K., and Forrest, R. E. (2010). "Life Histories, Population Dynamics, and Extinction Risks in Chondrichthyans.," in *Sharks and Their Relatives II: Biodiversity, Adaptive Physiology, and Conservation*. Eds. J. Carrier, J. Musick and M. Heithaus (Florida, USA: CRC Press), 655–696.

Dulvy, N. K., Pacoureau, N., Rigby, C. L., Pollom, R. A., Jabado, R. W., Ebert, D. A., et al. (2021). Overfishing Drives Over One-Third of All Sharks and Rays Toward a Global Extinction Crisis. *Curr. Biol.* 31, 1–15. doi: 10.1016/j.cub.2021.08.062

Espinoza, M., Matley, J., Heupel, M. R., Tobin, A. J., Fisk, A. T., and Simpfendorfer, C. A. (2019). Multi-Tissue Stable Isotope Analysis Reveals Resource Partitioning and Trophi(2019). Multi-Tissue Stable Isotope Analysis Reveals Resource Partitioning and Trophic Relationships of Large Reef-Associated Predators. *Mar. Ecol. Prog. Ser.* 615, 159–176. doi: 10.3354/meps12915

Fairclough, D. V., Clarke, K. R., Valesini, F. J., and Potter, I. C. (2008). Habitat Partitioning by Five Congeneric and Abundant Choerodon Species (Labridae) in a Large Subtropical Marine Embayment. *Estuar. Coast. Shelf Sci.* 77, 446–456. doi: 10.1016/j.ecss.2007.10.004

Ferrari, S. L. P., and Cribari-Neto, F. (2004). Beta Regression for Modelling Rates and Proportions. *J. Appl. Stat.* 31, 799–815. doi: 10.1080/0266476042000214501

Ferretti, F., Worm, B., Britten, G. L., Britten, G. L., and Lotze, H. K. (2010). Patterns and Ecosystem Consequences of Shark Declines in the Ocean. *K. Ecol. Lett.* 13, 1055–1071. doi: 10.1111/j.1461-0248.2010.01489.x

Filmalter, J. D., Cowley, P. D., Potier, M., Ménard, F., Smale, M. J., Cherel, Y., et al. (2017). Feeding Ecology of Silky Sharks Carcharhinus Falciformis Associated With Floating Objects in the Western Indian Ocean. *J. Fish. Biol.* 90, 1321–1337. doi: 10.1111/jfb.13241

Froese, R., and Pauly, D. (2021) *Fishbase* (World Wide Web electronic publication). Available at: http://www.fishbase.org (Accessed February 6, 2021).

Gupta, A. K., and Nadarajah, S. (2004). *Handbook of Beta Distribution and Its Applications. 1st Edn* (Boca Raton: CRC Press).

Hammerschlag, N. (2019). Quantifying Shark Predation Effects on Prey: Dietary Data Limitations and Study Approaches. *Endanger. Species Res.* 38, 147–151. doi: 10.3354/ESR00950

Hays, G. C. (2003). A Review of the Adaptive Significance and Ecosystem Consequences of Zooplankton Diel Vertical Migrations. *Hydrobiologia* 503, 163–170. doi: 10.1023/B:HYDR.0000008476.23617.b0

Hazen, E. L., and Johnson, D. W. (2010). Meridional Patterns in the Deep Scattering Layers and Top Predator Distribution in the Central Equatorial Pacific. *W. Fish. Oceanogr.* 19, 427–433. doi: 10.1111/j.1365-2419.2010.00561.x

Heithaus, M. R., Wirsing, A. J., and Dill, L. M. (2012). The Ecological Importance of Intact Top-Predator Populations: A Synthesis of 15 Years of Research in a Seagrass Ecosystem. *Mar. Freshw. Res.* 63, 1039–1050. doi: 10.1071/MF12024

Held, L., Schrödle, B., and Rue, H. (2010). "Posterior and Cross-Validatory Predictive Checks: A Comparison on MCMC and INLA," in *Statiscial Modelling and Regression Structures*. Eds. T. Kneib and G. Tutz (Berlin: Physica-Verlag), 111–131.

Horodysky, A. Z., Cooke, S. J., Graves, J. E., and Brill, R. W. (2016). Fisheries Conservation on the High Seas: Linking Conservation Physiology and Fisheries Ecology for the Management of Large Pelagic Fishes. *Conserv. Physiol.* 4, 1–18. doi: 10.1093/conphys/cov059

Howey, L. A., Tolentino, E. R., Papastamatiou, Y. P., Brooks, E. J., Abercrombie, D. L., Watanabe, Y. Y., et al. (2016). Into the Deep: The Functionality of Mesopelagic Excursions by an Oceanic Apex Predator. *Ecol. Evol.* 6, 5290–5304. doi: 10.1002/ece3.2260

Humphries, N. E., Simpson, S. J., Wearmouth, V. J., and Sims, D. W. (2016). Two's Company, Three's a Crowd: Fine-Scale Habitat Partitioning by Depth Among Sympatric Species of Marine Mesopredator. *Mar. Ecol. Prog. Ser.* 561, 173–187. doi: 10.3354/meps11937

Irigoien, X., Klevjer, T. A., Røstad, A., Martinez, U., Boyra, G., Acuña, J. L., et al. (2014). Large Mesopelagic Fishes Biomass and Trophic Efficiency in the Open Ocean. *Nat. Commun.* 5, 3271. doi: 10.1038/ncomms4271

Jackson, J. B. C., Kirby, M. X., Berger, W. H., Bjorndal, K. A., Botsford, L. W., Bourque, B. J., et al. (2001). Historical Overfishing and the Recent Collapse of Coastal Ecosystems. *Science* 293, 629–638. doi: 10.1126/science.1059199

Jorgensen, S. J., Anderson, S., Ferretti, F., Tietz, J. R., Chapple, T., Kanive, P., et al. (2019). Killer Whales Redistribute White Shark Foraging Pressure on Seals. *Sci. Rep.* 9 (6153), 1–9. doi: 10.1038/s41598-019-39356-2

Klevjer, T. A., Irigoien, X., Røstad, A., Fraile-Nuez, E., Benítez-Barrios, V. M., and Kaartvedt, S. (2016). Large Scale Patterns in Vertical Distribution and Behaviour of Mesopelagic Scattering Layers. *Sci. Rep.* 6, 19873. doi: 10.1038/srep19873

Kubodera, T., Watanabe, H., and Ichii, T. (2007). Feeding Habits of the Blue Shark, Prionace Glauca, and Salmon Shark, Lamna Ditropis, in the Transition Region of the Western North Pacific. *Rev. Fish. Biol. Fish.* 17, 111–124. doi: 10.1007/s11160-006-9020-z

Lear, K. O., Whitney, N. M., Morris, J. J., and Gleiss, A. C. (2021). Temporal Niche Partitioning as a Novel Mechanism Promoting Co-Existence of Sympatric Predators in Marine Systems. *Proc. R. Soc B.* 288, 20210816. doi: 10.1098/rspb.2021.0816

Le Bourg, B., Kiszka, J. J., Bustamante, P., Heithaus, M. R., Jaquemet, S., and Humber, F. (2019). Effect of Body Length, Trophic Position and Habitat Use on Mercury Concentrations of Sharks From Contrasted Ecosystems in the Southwestern Indian Ocean. *Environ. Res.* 169, 387–395. doi: 10.1016/j.envres.2018.11.024

Le Croizier, G., Lorrain, A., Sonke, J. E., Hoyos-Padilla, E. M., Galván-Magaña, F., Santana-Morales, O., et al. (2020a). The Twilight Zone as a Major Foraging Habitat and Mercury Source for the Great White Shark. *Environ. Sci. Technol.* 54, 15872–15882. doi: 10.1021/acs.est.0c05621

Le Croizier, G., Lorrain, A., Sonke, J. E., Jaquemet, S., Schaal, G., Renedo, M., et al. (2020b). Mercury Isotopes as Tracers of Ecology and Metabolism in Two Sympatric Shark Species. *Environ. Pollut.* 265, 114931. doi: 10.1016/j.envpol.2020.114931

Li, Y., Zhang, Y., and Dai, X. (2016). Trophic Interactions Among Pelagic Sharks and Large Predatory Teleosts in the Northeast Central Pacific. *J. Exp. Mar. Bio. Ecol.* 483, 97–103. doi: 10.1016/j.jembe.2016.04.013

Lowe, C. G., Wetherbee, B. M., Crow, G. L., and Tester, a. L. (1996). Ontogenetic Dietary Shifts and Feeding Behavior of the Tiger Shark, Galeocerdo Cuvier, in Hawaiian Waters. *L. Environ. Biol. Fishes* 47, 203–211. doi: 10.1007/BF00005044

Macena, B. C. L. (2016). *Habitats Adequados E Aspectos Ecológicos do Tubarão-Baleia (Rhincodon, Typus Smith 1828) No Oceano Atlântico Sudoeste E Equatorial* (Brazil: Universidade Federal de Pernambuco). Available at: https://repositorio.ufpe.br/bitstream/123456789/18654/1/Tese_B_Macena_Full_Tubaleia_oficial_FINAL_BIB.pdf.

Madigan, D. J., Li, M., Yin, R., Baumann, H., Snodgrass, O. E., Dewar, H., et al. (2018). Mercury Stable Isotopes Reveal Influence of Foraging Depth on Mercury Concentrations and Growth in Pacific Bluefin Tuna. *Environ. Sci. Technol.* 52, 6256–6264. doi: 10.1021/acs.est.7b06429

Madigan, D. J., Richardson, A. J., Carlisle, A. B., Weber, S. B., Brown, J., and Hussey, N. E. (2021). Water Column Structure Defines Vertical Habitat of Twelve Pelagic Predators in the South Atlantic. *ICES J. Mar. Sci.* 78, 867–883. doi: 10.1093/icesjms/fsaa222

Mangiafico, S. S. (2015). *An R Companion for the Handbook of Biological Statistics, version 1.3.2.* (New Brunswick (NJ, USA): Rutgers Cooperative Extension). Available at: rcompanion.org/rcompanion/.

Mendonça, S. A., Macena, B. C. L., Afonso, A. S., and Hazin, F. H. V. (2018). Seasonal Aggregation and Diel Activity by the Sicklefin Devil Ray Mobula Tarapacana Off a Small, Equatorial Outcrop of the Mid-Atlantic Ridge. *J. Fish. Biol.* 93, 1121–1129. doi: 10.1111/jfb.13829

Motta, P. J., Maslanka, M., Hueter, R. E., Davis, R. L., de la Parra, R., Mulvany, S. L., et al. (2010). Feeding Anatomy, Filter-Feeding Rate, and Diet of Whale Sharks Rhincodon Typus During Surface Ram Filter Feeding Off the Yucatan Peninsula, Mexico. *Zoology* 113, 199–212. doi: 10.1016/j.zool.2009.12.001

Mulas, A., Bellodi, A., Cannas, R., Carbonara, P., Cau, A., Marongiu, M. F., et al. (2019). Resource Partitioning Among Sympatric Elasmobranchs in the Central-Western Mediterranean Continental Shelf. *Mar. Biol.* 166, 153. doi: 10.1007/s00227-019-3607-0

Munroe, S. R. M., Simpfendorfer, C. A., and Heupel, M. R. (2014). Defining Shark Ecological Specialisation: Concepts, Context, and Examples. *Rev. Fish. Biol. Fish.* 24, 317–331. doi: 10.1007/s11160-013-9333-7

Musyl, M. K., Brill, R. W., Curran, D. S., Fragoso, N. M., McNaughton, L. M., Nielsen, A., et al. (2011). Postrelease Survival, Vertical and Horizontal Movements, and Thermal Habitats of Five Species of Pelagic Sharks in the Central Pacific Ocean. *Fish. Bull.* 109, 341–368. https://spo.nmfs.noaa.gov/sites/default/files/pdf-content/2011/1094/1094musyl.pdf

Nagelkerken, I., Goldenberg, S. U., Ferreira, C. M., Ullah, H., and Connell, S. D. (2020). Trophic Pyramids Reorganize When Food Webs Architecture Fails to Adjust to Ocean Change. *Science* 369, 829–832. doi: 10.1126/science.aax0621

Ogle, D. H., Doll, J. C., Wheeler, P., and Dinno, A. (2021) *R Package*. Available at: https://github.com/droglenc/FSA.

Olivar, M. P., Hulley, P. A., Castellón, A., Emelianov, M., López, C., Tuset, V. M., et al. (2017). Mesopelagic Fishes Across the Tropical and Equatorial Atlantic: Biogeographical and Vertical Patterns. *Prog. Oceanography* 151, 116–137. doi: 10.1016/j.pocean.2016.12.001

Ortiz, M., and Arocha, F. (2004). Alternative Error Distribution Models for Standardization of Catch Rates of Non-Target Species From a Pelagic Longline Fishery: Billfish Species in the Venezuelan Tuna Longline Fishery. *Fish. Res.* 70, 275–297. doi: 10.1016/j.fishres.2004.08.028

Pacoureau, N., Rigby, C. L., Kyne, P. M., Sherley, R. B., Winker, H., Carlson, J. K., et al. (2021). Half a Century of Global Decline in Oceanic Sharks and Rays. *Nature* 589, 567–571. doi: 10.1038/s41586-020-03173-9

Páez-Rosas, D., Insuasti-Zarate, P., Riofrío-Lazo, M., and Galván-Magaña, F. (2018). Feeding Behavior and Trophic Interaction of Three Shark Species in the Galapagos Marine Reserve. *PeerJ* 6, e4818. doi: 10.7717/peerj.4818

Papastamatiou, Y. P., Wetherbee, B. M., Lowe, C. G., and Crow, G. L. (2006). Distribution and Diet of Four Species of Carcharhinid Shark in the Hawaiian Islands: Evidence for Resource Partitioning and Competitive Exclusion. *Mar. Ecol. Prog. Ser.* 320, 239–251. doi: 10.3354/meps320239

Paradinas, I., Pennino, M. G., López-Quílez, A., Marín, M., Bellido, J. M., and Conesa, D. (2018). Modelling Spatially Sampled Proportion Processes. *REVSTAT Stat. J.* 16, 71–86. doi: 10.57805/revstat.v16i1.233

Pauly, D., Christensen, V., Dalsgaard, J., Froese, R., and Torres, (1998). Fishing Down Marine Food Webs. *Science* 279, 860–863. doi: 10.1126/science.279.5352.860

Pinela, A. M., Borrell, A., Cardona, L., and Aguilar, A. (2010). Stable Isotope Analysis Reveals Habitat Partitioning Among Marine Mammals Off the NW African Coast and Unique Trophic Niches for Two Globally Threatened Species. *Mar. Ecol. Prog. Ser.* 416, 295–306. doi: 10.3354/meps08790

Polovina, J. J., and Woodworth-Jefcoats, P. A. (2013). Fishery-Induced Changes in the Subtropical Pacific Pelagic Ecosystem Size Structure: Observations and Theory. *PLoS One* 8, e62341. doi: 10.1371/journal.pone.0062341

Proud, R., Cox, M. J., and Brierley, A. S. (2017). Biogeography of the Global Ocean's Mesopelagic Zone. *Curr. Biol.* 27, 113–119. doi: 10.1016/j.cub.2016.11.003

Queiroz, N., Humphries, N. E., Couto, A., Vedor, M., da Costa, I., Sequeira, A. M. M., et al. (2019). Global Spatial Risk Assessment of Sharks Under the Footprint of Fisheries. *Nature* 572, 461–466. doi: 10.1038/s41586-019-1444-4

R Core Team (2021). "*R: A Language and Environment for Statistical Computing*, (Vienna, Austria: R Foundation for Statistical Computing).

Receveur, A., Allain, V., Menard, F., Dhaussy, A. L., Laran, S., Ravache, A., et al. (2021). Modelling Marine Predator Habitat Using the Abundance of its Pelagic Prey in the Tropical South-Western Pacific. *Ecosystems* 1–23. doi: 10.1007/s10021-021-00685-x

Robinson, C., Steinberg, D. K., Anderson, T. R., Arístegui, J., Carlson, C. A., Frost, J. R., et al. (2010). Mesopelagic Zone Ecology and Biogeochemistry - A Synthesis. *Deep. Res. Part II Top. Stud. Oceanogr.* 57, 1504–1518. doi: 10.1016/j.dsr2.2010.02.018

Robison, B. H. (2009). Conservation of Deep Pelagic Biodiversity. *Conserv. Biol.* 23, 847–858. doi: 10.1111/j.1523-1739.2009.01219.x

Rohner, C. A., Couturier, L. I. E., Richardson, A. J., Pierce, S. J., Prebble, C. E. M., Gibbons, M. J., et al. (2013). Diet of Whale Sharks Rhincodon Typus Inferred From Stomach Content and Signature Fatty Acid Analyses. *Mar. Ecol. Prog. Ser.* 493, 219–235. doi: 10.3354/meps10500

Sabando, M. A., Rieucau, G., Bradley, D., Caselle, J. E., and Papastamatiou, Y. P. (2020). Habitat-Specific Inter and Intraspecific Behavioral Interactions Among Reef Sharks. *Oecologia* 193, 371–376. doi: 10.1007/s00442-020-04676-y

Santos, C. C., Domingo, A., Carlson, J., Natanson, L. J., Travassos, P., Macías, D., et al. (2021). Movements, Habitat Use, and Diving Behavior of Shortfin Mako in the Atlantic Ocean. *Front. Mar. Sci.* 8. doi: 10.3389/fmars.2021.686343

Santander-Neto, J., Barreto, R., Santana, F. M., and Lessa, R. P.T. (2021). Age, Growth and Demography of the Silky Shark Carcharhinus Falciformis From the Southwestern Atlantic. *Endang. Species Res.* 45, 237–49. doi: 10.3354/esr01131

Scheffer, M., Carpenter, S., and de Young, B. (2005). Cascading Effects of Overfishing Marine Systems. *Trends Ecol. Evol.* 20, 579–581. doi: 10.1016/j.tree.2005.08.018

Sequeira, A. M.M., Heupel, M. R., Lea, M. A., Eguíluz, V. M., Duarte, C. M., Meekan, M. G., et al. (2019). The Importance of Sample Size in Marine Megafauna Studies. *Ecol. Appl.* 29, e01947. doi: 10.1002/eap.1947

Smith, A. D., Houde, A. L. S., Neff, B., and Peres-Neto, P. R. (2017). Effects of Competition on Fitness-Related Traits. *Oecologia* 183, 701–713. doi: 10.1007/s00442-017-3816-5

Sutton, T. T. (2013). Vertical Ecology of the Pelagic Ocean: Classical Patterns and New Perspectives. *J. Fish. Biol.* 83, 1508–1527. doi: 10.1111/jfb.12263

Sutton, T. T., Wiebe, P. H., Madin, L., and Bucklin, A. (2010).). Diversity and Community Structure of Pelagic Fishes to 5000m Depth in the Sargasso Sea. *Deep. Res. Part II Top. Stud. Oceanogr.* 57, 2220–2233. doi: 10.1016/j.dsr2.2010.09.024

Thorrold, S. R., Afonso, P., Fontes, J., Braun, C. D., Santos, R. S., Skomal, G. B., et al. (2014). Extreme Diving Behaviour in Devil Rays Links Surface Waters and the Deep Ocean. *Nat. Commun.* 5 (4274), 1–7. doi: 10.1038/ncomms5274

Tillett, B. J., Meekan, M. G., and Field, I. C. (2014). Dietary Overlap and Partitioning Among Three Sympatric Carcharhinid Sharks. *Endanger. Species Res.* 25, 283–293. doi: 10.3354/esr00615

Trindade-Santos, I., Moyes, F., and Magurran, A. E. (2020). Global Change in the Functional Diversity of Marine Fisheries Exploitation Over the Past 65 Years. *Proc. R. Soc B. Biol. Sci.* 287, 20200889. doi: 10.1098/rspb.2020.0889

Tyminski, J. P., de la Parra-Venegas, R., Cano, J. G., and Hueter, R. E. (2015). Vertical Movements and Patterns in Diving Behavior of Whale Sharks as Revealed by Pop-Up Satellite Tags in the Eastern Gulf of Mexico. *PLoS One* 10, e0142156. doi: 10.1371/journal.pone.0142156

Vaske Júnior, T., Lessa, R. P., and Gadig, O. B. F. (2009a). Feeding Habits of the Blue Shark (*Prionace Glauca*) Off the Coast of Brazil. *Biota Neotrop.* 9, 55–60. doi: 10.1590/S1676-06032009000300004

Vaske Júnior, T., Vooren, C. M., and Lessa, R. P. (2009b). Feeding Strategy of the Night Shark (*Carcharhinus Signatus*) and Scalloped Hammerhead Shark (*Sphyrna Lewini*) Near Seamounts Off Northeastern Brazil. *Braz. J. Oceanogr.* 57, 97–104. doi: 10.1590/s1679-87592009000200002

Vedor, M., Mucientes, G., Hernández-Chan, S., Rosa, R., Humphries, N., Sims, D. W., et al. (2021). Oceanic Diel Vertical Movement Patterns of Blue Sharks Vary With Water Temperature and Productivity to Change Vulnerability to Fishing. *Front. Mar. Sci.* 8. doi: 10.3389/fmars.2021.688076

Vereshchaka, A., Abyzova, G., Lutina, A., and Musaeva, E. (2017). The Deep-Sea Zooplankton of the North, Central, and South Atlantic: Biomass, Abundance, Diversity. *Deep-Sea Res. II* 137, 89–101. doi: 10.1016/j.dsr2.2016.06.017

Young, J. W., Landsdell, M. J., Campbell, R. A., Cooper, S. P., Fuanes, F., and Guest, M. A. (2010). Feeding Ecology and Niche Segregation in Oceanic Top Predators Off Eastern Australia. *Mar. Biol.* 1157, 2347–2368. doi: 10.1007/s00227-010-1500-y

Conflict of Interest: The authors declare that the research was conducted in the absence of any commercial or financial relationships that could be construed as a potential conflict of interest.

frontiers | Frontiers in Marine Science

ORIGINAL RESEARCH
published: 30 June 2022
doi: 10.3389/fmars.2022.793248

Movement, Behavior, and Habitat Use of Whale Sharks (*Rhincodon typus*) in the Tropical Eastern Pacific Ocean

Hector M. Guzman[1]*, Caroline M. Collatos[2,3] and Catalina G. Gomez[4,5]

[1] Smithsonian Tropical Research Institute, Panama, Panama, [2] School for the Environment, University of Massachusetts, Boston, MA, United States, [3] Anderson Cabot Center for Ocean Life, New England Aquarium, Boston, MA, United States, [4] Centro de Ciencias del Mar y Limnología, Universidad de Panama, Panama, Panama, [5] Coiba Scientific Station (COIBA AIP), City of Knowledge, Panama, Panama

OPEN ACCESS

Edited by:
Mark Meekan,
Australian Institute of Marine Science (AIMS), Australia

Reviewed by:
Aaron Carlisle,
University of Delaware, United States
Abdul Hamid A. Toha,
University of Papua, Indonesia
Hawis Madduppa,
Bogor Agricultural University, Indonesia
David Morgan,
Murdoch University, Australia
Rob Harcourt, Macquarie University, Australia

***Correspondence:**
Hector M. Guzman
guzmanh@si.edu

Specialty section:
This article was submitted to Marine Megafauna, a section of the journal Frontiers in Marine Science

Received: 11 October 2021
Accepted: 27 May 2022
Published: 30 June 2022

Citation:
Guzman HM, Collatos CM and Gomez CG (2022) Movement, Behavior, and Habitat Use of Whale Sharks (Rhincodon typus) in the Tropical Eastern Pacific Ocean. Front. Mar. Sci. 9:793248. doi: 10.3389/fmars.2022.793248

Whale sharks (*Rhincodon typus*) are found circumglobally in tropical, subtropical, and warm temperate waters, and their known seasonal aggregations and migratory movements are influenced by factors such as ocean currents, thermobiological systems, and patterns of productivity. Several locations in the eastern tropical Pacific Ocean are known habitats for *R. typus*; Although it has long been known that whale sharks aggregate along the Panama coast, little is known in relation to their movement patterns, behavior, and habitat use. In this study, we investigated the movements and behaviors of *R. typus* tagged in Panama in relation to oceanographic variables and examined the overlap of foraging habitat and migratory routes with marine protected areas (MPAs), industrial fishing areas, and marine traffic. Satellite tracks from 30 *R. typus* tagged in the coastal waters of Panama were examined, including nine tags suspicious of earlier detachment. A hidden Markov model was then used to identify different behavioral states (foraging and migrating) and their relationships with environmental variables (sea surface temperature, primary productivity, chlorophyll-*a* concentrations, and eddy location/ speed) Tracks were also superimposed on maps of MPAs, industrial fishing areas, and regional marine vessel traffic to identify the degree of overlap. *Rhincodon typus* foraged mainly within the Panamanian exclusive economic zone but also moved north and south along the coast and out to the open ocean. Significant differences in environmental conditions were found between sites in which foraging and migrating behaviors were recorded. Higher productivity and chlorophyl concentration were associated with foraging behavior, while higher eddy speeds were observed when sharks migrated. *Rhincodon typus* used MPAs; however, there was a high degree of overlap between their habitat and areas of industrial fishing and marine vessel traffic. Our results highlight the use of the coastal waters of Panama, oceanic seamounts, and ridges, MPAs and industrial fishing areas by *R. typus* for foraging and migration. Additionally, our findings highlight the importance of satellite tracking studies for understanding the behavior and habitat use of highly mobile migratory species, such as *R. typus*.

Keywords: ***Rhincodon typus*, satellite tracks, habitat use, marine protected areas, migration, fisheries, Panama**

1 INTRODUCTION

Whale sharks (*Rhincodon typus)* are the largest fish species in the world (Colman, 1997; Rowat and Brooks, 2012), measuring up to 20 m in length (Chen et al., 1997). These filter feeders are found circumglobally in warm and temperate waters (Colman, 1997; Rowat and Brooks, 2012; Meekan et al., 2017; Norman et al., 2017; Guzman et al., 2021) and follow oceanic currents, undergoing vast transoceanic migrations of more than 20,000 km (Guzman et al., 2018). *Rhincodon typus* inhabits and seasonally aggregates in both coastal and oceanic areas; large seasonal aggregations have been documented in Madagascar, Mozambique, the Galapagos, the Seychelles, the Maldives, Ningaloo Reef in Australia, Isla Contoy off Mexico, and in the northern waters of the Gulf of Mexico (de la Parra Venegas et al., 2011; Rowat and Brooks, 2012; Meekan et al., 2017; Norman et al., 2017; Diamant et al., 2018). These seasonal aggregations and migration routes are largely driven by oceanic currents, plankton blooms, and fish and coral spawning events (Heyman et al., 2001; Riley et al., 2010).

Studies about *R. typus* aggregations and habitat use have been documented and studied around the globe and have been related to feeding areas (Ketchum et al., 2012; Acuña-Marrero et al., 2014), reproduction (Rowat and Brooks, 2012; Acuña-Marrero et al., 2014), and movements (Acuña-Marrero et al., 2014). However, the use of the coastal Pacific waters of Panama by this species is not well understood. *Rhincodon typus* was first documented in Panamanian waters as early as 1932 (Gudger, 1938; Hueter et al., 2013). Located off the Pacific coast off Panama, the Coiba National Park (CNP) is a habitat for *R. typus* during the months of December to March (Hearn et al., 2016; Guzman et al., 2018). During this time, *R. typus* appears to exhibit seasonal presence and is frequently observed in an area called Wahoo Rock in the CNP (Guzman et al., 2018). In 2011, Guzman et al. (2018) tagged three female *R. typus* with towed satellite transmitters in this area. One of these tagged sharks was detected in Panamanian coastal waters for a total of 116 d, spent 226 d between Panama and Clipperton Island, and completed a transpacific journey of over 20,000 km to the Marianas Trench in 841 d (Guzman et al., 2018). The Panamanian population of whale sharks has shown global genetic connectivity with the Arabian Gulf, Western Indian Ocean and Mexico (Guzman et al., 2021). While these results suggest that Panamanian waters are an important habitat for *R. typus*, there is still extremely limited research on their presence and movement in this area.

R. typus is highly threatened by illegal fishing, boating activity, and bycatch within Panamanian waters and adjacent coastal areas (Guzman H, personal observation). As elasmobranchs are slow-growing species with late maturity and relatively low fecundity (Hoenig and Gruber, 1990; Joung et al., 1996), *R. typus* is highly vulnerable to population decline and overfishing, and currently listed as 'globally endangered' on the IUCN Red List (Pierce and Norman, 2016). Thus, research focused on the population demographics, occurrence, movements, habitats, and overlap of *R. typus* with anthropogenic factors, such vessel traffic, and industrial fishing grounds, can further both local and global knowledge of this endangered species and aid conservation efforts.

To advance our understanding of the presence, habitat use, migratory movements, and potential overlap with marine protected areas (MPAs), industrial fishing areas, and marine traffic, this project deployed satellite tags on *R. typus* along the Pacific coast of Panama. The specific objectives of the study were to (1) present comparative analyses for the interpretation of presumably detached or fre-floating tags (*sensu* Hearn et al., 2013) trajectories synchronized with real-time surface currents and winds; (2) illustrate the use of the CNP and surrounding areas by *R. typus*; (3) investigate potential relationships between sea surface temperature (STT), chlorophyll-*a* concentrations, daily primary productivity, eddies, bathymetry, and *R. typus* movements; and (4) examine *R. typus* habit use and migration routes in relation to MPAs, industrial fishing areas, and regional marine traffic.

2 MATERIALS AND METHODS

2.1 Tagging Procedures

R. typus individuals were tagged between 2007 and 2012 at several locations in Pacific Panama with near real-time tether/towed satellite transmitters (model SPOT 253C; Wildlife Computers, Redmond, WA, USA). The tag model used specifies a battery life of 280 d, assuming 250 Argos transmissions per day, which occur only when the fish is swimming near the surface and the transmitter is exposed. To maximize battery life, transmitters were programmed to limit transmissions to a time block from 01:00 to 22:00 h every 2 d and to slow the repetition rate after 10 successive dry transmissions. The float tag was attached to the fish ca. 10 cm below the first dorsal fin by a 1.5 m tether made of stainless-steel cable and a 3.5 cm stainless steel dart using a 3.0-m Manny Puig^{TM} pole spear. Visibility and sea conditions precluded obtaining the sex and size estimates, important demography variables "to ascertain the conservation status and ensure persistence of the specie" (*sensu* Sequeira et al., 2016). The Animal Care and Use Committee of the Smithsonian Tropical Research Institute approved this sampling procedure.

2.2 Behavioral Models

ARGOS transmissions were filtered by deleting all transmissions in land (dry), quality "Z" and movements representing speeds over 100 km/day (6.4 km faster than the maximum speed reported by Eckert and Stewart, 2001). Two comparable analyses were performed: one using complete filtered transmission data (CD) of the animals and one with partially trimmed or removed trajectories (see l **Figures S1**) for suspicious of earlier detachment or freely floating tags (sensu Hearn et al., 2013). A Bayesian state-space random walk (SSRW) model for animal movement was used to optimize the obtained *R. typus* tracks based on ARGOS satellite tracking data error, which Vincent et al. (2002) calculated to be around 226 m for location class (LC) LC3, 372 m for LC2, and 757 m for LC1 and LC A. This model was used because it is useful when observations occur irregularly in time and when working with ARGOS transmission estimation errors (Jonsen et al., 2005). The model was run using the "fit_ssm" function in the "*bsam*" package (Jonsen, 2016) of R software (version 3.4.4; R Core

Team, 2018). The model was set to have four time-steps per day (tstep = 0.25), 5,000 samples during the adaptation and update phases, a thinning of 10 to minimize within-chain sample autocorrelation, and a span of 0.2 for the degree of smoothing.

Bayesian SSRW-corrected *R. typus* tracks were modeled with a hidden Markov model (HMM) to identify two different behavioral states—foraging and migratory behavior. The environmental variables described in **Table 1** were used as the model covariates. The HMM model was run using the "fitHMM" function in the "*moveHMM*" R package (Michelot et al., 2016). The initial values used to differentiate between foraging and migrating behavioral states were set to 5 ± 2 m and 30 ± 10 m for the step mean, respectively, and pi was set to 0 for the turning angle.

Foraging areas were identified and mapped by creating a kernel density plot (in ArcGIS v10.6) with all the modeled locations identified by the HMM model for that behavioral state. Low-use, medium-use, and high-use areas were determined based on the first, second, and third quartiles, respectively.

2.3 Environmental Variables, Fishing Effort, Vessel Traffic, and Protected Areas

2.3.1 Sea Surface Temperature (SST), Chlorophyll-a Concentration, and Daily Primary Productivity

Data were obtained from NOAA's Environmental Research Division ERDDAP server (NOAA, 2019). Chlorophyll-a concentrations (NOAA NMFS, 2019) were measured in mg m-3 with a monthly composite temporal resolution of 4.64 km (the most complete dataset in NOAA for the temporal and spatial scale of this study). The SST layer (NOAA NMFS, 2019) had a spatial resolution of 0.1° with a three-day composite analysis in °C. Primary productivity (NOAA NMFS, 2019) was measured as the net primary productivity of C per day (mg C m-2 d-1) with a spatial resolution of 0.0417° (**Table 1**). Data were paired (in time and space) to each modeled R. typus location using the "xtracto" function in the "*rerddapXtracto*" R software package (Xtractomatic, 2018).

2.3.2 Eddies, Currents, and Winds

R. typus locations were superimposed on previously identified eddies that overlapped the animal trajectories in time and space. The location, amplitude, speed, and type (cyclonic or anticyclonic) of eddies that occurred during the study period were obtained from the Mesoscale Eddy Trajectories Atlas [SSALTO/DUACS, 2019]. All *R. typus* locations that occurred within an eddy were identified by creating a circle around each eddy center (diameter equal to eddy amplitude) and extracting the eddy data for each *R. typus* location using the "Spatial Analyst tool" in ArcGIS (v10.6).

Daily marine currents (surface and 15 m depth at ¼ ° resolution) were obtained from Copernicus database named: MULTIOBS_GLO_PHY_NRT_015_003 (Global Total Surface and 15m Current (COPERNICUS-GLOBCURRENT) from Altimetric Geostrophic Current and Modeled Ekman Current Processing) available at: https://resources.marine.copernicus.eu/product-detail/MULTIOBS_GLO_PHY_NRT_015_003/DOCUMENTATION. We used 3-day wind diffusivity currents (WDC) obtained from Metop-A ASCAT, with a 0.25° resolution (**Table 1**) available at: https://coastwatch.pfeg.noaa.gov/erddap/griddap/erdQAekm3day.html. WDC is measured at 0 m elevation while just "wind" is measured at 10 m elevation. Current speed and WDC were calculated from V and U current vectors and overlapped spatially and temporary with whale shark transmissions (**Table 1**). Current speed, WDC, and whale shark traveling speed were correlated using Pearson method. Spatial data was overlapped using the Spatial Join function in ArcGIS Pro software (set to a search radio of 30 km) and temporal data and correlations were performed in R software.

2.3.3 Bathymetry, and Seamount Use

Rhincodon typus locations were overlaid on the Nibbon Foundation GEBCO gridded bathymetric dataset (GEBCO Bathymetric Compilation Group, 2020). Differences in water depth between behavioral states (migrating or foraging) were tested using the

TABLE 1 | Environmental variables obtained for each *Rhincodon typus* location.

Variable	Dataset name	Detailed name	Measured variable	Temporal resolution	Spatial resolution
Chlorophyll-*a* Concentration (NOAA NMFS, 2019)	erdMH1chlamday	Chlorophyll-a, Aqua MODIS, NPP, L3SMI, Global, Science Quality	Mean chlorophyll-*a* concentration (mg m^{-3})	Monthly composite	4.64 km
Sea Surface temperatura (NOAA NMFS, 2019)	erdAGssta3day	Sea Surface Temperature, POES AVHRR, GAC, Global, Day and Night		Three-day composite	0.1°
Primary Productivity (NOAA NMFS, 2019)	erdMH1pp1day	Primary Productivity, Aqua MODIS, NPP, Global, 1-Day, EXPERIMENTAL	Net primary productivity (mg C m^{-2} d^{-1})	One-day composite	0.0417°
Eddies (SSALTO/DUACS, 2019) The Mesoscale Eddy Trajectory Atlas	Global mesoscale eddy trajectory product	Global mesoscale eddy trajectory product	Amplitude (cm) Cyclonic type (+,-) Speed (cm/s)	Daily	0.01 m
Daily Marine Currents	MULTIOBS_GLO_PHY_NRT_015_003	Global Total Surface and 15m Current - COPERNICUS-GLOBCURRENT	U and V current vectors	Daily	0.25°
Wind Diffusivity Current	erdQAekm3day	Wind Diffusivity Current, Metop-A ASCAT, 0.25°, Global, Near Real Time, 2009-present (3 Day)	U and V wind current vectors (m/s)	3-day	0.25°
Bathymetry (GEBCO Bathymetric Compilation Group, 2020)	GEBCO_2020 grid, 15 arc-second intervals	GEBCO_2020 Grid, a continuous terrain model of the global oceans and land	Ocean depth (m)	Not temporal	15 arc-second intervals
Fishing Effort (Global Fishing Watch, 2020)	Global Fishing Watch	Fishing effort by flag state and gear type at 100th degree resolution	Fishing hours	Daily	0.01°

Wilcoxon test. We used a Resource Selection Model (Function "RSPF" in the Resource Selection R package) (Subhash et al. 2019) to evaluate the use of seamounts or underwater ridges during *R. typus* migration. The proportion of the oceanic areas (50 m away from shore) with depths above -1,000 m were quantified by extracting the depth of 50,000 random points from the GEBCO bathymetric dataset and modeled as "available resources", the "used resources" were given by the *R. typus* modeled locations above the -1,000m threshold.

2.3.4 Fishing Effort, Vessel Traffic Routes, and Marine Protected Areas Use

Fishing effort data were obtained from the Global Fishing Watch (GFW) dataset (Kroodsma et al., 2018). This dataset describes the number of fishing hours per square kilometer (h km^{-2}) based on the detection of > 70,000 unique AIS devices on fishing vessels from 2012 to 2016 (Kroodsma et al., 2018), and an updated version including data from 2017 and 2018. *Rhincodon typus* locations were overlaid onto the MPAs and industrial fishing areas. There was no temporal overlap between the fishing effort data (Kroodsma et al., 2018) and *R. typus* modeled locations; therefore, the quarterly mean of fishing effort was used as a reference. The fishing effort trimestral mean inside the study area was divided into three categories, low, medium, and high, corresponding to the first, second, and third quartiles of the data, respectively.

The location data also overlapped with regional marine vessel traffic. Long-range identification and tracking (LRIT) data were obtained from Pole Star Panama for all months in 2013 for the entire region. Pole Star is a leader company in maritime intelligence that monitors with satellite transmitters more than 34,000 ships worldwide. The impact of vessel traffic was estimated by creating a kernel density analysis weighted by vessel speed (speed reported by the Pole Star data) and identifying low-, medium-, and high-impact areas (based on kernel´s data quartiles of the combined effect of vessel density and traveling speed). *Rhincodon typus* locations that occurred inside a MPA were identified using the World Database on Protected Areas [administered by the United Nations Environment Program (UNEP) and the International Union for the Conservation of Nature (IUCN), managed by the UNEP World Conservation Monitoring Centre (UNEP-WCMC)]. All spatial analyses were performed using ArcGIS (v10.6).

2.4 Analyses of Potentially Detached or Freely Floating Tags

Hearn et al. (2018) determined detachment point of towed SPOT-5 satellite tags by comparing the trajectories of four tagged whale sharks (one individual with a SPLASH) that transmitted between 31 and 167 days and two deliberately floating tags. They concluded that detachment points can be usually identified by interpreting daily transmission times, class quality along with depth and temperature of the transmitted data. In addition, this interpretation can be facilitated with available information on general ocean circulation patterns (Hearn et al., 2018).

We used daily sequences of transmission times (*sensu* Hearn et al., 2013) to preliminary test those tags were attached to the sharks and not freely floating along the currents and winds (**Figure S1**). Shark traveling speed was calculated using filtered but unmodeled locations. Shark tracks (consecutive list of locations) were converted to ArcGIS line shapefiles using the Data Management tool "XY to Line", which created a line along chronological locations. Each track line was then split at each location point by using the ArcGIS tool "Split Line at Point", resulting in segmented tracks with individual lines between locations. The length (km) of each segment of the track was then calculated by using the "Calculate Geometry" tool available in the Attribute Table menu in ArcGIS. The difference in time (hr) between consecutive locations was calculated and used to estimate traveling speed (TS) between locations as: TS= Segment length (km)/time difference between consecutive points (hr).

Daily marine currents (surface and 15 m depth at ¼ ° resolution) were obtained from Copernicus database named: MULTIOBS_GLO_PHY_NRT_015_003 (Global Total Surface and 15m Current (COPERNICUS-GLOBCURRENT) from Altimetric Geostrophic Current and Modeled Ekman Current Processing. Current Speed (CS) was calculated from V and U current vectors using the Pythagorean theorem in where: CS=square root(V^2+U^2). Current speed, at ¼° resolution was overlapped spatially with whale shark locations by using the "Spatial Join" function in ArcGIS Pro software (set to a search radio of 30 km for each location). A temporal overlap was done by merging the two datasets (current speed and shark locations) by date in R software. Current speed (mean speed within 30 km around each location during the transmission day) and whale shark traveling speed (for the segment between two consecutive locations) were correlated using Pearson method **Figures S1, 2**). This correlation was analyzed independently when whale shark transmissions occurred inside an eddy as explained earlier in the manuscript.

3 RESULTS

3.1 *Rhincodon typus* Movements and Behavior

Solitary individuals were tagged sporadically between September 2007 and March 2012. A total of 32 *R. typus* were tagged along the Pacific coast of Panama; 25 were tagged in the Gulf of Chiriquí and 7 were tagged in the Las Perlas Archipelago, Gulf of Panama (**Table 2**). Two tags failed to transmit. A total of nine sharks showed dubious transmission times or detached shortly after tagging (**Figure S1**): five with long migrations and high frequency of transmission rates in morning hours (54741, 54745, 54764, 54878, 107719) were isolated from the analyses, and four tags with relative short movements were partially trimmed when transmission rates changed (107708, 54747, 54749, 54870). Those nine full trajectories, however, were modeled and analyzed for detachment by correlating sharks traveling speed with real-time marine current speed and wind current (see below). Accordingly, to compare analyses, results are presented for trimmed/removed data followed by full untrimmed data (30 tags) in parenthesis. Tagged sharks transmitted 51 d (498) with up to 307 (1,053) transmissions (**Table 2**). *Rhincodon typus*

TABLE 2 | *Rhincodon typus* tagged (30) in the Gulf of Panama (GP) and the Gulf of Chiriquí (GC), Satellite transmitter identification number (PTT).

PTT	Tagging area	Number of transmissions	Tagging date	Transmission days	% Days inside MPAs
54740	GC	147	March 18, 2011	24	87.5
54741*	GC	1,053	March 18, 2011	191	56.0
54744	GC	63	March 17, 2011	459	3.5
54745*	GC	938	February 7, 2011	173	27.7
54747***	GC	832 (931)	February 4, 2011	147 (169)	20.4 (85.2)
54748	GC	198	February 28, 2011	183	100
54749***	GC	34 (470)	March 20, 2011	18 (281)	38.9 (10.0)
54758**	GC	5	March 24, 2011	3	100
54763	GC	218	March 19, 2011	92	30.4
54764*	GC	868	March 2, 2011	184	2.2
54870***	GC	64 (636)	March 22, 2011	27 (178)	33.3 (17.4)
54875	GC	73	March 18, 2011	23	100
54878*	GC	693	March 19, 2011	202	20.3
66120	GP	294	September 7, 2007	81	80.2
66122	GC	82	February 25, 2010	16	50.0
66123	GP	14	September 6, 2007	498	0
66124**	GP	22	September 7, 2007	67	0
66125	GP	80	September 6, 2007	204	31.4
66126	GP	123	September 1, 2007	190	36.8
107707**	GC	29	December 12, 2011	148	18.2
107708***	GC	92 (291)	March 17, 2012	165 (280)	80.6 (100)
107710	GC	46	September 19, 2011	352	11.9
107712**	GC	9	December 12, 2011	34	29.4
107714	GC	33	December 14, 2011	32	100
107716	GC	38	February 14, 2012	30	60
107717**	GC	10	February 20, 2012	11	63.6
107718**	GC	174	September 19, 2011	171	52.6
107719*	GC	512	February 18, 2012	238	34.9
107722	GC	121	February 18, 2012	280	65.0
107725**	GC	31	December 19, 2011	20	100

In parentheses values for four tags before trimming data at detached point. Five tags assumed free-floating or drifting (*); tracks were not included in the model (**) and data only included in spatial analyses (% locations inside MPAs and maps); trajectories were trimmed at the assumed detaching points (***).

migrated north (to the Gulf of Tehuantepec, Mexico), south (to Ecuador), and to the open ocean (**Figure 1**).

A Pearson correlation test showed that the number of transmission days did not correlate with the number of transmissions ($r^2 = 0.05$). Transmitters need to be at the surface for a certain amount of time to send a correct location, and some *R. typus* may only surface sporadically or under rough sea conditions, meaning that while an individual shark's tag may be transmitting, received transmissions may be infrequent or sporadic.

The random walk state-space model was run for 18 (24) of the 30 tagged *R. typus*. Four sharks had information gaps > 100 without transmission, which impeded the ability of the model to run properly. For these four cases, the original data were split into 'before' and 'after' the data gap; these periods were modeled separately and then bound together to create a single modeled track. Seven sharks had too few transmission days or transmissions to run the model. These seven sharks were not included in the MHH model but were included in the estimation of % of locations inside MPAs, and in calculating the spatial and temporal overlap with vessel traffic and fishing grounds (see **Table 2**). From a total of 1,053 Argos locations, the Bayesian state-space random walk model (programed to estimate the location of each whale shark at four locations per day) resulted in 3,118 (9,968) modeled locations, now on referred to as "modeled locations". Based on these modeled locations sharks traveled at a mean speed of 8.5 (10.4) km/day with a maximum speed of 76.9 km/day (**Table 3**).

Based on the MHH model, *R. typus* spent equal amount of time foraging and migrating, with an average of 50% ± 6.5% (± SE) of their time foraging (range = 0%–100%) and 49.7% ± 6.5% of their time migrating (range = 0%–100%), contrary to the full trajectory data with an average of 76% ± 0.04% (± SE) foraging (range = 17%–100%) and 24% ± 0.04% migrating (range = 0%–83%) (**Table 4**, **Figure 2** top). Tagged *R. typus* foraged mainly inside the Panamanian Exclusive Economic Zone (EEZ) or the territorial waters in both the Gulf of Panama and the Gulf of Chiriquí and, to a lesser extent, parallel to 4°N, north and east of the Galapagos islands (**Figure 2** bottom).

3.2 *Rhincodon typus* and Environmental Variables

The MHH model results showed that environmental conditions were different for each behavior. Specifically, chlorophyll-*a* concentrations and primary productivity were significantly higher when *R. typus* were foraging ($p < 0.001$ in both cases). The SST did not differ significantly between the two behavioral states (**Table 5**). Mean water depths were significantly ($p < 0.05$) deeper when the tagged sharks were migrating -1,534.4 ± 41.3 m (-2,366.5 ± 20.9 m) than when they were foraging -765.6 ± 26.8 m (-1,015.5 ± 18.2 m) (**Table 5**), and most foraging locations 76.9% (66.5%) occurred in coastal waters (< 50 km from the

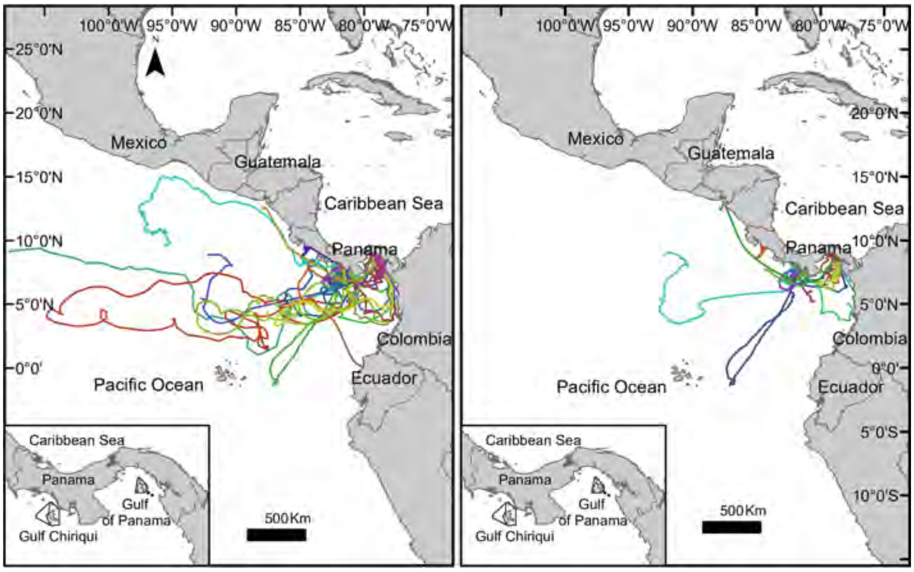

FIGURE 1 | Migratory tracks of 30 *Rhincodon typus* tagged with satellite transmitters off the Pacific coast of Panama: complete trajectories of 30 individuals (left plot); removed or partially trimmed of 25 individuals (right plot). Inset with map of the Pacific coast of Panama showing the *Rhincodon typus* tagging areas around Coiba National Park (Gulf of Chiriquí) and the northeast Las Perlas Archipelago (Gulf of Panama).

TABLE 3 | Mean, maximum and minimum traveling speed of 30 tagged whale sharks before and after the Bayesian State-Space Model for animal Movement (BSAM).

PTT	Data before modeling (Km/day)			Speed after BSAM model (Km/day)		
	Mean	Minimum	Maximum	Mean Speed	Minimum	Maximum
107707	13.4	0	50.6			
107708*	10.2 (18.3)	0	61.4 (75.9)	4.7 (8.4)	0.2 (0.2)	36.6 (73.2)
107710	5	0.1	28.8	7.3	0.0	32.7
107712	4.9	1.5	11			
107714	14	0.6	96	11.7	1.2	30.8
107716	7	0.2	26.9	4.5	0.6	14.0
107717	11.1	0.6	32.6			
107718	25.3	0.3	79.6			
107719**	33.5	0.4	80	16.9	0.4	32.1
107722	20.4	0.2	79.7	13.5	0.0	33.9
107725	22.7	0.9	86.3			
54740	13.8	0.4	67.9	7.9	0.4	32.0
54741**	26	0.4	79.4	15.0	0.3	31.7
54744	11.5	0.1	46.7	9.2	0.1	30.4
54745**	25	0.1	79	15.3	0.8	29.4
54747*	28.6 (23.6)	0.4 (0.2)	76.7 (76.7)	6.9 (12.0)	0.8 (0.4)	73.8 (74.5)
54748	20.7	0	79.8	7.1	0.2	29.0
54749*	13.4 (27.4)	0.2 (0.2)	74.7 (76.1)	6.7 (8.9)	0.0	18.5 (23.1)
54758	3.4	0.9	5.8			
54763	11.9	0	65.9	4.8	0.1	26.1
54764**	21.7	0.2	86.7	12.7	0.3	66.4
54870*	17.0 (10.9)	0.1 (0.0)	51.4 (51.4)	14.7 (14.7)	0.7 (0.7)	29.1 (29.1)
54875	19.3	0.6	69.7	7.8	0.1	20.2
54878**	15.6	0	78.8	10.7	0.0	31.8
66120	19.1	0	72.5	13.8	0.2	76.9
66122	17.7	1.9	62.2	11.0	1.5	23.8
66123	5.7	0.3	13.3			
66124	19.3	6.9	50.9			
66125	21.7	0.1	85.7	7.9	0.4	23.0
66126	16.8	0.1	86.4	5.5	0.1	56.4

Four trajectories were trimmed at the assumed detaching points (*). Five tags assumed free-floating or drifting (**). In parentheses speed values for the four tags before trimming data at detached point.

TABLE 4 | Percentage of *Rhincodon typus* locations for each behavioral state, within eddies, and within industrial fishing areas.

PTT	Behavioral state (%)		Locations within eddies (%)			Locations within fishing areas (%)		
	Foraging	Migrating	Overall	Cyclonic	Anti-cyclonic	Low effort	Mediumeffort	High effort
107707	3.45 (92)	96.55 (8)	0 (0)	0 (0)	0 (0)	96.6 (75)	3.4 (25)	0 (0)
107708*	97.87 (73)	2.13 (27)	0 (0)	0 (0)	0 (0)	98.8 (48)	1.2 (28)	0 (24)
107710	77.02 (96)	22.98 (4)	0 (0)	0 (0)	0 (0)	44.1 (15)	46 (54)	9.9 (31)
107712	0 (100)	100 (0)	0 (0)	0 (0)	0 (0)	100 (74)	0 (26)	0 (0)
107714	50.79 (100)	49.21 (0)	0 (0)	0 (0)	0 (0)	100 (73)	0 (27)	0 (0)
107716	100 (100)	0 (0)	0 (0)	0 (0)	0 (0)	100 (70)	0 (30)	0 (0)
107717	80 (100)	20 (0)	0 (0)	0 (0)	0 (0)	100 (30)	0 (70)	0 (0)
107718	42.2 (96)	57.8 (4)	2.3 (3)	2.4 (0)	0 (3)	41.6 (66)	17.3 (20)	41 (14)
107719*	(17)	(83)	(50)	(13)	(37)	(6)	(27)	(66)
107722	36.76 (45)	63.24 (55)	0 (0)	0 (0)	0 (0)	50.3 (21)	8.1 (16)	41.6 (63)
107725	6.45 (100)	93.55 (0)	0 (0)	0 (0)	0 (0)	100 (74)	0 (26)	0 (0)
54740	85.71 (100)	14.29 (0)	0 (0)	0 (0)	0 (0)	100 (98)	0 (2)	0 (0)
54741*	(037)	(63)	(20)	(5)	(15)	(15)	(15)	(71)
54744	42.5 (80)	57.50 (20)	0 (0)	0 (0)	0 (0)	95 (18)	5 (43)	0 (40)
54745*	(27)	(73)	(40)	(7)	(33)	(10)	(25)	(65)
54747*	47.97 (60)	52.03 (40)	8.1 (9)	2.7 (8)	6.2 (1)	86.2 (9)	11.4 (14)	2.4 (77)
54748	75.8 (89)	24.2 (11)	6.4 (5)	1.9 (3)	4.9 (1)	61.2 (6)	27 (20)	11.7 (74)
54749*	28 (39)	72 (61)	0 (0)	0 (0)	0 (0)	46.7 (42)	37.3 (26)	16 (32)
54758	60 (100)	40 (0)	0 (0)	0 (0)	0 (0)	100 (100)	0 (0)	0 (0)
54763	94.52 (100)	5.48 (0)	0 (0)	0 (0)	0 (0)	100 (62)	0 (38)	0 (0)
54764*	(74)	(26)	(31)	(31)	(0)	(58)	(30)	(12)
54870*	38.89 (71)	61.11 (29)	11.1 (4)	0 (3)	12.5 (0)	79.6 (4)	5.6 (45)	14.8 (52)
54875	51.06 (94)	48.94 (6)	0 (0)	0 (0)	0 (0)	66 (15)	34 (55)	0 (30)
54878*	(69)	(31)	(17)	(12)	(5)	(9)	(42)	(49)
66120	29.63 (74)	70.37 (26)	0 (0)	0 (0)	0 (0)	44.4 (5)	19.8 (18)	35.8 (77)
66122	21.88 (59)	78.13 (41)	0 (0)	0 (0)	0 (0)	68.8 (0)	31.3 (28)	0 (72)
66123	0 (50)	100 (50)	0 (0)	(0)	(0)	50 (50)	50 (0)	0 (50)
66124	18.18 (72)	81.82 (28)	0 (0)	0 (0)	0 (0)	68.2 (26)	0 (13)	31.8 (60)
66125	77.11 (90)	22.89 (10)	0.5 (0)	0.5 (0)	0 (0)	30.8 (25)	27.4 (27)	41.8 (48)
66126	90.33 (98)	9.67 (2)	0 (0)	0 (0)	0 (0)	23.3 (2)	13 (1)	63.7 (97)
Min.	0 (17)	0 (0)	0 (0)	0 (0)	0 (0)	23.3 (0)	0 (0)	0 (0)
Max.	100 (100)	100 (83)	11.11 (50.4)	2.65 (31)	12.50 (37)	100 (100)	50.0 (70)	63.7 (97)
Mean ± SE	50.2 ± 6.5 (76 ± 0.04)	49.75 ± 6.5 (24 ± 0.04)	1.14 ± 0.6 (6.2 ± 0.02)	0.30 ± 0.2 (3 ± 0.01)	0.95 ± 0.6 (3 ± 0.02)	74.1 ± 5.25 (37 ± 0.05)	13.5 ± 3.20 (27 ± 0.03)	12.4 ± 3.7 (37 ± 0.05)

In parentheses values for all 30 transmitters analyzed including partial and total removed data from assumed free-floating ones (*).

shore). Oceanic areas (50 km away from shore) shallower than 1,000 m were scarce within the study area, covering only 2.05% (3.64%) of the territory, however, up to 5.5% (19%) of the modeled locations occurred within these "shallow" areas indicating a significant use of seamounts and ridges by *R. typus* but only for the complete data (Resource Selection model, $p < 0.005$). The probability of changing between behavioral states (i.e., from migrating to foraging and *vice versa*), as well as the probability of staying in a particular state under the stationary distribution (**Figure 3**), was correlated with chlorophyll-*a*, productivity, and SST (**Table 6**).

There was a total of 24,437 eddies registered inside the study area between September 2007 and December 2012 (study period), only five of the analyzed shark tracks spend some time within an eddie, ranging from 0.5% to 11% of their time, especially in anticyclonic eddies (65%) (**Figure 4** top right, **Table 4**). However, full analyzed trajectories showed 10.25% of *R. typus* tracks overlapped temporal and spatially within them. On average, *R. typus* spent 6.2 ± 0.02% of their time within an eddy, although there was a high degree of variation among individuals. Six animals spent a significant amount of time (up to 50.4% in the case of individual 107719) within eddies. When foraging, an average of 10.9 ± 2.0% of the locations were within an eddy compared to 17.7% when migrating. When whale sharks were located inside an eddy, the eddy speeds (measured within the amplitude of an eddy) were significantly higher when *R. typus* were migrating ($p < 0.001$). There was not an apparent preference for staying in cyclonic or anticyclonic eddies, the frequency of whale sharks inside each these was 50%, both when calculated with the number of modeled locations or time spend inside the eddy (**Table 4**, **Figure 4** top left).

3.3 *Rhincodon typus* in Marine Protected Areas

R. typus visited a total of 10 (17) MPAs within three (five) countries (Mexico, Costa Rica, Panama, Colombia, and Ecuador) with 3.4% (22.6%) of the modeled locations occurring within an MPA, which accounted for a mean of 35.8 ± 5.4% (48 ± 6.3%) of their time; 97% (86%) of these locations occurred in Panama with higher rates in Parque Nacional Coiba and the recently expanded oceanic MPA Cordillera Coiba with nearly 68,000 km^2 (**Figure 4** bottom, **Tables 2**, **7**).

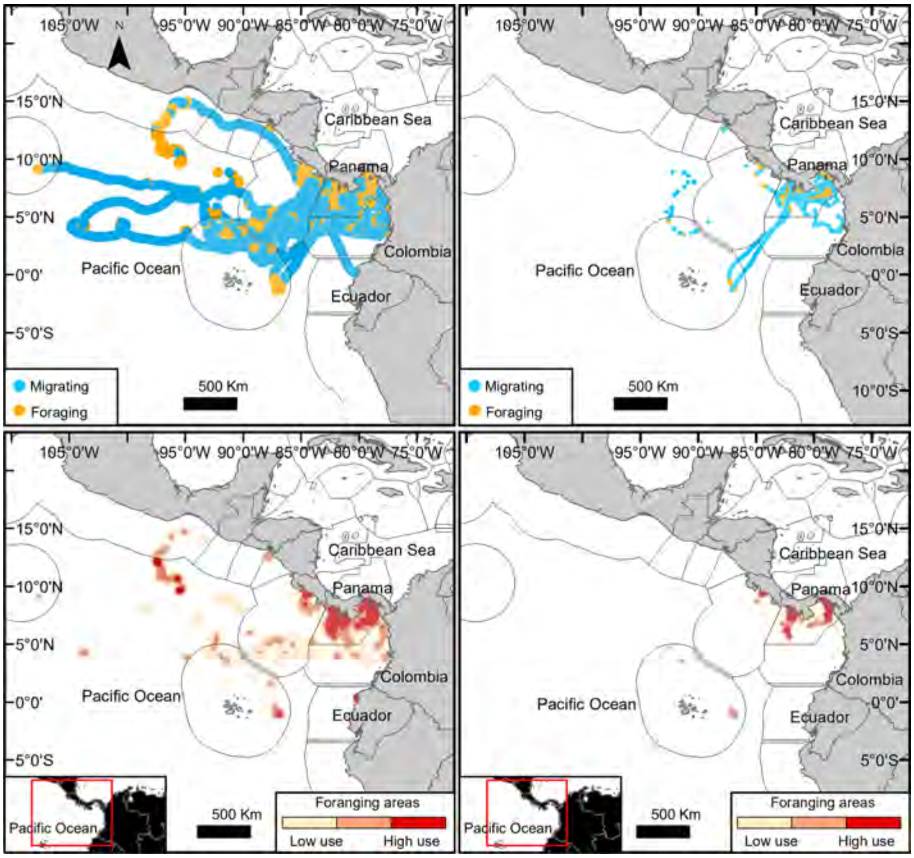

FIGURE 2 | *Rhincodon typus* behavioral states identified by a hidden Markov model: R. typus locations for two behavioral states—migrating (blue) and foraging (orange) (top plots); high-, medium-, and low-use (darkest to lighter) *R. typus* foraging areas (botton plots). Complete trajectories of 30 individuals (left plots); removed or partially trimmed of 25 individuals (right plots).

TABLE 5 | Mean (± SE) of environmental variables during each behavioral state (* indicates a significant difference between behaviors where p < 0.001).

Environmental variable	Foraging	Migrating
Sea surface temperature (°C)	28.1 ± 0.028	27.7 ± 0.04
	(27.94 ± 0.02)	(28.12 ± 0.02)
Chlorophyll (mg m^{-3})*	0.87 ± 0.02	0.54 ± 0.01
	(0.85 ± 0.02)	(0.35 ± 0.01)
Productivity (mg C m^{-2} d^{-1})*	1,055 ± 54.5	681 ± 12
	(1,024.29 ± 44.79)	(560.09 ± 4.63)
Eddy speed*	(32.90 ± 0.12)	(37.53 ± 0.17)
Depth (m)*	-765.6 ± 26.8	-1,534.4 ± 41.3
	(-2,366.5 ± 20.9)	(-1,015.5 ± 18.2)

In parentheses values for all 30 transmitters analyzed including partial and total removed data from assumed free-floating ones.

3.4 *Rhincodon typus* in Fishing Areas and Commercial Vessel Traffic

Of the areas occupied by tagged *R. typus*, 26.2% (50%) of all modeled locations occurred within high-effort fishing areas, 15% in medium-effort and 58% in low effort areas (**Figure 5 top**). In these areas, 86% of the fishing was tuna purse seines with a monthly average (mean ± SE) of 4,025 ± 1,417 fishing hours (503,987 fishing events between 2012 and 2018), and 13% were drifting longlines with a monthly average of 621.4 ± 157 fishing hours (174,701 fishing events). Purse seine effort did not differ significantly between the first, second, or fourth quarters (p > 0.05) but was lower during the third trimester (16%). Most of the drifting longline effort in the area occurred during the last quarter (53.2%). Vessels with a Colombian flag were the most common (25.2%, equivalent to an average of 1,170 fishing hours per month) followed by vessels from Mexico (24.26%), Venezuela (14.9%), and Panama (14.3%). The majority 70.9%

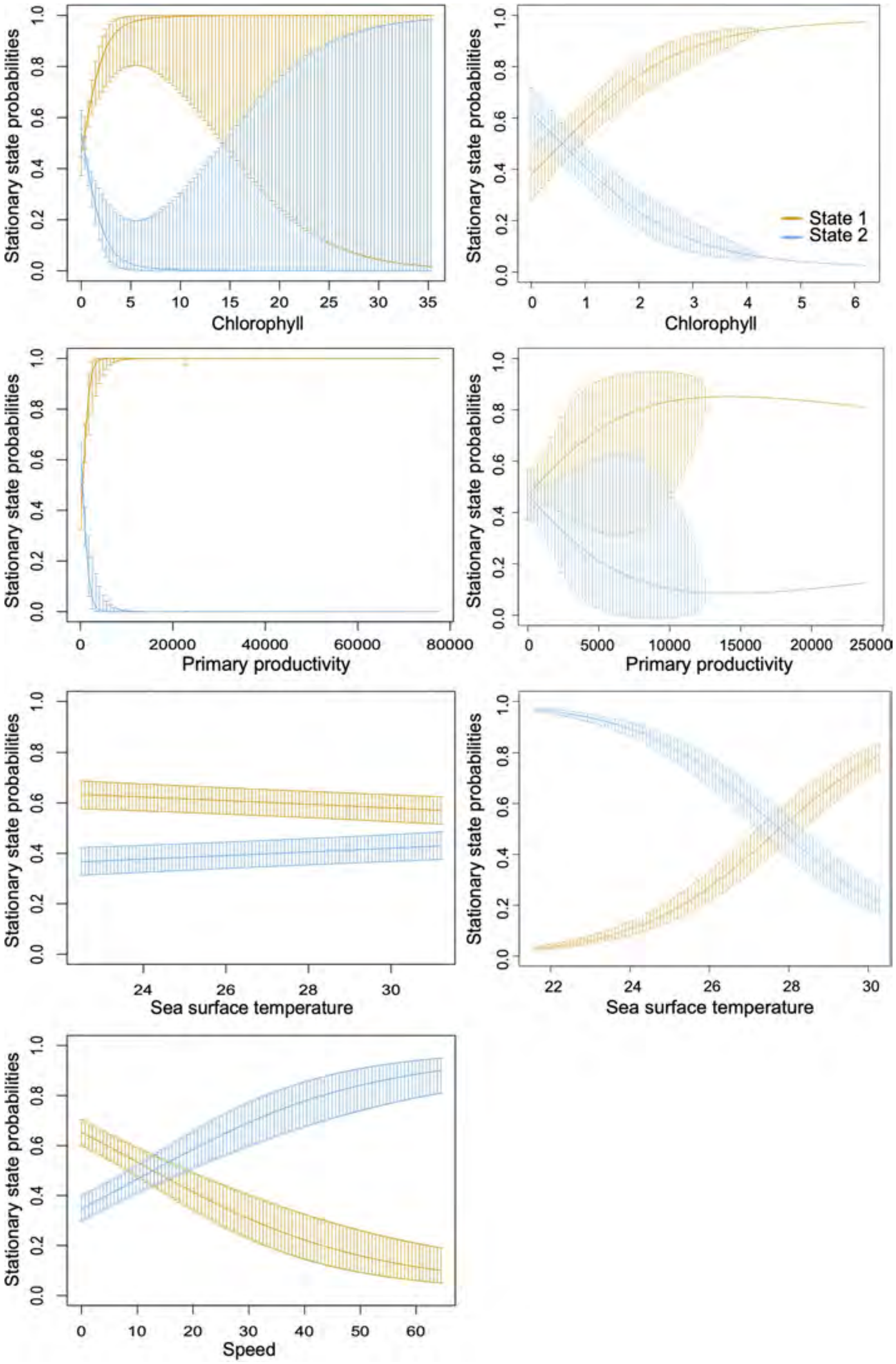

FIGURE 3 | Probabilities of remaining in a particular behavioral state calculated by the Hidden Markov Model (HMM) (state 1 = foraging, state 2 = migrating). Complete trajectories of 30 individuals (left plots); removed or partially trimmed of 25 individuals (right plots).

(88.8%) of *R. typus* modeled locations occurred within high-impact vessel traffic areas (areas with a higher density of vessels moving at higher speeds), 22% (11.2%) of the modeled locations occurred with medium impact areas, and 6.9% (0.0%) modeled locations occurred within low-impact areas (**Figure 5 bottom**).

3.5 Detached or Free-Floating Tags Versus Marine Currents and Winds

Traveling speed was not correlated to current speed (**Figures S1, 2**) at two different depths for any of the five suspicious whale shark trajectories: 107719 (R= 0.078, p>0.05 at surface; R=0.15,

TABLE 6 | Regression coefficients for the transition probabilities.

	From state 1 to 2	From state 2 to 1
Intercept	-2.913 (-1.6480)	-19.46 (-1.9842)
Chlorophyll-*a**	-0.156 (-0.8239)	0.7396 (0.1987)
Productivity*	-0.00007 (-0.0004)	0.0003 (0.0007)
Sea surface temperature*	-0.233 (-0.0128)	-0.578 (-0.0313)
Eddy speed	(0.0398)	(-0.0121)

State 1: foraging; state 2 migrating. (indicates a significant relationship where p < 0.001). In parentheses values for all 30 transmitters analyzed including partial and total removed data from assumed free-floating ones.*

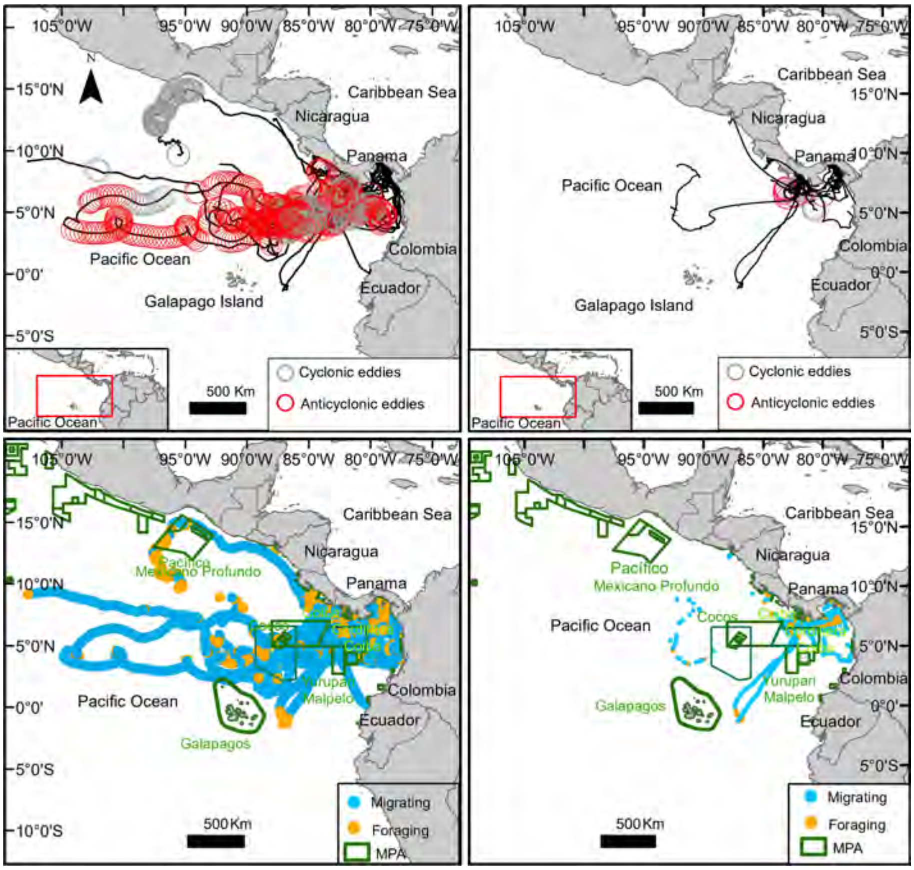

FIGURE 4 | *Rhincodon typus* tracks superimposed on real-time eddies (cyclonic in grey, anti-cyclonic in red) (top plots); *Rhincodon typus* modeled locations (blue = migrating and orange = foraging) superimposed on marine protected areas (MPAs) (botton plots). Complete trajectories of 30 individuals (left plots); removed or partially trimmed of 25 individuals (right plots).

p>0.005 at 15 m), 54741(R= -0.032, p>0.05; R=0.025, p>0.005), 54745 (R= -0.004, p>0.05; R=-0.1, p>0.005), 54764 (R= -0.2, p>0.05; R= 0.045, p>0.05), and 54878 (R= -0.2, p>0.05; R= -0.059, p>0.05). In addition, tag speed was tested for correlation with wind diffusivity current speed and marine currents, no correlation was found between these three variables, except for a significant correlation between tag speed and wind speed for tag 54764 (**Table 8**). These analyses suggest that those five tags were not floating on the surface, carried away by marine currents and winds, or detached from the animal.

4 DISCUSSION

For the first time, we investigated the movement, behavior, and habitat use of 30 *R. typus* individuals tagged in Panamanian waters. Our results indicate that the sharks spent the majority of their time foraging inside the Panamanian EEZ but also moved north to Mexico, south to Ecuador, and west to the open ocean. One female (PTT no. 107715) previously reported, traveled over 20,000 km to the western Indo-Pacific, which is the longest recorded trans-Pacific migration of an *R. typus* individual (also

TABLE 7 | Number and percentage of *Rhincodon typus* total modeled locations within marine protected areas (MPAs).

Country	MPA	Number of locations	Percentage
Colombia			**0.6 (8.1)**
	Malpelo	(74)	(3.2)
	Santuario de fauna y flora de Malpelo	(31)	(1.3)
	Encanto de los manglares del Bajo Baudo	1 (2)	0.0 (0.01)
	Golfo de Tribuga, Cabo Corrientes	(2)	(0.01)
	Yurupari - Malpelo	18 (74)	0.6 (3.3)
Costa Rica			**0.1 (1.6)**
	Isla del Coco	(6)	0.3)
	Área Marina de Manejo Montes Submarinos	2 (30)	0.1 (1.3)
Ecuador			**(0.5)**
	Galapagos	(4)	(0.2)
	Manglares Estuario del Rio Muisne	(8)	(0.4)
Mexico			**(3.5)**
	Pacifico Mexicano Profundo (RB PMP)	(79)	(3.5)
Panama			**(86.2)**
	Bahia de Panama	20 (52)	0.6 (2.3)
	Parque Nacional Coiba	574 (65)	18.4 (2.9)
	Golfo de Chiriquí	1 (5)	0.1 (0.22)
	Playa Boca Vieja	5 (6)	0.2 (0.26)
	Punta Patiño	3 (13)	0.1 (0.6)
	Zona especial de protección marina de Coiba	87 (1,117)	28 (49.5)
	Cordillera de Coiba	194 (690)	6.2 (30.5)

In parentheses values for all 30 transmitters analyzed including partial and total removed data from assumed free-floating ones. Bold values = Country total.

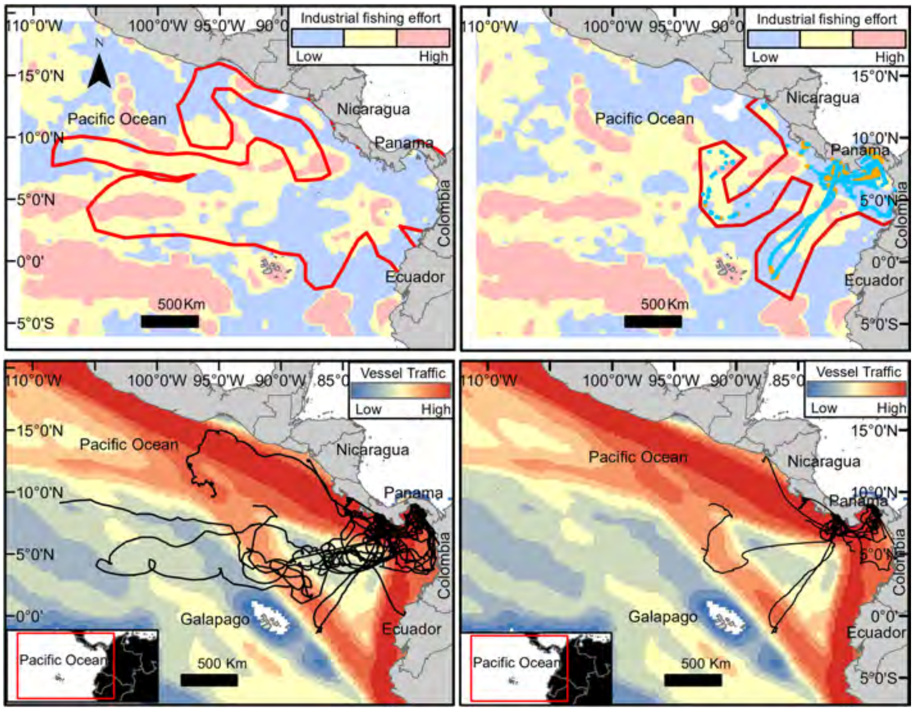

FIGURE 5 | Level of threat within areas used by *Rhincodon typus*: industrial fishing effort within *R. typus* habitat (red polygon) as the combined effect of density of fishing boats and fishing hours (top plots); vessel traffic, as the combined effect of density of vessels and their traveling speed (botton plots). Complete trajectories of 30 individuals (left plots); removed or partially trimmed of 25 individuals (right plots).

TABLE 8 | Correlations between tag, marine current, and wind diffusivity current speeds for five tags assumed to be detached or free-floating.

PTT	Variable 1	Variable 2	Correlation coefficient	P
107719	Current speed	Tag speed	0.078	0.482
	Current speed	Wind speed	0.025	0.828
	Tag speed	Wind speed	0.123	0.287
51741	Current speed	Tag speed	-0.032	0.744
	Current speed	Wind speed	0.006	0.959
	Tag speed	Wind speed	0.158	0.149
54745	Current speed	Tag speed	-0.004	0.967
	Current speed	Wind speed	0.042	0.718
	Tag speed	Wind speed	-0.069	0.550
54764	Current speed	Tag speed	-0.195	0.091
	Current speed	Wind speed	0.055	0.651
	Tag speed	Wind speed	-0.305	0.010*
54878	Current speed	Tag speed	-0.203	0.108
	Current speed	Wind speed	-0.156	0.246

(*) = Significant correlation (p < 0.05).

see Guzman et al., 2018). In comparison, tracking data from 27 adult female *R. typus* tagged near Darwin Island in the Galápagos archipelago revealed that individuals remained in the tagging area for short periods of time before moving into the open equatorial Pacific (Hearn et al., 2016). Similarly, immature individuals tagged in the Gulf of California largely remained in the Gulf, while adults moved out into the Pacific (Eckert and Stewart, 2001; Ramírez-Macías et al., 2017). Taken together, these studies indicate the importance of the coastal waters of the tropical eastern Pacific and the offshore areas of the Cocos and Galapagos islands as foraging and migratory habitats for *R. typus* (Acuña-Marrero et al., 2014). In addition, genetic connectivity between the biogeographic regions of the Eastern Pacific and the Indo-Pacific, particularly with the Western Indo-Pacific Ocean has been demonstrated for Panamanian transient individuals (Guzman et al., 2021), and as inferred migration route (Sequeira et al., 2013).

4.1 Analyses and Interpretation of Potential Detached or Free-Drifting Tags

We analyzed and plotted the individual tracks for all 30 animals. However, we paid particular attention to those five tags with the longest record (PTTS 107719, 54741, 54745, 54764, and 54878) that seem to suggest that they separated from the animal at some point and continued transmitting with the ocean currents. Hearn et al. (2013) recognized the small sample size used in the analyses, the "considerable variation among individuals in the length and time spent at the surface", and that data recorded by Argos satellite were intermittently with gaps of several days in some of the tagged animals. We cannot explain technically why transmissions in our longest records were at the same time on every day, and recognize this potential caveat. However, our analyses open the door to an alternative interpretation that could take more into account the animal's diving behavior (surface, vertical) while migrating or provisioning (feeding), and the lack of information on the movement and habitat use of whale sharks away from shallow coastal areas (Brunnschweiler et al., 2009). Graham et al. (2006) demonstrated that whale sharks could display "ultradian, diel and circa-lunar rhythmicity of diving behavior" during feeding. In addition, daily provisioning patterns change significantly during the day, apparently in response to changes in temperature and perhaps the size of the individual (Araujo et al., 2020).

Consequently, we argue that it is not easy to discern from the number and frequency of ARGOS transmissions alone the movement of whale sharks in an open ocean highly influenced by current, eddies, and sea surface height. Especially if it is considered that our data was properly filtered to correct potential satellite errors, went through two modeling processes (Bayesian and Markov models) to understand and interpret their trajectories and behaviors, and these trajectories, in turn, were analyzed with each individual's velocity information, current velocity and current velocity within the eddies. Hearn et al. (2018) showed floating tags drifting into open ocean at very different speeds and following an unmeasured current pattern into an eddy; we instead, measured animal movement in real-time and no relationship with surface currents and surface wind were observed, as previously reported for the species (Sleeman et al., 2010).

4.2 Environmental Variables and the Distribution of *Rhincodon typus*

Previous studies have shown that the distribution and aggregation of *R. typus* are associated with physical and biological oceanographic features relating to productivity (Stevens, 2007). Indeed, our results show that most inferred foraging occurred in shallower coastal waters, with a significant use of seamounts and ridges, and was significantly related to productivity and chlorophyll-*a* concentrations. This is in accordance with findings from other locations, where seasonal *R. typus* aggregations are typically associated with temporary increases in food resources (Stevens, 2007). In the tropical eastern Pacific, productivity is strongly influenced by the upwelling systems. Ryan et al. (2017) examined *R. typus* movements in relation to thermo-biological frontal systems in the eastern Pacific and found a strong association between individual movements and the northern equatorial upwelling front, with 80% of shark positions occurring within the front.

The same authors observed that seasonal movements between the equatorial and eastern boundary upwelling systems linked to productivity. Thus, our data indicate that *R. typus* in Panamanian waters exhibit similar foraging behaviors to individuals inhabiting the Pacific.

Migratory *R. typus* behavior has been linked to environmental factors such as water depth, SST, and eddy currents (Heyman et al., 2001; Riley et al., 2010). In our study, *R. typus* spent more time in eddies while migrating (17%) than foraging (10%), and when inside an eddy, eddy speed was significantly related to migratory behavior. Additionally, the two individual sharks that spent the most time within eddies were also those that spent the highest proportion of their time migrating (83% and 73%). Indeed, mesoscale eddies are important drivers of ocean ecosystem structure and are foraging hotspots for many marine animals in the eastern Pacific (Willett et al., 2006; Della Penna and Gaube, 2020). Eddy formation can drive the vertical movement of nutrients and phytoplankton and trap productive waters (Della Penna and Gaube, 2020). This may encourage *R. typus* to follow eddies during their migration to find food sources. Both anticyclonic eddies, which are associated with positive sea level anomalies (in the Tehuantepec and Papagayo eddy areas) and cyclonic eddies, which are associated with negative sea level anomalies (in the Humboldt Current), are linked to *R. typus* tracks (Revelles et al., 2007). Therefore, *R. typus* movement may not be specific to eddy type but more influenced by eddy speed. It has been suggested that the temperature gradients associated with eddies can be used for navigation by whale sharks (Sleeman et al., 2010). This might explain the observed association between higher eddy speeds and migratory behavior. However, it is important to note that seasonal and inter-annual variability in oceanographic conditions is characteristic of the eastern tropical Pacific, which may account for some of the variation between individuals and between regions.

4.3 *Rhincodon typus* Inside Marine Protected Areas

R. typus visited 17 MPAs within five countries, yet only 22.6% of the modeled locations occurred within an MPA. This may be considered an underestimation due to the ongoing increase of MPAs in the region. While MPAs are a valuable conservation tool, their effectiveness may be somewhat limited for highly mobile species (Norman, 1999; Reynolds et al., 2017). For migratory species such as *R. typus*, transboundary MPAs and MPA networks are especially important conservation approaches, as are efforts to protect oceanic areas (such as Cordillera de Coiba) and areas beyond national jurisdiction. In some areas, MPAs have been established to protect seasonal and year-round *R. typus* aggregations, such as South Ari Atoll in the Maldives and Ningaloo Reef in Australia. Additionally, the Marine Conservation Corridor of the Eastern Tropical Pacific (MCCETP) between the islands of Cocos, Galapagos, Malpelo, and Coiba was formally established in 2004 for the conservation and sustainable use of biodiversity in the equatorial eastern Pacific. Our observations highlight the importance of this area for *R. typus*. Adaptive management approaches and the use of dynamic MPAs that incorporate spatially dynamic ocean features, such as thermal fronts, are also important considerations given the importance of these features for *R. typus* and ongoing shifts in species distributions (Hooker et al., 2011).

4.4 *Rhincodon typus* Interactions With Fisheries

Injury and mortality because of interactions with fishing gear, including long lines (Wang et al., 2021), have emerged as key threat to many marine species, especially sharks and rays (Stevens et al., 2000). In our study, tagged *R. typus* transmitted from low-, medium-, and high-effort fishing areas, although approximately half of the modeled locations occurred from high-fishing-effort areas. The observed overlap with the tuna purse seine fishery is perhaps unsurprising given that purse seine fishing occurs more frequently in areas with high net primary productivity (Kroodsma et al., 2018), and tuna are often associated with other large species. Such fishing activities close to *R. typus* can lead to accidental capture and entanglement. Capietto et al. (2014) examined the spatial-temporal distribution of *R. typus* and fishery interaction hotspots in the Atlantic and Indian Oceans and recorded the number and fate of captured animals. They found high rates of incidental capture but low mortality because of these interactions. In contrast, high rates of mortality associated with fishing activities have been recorded in the Pacific Ocean (Western and Central Pacific Fisheries Commission, 2010). While we assessed fishing effort based on 70,000 out of 2.9 million motorized fishing vessels, small vessels (< 24 m) not equipped with an AIS system were not included (Kroodsma et al., 2018) despite also posing a threat. While there is a clear overlap between *R. typus* habitat use and fishing areas, long-term assessments of post-release survival are needed to obtain a clearer picture of the true impact of fishing on *R. typus* populations in the eastern Pacific (Capietto et al., 2014). Bycatch of juveniles and neonates in Peruvian waters is a clear example of the impact of fisheries on the species at any maturity stage (Pajuelo et al., 2018).

4.5 *Rhincodon typus* Interactions With Marine Traffic

As slow-moving surface dwellers, *R. typus* are vulnerable to collision with marine vessel traffic, and there is a high degree of global overlap between shipping activity and habitat use (Pirotta et al., 2019; Womersley et al., 2021; Womersley et al., 2022). Based on our observations, most modeled locations from tagged individuals occurred within high-impact vessel traffic areas, that is, a high density of vessels moving at high speed. Previous studies have found that individual *R. typus* spend approximately half of their time in surface waters (< 10 m depth) (Eckert and Stewart, 2001; Rowat and Gore, 2007; Womersley et al., 2021), and interactions with ships can result in behavioral modification, disturbance, displacement, injury, and even mortality (Pirotta et al., 2019; Womersley et al., 2021). Given the spatial overlap between marine vessels and *R. typus* habitat use, injury and mortality from ship collisions could be a significant factor in observed population declines (Womersley et al., 2022). Additional research is, therefore, needed to elucidate the extent of such interactions and their effects on *R. typus* fitness, survival, and, ultimately, population status.

Overall, this study shows that the coastal waters of Panama form an important foraging and migratory habitat for *R. typus* from which nomadic individuals move to other key areas in the eastern Pacific and the Indo-Pacific. Our observations highlight the need for further conservation of these habitats and the *R. typus* populations they support. Furthermore, we found that oceanographic processes are key determinants of *R. typus* distribution and behavior, primarily *via* influences on productivity, making *R. typus* vulnerable to changing climate conditions that can increase, water temperature, El Niño-Southern Oscillation events, ocean stratification and reduce productivity (Sequeira et al., 2014; Fiedler and Lavín, 2017; Riascos et al., 2019).

The high degree of overlap between *R. typus* habitat and human activities highlights the need for marine conservation planning approaches beyond MPAs at key aggregation sites, and the insights gleaned from this work can inform conservation planning at appropriate scales. More generally, our study highlights the value of satellite tracking studies for understanding the behavior, habitat use, and potential adaptation to climate change of highly mobile migratory species, such as *R. typus*.

Geopolitics have an impact in the conservation of transboundary species including marine protected areas where conflicts can be amplified (Harrison et al., 2018; Mackelworth et al., 2019). Our results suggest that this transboundary species could benefit from a regional conservation plan that includes high seas or international waters to improve its protection. Local regulations and management practices are in place in most countries along with the eastern Pacific offshore islands and some coastal areas, including fishing and product commercialization prohibitions and promoting ecotourism. Establishing a functional marine corridor or seaway (Migravia) was suggested (Guzman et al., 2021), and a plan for connecting EZZ waters of Ecuador, Colombia, Panama, and Costa Rica is in progress, but Peru must be included. The only existing corridor politically was established in 2014 along with six Central American countries, including Panama, Costa Rica, Nicaragua, Honduras, El Salvador, and Guatemala (OSPESCA, 2014). However, the protection of large high-seas areas, perhaps used along the shark's migratory routes for feeding and breeding as observed in this study, is not considered. We recommend the following actions: 1) Create a regional science-policy task force to coordinate the conservation of whale sharks in the eastern Pacific (Mexico-Peru minimum); 2) Develop marine territorial planning identifying critical aggregation areas potentially used for feeding and breeding; 3) Analyze migratory routes coupled with marine currents and vessel traffic routes to identify potential risk areas; 4) Increase satellite tagging efforts in the high-seas and coastal areas to understand the movement ecology of the species better.

AUTHOR'S NOTE

Global Fishing Watch has made every attempt to ensure the completeness, accuracy and reliability of the information provided on this Site. However, due to the nature and inherent limitations in source materials for information provided, Global Fishing Watch qualifies all designations of vessel fishing activity, including synonyms of the term "fishing activity", such as "fishing" or "fishing effort", as "apparent", rather than certain. And accordingly, the information is provided "as is" without warranty of any kind.

DATA AVAILABILITY STATEMENT

The raw data supporting the conclusions of this article will be made available by the authors, without undue reservation.

ETHICS STATEMENT

The animal study was reviewed and approved by Smithsonian Tropical Research Institute ACUC.

AUTHOR CONTRIBUTIONS

HG conceived the study, tagged all animals, and developed the research questions and analytical procedures. CG developed the statistical methods, programmed the R-codes, and performed the statistical analyses. HG, CG, and CC edited and approved the final version of the manuscript.

FUNDING

This research was partially funded by the MarViva Foundation (Panama), the International Community Foundation-CANDEO, the Secretaria Nacional de Ciencia, Tecnología e Innovación de Panamá (SENACYT), the Sistema Nacional de Investigadores from SENACYT, and the Smithsonian Tropical Research Institute.

ACKNOWLEDGMENTS

We thank C. Guevara and K. Mantel for their logistical assistance in the field. We also thank Marianne Fish and Editage (www.editage.com) for formatting and English language editing. We thanks five reviewers for the revision of the manuscript.

SUPPLEMENTARY MATERIAL

The Supplementary Material for this article can be found online at: https://www.frontiersin.org/articles/10.3389/fmars.2022.793248/full#supplementary-material

REFERENCES

Acuña-Marrero, D., Jiménez, J., Smith, F., Doherty, P. F.Jr, Hearn, A., Green, J. R., et al. (2014). Whale Shark (*Rhincodon Typus)* Seasonal Presence, Residence Time and Habitat Use at Darwin Island, Galapagos Marine Reserve. *PLos One* 9 (12), e115946. doi: 10.1371/journal.pone.0115946

Araujo, G., Labaja, J., Snow, S., Huveneers, C., and Ponzo, A. (2020). Changes in Diving Behaviour and Habitat Use of Provisioned Whale Sharks:

Implications for Management. *Sci. Rep.* 10 (1), 1–12. doi: 10.1038/s41598-020-73416-2

Brunnschweiler, J. M., Baensch, H., Pierce, S. J., and Sims, D. W. (2009). Deep-Diving Behaviour of a Whale Shark Rhincodon Typus During Long-Distance Movement in the Western Indian Ocean. *J. Fish Biol.* 74 (3), 706–714. doi: 10.1111/j.1095-8649.2008.02155.x

Capietto, A., Escalle, L., Chavance, P., Dubroca, L., Delgado de Molina, A., Murua, H., et al. (2014). Mortality of Marine Megafauna Induced by Fisheries: Insights From the Whale Shark, the World's Largest Fish. *Biol. Conserv.* 174, 147–151. doi: 10.1016/j.biocon.2014.03.024

Chen, C. T., Liu, K. M., and Joung, S. J. (1997). Preliminary Report on Taiwan's Whale Shark Fishery. *TRAFFIC Bull.* 17, 53–57. http://scholars.ntou.edu.tw/handle/123456789/16686

Colman, J. G. (1997). A Review of the Biology and Ecology of the Whale Shark. *J. Fish Biol.* 51, 1219–1234. doi: 10.1111/j.1095-8649.1997.tb01138.x

de la Parra Venegas, R., Hueter, R., González Cano, J., Tyminski, J., Gregorio Remolina, J., Maslanka, M., et al. (2011). An Unprecedented Aggregation of Whale Sharks, *Rhincodon Typus*, in Mexican Coastal Waters of the Caribbean Sea. *PLos One* 6, e18994. doi: 10.1371/journal.pone.0018994

Della Penna, A., and Gaube, P. (2020). Mesoscale Eddies Structure Mesopelagic Communities. *Front. Mar. Sci.* 7. doi: 10.3389/fmars.2020.00454

Diamant, S., Rohner, C. A., Kiszka, J. J., d'Echon, A. G., d'Echon, T. G., Sourisseau, E., et al. (2018). Movements and Habitat Use of Satellite-Tagged Whale Sharks Off Western Madagascar. *Endanger. Species Res.* 36, 49–58. doi: 10.3354/esr00889

Eckert, S. A., and Stewart, B. S. (2001). Telemetry and Satellite Tracking of Whale Sharks, *Rhincodon Typus*, in the Sea of Cortez, Mexico and the North Pacific Ocean. *Environ. Biol. Fish.* 60, 299–308. doi: 10.1023/A:1007674716437

E.U. Copernicus Marine Service Information (2022) *MULTIOBS_GLO_PHY_NRT_015_003 (Global Total Surface and 15m Current - COPERNICUS-GLOBCURRENT) From Altimetric Geostrophic Current and Modeled Ekman Current Processing).* Available at: https://resources.marine.copernicus.eu/product-detail/MULTIOBS_GLO_PHY_NRT_015_003/DOCUMENTATION (Accessed January 2022).

Fiedler, P. C., and Lavín, M. F. (2017). *Oceanographic Conditions of the Eastern Tropical Pacific in Coral Reefs of the Eastern Tropical.* Eds. P. W. Glynn, D. P. Manzello and I. C. Enochs (Netherlands: Springer), 59–83.

GEBCO Bathymetric Compilation Group (2020) *Grid. 2020*. Available at: https://dx.doi.org/10.5285/a29c5465-b138-234d-e053-6c86abc040b9 (Accessed May 7, 2021).

Global Fishing Watch. Available at: https://globalfishingwatch.org/ (Accessed November 30, 2020).

Graham, R. T., Roberts, C. M., and Smart, J. C. (2006). Diving Behaviour of Whale Sharks in Relation to a Predictable Food Pulse. *J. R. Soc Interface.* 3 (6), 109–116. doi: 10.1098/rsif.2005.0082

Gudger, E. W. (1938). A Whale Shark Rammed by a Vessel Off the Pacific Coast of Western Panama. *Nature* 141, 516. doi: 10.1038/141516a0

Guzman, H. M., Beaver, C. E., and Diaz-Ferguson, E. (2021). Novel Insights Into the Genetic Population Connectivity of Transient Whale Sharks (*Rhincodon Typus)* in Pacific Panama Provide Crucial Data for Conservation Efforts. *Frontier Mar. Sci.* 8, 744109. doi: 10.3389/fmars.2021.744109

Guzman, H. M., Gomez, C. G., Hearn, A., and Eckert, S. A. (2018). Longest Recorded Transpacific Migration of a Whale Shark (*Rhincodon Typus*). *Mar. Biodivers. Rec.* 11, 1–6. doi: 10.1186/s41200-018-0143-4

Harrison, A. L., Costa, D. P., Winship, A. J., Benson, S. R., Bograd, S. J., Antolos, M., et al. (2018). The Political Biogeography of Migratory Marine Predators. *Nat. Ecol. Evol.* 2 (10), 1571–1578. doi: 10.1038/s41559-018-0646-8

Hearn, A. R., Green, J. R., Espinoza, E., Peñaherrera, C., Acuña, D., and Klimley, A. P. (2013). Simple Criteria to Determine Detachment Point of Towed Satellite Tags Provide First Evidence of Return Migrations of Whale Sharks (*Rhincodon Typus*) at the Galapagos Islands, Ecuador. *Anim. Biotelemetry* 1, 1–10. doi: 10.1186/2050-3385-1-11

Hearn, A. R., Green, J., Román, M. H., Acuña-Marrero, D., Espinoza, E., and Klimley, A. P. (2016). Adult Female Whale Sharks Make Long-Distance Movements Past Darwin Island (Galapagos, Ecuador) in the Eastern Tropical Pacific. *Mar. Biol.* 163, 214. doi: 10.1007/s00227-016-2991-y

Heyman, W. D., Graham, R. T., Kjerfve, B., and Johannes, R. E. (2001). Whale Sharks *Rhincodon Typus* Aggregate to Feed on Fish Spawn in Belize. *Mar. Ecol. Prog. Ser.* 215, 275–282. doi: 10.3354/meps215275

Hoenig, J. M., and Gruber, S. H. (1990)Life-History Patterns in the Elasmobranchs: Implications for Fisheries Management in NOAA Tech. Rep. Nmfs. In: *Elasmobranchs as Living Resources: Advances in the Biology, Ecology, Systematics, and the Status of the Fisheries* (NOAA Technical Report NMFS). Available at: https://www.st.nmfs.noaa.gov/spo/SPO/tr90opt.pdf (Accessed May 10, 2021).

Hooker, S., Cañadas, A., Hyrenbach, K., Corrigan, C., Polovina, J., and Reeves, R. (2011). Making Protected Area Networks Effective for Marine Top Predators. *Endang. Species Res.* 13, 203–218. doi: 10.3354/esr00322

Hueter, R. E., Tyminski, J. P., and de la Parra, R. (2013). Horizontal Movements, Migration Patterns, and Population Structure of Whale Sharks in the Gulf of Mexico and Northwestern Caribbean Sea. *PLos One* 8, e71883. doi: 10.1371/journal.pone.0071883

Jonsen, I. (2016). Joint Estimation Over Multiple Individuals Improves Behavioural State Inference From Animal Movement Data. *Sci. Rep.* 6, 20625. doi: 10.1038/srep20625

Jonsen, I. D., Flemming, J. M., and Myers, R. A. (2005). Robust State-Space Modeling of Animal Movement Data. *Ecology* 86, 2874–2880. doi: 10.1890/04-1852

Joung, S. J., Chen, C. T., Clark, E., Uchida, S., and Huang, W. Y. P. (1996). The Whale Shark (*Rhincodon Typus*) is a Livebearer: 300 Embryos Found in One 'Megamamma' Supreme. *Environ. Biol. Fish.* 46, 219–223. doi: 10.1007/BF00004997

Ketchum, J. T., Galván-Magaña, F., and Klimley, A. P. (2012). Segregation and Foraging Ecology of Whale Sharks, *Rhincodon Typus*, in the Southwestern Gulf of California. *Environ. Biol. Fishes.* 96 (6), 779–795. doi: 10.1007/s10641-012-0071-9

Kroodsma, D. A., Mayorga, J., Hochberg, T., Miller, N. A., Boerder, K., Ferretti, F., et al. (2018). Tracking the Global Footprint of Fisheries. *Science* 359, 04–908. doi: 10.1126/science.aao5646

Mackelworth, P. C., Teff Seker, Y., Vega-Fernández, T., Marques, M., Lopes, F., D'Anna, G., et al. (2019). Geopolitics and Marine Conservation: Synergies and Conflicts. *Front. Mar. Sci.* 6. doi: 10.3389/fmars.2019.00759

Meekan, M., Austin, C. M., Tan, M. H., Wei, N. W. V., Miller, A., Pierce, S. J., et al. (2017). iDNA at Sea: Recovery of Whale Shark (*Rhincodon Typus*) Mitochondrial DNA Sequences From the Whale Shark Copepod (*Pandarus Rhincodonicus*) Confirms Global Population Structure. *Front. Mar. Sci.* 4. doi: 10.3389/fmars.2017.00420

Michelot, T., Langrock, R., and Patterson, T. A. (2016). moveHMM: An R Package for the Statistical Modelling of Animal Movement Data Using Hidden Markov Models. *Methods Ecol. Evol.* 7, 1308–1315. doi: 10.1111/2041-210X.12578

NOAA. ERDDAP. Available at: http://coastwatch.pfeg.noaa.gov/erddap/index.html (Accessed July 12, 2019).

NOAA NMFS *SWFSC ERD Chlorophyll-A (Erdmh1chlamday)*. Available at: https://coastwatch.pfeg.noaa.gov/erddap/search/index.html?page=1&itemsPerPage=1000&searchFor=erdMH1chlamday (Accessed July 12, 2019).

NOAA NMFS *SWFSC ERD Sea Surface Temperature*. Available at: https://coastwatch.pfeg.noaa.gov/erddap/search/index.html?page=1&itemsPerPage=1000&searchFor=erdAGssta3day (Accessed July 12, 2019).

NOAA NMFS *SWFSC ERD Primary Productivity*. Available at: https://coastwatch.pfeg.noaa.gov/erddap/search/index.html?page=1&itemsPerPage=1000&searchFor=erdMH1pp1day (Accessed July 12, 2019).

Norman, B. M. (1999). *Aspects of the Biology and Ecotourism Industry of the Whale Shark Rhincodon Typus in North-Western Australia* (Perth, Australia: Murdoch University).

Norman, B. M., Holmberg, J. A., Arzoumanian, Z., Reynolds, S. D., Wilson, R. P., Rob, D., et al. (2017). Undersea Constellations: The Global Biology of an Endangered Marine Mega-Vertebrate Further Informed Through Citizen Science. *BioScience* 67, 1029–1043. doi: 10.1093/biosci/bix127

OSPESCA (2014) *Reglamento Regional OSP-07-2014, Para Fortalecer La Sostenibilidad Poblacional Del Tiburón Ballena (Rhincodon Typus) En Los Países Miembros Del SICA. El Salvador*. Available at: http://www.fao.org/faolex/results/details/es/c/LEX-FAOC180626/.

Pajuelo, M., Alfaro-Shigueto, J., Romero, M., Pásara-Polack, A., Solano, A., Vela, G., et al. (2018). Occurrence and Bycatch of Juvenile and Neonate Whale Sharks (*Rhincodon Typus*) in Peruvian Waters. *Pac. Sci.* 72, 463–473. doi: 10.2984/72.4.6

Pierce, S. J., and Norman, B. (2016). e.T19488A2365291. Rhincodon typus. The IUCN Red List of Threatened Species 2016. doi: 10.2305/IUCN.UK.2016-1.RLTS.T19488A2365291.en. (Accessed November 4, 2020).

Pirotta, V., Grech, A., Jonsen, I. D., Laurance, W. F., and Harcourt, R. G. (2019). Consequences of Global Shipping Traffic for Marine Giants. *Front. Ecol. Environ.* 17, 39–47. doi: 10.1002/fee.1987

Protected planet - protected areas (WDPA). Available at: https://www.protectedplanet.net/en/search-areas?filters%5Bdb_type%5D%5B%5D=wdpa (Accessed June 1, 2020).

Ramírez-Macías, D., Queiroz, N., Pierce, S. J., Humphries, N. E., Sims, D. W., and Brunnschweiler, J. M. (2017). Oceanic Adults, Coastal Juveniles: Tracking the Habitat Use of Whale Sharks Off the Pacific Coast of Mexico. *PeerJ* 5, e3271. doi: 10.7717/peerj.3271

R Core Team (2018) *R: A Language and Environment for Statistical Computing* (Vienna: R Foundation for Statistical Computing). Available at: https://www.R-project.org/ (Accessed July 12, 2019).

Revelles, M., Isern-Fontanet, J., Cardona, L., San Félix, M., Carreras, C., and Aguilar, A. (2007). Mesoscale Eddies, Surface Circulation and the Scale of Habitat Selection by Immature Loggerhead Sea Turtles. *J. Exp. Mar. Biol. Ecol.* 347, 41–57. doi: 10.1016/j.jembe.2007.03.013

Reynolds, S. D., Norman, B. M., Beger, M., Franklin, C. E., and Dwyer, R. G. (2017). Movement, Distribution, and Marine Reserve Use by an Endangered Migratory Giant. *Divers. Distrib.* 23, 1268–1279. doi: 10.1111/ddi.12618

Riascos, J. M., Gutierrez, D., Ecribano, R., and Thatje, S. (2019). Editorial: El Niño-Southern Oscillation on a Changing Planet: Consequences for Coastal Ecosystems. *Front. Mar. Sci.* 6. doi: 10.3389/fmars.2019.00774

Riley, M. J., Hale, M. S., Harman, A., and Rees, R. G. (2010). Analysis of Whale Shark *Rhincodon Typus* Aggregations Near South Ari Atoll, Maldives Archipelago. *Aquat. Biol.* 8, 145–150. doi: 10.3354/ab00215

Rowat, D., and Brooks, K. S. (2012). A Review of the Biology, Fisheries and Conservation of the Whale Shark *Rhincodon Typus*. *J. Fish Biol.* 80, 1019–1056. doi: 10.1111/j.1095-8649.2012.03252.x

Rowat, D., and Gore, M. (2007). Regional Scale Horizontal and Local Scale Vertical Movements of Whale Sharks in the Indian Ocean Off Seychelles. *Fish. Res.* 84, 32–40. doi: 10.1016/j.fishres.2006.11.009

Ryan, J. P., Green, J. R., Espinoza, E., and Hearn, A. R. (2017). Association of Whale Sharks (*Rhincodon Typus*) With Thermo-Biological Frontal Systems of the Eastern Tropical Pacific. *PLos One* 12, e0182599. doi: 10.1371/journal.pone.0182599

Sequeira, A. M., Mellin, C., Fordham, D. A., Meekan, M. G., and Bradshaw, C. J. A. (2014). Predicting Current and Future Global Distributions of Whale Sharks. *Global Change Biol.* 20, 778–789. doi: 10.1111/gcb.12343

Sequeira, A. M., Mellin, C., Meekan, M. G., Sims, D. W., and Bradshaw, C. J. (2013). Inferred Global Connectivity of Whale Shark *Rhincodon Typus* Populations. *J. Fish Biol.* 82, 367–389. doi: 10.1111/jfb.12017

Sequeira, A. M., Thums, M., Brooks, K., and Meekan, M. G. (2016). Error and Bias in Size Estimates of Whale Sharks: Implications for Understanding Demography. *R. Soc Open Sci.* 3, 150668. doi: 10.1098/rsos.150668

Sleeman, J. C., Meekan, M. G., Wilson, S. G., Polovina, J. J., Stevens, J. D., Boggs, G. S., et al. (2010). To Go or Not to Go With the Flow: Environmental Influences on Whale Shark Movement Patterns. *J. Exp. Mar. Biol. Ecol.* 390, 84–98. doi: 10.1016/j.jembe.2010.05.009

SSALTO/DUACS (2019) *The Altimeter the Mesoscale Eddy Trajectory Atlas Products Were Produced by SSALTO/DUACS and Distributed by AVISO+ (Http://Www.Aviso.Altimetry.Fr/) With Support From CNES, in Collaboration With Oregon State University With Support From NASA*. Available at: https://www.aviso.altimetry.fr/en/data/products/value-added-products/global-mesoscale-eddy-trajectory-product.html (Accessed July, 2019).

Stevens, J. D. (2007). Whale Shark (*Rhincodon Typus*) Biology and Ecology: A Review of the Primary Literature. *Fish Res.* 84, 4–9. doi: 10.1016/j.fishres.2006.11.008

Stevens, J. D., Bonfil, R., Dulvy, N. K., and Walker, P. A. (2000). The Effects of Fishing on Sharks, Rays, and Chimaeras (Chondrichthyans), and the Implications for Marine Ecosystems. *ICES J. Mar. Sci.* 57, 476–494. doi: 10.1006/jmsc.2000.0724

Subhash, R. L., Jonah, L. K., and Solymos, P. (2019). ""ResourceSelection": Resource Selection (Probability) Functions for Use-Availability Data," in *R Package Version 0.3-5*. Available at: https://CRAN.R-project.org/package=ResourceSelection. Accessed: July 15, 2020).

Vincent, C., Mcconnell, B. J., Ridoux, V., and Fedak, M. A. (2002). Assessment of Argos Location Accuracy From Satellite Tags Deployed on Captive Gray Seals. *Marine Mammal Science*, 18(1):156–66.

Wang, J., Gao, C., Wu, F., Gao, X., Chen, J., Dai, X., et al (2021). The Discards and Bycatch of Chinese Tuna Longline Fleets in the Pacific Ocean From 2010 to 2018. *Biological Conservation*, 255:109011.

Western & Central Pacific Fisheries Commission (WCPFC) (2010) *Summary Information on Whale Shark and Cetacean Interactions in the Tropical WCPFC Purse Seine Fishery*. Available at: https://www.wcpfc.int/node/2670 (Accessed May 10, 2021).

Willett, C. S., Leben, R. R., and Lavín, M. F. (2006). Eddies and Tropical Instability Waves in the Eastern Tropical Pacific: A Review. *Prog. Oceanogr.* 69, 218–238. doi: 10.1016/j.pocean.2006.03.010

Womersley, F., Hancock, J., Cameron T. Perry, C. T., and Rowat, D. (2021). Wound-Healing Capabilities of Whale Sharks (*Rhincodon Typus*) and Implications for Conservation Management. *Conserv. Physiol.* 9, 1–17. doi: 10.1093/conphys/coaa120

Womersley, F. C., Humphries, N. E., Queiroz, N., Vedor, M., da Costa, I., Furtado, M., et al. (2002). Global Collision-Risk Hotspots of Marine Traffic and the World's Largest Fish, the Whale Shark. *Proc. Nat. Acad. Sci.* 119 (20), e2117440119. doi: 10.1073/pnas.2117440119

Xtractomatic, M. R. (2018) *Accessing Environmental Data From ERD's ERDDAP Server*. Available at: https://CRAN.R-project.org/package=xtractomatic (Accessed July 12, 2019).

Conflict of Interest: The authors declare that the research was conducted in the absence of any commercial or financial relationships that could be construed as a potential conflict of interest.

Frontiers in
Marine Science

Explores ocean-based solutions for emerging global challenges

The third most-cited marine and freshwater biology journal, advancing our understanding of marine systems and addressing global challenges including overfishing, pollution, and climate change.

Discover the latest Research Topics

See more →

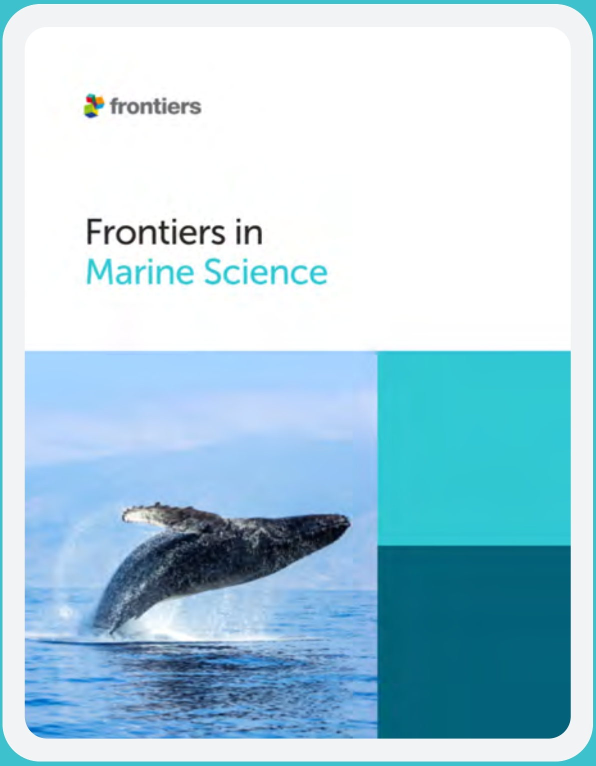
frontiers

Frontiers in
Marine Science

Frontiers

Avenue du Tribunal-Fédéral 34
1005 Lausanne, Switzerland
frontiersin.org

Contact us

+41 (0)21 510 17 00
frontiersin.org/about/contact